

PLANAR INDEX AND OUTERPLANAR INDEX OF ZERO-DIVISOR GRAPHS OF COMMUTATIVE RINGS WITHOUT IDENTITY

G. Kalaimurugan, P. Vignesh, M. Afkhami and Z. Barati

Received: 5 May 2021; Revised: 26 January 2022; Accepted: 7 March 2022

Communicated by Abdullah Harmancı

Dedicated to the memory of Professor Edmund R. Puczyłowski

ABSTRACT. Let R be a commutative ring without identity. The zero-divisor graph of R , denoted by $\Gamma(R)$ is a graph with vertex set $Z(R) \setminus \{0\}$ which is the set of all nonzero zero-divisor elements of R , and two distinct vertices x and y are adjacent if and only if $xy = 0$. In this paper, we characterize the rings whose zero-divisor graphs are ring graphs and outerplanar graphs. Further, we establish the planar index, ring index and outerplanar index of the zero-divisor graphs of finite commutative rings without identity.

Mathematics Subject Classification (2020): 05C10, 05C25, 05C75

Keywords: Zero-divisor graph, line graph, iterated line graph, planar index, outerplanar index, ring index

1. Introduction

Throughout this paper, R is a finite commutative ring without identity. Let $Z(R)$ be the set of all zero-divisors and $Z(R)^* = Z(R) \setminus \{0\}$. In [6], Beck defined a simple graph from commutative rings, the vertex set of that graph is formed by all the elements of a commutative ring R and two vertices x and y are adjacent if and only if $xy = 0$. In [3], Anderson and Livingston modified that graph structure and named it the zero-divisor graph $\Gamma(R)$ of R whose vertex set is $Z(R)^*$ and two distinct vertices x and y are adjacent if and only if $xy = 0$ for commutative rings. In [2], Anderson and Weber studied the zero-divisor graph of a commutative ring without identity.

Kuzmina and Maltsev characterized the planar zero-divisor graphs of nilpotent rings and non-nilpotent rings, in [11] and [12], respectively. In [4], Barati gave a full characterization of zero-divisor graphs associated to finite commutative rings with identity with respect to their planar index and outerplanar index.

A ring R is called *local* if it has a unique maximal ideal. If R is a non local commutative ring with identity, then $Z(R)$ need not be an ideal. For every commutative ring without identity, $Z(R) = R$, $Z(R)$ is an ideal. Therefore, if we focus the study of zero divisor graphs of commutative ring without identity, then it reveals the properties of commutative ring without identity. Thus, the zero-divisor graph of commutative rings without identity is a unique structure than commutative rings with identity. Moreover, we obtain the planar index, ring index and outerplanar index of the zero-divisor graphs of finite commutative rings without identity.

2. Preliminaries

Let G be a graph with n vertices and m edges. A *chord* is an edge joining any two non-adjacent vertices in a cycle. A *primitive cycle* is a cycle without chords. The *free rank* of G is the number of primitive cycles of G and it is denoted by $\text{frank}(G)$. The *cycle rank* of G is defined as $\text{rank}(G) = m - n + r$ where r is the number of connected components of G . Note that the cycle rank is the dimension of the cycle space of G and it satisfies the inequality $\text{rank}(G) \leq \text{frank}(G)$. The family of graphs satisfying that $\text{rank}(G) = \text{frank}(G)$ is called *ring graphs*.

The line graph of G (denoted by $L(G)$) is a graph whose vertex set consists of the set of all edges of G and two vertices of $L(G)$ are adjacent if the corresponding edges of G are adjacent. The k^{th} iterated line graph of G (denoted by $L^k(G)$) is defined as $L^k(G) = L(L^{k-1}(G))$, for every positive integer k . In particular, $L^0(G) = G$ and $L^1(G) = L(G)$. K_n and P_n denote the complete graph and the path of n vertices, respectively. A set of vertices of the graph G is called an *independent set* if no two vertices in the set are adjacent to each other. The join of two graphs $G_1 = (V_1, E_1)$ and $G_2 = (V_2, E_2)$ is a graph $G_1 + G_2$ whose vertex set is $V_1 \cup V_2$ and whose edge set contains the edges joining every vertex from V_1 to every vertex in V_2 . A vertex v is said to be a cut vertex if removal of the vertex v disconnects the graph G .

For a class of graphs \mathbb{G} , the graph G is said to be a *forbidden subgraph* for \mathbb{G} if no member of \mathbb{G} has G as an induced subgraph. We can say that G is a *minimal forbidden subgraph* for \mathbb{G} if it is a forbidden subgraph for \mathbb{G} but none of its proper induced subgraphs are forbidden subgraphs.

For a graph G , the *genus* of G is the minimum positive integer n such that G can be embedded in the surface S_n without edge crossings and it is denoted by $g(G)$. If a graph G can be embedded in the plane without edge crossings, then it is called *planar*, i.e., $g(G) = 0$. If $g(G) \neq 0$, then the graph G is non planar. An outerplanar

graph is a graph that can be embedded in the plane such that all vertices lie on the outer face of the drawing; otherwise, the graph is non-outerplanar.

The ring index of a graph G is the smallest integer k such that the k^{th} iterated line graph of G is not a ring graph and it is denoted by $\gamma_r(G)$. The planar index of a graph G is defined as the smallest k such that $L^k(G)$ is non-planar. We denote the planar index of G by $\gamma_p(G)$. The outerplanar index of a graph G is the smallest integer k such that the k^{th} iterated line graph of G is non-outerplanar and it is denoted by $\gamma_o(G)$. If $L^k(G)$ is outerplanar (respectively, ring graph or planar) for all $k \geq 0$, we define $\gamma_o(G) = \infty$ (respectively, $\gamma_r(G) = \infty$ or $\gamma_p(G) = \infty$).

Remark 2.1. In [10], I. Gitler et al. proved the relationship between outerplanar graph, ring graph and planar graph as follows:

$$\text{outerplanar} \Rightarrow \text{ring graph} \Rightarrow \text{planar}$$

(i.e. $\gamma_o(G) \leq \gamma_r(G) \leq \gamma_p(G)$).

In the literature, the notations for the commutative rings without identity are used in many ways. In this paper, we follow the notations used by Anderson and Weber in [2]. With respect to isomorphism, we identify the notations of the commutative rings without identity used in [2] and [11] as follow: $N_{0,2} \cong \mathbb{Z}_2^0$, $N_{0,3} \cong \mathbb{Z}_3^0$, $N_{0,4} \cong \mathbb{Z}_4^0$, $N_{0,5} \cong \mathbb{Z}_5^0$, $N_{2,2} \cong \frac{x\mathbb{Z}_2[x]}{x^3\mathbb{Z}_2[x]}$, $N_{3,3} \cong \frac{x\mathbb{Z}_3[x]}{x^3\mathbb{Z}_3[x]}$, $N_4 \cong \frac{x\mathbb{Z}[x]}{\langle 4x, x^2 - 2x \rangle}$, $N_9 \cong \frac{x\mathbb{Z}[x]}{\langle 9x, x^2 - 3x \rangle}$ and $N_{2,4} \cong \frac{x\mathbb{Z}[x]}{\langle 8x, x^2 - 2x \rangle}$. We denote the ring of integers modulo n by \mathbb{Z}_n and \mathbb{Z}_q^0 is the ring with additive group $(\mathbb{Z}_q, +_q)$ and trivial multiplication (i.e. $ab = 0$ for all $a, b \in \mathbb{Z}_q$). The following notations are useful for further reading of this paper.

$$Q_1 = \langle a, b \mid 4a = 0, 2b = 0, a^2 = b, ab = ba = 2a, b^2 = 0 \rangle;$$

$$Q_2 = \langle a, b \mid 4a = 0, 2b = 0, a^2 = 0, ab = ba = 2a, b^2 = 0 \rangle;$$

$$Q_3 = \langle a, b \mid 4a = 0, 2b = 0, a^2 = 2a, ab = ba = 2a, b^2 = 0 \rangle;$$

$$Q_4 = \langle a, b \mid 4a = 0, 2b = 0, a^2 = 2a, ab = ba = 0, b^2 = 2a \rangle;$$

$$Q_5 = \langle a, b, c \mid 2a = 2b = 2c = 0, a^2 = b, b^2 = 0, ab = c, c^2 = 0 \rangle;$$

$$Q_6 = \langle a, b, c \mid 2a = 2b = 2c = 0, a^2 = b^2 = 0, ab = -ba = c,$$

$$ac = ca = bc = cb = c^2 = 0 \rangle;$$

$$Q_7 = \langle a, b, c \mid 2a = 2b = 2c = 0, a^2 = c, ab = ba = 0, b^2 = c,$$

$$ac = ca = bc = cb = c^2 = 0 \rangle.$$

Remark 2.2. The characterization for planar zero-divisor graphs from all finite rings were obtained in [11, Theorem 3.1] and [12, Theorem 1 and 2]. In this characterization, we have exactly 24 (17 from Theorem 3.1 in [11] and 7 from Theorem 2 in [12]) non-isomorphic (up to isomorphism) commutative rings without identity whose zero-divisor graphs are planar.

We have restated the notations and combined the results from Theorem 3.1 in [11] and Theorem 2 in [12] with the restriction that rings are commutative without identity. From these evidence, we get the following theorem.

Theorem 2.3. *Let R be a finite commutative ring without identity and let \mathbb{F}_{p^n} be a finite field with p^n elements where p is a prime. Then $\Gamma(R)$ is planar if and only if R is isomorphic to one of the following rings:*

$\mathbb{Z}_2^0 \times \mathbb{Z}_2 \times \mathbb{Z}_2, \mathbb{Z}_2^0 \times \mathbb{F}_{p^n}, \mathbb{Z}_3^0 \times \mathbb{F}_{p^n}, \mathbb{Z}_2^0 \times \mathbb{Z}_4, \mathbb{Z}_2^0 \times \frac{\mathbb{Z}_2[x]}{\langle x^2 \rangle}, \mathbb{Z}_2 \times \frac{x\mathbb{Z}[x]}{\langle 4x, x^2 - 2x \rangle}, \mathbb{Z}_2 \times \frac{x\mathbb{Z}_2[x]}{x^3\mathbb{Z}_2[x]},$
 $\mathbb{Z}_2^0 \times \mathbb{Z}_2^0, \mathbb{Z}_2^0, \mathbb{Z}_3^0, \mathbb{Z}_4^0, \mathbb{Z}_5^0, \frac{x\mathbb{Z}_2[x]}{x^3\mathbb{Z}_2[x]}, \frac{x\mathbb{Z}_3[x]}{x^3\mathbb{Z}_3[x]}, \frac{x\mathbb{Z}[x]}{\langle 4x, x^2 - 2x \rangle}, \frac{x\mathbb{Z}[x]}{\langle 9x, x^2 - 3x \rangle}, \frac{x\mathbb{Z}[x]}{\langle 8x, x^2 - 2x \rangle}, \mathbb{Q}_i$
where $1 \leq i \leq 7$.

Let q be a prime number. Consider the ring $R = \mathbb{Z}_q^0 \times \mathbb{F}_{p^n}$. Note that $Z(R) = R$. Further, the subgraph of $\Gamma(R)$ induced by $(\mathbb{Z}_q^0)^* \times \{0\}$ is K_{q-1} and the subset $R \setminus (\mathbb{Z}_q^0 \times \{0\})$ with $(p^n - 1)q$ elements induces an independent set in $\Gamma(R)$. Also every element in $(\mathbb{Z}_q^0)^* \times \{0\}$ is adjacent with every element in $R \setminus (\mathbb{Z}_q^0 \times \{0\})$ in $\Gamma(R)$. Hence we have the following lemma, which gives the structure of $\Gamma(\mathbb{Z}_q^0 \times \mathbb{F}_{p^n})$.

Lemma 2.4. *Let p and q be prime numbers and $R = \mathbb{Z}_q^0 \times \mathbb{F}_{p^n}$. Then $\Gamma(R) \cong K_{q-1} + \overline{K_{(p^n-1)q}}$.*

Lemma 2.5. *Let R_1 and R_2 be finite commutative rings. If $\Gamma(R_1) \cong \Gamma(R_2)$, then $\Gamma(S \times R_1) \cong \Gamma(S \times R_2)$ for any commutative ring S .*

Proof. Let $\psi : \Gamma(R_1) \rightarrow \Gamma(R_2)$ be a graph isomorphism. Let S be a commutative ring. Consider $\phi : \Gamma(S \times R_1) \rightarrow \Gamma(S \times R_2)$ defined by $\phi((a, b)) = (a, \psi(b))$. Let (a, b) and (c, d) be two nonzero elements in $S \times R_1$ which are adjacent in $\Gamma(S \times R_1)$. From this $(ac, bd) = (0, 0)$ and so $\psi(bd) = \psi(b)\psi(d) = 0$. Now $\phi((ac, bd)) = (ac, \psi(bd)) = (ac, \psi(b)\psi(d)) = (0, 0)$ and so $(a, \psi(b))(c, \psi(d)) = (0, 0)$. Therefore, $\phi((a, b))\phi((c, d)) = (0, 0)$ and so $\phi((a, b))$ and $\phi((c, d))$ are adjacent in $\Gamma(S \times R_2)$. Similarly one can observe that $\phi((a, b))$ and $\phi((c, d))$ are not adjacent in $\Gamma(S \times R_1)$ whenever (a, b) and (c, d) are not adjacent in $\Gamma(S \times R_1)$. Since ψ is bijective, ϕ is bijective and so ϕ is a graph isomorphism. \square

The following is useful in the sequel of the paper.

Corollary 2.6. *Assume that R_1 and R_2 are finite commutative rings. If $\Gamma(R_1) \cong \Gamma(R_2)$, then $g(\Gamma(S \times R_1)) = g(\Gamma(S \times R_2))$ for any commutative ring S .*

3. The planar index of zero-divisor graphs

In [8], Ghebleh and Khatirinejad characterized connected graphs with respect to their planar index.

Theorem 3.1. [8, Theorem 10] *Let G be a connected graph. Then:*

- (a) $\gamma_p(G) = 0$ if and only if G is non-planar;
- (b) $\gamma_p(G) = \infty$ if and only if G is either a path, a cycle, or $K_{1,3}$;
- (c) $\gamma_p(G) = 1$ if and only if G is planar and either $\Delta(G) \geq 5$ or G has a vertex of degree 4 which is not a cut-vertex;
- (d) $\gamma_p(G) = 2$ if and only if $L(G)$ is planar and G contains one of the graphs H_i in Figure 1 as a subgraph;
- (e) $\gamma_p(G) = 4$ if and only if G is one of the graphs X_k or Y_k (Figure 1) for some $k \geq 2$;
- (f) $\gamma_p(G) = 3$ otherwise.

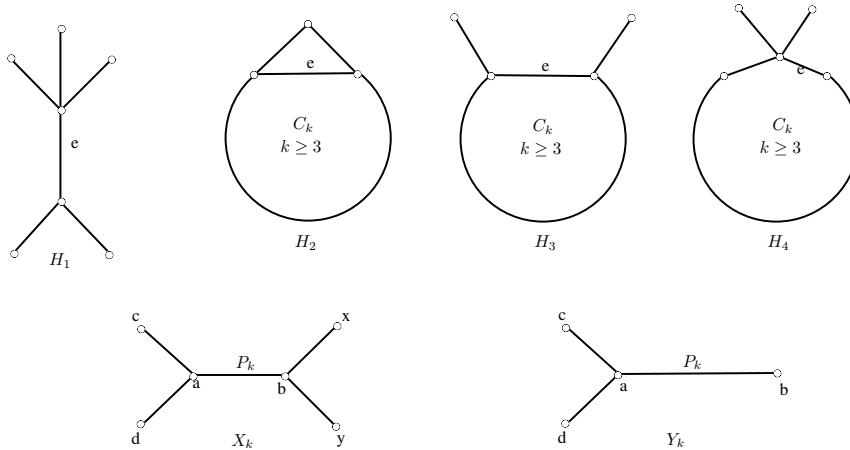


Figure 1

In [11] and [12], Kuzmina studied planarity for all finite rings. Specially, the planarity of zero divisor graphs with non zero identity was studied in [7] and according to these results, the planar index and outerplanar index of these graphs were studied in [4]. In this section, we characterize all zero divisor graphs with respect to the planar index when R is a commutative ring without identity.

Theorem 3.2. *Let R be a finite commutative ring without identity. Then*

- (1) $\gamma_p(\Gamma(R)) = \infty$ if and only if R is isomorphic to one of the following rings:

- (a) $\mathbb{Z}_2^0 \times \mathbb{Z}_2^0, \mathbb{Z}_2^0 \times \mathbb{Z}_2;$
- (b) $\mathbb{Z}_2^0, \mathbb{Z}_3^0, \mathbb{Z}_4^0, \frac{x\mathbb{Z}[x]}{\langle 4x, x^2-2x \rangle}, \frac{x\mathbb{Z}_2[x]}{x^3\mathbb{Z}_2[x]};$
- (2) $\gamma_p(\Gamma(R)) = 1$ if and only if R is isomorphic to one of the following rings:
 - (a) $\mathbb{Z}_2^0 \times \mathbb{Z}_2 \times \mathbb{Z}_2;$
 - (b) $\mathbb{Z}_2^0 \times \mathbb{F}_{p^n}$ with $p^n \geq 4, \mathbb{Z}_3^0 \times \mathbb{F}_{p^n}, \mathbb{Z}_2^0 \times \mathbb{Z}_4, \mathbb{Z}_2^0 \times \frac{\mathbb{Z}_2[x]}{\langle x^2 \rangle}, \mathbb{Z}_2 \times \frac{x\mathbb{Z}[x]}{\langle 4x, x^2-2x \rangle}, \mathbb{Z}_2 \times \frac{x\mathbb{Z}_2[x]}{x^3\mathbb{Z}_2[x]};$
 - (c) $\frac{x\mathbb{Z}[x]}{\langle 9x, x^2-3x \rangle}, \frac{x\mathbb{Z}_3[x]}{x^3\mathbb{Z}_3[x]}, \frac{x\mathbb{Z}[x]}{\langle 8x, x^2-2x \rangle}, Q_i$ where $1 \leq i \leq 7;$
- (3) $\gamma_p(\Gamma(R)) = 2$ if and only if R is isomorphic to $\mathbb{Z}_5^0;$
- (4) $\gamma_p(\Gamma(R)) = 3$ if and only if R is isomorphic to $\mathbb{Z}_2^0 \times \mathbb{Z}_3;$
- (5) $\gamma_p(\Gamma(R)) = 0$ otherwise.

Proof. For a non planar graph, the planar index is 0 because of Theorem 3.1. Therefore, we should focused on the case $\Gamma(R)$ is planar. Let R be a finite commutative ring without identity. Then $R \cong R_1 \times R_2 \times \dots \times R_n$ and R_i 's are indecomposable rings for all i such that $1 \leq i \leq n$. By Theorem 2.3, it is enough to consider $n \leq 3$.

Case 1. Suppose $n = 3$. By Theorem 2.3, $\Gamma(R_1 \times R_2 \times R_3)$ is planar if and only if $R \cong \mathbb{Z}_2^0 \times \mathbb{Z}_2 \times \mathbb{Z}_2$. By Figure 2, $\Delta(\Gamma(\mathbb{Z}_2^0 \times \mathbb{Z}_2 \times \mathbb{Z}_2)) = 6$. By Theorem 3.1, we have $\gamma_p(\Gamma(\mathbb{Z}_2^0 \times \mathbb{Z}_2 \times \mathbb{Z}_2)) = 1$.

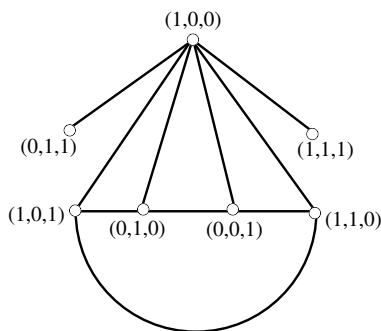


Figure 2. $\Gamma(\mathbb{Z}_2^0 \times \mathbb{Z}_2 \times \mathbb{Z}_2)$

Case 2. Suppose $n = 2$. By Theorem 2.3, $\Gamma(R_1 \times R_2)$ is planar if and only if R is isomorphic to one of the following rings: $\mathbb{Z}_2^0 \times \mathbb{Z}_2^0, \mathbb{Z}_2^0 \times \mathbb{F}_{p^n}, \mathbb{Z}_3^0 \times \mathbb{F}_{p^n}, \mathbb{Z}_2 \times \frac{x\mathbb{Z}[x]}{\langle 4x, x^2-2x \rangle}, \mathbb{Z}_2 \times \frac{x\mathbb{Z}_2[x]}{x^3\mathbb{Z}_2[x]}, \mathbb{Z}_2^0 \times \mathbb{Z}_4, \mathbb{Z}_2^0 \times \frac{\mathbb{Z}_2[x]}{\langle x^2 \rangle}.$

Suppose $R \cong \mathbb{Z}_2^0 \times \mathbb{Z}_2^0$. The products of trivial multiplication yields that $\Gamma(R) \cong K_3$. Now, by Theorem 3.1, we get that $\gamma_p(\Gamma(\mathbb{Z}_2^0 \times \mathbb{Z}_2^0)) = \infty$.

For $R \cong \mathbb{Z}_2^0 \times \mathbb{F}_{p^n}$, by Lemma 2.4, we have $\Gamma(\mathbb{Z}_2^0 \times \mathbb{F}_{p^n}) \cong K_{1,2p^n-2}$. If $p^n \geq 4$, then $\Delta(\Gamma(\mathbb{Z}_2^0 \times \mathbb{F}_{p^n})) \geq 6$. By Theorem 3.1, we have $\gamma_p(\Gamma(\mathbb{Z}_2^0 \times \mathbb{F}_{p^n})) = 1$ where $p^n \geq 4$. If $p^n = 3$, then $\Gamma(\mathbb{Z}_2^0 \times \mathbb{Z}_3) \cong K_{1,4}$. Since the line graph of any star

graph is complete, we have $L(\Gamma(\mathbb{Z}_2^0 \times \mathbb{Z}_3)) \cong K_4$ which is planar and H_2 is a subgraph of $L(\Gamma(\mathbb{Z}_2^0 \times \mathbb{Z}_3))$. By Theorem 3.1, $\gamma_p(L(\Gamma(\mathbb{Z}_2^0 \times \mathbb{Z}_3))) = 2$. It implies that $\gamma_p(\Gamma(\mathbb{Z}_2^0 \times \mathbb{Z}_3)) = 3$. Suppose $p^n = 2$. Then $R \cong \mathbb{Z}_2^0 \times \mathbb{Z}_2$. By Lemma 2.4, $\Gamma(R)$ is isomorphic to $K_{1,2}$. Since it is a path, we have $\gamma_p(\Gamma(\mathbb{Z}_2^0 \times \mathbb{Z}_2)) = \infty$.

Suppose $R \cong \mathbb{Z}_3^0 \times \mathbb{F}_{p^n}$. By Lemma 2.4, we have $\Gamma(\mathbb{Z}_3^0 \times \mathbb{F}_{p^n}) \cong K_2 + \overline{K_{3p^n-3}}$. Suppose $p^n \geq 3$. It is easy to see that the graph $\Gamma(\mathbb{Z}_3^0 \times \mathbb{F}_{p^n})$ is planar and $\Delta(\mathbb{Z}_3^0 \times \mathbb{F}_{p^n}) \geq 6$. By Theorem 3.1, $\gamma_p(\Gamma(\mathbb{Z}_3^0 \times \mathbb{F}_{p^n})) = 1$ for $p^n \geq 3$. Suppose $p^n = 2$ and $R \cong \mathbb{Z}_3^0 \times \mathbb{Z}_2$. By Lemma 2.4, $\Gamma(R)$ is isomorphic to $K_2 + \overline{K_3}$. It is a planar graph and it has two vertices of degree 4 which are not cut vertices. By Theorem 3.1, $\gamma_p(\Gamma(\mathbb{Z}_3^0 \times \mathbb{Z}_2)) = 1$.

It is not hard to see that

$$\Gamma(\mathbb{Z}_2^0 \times \mathbb{Z}_2) \cong \Gamma\left(\frac{x\mathbb{Z}[x]}{\langle 4x, x^2-2x \rangle}\right) \cong \Gamma\left(\frac{x\mathbb{Z}_2[x]}{x^3\mathbb{Z}_2[x]}\right).$$

By Corollary 2.6, we have that $\Gamma(\mathbb{Z}_2^0 \times \mathbb{Z}_2 \times \mathbb{Z}_2) \cong \Gamma(\mathbb{Z}_2 \times \mathbb{Z}_2^0 \times \mathbb{Z}_2) \cong \Gamma(\mathbb{Z}_2 \times \frac{x\mathbb{Z}[x]}{\langle 4x, x^2-2x \rangle}) \cong \Gamma(\mathbb{Z}_2 \times \frac{x\mathbb{Z}_2[x]}{x^3\mathbb{Z}_2[x]})$. We already proved that $\gamma_p(\Gamma(\mathbb{Z}_2^0 \times \mathbb{Z}_2 \times \mathbb{Z}_2)) = 1$. Therefore,

$$\gamma_p\left(\Gamma\left(\mathbb{Z}_2 \times \frac{x\mathbb{Z}[x]}{\langle 4x, x^2-2x \rangle}\right)\right) = \gamma_p\left(\Gamma\left(\mathbb{Z}_2 \times \frac{x\mathbb{Z}_2[x]}{x^3\mathbb{Z}_2[x]}\right)\right) = 1.$$

Assume that R is isomorphic to anyone of $\mathbb{Z}_2^0 \times \mathbb{Z}_4$ or $\mathbb{Z}_2^0 \times \frac{\mathbb{Z}_2[x]}{\langle x^2 \rangle}$. Then $\Gamma(R)$ is isomorphic to G_1 represented in Figure 3.

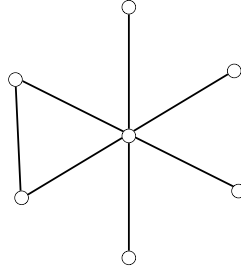


Figure 3. The graph G_1

The degree of the vertex $(1, 0)$ in the graphs $\Gamma(\mathbb{Z}_2^0 \times \mathbb{Z}_4)$ and $\Gamma(\mathbb{Z}_2^0 \times \frac{\mathbb{Z}_2[x]}{\langle x^2 \rangle})$ is 6. By Theorem 3.1, we have

$$\gamma_p(\Gamma(\mathbb{Z}_2^0 \times \mathbb{Z}_4)) = \gamma_p\left(\Gamma\left(\mathbb{Z}_2^0 \times \frac{\mathbb{Z}_2[x]}{\langle x^2 \rangle}\right)\right) = 1.$$

Case 3. Suppose $n = 1$. Since $\Gamma(R)$ is planar, by Theorem 2.3, R is isomorphic to one of the following rings: $\mathbb{Z}_2^0, \mathbb{Z}_3^0, \mathbb{Z}_4^0, \mathbb{Z}_5^0, \frac{x\mathbb{Z}[x]}{\langle 4x, x^2-2x \rangle}, \frac{x\mathbb{Z}_2[x]}{x^3\mathbb{Z}_2[x]}, \frac{x\mathbb{Z}[x]}{\langle 9x, x^2-3x \rangle}, \frac{x\mathbb{Z}_3[x]}{x^3\mathbb{Z}_3[x]}, \frac{x\mathbb{Z}[x]}{\langle 8x, x^2-2x \rangle}, Q_i$ where $1 \leq i \leq 7$.

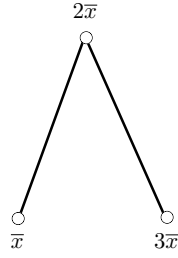


Figure 4(a). $\Gamma(\frac{x\mathbb{Z}[x]}{\langle 4x, x^2-2x \rangle})$

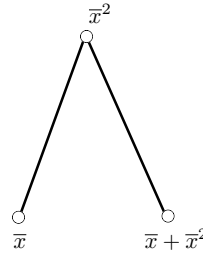


Figure 4(b). $\Gamma(\frac{x\mathbb{Z}_2[x]}{x^3\mathbb{Z}_2[x]})$

Suppose R is isomorphic to either \mathbb{Z}_2^0 or \mathbb{Z}_3^0 or \mathbb{Z}_4^0 or $\frac{x\mathbb{Z}[x]}{\langle 4x, x^2-2x \rangle}$ or $\frac{x\mathbb{Z}_2[x]}{x^3\mathbb{Z}_2[x]}$. The rings \mathbb{Z}_2^0 , \mathbb{Z}_3^0 and \mathbb{Z}_4^0 have the zero-divisor graphs K_1 , K_2 and K_3 respectively. Moreover, by Figure 4(a) and 4(b), we have that

$$\Gamma(\frac{x\mathbb{Z}[x]}{\langle 4x, x^2-2x \rangle}) \cong \Gamma(\frac{x\mathbb{Z}_2[x]}{x^3\mathbb{Z}_2[x]}) \cong K_{1,2}.$$

So, by Theorem 3.1, we can conclude that $\gamma_p(\Gamma(R)) = \infty$.

If $R \cong \mathbb{Z}_5^0$, then $\Gamma(\mathbb{Z}_5^0) \cong K_4$. By Theorem 3.1, we have $\gamma_p(\Gamma(\mathbb{Z}_5^0)) = 2$.

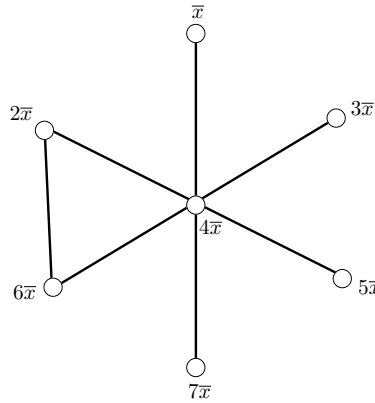
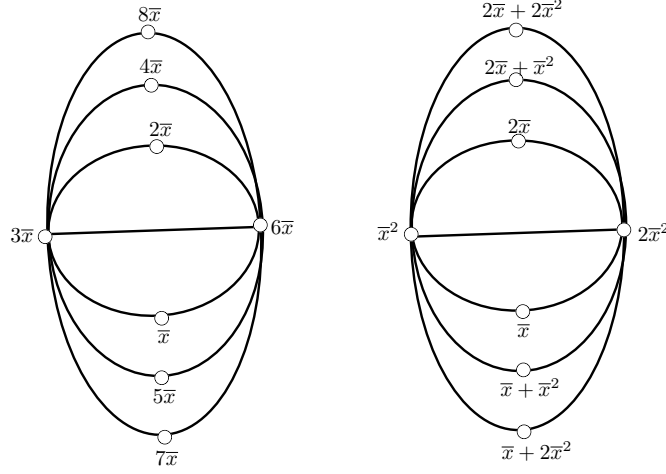


Figure 5. $\Gamma(\frac{x\mathbb{Z}[x]}{\langle 8x, x^2-2x \rangle})$

Suppose that R is isomorphic to either $\frac{x\mathbb{Z}[x]}{\langle 8x, x^2-2x \rangle}$ or Q_i for all i , $1 \leq i \leq 7$. Note that, $\Gamma(Q_1)$, $\Gamma(Q_2)$, $\Gamma(Q_3)$, $\Gamma(Q_4)$, $\Gamma(Q_5)$, $\Gamma(Q_6)$ and $\Gamma(Q_7)$ are illustrated in Figures 1.B, 2.A, 2.B, 3.A, 3.B, 4.A and 4.B of [11], respectively. From these Figures 1.B to 4.B and by Figure 5, one can easily check that $\Delta(\Gamma(R)) = 6$ and $\Gamma(R)$ is planar. By Theorem 3.1, $\gamma_p(\Gamma(R)) = 1$.

Figure 6(a). $\Gamma\left(\frac{x\mathbb{Z}[x]}{\langle 9x, x^2 - 3x \rangle}\right)$ Figure 6(b). $\Gamma\left(\frac{x\mathbb{Z}_3[x]}{x^3\mathbb{Z}_3[x]}\right)$

Suppose R is isomorphic to either $\frac{x\mathbb{Z}[x]}{\langle 9x, x^2 - 3x \rangle}$ or $\frac{x\mathbb{Z}_3[x]}{x^3\mathbb{Z}_3[x]}$. By Figures 6(a) and 6(b), $\Gamma(R) \cong K_2 + \overline{K_6}$. Clearly, $\Gamma\left(\frac{x\mathbb{Z}[x]}{\langle 9x, x^2 - 3x \rangle}\right)$ and $\Gamma\left(\frac{x\mathbb{Z}_3[x]}{x^3\mathbb{Z}_3[x]}\right)$ are planar and $\Delta\left(\Gamma\left(\frac{x\mathbb{Z}[x]}{\langle 9x, x^2 - 3x \rangle}\right)\right) = \Delta\left(\Gamma\left(\frac{x\mathbb{Z}_3[x]}{x^3\mathbb{Z}_3[x]}\right)\right) = 6$. By Theorem 3.1, we get that $\gamma_p\left(\Gamma\left(\frac{x\mathbb{Z}[x]}{\langle 9x, x^2 - 3x \rangle}\right)\right) = \gamma_p\left(\Gamma\left(\frac{x\mathbb{Z}_3[x]}{x^3\mathbb{Z}_3[x]}\right)\right) = 1$. \square

4. The ring index and outerplanar index of zero-divisor graphs

In this section, we characterize the rings whose zero-divisor graphs are either ring graphs or outerplanar graphs. Further, we give a full characterization of zero-divisor graphs with respect to their ring index and outerplanar index when R is a commutative ring without identity. In [9], Gitler et al. characterized the forbidden induced subgraphs for the family of ring graphs. We need some definitions to use their theorem.

Definition 4.1. (a) A *prism* is a graph consisting of two vertex-disjoint triangles $C_1 = (x_1, x_2, x_3, x_1)$ and $C_2 = (y_1, y_2, y_3, y_1)$, and three paths P_1, P_2 and P_3 pairwise vertex-disjoint, such that each P_i is a path between x_i and y_i for $i = 1, 2, 3$ and the subgraph induced by $V(P_i) \cup V(P_j)$ is a cycle for $1 \leq i < j \leq 3$ (Figure 7a).

(b) A *pyramid* is a graph consisting of a vertex w , a triangle $C = (z_1, z_2, z_3, z_1)$, and three paths P_1, P_2 and P_3 such that P_i is between w and z_i for $i = 1, 2, 3$; $V(P_i) \cap V(P_j) = w$ and the subgraph induced by $V(P_i) \cup V(P_j)$ is a cycle for $1 \leq i < j \leq 3$ and at least one of the P_1, P_2, P_3 has at least two edges (Figure 7b).

(c) A *theta* is a graph consisting of two non adjacent vertices x and y , and three paths P_1, P_2 and P_3 with ends x and y , such that the union of every two of P_1, P_2 and P_3 is an induced cycle (Figure 7c).

(d) A partial wheel is a graph consisting of a cycle C and a vertex z disjoint from C such that z is adjacent to some vertices of C . The cycle C is called the rim of W and z is called the center of W . A partial wheel T with rim C and center z is called a θ -*partial wheel* if $|V(C)| \geq 4$ and there exist two non adjacent vertices in $V(C) \cap N_T(z)$ (Figure 7d).

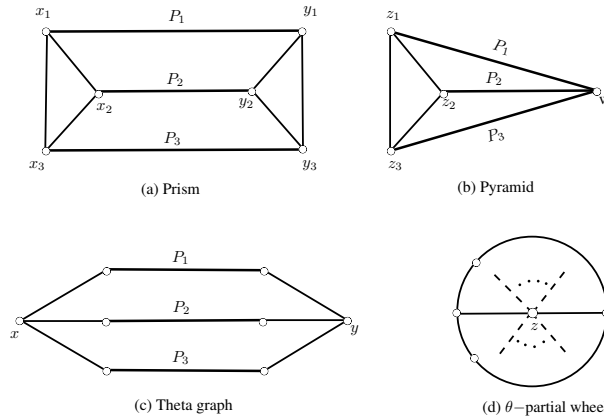


Figure 7

Theorem 4.2. [9, Corollary 4.13] *The minimal forbidden induced subgraphs for ring graphs are: prisms, pyramids, theta graphs, θ -partial wheels and K_4 .*

Let d_1, d_2, \dots, d_t are positive integers with $n \geq d_1 + d_2 + \dots + d_t$. We define $I(d_1, d_2, \dots, d_t)$ as the tree obtained from P_n by adding a leaf to each vertex of P_n that is at in distance of $d_1, d_1 + d_2, \dots, d_1 + d_2 + \dots + d_t$ (as in Figure 8). In [5], Barati completely characterized the graphs with respect to their ring index. It can be recalled in the following theorem.

Theorem 4.3. [5, Theorem 1.3] *Let G be a connected graph. Then:*

- (a) $\gamma_r(G) = 0$ if and only if G is not a ring graph if and only if it has an induced subgraph which is prism, pyramid, theta graph, θ -partial wheel or K_4 ;
- (b) $\gamma_r(G) = \infty$ if and only if G is either a path, a cycle, or $K_{1,3}$;
- (c) $\gamma_r(G) = 1$ if and only if G is a ring graph and G has a subgraph homeomorphic to $K_{1,4}$ or $K_1 + P_3$ in Figure 8;
- (d) $\gamma_r(G) = 2$ if and only if $L(G)$ is ring graph and G has a subgraph isomorphic to one of the graphs G_2 or G_3 in Figure 8;

- (e) $\gamma_r(G) = 3$ if and only if $G \in I(d_1, d_2, \dots, d_t)$ where $d_i \geq 2$ for $i = 2, \dots, t - 1$, and $d_1 \geq 1$ (Figure 8).

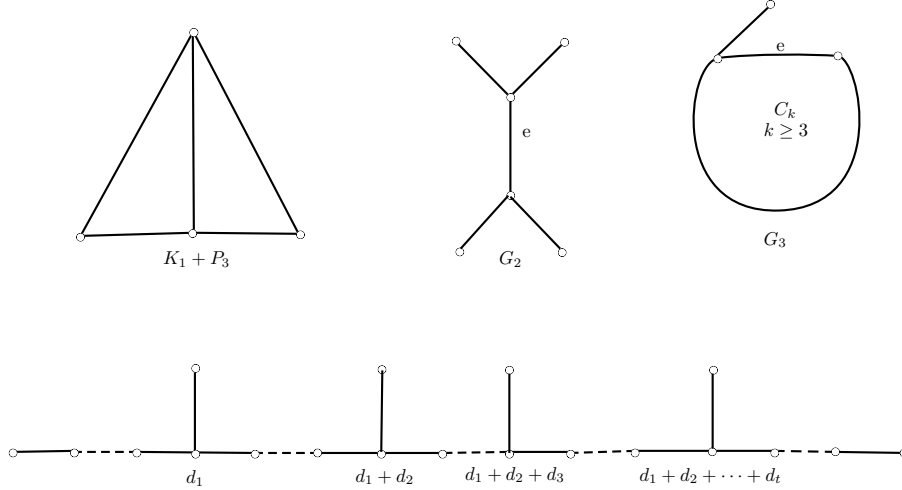


Figure 8

In [13], Lin et al. studied the outerplanarity of the iterated line graphs and they characterized all graphs with respect to their outerplanar index. Their theorem is recalled in the following theorem which is useful for further reading of this paper.

Theorem 4.4. [13, Theorem 3.4] *Let G be a connected graph. Then:*

- (a) $\gamma_o(G) = 0$ if and only if G is non-outerplanar;
- (b) $\gamma_o(G) = \infty$ if and only if G is either a path, a cycle, or $K_{1,3}$;
- (c) $\gamma_o(G) = 1$ if and only if G is planar and G has a subgraph homeomorphic to $K_{2,3}$, $K_{1,4}$ or $K_1 + P_3$ in Figure 8;
- (d) $\gamma_o(G) = 2$ if and only if $L(G)$ is planar and G has a subgraph isomorphic to one of the graphs G_2 or G_3 in Figure 8;
- (e) $\gamma_o(G) = 3$ if and only if $G \in I(d_1, d_2, \dots, d_t)$ where $d_i \geq 2$ for $i = 2, \dots, t - 1$, and $d_1 \geq 1$ (Figure 8).

In [1], Afkhami classified all finite commutative rings with identity whose zero-divisor graphs are ring graphs and outerplanar graphs. In the following theorems, we classify all finite commutative rings without identity whose zero-divisor graphs are ring graphs and outerplanar graphs.

Theorem 4.5. *Let R be a finite commutative ring without identity. Then $\Gamma(R)$ is a ring graph if and only if R is isomorphic to one of the following rings:*

$$\mathbb{Z}_2^0 \times \mathbb{Z}_2^0, \mathbb{Z}_2^0 \times \mathbb{F}_{p^n}, \mathbb{Z}_3^0 \times \mathbb{F}_{p^n}, \mathbb{Z}_2^0 \times \mathbb{Z}_4, \mathbb{Z}_2^0 \times \frac{\mathbb{Z}_2[x]}{\langle x^2 \rangle}, \mathbb{Z}_2^0, \mathbb{Z}_3^0, \mathbb{Z}_4^0, \frac{x\mathbb{Z}_2[x]}{x^3\mathbb{Z}_2[x]}, \frac{x\mathbb{Z}[x]}{\langle 4x, x^2 - 2x \rangle}, \frac{x\mathbb{Z}_3[x]}{x^3\mathbb{Z}_3[x]}, \frac{x\mathbb{Z}[x]}{\langle 9x, x^2 - 3x \rangle}, \frac{x\mathbb{Z}[x]}{\langle 8x, x^2 - 2x \rangle}, Q_1, Q_2, Q_5, Q_6.$$

Proof. Let $R \cong R_1 \times R_2 \times \cdots \times R_n$. We assume that $\Gamma(R)$ is a ring graph. Since every ring graph is planar, by Theorem 2.3, it is enough to consider $n \leq 3$.

Case 1. Assume that $n = 3$ and $R \cong R_1 \times R_2 \times R_3$. So $R \cong \mathbb{Z}_2^0 \times \mathbb{Z}_2 \times \mathbb{Z}_2$. Let $S = \{(1, 0, 1), (0, 1, 0), (1, 1, 0), (0, 0, 1), (1, 0, 0)\}$. Now, by Figure 2, it is easy to see that the induced subgraph of the graph $\Gamma(\mathbb{Z}_2^0 \times \mathbb{Z}_2 \times \mathbb{Z}_2)$ by the set S is isomorphic to a θ -partial wheel. By Theorem 4.2, $\Gamma(\mathbb{Z}_2^0 \times \mathbb{Z}_2 \times \mathbb{Z}_2)$ is not a ring graph.

Case 2. Assume that $n = 2$ and R is isomorphic to one of the following rings: $\mathbb{Z}_2^0 \times \mathbb{Z}_2^0$, $\mathbb{Z}_2^0 \times \mathbb{F}_{p^n}$, $\mathbb{Z}_3^0 \times \mathbb{F}_{p^n}$, $\mathbb{Z}_2^0 \times \mathbb{Z}_4$, $\mathbb{Z}_2^0 \times \frac{\mathbb{Z}_2[x]}{\langle x^2 \rangle}$.

Suppose $R \cong \mathbb{Z}_2^0 \times \mathbb{Z}_2^0$. Since the multiplication of R is trivial, $\Gamma(R)$ is isomorphic to K_3 . By Theorem 4.2, $\Gamma(R)$ is a ring graph.

By Lemma 2.4, the graph $\Gamma(\mathbb{Z}_2^0 \times \mathbb{F}_{p^n}) \cong K_1 + \overline{K_{2p^n-2}}$ and $\Gamma(\mathbb{Z}_3^0 \times \mathbb{F}_{p^n}) \cong K_2 + \overline{K_{3p^n-3}}$. Since $\Gamma(\mathbb{Z}_2^0 \times \mathbb{F}_{p^n})$ is a star graph, we can deduce that $\Gamma(\mathbb{Z}_2^0 \times \mathbb{F}_{p^n})$ is a ring graph. Also, it is not hard to see that $\text{rank}(\Gamma(\mathbb{Z}_3^0 \times \mathbb{F}_{p^n})) = \text{frank}(\Gamma(\mathbb{Z}_3^0 \times \mathbb{F}_{p^n})) = 3p^n - 3$. So, the graph $\Gamma(\mathbb{Z}_3^0 \times \mathbb{F}_{p^n})$ is a ring graph.

Suppose $R \cong \mathbb{Z}_2^0 \times \mathbb{Z}_4$. Then $\Gamma(R)$ is isomorphic to G_1 in Figure 2 and so $\text{rank}(\Gamma(R)) = \text{frank}(\Gamma(R)) = 1$. Therefore $\Gamma(\mathbb{Z}_2^0 \times \mathbb{Z}_4)$ is a ring graph. Since $\Gamma(\mathbb{Z}_4) \cong \Gamma(\frac{\mathbb{Z}_2[x]}{\langle x^2 \rangle})$, by Corollary 2.6, we get $\Gamma(\mathbb{Z}_2^0 \times \mathbb{Z}_4) \cong \Gamma(\mathbb{Z}_2^0 \times \frac{\mathbb{Z}_2[x]}{\langle x^2 \rangle})$. This implies that $\Gamma(\mathbb{Z}_2^0 \times \frac{\mathbb{Z}_2[x]}{\langle x^2 \rangle})$ is a ring graph.

We know that $\Gamma(\mathbb{Z}_2^0 \times \mathbb{Z}_2) \cong \Gamma(\frac{x\mathbb{Z}[x]}{\langle 4x, x^2-2x \rangle}) \cong \Gamma(\frac{x\mathbb{Z}_2[x]}{x^3\mathbb{Z}_2[x]})$. Now, by Corollary 2.6, $\Gamma(\mathbb{Z}_2^0 \times \mathbb{Z}_2 \times \mathbb{Z}_2) \cong \Gamma(\mathbb{Z}_2 \times \mathbb{Z}_2^0 \times \mathbb{Z}_2) \cong \Gamma(\mathbb{Z}_2 \times \frac{x\mathbb{Z}[x]}{\langle 4x, x^2-2x \rangle}) \cong \Gamma(\mathbb{Z}_2 \times \frac{x\mathbb{Z}_2[x]}{x^3\mathbb{Z}_2[x]})$. Since $\Gamma(\mathbb{Z}_2^0 \times \mathbb{Z}_2 \times \mathbb{Z}_2)$ is not a ring graph, we can conclude that the graphs $\Gamma(\mathbb{Z}_2 \times \frac{x\mathbb{Z}[x]}{\langle 4x, x^2-2x \rangle})$ and $\Gamma(\mathbb{Z}_2 \times \frac{x\mathbb{Z}_2[x]}{x^3\mathbb{Z}_2[x]})$ are not ring graphs.

Case 3. Assume that $n = 1$ and R is isomorphic to one of the following rings: \mathbb{Z}_2^0 , \mathbb{Z}_3^0 , \mathbb{Z}_4^0 , \mathbb{Z}_5^0 , $\frac{x\mathbb{Z}_2[x]}{x^3\mathbb{Z}_2[x]}$, $\frac{x\mathbb{Z}[x]}{\langle 4x, x^2-2x \rangle}$, $\frac{x\mathbb{Z}_3[x]}{x^3\mathbb{Z}_3[x]}$, $\frac{x\mathbb{Z}[x]}{\langle 9x, x^2-3x \rangle}$, $\frac{x\mathbb{Z}[x]}{\langle 8x, x^2-2x \rangle}$, Q_1 , Q_2 , Q_3 , Q_4 , Q_5 , Q_6 , Q_7 .

Since $\Gamma(\mathbb{Z}_n^0) \cong K_{n-1}$, by Theorem 4.2, the graphs $\Gamma(\mathbb{Z}_2^0)$, $\Gamma(\mathbb{Z}_3^0)$, $\Gamma(\mathbb{Z}_4^0)$ are ring graphs and the graph $\Gamma(\mathbb{Z}_5^0)$ is not a ring graph.

If R is isomorphic to either $\frac{x\mathbb{Z}_2[x]}{x^3\mathbb{Z}_2[x]}$ or $\frac{x\mathbb{Z}[x]}{\langle 4x, x^2-2x \rangle}$, then by Figure 4(a) and 4(b), $\Gamma(R)$ is isomorphic to P_3 . Therefore $\text{rank}(\Gamma(R)) = 0 = \text{frank}(\Gamma(R))$. So the graphs $\Gamma(\frac{x\mathbb{Z}_2[x]}{x^3\mathbb{Z}_2[x]})$ and $\Gamma(\frac{x\mathbb{Z}[x]}{\langle 4x, x^2-2x \rangle})$ are ring graphs.

Suppose R is isomorphic to either $\frac{x\mathbb{Z}_3[x]}{x^3\mathbb{Z}_3[x]}$ or $\frac{x\mathbb{Z}[x]}{\langle 9x, x^2-3x \rangle}$. By Figure 6(a) and 6(b), $\text{rank}(\Gamma(R)) = 6 = \text{frank}(\Gamma(R))$. Therefore $\Gamma(\frac{x\mathbb{Z}_3[x]}{x^3\mathbb{Z}_3[x]})$ and $\Gamma(\frac{x\mathbb{Z}[x]}{\langle 9x, x^2-3x \rangle})$ are ring graphs.

The zero-divisor graph of the rings $\frac{x\mathbb{Z}[x]}{\langle 8x, x^2-2x \rangle}$, Q_1 and Q_5 are isomorphic to the graph given in Figure 5 and Figures 1.B, 3.B of [11]. Note that rank and frank of

this graph is the same and both of them are equal to 1. So, these graphs are ring graphs.

Suppose R is isomorphic to either Q_2 or Q_6 . By Figure 2.A and 4.A of [11], we have $\text{rank}(\Gamma(R)) = 3 = \text{frank}(\Gamma(R))$. Hence $\Gamma(Q_2)$ and $\Gamma(Q_6)$ are ring graphs.

Suppose R is isomorphic to either Q_3 or Q_4 or Q_7 . By Figure 2.B, 3.A and 4.B of [11], the graphs $\Gamma(Q_3)$, $\Gamma(Q_4)$ and $\Gamma(Q_7)$ are isomorphic. Now, by setting $S = \{\bar{a}, 2\bar{a}, 3\bar{a}, \bar{a} + \bar{b}, 3\bar{a} + \bar{b}\}$, it is easy to see that the induced subgraph by the set S in the graph $\Gamma(Q_3)$ is a θ -partial wheel. So, the graphs $\Gamma(Q_3)$, $\Gamma(Q_4)$ and $\Gamma(Q_7)$ are not ring graphs.

By the above arguments and by Theorem 2.3, the result holds. \square

Theorem 4.6. *Let R be a commutative ring without identity. Then $\Gamma(R)$ is an outerplanar graph if and only if R is isomorphic to one of the following:*

$\mathbb{Z}_2^0 \times \mathbb{Z}_2^0$, $\mathbb{Z}_2^0 \times \mathbb{F}_{p^n}$, $\mathbb{Z}_2^0 \times \mathbb{Z}_4$, $\mathbb{Z}_2^0 \times \frac{\mathbb{Z}_2[x]}{\langle x^2 \rangle}$, \mathbb{Z}_2^0 , \mathbb{Z}_3^0 , \mathbb{Z}_4^0 , $\frac{x\mathbb{Z}_2[x]}{x^3\mathbb{Z}_2[x]}$, $\frac{x\mathbb{Z}[x]}{\langle 4x, x^2 - 2x \rangle}$, $\frac{x\mathbb{Z}[x]}{\langle 8x, x^2 - 2x \rangle}$, Q_1 , Q_2 , Q_5 , Q_6 .

Proof. Since every outerplanar graph is a ring graph, it is enough to consider the rings in Theorem 2.3 whose zero-divisor graphs are ring graphs. By similar arguments used in Theorem 4.5, we can verify that the zero-divisor graphs of the rings $\mathbb{Z}_2^0 \times \mathbb{Z}_2^0$, $\mathbb{Z}_2^0 \times \mathbb{F}_{p^n}$, $\mathbb{Z}_2^0 \times \mathbb{Z}_4$, $\mathbb{Z}_2^0 \times \frac{\mathbb{Z}_2[x]}{\langle x^2 \rangle}$, \mathbb{Z}_2^0 , \mathbb{Z}_3^0 , \mathbb{Z}_4^0 , $\frac{x\mathbb{Z}_2[x]}{x^3\mathbb{Z}_2[x]}$, $\frac{x\mathbb{Z}[x]}{\langle 4x, x^2 - 2x \rangle}$, $\frac{x\mathbb{Z}[x]}{\langle 8x, x^2 - 2x \rangle}$, Q_1 , Q_2 , Q_5 and Q_6 are outerplanar. Also, if R is isomorphic to either $\frac{x\mathbb{Z}_3[x]}{x^3\mathbb{Z}_3[x]}$ or $\frac{x\mathbb{Z}[x]}{\langle 9x, x^2 - 3x \rangle}$, then by Figures 7(a) and 7(b), $\Gamma(R)$ contains $K_{2,3}$ as a subgraph. Also, since $\Gamma(\mathbb{Z}_3^0 \times \mathbb{F}_{p^n}) \cong K_2 + \overline{K_{3p^n - 3}}$, the graph $\Gamma(\mathbb{Z}_3^0 \times \mathbb{F}_{p^n})$ has a copy of the graph $K_{2,3}$, too. So, we can deduce that the graphs $\Gamma(\frac{x\mathbb{Z}_3[x]}{x^3\mathbb{Z}_3[x]})$, $\Gamma(\frac{x\mathbb{Z}[x]}{\langle 9x, x^2 - 3x \rangle})$ and $\Gamma(\mathbb{Z}_3^0 \times \mathbb{F}_{p^n})$ are not outerplanar graphs. \square

In the rest of this section, we study the ring index and outerplanar index of the zero divisor graphs of commutative rings without identity. By Corollary 3.8 and Proposition 3.9 of [5], we conclude that the outerplanar index and ring index are the same when they are equal to 2,3 or ∞ . From this classification, we get the following theorem.

Theorem 4.7. *Let R be a finite commutative ring without identity. Then*

- (a) $\gamma_r(\Gamma(R)) = \infty$ if and only if R is isomorphic to one of the following: $\mathbb{Z}_2^0 \times \mathbb{Z}_2^0$, $\mathbb{Z}_2^0 \times \mathbb{Z}_2^0$, \mathbb{Z}_2^0 , \mathbb{Z}_3^0 , \mathbb{Z}_4^0 , $\frac{x\mathbb{Z}[x]}{\langle 4x, x^2 - 2x \rangle}$, $\frac{x\mathbb{Z}_2[x]}{x^3\mathbb{Z}_2[x]}$;
- (b) $\gamma_r(\Gamma(R)) = 1$ if and only if R is isomorphic to one of the following: $\mathbb{Z}_2^0 \times \mathbb{F}_{p^n}$ where $p^n \geq 3$, $\mathbb{Z}_3^0 \times \mathbb{F}_{p^n}$, $\mathbb{Z}_2^0 \times \mathbb{Z}_4$, $\mathbb{Z}_2^0 \times \frac{\mathbb{Z}_2[x]}{\langle x^2 \rangle}$, $\frac{x\mathbb{Z}_3[x]}{x^3\mathbb{Z}_3[x]}$, $\frac{x\mathbb{Z}[x]}{\langle 9x, x^2 - 3x \rangle}$, $\frac{x\mathbb{Z}[x]}{\langle 8x, x^2 - 2x \rangle}$, Q_1 , Q_2 , Q_5 , Q_6 ;
- (c) $\gamma_r(\Gamma(R)) = 0$ otherwise.

Proof. Let $R \cong R_1 \times R_2 \times \cdots \times R_n$. Since the planar index of a non planar graph is 0, we should focused on the case, $\Gamma(R)$ is planar. For any graph G , by Remark 2.1, $\gamma_r(G) \leq \gamma_p(G)$ together with Theorems 3.2 and Theorem 4.5, would prove assertion (b). So, it is enough to focus on the proof of assertion (a). By Theorem 4.5, we have the following cases.

Case 1. Suppose $n = 2$. Then R is isomorphic to one of the following rings: $\mathbb{Z}_2^0 \times \mathbb{Z}_2^0$, $\mathbb{Z}_2^0 \times \mathbb{Z}_2$.

If $R \cong \mathbb{Z}_2^0 \times \mathbb{Z}_2^0$, then $\Gamma(R) \cong K_3$. By Theorem 4.3, $\gamma_r(\Gamma(R)) = \infty$.

Now, suppose $R \cong \mathbb{Z}_2^0 \times \mathbb{F}_{p^n}$. By Lemma 2.4, $\Gamma(R)$ is isomorphic to $K_1 + \overline{K_{2p^n-2}}$. Therefore if $p^n = 2$, then $\gamma_r(\Gamma(\mathbb{Z}_2^0 \times \mathbb{Z}_2)) = \infty$.

Case 2. Suppose $n = 1$. Then R is isomorphic to one of the following rings: \mathbb{Z}_2^0 , \mathbb{Z}_3^0 , \mathbb{Z}_4^0 , $\frac{x\mathbb{Z}[x]}{\langle 4x, x^2-2x \rangle}$, $\frac{x\mathbb{Z}_2[x]}{x^3\mathbb{Z}_2[x]}$.

We know that if $R \cong \mathbb{Z}_n^0$, then $\Gamma(R)$ is a complete graph with $n - 1$ vertices. Then $\Gamma(\mathbb{Z}_2^0)$, $\Gamma(\mathbb{Z}_3^0)$ and $\Gamma(\mathbb{Z}_4^0)$ are isomorphic to either a path or a cycle, and so $\gamma_r(\Gamma(\mathbb{Z}_n^0)) = \infty$ where $n = 2, 3, 4$.

The graph $\Gamma(\frac{x\mathbb{Z}[x]}{\langle 4x, x^2-2x \rangle})$ and $\Gamma(\frac{x\mathbb{Z}_2[x]}{x^3\mathbb{Z}_2[x]})$ are represented in Figures 4(a) and 4(b). By Theorem 4.3, $\gamma_r(\Gamma(\frac{x\mathbb{Z}[x]}{\langle 4x, x^2-2x \rangle})) = \gamma_r(\Gamma(\frac{x\mathbb{Z}_2[x]}{x^3\mathbb{Z}_2[x]})) = \infty$. \square

In [4], Barati classified the outerplanar index of the zero divisor graphs of finite commutative rings with identity. In the following theorem, we establish the same idea for the zero divisor graphs of finite commutative rings without identity. In fact, we give a full characterization of the zero divisor graphs with respect to their outerplanar index when R is a finite commutative ring without identity.

Theorem 4.8. *Let R be a finite commutative ring without identity. Then*

- (a) $\gamma_o(\Gamma(R)) = \infty$ if and only if R is isomorphic to one of the following: $\mathbb{Z}_2^0 \times \mathbb{Z}_2$, $\mathbb{Z}_2^0 \times \mathbb{Z}_2^0$, \mathbb{Z}_2^0 , \mathbb{Z}_3^0 , \mathbb{Z}_4^0 , $\frac{x\mathbb{Z}[x]}{\langle 4x, x^2-2x \rangle}$, $\frac{x\mathbb{Z}_2[x]}{x^3\mathbb{Z}_2[x]}$;
- (b) $\gamma_o(\Gamma(R)) = 1$ if and only if R is isomorphic to one of the following: $\mathbb{Z}_2^0 \times \mathbb{F}_{p^n}$ where $p^n \geq 3$, $\mathbb{Z}_2^0 \times \mathbb{Z}_4$, $\mathbb{Z}_2^0 \times \frac{\mathbb{Z}_2[x]}{\langle x^2 \rangle}$, $\frac{x\mathbb{Z}[x]}{\langle 8x, x^2-2x \rangle}$, Q_1 , Q_2 , Q_5 , Q_6 ;
- (c) $\gamma_o(\Gamma(R)) = 0$ otherwise.

Proof. For any given graph G , by Remark 2.1 together with Theorems 4.4, 4.6 and 4.7, one can easily verify the assertion (b). By Theorems 4.3 and 4.4, for any graph G , if $\gamma_r(G) = \infty$, then $\gamma_o(G) = \infty$ and by Theorem 4.7, the assertion (a) holds. \square

5. Conclusion

In the literature, there are only some few research articles focusing on finite rings without assuming the multiplicative identity. This paper provides the characterization of commutative rings without identity whose zero-divisor graphs are ring graphs and outerplanar graphs. Also, we obtained the planar index, ring index and outerplanar index of the zero-divisor graphs of finite commutative rings without identity. The future work is to address the problem of obtaining various topological indices (like Steiner index, Wiener index, etc.,) for zero-divisor graphs from commutative ring without identity.

References

- [1] M. Afkhami, *When the comaximal and zero-divisor graphs are ring graphs and outerplanar*, Rocky Mountain J. Math., 44(6) (2014), 1745-1761.
- [2] D. F. Anderson and D. Weber, *The zero-divisor graph of a commutative ring without identity*, Int. Electron. J. Algebra, 23 (2018), 176-202.
- [3] D. F. Anderson and P. S. Livingston, *The zero-divisor graph of a commutative ring*, J. Algebra, 217(2) (1999), 434-447.
- [4] Z. Barati, *Planarity and outerplanarity indexes of the zero-divisor graphs*, Afr. Mat., 28(3-4) (2017), 505-514.
- [5] Z. Barati, *Ring index of a graph*, Bol. Soc. Mat. Mex., (3) 25(2) (2019), 225-236.
- [6] I. Beck, *Coloring of commutative rings*, J. Algebra, 116(1) (1988), 208-226.
- [7] R. Belshoff and J. Chapman, *Planar zero-divisor graphs*, J. Algebra, 316(1) (2007), 471-480.
- [8] M. Ghebleh and M. Khatirinejad, *Planarity of iterated line graphs*, Discrete Math., 308 (2008), 144-147.
- [9] I. Gitler, E. Reyes and J. A. Vega, *CIO and ring graphs: deficiency and testing*, J. Symbolic Comput., 79 (2017), 249-268.
- [10] I. Gitler, E. Reyes and R. H. Villarreal, *Ring graphs and complete intersection toric ideals*, Discrete Math., 310(3) (2010), 430-441.
- [11] A. S. Kuzmina and Y. N. Maltsev, *Nilpotent finite rings with planar zero-divisor graphs*, Asian-Eur. J. Math., 1(4) (2008), 565-574.
- [12] A. S. Kuzmina, *Description of finite nonnilpotent rings with planar zero-divisor graphs*, Discrete Math. Appl., 19(6) (2009), 601-617.
- [13] H. Lin, W. Yang, H. Zhang and J. Shu, *Outerplanarity of line graphs and iterated line graphs*, Appl. Math. Lett., 24(7) (2011), 1214-1217.

G. Kalaimurugan

Department of Mathematics
Thiruvalluvar University
Vellore 632 115, Tamil Nadu, India
e-mail: kalaimurugan@gmail.com

P. Vignesh

Department of Mathematics
Mepco Schlenk Engineering College
Sivakasi, Virudhunagar 626 005
Tamil Nadu, India
e-mail: paulvigneshphd@gmail.com, vignesh@mepcoeng.ac.in

M. Afkhami (Corresponding Author)

Department of Mathematics
University of Neyshabur
P.O.Box 91136-899, Neyshabur, Iran
e-mail: mojgan.afkhami@yahoo.com

Z. Barati

Department of Mathematics
Kosar University of Bojnord
Bojnord, Iran
e-mail: za.barati87@gmail.com

CAYLEY SUBSPACE SUM GRAPH OF VECTOR SPACES

G. Kalaimurugan, S. Gopinath and T. Tamizh Chelvam

Received: 18 July 2020; Accepted: 4 January 2022

Communicated by A. Çiğdem Özcan

Dedicated to the memory of Professor Edmund R. Puczyłowski

ABSTRACT. Let \mathbb{V} be a finite dimensional vector space over the field \mathbb{F} . Let $S(\mathbb{V})$ be the set of all subspaces of \mathbb{V} and $\mathbb{A} \subseteq S^*(\mathbb{V}) = S(\mathbb{V}) \setminus \{0\}$. In this paper, we define the Cayley subspace sum graph of \mathbb{V} , denoted by $\text{Cay}(S^*(\mathbb{V}), \mathbb{A})$, as the simple undirected graph with vertex set $S^*(\mathbb{V})$ and two distinct vertices X and Y are adjacent if $X+Z = Y$ or $Y+Z = X$ for some $Z \in \mathbb{A}$. Having defined the Cayley subspace sum graph, we study about the connectedness, diameter and girth of several classes of Cayley subspace sum graphs $\text{Cay}(S^*(\mathbb{V}), \mathbb{A})$ for a finite dimensional vector space \mathbb{V} and $\mathbb{A} \subseteq S^*(\mathbb{V}) = S(\mathbb{V}) \setminus \{0\}$.

Mathematics Subject Classification (2020): 05C10, 05C25, 05C75

Keywords: Cayley sum graph, vector space, subspace, diameter, girth, planar

1. Introduction

In recent years, lot of attention has been given for construction of graphs from algebraic structures. In particular, intersection graphs associated with subspaces of a vector space have been studied by many authors. The subspace inclusion graph of a vector space is introduced and studied by Das [9] and, further properties like Hamiltonian, Eulerian, planar, toroidal, independence number and domination number of the subspace inclusion graph have been studied in [11,13]. Also Das [11] posed four conjectures out of which two of them are solved by Wong [20] and remaining two are proved by Peter J. Cameron et al. [7]. Various other graphs associated with vector spaces like nonzero component union graph and nonzero component graph of finite dimensional vector spaces have been introduced and studied in [10,8,16,19]. The Cayley graph is a powerful tool to connect the algebra and graph theory and there are worthwhile applications for Cayley graphs like routing networks in parallel computing. The Cayley graph of finite groups and rings are well studied in the literature and one can see [1,2,4,12,14,17,15]. The both directed and undirected Cayley sum graph of ideals of commutative rings is defined in [3] and some basic properties such as connectivity, girth, clique number, planar

and outer planar are studied. Later Tamizh Chelvam et al. [18] studied about connectedness, Eulerian, Hamiltonian and toroidal properties of Cayley sum graph of ideals of commutative rings. Any interested reader can refer the monograph [5] for complete literature on graphs from rings.

2. Preliminaries

Throughout this paper, \mathbb{V} is a finite dimensional vector space of dimension n over the finite field \mathbb{F} containing q elements and $\mathfrak{B} = \{\alpha_1, \alpha_2, \dots, \alpha_n\}$ is a basis of \mathbb{V} . In this regard, $\mathfrak{B}(W)$ denotes a basis of a subspace W of \mathbb{V} in general $\mathfrak{B}(\mathbb{V})$ denotes a basis of \mathbb{V} . Let $S(\mathbb{V})$ be the set of all subspaces of \mathbb{V} and let \mathbb{A} be a subset of $S^*(\mathbb{V}) = S(\mathbb{V}) \setminus \{0\}$. The *Cayley subspace sum graph* of \mathbb{V} with respect to \mathbb{A} is the simple undirected graph with vertex set $S^*(\mathbb{V})$ and two distinct vertices X and Y are adjacent if and only if $X + Z = Y$ or $Y + Z = X$ for some $Z \in \mathbb{A}$ and the same is denoted as $\text{Cay}(S^*(\mathbb{V}), \mathbb{A})$. Any $k (\leq n)$ dimensional subspace W of \mathbb{V} spanned by $\{\beta_1, \dots, \beta_k\}$ is written as $\langle \beta_1, \dots, \beta_k \rangle$. When $\dim(V) = n$, the number of distinct subspaces of \mathbb{V} with $k \geq 1$ dimension is

$$\begin{bmatrix} n \\ k \end{bmatrix}_q = \frac{(q^n - 1)(q^{n-1} - 1) \dots (q^{n-k+1} - 1)}{(q^k - 1)(q^{k-1} - 1) \dots (q - 1)}.$$

Thus V has $\sum_{k=1}^n \begin{bmatrix} n \\ k \end{bmatrix}_q$ distinct non-zero subspaces and so the Cayley subspace sum graph $\text{Cay}(S^*(\mathbb{V}), \mathbb{A})$ contains $\sum_{k=1}^n \begin{bmatrix} n \\ k \end{bmatrix}_q$ vertices.

Now, we recall some definitions and notations on graphs. By a graph $G = (V, E)$, we mean a simple undirected graph with non-empty vertex set V and edge set E . The number of elements in V is called the order n of G and the number of elements in E is called the size m of G . A graph G is said to be complete if any two distinct vertices in G are adjacent and the complete graph of order n is denoted by K_n . A graph G is said to be bipartite if the vertex V can be partitioned into two disjoint subsets with no pair of vertices in one subset is adjacent. A star graph is a bipartite graph with any one of the subsets in the bipartite graph containing a single vertex and the same is called as the center of the star. A graph G is n -partite if the vertex V can be partitioned into n disjoint subsets with no pair of vertices in one subset is adjacent.

A walk in a graph G is a finite non-null sequence $W = v_0 e_1 v_1 e_2 \dots e_k v_k$, whose terms are alternatively vertices and edges, such that, for $1 \leq i \leq k$ and ends of

e_i are v_{i-1} and v_i . The walk W is said to be a trial if the edges e_1, \dots, e_k of the walk W are distinct. Further if vertices v_0, v_1, \dots, v_k are distinct, then W is called a path. A cycle is a path with starting and terminating vertex are same. A graph is said to be Hamiltonian if it contains a cycle containing all the vertices of G . A graph G is said to be connected if there exists a path between every pair of distinct vertices in G . The diameter of a connected graph is the supremum of the shortest distance between pairs of vertices in G and is denoted by $\text{diam}(G)$. The girth of G is defined as length of the shortest cycle in G and is denoted by $\text{gr}(G)$. We take $\text{gr}(G) = \infty$ if G contains no cycles. A complete subgraph of a graph G is called a clique. The clique number of G , written as $\omega(G)$, is the maximum size of a clique in G . A subset D of V is called dominating set if any vertex in $V \setminus D$ is adjacent with at least one vertex in D . The minimum cardinality of D is called domination number and it is denoted by $\gamma(G)$. A planar graph is a graph that can be embedded in the plane and the genus of planar graphs is zero. For undefined terms in graph theory, we refer [6].

3. Cayley subspace sum graph

Let \mathbb{V} be a finite dimensional vector space over a finite field \mathbb{F} , $S(\mathbb{V})$ be the set of all subspaces of \mathbb{V} and $\mathbb{A} \subseteq S^*(\mathbb{V}) = S(\mathbb{V}) \setminus \{0\}$. The Cayley subspace sum graph $\text{Cay}(S^*(\mathbb{V}), \mathbb{A}) = (V, E)$ is the simple undirected graph with vertex set $S^*(\mathbb{V})$ and two distinct vertices X and Y are adjacent $\text{Cay}(S^*(\mathbb{V}), \mathbb{A})$ if $X + Z = Y$ or $Y + Z = X$ for some $Z \in \mathbb{A}$. In this section, we observe some properties of $\text{Cay}(S^*(\mathbb{V}), \mathbb{A})$.

Theorem 3.1. *Let \mathbb{V} be an $n(\geq 2)$ dimensional vector space over a finite field with basis $\mathfrak{B} = \{\alpha_1, \dots, \alpha_n\}$ and $\mathbb{A} = \{W_1, \dots, W_k\} \subseteq S^*(\mathbb{V})$. Then $\text{Cay}(S^*(\mathbb{V}), \mathbb{A})$ is connected if and only if $\bigcup_{i=1}^k \mathfrak{B}(W_i) = \mathfrak{B}(\mathbb{V})$ where $\mathfrak{B}(W_i)$ is a basis of the subspace W_i of \mathbb{V} .*

Proof. Let $\text{Cay}(S^*(\mathbb{V}), \mathbb{A})$ be connected. Without loss of generality one can assume that $\mathfrak{B}(W_i) \subseteq \mathfrak{B}(\mathbb{V})$. Suppose $\bigcup_{i=1}^k \mathfrak{B}(W_i) \subset \mathfrak{B}(\mathbb{V})$. Then there exists at least one vector $\beta \in \mathbb{V}$ such that $\bigcup_{i=1}^k \mathfrak{B}(W_i) \cup \{\beta\} \subseteq \mathfrak{B}(\mathbb{V})$. Let $V_1 = \{X \in S^*(\mathbb{V}) : \beta_i \text{ and } \beta \text{ are linearly independent for all } \beta_i \in \mathfrak{B}(X)\}$ and $V_2 = S^*(\mathbb{V}) \setminus V_1$. For $X \in V_1$, we have $X + W_i = X' \in V_1$ for all $W_i \in \mathbb{A}, X \in V_1$ and $Y + W_i = Y' \in V_2$ for all $W_i \in \mathbb{A}, Y \in V_2$. This implies that two vertices in different partitions V_1 and V_2

of $S^*(\mathbb{V})$ are not connected by a path, which is a contradiction to the assumption that $\text{Cay}(S^*(\mathbb{V}), \mathbb{A})$ is connected. Hence $\bigcup_{i=1}^k \mathfrak{B}(W_i) = \mathfrak{B}(\mathbb{V})$.

Conversely, assume that $\bigcup_{i=1}^k \mathfrak{B}(W_i) = \mathfrak{B}(\mathbb{V})$ where $\mathbb{A} = \{W_1, \dots, W_k\} \subseteq S^*(\mathbb{V})$. For $X \in S^*(\mathbb{V})$, there exists a path $P = X - (X + W_1) - (X + W_1 + W_2) - \dots - (X + \sum_{i=1}^{\ell} W_i) - \dots - (X + \sum_{i=1}^{k-1} W_i) - \mathbb{V}$ between X and \mathbb{V} . Hence, every vertex $X \in S^*(\mathbb{V})$ is connected with \mathbb{V} so $\text{Cay}(S^*(\mathbb{V}), \mathbb{A})$ is connected. \square

Theorem 3.2. *Let \mathbb{V} be an $n(\geq 2)$ dimensional vector space over a finite field of order q with basis $\mathfrak{B} = \{\alpha_1, \dots, \alpha_n\}$ and $\mathbb{A} = \{W_1, \dots, W_k\} \subseteq S^*(\mathbb{V})$. If $\text{Cay}(S^*(\mathbb{V}), \mathbb{A})$ is connected then, it is not a path or cycle.*

Proof. Let $\text{Cay}(S^*(\mathbb{V}), \mathbb{A})$ be connected and $\mathbb{V}_{n-1} \subset S^*(\mathbb{V})$ be the set of all $n-1$ dimensional subspaces of \mathbb{V} . Then

$$|\mathbb{V}_{n-1}| = \begin{bmatrix} n \\ n-1 \end{bmatrix}_q = \frac{q^n - 1}{q - 1} \geq 3.$$

We claim that every vertex in \mathbb{V}_{n-1} is adjacent to \mathbb{V} . If not, there exists $X \in \mathbb{V}_{n-1}$ which is not adjacent to \mathbb{V} . This in turn implies that there exists $\beta \in \mathbb{V}$ such that $\mathfrak{B}(X) \cup \{\beta\} = \mathfrak{B}(\mathbb{V})$ and β is linearly independent with all the elements in $\mathfrak{B}(W_i)$ for all $W_i \in \mathbb{A}, 1 \leq i \leq k$. In this case $\bigcup_{i=1}^k \mathfrak{B}(W_i) \subset \mathfrak{B}(\mathbb{V})$, which is a contradiction to Theorem 3.1. Hence $\deg(\mathbb{V}) \geq |\mathbb{V}_{n-1}| = 3$ and so $\text{Cay}(S^*(\mathbb{V}), \mathbb{A})$ can never be a path or cycle. \square

Lemma 3.3. *Let \mathbb{V} be a finite dimensional vector space over a finite field \mathbb{F} . Then $\text{Cay}(S^*(\mathbb{V}), \mathbb{V})$ is a star graph.*

Proof. Let $W \in S^*(\mathbb{V})$ be a non-zero subspace of \mathbb{V} . Then $W + \mathbb{V} = \mathbb{V}$, i.e., \mathbb{V} is adjacent to all $W \in S^*(\mathbb{V})$. Hence $\text{Cay}(S^*(\mathbb{V}), \mathbb{V})$ is a star graph with \mathbb{V} as the central vertex. \square

Now, we observe certain instances where the Cayley subspace sum graph is connected and they are consequences of Theorem 3.1.

Corollary 3.4. *Let \mathbb{V} be an $n(\geq 2)$ dimensional vector space over a finite field. Then $\text{Cay}(S^*(\mathbb{V}), \mathbb{V})$ is connected and $\text{diam}(\text{Cay}(S^*(\mathbb{V}), \mathbb{V})) = 2$.*

Corollary 3.5. *Let \mathbb{V} be an $n(\geq 2)$ dimensional vector space over a finite field. Then $\text{Cay}(S^*(\mathbb{V}), S^*(\mathbb{V}))$ is connected and $\text{diam}(\text{Cay}(S^*(\mathbb{V}), S^*(\mathbb{V}))) = 2$.*

Corollary 3.6. *Let p be a prime number and $k \geq 1$ be an integer. Let \mathbb{V} be a two dimensional vector space over a finite field F of order $q = p^k$ with basis $\mathfrak{B} = \{\alpha_1, \alpha_2\}$. Then $\text{Cay}(S^*(\mathbb{V}), S^*(\mathbb{V})) = K_{1, q+1}$.*

Proof. Let $\mathfrak{B} = \{\alpha_1, \alpha_2\}$ be a basis for \mathbb{V} . The set of all non-zero one dimensional subspaces of \mathbb{V} are $V_1 = \{\langle \alpha_1 \rangle, \langle \alpha_2 \rangle, \langle \alpha_1 + a\alpha_2 \rangle\}$ for $0 \neq a \in \mathbb{F}$ where as \mathbb{V} is the only two dimensional trivial subspace of \mathbb{V} . Note that $|V_1| = p^k + 1$ and $|V_2| = 1$ and $\text{Cay}(S^*(\mathbb{V}), \mathbb{V}) = K_{1, q+1}$. \square

Now, we find the girth of $\text{Cay}(S^*(\mathbb{V}), S^*(\mathbb{V}))$.

Theorem 3.7. *Let \mathbb{V} be an $n(\geq 3)$ dimensional vector space over a finite field with basis $\mathfrak{B} = \{\alpha_1, \dots, \alpha_n\}$. Then the girth $gr(\text{Cay}(S^*(\mathbb{V}), S^*(\mathbb{V}))) = 3$.*

Proof. For an integer m , $1 \leq m \leq n-2$, let $X = \langle \alpha_1, \dots, \alpha_m \rangle$, $Y = \langle \alpha_1, \dots, \alpha_{m+1} \rangle$ and $Z = \langle \alpha_1, \dots, \alpha_{m+2} \rangle$ be m , $m+1$ and $m+2$ dimensional subspaces of \mathbb{V} respectively. Let $X' = \langle \alpha_{m+1} \rangle$, $Y' = \langle \alpha_{m+2} \rangle$ and $Z' = \langle \alpha_{m+1}, \alpha_{m+2} \rangle \in \mathbb{A}$. Then $X + X' = Y$, $Y + Y' = Z$ and $X + Z' = Z$. Hence $X - Y - Z - X$ is a cycle of length 3 in $\text{Cay}(S^*(\mathbb{V}), S^*(\mathbb{V}))$. \square

Theorem 3.8. *Let \mathbb{V} be a finite dimensional vector space of dimension $n(\geq 2)$ over a finite field \mathbb{F} and $\mathbb{A} \subseteq S^*(\mathbb{V})$. Then $\text{Cay}(S^*(\mathbb{V}), \mathbb{A})$ is an n -partite graph.*

Proof. Let S_m^* be the collection of all non-zero m -dimensional subspaces of \mathbb{V} . Then $\{S_m^* : 1 \leq m \leq n\}$ is a partition of $S^*(\mathbb{V})$. To conclude the proof, it is enough to prove that no two vertices in one partition S_m^* are adjacent in $\text{Cay}(S^*(\mathbb{V}), \mathbb{A})$. For, let $X, Y \in S_m^*$ for some m . Then $X = \langle \beta_1, \dots, \beta_m \rangle$ and $Y = \langle \beta'_1, \dots, \beta'_m \rangle$. Let $Z \in \mathbb{A}$ and $\dim(Z) = \ell$.

Case 1. If $Z \subseteq X$, then $X + Z = X$.

Case 2. If $Z \not\subseteq X$, then let $Y' = X + Z$. Note that $\dim(X \cap Z) < \ell$ and so $\dim(Y') = \dim(X) + \dim(Z) - \dim(X \cap Z) = m + \ell - \dim(X \cap Z) > m$. Hence $X + Z \neq Y$ for any $Z \in \mathbb{A}$ and so there exists no $Z \in \mathbb{A}$ such that $X + Z = Y$. \square

Using Theorem 3.8, we obtain the clique number of $\text{Cay}(S^*(\mathbb{V}), S^*(\mathbb{V}))$ where \mathbb{V} is a finite dimensional vector space.

Theorem 3.9. *Let \mathbb{V} be an $n(\geq 2)$ dimensional vector space over a finite field with basis $\mathfrak{B} = \{\alpha_1, \dots, \alpha_n\}$. Then $\omega(\text{Cay}(S^*(\mathbb{V}), S^*(\mathbb{V}))) = n$.*

Proof. Consider the set of subspaces $\{W_1, \dots, W_n\}$ where $W_i = \langle \alpha_1, \dots, \alpha_i \rangle$ is an i dimensional subspace of \mathbb{V} .

Given W_i, W_j $1 \leq i < j \leq n$, let $U_{ij} = \langle \alpha_{i+1}, \alpha_{i+2}, \dots, \alpha_{i+j} \rangle \in S^*(\mathbb{V})$. Then $W_i + U_{ij} = W_j$ and so the subgraph induced by $\{W_i : 1 \leq i \leq n\}$ is complete and so $\omega(\text{Cay}(S^*(\mathbb{V}), S^*(\mathbb{V}))) \geq n$. By Theorem 3.8, $\omega(\text{Cay}(S^*(\mathbb{V}), S^*(\mathbb{V}))) \leq n$. Hence $\omega(\text{Cay}(S^*(\mathbb{V}), S^*(\mathbb{V}))) = n$. \square

For a finite dimensional vector space \mathbb{V} over a finite field \mathbb{F} , the subspace inclusion graph $In(\mathbb{V})$ of \mathbb{V} was introduced and studied by Das [9]. The subspace inclusion graph $In(\mathbb{V})$ of \mathbb{V} is the simple undirected graph with the set of all nontrivial subspaces of \mathbb{V} as the vertex set and two vertices are adjacent if one is contained in other. If $\mathbb{V} \in \mathbb{A}$, then \mathbb{V} is adjacent to all the vertices in $\text{Cay}(S^*(\mathbb{V}), \mathbb{A})$. Hence it is necessary to study about the Cayley subspace sum graph by excluding by considering $\mathbb{V} \notin \mathbb{A}$. Let $S^{**}(\mathbb{V}) = S(\mathbb{V}) \setminus \{0, \mathbb{V}\}$ and $\mathbb{A} \subseteq S^{**}(\mathbb{V})$. Now we prove that the subspace inclusion graph $In(\mathbb{V})$ can be realized as a Cayley subspace sum graph with vertex set $S^{**}(\mathbb{V}) = S(\mathbb{V}) \setminus \{0, \mathbb{V}\}$.

Theorem 3.10. *Let \mathbb{V} be an $n(\geq 2)$ dimensional vector space over a finite field. Then $\text{Cay}(S^{**}(\mathbb{V}), S^{**}(\mathbb{V}))$ is isomorphic to $In(\mathbb{V})$.*

Proof. Note that the vertex sets of both $\text{Cay}(S^{**}(\mathbb{V}), S^{**}(\mathbb{V}))$ and $In(\mathbb{V})$ are nontrivial proper subspaces of \mathbb{V} . If X and Y are two adjacent vertices in the graph $\text{Cay}(S^{**}(\mathbb{V}), S^{**}(\mathbb{V}))$, by definition there exists some $Z \in S^{**}(\mathbb{V})$ such that $X + Z = Y$ or $Y + Z = X$. This gives that $X \subset Y$ or $Y \subset X$. Hence X and Y are adjacent in $In(\mathbb{V})$.

On the other hand, let X and Y be adjacent in $In(\mathbb{V})$. By definition either $X \subset Y$ or $Y \subset X$. Without loss of generality let us take $X \subset Y$. Then $X + W = Y$ where W is a subspace isomorphic to quotient space Y/X . From this X and Y are adjacent in $\text{Cay}(S^{**}(\mathbb{V}), S^{**}(\mathbb{V}))$. \square

Now we characterize all finite dimensional vector spaces \mathbb{V} for which $\text{Cay}(S^*(\mathbb{V}), S^*(\mathbb{V}))$ is planar. We recall the following well known characterization for planar graphs.

Theorem 3.11. ([6, Kuratowski's theorem pp. 151]) *A graph is planar if and only if it contains no subdivision of K_5 or $K_{3,3}$.*

Theorem 3.12. *Let \mathbb{V} be an $n(\geq 2)$ dimensional vector space over a finite field with basis $\mathfrak{B} = \{\alpha_1, \dots, \alpha_n\}$. Then $\text{Cay}(S^*(\mathbb{V}), S^*(\mathbb{V}))$ is planar if and only if $n = 2$.*

Proof. Assume that $\text{Cay}(S^*(\mathbb{V}), S^*(\mathbb{V}))$ is planar where \mathbb{V} is an n -dimensional vector space. Suppose $n \geq 3$. Let $\alpha_1, \alpha_2, \alpha_3 \in \mathfrak{B}(\mathbb{V})$. Consider the subspaces

$W_1 = \langle \alpha_1 \rangle$, $W_2 = \langle \alpha_2 \rangle$, $W_3 = \langle \alpha_3 \rangle$, $W_4 = \langle \alpha_1 + \alpha_2 \rangle$, $W_5 = \langle \alpha_1 + \alpha_3 \rangle$, $W_6 = \langle \alpha_2 + \alpha_3 \rangle$, $W_7 = \langle \alpha_1, \alpha_2 \rangle$, $W_8 = \langle \alpha_1, \alpha_3 \rangle$, $W_9 = \langle \alpha_2, \alpha_3 \rangle$, $W_{10} = \langle \alpha_1, \alpha_2 + \alpha_3 \rangle$, $W_{11} = \langle \alpha_2, \alpha_1 + \alpha_3 \rangle$, $W_{12} = \langle \alpha_3, \alpha_1 + \alpha_2 \rangle$. The subgraph H of $\text{Cay}(S^*(\mathbb{V}), S^*(\mathbb{V}))$ induced by $\{W_i : 1 \leq i \leq 12\}$ is given in Fig. 1.

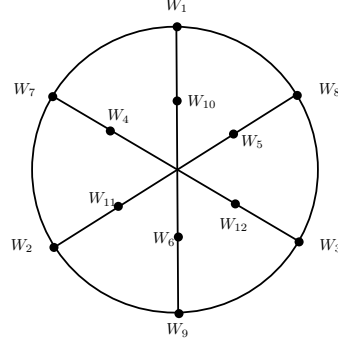


Fig. 1: The graph H

Note that the graph H is a subdivision graph of $K_{3,3}$ as given in Fig. 2.

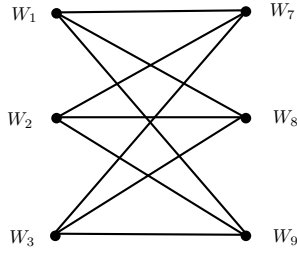


Fig. 2: $K_{3,3}$

From this $\text{Cay}(S^*(\mathbb{V}), S^*(\mathbb{V}))$ contains a subdivision of $K_{3,3}$ which is a contradiction to Theorem 3.11. Hence $n = 2$.

Conversely, assume that $n = 2$. By Corollary 3.6 $\text{Cay}(S^*(\mathbb{V}), S^*(\mathbb{V}))$ is a star graph and so planar. \square

4. Properties of $\text{Cay}(S^*(\mathbb{V}), \mathbb{A})$

In this section, we study $\text{Cay}(S^*(\mathbb{V}), \mathbb{A})$ where \mathbb{V} is an n -dimensional vector space over a finite field of order q with basis $\mathfrak{B} = \{\alpha_1, \alpha_2, \dots, \alpha_n\}$ and $\mathbb{A} = \{\langle \alpha_1 \rangle, \dots, \langle \alpha_n \rangle\}$. In view of Theorem 3.1, we have the following.

Lemma 4.1. *Let \mathbb{V} be an $n(\geq 2)$ dimensional vector space over a finite field with basis $\mathfrak{B} = \{\alpha_1, \dots, \alpha_n\}$ and $\mathbb{A} = \{\langle \alpha_1 \rangle, \dots, \langle \alpha_n \rangle\}$. Then $\text{Cay}(S^*(\mathbb{V}), \mathbb{A})$ is connected.*

Theorem 4.2. *Let \mathbb{V} be an $n(\geq 2)$ dimensional vector space over a finite field with basis $\mathfrak{B} = \{\alpha_1, \dots, \alpha_n\}$ and $\mathbb{A} = \{\langle \alpha_1 \rangle, \dots, \langle \alpha_n \rangle\}$. If X and Y are adjacent in $\text{Cay}(S^*(\mathbb{V}), \mathbb{A})$, then $|\dim(X) - \dim(Y)| = 1$.*

Proof. Let the vertices $X, Y \in S^*(\mathbb{V})$ be adjacent in $\text{Cay}(S^*(\mathbb{V}), \mathbb{A})$. By definition, there exists a subspace $\langle \alpha_i \rangle \in \mathbb{A}$ such that $X + \langle \alpha_i \rangle = Y$ or $Y + \langle \alpha_i \rangle = X$ for some $\alpha_i \in \mathfrak{B}$. Suppose $X + \langle \alpha_i \rangle = Y$ and $\dim(X) = k$. Then $\dim(Y) = \dim(X + \langle \alpha_i \rangle) = k + 1$. Hence $|\dim(X) - \dim(Y)| = |k - (k + 1)| = 1$. \square

Note that the converse of Theorem 4.2 is not true. For, let \mathbb{V} be an $n(\geq 2)$ dimensional vector space with basis $\mathfrak{B} = \{\alpha_1, \alpha_2, \alpha_3\}$ and $\mathbb{A} = \{\langle \alpha_1 \rangle, \langle \alpha_2 \rangle, \langle \alpha_3 \rangle\}$. Let $X = \langle \alpha_1 \rangle$ and $Y = \langle \alpha_1, \alpha_1 + \alpha_2 \rangle$. Then $|\dim(X) - \dim(Y)| = 1$ but there exists no $Z \in \mathbb{A}$ such that $X + Z = Y$ or $Y + Z = X$.

From Theorem 4.2, we have the following corollary.

Corollary 4.3. *Let \mathbb{V} be an $n(\geq 2)$ dimensional vector space over a finite field with basis $\mathfrak{B} = \{\alpha_1, \dots, \alpha_n\}$ and $\mathbb{A} = \{\langle \alpha_1 \rangle, \dots, \langle \alpha_n \rangle\}$. Then no two non-zero subspaces of same dimension are adjacent in $\text{Cay}(S^*(\mathbb{V}), \mathbb{A})$.*

Theorem 4.4. *Let \mathbb{V} be an $n(\geq 2)$ dimensional vector space over a finite field with basis $\mathfrak{B} = \{\alpha_1, \dots, \alpha_n\}$ and $\mathbb{A} = \{\langle \alpha_1 \rangle, \dots, \langle \alpha_n \rangle\}$. Then $\text{Cay}(S^*(\mathbb{V}), \mathbb{A})$ is a bipartite graph.*

Proof. Consider the partition $V_1 = \{X \in S^*(\mathbb{V}) : \dim(X) \text{ is odd}\}$ and $V_2 = \{X \in S^*(\mathbb{V}) : \dim(X) \text{ is even}\}$ of $S^*(\mathbb{V})$. Let X and Y be two vertices in the same partition V_i for $i = 1, 2$. If X and Y are of same dimension, then by Corollary 4.3, X and Y are not adjacent. If X and Y are of different dimension, then $|\dim(X) - \dim(Y)| \geq 2$. By Theorem 4.2, X and Y cannot be adjacent. Hence no two vertices in the same partition V_i for $i = 1, 2$ are adjacent in $\text{Cay}(S^*(\mathbb{V}), \mathbb{A})$. \square

Since a bipartite graph is bi-chromatic, we have the following corollary from Theorem 4.4.

Corollary 4.5. *Let \mathbb{V} be an $n(\geq 2)$ dimensional vector space over a finite field with basis $\mathfrak{B} = \{\alpha_1, \dots, \alpha_n\}$ and $\mathbb{A} = \{\langle \alpha_1 \rangle, \dots, \langle \alpha_n \rangle\}$. Then $\omega(\text{Cay}(S^*(\mathbb{V}), \mathbb{A})) = 2$.*

Also we have following corollary from Theorem 4.4.

Corollary 4.6. *Let \mathbb{V} be a two dimensional vector space over a finite field of order q with basis $\mathfrak{B} = \{\alpha_1, \alpha_2\}$ and $\mathbb{A} = \{\langle \alpha_1 \rangle, \langle \alpha_2 \rangle\}$. Then $\text{Cay}(S^*(\mathbb{V}), \mathbb{A})$ is the star graph $K_{1, q+1}$.*

Theorem 4.7. *Let \mathbb{V} be an $n(\geq 2)$ dimensional vector space over a finite field with basis $\mathfrak{B} = \{\alpha_1, \dots, \alpha_n\}$ and $\mathbb{A} = \{\langle \alpha_1 \rangle, \dots, \langle \alpha_n \rangle\}$. Then the girth of $\text{Cay}(S^*(\mathbb{V}), \mathbb{A})$ is given by*

$$\text{gr}(\text{Cay}(S^*(\mathbb{V}), \mathbb{A})) = \begin{cases} 4 & \text{if } n \geq 3; \\ \infty & \text{if } n = 2. \end{cases}$$

Proof. Case 1. Let \mathbb{V} be an $n \geq 3$ dimensional vector space with basis $\mathfrak{B} = \{\alpha_1, \dots, \alpha_n\}$. By Theorem 4.4, $\text{Cay}(S^*(\mathbb{V}), \mathbb{A})$ is a bipartite graph and so it contains no cycle of length 3. Consider the subspaces $W_1 = \langle \alpha_1 \rangle$, $W_2 = \langle \alpha_1, \alpha_2 \rangle$, $W_3 = \langle \alpha_1, \alpha_2, \alpha_3 \rangle$ and $W_4 = \langle \alpha_1, \alpha_3 \rangle$. Note that $W_1 - W_2 - W_3 - W_4 - W_1$ is a cycle of length 4 in $\text{Cay}(S^*(\mathbb{V}), \mathbb{A})$ and so $\text{gr}(\text{Cay}(S^*(\mathbb{V}), \mathbb{A})) = 4$.

Case 2. Let \mathbb{V} be a 2 dimensional vector space. By Theorem 4.6 $\text{Cay}(S^*(\mathbb{V}), \mathbb{A})$ is a star graph and so in this case $\text{gr}(\text{Cay}(S^*(\mathbb{V}), \mathbb{A}))$ is ∞ . \square

Theorem 4.8. *Let \mathbb{V} be an $n(\geq 2)$ dimensional vector space over a finite field with basis $\mathfrak{B} = \{\alpha_1, \dots, \alpha_n\}$ and $\mathbb{A} = \{\langle \alpha_1 \rangle, \dots, \langle \alpha_n \rangle\}$. Then $\text{diam}(\text{Cay}(S^*(\mathbb{V}), \mathbb{A})) = 2(n - 1)$.*

Proof. Let $X \in S^*(\mathbb{V})$. Assume that $\dim(X) = m \geq 1$ and $X = \langle \beta_1, \dots, \beta_m \rangle$. Without loss of generality one can assume that $\mathfrak{B}(X) \subseteq \mathfrak{B}(\mathbb{V})$ and $\mathfrak{B}(\mathbb{V})$ is obtained from $\mathfrak{B}(X)$ by adjoining $\gamma_1, \gamma_2, \dots, \gamma_{n-m}$.

Consider the trail $P : X - \langle \gamma_1, \beta_1, \dots, \beta_m \rangle - \langle \gamma_1, \gamma_2, \beta_1, \dots, \beta_m \rangle - \dots - \langle \gamma_1, \gamma_2, \dots, \gamma_{n-m}, \beta_1, \dots, \beta_m \rangle = \mathbb{V}$ from X to \mathbb{V} is of length $n - m$ which contains a (X, \mathbb{V}) path. Similarly, there exists a path of length at most $n - m$ for any other vertex Y to \mathbb{V} . From this, one can visualize a path of length at most $2(n - m)$ between X and Y in $\text{Cay}(S^*(\mathbb{V}), \mathbb{A})$. Hence $\text{diam}(\text{Cay}(S^*(\mathbb{V}), \mathbb{A})) \leq 2(n - m) \leq 2(n - 1)$.

Consider the two one dimensional subspaces $U = \langle \alpha_1 \rangle$ and $W = \langle \alpha_1 + \alpha_2 + \dots + \alpha_n \rangle$ of \mathbb{V} . Then $P : U - \langle \alpha_1, \alpha_2 \rangle - \langle \alpha_1, \alpha_2, \alpha_3 \rangle - \dots - \langle \alpha_1, \dots, \alpha_n \rangle$ is a path of length $n - 1$ between U and \mathbb{V} and so $d(U, \mathbb{V}) = n - 1$. On the other hand $Q : W - \langle \alpha_1, W \rangle - \langle \alpha_1, \alpha_2, W \rangle - \dots - \langle \alpha_1, \dots, \alpha_{n-1}, W \rangle$ is path of length $n - 1$ between Y and \mathbb{V} and so $d(W, \mathbb{V}) = n - 1$. Therefore $d(X, Y) = 2(n - 1)$ and so $\text{diam}(\text{Cay}(S^*(\mathbb{V}), \mathbb{A})) = 2(n - 1)$. \square

Now we characterize all finite dimensional vector spaces for which $\text{Cay}(S^*(\mathbb{V}), \mathbb{A})$ is planar.

Theorem 4.9. *Let \mathbb{V} be an $n(\geq 2)$ dimensional vector space over a finite field with basis $\mathfrak{B} = \{\alpha_1, \dots, \alpha_n\}$ and $\mathbb{A} = \{\langle \alpha_1 \rangle, \dots, \langle \alpha_n \rangle\}$. Then $\text{Cay}(S^*(\mathbb{V}), \mathbb{A})$ is planar if and only if $n = 2$.*

Proof. Suppose $n = 2$. By Theorem 3.12, $\text{Cay}(S^*(\mathbb{V}), S^*(\mathbb{V}))$ is planar. Thus $\text{Cay}(S^*(\mathbb{V}), \mathbb{A}) \subseteq \text{Cay}(S^*(\mathbb{V}), S^*(\mathbb{V}))$ is planar.

Conversely assume that $\text{Cay}(S^*(\mathbb{V}), \mathbb{A})$ is planar. Suppose $n \geq 3$. Consider the subspaces $W_1 = \langle \alpha_1 \rangle$, $W_2 = \langle \alpha_2 \rangle$, $W_3 = \langle \alpha_3 \rangle$, $W_4 = \langle \alpha_1 + \alpha_2 \rangle$, $W_5 = \langle \alpha_1 + \alpha_3 \rangle$, $W_6 = \langle \alpha_2 + \alpha_3 \rangle$, $W_7 = \langle \alpha_1 + \alpha_2 + \alpha_3 \rangle$, $W_8 = \langle \alpha_1, \alpha_2 \rangle$, $W_9 = \langle \alpha_1, \alpha_3 \rangle$, $W_{10} = \langle \alpha_2, \alpha_3 \rangle$, $W_{11} = \langle \alpha_1, \alpha_2 + \alpha_3 \rangle$, $W_{12} = \langle \alpha_2, \alpha_1 + \alpha_3 \rangle$, $W_{13} = \langle \alpha_3, \alpha_1 + \alpha_2 \rangle$, $W_{14} = \langle \alpha_1 + \alpha_2, \alpha_1 + \alpha_3 \rangle$ and $W_{15} = \langle \alpha_1, \alpha_2, \alpha_3 \rangle$. The induced subgraph H induced by $\{W_i : 1 \leq i \leq 15\}$ is a subgraph of $\text{Cay}(S^*(\mathbb{V}), \mathbb{A})$. The graph H is given in Fig. 3.

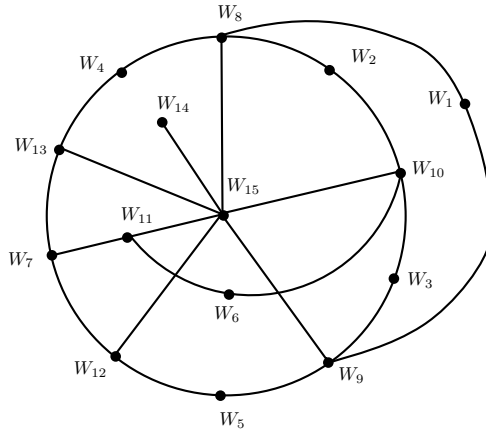


Fig. 3: Graph H

Now let us prove that the graph H cannot have a planar embedding. Note that the subgraph induced by $\{W_2, W_3, W_4, W_5, W_7, W_8, W_9, W_{10}, W_{12}, W_{13}\}$ is the cycle $C_1 = W_8 - W_2 - W_{10} - W_3 - W_9 - W_5 - W_{12} - W_7 - W_{13} - W_4 - W_8$.

Case 1. Let us place the vertex W_{15} in the interior face of C_1 as in Fig. 3. Now we get five cycles $C_2 = W_{13} - W_{15} - W_{12} - W_7 - W_{13}$, $C_3 = W_8 - W_{15} - W_{13} - W_4 - W_8$, $C_4 = W_{10} - W_{15} - W_8 - W_2 - W_{10}$, $C_5 = W_9 - W_{15} - W_{10} - W_3 - W_9$ and $C_6 = W_{12} - W_{15} - W_9 - W_5 - W_{12}$. Now one has to place the vertex W_{11} in an interior face of one of the cycles C_2, C_3, C_4, C_5 and C_6 . Without loss of generality let us place W_{11} in the interior face of C_2 as in the Fig. 3. Similarly place the vertex W_6 in one of the interior faces and without loss of generality let us place W_6 in the interior face of C_6 as in Fig. 3. Note that the vertex W_6 is adjacent to W_{10} and W_{11} . It is clear from Fig. 3 that one cannot draw the edges W_6W_{10} and W_6W_{11} without crossing another edge. Hence H is not planar.

Case 2. Now let us consider the possibility that the vertex W_{15} is placed in the outer face of C_1 . Note that the subgraph H' induced by $\{W_1, W_2, W_3, W_4, W_5, W_7, W_8, W_9, W_{10}, W_{11}, W_{12}, W_{13}, W_{15}\}$ is given in Fig. 4.

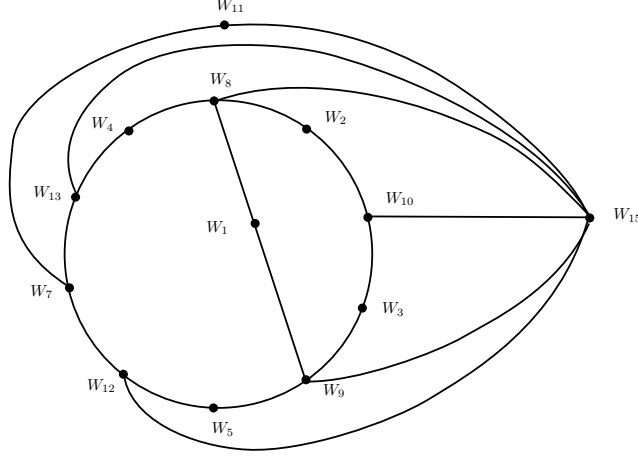


Fig. 4: H'

Consider the circle $C = W_1 - W_8 - W_{15} - W_9 - W_1$ in H' . The vertex W_{10} is inside C and W_{11} is outside the circle C . One cannot draw edges W_6W_{10} and W_6W_{11} in H' without crossings. Therefore the graph H is non-planar.

From the above $\text{Cay}(S^*(\mathbb{V}), S^*(\mathbb{V}))$ is non-planar, which is a contradiction. Hence $n = 2$. \square

5. Another class of $\text{Cay}(S^*(\mathbb{V}), \mathbb{A})$

In this section, we study $\text{Cay}(S^*(\mathbb{V}), \mathbb{A})$ where \mathbb{A} is set of all $m(1 \leq m < n)$ dimensional nonzero subspaces of \mathbb{V} for some fixed m .

Theorem 5.1. *Let \mathbb{V} be an $n(\geq 2)$ dimensional vector space over a finite field with basis $\mathfrak{B} = \{\alpha_1, \dots, \alpha_n\}$ and \mathbb{A} be the set of all $1 \leq m < n$ dimensional nonzero subspaces of \mathbb{V} . If X and Y are adjacent in $\text{Cay}(S^*(\mathbb{V}), \mathbb{A})$, then $|\dim(X) - \dim(Y)| \leq m$.*

Proof. Let $X, Y \in S^*(\mathbb{V})$ be adjacent in $\text{Cay}(S^*(\mathbb{V}), \mathbb{A})$. Then there exists some $Z \in \mathbb{A}$ such that $X + Z = Y$ or $Y + Z = X$. Without loss of generality, let us take $X + Z = Y$. Then $\dim(X + Z) = \dim(Y)$ and so

$$\begin{aligned} |\dim(X) - \dim(Y)| &= |\dim(X) - \dim(X + Z)| \\ &= |\dim(X) - (\dim(X) + \dim(Z) - \dim(X \cap Z))| \\ &= |\dim(Z) - \dim(X \cap Z)| \leq m. \end{aligned} \quad \square$$

Now, we have the following corollary for $n - 1$ dimensional subspaces of \mathbb{V} .

Corollary 5.2. *Let \mathbb{V} be an $n(\geq 2)$ dimensional vector space over a finite field with basis $\mathfrak{B} = \{\alpha_1, \dots, \alpha_n\}$ and \mathbb{A} be the set of all $n - 1$ dimensional nonzero subspaces of \mathbb{V} . Then \mathbb{V} is adjacent to all the vertices in $\text{Cay}(S^*(\mathbb{V}), \mathbb{A})$.*

Theorem 5.3. *Let \mathbb{V} be an $n(\geq 2)$ dimensional vector space over a finite field with basis $\mathfrak{B} = \{\alpha_1, \dots, \alpha_n\}$ and \mathbb{A} be the set of all $m(\geq 1)$ dimensional nonzero subspaces of \mathbb{V} . Then $\text{Cay}(S^*(\mathbb{V}), \mathbb{A})$ is connected.*

Proof. Let $X \in S^*(\mathbb{V})$. Assume that $\dim(X) = k$ and $\{\beta_1, \dots, \beta_k\}$ be a basis of X . By division algorithm, $n = mt + r$ where t and $r < m$ are integers. Then $P : X - \langle \beta_1, \dots, \beta_k, \alpha_1, \dots, \alpha_m \rangle - \langle \beta_1, \dots, \beta_k, \alpha_1, \dots, \alpha_{2m} \rangle - \dots - \langle \beta_1, \dots, \beta_k, \alpha_1, \dots, \alpha_{tm} \rangle - \mathbb{V}$ contains a path between the arbitrary vertex X and \mathbb{V} and so $\text{Cay}(S^*(\mathbb{V}), \mathbb{A})$ is connected. \square

Theorem 5.4. *Let \mathbb{V} be an $n(\geq 2)$ dimensional vector space over a finite field with basis $\mathfrak{B} = \{\alpha_1, \dots, \alpha_n\}$ and \mathbb{A} is the set of all $m(\geq 1)$ dimensional nonzero subspaces of \mathbb{V} . Then the girth of $\text{Cay}(S^*(\mathbb{V}), \mathbb{A})$ is 3.*

Proof. Let $X = \langle \beta_1, \dots, \beta_{m-1} \rangle, Y = \langle \beta_1, \dots, \beta_m \rangle$ and $Z = \langle \beta_1, \dots, \beta_{m+1} \rangle$ be subspaces of \mathbb{V} of dimension $m, m + 1$ and $m + 2$ respectively. Then the subspaces $X' = \langle \beta_1, \dots, \beta_m \rangle$ and $Y' = \langle \beta_2, \dots, \beta_{m+1} \rangle$ satisfy $X + X' = Y, Y + Y' = Z$ and $X + Y' = Z$. Hence $X - Y - Z - X$ is a cycle in $\text{Cay}(S^*(\mathbb{V}), \mathbb{A})$ of length 3 and so the girth of $\text{Cay}(S^*(\mathbb{V}), \mathbb{A})$ is 3. \square

Theorem 5.5. *Let \mathbb{V} be an $n(\geq 2)$ dimensional vector space over a finite field with basis $\mathfrak{B} = \{\alpha_1, \dots, \alpha_n\}$ and \mathbb{A} is the set of all $m(\geq 1)$ dimensional nonzero subspaces of \mathbb{V} . Then $\text{diam}(\text{Cay}(S^*(\mathbb{V}), \mathbb{A})) = 2\lceil \frac{n}{m} \rceil$.*

Proof. By division algorithm $n = tm + r$ where t, r be integers with $r < m$. Consider the subspaces $Y_k = \langle \alpha_{(k-1)m+1}, \alpha_{(k-1)m+2}, \dots, \alpha_{(k-1)m+m} \rangle$ for $1 \leq k \leq t$ of dimension m and $Y_{t+1} = \langle \alpha_{tm+1}, \alpha_{tm+2}, \dots, \alpha_n \rangle$ of \mathbb{V} of dimension r . For a nonzero subspace $X \in S^*(\mathbb{V})$, let $Z_0 = X$ and $Z_i = X + \sum_{j=1}^i Y_j$ for $i = 1, 2, \dots, t+1$. Then the trail $W : Z_0 - Z_1 - Z_2 - \dots - Z_{t+1} = \mathbb{V}$ from X to \mathbb{V} of length $t + 1 = \lceil \frac{n}{m} \rceil$ contains a (X, \mathbb{V}) path. Similarly a trail W' between another subspace $X' \in S^*(\mathbb{V})$ to \mathbb{V} of length $t + 1 = \lceil \frac{n}{m} \rceil$ contains a (X', \mathbb{V}) path. Hence there exists a path of length at most $2\lceil \frac{n}{m} \rceil$ between two arbitrary subspaces $X, X' \in S^*(\mathbb{V})$ and so $\text{Cay}(S^*(\mathbb{V}), \mathbb{A})$ is connected and $\text{diam}(\text{Cay}(S^*(\mathbb{V}), \mathbb{A})) \leq 2\lceil \frac{n}{m} \rceil$.

Consider the one dimensional subspaces $U = \langle \alpha_1 \rangle$ and $U' = \langle \alpha_1 + \alpha_2 + \dots + \alpha_n \rangle$ of \mathbb{V} . Then $P : Z_0 - Z_1 - Z_2 - \dots - Z_{t+1} = \mathbb{V}$ is a path of length $\lceil \frac{n}{m} \rceil$ between U and \mathbb{V} . Similarly $P' : U' - Z_1 - Z_2 - \dots - Z_{t+1} = \mathbb{V}$ is a path of length $\lceil \frac{n}{m} \rceil$ between U' and \mathbb{V} . Therefore $d(U, U') = 2\lceil \frac{n}{m} \rceil$ and so $\text{diam}(\text{Cay}(S^*(\mathbb{V}), \mathbb{A})) = 2\lceil \frac{n}{m} \rceil$. \square

6. Properties of $\text{Cay}(S^*(\mathbb{V}), \mathbb{A})$ where \mathbb{V} is 3 dimensional

In this section, we discuss some special properties of Cayley subspace sum graphs of three dimensional vector spaces over finite field. First we obtain some adjacency relations of $\text{Cay}(S^*(\mathbb{V}), \mathbb{A})$ for the different possibilities of \mathbb{A} . Let \mathbb{V} be the finite dimensional vector space with $\{\alpha_1, \alpha_2, \alpha_3\}$ as basis over the finite field \mathbb{F} of order q . One can see that the following are the complete list of non-zero subspaces of \mathbb{V} .

One dimensional subspaces

- (1) $\langle \alpha_i \rangle : i = 1, 2, 3;$
- (2) $\langle \alpha_i + a\alpha_j \rangle : i, j = 1, 2, 3; i \neq j, a \in \mathbb{F} \setminus \{0\};$
- (3) $\langle \alpha_1 + a\alpha_2 + b\alpha_3 \rangle : a, b \in \mathbb{F} \setminus \{0\}.$

Two dimensional subspaces

- (1) $\langle \alpha_i, \alpha_j \rangle : i, j = 1, 2, 3; i \neq j;$
- (2) $\langle \alpha_i, \alpha_j + a\alpha_k \rangle : i, j, k = 1, 2, 3; i \neq j \neq k, a \in \mathbb{F} \setminus \{0\};$
- (3) $\langle \alpha_1 + a\alpha_2, \alpha_1 + b\alpha_3 \rangle : a, b \in \mathbb{F} \setminus \{0\}.$

Note that total number of nonzero subspaces of \mathbb{V} is $2(q^2 + q) + 3$. Suppose $|V_i|$ is the number of i dimensional nonzero subspaces of \mathbb{V} , then $|V_1| = |V_2| = q^2 + q + 1$. Note that $\text{Cay}(S^{**}(\mathbb{V}), \mathbb{A})$ is a subgraph of $\text{Cay}(S^*(\mathbb{V}), \mathbb{A})$ with vertex set $S^{**}(\mathbb{V}) = S(\mathbb{V}) \setminus \{0, \mathbb{V}\}$.

Theorem 6.1. *Let \mathbb{V} be a three dimensional vector space over a finite field and \mathbb{A} be the set of all one dimensional non-zero proper subspaces of \mathbb{V} . Any two vertices in $\text{Cay}(S^{**}(\mathbb{V}), \mathbb{A})$ are adjacent if and only if one of them is properly contained in the other.*

Proof. Let X and Y be any two nonzero proper subspaces of \mathbb{V} and assume that they are adjacent in $\text{Cay}(S^{**}(\mathbb{V}), \mathbb{A})$. This implies there exists $Z \in \mathbb{A}$ such that $X + Z = Y$ or $Y + Z = X$. In the first case $X \subset Y$ where as in the second case $Y \subset X$.

Conversely, let X and Y be two nonzero proper subspaces of \mathbb{V} and $X \subset Y$. Without loss of generality $\dim(X)=1, \dim(Y)=2$ and so $X = \langle \beta \rangle$ and $Y = \langle \beta, \beta' \rangle$ for $\beta, \beta' \in \mathbb{V}^*$. Then $X + Z = Y$ where $Z = \langle \beta' \rangle \in \mathbb{A}$, i.e., X and Y are adjacent. \square

Theorem 6.2. *Let \mathbb{V} be a three dimensional vector space over a finite field and \mathbb{A} be the set of all two dimensional proper subspaces of \mathbb{V} . Any two subspaces are adjacent in $\text{Cay}(S^*(\mathbb{V}), \mathbb{A})$ if and only if one is properly contained in the other.*

Proof. The proof of “only if” part is similar to that of Theorem 6.1.

Conversely, let X and Y in $S^*(\mathbb{V})$ and $X \subset Y$. Then there are three possibilities. Suppose $\dim(X)=1$, $\dim(Y)=2$, $X = \langle \beta_1 \rangle$ and $Y = \langle \beta_1, \beta_2 \rangle$. Then $X + Y = Y$, i.e., X and Y are adjacent. Similar proof follows in the cases of $\dim(X)=1$, $\dim(Y)=3$; and $\dim(X)=2$, $\dim(Y)=3$. Thus in all the cases X and Y are adjacent. \square

Corollary 6.3. *Let \mathbb{V} be a three dimensional vector space over a finite field and \mathbb{A} be the set of all two dimensional proper subspaces of \mathbb{V} . Any two subspaces are adjacent in $\text{Cay}(S^{**}(\mathbb{V}), \mathbb{A})$ if and only if one is properly contained in the other.*

In similar to the proof of Theorem 6.2, one can prove the following.

Theorem 6.4. *Let \mathbb{V} be a four dimensional vector space over a finite field and \mathbb{A} be the set of all two dimensional proper subspaces of \mathbb{V} . Any two subspaces are adjacent in $\text{Cay}(S^{**}(\mathbb{V}), \mathbb{A})$ if and only if one is properly contained in the other.*

Remark 6.5. Let \mathbb{V} be a three dimensional vector space and \mathbb{A} be either the set of all one dimensional proper subspaces or the set of all two dimensional proper subspaces of \mathbb{V} . By Theorem 6.1 and Corollary 6.3, $\text{Cay}(S^{**}(\mathbb{V}), \mathbb{A})$ as same as $\text{In}(\mathbb{V})$. Let \mathbb{V} be a four dimensional vector space and \mathbb{A} be the set of all two dimensional proper subspaces of \mathbb{V} . By Theorem 6.4, $\text{Cay}(S^{**}(\mathbb{V}), \mathbb{A})$ as same as $\text{In}(\mathbb{V})$. This property is not true for four dimensional vector spaces with other choices for \mathbb{A} . For let \mathbb{A}_1 be set of all one dimensional proper subspaces and \mathbb{A}_2 be the set of all three dimensional proper subspaces of \mathbb{V} . Then the subspaces $\langle \alpha_1 \rangle$ and $\langle \alpha_1, \alpha_2, \alpha_3 \rangle$ are not adjacent in $\text{Cay}(S^{**}(\mathbb{V}), \mathbb{A}_1)$ even though $\langle \alpha_1 \rangle \subset \langle \alpha_1, \alpha_2, \alpha_3 \rangle$. Similarly $\langle \alpha_1 \rangle$ and $\langle \alpha_1, \alpha_2 \rangle$ are not adjacent in $\text{Cay}(S^{**}(\mathbb{V}), \mathbb{A}_2)$ even though $\langle \alpha_1 \rangle \subset \langle \alpha_1, \alpha_2 \rangle$.

Remark 6.6. By Theorem 6.4, $\text{Cay}(S^{**}(\mathbb{V}), \mathbb{A})$ is same as $\text{In}(\mathbb{V})$. Also, by [11, Corollary 6.3] $\text{Cay}(S^{**}(\mathbb{V}), \mathbb{A})$ is a $q + 1$ -regular graph.

Theorem 6.7. *Let \mathbb{V} be a three dimensional vector space over a field of order $q \in \{2, 3, 5, 8, 17\}$ and \mathbb{A} be the set of all two dimensional nonzero subspaces of \mathbb{V} . Then $\text{Cay}(S^*(\mathbb{V}), \mathbb{A})$ is Hamiltonian.*

Proof. By [11, Theorem 6.10], $\text{Cay}(S^{**}(\mathbb{V}), \mathbb{A})$ is Hamiltonian. Since \mathbb{V} is adjacent to all the elements in $\text{Cay}(S^*(\mathbb{V}), \mathbb{A})$, we see that $\text{Cay}(S^*(\mathbb{V}), \mathbb{A})$ is Hamiltonian. \square

Theorem 6.8. *Let \mathbb{V} be a three dimensional vector space over a field of order q and \mathbb{A} be the set of all one dimensional subspaces of \mathbb{V} . Then the domination number $\gamma(\text{Cay}(S^*(\mathbb{V}), \mathbb{A})) = q + 2$.*

Proof. Note that $\text{Cay}(S^*(\mathbb{V}), \mathbb{A})$ is a bipartite graph with vertex partition

$$V_1 = \mathbb{A} \cup \{\mathbb{V}\}$$

and

$$V_2 = \{\text{all two dimensional subspaces of } \mathbb{V}\}.$$

Consider the set $D = \{\langle \alpha_2, \alpha_1 + a\alpha_3 \rangle, \langle \alpha_2, \alpha_3 \rangle, \mathbb{V} \mid a \in \mathbb{F}\}$. Then the following are true.

- $\langle \alpha_i \rangle$ is dominated by $\langle \alpha_i, \alpha_j \rangle$ for $i, j = 1, 2, 3$ and $i \neq j$;
- $\langle \alpha_1 + a\alpha_2 \rangle$ and $\langle \alpha_2 + a\alpha_3 \rangle$ are dominated by $\langle \alpha_1, \alpha_2 \rangle$ and $\langle \alpha_2, \alpha_3 \rangle$ respectively;
- $\langle \alpha_1 + a\alpha_3 \rangle$ is dominated by $\langle \alpha_2, \alpha_1 + a\alpha_3 \rangle$;
- $\langle \alpha_1 + a\alpha_2 + b\alpha_3 \rangle$ is dominated by $\langle \alpha_2, \alpha_1 + b\alpha_3 \rangle$;
- Set of all two dimensional subspace are dominated by \mathbb{V} .

This shows that D is a dominating set of $\text{Cay}(S^*(\mathbb{V}), \mathbb{A})$ with $|D| = q + 2$. To conclude the proof, one has to show that $q + 1$ elements are not sufficient for a dominating set in $\text{Cay}(S^*(\mathbb{V}), \mathbb{A})$. Since \mathbb{V} dominates all two dimensional subspaces, for a minimal dominating set, one has to choose elements in V_2 which dominate all the elements in $V_1 \setminus \mathbb{V}$. By Remark 6.1, $\text{Cay}(S^{**}(\mathbb{V}), \mathbb{A})$ is a $q + 1$ -regular graph. Further $|V_1 \setminus \mathbb{V}| = q^2 + q + 1$ and $\frac{q^2 + q + 1}{q + 1} = q + \frac{1}{q + 1}$. This indicates that at least $q + 1$ elements from V_2 are needed to dominate all the elements in $V_1 \setminus \mathbb{V}$. Hence $\gamma(\text{Cay}(S^*(\mathbb{V}), \mathbb{A})) = q + 2$. \square

Now, we have the following corollary.

Corollary 6.9. *Let \mathbb{V} be a three dimensional vector space over a finite field of order q with basis $\mathfrak{B} = \{\alpha_1, \alpha_2, \alpha_3\}$ and $\mathbb{A} = \{\langle \alpha_1 \rangle, \langle \alpha_2 \rangle, \langle \alpha_3 \rangle\}$. Then $\gamma(\text{Cay}(S^*(\mathbb{V}), \mathbb{A})) = q + 2$.*

From Corollary 5.2, \mathbb{V} is adjacent to all the vertices and hence we have the following corollary regarding domination for two dimensional case.

Corollary 6.10. *Let \mathbb{V} be a three dimensional vector space over a field of order q with basis $\mathfrak{B} = \{\alpha_1, \alpha_2, \alpha_3\}$ and \mathbb{A} be the set of all two dimensional of \mathbb{V} . Then $\gamma(\text{Cay}(S^*(\mathbb{V}), \mathbb{A})) = 1$.*

Acknowledgement. The research work of T. Tamizh Chelvam is supported by CSIR Emeritus Scientist Scheme (No.21 (1123)/20/EMR-II) of Council of Scientific and Industrial Research, Government of India.

References

- [1] M. Afkhami, K. Khashyarmanesh and K. Nafar, *Generalized Cayley graphs associated to commutative rings*, Linear Algebra Appl., 437(3) (2012), 1040-1049.
- [2] M. Afkhami, M. R. Ahmadi, R. Jahani-Nezhad and K. Khashyarmanesh, *Cayley graphs of ideals in a commutative ring*, Bull. Malays. Math. Sci. Soc., 37(3) (2014), 833-843.
- [3] M. Afkhami, Z. Barati, K. Khashyarmanesh and N. Paknejad, *Cayley sum graphs of ideals of a commutative ring*, J. Aust. Math. Soc., 96(3) (2014), 289-302.
- [4] M. Afkhami, H. R. Barani, K. Khashyarmanesh and F. Rahbarnia, *A new class of Cayley graphs*, J. Algebra Appl. 15(4) (2016), 1650076 (8 pp).
- [5] D. F. Anderson, T. Asir, A. Badawi and T. Tamizh Chelvam, *Graphs from Rings*, First ed., Springer, Cham, 2021.
- [6] J. A. Bondy and U. S. R. Murty, *Graph Theory with Applications*, American Elsevier Publishing Co., Inc., New York, 1976.
- [7] P. J. Cameron, A. Das and H. K. Dey, *On some properties of vector space based graphs*, Linear Multilinear Algebra, <https://doi.org/10.1080/03081087.2022.2121370>, 2022.
- [8] A. Das, *Nonzero Component graph of a finite dimensional vector space*, Comm. Algebra, 44(9) (2016), 3918-3926.
- [9] A. Das, *Subspace inclusion graph of a vector space*, Comm. Algebra, 44(11) (2016), 4724-4731.
- [10] A. Das, *Non-zero component union graph of a finite-dimensional vector space*, Linear Multilinear Algebra, 65(6) (2017), 1276-1287.
- [11] A. Das, *On subspace inclusion graph of a vector space*, Linear Multilinear Algebra, 66(3) (2018), 554-564.
- [12] A. V. Kelarev, *On undirected Cayley graphs*, Australas. J. Combin., 25 (2002), 73-78.
- [13] C. Lanong and S. Dutta, *Some results on graphs associated with vector spaces*, J. Inf. Optim. Sci., 38(8) (2017), 1357-1368.

- [14] T. Tamizh Chelvam and S. Anukumar Kathirvel, *Generalized unit and unitary Cayley graphs of finite rings*, J. Algebra Appl., 18(1)(2019), 1950006 (21 pp).
- [15] T. Tamizh Chelvam and G. Kalaimurugan, *Bounds for domination parameters in Cayley graphs on Dihedral group*, Open J. Discrete Math., 2 (2012), 5-10.
- [16] T. Tamizh Chelvam and K. Prabha Ananthi, *The genus of graphs associated with vector spaces*, J. Algebra Appl., 19(5) (2020), 2050086 (11 pp).
- [17] T. Tamizh Chelvam, G. Kalaimurugan and W. Y. Chou, *The signed star domination number of Cayley graphs*, Discrete Math. Algorithms Appl., 4(2) (2012), 1250017 (10 pp).
- [18] T. Tamizh Chelvam, K. Selvakumar and V. Ramanathan, *Cayley sum graph of ideals of commutative rings*, J. Algebra Appl., 17(7) (2018), 1850125 (14 pp).
- [19] B. Tolve, *Vector Space semi-Cayley graphs*, Iran. J. Math. Sci. Inform., 13(2) (2018), 83-91.
- [20] D. Wong, X. Wang and C. Xia, *On two conjectures on the subspace inclusion graph of a vector space*, J. Algebra Appl., 17(10)(2018), 1850189 (9 pp).

G. Kalaimurugan

Department of Mathematics
Thiruvalluvar University
Vellore 632115, Tamil Nadu, India
ORCID:0000-0002-6736-2335
email: kalaimurugan@gmail.com

S. Gopinath

Department of Mathematics
Sri Sairam Institute of Technology
Chennai 60004, Tamil Nadu, India
ORCID:0000-0002-4063-8477
email: gopinathmathematics@gmail.com

T. Tamizh Chelvam (Corresponding Author)

Department of Mathematics
Manonmaniam Sundaranar University
Tirunelveli 627 012, Tamil Nadu, India
ORCID:0000-0002-1878-7847
email: tamche59@gmail.com



Finite-Time Synchronization for T–S Fuzzy Complex-Valued Inertial Delayed Neural Networks Via Decomposition Approach

S. Ramajayam¹ · S. Rajavel² · R. Samidurai¹ · Yang Cao³

Accepted: 10 December 2022

© The Author(s), under exclusive licence to Springer Science+Business Media, LLC, part of Springer Nature 2023

Abstract

This paper is mainly dedicated to the issue of finite-time synchronization of T–S fuzzy complex-valued neural networks with time-varying delays and inertial terms via directly constructing Lyapunov functions with separating the original complex-valued neural networks into two real-valued subsystems equivalently. First of all, to facilitate the analysis of the second-order derivative caused by the inertial term, two intermediate variables are introduced to transfer complex-valued inertial delayed neural networks (CVIDNNs) into the first-order differential equation form. Next, CVIDNNs are developed using T–S fuzzy rules. By using the Lyapunov stability theory, inequality scaling skills and adjustable algebraic criteria for T–S fuzzy CVIDNNs as well as the upper bound of the settling time for synchronization, are derived. Finally, one numerical example with simulations is given to illustrate the effectiveness of our theoretical results.

Keywords Complex-valued neural networks (CVNNs) · Inertial neural networks · T–S fuzzy · Finite-time Synchronization

1 Introduction

Dynamical behaviour analyzes for neural networks (NNs) have gotten a lot of interest in the last few years [1–4]. Particularly, the synchronization of NNs has attracted lots of attention of researchers due to its practical applications such as brain-like intelligence, image encryption and secure communication [5–12]. On the other hand, NNs with inertial items exist engineering and biological backgrounds [13, 14]. Unlike the traditional first-order NNs, inertial neural

✉ Yang Cao
caoyeacy@seu.edu.cn

R. Samidurai
samidurair@gmail.com

¹ Department of Mathematics, Thiruvalluvar University, Vellore 632 115, India

² Department of Mathematics, Adhiparasakthi College of Arts and Science (Autonomous), Ranipet 632 506, India

³ School of Cyber Science and Engineering, Southeast University, Nanjing 211189, China

networks (INNs), which are described by second-order derivative, can contribute to chaos and bifurcation [15]. It was discovered that INNs not only have more sophisticated dynamics than the traditional resistor-capacitor first-order model [16], but also have a diverse biological background. For instance, The membrane of a hair cell in semicircular canals of some animals, such as pigeons, appear to form circuits with inductance. According to researchers, INNs play an important role in many practical applications like signal processing, automatic control, and so on. As a result, it is critical to investigate the dynamics and control of INNs [17, 18]. Furthermore, in the actual models of the INNs, the introduction of the inertia term is generally reflected in inductance, contributing to the disordered search of memory and INNs can perfectly imitate the brain of human, so it is significance to research the dynamical properties of INNs. Therefore, such an issue is a meaningful topic that can be discussed in depth, which is a first motivation of this work.

Fuzzy logic systems or NNs have been proved to be universal approximators, i.e., they can approximate any nonlinear functions. Therefore, fuzzy logic systems and NNs have been widely adopted for nonlinear systems [19, 20]. In recent years, the fuzzy logic theory has been efficiently applied to many applications and it is an effective approach to modeling a complex nonlinear system and dealing with its stability. Takagi–Sugeno (T–S) fuzzy model [21–23] is generally known as an excellent mathematical model that allows many types of analyzes, of which synchronization is a promising issue in the fuzzy control field, particularly for nonlinear dynamics plants. Recently, the challenges of synchronization analysis for T–S fuzzy systems with NNs have been explored [24, 25]. Furthermore, T–S fuzzy models have been shown to be effective in dealing with nonlinear INNs. Few author studied the synchronization analysis for T–S fuzzy INNs [26, 27]. Compared with the asymptotic synchronization [28, 29], the finite-time synchronization is more attractive in some engineering fields [30, 31]. The finite-time synchronization of INNs was examined using some of the integral inequality and finite-time synchronization theorems given in [32–35]. Motivated by the above works, we will attempt to integrate the the T–S fuzzy logics, which could approximate nonlinear smooth functions with arbitrary accuracy using linear functions into INNs and take the IF–THEN rule into account to form a class of T–S fuzzy INNs with time-varying delays. This is our second motivation.

Motivated by the aforementioned results of real-valued NNs, we proposed in this paper to investigate results on complex-valued NNs (CVNNs). In addition, the above research results are all on the basis of the real-valued NNs model with real-valued activation functions, state variables and connection weights. CVNNs has more complex properties, not just simple extensions of real-valued one. It is very necessary to study this model into the study of the dynamic behaviors of nonlinear systems [36–38]. In many realistic systems CVNNs have been applied to deal with electromagnetic, light, quantum waves, optoelectronics, filtering, speech synthesis, remote sensing, signal processing, and so on. Nowadays, many of the researchers are interested to it and paid more attention to analyze the properties of CVNNs. CVNNs with complex-valued states, activation function, connection weight and input are an extension of real-valued NNs that have been one of the most important research topics in many applications [39–42]. In recent year, CVNNs with inertial terms have piqued the interest of researchers , but only a few results have been published. These two basic methods have also been applied to analyze the complex-valued INNs (CVINNs) with constant delays or time-varying delays and a number of meaningful works have been achieved, such as exponential/asymptotical stability [43], exponential/asymptotical stabilization [44]. The authors [43], adaptive synchronization problem was discussed for CVIDNNs by employing non-separation approach. In [44] analyzed the exponential synchronization of state-based switched CVIDNNs via decomposing approach. As stated in [45], in deep learning appli-

cation, NNs with complex-valued signals can realize more robust transmission of gradient information between layers, more accurate forgetting behavior, higher memory capacity and significantly reduced network scale. At the same time, CVNNs can be applied to handle with some practical problems which cannot be solved by a real-valued neuron [46]. In addition, handling the stability of CVINNs requires specific and completely different tools from real-valued INN ones. To our knowledge, there has been few developed achievements for CVINNs with time-varying delays and the result of finite-time synchronization problem has not been reported. Therefore, it is of great significance to study the dynamic behavior of CVINNs for extending the application scopes of NNs. In this paper is the main motivation.

Based on what has been discussed above, the main aim of this paper is to investigate finite-time synchronization for T–S fuzzy complex-valued inertial delayed neural networks via a decomposition approach with time-varying delays. The main highlights of this paper are as below.

1. This paper establishes a kind of T–S fuzzy CVIDNNs with inertial terms, fuzzy terms, and time-varying delays, and extends the previously published articles [43, 44]. This makes the model considered more versatile and practical in practical applications.
2. By dividing the fuzzy inertial complex-valued neural networks into real and imaginary parts, the model is converted into two fuzzy inertial real-valued NNs.
3. This paper combines with CVIDNNs and fuzzy IF-THEN rules to achieve the finite-time synchronization of T–S fuzzy CVIDNNs and the fuzzy-dependent technique is more adaptable and useful for reducing conservatism.
4. To finite-time synchronization of T–S fuzzy CVIDNNs, the linear feedback controller designed, which are general and different from the linear controllers in [26, 27].
5. Easily-verified algebraic criteria are performed to guarantee finite-time synchronization.
6. To highlight the usefulness of our theoretical result technique, a numerical example and comparison of synchronization scenarios are provided.

2 Problem Description

A class of T–S fuzzy CVDINNs with time delay is as follows:

$$\ddot{\gamma}_\alpha(t) = -\phi_\alpha \gamma_\alpha(t) - \psi_\alpha \dot{\gamma}_\alpha(t) + \sum_{\beta=1}^n \theta_{\alpha\beta}(\gamma_\alpha(t)) g_\beta(\gamma_\beta(t)) + \sum_{\beta=1}^n \omega_{\alpha\beta}(\gamma_\alpha(t)) g_\beta(\gamma_\beta(t - \sigma(t))), \tag{1}$$

with the initial condition: $\gamma(s) = \hat{\mu}(s) \in PC([-\sigma, 0], \mathbb{C}^n)$, $\gamma_\alpha(t) \in \mathbb{C}$ represents neuronal state, and its second derivative is known as the term of inertia.

$\phi_\alpha > 0$ and $\psi_\alpha > 0$ are feedback template components; $\theta_{\alpha\beta}(\gamma_\alpha(t))$ and $\omega_{\alpha\beta}(\gamma_\alpha(t))$ are complex-valued state-dependent connection weights; $\sigma(t)$ represent the time delays that satisfy $0 \leq \sigma(t) \leq \sigma_M$ and $\dot{\sigma}(t) \leq \sigma < 1$; $g_\beta(\cdot)$ is complex-valued activation function.

Suppose $\gamma_\alpha(t)$, $\theta_{\alpha\beta}(\gamma_\alpha(t))$, $\omega_{\alpha\beta}(\gamma_\alpha(t))$ and $g_\beta(\gamma_\beta(t))$ can be separated into real and imaginary parts; $\gamma_\alpha(t) = \gamma_\alpha^R(t) + i\gamma_\alpha^I(t)$, $\theta_{\alpha\beta}(\gamma_\alpha(t)) = \theta_{\alpha\beta}^R(\gamma_\alpha^R(t)) + i\theta_{\alpha\beta}^I(\gamma_\alpha^I(t))$, $\omega_{\alpha\beta}(\gamma_\alpha(t)) = \omega_{\alpha\beta}^R(\gamma_\alpha^R(t)) + i\omega_{\alpha\beta}^I(\gamma_\alpha^I(t))$, $g_\beta(\gamma_\beta(t)) = g_\beta^R(\gamma_\beta^R(t)) + ig_\beta^I(\gamma_\beta^I(t))$, in which $\gamma_\alpha^R(t)$, $\theta_{\alpha\beta}^R(\gamma_\alpha^R(t))$, $\omega_{\alpha\beta}^R(\gamma_\alpha^R(t))$ and $g_\beta^R(\gamma_\beta^R(t))$ are the real parts of $\gamma_\alpha(t)$, $\theta_{\alpha\beta}(\gamma_\alpha(t))$, $\omega_{\alpha\beta}(\gamma_\alpha(t))$ and $g_\beta(\gamma_\beta(t))$, respectively; $\gamma_\alpha^I(t)$, $\theta_{\alpha\beta}^I(\gamma_\alpha^I(t))$, $\omega_{\alpha\beta}^I(\gamma_\alpha^I(t))$ and $g_\beta^I(\gamma_\beta^I(t))$ are the imag-

inary parts of $\gamma_\alpha(t)$, $\theta_{\alpha\beta}(\gamma_\alpha(t))$, $\omega_{\alpha\beta}(\gamma_\alpha(t))$ and $g_\beta(\gamma_\beta(t))$, respectively. The following are the state-dependent coefficients: if $|\gamma_\alpha^R(t)| < \mathfrak{N}_\alpha$, $\theta_{\alpha\beta}^R(\gamma_\alpha^R(t))$, $\omega_{\alpha\beta}^R(\gamma_\alpha^R(t))$ are equal to $\hat{\theta}_{\alpha\beta}^R$, $\hat{\omega}_{\alpha\beta}^R$ and $\check{\theta}_{\alpha\beta}^R$, $\check{\omega}_{\alpha\beta}^R$ if $|\gamma_\alpha^I(t)| < \mathfrak{N}_\alpha$, $\theta_{\alpha\beta}^I(\gamma_\alpha^I(t))$, $\omega_{\alpha\beta}^I(\gamma_\alpha^I(t))$ are equal to $\hat{\theta}_{\alpha\beta}^I$, $\hat{\omega}_{\alpha\beta}^I$ and $\check{\theta}_{\alpha\beta}^I$, $\check{\omega}_{\alpha\beta}^I$ where $\mathfrak{N}_\alpha > 0$, $\mathfrak{N}_\alpha > 0$ denotes the threshold level, $\hat{\theta}_{\alpha\beta}^R$, $\hat{\omega}_{\alpha\beta}^R$, $\check{\theta}_{\alpha\beta}^R$, $\check{\omega}_{\alpha\beta}^R$; $\hat{\theta}_{\alpha\beta}^I$, $\hat{\omega}_{\alpha\beta}^I$, $\check{\theta}_{\alpha\beta}^I$, $\check{\omega}_{\alpha\beta}^I$ are constants. Let $\check{\theta}_{\alpha\beta}^R = \max\{|\hat{\theta}_{\alpha\beta}^R|, |\check{\theta}_{\alpha\beta}^R|\}$, $\check{\omega}_{\alpha\beta}^R = \max\{|\hat{\omega}_{\alpha\beta}^R|, |\check{\omega}_{\alpha\beta}^R|\}$, $\check{\theta}_{\alpha\beta}^I = \max\{|\hat{\theta}_{\alpha\beta}^I|, |\check{\theta}_{\alpha\beta}^I|\}$, $\check{\omega}_{\alpha\beta}^I = \max\{|\hat{\omega}_{\alpha\beta}^I|, |\check{\omega}_{\alpha\beta}^I|\}$.

Remark 2.1 Real-valued INNs have recently received a lot of attention due to their applications in engineering, and several results on secure communication have been published [17–19]. These results, however, are all based on real-valued systems. We know from Yu et al. [43] and Li et al. [44], that CVDINNs have several practical applications as well. To the best of the authors knowledge, there are limited results on CVDINNs, as inspired by Yu et al. [43] and Li et al. [44], As a result, this paper has significant implications for further research on CVDINNs.

Then, system (1) can be divided into two parts: real and imaginary, as shown below:

$$\begin{aligned} \ddot{\gamma}_\alpha^R(t) &= -\phi_\alpha \gamma_\alpha^R(t) - \psi_\alpha \dot{\gamma}_\alpha^R(t) + \sum_{\beta=1}^n \theta_{\alpha\beta}^R(\gamma_\alpha^R(t)) g_\beta^R(\gamma_\beta^R(t)) \\ &\quad - \sum_{\beta=1}^n \theta_{\alpha\beta}^I(\gamma_\alpha^I(t)) g_\beta^I(\gamma_\beta^I(t)) \\ &\quad + \sum_{\beta=1}^n \omega_{\alpha\beta}^R(\gamma_\alpha^R(t)) g_\alpha^R(\gamma_\alpha^R(t - \sigma(t))) \\ &\quad - \sum_{\beta=1}^n \omega_{\alpha\beta}^I(\gamma_\alpha^I(t)) g_\beta^I(\gamma_\beta^I(t - \sigma(t))), \end{aligned} \quad (2)$$

and

$$\begin{aligned} \ddot{\gamma}_\alpha^I(t) &= -\phi_\alpha \gamma_\alpha^I(t) - \psi_\alpha \dot{\gamma}_\alpha^I(t) + \sum_{\beta=1}^n \theta_{\alpha\beta}^R(\gamma_\alpha^R(t)) g_\beta^I(\gamma_\beta^I(t)) \\ &\quad + \sum_{\beta=1}^n \theta_{\alpha\beta}^I(\gamma_\alpha^I(t)) g_\beta^R(\gamma_\beta^R(t)) \\ &\quad + \sum_{\beta=1}^n \omega_{\alpha\beta}^R(\gamma_\alpha^R(t)) g_\beta^I(\gamma_\beta^I(t - \sigma(t))) \\ &\quad + \sum_{\beta=1}^n \omega_{\alpha\beta}^I(\gamma_\alpha^I(t)) g_\beta^R(\gamma_\beta^R(t - \sigma(t))). \end{aligned} \quad (3)$$

Systems (2) and (3) can be expressed as

$$\begin{aligned} \ddot{\Omega}(t) &= -\Phi \Omega(t) - \Psi \dot{\Omega}(t) + \Theta^{RI} G^R(t) + \Theta^{IR} G^I(t) \\ &\quad + W^{RI} G^R(t - \sigma(t)) + W^{IR} G^I(t - \sigma(t)), \end{aligned} \quad (4)$$

where $\Omega(t) = (\gamma_1^R(t), \dots, \gamma_n^R(t), \gamma_1^I(t), \dots, \gamma_n^I(t))^T$, $G^R(\cdot) = (g_1^R(\gamma_1^R(\cdot)), \dots, g_n^R(\gamma_n^R(\cdot)), g_1^R(\gamma_1^R(\cdot)), \dots, g_n^R(\gamma_n^R(\cdot)))^T$, $G^I(\cdot) = (g_1^I(\gamma_1^I(\cdot)), \dots, g_n^I(\gamma_n^I(\cdot)), g_1^I(\gamma_1^I(\cdot)), \dots, g_n^I(\gamma_n^I(\cdot)))^T$,

$$\Phi = \text{diag}\{\phi_1, \dots, \phi_n, \phi_1, \dots, \phi_n\}, \Psi = \text{diag}\{\psi_1, \dots, \psi_n, \psi_1, \dots, \psi_n\},$$

$$\begin{aligned} \Theta^{RI} &= \begin{pmatrix} (\theta_{\alpha\beta}^R(\gamma_{\alpha}^R(t)))_{n \times n} & 0 \\ 0 & (\theta_{\alpha\beta}^I(\gamma_{\alpha}^I(t)))_{n \times n} \end{pmatrix}, \\ \Theta^{IR} &= \begin{pmatrix} -(\theta_{\alpha\beta}^I(\gamma_{\alpha}^I(t)))_{n \times n} & 0 \\ 0 & (\theta_{\alpha\beta}^R(\gamma_{\alpha}^R(t)))_{n \times n} \end{pmatrix}, \\ W^{RI} &= \begin{pmatrix} (\omega_{\alpha\beta}^R(\gamma_{\alpha}^R(t)))_{n \times n} & 0 \\ 0 & (\omega_{\alpha\beta}^I(\gamma_{\alpha}^I(t)))_{n \times n} \end{pmatrix}, \\ W^{IR} &= \begin{pmatrix} -(\omega_{\alpha\beta}^I(\gamma_{\alpha}^I(t)))_{n \times n} & 0 \\ 0 & (\omega_{\alpha\beta}^R(\gamma_{\alpha}^R(t)))_{n \times n} \end{pmatrix}. \end{aligned}$$

Remark 2.2 The system model in this paper also considers complex domain, IF-THEN fuzzy, inertial item, time-varying delay, so the discussed CVINNs is a more general case than the existing system models, including the CVINNs without T-S fuzzy [13, 14], the CVINNs only with delay [43], the CVNNs without inertial items (see [36–42]) and so on. In additions, the theoretical results obtained in this work are established in a more general framework and has a wider field of actual applications such as secure communication compared to the results of the previous research works (see [36–42]).

Remark 2.3 Many mathematical models for real-world phenomena are inherently nonlinear, and nonlinear system stability analysis and synthesis problems are typically difficult. The fuzzy logic theory has been shown to be effective in dealing with a variety of complex nonlinear systems over the last few decades, and has thus received a great deal of attention in the literature. The T-S fuzzy INNs model is one of the most popular fuzzy models (see [26, 27]). A nonlinear system is represented in this type of fuzzy model by a set of local linear models smoothly connected by nonlinear membership functions, which has a convenient and simple dynamic structure, allowing the existing results for linear systems theory to be easily extended for this class of nonlinear systems. Therefore, it is of great significance to study the finite-time synchronization of T-S fuzzy CVINNs for extending the application scopes of T-S fuzzy INNs [26, 27].

T-S fuzzy sets are consider (4), as shown below:

Plant rule r: IF $k_1(t)$ is Υ_1^q , $k_2(t)$ is Υ_2^q , ..., $k_f(t)$ is Υ_f^q , THEN

$$\begin{aligned} \ddot{\Omega}(t) &= -\Phi^{(q)}\Omega(t) - \Psi^{(q)}\dot{\Omega}(t) + \Theta^{RI}G^R(t) + \Theta^{IR}G^I(t) \\ &+ W^{RI}G^R(t - \sigma(t)) + W^{IR}G^I(t - \sigma(t)), \end{aligned} \tag{5}$$

where $\Phi^{(q)} = \text{diag}\{\phi_1^{(q)}, \phi_2^{(q)}, \dots, \phi_n^{(q)}, \phi_1^{(q)}, \phi_2^{(q)}, \dots, \phi_n^{(q)}\}$, $\Psi^{(q)} = \text{diag}\{\psi_1^{(q)}, \psi_2^{(q)}, \dots, \psi_n^{(q)}, \psi_1^{(q)}, \psi_2^{(q)}, \dots, \psi_n^{(q)}\}$, Υ_p^q is fuzzy set, $k_p(t)$ is premise variable, $p \in \mathbb{N}_f$, $q \in \mathbb{N}_m$ and m is the number of fuzzy IF-THEN rules. System (5) can be inferred from the blending as

$$\begin{aligned} \ddot{\Omega}(t) &= \sum_{q=1}^m \Xi_q(k(t))[-\Phi^{(q)}\Omega(t) - \Psi^{(q)}\dot{\Omega}(t) + \Theta^{RI}G^R(t) + \Theta^{IR}G^I(t) \\ &+ W^{RI}G^R(t - \sigma(t)) + W^{IR}G^I(t - \sigma(t))], \end{aligned} \tag{6}$$

where $k(t) = (k_1(t), k_2(t), \dots, k_f(t))^T$, and

$$\Xi_q(k(t)) = \frac{\prod_{p=1}^f \Upsilon_p^q(k_p(t))}{\sum_{q=1}^m \prod_{p=1}^f \Upsilon_p^q(k_p(t))}$$

in which $\Upsilon_p^q(k_p(t))$ is the grade of membership of $k_p(t)$ in Υ_p^q . We know that based on fuzzy theory $\sum_{q=1}^m \Xi_q(k(t)) = 1$ and $\Xi_q(k(t)) \geq 0$ for $q \in \mathbb{N}_m$.

As a result of the drive system (6), the response system is as follows:

$$\begin{aligned} \ddot{\mathfrak{S}}(t) = & \sum_{q=1}^m \Xi_q(k(t))[-\Phi^{(q)}\mathfrak{S}(t) - \Psi^{(q)}\dot{\mathfrak{S}}(t) + \tilde{\Theta}^{RI}\tilde{G}^R(t) + \tilde{\Theta}^{IR}\tilde{G}^I(t) \\ & + \tilde{W}^{RI}\tilde{G}^R(t - \sigma(t)) + \tilde{W}^{IR}\tilde{G}^I(t - \sigma(t)) + \Lambda(t)], \end{aligned} \tag{7}$$

where $\Lambda(t) = (\varphi_1^R(t), \dots, \varphi_n^R(t), \varphi_1^I(t), \dots, \varphi_n^I(t))^T$ will be control designed later; $\mathfrak{S}(t) = (\hat{\gamma}_1^R(t), \dots, \hat{\gamma}_n^R(t), \hat{\gamma}_1^I(t), \dots, \hat{\gamma}_n^I(t))^T$ denotes the initial condition of the response system state variable: $\hat{\gamma}(s) = \check{\mu}(s) \in PC([- \sigma, 0], \mathbb{C}^n)$, $\tilde{G}^R(\cdot) = (g_1^R(\hat{\gamma}_1^R(\cdot)), \dots, g_n^R(\hat{\gamma}_n^R(\cdot)))$, $g_1^R(\hat{\gamma}_1^R(\cdot)), \dots, g_n^R(\hat{\gamma}_n^R(\cdot))^T$, $\tilde{G}^I(\cdot) = (g_1^I(\hat{\gamma}_1^I(\cdot)), \dots, g_n^I(\hat{\gamma}_n^I(\cdot)))$, $g_1^I(\hat{\gamma}_1^I(\cdot)), \dots, g_n^I(\hat{\gamma}_n^I(\cdot))^T$,

$$\begin{aligned} \tilde{\Theta}^{RI} &= \begin{pmatrix} (\theta_{\alpha\beta}^R(\hat{\gamma}_\alpha^R(t)))_{n \times n} & 0 \\ 0 & (\theta_{\alpha\beta}^I(\hat{\gamma}_\alpha^I(t)))_{n \times n} \end{pmatrix}, \\ \tilde{\Theta}^{IR} &= \begin{pmatrix} -(\theta_{\alpha\beta}^I(\hat{\gamma}_\alpha^I(t)))_{n \times n} & 0 \\ 0 & (\theta_{\alpha\beta}^R(\hat{\gamma}_\alpha^R(t)))_{n \times n} \end{pmatrix}, \\ \tilde{W}^{RI} &= \begin{pmatrix} (\omega_{\alpha\beta}^R(\hat{\gamma}_\alpha^R(t)))_{n \times n} & 0 \\ 0 & (\omega_{\alpha\beta}^I(\hat{\gamma}_\alpha^I(t)))_{n \times n} \end{pmatrix}, \\ \tilde{W}^{IR} &= \begin{pmatrix} -(\omega_{\alpha\beta}^I(\hat{\gamma}_\alpha^I(t)))_{n \times n} & 0 \\ 0 & (\omega_{\alpha\beta}^R(\hat{\gamma}_\alpha^R(t)))_{n \times n} \end{pmatrix}. \end{aligned}$$

We define $e_\alpha(t) = \hat{\gamma}_\alpha(t) - \gamma_\alpha(t)$ is the synchronization error as follows:

$$\begin{aligned} \ddot{\tilde{e}}(t) = & \sum_{q=1}^m \Xi_q(k(t))[-\Phi^{(q)}\tilde{e}(t) - \Psi^{(q)}\dot{\tilde{e}}(t) + \Theta^{RI}\tilde{H}^R(t) \\ & + \Theta^{IR}\tilde{H}^I(t) + W^{RI}\tilde{H}^R(t - \sigma(t)) + W^{IR}\tilde{H}^I(t - \sigma(t)) \\ & + \tilde{\Theta}^{RI}\tilde{H}^R(t) + \tilde{\Theta}^{IR}\tilde{H}^I(t) + \tilde{W}^{RI}\tilde{H}^R(t - \sigma(t)) \\ & + \tilde{W}^{IR}\tilde{H}^I(t - \sigma(t)) + \varphi(t)], \end{aligned} \tag{8}$$

where $\tilde{e}(t) = (e_1^R(t), \dots, e_n^R(t), e_1^I(t), \dots, e_n^I(t))^T$, $\tilde{H}^R(t) = ((H^R(t))^T, (H^R(t)^T))^T$, $\tilde{H}^I(t) = ((H^I(t))^T, (H^I(t)^T))^T$, $H^R(t) = (g_1^R(\hat{\gamma}_1^R(t)) - g_1^R(\gamma_1^R(t)), \dots, g_n^R(\hat{\gamma}_n^R(t)) - g_n^R(\gamma_n^R(t)))^T$, $H^I(t) = (g_1^I(\hat{\gamma}_1^I(t)) - g_1^I(\gamma_1^I(t)), \dots, g_n^I(\hat{\gamma}_n^I(t)) - g_n^I(\gamma_n^I(t)))^T$, $\tilde{\Theta}^{RI} = \Theta^{RI} - \tilde{\Theta}^{RI}$, $\tilde{\Theta}^{IR} = \Theta^{IR} - \tilde{\Theta}^{IR}$, $\tilde{W}^{RI} = W^{RI} - \tilde{W}^{RI}$, $\tilde{W}^{IR} = W^{IR} - \tilde{W}^{IR}$.

We designed the feedback controller $\varphi_\alpha(t) = \varphi_\alpha^R(t) + i\varphi_\alpha^I(t)$ is presented as follows:

$$\begin{cases} \varphi_\alpha^R(t) = -(k_\alpha^R(t)|\dot{e}_\alpha^R(t)|^{\hat{\zeta}} + \hat{k}_\alpha^R|e_\alpha^R(t)| + \zeta_\alpha^R(t)|e_\alpha^R(t)|^{\hat{\zeta}} + \hat{\rho}_\alpha^R|e_\alpha^R(t)| + \delta_\alpha^R) \text{sign}(\dot{e}_\alpha^R(t)), \\ \varphi_\alpha^I(t) = -(k_\alpha^I(t)|\dot{e}_\alpha^I(t)|^{\hat{\zeta}} + \hat{k}_\alpha^I|e_\alpha^I(t)| + \zeta_\alpha^I(t)|e_\alpha^I(t)|^{\hat{\zeta}} + \hat{\rho}_\alpha^I|e_\alpha^I(t)| + \delta_\alpha^I) \text{sign}(\dot{e}_\alpha^I(t)), \end{cases} \tag{9}$$

where $k_\alpha^R(t), \hat{k}_\alpha^R(t), \zeta_\alpha^R(t), \delta_\alpha^R(t), k_\alpha^I, \hat{k}_\alpha^I(t), \zeta_\alpha^I(t), \delta_\alpha^I$ are control gains and $\hat{k} = \hat{k}_\alpha^R = \hat{k}_\alpha^I$.

Assumption 2.4 The nonlinear functions $g_\alpha^R(\cdot)$ and $g_\alpha^I(\cdot)$ are differentiable, $|g_\alpha^R(\cdot)| \leq M_\alpha^R, |g_\alpha^I(\cdot)| \leq M_\alpha^I$ and there exists $\wp_\alpha^R > 0$ and $\wp_\alpha^I > 0$ such that

$$|g_\alpha^R(u) - g_\alpha^R(v)| \leq \wp_\alpha^R |u - v|, |g_\alpha^I(u) - g_\alpha^I(v)| \leq \wp_\alpha^I |u - v|, \forall u, v \in R.$$

Definition 2.5 CVIDNNs drive system (6) is said to be in finite-time synchronized with CVIDNNs response system (7), if there is a constant $t^*(\in (0)) > 0$ ($t^*(\in (0))$) based on the initial condition $\in (0)$ and $\in (t) = (\in_1^R(t), \in_2^R(t), \dots, \in_n^R(t), \in_1^I(t), \in_2^I(t), \dots, \in_m^I(t))^T$, such that $\lim_{t \rightarrow t^*} (\in(0)) ||\tilde{\in}(t)|| = 0$ and $||\tilde{\in}(t)|| \equiv 0$ for $\forall t > t^*(\in(0))$, where $t^*(\in(0))$ is referred as the settling time.

Lemma 2.6 If the following inequality holds for a continuous, positive definite function $\gamma(t)$

$$\dot{\gamma}(t) \leq -\iota \gamma^\varpi(t), \forall t \geq t_0, \gamma(t_0) \geq 0,$$

where $\iota > 0, 0 < \varpi < 1$ are constants. Then $\gamma(t)$ satisfies

$$\gamma^{1-\varpi}(t) \leq \gamma^{1-\varpi}(t_0) - \iota(1-\varpi)(t-t_0), t_0 \leq t \leq T,$$

and

$$\gamma(t_0) = 0, \forall t \geq T.$$

Also T given by

$$T = t_0 + \frac{\gamma^{1-\varpi}(t_0)}{\iota(1-\varpi)}.$$

3 Main Results

3.1 Finite-Time Synchronization via Feed-Back Controller

Theorem 3.1 Under Assumption 2.4, CVIDNNs drive system (6) is said to be in finite-time synchronized with CVIDNNs response system (7) are finite-time synchronized via feedback controller (9), if the following condition holds:

$$\left\{ \begin{array}{l} \text{(i)} \quad \left[\phi_\alpha^{(q)} + \sum_{\beta=1}^n (\check{\theta}_{\beta\alpha}^R \rho_\alpha^R + \check{\theta}_{\beta\alpha}^I \rho_\alpha^R) \right] \leq \hat{\rho}_\alpha^R \\ \text{(ii)} \quad \left[\phi_\alpha^{(q)} + \sum_{\beta=1}^n (\check{\theta}_{\beta\alpha}^I \rho_\alpha^R + \check{\theta}_{\beta\alpha}^R \rho_\alpha^I) \right] \leq \hat{\rho}_\alpha^I \\ \text{(iii)} \quad (1 - \psi_\alpha^q) \leq \hat{k}_\alpha \\ \text{(iv)} \quad \sum_{\beta=1}^n 2(|\hat{\theta}_{\alpha\beta}^R - \check{\theta}_{\alpha\beta}^R| + |\hat{\omega}_{\alpha\beta}^R - \check{\omega}_{\alpha\beta}^R|) M_\beta^R + \sum_{\beta=1}^n 2(|\hat{\theta}_{\alpha\beta}^I - \check{\theta}_{\alpha\beta}^I| \\ \quad + |\hat{\omega}_{\alpha\beta}^I - \check{\omega}_{\alpha\beta}^I|) M_\beta^I \leq \delta_\alpha^R + \delta_\alpha^I + \omega_\alpha^R + \omega_\alpha^I < 0, \end{array} \right. \tag{10}$$

and for $t \geq t^*$, the settling time $t^* = \frac{V^{1-\xi}(\in(0))}{\Omega_{min}^a(1-\xi)}$, where $\Omega_{min}^a = \min_{1 \leq \alpha \leq n} \{k_\alpha^R, k_\alpha^I, \zeta^R, \zeta^I\}$.

Proof Construct the Lyapunov-functional as:

$$V(t) = \sum_{\alpha=1}^n [|\in_\alpha^R(t)| + |\in_\alpha^I(t)| + |\dot{\in}_\alpha^R(t)| + |\dot{\in}_\alpha^I(t)|]. \tag{11}$$

We reach the following results by taking the time derivative of $V(t)$ along the trajectories of (8):

$$\begin{aligned}
D^+V(t) &= \sum_{\alpha=1}^n \{ \text{sign}(\epsilon_{\alpha}^R(t)) \dot{\epsilon}_{\alpha}^R(t) + \text{sign}(\epsilon_{\alpha}^I(t)) \dot{\epsilon}_{\alpha}^I(t) \\
&\quad + \text{sign}(\dot{\epsilon}_{\alpha}^R(t)) \ddot{\epsilon}_{\alpha}^R(t) + \text{sign}(\dot{\epsilon}_{\alpha}^I(t)) \ddot{\epsilon}_{\alpha}^I(t) \} \\
&\leq \sum_{\alpha=1}^n \sum_{q=1}^m \Xi_q(k(t)) \left\{ |\dot{\epsilon}_{\alpha}^R(t)| + |\dot{\epsilon}_{\alpha}^I(t)| \right. \\
&\quad + \phi_{\alpha}^{(q)} |\epsilon_{\alpha}^R(t)| - \psi_{\alpha}^{(q)} |\dot{\epsilon}_{\alpha}^R(t)| + \sum_{\beta=1}^n \check{\theta}_{\alpha\beta}^R |H_{\beta}^R(t)| \\
&\quad + \sum_{\beta=1}^n \check{\theta}_{\alpha\beta}^I |H_{\beta}^I(t)| + \sum_{\beta=1}^n \check{\omega}_{\alpha\beta}^R |H_{\beta}^R(t - \sigma(t))| \\
&\quad + \sum_{\beta=1}^n \check{\omega}_{\alpha\beta}^I |H_{\beta}^I(t - \sigma(t))| \\
&\quad + \sum_{\beta=1}^n |\theta_{\alpha\beta}^R(\gamma_{\alpha}^R(t)) - \theta_{\alpha\beta}^R(\gamma_{\alpha}^R(t))| |g_{\beta}^R(\gamma_{\beta}^R(t))| \\
&\quad + \sum_{\beta=1}^n |\theta_{\alpha\beta}^I(\gamma_{\alpha}^I(t)) - \theta_{\alpha\beta}^I(\gamma_{\alpha}^I(t))| |g_{\beta}^I(\gamma_{\beta}^I(t))| \\
&\quad + \sum_{\beta=1}^n |\omega_{\alpha\beta}^R(\gamma_{\alpha}^R(t)) - \omega_{\alpha\beta}^R(\gamma_{\alpha}^R(t))| |g_{\beta}^R(\gamma_{\beta}^R(t - \sigma(t)))| \\
&\quad + \sum_{\beta=1}^n |\omega_{\alpha\beta}^I(\gamma_{\alpha}^I(t)) - \omega_{\alpha\beta}^I(\gamma_{\alpha}^I(t))| |g_{\beta}^I(\gamma_{\beta}^I(t - \sigma(t)))| \\
&\quad - \text{sign}(\dot{\epsilon}_{\alpha}^R(t)) \phi_{\alpha}^R(t) + \phi_{\alpha}^{(q)} |\epsilon_{\alpha}^I(t)| - \psi_{\alpha}^{(q)} |\dot{\epsilon}_{\alpha}^I(t)| \\
&\quad + \sum_{\beta=1}^n \check{\theta}_{\alpha\beta}^R |H_{\beta}^I(t)| + \sum_{\beta=1}^n \check{\theta}_{\alpha\beta}^I |H_{\beta}^R(t)| \\
&\quad + \sum_{\beta=1}^n \check{\omega}_{\alpha\beta}^R |H_{\beta}^I(t - \sigma(t))| + \sum_{\beta=1}^n \check{\omega}_{\alpha\beta}^I |H_{\beta}^R(t - \sigma(t))| \\
&\quad + \sum_{\beta=1}^n |\theta_{\alpha\beta}^R(\gamma_{\alpha}^R(t)) - \theta_{\alpha\beta}^R(\gamma_{\alpha}^R(t))| |g_{\beta}^I(\gamma_{\beta}^I(t))| \\
&\quad + \sum_{\beta=1}^n |\theta_{\alpha\beta}^I(\gamma_{\alpha}^I(t)) - \theta_{\alpha\beta}^I(\gamma_{\alpha}^I(t))| |g_{\beta}^R(\gamma_{\beta}^R(t))| \\
&\quad + \sum_{\beta=1}^n |\omega_{\alpha\beta}^R(\gamma_{\alpha}^R(t)) - \omega_{\alpha\beta}^R(\gamma_{\alpha}^R(t))| |g_{\beta}^I(\gamma_{\beta}^I(t - \sigma(t)))|
\end{aligned}$$

$$\begin{aligned}
 & + \sum_{\beta=1}^n |\omega_{\alpha\beta}^I(\gamma_{\alpha}^I(t)) - \omega_{\alpha\beta}^I(\gamma_{\alpha}^I(t))| |g_{\beta}^R(\gamma_{\beta}^R(t - \sigma(t)))| \\
 & - \text{sign}(\dot{\epsilon}_{\alpha}^I(t)) \varphi_{\alpha}^I(t) \Big\}. \tag{12}
 \end{aligned}$$

It follows that the Assumption 2.4 and $0 \leq \sigma(t) \leq \sigma_M, \dot{\sigma} \leq \sigma \leq 1$, obtain that

$$\begin{aligned}
 D^+V(t) & \leq \sum_{\alpha=1}^n \sum_{q=1}^m \Xi_q(k(t)) \Big\{ |\dot{\epsilon}_{\alpha}^R(t)| + |\dot{\epsilon}_{\alpha}^I(t)| \\
 & + \phi_{\alpha}^{(q)} |\epsilon_{\alpha}^R(t)| - \psi_{\alpha}^{(q)} |\dot{\epsilon}_{\alpha}^R(t)| + \sum_{\beta=1}^n \check{\theta}_{\alpha\beta}^R \wp_{\beta}^R |\epsilon_{\beta}^R(t)| \\
 & + \sum_{\beta=1}^n \check{\theta}_{\alpha\beta}^I \wp_{\beta}^I |\epsilon_{\beta}^I(t)| + \sum_{\beta=1}^n |\hat{\theta}_{\alpha\beta}^R - \check{\theta}_{\alpha\beta}^R| M_{\beta}^R + \sum_{\beta=1}^n |\hat{\theta}_{\alpha\beta}^I - \check{\theta}_{\alpha\beta}^I| M_{\beta}^I \\
 & + \sum_{\beta=1}^n |\hat{\omega}_{\alpha\beta}^R - \check{\omega}_{\alpha\beta}^R| M_{\beta}^R + \sum_{\beta=1}^n |\hat{\omega}_{\alpha\beta}^I - \check{\omega}_{\alpha\beta}^I| M_{\beta}^I \\
 & - \text{sign}(\dot{\epsilon}_{\alpha}^R(t)) \varphi_{\alpha}^R(t) + \phi_{\alpha}^{(q)} |\epsilon_{\alpha}^I(t)| - \psi_{\alpha}^{(q)} |\dot{\epsilon}_{\alpha}^I(t)| \\
 & + \sum_{\beta=1}^n \check{\theta}_{\alpha\beta}^R \wp_{\beta}^I |\epsilon_{\beta}^I(t)| + \sum_{\beta=1}^n \check{\theta}_{\alpha\beta}^I \wp_{\beta}^R |\epsilon_{\beta}^R(t)| + \sum_{\beta=1}^n |\hat{\theta}_{\alpha\beta}^R - \check{\theta}_{\alpha\beta}^R| M_{\beta}^I \\
 & + \sum_{\beta=1}^n |\hat{\theta}_{\alpha\beta}^I - \check{\theta}_{\alpha\beta}^I| M_{\beta}^R + \sum_{\beta=1}^n |\hat{\omega}_{\alpha\beta}^R - \check{\omega}_{\alpha\beta}^R| M_{\beta}^I \\
 & + \sum_{\beta=1}^n |\hat{\omega}_{\alpha\beta}^I - \check{\omega}_{\alpha\beta}^I| M_{\beta}^R - \text{sign}(\dot{\epsilon}_{\alpha}^I(t)) \varphi_{\alpha}^I(t) \Big\} \\
 & \leq \sum_{\alpha=1}^n \sum_{q=1}^m \Xi_q(k(t)) \Big\{ (1 - \psi_{\alpha}^{(q)}) |\dot{\epsilon}_{\alpha}^R(t)| + (1 - \psi_{\alpha}^{(q)}) |\dot{\epsilon}_{\alpha}^I(t)| \\
 & + \left[\phi_{\alpha}^{(q)} + \sum_{\beta=1}^n (\check{\theta}_{\beta\alpha}^R \wp_{\alpha}^R + \check{\theta}_{\beta\alpha}^I \wp_{\alpha}^I) \right] |\epsilon_{\alpha}^R(t)| \\
 & + \sum_{\beta=1}^n 2(|\hat{\theta}_{\alpha\beta}^R - \check{\theta}_{\alpha\beta}^R|) M_{\beta}^R \\
 & + \sum_{\beta=1}^n 2(|\hat{\theta}_{\alpha\beta}^I - \check{\theta}_{\alpha\beta}^I| + |\hat{\omega}_{\alpha\beta}^I - \check{\omega}_{\alpha\beta}^I|) M_{\beta}^I \\
 & - \text{sign}(\dot{\epsilon}_{\alpha}^R(t)) \varphi_{\alpha}^R(t) + \left[\phi_{\alpha}^{(q)} + \sum_{\beta=1}^n (\check{\theta}_{\beta\alpha}^I \wp_{\alpha}^I + \check{\theta}_{\beta\alpha}^R \wp_{\alpha}^R) \right] |\epsilon_{\alpha}^I(t)| \\
 & - \text{sign}(\dot{\epsilon}_{\alpha}^I(t)) \varphi_{\alpha}^I(t) \Big\}. \tag{13}
 \end{aligned}$$

The feedback controller (9), it follows that,

$$\begin{aligned}
 D^+V(t) \leq & \sum_{\alpha=1}^n \sum_{q=1}^m \Xi_q(k(t)) \left\{ (1 - \psi_\alpha^{(q)}) |\dot{\epsilon}_\alpha^R(t)| + (1 - \psi_\alpha^{(q)}) |\dot{\epsilon}_\alpha^I(t)| \right. \\
 & + \left[\phi_\alpha^{(q)} + \sum_{\beta=1}^n (\check{\theta}_{\beta\alpha}^R \varrho_\alpha^R + \check{\theta}_{\beta\alpha}^I \varrho_\alpha^R) \right] | \epsilon_\alpha^R(t) | \\
 & + \sum_{\beta=1}^n 2(|\hat{\theta}_{\alpha\beta}^R - \check{\theta}_{\alpha\beta}^R| + |\hat{\omega}_{\alpha\beta}^R - \check{\omega}_{\alpha\beta}^R|) M_\beta^R \\
 & + \sum_{\beta=1}^n 2(|\hat{\theta}_{\alpha\beta}^I - \check{\theta}_{\alpha\beta}^I| + |\hat{\omega}_{\alpha\beta}^I - \check{\omega}_{\alpha\beta}^I|) M_\beta^I \\
 & - k_\alpha^R(t) |\dot{\epsilon}_\alpha^R(t)|^{\hat{\zeta}} - \hat{k}_\alpha^R |\dot{\epsilon}_\alpha^R(t)| - \zeta_\alpha^R(t) | \epsilon_\alpha^R(t) |^{\hat{\zeta}} - \omega_\alpha^R \\
 & + \left[\phi_\alpha^{(q)} + \sum_{\beta=1}^n (\check{\theta}_{\beta\alpha}^I \varrho_\alpha^I + \check{\theta}_{\beta\alpha}^R \varrho_\alpha^I) \right] | \epsilon_\alpha^I(t) | - \hat{\rho}_\alpha^R | \epsilon_\alpha^R(t) | - \hat{\rho}_\alpha^I | \epsilon_\alpha^I(t) | \\
 & \left. - k_\alpha^I(t) |\dot{\epsilon}_\alpha^I(t)|^{\hat{\zeta}} - \hat{k}_\alpha^I |\dot{\epsilon}_\alpha^I(t)| - \zeta_\alpha^I(t) | \epsilon_\alpha^I(t) |^{\hat{\zeta}} - \omega_\alpha^I \right\}.
 \end{aligned}$$

Then,

$$\begin{aligned}
 D^+V(t) \leq & \sum_{\alpha=1}^n \sum_{\beta=1}^m \Xi_q(k(t)) \left\{ (1 - \psi_\alpha^{(q)}) |\dot{\epsilon}_\alpha^R(t)| + (1 - \psi_\alpha^{(q)}) |\dot{\epsilon}_\alpha^I(t)| \right. \\
 & + \left[\phi_\alpha^{(q)} + \sum_{\beta=1}^n (\check{\theta}_{\beta\alpha}^R \rho_\alpha^R + \check{\theta}_{\beta\alpha}^I \rho_\alpha^R) \right] | \epsilon_\alpha^R(t) | \\
 & + \left[\phi_\alpha^{(q)} + \sum_{\beta=1}^n (\check{\theta}_{\beta\alpha}^I \rho_\alpha^I + \check{\theta}_{\beta\alpha}^R \rho_\alpha^I) \right] | \epsilon_\alpha^I(t) | \\
 & - k_\alpha^R |\dot{\epsilon}_\alpha^R(t)|^{\hat{\zeta}} - k_\alpha^I |\dot{\epsilon}_\alpha^I(t)|^{\hat{\zeta}} - \hat{k}_\alpha |\dot{\epsilon}^R(t)| - \hat{k}_\alpha |\dot{\epsilon}^I(t)| \\
 & - \hat{\rho}_\alpha^R | \epsilon_\alpha^R(t) | - \hat{\rho}_\alpha^I | \epsilon_\alpha^I(t) | - \zeta_\alpha^R | \epsilon_\alpha^R(t) |^{\hat{\zeta}} - \zeta_\alpha^I | \epsilon_\alpha^I(t) |^{\hat{\zeta}} \\
 & + \sum_{\beta=1}^n 2(|\hat{\theta}_{\alpha\beta}^R - \check{\theta}_{\alpha\beta}^R| + |\hat{\omega}_{\alpha\beta}^R - \check{\omega}_{\alpha\beta}^R|) M_\beta^R \\
 & \times \sum_{\beta=1}^n 2(|\hat{\theta}_{\alpha\beta}^I - \check{\theta}_{\alpha\beta}^I| + |\hat{\omega}_{\alpha\beta}^I - \check{\omega}_{\alpha\beta}^I|) M_\beta^I - \omega_\alpha^R - \omega_\alpha^I \left. \right\}. \quad (14)
 \end{aligned}$$

If the condition (10) holds, we obtain that

$$\begin{aligned}
 D^+V(t) & \leq -k_\alpha^R |\dot{\epsilon}_\alpha^R(t)|^{\hat{\zeta}} - k_\alpha^I |\dot{\epsilon}_\alpha^I(t)|^{\hat{\zeta}} - \zeta_\alpha^R | \epsilon_\alpha^R(t) |^{\hat{\zeta}} - \zeta_\alpha^I | \epsilon_\alpha^I(t) |^{\hat{\zeta}} \\
 & \leq -\min_{1 \leq \alpha \leq n} \{k_\alpha^R, k_\alpha^I, \zeta_\alpha^R, \zeta_\alpha^I\} \{ | \epsilon_\alpha^R(t) |^{\hat{\zeta}} + | \epsilon_\alpha^I(t) |^{\hat{\zeta}} + | \dot{\epsilon}_\alpha^R(t) |^{\hat{\zeta}} + | \dot{\epsilon}_\alpha^I(t) |^{\hat{\zeta}} \} \\
 & \leq -\Omega_{\min}^{(a)} V^{\hat{\zeta}}(t)
 \end{aligned}$$

where $\Omega_{min}^{(a)} > 0$, $0 < \hat{\zeta} < 1$ are constants. Therefore, we get $V(\in(t)) = 0, \forall t \geq t^*$ and the settling time $t^* = \frac{V^{1-\hat{\zeta}}(\in(0))}{\Omega_{min}^{(a)}(1-\hat{\zeta})}$.

By Definition 2.5, we conclude that the CVIDNNs drive system (6) can be achieved finite-time synchronized with CVIDNNs response system (7) and the setting time $t^* = \frac{V^{1-\hat{\zeta}}(\in(0))}{\Omega_{min}^{(a)}(1-\hat{\zeta})}$. □

Remark 3.2 Unlike the results for asymptotical and exponential synchronization of CVIDNNs with and without separate real and imaginary parts in [43, 44], this paper studies finite-time synchronization of the T-S fuzzy CVIDNNs drive system (6) and CVIDNNs response system (7) under feed-back controller. Different from previous work which focus on the asymptotical and exponential synchronization, we care more about the length of convergence time and design a controller to make it be able to adjust to an arbitrary length. It has been proved that finite-time synchronization has better application in the practical fields, such as signal processing, pattern recognition, associative memories and optimization problems. Then, by light of the proposed settling-time techniques in (10), our goal is achieved. Theorem 3.1 gives the sufficient conditions on finite-time synchronization of T-S fuzzy CVIDNNs with time-varying delays. The settling time function is bounded above by a priori value that depends on the design parameters, which is associated to initial conditions. It shows that the reaching time is secured during a prescribed manner. According to the settling time formula (10), we know that t^* is inversely proportional to $\hat{\zeta}, \zeta^R, \zeta^I, k_\alpha^R$, and k_α^I .

3.2 Asymptotically Synchronization Via Feed-Back Controller

Next, we investigated asymptotically the synchronization of the CVIDNNs drive system (6) and CVIDNNs response system (7), under feed-back controller is equivalent to the stability of error system (8).

The feedback controller designed as

$$\begin{cases} \phi_\alpha^R(t) = -(\hat{k}_\alpha^R |\dot{\epsilon}_\alpha^R(t)| + \hat{\rho}_\alpha^R |\epsilon^R(t)| + \delta_\alpha^R) \text{sign}(\dot{\epsilon}_\alpha^R) \\ \phi_\alpha^I(t) = -(\hat{k}_\alpha^I |\dot{\epsilon}_\alpha^I(t)| + \hat{\rho}_\alpha^I |\epsilon^I(t)| + \delta_\alpha^I) \text{sign}(\dot{\epsilon}_\alpha^I) \end{cases} \tag{15}$$

where $\hat{k}_\alpha^R, \hat{k}_\alpha^I, \hat{\rho}_\alpha^R, \hat{\rho}_\alpha^I, \delta_\alpha^R, \delta_\alpha^I$ are gains.

Theorem 3.3 Under Assumption 2.4, the CVIDNNs drive system (6) and the CVIDNNs response system (7) can be achieved asymptotically synchronized via controller (15), if the following condition are satisfied as follows:

$$\begin{cases} \text{(i)} \quad \hat{k}_\alpha^R \geq 1 - \min_{1 \leq q \leq m} \{ \psi_\alpha^{(q)} \} \\ \text{(ii)} \quad \hat{k}_\alpha^I \geq 1 - \min_{1 \leq q \leq m} \{ \psi_\alpha^{(q)} \} \\ \text{(iii)} \quad \hat{\rho}_\alpha^R \geq \max_{1 \leq q \leq m} \{ \phi_\alpha^{(q)} \} + \sum_{\beta=1}^n (\check{\theta}_{\beta\alpha}^R \rho_\alpha^R + \check{\theta}_{\beta\alpha}^I \rho_\alpha^R) \\ \text{(iv)} \quad \hat{\rho}_\alpha^I \geq \max_{1 \leq q \leq m} \{ \phi_\alpha^{(q)} \} + \sum_{\beta=1}^n (\check{\theta}_{\beta\alpha}^I \rho_\alpha^R + \check{\theta}_{\beta\alpha}^R \rho_\alpha^I) \\ \text{(v)} \quad \delta_\alpha^R + \delta_\alpha^I \geq \sum_{\beta=1}^n 2(|\hat{\theta}_{\alpha\beta}^R - \check{\theta}_{\alpha\beta}^R| + |\hat{\omega}_{\alpha\beta}^R - \check{\omega}_{\alpha\beta}^R|) M_\beta^R \\ \quad + \sum_{\beta=1}^n 2(|\hat{\theta}_{\alpha\beta}^I - \check{\theta}_{\alpha\beta}^I| + |\hat{\omega}_{\alpha\beta}^I - \check{\omega}_{\alpha\beta}^I|) M_\beta^R \end{cases} \tag{16}$$

Proof We choose Lyapunov-function same as in (11) and time derivative of $V(t)$, obtain that

$$D^+ V(t) \leq \sum_{\alpha=1}^n \sum_{q=1}^m \Xi_q(k(t)) \left\{ (1 - \psi_\alpha^q) |\dot{\epsilon}_\alpha^R(t)| + (1 - \psi_\alpha^q) |\dot{\epsilon}_\alpha^I(t)| \right\}$$

$$\begin{aligned}
& + \left[\phi_\alpha^q + \sum_{\beta=1}^n (\check{\theta}_{\beta\alpha}^R \rho_\alpha^R + \check{\theta}_{\beta\alpha}^I \rho_\alpha^R) \right] | \in_\alpha^R(t) | \\
& + \left[\phi_\alpha^q + \sum_{\beta=1}^n (\check{\theta}_{\beta\alpha}^I \rho_\alpha^R + \check{\theta}_{\beta\alpha}^R \rho_\alpha^I) \right] | \in_\alpha^I(t) | \\
& + \sum_{\beta=1}^n 2(|\hat{\theta}_{\alpha\beta}^R - \check{\theta}_{\alpha\beta}^R| + |\hat{\omega}_{\alpha\beta}^R - \check{\omega}_{\alpha\beta}^R|) M_\beta^R \\
& + \sum_{\beta=1}^n 2(|\hat{\theta}_{\alpha\beta}^I - \check{\theta}_{\alpha\beta}^I| + |\hat{\omega}_{\alpha\beta}^I - \check{\omega}_{\alpha\beta}^I|) M_\beta^I \\
& - \omega_\alpha^R - \omega_\alpha^I - \hat{k}_\alpha^R |\dot{\in}_\alpha^R(t)| - \hat{k}_\alpha^I |\dot{\in}_\alpha^I(t)| - \hat{\rho}_\alpha^R | \in_\alpha^R(t) | - \hat{\rho}_\alpha^I | \in_\alpha^I(t) | \Big\}. \quad (17)
\end{aligned}$$

Then,

$$\begin{aligned}
D^+V(t) & \leq \sum_{\alpha=1}^n \sum_{q=1}^m \Xi_q(k(t)) \left\{ (1 - \psi_\alpha^{(q)} - \hat{k}_\alpha^R) |\dot{\in}_\alpha^R(t)| + (1 - \psi_\alpha^{(q)} - \hat{k}_\alpha^I) |\dot{\in}_\alpha^I(t)| \right. \\
& + \left[\phi_\alpha^{(q)} + \sum_{\beta=1}^n (\check{\theta}_{\beta\alpha}^R \rho_\alpha^R + \check{\theta}_{\beta\alpha}^I \rho_\alpha^R) - \hat{\rho}_\alpha^R \right] | \in_\alpha^R(t) | \\
& + \left[\phi_\alpha^{(q)} + \sum_{\beta=1}^n (\check{\theta}_{\beta\alpha}^I \rho_\alpha^I + \check{\theta}_{\beta\alpha}^R \rho_\alpha^I) - \hat{\rho}_\alpha^I \right] | \in_\alpha^I(t) | \\
& + \sum_{\beta=1}^n 2(|\hat{\theta}_{\alpha\beta}^R - \check{\theta}_{\alpha\beta}^R| + |\hat{\omega}_{\alpha\beta}^R - \check{\omega}_{\alpha\beta}^R|) M_\beta^R \\
& + \sum_{\beta=1}^n 2(|\hat{\theta}_{\alpha\beta}^I - \check{\theta}_{\alpha\beta}^I| + |\hat{\omega}_{\alpha\beta}^I - \check{\omega}_{\alpha\beta}^I|) M_\beta^I - \omega_\alpha^R - \omega_\alpha^I \Big\}. \quad (18)
\end{aligned}$$

If the condition (16) are satisfied, then $D^+V(t) \leq 0, \forall t \geq 0$. Therefore, the error system (8) are asymptotically stable, i.e; the CVIDNNs response system (6) can synchronized with the CVIDNNs drive system (7) via controller (15). \square

Remark 3.4 Compared with [43] where the exponential synchronization of CVIDNNs, where the exponential stabilization of CVIDNNs [44] are studied, we achieve the finite-time synchronization of the T–S fuzzy CVIDNNs in this paper. Unlike previous research results, which has focused on asymptotical or exponential stabilization and synchronization, we are more concerned with the length of convergence time and have designed a controller that can adjust to an arbitrary duration. Many author, it has been demonstrated that finite-time synchronization is more useful in practical applications such as secure communication.

4 Numerical Examples

In this section, a numerical example is provided to demonstrate the validity of the main results of Theorem 3.1.

Example 1 Consider the following drive-response T-S fuzzy CVIDNNs, as well as the two fuzzy rules:

$$\begin{aligned} \ddot{\gamma}_\alpha(t) = & \sum_{q=1}^2 \Xi_q(k(t)) \left\{ [-\phi_\alpha^{(q)} \gamma_\alpha(t) - \psi_\alpha^{(q)} \dot{\gamma}_\alpha(t)] \right. \\ & + \sum_{\beta=1}^2 \theta_{\alpha\beta}(\gamma_\alpha(t)) g_\beta(\gamma_\beta(t)) \\ & \left. + \sum_{\beta=1}^2 \omega_{\alpha\beta}(\gamma_\alpha(t)) g_\beta(\gamma_\beta(t - \sigma(t))) \right\}, \end{aligned} \tag{19}$$

and

$$\begin{aligned} \ddot{\hat{\gamma}}_\alpha(t) = & \sum_{q=1}^2 \Xi_q(k(t)) \left\{ -\phi_\alpha^{(q)} \hat{\gamma}_\alpha(t) - \psi_\alpha^{(q)} \dot{\hat{\gamma}}_\alpha(t) \right. \\ & + \sum_{\beta=1}^2 \theta_{\alpha\beta}(\hat{\gamma}_\alpha(t)) g_\beta(\hat{\gamma}_\beta(t)) \\ & \left. + \sum_{\beta=1}^2 \omega_{\alpha\beta}(\hat{\gamma}_\alpha(t)) g_\beta(\hat{\gamma}_\beta(t - \sigma(t))) + \varphi_l(t) \right\}, \end{aligned} \tag{20}$$

$\alpha = 1, 2$, time delays $\sigma(t) = \frac{e^t}{1+e^t}$ with $\sigma_M = 0.78$, $\phi_1^{(1)} = \psi_2^{(1)} = \phi_2^{(1)} = \psi_2^{(1)} = 2.72$, $\phi_1^{(2)} = \psi_2^{(2)} = \phi_2^{(2)} = \psi_2^{(2)} = 3.91$, $\check{\theta}_{11}^R = -1.04$, $\hat{\theta}_{11}^R = -1.70$, $\check{\theta}_{12}^R = 2.01$, $\hat{\theta}_{12}^R = -0.92$, $\check{\theta}_{21}^R = 2.33$, $\hat{\theta}_{21}^R = -1.18$, $\check{\theta}_{22}^R = 2.69$, $\hat{\theta}_{22}^R = -1.87$, $\check{\theta}_{22}^R = 1.04$, $\check{\theta}_{11}^I = -1.27$, $\hat{\theta}_{11}^I = -0.15$, $\check{\theta}_{12}^I = 1.40$, $\hat{\theta}_{12}^I = -1.24$, $\check{\theta}_{21}^I = 0.49$, $\hat{\theta}_{21}^I = 1.50$, $\check{\theta}_{22}^I = 0.31$, $\hat{\theta}_{22}^I = -2.19$, $\check{\omega}_{11}^R = -2.13$, $\hat{\omega}_{11}^R = -0.92$, $\check{\omega}_{12}^R = -2.13$, $\hat{\omega}_{12}^R = 1.24$, $\check{\omega}_{21}^R = -0.52$, $\hat{\omega}_{21}^R = 1.49$, $\check{\omega}_{22}^R = -2.04$, $\hat{\omega}_{22}^R = -2.57$, $\check{\omega}_{11}^I = 2.10$, $\hat{\omega}_{11}^I = -3.21$, $\check{\omega}_{12}^I = 1.40$, $\hat{\omega}_{12}^I = 4.12$, $\check{\omega}_{21}^I = 3.01$, $\hat{\omega}_{21}^I = 2.27$, $\check{\omega}_{22}^I = 3.37$, $\hat{\omega}_{22}^I = -3.26$, activation function $g_\beta(\cdot) = \tan 3h(\cdot) + \tan 5h(\cdot)i$ and membership functions $\Xi_1(k(t)) = e^{9|k(t)|}/(1 + e^{9|k(t)|})$, $\Xi_2(k(t)) = 1/(1 + e^{9|k(t)|})$, where $k(t)$ takes $\gamma_1(t)$ and $\hat{\gamma}_1(t)$ in the drive and response systems, respectively.

Under the initial values $\gamma_1(s) = 2.4 - 3.1i$, $\gamma_2(s) = -1.3 + 2.0i$, $\dot{\gamma}_1 = -2.5 - 3.1i$, $\dot{\gamma}_2(s) = 2.6 - 5.1i$, $\hat{\gamma}_1(s) = -1.2 + 0.3i$, $\hat{\gamma}_2(s) = 2.1 + 1.7i$, $\dot{\gamma}_1(s) = -0.3 - 2.8i$, $\dot{\gamma}_2(s) = 2.5 - 2.8i$, $s \in [-1, 0)$, the drive-response CVIDNNs (19) and (20) are unsynchronized without control, as illustrated in Figs. 1, 2, 3 and 4.

Next we designed controller from (9), we select control parameters, $k_1^R = 1.2$, $k_2^R = 2.3$, $k_1^I = 0.7$, $k_2^I = -0.9$, $\zeta_1^R = -2.3$, $\zeta_2^R = -4.5$, $\zeta_1^I = 0.9$, $\zeta_2^I = 1.3$, $\hat{\rho}_1^R = 3.5$, $\hat{\rho}_2^R = -3.9$, $\hat{\rho}_1^I = -5.6$, $\hat{\rho}_2^I = 0.6$, $\hat{k}_1 = 1.7$, $\hat{k}_2 = 0.8$, $\delta_1^R = -3.5$, $\delta_2^R = -4.5$, $\delta_1^I = -7.3$, $\delta_2^I = 2.1$.

Then, according condition (10) is satisfied. It can be obtained from Theorem 3.1 that the drive system (19) and response system (20) with above parameters can achieve synchronized in finite-time. Figure 5 and Fig. 6 show the synchronization error trajectories of real and imaginary part for drive system (19) and response system (20) via the controller (9).

Furthermore, the estimated setting time is obtained as $t^* = \frac{V^{1-\hat{\zeta}}(\epsilon(0))}{\Omega_{min}^\alpha(1-\hat{\zeta})} = 0.9372$.

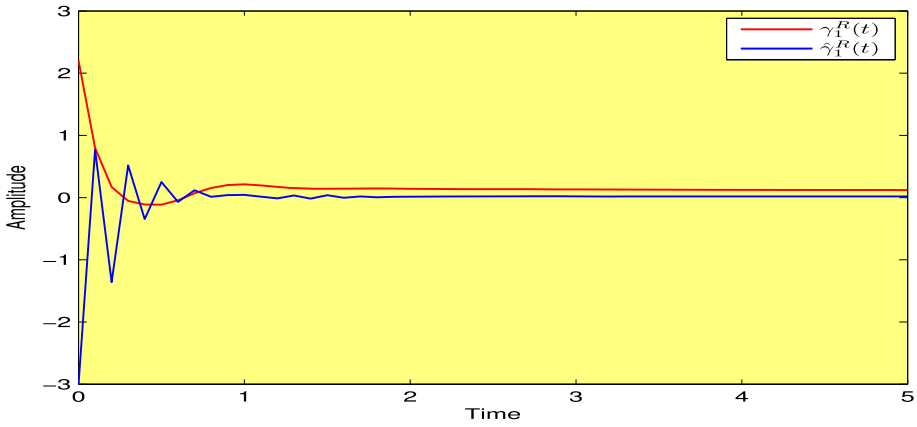


Fig. 1 Time evolutions of the states $\gamma_1^R(t)$ and $\hat{\gamma}_1^R(t)$ for drive-response system (19) and (20) without controller

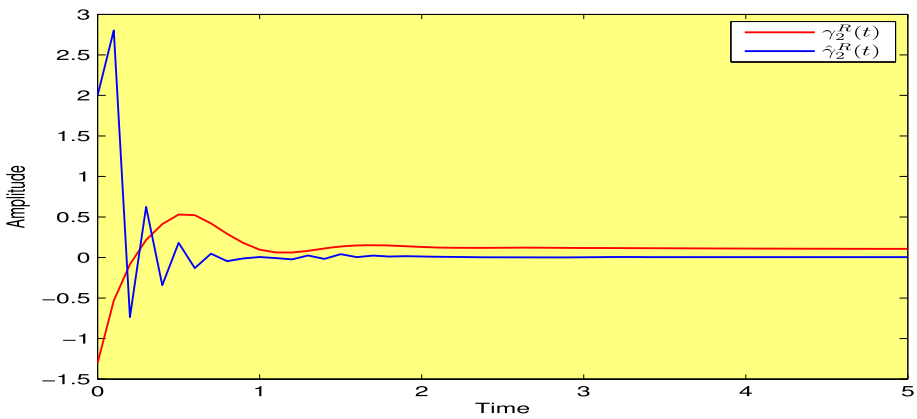


Fig. 2 Time evolutions of the states $\gamma_2^R(t)$ and $\hat{\gamma}_2^R(t)$ for drive-response system (19) and (20) without controller

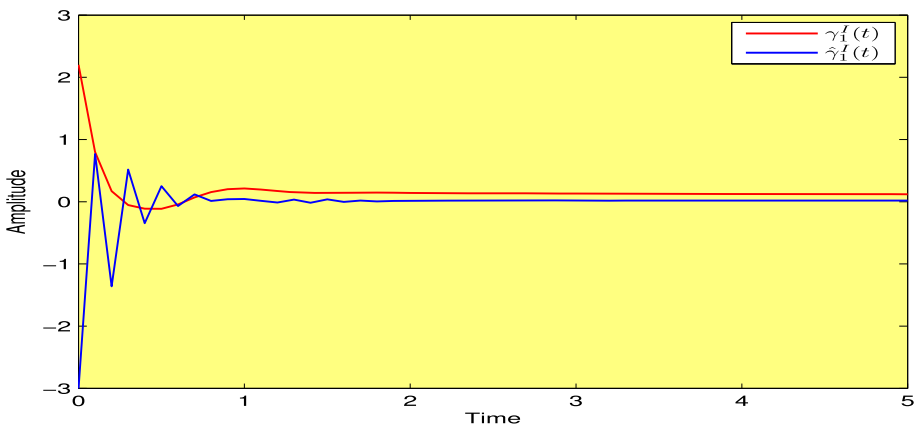


Fig. 3 Time evolutions of the states $\gamma_1^I(t)$ and $\hat{\gamma}_1^I(t)$ for drive-response system (19) and (20) without controller

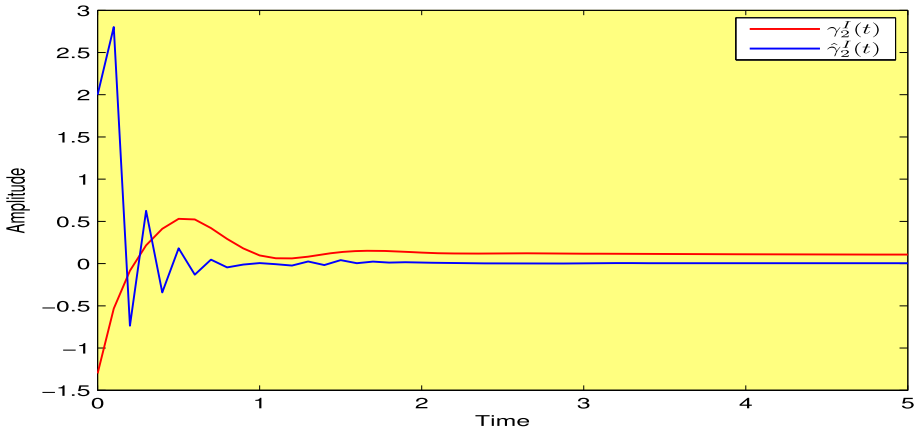


Fig. 4 Time evolutions of the states $\gamma_2^I(t)$ and $\hat{\gamma}_2^I(t)$ for drive-response system (19) and (20) without controller

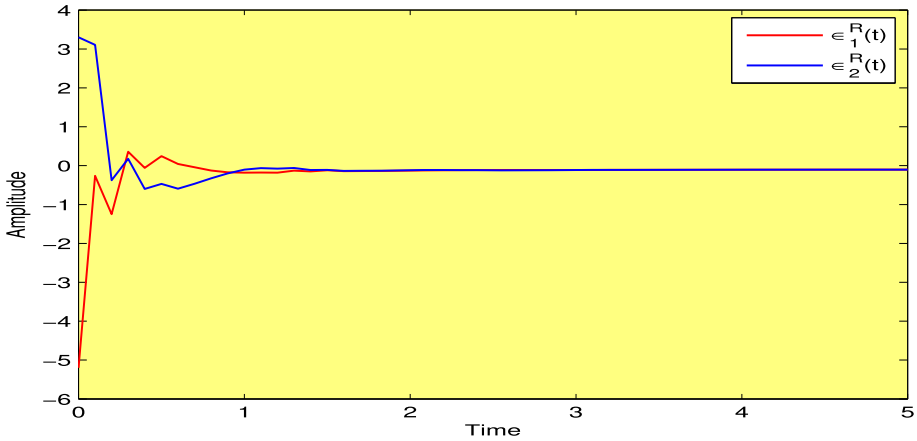


Fig. 5 Synchronization error trajectories $\epsilon_1^R(t)$, $\epsilon_2^R(t)$ under controller (9)

Remark 4.1 From Figs. 5 and 6, we find the T-S fuzzy CVIDNNs drive system (19) and response system (20) successfully realizes the finite-time synchronized under the feed-back controller (9). From Figs. 7 and 8, we find, the asymptotically synchronized when T-S fuzzy CVIDNNs drive system (19) and response system (20) via controller (15) is unstable, we enhance the control strength. The control strength weakens with the T-S fuzzy CVIDNNs drive system (19) and response system (20) achieving the finite-time synchronized.

Remark 4.2 In the compare with controllers (see [43, 44]), the sufficiently small gains would lead to small control inputs, but the required synchronization speed may be quite slow. Our controller designed to achieve synchronization, the controller (10) with parameters $\hat{\zeta}$, ζ^R , ζ^I , k_α^R , and k_α^I should be selected in accordance with the synchronization speed to be quick and the control input not to be very large, considering the designer requirements.

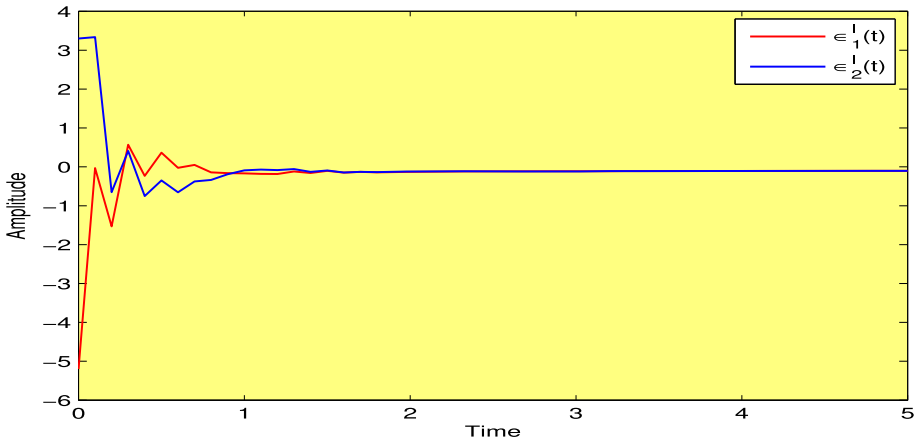


Fig. 6 Synchronization error trajectories $e_1^I(t)$, $e_2^I(t)$ under controller (9)

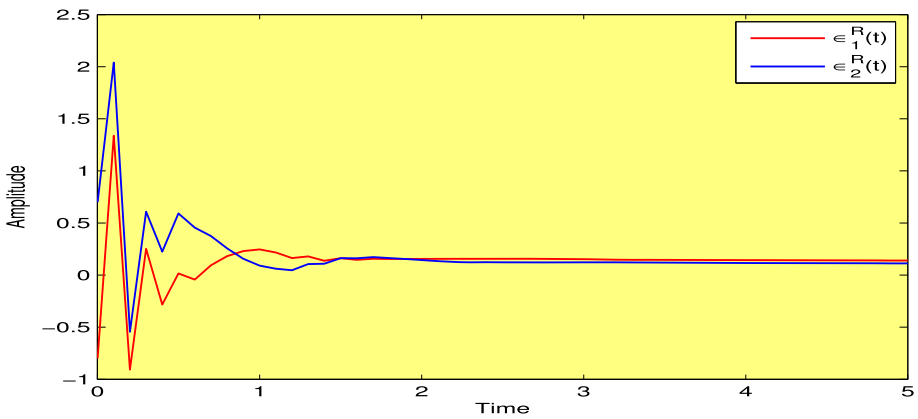


Fig. 7 Synchronization error trajectories $e_1^R(t)$, $e_2^R(t)$ under controller (15)

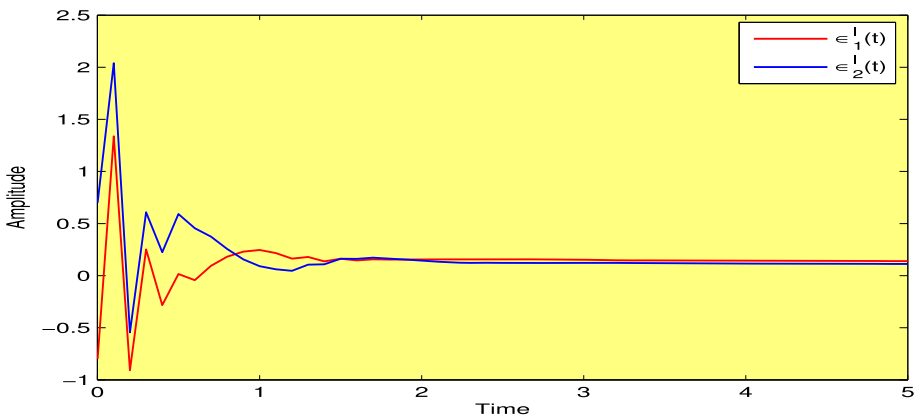


Fig. 8 Synchronization error trajectories $e_1^I(t)$, $e_2^I(t)$ under controller (15)

5 Conclusion

We investigated the finite-time synchronization problem for T–S fuzzy of CVIDNNs in this study by divided into the real and imaginary parts of complex-valued values. Some easily verified algebraic criteria to ensure the finite-time synchronization of CVIDNNs are established by utilizing the Lyapunov function and inequality analytical techniques. A numerical example showed the validity of our theoretical results. For further works, we will study the sampled-data event triggered control of CVIDNNs with time delays.

Acknowledgements This work was supported by the National Board Higher Mathematics, Mumbai, India, under the Sanctioned No. 02011/10/2019/NBHM(R.P)/R D II / 1242 and the National Natural Science Foundation of China under Grant No. 62103103, and the Natural Science Foundation of Jiangsu Province of China under Grant No. BK20210223.

Declarations

Conflict of interest The authors have no conflicts of interest to declare. All co-authors have seen and agree with the contents of the manuscript and there is no financial interest to report.

References

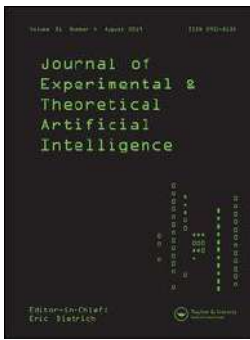
1. Rajivganthi C, Rihan A, Lakshmanan S, Rakkiyappan R, Muthukumar P (2016) Synchronization of memristor-based delayed BAM neural networks with fractional-order derivatives. *Complexity* 21:412–426
2. Pratap A, Raja R, Cao J, Rihan FA, Seadawy AR (2020) Quasi-pinning synchronization and stabilization of fractional order BAM neural networks with delays and discontinuous neuron activations. *Chaos, Solitons Fractals* 131:109491
3. Du Y, Zhong S, Zhou N (2014) Global asymptotic stability of Markovian jumping stochastic Cohen–Grossberg BAM neural networks with discrete and distributed time-varying delays. *Appl Math Comput* 243:624–636
4. Xiao J, Wen S, Yang X, Zhong S (2020) New approach to global Mittag–Leffler synchronization problem of fractional-order quaternion-valued BAM neural networks based on a new inequality. *Neural Netw* 122:320–337
5. Lv X, Li X, Cao J, Perc M (2018) Dynamical and static multisynchronization of coupled multistable neural networks via impulsive control. *IEEE Trans Neural Netw Learn Syst* 29:6062–6072
6. Zhuang J, Cao J, Tang L, Xia Y, Perc M (2020) Synchronization analysis for stochastic delayed multilayer network with additive couplings. *IEEE Trans Syst, Man, Cybern: Syst* 50:4807–4816
7. Zhang W, Wang X, You W, Chen J, Dai P, Zhang P (2019) RESLS: region and edge synergetic level set framework for image segmentation. *IEEE Trans Image Process* 29:57–71
8. Ngo L, Cha J, Han JH (2019) Deep neural network regression for automated retinal layer segmentation in optical coherence tomography images. *IEEE Trans Image Process* 29:303–312
9. Zhou Z, Zhang B, Yu X (2021) Infrared handprint classification using deep convolution neural network. *Neural Process Lett* 53:1065–1079
10. Xiao Y, Zijie Z (2020) Infrared image extraction algorithm based on adaptive growth immune field. *Neural Process Lett* 51:2575–2587
11. He K, Cao X, Shi Y, Nie D, Gao Y, Shen D (2019) Pelvic organ segmentation using distinctive curve guided fully convolutional networks. *IEEE Trans Med Imaging* 38:585–595
12. Yu X, Ye X, Zhang S (2022) Floating pollutant image target extraction algorithm based on immune extremum region. *Digit Signal Process* 123:103442
13. Long C, Zhang G, Hu J (2021) Fixed-time synchronization for delayed inertial complex-valued neural networks. *Appl Math Comput* 405:126272
14. Long C, Zhang G, Zeng Z, Hu J (2022) Finite-time stabilization of complex-valued neural networks with proportional delays and inertial terms: a non-separation approach. *Neural Netw* 148:86–95
15. Huang C, Liu B (2019) New studies on dynamic analysis of inertial neural networks involving non-reduced order method. *Neurocomputing* 325:283–287

16. Wheeler DW, Schieve WC (1997) Stability and chaos in an inertial two-neuron system. *Physica D* 105:267–284
17. Alimi AM, Aouiti C, Assali EA (2019) Finite-time and fixed-time synchronization of a class of inertial neural networks with multi-proportional delays and its application to secure communication. *Neurocomputing* 332:29–43
18. Lakshmanan S, Prakash M, Lim CP, Rakkiyappan R, Balasubramaniam P, Nahavandi S (2018) Synchronization of an inertial neural network with time-varying delays and its application to secure communication. *IEEE Trans Neural Netw Learn Syst* 29:195–207
19. Prakash M, Balasubramaniam P, Lakshmanan S (2016) Synchronization of Markovian jumping inertial neural networks and its applications in image encryption. *Neural Netw* 83:86–93
20. Muralisankar S, Gopalakrishnan N, Balasubramaniam P (2012) An LMI approach for global robust dissipativity analysis of T–S fuzzy neural networks with interval time-varying delays. *Expert Syst Appl* 39:3345–3355
21. Tan Y, Du D, Fei S (2018) Quantized filtering for T–S fuzzy networked systems with saturation non linearities: an output-dependent triggering method. *ISA Trans* 72:122–137
22. Liu Y, Lee S (2016) Stability and stabilization of Takagi–Sugeno fuzzy systems via sampled-data and state quantized controller. *IEEE Trans Fuzzy Syst* 24:635–644
23. Yue D, Tian E, Zhang Y, Peng C (2009) Delay-distribution-dependent stability and stabilization of T–S fuzzy systems with probabilistic interval delay. *IEEE Trans Syst Man Cybern* 39:503–516
24. Tan Y, Liu Y, Niu B, Fei S (2020) Event-triggered synchronization control for T–S fuzzy neural networked systems with time delay. *J Franklin Inst* 357:5934–5953
25. Tong D, Zhu Q, Zhou W, Xu Y, Fang J (2013) Adaptive synchronization for stochastic T–S fuzzy neural networks with time-delay and Markovian jumping parameters. *Neurocomputing* 117:91–97
26. Duan L, Li J (2021) Fixed-time synchronization of fuzzy neutral-type BAM memristive inertial neural networks with proportional delays. *Inf Sci* 576:522–541
27. Jian J, Duan L (2020) Finite-time synchronization for fuzzy neutral-type inertial neural networks with time-varying coefficients and proportional delays. *Fuzzy Sets Syst* 381:51–67
28. Hao Z, Xing-yuan W, Peng-fei Y, Yu-jie Sun (2020) Combination synchronization and stability analysis of time-varying complex-valued neural networks. *Chaos, Solitons Fractals* 131:109485
29. Zhang B, Deng F, Xie S, Luo S (2018) Exponential synchronization of stochastic time-delayed memristor-based neural networks via distributed impulsive control. *Neurocomputing* 286:41–50
30. Shi Y, Zhu P (2016) Finite-time synchronization of stochastic memristor-based delayed neural networks. *Neural Comput Appl* 29:293–301
31. Jiang M, Wang S, Mei J, Shen Y (2015) Finite-time synchronization control of a class of memristor-based recurrent neural networks. *Neural Netw* 63:133–140
32. Zhang ZQ, Cao JD (2018) Novel finite-time synchronization criteria for inertial neural networks with time delays via integral inequality method. *IEEE Trans Neural Netw Learn Syst* 30:1476–1485
33. Hu LF, Zhong SM, Shi KB, Zhang XJ (2020) Further results on finite-time synchronization of delayed inertial memristive neural networks via a novel analysis method. *Neural Netw* 127:45–47
34. Long CQ, Zhang GD, Zeng ZG, Hu JH (2021) Finite-time lag synchronization of inertial neural networks with mixed infinite time-varying delays and state-dependent switching. *Neurocomputing* 433:50–58
35. Wu YB, Gao YX, Li WX (2020) Finite-time synchronization of switched neural networks with state-dependent switching via intermittent control. *Neurocomputing* 384:325–334
36. Bohner M, Rao VSH, Sanyal S (2011) Global stability of complex-valued neural networks on time scales. *Differ Equ Dyn Syst* 19:3–11
37. Rajchakit G, Sriraman R (2021) Robust passivity and stability analysis of uncertain complex-valued impulsive neural networks with time-varying delays. *Neural Process Lett* 53:581–606
38. Chanthorn P, Rajchakit G, Ramalingam S, Lim CP, Ramachandran R (2020) Robust dissipativity analysis of hopfield-type complex-valued neural networks with time-varying delays and linear fractional uncertainties. *Mathematics* 8:595
39. Samidurai R, Sriraman R, Zhu S (2019) Leakage delay-dependent stability analysis for complex-valued neural networks with discrete and distributed time-varying delays. *Neurocomputing* 338:262–273
40. Chen X, Zhao Z, Song Q, Hu J (2017) Multistability of complex-valued neural networks with time-varying delays. *Appl Math Comput* 294:18–35
41. Zhang Z, Liu X, Chen J, Guo G, Zhou S (2011) Further stability analysis for delayed complex-valued recurrent neural networks. *Neurocomputing* 251:81–89
42. Liang J, Gong W, Huang H (2016) Multistability of complex-valued neural networks with discontinuous activation functions. *Neural Netw* 84:125–142
43. Yu J, Hu C, Jiang H, Wang L (2020) Exponential and adaptive synchronization of inertial complex-valued neural networks: a non-reduced order and non-separation approach. *Neural Netw* 124:50–59

44. Li X, Fang J, Huang T (2020) Event-triggered exponential stabilization for state-based switched inertial complex-valued neural networks with multiple delays. *IEEE Trans Cybern.* <https://doi.org/10.1109/TCYB.2020.3031379>
45. Amin MdF, Murase K (2009) Single-layered complex-valued neural network for real-valued classification problems. *Neurocomputing* 72:945–955
46. Velmurugan G, Rakkiyappan R, Lakshmanan S (2015) Passivity analysis of memristor-based complex-valued neural networks with time-varying delays. *Neural Process Lett* 42:517–540

Publisher's Note Springer Nature remains neutral with regard to jurisdictional claims in published maps and institutional affiliations.

Springer Nature or its licensor (e.g. a society or other partner) holds exclusive rights to this article under a publishing agreement with the author(s) or other rightsholder(s); author self-archiving of the accepted manuscript version of this article is solely governed by the terms of such publishing agreement and applicable law.



Robust H_∞ performance for discrete time T-S fuzzy switched memristive stochastic neural networks with mixed time-varying delays

R. Vadivel, M. Syed Ali & Young Hoon Joo

To cite this article: R. Vadivel, M. Syed Ali & Young Hoon Joo (2020): Robust H_∞ performance for discrete time T-S fuzzy switched memristive stochastic neural networks with mixed time-varying delays, Journal of Experimental & Theoretical Artificial Intelligence, DOI: [10.1080/0952813X.2020.1725649](https://doi.org/10.1080/0952813X.2020.1725649)

To link to this article: <https://doi.org/10.1080/0952813X.2020.1725649>



Published online: 16 Feb 2020.



Submit your article to this journal [↗](#)



Article views: 7



View related articles [↗](#)



View Crossmark data [↗](#)



Robust H_∞ performance for discrete time T-S fuzzy switched memristive stochastic neural networks with mixed time-varying delays

R. Vadivel^{a,b}, M. Syed Ali^a and Young Hoon Joo^c

^aDepartment of Mathematics, Thiruvalluvar University, Vellore, India; ^bDepartment of Mathematics, Phuket Rajabhat University, Phuket, Thailand; ^cThe School of IT Information and Control Engineering, Kunsan National University, Gunsan, Republic of Korea

ABSTRACT

In this paper, we study the robust H_∞ performance for discrete-time T-S fuzzy switched memristive stochastic neural networks with mixed time-varying delays and switching signal design. The neural network under consideration is subject to time-varying and norm bounded parameter uncertainties. Decomposing of the delay interval approach is employed in both the discrete delays and distributed delays. By constructing a proper Lyapunov-Krasovskii functional (LKF) with triple summation terms and using an improved summation inequality techniques. Sufficient conditions are derived in terms of linear matrix inequalities (LMIs) to guarantee the considered discrete-time neural networks to be exponentially stable. Finally, numerical examples with simulation results are given to illustrate the effectiveness of the developed theoretical results.

ARTICLE HISTORY

Received 1 November 2018
Accepted 30 January 2020

KEYWORDS

Switched; memristive; H_∞ performance; Lyapunov-Krasovskii functional; neural networks

Introduction

As it is well known, in the theoretical modelling of traditional neural circuits, the system parameters are determined by the electric components such as capacitance and resistance. Recently, the memristor has received increasing research attention due to its advantages over resistance such as small size, low energy consumption and storage capacity (Chua, 1971; Strukov, Snider, Stewart, & Williams, 2008). Due to the rapid development of the memristor, the memristive NNs have stirred a great deal of research interests and considerable research efforts have been made on the dynamical behaviour analysis issues of memristive NNs such as stability issues (Anbuviya, Mathiyalagan, Sakthivel, & Prakash, 2016; Li et al., 2017b; Mathiyalagan, Anbuviya, Sakthivel, Park, & Prakash, 2016) and synchronisation problems (Li et al., 2017a; Que et al., 2010; Yang, Luo, Liu, & Li, 2017). It should be pointed out that, in the existing literature, almost all the memristive NNs concerned are of continuous time. Actually, the discrete-time NNs could be more suitable to the model digitally transmitted signals in a dynamical way. Therefore, the memristive NNs of discrete-time case are of great importance for both theoretical and practical reasons. Very recently, rich body of works have been done on the dynamic behaviour of the switched NNs, especially for the memristive system (Gao, Zhu, Alsaedi, Alsaedi, & Hayat, 2017; Jiang & Li, 2016; Syed Ali & Saravanan, 2018).

In the past several decades, memristive NNs have attracted an ever-increasing research interest due to their superior performance for advanced challenges in applications such as signal processing, pattern recognition, image processing, associative memory and power systems. In this applications, most of the NNs are implemented by digital computer, including microprocessor and

microcontrollers, with necessary input/output hardware. As we know, the fundamental character of digital computer is that it processes information in discrete steps. Therefore, discrete-time NNs are better matched than their continuous-time analogs in today's digital world (Jin, Hen, & Wu, 2016; Song, Gao, & Zheng, 2009; Song & Wang, 2007). Hence, it is essential to study the dynamical behaviour of discrete-time NNs. Moreover, time delays are frequently encountered in various engineering, biological and economic systems. Due to the finite speed of information processing and the inherent communication time of neurons, the existence of time delays usually causes oscillation, divergence, or even instability of NNs. Therefore, it is of both theoretical and practical importance to study the dynamical behaviour of discrete-time system with time delays (Lin, Wu, & Li, 2016; Liu, Wang, & Shu, 2016; Wang, Xue, Fei, & Li, 2013; Wu, Liu, Shi, He, & Yokoyama, 2008; Wu, Su, Chu, & Zhou, 2010; Yu, Zhang, & Fei, 2010; Zhang, Xu, & Zou, 2008).

In the last few years, the problem of stability analysis of both continuous-time and discrete-time stochastic NNs has been the crucial topic for researchers (Maharajan, Raja, Cao, & Rajchakit, 2019; Sowmiya, Raja, Cao, Li, & Rajchakit, 2018; Syed Ali & Marudai, 2011). In practice, the stochastic disturbances which certainly existed in the NNs are the main source of disturbances. When compared with the typical neural networks, the stochastic NNs have more practical significance when the stochastic effects are taken into account (see (Chinnamuniyandi, Raja, Cao, Rajchakit, & Li, 2018; Deng, Hua, Liu, Peng, & Fei, 2011; Hua, Liu, Deng, & Fei, 2010; Maharajan, Raja, Cao, Ravi, & Rajchakit, 2018; Selvaraj, Sakthivel, & Kwon, 2018; Sowmiya, Raja, Zhu, & Rajchakit, 2019)). However, it is well known that the stability of a well-designed neural network may often be destroyed by its unavoidable uncertainty. In practice, uncertainties often exist in most engineering and communication systems and may cause undesirable dynamic network behaviours. More specifically, the connection weights of the neurons are inherently dependent on certain resistance and capacitance values that inevitably bring in uncertainties during the parameter identification process. The deviations and perturbations in parameters are the main sources of uncertainty. So, it is important to study the dynamical behaviours of NNs by taking the uncertainty into account (Jarina Banu, Balasubramaniam, & Ratnavelu, 2015; Kwon, Lee, & Park, 2012; Li & Cao, 2016). A switched system is a hybrid system which consists of several subsystems and a switching signal that handle the switching among them (Arunkumar et al., 2012; Liberzon, 2003; Zhang & Yu, 2009). Switching among systems may produce many complicated nonlinear system behaviours, such as multiple limit cycles and chaos. However, it should be mentioned that all these existing studies about the stability analysis are performed for switched system using the Lyapunov asymptotic stability theory, which is defined over the infinite-time interval. But in many practical applications, the transient behaviour of system is concerned over a fixed time interval, in which the system states need to grip below a prescribed upper bound and larger values are not permitted during this time-interval. Recently, many biologists are focusing on the transient values of the actual network states. Practical examples for switched systems are automated highway systems, automotive engine control system, chemical process, constrained robotics, power systems and power electronics, robot manufacture and stepper motors (Hou, Zong, & Wu, 2011; Phat & Ratchagit, 2011). Recently, there are many results that have been reported for switched discrete-time NNs along with switching signal (see (Lien, Yu, Chang, Chung, & Chen, 2012; 2013, 2014) and references therein).

On the other hand, H_∞ concept was proposed to reduce the effect of the disturbance input on the regulated output to within a prescribed level. Analysis and synthesis in H_∞ setting have good advantages such as effective disturbance attenuation, less sensitivity to uncertainties and many practical applications (Zha, Fang, Li, & Liu, 2017; Zhang, Shi, & Shi, 2017; Zhao & Hu, 2017). It is well known that the H_∞ performance is closely related to the capability of disturbance rejection. On another research direction, Takagi-Sugeno (T-S) fuzzy systems have been verified to be a powerful tool for controlling nonlinear systems owing to their universal approximation characteristics. The T-S fuzzy model approach combines the flexible fuzzy logic theory and successful linear system theory into a uniform framework to approximate a broad range of complex nonlinear systems. The advantages in using a small number of rules to model higher-order nonlinear systems based on T-S fuzzy model were

exposed in (Dong, Fang, Shi, & Wu, 2019; Qiu, Gao, & Ding, 2016; Takagi & Sugeno, 1985; Tian, Yue, & Zhang, 2009; Wu, Dong, Shi, Zhang, & Huang, 2019). In general, the switched signals with local input–output relations are represented by T-S fuzzy systems which can be described by fuzzy IF-THEN rules. Noting the importance of switching signal design, it is natural to wonder how to address the discrete-time problem for stochastic NNs by T-S fuzzy approach. The advantages of the memristors good features such as small scale, pinched hysteresis and plasticity. If the synapses of the neural network is imitated by memristors, the induced switched memristive NNs become more complicate. One of the reasons comes from that the memristor circuit itself exhibits some switching behaviours depending on states. The study on discrete-time T-S fuzzy switched memristor-based on delayed NNs is of interest and significance. But the research on this field has not been fully covered so far.

Besides, discrete-time switched memristive NNs based on T-S fuzzy approaches are often subject to instantaneous perturbation and abrupt change, i.e., disturbance, at certain moments. This can be caused by environmental noises, switching behaviour and control effects in a dynamic system. Noise can affect dynamical behaviours of the neuron systems. Due to possible faults, time delays and disturbances, some subsystems of a switched memristive neural network may be unstable. Therefore, how to stabilise the discrete-time T-S fuzzy switched memristor-based with unstable subsystems is a challenge. However, to the best of the authors knowledge, the H_∞ performance for switched T-S fuzzy discrete-time memristive stochastic NNs with switching signal has not been adequately addressed in the literature yet, not to mention that the H_∞ performance index is imposed simultaneously. It is, therefore, the purpose of this paper is to fill such a gap.

Based on the aforementioned factors, we study the problem of robust H_∞ analysis for discrete-time switched memristive stochastic NNs with mixed time varying delay. To guarantee the exponential stability and disturbance attenuation performance, the Lyapunov functional method and some summation analysis techniques are utilised. The major contributions of this paper are summarised as follows.

- (1) The discrete-time switched memristive stochastic NNs with time-varying discrete delay and bounded distributed delay are firstly proposed.
- (2) By constructing a new Lyapunov-Krasovskii functional which including the lower and upper delay bounds of interval time-varying delays new sufficient conditions that guarantee the exponential stability are established in terms of linear matrix inequities (LMIs).
- (3) Based on the novel summation inequality technique, a new switching signal design approach is developed to guarantee the H_∞ performance for consider NNs.
- (4) Finally, the effectiveness and advantages of the derived results are demonstrated by numerical examples.

Notation: Throughout this paper, \mathbb{N} stands for the set of positive integers, \mathbb{R}^n denotes the n -dimensional Euclidean space, $\mathbb{R}^{n \times m}$ is the set of $n \times m$ real matrices. For a matrix B and two symmetric matrices A and C , $\begin{bmatrix} A & B \\ * & C \end{bmatrix}$ denote the symmetric matrix, where the notation $*$ represents the entries implied by symmetry. For $X \in \mathbb{R}^{n \times m}$, the notation $X > 0$ (respectively, $X \geq 0$) means that the matrix X is a real symmetric positive definite (positive semi-definite). The superscript T represents the transpose of the matrix (or vector). I denotes the identity matrix of the compatible dimensions, $\text{diag}\{ \dots \}$ denotes the block-diagonal matrix and $\| \cdot \|$ is the Euclidean norm in \mathbb{R}^n . λ_{\max} and λ_{\min} denote the maximum and minimum eigenvalues respectively. $l_2[0, \infty)$ is the space of square-summable infinite vector sequences over $[0, \infty)$.

Problem description and preliminaries

We consider the following switched memristor discrete-time stochastic NNs with time varying delay which is represented by a T-S fuzzy model composed of a set of fuzzy implications and each implication is expressed as a linear system model Wu et al. (2019).

Plant Rule ℓ : IF $\hat{y}_1(k)$ is $\hat{\pi}_1^\ell$, $\hat{y}_2(k)$ is $\hat{\pi}_2^\ell$ and \dots and $\hat{y}_r(k)$ is $\hat{\pi}_r^\ell$

THEN

$$\begin{cases} u(k+1) &= A^\ell(u(k))u(k) + B^\ell(u(k))f(u(k)) + C^\ell(u(k))f(u(k-d(k))) \\ &+ D^\ell(u(k))\sum_{i=1}^{\tau(k)} f(u(k-i)) + E^\ell v(k) + \sigma^\ell(k, u(k), u(k-d(k)))w(k), \\ y(k) &= A_1^\ell u(k) + D_1^\ell u(k-d(k)) + G^\ell v(k), \\ u(l) &= \varphi(l), l = k_0 - d_2, \dots, k_0, \end{cases} \quad (1)$$

where $u(k) = [u_1(k), u_2(k), \dots, u_n(k)]^T$ is the state vector with n neurons; $f(u(k)) = [f_1(u_1(k)), f_2(u_2(k)), \dots, f_n(u_n(k))]$ denotes the neuron activation function; $v(k) \in \mathbb{R}^n$ is the disturbance input which belongs to $l_2[0, \infty)$; $y(k) \in \mathbb{R}^m$ is the measurement output; $d(k)$ and $\tau(k)$ denote the discrete delay and the finite-distributed delay, respectively, and satisfy $d_1 \leq d(k) \leq d_2$ and $\tau_1 \leq \tau(k) \leq \tau_2$, where $d_2 \geq d_1 > 0$ and $\tau_2 \geq \tau_1 > 0$ are prescribed integers; $A^\ell(u(k)) = \text{diag}\{a_1^\ell(u_1(k)), a_2^\ell(u_2(k)), \dots, a_n^\ell(u_n(k))\}$ is the state feedback matrix; $B^\ell(u(k)) = (b_{ij}^\ell(u_i(k)))_{n \times n}$, $C^\ell(u(k)) = (c_{ij}^\ell(u_i(k)))_{n \times n}$ and $D^\ell(u(k)) = (d_{ij}^\ell(u_i(k)))_{n \times n}$ represents the connection weight matrices. E^ℓ , G^ℓ , A_1^ℓ , D_1^ℓ are known constant matrices with appropriate dimensions; $\varphi(l)$ is a given initial condition sequence.

In the system (1), the stochastic disturbance term $\sigma(k, u(k), u(k-d(k)))w(k)$ can be viewed as stochastic perturbations on the neuron states and delayed neuron states with

$$\mathbb{E}\{w(k)\} = 0, \mathbb{E}\{w^2(k)\} = 1, \mathbb{E}\{w(j)w(j)\} = 0 \quad (i \neq j).$$

The function $\sigma(k, u, y) : \mathbb{R} \times \mathbb{R}^n \times \mathbb{R}^n \rightarrow \mathbb{R}^n$ is Borel measurable and is locally Lipschitz continuous, satisfying the following Assumption 2.1:

Assumption 2.1. There exist two positive constants $\hat{\rho}_1$ and $\hat{\rho}_2$ such that

$$\sigma^T(k, u, y)\sigma(k, u, y) \leq \hat{\rho}_1 u^T u + \hat{\rho}_2 y^T y, \forall k \geq 0, u, y \in \mathbb{R}^n. \quad (2)$$

where $\hat{\pi}_j^\ell$ ($j = 1, 2, \dots, r$) is the fuzzy set, $\hat{y}(k) = [\hat{y}_1(k) \hat{y}_2(k) \dots \hat{y}_r(k)]^T$ is the premise variable vector and q is the number of **IF – THEN** rules.

Now, the defuzzified output of the T-S fuzzy model (2) is represented as follows:

$$\begin{cases} u(k+1) &= \sum_{l=1}^q \phi^l(\hat{y}(k)) [A^\ell(u(k))u(k) + B^\ell(u(k))f(u(k)) + C^\ell(u(k))f(u(k-d(k))) \\ &+ D^\ell(u(k))\sum_{i=1}^{\tau(k)} f(u(k-i)) + E^\ell v(k) + \sigma^\ell(k, u(k), u(k-d(k)))w(k)], \\ y(k) &= \sum_{l=1}^q \phi^l(\hat{y}(k)) [A_1^\ell u(k) + D_1^\ell u(k-d(k)) + G^\ell v(k)], \\ u(l) &= \varphi(l), l = k_0 - d_2, \dots, k_0, \end{cases} \quad (3)$$

where $\phi^l(\hat{y}(k)) = \frac{\rho^l(\hat{y}(k))}{\sum_{l=1}^q \rho^l(\hat{y}(k))}$, $\rho^l(\hat{y}(k)) = \prod_{s=1}^r \hat{\pi}_s^l(\gamma_s(k))$, in which $\hat{\pi}_s^l(\gamma_s(k))$ is the grade of the membership function of $\gamma_s(k)$ in $\hat{\pi}_s^l$. According to the theory of fuzzy sets, we have $\rho^l(\hat{y}(k)) \geq 0, l = 1, 2, \dots, q$, $\sum_{l=1}^q \rho^l(\hat{y}(k)) > 0 \forall k$ and $\phi^l(\hat{y}(k))$ satisfies $\phi^l(\hat{y}(k)) \geq 0, l = 1, 2, \dots, q$ and $\sum_{l=1}^q \phi^l(\hat{y}(k)) = 1 \forall k$.

Assumption 2.2. Given any $x, y \in \mathbb{R}(x \neq y), j \in \{1, 2, \dots, n\}$, the activation functions $f_j(\cdot)$ is continuous and bounded, and there exist constants F_j^-, F_j^+ as well as $F^+ = \text{diag}\{F_1^+, F_2^+, \dots, F_n^+\}$ and $F^- = \text{diag}\{F_1^-, F_2^-, \dots, F_n^-\}$ such that the following condition holds:

$$F_j^- \leq \frac{f_j(y) - f_j(x)}{y - x} \leq F_j^+. \quad (4)$$

According to current-voltage characteristics of memristor Chua (1971), the definition of $a_i(u_i(k)), b_{ij}(u_i(k)), c_{ij}(u_i(k))$ and $d_{ij}(u_i(k))$ are considered as follows

$$\begin{aligned} a_i(u_i(k)) &= \begin{cases} \hat{a}_i, & |u_i(k)| \leq k_i, \\ \check{a}_i, & |u_i(k)| > k_i, \end{cases} \\ b_{ij}(u_i(k)) &= \begin{cases} \hat{b}_{ij}, & |u_i(k)| \leq k_i, \\ \check{b}_{ij}, & |u_i(k)| > k_i, \end{cases} \\ c_{ij}(u_i(k)) &= \begin{cases} \hat{c}_{ij}, & |u_i(k)| \leq k_i, \\ \check{c}_{ij}, & |u_i(k)| > k_i, \end{cases} \\ d_{ij}(u_i(k)) &= \begin{cases} \hat{d}_{ij}, & |u_i(k)| \leq k_i, \\ \check{d}_{ij}, & |u_i(k)| > k_i, \end{cases} \end{aligned} \quad (5)$$

in which switching jumps $k_i > 0, |\hat{a}_i| < 1, |\check{a}_i| < 1, \hat{b}_{ij}, \check{b}_{ij}, \hat{c}_{ij}, \check{c}_{ij}, \hat{d}_{ij}, \check{d}_{ij}, i, j = 1, 2, \dots, n$ are known constants with respect to memristances.

$$\begin{aligned} a_i(u_i(k)) &= \frac{1}{C_i} \left[\sum_{j=1}^n (M_{ij} + W_{ij}) \times \text{sgn}_{ij} + \frac{1}{R_i} \right] \\ b_{ij}(u_i(k)) &= \frac{M_{ij}}{C_i} \times \text{sgn}_{ij}, c_{ij}(u_i(k)) = \frac{M_{ij}}{C_i} \times \text{sgn}_{ij}, d_{ij}(u_i(k)) = \frac{M_{ij}}{C_i} \times \text{sgn}_{ij}. \end{aligned} \quad (6)$$

where $\text{sgn}_{ij} = 1$, if $i \neq j$ holds, otherwise, -1 ; C_i and R_i stand for the capacitor and resistor, respectively; M_{ij} and W_{ij} are the memductances of memristors. Since the memductance cannot be negative, it is clear from the description that $b_{ij}(\cdot), c_{ij}(\cdot)$ and $d_{ij}(\cdot)$ are nonpositive if $i = j$ holds, otherwise, nonnegative.

$$\begin{aligned} a_i^- &= \min\{\hat{a}_i, \check{a}_i\}, a_i^+ = \max\{\hat{a}_i, \check{a}_i\}, \\ b_{ij}^- &= \min\{\hat{b}_{ij}, \check{b}_{ij}\}, b_{ij}^+ = \max\{\hat{b}_{ij}, \check{b}_{ij}\}, \\ c_{ij}^- &= \min\{\hat{c}_{ij}, \check{c}_{ij}\}, c_{ij}^+ = \max\{\hat{c}_{ij}, \check{c}_{ij}\}, \\ d_{ij}^- &= \min\{\hat{d}_{ij}, \check{d}_{ij}\}, d_{ij}^+ = \max\{\hat{d}_{ij}, \check{d}_{ij}\}, \\ A^- &= \text{diag}\{a_1^-, a_2^-, \dots, a_n^-\}, A^+ = \text{diag}\{a_1^+, a_2^+, \dots, a_n^+\}, \\ B^- &= (b_{ij}^-)_{(n \times n)}, B^+ = (b_{ij}^+)_{(n \times n)}, \\ C^- &= (c_{ij}^-)_{(n \times n)}, C^+ = (c_{ij}^+)_{(n \times n)}, \\ D^- &= (d_{ij}^-)_{(n \times n)}, D^+ = (d_{ij}^+)_{(n \times n)}. \end{aligned} \quad (7)$$

It is clear that $A^\ell(u(k)) \in [A^-, A^+]$, $B^\ell(u(k)) \in [B^-, B^+]$, $C^\ell(u(k)) \in [C^-, C^+]$ and $D^\ell(u(k)) \in [d^-, d^+]$. Define

$$\tilde{A} = \frac{A^- + A^+}{2} = \text{diag}\left\{\frac{a_1^+ + a_1^-}{2}, \frac{a_2^+ + a_2^-}{2}, \dots, \frac{a_n^+ + a_n^-}{2}\right\},$$

$$\tilde{B} = \frac{B^- + B^+}{2} = \left(\frac{b_{ij}^+ + b_{ij}^-}{2} \right)_{n \times n}, \tilde{C} = \frac{C^- + C^+}{2} = \left(\frac{c_{ij}^+ + c_{ij}^-}{2} \right)_{n \times n},$$

$$\tilde{D} = \frac{D^- + D^+}{2} = \left(\frac{d_{ij}^+ + d_{ij}^-}{2} \right)_{n \times n}.$$

The matrices $A^\ell(u(k))$, $B^\ell(u(k))$, $C^\ell(u(k))$, and $D^\ell(u(k))$ can be written as $A^\ell(u(k)) = \tilde{A}^\ell + \Delta A^\ell(k)$, $B^\ell(u(k)) = \tilde{B}^\ell + \Delta B^\ell(k)$, $C^\ell(u(k)) = \tilde{C}^\ell + \Delta C^\ell(k)$, $D^\ell(u(k)) = \tilde{D}^\ell + \Delta D^\ell(k)$. Therefore we have

$$\begin{cases} u(k+1) = \sum_{i=1}^q \phi^i(\hat{y}(k)) \{ [\tilde{A}^\ell + \Delta A^\ell(k)]u(k) + [\tilde{B}^\ell + \Delta B^\ell(k)]f(u(k)) \\ \quad + [\tilde{C}^\ell + \Delta C^\ell(k)]f(u(k-d(k))) + [\tilde{D}^\ell + \Delta D^\ell(k)] \sum_{i=1}^{\tau(k)} f(u(k-i)) + E^\ell v(k) \\ \quad + \sigma^\ell(k, u(k), u(k-d(k)))w(k) \}, \\ y(k) = \sum_{i=1}^q \phi^i(\hat{y}(k)) \{ A_{1\sigma(k)}^\ell u(k) + D_{1\sigma(k)}^\ell u(k-d(k)) + G^\ell v(k) \}, \\ u(l) = \varphi(l), l = k_0 - d_2, \dots, k_0, \end{cases} \quad (8)$$

where $\Delta A^\ell(k) = \sum_{i=1}^n k_i v_i(k) k_i^T$, $\Delta B^\ell(k) = \sum_{i,j=1}^n k_{ij} t_{ij}(k) k_j^T$, $\Delta C^\ell(k) = \sum_{i=1}^n k_i g_{ij}(k) k_j^T$ and $\Delta D^\ell(k) = \sum_{i,j=1}^n k_{ij} s_{ij}(k) k_j^T$, $k_n \in \mathbb{R}^n$ is the column vector with the n th element being 1 and others being 0, $v_i(k)$, t_{ij} , g_{ij} and s_{ij} are unknown scalars satisfying $|v_i(k)| \leq \tilde{a}_i$, $|t_{ij}(k)| \leq \tilde{b}_{ij}$, $|g_{ij}(k)| \leq \tilde{c}_{ij}$ and $|s_{ij}(k)| \leq \tilde{d}_{ij}$ with $\tilde{a}_j = \frac{a_j^+ - a_j^-}{2}$, $\tilde{b}_{ij} = \frac{b_{ij}^+ - b_{ij}^-}{2}$, $\tilde{c}_{ij} = \frac{c_{ij}^+ - c_{ij}^-}{2}$ and $\tilde{d}_{ij} = \frac{d_{ij}^+ - d_{ij}^-}{2}$. $\Delta A^\ell(k)$, $\Delta B^\ell(k)$, $\Delta C^\ell(k)$ and $\Delta D^\ell(k)$ are the parameter matrices of the following structures

$$\Delta A^\ell(k) = \mathcal{E}^\ell \mathcal{F}^\ell(k) N_1^\ell, \Delta B^\ell(k) = \mathcal{E}^\ell \mathcal{F}^\ell(k) N_2^\ell, \Delta C^\ell(k) = \mathcal{E}^\ell \mathcal{F}^\ell(k) N_3^\ell, \Delta D^\ell(k) = \mathcal{E}^\ell \mathcal{F}^\ell(k) N_4^\ell. \quad (9)$$

where \mathcal{E}^ℓ , N_1^ℓ , N_2^ℓ , N_3^ℓ , N_4^ℓ are known real constant matrices. $\mathcal{F}^\ell(k)$ are unknown time-varying matrices and satisfy $\mathcal{F}^{\ell T}(k) \mathcal{F}^\ell(k) \leq I$, where I is the identity matrix with appropriate dimension.

Switched memristive stochastic NNs

Consider the memristive based switched stochastic NNs based on the system (8) as follows:

$$\begin{aligned} u(k+1) &= \sum_{i=1}^q \phi^i(\hat{y}(k)) \{ A_{\sigma(k)}^\ell(u(k))u(k) + B_{\sigma(k)}^\ell(u(k))f(u(k)) + C_{\sigma(k)}^\ell(u(k))f(u(k-d(k))) \\ &\quad + D_{\sigma(k)}^\ell(u(k)) \sum_{i=1}^{\tau(k)} f(u(k-i)) + E_{\sigma(k)}^\ell v(k) + \sigma^\ell(k, u(k), u(k-d(k)))w(k) \}, \\ y(k) &= \sum_{i=1}^q \phi^i(\hat{y}(k)) \{ A_{1\sigma(k)}^\ell u(k) + D_{1\sigma(k)}^\ell u(k-d(k)) + G_{\sigma(k)}^\ell v(k) \}, \\ u(l) &= \varphi(l), l = k_0 - d_2, \dots, k_0 \end{aligned} \quad (10)$$

The switching signal $\sigma(k) : \mathbb{R}^n \rightarrow \tilde{\mathcal{U}} = \{1, 2, \dots, N\}$ is the switching rule, which is a function depending on the state at each time and will be designed. A switching function is a rule which determines a switching sequence for a given switching system. Moreover, $\sigma(k) = i$ means that the i^{th} subsystem is activated. N is the number of subsystems of the switched system. Firstly, we will introduce the switching regions and the corresponding switching law. Given $P > 0$ and $\hat{U} > 0$, define the domains by

$$\Omega_i(P, \hat{U}, A_i^\ell) = \{u(k) \in \mathbb{R}^n : u^T(k) \hat{Y}_i u(k) < 0\}, \quad (11)$$

where $\hat{Y}_i = A_i^{\rho T} P A_i^{\rho} - \hat{U}$, $i \in \tilde{\mathcal{U}}$. From the similar proof of Lien et al. (2012); Phat and Ratchagit (2011), it can be easily obtained that

$$\bigcup_{i=1}^N \Omega_i = \mathbb{R}^n \setminus \{0\}. \quad (12)$$

Construct the following switching region:

$$\tilde{\Omega}_1 = \Omega_1, \tilde{\Omega}_2 = \Omega_2 \setminus \tilde{\Omega}_1, \tilde{\Omega}_3 = \Omega_3 \setminus \tilde{\Omega}_1 \setminus \tilde{\Omega}_2, \dots, .$$

We can obtain $\bigcup_{i=1}^N \tilde{\Omega}_i = \mathbb{R}^n \setminus \{0\}$ and $\tilde{\Omega}_i \cap \tilde{\Omega}_j = \bar{\phi}$, for all $i \neq j$, where $\bar{\phi}$ is an empty set.

After dividing the whole state space \mathbb{R}^n into N sub regions, we construct the switching signal as follows:

$$\sigma(u(k)) = i, \forall u(k) \in \tilde{\Omega}_i (i \in \tilde{\mathcal{U}}) \quad (13)$$

Definition 2.3. (Zhang & Yu, 2009) The system (1) is said to be exponentially stable, if there exist a switching function $\sigma(\cdot)$ and positive number c such that any solution $u(k, \phi)$ of the system satisfies

$$\|u(k)\| \leq c \lambda^{k-k_0} \|\phi\|_s, \forall k \geq k_0, \quad (14)$$

for any initial conditions $(k_0, \phi) \in \mathbb{R}^+ \times \mathbb{C}^n$. $c > 0$ is the decay coefficient, $0 < \lambda \leq 1$ is the decay rate, and $\|\phi\|_s = \sup\{\|\phi(l)\|, l = k_0 - d_2, k_0 - d_2 + 1, \dots, k_0\}$.

Definition 2.4. (Phat & Ratchagit, 2011) The system of matrices $u \in \mathbb{R}^n \setminus \{0\}$ is said to be strictly complete if, for every $u \in \mathbb{R}^n \setminus \{0\}$, such that $u^T H_i u < 0$.

It is easy to see that the system of matrices $\{H_i\} (i \in \tilde{\mathcal{U}})$ is strictly complete iff $\bigcup_{i=1}^N \Omega_i = \mathbb{R}^n \setminus \{0\}$, where $\Omega_i = \{u \in \mathbb{R}^n : u^T H_i u < 0\} (i \in \tilde{\mathcal{U}})$.

Definition 2.5. (Lien et al., 2014) Consider system (10) with the switching signal in (13) and the following conditions.

- (i) With $v(k) = 0$, the system (10) is exponentially stable with convergence rate $0 < \alpha < 1$.
- (ii) With zero initial conditions, the signals $v(k)$ and $y(k)$ are bounded by

$$\sum_{k=0}^{\infty} \alpha^{-2k} y^T(k) y(k) \leq \kappa^2 \sum_{k=0}^{\infty} \alpha^{-2k} v^T(k) v(k),$$

for all $v \in L_2(\alpha, 0, \infty)$, $v \neq 0$ for constants $\kappa > 0$ and $0 < \alpha < 1$. In the above conditions, the system (1) is exponentially stabilisable with H_{∞} performance κ and convergence rate α by switching signal in (13).

Lemma 2.6. (Lien et al., 2013) The system of matrices $\{H_i\} (i \in \tilde{\mathcal{U}})$ is strictly complete if there exists $\hat{\alpha}_i \geq 0$, $\sum_{i=1}^N \hat{\alpha}_i$ such that $\sum_{i=1}^N \hat{\alpha}_i H_i < 0$. If $N = 2$; then the above condition is also necessary for the strict completeness.

Lemma 2.7. (Liu et al., 2016) Let $R_2 \in \mathbb{R}^{n \times n}$ be a given positive definite matrix. Then for all $y_0, y_1, y_2, \dots, y_n \in \mathbb{R}^n$, the following inequality holds

$$\sum_{k=0}^n Y y_k^T R_2 Y y_k \geq \frac{1}{n+1} (y_{n+1} - y_0)^T R_2 (y_{n+1} - y_0) + \frac{3}{n+1} \pi_1^T \frac{n+2}{n} R_2 \pi_1,$$

where $Y y_k = y_{k+1} - y_k$ and $\pi_1 = y_{n+1} + y_0 - \frac{2}{n+2} \sum_{k=0}^{n+1} y_k$.

Lemma 2.8. (Jin et al., 2016) For a positive definite symmetric matrix Z_2 , any matrix \tilde{J} , $\tau(k) \in [d_1, d_2]$ and $\eta(k) = u(k+1) - u(k)$, the sum term $\mathfrak{R}(k)$ given as $\mathfrak{R}(k) = \sum_{\theta=k-d_1}^{k-d_1-1} \eta^T(\theta)Z_2\eta(\theta) + \sum_{\theta=k-d_2}^{k-d(k)-1} \eta^T(\theta)Z_2\eta(\theta)$ can be estimated as

$$d_{12}\mathfrak{R}(k) \geq \tilde{\zeta}^T(t) \left(\begin{bmatrix} \hat{\Gamma}_1 \\ \hat{\Gamma}_2 \end{bmatrix}^T \begin{bmatrix} \tilde{R} & \tilde{J} \\ * & \tilde{R} \end{bmatrix} + \begin{bmatrix} \frac{d_2-d(k)}{d_{12}}\hat{M}_1 & 0 \\ * & \frac{d(k)-d_1}{d_{12}}\hat{M}_2 \end{bmatrix} \right) \hat{\zeta}(t) \begin{bmatrix} \hat{\Gamma}_1 \\ \hat{\Gamma}_2 \end{bmatrix}.$$

where

$$\tilde{R} = \text{diag}\{Z_2, 3Z_2\}, \hat{M}_1 = \tilde{R} - \tilde{J}\tilde{R}^{-1}\tilde{J}^T, \hat{M}_2 = \tilde{R} - \tilde{J}^T\tilde{R}^{-1}\tilde{J}, d_{12} = d_2 - d_1,$$

$$\zeta(t) = [u^T(k), u^T(k-d_1), u^T(k-d(k)), u^T(k-d_2), \hat{b}_1^T(t), \hat{b}_2^T(t), \hat{b}_3^T(t)]^T,$$

$$\hat{b}_1^T(t) = \sum_{\theta=k-d_1}^k \frac{u(\theta)}{d_1+1}, \hat{b}_2^T(t) = \sum_{\theta=k-d(k)}^{k-d_1} \frac{u(\theta)}{d(k)-d_1+1}, \hat{b}_3^T(t) = \sum_{\theta=k-d_2}^{k-d(k)} \frac{u(\theta)}{d_2-d(k)+1},$$

$$\hat{\Gamma}_1 = \begin{bmatrix} \check{e}_2 - \check{e}_3 \\ \check{e}_2 + \check{e}_3 - 2\check{e}_6 \end{bmatrix}, \hat{\Gamma}_2 = \begin{bmatrix} \check{e}_3 - \check{e}_4 \\ \check{e}_3 + \check{e}_4 - 2\check{e}_7 \end{bmatrix},$$

$$\check{e}_s = [0_{n \times (s-1)n}, I_{n \times n}, 0_{n \times (7-s)n}], s = 1, 2, 3, \dots, 7.$$

Lemma 2.9. (Arunkumar et al., 2012) For any symmetric positive-definite matrix $Z_1 \in \mathbb{R}^{n \times n}$, the integers τ_2 and τ_1 , ($\tau_2 \geq \tau_1$), $x(t) : \{\tau_1, \tau_1+1, \dots, \tau_2\} \rightarrow \mathbb{R}^n$, such that the following sums are well defined, then

$$\left(\sum_{t=\tau_1}^{\tau_2} x(t) \right)^T Z_1 \left(\sum_{t=\tau_1}^{\tau_2} x(t) \right) \leq \bar{\tau} \sum_{t=\tau_1}^{\tau_2} x(t)^T Z_1 x(t), \tag{15}$$

holds, where $\bar{\tau} = \tau_2 - \tau_1 + 1$.

Lemma 2.10. (Syed Ali & Marudai, 2011) Given constant matrices $\delta_1, \delta_2, \delta_3$, where $\delta_1 = \delta_1^T > 0$ and $\delta_2 = \delta_2^T > 0$ then $\delta_1 + \delta_3^T \delta_2^{-1} \delta_3 < 0$ if and only if $\begin{bmatrix} \delta_1 & \delta_3^T \\ \delta_3 & -\delta_2 \end{bmatrix} < 0$.

Lemma 2.11. (Arunkumar et al., 2012) For any vector $x, y \in \mathbb{R}^n$, matrices A, P, D, E and F are real matrices of appropriate dimensions with $P > 0, F^T F \leq I$ and scalar $\epsilon > 0$, the following inequalities hold:

- (i) $2x^T DFEy \leq \epsilon^{-1} x^T D D^T x + \epsilon y^T E^T E y$.
- (ii) If $P - \epsilon D D^T > 0$, then $(A + DFE)^T P^{-1} (A + DFE) \leq A^T (P - \epsilon D D^T)^{-1} A + \epsilon^{-1} E^T E$.

Main results

We design a switching rule for memristive discrete-time stochastic NNs (1) with mixed time-varying delay and derive the condition to guarantee that the system is exponentially stable. In order to discuss robust exponential stability of system (1), we consider the following nominal system without parametric uncertainties:

$$\begin{aligned}
 u(k+1) &= \sum_{l=1}^q \phi^l(\hat{y}(k)) \{ \tilde{A}_i^\ell u(k) + \tilde{B}_i^\ell(u(k))f(u(k)) + \tilde{C}_i^\ell f(u(k-d(k))) \\
 &\quad + \tilde{D}_i^\ell \sum_{i=1}^{\infty} \mu_i f(u(k-i)) + E_i^\ell v(k) + \sigma(k, u(k), u(k-d(k)))w(k) \}, \\
 y(k) &= \sum_{l=1}^q \phi^l(\hat{y}(k)) \{ A_{1i}^\ell u(k) + D_{1i}^\ell u(k-d(k)) + G_i^\ell v(k) \}, \\
 u(l) &= \varphi(l), l = k_0 - d_2, \dots, k_0.
 \end{aligned} \tag{16}$$

The following theorem gives a sufficient condition for the existence of an admissible reasonable switching rule for system (16) with disturbance input $v(k) = 0$ to be exponentially stable. At first, in order to make the presentation more sententious, we define:

$$\begin{aligned}
 \Delta_1 &= \frac{d_1 + 1}{d_1 - 1}, \Delta_2 = \frac{(d_2 - d_1 + 1)}{(d(k) - d_1)(d(k) - d_1 - 1)}, \Delta_3 = \frac{(d_2 - d(k))}{(d_2 - d_1)}, \\
 \Delta_5 &= \frac{(d(k) - d_1)}{(d_2 - d_1)}, \Delta_6 = \frac{(d_2 - d_1 + 1)}{(d(k) - d_1)(d(k) - d_1 - 1)^2}, \bar{\eta}^T = \{u^T(k) f^T(u(k))\}.
 \end{aligned}$$

Theorem 3.1. For some constants $\alpha \in (0, 1]$, d_1, d_2, τ_1, τ_2 and $0 \leq \gamma_i \leq 1, i \in \tilde{\mathcal{U}}, \sum_{i=1}^N \gamma_i = 1$, if there exist positive definite symmetric matrices $P, Z_1, Z_2, R_2, R_3, S, \hat{U}$ and $Q = \begin{bmatrix} T_2 & W \\ W^T & T_4 \end{bmatrix}$, the diagonal matrices $U_i (i = 1, 2)$ such that the following LMIs hold:

$$P < \lambda^* I \tag{17}$$

$$\Phi = \begin{bmatrix} \Psi_{14,14} & \tilde{\Gamma}_2 & \tilde{\Gamma}_3 & \tilde{\Gamma}_4 \\ * & -Z_1 & 0 & 0 \\ * & * & -Z_2 & 0 \\ * & * & * & -R_2 \end{bmatrix} < 0, \tag{18}$$

$$\sum_{i=1}^N \gamma_i (\tilde{A}_i^\ell)^T P \tilde{A}_i^\ell < \hat{U}, \tag{19}$$

then the system (16) with time-varying delay is globally exponentially stable with convergence rate $\hat{\lambda} = \sqrt{\alpha}$ by the switching signal designed by (13).

$$\Psi_{11} = \hat{U} - \alpha P + (d_2 - d_1 + 1)\alpha^{d_1} T_2 - R_2 \alpha^{d_1} - 3\alpha^{d_1} \Delta_1 R_2 + \lambda^* \hat{\rho}_1 - \alpha^{d_1} Z_1 - F_1 U_1 - 3\alpha^{d_1} \Delta_1 Z_1 + d_{12}^2 R_3,$$

$$\Psi_{12} = -R_2 \alpha^{d_1} - 3\alpha^{d_1} \Delta_1 R_2, \Psi_{13} = \alpha^{d_1} Z_1 - 3\alpha^{d_1} \Delta_1 Z_1, \Psi_{15} = \tilde{A}_i^{\ell T} P \tilde{B}_i^\ell + \alpha^{d_1} (d_2 - d_1 + 1)W + F_2 U_1,$$

$$\Psi_{16} = \tilde{A}_i^{\ell T} P \tilde{C}_i^\ell, \Psi_{17} = \frac{3}{d_1 - 1} R_2 \alpha^{d_1} + \frac{3}{d_1 - 1} R_2^T \alpha^{d_1}, \Psi_{19} = 3\alpha^{d_1} \frac{Z_1}{d_1 - 1} + 3\alpha^{d_1} \frac{Z_1^T}{d_1 - 1},$$

$$\Psi_{1,12} = \tilde{A}_i^{\ell T} P \tilde{D}_i^\ell, \Psi_{22} = -R_2 \alpha^{d_1} - 3\alpha^{d_1} \Delta_1 R_2 + \lambda^* \hat{\rho}_2 - 3\Delta_2 \alpha^{d_1} R_2 - (Z_2 + \Delta_3 Z_2) \frac{\alpha^{d_2}}{(d_2 - d_1)}$$

$$- (3Z_2 + 3\Delta_3 Z_2) \frac{\alpha^{d_2}}{(d_2 - d_1)} - \frac{\alpha^{d_1}}{d(k) - d_1} R_2, \Psi_{23} = \frac{\alpha^{d_1}}{d(k) - d_1} R_2 - 3\Delta_2 \alpha^{d_1} R_2$$

$$+ (Z_2 + \Delta_3 Z_2) \frac{\alpha^{d_2}}{(d_2 - d_1)} - (3Z_2 + 3\Delta_3 Z_2) \frac{\alpha^{d_2}}{(d_2 - d_1)}, \Psi_{27} = 3\alpha^{d_1} \frac{R_2}{d_1 - 1} + 3\alpha^{d_1} \frac{R_2^T}{d_1 - 1},$$

$$\Psi_{28} = 3\Delta_2 \alpha^{d_1} R_2 + 3\Delta_6 \alpha^{d_1} R_2^T, \Psi_{210} = (3Z_2 + 3\Delta_3 Z_2) \frac{\alpha^{d_2}}{(d_2 - d_1)} + (3Z_2^T + 3\Delta_3 Z_2^T) \frac{\alpha^{d_2}}{(d_2 - d_1)},$$

$$\Psi_{33} = \frac{\alpha^{d_1}}{d(k) - d_1} R_2 - 3\Delta_2 \alpha^{d_1} R_2 - \alpha^{d_2} T_2 - F_1 U_2 - \alpha^{d_1} Z_1 - 3\alpha^{d_1} \Delta_1 Z_1 - (Z_2 + \Delta_3 Z_2) \frac{\alpha^{d_2}}{(d_2 - d_1)} \\ - (3Z_2^T + \Delta_3 Z_2^T) \frac{\alpha^{d_2}}{(d_2 - d_1)} - (Z_2 + \Delta_5 Z_2) \frac{\alpha^{d_2}}{(d_2 - d_1)},$$

$$\Psi_{34} = \frac{d_1}{d_1 - d(k)} \alpha^{d_1} Z_1 - \frac{3d_1}{d_1 - d(k)} \Delta_4 \alpha^{d_1} Z_1 + (Z_2 + \Delta_5 Z_2) \frac{\alpha^{d_2}}{(d_2 - d_1)} - (3Z_2 + 3\Delta_5 Z_2) \frac{\alpha^{d_2}}{(d_2 - d_1)},$$

$$\Psi_{36} = -\alpha^{d_2} W + F_2 U_2, \Psi_{38} = 3\Delta_6 \alpha^{d_1} R_2 + 3\Delta_6 \alpha^{d_1} R_2^T, \Psi_{39} = 3\alpha^{d_1} \frac{Z_1}{d_1 - 1} + 3\alpha^{d_1} \frac{Z_1^T}{d_1 - 1},$$

$$\Psi_{310} = (3Z_2 + 3\Delta_3 Z_2) \frac{\alpha^{d_2}}{(d_2 - d_1)} + (3Z_2^T + 3\Delta_3 Z_2^T) \frac{\alpha^{d_2}}{(d_2 - d_1)},$$

$$\Psi_{312} = (3Z_2 + 3\Delta_5 Z_2) \frac{\alpha^{d_2}}{(d_2 - d_1)} + (3Z_2^T + 3\Delta_5 Z_2^T) \frac{\alpha^{d_2}}{(d_2 - d_1)},$$

$$\Psi_{44} = -(3Z_2 + 3\Delta_5 Z_2) \frac{\alpha^{d_2}}{(d_2 - d_1)} - \frac{d_1}{d_1 - d(k)} 3\Delta_4 \alpha^{d_1} Z_1 - (Z_2 + \Delta_5 Z_2) \frac{\alpha^{d_2}}{(d_2 - d_1)},$$

$$\Psi_{411} = -(3Z_2 + 3\Delta_5 Z_2) \frac{\alpha^{d_2}}{(d_2 - d_1)} + (3Z_2^T + 3\Delta_5 Z_2^T) \frac{\alpha^{d_2}}{(d_2 - d_1)},$$

$$\Psi_{55} = \tilde{B}_i^{\ell T} P \tilde{B}_i^{\ell} + \alpha^{d_1} (d_2 - d_1 + 1) T_4 + \frac{\tau_2 (\tau_2 + \tau_1) (\tau_2 - \tau_1 + 1)}{2} S - U_1, \Psi_{56} = \tilde{B}_i^{\ell T} P \tilde{C}_i^{\ell},$$

$$\Psi_{512} = \tilde{B}_i^{\ell T} P \tilde{D}_i^{\ell}, \Psi_{66} = \tilde{C}_i^{\ell T} P \tilde{C}_i^{\ell} - U_2 - \alpha^{d_2} T_4, \Psi_{612} = \tilde{C}_i^{\ell T} P \tilde{D}_i^{\ell}, \Psi_{77} = -12\alpha^{d_1} \frac{R_2}{(d_1 + 1)(d_1 - 1)},$$

$$\Psi_{88} = 3 \frac{(d_2 - d_1 - 1)}{(d(k) - d_1)(d(k) - d_1 + 1)^3} \alpha^{d_1} R_2, \Psi_{99} = -12\alpha^{d_1} \frac{Z_1}{(d_1 + 1)(d_1 - 1)},$$

$$\Psi_{1010} = -12(3Z_2 + 3\Delta_3 Z_2) \frac{\alpha^{d_2}}{(d_2 - d_1)}, \Psi_{1111} = -4(3Z_2 + 3\Delta_5 Z_2) \frac{\alpha^{d_2}}{(d_2 - d_1)},$$

$$\Psi_{1212} = -S + \tilde{D}_i^{\ell T} P \tilde{D}_i^{\ell}, W_4 = \text{diag}\{Z_2, 3Z_2\}, \lambda^* = \lambda_{\max} P,$$

$$\Psi_{1313} = -\alpha^{d_2} R_3, \Psi_{1314} = -\alpha^{d_2} W_2, \Psi_{1414} = -\alpha^{d_2} R_3, \tilde{\Gamma}_2 = [d_1 \Xi_1^T Z_1], \tilde{\Gamma}_3 = [(d_2 - d_1) \Xi_1^T Z_2],$$

$$\tilde{\Gamma}_4 = [\sqrt{d_1} \tilde{\Xi}_1^T R_2], \tilde{\Xi}_1 = [W_{p1} - W_{p2}], W_{p1} = [\tilde{A}_i^\ell \ 0 \ 0 \ 0 \ \tilde{B}_i^\ell \ \tilde{C}_i^\ell \ \underbrace{0 \ 0 \ 0}_{5 \text{ times}} \ \tilde{D}_i^\ell \ 0 \ 0], W_{p2} = [I \ \underbrace{0 \ 0 \ 0}_{13 \text{ times}}]. \quad (20)$$

Proof. We consider the Lyapunov-Krasovskii functional for model in (16) as

$$V(k, u(k)) = \sum_{i=1}^6 V_i(k, u(k)), \quad (21)$$

where

$$V_1(k, u(k)) = u(k) P u(k),$$

$$V_2(k, u(k)) = d_1 \sum_{i=-d_1+1}^0 \sum_{j=k+i-1}^{k-1} \alpha^{k-1-j} \eta^T(j) Z_1 \eta(j),$$

$$V_3(k, u(k)) = d_{12} \sum_{i=-d_2+1}^{-d_1} \sum_{j=k+i-1}^{k-1} \alpha^{k-1-j} \eta^T(j) Z_2 \eta(j),$$

$$V_4(k, u(k)) = \sum_{i=-d(k)}^{-1} \sum_{j=k+i}^{k-1} \alpha^{k-1-j} \eta^T(j) R_2 \eta(j),$$

$$V_5(k, u(k)) = \sum_{j=k-d(k)}^{k-1} \alpha^{k-1-j} \begin{bmatrix} u(j) \\ f(u(j)) \end{bmatrix}^T Q \begin{bmatrix} u(j) \\ f(u(j)) \end{bmatrix}$$

$$+ \sum_{i=-d_2}^{-d_1-1} \sum_{j=k+i}^{k-1} \alpha^{k-1-j} \begin{bmatrix} u(j) \\ f(u(j)) \end{bmatrix}^T Q \begin{bmatrix} u(j) \\ f(u(j)) \end{bmatrix},$$

$$V_6(k, u(k)) = d_{12} \sum_{i=-d_2}^{-d_1-1} \sum_{j=k+i}^{k-1} \alpha^{k-1-j} u(j) R_3 u(j) + \tau_2 \sum_{\beta=\tau_1}^{\tau_2} \sum_{v=1}^{\beta} \sum_{j=k-v}^{k-1} \alpha^{k-1-j} f^T(u(j)) S f(u(j)),$$

where $\eta(k) = u(k+1) - u(k)$. Next, we will show the decay estimation of $V(k, u(k))$ in (21) along the state trajectory of system (16). To this end, define $V(k+1) - V(k) = \sum_{j=1}^6 \tilde{\Delta} V_j(k)$, then we have

$$\tilde{\Delta} V_1(k) = u^T(k+1) P u(k+1) - \alpha u^T(k) P u(k),$$

$$= [\tilde{A}_i^\ell u(k) + \tilde{B}_i^\ell(u(k)) f(u(k)) + \tilde{C}_i^\ell f(u(k-d(k))) + \tilde{D}_i^\ell \sum_{i=1}^{\infty} \mu_i f(u(k-i))$$

$$+ \sigma_i^\ell(k, u(k), u(k-d(k))) w(k)]^T P [\tilde{A}_i^\ell u(k) + \tilde{B}_i^\ell(u(k)) f(u(k)) + \tilde{C}_i^\ell f(u(k-d(k)))$$

$$+ \tilde{D}_i^\ell \sum_{i=1}^{\infty} \mu_i f(x(k-i)) + \sigma_i^\ell(k, x(k), x(k-d(k))) w(k)] - \alpha u^T(k) P u(k).$$

From Assumption 2.1 and condition (17), we have

$$\sigma_i^{\ell T}(k, u(k), u(k-d(k))) P \sigma_i^\ell(k, u(k), u(k-d(k)))$$

$$\begin{aligned}
&\leq \lambda_{\max}(P)\sigma_i^{\ell T}(k, u(k), u(k-d(k)))\sigma_i^{\ell}(k, u(k), u(k-d(k))) \\
&\leq \lambda^*(\hat{\rho}_1 u^T(k)u(k) + \hat{\rho}_2 u^T(k-d(k))u(k-d(k))), \\
\tilde{\Delta}V_2(k) &= d_1 \sum_{i=-d_1+1}^0 \left\{ \sum_{j=k+i}^k \alpha^{k-j} \eta^T(j) Z_1 \eta(j) - \sum_{j=k+i-1}^{k-1} \alpha^{k-j-1} \eta^T(j) Z_1 \eta(j) \right\} \\
&= d_1 \sum_{i=-d_1+1}^0 \left\{ \eta^T(k) Z_1 \eta(k) + \sum_{j=k+i}^{k-1} \alpha^{k-j} \eta^T(j) Z_1 \eta(j) - \sum_{j=k+i}^{k-1} \alpha^{k-j} \eta^T(j) Z_1 \eta(j) \right. \\
&\quad \left. - \eta^T(k+i-1) Z_1 \alpha^{-i} \eta(k+i-1) \right\} \\
&= d_1^2 \eta^T(k) Z_1 \eta(k) - d_1 \sum_{i=-d_1+1}^0 \eta^T(k+i-1) Z_1 \alpha^{-i} \eta(k+i-1) \\
&= d_1^2 \eta^T(k) Z_1 \eta(k) - d_1 \sum_{j=k-d_1}^{k-1} \eta^T(j) Z_1 \alpha^{k-j} \eta(j), \\
\tilde{\Delta}V_3(k) &= (d_2 - d_1) \sum_{i=d_2+1}^{-d_1} \left\{ \sum_{j=k+i}^k \alpha^{k-j} \eta^T(j) Z_2 \eta(j) - \sum_{j=k+i-1}^{k-1} \alpha^{k-1-j} \eta^T(j) Z_2 \eta(j) \right\} \\
&= (d_2 - d_1) \sum_{i=d_2+1}^{-d_1} \left\{ \eta^T(k) Z_2 \eta(k) + \sum_{j=k+i}^{k-1} \alpha^{k-j} \eta^T(j) Z_2 \eta(j) - \alpha^{-i} \eta^T(k+i-1) Z_2 \eta(k+i-1) \right. \\
&\quad \left. - \sum_{j=k+i}^{k-1} \alpha^{k-j} \eta^T(j) Z_2 \eta(j) \right\} \\
&= (d_2 - d_1)^2 \eta^T(k) Z_2 \eta(k) - (d_2 - d_1) \sum_{j=k-d_2}^{k-d_1-1} \alpha^{k-j} \eta^T(j) Z_2 \eta(j), \\
\tilde{\Delta}V_4(k) &= \sum_{i=-d(k)}^{-1} \left\{ \sum_{j=k+i+1}^k \alpha^{k-j} \eta^T(j) R_2 \eta(j) - \sum_{j=k+i}^{k-1} \alpha^{k-1-j} \eta^T(j) R_2 \eta(j) \right\} \\
&= \sum_{i=-d(k)}^{-1} \left\{ \eta^T(k) R_2 \eta(k) + \sum_{j=k+i+1}^{k-1} \alpha^{k-j} \eta^T(j) R_2 \eta(j) - \sum_{j=k+i+1}^{k-1} \alpha^{k-j} \eta^T(j) R_2 \eta(j) \right. \\
&\quad \left. - \alpha^{-i-1} \eta^T(k+i) R_2 \eta(k+i) \right\} \\
&= d(k) \eta^T(k) R_2 \eta(k) - \sum_{j=k-d(k)}^{k-1} \alpha^{k-j} \eta^T(j) R_2 \eta(j),
\end{aligned}$$

$$\begin{aligned}
 \tilde{\Delta}V_5(k) &= \sum_{j=k-d(k+1)+1}^k \alpha^{k-j} \tilde{\eta}^T(j) Q \tilde{\eta}(j) - \sum_{j=k-d(k)}^{k-1} \alpha^{k-1-j} \tilde{\eta}^T(j) Q \tilde{\eta}(j) \\
 &\quad + \sum_{i=-d_2}^{-d_1-1} \left\{ \sum_{j=k+i+1}^k \alpha^{k-j} \tilde{\eta}^T(j) Q \tilde{\eta}(j) - \sum_{j=k+i}^{k-1} \alpha^{k-1-j} \tilde{\eta}^T(j) Q \tilde{\eta}(j) \right\} \\
 &= \tilde{\eta}^T(k) Q \tilde{\eta}(k) + \sum_{j=k-d(k+1)+1}^{k-1} \alpha^{k-j} \tilde{\eta}^T(j) Q \tilde{\eta}(j) - \alpha^{d(k)} \tilde{\eta}^T(k-d(k)) Q \tilde{\eta}(k-d(k)) \\
 &\quad - \sum_{j=k-d(k+1)+1}^{k-1} \alpha^{k-j} \tilde{\eta}^T(j) Q \tilde{\eta}(j) + \sum_{i=-d_2}^{-d_1-1} \left\{ \tilde{\eta}^T(k) Q \tilde{\eta}(k) + \sum_{j=k+i+1}^{k-1} \alpha^{k-j} \tilde{\eta}^T(j) Q \tilde{\eta}(j) \right. \\
 &\quad \left. - \alpha^{i-1} \tilde{\eta}^T(k+i) Q \tilde{\eta}(k+i) - \sum_{j=k+i+1}^{k-1} \alpha^{k-j} \tilde{\eta}^T(j) Q \tilde{\eta}(j) \right\} \\
 &\leq (d_{12} + 1) \tilde{\eta}^T(k) Q \tilde{\eta}(k) - \alpha^{d_2} \tilde{\eta}^T(k-d(k)) Q \tilde{\eta}(k-d(k)), \\
 \bar{\Delta}V_6(k) &= \sum_{i=d_2}^{-d_1-1} \left\{ \sum_{j=k+i+1}^k \alpha^{k-j} u^T(k) R_3 u(k) - \sum_{j=k+i}^{k-1} \alpha^{k-1-j} u^T(k) R_3 u(k) \right\} \\
 &\quad + v_1 f(u(k))^T S f(u(k)) - \tau_2 \sum_{\beta=\tau_1}^{\tau_2} \sum_{v=1}^{\beta} \alpha^{\tau_2} f^T(u(k-v)) S f(u(k-v)), \\
 &= d_{12}^2 u^T(k) R_3 u(k) - d_{12} \sum_{j=k-d_2}^{k-d_1-1} \alpha^{k-j} u^T(j) R_3 u(j) + v_1 f(u(k))^T S f(u(k)) \\
 &\quad - \tau_2 \sum_{v=1}^{\tau(k)} \alpha^{\tau_2} f^T(u(k-v)) S f(u(k-v)), \\
 &= d_{12}^2 u^T(k) R_3 u(k) - d_{12} \sum_{j=k-d_2}^{k-d_1-1} \alpha^{k-j} u^T(j) R_3 u(j) + v_1 f(u(k))^T S f(u(k)) \\
 &\quad - \sum_{v=1}^{\tau(k)} \alpha^{\tau_2} f^T(u(k-v)) S \sum_{v=1}^{\tau(k)} f(u(k-v)). \tag{22}
 \end{aligned}$$

While

$$\sum_{j=k-d(k)}^{k-1} \alpha^{k-j} \eta^T(j) R_2 \eta(j) = \sum_{j=k-d_1}^{k-1} \alpha^{k-j} \eta^T(j) R_2 \eta(j) + \sum_{j=k-d(k)}^{k-d_1-1} \alpha^{k-j} \eta^T(j) R_2 \eta(j). \tag{23}$$

Using Lemma 2.7, we have

$$\begin{aligned}
& -d_1 \sum_{j=k-d_1}^{k-1} \eta^T(j) Z_1 \alpha^{k-j} \eta(j) \leq -\alpha^{d_1} [u(k) - u(k-d_1)]^T Z_1 [u(k) - u(k-d_1)] \\
& - 3\alpha^{d_1} \left[u(k) + u(k-d_1) - \frac{2}{d_1+1} \sum_{i=k-d_1}^k u(i) \right]^T \\
& Z_1 \frac{d_1+1}{d_1-1} \left[u(k) + u(k-d_1) - \frac{2}{d_1+1} \sum_{i=k-d_1}^k u(i) \right], \\
& = -\xi^T(k) \Pi_1^T \begin{bmatrix} Z_1 & 0 \\ 0 & 3 \frac{d_1+1}{(d_1-1)} Z_1 \end{bmatrix} \Pi_1 \xi(k),
\end{aligned} \tag{24}$$

where $e_i = [0_{n \times (i-1)n}, I, 0_{n \times (14-i)n}]_{n \times 14n}$, $i = 1, 2, \dots, 14$ and $\Pi_1 = [e_1^T - e_3^T, e_1^T + e_3^T - 2e_9^T]$.

$$\begin{aligned}
& - \sum_{j=k-d(k)}^{k-d_1-1} \alpha^{k-j} \eta^T(j) R_2 \eta(j) \leq \alpha^{d_1} \frac{-1}{d(k)-d_1} [u(k-d_1) - u(k-d(k))]^T R_2 [u(k-d_1) - u(k-d(k))] \\
& - \alpha^{d_1} \frac{3(d(k)-d_1+1)}{(d(k)-d_1)(d(k)-d_1-1)} [u(k-d_1) + u(k-d(k))] \\
& - \frac{2}{d(k)-d_1+1} \sum_{j=k-d(k)}^{k-d_1} u(j)]^T R_2 [u(k-d_1) + u(k-d(k))] \\
& - \frac{2}{d(k)-d_1+1} \sum_{j=k-d(k)}^{k-d_1} u(j)]. \\
& \sum_{j=k-d_1}^{k-1} \alpha^{k-j} \eta^T(j) R_2 \eta(j) \leq \alpha^{d_1} \begin{bmatrix} u(k) - u(k-d_1) \\ u(k) + u(k-d_1) - \frac{2}{d_1+1} \sum_{j=k-d_1}^k u(j) \end{bmatrix}^T \begin{bmatrix} -\frac{R_2}{d_1} & 0 \\ 0 & -3 \frac{d_1+1}{d_1(d_1-1)} R_2 \end{bmatrix} \\
& \begin{bmatrix} u(k) - u(k-d_1) \\ u(k) + u(k-d_1) - \frac{2}{d_1+1} \sum_{j=k-d_1}^k u(j) \end{bmatrix}.
\end{aligned} \tag{25}$$

According to Lemma 2.9, we have

$$- \sum_{j=k-d_2}^{k-d_1-1} \alpha^{k-j} u^T(j) R_3 u(j) \leq -\xi^T(k) \begin{bmatrix} e_{13} \\ e_{14} \end{bmatrix}^T \begin{bmatrix} R_3 & W_2 \\ * & R_3 \end{bmatrix} \begin{bmatrix} e_{13} \\ e_{14} \end{bmatrix} \xi(k). \tag{26}$$

Then, for any matrix W_4 , the improved summation inequality in Lemma 2.8 is employed to estimate other sum terms possessed time-varying delay $d(k)$ in $\Delta V_3(k, u(k))$, we have

$$\begin{aligned}
& (d_2 - d_1) \alpha^{d_2} \sum_{i=k-d_2}^{k-d_1-1} \eta^T(i) Z_2 \eta(i) = \alpha^{d_2} \left\{ \sum_{i=k-d_2}^{k-d(k)-1} \eta^T(i) Z_2 \eta(i) + \sum_{i=k-d(k)}^{k-d_1-1} \eta^T(i) Z_2 \eta(i) \right\}, \\
& \leq \Lambda_2(k).
\end{aligned}$$

Where

$$\Lambda_2(k) = \begin{bmatrix} \hat{\Gamma}_1 \\ \hat{\Gamma}_2 \end{bmatrix}^T \left(\begin{bmatrix} W_4 & V_2 \\ * & W_4 \end{bmatrix} + \begin{bmatrix} \frac{d_2-d(k)}{d_2-d_1} (W_4 - V_2 W_4^{-1} V_2^T) & 0 \\ 0 & \frac{d(k)-d_1}{d_2-d_1} (W_4 - V_2^T W_4^{-1} V_2) \end{bmatrix} \right) \begin{bmatrix} \hat{\Gamma}_1 \\ \hat{\Gamma}_2 \end{bmatrix}.$$

Thus, it is clear that

$$\Delta V_{4i}(k) \leq (d_2 - d_1)^2 \eta^T(k) Z_2 \eta(k) - \Lambda_2(k). \quad (27)$$

where $j = 1, 2, \dots, n$ thus, there exist matrices $U_1 = \text{diag}\{u_{11}, u_{12}, \dots, u_{1n}\} > 0$, $U_2 = \text{diag}\{u_{21}, u_{22}, \dots, u_{2n}\} > 0$, such that

$$\sum_{j=1}^n r_j \begin{bmatrix} u(k) \\ f(u(k)) \end{bmatrix}^T \begin{bmatrix} F_j^- F_j^+ \kappa_j \kappa_j^T & -\frac{F_j^- + F_j^+}{2} \kappa_j \kappa_j^T \\ -\frac{F_j^- + F_j^+}{2} \kappa_j \kappa_j^T & \kappa_j \kappa_j^T \end{bmatrix} \begin{bmatrix} u(k) \\ f(u(k)) \end{bmatrix} \leq 0,$$

$$\begin{bmatrix} u(k) \\ f(u(k)) \end{bmatrix}^T \begin{bmatrix} U_1 F_1 & -U_1 F_2 \\ -U_1 F_2 & U_1 \end{bmatrix} \begin{bmatrix} u(k) \\ f(u(k)) \end{bmatrix} \leq 0.$$

Similar to this, one can get

$$\begin{bmatrix} u(k-d(k)) \\ f(u(k-d(k))) \end{bmatrix}^T \begin{bmatrix} U_2 F_1 & -U_2 F_2 \\ -U_2 F_2 & U_2 \end{bmatrix} \begin{bmatrix} u(k-d(k)) \\ f(u(k-d(k))) \end{bmatrix} \leq 0. \quad (28)$$

Combining (21) to (28) and using Schur complement Lemma, it yields

$$\tilde{\Delta}_j(k) \leq \xi^T(k) \begin{bmatrix} \Psi_{14,14} & \tilde{\Gamma}_2 & \tilde{\Gamma}_3 & \tilde{\Gamma}_4 \\ * & -Z_1 & 0 & 0 \\ * & * & -Z_2 & 0 \\ * & * & * & -R_2 \end{bmatrix} \xi(k) + u^T(k) \hat{Y}_i u(k),$$

$$\xi^T(k) = [u^T(k) \ u^T(k-d_1) \ u^T(k-d(k)) \ u^T(k-d_2) \ f^T(u(k)) \ f^T(u(k-d(k)))]$$

$$\sum_{i=k-d_1}^k u^T(i) \sum_{i=k-d(k)+1}^{k-d_1-1} u^T(i) \sum_{i=k-d(k)}^k u^T(i) \sum_{i=k-d(k)}^{k-d_1} u^T(i) \sum_{i=k-d_2}^{k-d(k)} u^T(i)$$

$$\left[\sum_{v=1}^{\tau(k)} f^T(u(k-v)) \sum_{i=k-d(k)}^{k-d_1-1} u^T(i) \sum_{i=k-d_2}^{k-d(k)-1} u^T(i) \right].$$

By using Definition 2.4 and condition (19), we know that the system of matrices $\hat{Y}_i = (\tilde{A}_i^\ell)^T P \tilde{A}_i^\ell - \hat{U}$, $i \in \tilde{\mathcal{O}}$ is strictly complete, and the sets Ω_i and $\tilde{\Omega}_i$ are well defined, such that

$$\bigcup_{i=1}^N \Omega_i = \mathbb{R}^n \setminus \{0\}, \quad \bigcup_{i=1}^N \tilde{\Omega}_i = \mathbb{R}^n \setminus \{0\},$$

$$\tilde{\Omega}_i \cap \tilde{\Omega}_j = \Phi, \quad i \neq j.$$

Therefore, for any $u(k) \in \mathbb{R}^n$, $k > 0$, there always exists an $i \in \{1, 2, \dots, N\}$ such that $u(k) \in \tilde{\Omega}_i$. Choosing the switching rule (13) with condition (19), leads to

$$\Delta V(k)|_{v(k)=0} = V(k+1) - V(k) \leq 0,$$

$$V(k + 1) \leq V(k), \tag{29}$$

From (21), there exist two positive constants c_1 and c_2 , such that

$$c_1 \|u(k)\|^2 \leq V(k), \quad V(0) \leq c_2 \|u(0)\|^2. \tag{30}$$

Where

$$\begin{aligned} c_1 &= \lambda_{\min}(P) \\ c_2 &= \lambda_{\max}(P) + 4d_1^2\lambda_{\max}(Z_1) + 4(d_2 - d_1)^2\lambda_{\max}(Z_2) + d_1\lambda_{\max}(R_2) \\ &\quad + (1 + d_2 - d_1)\lambda_{\max}(Q) + 2d_1^2\lambda_{\max}(R_3) + d_2\lambda_{\max}(S). \end{aligned}$$

From (29) and (30), one obtains

$$\|u(k)\| \leq \sqrt{\frac{c_2}{\lambda_{\min}(P)}} \alpha^k \|u(0)\|_s. \tag{31}$$

By Definition 2.3, we know that the system (16) is exponentially stable with decay rate $\lambda = \sqrt{\alpha}$. This completes the proof. \square

Theorem 3.2. For some constants $\alpha \in (0, 1]$, d_1, d_2, τ_1, τ_2 and $0 \leq \gamma_i \leq 1, \sum_{i=1}^N \gamma_i = 1 (i \in \tilde{U})$, if there exist positive definite symmetric matrices $P, Z_1, Z_2, R_2, R_3, \hat{U}, Q = \begin{bmatrix} T_2 & W \\ W^T & T_4 \end{bmatrix}, S$, the diagonal matrices $U_i (i = 1, 2)$ such that the following LMIs hold:

$$P < \lambda^* I \tag{32}$$

$$\Phi = \begin{bmatrix} \Psi_{14,14} & \gamma_a & \tilde{\Gamma}_2 & \tilde{\Gamma}_3 & \tilde{\Gamma}_4 & \gamma_b & 0 \\ * & \Psi_{15,15} & 0 & 0 & 0 & 0 & 0 \\ * & * & -Z_1 & 0 & 0 & 0 & 0 \\ * & * & * & -Z_2 & 0 & 0 & 0 \\ * & * & * & * & -R_2 & 0 & 0 \\ * & * & * & * & * & -I & 0 \\ * & * & * & * & * & * & -\kappa^2 \end{bmatrix} < 0, \tag{33}$$

$$\sum_{i=1}^N \gamma_i (\tilde{A}_i^\ell)^T P \tilde{A}_i^\ell < \hat{U}, \tag{34}$$

then the system (16) is globally exponentially stable with convergence rate $\hat{\lambda} = \sqrt{\alpha}$ and H_∞ performance κ by the switching signal designed by (13).

Here

$$\gamma_a^T = [\gamma_{a1}^T \ 0 \ 0 \ 0 \ \underbrace{\gamma_{e1}^T \ \gamma_{f1}^T \ 0 \ 0 \ 0}_{5 \text{ times}} \ \gamma_{g1}^T \ 0 \ 0], \gamma_b = [\underbrace{A_{1i}^\ell \ 0 \ D_{1i}}_{11 \text{ times}} \ G_i]^T, \gamma_{a1} = \tilde{A}_i^\ell T P E_i^\ell,$$

$$\gamma_{e1} = \tilde{B}_i^\ell T P E_i^\ell, \gamma_{f1} = \tilde{C}_i^\ell T P E_i^\ell, \gamma_{g1} = \tilde{D}_i^\ell T P E_i^\ell, \Psi_{15,15} = E_i^\ell T P E_i^\ell. \tag{35}$$

Proof. In the case of the initial condition is zero, consider the performance index,

$$J(n) = \sum_{k=0}^{\infty} [y^T(k)y(k) - \kappa^2 v^T(k)v(k)], \quad (36)$$

for all non zero $v(k)$, by following the proof of Theorem 3.1, the performance index can be converted to

$$J(n) = \sum_{k=0}^{\infty} [y^T(k)y(k) - \kappa^2 v^T(k)v(k) + \Delta V_j(k)] \leq \xi_2^T(t)\Psi\xi_2(t), \quad (37)$$

where $\xi_2^T(t) = [\xi^T(t) \ v^T(t)]^T$. In the view of LMI (33), we have $J(n) \leq 0$, that is,

$$\sum_{k=0}^{\infty} [y^T(k)y(k) - \kappa^2 v^T(k)v(k)] \leq 0,$$

$$\sum_{k=0}^{\infty} y^T(k)y(k) \leq \sum_{k=0}^{\infty} \kappa^2 v^T(k)v(k), \forall v(k) \in L_2(\alpha, 0, \infty). \quad (38)$$

By Definition 2.5, the system (16) is exponentially stable with convergence rate $0 < \alpha < 1$ and H_∞ performance index $\lambda = \sqrt{\alpha}$. \square

Robust switched memristive stochastic nns

Now, we can extend Theorem 3.1 and 3.2 to obtain the corresponding results for switched uncertain memristive NNs (10), set

$$[\Delta A_i^\ell \ \Delta B_i^\ell \ \Delta C_i^\ell \ \Delta D_i^\ell] = \mathcal{E}_i^\ell \mathcal{F}_i^\ell(k) [N_{1i}^\ell \ N_{2i}^\ell \ N_{3i}^\ell \ N_{4i}^\ell]. \quad (39)$$

The following theorem provides the robust exponential stability conditions for uncertain switched memristive stochastic NNs (10).

Theorem 3.3. For some constants $\alpha \in (0, 1]$, d_1, d_2, τ_1, τ_2 , and $0 \leq \gamma_i \leq 1, \sum_{i=1}^N \gamma_i = 1 (i \in \mathcal{I})$, if there exist positive definite symmetric matrices $P, Z_1, Z_2, R_2, R_3, Q = \begin{bmatrix} T_2 & W \\ W^T & T_4 \end{bmatrix}$, the diagonal matrices $U_i (i = 1, 2)$ and scalars $\epsilon_{1i} > 0, \epsilon_{2i} > 0$ such that the following LMIs hold:

$$P < \lambda^* I \quad (40)$$

$$\Phi = \begin{bmatrix} \Psi_{14,14} & \Upsilon_a & 0 & \tilde{\Gamma}_{17} & \tilde{\Gamma}_{18} & \Upsilon_b & \Upsilon_c & \Upsilon_d \\ * & \Psi_{15,15} & 0 & 0 & 0 & 0 & 0 & 0 \\ * & * & -\kappa^2 & 0 & 0 & 0 & 0 & 0 \\ * & * & * & \tilde{\Gamma}_{16,16} & 0 & 0 & 0 & 0 \\ * & * & * & * & \tilde{\Gamma}_{17,17} & 0 & 0 & 0 \\ * & * & * & * & * & -I & 0 & 0 \\ * & * & * & * & * & * & -\epsilon_{1i} & 0 \\ * & * & * & * & * & * & * & -\epsilon_{2i} \end{bmatrix} < 0, \quad (41)$$

then the system (10) is globally exponentially stable with convergence rate $\hat{\lambda} = \sqrt{\alpha}$ and H_∞ performance κ by the switching signal designed by (13).

Where

$$\begin{aligned}
\tilde{\Gamma}_{17} &= [\tilde{A}_i^\ell \ 0 \ 0 \ 0 \ \tilde{B}_i^\ell \ \tilde{C}_i^\ell \ \underbrace{0 \ 0 \ 0}_{5 \text{ times}} \ \tilde{D}_i^\ell \ 0 \ 0 \ E_i^\ell], \tilde{\Gamma}_{18} = [\tilde{A}_i^\ell - I \ 0 \ 0 \ 0 \ \tilde{B}_i^\ell \ \tilde{C}_i^\ell \ \underbrace{0 \ 0 \ 0}_{5 \text{ times}} \ \tilde{D}_i^\ell \ 0 \ 0 \ E_i^\ell], \\
W_{p2} &= [I \ \underbrace{0 \ 0 \ 0}_{7 \text{ times}} \ \underbrace{0 \ 0 \ 0}_{6 \text{ times}}], \tilde{\Gamma}_{16,16} = -P + \epsilon_1 \mathcal{E}_i \mathcal{E}_i^T, \tilde{\Gamma}_{17,17} = -W + \epsilon_2 \mathcal{E}_i \mathcal{E}_i^T, \\
W &= d_1 Z_1 + (d_2 - d_1)^2 Z_2 + R_2, Y_c = [N_{1i}^\ell \ 0 \ 0 \ 0 \ N_{2i}^\ell \ N_{3i}^\ell \ \underbrace{0 \ 0 \ 0}_{5 \text{ times}} \ N_{4i}^\ell \ 0 \ 0 \ 0], \\
Y_d &= [N_{1i}^\ell \ 0 \ 0 \ 0 \ N_{2i}^\ell \ N_{3i}^\ell \ \underbrace{0 \ 0 \ 0}_{5 \text{ times}} \ N_{4i}^\ell \ 0 \ 0 \ 0].
\end{aligned} \tag{42}$$

and the remaining terms are defined in Theorem 3.1.

Proof. The result is carried out by using the techniques and the similar lines of proof in Theorem 3.1 and 3.2. Thus we have,

$$\begin{aligned}
\tilde{\Delta}_j(k) + y^T(k)y(k) - \kappa^2 v^T(k)v(k) &\leq \xi_2^T(k) \begin{bmatrix} \Psi^{14,14} & Y_a \\ * & \Psi_{15,15} \end{bmatrix} \xi_2(k) + \eta^T(k)W\eta(k) \\
&+ u^T(k+1)Pu(k+1) + y^T(k)y(k) - \kappa^2 v^T(k)v(k),
\end{aligned} \tag{43}$$

here

$$\begin{aligned}
u^T(k+1)Pu(k+1) &= [[\tilde{A}_i^\ell + \Delta A_i^\ell(k)]u(k) + [\tilde{B}_i^\ell + \Delta B_i^\ell(k)]f(u(k)) + [\tilde{C}_i^\ell + \Delta C_i^\ell(k)]f(u(k-d(k))) \\
&+ [\tilde{D}_i^\ell + \Delta D_i^\ell(k)] \sum_{i=1}^{\tau(k)} f(u(k-i)) + E_i^\ell v(k) + \sigma(k, u(k), u(k-d(k)))w(k)]^T P \\
&[[\tilde{A}_i^\ell + \Delta A_i^\ell(k)]u(k) + [\tilde{B}_i^\ell + \Delta B_i^\ell(k)]f(u(k)) + [\tilde{C}_i^\ell + \Delta C_i^\ell(k)]f(u(k-d(k))) \\
&+ [\tilde{D}_i^\ell + \Delta D_i^\ell(k)] \sum_{i=1}^{\tau(k)} f(u(k-i)) + E_i^\ell v(k) + \sigma(k, u(k), u(k-d(k)))w(k)] \\
&= [\tilde{A}_i^\ell u(k) + \tilde{B}_i^\ell f(u(k)) + \tilde{C}_i^\ell f(u(k-d(k))) + \tilde{D}_i^\ell \sum_{i=1}^{\tau(k)} f(u(k-i)) + E_i^\ell v(k) \\
&+ \sigma(k, u(k), u(k-d(k)))w(k)]^T (P^{-1} - \epsilon_{1i} \mathcal{E}_i^\ell \mathcal{E}_i^T)^{-1} [\tilde{A}_i^\ell u(k) + \tilde{B}_i^\ell f(u(k)) \\
&+ \tilde{C}_i^\ell f(u(k-d(k))) + \tilde{D}_i^\ell \sum_{i=1}^{\tau(k)} f(u(k-i)) + E_i^\ell v(k) + \sigma(k, u(k), u(k-d(k)))w(k)],
\end{aligned} \tag{44}$$

Similarly,

$$\begin{aligned}
\eta^T(k)W\eta(k) &= [\tilde{A}_i^\ell u(k) + \tilde{B}_i^\ell f(u(k)) + \tilde{C}_i^\ell f(u(k-d(k))) + \tilde{D}_i^\ell \sum_{i=1}^{\tau(k)} f(x(k-i)) + E_i^\ell v(k) \\
&+ \sigma(k, x(k), x(k-d(k)))w(k) - u(k)]^T (W^{-1} - \epsilon_{2i} \mathcal{E}_i \mathcal{E}_i^T)^{-1} [\tilde{A}_i^\ell u(k) + \tilde{B}_i^\ell f(u(k)) \\
&+ \tilde{C}_i^\ell f(u(k-d(k))) + \tilde{D}_i^\ell \sum_{i=1}^{\tau(k)} f(x(k-i)) + E_i^\ell v(k) + \sigma(k, x(k), x(k-d(k)))w(k) - u(k)].
\end{aligned} \tag{45}$$

Combining (43)–(45), using Schur complement Lemma and following the ideas in proof Theorem 3.1, we get (41). This completes the proof. \square

Remark 3.4. In Theorems 3.1 and 3.3, the criteria that ensure the exponential stability of discrete time neural networks with time-varying delay are established in terms of LMIs. If there is no parametric uncertainties, stochastic terms, T-S fuzzy and switching signals then the DNNs (1) is reduced to the following neural network model

$$u(k+1) = Au(k) + Bf(u(k)) + Cf(u(k-d(k))), \quad (46)$$

where the time varying delay $d(k)$ satisfies $d_1 \leq d(k) \leq d_2$, where d_1 and d_2 are constants. According to Theorem 3.1, we have the following Corollary 3.5, for the asymptotic stability of discrete time NNs (46).

Corollary 3.5. For some constants d_1, d_2, τ_1, τ_2 , if there exist positive definite symmetric matrices P, Z_1, Z_2, R_2, R_3 , and $Q = \begin{bmatrix} T_2 & W \\ W^T & T_4 \end{bmatrix}$, the diagonal matrices $U_i (i = 1, 2)$ such that the following LMIs hold:

$$\Phi = \begin{bmatrix} \Psi_{13,13} & \tilde{\Gamma}_2 & \tilde{\Gamma}_3 & \tilde{\Gamma}_4 \\ * & -Z_1 & 0 & 0 \\ * & * & -Z_2 & 0 \\ * & * & * & -R_2 \end{bmatrix} < 0, \quad (47)$$

where

$$\Psi_{11} = (d_2 - d_1 + 1)\alpha^{d_1}T_2 - R_2\alpha^{d_1} - 3\alpha^{d_1}\Delta_1R_2 - \alpha^{d_1}Z_1 - F_1U_1 - 3\alpha^{d_1}\Delta_1Z_1 + d_1^2R_3,$$

$$\Psi_{12} = -R_2\alpha^{d_1} - 3\alpha^{d_1}\Delta_1R_2, \Psi_{13} = \alpha^{d_1}Z_1 - 3\alpha^{d_1}\Delta_1Z_1, \Psi_{15} = A^T P B^\ell + \alpha^{d_1}(d_2 - d_1 + 1)W + F_2U_1,$$

$$\Psi_{16} = A^T P C^\ell, \Psi_{17} = \frac{3}{d_1 - 1}R_2\alpha^{d_1} + \frac{3}{d_1 - 1}R_2^T\alpha^{d_1}, \Psi_{19} = 3\alpha^{d_1}\frac{Z_1}{d_1 - 1} + 3\alpha^{d_1}\frac{Z_1^T}{d_1 - 1},$$

$$\Psi_{22} = -R_2\alpha^{d_1} - 3\alpha^{d_1}\Delta_1R_2 - 3\Delta_2\alpha^{d_1}R_2 - (Z_2 + \Delta_3Z_2)\frac{\alpha^{d_2}}{(d_2 - d_1)} - (3Z_2 + 3\Delta_3Z_2)\frac{\alpha^{d_2}}{(d_2 - d_1)}$$

$$- \frac{\alpha^{d_1}}{d(k) - d_1}R_2, \Psi_{23} = \frac{\alpha^{d_1}}{d(k) - d_1}R_2 - 3\Delta_2\alpha^{d_1}R_2 + (Z_2 + \Delta_3Z_2)\frac{\alpha^{d_2}}{(d_2 - d_1)}$$

$$- (3Z_2 + 3\Delta_3Z_2)\frac{\alpha^{d_2}}{(d_2 - d_1)}, \Psi_{27} = 3\alpha^{d_1}\frac{R_2}{d_1 - 1} + 3\alpha^{d_1}\frac{R_2^T}{d_1 - 1},$$

$$\Psi_{28} = 3\Delta_2\alpha^{d_1}R_2 + 3\Delta_6\alpha^{d_1}R_2^T, \Psi_{210} = (3Z_2 + 3\Delta_3Z_2)\frac{\alpha^{d_2}}{(d_2 - d_1)} + (3Z_2^T + 3\Delta_3Z_2^T)\frac{\alpha^{d_2}}{(d_2 - d_1)},$$

$$\Psi_{33} = \frac{\alpha^{d_1}}{d(k) - d_1}R_2 - 3\Delta_2\alpha^{d_1}R_2 - \alpha^{d_2}T_2 - F_1U_2 - \alpha^{d_1}Z_1 - 3\alpha^{d_1}\Delta_1Z_1 - (Z_2 + \Delta_3Z_2)\frac{\alpha^{d_2}}{(d_2 - d_1)}$$

$$- (3Z_2^T + \Delta_3Z_2^T)\frac{\alpha^{d_2}}{(d_2 - d_1)} - (Z_2 + \Delta_5Z_2)\frac{\alpha^{d_2}}{(d_2 - d_1)},$$

$$\Psi_{34} = \frac{d_1}{d_1 - d(k)}\alpha^{d_1}Z_1 - \frac{3d_1}{d_1 - d(k)}\Delta_4\alpha^{d_1}Z_1 + (Z_2 + \Delta_5Z_2)\frac{\alpha^{d_2}}{(d_2 - d_1)} - (3Z_2 + 3\Delta_5Z_2)\frac{\alpha^{d_2}}{(d_2 - d_1)},$$

$$\Psi_{36} = -\alpha^{d_2} W + F_2 U_2, \Psi_{38} = 3\Delta_6 \alpha^{d_1} R_2 + 3\Delta_6 \alpha^{d_1} R_2^T, \Psi_{39} = 3\alpha^{d_1} \frac{Z_1}{d_1 - 1} + 3\alpha^{d_1} \frac{Z_1^T}{d_1 - 1},$$

$$\Psi_{3_{10}} = (3Z_2 + 3\Delta_3 Z_2) \frac{\alpha^{d_2}}{(d_2 - d_1)} + (3Z_2^T + 3\Delta_3 Z_2^T) \frac{\alpha^{d_2}}{(d_2 - d_1)},$$

$$\Psi_{44} = -(3Z_2 + 3\Delta_5 Z_2) \frac{\alpha^{d_2}}{(d_2 - d_1)} - \frac{d_1}{d_1 - d(k)} 3\Delta_4 \alpha^{d_1} Z_1 - (Z_2 + \Delta_5 Z_2) \frac{\alpha^{d_2}}{(d_2 - d_1)},$$

$$\Psi_{4_{11}} = -(3Z_2 + 3\Delta_5 Z_2) \frac{\alpha^{d_2}}{(d_2 - d_1)} + (3Z_2^T + 3\Delta_5 Z_2^T) \frac{\alpha^{d_2}}{(d_2 - d_1)},$$

$$\Psi_{55} = \tilde{B}_i^{\ell T} P \tilde{B}_i^{\ell} + \alpha^{d_1} (d_2 - d_1 + 1) T_4 + \frac{\tau_2 (\tau_2 + \tau_1) (\tau_2 - \tau_1 + 1)}{2} S - U_1, \Psi_{56} = \tilde{B}_i^{\ell T} P \tilde{C}_i^{\ell},$$

$$\Psi_{66} = \tilde{C}_i^{\ell T} P \tilde{C}_i^{\ell} - U_2 - \alpha^{d_2} T_4, \Psi_{77} = -12\alpha^{d_1} \frac{R_2}{(d_1 + 1)(d_1 - 1)},$$

$$\Psi_{88} = 3 \frac{(d_2 - d_1 - 1)}{(d(k) - d_1)(d(k) - d_1 + 1)^3} \alpha^{d_1} R_2, \Psi_{99} = -12\alpha^{d_1} \frac{Z_1}{(d_1 + 1)(d_1 - 1)},$$

$$\Psi_{10_{10}} = -12(3Z_2 + 3\Delta_3 Z_2) \frac{\alpha^{d_2}}{(d_2 - d_1)}, \Psi_{11_{11}} = -4(3Z_2 + 3\Delta_5 Z_2) \frac{\alpha^{d_2}}{(d_2 - d_1)},$$

$$\Psi_{12_{12}} = -\alpha^{d_2} R_3, \Psi_{12_{13}} = -\alpha^{d_2} W_2, \Psi_{13_{13}} = -\alpha^{d_2} R_3.$$

and the other terms are same as defined in Theorem 3.1.

Proof. Consider the same L-K functional as defined in Theorem 3.1. The proof immediately Follows From The Similar Way Of Proof of Theorem 3.1, hence it is omitted. \square

Remark 3.6. The Equation (1) is described by a discrete-time T-S fuzzy switched memristive neural networks modelled in (10). In this model the system dynamics are captured by a set of fuzzy IF-THEN rules with switching signals that represent local linear input-output relations of a nonlinear system.

Remark 3.7. Primarily, computational complexity will be a big issue based on how large are the LMIs and how more are the decision variables. In Theorems 3.1 and 3.3 we have used maximum number of decision variables in our LMIs. However, large size of LMIs yield better performance. The results in Theorems 3.1 and 3.3 are derived based on the construction of proper L-K functional with quadratic, triple summation terms, and by using a newly introduced summation inequality techniques which produces tighter bounds than what the existing ones such as the Auxiliary function based integral inequality and Reciprocally convex approach produce. It should be mentioned that the obtained H_∞ performance for the considered NNs with switching signal and mixed time-varying delays are less conservative than the existing ones in the literature, it is easy to see in Table 1. Meanwhile, it should also be noticed that the relaxation of the derived results is acquired at the cost of more number of decision variables. As far the results to be efficient enough it is more comfortable to have larger maximum allowable upper bounds but still in order to reduce computation complexity burden and time computation, our future work will be reducing the number of decision variables by applying Finsler's Lemma in our work

Remark 3.8. *Theorem 3.1 develops a globally exponentially stability criterion of discrete-time T-S fuzzy switched memristive stochastic NNs. Theorem 3.1 makes full use of the information of the subsystems upper bounds of the time-varying delays, which also brings us the less conservativeness.*

Remark 3.9. *It is very interesting to note that, in this paper, the reduced conservatism is primarily from the construction of the suitable Lyapunov-Krasovskii functional and the use of bounding techniques in summation terms. In recent years, some researchers have used the inequality techniques, such as Wirtinger based integral inequality and novel summation inequality techniques. These two inequalities are the best techniques to reduce conservatism. In addition, these above summation technique is given to take fully the relationship between the terms in the frame work of linear matrix inequalities (LMIs) into account, which gives the conservatism of our results.*

Remark 3.10. *Generally, switching signal design with memristive concept, T-S fuzzy and uncertain parameters are not simply applied to stochastic NNs in discrete time case. Some research publications have tackled such problems. However, the authors used very simple LKFs to solve the stability problems in those articles. A new LKF with the information of time-varying delay (like discrete, distributed delay involving both upper and lower bounds, i.e., $\tau_1 \leq \tau(k) \leq \tau_2$, $d_1 \leq d(k) \leq d_2$) is proposed for the stability analysis of H_∞ performance with switching signal in this paper, considering that some computational complexity can occur in our method. However, Robust H_∞ performance for discrete time T-S fuzzy switched memristive was completely studied for stochastic NNs with mixed time delays, which is the main contribution and motivation of our work.*

Remark 3.11. *It should be highly pointed out that, in the previous literature authors in [12,13,15,16] investigated the problems with simple delayed NNs with various stability criteria. So far, it is noted that unfortunately in the existing literature memristive stochastic NNs with the presence of T-S fuzzy, switching signal, and uncertain parameters has not been considered yet. The model considered in the present study is more practical than that proposed by [23,38,39], because they consider only stochastic NNs with switching signal design, but in this paper they consider both memristive and uncertain parameters with switching signal for the available neural network model. Moreover, in the proof of theorems and corollaries, we utilise the Wirtinger and novel summation inequality technique has been widely employed to tackle time-varying delay such as defined in $V_s(k, u(k))$ ($s = 3, 4$) and was shown more tighter than the ones based on Jensen's inequality formula.*

Numerical examples

In this section, we provide numerical examples with simulation results to illustrate the effectiveness and advantages of the proposed theory.

Example 4.1. Consider the following T-S fuzzy memristor based stochastic uncertain NNs with time varying delays and switching signal:

$$\begin{aligned}
 u(k+1) = & \sum_{l=1}^q \phi^l(\hat{y}(k)) [\tilde{A}_i^\ell + \Delta A_i^\ell(k)] u(k) + [\tilde{B}_i^\ell + \Delta B_i^\ell(k)] f(u(k)) + [\tilde{C}_i^\ell + \Delta C_i^\ell(k)] f(u(k-d(k))) \\
 & + [\tilde{D}_i^\ell + \Delta D_i^\ell(k)] \sum_{i=1}^{\tau(k)} f(u(k-i)) + E_i^\ell v(k) + \sigma(k, x(k), x(k-d(k))) w(k),
 \end{aligned}$$

$$y(k) = \sum_{l=1}^q \phi^l(\hat{y}(k)) [A_{1l}^\ell u(k) + D_{1l}^\ell u(k-d(k)) + G_l^\ell v(k)],$$

$$u(l) = \phi(l), \quad l = k_0 - d_2, \dots, k_0. \quad (48)$$

The parameters of the first subsystem are

$$\begin{aligned} a_1^1(u_1(\cdot)) &= \begin{cases} 0.4, & |u_1(\cdot) \leq 1|, \\ 0.6, & |u_1(\cdot) > 1|, \end{cases} & a_2^1(u_2(\cdot)) &= \begin{cases} 0.4, & |u_2(\cdot) \leq 1|, \\ 0.6, & |u_2(\cdot) > 1|, \end{cases} \\ b_{11}^1(u_1(\cdot)) &= \begin{cases} 0.5, & |u_1(\cdot) \leq 1|, \\ 0.2, & |u_1(\cdot) > 1|, \end{cases} & b_{12}^1(u_1(\cdot)) &= \begin{cases} 0.2, & |u_1(\cdot) \leq 1|, \\ -0.3, & |u_1(\cdot) > 1|, \end{cases} \\ b_{21}^1(u_2(\cdot)) &= \begin{cases} 0.3, & |u_2(\cdot) \leq 1|, \\ 0.15, & |u_2(\cdot) > 1|, \end{cases} & b_{22}^1(u_2(\cdot)) &= \begin{cases} 0.6, & |u_2(\cdot) \leq 1|, \\ -0.18, & |u_2(\cdot) > 1|, \end{cases} \\ c_{11}^1(u_1(\cdot)) &= \begin{cases} 0.2, & |u_1(\cdot) \leq 1|, \\ 0.5, & |u_1(\cdot) > 1|, \end{cases} & c_{12}^1(u_1(\cdot)) &= \begin{cases} 0.3, & |u_1(\cdot) \leq 1|, \\ 0.2, & |u_1(\cdot) > 1|, \end{cases} \\ c_{21}^1(u_2(\cdot)) &= \begin{cases} 0.2, & |u_2(\cdot) \leq 1|, \\ -0.1, & |u_2(\cdot) > 1|, \end{cases} & c_{22}^1(u_2(\cdot)) &= \begin{cases} -0.3, & |u_2(\cdot) \leq 1|, \\ 0.1, & |u_2(\cdot) > 1|, \end{cases} \\ d_{11}^1(u_1(\cdot)) &= \begin{cases} -0.8, & |u_1(\cdot) \leq 1|, \\ -0.7, & |u_1(\cdot) > 1|, \end{cases} & d_{12}^1(u_1(\cdot)) &= \begin{cases} 0.6, & |u_1(\cdot) \leq 1|, \\ 0.7, & |u_1(\cdot) > 1|, \end{cases} \\ d_{21}^1(u_2(\cdot)) &= \begin{cases} 0.8, & |u_2(\cdot) \leq 1|, \\ 0.9, & |u_2(\cdot) > 1|, \end{cases} & d_{22}^1(u_2(\cdot)) &= \begin{cases} -0.9, & |u_2(\cdot) \leq 1|, \\ -1.0, & |u_2(\cdot) > 1|, \end{cases} \\ a_1^2(u_1(\cdot)) &= \begin{cases} 0.5, & |u_1(\cdot) \leq 1|, \\ 0.7, & |u_1(\cdot) > 1|, \end{cases} & a_2^2(u_2(\cdot)) &= \begin{cases} 0.45, & |u_2(\cdot) \leq 1|, \\ 0.8, & |u_2(\cdot) > 1|, \end{cases} \\ b_{11}^2(u_1(\cdot)) &= \begin{cases} 0.6, & |u_1(\cdot) \leq 1|, \\ 0.3, & |u_1(\cdot) > 1|, \end{cases} & b_{12}^2(u_1(\cdot)) &= \begin{cases} 0.3, & |u_1(\cdot) \leq 1|, \\ -0.4, & |u_1(\cdot) > 1|, \end{cases} \\ b_{21}^2(u_2(\cdot)) &= \begin{cases} 0.14, & |u_2(\cdot) \leq 1|, \\ 0.15, & |u_2(\cdot) > 1|, \end{cases} & b_{22}^2(u_2(\cdot)) &= \begin{cases} 0.7, & |u_2(\cdot) \leq 1|, \\ -0.2, & |u_2(\cdot) > 1|, \end{cases} \\ c_{11}^2(u_1(\cdot)) &= \begin{cases} 0.3, & |u_1(\cdot) \leq 1|, \\ 0.4, & |u_1(\cdot) > 1|, \end{cases} & c_{12}^2(u_1(\cdot)) &= \begin{cases} 0.4, & |u_1(\cdot) \leq 1|, \\ 0.3, & |u_1(\cdot) > 1|, \end{cases} \\ c_{21}^2(u_2(\cdot)) &= \begin{cases} 0.4, & |u_2(\cdot) \leq 1|, \\ -0.2, & |u_2(\cdot) > 1|, \end{cases} & c_{22}^2(u_2(\cdot)) &= \begin{cases} -0.2, & |u_2(\cdot) \leq 1|, \\ 0.3, & |u_2(\cdot) > 1|, \end{cases} \\ d_{11}^2(u_1(\cdot)) &= \begin{cases} -0.7, & |u_1(\cdot) \leq 1|, \\ -0.8, & |u_1(\cdot) > 1|, \end{cases} & d_{12}^2(u_1(\cdot)) &= \begin{cases} 0.8, & |u_1(\cdot) \leq 1|, \\ 0.9, & |u_1(\cdot) > 1|, \end{cases} \\ d_{21}^2(u_2(\cdot)) &= \begin{cases} 0.72, & |u_2(\cdot) \leq 1|, \\ 0.8, & |u_2(\cdot) > 1|, \end{cases} & d_{22}^2(u_2(\cdot)) &= \begin{cases} -0.8, & |u_2(\cdot) \leq 1|, \\ -1.0, & |u_2(\cdot) > 1|, \end{cases} \end{aligned}$$

The parameters of the second subsystem are

$$a_1^3(u_1(\cdot)) = \begin{cases} 0.6, & |u_1(\cdot) \leq 1|, \\ 0.85, & |u_1(\cdot) > 1|, \end{cases} \quad a_2^3(u_2(\cdot)) = \begin{cases} 0.34, & |u_2(\cdot) \leq 1|, \\ 0.7, & |u_2(\cdot) > 1|, \end{cases}$$

$$b_{11}^3(u_1(\cdot)) = \begin{cases} 0.55, & |u_1(\cdot) \leq 1|, \\ 0.4, & |u_1(\cdot) > 1|, \end{cases} \quad b_{12}^3(u_1(\cdot)) = \begin{cases} 0.4, & |u_1(\cdot) \leq 1|, \\ -0.64, & |u_1(\cdot) > 1|, \end{cases}$$

$$b_{21}^3(u_2(\cdot)) = \begin{cases} 0.25, & |u_2(\cdot) \leq 1|, \\ 0.5, & |u_2(\cdot) > 1|, \end{cases} \quad b_{22}^3(u_2(\cdot)) = \begin{cases} 0.6, & |u_2(\cdot) \leq 1|, \\ -0.35, & |u_2(\cdot) > 1|, \end{cases}$$

$$c_{11}^3(u_1(\cdot)) = \begin{cases} 0.5, & |u_1(\cdot) \leq 1|, \\ 0.2, & |u_1(\cdot) > 1|, \end{cases} \quad c_{12}^3(u_1(\cdot)) = \begin{cases} 0.6, & |u_1(\cdot) \leq 1|, \\ 0.45, & |u_1(\cdot) > 1|, \end{cases}$$

$$c_{21}^3(u_2(\cdot)) = \begin{cases} 0.5, & |u_2(\cdot) \leq 1|, \\ -0.35, & |u_2(\cdot) > 1|, \end{cases} \quad c_{22}^3(u_2(\cdot)) = \begin{cases} -0.56, & |u_2(\cdot) \leq 1|, \\ 0.45, & |u_2(\cdot) > 1|, \end{cases}$$

$$d_{11}^3(u_1(\cdot)) = \begin{cases} -0.6, & |u_1(\cdot) \leq 1|, \\ -0.45, & |u_1(\cdot) > 1|, \end{cases} \quad d_{12}^3(u_1(\cdot)) = \begin{cases} 0.6, & |u_1(\cdot) \leq 1|, \\ -0.55, & |u_1(\cdot) > 1|, \end{cases}$$

$$d_{21}^3(u_2(\cdot)) = \begin{cases} 0.01, & |u_2(\cdot) \leq 1|, \\ 0.3, & |u_2(\cdot) > 1|, \end{cases} \quad d_{22}^3(u_2(\cdot)) = \begin{cases} -0.6, & |u_2(\cdot) \leq 1|, \\ 0.8, & |u_2(\cdot) > 1|, \end{cases}$$

$$a_1^4(u_1(\cdot)) = \begin{cases} 0.46, & |u_1(\cdot) \leq 1|, \\ 0.8, & |u_1(\cdot) > 1|, \end{cases} \quad a_2^4(u_2(\cdot)) = \begin{cases} 0.35, & |u_2(\cdot) \leq 1|, \\ 0.6, & |u_2(\cdot) > 1|, \end{cases}$$

$$b_{11}^4(u_1(\cdot)) = \begin{cases} 0.54, & |u_1(\cdot) \leq 1|, \\ -0.3, & |u_1(\cdot) > 1|, \end{cases} \quad b_{12}^4(u_1(\cdot)) = \begin{cases} 0.4, & |u_1(\cdot) \leq 1|, \\ -0.65, & |u_1(\cdot) > 1|, \end{cases}$$

$$b_{21}^4(u_2(\cdot)) = \begin{cases} 0.34, & |u_2(\cdot) \leq 1|, \\ 0.64, & |u_2(\cdot) > 1|, \end{cases} \quad b_{22}^4(u_2(\cdot)) = \begin{cases} 0.5, & |u_2(\cdot) \leq 1|, \\ -0.43, & |u_2(\cdot) > 1|, \end{cases}$$

$$c_{11}^4(u_1(\cdot)) = \begin{cases} 0.23, & |u_1(\cdot) \leq 1|, \\ 0.54, & |u_1(\cdot) > 1|, \end{cases} \quad c_{12}^4(u_1(\cdot)) = \begin{cases} -0.3, & |u_1(\cdot) \leq 1|, \\ 0.3, & |u_1(\cdot) > 1|, \end{cases}$$

$$c_{21}^4(u_2(\cdot)) = \begin{cases} 0.67, & |u_2(\cdot) \leq 1|, \\ -1.2, & |u_2(\cdot) > 1|, \end{cases} \quad c_{22}^4(u_2(\cdot)) = \begin{cases} -1.2, & |u_2(\cdot) \leq 1|, \\ 1.3, & |u_2(\cdot) > 1|, \end{cases}$$

$$d_{11}^4(u_1(\cdot)) = \begin{cases} -1.2, & |u_1(\cdot) \leq 1|, \\ -1.8, & |u_1(\cdot) > 1|, \end{cases} \quad d_{12}^4(u_1(\cdot)) = \begin{cases} 0.2, & |u_1(\cdot) \leq 1|, \\ 0.3, & |u_1(\cdot) > 1|, \end{cases}$$

$$d_{21}^4(u_2(\cdot)) = \begin{cases} 0.54, & |u_2(\cdot) \leq 1|, \\ 0.67, & |u_2(\cdot) > 1|, \end{cases} \quad d_{22}^4(u_2(\cdot)) = \begin{cases} -0.6, & |u_2(\cdot) \leq 1|, \\ -2.0, & |u_2(\cdot) > 1|, \end{cases}$$

$$\mathcal{E}_1 = \begin{bmatrix} 1 & 0 \\ 0 & 1 \end{bmatrix}, \mathcal{E}_2 = \begin{bmatrix} 0.5 & 0 \\ 0 & 0.5 \end{bmatrix}, N_{11} = N_{21} = N_{31} = N_{41} = \text{diag}\{0.1, 0.1\},$$

$$N_{12} = N_{22} = N_{32} = N_{42} = \text{diag}\{0.2, 0.2\}.$$

The membership functions for Rules 1 and 2 are $\phi^1(u_1(k)) = 1/\exp(-2u_1(k))$, $\phi^2(u_1(k)) = 1 - \phi^1(u_1(k))$. The activation functions are described by $f_1(y) = \frac{1}{20}(|a+1| + |a-1|)$, $f_2(y) = \frac{1}{10}(|a+1| + |a-1|)$. It can be verified that Assumption 2.1 is satisfied with $F_1^- = -0.1, F_1^+ = 0.1, F_2^- = -0.2, F_2^+ = 0.2$. Therefore, we can obtain

$$F_1 = \begin{bmatrix} -0.01 & 0 \\ 0 & -0.04 \end{bmatrix}, F_2 = \begin{bmatrix} 0 & 0 \\ 0 & 0 \end{bmatrix}.$$

If we choose $\hat{\rho}_1 = \hat{\rho}_2 = 0.1, \alpha = 0.5$, assumed that the distributed delay $\tau(k)$ satisfies $5 \leq \tau(k) \leq 9$, that is, $\tau_1 = 5$ and $\tau_2 = 9$ and the time delay lower bound $d_1 = 2$ and upper bound $d_2 = 8$, then by solving the LMIs in Theorem 3.3 using Matlab-LMI control toolbox, we get the feasible solutions are as follows:

$$P = 10^4 \begin{bmatrix} 7.6469 & 0.0007 \\ 0.0007 & 7.6525 \end{bmatrix}, Z_1 = \begin{bmatrix} 76.6670 & 0.5967 \\ 0.5967 & 81.6048 \end{bmatrix}, Z_2 = 10^3 \begin{bmatrix} 4.9264 & 0.0027 \\ 0.0027 & 4.9477 \end{bmatrix},$$

$$T_2 = \begin{bmatrix} 26.8707 & -0.0241 \\ -0.0241 & 26.6600 \end{bmatrix}, T_4 = \begin{bmatrix} 980.7714 & -0.8760 \\ -0.8760 & 971.1925 \end{bmatrix}, W = \begin{bmatrix} 95.1496 & -0.1099 \\ -0.1099 & 94.2281 \end{bmatrix},$$

$$R_2 = 10^4 \begin{bmatrix} 136.6891 & 0.3123 \\ 0.3123 & 139.2056 \end{bmatrix}, R_3 = \begin{bmatrix} 6.9083 & -0.0061 \\ -0.0061 & 6.8549 \end{bmatrix}, S = 10^3 \begin{bmatrix} 2.2745 & -0.0020 \\ -0.0020 & 2.2571 \end{bmatrix},$$

$$U_1 = 10^4 \begin{bmatrix} 1.7314 & 0 \\ 0 & 1.7209 \end{bmatrix}, U_2 = 10^4 \begin{bmatrix} 8.0768 & 0 \\ 0 & 8.0766 \end{bmatrix}, \epsilon_1 = 10^4 \times 8.3494,$$

$$\epsilon_2 = 10^4 \times 6.4585, \lambda^* = 10.5241.$$

Select the switching signal by $\sigma(u(k)) = i, u(k) \in \bar{\Omega}_i, i = 1, 2$. Therefore, it follows from Theorem 3.3 that the memristive based stochastic neural network (48) with switching signal and T-S fuzzy effect is exponentially stable. For given initial state $[2, -2]^T$, Figure 1 shows that the state trajectories of the considered neural network converges, which provides that the discrete time stochastic neural network is stable.

Example 4.2. Consider the following memristive based stochastic NNs with time varying delays and switching signal:

$$u(k+1) = A_i u(k) + B_i(u(k))f(u(k)) + C_i f(u(k-d(k)))$$

$$+ D_i \sum_{i=1}^{\infty} \mu_i f(u(k-i)) + E_i v(k) + \sigma(k, x(k), x(k-d(k)))w(k),$$

$$y(k) = A_{1i} u(k) + D_{1i} u(k-d(k)) + G_i v(k),$$

$$u(l) = \phi(l), l = k_0 - d_2, \dots, k_0$$

Consider the same input known matrices from Example 4.1 and let $d_1 = 2, d_2 = 8$, the activation function are taken as follows: $f_1(y) = f_2(y) = \tanh(y)$. It can be verified that Assumption 2.1 is satisfied with $F_1^- = 0, F_1^+ = 0, F_2^- = 1, F_2^+ = 1$. Thus,

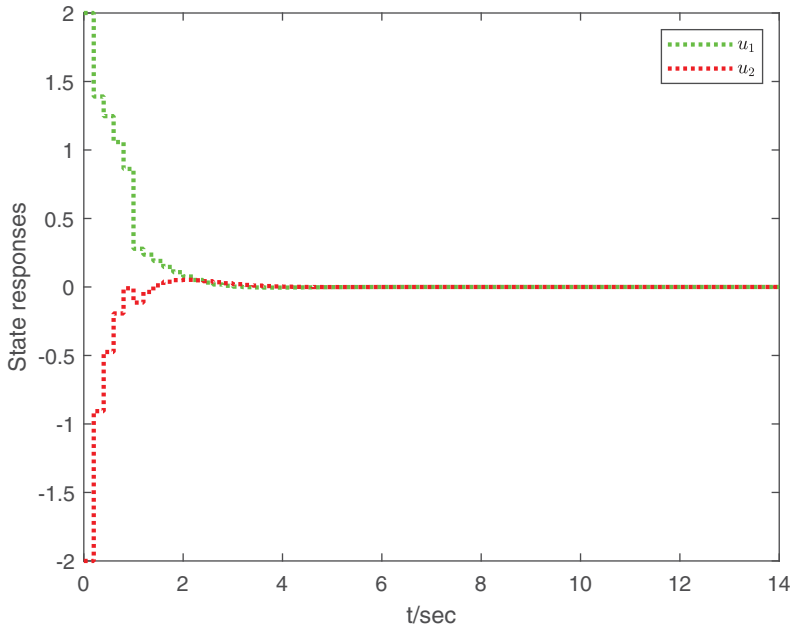


Figure 1. State responses of MNNs (46) in Example 4.1.

$$F_1 = \begin{bmatrix} 0 & 0 \\ 0 & 0 \end{bmatrix}, F_2 = \begin{bmatrix} 0.5 & 0 \\ 0 & 0.5 \end{bmatrix}.$$

By using the Matlab LMI control Toolbox solve the LMIs in Theorem 3.1, we obtain a set of feasible solutions as

$$P = 10^4 \begin{bmatrix} 3.1010 & 0.0001 \\ 0.0001 & 3.1020 \end{bmatrix}, Z_1 = \begin{bmatrix} 49.9511 & -0.0656 \\ -0.0656 & 49.8721 \end{bmatrix}, Z_2 = 10^3 \begin{bmatrix} 2.2342 & -0.0020 \\ -0.0020 & 2.2284 \end{bmatrix},$$

$$T_2 = \begin{bmatrix} 28.5132 & 0.0034 \\ 0.0034 & 28.4704 \end{bmatrix}, T_4 = \begin{bmatrix} 994.3211 & 0.1083 \\ 0.1083 & 991.3597 \end{bmatrix}, W = \begin{bmatrix} 95.8580 & 0.0024 \\ 0.0024 & 95.5614 \end{bmatrix},$$

$$R_2 = 10^4 \begin{bmatrix} 88.1245 & -0.0655 \\ -0.0655 & 87.8132 \end{bmatrix}, R_3 = 10^3 \begin{bmatrix} 4.2691 & 0.0004 \\ 0.0004 & 4.2630 \end{bmatrix}, S = 10^3 \begin{bmatrix} 1.8646 & 0.0002 \\ 0.0002 & 1.8619 \end{bmatrix},$$

$$U_1 = 10^4 \begin{bmatrix} 1.0344 & 0 \\ 0 & 1.0317 \end{bmatrix}, U_2 = 10^4 \begin{bmatrix} 3.1824 & 0 \\ 0 & 3.1821 \end{bmatrix}, \lambda^* = 15.3742.$$

select the switching signal by $\sigma(u(k)) = i, u(k) \in \bar{\Omega}_i, i = 1, 2$. On the other side, by setting the upper delay bound $d_2 = 8$, we have the H_∞ performance $\kappa = 0.8947$. Thus, it can be concluded that the memristive stochastic NNs (16) is exponentially stable and the state trajectories of the dynamical system are converge to the zero equilibrium point with an initial state $[3, -3]^T$, it is shown in [Figure 2](#).

Example 4.3. Consider the following discrete NNs (46) with the following parameters:

$$A = \begin{bmatrix} 0.1 & 0 \\ 0 & 0.3 \end{bmatrix}, B = \begin{bmatrix} 0.02 & 0 \\ 0 & 0.004 \end{bmatrix}, C = \begin{bmatrix} -0.01 & 0.01 \\ -0.02 & -0.01 \end{bmatrix}.$$

and the activation function satisfies $f(k) = \begin{bmatrix} \tanh(k_1) \\ \tanh(k_2) \end{bmatrix}$ satisfies Assumption 2.2.

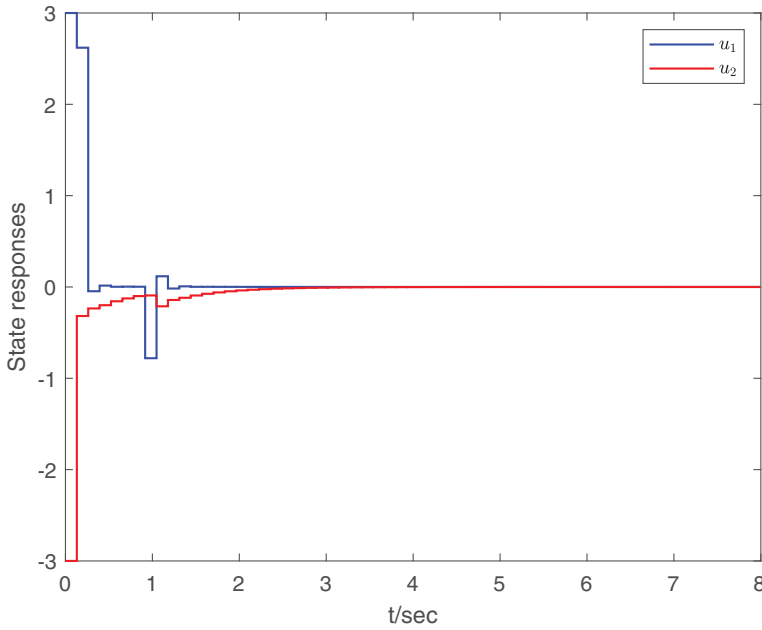


Figure 2. State responses of MNNs (16) in Example 4.2.

Table 1. Calculated maximum d_2 for given d_1 for Example 4.3.

d_1	2	4	6	8
(Wang et al., 2013)	13	16	17	19
(Wu et al., 2010)	15	17	18	20
(Jarina Banu et al., 2015)	30	32	34	36
Corollary 3.5	32	34	35	38

For different values of d_1 , the upper bounds of delay d_2 are obtained by various approaches, which guarantee the asymptotic stability of the NNs (46). From the values listed in Table 1, one can easily see that the stability criterion proposed in Corollary 3.5 is less conservative than those in Refs. Jarina Banu et al. (2015); Wang et al. (2013); Wu et al. (2010).

Example 4.4. Consider the following discrete NNs (46) with the following parameters:

$$A = \begin{bmatrix} 0.8 & 0 \\ 0 & 0.9 \end{bmatrix}, B = \begin{bmatrix} 0.001 & 0 \\ 0 & 0.005 \end{bmatrix}, C = \begin{bmatrix} -0.1 & 0.01 \\ -0.2 & -0.1 \end{bmatrix}.$$

and the activation functions satisfy Assumption 2.2 with $F_1^- = F_2^- = 0, F_1^+ = F_2^+ = 1$. By using the MATLAB LMI toolbox, we can solve the LMI in Corollary 3.5. This ensures the asymptotic stability of the system (46). For different values of d_1 , the allowable upper bounds of time delay d_2 are obtained by various approaches, and they are listed in Table 3. Moreover, the number of decision variables in (Jarina Banu et al., 2015; Kwon et al., 2012; Selvaraj et al., 2018) are $15n^2 + 5n, 17.5n^2 + 4.5n$ and $28.5n^2 + 7.5n$. In this paper, the number of decision variables of Corollary 3.5 is $4n^2 + 6n$. Therefore, from the values listed in Table 3 and number of decision variables in Table 2, one can easily see that the stability criterion proposed in Corollary 3.5 yields less conservatism than those in Jarina Banu et al. (2015); Kwon et al. (2012); Lin et al. (2016); Selvaraj et al. (2018); Song et al. (2009); Song and Wang (2007); Wu et al. (2008); Yu et al. (2010).

Table 2. Number of decision variables involved in various papers.

	No of decision variables
(Selvaraj et al., 2018)	$15n^2 + 5n$
(Jarina Banu et al., 2015)	$17.5n^2 + 4.5n$
(Kwon et al., 2012)	$28.5n^2 + 7.5n$
This paper	$4n^2 + 6n$

Table 3. Calculated maximum d_2 for given d_1 for Example 4.4.

d_1	2	4	6	8
(Song et al., 2009)	11	11	12	13
(Song & Wang, 2007)	11	12	13	14
(Wu et al., 2008)	15	16	17	18
(Yu et al., 2010)	13	15	17	19
(Lin et al., 2016)	15	17	18	19
Corollary 3.5	18	19	21	22

Conclusion

In this paper, the problem of robust H_∞ performance for discrete-time T-S fuzzy switched memristive stochastic NNs with mixed time varying delays. By employing, some novel summation inequality techniques and LMI approach, we designed switching signal such that the resulting closed-loop neural network is robustly exponential stable with a prescribed H_∞ performance. The obtained results are all in the form of an effective linear matrix inequality (LMI), which can be easily optimised by MATLAB-LMI control toolbox. Finally, numerical examples are given to show the superiority of our proposed stability conditions. In the end, we would like to conclude that the results we presented here are quite general and the conditions are relatively easy to check. Therefore, it is believed that all the results obtained in this paper can be extendable to complex-valued NNs and state estimation issues of general-switched systems with multiple channels subject to random packet dropouts. Moreover, the model proposed in this work can be also extended event-triggered mechanism to the coupled NNs with imperfect communication, such as packet dropouts and quantisation. We will also target on the complex phenomena like the randomly occurring uncertainties, incomplete measurements, MJSs with repeated scalar nonlinearities, T-S fuzzy-based piecewise Lyapunov function and decentralised event triggered with asynchronous sampling. Which makes the model more practical. Which will be investigated in our future work.

Acknowledgement

The work of second author was supported by the CSIR project No. 25(0274)/17/EMR-II dated 27/04/2017. Also, the work of third author was supported by the Basic Science Research Program through the National Research Foundation of Korea (NRF) funded by the Ministry of Education (NRF-2016R1A6A1A03013567) and by the Korea Institute of Energy Technology Evaluation and Planning (KETEP) and the Ministry of Trade, Industry & Energy (MOTIE) of the Republic of Korea (No. 20,174,030,201,670).

Disclosure statement

No potential conflict of interest was reported by the authors.

Funding

This work was supported by the Council of Scientific and Industrial Research, India [CSIR . 25(0274)/17/EMR-II dated 27/04/2017].

References

- Anbuvithya, R., Mathiyalagan, K., Sakthivel, R., & Prakash, P. (2016). Passivity of memristor-based BAM neural networks with different memductance and uncertain delays. *Cognitive Neurodynamics*, *10*, 339–351.
- Arunkumar, A., Sakthivel, R., Mathiyalagan, K., & Marshal Anthoni, S. (2012). Robust stability criteria for discrete-time switched neural networks with various activation functions. *Applied Mathematics and Computation*, *218*(22), 10803–10816.
- Chinnamuniyandi, M., Raja, R., Cao, J., Rajchakit, G., & Li, X. (2018). A new global robust exponential stability criterion for H_∞ control of uncertain stochastic neutral-type neural networks with both time varying delays. *International Journal of Control, Automation and Systems*, *16*, 726–738.
- Chua, L. (1971). Memristor—the missing circuit element. *IEEE Transactions on Circuit Theory*, *18*, 507–519.
- Deng, F., Hua, M., Liu, X., Peng, Y., & Fei, J. (2011). Robust delay-dependent exponential stability for uncertain stochastic neural networks with mixed delays. *Neurocomputing*, *10*, 1503–1509.
- Dong, S., Fang, M., Shi, P., & Wu, Z. G. (2019). Dissipativity-based control for fuzzy systems with asynchronous modes and intermittent measurements. *IEEE Transactions on Cybernetics*. doi:10.1109/TCYB.2018.2887060
- Gao, J., Zhu, P., Alsaedi, A., Alsaadi, F. E., & Hayat, T. (2017). A new switching control for finite-time synchronization of memristor-based recurrent neural networks. *Neural Networks*, *86*, 1–9.
- Hou, L., Zong, G., & Wu, Y. (2011). Robust exponential stability analysis of discrete-time switched Hopfield neural networks with time delay. *Nonlinear Analysis: Hybrid Systems*, *5*(3), 525–534.
- Hua, M., Liu, X., Deng, F., & Fei, J. (2010). New results on robust exponential stability of uncertain stochastic neural networks with mixed time-varying delays. *Neural Processing Letters*, *32*, 219–233.
- Jarina Banu, L., Balasubramaniam, P., & Ratnavelu, K. (2015). Robust stability analysis for discrete-time uncertain neural networks with leakage time-varying delay. *Neurocomputing*, *151*, 7808–7816.
- Jiang, Y., & Li, C. (2016). Exponential stability of memristor-based synchronous switching neural networks with time delays. *International Journal of Biomathematics*, *9*, 1650016.
- Jin, L., Hen, Y., & Wu, M. (2016). Improved delay-dependent stability analysis of discrete-time neural networks with time-varying delay. *Journal of the Franklin Institute*, *354*(4), 1922–1936.
- Kwon, O. M., Lee, S. M., & Park, J. H. (2012). On improved passivity criteria of uncertain neural networks with time-varying delays. *Nonlinear Dynamics*, *67*, 1261–1271.
- Li, R., & Cao, J. (2016). Dissipativity analysis of memristive neural networks with time-varying delays and randomly occurring uncertainties. *Mathematical Methods in the Applied Sciences*, *39*, 2896–2915.
- Li, R., Cao, J., Alsaedi, A., & Hayat, T. (2017a). Non-fragile state observation for delayed memristive neural networks: continuous-time case and discrete-time case. *Neurocomputing*, *245*, 102–113.
- Li, X., Fang, J., & Li, H. (2017b). Master-slave exponential synchronization of delayed complex-valued memristor-based neural networks via impulsive control. *Neural Networks*, *93*, 165–175.
- Liberzon, D. (2003). *Switching in systems and control*. Basel: Birkhauser.
- Lien, C., Yu, K., Wu, L., Chung, L., & Chen, J. (2014). Robust H_∞ switching control and switching signal design for uncertain discrete switched systems with interval time-varying delay. *Journal of the Franklin Institute*, *351*(1), 565–578.
- Lien, C. H., Yu, K. W., Chang, H. C., Chung, L. Y., & Chen, J. D. (2012). Switching signal design for exponential stability of discrete switched systems with interval time-varying delay. *Journal of the Franklin Institute*, *349*(6), 2182–2192.
- Lien, C. H., Yu, K. W., Chung, L. Y., & Chen, J. D. (2013). H_∞ performance for uncertain discrete switched systems with interval time-varying delay via switching signal design. *Applied Mathematical Modelling*, *37*(4), 2484–2494.
- Lin, D. H., Wu, J., & Li, J. N. (2016). Less conservative stability condition for uncertain discrete-time recurrent neural networks with time-varying delays. *Neurocomputing*, *173*, 1578–1588.
- Liu, X. G., Wang, F. X., & Shu, Y. J. (2016). A novel summation inequality for stability analysis of discrete-time neural networks. *Journal of Computational and Applied Mathematics*, *304*, 160–171.
- Maharajan, C., Raja, R., Cao, J., & Rajchakit, G. (2019). Fractional delay segments method on time-delayed recurrent neural networks with impulsive and stochastic effects: An exponential stability approach. *Neurocomputing*, *323*, 277–298.
- Maharajan, C., Raja, R., Cao, J., Ravi, G., & Rajchakit, G. (2018). Global exponential stability of Markovian jumping stochastic impulsive uncertain BAM neural networks with leakage, mixed time delays, and α -inverse Holder activation functions. *Advances in Difference Equations*, *118*. doi:10.1186/s13662-018-1553-7
- Mathiyalagan, K., Anbuvithya, R., Sakthivel, R., Park, J. H., & Prakash, P. (2016). Non-fragile H_∞ synchronization of memristor-based neural networks using passivity theory. *Neural Networks*, *74*, 85–100.
- Phat, V. N., & Ratchagit, K. (2011). Stability and stabilization of switched linear discrete-time systems with interval time varying delay. *Nonlinear Analysis: Hybrid Systems*, *5*(4), 605–612.
- Qiu, J., Gao, H., & Ding, S. X. (2016). Recent advances on fuzzy-model-based nonlinear networked control systems: A survey. *IEEE Transactions on Industrial Electronics*, *63*(2), 1207–1217.
- Que, H., Fang, M., Wu, Z. G., Su, H., Huang, T., & Zhang, D. (2010). Exponential synchronization via aperiodic sampling of complex delayed networks. *IEEE Transactions on Systems, Man, and Cybernetics: Systems*, *49*(7), 1399–1407.

- Selvaraj, P., Sakthivel, R., & Kwon, M. O. (2018). Finite-time synchronization of stochastic coupled neural networks subject to Markovian switching and input saturation. *Neural Networks*, 105, 154–165.
- Song, C., Gao, H., & Zheng, W. X. (2009). A new approach to stability analysis of discrete-time recurrent neural networks with time-varying delay. *Neurocomputing*, 72, 2563–2568.
- Song, Q., & Wang, Z. (2007). A delay-dependent LMI approach to dynamics analysis of discrete-time recurrent neural networks with time-varying delays. *Physics Letters A*, 368(1–2), 134–145.
- Sowmiya, C., Raja, R., Cao, J., Li, X., & Rajchakit, G. (2018). Discrete-time stochastic impulsive BAM neural networks with leakage and mixed time delays: An exponential stability problem. *Journal of the Franklin Institute*, 355(10), 4404–4435.
- Sowmiya, C., Raja, R., Zhu, Q., & Rajchakit, G. (2019). Further mean-square asymptotic stability of impulsive discrete-time stochastic BAM neural networks with Markovian jumping and multiple time-varying delays. *Journal of the Franklin Institute*, 356(1), 561–591.
- Strukov, D., Snider, G., Stewart, D., & Williams, R. (2008). The missing memristor found. *Nature*, 453, 80–83.
- Syed Ali, M., & Marudai, M. (2011). Stochastic stability of discrete-time uncertain recurrent neural networks with Markovian jumping and time-varying delays. *Mathematical and Computer Modelling*, 54(9–10), 1979–1988.
- Syed Ali, M., & Saravanan, S. (2018). Finite-time stability for memristor based switched neural networks with time-varying delays via average dwell time approach. *Neurocomputing*, 275, 1637–1649.
- Takagi, T., & Sugeno, M. (1985). Fuzzy identification of systems and its applications to modeling and control. *IEEE Transactions on Systems, Man, and Cybernetics*, 15(1), 116–132.
- Tian, E., Yue, D., & Zhang, Y. (2009). Delay-dependent robust H_∞ control for T-S fuzzy system with interval time-varying delay. *Fuzzy Sets and Systems*, 160(12), 1708–1719.
- Wang, T., Xue, M., Fei, S., & Li, T. (2013). Triple Lyapunov functional technique on delay-dependent stability for discrete-time dynamical networks. *Neurocomputing*, 122, 221–228.
- Wu, M., Liu, F., Shi, P., He, Y., & Yokoyama, R. (2008). Improved free-weighting matrix approach for stability analysis of discrete-time recurrent neural networks with time-varying delay. *IEEE Transactions on Circuits and Systems-II: Express Briefs*, 55(7), 690–694.
- Wu, Z., Su, H., Chu, J., & Zhou, W. (2010). Improved delay-dependent stability condition of discrete recurrent neural networks with time varying delays. *IEEE Transactions on Neural Networks*, 21(4), 692–697.
- Wu, Z. G., Dong, S., Shi, P., Zhang, D., & Huang, T. (2019). Reliable filter design of Takagi-Sugeno fuzzy switched systems with imprecise modes. *IEEE Transactions on Cybernetics*, 1–11. doi:10.1109/TCYB.2018.2885505
- Yang, Z., Luo, B., Liu, D., & Li, Y. (2017). Pinning synchronization of memristor-based neural networks with time-varying delays. *Neural Networks*, 93, 143–151.
- Yu, J., Zhang, K., & Fei, S. (2010). Exponential stability criteria for discrete-time recurrent neural networks with time-varying delay. *Nonlinear Analysis: Real World Applications*, 11(1), 207–216.
- Zha, L., Fang, J., Li, X., & Liu, J. (2017). Event-triggered output feedback H_∞ control for networked Markovian jump systems with quantizations. *Nonlinear Analysis: Hybrid Systems*, 24, 146–158.
- Zhang, B., Xu, S., & Zou, Y. (2008). Improved delay-dependent exponential stability criteria for discrete-time recurrent neural networks with time-varying delays. *Neurocomputing*, 72, 321–330.
- Zhang, W., & Yu, L. (2009). Stability analysis for discrete-time switched time-delay systems. *Automatica*, 45(10), 2265–2271.
- Zhang, Y., Shi, Y., & Shi, P. (2017). Resilient and robust finite-time H_∞ control for uncertain discrete-time jump nonlinear systems. *Applied Mathematical Modelling*, 49, 612–629.
- Zhao, J., & Hu, Z. (2017). Exponential H_∞ control for singular systems with time-varying delay. *International Journal of Control, Automation and Systems*, 15, 1–8.



\mathcal{H}_∞ /passive non-fragile synchronisation of Markovian jump stochastic complex dynamical networks with time-varying delays

M. Syed Ali, M. Usha, O. M. Kwon, Nallappan Gunasekaran & Ganesh Kumar Thakur

To cite this article: M. Syed Ali, M. Usha, O. M. Kwon, Nallappan Gunasekaran & Ganesh Kumar Thakur (2021) \mathcal{H}_∞ /passive non-fragile synchronisation of Markovian jump stochastic complex dynamical networks with time-varying delays, International Journal of Systems Science, 52:7, 1270-1283, DOI: [10.1080/00207721.2020.1856445](https://doi.org/10.1080/00207721.2020.1856445)

To link to this article: <https://doi.org/10.1080/00207721.2020.1856445>



Published online: 29 Dec 2020.



Submit your article to this journal [↗](#)



Article views: 66



View related articles [↗](#)



View Crossmark data [↗](#)



Citing articles: 1 View citing articles [↗](#)



\mathcal{H}_∞ /passive non-fragile synchronisation of Markovian jump stochastic complex dynamical networks with time-varying delays

M. Syed Ali^a, M. Usha^a, O. M. Kwon^b, Nallappan Gunasekaran^c and Ganesh Kumar Thakur^d

^aDepartment of Mathematics, Thiruvalluvar University, Vellore, India; ^bSchool of Electrical Engineering, Chungbuk National University, Cheongju, Republic of Korea; ^cDepartment of Mathematical Sciences, Shibaura Institute of Technology, Saitama, Japan; ^dDepartment of Applied sciences, Krishna Engineering College, Ghaziabad, India

ABSTRACT

This paper deals with the problem of \mathcal{H}_∞ /passive non-fragile synchronisation for a class of complex dynamical networks subject to Markovian jumping time-varying coupling delays. Gain variation is represented by a stochastic variable that is assumed to satisfy the Bernoulli distribution with white sequences. The synchronisation error system became stable through our designed controller. By Lyapunov–Krasovskii stability theory, a new stochastic synchronisation criterion is established for the considered network in terms of linear matrix inequality (LMI). An illustration is given to show effectiveness of the proposed theoretical results.

ARTICLE HISTORY

Received 29 March 2019
Accepted 22 November 2020

KEYWORDS

Synchronization; complex dynamical networks; non-fragile control; Markov jump parameters; stochastic noise; time-varying delays

1. Introduction

In the last few years, the spearheading works of Watts and Strogatz in Watts and Strogatz (1998), Newman (2003), Syed Ali and Yogambigai (2016), and X. Wang and Chen (2003), which investigated complex networks have gained much attention as a result of its theoretical relevance and potential applications in most significant real-world networks, such as transportation networks, communication networks, social networks, biological networks, electric power grids and others. Complex network is commonly envisaged as a large set of interconnected nodes, in which each node represents a dynamical system and the edges represent connections. Particularly, the unpredictable system seen has ended up being very productive and turns into a key way to deal with researching complex networks of connecting objects. Thus, studies of complex behaviours in complex systems have in the fields of science and engineering (see Abhijit & Lewis, 2010; W. Guo et al., 2010; Lu & Ho, 2010; Qiu et al., 2020, 2019; Strogatz, 2001; Sun et al., 2020; M. Wang et al., 2020, 2018a, 2018b; Wu, Shi, et al., 2013; Yu et al., 2011; W. Zhang et al., 2014, and references therein).

Synchronization as a collective behaviour of networks, appears in a widespread field, ranging from natural networks to artificial networks such as flashing fireflies, brain web, yeast cell, semiconductor lasers, sensor networks. Because of the ubiquitousness of synchronisation, scientists attempt to understand the mechanism behind the phenomena and the way it works to get its advantages. For example, in sensor networks, the clock should be synchronised so that the sensor network can process data more correctly and in semiconductor lasers, they need to be synchronised in order to generate large power lasers (Behinfaraz & Badamchizadeh, 2018; Behinfaraz et al., 2019; Yu et al., 2011). Consisting of large amount of nodes, complex dynamical networks (CDNs) have been observed to show synchronisation in many cases, including both the manmade and the natural networks. Thus, the synchronisation phenomenon has received much attention among researchers (Cai et al., 2016; Du & Xu, 2014; Karimi & Gao, 2010; Lee et al., 2012; Qi et al., 2010; Yu & Cao, 2007; Yue & Lam, 2005; Zeng & Cao, 2011; Zhao & Zeng, 2010).

\mathcal{H}_∞ synchronisation control is an available mechanism for attenuating the effect of disturbances in

networks (X. G. Guo et al., 2015; H. Shen et al., 2015). \mathcal{H}_∞ synchronisation control is generally applied to the problem of optimal control. Designing an \mathcal{H}_∞ synchronisation controller for the stability of error system will refrain the interference. For example, \mathcal{H}_∞ synchronisation of complex networks the studied in B. Shen et al. (2011). Passive synchronisation analysis and design of complex systems, have paid much attention in the last decades (Selivanov et al., 2015). In Yao et al. (2009), passivity analysis for complex dynamical systems with and without coupling delay was investigated. The passivity theory becomes a powerful mechanism to synthesising complex neurons (Gao et al., 2007). Research on the \mathcal{H}_∞ and passive filtering, for a more flexible design where studied by many authors (Fang & Park, 2013; Wu, Park, Su, Song, et al., 2013; Yang et al., 2013).

On the other hand, Markovian jump systems introduced by Krasovskii and Lidskii (1961) have a crucial role in the area of control and operations research communities. Dynamic systems can be modelled by a special class of hybrid system such as Markovian jump complex dynamical networks. Markovian jumping systems have been one of the important research topics in the area of signal processing, control systems, and a good deal of results were available in the literature (see Alfa, 2004; Asmussenn & Kella, 2000; Barron, 2018a, 2018b, 2019; Barron & Yechiali, 2017; Breuer, 2010; Ross, 1969; Ruiz-Castro, 2016; Yang et al., 2013 and references therein). Markov jump systems are a class of hybrid systems and have attracted considerable attention because of their extensive application in modelling many practical systems with random abrupt changes in their structure and parameters including manufacturing systems, aerospace systems, etc. In Desouza and Fragoso (1993) and Wu et al. (2011), it has been shown that the switching between different modes can be governed by a Markovian chain and hence the neural networks with such a jumping character are actually a class of special Markovian jumping system (Dong et al., 2012). So far, a lot of results have been obtained on various analysis problems for Markovian jumping neural networks, for stability analysis and for passivity analysis. In literature, several works have been illustrated on Markovian jump complex dynamical networks (see Ma & Zheng, 2015; Yi et al., 2013 and references therein).

Actually, the evolution of many practical systems is always affected by various stochastic disturbances and uncertainties from unpredictable environmental conditions. Thus, stochastic modelling has been of great consequence in branches such as neurotransmitters. Dynamical behaviours of complex systems are mainly affected by the external disturbances. Therefore, synchronisation analysis for stochastic systems has received much research interest. A robust resilient control problem of discrete-time Markov jump nonlinear systems has been solved by employing the linear matrix inequality and stochastic analysis techniques (Y. Zhang et al., 2017). Based on the dissipative theory and the event-triggered sampling scheme, the non-fragile control design problem for a class of network-based singular systems with input time-varying delay and external disturbances has been addressed (Sakthivel et al., 2017). Therefore, it is reasonable to consider the non-fragile control design in the study of synchronisation of CDNs. Consequently, so far, investigations on \mathcal{H}_∞ /passive non-fragile synchronisation of Markovian jump stochastic complex dynamical networks with time-varying delays have not been considered until, now, which motivates this study.

This Motivates to study the \mathcal{H}_∞ /passive non-fragile synchronisation of Markovian jump stochastic CDNs with time-varying delays.

- (1) We proposed a mixed \mathcal{H}_∞ and passive performance index for dealing with the synchronisation control problem for CDNs. The synchronisation control problem based on the proposed index is a more general case.
- (2) The role of the designed controllers is analysed in detail by constructing a suitable comparison system.
- (3) The synchronisation criteria are derived according to whether the node systems in the CDNs or the goal system satisfies the corresponding conditions.
- (4) A novel Lyapunov functional is constructed which includes details of time-varying and non-fragile state feedback controllers.
- (5) Finally, an example is given to illustrate the effectiveness of our proposed method.

Notation: \mathbb{R}^n denotes the n -dimensional Euclidean space and $\mathbb{R}^{m \times n}$ is the $m \times n$ real matrices, respectively. $\mathcal{T}_1 > 0$ is real symmetric and positive definite.

A^T means the transpose of matrix A and the asterisk ‘*’ in a matrix is used to represent the term which is induced by symmetry. I is the identity matrix with compatible dimension. The symbol ‘ \otimes ’ stands for Kronecker product. \mathbb{E} is the mathematical expectation operator. Let $(\Gamma, \mathcal{E}, \mathcal{Q})$ be a Complete probability space which relatives to an increasing family $(\mathcal{E}_t)_{t>0}$ of σ -algebras $(\mathcal{E}_t)_{t>0} \subset \mathcal{E}$, where Γ is the sample space, \mathcal{E} is σ -algebra of subsets of the sample space and \mathcal{Q} is the probability measure on \mathcal{E} .

2. Problem formulation and preliminaries

The complex dynamical networks (CDNs) with Markovian jump parameters, outer coupling and stochastic noise, which consists of N identical nodes and is defined over the Wiener process is described as

$$\begin{aligned} dx_i(t) = & \left[\mathcal{A}(\eta(t))x_i(t) + f(t, x_i(t)) \right. \\ & + \sum_{j=1}^N E_{ij}C(\eta(t))x_j(t - \flat(t)) \\ & \left. + u_i(t) + w_i(t) \right] dt \\ & + \sigma(t, x_i(t), x_i(t - \flat(t)))d\omega(t), \\ Z(t) = & \mathcal{J}(\eta(t))x_i(t), \quad i = 1, 2, \dots, N, \end{aligned} \tag{1}$$

where $x_i(t) \in \mathbb{R}^n$ is the state variables of the i th node of the network and $u_i(t) \in \mathbb{R}^n$ is the control input of the i th node; $Z(t)$ is the output; $f(\cdot, \cdot) \in \mathbb{R}^n$ represents a non-linear vector-valued function; $\{\eta(t) \ (t > 0)\}$ is the continuous-time Markov process which describes the evolution of the mode at time t ; $\mathcal{A}(\eta(t))$ is a constant matrix with suitable dimensions; the function $\sigma(\cdot, \cdot, \cdot) : \mathbb{R} \times \mathbb{R}^n \times \mathbb{R}^n \rightarrow \mathbb{R}^n$ is the noise intensity vector-valued function; $\omega(t) = [\omega_1(t), \omega_2(t), \dots, \omega_m(t)]^T \in \mathbb{R}^m$ is an m -dimensional Brownian motion defined on the probability space $(\Gamma, \mathcal{E}, \mathcal{Q})$ with $\mathbb{E}\{\omega(t)\} = 0, \mathbb{E}\{\omega^2(t)\} = 1$ and $\mathbb{E}\{\omega(s)\omega(t)\} = 0$ for $s \neq t$, where \mathbb{E} is the mathematical expectation; $C(\eta(t)) \in \mathbb{R}^{n \times n}$ is a constant inner-coupling matrix of the nodes; $E = (E_{ij})_{N \times N}$ matrix of the outer-coupling matrix representing the topological structure of the complex networks; $w_i(t) \in \mathbb{R}^p$ stands for external disturbance which belongs to

$\mathcal{L}_2[0, \infty)$, $\mathcal{J}(\eta(t))$ is a known matrix with appropriate dimension. Which is defined as follows: if there is a connection between node i and j ($i \neq j$), then $E_{ij} = 1$, if i and j has connection ($i \neq j$), if there is no connection $E_{ij} = 0$.

The matrix E of diagonal elements for $i = 1, 2, \dots, N$ is defined as

$$E_{ii} = - \sum_{j=1, j \neq i}^N E_{ij}. \tag{2}$$

The function $\flat(t)$ satisfies,

$$0 \leq \flat_1 \leq \flat(t) \leq \flat_2, \quad 0 \leq \dot{\flat}(t) \leq \mu, \tag{3}$$

with \flat_1, \flat_2, μ , are scalars.

The process $\{\eta(t), t \geq 0\}$ is a right continuous-time homogeneous Markovian process, it takes values $\mathcal{S} = \{1, 2, \dots, \mathcal{N}\}$. More precisely, $\eta(t)$ is associated with the transition probability matrix $\Theta = \{\pi_{\rho j}\}, \forall \rho, j \in \mathcal{S}$ which is given by the following transition rates:

$$\begin{aligned} Pr(\eta(t + \Delta t) = j | \eta(t) = \rho) \\ = \begin{cases} \pi_{\rho j} \Delta t + o(\Delta t), & \text{if } \rho \neq j \\ 1 + \pi_{\rho \rho} \Delta t + o(\Delta t), & \text{if } \rho = j, \end{cases} \end{aligned} \tag{4}$$

where $\Delta t > 0$ and $\lim_{\Delta t \rightarrow 0} (o(\Delta t)/\Delta t) = 0$ and $\pi_{\rho j} \geq 0$ for $\rho \neq j$ is the transition rate from mode ρ at time t to mode j at time $t + \Delta$ and $\pi_{\rho \rho} = - \sum_{j=1, j \neq \rho}^{\mathcal{N}} \pi_{\rho j}$.

For convenience, each possible value of $\eta(t)$ is denoted by $\rho, \rho \in \mathcal{S}$ in the sequel. Then we have

$$\mathcal{A}(\eta(t)) = \mathcal{A}_\rho, \quad C(\eta(t)) = C_\rho, \quad \mathcal{J}(\eta(t)) = \mathcal{J}_\rho,$$

where $\mathcal{A}_\rho, C_\rho, \mathcal{J}_\rho$, for any $\rho \in \mathcal{S}$, are known constant matrices of appropriate dimensions.

$$\begin{aligned} dx_i(t) = & \left[\mathcal{A}_\rho x_i(t) + f(t, x_i(t)) \right. \\ & + \sum_{j=1}^N E_{ij}C_\rho x_j(t - \flat(t)) \\ & \left. + u_i(t) + w_i(t) \right] dt \\ & + \sigma(t, x_i(t), x_i(t - \flat(t)))d\omega(t), \\ Z(t) = & \mathcal{J}_\rho x_i(t), \quad i = 1, 2, \dots, N, \end{aligned} \tag{5}$$

To synchronise all the N identical nodes in the network (5) to a common value, let us define the synchronisation error vector as $e_i(t) = x_i(t) - s(t)$, where $s(t) \in \mathbb{R}^n$ is the state vector of the unforced isolated node that can be expressed as

$$ds(t) = [A_\rho s(t) + f(t, s(t))]dt, \quad (6)$$

and is assumed to be noise-free, that is, $\sigma(t, s(t), s(t) - \mathfrak{p}(t)) = 0$. Based on this error vector, we now choose a robust state feedback controller (1), which is insensitive to the uncertain perturbations or gain fluctuations and of the form:

$$u_i(t) = (K_\rho + \beta(t)\Delta K_\rho(t))e_i(t), \quad i = 1, 2, \dots, N, \quad (7)$$

where K_ρ is the controller gain matrix that is to be determined in the forthcoming section, The real-valued matrix $\Delta K_\rho(t)$ representing the controller gain fluctuations, and $\beta(t)$ is a stochastic variable describing the randomly occurring controller gain fluctuations. It is here assumed that $\Delta K_\rho(t)$ takes the form $\Delta K_\rho(t) = \mathcal{M}_\rho \Gamma_\rho(t) \mathcal{N}_\rho$, where \mathcal{M}_ρ and \mathcal{N}_ρ are known real constant matrices and $\Gamma_\rho(t)$ is an unknown time-varying matrix satisfying $\Gamma_\rho^T(t) \Gamma_\rho(t) \leq I$. Further, it is assumed that the stochastic variable $\beta(t)$ obeys the Bernoulli distribution with the following probability rules: (i) $\text{Prob}\{\beta(t) = 1\} = \mathbb{E}\{\beta(t)\} = \bar{\beta}$, and (ii) $\text{Prob}\{\beta(t) = 0\} = 1 - \mathbb{E}\{\beta(t)\} = 1 - \bar{\beta}$, where $\bar{\beta} \in [0, 1]$.

Subtracting (6) from (5) then by using (7), we can obtain the following closed-loop form of the error systems:

$$\begin{aligned} de_i(t) = & \left[A_\rho e_i(t) + g(t, e_i(t)) \right. \\ & + \sum_{j=1}^N E_{ij} C_\rho e_j(t - \mathfrak{p}(t)) + (K_\rho \\ & + \beta(t)\Delta K_\rho(t))e_i(t) + w_i(t) \left. \right] dt \\ & + \hat{\sigma}(t, e_i(t), e_i(t) - \mathfrak{p}(t))d\omega(t), \\ \hat{Z}(t) = & \mathcal{J}_\rho e_i(t), \quad i = 1, 2, \dots, N, \end{aligned} \quad (8)$$

where $g(t, e_i(t)) = f(t, x_i(t)) - f(t, s(t))$ and $\hat{\sigma}(t, e_i(t), e_i(t) - \mathfrak{p}(t)) = \sigma(t, x_i(t), x_i(t) - \mathfrak{p}(t)) - \sigma(t, s(t), s(t) - \mathfrak{p}(t))$. By using the Kronecker product

properties and mathematical manipulations, the error system (8) can be written in the following compact form:

$$\begin{aligned} de(t) = & \left[(A_\rho + K_\rho + \bar{\beta}\mathcal{M}_\rho \Gamma_\rho(t) \mathcal{N}_\rho \right. \\ & + (\beta(t) - \bar{\beta})\mathcal{M}_\rho \Gamma_\rho(t) \mathcal{N}_\rho)e(t) + G(t, e(t)) \\ & + (E \otimes C_\rho)e(t - \mathfrak{p}(t)) + w(t) \left. \right] dt \\ & + \hat{\sigma}(t, e(t), e(t) - \mathfrak{p}(t))d\omega(t), \\ \tilde{Z}(t) = & \mathcal{J}_\rho e(t), \end{aligned} \quad (9)$$

where

$$e(t) := \left[e_1^T(t), e_2^T(t), \dots, e_N^T(t) \right]^T,$$

$$\begin{aligned} G(t, e(t)) := & \left[g^T(t, e_1(t)), g^T(t, e_2(t)), \right. \\ & \left. \times \dots, g^T(t, e_N(t)) \right]^T, \end{aligned}$$

$$\begin{aligned} \hat{\sigma}(t, e(t), e(t) - \mathfrak{p}(t)) := & \left[\hat{\sigma}^T(t, e_1(t), e_1(t) - \mathfrak{p}(t)), \right. \\ & \times \hat{\sigma}^T(t, e_2(t), e_2(t) - \mathfrak{p}(t)), \\ & \times \dots, \hat{\sigma}^T(t, e_N(t), \\ & \left. \times e_N(t) - \mathfrak{p}(t)) \right]^T, \end{aligned}$$

$$w(t) := \left[w_1^T(t), w_2^T(t), \dots, w_N^T(t) \right]^T.$$

Assumption 2.1 (Syed Ali, 2014): The noise intensity function $\sigma(\cdot, \cdot, \cdot) : \mathbb{R}^+ \times \mathbb{R}^n \times \mathbb{R}^n \rightarrow \mathbb{R}^{n \times m}$ is uniformly Lipschitz continuous and also satisfies the linear growth conditions. Moreover,

$$\begin{aligned} & \text{Trace} \left\{ \hat{\sigma}^T(t, x_i(t), x_i(t) - \mathfrak{p}(t)) \right. \\ & \quad \left. \hat{\sigma}(t, x_i(t), x_i(t) - \mathfrak{p}(t)) \right\} \\ & \leq x_i^T(t) X x_i(t) + x_i^T(t - \mathfrak{p}(t)) Y x_i(t - \mathfrak{p}(t)), \end{aligned}$$

where X and Y are positive diagonal matrices with appropriate dimensions.

Assumption 2.2 (Z. Wang et al., 2006): For any $j \in \{1, 2, \dots, n\}$, $f_j(0) = 0$ and there exist constants F_j^- and F_j^+ such that

$$F_j^- \leq \frac{f_j(\alpha_1) - f_j(\alpha_2)}{\alpha_1 - \alpha_2} \leq F_j^+, \quad \forall \alpha_1 \neq \alpha_2. \quad (10)$$

Definition 2.1 (Joby et al., 2016): Given a weighting scalar $\sigma \in [0, 1]$, the synchronisation error system (9) is said to be asymptotically stable with a prescribed \mathcal{H}_∞ performance $\delta > 0$ if for all non-zero $w(t) \in \mathcal{L}_2[0, \infty)$, the response $\tilde{Z}(t)$ under the initial condition satisfies

$$\begin{aligned} & \int_0^{\mathcal{T}_p} \left[-\sigma \tilde{Z}^T(t) \tilde{Z}(t) + 2(1 - \sigma) \delta \tilde{Z}^T(t) w(t) \right] dt \\ & \geq -\delta^2 \int_0^{\mathcal{T}_p} [w^T(t) w(t)] dt, \end{aligned} \quad (11)$$

for any $\mathcal{T}_p \geq 0$ and any non-zero $w(t) \in \mathcal{L}_2[0, \infty)$.

Remark 2.1: It should be pointed out that the performance index in (11) is a mixed \mathcal{H}_∞ /passive index, which may reduce to the \mathcal{H}_∞ performance index or the passivity performance by tuning the weighting parameter σ . More specifically, when $\sigma = 0$, the expression in (11) becomes the passivity performance index; and when $\sigma = 1$, the expression in (11) degenerates into the \mathcal{H}_∞ performance index. When $\sigma \in (0, 1)$, the expression (11) stands for the mixed \mathcal{H}_∞ /passive performance index. Therefore, from an application viewpoint, our mixed \mathcal{H}_∞ /passive non-fragile controller design method is more convenient for users than some existing passive non-fragile controller design methods or \mathcal{H}_∞ non-fragile controller design methods.

Remark 2.2: The authors in Xu et al. (2006) and Lien et al. (2007), studied the non-fragile control for dynamical systems with time delays. In Xu et al. (2006), authors discussed the stabilisation and \mathcal{H}_∞ control for uncertain stochastic time delay systems via non-fragile controllers. The non-fragile observer-based control for linear systems via LMI approach was investigated in Lien et al. (2007). In Chen et al. (2011), authors pointed out the non-fragile observer-based \mathcal{H}_∞ control for neutral stochastic hybrid systems with time-varying delay. The non-fragile synchronisation of neural networks with time-varying delay and randomly occurring controller gain fluctuation have been studied in Fang and Park (2013). In Wu, Park, Su, and Chu (2013), authors analysed the non-fragile synchronisation control for complex networks with missing data. But in this paper, we have introduced the synchronisation for Markovian jumping CDNs with time-varying coupling delays. Moreover, we have introduced the non-fragile controller

and derived the sufficient conditions in terms of LMIs, using \mathcal{H}_∞ /passive synchronisation of stochastic analysis technique which makes the results less conservative.

Remark 2.3: The stochastic variable $\beta(t)$ is introduced by the motivation of Li et al. (2012), wherein the Bernoulli distributed sequence $\beta(t)$ was used to model the missing information of the system. In our work, we have used this to describe the probability of the random time-varying delay in different intervals.

Remark 2.4: It should be noted that, so far in the literature, several control approaches have been proposed for the synchronisation problem of several CDNs (Cai et al., 2016; Lee et al., 2012; M. J. Park et al., 2012), wherein the interconnection topology among the nodes are assumed to be fixed. However, in practice, this assumption is practically difficult or even impossible. However, yet now, there were no results reported in the existing literature for the synchronisation analysis of stochastic CDNs with Markovian jump parameters. According to this fact, in this paper, \mathcal{H}_∞ /passive synchronisation problem of Markovian jump stochastic CDNs with time-varying delays is investigated. Furthermore, due to random behaviour in the dynamics of stochastic CDNs, it is very difficult to determine the exact fixed control value. Therefore, in this paper, the feedback control gain is considered with uncertain terms, which is more significant to reflect the realistic scenarios.

Remark 2.5: As like the system defined in Syed Ali and Yogambigai (2018), my problem also contains the same system but by employing the innovative LKFs and utilising the Lemmas name we get the less conservative results.

Lemma 2.2 (N. Wang et al., 2016): For any constant matrix $M \in \mathbb{R}^{n \times n}$, $M^T = M > 0$, scalars α and β with $\alpha > \beta$ and vector $x : [\beta, \alpha] \rightarrow \mathbb{R}^n$, such that the following integrations are well defined, then

$$\begin{aligned} & -(\alpha - \beta) \int_\beta^\alpha x^T(s) M x(s) ds \\ & \leq - \left(\int_\beta^\alpha x(s) ds \right)^T M \left(\int_\beta^\alpha x(s) ds \right), \end{aligned}$$

$$\begin{aligned}
& -\frac{(\alpha - \beta)^2}{2} \int_{\beta}^{\alpha} \int_u^{\alpha} x^T(s) \mathcal{M}x(s) \mathrm{d}s \mathrm{d}u \\
& \leq -\left(\int_{\beta}^{\alpha} \int_u^{\alpha} x(s) \mathrm{d}s \mathrm{d}u \right)^T \\
& \quad \times \mathcal{M} \left(\int_{\beta}^{\alpha} \int_u^{\alpha} x(s) \mathrm{d}s \mathrm{d}u \right).
\end{aligned}$$

Lemma 2.3 (P. Park et al., 2011): Assume that Ω , \mathbf{M}_i and \mathbf{E}_i are real matrices with appropriate dimensions and $\mathbf{F}_i^T \mathbf{F}_i \leq I$. Then, the inequality $\Omega + \mathbf{M}_i \mathbf{F}_i \mathbf{E}_i + \mathbf{E}_i^T \mathbf{F}_i^T \mathbf{M}_i^T < 0$ holds if and only if there exists a scalar $\epsilon > 0$ satisfying $\Omega + \epsilon^{-1} \mathbf{M}_i \mathbf{M}_i^T + \epsilon \mathbf{E}_i^T \mathbf{E}_i < 0$ or equivalently

$$\begin{bmatrix} \Omega & \mathbf{M}_i & \epsilon \mathbf{E}_i^T \\ * & -\epsilon I & 0 \\ * & * & -\epsilon I \end{bmatrix} < 0. \quad (12)$$

Lemma 2.4 (Langville & Stewart, 2004): The properties of Kronecker product have the following properties:

- (1) $(\beta X) \otimes Y = X \otimes (\beta Y)$;
- (2) $(X + Y) \otimes Z = X \otimes Z + Y \otimes Z$;
- (3) $(X \otimes Y)(Z \otimes W) = (XZ) \otimes (YW)$;
- (4) $(X \otimes Y)^T = X^T \otimes Y^T$.

3. Main results

In this section, we present results for non-fragile synchronisation of complex dynamical networks with Markovian jumping parameters and stochastic noise.

Theorem 3.1: For given positive scalars $Q_1, Q_2, \mu, \delta, \bar{\beta} \in [0, 1]$, matrices \mathcal{J}_ρ , the network (9) is asymptotically stable in mean square with prescribed mixed \mathcal{H}_∞ and passivity performance level $\delta > 0$ under the non-fragile control (7), if there exist matrices $\mathcal{P}_\rho > 0, \mathcal{T}_1 > 0, \mathcal{T}_2 > 0, \mathcal{T}_3 > 0, \mathcal{U}_1 > 0, \mathcal{U}_2 > 0, \mathcal{U}_3 > 0, \mathcal{L}_1 > 0$, positive diagonal matrix \mathcal{Y} , and positive scalars λ_1, ϵ_1 such that the following matrix inequalities hold:

$$\mathcal{P}_\rho < \lambda_1 I, \quad \rho \in \mathcal{S} \quad (13)$$

$$\bar{\Omega}_\rho = \begin{bmatrix} [\Omega_{\rho lm}]_{10 \times 10} & \epsilon_1 \vartheta_\rho & \nu_\rho^T \\ * & -\epsilon_1 I & 0 \\ * & * & -\epsilon_1 I \end{bmatrix} < 0, \quad (14)$$

where

$$\begin{aligned}
\Omega_{\rho 11} &= \mathcal{P}_\rho \mathcal{A}_\rho + \mathcal{A}_\rho^T \mathcal{P}_\rho^T + \mathcal{P}_\rho \mathcal{K}_\rho + \mathcal{K}_\rho^T \mathcal{P}_\rho^T \\
&+ \sum_{j=1}^N \pi_{\rho j} \mathcal{P}_j + \lambda_1 \mathcal{R}_3 + \mathcal{T}_1 + \mathcal{T}_2 + \mathcal{T}_3 \\
&+ Q_1^2 \mathcal{U}_1 + Q_2^2 \mathcal{U}_2 + Q_2^2 \mathcal{U}_3 - \mathcal{F}_1 \mathcal{Y} + 2\sigma \mathcal{J}_\rho^T \mathcal{J}_\rho,
\end{aligned}$$

$$\Omega_{\rho 12} = \mathcal{P}_\rho (E \otimes C_\rho), \quad \Omega_{\rho 15} = \mathcal{P}_\rho + \mathcal{F}_2 \mathcal{Y},$$

$$\Omega_{\rho 19} = \mathcal{P}_\rho - 2(1 - \sigma) \delta \mathcal{J}_\rho^T,$$

$$\Omega_{\rho 22} = \lambda_1 \mathcal{R}_4 - (1 - \mu) \mathcal{T}_3,$$

$$\Omega_{\rho 33} = -\mathcal{T}_1 + Q_{12}^2 \mathcal{L}_1, \quad \Omega_{\rho 44} = -\mathcal{T}_2, \quad \Omega_{\rho 55} = -\mathcal{Y},$$

$$\Omega_{\rho 66} = -\mathcal{U}_1, \quad \Omega_{\rho 77} = -(1 - \mu) \mathcal{U}_2, \quad \Omega_{\rho 88} = -\mathcal{U}_3,$$

$$\Omega_{\rho 99} = -\delta^2 I, \quad \Omega_{\rho 1010} = -\mathcal{L}_1, \quad Q_{12} = Q_2 - Q_1,$$

$$\vartheta_\rho = [\bar{\beta} \mathcal{P}_\rho \mathcal{M}_\rho \quad 0 \quad 0 \quad 0 \quad 0 \quad 0 \quad 0 \quad 0 \quad 0 \quad 0]^T,$$

$$\nu_\rho = [\mathcal{N}_\rho \quad 0 \quad 0 \quad 0 \quad 0 \quad 0 \quad 0 \quad 0 \quad 0 \quad 0].$$

Proof: For each $\rho \in \mathcal{S}$, define $e_t = e(t + s)$, $-\mathfrak{b}_2 \leq s \leq 0$. Construct Lyapunov–Krasovskii functional as

$$V(e_t, \mathfrak{t}, \rho) = \sum_{n=1}^4 V_n(e_t, \mathfrak{t}, \rho), \quad (15)$$

where,

$$V_1(e_t, \mathfrak{t}, \rho) = e^T(\mathfrak{t}) \mathcal{P}_\rho e(\mathfrak{t}), \quad (16)$$

$$\begin{aligned}
V_2(e_t, \mathfrak{t}, \rho) &= \int_{\mathfrak{t}-\mathfrak{b}_1}^{\mathfrak{t}} e^T(s) \mathcal{T}_1 e(s) \mathrm{d}s \\
&+ \int_{\mathfrak{t}-\mathfrak{b}_2}^{\mathfrak{t}} e^T(s) \mathcal{T}_2 e(s) \mathrm{d}s \\
&+ \int_{\mathfrak{t}-\mathfrak{b}(\mathfrak{t})}^{\mathfrak{t}} e^T(s) \mathcal{T}_3 e(s) \mathrm{d}s, \quad (17)
\end{aligned}$$

$$\begin{aligned}
V_3(e_t, \mathfrak{t}, \rho) &= \mathfrak{b}_1 \int_{-\mathfrak{b}_1}^0 \int_{\mathfrak{t}+\theta}^{\mathfrak{t}} e^T(s) \mathcal{U}_1 e(s) \mathrm{d}s \mathrm{d}\theta \\
&+ \mathfrak{b}_{12} \int_{-\mathfrak{b}_2}^{-\mathfrak{b}_1} \int_{\mathfrak{t}+\theta}^{\mathfrak{t}-\mathfrak{b}_1} e^T(s) \mathcal{L}_1 e(s) \mathrm{d}s \mathrm{d}\theta, \quad (18)
\end{aligned}$$

$$\begin{aligned}
V_4(e_t, \mathfrak{t}, \rho) &= \mathfrak{b}_2 \int_{-\mathfrak{b}(\mathfrak{t})}^0 \int_{\mathfrak{t}+\theta}^{\mathfrak{t}} e^T(s) \mathcal{U}_2 e(s) \mathrm{d}s \mathrm{d}\theta \\
&+ \mathfrak{b}_2 \int_{-\mathfrak{b}_2}^0 \int_{\mathfrak{t}+\theta}^{\mathfrak{t}} e^T(s) \mathcal{U}_3 e(s) \mathrm{d}s \mathrm{d}\theta, \quad (19)
\end{aligned}$$

with $\mathcal{P}_\rho > 0, \mathcal{T}_v (v = 1, 2, 3), \mathcal{U}_v (v = 1, 2, 3), \mathcal{L}_1, \mathfrak{b}_{12} = \mathfrak{b}_2 - \mathfrak{b}_1$. ■

Based on Ito’s differential formula (He et al., 2016), stochastic derivative of $V(e_t, t, \rho)$ can be calculated by

$$dV(e_t, t, \rho) = \mathcal{L}V(e_t, t, \rho) + V_e(e_t, t, \rho)\sigma(t, e(t)) \times e(t - \mathfrak{p}(t))d\mathfrak{w}(t), \tag{20}$$

where

$$\begin{aligned} \mathcal{L}V(e_t, t, \rho) &= \mathcal{L}V_1(e_t, t, \rho) + \mathcal{L}V_2(e_t, t, \rho) \\ &\quad + \mathcal{L}V_3(e_t, t, \rho) + \mathcal{L}V_4(e_t, t, \rho) \quad \text{and} \\ V_e(e_t, t, \rho) &= \frac{\partial V(e_t, t, \rho)}{\partial e}. \end{aligned}$$

The derivative of $V(e_t, t, \rho)$ along trajectories of (9), can be calculated as,

$$\begin{aligned} \mathcal{L}V_1(e_t, t, \rho) &= 2e^T(t)\mathcal{P}_\rho[(\mathcal{A}_\rho + \mathcal{K}_\rho \\ &\quad + \beta(t)(\mathcal{M}_\rho\Gamma_\rho(t)\mathcal{N}_\rho) \\ &\quad + (\beta(t) - \bar{\beta})(\mathcal{M}_\rho\Gamma_\rho(t)\mathcal{N}_\rho)e(t) \\ &\quad + G(t, e(t)) + (E \otimes \mathcal{C}_\rho)e(t - \mathfrak{p}(t)) \\ &\quad + w(t)]d\mathfrak{t} + \sum_{j=1}^N \pi_{\rho j}e^T(t)\mathcal{P}_j e(t) \\ &\quad + \text{Trace}\left\{\hat{\sigma}^T(t, e(t), e(t - \mathfrak{p}(t))) \right. \\ &\quad \left. \times \mathcal{P}_\rho \hat{\sigma}(t, e(t), e(t - \mathfrak{p}(t)))\right\}, \tag{21} \end{aligned}$$

$$\begin{aligned} \mathcal{L}V_2(e_t, t, \rho) &\leq e^T(t)(\mathcal{T}_1 + \mathcal{T}_2 + \mathcal{T}_3)e(t) \\ &\quad - e^T(t - \mathfrak{p}_1)\mathcal{T}_1 e(t - \mathfrak{p}_1) \\ &\quad - e^T(t - \mathfrak{p}_2)\mathcal{T}_2 e(t - \mathfrak{p}_2) \\ &\quad - (1 - \mu)e^T(t - \mathfrak{p}(t))\mathcal{T}_3 e(t - \mathfrak{p}(t)), \tag{22} \end{aligned}$$

$$\begin{aligned} \mathcal{L}V_3(e_t, t, \rho) &= \mathfrak{p}_1^2 e^T(t)\mathcal{U}_1 e(t) \\ &\quad - \mathfrak{p}_1 \int_{t-\mathfrak{p}_1}^t e^T(s)\mathcal{U}_1 e(s)d\mathfrak{s} \\ &\quad + \mathfrak{p}_{12}^2 e^T(t - \mathfrak{p}_1)\mathcal{L}_1 e(t - \mathfrak{p}_1) \\ &\quad - \mathfrak{p}_{12} \int_{t-\mathfrak{p}_2}^{t-\mathfrak{p}_1} e^T(s)d\mathfrak{s}\mathcal{L}_1 e(s)d\mathfrak{s}, \tag{23} \end{aligned}$$

$$\begin{aligned} \mathcal{L}V_4(e_t, t, \rho) &= \mathfrak{p}_2^2 e^T(t)(\mathcal{U}_2 + \mathcal{U}_3)e(t) \\ &\quad - \mathfrak{p}_2(1 - \mu) \int_{t-\mathfrak{p}(t)}^t e^T(s)\mathcal{U}_2 e(s)d\mathfrak{s} \\ &\quad - \mathfrak{p}_2 \int_{t-\mathfrak{p}_2}^t e^T(s)\mathcal{U}_3 e(s)d\mathfrak{s}. \tag{24} \end{aligned}$$

Further, by using Jensen’s single integral inequality (N. Wang et al., 2016) in (24) and (25), we can get the following inequalities:

$$\begin{aligned} &- \mathfrak{p}_1 \int_{t-\mathfrak{p}_1}^t e^T(s)\mathcal{U}_1 e(s)d\mathfrak{s} \\ &\leq - \int_{t-\mathfrak{p}_1}^t e^T(s)d\mathfrak{s}\mathcal{U}_1 \int_{t-\mathfrak{p}_1}^t e(s)d\mathfrak{s}, \tag{25} \end{aligned}$$

$$\begin{aligned} &- \mathfrak{p}_{12} \int_{t-\mathfrak{p}_2}^{t-\mathfrak{p}_1} e^T(s)d\mathfrak{s}\mathcal{L}_1 e(s)d\mathfrak{s} \\ &\leq - \int_{t-\mathfrak{p}_2}^{t-\mathfrak{p}_1} e^T(s)d\mathfrak{s}\mathcal{L}_1 \int_{t-\mathfrak{p}_2}^{t-\mathfrak{p}_1} e(s)d\mathfrak{s}, \tag{26} \end{aligned}$$

$$\begin{aligned} &- \mathfrak{p}_2 \int_{t-\mathfrak{p}(t)}^t e^T(s)\mathcal{U}_2 e(s)d\mathfrak{s} \\ &\leq - \int_{t-\mathfrak{p}(t)}^t e^T(s)d\mathfrak{s}\mathcal{U}_2 \int_{t-\mathfrak{p}(t)}^t e(s)d\mathfrak{s}, \tag{27} \end{aligned}$$

$$\begin{aligned} &- \mathfrak{p}_2 \int_{t-\mathfrak{p}_2}^t e^T(s)\mathcal{U}_3 e(s)d\mathfrak{s} \\ &\leq - \int_{t-\mathfrak{p}_2}^t e^T(s)d\mathfrak{s}\mathcal{U}_3 \int_{t-\mathfrak{p}_2}^t e(s)d\mathfrak{s}. \tag{28} \end{aligned}$$

On the other hand, Assumption 2.1 and condition (13) gives that

$$\begin{aligned} &\text{Trace}\left\{\sigma^T(t, (t), e(t - \mathfrak{p}(t)))\mathcal{P}_\rho \cdot \sigma(t, (t) \right. \\ &\quad \left. \times, e(t - \mathfrak{p}(t)))\right\} \\ &\leq \lambda_1 \cdot \text{Trace}\left\{\sigma^T(t, (t), e(t - \mathfrak{p}(t)))\sigma(t, (t), \right. \\ &\quad \left. \times e(t - \mathfrak{p}(t)))\right\} \\ &\leq \lambda_1 \cdot \left[e^T(t)\mathcal{R}_3 e(t) + e^T(t - \mathfrak{p}(t)) \right. \\ &\quad \left. \times \mathcal{R}_4 e(t - \mathfrak{p}(t)) \right], \tag{29} \end{aligned}$$

where λ_1 are positive scalars and $\mathcal{R}_3, \mathcal{R}_4$ are known constant matrices.

Moreover, according to Assumption 2.2, for positive diagonal matrix \mathcal{Y} , the following inequality hold:

$$\begin{aligned} &\begin{bmatrix} e(t) \\ F(t, e(t)) \end{bmatrix}^T \begin{bmatrix} F_1\mathcal{Y} & -F_2\mathcal{Y} \\ -F_2\mathcal{Y} & \mathcal{Y} \end{bmatrix} \begin{bmatrix} e(t) \\ F(t, e(t)) \end{bmatrix} \leq 0. \tag{30} \end{aligned}$$

From, (20)–(30), taking both sides mathematical expectation we get,

$$\begin{aligned} \mathbb{E} \left[\frac{dV(e_t, t, \rho)}{dt} \right] &= \mathbb{E}[\mathcal{L}V(e_t, t, \rho)], \\ &= \mathbb{E} \left[\eta^T(t) \left(\widehat{\Theta} + \vartheta_\rho \Gamma_\rho(t) \nu_\rho \right. \right. \\ &\quad \left. \left. + (\vartheta_\rho \Gamma_\rho(t) \nu_\rho)^T \right) \eta(t) \right], \end{aligned} \quad (31)$$

where

$$\widehat{\Theta} = \left[\widehat{\Theta}_{l,m} \right], \quad l, m = 1, 2, \dots, 10,$$

with

$$\begin{aligned} \widehat{\Theta}_{11} &= \mathcal{P}_\rho \mathcal{A}_\rho + \mathcal{A}_\rho^T \mathcal{P}_\rho^T + \mathcal{P}_\rho \mathcal{K}_\rho + \mathcal{K}_\rho^T \mathcal{P}_\rho^T \\ &\quad + \sum_{j=1}^N \pi_{\rho_j} \mathcal{P}_j + \lambda_1 \mathcal{R}_3 + \mathcal{T}_1 + \mathcal{T}_2 + \mathcal{T}_3 \\ &\quad + \mathfrak{b}_1^2 \mathcal{U}_1 + \mathfrak{b}_2^2 \mathcal{U}_2 + \mathfrak{b}_2^2 \mathcal{U}_3 - \mathcal{F}_1 \mathcal{Y}, \\ \widehat{\Theta}_{12} &= \mathcal{P}_\rho (E \otimes C_\rho), \quad \widehat{\Theta}_{15} = \mathcal{P}_\rho + \mathcal{F}_2 \mathcal{Y}, \\ \widehat{\Theta}_{19} &= \mathcal{P}_\rho, \quad \widehat{\Theta}_{22} = \lambda_1 \mathcal{R}_4 - (1 - \mu) \mathcal{T}_3, \\ \widehat{\Theta}_{33} &= -\mathcal{T}_1 + \mathfrak{b}_1^2 \mathcal{L}_1, \quad \widehat{\Theta}_{44} = -\mathcal{T}_2, \\ \widehat{\Theta}_{55} &= -\mathcal{Y}, \quad \widehat{\Theta}_{66} = -\mathcal{U}_1, \quad \widehat{\Theta}_{77} = -(1 - \mu) \mathcal{U}_2, \\ \widehat{\Theta}_{88} &= -\mathcal{U}_3, \quad \widehat{\Theta}_{99} = 0, \widehat{\Theta}_{1010} = -\mathcal{L}_1, \\ \mathfrak{b}_{12} &= \mathfrak{b}_2 - \mathfrak{b}_1. \end{aligned}$$

Based on Lemma 2.3 for any positive scalar ϵ_1 , the right-hand side of (31) can equivalently be written as

$$\begin{aligned} &\widehat{\Theta}_{10 \times 10} + \vartheta_\rho \Gamma_\rho(t) \nu_\rho + (\vartheta_\rho \Gamma_\rho(t) \nu_\rho)^T \\ &\leq \widehat{\Theta}_{10 \times 10} + \epsilon_1 \vartheta_\rho \nu_\rho + \epsilon_1 \vartheta_\rho^T \nu_\rho. \end{aligned} \quad (32)$$

By applying Schur complement Lemma, the inequalities (32) becomes,

$$\bar{\Theta}_\rho = \begin{bmatrix} \widehat{\Theta}_{10 \times 10} & \epsilon_1 \vartheta_\rho & \nu_\rho^T \\ * & -\epsilon_1 I & 0 \\ * & * & -\epsilon_1 I \end{bmatrix} < 0, \quad (33)$$

we get

$$\mathbb{E}[\mathcal{L}V(e_t, t, \rho)] \leq \mathbb{E} \left[\eta^T(t) \bar{\Theta}_\rho \eta(t) \right] < 0. \quad (34)$$

Hence, using Lyapunov stability approach, we can conclude, the stochastic system (9) is asymptotically stable in mean square.

Next, we study the mixed \mathcal{H}_∞ passivity performance of system (9) with non-zero disturbance input ($w(t) \neq 0$) for any $t > 0$. Now, we define

$$\begin{aligned} J_{zv}(t) &= \mathbb{E} \left\{ \int_0^{T_p} \left[\sigma \tilde{Z}^T(t) \tilde{Z}(t) - 2(1 - \sigma) \delta \tilde{Z}^T(t) w(t) \right. \right. \\ &\quad \left. \left. - \delta^2 w^T(t) w(t) \right] dt \right\}, \quad t \geq 0, \end{aligned} \quad (35)$$

and we can see that,

$$\begin{aligned} J_{zv}(t) &= \mathbb{E} \left\{ \int_0^{T_p} \left[\sigma \tilde{Z}^T(t) \tilde{Z}(t) - 2(1 - \sigma) \delta \tilde{Z}^T(t) w(t) \right. \right. \\ &\quad \left. \left. - \delta^2 w^T(t) w(t) + \mathcal{L}V(e_t, t, \rho) \right] dt \right\} \\ &= \mathbb{E} \left[\int_0^t \eta^T(s) \bar{\Omega}_\rho \eta(s) ds \right], \end{aligned} \quad (36)$$

where

$$\begin{aligned} \eta(t) &= \begin{bmatrix} e^T(t) & e^T(t - \mathfrak{b}(t)) & e^T(t - \mathfrak{b}_1) \\ e^T(t - \mathfrak{b}_2) & F^T(t, e(t)) & \int_{t-\mathfrak{b}_1}^t e^T(s) ds \\ \int_{t-\mathfrak{b}(t)}^t e^T(s) ds & \int_{t-\mathfrak{b}_2}^t e^T(s) ds \\ w^T(t) & \int_{t-\mathfrak{b}_2}^{t-\mathfrak{b}_1} e^T(s) ds \end{bmatrix}^T, \end{aligned}$$

and $\bar{\Omega}_\rho$ is given (14). Hence for $w(t) \neq 0$ we get, $J_{zv}(t) < 0$, and (11) satisfies. Therefore, for any non-zero $w(t) \in [0, \infty)$, (11) holds for all $t > 0$.

Hence by Definition 2.1, gives the asymptotic stability in mean square of the system (9).

Theorem 3.2: For given positive scalars $Q_1, Q_2, \mu, \delta, \bar{\beta} \in [0, 1]$, matrices \mathcal{T}_ρ , the network (9) is asymptotically stable in mean square with prescribed mixed \mathcal{H}_∞ and passivity performance level δ under the non-fragile control (7), if there exist symmetric matrices $\mathcal{X}_\rho > 0, \widehat{\mathcal{P}}_\rho > 0, \widehat{\mathcal{T}}_\rho > 0$ ($l = 1, 2, 3$), $\widehat{\mathcal{U}}_{\nu\rho} > 0$ ($\nu = 1, 2, 3$), $\widehat{\mathcal{L}}_{1\rho} > 0$, any matrices \mathcal{Z}_ρ with appropriate dimensions, positive diagonal matrix \mathcal{Y} , and positive scalars $\widehat{\lambda}_1 > 0, \epsilon_1$ such that the following matrix inequalities hold:

$$\mathcal{X}_\rho - \widehat{\lambda}_1 I > 0, \quad \rho \in \mathcal{S}, \quad (37)$$

$$\widehat{\bar{\Omega}}_\rho = \left[\widehat{\bar{\Omega}}_{\rho lm} \right]_{15 \times 15} < 0, \quad (38)$$

where

$$\begin{aligned}\widehat{\Omega}_{\rho 11} &= \mathcal{A}_\rho \mathcal{X}_\rho + \mathcal{X}_\rho \mathcal{A}_\rho^T + \mathcal{Z}_\rho + \mathcal{Z}_\rho^T + \widehat{\mathcal{T}}_{1\rho} + \widehat{\mathcal{T}}_{2\rho} \\ &\quad + \widehat{\mathcal{T}}_{3\rho} + Q_1^2 \widehat{\mathcal{U}}_{1\rho} + Q_2^2 \widehat{\mathcal{U}}_{2\rho} + Q_3^2 \widehat{\mathcal{U}}_{3\rho} - F_1 \widehat{\mathcal{Y}} \\ &\quad + \pi_{\rho\rho}(h) \mathcal{X}_\rho, \quad \widehat{\Omega}_{\rho 12} = (E \otimes \mathcal{C}_\rho) \mathcal{X}_\rho, \\ \widehat{\Omega}_{\rho 15} &= \widehat{\mathcal{P}}_\rho + F_2 \widehat{\mathcal{Y}}, \quad \widehat{\Omega}_{\rho 19} = I - 2(1 - \sigma) \delta \mathcal{X}_\rho \mathcal{J}_\rho^T, \\ \widehat{\Omega}_{\rho 111} &= \bar{\beta} \mathcal{M}_\rho, \quad \widehat{\Omega}_{\rho 112} = \mathcal{X}_\rho \mathcal{N}_\rho, \quad \widehat{\Omega}_{\rho 113} = \mathcal{X}_\rho \sqrt{\mathcal{R}_3}, \\ \widehat{\Omega}_{\rho 114} &= \left[\sqrt{\pi_{\rho 1}} \mathcal{X}_\rho^T, \dots, \sqrt{\pi_{\rho(\rho-1)}} \mathcal{X}_\rho^T, \right. \\ &\quad \left. \times \sqrt{\pi_{\rho(\rho+1)}} \mathcal{X}_\rho^T, \dots, \sqrt{\pi_{\rho N}} \mathcal{X}_\rho^T \right], \\ \widehat{\Omega}_{\rho 115} &= \mathcal{X}_\rho \mathcal{J}_\rho, \quad \widehat{\Omega}_{\rho 22} = -(1 - \mu) \widehat{\mathcal{T}}_{3\rho}, \\ \widehat{\Omega}_{\rho 213} &= \mathcal{X}_\rho \sqrt{\mathcal{R}_4}, \quad \widehat{\Omega}_{\rho 33} = -\widehat{\mathcal{T}}_{1\rho} + Q_{12}^2 \widehat{\mathcal{L}}_{1\rho}, \\ \widehat{\Omega}_{\rho 44} &= -\widehat{\mathcal{T}}_{2\rho}, \quad \widehat{\Omega}_{\rho 55} = \widehat{\mathcal{Y}}, \quad \widehat{\Omega}_{\rho 66} = -\widehat{\mathcal{U}}_{1\rho}, \\ \widehat{\Omega}_{\rho 77} &= -(1 - \mu) \widehat{\mathcal{U}}_{2\rho}, \quad \widehat{\Omega}_{\rho 88} = -\widehat{\mathcal{U}}_{3\rho}, \\ \widehat{\Omega}_{\rho 99} &= -\delta^2 I, \quad \widehat{\Omega}_{\rho 1010} = -\widehat{\mathcal{L}}_{1\rho}, \quad \widehat{\Omega}_{\rho 1111} = -\epsilon_1 I, \\ \widehat{\Omega}_{\rho 1212} &= -\epsilon_1 I, \quad \widehat{\Omega}_{\rho 1313} = -\widehat{\lambda}_1 I, \\ \widehat{\Omega}_{\rho 1414} &= -\text{diag} \left[\mathcal{X}_1, \dots, \mathcal{X}_{\rho-1}, \right. \\ &\quad \left. \times \mathcal{X}_{\rho+1}, \dots, \mathcal{X}_N \right], \\ \widehat{\Omega}_{\rho 1515} &= -\sigma I, \quad \widehat{\lambda}_1 = -\frac{1}{\lambda_1},\end{aligned}$$

Other terms $\widehat{\Omega}_{\rho lm}$ are defined in Theorem 3.2. The feedback controller gain matrices in (7) are computed by $\mathcal{K}_\rho = \mathcal{Z}_\rho \mathcal{X}_\rho^{-1}$.

Proof: Let $\mathcal{X}_\rho = \mathcal{P}_\rho^{-1}$ and pre and post multiply the matrix $\widehat{\Omega}_\rho$ by $\text{diag}\{\mathcal{X}_\rho, \mathcal{X}_\rho, \mathcal{X}_\rho, \mathcal{X}_\rho, \mathcal{X}_\rho, \mathcal{X}_\rho, \mathcal{X}_\rho, \mathcal{X}_\rho, I, \mathcal{X}_\rho, I, I\}$.

Now, we introduce the following new variables: $\mathcal{X}_\rho \widehat{\mathcal{T}}_l \mathcal{X}_\rho = \widehat{\mathcal{T}}_{l\rho}$ ($l = 1, 2, 3$), $\mathcal{X}_\rho \mathcal{U}_v \mathcal{X}_\rho = \widehat{\mathcal{U}}_{v\rho}$ ($v = 1, 2, 3$), $\mathcal{X}_\rho \mathcal{L}_1 \mathcal{X}_\rho = \widehat{\mathcal{L}}_{1\rho}$, $\mathcal{X}_\rho \mathcal{P}_\rho \mathcal{X}_\rho = \widehat{\mathcal{P}}_\rho$ and $\mathcal{Z}_\rho = \mathcal{K}_\rho \mathcal{X}_\rho$.

Moreover, the conditions in (37) can be obtained from (13), (14), respectively, which are the desired conditions. Hence, the proof is completed. ■

Remark 3.1: The two stochastic variables satisfying Bernoulli random binary distributions are adopted to character the randomly occurring phenomena in the synchronisation problem for complex dynamical networks. It can be observed that when $\bar{\beta} = 1$, the controllers (9) are degenerated to the general non-fragile controllers. By utilising the stochastic information, a

better synchronisation performance can be obtained with less conservatism.

Remark 3.2: It is noted that the non-fragile stochastic Markov jump synchronisation problem for CDNs (9) in Theorem 3.2 and the desired controllers can be obtained when LMIs (36) are feasible then it is solvable (Figure 1).

4. Numerical example

In this section, a numerical example is presented to demonstrate the effectiveness of the proposed synchronisation control scheme for the complex dynamical network (9).

Example 4.1: Stochastic Markov jump CDNs with 3-nodes and modes 2, is considered as

$$\begin{aligned}d[e(t)] &= \left[(\mathcal{A}_\rho + \mathcal{K}_\rho + \bar{\beta} \mathcal{M}_\rho \Gamma_\rho(t) \mathcal{N}_\rho \right. \\ &\quad \left. + (\beta(t) - \bar{\beta}) \mathcal{M}_\rho \Gamma_\rho(t) \mathcal{N}_\rho) e(t) + G(t, e(t)) \right. \\ &\quad \left. + (E \otimes \mathcal{C}_\rho) e(t - \mathfrak{p}(t)) + w(t) \right] dt \\ &\quad + \hat{\rho}(t, e(t), e(t - \mathfrak{p}(t))) d\omega(t),\end{aligned}$$

$$\tilde{Z}(t) = \mathcal{J}_\rho e(t),$$

with the parameters

$$\begin{aligned}\mathcal{A}_1 &= \begin{bmatrix} 0.5 & 0 \\ 0 & 0.5 \end{bmatrix}, \quad \mathcal{C}_1 = \begin{bmatrix} 0.3 & 0 \\ 0 & 0.3 \end{bmatrix}, \\ \mathcal{A}_2 &= \begin{bmatrix} 2.5 & 0 \\ 0 & 2.5 \end{bmatrix}, \quad \mathcal{C}_2 = \begin{bmatrix} 0.2 & 0 \\ 0 & 0.4 \end{bmatrix}, \\ \mathcal{F}_2 &= \begin{bmatrix} 0.5 & 0 \\ 0 & 0.5 \end{bmatrix}.\end{aligned}$$

It is clear to see that $f(t, x_i(t))$ satisfies Assumption 2.2, and $\mathcal{F}_1 = 0$. In this example, we consider the Markov jump topology with two modes, the outer coupling matrix is assumed to be

$$E = \begin{bmatrix} -2 & 1 & 1 \\ 1 & -1 & 0 \\ 1 & 0 & -1 \end{bmatrix}.$$

Then it is easy to verify that $\mathfrak{p}_1 = 0.1327$, $\mathfrak{p}_2 = 0.04$, $\sigma = 0.5$, $\mu = 0.01$, $\delta = 0.4036$ and

$$\begin{aligned}\mathcal{R}_3 &= \begin{bmatrix} 0.5 & 0 \\ 0 & 0.5 \end{bmatrix}, \quad \mathcal{R}_4 = \begin{bmatrix} 0.6 & 0 \\ 0 & 0.6 \end{bmatrix}, \\ \mathcal{J}_1 &= \begin{bmatrix} 2 & 4 \\ 3 & 4 \end{bmatrix}.\end{aligned}$$

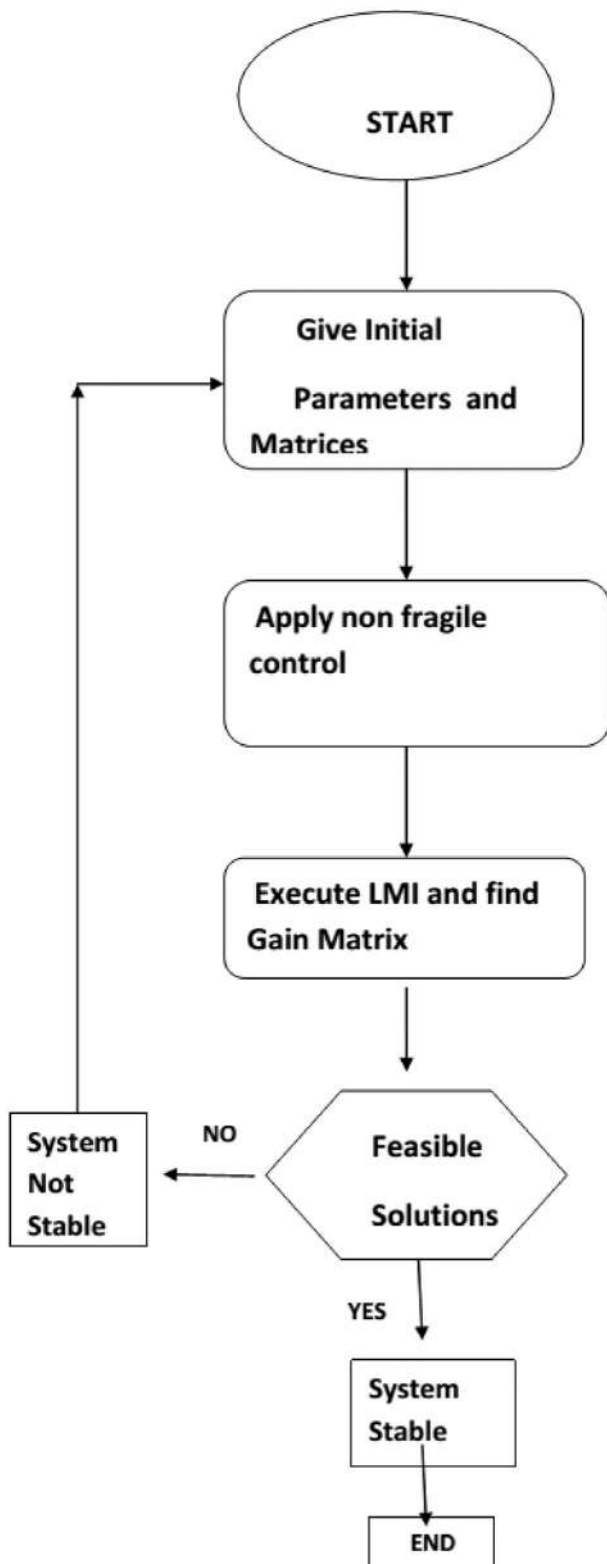


Figure 1. Flow graph of the proposed method.

The stochastic variable representing the controller gain fluctuations is chosen as $\beta(t) = 0.25 + 0.25 \sin(t)$. Furthermore, the uncertain matrices in the control gain are taken as

$$\mathcal{M}_1 = \begin{bmatrix} 0.01 & 0.1 \\ 0.02 & 0.02 \end{bmatrix}, \quad \mathcal{M}_2 = \begin{bmatrix} 0.02 & 0.02 \\ 0.03 & 0.01 \end{bmatrix},$$

$$\mathcal{N}_1 = \begin{bmatrix} 0.01 & 0.02 \\ 0.01 & 0.03 \end{bmatrix}, \quad \mathcal{N}_2 = \begin{bmatrix} 0.02 & 0.01 \\ 0.01 & 0.01 \end{bmatrix},$$

and $\Gamma_\rho(t) = \sin(t)$. By solving (37), (38) we get the following solutions:

$$\mathcal{P}_1 = \begin{bmatrix} -5.7174 & 0.0044 \\ 0.0044 & -5.7131 \end{bmatrix},$$

$$\mathcal{P}_2 = \begin{bmatrix} -5.7136 & 0.0033 \\ 0.0033 & -5.7163 \end{bmatrix},$$

$$\mathcal{Y} = \begin{bmatrix} 11.9073 & 0 \\ 0 & 11.9073 \end{bmatrix},$$

$$\mathcal{T}_{11} = \begin{bmatrix} 10.6298 & 0.0214 \\ 0.0214 & 10.5908 \end{bmatrix},$$

$$\mathcal{T}_{21} = \begin{bmatrix} 10.5379 & 0.0214 \\ 0.0214 & 10.4989 \end{bmatrix},$$

$$\mathcal{T}_{31} = \begin{bmatrix} 10.5645 & -0.0288 \\ -0.0288 & 10.5385 \end{bmatrix},$$

$$\mathcal{T}_{12} = \begin{bmatrix} 10.6007 & 0.0270 \\ 0.0270 & 10.6096 \end{bmatrix},$$

$$\mathcal{T}_{22} = \begin{bmatrix} 10.5088 & 0.0270 \\ 0.0270 & 10.5178 \end{bmatrix},$$

$$\mathcal{T}_{32} = \begin{bmatrix} 10.5097 & -0.0484 \\ -0.0484 & 10.5345 \end{bmatrix},$$

$$\mathcal{U}_{11} = \begin{bmatrix} 11.4159 & 0.0004 \\ 0.0004 & 11.4152 \end{bmatrix},$$

$$\mathcal{U}_{21} = \begin{bmatrix} 11.5294 & 0.0000 \\ 0.0000 & 11.5293 \end{bmatrix},$$

$$\mathcal{U}_{31} = \begin{bmatrix} 11.4159 & 0.0004 \\ 0.0004 & 11.4152 \end{bmatrix},$$

$$\mathcal{U}_{12} = \begin{bmatrix} 11.4153 & 0.0005 \\ 0.0005 & 11.4155 \end{bmatrix},$$

$$\mathcal{U}_{22} = \begin{bmatrix} 11.5293 & 0.0001 \\ 0.0001 & 11.5293 \end{bmatrix},$$

$$\mathcal{U}_{32} = \begin{bmatrix} 11.4153 & 0.0005 \\ 0.0005 & 11.4155 \end{bmatrix},$$

$$\mathcal{Z}_1 = \begin{bmatrix} -25.7784 & 1.2256 \\ 1.2256 & -26.9589 \end{bmatrix},$$

$$\mathcal{Z}_2 = \begin{bmatrix} -26.7399 & 1.5280 \\ 1.5280 & -26.3696 \end{bmatrix},$$

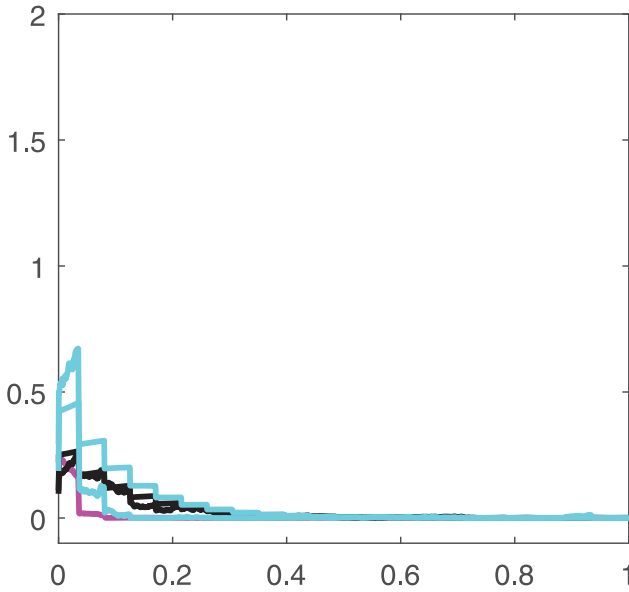


Figure 2. Error trajectories of the system in Example with node 3.

$$\mathcal{X}_1 = \begin{bmatrix} 0.1391 & 0.1353 \\ 0.1353 & 0.1384 \end{bmatrix},$$

$$\mathcal{X}_2 = \begin{bmatrix} 0.1033 & 0.0990 \\ 0.0990 & 0.1018 \end{bmatrix},$$

$$\mathcal{L}_{11} = \begin{bmatrix} 11.4178 & 0.0002 \\ 0.0002 & 11.4175 \end{bmatrix},$$

$$\mathcal{L}_{12} = \begin{bmatrix} 11.4175 & 0.0003 \\ 0.0003 & 11.4176 \end{bmatrix}.$$

The corresponding non-fragile controller gain matrices obtained are as follows (Figure 2):

$$\mathcal{K}_1 = 10^3 \begin{bmatrix} -3.9494 & 3.8698 \\ 4.0378 & -4.1422 \end{bmatrix},$$

$$\mathcal{K}_2 = 10^3 \begin{bmatrix} -4.0304 & 3.9358 \\ 3.8810 & -4.0340 \end{bmatrix},$$

$$\epsilon_1 = 12.2138, \quad \hat{\lambda}_1 = -\frac{1}{\lambda_1} = 12.0978.$$

Remark 4.1: In Examples of Sakthivel et al. (2018), authors have taken the discrete time-varying delays as $\tau_1(t_j) = \sin(t_j)$, $\tau_2(t_j) = \sin(t_j)$. It followed that $\mu = 0.5$ and Bernoulli distributed sequence $\bar{\beta} = 0.9$. But in this paper, in Example 4.1 discrete time-varying delays are chosen as $\beta_1(t_j) = 0.1327 + \sin(t_j)$, $\beta_2(t_j) = 0.04 + \sin(t_j)$, $\sigma = 0.5$, $\mu = 0.01$, $\delta = 0.4036$, we can conclude that our results are better than those in Sakthivel et al. (2018)

5. Conclusion

In this study, \mathcal{H}_∞ and passive non-fragile synchronisation of Markovian jump stochastic CDNs with time-varying delays, randomly occurring gain variation and stochastic noise is investigated. Moreover, we have introduced a stochastic variable satisfying the Bernoulli distribution to represent the random gain variations in the non-fragile controller. Lyapunov–Krasovskii stability theory and some stochastic techniques are employed. We developed a new \mathcal{H}_∞ and passive performance stochastic synchronisation criterion for the investigated system in terms of LMIs and given a design algorithm for the proposed non-fragile state feedback controller to a solution of the attain set of LMIs. At long last, a numerical example is given to validate the efficiency and feasibility of these technique expected in this paper. We can extend the present results to the analysis of synchronization of \mathcal{H}_∞ filter design with discrete-time Markovian jump CDNs.

Disclosure statement

No potential conflict of interest was reported by the author(s).

Funding

This work is supported by NBHM [grant number 2–48(5)/2016/NBHM/R.P/-R-D II/14088], and the Jiangsu Provincial Key Laboratory of Networked Collective Intelligence [grant number BM2017002]. The work of O.M. Kwon was supported in part by the Basic Science Research Program through the National Research Foundation of Korea (NRF) funded by the Ministry of Education [grant number NRF-2019R1I1A3A02058096], [grant number NRF-2020R1A6A1-A12047945], in part by the Brain Research Program through the National Research Foundation of Korea (NRF) funded by the Ministry of Science, ICT & Future Planning [grant number NRF-2017M3C7A1044815] and in part by the MSIT (Ministry of Science and ICT), Korea, under the ITRC (Information Technology Research Center) support program [grant number IITP-2020-1711120023] supervised by the IITP (Institute for Information & Communications Technology Planning & Evaluation).

References

- Abhijit, D., & Lewis, F. (2010). Distributed adaptive control for synchronization of unknown non-linear networked systems. *Automatica*, 46(12), 2014–2021. <https://doi.org/10.1016/j.automatica.2010.08.008>

- Alfa, A. S. (2004). Markov chain representations of discrete distributions applied to queueing models. *Computers & Operations Research*, 31(14), 2365–2385. [https://doi.org/10.1016/S0305-0548\(03\)00192-8](https://doi.org/10.1016/S0305-0548(03)00192-8)
- Asmussenn, S., & Kella, O. (2000). A multi-dimensional martingale for Markov additive processes and its applications. *Advances in Applied Probability*, 32(2), 376–393. <https://doi.org/10.1239/aap/1013540169>
- Barron, Y. (2018a). An order-revenue inventory model with returns and sudden obsolescence. *Operations Research Letters*, 46(1), 88–92. <https://doi.org/10.1016/j.orl.2017.11.005>
- Barron, Y. (2018b). Group maintenance policies for an R-out-of-N system with phase-type distribution. *Annals of Operations Research*, 261, 79–105. <https://doi.org/10.1007/s10479-017-2617-x>
- Barron, Y. (2019). A threshold policy in a Markov-modulated production system with server vacation: The case of continuous and batch supplies. *Advances in Applied Probability*, 50(4), 1246–1274. <https://doi.org/10.1017/apr.2018.59>
- Barron, Y., & Yechiali, U. (2017). Generalized control-limit preventive repair policies for deteriorating cold and warm standby Markovian systems. *IIEE Transactions*, 49(11), 1031–1049. <https://doi.org/10.1080/24725854.2017.1335919>
- Behinfaraz, R., & Badamchizadeh, M. A. (2018). Synchronization of different fractional order chaotic systems with time-varying parameter and orders. *ISA Transactions*, 80, 399–410. <https://doi.org/10.1016/j.isatra.2018.07.014>
- Behinfaraz, R., Ghaemi, S., & Khanmohammadi, S. (2019). Risk assessment in control of fractional-order coronary artery system in the presence of external disturbance with different proposed controllers. *Applied Soft Computing*, 77, 290–299. <https://doi.org/10.1016/j.asoc.2018.12.014>
- Breuer, L. (2010). A quintuple law for Markov additive processes with phase-type jumps. *Journal of Applied Probability*, 47(2), 441–458. <https://doi.org/10.1239/jap/1276784902>
- Cai, S., Lei, X., & Liu, Z. (2016). Outer synchronization between two hybrid-coupled delayed dynamical networks via aperiodically adaptive intermittent pinning control. *Complexity*, 21(S2), 593–605. <https://doi.org/10.1002/cplx.v21.S2>
- Chen, G., Shen, Y., & Zhu, S. (2011). Non-fragile observer based h_8 control for neutral stochastic hybrid systems with time-varying delay. *Neural Computing and Applications*, 20, 1149–1158. <https://doi.org/10.1007/s00521-010-0471-8>
- Desouza, C. E., & Fragoso, M. D. (1993). H_∞ control for linear system with Markovian jumping parameters. *Control Theory and Technology*, 9(2), 457–466.
- Dong, H., Wang, Z., & Gao, H. (2012). Distributed filtering for a class of time-varying system over sensor networks with quantization errors and successive packet dropouts. *IEEE Transactions on Signal Processing*, 60(6), 3161–3173. <https://doi.org/10.1109/TSP.2012.2190599>
- Du, Y., & Xu, R. (2014). Robust synchronization of an array of neural networks with hybrid coupling and mixed time delays. *ISA Transactions*, 53(4), 1015–1023. <https://doi.org/10.1016/j.isatra.2014.03.005>
- Fang, M., & Park, J. H. (2013). Non-fragile synchronization of neural networks with time-varying delay and randomly occurring controller gain fluctuation. *Applied Mathematics and Computation*, 219(15), 8009–8017. <https://doi.org/10.1016/j.amc.2013.02.030>
- Gao, H., Chen, T., & Chai, T. (2007). Passivity and passification for networked control systems. *SIAM Journal on Control and Optimization*, 46(4), 1299–1322. <https://doi.org/10.1137/060655110>
- Guo, W., Austin, F., & Chen, S. (2010). Global synchronization of nonlinearly coupled complex networks with non-delayed coupling. *Communications in Nonlinear Science and Numerical Simulation*, 15(6), 1631–1639. <https://doi.org/10.1016/j.cnsns.2009.06.016>
- Guo, X. G., Wang, J. L., Liao, F., & Wang, D. (2015). Quantized H_∞ consensus of multi-agent systems with quantization mismatch under switching weighted topologies. *IEEE Transactions on Control of Network Systems*, 4(2), 202–212. <https://doi.org/10.1109/TCNS.2015.2489338>
- He, G., Fang, J. A., Zhang, W., & Li, Z. (2016). Synchronization of switched complex dynamical networks with non-synchronised subnetworks and stochastic disturbances. *Neurocomputing*, 171, 39–47. <https://doi.org/10.1016/j.neucom.2015.05.068>
- Joby, M., Sakthivel, R., Mathiyalagan, K., & Marshal Anthoni, S. (2016). Fault-Tolerant sampled-Data mixed H_∞ and passivity control of stochastic systems and its application. *Complexity*, 21, 420–429. <https://doi.org/10.1002/cplx.v21.6>
- Karimi, H., & Gao, H. (2010). New delay-dependent exponential synchronization for uncertain neural networks with mixed time delays. *IEEE Transactions on Systems, Man, and Cybernetics, Part B (Cybernetics)*, 40(1), 173–185. <https://doi.org/10.1109/TSMCB.2009.2024408>
- Krasovskii, N. N., & Lidskii, E. A. (1961). Analysis and design of controllers in systems with random attributes. *Automatic Remote Control*, 22, 1021–1025.
- Langville, A. N., & Stewart, W. J. (2004). The Kronecker product and stochastic automata networks. *Journal of Computational and Applied Mathematics*, 167(2), 429–447. <https://doi.org/10.1016/j.cam.2003.10.010>
- Lee, T. H., Park, J. H., Ji, D. H., Kwon, O. M., & Lee, S. M. (2012). Guaranteed cost synchronization of a complex dynamical network via dynamic feedback control. *Applied Mathematics and Computation*, 218(11), 6469–6481. <https://doi.org/10.1016/j.amc.2011.11.112>
- Li, H., Wong, W. K., & Tang, Y. (2012). Global synchronization stability for stochastic complex dynamical networks with probabilistic interval time-varying delays. *Journal of Optimization Theory and Applications*, 152, 496–516. <https://doi.org/10.1007/s10957-011-9917-0>
- Lien, C. H., Cheng, W. C., Tsai, C. H., & Yu, K. W. (2007). Non-fragile observer based controls of linear systems via LMI approach. *Chaos, Solitons & Fractals*, 32, 1530–1537. <https://doi.org/10.1016/j.chaos.2005.11.092>
- Lu, J., & Ho, D. W. C. (2010). Globally exponential synchronization and synchronizability for general dynamical networks. *IEEE Transactions on Systems, Man, and Cybernetics, Part B (Cybernetics)*, 40(2), 350–361. <https://doi.org/10.1109/TSMCB.2009.2023509>

- Ma, Y., & Zheng, Y. (2015). Synchronization of continuous time Markovian jumping singular complex networks with mixed mode-dependent time delays. *Neurocomputing*, 156, 52–59. <https://doi.org/10.1016/j.neucom.2015.01.001>
- Newman, M. E. J. (2003). The structure and function of complex networks. *SIAM Review*, 45, 167–256. <https://doi.org/10.1137/S003614450342480>
- Park, P., Ko, J., & Jeong, C. (2011). Reciprocally convex approach to stability of systems with time-varying delays. *Automatica*, 47(1), 235–238. <https://doi.org/10.1016/j.automatica.2010.10.014>
- Park, M. J., Kwon, O. M., Park, J. H., Lee, S. M., & Cha, E. J. (2012). Synchronization criteria of fuzzy complex dynamical networks with interval time-varying delays. *Applied Mathematics and Computation*, 218(23), 11634–11647. <https://doi.org/10.1016/j.amc.2012.05.046>
- Qi, D., Liu, M., Qiu, M., & Zhang, S. (2010). Exponential synchronization of general discrete-time chaotic neural networks with or without time delays. *IEEE Transactions on Neural Networks*, 21(8), 1358–1365. <https://doi.org/10.1109/TNN.2010.2050904>
- Qiu, J., Sun, K., Rudas, I. J., & Gao, H. (2020). Command filter-based adaptive NN control for MIMO nonlinear systems with full-state constraints and actuator hysteresis. *IEEE Transactions on Cybernetics*, 50(7), 2905–2915. <https://doi.org/10.1109/TCYB.6221036>
- Qiu, J., Sun, K., Wang, T., & Gao, H. (2019). Observer-based fuzzy adaptive event-triggered control for pure-feedback nonlinear systems with prescribed performance. *IEEE Transactions on Fuzzy Systems*, 27(11), 2152–2162. <https://doi.org/10.1109/TFUZZ.91>
- Ross, S. M. (1969). A Markovian replacement model with generalization to include stocking. *Management Science*, 15, 702–715. <https://doi.org/10.1287/mnsc.15.11.702>
- Ruiz-Castro, J. E. (2016). Complex multi-state systems modelled through marked Markovian arrival processes. *European Journal of Operational Research*, 252, 852–865. <https://doi.org/10.1016/j.ejor.2016.02.007>
- Sakthivel, R., Sakthivel, R., Kaviarasan, B., Wang, C., & Ma, Y. K. (2018). Finite-Time nonfragile synchronization of stochastic complex dynamical networks with semi-Markov switching outer coupling. *Complexity*, 2018, 1–13. <https://doi.org/10.1155/2018/8546304>
- Sakthivel, R., Santra, S., Kaviarasan, B., & Venkatanareshbabu, K. (2017). Dissipative analysis for network-based singular systems with non-fragile controller and event-triggered sampling scheme. *Journal of the Franklin Institute*, 354(12), 4739–4761. <https://doi.org/10.1016/j.jfranklin.2017.05.026>
- Selivanov, A., Fradkov, A., & Fridman, E. (2015). Passification-based decentralized adaptive synchronization of dynamical networks with time-varying delays. *Journal of the Franklin Institute*, 352(1), 52–72. <https://doi.org/10.1016/j.jfranklin.2014.10.007>
- Shen, H., Park, J. H., Wu, Z. G., & Zhang, Z. (2015). Finite-time H_∞ synchronization for complex networks with semi-markov jump topology. *Communications in Nonlinear Science and Numerical Simulation*, 24(1), 40–51. <https://doi.org/10.1016/j.cnsns.2014.12.004>
- Shen, B., Wang, Z., & Liu, X. (2011). Bounded H_∞ synchronization and state estimation for discrete time-varying stochastic complex networks over a finite horizon. *IEEE Transactions on Neural Networks and Learning Systems*, 22(1), 145–157. <https://doi.org/10.1109/TNN.2010.2090669>
- Strogatz, S. (2001). Exploring complex networks. *Nature*, 410, 268–276. <https://doi.org/10.1038/35065725>
- Sun, K., Liu, L., Qiu, J., & Feng, G. (2020). Fuzzy adaptive finite-time fault-tolerant control for strict-feedback nonlinear systems. *IEEE Transactions on Fuzzy Systems*, 1–11. <https://doi.org/10.1109/TFUZZ.2020.2965890>
- Syed Ali, M. (2014). Robust stability of stochastic uncertain recurrent neural networks with Markovian jumping parameters and time-varying delays. *International Journal of Machine Learning and Cybernetics*, 5, 13–22. <https://doi.org/10.1007/s13042-012-0124-6>
- Syed Ali, M., & Yogambigai, J. (2016). Synchronization of complex dynamical networks with hybrid coupling delays on time scales by handling multitude Kronecker product terms. *Applied Mathematics and Computation*, 291, 244–258. <https://doi.org/10.1016/j.amc.2016.06.046>
- Syed Ali, M., & Yogambigai, J. (2018). Extended dissipative synchronization of complex dynamical networks with additive time-varying delay and discrete-time information. *Journal of Computational and Applied Mathematics*, 348, 328–341. <https://doi.org/10.1016/j.cam.2018.06.003>
- Wang, X., & Chen, G. (2003). Complex networks: Small-world, scale-free and beyond. *IEEE Circuits and Systems Magazine*, 3(1), 6–20. <https://doi.org/10.1109/MCAS.2003.1228503>
- Wang, M., Feng, G., & Qiu, J. B. (2020). Finite frequency fuzzy output feedback controller design for Roesser-type two-dimensional nonlinear systems. *IEEE Transactions on Fuzzy Systems*. <https://doi.org/10.1109/TFUZZ.2020.2966155>
- Wang, Z., Liu, Y., Yu, L., & Liu, X. (2006). Exponential stability of delayed recurrent neural networks with Markovian jumping parameters. *Physics Letters A*, 356(4-5), 346–352. <https://doi.org/10.1016/j.physleta.2006.03.078>
- Wang, N., Qian, C. J., Sun, J. C., & Liu, Y. C. (2016). Adaptive robust finite-time trajectory tracking control of fully actuated marine surface vehicles. *IEEE Transactions on Control Systems Technology*, 24(4), 1454–1462. <https://doi.org/10.1109/TCST.2015.2496585>
- Wang, M., Qiu, J., & Feng, G. (2018a). Finite frequency filtering design for uncertain discrete-time systems using past output measurements. *IEEE Transactions on Circuits and Systems I: Regular Papers*, 65(9), 3005–3013. <https://doi.org/10.1109/TCSI.8919>
- Wang, M., Qiu, J., & Feng, G. (2018b). Finite frequency memory output feedback controller design for T-S fuzzy dynamical systems. *IEEE Transactions on Fuzzy Systems*, 26(6), 3301–3313. <https://doi.org/10.1109/TFUZZ.2018.2821654>
- Watts, D. J., & Strogatz, S. H. (1998). Collective dynamics of small-world networks. *Nature*, 393(6684), 440–442. <https://doi.org/10.1038/30918>

- Wu, Z. G., Park, J. H., Su, H., & Chu, J. (2013). Non-fragile synchronization control for complex networks with missing data. *International Journal of Control*, 86, 555–566. <https://doi.org/10.1080/00207179.2012.747704>
- Wu, Z. G., Park, J. H., Su, H., Song, B., & Chu, J. (2013). Mixed H_∞ and passive filtering for singular systems with time delays. *Signal Processing*, 93(7), 1705–1711. <https://doi.org/10.1016/j.sigpro.2013.01.003>
- Wu, Z. G., Shi, P., Su, H., & Chu, J. (2011). Passivity analysis for discrete-time stochastic Markovian jump neural networks with mixed time delays. *IEEE Transactions on Neural Networks and Learning Systems*, 22(10), 1566–1575. <https://doi.org/10.1109/TNN.2011.2163203>
- Wu, Z. G., Shi, P., Su, H., & Chu, J. (2013). Sampled-data exponential synchronization of complex dynamical networks with time-varying coupling delay. *IEEE Transactions on Neural Networks and Learning Systems*, 24(8), 1177–1187. <https://doi.org/10.1109/TNNLS.2013.2253122>
- Xu, S., Lam, L., Yang, G. H., & Wang, J. (2006). Stabilization and H_∞ control for uncertain stochastic time-delay systems via non-fragile controllers. *Asian Journal of Control*, 8(2), 197–200. <https://doi.org/10.1111/asjc.2006.8.issue-2>
- Yang, X., Cao, J., & Lu, J. (2013). Synchronization of randomly coupled neural networks with Markovian jumping and time-delay. *IEEE Transactions on Circuits and Systems I: Regular Papers*, 60(2), 363–376. <https://doi.org/10.1109/TCSI.2012.2215804>
- Yao, J., Guan, Z. H., & Hill, D. J. (2009). Passivity-based control and synchronization of general complex dynamical networks. *Automatica*, 45(9), 2107–2113. <https://doi.org/10.1016/j.automatica.2009.05.006>
- Yi, J. W., Wang, Y. W., Xiao, J. W., & Huang, Y. (2013). Exponential synchronization of complex dynamical networks with Markovian jumping parameters and stochastic delays and its application to multi-agent systems. *Communications in Nonlinear Science and Numerical Simulation*, 18(5), 1175–1192. <https://doi.org/10.1016/j.cnsns.2012.09.031>
- Yu, W., & Cao, J. (2007). Adaptive synchronization and lag synchronization of uncertain dynamical system with time delay based on parameter identification. *Physica A: Statistical Mechanics and Its Applications*, 375(2), 467–482. <https://doi.org/10.1016/j.physa.2006.09.020>
- Yu, W., Chen, G., & Cao, J. (2011). Adaptive synchronization of uncertain coupled stochastic complex networks. *Asian Journal of Control*, 13(3), 418–429. <https://doi.org/10.1002/asjc.v13.3>
- Yue, D., & Lam, J. (2005). Non-fragile guaranteed cost control for uncertain descriptor system with time varying state and input delays. *Optimal Control Applications and Methods*, 26(2), 85–105. [https://doi.org/10.1002/\(ISSN\)1099-1514](https://doi.org/10.1002/(ISSN)1099-1514)
- Zeng, J., & Cao, J. (2011). Synchronization in singular hybrid complex networks with delayed coupling. *International Journal of Systems, Control and Communications*, 3(2), 144–157. <https://doi.org/10.1504/IJSCC.2011.039865>
- Zhang, Y., Shi, Y., & Shi, P. (2017). Robust and non-fragile finite-time H_∞ control for uncertain Markovian jump non-linear systems. *Applied Mathematics and Computation*, 279, 125–138. <https://doi.org/10.1016/j.amc.2016.01.012>
- Zhang, W., Tang, Y., Wu, X., & Fang, J. A. (2014). Synchronization of nonlinear dynamical networks with heterogeneous impulses. *IEEE Transactions on Circuits and Systems I: Regular Papers*, 61(4), 1220–1228. <https://doi.org/10.1109/TCSI.2013.2286027>
- Zhao, X., & Zeng, Q. (2010). New robust delay-dependent stability and H_∞ analysis for uncertain Markovian jump systems with time-varying delays. *Journal of the Franklin Institute*, 347(5), 863–874. <https://doi.org/10.1016/j.jfranklin.2010.03.009>

Received August 25, 2021, accepted September 16, 2021, date of publication September 20, 2021, date of current version September 29, 2021.

Digital Object Identifier 10.1109/ACCESS.2021.3113915

Adaptive Fuzzy Feedback Controller Design for Finite-Time Mittag-Leffler Synchronization of Fractional-Order Quaternion-Valued Reaction-Diffusion Fuzzy Molecular Modeling of Delayed Neural Networks

G. NARAYANAN¹, M. SYED ALI¹, MD IRSHAD ALAM², GRIENGGRAI RAJCHAKIT³, NATTAKAN BOONSATIT⁴, PANKAJ KUMAR⁵, AND PORPATTAMA HAMMACHUKIATTIKUL⁶

¹Complex Systems and Networked Science Laboratory, Department of Mathematics, Thiruvalluvar University, Vellore 632115, India

²Department of Electrical Engineering, Sitamarhi Institute of Technology, Sitamarhi, Bihar 843302, India

³Department of Mathematics, Faculty of Science, Maejo University, San Sai, Chiang Mai 50290, Thailand

⁴Department of Mathematics, Faculty of Science and Technology, Rajamangala University of Technology Suvarnabhumi, Nonthaburi 11000, Thailand

⁵Department of Computer Science and Engineering, Noida Institute of Engineering and Technology, Greater Noida, Uttar Pradesh 201306, India

⁶Department of Mathematics, Faculty of Science, Phuket Rajabhat University (PKRU), Ratsada, Phuket 83000, Thailand

Corresponding author: Nattakan Boonsatit (nattakan.b@rmutsb.ac.th)

ABSTRACT This paper addresses an adaptive fuzzy feedback controller design problem for finite-time Mittag-Leffler synchronization (FTMLS) of fractional-order quaternion-valued reaction-diffusion T-S fuzzy molecular modeling of delayed neural networks. A novel approach is proposed to effectively deal with the joint effects from fuzzy rules and reaction-diffusion terms for the class of T-S fuzzy fractional-order reaction-diffusion delayed quaternion-valued neural networks (FORDDQVNNs) under consideration. By employing Lyapunov stability theory, Caputo fractional derivative, several algebraic criteria are established to guarantee the FTMLS of T-S fuzzy FORDDQVNNs via designed fuzzy feedback controller. Moreover, the adaptive controller and parameter update laws are designed via adaptive control methods. Compared with existing results in the literature, we also show that our results are less conservative than existing ones with these illustrative T-S fuzzy FORDDQVNNs. A numerical example is presented to verify the analysis results and illustrate the effectiveness of the proposed FTMLS conditions.

INDEX TERMS Quaternion-valued neural networks (QVNNs), fractional derivatives, reaction-diffusion terms, Takagi-Sugeno fuzzy, adaptive control law.

I. INTRODUCTION

Based on these biological knowledge, the stability of molecular models of genetic regulatory networks, neural networks (NNs) and etc., has received more and more attention [1]–[3]. Note that these applications have important relationships with their dynamic behaviors, the internal dynamics of NNs, such as stability, multistability, synchronization, and so on, and have received increasing attention in past decades [4], [5]. In order to describe physical

phenomena more accurately, fractional-order neural networks (FONNs) are recognized as a significant improvement over the integer-order NNs because of their long-term memory and hereditary properties [6], [7]. Subsequently, FONNs as a kind of important biological networks, have attracted increasing interests [8], [9]. In the study of FONNs, the discussion of dynamical behaviors is always a hot topic, such as Mittag-Leffler synchronization [10], stability [11] and so forth [12], [13]. Time delays, such as leakage delays, distributed delays, discrete delays, and neutral delays are widespread and inevitable in NNs [14]–[17]. It is a source of oscillation, divergence, instability, chaos and

The associate editor coordinating the review of this manuscript and approving it for publication was Seyedali Mirjalili¹.

poor performance. Therefore, investigation of delayed NNs is not only of theoretical significance but also of practical significance.

As a typical collective behavior, synchronization has attracted considerable attention due to its theoretical importance and practical applications in various fields such as the modeling brain activity, cryptography, clock synchronization of sensor networks [18]–[20]. Until now, the problem of synchronization for fractional-order systems, particularly, dynamical networks [21] has been much analyzed, and widely control strategies, including the sliding mode control [22], impulsive control [23], the pinning control [24], and the adaptive control [10] have been concentrated on this topic. The above mentioned types of synchronization are shows that the trajectories of the response system can reach the trajectories of deriving system over the infinite horizon. In the application point of view, the synchronization should be realized in finite-time which is more and more important. Thus, it is necessary to analyze the finite-time synchronization of FONNs. Recently, many authors have paid their attention and interest for the analysis of finite-time synchronization of FONNs and some good results has been reported in [25]–[27]. For instance, the author [28] investigated the FTMLS of memristive BAM FONNs with time delays via state-feedback control. Chen *et al.* [29] studied FTMLS of memristor-based FONNs with parameters uncertainty by using Lyapunov-like method.

Reaction-diffusion NNs (RDNNs), in which the neuron states are dependent on both time and space, can perfectly describe the time and spatial evolutions. In comparison with the traditional NNs, RDNNs could realize better approximations of actual systems. It is thus reasonable and important to consider NNs with diffusion effects. Recently, many elegant achievements on qualitative analysis of dynamical behaviors for various RDNN models have been reported in [30]–[32]. In recent years, many efforts have been dedicated to investigating synchronization of RDNNs with time delays [33]–[35]. Also, relatively recently, reaction-diffusion terms have been incorporated into some fractional-order models [36], [37]. For example, Stamova and Stamo [38] developed impulsive control on Mittag-Leffler synchronization of FONNs with time-varying delays and reaction-diffusion terms. On the other hand, recent years have witnessed a rapid growing interest in adaptive control [39], [40] which is an important control technique and has been widely used to synchronization of NNs with reaction effects. These days, adaptive control has been applied to adjust control gains to achieve synchronization of FONNs with reaction effects. Based on the Caputo partial fractional derivative and adaptive control technique, some sufficient conditions for ensuring coupled networks synchronization of fractional-order reaction-diffusion systems were discussed in [41].

Takagi-Sugeno (T-S) fuzzy model [42] is widely recognized as an effective mathematical model, which supports various kinds of analyzes of which synchronization is

a promising topic in the fuzzy control community, especially for nonlinear systems. Among various kinds of fuzzy methods, the T-S fuzzy systems are widely accepted as a useful tool for design and analysis of fuzzy control system [43]–[45]. Recently, the T-S fuzzy rules have been connected with the RDNNs and several accomplishments have been achieved. Based on the T-S fuzzy model, a fuzzy controller of state-feedback type was considered for fuzzy memristive-based RDNNs in [46]. In [47], the fuzzy adaptive stabilization problem was discussed for T-S fuzzy memristive RDNNs by employing the event-triggered sampled-data control. Authors in [48] analyzed the synchronization of RDNNs subject to partial couplings and T-S fuzzy nodes under pinning control. In [49], another fuzzy sampled-data controller was adopted to deal with the synchronization of T-S fuzzy RDNNs.

Above all, although the corresponding methods and techniques for studying real-valued NNs (RVNNs) or complex-valued NNs (CVNNs) cannot be directly used to investigate QVNNs, QVNNs can be converted into four real-valued systems by applying Hamilton rules to quaternion multiplication [50], [51]. Considering the simple representation of quaternion, which is easy to understand the geometrical meanings, QVNNs can be applied to various fields of science and engineering. Up to now, direct quaternion approach [52], plural decomposition approach [53], real decomposition approach [54], and have been proposed to investigate the dynamical analysis and synchronization for integer-order QVNNs. Recently, some researchers attempted to investigate the advantages of quaternions into FONNs. It is also necessary to point out that fractional-order QVNNs have many applications in engineering and science, such as wave propagation, electromagnetic waves, diffusion, and viscoelastic systems. So far, there have been some results on the dynamic properties of fractional-order QVNNs, but there are few results to propose Mittag-Leffler synchronization criteria for fractional-order QVNNs [55]–[57]. Furthermore, the FTMLS problem of fractional-order QVNNs by using linear feedback controllers have been investigated [58]. Since reaction-diffusion of CVNNs and QVNNs have storage capacity advantages in comparison to RVNNs, the synchronization issues of CVNNs and QVNNs with reaction-diffusion terms have received growing research interest in recent years [59]–[62]. However, to the best of our knowledge, these results are under the assumption that the reaction-diffusion QVNNs are of integer-order, and there are no results on the FTMLS of fractional-order systems via adaptive fuzzy feedback controller. Therefore, it is highly important and indeed imperative to study the FTMLS problem of FORDDQVNNs both in theoretical interest and practical applications.

Inspired by the above-mentioned arguments, in this paper aims to design an adaptive fuzzy feedback controller scheme for FTMLS problem of T-S fuzzy FORDDQVNNs. By virtue of the Green formula, Caputo fractional derivative and inequality technique, several algebraic criteria are

established to guarantee the FTMLS problem of the proposed model. The main contributions of this paper are listed as below:

(i) First, the quaternion algebra is introduced in fractional-order reaction-diffusion system. To avoid the non-commutativity of quaternion multiplication, the QVNNs are decomposed into four RVNNs by using plural decomposition approach based on Hamilton rules: $i^2 = -1, j^2 = -1, k^2 = -1, ij = k, ji = -k, jk = i, kj = -i, ki = j, ik = -j$.

(ii) This paper is one of the first paper that combines the fuzzy IF-THEN rules and the quaternion algebra with fractional-order RDNNs and attempts to achieve the FTMLS of T-S fuzzy FORDDQVNNs and the fuzzy-dependent adjustable matrix inequality technique is more flexible and helpful to reduce the conservatism.

(iii) By the construction of fuzzy feedback controller, Lyapunov functional, and some novel easily verifiable algebraic inequality conditions is established to achieve the FTMLS of T-S fuzzy FORDDQVNNs. It is worth noting that the effect of the reaction-diffusion on the FTMLS is considered in our results. Also the suitable adaptive controller is designed with adaptive law which guarantees the FTMLS of the proposed model.

(iv) Based on the previous papers on QVNNs, such as without reaction-diffusion terms [50]–[58], without fuzzy rules in [62], and without fractional-order [62], the effects of reaction-diffusion on the fractional-order system are additionally proposed in this paper, which means that our considered QVNNs are more general and may better meet practical requirements. Several corollaries are provided to show the advantages of the obtained results. It is noted that our results are comprehensive and include some existing ones [59]–[61] as special cases.

(v) To further illustrate the effectiveness of our theoretical result approach is demonstrated by numerical example and from the simulation results to comparing control scenarios are given.

Notation: Real numbers, complex numbers, and quaternion numbers are referred as \mathbb{R}, \mathbb{C} , and \mathbb{Q} respectively. $\mathbb{R}^{n \times n}, \mathbb{C}^{n \times n}, \mathbb{Q}^{n \times n}$ represents the set of all $n \times n$ real-valued, complex-valued, quaternion-valued matrices, respectively. The Caputo fractional derivative operator ${}^C D_0^\lambda$ is chosen for fractional-order derivative with order λ . For $\wp = (\wp_1, \wp_2, \dots, \wp_n)^T \in \mathbb{Q}^n$, let $|\wp| = (|\wp_1|, |\wp_2|, \dots, |\wp_n|)^T$ be the modulus of \wp , and $\|\wp\| = (\sum_{\theta=1}^n |\wp_\theta|^2)^{\frac{1}{2}}$ be the norm of \wp .

II. MODEL DESCRIPTION AND PRELIMINARIES

A. QUATERNION ALGEBRA

Quaternions are an associative algebra defined over the real field \mathbb{R} . A real quaternion, simply called quaternion, can be written in the form

$$h = h^r + h^i i + h^j j + h^k k \in \mathbb{Q}$$

with real coefficients h^r, h^i, h^j and h^k comprises a real part denoted by $\mathcal{R}(h) = h^r$, and a vector part with three imaginary components, denoted by $\mathcal{I}(h) = h^i i + h^j j + h^k k$.

The imaginary units, i, j , and k obey the following rules:

$$\begin{aligned} i^2 &= j^2 = k^2 = -1, \\ ij &= -ji = k, \\ jk &= -kj = i, \\ ki &= -ik = j, \end{aligned}$$

which implies immediately that the quaternion multiplication is not commutative.

For two quaternions $p = p^r + p^i i + p^j j + p^k k$ and $h = h^r + h^i i + h^j j + h^k k$, the addition between them is defined by

$$p+h = (p^r+h^r)+(p^i+h^i)i+(p^j+h^j)j+(p^k+h^k)k.$$

The product between them is defined as

$$\begin{aligned} ph &= (p^r h^r - p^i h^i - p^j h^j - p^k h^k) \\ &+ (p^r h^i + p^i h^r) + p^j h^k - p^k h^j) i \\ &+ (p^r h^j + p^j h^r - p^i h^k + p^k h^i) j \\ &+ (p^r h^k + p^k h^r + p^i h^j - p^j h^i) k. \end{aligned}$$

For a quaternion $h = h^r + h^i i + h^j j + h^k k$, the conjugate of h , denoted by h^* or \bar{h} , is defined as

$$h^* = \bar{h} = h^r - h^i i - h^j j - h^k k,$$

and the modulus of h , denoted by $|h|$, is defined as

$$|h| = \sqrt{h h^*} = \sqrt{(h^r)^2 + (h^i)^2 + (h^j)^2 + (h^k)^2}.$$

Definition 1 [38]: For any $t > 0$, Caputo fractional derivative of order $\lambda (0 < \lambda < 1)$ for a function $\chi(t, z) \in \mathbb{C}^1[[0, b] \times \Omega, \mathbb{R}]$ is defined by

$$\frac{\partial^\lambda \chi(t, z)}{\partial t^\lambda} = \frac{1}{\Gamma(1-\lambda)} \int_0^t \frac{\partial \chi(s, z)}{\partial s} \frac{ds}{(t-s)^\lambda},$$

where $\Gamma(v) = \int_0^\infty e^{-t} t^{v-1} dt$. In the case when, $\frac{\partial^\lambda \chi(t, \cdot)}{\partial t^\lambda} = \frac{d^\lambda \chi(t)}{dt^\lambda} = {}^C D_0^\lambda \chi(t)$.

Definition 2 [10]: The one-parameter Mittag-Leffler function is defined as

$$\mathbb{E}_\lambda(x) = \sum_{n=0}^\infty \frac{x^n}{\Gamma(n\lambda+1)},$$

where $\lambda > 0$, and $x \in \mathbb{C}$.

In this paper, the fractional-order quaternion-valued reaction-diffusion molecular model of neural networks with time delay is considered as the following form:

$$\begin{aligned} \frac{\partial^\lambda \mathfrak{S}_\theta(t, z)}{\partial t^\lambda} &= \sum_{\alpha=1}^m \frac{\partial}{\partial z_\alpha} \left(q_{\theta\alpha} \frac{\partial \mathfrak{S}_\theta(t, z)}{\partial z_\alpha} \right) \\ &- a_\theta \mathfrak{S}_\theta(t, z) + \sum_{\varphi=1}^n b_{\theta\varphi} f_\varphi(\mathfrak{S}_\varphi(t, z)) \\ &+ \sum_{\varphi=1}^n d_{\theta\varphi} g_\varphi(\mathfrak{S}_\varphi(t-\sigma(t), z)) + \mathcal{I}_\theta, \end{aligned}$$

(or) the vector form

$$\frac{\partial^\lambda \mathfrak{S}(t, z)}{\partial t^\lambda} = \Delta \mathfrak{S}(t, z) - \mathcal{A} \mathfrak{S}(t, z) + \mathcal{B} F(\mathfrak{S}(t, z)) + \mathcal{D} G(\mathfrak{S}(t - \sigma(t), z)) + \mathcal{I}, \quad (1)$$

where $\lambda \in (0, 1)$, $\theta = 1, 2, \dots, n$; Ω is a bounded domain with smooth boundary $\partial\Omega$ in \mathbb{R}^m , and the space vector $z = (z_1, z_2, \dots, z_m) \in \Omega$; $\mathfrak{S}(t, z) = (\mathfrak{S}_1(t, z), \mathfrak{S}_2(t, z), \dots, \mathfrak{S}_n(t, z))^T \in \mathbb{Q}^n$; $\Delta \mathfrak{S}(t, z) = \sum_{\alpha=1}^m \frac{\partial}{\partial z_\alpha} \left(\mathcal{Q} \frac{\partial \mathfrak{S}_\theta(t, z)}{\partial z_\alpha} \right)$; $\mathcal{Q} = \text{diag}(q_{1\alpha}, q_{2\alpha}, \dots, q_{n\alpha}) \in \mathbb{R}^{n \times n}$ with $\mathcal{Q} > 0$ is transmission diffusion operator; $\mathcal{A} = \text{diag}(a_1, a_2, \dots, a_n) \in \mathbb{R}^{n \times n}$ with $a_\theta > 0$; $\mathcal{B} = (b_{\theta\varphi})_{n \times n} \in \mathbb{Q}^{n \times n}$ and $\mathcal{D} = (d_{\theta\varphi})_{n \times n} \in \mathbb{Q}^{n \times n}$ are stands for the interconnection weight matrix; $F(\mathfrak{S}(t, z)) = (f_1(\mathfrak{S}_1(t, z)), f_2(\mathfrak{S}_2(t, z)), \dots, f_n(\mathfrak{S}_n(t, z)))^T \in \mathbb{Q}^n$ and $G(\mathfrak{S}(t - \sigma(t), z)) = (g_1(\mathfrak{S}_1(t - \sigma(t), z)), g_2(\mathfrak{S}_2(t - \sigma(t), z)), \dots, g_n(\mathfrak{S}_n(t - \sigma(t), z)))^T \in \mathbb{Q}^n$ define without and with time delay, the activation function respectively; $\mathcal{I} = (\mathcal{I}_1, \mathcal{I}_2, \dots, \mathcal{I}_n) \in \mathbb{Q}^n$ is the external input; $\mathfrak{S}_\theta(t, z) \in \mathbb{Q}$ is the quaternion-valued state variable for the θ th unit at time t and in space z and obesisously, $\mathfrak{S}_\theta = \mathfrak{S}_\theta^r i + \mathfrak{S}_\theta^j j + \mathfrak{S}_\theta^k k$; $b_{\theta\varphi} = b_{\theta\varphi}^r i + b_{\theta\varphi}^j j + b_{\theta\varphi}^k k$; $d_{\theta\varphi} = d_{\theta\varphi}^r i + d_{\theta\varphi}^j j + d_{\theta\varphi}^k k$; $f_\varphi(\mathfrak{S}_\varphi(t, z)) = f_\varphi^r(\mathfrak{S}_\varphi^r(t, z)) + f_\varphi^i(\mathfrak{S}_\varphi^i(t, z))i + f_\varphi^j(\mathfrak{S}_\varphi^j(t, z))j + f_\varphi^k(\mathfrak{S}_\varphi^k(t, z))k$; $g_\varphi(\mathfrak{S}_\varphi(t - \sigma(t), z)) = g_\varphi^r(\mathfrak{S}_\varphi^r(t - \sigma(t), z)) + g_\varphi^i(\mathfrak{S}_\varphi^i(t - \sigma(t), z))i + g_\varphi^j(\mathfrak{S}_\varphi^j(t - \sigma(t), z))j + g_\varphi^k(\mathfrak{S}_\varphi^k(t - \sigma(t), z))k$; $\mathcal{I}_\theta = \mathcal{I}_\theta^r i + \mathcal{I}_\theta^j j + \mathcal{I}_\theta^k k$. The initial and boundary values of (1) are set as

$$\begin{cases} \mathfrak{S}(t, z) = 0, & (t, z) \in [-\sigma, +\infty) \times \partial\Omega, \\ \mathfrak{S}(s, z) = \psi^l(s, z), & (s, z) \in [-\sigma, 0] \times \Omega, \end{cases}$$

where $\psi^l(s, z)$ is bounded and continuous on $[-\sigma, 0] \times \Omega$, $\psi^l(s, z) = (\psi_1^l(s, z), \psi_2^l(s, z), \dots, \psi_n^l(s, z))^T$; $\psi^l(s, z) = \psi^{lr}(s, z) + \psi^{li}(s, z)i + \psi^{lj}(s, z)j + \psi^{lk}(s, z)k$.

Viewing system (1) as the drive system, we introduce the response system as

$$\begin{aligned} \frac{\partial^\lambda \mathfrak{Z}_\theta(t, z)}{\partial t^\lambda} &= \sum_{\alpha=1}^m \frac{\partial}{\partial z_\alpha} \left(q_{\theta\alpha} \frac{\partial \mathfrak{Z}_\theta(t, z)}{\partial z_\alpha} \right) \\ &\quad - a_\theta \mathfrak{Z}_\theta(t, z) + \sum_{\varphi=1}^n b_{\theta\varphi} f_\varphi(\mathfrak{Z}_\varphi(t, z)) \\ &\quad + \sum_{\varphi=1}^n d_{\theta\varphi} g_\varphi(\mathfrak{Z}_\varphi(t - \sigma(t), z)) + \mathcal{I}_\theta + u_\theta(t, z), \end{aligned}$$

(or) the vector form

$$\frac{\partial^\lambda \mathfrak{Z}(t, z)}{\partial t^\lambda} = \Delta \mathfrak{Z}(t, z) - \mathcal{A} \mathfrak{Z}(t, z) + \mathcal{B} F(\mathfrak{Z}(t, z)) + \mathcal{D} G(\mathfrak{Z}(t - \sigma(t), z)) + \mathcal{I} + \hat{u}(t, z), \quad (2)$$

where $\lambda \in (0, 1)$, $\Delta \mathfrak{Z}(t, z) = \sum_{\alpha=1}^m \left(q_{\theta\alpha} \frac{\partial \mathfrak{Z}_\theta(t, z)}{\partial z_\alpha} \right)$; $\mathfrak{Z}(t, z) = (\mathfrak{Z}_1(t, z), \dots, \mathfrak{Z}_n(t, z))^T \in \mathbb{Q}^n$; $\hat{u}(t, z) = (u_1(t, z), \dots, u_n(t, z))^T \in \mathbb{Q}^n$ is the controller which will be designed.

Moreover,

$$\begin{cases} \mathfrak{Z}(t, z) = 0, & (t, z) \in [-\sigma, +\infty) \times \partial\Omega, \\ \mathfrak{Z}(s, z) = \psi^s(s, z), & (s, z) \in [-\sigma, 0] \times \Omega, \end{cases}$$

where $\psi^s(s, z)$ is bounded and continuous on $[-\sigma, 0] \times \Omega$, $\psi^s(s, z) = (\psi_1^s(s, z), \psi_2^s(s, z), \dots, \psi_n^s(s, z))^T$; $\psi^s(s, z) = \psi^{sr}(s, z) + \psi^{si}(s, z)i + \psi^{sj}(s, z)j + \psi^{sk}(s, z)k$.

B. FUZZY LOGIC MOLECULAR MODELING

A fuzzy dynamic model has been proposed by Takagi and Sugeno [42] to represent different linear/nonlinear systems of different rules. Based on this, we shall construct T-S fuzzy system to describe molecular model of FOQVRDNNs structure. Similar to [47]–[49], we consider a T-S fuzzy molecular model, in which the ξ th rule is formulated in the following form:

Plant rule ξ : If $\beta_1(t)$ is Ξ_1^ξ , $\beta_2(t)$ is Ξ_2^ξ , ..., $\beta_r(t)$ is Ξ_r^ξ .

Then

$$\begin{cases} \frac{\partial^\lambda \mathfrak{Z}(t, z)}{\partial t^\lambda} = \Delta \mathfrak{Z}(t, z) - \mathcal{A}_\xi \mathfrak{Z}(t, z) + \mathcal{B}_\xi F(\mathfrak{Z}(t, z)) \\ \quad + \mathcal{D}_\xi G(\mathfrak{Z}(t - \sigma(t), z)) + \mathcal{I}, \\ \mathfrak{Z}(t, z) = 0, & (t, z) \in [-\sigma, +\infty) \times \partial\Omega, \\ \mathfrak{Z}(s, z) = \psi^l(s, z), & (s, z) \in [-\sigma, 0] \times \Omega, \end{cases} \quad (3)$$

where $\beta_\ell(t)$ ($\ell = 1, 2, \dots, r$) and Ξ_ℓ^ξ ($\xi = 1, 2, \dots, \zeta$) show the premise variable vectors and fuzzy sets, respectively; ζ is the number of fuzzy If-Then rules; $\mathcal{A}_\xi = \text{diag}(a_{\xi 1}, a_{\xi 2}, \dots, a_{\xi n})$ with $\mathcal{A}_\xi > 0$; $\mathcal{B}_\xi = (b_{\xi\theta\varphi}) \in \mathbb{Q}^{n \times n}$; $\mathcal{D}_\xi = (d_{\xi\theta\varphi}) \in \mathbb{Q}^{n \times n}$.

By employing the weighted average fuzzy blending approach, the overall T-S fuzzy FORDDQVNNs (3) can be described as

$$\begin{cases} \frac{\partial^\lambda \mathfrak{Z}(t, z)}{\partial t^\lambda} = \sum_{\xi=1}^{\zeta} \Psi_\xi(\beta(t)) \{ \Delta \mathfrak{Z}(t, z) - \mathcal{A}_\xi \mathfrak{Z}(t, z) \\ \quad + \mathcal{B}_\xi F(\mathfrak{Z}(t, z)) + \mathcal{D}_\xi G(\mathfrak{Z}(t - \sigma(t), z)) + \mathcal{I} \}, \\ \mathfrak{Z}(t, z) = 0, & (t, z) \in [-\sigma, +\infty) \times \partial\Omega, \\ \mathfrak{Z}(s, z) = \psi^l(s, z), & (s, z) \in [-\sigma, 0] \times \Omega, \end{cases} \quad (4)$$

where $\beta(t) = (\beta_1(t), \beta_2(t), \dots, \beta_r(t))^T$, $\Psi_\xi(\beta(t)) = \frac{\prod_{\ell=1}^r \Xi_\ell^\xi(\beta_\ell(t))}{\sum_{\xi=1}^{\zeta} \prod_{\ell=1}^r \Xi_\ell^\xi(\beta_\ell(t))}$, in which $\Xi_\ell^\xi(\beta_\ell(t))$ is the grade of membership of $\beta_\ell(t)$ is Ξ_ℓ^ξ . According to the fuzzy theory it follows that $\sum_{\xi=1}^{\zeta} \Psi_\xi(\beta(t)) = 1$ and $\Psi_\xi(\beta(t)) \geq 0$ for ($\xi = 1, 2, \dots, \zeta$).

The considered T-S fuzzy response (2) is in the similar form (4),

$$\begin{cases} \frac{\partial^\lambda \mathfrak{Z}(t, z)}{\partial t^\lambda} = \sum_{\xi=1}^{\zeta} \Psi_\xi(\beta(t)) \{ \Delta \mathfrak{Z}(t, z) - \mathcal{A}_\xi \mathfrak{Z}(t, z) \\ \quad + \mathcal{B}_\xi F(\mathfrak{Z}(t, z)) + \mathcal{D}_\xi G(\mathfrak{Z}(t - \sigma(t), z)) \\ \quad + \mathcal{I} + \hat{u}_\xi(t, z) \}, \\ \mathfrak{Z}(t, z) = 0, & (t, z) \in [-\sigma, +\infty) \times \partial\Omega, \\ \mathfrak{Z}(s, z) = \psi^k(s, z), & (s, z) \in [-\sigma, 0] \times \Omega, \end{cases} \quad (5)$$

where $\hat{u}_\xi = (u_{\xi 1}, u_{\xi 2}, \dots, u_{\xi n})^T$.

By applying the non-commutativity of quaternion multiplication with hamiltonian rules (4) and (5) be rewritten as the following four real-valued equations

$$\begin{aligned} & \frac{\partial^\lambda \mathfrak{S}^r(t, z)}{\partial t^\lambda} \\ &= \sum_{\xi=1}^{\zeta} \Psi_{\xi}(\beta(t)) \{ \Delta \mathfrak{S}^r(t, z) - \mathcal{A}_{\xi} \mathfrak{S}^r(t, z) + \mathcal{B}_{\xi}^r F^r(\mathfrak{S}^r(t, z)) \\ & \quad - \mathcal{B}_{\xi}^i F^i(\mathfrak{S}^i(t, z)) - \mathcal{B}_{\xi}^j F^j(\mathfrak{S}^j(t, z)) - \mathcal{B}_{\xi}^k F^k(\mathfrak{S}^k(t, z)) \\ & \quad + \mathcal{D}_{\xi}^r G^r(\mathfrak{S}^r(t-\sigma(t), z)) - \mathcal{D}_{\xi}^i G^i(\mathfrak{S}^i(t-\sigma(t), z)) \\ & \quad - \mathcal{D}_{\xi}^j G^j(\mathfrak{S}^j(t-\sigma(t), z)) - \mathcal{D}_{\xi}^k G^k(\mathfrak{S}^k(t-\sigma(t), z)) \\ & \quad + \mathcal{I}^r \}, \end{aligned} \tag{6}$$

$$\begin{aligned} & \frac{\partial^\lambda \mathfrak{S}^i(t, z)}{\partial t^\lambda} \\ &= \sum_{\xi=1}^{\zeta} \Psi_{\xi}(\beta(t)) \{ \Delta \mathfrak{S}^i(t, z) - \mathcal{A}_{\xi} \mathfrak{S}^i(t, z) + \mathcal{B}_{\xi}^r F^i(\mathfrak{S}^i(t, z)) \\ & \quad + \mathcal{B}_{\xi}^i F^r(\mathfrak{S}^r(t, z)) + \mathcal{B}_{\xi}^j F^k(\mathfrak{S}^k(t, z)) - \mathcal{B}_{\xi}^k F^j(\mathfrak{S}^j(t, z)) \\ & \quad + \mathcal{D}_{\xi}^r G^i(\mathfrak{S}^i(t-\sigma(t), z)) + \mathcal{D}_{\xi}^i G^r(\mathfrak{S}^r(t-\sigma(t), z)) \\ & \quad + \mathcal{D}_{\xi}^j G^k(\mathfrak{S}^k(t-\sigma(t), z)) - \mathcal{D}_{\xi}^k G^j(\mathfrak{S}^j(t-\sigma(t), z)) \\ & \quad + \mathcal{I}^i \}, \end{aligned} \tag{7}$$

$$\begin{aligned} & \frac{\partial^\lambda \mathfrak{S}^j(t, z)}{\partial t^\lambda} \\ &= \sum_{\xi=1}^{\zeta} \Psi_{\xi}(\beta(t)) \{ \Delta \mathfrak{S}^j(t, z) - \mathcal{A}_{\xi} \mathfrak{S}^j(t, z) + \mathcal{B}_{\xi}^r F^j(\mathfrak{S}^j(t, z)) \\ & \quad - \mathcal{B}_{\xi}^i F^k(\mathfrak{S}^k(t, z)) + \mathcal{B}_{\xi}^j F^r(\mathfrak{S}^r(t, z)) + \mathcal{B}_{\xi}^k F^i(\mathfrak{S}^i(t, z)) \\ & \quad + \mathcal{D}_{\xi}^r G^j(\mathfrak{S}^j(t-\sigma(t), z)) - \mathcal{D}_{\xi}^i G^k(\mathfrak{S}^k(t-\sigma(t), z)) \\ & \quad + \mathcal{D}_{\xi}^j G^r(\mathfrak{S}^r(t-\sigma(t), z)) + \mathcal{D}_{\xi}^k G^i(\mathfrak{S}^i(t-\sigma(t), z)) \\ & \quad + \mathcal{I}^j \}, \end{aligned} \tag{8}$$

$$\begin{aligned} & \frac{\partial^\lambda \mathfrak{S}^k(t, z)}{\partial t^\lambda} \\ &= \sum_{\xi=1}^{\zeta} \Psi_{\xi}(\beta(t)) \{ \Delta \mathfrak{S}^k(t, z) - \mathcal{A}_{\xi} \mathfrak{S}^k(t, z) + \mathcal{B}_{\xi}^r F^k(\mathfrak{S}^k(t, z)) \\ & \quad + \mathcal{B}_{\xi}^i F^j(\mathfrak{S}^j(t, z)) - \mathcal{B}_{\xi}^j F^i(\mathfrak{S}^i(t, z)) + \mathcal{B}_{\xi}^k F^r(\mathfrak{S}^r(t, z)) \\ & \quad + \mathcal{D}_{\xi}^r G^k(\mathfrak{S}^k(t-\sigma(t), z)) + \mathcal{D}_{\xi}^i G^j(\mathfrak{S}^j(t-\sigma(t), z)) \\ & \quad - \mathcal{D}_{\xi}^j G^i(\mathfrak{S}^i(t-\sigma(t), z)) + \mathcal{D}_{\xi}^k G^r(\mathfrak{S}^r(t-\sigma(t), z)) \\ & \quad + \mathcal{I}^k \}, \end{aligned} \tag{9}$$

(or) two complex-valued equations of drive system

$$\begin{aligned} & \frac{\partial^\lambda \mathfrak{S}^R(t, z)}{\partial t^\lambda} = \sum_{\xi=1}^{\zeta} \Psi_{\xi}(\beta(t)) \{ \Delta \mathfrak{S}^R(t, z) - \mathcal{A}_{\xi} \mathfrak{S}^R(t, z) \\ & \quad + \mathcal{B}_{\xi}^R F^R(\mathfrak{S}^R(t, z)) - \mathcal{B}_{\xi}^I F^I(\mathfrak{S}^I(t, z)) \\ & \quad + \mathcal{D}_{\xi}^R G^R(\mathfrak{S}^R(t-\sigma(t), z)) \\ & \quad - \mathcal{D}_{\xi}^I G^I(\mathfrak{S}^I(t-\sigma(t), z)) + \mathcal{I}^R \}, \end{aligned} \tag{10}$$

$$\begin{aligned} & \frac{\partial^\lambda \mathfrak{S}^I(t, z)}{\partial t^\lambda} = \sum_{\xi=1}^{\zeta} \Psi_{\xi}(\beta(t)) \{ \Delta \mathfrak{S}^I(t, z) - \mathcal{A}_{\xi} \mathfrak{S}^I(t, z) \\ & \quad + \mathcal{B}_{\xi}^R F^I(\mathfrak{S}^I(t, z)) + \mathcal{B}_{\xi}^I F^R(\mathfrak{S}^R(t, z)) \\ & \quad + \mathcal{D}_{\xi}^R G^I(\mathfrak{S}^I(t-\sigma(t), z)) \\ & \quad + \mathcal{D}_{\xi}^I G^R(\mathfrak{S}^R(t-\sigma(t), z)) + \mathcal{I}^I \}, \end{aligned} \tag{11}$$

and

$$\begin{aligned} & \frac{\partial^\lambda \mathfrak{Z}^r(t, z)}{\partial t^\lambda} \\ &= \sum_{\xi=1}^{\zeta} \Psi_{\xi}(\beta(t)) \{ \Delta \mathfrak{Z}^r(t, z) - \mathcal{A}_{\xi} \mathfrak{Z}^r(t, z) \\ & \quad + \mathcal{B}_{\xi}^r F^r(\mathfrak{Z}^r(t, z)) - \mathcal{B}_{\xi}^i F^i(\mathfrak{Z}^i(t, z)) - \mathcal{B}_{\xi}^j F^j(\mathfrak{Z}^j(t, z)) \\ & \quad - \mathcal{B}_{\xi}^k F^k(\mathfrak{Z}^k(t, z)) + \mathcal{D}_{\xi}^r G^r(\mathfrak{Z}^r(t-\sigma(t), z)) \\ & \quad - \mathcal{D}_{\xi}^i G^i(\mathfrak{Z}^i(t-\sigma(t), z)) - \mathcal{D}_{\xi}^j G^j(\mathfrak{Z}^j(t-\sigma(t), z)) \\ & \quad - \mathcal{D}_{\xi}^k G^k(\mathfrak{Z}^k(t-\sigma(t), z)) + \mathcal{I}^r + \hat{u}_{\xi}^r(t, z) \}, \end{aligned} \tag{12}$$

$$\begin{aligned} & \frac{\partial^\lambda \mathfrak{Z}^i(t, z)}{\partial t^\lambda} \\ &= \sum_{\xi=1}^{\zeta} \Psi_{\xi}(\beta(t)) \{ \Delta \mathfrak{Z}^i(t, z) - \mathcal{A}_{\xi} \mathfrak{Z}^i(t, z) \\ & \quad + \mathcal{B}_{\xi}^r F^i(\mathfrak{Z}^i(t, z)) + \mathcal{B}_{\xi}^i F^r(\mathfrak{Z}^r(t, z)) + \mathcal{B}_{\xi}^j F^k(\mathfrak{Z}^k(t, z)) \\ & \quad - \mathcal{B}_{\xi}^k F^j(\mathfrak{Z}^j(t, z)) + \mathcal{D}_{\xi}^r G^i(\mathfrak{Z}^i(t-\sigma(t), z)) \\ & \quad + \mathcal{D}_{\xi}^i G^r(\mathfrak{Z}^r(t-\sigma(t), z)) + \mathcal{D}_{\xi}^j G^k(\mathfrak{Z}^k(t-\sigma(t), z)) \\ & \quad - \mathcal{D}_{\xi}^k G^j(\mathfrak{Z}^j(t-\sigma(t), z)) + \mathcal{I}^i + \hat{u}_{\xi}^i(t, z) \}, \end{aligned} \tag{13}$$

$$\begin{aligned} & \frac{\partial^\lambda \mathfrak{Z}^j(t, z)}{\partial t^\lambda} \\ &= \sum_{\xi=1}^{\zeta} \Psi_{\xi}(\beta(t)) \{ \Delta \mathfrak{Z}^j(t, z) - \mathcal{A}_{\xi} \mathfrak{Z}^j(t, z) \\ & \quad + \mathcal{B}_{\xi}^r F^j(\mathfrak{Z}^j(t, z)) - \mathcal{B}_{\xi}^i F^k(\mathfrak{Z}^k(t, z)) + \mathcal{B}_{\xi}^j F^r(\mathfrak{Z}^r(t, z)) \\ & \quad + \mathcal{B}_{\xi}^k F^i(\mathfrak{Z}^i(t, z)) + \mathcal{D}_{\xi}^r G^j(\mathfrak{Z}^j(t-\sigma(t), z)) \\ & \quad - \mathcal{D}_{\xi}^i G^k(\mathfrak{Z}^k(t-\sigma(t), z)) + \mathcal{D}_{\xi}^j G^r(\mathfrak{Z}^r(t-\sigma(t), z)) \\ & \quad + \mathcal{D}_{\xi}^k G^i(\mathfrak{Z}^i(t-\sigma(t), z)) + \mathcal{I}^j + \hat{u}_{\xi}^j(t, z) \}, \end{aligned} \tag{14}$$

$$\begin{aligned} & \frac{\partial^\lambda \mathfrak{Z}^k(t, z)}{\partial t^\lambda} \\ &= \sum_{\xi=1}^{\zeta} \Psi_{\xi}(\beta(t)) \{ \Delta \mathfrak{Z}^k(t, z) - \mathcal{A}_{\xi} \mathfrak{Z}^k(t, z) \\ & \quad + \mathcal{B}_{\xi}^r F^k(\mathfrak{Z}^k(t, z)) + \mathcal{B}_{\xi}^i F^j(\mathfrak{Z}^j(t, z)) - \mathcal{B}_{\xi}^j F^i(\mathfrak{Z}^i(t, z)) \\ & \quad + \mathcal{B}_{\xi}^k F^r(\mathfrak{Z}^r(t, z)) + \mathcal{D}_{\xi}^r G^k(\mathfrak{Z}^k(t-\sigma(t), z)) \\ & \quad + \mathcal{D}_{\xi}^i G^j(\mathfrak{Z}^j(t-\sigma(t), z)) - \mathcal{D}_{\xi}^j G^i(\mathfrak{Z}^i(t-\sigma(t), z)) \\ & \quad + \mathcal{D}_{\xi}^k G^r(\mathfrak{Z}^r(t-\sigma(t), z)) + \mathcal{I}^k + \hat{u}_{\xi}^k(t, z) \}, \end{aligned} \tag{15}$$

(or) two complex-valued equations of response system

$$\frac{\partial^\lambda \mathfrak{Z}^R(t, z)}{\partial t^\lambda} = \sum_{\xi=1}^{\zeta} \Psi_{\xi}(\beta(t)) \{ \Delta \mathfrak{Z}^R(t, z) - \mathcal{A}_{\xi} \mathfrak{Z}^R(t, z) + \mathcal{B}_{\xi}^R F^R(\mathfrak{Z}^R(t, z)) - \mathcal{B}_{\xi}^I F^I(\mathfrak{Z}^I(t, z)) + \mathcal{D}_{\xi}^R G^R(\mathfrak{Z}^R(t - \sigma(t), z)) - \mathcal{D}_{\xi}^I G^I(\mathfrak{Z}^I(t - \sigma(t), z)) + \mathcal{I}^R + \hat{u}_{\xi}^R(t, z) \}, \quad (16)$$

$$\frac{\partial^\lambda \mathfrak{Z}^I(t, z)}{\partial t^\lambda} = \sum_{\xi=1}^{\zeta} \Psi_{\xi}(\beta(t)) \{ \Delta \mathfrak{Z}^I(t, z) - \mathcal{A}_{\xi} \mathfrak{Z}^I(t, z) + \mathcal{B}_{\xi}^R F^I(\mathfrak{Z}^I(t, z)) + \mathcal{B}_{\xi}^I F^R(\mathfrak{Z}^R(t, z)) + \mathcal{D}_{\xi}^R G^I(\mathfrak{Z}^I(t - \sigma(t), z)) + \mathcal{D}_{\xi}^I G^R(\mathfrak{Z}^R(t - \sigma(t), z)) + \mathcal{I}^I + \hat{u}_{\xi}^I(t, z) \}. \quad (17)$$

Associated with system (6)-(9) and (12)-(15), initial and boundary value conditions are as follows

$$\begin{cases} \mathfrak{Z}^{\eta}(t, z) = 0, & (t, z) \in [-\sigma, +\infty) \times \partial\Omega, \\ \mathfrak{Z}^{\eta}(s, z) = \psi^{\eta}(s, z), & (s, z) \in [-\sigma, 0] \times \Omega, \\ \mathfrak{Z}^{\eta}(t, z) = 0, & (t, z) \in [-\sigma, +\infty) \times \partial\Omega, \\ \mathfrak{Z}^{\eta}(s, z) = \psi^{\eta}(s, z), & (s, z) \in [-\sigma, 0] \times \Omega. \end{cases} \quad (18)$$

Assumption 1: Throughout, this paper, we assume that $f_{\theta}^{\eta}(\cdot)$ and $g_{\theta}^{\eta}(\cdot)$ ($\theta = 1, 2, \dots, n, \eta = r, i, j, k$) are respectively of function $f_{\theta}(\cdot)$ and $g_{\theta}(\cdot)$ satisfy the following inequalities for any $\vartheta_1, \vartheta_2 \in \mathbb{R}$,

$$\begin{aligned} |f_{\theta}^{\eta}(\vartheta_1) - f_{\theta}^{\eta}(\vartheta_2)| &\leq \mathcal{F}_{\theta}^{\eta} |\vartheta_1 - \vartheta_2|, \\ |g_{\theta}^{\eta}(\vartheta_1) - g_{\theta}^{\eta}(\vartheta_2)| &\leq \mathcal{G}_{\theta}^{\eta} |\vartheta_1 - \vartheta_2|, \end{aligned}$$

where $\mathcal{F}_{\theta}^{\eta}, \mathcal{G}_{\theta}^{\eta}$ ($\eta = r, i, j, k$) are positive constants.

Assumption 2: For any $\theta = 1, 2, \dots, n, \alpha = 1, 2, \dots, m$, the constants $q_{\theta\alpha}$ are such that $q_{\theta\alpha} > \hat{q}_{\theta\alpha} \geq 0$.

Now define the error $\wp(t, z) = \mathfrak{Z}(t, z) - \mathfrak{S}(t, z) \triangleq \wp^r(t, z) + i\wp^i(t, z) + j\wp^j(t, z) + k\wp^k(t, z)$, namely $\wp^r(t, z) = \mathfrak{Z}^r(t, z) - \mathfrak{S}^r(t, z)$, $\wp^i(t, z) = \mathfrak{Z}^i(t, z) - \mathfrak{S}^i(t, z)$, $\wp^j(t, z) = \mathfrak{Z}^j(t, z) - \mathfrak{S}^j(t, z)$, $\wp^k(t, z) = \mathfrak{Z}^k(t, z) - \mathfrak{S}^k(t, z)$. Simplicity we denote $t_{\sigma} = t - \sigma(t)$. Then the error dynamics system between (6)-(9) and (12)-(15), can be obtained with four parts as:

$$\begin{aligned} \frac{\partial^\lambda \wp^r(t, z)}{\partial t^\lambda} &= \sum_{\xi=1}^{\zeta} \Psi_{\xi}(\beta(t)) \{ \Delta \wp^r(t, z) - \mathcal{A}_{\xi} \wp^r(t, z) + \mathcal{B}_{\xi}^R [F^r(\mathfrak{Z}^r(t, z)) - F^r(\mathfrak{S}^r(t, z))] - \mathcal{B}_{\xi}^I [F^i(\mathfrak{Z}^i(t, z)) - F^i(\mathfrak{S}^i(t, z))] - \mathcal{B}_{\xi}^j [F^j(\mathfrak{Z}^j(t, z)) - F^j(\mathfrak{S}^j(t, z))] - \mathcal{B}_{\xi}^k [F^k(\mathfrak{Z}^k(t, z)) - F^k(\mathfrak{S}^k(t, z))] + \mathcal{D}_{\xi}^R [G^r(\mathfrak{Z}^r(t_{\sigma}, z)) - G^r(\mathfrak{S}^r(t_{\sigma}, z))] - \mathcal{D}_{\xi}^I [G^i(\mathfrak{Z}^i(t_{\sigma}, z)) - G^i(\mathfrak{S}^i(t_{\sigma}, z))] - \mathcal{D}_{\xi}^j [G^j(\mathfrak{Z}^j(t_{\sigma}, z)) - G^j(\mathfrak{S}^j(t_{\sigma}, z))] - \mathcal{D}_{\xi}^k [G^k(\mathfrak{Z}^k(t_{\sigma}, z)) - G^k(\mathfrak{S}^k(t_{\sigma}, z))] + \hat{u}_{\xi}^r(t, z) \}, \end{aligned} \quad (19)$$

$$\begin{aligned} \frac{\partial^\lambda \wp^i(t, z)}{\partial t^\lambda} &= \sum_{\xi=1}^{\zeta} \Psi_{\xi}(\beta(t)) \{ \Delta \wp^i(t, z) - \mathcal{A}_{\xi} \wp^i(t, z) + \mathcal{B}_{\xi}^R [F^i(\mathfrak{Z}^i(t, z)) - F^i(\mathfrak{S}^i(t, z))] + \mathcal{B}_{\xi}^I [F^r(\mathfrak{Z}^r(t, z)) - F^r(\mathfrak{S}^r(t, z))] + \mathcal{B}_{\xi}^j [F^k(\mathfrak{Z}^k(t, z)) - F^k(\mathfrak{S}^k(t, z))] - \mathcal{B}_{\xi}^k [F^j(\mathfrak{Z}^j(t, z)) - F^j(\mathfrak{S}^j(t, z))] + \mathcal{D}_{\xi}^R [G^i(\mathfrak{Z}^i(t_{\sigma}, z)) - G^i(\mathfrak{S}^i(t_{\sigma}, z))] + \mathcal{D}_{\xi}^I [G^r(\mathfrak{Z}^r(t_{\sigma}, z)) - G^r(\mathfrak{S}^r(t_{\sigma}, z))] + \mathcal{D}_{\xi}^j [G^k(\mathfrak{Z}^k(t_{\sigma}, z)) - G^k(\mathfrak{S}^k(t_{\sigma}, z))] - \mathcal{D}_{\xi}^k [G^j(\mathfrak{Z}^j(t_{\sigma}, z)) - G^j(\mathfrak{S}^j(t_{\sigma}, z))] + \hat{u}_{\xi}^i(t, z) \}, \end{aligned} \quad (20)$$

$$\begin{aligned} \frac{\partial^\lambda \wp^j(t, z)}{\partial t^\lambda} &= \sum_{\xi=1}^{\zeta} \Psi_{\xi}(\beta(t)) \{ \Delta \wp^j(t, z) - \mathcal{A}_{\xi} \wp^j(t, z) + \mathcal{B}_{\xi}^R [F^j(\mathfrak{Z}^j(t, z)) - F^j(\mathfrak{S}^j(t, z))] - \mathcal{B}_{\xi}^I [F^k(\mathfrak{Z}^k(t, z)) - F^k(\mathfrak{S}^k(t, z))] + \mathcal{B}_{\xi}^j [F^r(\mathfrak{Z}^r(t, z)) - F^r(\mathfrak{S}^r(t, z))] + \mathcal{B}_{\xi}^k [F^i(\mathfrak{Z}^i(t, z)) - F^i(\mathfrak{S}^i(t, z))] + \mathcal{D}_{\xi}^R [G^j(\mathfrak{Z}^j(t_{\sigma}, z)) - G^j(\mathfrak{S}^j(t_{\sigma}, z))] - \mathcal{D}_{\xi}^I [G^k(\mathfrak{Z}^k(t_{\sigma}, z)) - G^k(\mathfrak{S}^k(t_{\sigma}, z))] + \mathcal{D}_{\xi}^j [G^r(\mathfrak{Z}^r(t_{\sigma}, z)) - G^r(\mathfrak{S}^r(t_{\sigma}, z))] + \mathcal{D}_{\xi}^k [G^i(\mathfrak{Z}^i(t_{\sigma}, z)) - G^i(\mathfrak{S}^i(t_{\sigma}, z))] + \hat{u}_{\xi}^j(t, z) \}, \end{aligned} \quad (21)$$

$$\begin{aligned} \frac{\partial^\lambda \wp^k(t, z)}{\partial t^\lambda} &= \sum_{\xi=1}^{\zeta} \Psi_{\xi}(\beta(t)) \{ \Delta \wp^k(t, z) - \mathcal{A}_{\xi} \wp^k(t, z) + \mathcal{B}_{\xi}^R [F^k(\mathfrak{Z}^k(t, z)) - F^k(\mathfrak{S}^k(t, z))] + \mathcal{B}_{\xi}^I [F^j(\mathfrak{Z}^j(t, z)) - F^j(\mathfrak{S}^j(t, z))] - \mathcal{B}_{\xi}^j [F^i(\mathfrak{Z}^i(t, z)) - F^i(\mathfrak{S}^i(t, z))] + \mathcal{B}_{\xi}^k [F^r(\mathfrak{Z}^r(t, z)) - F^r(\mathfrak{S}^r(t, z))] + \mathcal{D}_{\xi}^R [G^k(\mathfrak{Z}^k(t_{\sigma}, z)) - G^k(\mathfrak{S}^k(t_{\sigma}, z))] + \mathcal{D}_{\xi}^I [G^j(\mathfrak{Z}^j(t_{\sigma}, z)) - G^j(\mathfrak{S}^j(t_{\sigma}, z))] - \mathcal{D}_{\xi}^j [G^i(\mathfrak{Z}^i(t_{\sigma}, z)) - G^i(\mathfrak{S}^i(t_{\sigma}, z))] + \mathcal{D}_{\xi}^k [G^r(\mathfrak{Z}^r(t_{\sigma}, z)) - G^r(\mathfrak{S}^r(t_{\sigma}, z))] + \hat{u}_{\xi}^k(t, z) \}. \end{aligned} \quad (22)$$

The initial and boundary values of (19)-(22) are set as

$$\begin{cases} \wp^{\eta}(t, z) = 0, & (t, z) \in [-\sigma, +\infty) \times \partial\Omega, \\ \wp^{\eta}(s, z) = \hat{\psi}^{\eta}(s, z), & (s, z) \in [-\sigma, 0] \times \Omega, \end{cases}$$

where $\hat{\psi}^{\eta}(s, z) = \psi^{\eta}(s, z) - \psi^{\eta}(s, z)$ ($\eta = r, i, j, k$). We define, $\wp(t, z) = ((\wp^r(t, z))^T, (\wp^i(t, z))^T, (\wp^j(t, z))^T, (\wp^k(t, z))^T)^T$, $\Delta \wp(t, z) = ((\Delta \wp^r(t, z))^T, (\Delta \wp^i(t, z))^T, (\Delta \wp^j(t, z))^T, (\Delta \wp^k(t, z))^T)^T$, $\hat{U}_{\xi}(t, z) = ((\hat{u}_{\xi}^r(t, z))^T, (\hat{u}_{\xi}^i(t, z))^T, (\hat{u}_{\xi}^j(t, z))^T, (\hat{u}_{\xi}^k(t, z))^T)^T$.

$$(\hat{u}_\xi^i(t, z))^T, (\hat{u}_\xi^j(t, z))^T, (\hat{u}_\xi^k(t, z))^T, \hat{F}(\hat{\rho}(t, z)) = ((F^r(\mathfrak{Z}^r(t, z)) - F^r(\mathfrak{S}^r(t, z)))^T, (F^i(\mathfrak{Z}^i(t, z)) - F^i(\mathfrak{S}^i(t, z)))^T, (F^j(\mathfrak{Z}^j(t, z)) - F^j(\mathfrak{S}^j(t, z)))^T, (F^k(\mathfrak{Z}^k(t, z)) - F^k(\mathfrak{S}^k(t, z)))^T)^T, \hat{G}(\hat{\rho}(t_\sigma, z)) = ((G^r(\mathfrak{Z}^r(t_\sigma, z)) - G^r(\mathfrak{S}^r(t_\sigma, z)))^T, (G^i(\mathfrak{Z}^i(t_\sigma, z)) - G^i(\mathfrak{S}^i(t_\sigma, z)))^T, (G^j(\mathfrak{Z}^j(t_\sigma, z)) - G^j(\mathfrak{S}^j(t_\sigma, z)))^T, (G^k(\mathfrak{Z}^k(t_\sigma, z)) - G^k(\mathfrak{S}^k(t_\sigma, z)))^T)^T,$$

$$\hat{A}_\xi = \text{diag}(\mathcal{A}_\xi, \mathcal{A}_\xi, \mathcal{A}_\xi, \mathcal{A}_\xi),$$

$$\hat{B}_\xi = \begin{bmatrix} \mathcal{B}_\xi^r & -\mathcal{B}_\xi^i & -\mathcal{B}_\xi^j & -\mathcal{B}_\xi^k \\ \mathcal{B}_\xi^i & \mathcal{B}_\xi^r & -\mathcal{B}_\xi^k & \mathcal{B}_\xi^j \\ \mathcal{B}_\xi^j & \mathcal{B}_\xi^k & \mathcal{B}_\xi^r & -\mathcal{B}_\xi^i \\ \mathcal{B}_\xi^k & -\mathcal{B}_\xi^j & \mathcal{B}_\xi^i & \mathcal{B}_\xi^r \end{bmatrix},$$

$$\hat{C}_\xi = \begin{bmatrix} \mathcal{C}_\xi^r & -\mathcal{C}_\xi^i & -\mathcal{C}_\xi^j & -\mathcal{C}_\xi^k \\ \mathcal{C}_\xi^i & \mathcal{C}_\xi^r & -\mathcal{C}_\xi^k & \mathcal{C}_\xi^j \\ \mathcal{C}_\xi^j & \mathcal{C}_\xi^k & \mathcal{C}_\xi^r & -\mathcal{C}_\xi^i \\ \mathcal{C}_\xi^k & -\mathcal{C}_\xi^j & \mathcal{C}_\xi^i & \mathcal{C}_\xi^r \end{bmatrix}.$$

Then the system (19)-(22) can be expressed as

$$\frac{\partial^\lambda \rho(t, z)}{\partial t^\lambda} = \sum_{\xi=1}^{\zeta} \Psi_\xi(\beta(t)) \{ \Delta \rho(t, z) - \hat{A}_\xi \rho(t, z) + \hat{B}_\xi \hat{F}(\hat{\rho}(t, z)) + \hat{C}_\xi \hat{G}(\hat{\rho}(t_\sigma, z)) + \hat{U}_\xi(t, z) \}. \quad (23)$$

The initial and boundary values related to system (23) are of the form

$$\begin{cases} \rho(t, z) = 0, & (t, z) \in [-\sigma, +\infty) \times \partial\Omega, \\ \rho(s, z) = \hat{\psi}(s, z), & (s, z) \in [-\sigma, 0] \times \Omega, \end{cases} \quad (24)$$

where $\hat{\psi}(s, z) = ((\hat{\psi}^r(s, z))^T, (\hat{\psi}^i(s, z))^T, (\hat{\psi}^j(s, z))^T, (\hat{\psi}^k(s, z))^T)^T$.

Definition 3 [60]: The drive system (4) is said to be finite-time Mittag-Leffler synchronized with response system (5) for proposed controllers. That is, the state of error system (23) is said to be Mittag-Leffler stable in finite-time under initial condition (24), if there exist positive constants $\{\delta^\eta, \epsilon^\eta, \Theta, \omega, T\}$ ($\eta = r, i, j, k$), $\delta = \sum_{\eta=r,i}^{j,k} \{\delta^\eta\}$, $\epsilon = \sum_{\eta=r,i}^{j,k} \{\epsilon^\eta\}$, $\epsilon > \delta$, $\|\hat{\psi}(s, z)\| \leq \delta^\eta$, and $\|\hat{\psi}(s, z)\| \leq \delta$, such that $\|\rho^\eta(t, z)\| \leq \epsilon^\eta$ and $\|\rho(t, z)\| \leq \|\hat{\psi}(s, z)\| \{\mathbb{E}_\lambda(-\Theta t^\lambda)\}^\omega < \epsilon$, hold ($t \geq 0, t \in F$ and F is the interval $[0, T)$).

Lemma 1 [36]: For a continuously differentiable with respect to its first argument function $\rho : [0, v] \times \Omega \rightarrow \mathbb{R}$, $v > 0$, we have

$$\frac{1}{2} \frac{\partial^\lambda \rho^2(t, z)}{\partial t^\lambda} \leq \rho(t, z) \frac{\partial^\lambda \rho(t, z)}{\partial t^\lambda}, \quad t \geq 0, z \in \Omega,$$

where $0 < \lambda < 1$.

Lemma 2 [36]: Let Ω be cube $|z_k| < l_k$ ($k = 1, 2, \dots, m$) and $\vartheta(z) = \vartheta(z_1, z_2, \dots, z_m)$ be a real-valued function which defines on $\vartheta(z) \in \mathbb{C}^1(\Omega)$ and it vanishes on the boundary $\partial\Omega$ of Ω , i.e., $\vartheta(z)|_{z \in \partial\Omega} = 0$. Then

$$\int_\Omega \vartheta^2(z) dz \leq l_k^2 \int_\Omega \left(\frac{\partial \vartheta(z)}{\partial z_k} \right)^2 dz.$$

Lemma 3 [38]: Assume that the function $\mathbb{V} \in \mathbb{V}_0$ is such that for $t > 0$ and the inequality ${}^C D_0^\lambda \mathbb{V}(t, \hat{\rho}(t, z)) \leq -\hat{\pi} \mathbb{V}(t, \hat{\rho}(t, z))$, where $\lambda \in (0, 1)$ and $\hat{\pi} > 0$. Then

$$\mathbb{V}(t, \hat{\rho}(t, z)) \leq \sup_{-\sigma \leq s \leq 0} \mathbb{V}(0, \hat{\rho}(0, z)) \mathbb{E}_\lambda(\hat{\pi} t^\lambda), \quad t > 0.$$

III. MAIN RESULTS

In this section, some sufficient conditions are derived by designing suitable controllers respectively to achieve FTMLS of the drive-response system (4) and (5). To achieve the FTMLS of drive-response system, the following controllers are designed

$$\hat{u}_\xi^\eta(t, z) = -\mu_{\xi\theta}^\eta \rho_\theta^\eta(t, z), \quad (25)$$

where $\xi = 1, 2, \dots, \zeta$; $\mu_{\xi\theta}^\eta$ ($\eta = r, i, j, k$) are fuzzy feedback control gains to be determined later.

Remark 1: The control gains $\mu_{\xi\theta}^\eta$ are considered to be not same in $\hat{u}_\xi^r, \hat{u}_\xi^i, \hat{u}_\xi^j$ and \hat{u}_ξ^k , so the conservatism can be improved.

Theorem 1: Under Assumption 1 and 2, the system (4) and (5) achieve the FTMLS via controller (25) if the following conditions holds:

$$(i) \quad \Theta = (\mathbb{U} - \mathbb{L}) > 0, \quad (26)$$

$$(ii) \quad \mathbb{E}_\lambda(-\Theta t^\lambda) < \frac{\epsilon^2}{\delta^2}, \quad (27)$$

where,

$$\mathbb{U} = \min_{1 \leq \theta \leq n} \{\mathbb{U}_\theta^r, \mathbb{U}_\theta^i, \mathbb{U}_\theta^j, \mathbb{U}_\theta^k\}, \quad \mathbb{L} = \max_{1 \leq \theta \leq n} \{\mathbb{L}_\theta^r, \mathbb{L}_\theta^i, \mathbb{L}_\theta^j, \mathbb{L}_\theta^k\},$$

$$\hat{\mathbb{Q}} = \frac{\hat{q}_{\theta\alpha}}{l_\alpha^2},$$

$$\mathbb{U}_\theta^r = \min_{1 \leq \theta \leq n} \left\{ \frac{1}{2} [2(a_{\xi\theta} + \hat{\mathbb{Q}} + \mu_{\xi\theta}^r) - \sum_{\varphi=1}^n (\mathcal{F}_\varphi^r |b_{\xi\theta\varphi}^r| - \mathcal{F}_\varphi^i |b_{\xi\theta\varphi}^i| - \mathcal{F}_\varphi^j |b_{\xi\theta\varphi}^j| - \mathcal{F}_\varphi^k |b_{\xi\theta\varphi}^k| + \mathcal{F}_\varphi^r (|b_{\xi\theta\varphi}^r| + |b_{\xi\theta\varphi}^i| + |b_{\xi\theta\varphi}^j| + |b_{\xi\theta\varphi}^k|) + \mathcal{G}_\varphi^i |d_{\xi\theta\varphi}^r| - \mathcal{G}_\varphi^j |d_{\xi\theta\varphi}^i| - \mathcal{G}_\varphi^k |d_{\xi\theta\varphi}^j|)] \right\},$$

$$\mathbb{U}_\theta^i = \min_{1 \leq \theta \leq n} \left\{ \frac{1}{2} [2(a_{\xi\theta} + \hat{\mathbb{Q}} + \mu_{\xi\theta}^i) - \sum_{\varphi=1}^n (\mathcal{F}_\varphi^i |b_{\xi\theta\varphi}^r| + \mathcal{F}_\varphi^r |b_{\xi\theta\varphi}^i| + \mathcal{F}_\varphi^k |b_{\xi\theta\varphi}^j| - \mathcal{F}_\varphi^j |b_{\xi\theta\varphi}^k| + \mathcal{F}_\varphi^i (|b_{\xi\theta\varphi}^r| - |b_{\xi\theta\varphi}^i| + |b_{\xi\theta\varphi}^k| - |b_{\xi\theta\varphi}^j|) + \mathcal{G}_\varphi^i |d_{\xi\theta\varphi}^r| + \mathcal{G}_\varphi^r |d_{\xi\theta\varphi}^i| + \mathcal{G}_\varphi^k |d_{\xi\theta\varphi}^j| - \mathcal{G}_\varphi^j |d_{\xi\theta\varphi}^k|)] \right\},$$

$$\mathbb{U}_\theta^j = \min_{1 \leq \theta \leq n} \left\{ \frac{1}{2} [2(a_{\xi\theta} + \hat{\mathbb{Q}} + \mu_{\xi\theta}^j) - \sum_{\varphi=1}^n (\mathcal{F}_\varphi^j |b_{\xi\theta\varphi}^r| - \mathcal{F}_\varphi^k |b_{\xi\theta\varphi}^i| + \mathcal{F}_\varphi^r |b_{\xi\theta\varphi}^j| + \mathcal{F}_\varphi^i |b_{\xi\theta\varphi}^k| + \mathcal{F}_\varphi^j (|b_{\xi\theta\varphi}^r| - |b_{\xi\theta\varphi}^i| - |b_{\xi\theta\varphi}^k| + |b_{\xi\theta\varphi}^j|) + \mathcal{G}_\varphi^i |d_{\xi\theta\varphi}^r| - \mathcal{G}_\varphi^k |d_{\xi\theta\varphi}^i| + \mathcal{G}_\varphi^r |d_{\xi\theta\varphi}^j| + \mathcal{G}_\varphi^i |d_{\xi\theta\varphi}^k|)] \right\},$$

$$\begin{aligned} \mathcal{U}_\theta^k &= \min_{1 \leq \theta \leq n} \left\{ \frac{1}{2} [2(a_{\xi\theta} + \widehat{Q} + \mu_{\xi\theta}^k) - \sum_{\varphi=1}^n (\mathcal{F}_\varphi^k |b_{\xi\theta\varphi}^r| \right. \\ &\quad + \mathcal{F}_\varphi^j |b_{\xi\theta\varphi}^i| - \mathcal{F}_\varphi^i |b_{\xi\theta\varphi}^j| + \mathcal{F}_\varphi^r |b_{\xi\theta\varphi}^k| + \mathcal{F}_\varphi^k (|b_{\xi\theta\varphi}^r| \\ &\quad - |b_{\xi\theta\varphi}^k| + |b_{\xi\theta\varphi}^j| - |b_{\xi\theta\varphi}^i|) + \mathcal{G}_\varphi^k |d_{\xi\theta\varphi}^r| + \mathcal{G}_\varphi^j |d_{\xi\theta\varphi}^i| \\ &\quad \left. - \mathcal{G}_\varphi^i |d_{\xi\theta\varphi}^j| + \mathcal{G}_\varphi^r |d_{\xi\theta\varphi}^k|) \right\}, \\ \mathcal{L}_\theta^r &= \max_{1 \leq \theta \leq n} \left\{ \frac{1}{2} \sum_{\varphi=1}^n \mathcal{G}_\varphi^r (|d_{\xi\theta\varphi}^r| + |d_{\xi\theta\varphi}^i| + |d_{\xi\theta\varphi}^j| + |d_{\xi\theta\varphi}^k|) \right\}, \\ \mathcal{L}_\theta^i &= \max_{1 \leq \theta \leq n} \left\{ \frac{1}{2} \sum_{\varphi=1}^n \mathcal{G}_\varphi^i (|d_{\xi\theta\varphi}^r| - |d_{\xi\theta\varphi}^i| - |d_{\xi\theta\varphi}^j| + |d_{\xi\theta\varphi}^k|) \right\}, \\ \mathcal{L}_\theta^j &= \max_{1 \leq \theta \leq n} \left\{ \frac{1}{2} \sum_{\varphi=1}^n \mathcal{G}_\varphi^j (|d_{\xi\theta\varphi}^r| + |d_{\xi\theta\varphi}^i| - |d_{\xi\theta\varphi}^j| - |d_{\xi\theta\varphi}^k|) \right\}, \\ \mathcal{L}_\theta^k &= \max_{1 \leq \theta \leq n} \left\{ \frac{1}{2} \sum_{\varphi=1}^n \mathcal{G}_\varphi^k (|d_{\xi\theta\varphi}^r| - |d_{\xi\theta\varphi}^i| + |d_{\xi\theta\varphi}^j| - |d_{\xi\theta\varphi}^k|) \right\}. \end{aligned}$$

Proof: Consider a Lyapunov function as follows

$$\mathbb{V}(t, \wp(t, z)) = \sum_{\eta=r,i}^{j,k} \int_{\Omega} \sum_{\theta=1}^n \frac{1}{2} (\wp_\theta^\eta)^2(t, z) dz. \quad (28)$$

By calculating the Caputo fractional derivative of $\mathbb{V}(t, \wp(t, z))$ with $\lambda \in (0, 1)$, along the trajectory of the error system, we can obtain

$$\begin{aligned} \frac{d^\lambda \mathbb{V}(t, \wp(t, z))}{dt^\lambda} &= \sum_{\eta=r,i}^{j,k} \left\{ \frac{1}{2} \frac{d^\lambda}{dt^\lambda} \left(\int_{\Omega} \sum_{\theta=1}^n (\wp_\theta^\eta)^2(t, z) dz \right) \right\} \\ &= \sum_{\eta=r,i}^{j,k} \frac{1}{2} \sum_{\theta=1}^n \left\{ \frac{d^\lambda}{dt^\lambda} \left(\int_{\Omega} (\wp_\theta^\eta)^2(t, z) dz \right) \right\}. \end{aligned} \quad (29)$$

In particular, we have

$$\begin{aligned} \frac{d^\lambda}{dt^\lambda} \left(\int_{\Omega} (\wp_\theta^\eta)^2(t, z) dz \right) &= \frac{1}{\Gamma(1-\lambda)} \int_0^t \left(\frac{d}{ds} \int_{\Omega} (\wp_\theta^\eta)^2(t, z) dz \right) \frac{ds}{(t-s)^\lambda} \\ &= \int_{\Omega} \frac{1}{\Gamma(1-\lambda)} \left(\int_0^t \frac{\partial (\wp_\theta^\eta)^2(t, z)}{\partial s} \frac{ds}{(t-s)^\lambda} \right) dz \\ &= \int_{\Omega} \frac{\partial^\lambda (\wp_\theta^\eta)^2(t, z)}{\partial t^\lambda} dz. \end{aligned} \quad (30)$$

From (29) and (30), we get

$$\frac{d^\lambda \mathbb{V}(t, \wp(t, z))}{dt^\lambda} = \sum_{\eta=r,i}^{j,k} \left\{ \frac{1}{2} \sum_{\theta=1}^n \int_{\Omega} \frac{\partial^\lambda (\wp_\theta^\eta)^2(t, z)}{\partial t^\lambda} dz \right\}.$$

It follows from Lemma 1 that

$$\frac{d^\lambda \mathbb{V}(t, \wp(t, z))}{dt^\lambda} \leq \sum_{\eta=r,i}^{j,k} \left\{ \sum_{\theta=1}^n \int_{\Omega} \wp_\theta^\eta(t, z) \frac{\partial^\lambda \wp_\theta^\eta(t, z)}{\partial t^\lambda} dz \right\}.$$

That is,

$$\begin{aligned} {}^C D_0^\lambda \mathbb{V}(t, \wp(t, z)) &\leq \sum_{\theta=1}^n \int_{\Omega} \wp_\theta^r(t, z) \frac{\partial^\lambda \wp_\theta^r(t, z)}{\partial t^\lambda} dz \\ &\quad + \sum_{\theta=1}^n \int_{\Omega} \wp_\theta^i(t, z) \frac{\partial^\lambda \wp_\theta^i(t, z)}{\partial t^\lambda} dz \\ &\quad + \sum_{\theta=1}^n \int_{\Omega} \wp_\theta^j(t, z) \frac{\partial^\lambda \wp_\theta^j(t, z)}{\partial t^\lambda} dz \\ &\quad + \sum_{\theta=1}^n \int_{\Omega} \wp_\theta^k(t, z) \frac{\partial^\lambda \wp_\theta^k(t, z)}{\partial t^\lambda} dz. \end{aligned}$$

We denote,

$$\begin{aligned} \mathbb{W}_1 &= \sum_{\theta=1}^n \int_{\Omega} \wp_\theta^r(t, z) \frac{\partial^\lambda \wp_\theta^r(t, z)}{\partial t^\lambda} dz, \\ \mathbb{W}_2 &= \sum_{\theta=1}^n \int_{\Omega} \wp_\theta^i(t, z) \frac{\partial^\lambda \wp_\theta^i(t, z)}{\partial t^\lambda} dz, \\ \mathbb{W}_3 &= \sum_{\theta=1}^n \int_{\Omega} \wp_\theta^j(t, z) \frac{\partial^\lambda \wp_\theta^j(t, z)}{\partial t^\lambda} dz, \\ \mathbb{W}_4 &= \sum_{\theta=1}^n \int_{\Omega} \wp_\theta^k(t, z) \frac{\partial^\lambda \wp_\theta^k(t, z)}{\partial t^\lambda} dz. \end{aligned}$$

Then,

$$\begin{aligned} \mathbb{W}_1 &\leq \sum_{\xi=1}^{\zeta} \Psi_\xi(\beta(t)) \sum_{\theta=1}^n \int_{\Omega} \wp_\theta^r(t, z) \left\{ \sum_{\alpha=1}^m \frac{\partial}{\partial z_\alpha} (q_{\theta\alpha} \frac{\partial \wp_\theta^r(t, z)}{\partial z_\alpha}) \right. \\ &\quad - a_{\xi\theta} \wp_\theta^r(t, z) + \sum_{\varphi=1}^n b_{\xi\theta\varphi}^r [f_\varphi^r(\mathfrak{Z}_\varphi^r(t, z)) - f_\varphi^r(\mathfrak{N}_\varphi^r(t, z))] \\ &\quad - \sum_{\varphi=1}^n b_{\xi\theta\varphi}^i [f_\varphi^i(\mathfrak{Z}_\varphi^i(t, z)) - f_\varphi^i(\mathfrak{N}_\varphi^i(t, z))] \\ &\quad - \sum_{\varphi=1}^n b_{\xi\theta\varphi}^j [f_\varphi^j(\mathfrak{Z}_\varphi^j(t, z)) - f_\varphi^j(\mathfrak{N}_\varphi^j(t, z))] \\ &\quad - \sum_{\varphi=1}^n b_{\xi\theta\varphi}^k [f_\varphi^k(\mathfrak{Z}_\varphi^k(t, z)) - f_\varphi^k(\mathfrak{N}_\varphi^k(t, z))] \\ &\quad + \sum_{\varphi=1}^n d_{\xi\theta\varphi}^r [g_\varphi^r(\mathfrak{Z}_\varphi^r(t_\sigma, z)) - g_\varphi^r(\mathfrak{N}_\varphi^r(t_\sigma, z))] \\ &\quad - \sum_{\varphi=1}^n d_{\xi\theta\varphi}^i [g_\varphi^i(\mathfrak{Z}_\varphi^i(t_\sigma, z)) - g_\varphi^i(\mathfrak{N}_\varphi^i(t_\sigma, z))] \\ &\quad - \sum_{\varphi=1}^n d_{\xi\theta\varphi}^j [g_\varphi^j(\mathfrak{Z}_\varphi^j(t_\sigma, z)) - g_\varphi^j(\mathfrak{N}_\varphi^j(t_\sigma, z))] \\ &\quad - \sum_{\varphi=1}^n d_{\xi\theta\varphi}^k [g_\varphi^k(\mathfrak{Z}_\varphi^k(t_\sigma, z)) - g_\varphi^k(\mathfrak{N}_\varphi^k(t_\sigma, z))] \\ &\quad \left. - \mu_{\xi\theta}^r \wp_\theta^r(t, z) \right\}. \end{aligned} \quad (31)$$

By the boundary conditions and Green's formula, we have

$$\sum_{\alpha=1}^m \int_{\Omega} \wp_{\theta}^r(t, z) \frac{\partial}{\partial z_{\alpha}} \left(q_{\theta\alpha} \frac{\partial \wp_{\theta}^r(t, z)}{\partial z_{\alpha}} \right) dz = - \sum_{\alpha=1}^m \int_{\Omega} q_{\theta\alpha} \left(\frac{\partial \wp_{\theta}^r(t, z)}{\partial z_{\alpha}} \right)^2 dz.$$

By using Assumption 2 and the light of Lemma 2, we have

$$\begin{aligned} & \sum_{\alpha=1}^m \int_{\Omega} \wp_{\theta}^r(t, z) \frac{\partial}{\partial z_{\alpha}} \left(q_{\theta\alpha} \frac{\partial \wp_{\theta}^r(t, z)}{\partial z_{\alpha}} \right) dz \\ & \leq - \sum_{\alpha=1}^m \int_{\Omega} \hat{q}_{\theta\alpha} \left(\frac{\partial \wp_{\theta}^r(t, z)}{\partial z_{\alpha}} \right)^2 dz \\ & \leq - \sum_{\alpha=1}^m \int_{\Omega} \frac{\hat{q}_{\theta\alpha}}{l_{\alpha}^2} (\wp_{\theta}^r)^2(t, z) dz \\ & \leq - \hat{Q} \int_{\Omega} (\wp_{\theta}^r)^2(t, z) dz. \end{aligned} \tag{32}$$

According to Assumption 1 and the inequality $2|x||y| \leq x^2+y^2$, we have

$$\begin{aligned} & \sum_{\varphi=1}^n b_{\xi\theta\varphi}^r \int_{\Omega} \wp_{\theta}^r(t, z) [f_{\varphi}^r(\mathfrak{Z}_{\varphi}^r(t, z)) - f_{\varphi}^r(\mathfrak{S}_{\varphi}^r(t, z))] dz \\ & \leq \sum_{\varphi=1}^n \mathcal{F}_{\varphi}^r |b_{\xi\theta\varphi}^r| \int_{\Omega} |\wp_{\theta}^r(t, z)| |\wp_{\varphi}^r(t, z)| dz \\ & \leq \frac{1}{2} \sum_{\varphi=1}^n \mathcal{F}_{\varphi}^r |b_{\xi\theta\varphi}^r| \int_{\Omega} ((\wp_{\theta}^r)^2(t, z) + (\wp_{\varphi}^r)^2(t, z)) dz, \end{aligned} \tag{33}$$

$$\begin{aligned} & \sum_{\varphi=1}^n b_{\xi\theta\varphi}^i \int_{\Omega} \wp_{\theta}^i(t, z) [f_{\varphi}^i(\mathfrak{Z}_{\varphi}^i(t, z)) - f_{\varphi}^i(\mathfrak{S}_{\varphi}^i(t, z))] dz \\ & \leq \frac{1}{2} \sum_{\varphi=1}^n \mathcal{F}_{\varphi}^i |b_{\xi\theta\varphi}^i| \int_{\Omega} ((\wp_{\theta}^i)^2(t, z) + (\wp_{\varphi}^i)^2(t, z)) dz, \end{aligned} \tag{34}$$

$$\begin{aligned} & \sum_{\varphi=1}^n b_{\xi\theta\varphi}^j \int_{\Omega} \wp_{\theta}^j(t, z) [f_{\varphi}^j(\mathfrak{Z}_{\varphi}^j(t, z)) - f_{\varphi}^j(\mathfrak{S}_{\varphi}^j(t, z))] dz \\ & \leq \frac{1}{2} \sum_{\varphi=1}^n \mathcal{F}_{\varphi}^j |b_{\xi\theta\varphi}^j| \int_{\Omega} ((\wp_{\theta}^j)^2(t, z) + (\wp_{\varphi}^j)^2(t, z)) dz, \end{aligned} \tag{35}$$

$$\begin{aligned} & \sum_{\varphi=1}^n b_{\xi\theta\varphi}^k \int_{\Omega} \wp_{\theta}^k(t, z) [f_{\varphi}^k(\mathfrak{Z}_{\varphi}^k(t, z)) - f_{\varphi}^k(\mathfrak{S}_{\varphi}^k(t, z))] dz \\ & \leq \frac{1}{2} \sum_{\varphi=1}^n \mathcal{F}_{\varphi}^k |b_{\xi\theta\varphi}^k| \int_{\Omega} ((\wp_{\theta}^k)^2(t, z) + (\wp_{\varphi}^k)^2(t, z)) dz, \end{aligned} \tag{36}$$

$$\begin{aligned} & \sum_{\varphi=1}^n d_{\xi\theta\varphi}^r \int_{\Omega} \wp_{\theta}^r(t, z) [g_{\varphi}^r(\mathfrak{Z}_{\varphi}^r(t_{\sigma}, z)) - g_{\varphi}^r(\mathfrak{S}_{\varphi}^r(t_{\sigma}, z))] dz \\ & \leq \frac{1}{2} \sum_{\varphi=1}^n \mathcal{G}_{\varphi}^r |d_{\xi\theta\varphi}^r| \int_{\Omega} ((\wp_{\theta}^r)^2(t, z) + (\wp_{\varphi}^r)^2(t_{\sigma}, z)) dz, \end{aligned} \tag{37}$$

$$\sum_{\varphi=1}^n d_{\xi\theta\varphi}^i \int_{\Omega} \wp_{\theta}^i(t_{\sigma}, z) [g_{\varphi}^i(\mathfrak{Z}_{\varphi}^i(t_{\sigma}, z)) - g_{\varphi}^i(\mathfrak{S}_{\varphi}^i(t_{\sigma}, z))] dz$$

$$\leq \frac{1}{2} \sum_{\varphi=1}^n \mathcal{G}_{\varphi}^i |d_{\xi\theta\varphi}^i| \int_{\Omega} ((\wp_{\theta}^i)^2(t, z) + (\wp_{\varphi}^i)^2(t_{\sigma}, z)) dz, \tag{38}$$

$$\begin{aligned} & \sum_{\varphi=1}^n d_{\xi\theta\varphi}^j \int_{\Omega} \wp_{\theta}^j(t_{\sigma}, z) [g_{\varphi}^j(\mathfrak{Z}_{\varphi}^j(t_{\sigma}, z)) - g_{\varphi}^j(\mathfrak{S}_{\varphi}^j(t_{\sigma}, z))] dz \\ & \leq \frac{1}{2} \sum_{\varphi=1}^n \mathcal{G}_{\varphi}^j |d_{\xi\theta\varphi}^j| \int_{\Omega} ((\wp_{\theta}^j)^2(t, z) + (\wp_{\varphi}^j)^2(t_{\sigma}, z)) dz, \end{aligned} \tag{39}$$

$$\begin{aligned} & \sum_{\varphi=1}^n d_{\xi\theta\varphi}^k \int_{\Omega} \wp_{\theta}^k(t_{\sigma}, z) [g_{\varphi}^k(\mathfrak{Z}_{\varphi}^k(t_{\sigma}, z)) - g_{\varphi}^k(\mathfrak{S}_{\varphi}^k(t_{\sigma}, z))] dz \\ & \leq \frac{1}{2} \sum_{\varphi=1}^n \mathcal{G}_{\varphi}^k |d_{\xi\theta\varphi}^k| \int_{\Omega} ((\wp_{\theta}^k)^2(t, z) + (\wp_{\varphi}^k)^2(t_{\sigma}, z)) dz. \end{aligned} \tag{40}$$

Substituting (32)-(40) into (31), we obtain that

$$\begin{aligned} \mathbb{W}_1 & \leq \sum_{\xi=1}^{\zeta} \Psi_{\xi}(\beta(t)) \left\{ -\frac{1}{2} \sum_{\theta=1}^n [2(a_{\xi\theta} + \hat{Q} + \mu_{\xi\theta}^r)] \right. \\ & \quad - \sum_{\varphi=1}^n (\mathcal{F}_{\varphi}^r |b_{\xi\theta\varphi}^r| - \mathcal{F}_{\varphi}^i |b_{\xi\theta\varphi}^i| - \mathcal{F}_{\varphi}^j |b_{\xi\theta\varphi}^j| - \mathcal{F}_{\varphi}^k |b_{\xi\theta\varphi}^k| \\ & \quad + \mathcal{F}_{\varphi}^r |b_{\xi\theta\varphi}^r| + \mathcal{G}_{\varphi}^r |d_{\xi\theta\varphi}^r| - \mathcal{G}_{\varphi}^i |d_{\xi\theta\varphi}^i| - \mathcal{G}_{\varphi}^j |d_{\xi\theta\varphi}^j| \\ & \quad \left. - \mathcal{G}_{\varphi}^k |d_{\xi\theta\varphi}^k|) \int_{\Omega} (\wp_{\theta}^r)^2(t, z) dz \right. \\ & \quad - \frac{1}{2} \sum_{\theta=1}^n \sum_{\varphi=1}^n \mathcal{F}_{\theta}^i |b_{\xi\theta\varphi}^i| \int_{\Omega} (\wp_{\theta}^i)^2(t, z) dz \\ & \quad - \frac{1}{2} \sum_{\theta=1}^n \sum_{\varphi=1}^n \mathcal{F}_{\theta}^j |b_{\xi\theta\varphi}^j| \int_{\Omega} (\wp_{\theta}^j)^2(t, z) dz \\ & \quad - \frac{1}{2} \sum_{\theta=1}^n \sum_{\varphi=1}^n \mathcal{F}_{\theta}^k |b_{\xi\theta\varphi}^k| \int_{\Omega} (\wp_{\theta}^k)^2(t, z) dz \\ & \quad + \frac{1}{2} \sum_{\theta=1}^n \sum_{\varphi=1}^n \mathcal{G}_{\theta}^r |d_{\xi\theta\varphi}^r| \int_{\Omega} (\wp_{\theta}^r)^2(t_{\sigma}, z) dz \\ & \quad - \frac{1}{2} \sum_{\theta=1}^n \sum_{\varphi=1}^n \mathcal{G}_{\theta}^i |d_{\xi\theta\varphi}^i| \int_{\Omega} (\wp_{\theta}^i)^2(t_{\sigma}, z) dz \\ & \quad - \frac{1}{2} \sum_{\theta=1}^n \sum_{\varphi=1}^n \mathcal{G}_{\theta}^j |d_{\xi\theta\varphi}^j| \int_{\Omega} (\wp_{\theta}^j)^2(t_{\sigma}, z) dz \\ & \quad \left. - \frac{1}{2} \sum_{\theta=1}^n \sum_{\varphi=1}^n \mathcal{G}_{\theta}^k |d_{\xi\theta\varphi}^k| \int_{\Omega} (\wp_{\theta}^k)^2(t_{\sigma}, z) dz \right\}. \end{aligned} \tag{41}$$

Similarly,

$$\begin{aligned} \mathbb{W}_2 & \leq \sum_{\xi=1}^{\zeta} \Psi_{\xi}(\beta(t)) \left\{ \frac{1}{2} \sum_{\theta=1}^n \sum_{\varphi=1}^n \mathcal{F}_{\theta}^r |b_{\xi\theta\varphi}^r| \int_{\Omega} (\wp_{\theta}^r)^2(t, z) dz \right. \\ & \quad - \frac{1}{2} \sum_{\theta=1}^n [2(a_{\xi\theta} + \hat{Q} + \mu_{\xi\theta}^i) - \sum_{\varphi=1}^n (\mathcal{F}_{\varphi}^i |b_{\xi\theta\varphi}^i| \\ & \quad + \mathcal{F}_{\varphi}^r |b_{\xi\theta\varphi}^r| + \mathcal{F}_{\varphi}^k |b_{\xi\theta\varphi}^k| - \mathcal{F}_{\varphi}^j |b_{\xi\theta\varphi}^j| + \mathcal{F}_{\theta}^i |b_{\xi\theta\varphi}^i| \\ & \quad + \mathcal{G}_{\varphi}^i |d_{\xi\theta\varphi}^i| + \mathcal{G}_{\varphi}^r |d_{\xi\theta\varphi}^r| + \mathcal{G}_{\varphi}^k |d_{\xi\theta\varphi}^k| \\ & \quad \left. - \mathcal{G}_{\varphi}^j |d_{\xi\theta\varphi}^j|) \int_{\Omega} (\wp_{\theta}^i)^2(t, z) dz \right. \\ & \quad - \frac{1}{2} \sum_{\theta=1}^n \sum_{\varphi=1}^n \mathcal{F}_{\theta}^j |b_{\xi\theta\varphi}^j| \int_{\Omega} (\wp_{\theta}^j)^2(t, z) dz \\ & \quad - \frac{1}{2} \sum_{\theta=1}^n \sum_{\varphi=1}^n \mathcal{F}_{\theta}^k |b_{\xi\theta\varphi}^k| \int_{\Omega} (\wp_{\theta}^k)^2(t, z) dz \\ & \quad \left. + \frac{1}{2} \sum_{\theta=1}^n \sum_{\varphi=1}^n \mathcal{G}_{\theta}^i |d_{\xi\theta\varphi}^i| \int_{\Omega} (\wp_{\theta}^i)^2(t_{\sigma}, z) dz \right. \\ & \quad + \frac{1}{2} \sum_{\theta=1}^n \sum_{\varphi=1}^n \mathcal{G}_{\theta}^r |d_{\xi\theta\varphi}^r| \int_{\Omega} (\wp_{\theta}^r)^2(t_{\sigma}, z) dz \\ & \quad \left. + \frac{1}{2} \sum_{\theta=1}^n \sum_{\varphi=1}^n \mathcal{G}_{\theta}^k |d_{\xi\theta\varphi}^k| \int_{\Omega} (\wp_{\theta}^k)^2(t_{\sigma}, z) dz \right\}. \end{aligned}$$

$$\begin{aligned}
 & -\mathcal{G}_\varphi^j |d_{\xi\theta\varphi}^k| \int_{\Omega} (\wp_\theta^i)^2(t, z) dz \\
 & -\frac{1}{2} \sum_{\theta=1}^n \sum_{\varphi=1}^n \mathcal{F}_\theta^j |b_{\xi\varphi\theta}^k| \int_{\Omega} (\wp_\theta^j)^2(t, z) dz \\
 & +\frac{1}{2} \sum_{\theta=1}^n \sum_{\varphi=1}^n \mathcal{F}_\theta^k |b_{\xi\varphi\theta}^j| \int_{\Omega} (\wp_\theta^k)^2(t, z) dz \\
 & +\frac{1}{2} \sum_{\theta=1}^n \sum_{\varphi=1}^n \mathcal{G}_\theta^r |d_{\xi\varphi\theta}^i| \int_{\Omega} (\wp_\theta^r)^2(t_\sigma, z) dz \\
 & +\frac{1}{2} \sum_{\theta=1}^n \sum_{\varphi=1}^n \mathcal{G}_\theta^i |d_{\xi\varphi\theta}^r| \int_{\Omega} (\wp_\theta^i)^2(t_\sigma, z) dz \\
 & -\frac{1}{2} \sum_{\theta=1}^n \sum_{\varphi=1}^n \mathcal{G}_\theta^j |d_{\xi\varphi\theta}^k| \int_{\Omega} (\wp_\theta^j)^2(t_\sigma, z) dz \\
 & +\frac{1}{2} \sum_{\theta=1}^n \sum_{\varphi=1}^n \mathcal{G}_\theta^k |d_{\xi\varphi\theta}^i| \int_{\Omega} (\wp_\theta^k)^2(t_\sigma, z) dz \}, \quad (42)
 \end{aligned}$$

$$\begin{aligned}
 \mathbb{W}_3 \leq & \sum_{\xi=1}^{\zeta} \Psi_\xi(\beta(t)) \left\{ \frac{1}{2} \sum_{\theta=1}^n \sum_{\varphi=1}^n \mathcal{F}_\theta^r |b_{\xi\varphi\theta}^j| \int_{\Omega} (\wp_\theta^r)^2(t, z) dz \right. \\
 & +\frac{1}{2} \sum_{\theta=1}^n \sum_{\varphi=1}^n \mathcal{F}_\theta^j |b_{\xi\varphi\theta}^k| \int_{\Omega} (\wp_\theta^j)^2(t, z) dz -\frac{1}{2} \sum_{\theta=1}^n [2(a_{\xi\theta} \\
 & +\widehat{\mathcal{Q}}+\mu_{\xi\theta}^j) - \sum_{\varphi=1}^n (\mathcal{F}_\varphi^j |b_{\xi\theta\varphi}^r| - \mathcal{F}_\varphi^k |b_{\xi\theta\varphi}^i| + \mathcal{F}_\varphi^r |b_{\xi\theta\varphi}^j| \\
 & + \mathcal{F}_\varphi^i |b_{\xi\theta\varphi}^k| + \mathcal{F}_\varphi^j |b_{\xi\theta\varphi}^r| + \mathcal{G}_\varphi^j |d_{\xi\theta\varphi}^r| - \mathcal{G}_\varphi^k |d_{\xi\theta\varphi}^i| \\
 & + \mathcal{G}_\varphi^r |d_{\xi\theta\varphi}^j| + \mathcal{G}_\varphi^i |d_{\xi\theta\varphi}^k|)] \int_{\Omega} (\wp_\theta^j)^2(t, z) dz \\
 & -\frac{1}{2} \sum_{\theta=1}^n \sum_{\varphi=1}^n \mathcal{F}_\theta^k |b_{\xi\varphi\theta}^j| \int_{\Omega} (\wp_\theta^k)^2(t, z) dz \\
 & +\frac{1}{2} \sum_{\theta=1}^n \sum_{\varphi=1}^n \mathcal{G}_\theta^r |d_{\xi\varphi\theta}^i| \int_{\Omega} (\wp_\theta^r)^2(t_\sigma, z) dz \\
 & +\frac{1}{2} \sum_{\theta=1}^n \sum_{\varphi=1}^n \mathcal{G}_\theta^i |d_{\xi\varphi\theta}^r| \int_{\Omega} (\wp_\theta^i)^2(t_\sigma, z) dz \\
 & +\frac{1}{2} \sum_{\theta=1}^n \sum_{\varphi=1}^n \mathcal{G}_\theta^j |d_{\xi\varphi\theta}^k| \int_{\Omega} (\wp_\theta^j)^2(t_\sigma, z) dz \\
 & \left. -\frac{1}{2} \sum_{\theta=1}^n \sum_{\varphi=1}^n \mathcal{G}_\theta^k |d_{\xi\varphi\theta}^i| \int_{\Omega} (\wp_\theta^k)^2(t_\sigma, z) dz \right\}, \quad (43)
 \end{aligned}$$

and

$$\begin{aligned}
 \mathbb{W}_4 \leq & \sum_{\xi=1}^{\zeta} \Psi_\xi(\beta(t)) \left\{ \frac{1}{2} \sum_{\theta=1}^n \sum_{\varphi=1}^n \mathcal{F}_\theta^r |b_{\xi\varphi\theta}^k| \int_{\Omega} (\wp_\theta^r)^2(t, z) dz \right. \\
 & \left. -\frac{1}{2} \sum_{\theta=1}^n \sum_{\varphi=1}^n \mathcal{F}_\theta^i |b_{\xi\varphi\theta}^j| \int_{\Omega} (\wp_\theta^i)^2(t, z) dz \right.
 \end{aligned}$$

$$\begin{aligned}
 & +\frac{1}{2} \sum_{\theta=1}^n \sum_{\varphi=1}^n \mathcal{F}_\theta^j |b_{\xi\varphi\theta}^i| \int_{\Omega} (\wp_\theta^j)^2(t, z) dz \\
 & -\frac{1}{2} \sum_{\theta=1}^n [2(a_{\xi\theta} + \mathcal{Q}_\theta + \mu_{\xi\theta}^k) - \sum_{\varphi=1}^n (\mathcal{F}_\varphi^k |b_{\xi\theta\varphi}^k| \\
 & + \mathcal{F}_\varphi^j |b_{\xi\theta\varphi}^i| - \mathcal{F}_\varphi^i |b_{\xi\theta\varphi}^j| + \mathcal{F}_\varphi^r |b_{\xi\theta\varphi}^k| + \mathcal{F}_\varphi^i |b_{\xi\theta\varphi}^r| \\
 & + \mathcal{G}_\varphi^k |d_{\xi\theta\varphi}^r| + \mathcal{G}_\varphi^j |d_{\xi\theta\varphi}^i| - \mathcal{G}_\varphi^i |d_{\xi\theta\varphi}^j| \\
 & + \mathcal{G}_\varphi^r |d_{\xi\theta\varphi}^k|)] \int_{\Omega} (\wp_\theta^k)^2(t, z) dz \\
 & +\frac{1}{2} \sum_{\theta=1}^n \sum_{\varphi=1}^n \mathcal{G}_\theta^r |d_{\xi\varphi\theta}^k| \int_{\Omega} (\wp_\theta^r)^2(t_\sigma, z) dz \\
 & -\frac{1}{2} \sum_{\theta=1}^n \sum_{\varphi=1}^n \mathcal{G}_\theta^j |d_{\xi\varphi\theta}^i| \int_{\Omega} (\wp_\theta^j)^2(t_\sigma, z) dz \\
 & +\frac{1}{2} \sum_{\theta=1}^n \sum_{\varphi=1}^n \mathcal{G}_\theta^i |d_{\xi\varphi\theta}^r| \int_{\Omega} (\wp_\theta^i)^2(t_\sigma, z) dz \\
 & \left. +\frac{1}{2} \sum_{\theta=1}^n \sum_{\varphi=1}^n \mathcal{G}_\theta^k |d_{\xi\varphi\theta}^r| \int_{\Omega} (\wp_\theta^k)^2(t_\sigma, z) dz \right\}. \quad (44)
 \end{aligned}$$

Combining from (41)-(44), we have

$$\begin{aligned}
 & C_{D_0} \lambda \mathbb{V}(t, \wp(t, z)) \\
 & \leq \sum_{\xi=1}^{\zeta} \Psi_\xi(\beta(t)) \left\{ -\frac{1}{2} \sum_{\theta=1}^n [2(a_{\xi\theta} + \widehat{\mathcal{Q}} + \mu_{\xi\theta}^r) \right. \\
 & - \sum_{\varphi=1}^n (\mathcal{F}_\varphi^r |b_{\xi\theta\varphi}^r| - \mathcal{F}_\varphi^i |b_{\xi\theta\varphi}^j| - \mathcal{F}_\varphi^j |b_{\xi\theta\varphi}^i| - \mathcal{F}_\varphi^k |b_{\xi\theta\varphi}^k| \\
 & + \mathcal{F}_\varphi^r (|b_{\xi\theta\varphi}^r| + |b_{\xi\theta\varphi}^i| + |b_{\xi\theta\varphi}^j| + |b_{\xi\theta\varphi}^k|) + \mathcal{G}_\varphi^r |d_{\xi\theta\varphi}^r| \\
 & \left. - \mathcal{G}_\varphi^i |d_{\xi\theta\varphi}^j| - \mathcal{G}_\varphi^j |d_{\xi\theta\varphi}^i| - \mathcal{G}_\varphi^k |d_{\xi\theta\varphi}^k|)] \int_{\Omega} (\wp_\theta^r)^2(t, z) dz \right. \\
 & -\frac{1}{2} \sum_{\theta=1}^n [2(a_{\xi\theta} + \widehat{\mathcal{Q}} + \mu_{\xi\theta}^i) - \sum_{\varphi=1}^n (\mathcal{F}_\varphi^i |b_{\xi\theta\varphi}^r| + \mathcal{F}_\varphi^r |b_{\xi\theta\varphi}^i| \\
 & + \mathcal{F}_\varphi^k |b_{\xi\theta\varphi}^j| - \mathcal{F}_\varphi^j |b_{\xi\theta\varphi}^k| + \mathcal{F}_\varphi^i (|b_{\xi\theta\varphi}^r| - |b_{\xi\theta\varphi}^i| + |b_{\xi\theta\varphi}^k| \\
 & - |b_{\xi\theta\varphi}^j|) + \mathcal{G}_\varphi^i |d_{\xi\theta\varphi}^r| + \mathcal{G}_\varphi^r |d_{\xi\theta\varphi}^i| + \mathcal{G}_\varphi^k |d_{\xi\theta\varphi}^j| - \mathcal{G}_\varphi^j |d_{\xi\theta\varphi}^k|)] \\
 & \times \int_{\Omega} (\wp_\theta^i)^2(t, z) dz -\frac{1}{2} \sum_{\theta=1}^n [2(a_{\xi\theta} + \widehat{\mathcal{Q}} + \mu_{\xi\theta}^j) \\
 & - \sum_{\varphi=1}^n (\mathcal{F}_\varphi^j |b_{\xi\theta\varphi}^r| - \mathcal{F}_\varphi^k |b_{\xi\theta\varphi}^i| + \mathcal{F}_\varphi^r |b_{\xi\theta\varphi}^j| + \mathcal{F}_\varphi^i |b_{\xi\theta\varphi}^k| \\
 & + \mathcal{F}_\varphi^j (|b_{\xi\theta\varphi}^r| - |b_{\xi\theta\varphi}^i| - |b_{\xi\theta\varphi}^k| + |b_{\xi\theta\varphi}^j|) + \mathcal{G}_\varphi^j |d_{\xi\theta\varphi}^r| \\
 & \left. - \mathcal{G}_\varphi^k |d_{\xi\theta\varphi}^i| + \mathcal{G}_\varphi^r |d_{\xi\theta\varphi}^j| - \mathcal{G}_\varphi^i |d_{\xi\theta\varphi}^k|)] \int_{\Omega} (\wp_\theta^j)^2(t, z) dz \right. \\
 & \left. -\frac{1}{2} \sum_{\theta=1}^n [2(a_{\xi\theta} + \widehat{\mathcal{Q}} + \mu_{\xi\theta}^k) - \sum_{\varphi=1}^n (\mathcal{F}_\varphi^k |b_{\xi\theta\varphi}^r| + \mathcal{F}_\varphi^j |b_{\xi\theta\varphi}^i| \right. \\
 & - \mathcal{F}_\varphi^i |b_{\xi\theta\varphi}^j| + \mathcal{F}_\varphi^r |b_{\xi\theta\varphi}^k| + \mathcal{F}_\varphi^k (|b_{\xi\theta\varphi}^r| - |b_{\xi\theta\varphi}^i| + |b_{\xi\theta\varphi}^j| \\
 & \left. - |b_{\xi\theta\varphi}^k|) + \mathcal{G}_\varphi^k |d_{\xi\theta\varphi}^r| + \mathcal{G}_\varphi^j |d_{\xi\theta\varphi}^i| - \mathcal{G}_\varphi^i |d_{\xi\theta\varphi}^j| + \mathcal{G}_\varphi^r |d_{\xi\theta\varphi}^k|)] \int_{\Omega} (\wp_\theta^k)^2(t, z) dz \right\}
 \end{aligned}$$

$$\begin{aligned} & \times \int_{\Omega} (\wp_{\theta}^k)^2(t, z) dz + \frac{1}{2} \sum_{\theta=1}^n \sum_{\varphi=1}^n \mathcal{G}_{\theta}^r (|d_{\xi\varphi\theta}^r| + |d_{\xi\varphi\theta}^i| \\ & + |d_{\xi\varphi\theta}^j| + |d_{\xi\varphi\theta}^k|) \int_{\Omega} (\wp_{\theta}^r)^2(t_{\sigma}, z) dz + \frac{1}{2} \sum_{\theta=1}^n \sum_{\varphi=1}^n \mathcal{G}_{\theta}^i \\ & \times (|d_{\xi\varphi\theta}^r| - |d_{\xi\varphi\theta}^i| - |d_{\xi\varphi\theta}^j| + |d_{\xi\varphi\theta}^k|) \int_{\Omega} (\wp_{\theta}^i)^2(t_{\sigma}, z) dz \\ & + \frac{1}{2} \sum_{\theta=1}^n \sum_{\varphi=1}^n \mathcal{G}_{\theta}^j (|d_{\xi\varphi\theta}^r| + |d_{\xi\varphi\theta}^i| - |d_{\xi\varphi\theta}^j| - |d_{\xi\varphi\theta}^k|) \\ & \times \int_{\Omega} (\wp_{\theta}^j)^2(t_{\sigma}, z) dz + \frac{1}{2} \sum_{\theta=1}^n \sum_{\varphi=1}^n \mathcal{G}_{\theta}^k (|d_{\xi\varphi\theta}^r| - |d_{\xi\varphi\theta}^i| \\ & + |d_{\xi\varphi\theta}^j| - |d_{\xi\varphi\theta}^k|) \int_{\Omega} (\wp_{\theta}^k)^2(t_{\sigma}, z) dz \}. \end{aligned}$$

Thus,

$$\begin{aligned} & {}^C D_0^{\lambda} \mathbb{V}(t, \wp(t, z)) \\ & \leq \sum_{\xi=1}^{\zeta} \Psi_{\xi}(\beta(t)) \left\{ -\frac{1}{2} \sum_{\theta=1}^n \mathcal{U}_{\theta}^r \int_{\Omega} (\wp_{\theta}^r)^2(t, z) dz \right. \\ & - \frac{1}{2} \sum_{\theta=1}^n \mathcal{U}_{\theta}^i \int_{\Omega} (\wp_{\theta}^i)^2(t, z) dz - \frac{1}{2} \sum_{\theta=1}^n \mathcal{U}_{\theta}^j \int_{\Omega} (\wp_{\theta}^j)^2(t, z) dz \\ & - \frac{1}{2} \sum_{\theta=1}^n \mathcal{U}_{\theta}^k \int_{\Omega} (\wp_{\theta}^k)^2(t, z) dz + \frac{1}{2} \sum_{\theta=1}^n \mathcal{L}_{\theta}^r \int_{\Omega} (\wp_{\theta}^r)^2(t_{\sigma}, z) dz \\ & + \frac{1}{2} \sum_{\theta=1}^n \mathcal{L}_{\theta}^i \int_{\Omega} (\wp_{\theta}^i)^2(t_{\sigma}, z) dz + \frac{1}{2} \sum_{\theta=1}^n \mathcal{L}_{\theta}^j \int_{\Omega} (\wp_{\theta}^j)^2(t_{\sigma}, z) dz \\ & \left. + \frac{1}{2} \sum_{\theta=1}^n \mathcal{L}_{\theta}^k \int_{\Omega} (\wp_{\theta}^k)^2(t_{\sigma}, z) dz \right\} \\ & \leq -\mathcal{U} \sum_{\eta=r,i}^{j,k} \int_{\Omega} \sum_{\theta=1}^n \frac{1}{2} (\wp_{\theta}^{\eta})^2(t, z) dz \\ & + \mathcal{L} \sum_{\eta=r,i}^{j,k} \int_{\Omega} \sum_{\theta=1}^n \frac{1}{2} (\wp_{\theta}^{\eta})^2(t_{\sigma}, z) dz \\ & \leq -\mathcal{U} \mathbb{V}(t, \wp(t, z)) + \sup_{t_{\sigma} \leq s \leq t} \mathcal{L} \mathbb{V}(t_{\sigma}, \wp(t_{\sigma}, z)). \end{aligned} \tag{45}$$

As the above inequality satisfies the Razumikhin condition [11], we have

$$\mathbb{V}(s, \wp(s, z)) \leq \mathbb{V}(t, \wp(t, z)), \quad t_{\sigma} \leq s \leq t, \quad t \geq 0. \tag{46}$$

From (45) and (46), we have

$${}^C D_0^{\lambda} \mathbb{V}(t, \wp(t, z)) \leq -\Theta \mathbb{V}(t, \wp(t, z)). \tag{47}$$

Applying Lemma 3 in inequality (47), it follows that

$$\mathbb{V}(t, \wp(t, z)) \leq \sup_{\sigma \leq s \leq 0} \mathbb{V}(0, \hat{\psi}(s, \cdot)) \mathbb{E}_{\lambda}(-\Theta t^{\lambda}), \quad t > 0.$$

So, the equivalent inequality (28) can be derived as follows

$$\begin{aligned} & \sum_{\eta=r,i}^{j,k} \int_{\Omega} \sum_{\theta=1}^n (\wp_{\theta}^{\eta})^2(t, z) dz \\ & \leq \sum_{\eta=r,i}^{j,k} \left(\sup_{\sigma \leq s \leq 0} \int_{\Omega} \sum_{\theta=1}^n (\hat{\psi}_{\theta}^{\eta})^2(s, z) dz \right) \mathbb{E}_{\lambda}(-\Theta t^{\lambda}). \end{aligned}$$

Denote $\|\hat{\psi}^{\eta}(s, z)\| = \left(\sup_{\sigma \leq s \leq 0} \int_{\Omega} \sum_{\theta=1}^n (\hat{\psi}_{\theta}^{\eta})^2(s, z) dz \right)^{\frac{1}{2}}$, then

$$\sum_{\eta=r,i}^{j,k} \int_{\Omega} \sum_{\theta=1}^n (\wp_{\theta}^{\eta})^2(t, z) dz \leq \sum_{\eta=r,i}^{j,k} \|\hat{\psi}^{\eta}(s, z)\|^2 \mathbb{E}_{\lambda}(-\Theta t^{\lambda}).$$

According to inequality (27) and Definition 3, it follows that

$$\sum_{\eta=r,i}^{j,k} \|\wp^{\eta}(t, z)\|^2 \leq \delta^2 \frac{\epsilon^2}{\delta^2}.$$

Therefore,

$$\sum_{\eta=r,i}^{j,k} \|\wp^{\eta}(t, z)\| \leq \epsilon. \tag{48}$$

Based on Definition 3, and the inequality (48), we can conclude that the system (4) is said to be FTMLS with the system (5) under controllers (25). \square

Remark 2: Compared with the results in [62], the model in this paper has the fuzzy rules, fractional-order case and thus, our models are new and more general. Although Song et al. [62] studied finite-time anti-synchronization of memristive QVNNs with reaction-diffusion, and the controller was state feedback controller not adaptive fuzzy controller. Thus, to efficiently adjust the fuzzy control gains so that save control cost, we introduce adaptive control approach in (49). This is the first time to use an adaptive control method to study the FTMLS of T-S FORDDQVNNs.

The adaptive fuzzy controller is presented as follows:

$$\begin{cases} \hat{u}_{\xi}^{\eta}(t, z) = -\varpi_{\xi\theta}^{\eta} \wp_{\theta}^{\eta}(t, z), \\ {}^C D_0^{\lambda} \varpi_{\xi\theta}^{\eta} = \gamma_{\xi\theta}^{\eta} (\wp_{\theta}^{\eta})^2(t, z) - \frac{\varrho^{\eta}}{2} (\varpi_{\xi\theta}^{\eta}(t) - \varpi^{\eta})^2, \end{cases} \tag{49}$$

for $\theta = 1, 2, \dots, n$; $\xi = 1, 2, \dots, \zeta$, where $\varpi^{\eta} > 0$ are tunable constants, $\varpi_{\xi\theta}^{\eta}(t) > 0$ are tunable functions, $\varrho^{\eta} > 0$ and $\gamma_{\xi\theta}^{\eta} > 0$ are constants.

Theorem 2: Under Assumption 1 and 2, the system (4) and (5) achieve the FTMLS via adaptive controller (49) if the following conditions holds:

$$(i) \quad \Phi = \mathfrak{N} - \hat{\varrho} > 0, \tag{50}$$

$$(ii) \quad \mathbb{E}_{\lambda}(-\Phi t^{\lambda}) < \frac{\epsilon^2}{\mathcal{K} \delta^2}. \tag{51}$$

where,

$$\mathfrak{N} = \hat{\mathfrak{K}} - \hat{\mathfrak{F}}, \hat{\varrho} = \min\{\varrho^r, \varrho^i, \varrho^j, \varrho^k\}, \hat{\mathcal{Q}} = \frac{\hat{q}_{\theta\alpha}}{l_{\alpha}^2},$$

$$\begin{aligned}
 & -|b_{\xi\varphi\theta}^i| + \mathcal{G}_\varphi^k |d_{\xi\varphi\theta}^r| + \mathcal{G}_\varphi^j |d_{\xi\varphi\theta}^i| - \mathcal{G}_\varphi^i |d_{\xi\varphi\theta}^j| + \mathcal{G}_\varphi^r |d_{\xi\varphi\theta}^k| \\
 & \times \int_{\Omega} (\wp_{\theta}^k)^2(t, z) dz - \int_{\Omega} \sum_{\theta=1}^n \wp_{\xi\theta}^r (\wp_{\theta}^r)^2(t, z) dz \\
 & - \int_{\Omega} \sum_{\theta=1}^n \wp_{\xi\theta}^i (\wp_{\theta}^i)^2(t, z) dz - \int_{\Omega} \sum_{\theta=1}^n \wp_{\xi\theta}^j (\wp_{\theta}^j)^2(t, z) dz \\
 & - \int_{\Omega} \sum_{\theta=1}^n \wp_{\xi\theta}^k (\wp_{\theta}^k)^2(t, z) dz + \frac{1}{2} \sum_{\theta=1}^n \sum_{\varphi=1}^n \mathcal{G}_\theta^r (|d_{\xi\varphi\theta}^r| \\
 & + |d_{\xi\varphi\theta}^i| + |d_{\xi\varphi\theta}^j| + |d_{\xi\varphi\theta}^k|) \int_{\Omega} (\wp_{\theta}^r)^2(t_{\sigma}, z) dz \\
 & + \frac{1}{2} \sum_{\theta=1}^n \sum_{\varphi=1}^n \mathcal{G}_\theta^i (|d_{\xi\varphi\theta}^r| - |d_{\xi\varphi\theta}^i| - |d_{\xi\varphi\theta}^j| + |d_{\xi\varphi\theta}^k|) \\
 & \times \int_{\Omega} (\wp_{\theta}^i)^2(t_{\sigma}, z) dz + \frac{1}{2} \sum_{\theta=1}^n \sum_{\varphi=1}^n \mathcal{G}_\theta^j (|d_{\xi\varphi\theta}^r| + |d_{\xi\varphi\theta}^i| \\
 & - |d_{\xi\varphi\theta}^j| - |d_{\xi\varphi\theta}^k|) \int_{\Omega} (\wp_{\theta}^j)^2(t_{\sigma}, z) dz + \frac{1}{2} \sum_{\theta=1}^n \sum_{\varphi=1}^n \mathcal{G}_\theta^k \\
 & (-|d_{\xi\varphi\theta}^j| - |d_{\xi\varphi\theta}^k|) \int_{\Omega} (\wp_{\theta}^k)^2(t_{\sigma}, z) dz + \frac{1}{2} \sum_{\theta=1}^n \sum_{\varphi=1}^n \mathcal{G}_\theta^k \\
 & \times (|d_{\xi\varphi\theta}^r| - |d_{\xi\varphi\theta}^i| + |d_{\xi\varphi\theta}^j| - |d_{\xi\varphi\theta}^k|) \int_{\Omega} (\wp_{\theta}^k)^2(t_{\sigma}, z) dz \}.
 \end{aligned}$$

Next,

$$\begin{aligned}
 & \widehat{W}_2 \\
 & \leq \sum_{\xi=1}^{\zeta} \Psi_{\xi}(\beta(t)) \left\{ \int_{\Omega} \left(\sum_{\theta=1}^n \frac{1}{\gamma_{\xi\theta}^r} (\wp_{\xi\theta}^r(t) - \wp^r)^C D_0^{\lambda} \wp_{\xi\theta}^r(t) \right) dz \right. \\
 & + \int_{\Omega} \left(\sum_{\theta=1}^n \frac{1}{\gamma_{\xi\theta}^i} (\wp_{\xi\theta}^i(t) - \wp^i)^C D_0^{\lambda} \wp_{\xi\theta}^i(t) \right) dz \\
 & + \int_{\Omega} \left(\sum_{\theta=1}^n \frac{1}{\gamma_{\xi\theta}^j} (\wp_{\xi\theta}^j(t) - \wp^j)^C D_0^{\lambda} \wp_{\xi\theta}^j(t) \right) dz \\
 & \left. + \int_{\Omega} \left(\sum_{\theta=1}^n \frac{1}{\gamma_{\xi\theta}^k} (\wp_{\xi\theta}^k(t) - \wp^k)^C D_0^{\lambda} \wp_{\xi\theta}^k(t) \right) dz \right\} \\
 & \leq \sum_{\xi=1}^{\zeta} \Psi_{\xi}(\beta(t)) \left\{ \int_{\Omega} \sum_{\theta=1}^n \frac{1}{\gamma_{\xi\theta}^r} (\wp_{\xi\theta}^r(t) - \wp^r) \right. \\
 & \times \left\{ \gamma_{\xi\theta}^r (\wp_{\theta}^r)^2(t, z) - \frac{\varrho^r}{2} (\wp_{\xi\theta}^r - \wp^r) \right\} dz \\
 & + \int_{\Omega} \sum_{\theta=1}^n \frac{1}{\gamma_{\xi\theta}^i} (\wp_{\xi\theta}^i(t) - \wp^i) \left\{ \gamma_{\xi\theta}^i (\wp_{\theta}^i)^2(t, z) \right. \\
 & \left. - \frac{\varrho^i}{2} (\wp_{\xi\theta}^i - \wp^i) \right\} dz + \int_{\Omega} \sum_{\theta=1}^n \frac{1}{\gamma_{\xi\theta}^j} (\wp_{\xi\theta}^j(t) - \wp^j) \\
 & \times \left\{ \gamma_{\xi\theta}^j (\wp_{\theta}^j)^2(t, z) - \frac{\varrho^j}{2} (\wp_{\xi\theta}^j - \wp^j) \right\} dz \\
 & + \int_{\Omega} \sum_{\theta=1}^n \frac{1}{\gamma_{\xi\theta}^k} (\wp_{\xi\theta}^k(t) - \wp^k) \left\{ \gamma_{\xi\theta}^k (\wp_{\theta}^k)^2(t, z) \right. \\
 & \left. - \frac{\varrho^k}{2} (\wp_{\xi\theta}^k - \wp^k) \right\} dz \}.
 \end{aligned}$$

$$\begin{aligned}
 & \leq \sum_{\xi=1}^{\zeta} \Psi_{\xi}(\beta(t)) \left\{ \int_{\Omega} \sum_{\theta=1}^n (\wp_{\xi\theta}^r(t) - \wp^r) (\wp_{\theta}^r)^2(t, z) dz \right. \\
 & + \int_{\Omega} \sum_{\theta=1}^n (\wp_{\xi\theta}^i(t) - \wp^i) (\wp_{\theta}^i)^2(t, z) dz \\
 & + \int_{\Omega} \sum_{\theta=1}^n (\wp_{\xi\theta}^j(t) - \wp^j) (\wp_{\theta}^j)^2(t, z) dz \\
 & + \int_{\Omega} \sum_{\theta=1}^n (\wp_{\xi\theta}^k(t) - \wp^k) (\wp_{\theta}^k)^2(t, z) dz \\
 & - \varrho^r \int_{\Omega} \sum_{\theta=1}^n \frac{1}{2\gamma_{\xi\theta}^r} (\wp_{\xi\theta}^r(t) - \wp^r)^2 dz \\
 & - \varrho^i \int_{\Omega} \sum_{\theta=1}^n \frac{1}{2\gamma_{\xi\theta}^i} (\wp_{\xi\theta}^i(t) - \wp^i)^2 dz \\
 & - \varrho^j \int_{\Omega} \sum_{\theta=1}^n \frac{1}{2\gamma_{\xi\theta}^j} (\wp_{\xi\theta}^j(t) - \wp^j)^2 dz \\
 & \left. - \varrho^k \int_{\Omega} \sum_{\theta=1}^n \frac{1}{2\gamma_{\xi\theta}^k} (\wp_{\xi\theta}^k(t) - \wp^k)^2 dz \right\}.
 \end{aligned}$$

On the basis of above mentioned work, we can drive that

$$\begin{aligned}
 & C D_0^{\lambda} \mathbb{V}(t, \wp(t, z)) \\
 & \leq \sum_{\xi=1}^{\zeta} \Psi_{\xi}(\beta(t)) \left\{ -\frac{1}{2} \sum_{\theta=1}^n [2(a_{\xi\theta} + \widehat{Q} + \wp^r) \right. \\
 & - \sum_{\varphi=1}^n (\mathcal{F}_{\varphi}^r |b_{\xi\varphi\theta}^r| - \mathcal{F}_{\varphi}^i |b_{\xi\varphi\theta}^i| - \mathcal{F}_{\varphi}^j |b_{\xi\varphi\theta}^j| - \mathcal{F}_{\varphi}^k |b_{\xi\varphi\theta}^k| \\
 & + \mathcal{F}_{\varphi}^r (|b_{\xi\varphi\theta}^r| + |b_{\xi\varphi\theta}^i| + |b_{\xi\varphi\theta}^j| + |b_{\xi\varphi\theta}^k|) + \mathcal{G}_{\varphi}^r |d_{\xi\varphi\theta}^r| \\
 & - \mathcal{G}_{\varphi}^i |d_{\xi\varphi\theta}^i| - \mathcal{G}_{\varphi}^j |d_{\xi\varphi\theta}^j| - \mathcal{G}_{\varphi}^k |d_{\xi\varphi\theta}^k|) \int_{\Omega} (\wp_{\theta}^r)^2(t, z) dz \\
 & - \frac{1}{2} \sum_{\theta=1}^n [2(a_{\xi\theta} + \widehat{Q} + \wp^i) - \sum_{\varphi=1}^n (\mathcal{F}_{\varphi}^i |b_{\xi\varphi\theta}^i| + \mathcal{F}_{\varphi}^r |b_{\xi\varphi\theta}^r| \\
 & + \mathcal{F}_{\varphi}^k |b_{\xi\varphi\theta}^k| - \mathcal{F}_{\varphi}^j |b_{\xi\varphi\theta}^j| - |b_{\xi\varphi\theta}^i| + |b_{\xi\varphi\theta}^k| \\
 & - |b_{\xi\varphi\theta}^j|) + \mathcal{G}_{\varphi}^i |d_{\xi\varphi\theta}^i| + \mathcal{G}_{\varphi}^r |d_{\xi\varphi\theta}^r| + \mathcal{G}_{\varphi}^k |d_{\xi\varphi\theta}^k| - \mathcal{G}_{\varphi}^j |d_{\xi\varphi\theta}^j|) \int_{\Omega} (\wp_{\theta}^i)^2(t, z) dz \\
 & - \frac{1}{2} \sum_{\theta=1}^n [2(a_{\xi\theta} + \widehat{Q} + \wp^j) \\
 & - \sum_{\varphi=1}^n (\mathcal{F}_{\varphi}^j |b_{\xi\varphi\theta}^j| - \mathcal{F}_{\varphi}^i |b_{\xi\varphi\theta}^i| + \mathcal{F}_{\varphi}^r |b_{\xi\varphi\theta}^r| + \mathcal{F}_{\varphi}^k |b_{\xi\varphi\theta}^k| \\
 & + \mathcal{F}_{\varphi}^i (|b_{\xi\varphi\theta}^r| - |b_{\xi\varphi\theta}^j| - |b_{\xi\varphi\theta}^k| + |b_{\xi\varphi\theta}^i|) + \mathcal{G}_{\varphi}^j |d_{\xi\varphi\theta}^j| \\
 & - \mathcal{G}_{\varphi}^i |d_{\xi\varphi\theta}^i| + \mathcal{G}_{\varphi}^r |d_{\xi\varphi\theta}^r| + \mathcal{G}_{\varphi}^k |d_{\xi\varphi\theta}^k|) \int_{\Omega} (\wp_{\theta}^j)^2(t, z) dz \\
 & - \frac{1}{2} \sum_{\theta=1}^n [2(a_{\xi\theta} + \widehat{Q} + \wp^k) - \sum_{\varphi=1}^n (\mathcal{F}_{\varphi}^k |b_{\xi\varphi\theta}^k| + \mathcal{F}_{\varphi}^i |b_{\xi\varphi\theta}^i| \\
 & - \mathcal{F}_{\varphi}^j |b_{\xi\varphi\theta}^j| + \mathcal{F}_{\varphi}^r |b_{\xi\varphi\theta}^r| - |b_{\xi\varphi\theta}^k| + |b_{\xi\varphi\theta}^i| \\
 & - |b_{\xi\varphi\theta}^j|) + \mathcal{G}_{\varphi}^k |d_{\xi\varphi\theta}^k| + \mathcal{G}_{\varphi}^i |d_{\xi\varphi\theta}^i| - \mathcal{G}_{\varphi}^j |d_{\xi\varphi\theta}^j| + \mathcal{G}_{\varphi}^r |d_{\xi\varphi\theta}^r|) \int_{\Omega} (\wp_{\theta}^k)^2(t, z) dz \}.
 \end{aligned}$$

$$\begin{aligned}
 & \times \int_{\Omega} (\wp_{\theta}^k)^2(t, z) dz + \frac{1}{2} \sum_{\theta=1}^n \sum_{\varphi=1}^n \mathcal{G}_{\theta}^r (|d_{\xi\varphi\theta}^r| + |d_{\xi\varphi\theta}^i| + |d_{\xi\varphi\theta}^j| \\
 & + |d_{\xi\varphi\theta}^k|) \int_{\Omega} (\wp_{\theta}^r)^2(t_{\sigma}, z) dz + \frac{1}{2} \sum_{\theta=1}^n \sum_{\varphi=1}^n \mathcal{G}_{\theta}^i (|d_{\xi\varphi\theta}^r| \\
 & - |d_{\xi\varphi\theta}^i| - |d_{\xi\varphi\theta}^j| + |d_{\xi\varphi\theta}^k|) \int_{\Omega} (\wp_{\theta}^j)^2(t_{\sigma}, z) dz \\
 & + \frac{1}{2} \sum_{\theta=1}^n \sum_{\varphi=1}^n \mathcal{G}_{\theta}^j (|d_{\xi\varphi\theta}^r| + |d_{\xi\varphi\theta}^i| - |d_{\xi\varphi\theta}^j| - |d_{\xi\varphi\theta}^k|) \\
 & \times \int_{\Omega} (\wp_{\theta}^j)^2(t_{\sigma}, z) dz + \frac{1}{2} \sum_{\theta=1}^n \sum_{\varphi=1}^n \mathcal{G}_{\theta}^k (|d_{\xi\varphi\theta}^r| - |d_{\xi\varphi\theta}^i| \\
 & + |d_{\xi\varphi\theta}^j| - |d_{\xi\varphi\theta}^k|) \int_{\Omega} (\wp_{\theta}^k)^2(t_{\sigma}, z) dz \\
 & - \varrho^r \int_{\Omega} \sum_{\theta=1}^n \frac{1}{2\gamma_{\xi\theta}^r} (\varpi_{\xi\theta}^r(t) - \varpi^r)^2 dz \\
 & - \varrho^i \int_{\Omega} \sum_{\theta=1}^n \frac{1}{2\gamma_{\xi\theta}^i} (\varpi_{\xi\theta}^i(t) - \varpi^i)^2 dz \\
 & - \varrho^j \int_{\Omega} \sum_{\theta=1}^n \frac{1}{2\gamma_{\xi\theta}^j} (\varpi_{\xi\theta}^j(t) - \varpi^j)^2 dz \\
 & - \varrho^k \int_{\Omega} \sum_{\theta=1}^n \frac{1}{2\gamma_{\xi\theta}^k} (\varpi_{\xi\theta}^k(t) - \varpi^k)^2 dz \} \\
 & \leq \sum_{\xi=1}^{\zeta} \Psi_{\xi}(\beta(t)) \left\{ -\frac{1}{2} \sum_{\theta=1}^n \mathfrak{K}_{\theta}^r \int_{\Omega} (\wp_{\theta}^r)^2(t, z) dz \right. \\
 & - \frac{1}{2} \sum_{\theta=1}^n \mathfrak{K}_{\theta}^i \int_{\Omega} (\wp_{\theta}^i)^2(t, z) dz - \frac{1}{2} \sum_{\theta=1}^n \mathfrak{K}_{\theta}^j \int_{\Omega} (\wp_{\theta}^j)^2(t, z) dz \\
 & - \frac{1}{2} \sum_{\theta=1}^n \mathfrak{K}_{\theta}^k \int_{\Omega} (\wp_{\theta}^k)^2(t, z) dz + \frac{1}{2} \sum_{\theta=1}^n \mathfrak{P}_{\theta}^r \int_{\Omega} (\wp_{\theta}^r)^2(t_{\sigma}, z) dz \\
 & + \frac{1}{2} \sum_{\theta=1}^n \mathfrak{P}_{\theta}^i \int_{\Omega} (\wp_{\theta}^i)^2(t_{\sigma}, z) dz + \frac{1}{2} \sum_{\theta=1}^n \mathfrak{P}_{\theta}^j \int_{\Omega} (\wp_{\theta}^j)^2(t_{\sigma}, z) dz \\
 & + \frac{1}{2} \sum_{\theta=1}^n \mathfrak{P}_{\theta}^k \int_{\Omega} (\wp_{\theta}^k)^2(t_{\sigma}, z) dz \\
 & - \varrho^r \int_{\Omega} \sum_{\theta=1}^n \frac{1}{2\gamma_{\xi\theta}^r} (\varpi_{\xi\theta}^r(t) - \varpi^r)^2 dz \\
 & - \varrho^i \int_{\Omega} \sum_{\theta=1}^n \frac{1}{2\gamma_{\xi\theta}^i} (\varpi_{\xi\theta}^i(t) - \varpi^i)^2 dz \\
 & - \varrho^j \int_{\Omega} \sum_{\theta=1}^n \frac{1}{2\gamma_{\xi\theta}^j} (\varpi_{\xi\theta}^j(t) - \varpi^j)^2 dz \\
 & \left. - \varrho^k \int_{\Omega} \sum_{\theta=1}^n \frac{1}{2\gamma_{\xi\theta}^k} (\varpi_{\xi\theta}^k(t) - \varpi^k)^2 dz \right\} \\
 & \leq -\widehat{\mathfrak{K}} \sum_{\eta=r,i}^{j,k} \int_{\Omega} \sum_{\theta=1}^n \frac{1}{2} (\wp_{\theta}^{\eta})^2(t, z) dz
 \end{aligned}$$

$$\begin{aligned}
 & + \widehat{\mathfrak{P}} \sum_{\eta=r,i}^{j,k} \int_{\Omega} \sum_{\theta=1}^n \frac{1}{2} (\wp_{\theta}^{\eta})^2(t_{\sigma}, z) dz \\
 & - \widehat{\varrho} \sum_{\eta=r,i}^{j,k} \int_{\Omega} \sum_{\theta=1}^n \frac{1}{2\gamma_{\xi\theta}^{\eta}} \sum_{\xi=1}^{\zeta} \Psi_{\xi}(\beta(t)) (\varpi_{\xi\theta}^{\eta}(t) - \varpi^k)^2 dz \\
 & \leq -\widehat{\mathfrak{K}} \widehat{\mathbb{V}}(t, \wp(t, z)) + \widehat{\mathfrak{P}} \sup_{t_{\sigma} \leq s \leq t} \widehat{\mathbb{V}}(t_{\sigma}, \wp(t_{\sigma}, z)) \\
 & - \widehat{\varrho} \widehat{\mathbb{W}}(t, \wp(t, z)).
 \end{aligned}$$

For $t_{\sigma} \leq s \leq t, t \geq 0$, based on the above inequality, the error state $\wp(t, z)$ satisfies the Razumikhin condition [11], which gives,

$$\begin{aligned}
 {}^C D_0^{\lambda} \mathbb{V}(t, \wp(t, z)) & \leq -(\widehat{\mathfrak{K}} - \widehat{\mathfrak{P}}) \widehat{\mathbb{V}}(t, \wp(t, z)) - \widehat{\varrho} \widehat{\mathbb{W}}(t, \wp(t, z)) \\
 & \leq -\mathfrak{N} \widehat{\mathbb{V}}(t, \wp(t, z)) - \widehat{\varrho} \widehat{\mathbb{W}}(t, \wp(t, z)) \\
 & \leq -\Phi \mathbb{V}(t, \wp(t, z)).
 \end{aligned}$$

From Lemma 3, we have that

$$\mathbb{V}(t, \wp(t, z)) \leq \sup_{\sigma \leq s \leq 0} \mathbb{V}(0, \hat{\psi}(s, z)) \mathbb{E}_{\lambda}(-\Phi t^{\lambda}), \quad t > 0.$$

It means that

$$\begin{aligned}
 & \sum_{\eta=r,i}^{j,k} \int_{\Omega} \sum_{\theta=1}^n \frac{1}{2} (\wp_{\theta}^{\eta})^2(t, z) dz \\
 & \leq \sum_{\eta=r,i}^{j,k} \int_{\Omega} \sum_{\theta=1}^n \frac{1}{2} (\wp_{\theta}^{\eta})^2(t, z) dz + \sum_{\eta=r,i}^{j,k} \int_{\Omega} \sum_{\theta=1}^n \frac{1}{2\gamma_{\xi\theta}^{\eta}} \\
 & \times \left(\sum_{\xi=1}^{\zeta} \Psi_{\xi}(\beta(t)) (\varpi_{\xi\theta}^{\eta}(t) - \varpi^{\eta})^2 \right) dz \\
 & \leq \left\{ \sum_{\eta=r,i}^{j,k} \left(\sup_{\sigma \leq s \leq 0} \int_{\Omega} \sum_{\theta=1}^n (\hat{\psi}_{\theta}^{\eta})^2(s, z) dz \right) + \sum_{\eta=r,i}^{j,k} \int_{\Omega} \sum_{\theta=1}^n \frac{1}{2\gamma_{\xi\theta}^{\eta}} \right. \\
 & \left. \times \left(\sum_{\xi=1}^{\zeta} \Psi_{\xi}(\beta(t)) (\varpi_{\xi\theta}^{\eta}(0) - \varpi^{\eta})^2 \right) dz \right\} \mathbb{E}_{\lambda}(-\Phi t^{\lambda}).
 \end{aligned}$$

In view of $(\varpi_{\xi\theta}^{\eta}(0) - \varpi^{\eta})$ is finite, it is obvious that there exists a positive constant \mathcal{K} leading to

$$\begin{aligned}
 & \sum_{\eta=r,i}^{j,k} \left(\sup_{\sigma \leq s \leq 0} \int_{\Omega} \sum_{\theta=1}^n (\hat{\psi}_{\theta}^{\eta})^2(s, z) dz \right) + \sum_{\eta=r,i}^{j,k} \int_{\Omega} \sum_{\theta=1}^n \frac{1}{2\gamma_{\xi\theta}^{\eta}} \\
 & \times \left(\sum_{\xi=1}^{\zeta} \Psi_{\xi}(\beta(t)) (\varpi_{\xi\theta}^{\eta}(0) - \varpi^{\eta})^2 \right) dz \\
 & \leq \mathcal{K} \sum_{\eta=r,i}^{j,k} \left(\sup_{\sigma \leq s \leq 0} \int_{\Omega} \sum_{\theta=1}^n (\hat{\psi}_{\theta}^{\eta})^2(s, z) dz \right).
 \end{aligned}$$

Finally, we obtain that

$$\begin{aligned}
 & \sum_{\eta=r,i}^{j,k} \int_{\Omega} \sum_{\theta=1}^n \frac{1}{2} (\wp_{\theta}^{\eta})^2(t, z) dz \\
 & \leq \mathcal{K} \sum_{\eta=r,i}^{j,k} \left(\sup_{\sigma \leq s \leq 0} \int_{\Omega} \sum_{\theta=1}^n (\hat{\psi}_{\theta}^{\eta})^2(s, z) dz \right) \mathbb{E}_{\lambda}(-\Phi t^{\lambda}).
 \end{aligned}$$

According to inequality (51) and Definition 3, it follows that

$$\sum_{\eta=r,i}^{j,k} \|\varphi^\eta(t, z)\|^2 \leq \mathcal{K}\delta^2 \frac{\epsilon^2}{\mathcal{K}\delta^2}.$$

That is

$$\sum_{\eta=r,i}^{j,k} \|\varphi^\eta(t, z)\| \leq \epsilon.$$

According to Definition 3, we can conclude that the drive system (4) is said to be FTMLS with the response system (5) under adaptive controllers (49). \square

Remark 3: Most industrial processes are spatiotemporal in nature, and the mathematical models of these nonlinear processes are generally expressed by nonlinear PDEs. In this paper, we designed adaptive fuzzy feedback controller scheme for FTMLS problem of T-S fuzzy FORDDQVNNs. Up to now, many interesting works concerning the property of fractional-order QVNNs without reaction-diffusion terms and fuzzy rules have been obtained, see [50]–[57]. Furthermore, the FTMLS problem of fractional-order QVNNs by using linear feedback controllers have been investigated [58]. In [62], finite/fixed-time synchronization problem was discussed for memristive QVNNs with integer-order case. To the best of our knowledge, the present study is the first attempt to analyze the FTMLS of T-S fuzzy FORDDQVNNs under adaptive fuzzy feedback controller scheme. Therefore, the theoretical results established in this paper are new and extend some previous ones.

Remark 4: In the implementation, due to the restrictions of equipments and influence of the environment, the reaction-diffusion phenomenon and fuzzy rules in CVNNs. Different from the existing reaction-diffusion CVNNs and without T-S fuzzy rules in [59]–[61], reaction-diffusion CVNNs without fractional-order case in [59]–[61], and the T-S fuzzy fractional-order reaction-diffusion CVNNs is newly built in (10), (11) and (16), (17), which not only considers the effect of the reaction-diffusion phenomenon but the fuzzy-dependent adjustable matrix inequality technique is more flexible and helpful to reduce the conservatism and compared with integer-order neurons, fractional-order neurons are helpful for effective signal detection and extraction. Thus, compared with the models in [59]–[61], the model in (10), (11) and (16), (17) is more applicable. T-S fuzzy FORDDQVNNs can be regarded as a generalization of fractional-order reaction-diffusion CVNNs, thus Theorem 1 and Theorem 2 can be used to estimate the FTMLS of T-S fuzzy fractional-order reaction-diffusion CVNNs.

Combining (10), (11) and (16), (17), can derive the following error system

$$\frac{\partial^\lambda \varphi^R(t, z)}{\partial t^\lambda} = \sum_{\xi=1}^{\zeta} \Psi_\xi(\beta(t)) \{ \Delta \varphi^R(t, z) - \mathcal{A}_\xi \varphi^R(t, z) + \mathcal{B}_\xi^R [F^R(\mathfrak{Z}^R(t, z)) - F^R(\mathfrak{Z}^I(t, z))] \}$$

$$\begin{aligned} & -\mathcal{B}_\xi^I [F^I(\mathfrak{Z}^I(t, z)) - F^I(\mathfrak{Z}^I(t, z))] \\ & + \mathcal{D}_\xi^R [G^R(\mathfrak{Z}^R(t_\sigma, z)) - G^R(\mathfrak{Z}^R(t_\sigma, z))] \\ & - \mathcal{D}_\xi^I [G^I(\mathfrak{Z}^I(t_\sigma, z)) - G^I(\mathfrak{Z}^I(t_\sigma, z))] \\ & + \hat{u}_\xi^R(t, z), \end{aligned} \tag{52}$$

$$\begin{aligned} \frac{\partial^\lambda \varphi^I(t, z)}{\partial t^\lambda} & = \sum_{\xi=1}^{\zeta} \Psi_\xi(\beta(t)) \{ \Delta \varphi^I(t, z) - \mathcal{A}_\xi \varphi^I(t, z) \\ & + \mathcal{B}_\xi^R [F^I(\mathfrak{Z}^I(t, z)) - F^I(\mathfrak{Z}^I(t, z))] \\ & + \mathcal{B}_\xi^I [F^R(\mathfrak{Z}^R(t, z)) - F^R(\mathfrak{Z}^R(t, z))] \\ & + \mathcal{D}_\xi^R [G^I(\mathfrak{Z}^I(t_\sigma, z)) - G^I(\mathfrak{Z}^I(t_\sigma, z))] \\ & + \mathcal{D}_\xi^I [G^R(\mathfrak{Z}^R(t_\sigma, z)) - G^R(\mathfrak{Z}^R(t_\sigma, z))] \\ & + \hat{u}_\xi^I(t, z) \}. \end{aligned} \tag{53}$$

According to (52) and (53) can be rewritten as

$$\frac{\partial^\lambda \tilde{\varphi}(t, z)}{\partial t^\lambda} = \sum_{\xi=1}^{\zeta} \Psi_\xi(\beta(t)) \{ \Delta \tilde{\varphi}(t, z) - \tilde{\mathcal{A}}_\xi \tilde{\varphi}(t, z) + \tilde{\mathcal{B}}_\xi \tilde{F}(\tilde{\varphi}(t, z)) + \tilde{\mathcal{C}}_\xi \tilde{G}(\tilde{\varphi}(t_\sigma, z)) + \tilde{U}_\xi(t, z) \}, \tag{54}$$

where, $\tilde{\varphi}(t, z) = ((\varphi^R(t, z))^T, (\varphi^I(t, z))^T)^T$, $\Delta \tilde{\varphi}(t, z) = ((\Delta \varphi^R(t, z))^T, (\Delta \varphi^I(t, z))^T)^T$, $\tilde{F}(\tilde{\varphi}(t, z)) = ((F^R(\mathfrak{Z}^R(t, z)) - F^R(\mathfrak{Z}^I(t, z)))^T, (F^I(\mathfrak{Z}^I(t, z)) - F^I(\mathfrak{Z}^I(t, z)))^T)^T$, $\tilde{G}(\tilde{\varphi}(t_\sigma, z)) = ((G^R(\mathfrak{Z}^R(t_\sigma, z)) - G^R(\mathfrak{Z}^I(t_\sigma, z)))^T, (G^I(\mathfrak{Z}^I(t_\sigma, z)) - G^I(\mathfrak{Z}^I(t_\sigma, z)))^T)^T$, $\tilde{U}_\xi(t, z) = ((\hat{u}_\xi^R(t, z))^T, (\hat{u}_\xi^I(t, z))^T)^T$, $\tilde{\mathcal{A}}_\xi = \text{diag}(\mathcal{A}_\xi, \mathcal{A}_\xi)$, $\tilde{\mathcal{B}}_\xi = \begin{bmatrix} \mathcal{B}_\xi^R & -\mathcal{B}_\xi^I \\ \mathcal{B}_\xi^I & \mathcal{B}_\xi^R \end{bmatrix}$, $\tilde{\mathcal{C}}_\xi = \begin{bmatrix} \mathcal{C}_\xi^R & -\mathcal{C}_\xi^I \\ \mathcal{C}_\xi^I & \mathcal{C}_\xi^R \end{bmatrix}$.

In the following, we use the fuzzy feedback scheme to realize FTMLS between the system (54), then the controller can be designed as

$$\hat{u}_\xi^R(t, z) = -\hat{\mu}_{\xi\theta}^R \tilde{\varphi}_\theta^R(t, z), \quad \hat{u}_\xi^I(t, z) = -\hat{\mu}_{\xi\theta}^I \tilde{\varphi}_\theta^I(t, z), \tag{55}$$

where $\hat{\mu}_{\xi\theta}^R$ and $\hat{\mu}_{\xi\theta}^I$ represents the control gain.

Corollary 1: Under Assumption 1 and 2, the system (54) achieve the FTMLS via controller (55) if the following conditions holds:

- (i) $\Lambda = (\mathfrak{B} - \mathfrak{E}) > 0$,
- (ii) $\mathbb{E}_\lambda(-\Lambda t^\lambda) < \frac{\epsilon^2}{\delta^2}$,

where,

$$\begin{aligned} \mathfrak{B} & = \min_{1 \leq \theta \leq n} \{ \mathfrak{B}_\theta^R, \mathfrak{B}_\theta^I \}, \quad \mathfrak{E} = \max_{1 \leq \theta \leq n} \{ \mathfrak{E}_\theta^R, \mathfrak{E}_\theta^I \}, \\ \mathfrak{B}_\theta^R & = \min_{1 \leq \theta \leq n} \left\{ \frac{1}{2} [2(a_{\xi\theta} + \hat{Q} + \hat{\mu}_{\xi\theta}^R) - \sum_{\varphi=1}^n (\mathcal{F}_\varphi^R |b_{\xi\theta\varphi}^R| \right. \\ & \quad - \mathcal{F}_\varphi^I |b_{\xi\theta\varphi}^I| + \mathcal{F}_\varphi^R (|b_{\xi\varphi\theta}^R| + |b_{\xi\varphi\theta}^I|) + \mathcal{G}_\varphi^R |d_{\xi\theta\varphi}^R| \\ & \quad \left. - \mathcal{G}_\varphi^I |d_{\xi\theta\varphi}^I|) \right\}, \end{aligned}$$

$$\mathfrak{B}_\theta^I = \min_{1 \leq \theta \leq n} \left\{ \frac{1}{2} [2(a_{\xi\theta} + \widehat{Q} + \tilde{\mu}_{\xi\theta}^I) - \sum_{\varphi=1}^n (\mathcal{F}_\varphi^I |b_{\xi\theta\varphi}^R| + \mathcal{F}_\varphi^R |b_{\xi\theta\varphi}^I| + \mathcal{F}_\theta^I (|d_{\xi\varphi\theta}^R| - |b_{\xi\varphi\theta}^I|) + \mathcal{G}_\varphi^I |d_{\xi\theta\varphi}^R| + \mathcal{G}_\varphi^R |d_{\xi\theta\varphi}^I|)] \right\},$$

$$\mathfrak{C}_\theta^R = \max_{1 \leq \theta \leq n} \left\{ \frac{1}{2} \sum_{\varphi=1}^n \mathcal{G}_\theta^R (|d_{\xi\varphi\theta}^R| + |d_{\xi\varphi\theta}^I|) \right\},$$

$$\mathfrak{C}_\theta^I = \max_{1 \leq \theta \leq n} \left\{ \frac{1}{2} \sum_{\varphi=1}^n \mathcal{G}_\theta^I (|d_{\xi\varphi\theta}^R| - |d_{\xi\varphi\theta}^I|) \right\}.$$

Designing an adaptive controller $\hat{u}_\xi^R(t, z)$ and $\hat{u}_\xi^I(t, z)$ as follows:

$$\begin{cases} \hat{u}_\xi^R(t, z) = -\varpi_{\xi\theta}^R \varrho_\theta^\eta(t, z), \\ \hat{u}_\xi^I(t, z) = -\varpi_{\xi\theta}^I \varrho_\theta^\eta(t, z), \\ {}^C D_0^\lambda \varpi_{\xi\theta}^R = \gamma_{\xi\theta}^R (\varrho_\theta^R)^2(t, z) - \frac{\varrho^R}{2} (\varpi_{\xi\theta}^R(t) - \varpi^R)^2, \\ {}^C D_0^\lambda \varpi_{\xi\theta}^I = \gamma_{\xi\theta}^I (\varrho_\theta^I)^2(t, z) - \frac{\varrho^I}{2} (\varpi_{\xi\theta}^I(t) - \varpi^I)^2, \end{cases} \quad (56)$$

for $\theta = 1, 2, \dots, n$; $\xi = 1, 2, \dots, \zeta$, where $\varpi^R > 0$, $\varpi^I > 0$ are tunable constants; $\varpi_{\xi\theta}^R(t) > 0$, $\varpi_{\xi\theta}^I(t) > 0$ are tunable functions; $\varrho^R > 0$, $\varrho^I > 0$ and $\gamma_{\xi\theta}^R > 0$, $\gamma_{\xi\theta}^I > 0$ are constants.

Corollary 2: Under Assumption 1 and 2, the system (54) achieve the FTMLS via adaptive controller (56) if the following conditions holds:

- (i) $\widehat{\Phi} = \mathfrak{T} - \bar{\varrho} > 0$,
- (ii) $\mathbb{E}_\lambda(-\widehat{\Phi}t^\lambda) < \frac{\epsilon^2}{\mathcal{K}\delta^2}$.

where,

$$\mathfrak{T} = \widehat{\mathcal{S}} - \widehat{\mathcal{Z}}, \widehat{\mathcal{S}} = \min_{1 \leq \theta \leq n} \{\mathcal{S}_\theta^R, \mathcal{S}_\theta^I\},$$

$$\widehat{\mathcal{Z}} = \max_{1 \leq \theta \leq n} \{\mathcal{Z}_\theta^R, \mathcal{Z}_\theta^I\}, \bar{\varrho} = \min\{\varrho^R, \varrho^I\},$$

$$\mathcal{S}_\theta^R = \min_{1 \leq \theta \leq n} \left\{ \frac{1}{2} [2(a_{\xi\theta} + \widehat{Q} + \varpi^R) - \sum_{\varphi=1}^n (\mathcal{F}_\varphi^R |b_{\xi\theta\varphi}^R| - \mathcal{F}_\varphi^I |b_{\xi\theta\varphi}^I| + \mathcal{F}_\theta^R (|b_{\xi\varphi\theta}^R| + |b_{\xi\varphi\theta}^I|) + \mathcal{G}_\varphi^R |d_{\xi\theta\varphi}^R| - \mathcal{G}_\varphi^I |d_{\xi\theta\varphi}^I|)] \right\},$$

$$\mathcal{S}_\theta^I = \min_{1 \leq \theta \leq n} \left\{ \frac{1}{2} [2(a_{\xi\theta} + \widehat{Q} + \varpi^I) - \sum_{\varphi=1}^n (\mathcal{F}_\varphi^I |b_{\xi\theta\varphi}^R| + \mathcal{F}_\varphi^R |b_{\xi\theta\varphi}^I| + \mathcal{F}_\theta^I (|b_{\xi\varphi\theta}^R| - |b_{\xi\varphi\theta}^I|) + \mathcal{G}_\varphi^I |d_{\xi\theta\varphi}^R| + \mathcal{G}_\varphi^R |d_{\xi\theta\varphi}^I|)] \right\},$$

$$\mathcal{Z}_\theta^R = \max_{1 \leq \theta \leq n} \left\{ \frac{1}{2} \sum_{\varphi=1}^n \mathcal{G}_\theta^R (|d_{\xi\varphi\theta}^R| + |d_{\xi\varphi\theta}^I|) \right\},$$

$$\mathcal{Z}_\theta^I = \max_{1 \leq \theta \leq n} \left\{ \frac{1}{2} \sum_{\varphi=1}^n \mathcal{G}_\theta^I (|d_{\xi\varphi\theta}^R| - |d_{\xi\varphi\theta}^I|) \right\}.$$

Remark 5: The result of Corollary 1 and 2 can also be applied to T-S fuzzy fractional-order reaction-diffusion CVNNs. Moreover, T-S fuzzy fractional-order reaction-diffusion RVNNs are also applicable to the results in this paper. This shows that the outcomes of this paper are more general.

If transmission delay term are not considered, T-S fuzzy FORDDQVNNs (4) is reduced to T-S fuzzy fractional-order reaction-diffusion QVNNs

$$\frac{\partial^\lambda \mathfrak{Z}(t, z)}{\partial t^\lambda} = \sum_{\xi=1}^{\zeta} \Psi_\xi(\beta(t)) \{ \Delta \mathfrak{Z}(t, z) - \mathcal{A}_\xi \mathfrak{Z}(t, z) + \mathcal{B}_\xi F(\mathfrak{Z}(t, z)) + \mathcal{I} \}. \quad (57)$$

and T-S FORDDQVNNs (5) is reduced to the controlled T-S fuzzy fractional-order reaction-diffusion QVNNs,

$$\frac{\partial^\lambda \mathfrak{Z}(t, z)}{\partial t^\lambda} = \sum_{\xi=1}^{\zeta} \Psi_\xi(\beta(t)) \{ \Delta \mathfrak{Z}(t, z) - \mathcal{A}_\xi \mathfrak{Z}(t, z) + \mathcal{B}_\xi F(\mathfrak{Z}(t, z)) + \mathcal{I} + \hat{u}_\xi(t, z) \}. \quad (58)$$

In this case, we have the following corollary.

Corollary 3: Under Assumption 1 and 2, the system (57) and (58) achieve the FTMLS via controller (25) if the following conditions holds:

- (i) $\Psi > 0$,
- (ii) $\mathbb{E}_\lambda(-\Psi t^\lambda) < \frac{\epsilon^2}{\delta^2}$,

where,

$$\Psi = \min_{1 \leq \theta \leq n} \{\mathfrak{N}_\theta^r, \mathfrak{N}_\theta^i, \mathfrak{N}_\theta^j, \mathfrak{N}_\theta^k\},$$

$$\mathfrak{N}_\theta^r = \frac{1}{2} [2(a_{\xi\theta} + \widehat{Q} + \mu_{\xi\theta}^r) - \sum_{\varphi=1}^n (\mathcal{F}_\varphi^r |b_{\xi\theta\varphi}^r| - \mathcal{F}_\varphi^i |b_{\xi\theta\varphi}^i| - \mathcal{F}_\varphi^j |b_{\xi\theta\varphi}^j| - \mathcal{F}_\varphi^k |b_{\xi\theta\varphi}^k| + \mathcal{F}_\theta^r (|b_{\xi\varphi\theta}^r| + |b_{\xi\varphi\theta}^i| + |b_{\xi\varphi\theta}^j| + |b_{\xi\varphi\theta}^k|))],$$

$$\mathfrak{N}_\theta^i = \frac{1}{2} [2(a_{\xi\theta} + \widehat{Q} + \mu_{\xi\theta}^i) - \sum_{\varphi=1}^n (\mathcal{F}_\varphi^i |b_{\xi\theta\varphi}^r| + \mathcal{F}_\varphi^r |b_{\xi\theta\varphi}^i| + \mathcal{F}_\varphi^j |b_{\xi\theta\varphi}^j| - \mathcal{F}_\varphi^k |b_{\xi\theta\varphi}^k| + \mathcal{F}_\theta^i (|b_{\xi\varphi\theta}^r| - |b_{\xi\varphi\theta}^i| + |b_{\xi\varphi\theta}^j| - |b_{\xi\varphi\theta}^k|))],$$

$$\mathfrak{N}_\theta^j = \frac{1}{2} [2(a_{\xi\theta} + \widehat{Q} + \mu_{\xi\theta}^j) - \sum_{\varphi=1}^n (\mathcal{F}_\varphi^j |b_{\xi\theta\varphi}^r| - \mathcal{F}_\varphi^k |b_{\xi\theta\varphi}^i| + \mathcal{F}_\varphi^r |b_{\xi\theta\varphi}^r| + \mathcal{F}_\varphi^i |b_{\xi\theta\varphi}^i| + \mathcal{F}_\varphi^j |b_{\xi\theta\varphi}^j| - \mathcal{F}_\varphi^k |b_{\xi\theta\varphi}^k| - |b_{\xi\varphi\theta}^k| + |b_{\xi\varphi\theta}^i|))],$$

$$\mathfrak{N}_\theta^k = \frac{1}{2} [2(a_{\xi\theta} + \widehat{Q} + \mu_{\xi\theta}^k) - \sum_{\varphi=1}^n (\mathcal{F}_\varphi^k |b_{\xi\theta\varphi}^r| + \mathcal{F}_\varphi^i |b_{\xi\theta\varphi}^i| - \mathcal{F}_\varphi^j |b_{\xi\theta\varphi}^j| + \mathcal{F}_\varphi^r |b_{\xi\theta\varphi}^r| + \mathcal{F}_\varphi^i |b_{\xi\theta\varphi}^i| + \mathcal{F}_\varphi^j |b_{\xi\theta\varphi}^j| - \mathcal{F}_\varphi^k |b_{\xi\theta\varphi}^k| + |b_{\xi\varphi\theta}^j| - |b_{\xi\varphi\theta}^i|))].$$

Corollary 4: Under Assumption 1 and 2, the system (57) and (58) achieve the FTMLS via adaptive controller (49) if the following conditions holds:

- (i) $\Upsilon = \widehat{\mathfrak{J}} - \widehat{\varrho} > 0$,
- (ii) $\mathbb{E}_\lambda(-\Upsilon r^\lambda) < \frac{\epsilon^2}{\mathcal{K}\delta^2}$.

where,

$$\begin{aligned} \widehat{\mathfrak{J}} &= \min_{1 \leq \theta \leq n} \{\widehat{\mathfrak{J}}_\theta^r, \widehat{\mathfrak{J}}_\theta^i, \widehat{\mathfrak{J}}_\theta^j, \widehat{\mathfrak{J}}_\theta^k\}, \widehat{\varrho} = \{\varrho^r, \varrho^i, \varrho^j, \varrho^k\}, \\ \widehat{\mathfrak{J}}_\theta^r &= \frac{1}{2} \left[2(a_{\xi\theta} + \mathcal{Q}_\theta + \varpi^r) - \sum_{\varphi=1}^n (\mathcal{F}_\varphi^r |b_{\xi\theta\varphi}^r| - \mathcal{F}_\varphi^i |b_{\xi\theta\varphi}^i| \right. \\ &\quad \left. - \mathcal{F}_\varphi^j |b_{\xi\theta\varphi}^j| - \mathcal{F}_\varphi^k |b_{\xi\theta\varphi}^k| + \mathcal{F}_\varphi^r (|b_{\xi\varphi\theta}^r| + |b_{\xi\varphi\theta}^i| \right. \\ &\quad \left. + |b_{\xi\varphi\theta}^j| + |b_{\xi\varphi\theta}^k|) \right], \\ \widehat{\mathfrak{J}}_\theta^i &= \frac{1}{2} \left[2(a_{\xi\theta} + \mathcal{Q}_\theta + \varpi^i) - \sum_{\varphi=1}^n (\mathcal{F}_\varphi^i |b_{\xi\theta\varphi}^r| + \mathcal{F}_\varphi^r |b_{\xi\theta\varphi}^i| \right. \\ &\quad \left. + \mathcal{F}_\varphi^k |b_{\xi\theta\varphi}^j| - \mathcal{F}_\varphi^j |b_{\xi\theta\varphi}^k| + \mathcal{F}_\varphi^i (|b_{\xi\varphi\theta}^r| - |b_{\xi\varphi\theta}^i| \right. \\ &\quad \left. + |b_{\xi\varphi\theta}^k| - |b_{\xi\varphi\theta}^j|) \right], \\ \widehat{\mathfrak{J}}_\theta^j &= \frac{1}{2} \left[2(a_{\xi\theta} + \mathcal{Q}_\theta + \varpi^j) - \sum_{\varphi=1}^n (\mathcal{F}_\varphi^j |b_{\xi\theta\varphi}^r| - \mathcal{F}_\varphi^k |b_{\xi\theta\varphi}^i| \right. \\ &\quad \left. + \mathcal{F}_\varphi^r |b_{\xi\theta\varphi}^j| + \mathcal{F}_\varphi^i |b_{\xi\theta\varphi}^k| + \mathcal{F}_\varphi^j (|b_{\xi\varphi\theta}^r| - |b_{\xi\varphi\theta}^i| \right. \\ &\quad \left. - |b_{\xi\varphi\theta}^k| + |b_{\xi\varphi\theta}^j|) \right], \\ \widehat{\mathfrak{J}}_\theta^k &= \frac{1}{2} \left[2(a_{\xi\theta} + \widehat{\mathcal{Q}} + \varpi^k) - \sum_{\varphi=1}^n (\mathcal{F}_\varphi^k |b_{\xi\theta\varphi}^r| + \mathcal{F}_\varphi^i |b_{\xi\theta\varphi}^j| \right. \\ &\quad \left. - \mathcal{F}_\varphi^i |b_{\xi\theta\varphi}^k| + \mathcal{F}_\varphi^r |b_{\xi\theta\varphi}^j| + \mathcal{F}_\varphi^k (|b_{\xi\varphi\theta}^r| - |b_{\xi\varphi\theta}^i| \right. \\ &\quad \left. + |b_{\xi\varphi\theta}^j| - |b_{\xi\varphi\theta}^k|) \right]. \end{aligned}$$

IV. NUMERICAL EXAMPLE

In this section, we present a example to demonstrate our main results. In order to verify the effectiveness of the proposed control strategies for the synchronization between drive system (59) and response system (60).

Example: Consider the following 2D-dimensional drive system with two plant rules.

$$\frac{\partial^\lambda \mathfrak{Z}(t, z)}{\partial t^\lambda} = \sum_{\xi=1}^{\zeta} \Psi_\xi(\beta(t)) \{ \Delta \mathfrak{Z}(t, z) - \mathcal{A}_\xi \mathfrak{Z}(t, z) + \mathcal{B}_\xi F(\mathfrak{Z}(t, z)) + \mathcal{D}_\xi G(\mathfrak{Z}(t - \sigma(t), z)) + \mathcal{I} \}. \quad (59)$$

Plant Rule 1: If $\beta_1(t)$ is Ξ_1^1 , then,

$$\frac{\partial^\lambda \mathfrak{Z}(t, z)}{\partial t^\lambda} = \sum_{\xi=1}^{\zeta} \Psi_\xi(\beta(t)) \{ \Delta \mathfrak{Z}(t, z) - \mathcal{A}_1 \mathfrak{Z}(t, z) + \mathcal{B}_1 F(\mathfrak{Z}(t, z)) + \mathcal{D}_1 G(\mathfrak{Z}(t - \sigma(t), z)) + \mathcal{I} \}.$$

Plant Rule 2: If $\beta_2(t)$ is Ξ_2^2 , then,

$$\frac{\partial^\lambda \mathfrak{Z}(t, z)}{\partial t^\lambda} = \sum_{\xi=1}^{\zeta} \Psi_\xi(\beta(t)) \{ \Delta \mathfrak{Z}(t, z) - \mathcal{A}_2 \mathfrak{Z}(t, z) + \mathcal{B}_2 F(\mathfrak{Z}(t, z)) + \mathcal{D}_2 G(\mathfrak{Z}(t - \sigma(t), z)) + \mathcal{I} \}.$$

The parameters are as follows

$$\begin{aligned} \Delta \mathfrak{Z}(t, z) &= \sum_{\alpha=1}^m \left(q_{\theta\alpha} \frac{\partial \mathfrak{Z}(t, z)}{\partial z_\alpha} \right), m = n = 2, \\ l_1 &= 3, l_2 = 5, \Omega = \{z : z = (z_1, z_2)^T, |z_\alpha| < 1\}, \alpha = 1, 2, \lambda = 0.93, \mathcal{A}_1 = \text{diag}(3.2, 3.9), \mathcal{A}_2 = \text{diag}(4.7, 4.3), \mathfrak{Z}(t, z) = \mathfrak{Z}^r(t, z) + \mathfrak{Z}^i(t, z) + \mathfrak{Z}^j(t, z) + \mathfrak{Z}^k(t, z), F(\mathfrak{Z}(t, z)) = ((f_1(\mathfrak{Z}(t, z)))^T, (f_2(\mathfrak{Z}(t, z)))^T)^T, G(\mathfrak{Z}(t - \sigma(t), z)) = ((g_1(\mathfrak{Z}(t - \sigma(t), z)))^T, (g_2(\mathfrak{Z}(t - \sigma(t), z)))^T)^T, \sigma(t) = \frac{3e^t}{10+7e^t}, \Psi_1(\beta(t)) = \cos^2(5 \tanh(\|\mathfrak{Z}_1\| + \|\mathfrak{Z}_2\|)), \Psi_2(\beta(t)) = \sin^2(5 \tanh(\|\mathfrak{Z}_1\| + \|\mathfrak{Z}_2\|)), \mathcal{I}(t) = \begin{bmatrix} 2\cos(t) - 3\sin(t)i - \cos(t)j + 2\sin(t)k \\ 3\sin(t) + \cos(t)i + 2\cos(t)j - \sin(t)k \end{bmatrix}, \\ (q_{\theta\alpha})_{2 \times 2} &= \begin{bmatrix} 1.9 & 0.2 \\ 0.2 & 2.9 \end{bmatrix}, \mathcal{B}_1 = \begin{bmatrix} b_{111} & b_{112} \\ b_{121} & b_{122} \end{bmatrix}, \mathcal{B}_2 = \begin{bmatrix} b_{211} & b_{212} \\ b_{221} & b_{222} \end{bmatrix}, \mathcal{D}_1 = \begin{bmatrix} d_{111} & d_{112} \\ d_{121} & d_{122} \end{bmatrix}, \mathcal{D}_2 = \begin{bmatrix} d_{211} & d_{212} \\ d_{221} & d_{222} \end{bmatrix}, \end{aligned}$$

where,

$b_{111} = 1.3 - 0.9i - 1.3j + 0.9k$, $b_{112} = 2.1 + 1.2i - 0.9j - 2.1k$, $b_{121} = -1.9 + 2.3i + 1.9j - 2.3k$, $b_{122} = -1.4 + 0.9i + 1.1j + 0.9k$, $b_{211} = 2.3 - 1.9i + 1.3j + 0.7k$, $b_{212} = -1.3 + 0.9i - 2.3j + 1.9k$, $b_{221} = 2.1 - 1.7i - 1.3j - 0.9k$, $b_{222} = 0.9 + 1.9i + 2.3j - 1.5k$, $d_{111} = -3.7 + 2.9i - 3.3j - 2.9k$, $d_{112} = 3.1 - 3.3i + 2.9j - 3.1k$, $d_{121} = 1.9 - 2.7i + 1.9j - 2.7k$, $d_{122} = 2.4 - 1.9i - 2.1j - 1.9k$, $d_{211} = 3.3 - 2.9i + 2.3j + 2.7k$, $d_{212} = 2.9 + 2.3i - 2.9j - 2.3k$, $d_{221} = 2.1 + 1.7i + 1.3j + 2.9k$, $d_{222} = 2.9 - 3.9i + 1.3j + 1.7k$. With the original initial conditions set as $\mathfrak{Z}_1(0, z) = -3.1 \cos(z) + 2.3 \cos(z)i + 1.8 \sin(z)j - 1.6 \cos(z)k$ and $\mathfrak{Z}_2(0, z) = 2.4 \sin(z) - 3.1 \cos(z)i + 2.6 \sin(z)j + 0.6 \sin(z)k$, the drive system state trajectories can be described as in Fig. 1.

The controlled response system is depicted by

$$\frac{\partial^\lambda \mathfrak{Z}(t, z)}{\partial t^\lambda} = \sum_{\xi=1}^{\zeta} \Psi_\xi(\beta(t)) \{ \Delta \mathfrak{Z}(t, z) - \mathcal{A}_\xi \mathfrak{Z}(t, z) + \mathcal{B}_\xi F(\mathfrak{Z}(t, z)) + \mathcal{D}_\xi G(\mathfrak{Z}(t - \sigma(t), z)) + \mathcal{I} + \widehat{U}_\xi(t, z) \}, \quad (60)$$

where $\lambda = 0.93$, other parameters are the same as of as drive system (59).

Case 1: We choose $f_\varphi^r(\cdot) = g_\varphi^r(\cdot) = 2.17 \tanh(\cdot) + 0.03 \text{sign}(\cdot)$, $f_\varphi^i(\cdot) = g_\varphi^i(\cdot) = 1.49 \tanh(\cdot) + 0.01 \text{sign}(\cdot)$, $f_\varphi^j(\cdot) = g_\varphi^j(\cdot) = 2.17 \tanh(\cdot) + 0.03 \text{sign}(\cdot)$, $f_\varphi^k(\cdot) = g_\varphi^k(\cdot) = 1.49 \tanh(\cdot) + 0.01 \text{sign}(\cdot)$, as the activation function. Thus, Assumption (\mathcal{H}_1) are $\mathcal{F}_\varphi^r = \frac{1}{4}$, $\mathcal{F}_\varphi^i = \frac{1}{2}$, $\mathcal{F}_\varphi^j = \frac{1}{4}$, $\mathcal{F}_\varphi^k = \frac{1}{2}$, $\mathcal{G}_\varphi^r = 0$, $\mathcal{G}_\varphi^i = \frac{1}{2}$, $\mathcal{G}_\varphi^j = 0$, $\mathcal{G}_\varphi^k = \frac{1}{2}$, ($\varphi = 1, 2$) and also (\mathcal{H}_2) are $\hat{q}_{11} = 1.7$, $\hat{q}_{22} = 2.7$, $\hat{q}_{12} = \hat{q}_{21} = 0$.

Then, for controller (25), the parameters are designed as $\mu_{11}^r = 3.7$, $\mu_{12}^r = 3.1$, $\mu_{21}^r = 2.5$, $\mu_{22}^r = 2.9$, $\mu_{11}^i = 2.3$, $\mu_{12}^i = 3.5$, $\mu_{21}^i = 2.7$, $\mu_{22}^i = 3.7$, $\mu_{11}^j = 2.7$,

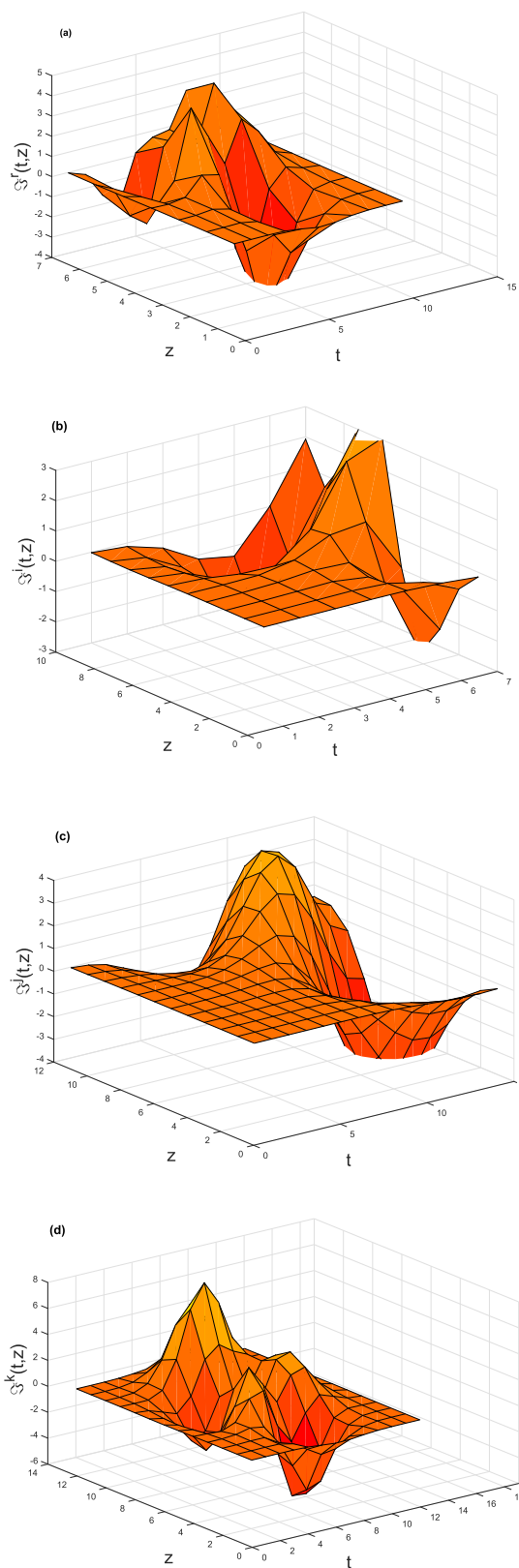


FIGURE 1. State trajectory of (a) $\mathfrak{Z}^r(t, z)$, (b) $\mathfrak{Z}^i(t, z)$, (c) $\mathfrak{Z}^j(t, z)$, and (d) $\mathfrak{Z}^k(t, z)$ of system (59) without control.

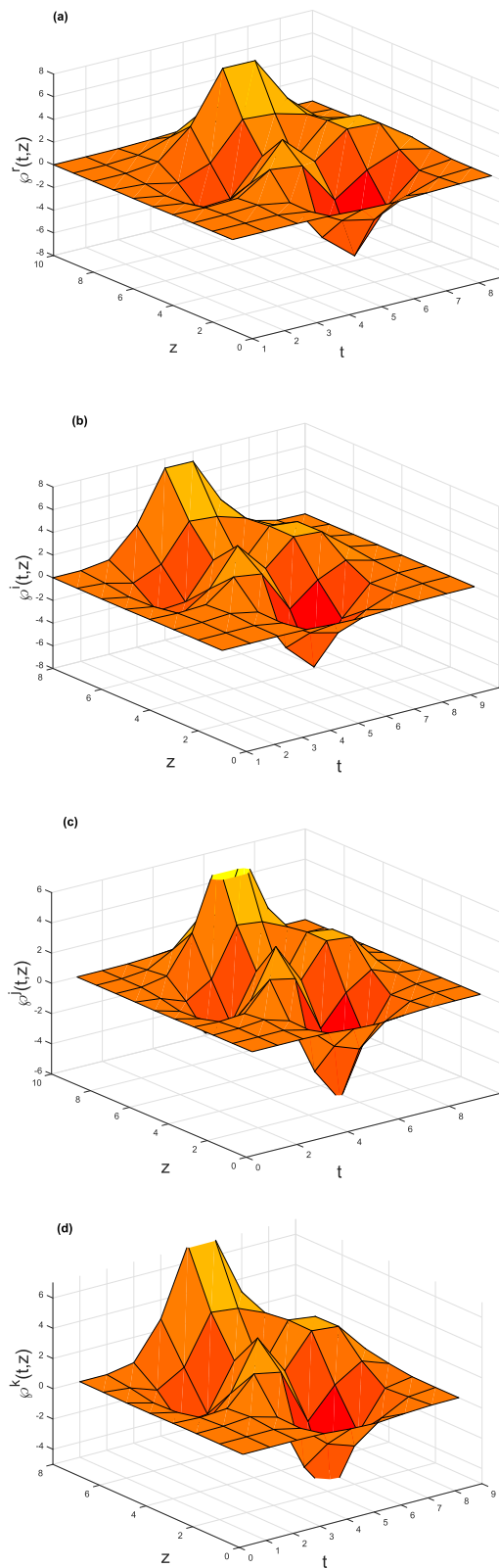


FIGURE 2. Synchronization error (a) $\phi^r(t, z)$, (b) $\phi^i(t, z)$, (c) $\phi^j(t, z)$, and (d) $\phi^k(t, z)$ of system (59) and (60) via fuzzy feedback controller (25) with fractional-order $\lambda = 0.93$.

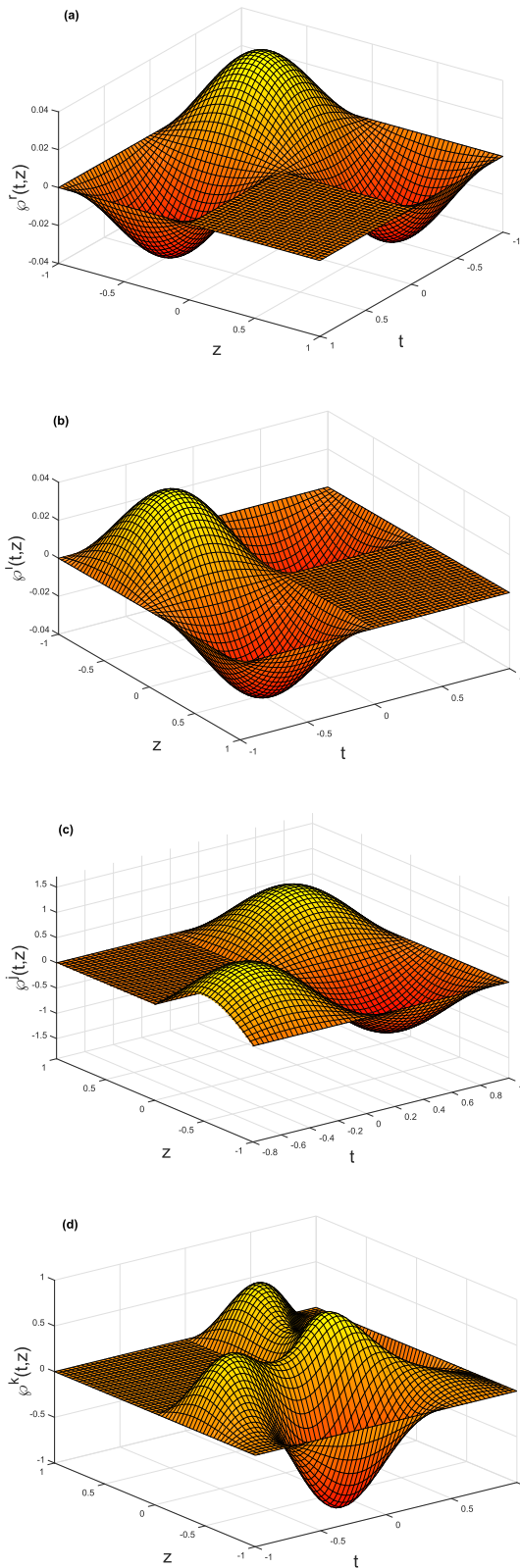


FIGURE 3. Synchronization error (a) $\phi^r(t, z)$, (b) $\phi^i(t, z)$, (c) $\phi^j(t, z)$, and (d) $\phi^k(t, z)$ of system (59) and (60) via adaptive controller (49) with fractional-order $\lambda = 0.93$.

$\mu_{12}^j = 4.1, \mu_{21}^j = 3.1, \mu_{22}^j = 2.8, \mu_{11}^k = 1.7, \mu_{12}^k = 2.7, \mu_{21}^k = 3.2,$ and $\mu_{22}^k = 3.9,$ combining with the proposed criteria in Theorem 1, one obtains the following results:

$$\begin{aligned} \mathcal{U}_\theta^r &= 9.4550, \mathcal{U}_\theta^i = 1.1525, \mathcal{U}_\theta^j = 4.8025, \mathcal{U}_\theta^k = 4.0025, \\ \mathcal{L}_\theta^r &= 0, \mathcal{L}_\theta^i = 1.4000, \mathcal{L}_\theta^j = 0, \mathcal{L}_\theta^k = 0.0025, \end{aligned}$$

and, $\Theta = (\mathcal{U} - \mathcal{L}) = 0.2400 > 0,$ holds and we can evaluate the finite time is about $t = 2.5$ according to the condition $\mathbb{E}_\lambda(-\Theta t^\lambda) < \frac{\epsilon^2}{\delta^2},$ when we assume $\epsilon = 6.70, \delta = 1.5.$ Therefore, the drive system (59) can achieve FTMLS with response system (60) under the designed controller (25). Fig. 2 are synchronization errors $\phi^\eta(t, z)$ ($\eta = r, i, j, k$) respectively, which have verified the feasibility and validness of the established theoretical results.

Case 2: We choose same as the activation function in case 1. Thus, Assumption (\mathcal{H}_1) are $\mathcal{F}_\varphi^r = 1, \mathcal{F}_\varphi^i = 0, \mathcal{F}_\varphi^j = 1, \mathcal{F}_\varphi^k = 0, \mathcal{G}_\varphi^r = 0, \mathcal{G}_\varphi^i = \frac{2}{5}, \mathcal{G}_\varphi^j = 0, \mathcal{G}_\varphi^k = \frac{2}{5},$ ($\varphi = 1, 2$) and (\mathcal{H}_2) are $\hat{q}_{11} = 1.5, \hat{q}_{22} = 2, \hat{q}_{12} = \hat{q}_{21} = 0.$

Then, for adaptive controller (49), the parameters are designed as $\gamma_{11}^r = 4.09, \gamma_{12}^r = 2.70, \gamma_{21}^r = 2.08, \gamma_{22}^r = 3.10, \gamma_{11}^i = 2.53, \gamma_{12}^i = 3.70, \gamma_{21}^i = 3.07, \gamma_{22}^i = 4.07, \gamma_{11}^j = 3.11, \gamma_{12}^j = 3.97, \gamma_{21}^j = 4.13, \gamma_{22}^j = 2.97, \gamma_{11}^k = 3.63, \gamma_{12}^k = 3.07, \gamma_{21}^k = 3.80, \gamma_{22}^k = 3.36, \varpi^r = 2.71, \varpi^i = 0.93, \varpi^j = 1.57, \varpi^k = 0.89, \varrho^r = 0.73, \varrho^i = 0.21, \varrho^j = 0.97,$ and $\varrho^k = 1.03.$ By Theorem 2, we obtains the results:

$$\begin{aligned} \hat{\mathcal{R}}_\alpha^r &= 1.5200, \hat{\mathcal{R}}_\alpha^i = 2.1700, \hat{\mathcal{R}}_\alpha^j = 1.7800, \hat{\mathcal{R}}_\alpha^k = 1.5900, \\ \mathfrak{P}_\alpha^r &= 0, \mathfrak{P}_\alpha^i = 1.1200, \mathfrak{P}_\alpha^j = 0, \mathfrak{P}_\alpha^k = 0.0400, \end{aligned}$$

$\mathfrak{N} = \hat{\mathcal{R}} - \hat{\mathfrak{P}} = 0.4000,$ and $\Phi = \mathfrak{N} - \hat{\varrho} = 0.1900 > 0$ holds, we can evaluate the finite-time is about $t = 0.6$ according to the condition $\mathbb{E}_\lambda(-\Phi t^\lambda) < \frac{\epsilon^2}{\mathcal{K}\delta^2},$ when we assume $\epsilon = 7.23, \delta = 1.9, \mathcal{K} = 1.05.$ Therefore, the drive system (59) can achieve FTMLS with response system (60) under the designed controller (49). The simulation results are shown in Fig. 3, where the synchronization errors $\phi^\eta(t, z)$ ($\eta = r, i, j, k$), trend to be zero quickly with regard to time $t.$

V. CONCLUSION

In this paper, we introduces adaptive fuzzy feedback control schemes to investigate the FTMLS of T-S fuzzy FORDQVNNs. First, mainly by employing Hamilton rules, the studied multidimensional systems have been divided into the relevant real-valued ones. By designing new state-feedback controller and fuzzy adaptive controllers, then constructing a suitable Lyapunov functional and employing algebraic inequality methods, a novel FTMLS criterion of the proposed system can be obtained. Finally, a simulation example has been given to demonstrate the merits of the proposed approach. However, there are still two unsolved problems in this paper: (i) Stochastic factors are not considered in modeling, which is not consistent with some actual systems, and (ii) The impulsive controller would further reduce the

contact consumption of the system compared to the continuous controllers. Therefore, inspired by [4], [32], [36], the FTMLS problem of stochastic FORDQVNNs via impulsive controller scheme will be studied in our future work.

REFERENCES

- [1] M. Xiao, W. X. Zheng, and G. Jiang, "Bifurcation and oscillatory dynamics of delayed cyclic gene networks including small RNAs," *IEEE Trans. Cybern.*, vol. 49, no. 3, pp. 883–896, Mar. 2019.
- [2] H. Shen, Y. Zhu, L. Zhang, and J. H. Park, "Extended dissipative state estimation for Markov jump neural networks with unreliable links," *IEEE Trans. Neural Netw. Learn. Syst.*, vol. 28, no. 2, pp. 346–358, Feb. 2017.
- [3] M. S. Ali, N. Gunasekaran, C. K. Ahn, and P. Shi, "Sampled-data stabilization for fuzzy genetic regulatory networks with leakage delays," *IEEE/ACM Trans. Comput. Biol. Bioinf.*, vol. 15, no. 1, pp. 271–285, Jan. 2018.
- [4] Q. Zhu and J. Cao, "Stability analysis of Markovian jump stochastic BAM neural networks with impulse control and mixed time delays," *IEEE Trans. Neural Netw. Learn. Syst.*, vol. 23, no. 3, pp. 467–479, Mar. 2012.
- [5] H. Shen, Z. Huang, J. Cao, and J. H. Park, "Exponential H_∞ filtering for continuous-time switched neural networks under persistent dwell-time switching regularity," *IEEE Trans. Cybern.*, vol. 50, no. 6, pp. 2440–2449, Jun. 2020.
- [6] Z. Ding, Z. Zeng, and L. Wang, "Exponential H_∞ filtering for continuous-time switched neural networks under persistent dwell-time switching regularity," *IEEE Trans. Neural Netw. Learn. Syst.*, vol. 29, pp. 1477–1490, 2018.
- [7] E. Arslan, G. Narayanan, M. S. Ali, S. Arik, and S. Saroha, "Controller design for finite-time and fixed-time stabilization of fractional-order memristive complex-valued BAM neural networks with uncertain parameters and time-varying delays," *Neural Netw.*, vol. 130, pp. 60–74, Oct. 2020.
- [8] Y. Qiao, H. Yan, L. Duan, and J. Miao, "Finite-time synchronization of fractional-order gene regulatory networks with time delay," *Neural Netw.*, vol. 126, pp. 1–10, Jun. 2020.
- [9] T. Stamov and I. Stamova, "Design of impulsive controllers and impulsive control strategy for the Mittag-Leffler stability behavior of fractional gene regulatory networks," *Neurocomputing*, vol. 424, pp. 54–62, Feb. 2021.
- [10] Y. Kao, Y. Li, J. H. Park, and X. Chen, "Mittag-Leffler synchronization of delayed fractional memristor neural networks via adaptive control," *IEEE Trans. Neural Netw. Learn. Syst.*, vol. 32, no. 5, pp. 2279–2284, May 2021, doi: 10.1109/TNNLS.2020.2995718.
- [11] M. S. Ali, G. Narayanan, V. Shekher, A. Alsaedi, and B. Ahmad, "Global Mittag-Leffler stability analysis of impulsive fractional-order complex-valued BAM neural networks with time varying delays," *Commun. Nonlinear Sci. Numer. Simul.*, vol. 83, Apr. 2020, Art. no. 105088.
- [12] Z. Tang, J. H. Park, and J. Feng, "Impulsive effects on quasi-synchronization of neural networks with parameter mismatches and time-varying delay," *IEEE Trans. Neural Netw. Learn. Syst.*, vol. 29, no. 4, pp. 908–919, Jan. 2018.
- [13] J. Jia, X. Huang, Y. Li, J. Cao, and A. Alsaedi, "Global stabilization of fractional-order memristor-based neural networks with time delay," *IEEE Trans. Neural Netw. Learn. Syst.*, vol. 31, pp. 907–1009, 2020.
- [14] M. S. Ali, G. Narayanan, V. Shekher, H. Alsulami, and T. Saeed, "Dynamic stability analysis of stochastic fractional-order memristor fuzzy BAM neural networks with delay and leakage terms," *Appl. Math. Comput.*, vol. 369, Mar. 2020, Art. no. 124896.
- [15] L. Hua, H. Zhu, K. Shi, S. Zhong, Y. Tang, and Y. Liu, "Novel finite-time reliable control design for memristor-based inertial neural networks with mixed time-varying delays," *IEEE Trans. Circuits Syst. I, Reg. Papers*, vol. 68, no. 4, pp. 1599–1609, Apr. 2021.
- [16] X. Li and S. Song, "Impulsive control for existence, uniqueness, and global stability of periodic solutions of recurrent neural networks with discrete and continuously distributed delays," *IEEE Trans. Neural Netw. Learn. Syst.*, vol. 24, no. 6, pp. 868–877, Jun. 2013.
- [17] W. Huang, Q. Song, Z. Zhao, Y. Liu, and F. E. Alsaadi, "Robust stability for a class of fractional-order complex-valued projective neural networks with neutral-type delays and uncertain parameters," *Neurocomputing*, vol. 450, pp. 399–410, Aug. 2021.
- [18] H. Bao, J. H. Park, and J. Cao, "Exponential synchronization of coupled stochastic memristor-based neural networks with time-varying probabilistic delay coupling and impulsive delay," *IEEE Trans. Neural Netw. Learn. Syst.*, vol. 27, no. 1, pp. 190–201, Jan. 2016.
- [19] W. H. Chen, X. Lu, and W. X. Zheng, "Impulsive stabilization and impulsive synchronization of discrete-time delayed neural networks," *IEEE Trans. Neural Netw. Learn. Syst.*, vol. 26, pp. 734–738, 2015.
- [20] H. Bao, J. H. Park, and J. Cao, "Synchronization of fractional-order complex-valued neural networks with time delay," *Neural Netw.*, vol. 81, pp. 16–28, Sep. 2016.
- [21] I. Stamova, "Global Mittag-Leffler stability and synchronization of impulsive fractional-order neural networks with time-varying delays," *Nonlinear Dyn.*, vol. 77, no. 4, pp. 1251–1260, Sep. 2014.
- [22] H. Liu, Y. Pan, S. Li, and Y. Chen, "Synchronization for fractional-order neural networks with full/under-actuation using fractional-order sliding mode control," *Int. J. Mach. Learn. Cybern.*, vol. 9, no. 7, pp. 1219–1232, Jul. 2018.
- [23] X. Yang, C. Li, T. Huang, Q. Song, and J. Huang, "Global Mittag-Leffler synchronization of fractional-order neural networks via impulsive control," *Neural Process. Lett.*, vol. 48, no. 1, pp. 459–479, Aug. 2018.
- [24] H.-L. Li, C. Hu, H. Jiang, Z. Teng, and Y.-L. Jiang, "Synchronization of fractional-order complex dynamical networks via periodically intermittent pinning control," *Chaos, Solitons Fractals*, vol. 103, pp. 357–363, Oct. 2017.
- [25] X. Peng, H. Wu, and J. Cao, "Global nonfragile synchronization in finite time for fractional-order discontinuous neural networks with nonlinear growth activations," *IEEE Trans. Neural Netw. Learn. Syst.*, vol. 30, no. 7, pp. 2123–2137, Jul. 2019.
- [26] G. Velmurugan, R. Rakkiyappan, and J. D. Cao, "Finite-time synchronization of fractional-order memristor-based neural networks with time delays," *Neural Netw.*, vol. 73, pp. 36–46, Jan. 2016.
- [27] X. Li, J.-A. Fang, W. Zhang, and H. Li, "Finite-time synchronization of fractional-order memristive recurrent neural networks with discontinuous activation functions," *Neurocomputing*, vol. 316, pp. 284–293, Nov. 2018.
- [28] J. Xiao, S. Zhong, Y. Li, and F. Xu, "Finite-time Mittag-Leffler synchronization of fractional-order memristive BAM neural networks with time delays," *Neurocomputing*, vol. 219, pp. 431–439, Jan. 2016.
- [29] C. Chen, Z. Ding, S. Li, and L. Wang, "Finite-time Mittag-Leffler synchronization of fractional-order delayed memristive neural networks with parameters uncertainty and discontinuous activation functions," *Chin. Phys. B*, vol. 29, no. 4, Apr. 2020, Art. no. 040202.
- [30] X. Lu, W.-H. Chen, Z. Ruan, and T. Huang, "A new method for global stability analysis of delayed reaction-diffusion neural networks," *Neurocomputing*, vol. 317, pp. 127–136, Nov. 2018.
- [31] Y. Cao, Y. Cao, S. Wen, T. Huang, and Z. Zeng, "Passivity analysis of delayed reaction-diffusion memristor-based neural networks," *Neural Netw.*, vol. 109, pp. 159–167, Jan. 2019.
- [32] T. Wei, P. Lin, Y. Wang, and L. Wang, "Stability of stochastic impulsive reaction-diffusion neural networks with S-type distributed delays and its application to image encryption," *Neural Netw.*, vol. 116, pp. 35–45, Aug. 2019.
- [33] C. Hu, H. Jiang, and Z. Teng, "Impulsive control and synchronization for delayed neural networks with reaction-diffusion terms," *IEEE Trans. Neural Netw.*, vol. 21, no. 1, pp. 67–81, Jan. 2010.
- [34] Z. Wang, J. Cao, Z. Cai, and L. Rutkowski, "Anti-synchronization in fixed time for discontinuous reaction-diffusion neural networks with time-varying coefficients and time delay," *IEEE Trans. Cybern.*, vol. 50, no. 6, pp. 2758–2769, Jun. 2020.
- [35] D. Zeng, R. Zhang, J. H. Park, Z. Pu, and Y. Liu, "Pinning synchronization of directed coupled reaction-diffusion neural networks with sampled-data communications," *IEEE Trans. Neural Netw. Learn. Syst.*, vol. 31, no. 6, pp. 2092–2103, Jun. 2020.
- [36] J. Cao, G. Stamov, I. Stamova, and S. Simeonov, "Almost periodicity in impulsive fractional-order reaction-diffusion neural networks with time-varying delays," *IEEE Trans. Cybern.*, vol. 51, no. 1, pp. 151–161, Jan. 2021.
- [37] X. Wu, S. Liu, and Y. Wang, "Stability analysis of Riemann-Liouville fractional-order neural networks with reaction-diffusion terms and mixed time-varying delays," *Neurocomputing*, vol. 431, pp. 169–178, Mar. 2021.
- [38] I. Stamova and G. Stamov, "Mittag-leffler synchronization of fractional neural networks with time-varying delays and reaction-diffusion terms using impulsive and linear controllers," *Neural Netw.*, vol. 96, pp. 22–32, Dec. 2017.
- [39] L. Shanmugam, P. Mani, R. Rajan, and Y. H. Joo, "Adaptive synchronization of reaction-diffusion neural networks and its application to secure communication," *IEEE Trans. Cybern.*, vol. 50, no. 3, pp. 911–922, Mar. 2020.

- [40] J.-L. Wang, H.-N. Wu, and L. Guo, "Novel adaptive strategies for synchronization of linearly coupled neural networks with reaction-diffusion terms," *IEEE Trans. Neural Netw. Learn. Syst.*, vol. 25, no. 2, pp. 429–440, Feb. 2014.
- [41] Y. Lv, C. Hu, J. Yu, H. Jiang, and T. Huang, "Edge-based fractional-order adaptive strategies for synchronization of fractional-order coupled networks with reaction-diffusion terms," *IEEE Trans. Cybern.*, vol. 50, no. 4, pp. 1582–1594, Apr. 2020.
- [42] C. Huang, X. Zhang, H.-K. Lam, and S.-H. Tsai, "Synchronization analysis for nonlinear complex networks with reaction-diffusion terms using fuzzy-model-based approach," *IEEE Trans. Fuzzy Syst.*, vol. 29, no. 6, pp. 1350–1362, Jun. 2021.
- [43] H. Shen, F. Li, H. Yan, H. R. Karimi, and H. K. Lam, "Finite-time event-triggered H_∞ control for T-S fuzzy Markov jump systems," *IEEE Trans. Fuzzy Syst.*, vol. 26, pp. 3122–3135, 2018.
- [44] K. Shi, J. Wang, Y. Tang, and S. Zhong, "Reliable asynchronous sampled-data filtering of T-S fuzzy uncertain delayed neural networks with stochastic switched topologies," *Fuzzy Sets Syst.*, vol. 381, pp. 1–25, Feb. 2020.
- [45] H. Shen, Y. Men, Z. Wu, and J. H. Park, "Nonfragile H_∞ control for fuzzy Markovian jump systems under fast sampling singular perturbation," *IEEE Trans. Syst., Man, Cybern., Syst.*, vol. 48, pp. 2058–2069, 2018.
- [46] L. Wang, H. He, Z. Zeng, and C. Hu, "Global stabilization of fuzzy memristor-based Reaction-Diffusion neural networks," *IEEE Trans. Cybern.*, vol. 50, no. 11, pp. 4658–4669, Nov. 2020.
- [47] R. Zhang, D. Zeng, J. H. Park, H.-K. Lam, and S. Zhong, "Fuzzy adaptive event-triggered sampled-data control for stabilization of T-S fuzzy memristive neural networks with reaction-diffusion terms," *IEEE Trans. Fuzzy Syst.*, vol. 29, no. 7, pp. 1775–1785, Jul. 2021, doi: 10.1109/TFUZZ.2020.2985334.
- [48] J. Wang, X. Wang, N. Xie, J. Xia, and H. Shen, "Fuzzy model-based H_∞ pinning synchronization for coupled neural networks subject to reaction-diffusion," *IEEE Trans. Fuzzy Syst.*, early access, Nov. 9, 2020, doi: 10.1109/TFUZZ.2020.3036697.
- [49] R. Zhang, D. Zeng, J. H. Park, H.-K. Lam, and X. Xie, "Fuzzy sampled-data control for synchronization of T-S fuzzy reaction-diffusion neural networks with additive time-varying delays," *IEEE Trans. Cybern.*, vol. 51, no. 5, pp. 2384–2397, May 2021.
- [50] X. Chen and C. Song, "State estimation for quaternion-valued neural networks with multiple time delays," *IEEE Trans. Syst., Man, Cybern., Syst.*, vol. 49, no. 11, pp. 2278–2287, Nov. 2019.
- [51] X. Chen, Q. Song, and Z. Li, "Design and analysis of quaternion-valued neural networks for associative memories," *IEEE Trans. Syst., Man, Cybern., Syst.*, vol. 48, no. 12, pp. 2305–2314, Dec. 2018.
- [52] Z. Tu, J. Cao, A. Alsaedi, and T. Hayat, "Global dissipativity analysis for delayed quaternion-valued neural networks," *Neural Netw.*, vol. 89, pp. 97–104, May 2017.
- [53] Q. Song and X. Chen, "Multistability analysis of quaternion-valued neural networks with time delays," *IEEE Trans. Neural Netw. Learn. Syst.*, vol. 29, no. 11, pp. 5430–5440, Nov. 2018.
- [54] Y. Liu, D. Zhang, J. Lou, J. Lu, and J. Cao, "Stability analysis of quaternion-valued neural networks: Decomposition and direct approaches," *IEEE Trans. Neural Netw. Learn. Syst.*, vol. 29, no. 9, pp. 4201–4211, Sep. 2017.
- [55] X. Yang, C. Li, Q. Song, J. Chen, and J. Huang, "Global Mittag-Leffler stability and synchronization analysis of fractional-order quaternion-valued neural networks with linear threshold neurons," *Neural Netw.*, vol. 105, pp. 88–103, Sep. 2018.
- [56] H.-L. Li, L. Zhang, C. Hu, H. Jiang, and J. Cao, "Global Mittag-Leffler synchronization of fractional-order delayed quaternion-valued neural networks: Direct quaternion approach," *Appl. Math. Comput.*, vol. 373, May 2020, Art. no. 125020.
- [57] J. Xiao, J. Cao, J. Cheng, S. Wen, R. Zhang, and S. Zhong, "Novel inequalities to global Mittag-Leffler synchronization and stability analysis of fractional-order quaternion-valued neural networks," *IEEE Trans. Neural Netw. Learn. Syst.*, vol. 32, no. 8, pp. 3700–3709, Aug. 2021, doi: 10.1109/TNNLS.2020.3015952.
- [58] J. Xiao, J. Cao, J. Cheng, S. Zhong, and S. Wen, "Novel methods to finite-time Mittag-Leffler synchronization problem of fractional-order quaternion-valued neural networks," *Inf. Sci.*, vol. 526, pp. 221–244, Jul. 2020.
- [59] X. Song, J. Man, S. Song, Y. Zhang, and Z. Ning, "Finite/fixed-time synchronization for Markovian complex-valued memristive neural networks with reaction-diffusion terms and its application," *Neurocomputing*, vol. 414, pp. 131–142, Nov. 2020.
- [60] Y. Huang, J. Hou, and E. Yang, "Passivity and synchronization of coupled reaction-diffusion complex-valued memristive neural networks," *Appl. Math. Comput.*, vol. 379, Aug. 2020, Art. no. 125271.
- [61] L. Duan, M. Shi, C. Huang, and X. Fang, "Synchronization in finite/fixed-time of delayed diffusive complex-valued neural networks with discontinuous activations," *Chaos, Solitons Fractals*, vol. 142, Jan. 2021, Art. no. 110386.
- [62] X. Song, J. Man, S. Song, and C. K. Ahn, "Finite/fixed-time anti-synchronization of inconsistent Markovian quaternion-valued memristive neural networks with reaction-diffusion terms," *IEEE Trans. Circuits Syst. I, Reg. Papers*, vol. 68, no. 1, pp. 363–375, Jan. 2021.



G. NARAYANAN was born in 1994. He received the B.Sc. degree in mathematics from C. Abdul Hakeem College, Melvisharam, Vellore, Tamil Nadu, India, affiliated to Thiruvalluvar University, Vellore, in 2015, and the master's degree in mathematics from Thiruvalluvar University, in 2018, where he is currently pursuing the Ph.D. degree with the Department of Mathematics. His research interests include fractional differential equations, wind turbine systems, cyber security control, complex-valued and quaternion-valued of molecular systems, and multi-agent networked systems.



M. SYED ALI graduated from the Department of Mathematics, Gobi Arts and Science College, affiliated to Bharathiar University, Coimbatore, Tamil Nadu, India, in 2002, received the master's degree in mathematics from Sri Ramakrishna Mission Vidyalyaya College of Arts and Science, affiliated to Bharathiar University, in 2005, the Master of Philosophy degree in mathematics from Gandhigram Rural University, Gandhigram, India, in 2006, with a focus on numerical analysis, and the Doctor of Philosophy degree in mathematics from Gandhigram Rural University, in 2010, with a focus on fuzzy neural networks. In 2010, he was selected as a Postdoctoral Fellow for promoting his research in the field of mathematics at Bharathidasan University, Trichy, Tamil Nadu, where he worked, from November 2010 to February 2011. Since March 2011, he has been working as an Assistant Professor with the Department of Mathematics, Thiruvalluvar University, Vellore, Tamil Nadu. He has published more than 130 research articles in various SCI journals holding impact factors. He has also published research articles in national journals and international conference proceedings. His research interests include stochastic differential equations, dynamical systems, fuzzy neural networks, complex networks, and cryptography. He also serves as a reviewer for several SCI journals. He was awarded Young Scientist Award 2016 by The Academy of Sciences, Chennai.



MD IRSHAD ALAM received the B.Tech. degree from MIT, Muzaffarpur, the Master of Technology degree from BIT Sindri, Dhanbad, under Vinoba Bhave University, in 2011, and the Ph.D. degree in electrical engineering from B. R. Ambedkar Bihar University, in 2014. He is currently working as an Assistant Professor with the Electrical Engineering Department, Sitamarhi Institute of Technology, Sitamarhi, Bihar, India. His research interests include power systems, control systems, and organic semiconductor materials.



GRIENGGRAI RAJCHAKIT was born in 1981. He received the B.S. degree in mathematics from Thammasat University, Bangkok, Thailand, in 2003, the M.S. degree in applied mathematics from Chiang Mai University, Chiang Mai, Thailand, in 2005, and the Ph.D. degree in applied mathematics from King Mongkut's University of Technology Thonburi, Bangkok, with a focus on mathematics with specialized area of stability and control of neural networks. He is currently working

as a Lecturer with the Department of Mathematics, Faculty of Science, Maejo University, Chiang Mai. He has authored or coauthored of more than 133 research articles in various SCI journals. His research interests include complex-valued NNs, complex dynamical networks, control theory, stability analysis, sampled-data control, multi-agent systems, T-S fuzzy theory, and cryptography. He serves as a reviewer for various SCI journals. He was a recipient of Thailand Frontier Author Award by Thomson Reuters Web of Science, in 2016, TRF-OHEC-Scopus Researcher Award by The Thailand Research Fund (TRF), Office of the Higher Education Commission (OHEC), and Scopus, in 2016.



NATTAKAN BOONSATIT received the M.Sc. degree in applied mathematics from King Mongkut's University of Technology North Bangkok (KMUTNB), Bangkok, Thailand. She is currently working with the Department of Mathematics, Faculty of Science and Technology, Rajamangala University of Technology Suvarnabhumi, Nonthaburi, Thailand. Her research interests include mathematic model, climate change, atmospheric model, Lyapunov theory and

neural networks, stability analysis of dynamical systems, synchronization, and chaos theory.



PANKAJ KUMAR is currently working as an Assistant Professor with the Department of Computer Science and Engineering, Noida Institute of Engineering and Technology, Greater Noida. He has served as a Faculty Member for various institutes, such as IGIT, New Delhi, and DataPro InfoWorld Ltd., Hazaribagh. He has more than 11 years of experiences in teaching, research, and industry. He taught a wide spectrum of courses related to web technology, software engineering,

AOP, and soft computing. He has supervised nine M.Tech. dissertations and various B.Tech. projects. His major research interests include organic semiconductor materials, software engineering focusing on software quality and aspect-oriented programming, and neural networks. He is currently on the panel of various reputed international journals as a reviewer. He has actively associated with various professional bodies.



PORPATTAMA HAMMACHUKIATTIKUL received the Ph.D. degree in applied mathematics from King Mongkut's University of Technology Thonburi (KMUTT), Bangkok, Thailand. She is currently working with the Department of Mathematics, Phuket Rajabhat University (PKRU), Phuket, Thailand. Her research interests include mathematic model, climate change, atmospheric model, Lyapunov theory and neural networks, stability analysis of dynamical systems, synchronization, and chaos theory.

...

REPPRESSED VOICES OF MIGRATION: DISPLACEMENT AS A SYMBOLIC
REPRESENTATION OF EXPLOITATION OF NATURE AND WOMEN IN RAJAM
KRISHNAN'S *WHEN THE KURUNCHI BLOOMS*.

S. Julia Selva Sundari Ph.D. Research Scholar (PT) Department of English, Thiruvalluvar
University, Serkadu, Vellore
Dr.C.Anita Assistant Professor Department of English, Thiruvalluvar University,
Serkadu, Vellore

Abstract

Migration has displaced families from its root and has disrupted peaceful living. Men and women share varied perceptions of the need for migration. Men, by their urge to explore, welcome migration as a positive change befitting a convenient life. Whereas Women who are rooted in their culture resist it as a factor of exploitation of women and Nature. The industrial revolution and climate change have initiated displacement and boosted hopefulness for better prospects, but it has hidden the agenda that vulgarize women's freedom and ransacks the resources of Nature. This article analyses and understands the truthfulness of gender issues in migration, shared as a bold voice of women in repression. Rajam Krishnan uses displacement and migration in *When the Kurunchi Blooms*, to symbolically represent the endangerment of the ecoregion and suppression of women in a tribal community.

Keywords: Migration, Displacement, Badagas, Tribal Community, Kurunchi

The new age evolution has witnessed Man exploring the various possibilities of advancement in the light of the industrial and green revolution and the initiation of unique and unconventional practices in society that mitigated the change. The scope of Migration has been historically withheld as a rare phenomenon that began as means of finding new habitats due to colossal disasters and invasions of land. The movement of the Homo erectus from Africa, migration to the Americas, Neolithic revolution, Indo-European invasion, Turkie expansion are a few notable instances in early history when the large community moved to new places. Colonialism displaced a more prominent sect of humans either voluntarily or involuntarily. People moved voluntarily to seek better prospects to end poverty and gain financial stability, while the involuntary movement is characterized by refugees, the slave trade, and human trafficking. The UN Migration Agency (IOM) defines a migrant as "any person who is moving or has moved across an international border or within a State away from his/her habitual place of residence, regardless of (1) the person's legal status, (2) whether the movement is voluntary or involuntary; (3) what the causes for the movement are; or (4) what the length of the stay is." The defining factor in migration is in the fundamentality of the initiation, whether it is a voluntary action or enabled by involuntary means.

The early half of the twentieth century witnessed displacement due to world war and post-world war migration birthed by decolonization agreements. India Partition, the Polish movement, and the Potsdam agreement, which displaced twenty million Germans, is the largest in modern history. War, agreements, and peace treaties have politicized the movement of people. The non-politized are mitigated through climatic changes and incompetent governance of natural resources. Industrialization and Urbanization initiated large displacements during the second half of the twentieth century. Post world war quickened the process of displacement by luring the human mind to explore newer frontiers of possibilities. Science and technology required people to displace from their original habitats for higher education and career prospects. Development and economic preference turned people away from their practice of belonging to their native settlements.

Migration can be characterized based on locale and permanence. People begin their movement within states and have continued moving between states and emigrating to other countries. Inter-state and within-country movements are chiefly categorized as a pattern of Urban-Rural movement or Urban to Urban movement. Rural populations move to towns and cities for work, while urban to urban migration happens

ECOLOGICAL CONCERNS IN THE SELECT WORKS OF AMITAV GHOSH

Dr. C. Anita, Assistant Professor of English, Thiruvalluvar University
Dr. S. Sasikumar, Assistant Professor of English, K M G College of Arts and Science, (Affiliated to Thiruvalluvar University)

ABSTRACT

The first and foremost concern of ecocriticism is environmentalism. It should be understood as a political and ethical movement that seeks to improve and protect the quality of the environment through the adoption of forms of political, economic, or social organisations that are taught to be necessary for, at least, conducive to the benign treatment of the environment by humans, and through a reassessment of humanity's relationship with nature. Environmentalists known as "eco warriors" try to raise awareness among people that the human race's and other species' lives are in jeopardy if they do not value the biosphere's indispensability.

Environmentalism, Bioregionalism, Deep Ecology, Eco Marxism, and Eco Feminism are some of the subtopics found in ecocriticism in a nutshell. Bioregionalism thinks globally and acts locally. Colonization may also have specific goals such as obtaining cheap new materials, cheap labor, and a captive market for product manufacturing; in this case, colonisation is a growth to the exploitation of the environment. Globalisation has accelerated biodiversity destruction also. It turns all forests and farms into industrial monocultures, which destroy both the biodiversity and the cultural diversity of local communities.

Keywords: Ecology, Exploitation, Colonisation of Land and Biodiversity Destruction

In recent times, literature envisages itself as a multi-dispersary forum, enabling and incorporating cultural studies as a discipline of social science, such as anthropology, socio-psychology, new historicism, neo-modernism, environmentalism, and so on. The present paper proposes to take up environmental issue represented in the literature.

The term "ecocriticism," which is a combination of two words, "eco" and "critic," is derived from Greek. In Greek, eco and critic mean "house" and "judge," which imply that "a person who judges the merits and faults of writings that debit the effect of culture upon nature, with a view toward celebrating nature, berating its despoilers, and revising their harm through political action" (Glotfelty, 69). The term was first coined by William Rueckert in this essay "Literature and Ecology, an experiment: Ecocriticism" and terms Ecocriticism as "the application of ecology and ecological concepts to the study of literature" ("Home and Gasmere; ecological Holiness", 112). Ecocriticism is known in different forms as "Ecopoetics", "Ecoterriosm", "Environmental literary criticism", "Green cultural studies", "Landscape criticism". Although ecocriticism is branded as environmentalism, there is a major difference between the terms "Eco" and "Enviro." "Eco" implies interdependent communities, integrated systems and strong connections among constituent parts. "Enviro" is anthropocentric and dualistic, implying human beings are at the centre, surrounded by everything else that is not human. Ecocriticism thus brings about a radical shift from anthropocentrism to biocentrism.

The first and foremost concern of ecocriticism is environmentalism. It should be understood as a political and ethical movement that seeks to improve and protect the quality of the environment through the adoption of forms of political, economic, or social organisations that are taught to be necessary for, at least, conducive to the benign treatment of the environment by humans, and through a reassessment of humanity's relationship with nature. Garrad defines environmentalists as those "who are concerned with environmental issues such as global warming and pollution, but who wish to maintain or improve



JOURNAL OF EMERGING TECHNOLOGIES AND INNOVATIVE RESEARCH (JETIR)

An International Scholarly Open Access, Peer-reviewed, Refereed Journal

Fractured Identity in K. A. Gunasekaran's *The Scar*

M. Muniyappan
M.Phil Research Scholar
Dept. of English
Thiruvalluvar University
Serkadu-632115

Dr. C. Anitha
Assistant Professor
Dept. of English
Thiruvalluvar University
Serkadu-632115

Abstract

This article entitled "Fractured Identity in K. A. Gunasekaran's *The Scar*". Focuses on the fractured identity of Dalits through in the fiction *The Scar* by K. A. Gunasekaran. Dalit Autobiography has emerged out to be not only a part of the Dalit history but also an important node of Dalit Literature. It is a historical act of the Dalits to achieve a sense of identity and mobilize resistance against different forms of oppression. This article seeks to examine the status and sufferings of Dalits and their survival in the caste Hindu society in the context of K. A. Gunasekaran's Tamil autobiography 'Vadu' which is available in English translation and adaptation (2009) by V. Kadamban. By writing his autobiography Gunasekaran thus challenged the traditional narrative of Dalit history and propagated by mainstream writers. Not only it is a record of his experiences but it is also a reflection of a certain time. It talks about his life up to his graduation. The narrative evokes a mixture of Hinduism, Islam and Christianity. This autobiography shows the curse of untouchability that has inflicted ethnic and physical wounds in the minds of the so called outcasts. The paper examines how this autobiography could be used for our understanding of their hurdles of faced challenges by the Dalits and the caste system.

Keywords: Dalit, Auto Biography, Fractured Identity, untouchability

Dalit autobiography plays a vital role in the upliftment of Dalits. It brings out the true evidence of discrimination against Dalits in the name of caste and it also highlights the duality of the Dalits in treating themselves. The author evidences the double standards of Indian villages' cruelty and lack of consciousness towards Dalits. K. A. Gunasekaran duels in the subject casteism which is widespread in every part of Indian village.



'ECOFEMINISM AND WILDERNESS THERAPY': THE INSEPARABLE BIPARTITE IN THE JOURNEY TO SELF-REALIZATION AND ARTICULATION IN AMBAI'S "FOREST."

S. Julia Selva Sundari Ph.D. Research Scholar (PT) Department of English, Thiruvalluvar University, Serkadu, Vellore

Dr.C.Anita Assistant Professor Department of English, Thiruvalluvar University, Serkadu, Vellore.

Abstract

The need to conquer the fear of self-worth is a mandate in a male-centric society. Women as victims of patriarchal misogyny require a trustworthy therapist to treat and heal. Ecofeminism understands the common source of contention evident in the subjugation of women and exploitation of nature. Wilderness therapy addresses the innate pain of women as they take a journey into the unexplored territories of the deep forest. It is comparable to the journey into the depth of oneself to understand the crux of the issue. The article Ecofeminism and Wilderness Therapy explores the tenets of Wilderness therapy and discusses the journey of Chentiru. Her interaction in the Wilderness provides her clarity. Ambai uses the mythical character Sita as a parallel plot and compares the similarity between Chentiru and Sita in the Wilderness. Sita and Chentiru understand the core of the issue that has structured their life. They acquire the courage to articulate the pain which has been thrust on them. The journey into the Wilderness has brought about a change, making a strong recommendation to every woman in distress.

Keywords: Wilderness Therapy, Ecofeminism, Forest, Patriarchal Misogyny

The subaltern voices have chiseled the pre and post-independent Indian history. This voice of the oppressed arose out of their dire need to claim their prominence as natives and compatriots. The consequence of British hegemony incarcerated the Indian nationals. Imperialism enslaved the Indians under British supremacy, while casteism subdued them under class dominancy. Among the vast majority of the subaltern lies the marginalized subset of womanhood. The voice of Indian women is ever considered an abomination in a patriarchal community. The Indian subcontinent in a totalitarian front has lost its roots and relevance in the realm of colonization under the British Raj, and women lost their equitable position to the egregious practice of patriarchy and anarchy together. Subjugation is a forced ordeal thrust upon women. The decline of the status of women in society began when the ideology of equal share in labour diversified into a commodity, asset, and claim over private property.

The subservience of women began with stereotyping. They held roles that made a lesser contribution to economic upliftment. Women's roles are characterized by childcare and homemaking. In class, caste, and imperialistic sovereignty, the subordination of women has permitted oppressive and toxic practices such as child marriage, illiteracy, juvenile pregnancy, partiality in law and governance, polygamy, and economic dependency. These venomous doctrines silenced women's voices, causing detrimental social stratification against equality and compatibility. In India, humanity stooped to its lowest point with the acceptance of systems like Sati, female infanticide, the Devadasi system, dowry harassment, and honour killing.

Narrative- A blend of Modern and Traditional: A Study of Ben

Okri's Select Novels

S S Sathishkumar,
Ph D Research Scholar,
Department of English,
Thiruvalluvar University,
Vellore, Tamilnadu,
India

Dr C Anita,
Assistant Professor,
Department of English,
Thiruvalluvar University,
Vellore, Tamilnadu,
India.

Abstract:

Okri employs a narrative style a mixture of reality and imaginary. He uses African oral tradition and bond with modern technique 'Magical Realism'. Though Okri's works deal with magical realism, he refuses to be called him as pure magical realist writer. The reason for Okri, to adopt magical realism in his works, is the inadequacy of narrative techniques to express the neo-colonial aspects in African literature. He employs the narrative technique in his *Abiku Trilogy*.

Key words: Ben Okri, narrative style, magical realism, Abiku Trilogy, African oral tradition

Okri's narrative style is a mixture of reality with the imaginary facts. He utilises African oral tradition with magical realism. Critics state that Okri as a magical realist but in an interview he strongly declines to be categorized as clean magical realist writer. The chapter focuses only on the narrative style with the merge of magical elements and oral tradition found in Okri's select novels. The narrative techniques uses by Okri illustrate the life and the consequences faced by people in post independent Nigeria.

<http://infokara>

Abstract:

The biggest challenge women faced in Indian social history is patriarchy. India has age old rigidly built patriarchal structure. In a male chauvinist society, the power of decision making is handed to men and women are same. A woman born in a patriarchal society tend to suffer because of the ruling rules. Rabindranath Tagore's play *The King and the Queen* the theme placed in one such society. The protagonist Sumitra is seen struggling against the male-dominated society. Tagore message to the society through Sumitra's role is that women are the grip of social ills such as fear, injustice and gender discrimination. Protagonist Sumitra is dead against that. The dramatist ends the play by making Sumitra a fierce rebel fighting against her own husband for the sake of her country and its people.

Keywords: Political Identity, Right for Equality, Pre Independent India.

Tagore defines the Indian philosophy of *Rajdharm* in the play *The King and the Queen*. *Rajdharm* means the king does his duties and helps the poor who are in the emperor. King Vikram does not recognise his *Rajdharm* as his emperor. He neglects his royal duties because of his passionate attachment with the queen "VIKRAM. No more vain words, queen. The bird's nests are silent with love. Lips keep guard upon lips and allow no word to clamour" (*KQ*, 94). Sumitra requests Vikram to do his kingly duties. She advises the people of the kingdom are dying by the hunger for his negligence. She tells him to save the people from dicots. Vikram gets infuriated by Sumitra's words and he replies to his wife, he knows when and what to do for the people. He says that to keep silent like birds are always living silently in their nest. Psychologically he has a mentality of nothing to do if a woman accuses him, even if he refused to fight with foes. She worries that he is not able to understand his relationship and responsibilities. He acted as a sensuous man.

Tagore suited the title of the play *Raja O Rani* published in Bengali 1889. He translated the play into English with the title *The King and the Queen*. He has written the play during the early twentieth century scenario — political and social upheavals in colonial India. The period the Bengal partition is the backdrop of the play. He opposed the British Raj and split off Bengal. In the play, he places Sumitra's role during the political upheavals were going on in pre-independence India. He represents the period Indian women participated in freedom fighting. Through the play, he mentioned Indian men and their sacrifice occupy a foremost place in Indian freedom history.

Queen Sumitra discomforts and restlessness gets echoed in the play. Tagore's king Vikram represents his authority over the country, sensible duties and also how he lived a self-centred life:

VIKRAM. Why have you delayed in coming to me for so long, my love?

SUMITRA. Do you not know, my king that I am utterly yours wherever I am? It

was your house and its service that kept me away from your presence, but not from you

(*The King and the Queen*, 93)

The scene opens with the husband questioning his wife. Vikram enquires his wife Sumitra for being late in the king's court. She replies that wherever she may be her mind contemplates on him. She says that the king's palace is not her palace; it is the King's palace. She expresses her feelings that she maintains a distance from the King to do his kingly duties because she understands the role of personal space in a relationship. She keeps him at a distance but she takes care of him. Vikram treats his wife as inferior. His behaviour resembles, he is a ruling master of Sumitra that she lives in the shackled condition in the palace.

The traditional duty of a married woman through Sumitra dialogue is understood. She is not the ruler of a country but is dependent on the King. She cannot realise her wish without her husband.

Copyright @ 2020 Author

Subverting the Gender Stereotype in Mahesh Dattani's Select plays

B.Anitha

PhD Fellow, scholar (P/T)
Department of English,
Thiruvalluvar University,
Tiruchirappalli, Vellore.

Dr.C.Anita

Assistant professor
Department of English,
Thiruvalluvar University,
Tiruchirappalli, Vellore.

Abstract

Subverting the Gender Stereotype examine the issues of femininity in the urban context, the complex relationship between men and women in the modern urban family and their trials and tribulations and gender inequalities through the plays *Bravely Fought the Queen* and *Clearing the Rubble*. The modern urban families and their trials and tribulations often form the crux of Mahesh Dattani's works. Urban issues are dealt with at most sincerity and close to reality.

Keywords: Stereotype, Gender, Feminism, Urban, Modern, Mahesh Dattani.

Patriarchal -

The eminent theatre director Frin Mee observes, "Mahesh Dattani frequent takes as his subject the complicated dynamic of the modern urban family" (Note 3). But even though the setting of his plays is mainly urban, the issues he deals with are varied. Mahesh Dattani, through his themes and characters, almost defies gender categorization. But it can be said without a doubt that he is a writer who depicts the oppressed and the marginalised and the stereotyped. Gender stereotyping and its consequent

SELF-CONFINEMENT OF MASHA IN CHEKHOV'S *THREE SISTERS*

M. Hassan
Ph.D. Research Scholar
Dept. of English
Thiruvalluvar University
Serkkadu, Vellore-115

Dr. C. Anita
Assistant Professor
Dept. of English
Thiruvalluvar University
Serkkadu, Vellore-115

Anton Pavlovich Chekhov is a cardinal literary figure in Russia. He is known to Russia through his short stories and became popular very much with his plays. He has written many plays among them a few plays became very popular they are *Three Sisters* and *The Cherry Orchard*. This article analyses the character of Masha in *Three Sisters*. This play has published in the year 1901.

The book *Nineteenth century Russian literature* has written by a famous British historian of medieval Russian history and of Russian literature John Fennell. He points out that the common purports of Chekhov stories and dramas in the following lines.

It is to a study of the state of man's consciousness that the whole of Chekhov's nature work, including the drama is devoted, indeed the majority of the Chekhov stories may, in retrospect, be seen as falling within the same pattern. His subject is contemporary Russia, his meaning is universal. (323)

According to Fennell the concept of Chekhov's short stories and dramas reflect the life style of Russians. A century back Russians lived a life of much emotions and turbulence. The beginning of twentieth century Russians were suffered by civil war and Industrial Development such as high taxes, loss of jobs, and rampant hunger. During Industrial Revolution the working class people and peasants suffered more than nobles. This was a traumatic period for the Russians.

Depression occurs in both the genders. Women are affected more comparatively worse than men. Depression impacts in all area in women's life. For an example when a girl is depressed denied higher education she goes to the depression state. A married woman is also depressed when she is bounded with responsibilities such as take care and responsibility for her

TERMINATION OF THE TRADITIONAL FOREST: A STUDY OF BEN OKRI'S *THE FAMISHED ROAD*

K.Sathishkumar Ph.D Research Scholar Department of English Thiruvalluvar University Vellore,
Tamilnadu India

Dr.C.Anita Assistant Professor Department of English Thiruvalluvar University Vellore,
Tamilnadu India

Abstract:

Nigeria has an indigenous identity for its natural resources. The forest is attached with the culture and tradition of Nigeria. Ben Okri is a Nigerian writer who illustrates the degeneration of natural forest in his novel *The Flowers and Shadows*. He brings out the negative faces of globalization and modernization. The process of globalization gradually destructs the natural resources by means of expanding the civilization and industries. Okri focuses on forest's ecological value by highlighting the significant role of the forest in African culture and financial system. Okri creates awareness to regenerate the forest for future generation.

Keywords: Ben Okri, Nigeria, natural resources, forest, tradition, globalization, modernization,

Forest is the basis of the environment. Forest sticks to great values in every group of people. The world without trees, plants and shrubs become bare land with stones and mountains. The beauty of natural landscape is lost and cause impairment to the health of human being and other creatures. African continent is widely known for its vast spreading forest which is filled with thousands of species ranging from trees, shrubs, parasites, animals, humans. Forest affords food resources, habitats for inhabitation for humans and other animals. The forest plays a vital role in regulating climate and prevents erosion. The African forest has precious resources. In the Westerners point of view, the African forest has valuable resources to be exploited by the European colonisers. Writers from Africa signify the importance of preserving forests in their works. Chinua Achebe in his *Things Fall Apart* has "given the alarming statistics on the current state of forests in Nigeria" (Gillian Gane 40). Ben Okri's *The Famished Road* depicts the devastating effects of development on forest. While moving further into the research, a brief explanation of Ben Okri is essential. Okri was born in 1959 in northern Nigeria to an Urhobo father and Igbo mother. His father decided to study law so he finally left for London. Okri spent his childhood in England. At the age of seven Okri returned to Nigeria in 1968 at the time of Biafra War. Okri returned to England for his university degree B.A in Creative literature. He was working as a journalist and began writing essays and short stories. His earlier works focus on life in modern day Nigeria. Okri, being a diasporic writer, wrote about the problems which beset his homeland. His writings depict poverty, famine and political corruption. He combines western literary techniques with the elements of traditional African folklore and myth. It is imperative to discuss about Chinua Achebe's the theme of forest in his novel *Things Fall Apart*. Achebe uses the term 'Evil Forest' in this novel. He stresses the significant of forest. The forest is essential for the Igbo since it conserves Igbo's social and religious order. In *Things Fall Apart*, reference to the forest is given as "Evil Forest" where the disgraced people are buried after death.

In it were buried all those who died of the really evil diseases, like leprosy and smallpox. It was also the dumping ground for the potent fetishes of great medicine men when they died. An 'evil forest' was, therefore, alive with sinister forces and powers of darkness (Achebe 148).

Evil forest is a region where contaminants of leprosy and smallpox are buried. Evil forest serves as a safety regulator to remove the noxious elements that are hazardous to the society. In the context of neocolonial and globalization manipulation, shows how human being is a weakening force to natural resources. Okri focuses on forest's ecological value by highlighting the significant role of the forest in African culture and financial system. In *The Famished Road* the text is a reminder of the steady disappearance of both natural resources and traditional credence in

Asynchronous Extended Dissipative Filtering for T–S Fuzzy Markov Jump Systems

Yufeng Tian¹ and Zhanshan Wang¹, *Senior Member, IEEE*

Abstract—This article is concerned with the asynchronous reliable extended dissipative filtering problem for a class of continuous-time T–S fuzzy Markov jump systems. The modes of the encountered sensor failures and the designed filter are considered to be asynchronous with the original systems, which can be described by two mutually independent hidden Markov processes. By proposing double variables-based decoupling principle and variable substitution principle, a new condition is presented to guarantee the filtering error system to be stochastically stable and extended dissipative. Compared with the existing works, the proposed method does not impose constraints on Lyapunov variables and slack variables, and some unnecessary constraints on the system structure are removed. These directly lead to less conservative and more general results. An example is provided to illustrate the effectiveness of the proposed design method.

Index Terms—Asynchronous reliable extended dissipative filtering, double variables-based decoupling principle (DVDP), Takagi–Sugeno (T–S) fuzzy Markov jump systems (MJSS), variable substitution principle (VSP).

I. INTRODUCTION

SINCE many mathematical models of physical systems are nonlinear with complex uncertainties, causing many difficulties in the control and analysis, researchers have been trying to seek effective methods for controlling nonlinear systems [1]–[3]. It is known that Takagi–Sugeno (T–S) fuzzy inference plays a popular way in modeling nonlinearities, such as saturations and dead zones [4], [5]. It has been shown that a complex nonlinear system can be described in terms of a family of IF-THEN rules since the T–S model behaves like a linear system [6]. On this basis, many works for stability analysis and the controller/filter design problems have been published [7]–[9].

Manuscript received January 23, 2020; revised July 25, 2020 and March 28, 2021; accepted May 5, 2021. This work was supported in part by the National Natural Science Foundation of China under Grant 61973070; in part by Liaoning Revitalization Talents Program under Grant XLYC1802010; in part by SAPI Fundamental Research Funds under Grant 2018ZCX22; and in part by Fundamental Research Funds for the Central Universities under Grant N2104003. This article was recommended by Associate Editor Y.-J. Liu. (Corresponding author: Zhanshan Wang.)

The authors are with the State Key Laboratory of Synthetical Automation for Process Industries, Northeastern University, 2011DA105325, Shenyang 110819, China, and also with the College of Information Science and Engineering, Northeastern University, Shenyang 110819, China (e-mail: tyf_tyf@163.com; zhanshan_wang@163.com).

Color versions of one or more figures in this article are available at <https://doi.org/10.1109/TSMC.2021.3079464>.

Digital Object Identifier 10.1109/TSMC.2021.3079464

Markov jump systems (MJSs) experience abrupt changes in their parameters and structure, and have been an attractive research topic [10]–[14]. A lot of results have been reported to solve filtering problems [15]–[17]. In [17], the reliable exponential H_∞ filtering problem has been studied for singular MJSs with sensor failures. Sensor failures may arise unexpectedly and they can affect system performance or even bring about damages. Thus, plenty of literature on reliable filtering for MJSs has been reported [9], [18]. It is worth pointing out that the aforementioned results were developed in the context of linear MJSs. With rapid development of fuzzy system theory, more and more problems of T–S fuzzy MJSs have been studied [19]–[21], in which the system mode is assumed to be available to the filters at any time through the sensor. Unfortunately, utilization of mode will be limited because of some deviant behaviors, such as time-delays and data dropouts. Unlike some published papers [15]–[21], another nonsynchronous mechanism has been applied to deal with some concerned asynchronous phenomena, namely, hidden Markov model (HMM) [22]. Afterward, the asynchronous filtering by HMM has been extended to many works [23]–[28]. Although a number of results on the asynchronous filtering have been achieved for T–S fuzzy MJSs, few results focus on the asynchronous reliable filtering for T–S fuzzy MJSs except [23]. In [23], the asynchronous reliable $L_2 - L_\infty$ filtering problem for T–S fuzzy MJSs with sensor failures has been considered. However, the constrained structure of Lyapunov variables (such as $P_d = \begin{bmatrix} P_{1d} & P_2 \\ P_2^T & P_2 \end{bmatrix}$) may bring conservativeness. Although the constrained Lyapunov variables can be avoided by introducing slack variables (Finsler’s lemma), such as in [24]–[26], the introduced slack matrices are still constrained (such as $G_s = \begin{bmatrix} G_{1s} & X_s \\ G_{2s} & X_s \end{bmatrix}$ in [25]). It may also lead to conservativeness.

On the other hand, the extended dissipative filtering, which includes H_∞ , $L_2 - L_\infty$, passive, and dissipative filtering by tuning weighting parameters, is first proposed for continuous-time MJSs in [29]. Afterward, the extended dissipative filtering problem for continuous-time dynamic systems has been widely investigated [30]–[33]. For example, Li *et al.* [30] investigated the extended dissipative filter design problems for continuous-time fuzzy systems with time-varying delays. However, some unnecessary constraints on the filtering error system have to be imposed, which may lead to some limitations in practical applications. Moreover, the above mentioned works [29]–[32] only focus on the synchronous cases. Thus, without constraints,

how to handle the asynchronous extended dissipative filtering for continuous-time T-S fuzzy MJSs is an important topic.

Summarizing the above discussions, this article studies the problem of the asynchronous reliable extended dissipative filtering for T-S fuzzy MJSs. First, by employing HMM, two independently stochastic variables are introduced to describe the encountered sensor failures and filter, respectively. Second, a new condition, associated with the modes of plant, sensor failures, and filter are proposed to ensure the stochastic stability and extended dissipativity of the filtering error systems. The main contributions and novelty are given as follows.

- 1) By proposing double variables-based decoupling principle (DVDP) and variable substitution principle (VSP), the asynchronous reliable extended dissipative filter design condition is presented for T-S fuzzy MJSs. Compared with the existing methods [23]–[26], this article fully considers the free structure of Lyapunov variables and slack variables, which provides extra free dimensions in the solution space. It directly leads to the reduction of conservativeness in the filtering solution.
- 2) Compared with the existing works [29]–[32], some unnecessary constraints on the system structure are relaxed by introducing a set of positive scalars and symmetric positive matrices with the aid of S-procedure lemma, which leads to more general results.
- 3) Based on 1) and 2), the asynchronous reliable extended dissipative filtering is achieved for T-S fuzzy MJSs, which unifies the reliable filtering, extended dissipative filtering, and asynchronous filtering in a framework.

The remainder of this article is organized as follows. System description and preliminaries are presented in Section II and the main results are discussed in Section III. In Section IV, an example is provided and conclusions are presented in Section V.

Notation: Throughout this article, \mathcal{R}^n represents the n -dimensional Euclidean space; X^T denotes the transpose of X ; “*” in LMIs represents the symmetric term of the matrix; $\text{Sym}[X]$ means $X + X^T$; $\lambda_{\max}(X)$ represents the maximum eigenvalue of X ; $\mathcal{E}(X)$ denotes the mathematical expectation operator of X ; $\mathcal{L}_2[0, \infty)$ refers to the space of square-integrable vector functions over $[0, \infty)$; $\|X\|$ denotes the Euclidean norm for vectors of X ; $\text{col}[X, Y]$ denotes $[X^T, Y^T]^T$; $\text{diag}\{\dots\}$ represents a block diagonal matrix; and $\text{vec}[X, Y]$ represents $[X, Y]^T$.

II. SYSTEM DESCRIPTION AND PRELIMINARIES

Consider the following T-S fuzzy MJSs.

Plant Rule i : IF $\theta_1(t)$ is $\Gamma_{i1}, \dots, \theta_p(t)$ is Γ_{ip} , then

$$\begin{cases} \dot{x}(t) = A_{q(t)i}x(t) + B_{q(t)i}w(t) \\ y(t) = C_{q(t)i}x(t) + D_{q(t)i}w(t) \\ z(t) = E_{q(t)i}x(t) + F_{q(t)i}w(t) \end{cases} \quad (1)$$

where $\Gamma_{ij}(i \in \mathbb{V} = \{1, 2, \dots, v\}, j \in \{1, 2, \dots, p\})$ and $\theta_j(t)$ are fuzzy set with v fuzzy rules and the premise variable, respectively. $A_{q(t)i}, B_{q(t)i}, C_{q(t)i}, D_{q(t)i}, E_{q(t)i}$, and $F_{q(t)i}$ are known system matrices. $x(t) \in \mathcal{R}^n$, $y(t) \in \mathcal{R}^m$, $z(t) \in \mathcal{R}^p$, and $w(t) \in \mathcal{R}^q$ (belongs to $\mathcal{L}_2[0, \infty)$) are the system state, the measurement output, and the disturbance input, respectively. The

variable $q(t)$ stands for a continuous-time Markov jump process with TRM $\Lambda = [\lambda_{qc}]$. It takes value in $\mathbb{Q} = \{1, 2, \dots, Q\}$ with TPs given by

$$\Pr\{q(t+b) = c | q(t) = q\} = \begin{cases} \lambda_{qc}b + o(b), & q \neq c \\ 1 + \lambda_{cc}b + o(b), & q = c \end{cases}$$

where $\lambda_{cc} = -\sum_{c=1, q \neq c}^Q \lambda_{qc}$, $\sum_{c=1}^Q \lambda_{qc} = 0$, and $\lim_{\Delta \rightarrow 0} (o(b)/b) = 0$.

When $q(t) = q$, the overall fuzzy model is obtained by T-S fuzzy inference method

$$\begin{cases} \dot{x}(t) = A_q(h)x(t) + B_q(h)w(t) \\ y(t) = C_q(h)x(t) + D_q(h)w(t) \\ z(t) = E_q(h)x(t) + F_q(h)w(t) \end{cases} \quad (2)$$

where

$$\begin{aligned} A_q(h) &= \sum_{i=1}^v h_i(\theta(t))A_{qi}, B_q(h) = \sum_{i=1}^v h_i(\theta(t))B_{qi} \\ C_q(h) &= \sum_{i=1}^v h_i(\theta(t))C_{qi}, D_q(h) = \sum_{i=1}^v h_i(\theta(t))D_{qi} \\ E_q(h) &= \sum_{i=1}^v h_i(\theta(t))E_{qi}, F_q(h) = \sum_{i=1}^v h_i(\theta(t))F_{qi} \\ h_i(\theta(t)) &= \frac{\prod_{j=1}^p \Gamma_{ij}(\theta_j(t))}{\sum_{i=1}^v \prod_{j=1}^p \Gamma_{ij}(\theta_j(t))} \\ \theta(t) &= [\theta_1(t), \theta_2(t), \dots, \theta_p(t)] \end{aligned}$$

where $h_i(\theta(t))$ and $\Gamma_{ij}(\theta_j(t))$ represent the normalized fuzzy weighting function and grade of membership of $\theta_j(t)$ in Γ_{ij} , respectively. For $\forall t > 0$, we assume $\prod_{j=1}^p \Gamma_{ij}(\theta_j(t)) > 0$. It implies $h_i(\theta(t)) > 0$ and $\sum_{i=1}^v h_i(\theta(t)) = 1$.

When the sensors experience failures, the following sensor failure model is adopted in this article:

$$y_i^F = f_{\rho(t)i}(t)y_i(t), i \in \{1, 2, \dots, m\} \quad (3)$$

where y_i^F is the attainable signal from the i th sensor. The stochastic failure phenomenon can be described by variable $s(t) \in \mathbb{S} = \{1, 2, \dots, S\}$, which applies to HMM theory with the conditional probability matrix (CPM) $\mathcal{S} = [\rho_{qs}]$ ($\rho_{qs} > 0$) satisfying $\Pr\{s(t) = s | q(t) = q\} = \rho_{qs}$, where $\sum_{s=1}^S \rho_{qs} = 1$. Besides, the variable $f_{si}(t)$ ($s(t) = s$) describes the i th failure level under the s th mode satisfying

$$0 \leq f_{-si} \leq f_{si} \leq \bar{f}_{si} \leq 1 \quad (4)$$

where f_{-si} and \bar{f}_{si} represent the given lower and upper bounds of f_{si} , respectively. If $f_{-si} = \bar{f}_{si} = 0$ [i.e., $f_{si}(t) = 0$], the i th sensor under the s th mode loses its function and outage happens. When $f_{-si} = \bar{f}_{si} = 1$ [i.e., $f_{si}(t) = 1$], it works efficiently without failures. Partial failures will occur if $0 < f_{si}(t) < 1$. In this case, $f_{si}(t)$ can be described as

$$f_{si}(t) = \hat{f}_{si} + \delta_{si}(t) \quad (5)$$

where $\hat{f}_{si} = (f_{-si} + \bar{f}_{si})/2$. We can conclude

$$y^F(t) = F_s(t)y(t) = (\hat{F}_s + \Delta_s(t))y(t) \quad (6)$$

where

$$\begin{aligned}\Delta_s(t) &= \text{diag}\{\delta_{s1}(t), \delta_{s2}(t), \dots, \delta_{sm}(t)\} \\ \hat{F}_s(t) &= \text{diag}\{\hat{f}_{s1}, \hat{f}_{s2}, \dots, \hat{f}_{sm}\} \\ \check{F}_s(t) &= \text{diag}\{\check{f}_{s1}, \check{f}_{s2}, \dots, \check{f}_{sm}\} \\ \Delta_s^T(t)\Delta_s(t) &\leq \check{F}_s^T \check{F}_s \leq I.\end{aligned}$$

In this article, the HMM theory is used to design an asynchronous filter for estimating the plant. $\kappa(t) (\kappa(t) \in \mathbb{K} = \{1, 2, \dots, K\})$ is used to depict this situation. Furthermore, it has the same features with $s(t)$. That is, it satisfies the CPM $\mathcal{K} = [\tau_{qk}] (\tau_{qk} > 0)$ with $\Pr\{\kappa(t) = k | q(t) = q\} = \tau_{qk}$, where $\sum_{k=1}^K \tau_{qk} = 1$. Although asynchronous modes of the sensor and the filter are controlled by the plant mode directly, they are conditionally independent, i.e.,

$$\begin{aligned}\Pr\{s(t) = s, k(t) = k | q(t) = q\} \\ &= \Pr\{s(t) = s | q(t) = q\} \times \Pr\{k(t) = k | q(t) = q\} \\ &= \rho_{qs} \tau_{qk}.\end{aligned}\quad (7)$$

In order to estimate the signal $z(t)$ in system (2), the following asynchronously reliable filter is designed with $k(t) = k$ and $h_i(\theta(t)) = h_i$:

$$\begin{cases} \dot{x}_f(t) = A_k(h)x_f(t) + B_k(h)y^F(t) \\ z_f(t) = E_k(h)x_f(t) \end{cases}\quad (8)$$

where

$$\begin{aligned}A_k(h) &= \sum_{i=1}^v h_i A_{ki}, B_k(h) = \sum_{i=1}^v h_i B_{ki} \\ E_k(h) &= \sum_{i=1}^v h_i E_{ki}.\end{aligned}$$

Defining $\bar{x}(t) = [x^T(t), x_f^T(t)]^T$ and $\bar{z}(t) = z(t) - z_f(t)$, combining (2), (6), and (8), the filtering error system can be given as

$$\begin{cases} \dot{\bar{x}}(t) = (\bar{A}_{qsk}(h) + \bar{B}_{1k}(h)\Delta_s(t)\bar{C}_q(h))\bar{x}(t) \\ \quad + (\bar{B}_{2qsk}(h) + \bar{B}_{1k}(h)\Delta_s(t)\bar{D}_q(h))w(t) \\ \bar{z}(t) = \bar{E}_{qk}(h)\bar{x}(t) + \bar{F}_{qk}(h)w(t) \end{cases}\quad (9)$$

where

$$\begin{aligned}\bar{A}_{qsk}(h) &= \begin{bmatrix} \bar{A}_{qsk}^1(h) \\ \bar{A}_{qsk}^2(h) \end{bmatrix} = \sum_{i=1}^v \sum_{j=1}^v h_i h_j \bar{A}_{qskij} \\ \bar{A}_{qskij} &= \begin{bmatrix} A_{qi} & 0 \\ B_{kj} \check{F}_s C_{qi} & A_{kj} \end{bmatrix} \\ \bar{B}_{2qsk}(h) &= \begin{bmatrix} \bar{B}_{2qsk}^1(h) \\ \bar{B}_{2qsk}^2(h) \end{bmatrix} = \sum_{i=1}^v \sum_{j=1}^v h_i h_j \bar{B}_{2qskij} \\ \bar{B}_{2qskij} &= \begin{bmatrix} B_{qi} \\ B_{kj} \check{F}_s D_{qi} \end{bmatrix} \\ \bar{B}_{1k}(h) &= \begin{bmatrix} \bar{B}_{1k}^1(h) \\ \bar{B}_{1k}^2(h) \end{bmatrix} = \sum_{j=1}^v h_j \bar{B}_{1kj}, \bar{B}_{1kj} = \begin{bmatrix} 0 \\ B_{kj} \end{bmatrix} \\ \bar{E}_{qk}(h) &= \sum_{j=1}^v \sum_{i=1}^v h_i h_j \bar{E}_{qkij}, \bar{E}_{qkij} = \begin{bmatrix} E_{qi} & -E_{kj} \end{bmatrix}\end{aligned}$$

$$\begin{aligned}\bar{C}_q(h) &= \sum_{i=1}^v h_i \bar{C}_{qi}, \bar{C}_q(h) = \begin{bmatrix} C_{qi} & 0 \end{bmatrix} \\ \bar{D}_q(h) &= \sum_{i=1}^v h_i \bar{D}_{qi}, \bar{F}_q(h) = \sum_{i=1}^v h_i \bar{F}_{qi}.\end{aligned}$$

Remark 1: Note that actual factors, such as time delays and data dropouts make synchronization hard to maintain. In [10], the piecewise homogeneous Markov jump principle has been adopted to describe asynchronization of nonlinear MJSs. Compared with the piecewise homogeneous Markov principle in [10], HMM is only dependent on the current mode of original system (9). And HMM approach just requires a conditional transition probability matrix to characterize the asynchronous phenomenon instead of several transition probability matrices in [10]. Thus, HMM has a simpler structure and is easier to understand.

The aim of this article is to design an asynchronous reliable extended dissipative filter (8) such that (9) is stochastically stable and extended dissipative. For the simplicity of analysis, we establish the following block matrix:

$$\begin{bmatrix} \mathfrak{A}^1(h) \\ \mathfrak{A}^2(h) \end{bmatrix} = \begin{bmatrix} A_{qsk}^1(h) & B_{2qsk}^1(h) & B_{1k}^1(h) \\ A_{qsk}^2(h) & B_{2qsk}^2(h) & B_{1k}^2(h) \end{bmatrix}.\quad (10)$$

The advantage of the structure of the block matrix lies in separation of system matrices $\mathfrak{A}^1(h)$ and filter matrices $\mathfrak{A}^2(h)$, which enables us to parameterize filter matrices by slack matrices in next section. Before ending this section, some technical preconditions are introduced for easily deriving LMI filter design conditions.

Assumption 1: Matrices $\Psi_1, \Psi_2, \Psi_3 = \Psi_3^T$, and Φ satisfying the following conditions.

- 1) $\Psi_1 = \Psi_1^T = -\Psi_1^T \Psi_1$ with $\bar{\Psi}_1 \geq 0$.
- 2) $\Phi = \Phi^T = \bar{\Phi}^T \bar{\Phi}$ with $\bar{\Phi} \geq 0$.
- 3) $B_2^T \Psi_1 B_2 + He[B_2^T \Psi_2] + \Psi_3 > 0$.
- 4) $(\|\Psi_1\| + \|\Psi_2\|) \cdot \|\Phi\| = 0$.

Definition 1 [29]: For prescribed matrices Ψ_1, Ψ_2, Ψ_3 , and Φ satisfying Assumption 1, filtering error system (9) is said to be extended dissipative, if there exists a scalar ϱ such that the following inequality holds for $w(t) \in \mathcal{L}_2[0, +\infty)$ and any $t_f > 0$:

$$\int_0^{t_f} J(s) ds \geq \bar{z}^T(t) \Phi \bar{z}(t) + \varrho \quad (11)$$

where

$$J(s) = \bar{z}^T(s) \Psi_1 \bar{z}(s) + 2\bar{z}^T(s) \Psi_2 w(s) + w^T(s) \Psi_3 w(s). \quad (12)$$

Remark 2: The asynchronous extended dissipative filtering considered in this article can be reduced to the synchronous extended dissipative filtering investigated in [29]–[32] if $\mathbb{Q} = \mathcal{K}$ and $\tau_{qq} = 1$. It can be concluded that the asynchronous extended dissipative filtering can be reduced to the asynchronous H_∞ filtering, the asynchronous $L_2 - L_\infty$ filtering, the asynchronous passive filtering, and the asynchronous dissipative filtering by tuning parameters Ψ_1, Ψ_2, Ψ_3 , and Φ , respectively, (shown in Table I).

TABLE I
EXTENDED DISSIPATIVE PERFORMANCE

Performance	Φ	Ψ_1	Ψ_2	Ψ_3
H_∞	0	-I	0	$\gamma^2 I$
$L_2 - L_\infty$	I	0	0	$\gamma^2 I$
Passivity	0	0	I	γI
Dissipativity	0	-I	I	$2I - \gamma I$

Lemma 1 (Double Variables-Based Decoupling Principle):

For a scalar $\beta \neq 0$, matrices A , M , T , F , and N with appropriate dimensions, the following propositions are equivalent:

$$\wp_1 \triangleq T + MA + A^T M^T < 0 \quad (13)$$

$$\wp_2 \triangleq \begin{bmatrix} T + He[FA] & \beta(M - F) + A^T N^T \\ * & -\beta N - \beta N^T \end{bmatrix} < 0. \quad (14)$$

Proof: Two steps will be given as follows.

1) $\wp_1 \Rightarrow \wp_2$: Inequality (13) holds, then there exist scalars β and λ such that

$$\begin{bmatrix} T + He[A^T M^T] - \frac{\lambda}{\beta} A^T A & \lambda A^T \\ * & -\beta \lambda I \end{bmatrix} < 0. \quad (15)$$

Setting $F^T = M^T - (1/2\beta)\lambda A$, $N = (1/2\lambda)I$, then (14) is obtained.

2) $\wp_2 \Rightarrow \wp_1$: Pre- and post-multiplying (14) by $[I, (1/\beta)A^T]$ and its transpose, respectively, the inequality (13) is obtained. This proof of the equivalence is completed. ■

Remark 3: In order to decouple the cross terms between A and M , different from the existing methods (Finsler's lemma) in [24]–[26], a new decoupling principle is proposed in this article by introducing two slack variables F and N in (14), which can be named DVDP. In the DVDP, two slack variables F and N are independent from each other. Thus, some stability criteria, controller design or filter design conditions with less conservatism can be obtained by choosing free and independent variables F and N . Compared with the single variable-based decoupling principles (SVDPs) by introducing a variable N in [15], [20], [34]–[36], three advantages of Lemma 1 in this article are shown as follows: 1) the mathematical proof of the necessity and sufficiency is provided; 2) DVDP provides more degrees of freedom than SVDPs; and 3) SVDPs are special cases of the DVDP. For example, if $F = 0$, then Lemma 1 of present article reduces to that in [15] and [20]. If $F = 0$, $\beta = 1$, then Lemma 1 of present article reduces to that in [34]. If $T < 0$, $F = 0$, then Lemma 1 of present article reduces to that in [35], [36].

Lemma 2 (Variable Substitution Principle): Given matrix N , symmetric matrices M_1 and M_2 with appropriate dimensions, if there exist matrices Q_1 , Q_2 , and R satisfying

$$J_1 \triangleq \begin{bmatrix} Q_1 & R - N \\ * & Q_2 \end{bmatrix} \geq 0 \quad (16)$$

$$J_2 \triangleq \begin{bmatrix} M_1 + Q_1 & R \\ * & M_2 + Q_2 \end{bmatrix} < 0 \quad (17)$$

Algorithm 1 Infinite Iteration Algorithm

Relax N in (18)

Step 1: Let (18i) be (18). Relax N in (18i) by (16) and (17). Let (16i) be (16) and (17) be (17i).

Step 2: Store (17i). Let (18ii) be (16i). Relax N in (18ii) by (16ii) and (17ii).

Step 3: Store (17ii). Repeat Step 2 for n times. Store (17iii), ..., (17n), and (16n).

Step 4: Obtain the relaxed conditions (17i), (17ii), ..., (17n), and (16n).

then the following inequality holds:

$$J_3 \triangleq \begin{bmatrix} M_1 & N \\ * & M_2 \end{bmatrix} < 0. \quad (18)$$

Proof: Noticing the fact $J_2 = J_1 + J_3$, from $J_1 \geq 0$ and $J_2 < 0$, it yields $J_3 < 0$. But not vice versa. ■

Remark 4: Note that a fixed N in J_3 will lead to some inflexibility, so a slack variable R is introduced to relax J_3 , which yields J_2 . Variable R can be chosen freely, which is independent of fixed variable N . Thus, we name Lemma 2 (VSP). Compared with J_3 , J_2 is more general and flexible. If $J_1 = 0$, then J_2 reduces to J_3 . Different from the DVDP/SVDPs in Lemma 1 of present article and [15], [20], [34]–[36] separating the product terms (i.e., AM in Lemma 1), the VSP is used to substitute a fixed matrix N by a slack variable R . Although VSP can increase the flexibility of the final conditions, there still exists some room to be further improved. For example, the following algorithm is one of them. From Algorithm 1, it can be seen that if $n \rightarrow +\infty$, then fixed matrix N may be removed.

III. MAIN RESULTS

Note that many works on extended dissipative filtering for continuous-time MJSs have been reported [29]–[32]. However, these works assume that the modes of the filter and plant are synchronous. It is known that synchronization becomes unrealistic since there exist some practical factors, such as data dropouts and time delays. Thus, in this section, the asynchronous reliable extended dissipative filtering will be developed. First, we will analyze the stochastic stability and extended dissipativity for system (9).

Theorem 1: Given scalars $\vartheta > 0$, $\alpha_q \neq 0$, $\beta_q \neq 0$, matrices \hat{F}_s , \check{F}_s , and $\bar{\Psi}_1$, Ψ_2 , Ψ_3 , $\bar{\Phi}$ satisfying Assumption 1, system (9) is stochastically stable and extended dissipative if there exist scalars $\vartheta_q \leq \vartheta$, $\rho_q > 0$, symmetric positive definite matrices U_q , P_q , matrices $W_q(h)$, M_{1q} , M_{2q} , Θ_q , Y_{q1} , Y_{q2} , N , \hat{A}_{ki} , \hat{B}_{ki} , \hat{E}_{ki} , and diagonal positive definite matrices R_s such that the following inequalities hold for $q \in \mathbb{Q}$, $s \in \mathbb{S}$, and $k \in \mathbb{K}$:

$$P_q - \vartheta G_q + \rho_q I > 0 \quad (19)$$

$$\Xi_{qsk}(h) < 0 \quad (20)$$

$$\Omega_{qsk}(h) < 0 \quad (21)$$

$$\Upsilon_{qk}(h) < 0 \quad (22)$$

where

$$\begin{aligned}\Xi_{qsk}(h) &= \sum_{s=1}^K \sum_{k=1}^S \rho_{qs} \tau_{qk} \text{Sym} \left[\Theta_q \tilde{\mathfrak{A}}_F^2(h) \right] - W_q(h) \\ \Omega_{qsk}(h) &= \begin{bmatrix} \Omega_{qsk}^{11}(h) & \Omega_{qsk}^{12}(h) & \Omega_{qsk}^{13}(h) \\ * & -\beta_q N - \beta_q N & 0 \\ * & * & -I \end{bmatrix} \\ \Upsilon_{qk}(h) &= \begin{bmatrix} -\vartheta_q I & \Upsilon_q^{12}(h) \bar{\Phi}^T & \Upsilon_q^{13}(h) \bar{\Phi}^T \\ * & -P_q & 0 \\ * & * & -U_q \end{bmatrix} \\ \Omega_{qsk}^{11}(h) &= \Psi_{qsk}(h) + W_q(h) \\ \Omega_{qsk}^{12}(h) &= \beta_q (\Lambda_q - \Theta_q) + \left[\tilde{\mathfrak{A}}_F^2(h) \right]^T N^T \\ \Omega_{qsk}^{13}(h) &= \text{vec} \left[\bar{E}_{qk}^T(h) \bar{\Psi}_1^T, \bar{F}_q^T(h) \bar{\Psi}_1^T, 0_4 \right] \\ \Psi_{qsk}(h) &= \begin{bmatrix} \Psi_{1qsk}(h) & \alpha_q (\mathcal{P}_q - M_q) + \left[\tilde{\mathfrak{A}}^1(h) \right]^T Y_{q1}^T \\ * & -\alpha_q Y_q - \alpha_q Y_q^T \end{bmatrix} \\ \Psi_{1qsk}(h) &= \Phi_{qsk}(h) + \text{Sym} \left[M_{q1} \tilde{\mathfrak{A}}^1(h) \right] \\ \Phi_{qsk}(h) &= \begin{bmatrix} \sum_{c=1}^Q \lambda_{qc} P_c & -\bar{E}_{q1}^T \Psi_2 & 0 & \bar{C}_q^T(h) R_s \\ * & \Phi_q^{22}(h) & 0 & \bar{D}_q^T(h) R_s \\ * & * & -R_s & 0 \\ * & * & * & -R_s \end{bmatrix} \\ \Phi_q^{22}(h) &= -\text{Sym} \left[\bar{F}_q^T(h) \Psi_2 \right] - \Psi_3, \tilde{\mathfrak{A}}_F^2(h) = \left[\tilde{\mathfrak{A}}_F^2(h), 0_3 \right] \\ \tilde{\mathfrak{A}}_F^2(h) &= \left[\bar{A}_{qsk}^2(h), \bar{B}_{2qsk}^2(h), \bar{B}_{1k}^2(h) \check{F}_s \right] \\ \mathcal{P}_q &= \text{vec} [P_q, 0_3], \Lambda_q = \text{vec} [M_{q2}, Y_{q2}] \\ M_{q2} &= \text{vec} [M_{q21}, M_{q22}, M_{q23}, M_{q24}] \\ Y_q &= \begin{bmatrix} Y_{q1} & Y_{q2} \end{bmatrix} = \begin{bmatrix} Y_{q11} & Y_{q12} \\ Y_{q12}^T & Y_{q13} \end{bmatrix} \\ M_{q1} &= \text{vec} [M_{q11}, M_{q12}, M_{q13}, M_{q14}] \\ \Upsilon_q^{12}(h) &= \left[\sqrt{\tau_{q1}} \bar{E}_{q1}^T(h), \dots, \sqrt{\tau_{qK}} \bar{E}_{qK}^T(h) \right] \\ \Upsilon_q^{13}(h) &= \left[\sqrt{\tau_{q1}} \bar{F}_{q1}^T(h), \dots, \sqrt{\tau_{qK}} \bar{F}_{qK}^T(h) \right] \\ \tilde{\mathfrak{A}}^1(h) &= \left[\mathfrak{A}^1(h), 0 \right].\end{aligned}$$

Proof: The proof will be completed by the following three steps. For simplicity, set $\sum_{s,k} \rho_s \tau_k = \sum_{s=1}^K \sum_{k=1}^S \rho_{qs} \tau_{qk}$.

1) *Two-Step Decoupling:* By Schur complement, it follows from (21):

$$\bar{\Omega}_{qsk}(h) = \begin{bmatrix} \bar{\Omega}_{qsk}^{11}(h) & \Omega_{qsk}^{12}(h) \\ * & -\beta_q N - \beta_q N \end{bmatrix} < 0 \quad (23)$$

where

$$\bar{\Omega}_{qsk}^{11}(h) = \Psi_{qsk}(h) + W_q(h) + \Omega_{qk}^{13}(h) \left[\Omega_{qk}^{13}(h) \right]^T.$$

Combining $\sum_{s=1}^S \rho_{qs} = 1$, $\sum_{k=1}^K \tau_{qk} = 1$, and (20), we have

$$\tilde{\Omega}_{qsk}(h) = \sum_{s,k} \rho_s \tau_k \begin{bmatrix} \tilde{\Omega}_{qsk}^{11}(h) & \Omega_{qsk}^{12}(h) \\ * & -\beta_q N - \beta_q N \end{bmatrix} < 0 \quad (24)$$

where

$$\tilde{\Omega}_{qsk}^{11}(h) = \Psi_{qsk}(h) + \Omega_{qk}^{13}(h) \left[\Omega_{qk}^{13}(h) \right]^T + \text{Sym} \left[\Theta_q \tilde{\mathfrak{A}}_F^2(h) \right].$$

By Lemma 1 for the first time, we have

$$\tilde{\Psi}_{qsk}(h) = \sum_{s,k} \rho_s \tau_k \left\{ \left[\Psi_{qsk}(h) + \Omega_{qk}^{13}(h) \left[\Omega_{qk}^{13}(h) \right]^T + \text{Sym} \left[\Lambda_q \tilde{\mathfrak{A}}_F^2(h) \right] \right\} < 0. \quad (25)$$

It equals

$$\tilde{\Psi}_{qsk}(h) = \sum_{s,k} \rho_s \tau_k \begin{bmatrix} \tilde{\Psi}_{qsk}^{11}(h) & \tilde{\Psi}_{qsk}^{12}(h) \\ * & -\alpha_q Y_q - \alpha_q Y_q^T \end{bmatrix} < 0$$

where

$$\begin{aligned}\tilde{\Psi}_{qsk}^{11}(h) &= \Phi_{qsk}(h) + \tilde{\Psi}_{qk}^{13}(h) \left[\tilde{\Psi}_{qk}^{13}(h) \right]^T \\ &\quad + \text{Sym} \left[M_{q1} \mathfrak{A}^1(h) \right] + \text{Sym} \left[M_{q2} \tilde{\mathfrak{A}}^2(h) \right] \\ \tilde{\Psi}_{qsk}^{12}(h) &= \alpha_q (\mathcal{P}_q - M_q) + \left[\mathfrak{A}^1(h) \right]^T Y_{q1}^T + \left[\tilde{\mathfrak{A}}_F^2(h) \right]^T Y_{q2}^T \\ \tilde{\Psi}_{qk}^{13}(h) &= \text{vec} \left[\bar{E}_{qk}^T(h) \bar{\Psi}_1^T, \bar{F}_q^T(h) \bar{\Psi}_1^T, 0_2 \right].\end{aligned}$$

From $M_q = \text{vec} [M_{q1}, M_{q2}]$ and $Y_q = \text{vec} [Y_{q1}, Y_{q2}]$, we have

$$\begin{aligned}\tilde{\Psi}_{qsk}^{11}(h) &= \Phi_{qsk}(h) + \tilde{\Psi}_{qk}^{13}(h) \left[\tilde{\Psi}_{qk}^{13}(h) \right]^T + \text{Sym} \left[M_q \mathfrak{R}(h) \right] \\ \tilde{\Psi}_{qsk}^{12}(h) &= \alpha_q (\mathcal{P}_q - M_q) + \mathfrak{R}^T(h) Y_q^T \\ \mathfrak{R}(h) &= \begin{bmatrix} \mathfrak{A}^1(h) \\ \tilde{\mathfrak{A}}_F^2(h) \end{bmatrix} = \begin{bmatrix} \bar{A}_{qsk}(h), \bar{B}_{2qsk}(h), \bar{B}_{1k}(h) \check{F}_s \end{bmatrix}.\end{aligned}$$

By Lemma 1 for the second time, we can get

$$\hat{\Psi}_{qsk}(h) = \sum_{s,k} \rho_s \tau_k \left\{ \Phi_{qsk}(h) + \tilde{\Psi}_{qk}^{13}(h) \left[\tilde{\Psi}_{qk}^{13}(h) \right]^T + \text{Sym} \left[\mathcal{P}_q \mathfrak{R}(h) \right] \right\} < 0. \quad (26)$$

By Schur complement lemma, $\hat{\Psi}_{qsk}(h) < 0$ can be transformed as

$$\bar{\Psi}_{qsk}(h) < 0 \quad (27)$$

where

$$\bar{\Psi}_{qsk}(h) = \sum_{s,k} \rho_s \tau_k \begin{bmatrix} \Psi_{qsk}^1(h) & \Psi_{qk}^2(h) \check{F}_s & \Psi_q^3(h) R_s \\ * & -R_s & 0 \\ * & * & -R_s \end{bmatrix}$$

$$\Psi_{qsk}^1(h) = \begin{bmatrix} \Psi_{qsk}^{11}(h) & \Psi_{qsk}^{12}(h) \\ * & \Psi_q^{22}(h) \end{bmatrix}$$

$$\Psi_{qk}^2(h) = \begin{bmatrix} P_q \bar{B}_{1k}(h) \\ 0 \end{bmatrix}, \Psi_q^3(h) = \begin{bmatrix} \bar{C}_q^T(h) \\ \bar{D}_q^T(h) \end{bmatrix}$$

$$\Psi_{qsk}^{11}(h) = P_q \bar{A}_{qsk}(h) + \sum_{c=1}^Q \lambda_{qc} P_c - \bar{E}_{qk}^T(h) \Psi_1 \bar{E}_{qk}^T(h)$$

$$\Psi_{qsk}^{12}(h) = P_q \bar{B}_{2qsk}(h) - \bar{E}_{qk}^T(h) \Psi_1 \bar{F}_q^T(h) - \bar{E}_{qk}^T(h) \Psi_2$$

$$\Psi_q^{22}(h) = -\bar{F}_q^T(h) \Psi_1 \bar{F}_q(h) - \text{Sym} \left[\bar{F}_q^T(h) \Psi_2 \right] - \Psi_3.$$

By Schur complement, it follows from (27):

$$\sum_{s,k} \rho_s \tau_k \left\{ \Psi_{qsk}^1(h) + \Psi_{qk}^2(h) \check{F}_s R_s^{-1} \check{F}_s \left[\Psi_{qk}^2(h) \right]^T \right. \\ \left. + \Psi_q^3(h) R_s \left[\Psi_q^3(h) \right]^T \right\} < 0. \quad (28)$$

From $\Delta_s^T(t) \Delta_s(t) \leq \check{F}_s^T \check{F}_s \leq I$, it follows:

$$\sum_{s,k} \rho_s \tau_k \left\{ \Psi_{qsk}^1(h) + \Psi_{qk}^2(h) \Delta_s(t) R_s^{-1} \Delta_s(t) \left[\Psi_{qk}^2(h) \right]^T \right. \\ \left. + \Psi_q^3(h) R_s \left[\Psi_q^3(h) \right]^T \right\} < 0. \quad (29)$$

Then, we obtain

$$\sum_{s,k} \rho_s \tau_k \left\{ \Psi_{qsk}^1(h) + \text{Sym} \left[\Psi_{qk}^2(h) \Delta_s(t) \left[\Psi_q^3(h) \right]^T \right] \right\} < 0. \quad (30)$$

Recalling (27), we have

$$\sum_{s,k} \rho_s \tau_k \begin{bmatrix} \bar{\Phi}_{qsk}^{11}(h) & \bar{\Phi}_{qsk}^{12}(h) \\ 0 & \Psi_q^{22}(h) \end{bmatrix} < 0 \quad (31)$$

where

$$\bar{\Phi}_{qsk}^{11}(h) = P_q (\bar{A}_{qsk}(h) + \bar{B}_{1k}(h) \Delta_s(t) \bar{C}_q(h)) \\ + \sum_{c=1}^Q \lambda_{qc} P_c - \bar{E}_{qk}^T(h) \Psi_1 \bar{E}_{qk}^T(h) \\ \bar{\Phi}_{qsk}^{12}(h) = P_q (\bar{B}_{2qsk}(h) + \bar{B}_{1k}(h) \Delta_s(t) \bar{C}_q(h)) \\ - \bar{E}_{qk}^T(h) \Psi_1 \bar{F}_q^T(h) - \bar{E}_{qk}^T(h) \Psi_2.$$

2) *Stochastic Stability Analysis*: Construct the following mode-dependent Lyapunov functional for system (9):

$$V(t) = \bar{x}^T(t) P_q \bar{x}(t). \quad (32)$$

Let \mathcal{L} be the weak infinitesimal generator of the stochastic process $\{x(t), q(t)\}$. Setting $\eta(t) = [\bar{x}^T(t), w^T(t)]^T$, we have

$$\mathcal{L}V(t) = \eta^T(t) \sum_{s,k} \rho_s \tau_k \begin{bmatrix} \bar{\Phi}_{qsk}^{11}(h) & \bar{\Phi}_{qsk}^{12}(h) \\ 0 & 0 \end{bmatrix} \eta(t) \quad (33)$$

where

$$\bar{\Phi}_{qsk}^{11}(h) = P_q (\bar{A}_{qsk}(h) + \bar{B}_{1k}(h) \Delta_s(t) \bar{C}_q(h)) + \sum_{c=1}^Q \lambda_{qc} P_c \\ \bar{\Phi}_{qsk}^{12}(h) = P_q (\bar{B}_{2qsk}(h) + \bar{B}_{1k}(h) \Delta_s(t) \bar{C}_q(h)).$$

From (31) with $w(t) = 0$, we have $\mathcal{E}\{\mathcal{L}V(t)\} < 0$, which implies the stochastic stability of system (9).

3) *Extended Dissipativity Analysis*: The following equality is true:

$$\mathcal{E}\{\bar{z}^T(t) \Phi \bar{z}(t)\} = \eta^T(t) Z_{qk}(h) \eta(t) \quad (34)$$

where

$$Z_{qk}(h) = \sum_{k=1}^K \tau_{qk} \begin{bmatrix} \bar{E}_{qk}^T(h) \Phi \bar{E}_{qk}(h) & \bar{E}_{qk}^T(h) \Phi \bar{F}_q(h) \\ * & \bar{F}_q^T(h) \Phi \bar{F}_q(h) \end{bmatrix}.$$

By Schur complement, it follows from $\Phi = \bar{\Phi}^T \bar{\Phi}$ and (22):

$$Z_{qk}(h) < \vartheta_q \begin{bmatrix} G_q & 0 \\ 0 & U_q \end{bmatrix}. \quad (35)$$

Combining with (34), it follows:

$$\mathcal{E}\{\bar{z}^T(t) \Phi \bar{z}(t)\} < \mathcal{E}\{\vartheta_q \bar{x}^T(t) G_q \bar{x}(t)\} + \vartheta_q w^T(t) U_q w(t).$$

From $\vartheta_q \leq \vartheta$, we have

$$\mathcal{E}\{\vartheta \bar{x}^T(t) G_q \bar{x}(t)\} + \vartheta_q w^T(t) U_q w(t) - \mathcal{E}\{\bar{z}^T(t) \Phi \bar{z}(t)\} > 0.$$

By S-procedure lemma, there exists scalar $\rho_q > 0$ such that

$$\mathcal{E}\{\vartheta \bar{x}^T(t) G_q \bar{x}(t)\} + \vartheta_q w^T(t) U_q w(t) \\ - \mathcal{E}\{\bar{z}^T(t) \Phi \bar{z}(t)\} - \mathcal{E}\{\rho_q \bar{x}^T(t) \bar{x}(t)\} > 0. \quad (36)$$

In view of (31) and (33), we have

$$\mathcal{L}V(t) < J(t). \quad (37)$$

By Dynkin's formula, we have

$$\mathcal{E}\left\{\int_0^t J(s) ds\right\} \geq \mathcal{E}\{\bar{x}^T(t) P_q \bar{x}(t)\} - V(0). \quad (38)$$

Combining (19), (36), and (38), it yields

$$\mathcal{E}\left\{\int_0^t J(s) ds\right\} - \mathcal{E}\{\bar{z}^T(t) \Phi \bar{z}(t)\} \\ \geq -w^T(t) \vartheta_q U_q w(t) - V(0). \quad (39)$$

Setting

$$\varrho = -\sup_{t,q} \left\{ |\vartheta_q| \cdot \|U_q\| \cdot |w(t)|^2 - \|P_q\| \cdot |\bar{x}(t)|^2 \right\} - V(0)$$

the following inequality holds:

$$\mathcal{E}\left\{\int_0^t J(s) ds\right\} - \mathcal{E}\{\bar{z}^T(t) \Phi \bar{z}(t)\} \geq \varrho. \quad (40)$$

In order to prove the extended dissipativity of system (9), we need to verify the following inequality for any $t_f \geq t \geq 0$:

$$\mathcal{E}\left\{\int_0^{t_f} J(s) ds\right\} - \sup_{0 \leq t \leq t_f} \mathcal{E}\{\bar{z}^T(t) \Phi \bar{z}(t)\} \geq \varrho. \quad (41)$$

For this purpose, we will prove the two cases, namely, $\|\Phi\| = 0$ and $\|\Phi\| \neq 0$, respectively.

1) $\|\Phi\| = 0$, from (40), for any $t_f \geq t \geq 0$, it follows:

$$\mathcal{E}\left\{\int_0^{t_f} J(s) ds\right\} \geq \varrho \quad (42)$$

which implies (41).

2) $\|\Phi\| \neq 0$, we know $\Psi_1 = 0$ and $\Psi_2 = 0$ by Assumption 1–3). From $\Omega_q^{22}(h) < 0$ in (21), we have $\Psi_3 > 0$ which implies $J(s) = w^T(s) \Psi_3 w(s) \geq 0$. Thus, the following inequalities hold for $t_f \geq t \geq 0$:

$$\mathcal{E}\left\{\int_0^{t_f} J(s) ds\right\} \geq \mathcal{E}\left\{\int_0^t J(s) ds\right\} \quad (43)$$

$$\sup_{0 \leq t \leq t_f} \mathcal{E}\{\bar{z}^T(t) \Phi \bar{z}(t)\} \geq \mathcal{E}\{\bar{z}^T(t) \Phi \bar{z}(t)\}. \quad (44)$$

It is clearly seen that (41) holds from (40). Then, the extended dissipativity is proven. Summarized the above three steps, the proof is completed. ■

Remark 5: Note that in the existing works [29]–[32], $\bar{F}_{qk}(h)$, Ψ_1 , Ψ_2 , Ψ_3 , and Φ are presumed to satisfy Assumption 1 of present article and the following constraint:

$$\|\bar{F}_{qk}(h)\| \cdot \|\Phi\| = 0. \quad (45)$$

That is, the structure of the filtering error system (9) is constrained (similar cases see [29]–[32] for details). In this article, it is removed by introducing symmetric positive definite matrices U_q and positive scalars ϑ_q (see step 3) in this article for details). Of course, if constraint (45) is utilized in this article, that is, $\bar{F}_{qk}(h) = 0$, then we can get

$$\Upsilon_{qk}(h) = \begin{bmatrix} -\vartheta_q I & \Upsilon_q^{12}(h)\bar{\Phi}^T \\ * & -P_q \end{bmatrix} < 0. \quad (46)$$

Moreover, if $\vartheta_q = 1$, $\mathbb{Q} = \mathcal{K}$, and $\tau_{qq} = 1$, then (46) reduces to the results in [29]–[32]. Thus, the proposed method of present article is more applicable and general than the existing works [29]–[32].

Remark 6: Note that the free-weighting method is used to separate the system (filter) matrices and the Lyapunov variables in this article, which can avoid the constraints on Lyapunov variables. Otherwise, if free-weighting method is not used in this article, matrix transformation can be used, such as in [31]. In this case, constraints on some Lyapunov variables are inevitable, such as $Z_i = \text{diag}\{\tilde{Z}_{1i}, \tilde{Z}_{2i}\}$ in [31], which results in underutilization of full relationships on system information. Moreover, free-weighting method has been widely utilized to construct LKF, such as in [37], which can be used to relax the positive definite requirements for some matrices. Thus, by using free-weighting method, additional degree of freedom can be obtained in the final conditions. It is an efficient way to reduce conservatism.

Remark 7: In [23], the asynchronous reliable $L_2 - L_\infty$ filtering problem of system (1) has been investigated, but the Lyapunov variables are constrained (see P_d in [23] for details). In [24]–[26], by using Finsler's lemma, the constraints on Lyapunov variables can be overcome by introducing some slack matrices, but the introduced slack variables are also constrained (see G_s and R_s in [25] for details). Similarity, by using SVDPs [19], such constraints are also inevitable. In this article, the constraints on Lyapunov variables and slack variables are removed in Theorem 1 of present article by using a two-step decoupling technique (by using DVDP twice times), the two steps are simplified as follows.

- 1) *First Step:* By using the DVDP for the first time, the constraints on Lyapunov variables in [23] are avoided [see condition (25) for details].
- 2) *Second Step:* By using the DVDP for the second time, the constraints on slack variables in [24]–[26] are overcome [see condition (26) for details].

Based on Theorem 1 and Lemma 2, less conservative solutions to the filter matrices will be given as follows.

Theorem 2: Given scalars $\vartheta > 0$, $\alpha_q \neq 0$, $\beta_q \neq 0$, $\iota_{mq}(m = 1, 2, 3, 4)$, matrices \hat{F}_s , \hat{F}_s , and Ψ_1 , Ψ_2 , Ψ_3 , Φ satisfying Assumption 1, system (9) is stochastically stable and extended dissipative if there exist scalars $\vartheta_q \leq \vartheta$, $\rho_q > 0$, symmetric positive definite matrices P_{1q} , P_{3q} , G_{1q} , G_{3q} , U_q , matrices W_{1qij} , W_{2qij} , W_{3qij} , Θ_q , P_{2q} , G_{2q} , M_{q1} , M_{q2} , Y_{q1} , Y_{q2} ,

N , \hat{A}_{ki} , \hat{B}_{ki} , E_{ki} , and diagonal positive definite matrix R_s such that the following inequalities hold for $i, j \in \mathbb{V}$, $q \in \mathbb{Q}$, $s \in \mathbb{S}$, and $k \in \mathbb{K}$:

$$F_q > 0 \quad (47)$$

$$\mathbb{V}_q \geq 0 \quad (48)$$

$$\Xi_{qskii} < 0 \quad (49)$$

$$\Xi_{qskij} + \Xi_{qskji} < 0 \quad (50)$$

$$\Omega_{qskii} < 0 \quad (51)$$

$$\Omega_{qskij} + \Omega_{qskji} < 0 \quad (52)$$

$$\Upsilon_{qkii} < 0 \quad (53)$$

$$\Upsilon_{qkij} + \Upsilon_{qkji} < 0 \quad (54)$$

where

$$F_q = \begin{bmatrix} P_{1q} - \vartheta G_{1q} + \rho_q I & P_{2q} - \vartheta G_{2q} \\ * & P_{3q} - \vartheta G_{3q} + \rho_q I \end{bmatrix}$$

$$\mathbb{V}_q = \begin{bmatrix} V_{q1} & \beta_q(\mathcal{I}_q N - \Theta_q) \\ * & V_{q2} \end{bmatrix}$$

$$\Xi_{qskij} = \sum_{s=1}^K \sum_{l=1}^S \rho_{qs} \tau_{qk} \text{Sym}[\mathcal{I}_q \hat{\mathfrak{X}}_{ij}^2] - W_{qij}$$

$$\Omega_{qskij} = \begin{bmatrix} \Omega_{qskij}^{11} & \beta_q(\Lambda_q - \Theta_q) + (\hat{\mathfrak{X}}_{ij}^2)^T & \Omega_{qkij}^{13} \\ * & -\beta_q N - \beta_q N + V_{2q} & 0 \\ * & * & -I \end{bmatrix}$$

$$\Upsilon_{qkij} = \begin{bmatrix} -\vartheta_q I & \Upsilon_{qi}^{12} \bar{\Phi}^T & \Upsilon_{qi}^{13} \bar{\Phi}^T & \Upsilon_{qi}^{14} \bar{\Phi}^T \\ * & -G_{1q} & -G_{2q} & 0 \\ * & * & -G_{3q} & 0 \\ * & * & * & -U_q \end{bmatrix}$$

$$\Omega_{qskij}^{11} = \Psi_{qskij} + W_{qij} + V_{q1}$$

$$\Omega_{qkij}^{13} = \text{vec}[-E_{qi}^T \bar{\Psi}_1^T, E_{kj}^T \bar{\Psi}_1^T, F_{qi}^T \bar{\Psi}_1^T, 0_3]$$

$$\Psi_{qskij} = \begin{bmatrix} \Psi_{qskij}^{11} & \alpha_q(P_q - M_q) + (\hat{\mathfrak{X}}_{ij}^1)^T Y_{q1} \\ * & -\alpha_q Y_q - \alpha_q Y_q^T \end{bmatrix}$$

$$\Psi_{qskij}^{11} = \Phi_{qskij} + \text{Sym}[M_{q1} \hat{\mathfrak{X}}_{ij}^1]$$

$$\Phi_{qskij} = \begin{bmatrix} \sum_{c=1}^Q \lambda_{qc} P_c & \Phi_{qkij}^{12} & 0 & \Phi_{qs}^{14} \\ * & \Phi_{qi}^{22} & 0 & D_{qi}^T R_s \\ * & * & -R_s & 0 \\ * & * & * & -R_s \end{bmatrix}$$

$$\Phi_{qkij}^{12} = \begin{bmatrix} -E_{qi}^T \Psi_2 \\ E_{kj}^T \Psi_2 \end{bmatrix}, \Phi_{qs}^{14} = \begin{bmatrix} C_{qi}^T R_s \\ 0 \end{bmatrix}$$

$$\Phi_{qi}^{22} = -\text{Sym}[F_{qi}^T \Psi_2] - \Psi_3, \hat{\mathfrak{X}}_{ij}^2 = [\hat{\mathfrak{X}}_{1ij}^2, 0_3]$$

$$\hat{\mathfrak{X}}_{ij}^2 = [\hat{B}_{kj} \hat{F}_s C_{qi}, \hat{A}_{kj}, \hat{B}_{kj} \hat{F}_s D_{qi}, \hat{B}_{ki} \hat{F}_s]$$

$$\mathfrak{X}_{qi}^1 = [A_{qi}, 0, B_{qi}, 0, 0], \mathcal{P}_q = \text{vec}[P_q, 0, 0]$$

$$\mathcal{I}_q = \text{vec}[\iota_{1q} I, \iota_{2q} I, \iota_{3q} \Gamma_{1q} I, \iota_{4q} \Gamma_{2q} I, 0_3]$$

$$\Upsilon_{qi}^{12} = [\sqrt{\tau_{q1}} E_{qi}^T, \dots, \sqrt{\tau_{qK}} E_{qi}^T]^T$$

$$\Upsilon_{qi}^{13} = [\sqrt{\tau_{q1}} E_{1j}^T, \dots, \sqrt{\tau_{qK}} E_{Kj}^T]^T$$

$$\Upsilon_{qi}^{14} = [\sqrt{\tau_{q1}} F_{qi}^T, \dots, \sqrt{\tau_{qK}} F_{qi}^T]^T$$

$$\begin{aligned} M_{q1} &= \text{vec}[M_{q11}, M_{q12}, M_{q13}, M_{q14}] \\ M_{q11} &= \text{vec}[M_{q111}, M_{q112}] \end{aligned}$$

the other notations are the same those in Theorem 1. Meanwhile, the desired filter matrices can be computed by

$$A_{ki} = N^{-1}\hat{A}_{ki}, B_{ki} = N^{-1}\hat{B}_{ki}, E_{ki} = E_{ki}. \quad (55)$$

Proof: By Schur complement lemma, it follows from Ω_{qskij} :

$$\tilde{\Omega}_{qskij} = \begin{bmatrix} \tilde{\Omega}_{qskij}^{11} & \beta_q(\Lambda_q - \Theta_q) + [\hat{\mathfrak{X}}_{ij}^2]^T \\ * & -\beta_q N - \beta_q N + V_{2q} \end{bmatrix} \quad (56)$$

where

$$\tilde{\Omega}_{qskij}^{11} = \Psi_{qskij} + W_{qij} + V_{q1} + \Omega_{qkij}^{15} \left(\Omega_{qkij}^{15} \right)^T.$$

By Lemma 2, it follows from (48) and (56):

$$\tilde{\Omega}_{qskij} = \begin{bmatrix} \tilde{\Omega}_{qskij}^{11} & \beta_q(N - \Theta_q) + [\hat{\mathfrak{X}}_{ij}^2]^T \\ * & -\beta_q N - \beta_q N \end{bmatrix} \quad (57)$$

where

$$\tilde{\Omega}_{qskij}^{11} = \Psi_{qskij} + W_{qij} + \Omega_{qkij}^{15} \left(\Omega_{qkij}^{15} \right)^T.$$

Recalling (55), we have

$$\hat{A}_{ki} = NA_{ki}, \hat{B}_{ki} = NB_{ki}. \quad (58)$$

Submitting (58) into $\tilde{\Omega}_{qskij}$ and Ξ_{qskij} , we can, respectively, obtain

$$\begin{aligned} \hat{\Omega}_{qskij} &= \begin{bmatrix} \hat{\Omega}_{qskij}^{11} & \beta_q(\mathcal{I}_q N - \Theta_q) + [\mathfrak{X}_{ij}^2]^T N^T \\ * & -\beta_q N - \beta_q N \end{bmatrix} \\ \Xi_{qskij} &= \sum_{s,k} \text{Sym} \left(\rho_s \tau_k \mathcal{I}_q N [\mathfrak{X}_{ij}^2]^T \right) - W_{qij} \end{aligned}$$

where

$$\begin{aligned} \hat{\Omega}_{qskij}^{11} &= \Psi_{qskij} + W_{qij} + \Omega_{qkij}^{15} \left(\Omega_{qkij}^{15} \right)^T \\ \mathfrak{X}_{ij}^2 &= \text{vec} \left[B_{kj} \hat{F}_s C_{qi}, A_{kj}, B_{kj} \hat{F}_s D_{qi}, B_{ki} \check{F}_s \right]. \end{aligned}$$

Setting

$$W_q(h) = \sum_{i=1}^{r-1} \sum_{j=i+1}^r h_i h_j W_{qij} \quad (59)$$

based on the fuzzy inference, (9) and (55), it yields

$$\begin{aligned} \Xi_{qsk}(h) &= \sum_{i=1}^r h_i^2 \Xi_{qskii} + \sum_{i=1}^{r-1} \sum_{j=i+1}^r h_i h_j (\Xi_{qskij} + \Xi_{qskji}) \\ \Omega_{qsk}(h) &= \sum_{i=1}^r h_i^2 \Omega_{qskii} + \sum_{i=1}^{r-1} \sum_{j=i+1}^r h_i h_j (\Omega_{qskij} + \Omega_{qskji}) \\ \Upsilon_{qk}(h) &= \sum_{i=1}^r h_i^2 \Upsilon_{qi} + \sum_{i=1}^{r-1} \sum_{j=i+1}^r h_i h_j (\Upsilon_{qkij} + \Upsilon_{qkji}). \end{aligned}$$

Hence, we can conclude that: (20) is guaranteed by (48) and (50). Equation (21) is guaranteed by (51) and (52). Equation (22) is guaranteed by (53) and (54). Thus, the

stochastic stability and extended dissipativity of system (9) are ensured. The proof is completed. ■

Remark 8: Note that in some existing works, such as in [31], each filter matrix should be considered independently, such as A_{kj} and B_{kj} . In this article, with the construction of the block matrix (10), we just need to focus on sub-block matrices $\mathfrak{A}^1(h)$ and $\mathfrak{A}^2(h)$ in (10) instead of each filter matrix, which is easier to obtain the final conditions.

Remark 9: Note that Theorem 1 cannot be directly solved by LMI approach due to the cross terms $\Theta_q \tilde{\mathfrak{X}}^2(h)$ and $N \tilde{\mathfrak{X}}^2(h)$. From the structure of the product terms, if we set

$$\Theta_q = [N, N, \Gamma_{1q} N, \Gamma_{2q} N, 0, 0, 0] \quad (60)$$

then Theorem 1 can be solved. However, the structure of Θ_q in (60) established by a series of fixed matrices N may also lead to conservativeness. With the help of VSP, the constrained structure in (60) is relaxed in Theorem 2. Concretely, Θ_q is replaced by a series of slack variables with free structure, which leads to more flexible solutions. Moreover, slack matrices Γ_{1q} , Γ_{2q} instead of the fixed ones in [34] and [36], and slack scalars α_q , β_q , and ι_{mq} ($m = 1, 2, \dots, 5$) introduced in LMIs make Theorem 2 more flexible.

Remark 10: Note that the parameter β_q is chosen first in Theorems 1 and 2, in which the optimal value can be found by the approach stated in [15] (Remark 9). The numerical solution to this problem can be obtained by using a numerical optimization algorithm, such as the program *fminsearch* in the Optimization Toolbox of MATLAB.

Remark 11: Theorem 2 of present article can be reduced to [23, Th. 2] as its special case, the detailed procedure is given as follows. Without the use of the DVDP and the VSP, then (48) can be canceled. Set $\rho_q \geq (\gamma^2 - 1) \max_q \lambda_{\max}(P_q)$ in (47), $\tilde{\Psi}_1 = 0$, $\Psi_2 = 0$, $\Psi_3 = \gamma^2 I$ in (51) and (52), and $\Phi = 1$, $\vartheta_q = \gamma^2$, $G_q = P_q$ in (53) and (54), then Theorem 2 of present article reduces to [23, Th. 2].

Remark 12: It should be pointed out that the proposed methods in this article mainly focus on the separation of the system matrices and the Lyapunov variables for filter design of T-S fuzzy MJSs. Thus, it can be also applied to separate the system matrices and the Lyapunov variables for some more complicated and general situations, such as finite-time filter design for nonhomogeneous T-S fuzzy MJSs [38] and event-triggered reliable H_∞ filtering for nonlinear parabolic PDE systems with Markovian jumping sensor faults [9].

IV. EXAMPLES

In the section, an example will be given to show the effectiveness of proposed design method.

Consider a tunnel diode circuit [23], which is shown in Fig. 1. The system parameters are given as

$$\begin{aligned} A_1(1) &= \begin{bmatrix} -0.1 & 50 \\ -1 & -10 \end{bmatrix}, A_1(2) = \begin{bmatrix} -4.6 & 50 \\ -1 & -10 \end{bmatrix} \\ A_2(1) &= \begin{bmatrix} -0.11 & 50.1 \\ -1 & -10.1 \end{bmatrix}, A_2(2) = \begin{bmatrix} -4.5 & 50 \\ -1.1 & -10 \end{bmatrix} \\ B_1(1) &= \begin{bmatrix} 0 \\ 1 \end{bmatrix}, B_1(2) = \begin{bmatrix} 0 \\ 1 \end{bmatrix} \end{aligned}$$

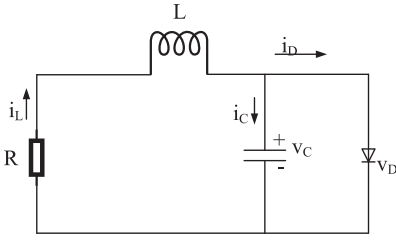


Fig. 1. Tunnel diode circuit.

TABLE II
OPTIMIZED VARIABLE FOR EACH CASE

Performance	H_∞	$L_2 - L_\infty$	Passivity	Dissipativity
$\bar{\gamma}$	1.0395	0.3162	0.8285	1.1389

$$B_2(1) = \begin{bmatrix} 0 \\ 1.1 \end{bmatrix}, B_2(2) = \begin{bmatrix} 0 \\ 0.9 \end{bmatrix}$$

$$E_1(1) = E_1(2) = E_2(2) = \begin{bmatrix} 1 & 0 \end{bmatrix}, E_2(1) = \begin{bmatrix} 1.5 & 0 \end{bmatrix}$$

$$C_1(1) = C_1(2) = \begin{bmatrix} 1 & 0 \end{bmatrix}, C_2(1) = \begin{bmatrix} 1.1 & 0 \end{bmatrix}$$

$$C_2(2) = \begin{bmatrix} 0.9 & 0 \end{bmatrix}, D_q(h) = 1, F_q(h) = 0.1, q, h = 1, 2$$

$$h_1 = \begin{cases} 0, & x_1(t) < 3 \\ (3 + x_1(t))/3, & x_1(t) \in [-3, 0] \\ (3 - x_1(t))/3, & x_1(t) \in [0, 3] \\ 0, & x_1(t) > 3 \end{cases}$$

$$h_2 = 1 - h_1.$$

The TRM of the original system is given as

$$\Lambda = \begin{bmatrix} -6 & 6 \\ 4 & -4 \end{bmatrix}.$$

Two sensor failure modes are assumed by

$$\hat{F}_1 = 0.8, \check{F}_1 = 0.05, \Delta_1(t) = 0.05\sin(t)$$

$$\hat{F}_2 = 0.9, \check{F}_2 = 0.05, \Delta_2(t) = 0.05\cos(t)$$

and the CPM of sensor and the filter are assumed by

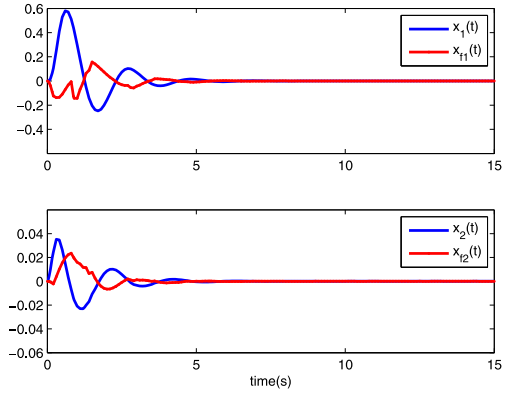
$$S = \begin{bmatrix} 0.2 & 0.8 \\ 0.5 & 0.5 \end{bmatrix}, \mathcal{K} = \begin{bmatrix} 0.4 & 0.6 \\ 0.6 & 0.4 \end{bmatrix}.$$

Choose $\alpha_q = \beta_q = \alpha$, $\alpha = \iota_{mq} = 1 (m = 1, 2, 3, 4)$, $\vartheta = 5$, and $\Gamma_{1q} = \Gamma_{2q} = [1, 0]$. Based on the above parameters, by solving Theorem 2 of present article, the optimized variables of the four performance shown in Table I are given in Table II. By using [23, Th. 2], the optimized $L_2 - L_\infty$ index is $\bar{\gamma} = 0.6355$ under the same parameters while the optimized $L_2 - L_\infty$ index is $\bar{\gamma} = 0.3162$ by Theorem 2 of present article. It can be concluded that the proposed method in this article is less conservative than that in [23]. Recalling Remark 10, we can find the optimal parameter $\alpha = 2.1$. And the corresponding optimal index is $\bar{\gamma} = 0.3109$ by using Theorem 2, which shows the effectiveness of the slack scalars.

To validate the effectiveness of the proposed filter design condition, as special cases, by using Theorem 2 of present article, the H_∞ filter matrices and $L_2 - L_\infty$ filter matrices will be given as follows, respectively.

1) H_∞ Filter Matrices:

$$A_{f1}(1) = \begin{bmatrix} -8.2890 & 28.8471 \\ -0.0106 & -0.9632 \end{bmatrix}$$

Fig. 2. Estimation signal $x(t)$ and the H_∞ filter output signal $x_f(t)$.

$$B_{f1}(1) = \begin{bmatrix} -4.1735 \\ -0.0540 \end{bmatrix}, E_{f1}(1) = \begin{bmatrix} -0.6631 & -3.6937 \end{bmatrix}$$

$$A_{f2}(1) = \begin{bmatrix} -5.8028 & 25.3703 \\ 0.0041 & -2.2209 \end{bmatrix}$$

$$B_{f2}(1) = \begin{bmatrix} -1.6576 \\ 0.0999 \end{bmatrix}, E_{f2}(1) = \begin{bmatrix} -0.3709 & 4.0869 \end{bmatrix}$$

$$A_{f1}(2) = \begin{bmatrix} -11.3113 & 9.7596 \\ 0.0019 & -0.5457 \end{bmatrix}$$

$$B_{f1}(2) = \begin{bmatrix} -5.9816 \\ 0.0278 \end{bmatrix}, E_{f1}(2) = \begin{bmatrix} -0.6406 & -1.6642 \end{bmatrix}$$

$$A_{f2}(2) = \begin{bmatrix} -3.8796 & 63.8811 \\ -0.0210 & -2.9155 \end{bmatrix}$$

$$B_{f2}(2) = \begin{bmatrix} 4.0028 \\ -0.0449 \end{bmatrix}, E_{f2}(2) = \begin{bmatrix} -0.4359 & 0.5256 \end{bmatrix}.$$

2) $L_2 - L_\infty$ Filter Matrices:

$$A_{f1}(1) = \begin{bmatrix} -0.6167 & 22.3050 \\ -0.2582 & -3.2601 \end{bmatrix}$$

$$B_{f1}(1) = \begin{bmatrix} -0.8053 \\ -0.2168 \end{bmatrix}, E_{f1}(1) = \begin{bmatrix} -0.0571 & 0.0140 \end{bmatrix}$$

$$A_{f2}(1) = \begin{bmatrix} -0.2998 & 39.0939 \\ -0.2290 & -5.2405 \end{bmatrix}$$

$$B_{f2}(1) = \begin{bmatrix} 1.4295 \\ -0.0259 \end{bmatrix}, E_{f2}(1) = \begin{bmatrix} -0.0527 & 0.0129 \end{bmatrix}$$

$$A_{f1}(2) = \begin{bmatrix} -1.6084 & 45.2664 \\ -0.3427 & -2.9667 \end{bmatrix}$$

$$B_{f1}(2) = \begin{bmatrix} 1.4290 \\ -0.2946 \end{bmatrix}, E_{f1}(2) = \begin{bmatrix} -0.0439 & 0.0108 \end{bmatrix}$$

$$A_{f2}(2) = \begin{bmatrix} -1.5120 & 28.7261 \\ -0.1265 & -5.9214 \end{bmatrix}$$

$$B_{f2}(2) = \begin{bmatrix} 0.4735 \\ -0.0456 \end{bmatrix}, E_{f2}(2) = \begin{bmatrix} -0.0439 & 0.0108 \end{bmatrix}.$$

Choosing disturbance input as $w(t) = \sin(3t)e^{-0.9t}$, initial states as $\bar{x}(0) = \text{col}[0, 0, 0, 0]$, and initial mode as $r_0 = 1$. From Figs. 2–5, one can observe that the state error and filtering error eventually tend to zero, which imply that the filtering error system is stable. Moreover, the evolution of system mode and filter mode is plotted in Figs. 3 and 5. Pertaining to this

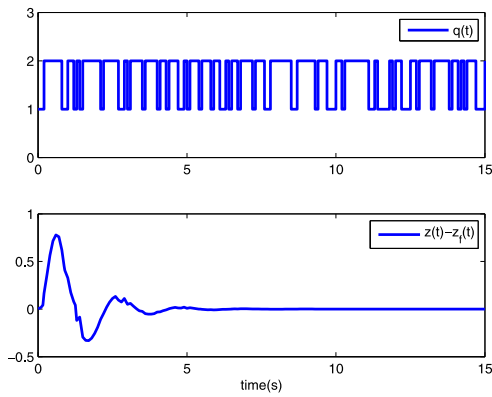


Fig. 3. One possible switching signals and estimation error $\bar{z}(t)$ of H_∞ filter.

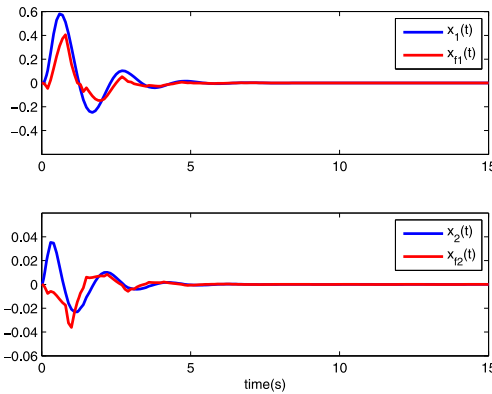


Fig. 4. Estimation signal $x(t)$ and the $L_2 - L_\infty$ filter output signal $x_f(t)$.

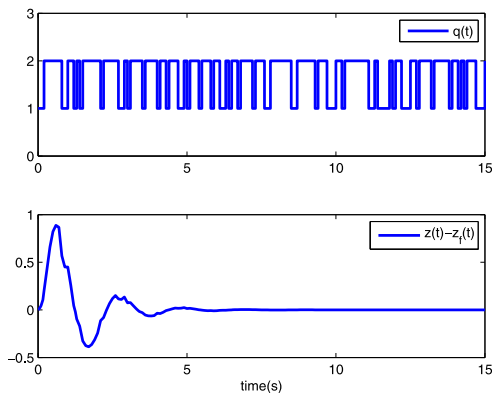


Fig. 5. One possible switching signals and estimation error $\bar{z}(t)$ of $L_2 - L_\infty$ filter.

example, it is seen that the designed filtering method in this article is effective.

V. CONCLUSION

In this article, the asynchronous reliable extended dissipative filtering problem, which includes H_∞ , $L_2 - L_\infty$, passive, and dissipative filters in a unified frameworks has been investigated for a class of T-S fuzzy MJSs. Based on HMM theory, the encountered sensor failures and filter are describer by two stochastic variables, which are dependent on the plant mode. A novel condition, associated with the modes of plant, sensor failures, and the filter have been proposed to ensure the

stochastic stability and extended dissipativity of filtering error system by proposing the DVDP and the VSP. Compared with the existing works, the free structure of Lyapunov variables and slack variables have been fully utilized. Moreover, some unnecessary constraints on filtering error system have been removed in this article. These directly lead to less conservative and more general results. An example has been provided to show the effectiveness of the design approach. In the future, we will extend the obtained results to more general situations, such as finite-time filtering [12] and sliding mode control [39] for T-S fuzzy MJSs.

REFERENCES

- [1] Q. Song and X. Chen, "Multistability analysis of quaternion-valued neural networks with time delays," *IEEE Trans. Neural Netw. Learn. Syst.*, vol. 29, no. 11, pp. 5430–5440, Nov. 2018.
- [2] X. Chen and Q. Song, "State estimation for quaternion-valued neural networks with multiple time delays," *IEEE Trans. Syst., Man, Cybern., Syst.*, vol. 49, no. 11, pp. 2278–2287, Nov. 2019.
- [3] Y. Tian and Z. Wang, " H_∞ performance state estimation for static neural networks with time-varying delays via two improved inequalities," *IEEE Trans. Circuits Syst. II, Exp. Briefs*, vol. 68, no. 1, pp. 321–325, Jan. 2021.
- [4] X. Zhao, X. Wang, L. Ma, and G. Zong, "Fuzzy approximation based asymptotic tracking control for a class of uncertain switched nonlinear systems," *IEEE Trans. Fuzzy Syst.*, vol. 28, no. 4, pp. 632–644, Apr. 2020.
- [5] L. Ma, X. Huo, X. Zhao, and G. Zong, "Adaptive fuzzy tracking control for a class of uncertain switched nonlinear systems with multiple constraints: A small-gain approach," *Int. J. Fuzzy Syst.*, vol. 21, no. 8, pp. 2609–2624, Nov. 2019.
- [6] Y. Tian and Z. Wang, "Composite slack-matrix-based integral inequality and its application to stability analysis of time-delay systems," *Appl. Math. Lett.*, vol. 120, Oct. 2021, Art. no. 107252, doi: 10.1016/j.aml.2021.107252.
- [7] X.-H. Chang, L. Zhang, and J. H. Park, "Robust static output feedback H_∞ control for uncertain fuzzy systems," *Fuzzy Sets Syst.*, vol. 273, pp. 87–104, Aug. 2015.
- [8] X.-H. Chang, Z.-M. Li, and J. H. Park, "Fuzzy generalized H_2 filtering for nonlinear discrete-time systems with measurement quantization," *IEEE Trans. Syst., Man, Cybern., Syst.*, vol. 48, no. 2, pp. 2419–2430, Dec. 2018.
- [9] X. Song, M. Wang, B. Zhang, and S. Song, "Event-triggered reliable H_∞ fuzzy filtering for nonlinear parabolic PDE systems with Markovian jumping sensor faults," *Inf. Sci.*, vol. 510, no. 8, pp. 50–69, Feb. 2020.
- [10] Z.-G. Wu, P. Shi, H. Su, and J. Chu, "Asynchronous $l_2 - l_\infty$ filtering for discrete-time stochastic Markov jump systems with randomly occurred sensor nonlinearities," *Automatica*, vol. 50, no. 1, pp. 180–186, 2014.
- [11] Y. Tian and Z. Wang, "Extended dissipativity analysis for Markovian jump neural networks via double integral-based delay-product-type Lyapunov functional," *IEEE Trans. Neural Netw. Learn. Syst.*, early access, Jul. 23, 2020, doi: 10.1109/TNNLS.2020.3008691.
- [12] X. Song, J. Man, S. Song, and Z. Wang, "Finite-time nonfragile time-varying proportional retarded synchronization for Markovian Inertial Memristive NNs with reaction-diffusion items," *Neural Netw.*, vol. 123, pp. 317–330, Mar. 2020.
- [13] M. Fang, L. Wang, and Z. Wu, "Asynchronous stabilization of Boolean control networks with stochastic switched signals," *IEEE Trans. Syst., Man, Cybern., Syst.*, vol. 51, no. 4, pp. 2425–2432, Apr. 2021.
- [14] C. Ren, S. He, X. Luan, F. Liu, and H. R. Karimi, "Finite-time L_2 -gain asynchronous control for continuous-time positive hidden Markov jump systems via T-S fuzzy model approach," *IEEE Trans. Cybern.*, vol. 51, no. 1, pp. 77–87, Jan. 2021.
- [15] J. Wang, S. Ma, C. Zhang, and M. Fu, " H_∞ state estimation via asynchronous filtering for descriptor Markov jump systems with packet losses," *Signal Process.*, vol. 154, pp. 159–167, Sep. 2019.
- [16] Y. Tian and Z. Wang, "A switched fuzzy filter approach to H_∞ filtering for Takagi-Sugeno fuzzy Markov jump systems with time delay: The continuous-time case," *Inf. Sci.*, vol. 557, pp. 236–249, May 2021.

- [17] G. Liu, S. Xu, J. Park, and G. Zhuang, "Reliable exponential H_∞ filtering for singular Markovian jump systems with time-varying delays and sensor failures," *Int. J. Robust Nonlinear Control*, vol. 28, no. 14, pp. 4230–4245, Sep. 2018.
- [18] H. Shen, Z.-G. Wu, and J. H. Park, "Reliable mixed passive and H_∞ filtering for semi-Markov jump systems with randomly occurring uncertainties and sensor failures," *Int. J. Robust Nonlinear Control*, vol. 25, no. 17, pp. 3231–3251, Nov. 2015.
- [19] Y. Yin, P. Shi, F. Liu, K. L. Teo, and C.-C. Lim, "Robust filtering for nonlinear nonhomogeneous Markov jump systems by fuzzy approximation approach," *IEEE Trans. Cybern.*, vol. 45, no. 9, pp. 1706–1716, Sep. 2015.
- [20] J. Wang, S. Ma, C. Zhang, and M. Fu, "Finite-time H_∞ filtering for nonlinear singular systems with nonhomogeneous Markov jumps," *IEEE Trans. Cybern.*, vol. 49, no. 6, pp. 2133–2144, Jun. 2019.
- [21] H. Shen, F. Li, Z.-G. Wu, J. H. Park, and V. Sreeram, "Fuzzy-model-based nonfragile control for nonlinear singularly perturbed systems with semi-Markov jump parameters," *IEEE Trans. Fuzzy Syst.*, vol. 26, no. 6, pp. 3428–3439, Dec. 2018.
- [22] Z.-G. Wu, P. Shi, Z. Shu, H. Su, and R. Lu, "Passivity-based asynchronous control for Markov jump systems," *IEEE Trans. Autom. Control*, vol. 62, no. 4, pp. 2020–2025, Apr. 2017.
- [23] Z.-G. Wu, S. Dong, P. Shi, H. Su, and T. Huang, "Reliable filtering of nonlinear Markovian jump systems: The continuous-time case," *IEEE Trans. Syst., Man, Cybern., Syst.*, vol. 49, no. 2, pp. 386–393, Feb. 2019.
- [24] J. Tao, R. Lu, H. Su, P. Shi, and Z.-G. Wu, "Asynchronous filtering of nonlinear Markov jump systems with randomly occurred quantization via T-S fuzzy models," *IEEE Trans. Fuzzy Syst.*, vol. 26, no. 4, pp. 1866–1877, Aug. 2018.
- [25] S. Dong, Z.-G. Wu, Y.-J. Pan, H. Su, and Y. Liu, "Hidden-Markov-model-based asynchronous filter design of nonlinear Markov jump systems in continuous-time domain," *IEEE Trans. Cybern.*, vol. 49, no. 6, pp. 2294–2304, Jun. 2019.
- [26] Y. Shen, Z. Wu, P. Shi, H. Su, and T. Huang, "Asynchronous filtering for Markov jump neural networks with quantized outputs," *IEEE Trans. Syst., Man, Cybern., Syst.*, vol. 49, no. 2, pp. 433–443, Feb. 2019.
- [27] Y. Shen, Z. Wu, P. Shi, and G. Wen, "Dissipativity based fault detection for 2D Markov jump systems with asynchronous modes," *Automatica*, vol. 106, pp. 8–17, Aug. 2019.
- [28] Z. Wu, Y. Shen, P. Shi, Z. Shu, and H. Su, " H_∞ control for 2D Markov jump systems in Roesser model," *IEEE Trans. Autom. Control*, vol. 64, no. 1, pp. 427–432, Jan. 2019.
- [29] B. Zhang, W. X. Zheng, and S. Xu, "Filtering of Markovian jump delay systems based on a new performance index," *IEEE Trans. Circuits Syst. I, Reg. Papers*, vol. 60, no. 5, pp. 1250–1263, May 2013.
- [30] J. Li, X. Huang, and Z. Li, "Extended dissipative filtering of fuzzy systems with time-varying delay under imperfect premise matching," *Int. J. Syst. Sci.*, vol. 48, no. 8, pp. 1731–1743, Dec. 2017.
- [31] G. Zhuang, S. Xu, B. Zhang, J. Xia, Y. Chu, and Y. Zou, "Unified filters design for singular Markovian jump systems with time-varying delays," *J. Franklin Inst.*, vol. 353, no. 15, pp. 3739–3768, Oct. 2016.
- [32] W. Xia, W. Zheng, and S. Xu, "Extended dissipativity analysis of digital filters with time delay and Markovian jumping parameters," *Signal Process.*, vol. 152, pp. 247–254, Nov. 2018.
- [33] H. Shen, M. Xing, H. Yan, and J. H. Park, "Extended dissipative filtering for persistent dwell-time switched systems with packet dropouts," *IEEE Trans. Syst., Man, Cybern., Syst.*, vol. 50, no. 11, pp. 4796–4806, Nov. 2020.
- [34] X. Jiang, G. Xia, and Z. Feng, "Some improvements on 'homogenous polynomial H_∞ filtering for uncertain discrete-time systems: A descriptor approach,'" *Int. J. Adapt. Control Signal Process.*, vol. 32, no. 2, pp. 1715–1730, Dec. 2018.
- [35] X.-H. Chang, J. H. Park, and J. Zhou, "Robust static output feedback H_∞ control design for linear systems with polytopic uncertainties," *Syst. Control Lett.*, vol. 85, pp. 23–32, Nov. 2015.
- [36] X.-H. Chang, J. H. Park, and Z. Tang, "New approach to H_∞ filtering for discrete-time systems with polytopic uncertainties," *Signal Process.*, vol. 113, pp. 147–158, Aug. 2015.
- [37] Y. Tian and Z. Wang, "Stability analysis and generalised memory controller design for delayed T-S fuzzy systems via flexible polynomial-based functions," *IEEE Trans. Fuzzy Syst.*, early access, Dec. 21, 2020, doi: [10.1109/TFUZZ.2020.3046338](https://doi.org/10.1109/TFUZZ.2020.3046338).
- [38] Y. Tian and Z. Wang, "Finite-time extended dissipative filtering for singular T-S fuzzy systems with nonhomogeneous Markov jumps," *IEEE Trans. Cybern.*, early access, Nov. 18, 2020, doi: [10.1109/TCYB.2020.3030503](https://doi.org/10.1109/TCYB.2020.3030503).
- [39] R. Nie, S. He, F. Liu, and X. Luan, "Sliding mode controller design for conic-type nonlinear semi-Markovian jumping systems of time-delayed Chua's circuit," *IEEE Trans. Syst., Man, Cybern., Syst.*, vol. 51, no. 4, pp. 2467–2475, Apr. 2021.



Yufeng Tian received the B.Sc. degree in information and computing science and the M.Sc. degree in system theory from Northeastern University, Shenyang, China, in 2016 and 2018, respectively, where he is currently pursuing the Ph.D. degree in control theory and control engineering.

His research interests include neural networks, stochastic system, and control system theory.



Zhanshan Wang (Senior Member, IEEE) received the M.S. degree in control theory and control engineering from Liaoning Shihua University, Fushun, China, in 2001, and the Ph.D. degree in control theory and control engineering from Northeastern University, Shenyang, China, in 2006.

He has been a Professor with Northeastern University since 2010. He has authored or coauthored over 150 journal and conference papers and five monographs. He holds ten patents. His current research interests include the stability analysis of

recurrent neural networks, fault diagnosis, fault tolerant control, intelligent automation and their applications in power systems, and smart grid.

Prof. Wang was an Associate Editor of the IEEE TRANSACTIONS ON NEURAL NETWORKS AND LEARNING SYSTEMS and *Acta Automatica Sinica*. He is currently an Associate Editor of *Neural Processing and Letters*.

See discussions, stats, and author profiles for this publication at: <https://www.researchgate.net/publication/365105281>

Fuzzy observer-based consensus tracking control for fractional-order multi-agent systems under cyber-attacks and its application to electronic circuits

Article in IEEE Transactions on Network Science and Engineering · January 2022

DOI: 10.1109/TNSE.2022.3217618

CITATION

1

READS

64

5 authors, including:



Govindasamy Narayanan

Kunsan National University

18 PUBLICATIONS 332 CITATIONS

[SEE PROFILE](#)



M. Syed Ali

Thiruvalluvar University

190 PUBLICATIONS 3,675 CITATIONS

[SEE PROFILE](#)



Quanxin Zhu

Hunan Normal University

349 PUBLICATIONS 8,524 CITATIONS

[SEE PROFILE](#)



Ganesh Kumar Thakur

ABES Engineering College

23 PUBLICATIONS 86 CITATIONS

[SEE PROFILE](#)

Some of the authors of this publication are also working on these related projects:



Special Issue "Advanced Symmetry Methods for Dynamics, Control, Optimization and Applications" [View project](#)



Stability and control of stochastic differential equations [View project](#)

Fuzzy observer-based consensus tracking control for fractional-order multi-agent systems under cyber-attacks and its application to electronic circuits

G. Narayanan, M. Syed Ali, Quanxin Zhu*, Bandana Priya, Ganesh Kumar Thakur

Abstract—Consensus control of multi-agent systems (MASs) has applications in various domains. As MASs work in networked environments, their security control becomes critically desirable in response to cyber-attacks. In this paper, the observer-based consensus tracking control problem is investigated for a class of Takagi-Sugeno fuzzy fractional-order multi-agent systems (FOMASs) under cyber-attacks. The malicious cyber attacks can impact the security of topologies of the communication networks of both controllers and observers. To estimate unmeasurable system states, a fuzzy observer is built. It is found that the topology of contact for observer states may be different from that of the feedback signals. A novel mathematical model for T-S fuzzy FOMASs with cyber-attacks is proposed. By using algebraic graph theory, Lyapunov functional, and fractional calculus theory, a distributed feed-back controller is developed for each agent, which guarantee the secure performance of tracking consensus error and observer error. Finally, two numerical examples demonstrate the effectiveness of the suggested control scheme, and the controller design for electronic network circuits shows the applicability of the proposed theoretical results. Simulations results for different differential-orders and coupling strength scenarios are given.

Index Terms—Fractional-order, Takagi-Sugeno model, Multi-agent systems, Cyber-attacks, Distributed control.

I. INTRODUCTION

The distributed coordinated control of MASs have gained wider and wider attention due to its potential applications in several disciplines such as robotics [1], aircraft control [2], unmanned air vehicles [3], smart grids [4], and sensor networks [5]. We should note that much of the existing

This work was jointly supported by the National Natural Science Foundation of China (62173139) and the Science and Technology Innovation Program of Hunan Province (2021RC4030). The author G. Narayanan, wishes to thank the Center for Nonlinear Systems, Chennai Institute of Technology, India, vide funding number CIT/CNS/2022/RD/003 for partially funded of this work. The corresponding author is Quanxin Zhu.

G. Narayanan is with Center for Computational Modeling, Chennai Institute of Technology, Chennai-600069, India. M. Syed Ali is with Department of Mathematics, Thiruvalluvar University, Vellore-632115, Tamil Nadu, India. Quanxin Zhu is with School of Mathematics and Statistics, Hunan Normal University, Changsha, Hunan, 410081, China and also with the Key Laboratory of Control and Optimization of Complex Systems, College of Hunan Province, Hunan Normal University, Changsha 410081, China. Bandana Priya is Department of Applied Science, G L Bajaj institute of Technology and Management, Greater Noida, Uttar Pradesh, India. Ganesh Kumar Thakur is with ABES Engineering College, Ghaziabad, UP, India. Emails: zqx22@126.com (Quanxin Zhu), syedgru@gmail.com (M. Syed Ali), narayananvu@gmail.com (G. Narayanan).

research on MASs consensus focuses on integer-order dynamics ([6]-[9]). The importance of dealing with fractional-order derivatives is the involvement of memory and hereditary properties that gives a more realistic way to fractional-order models ([10], [11]). Due to the memory effect, the non-integer models integrate all previous information from the past that makes it to predict and translate the fractional-order models more accurately. It has been discovered, in particular, that fractional-order systems, which are acknowledged as a major advance over integer-order systems, could be applied in a growing number of engineering application fields ([12]-[14]). Despite the fact that there are many studies on the consensus of MASs in integer-order case, there are few results on FOMASs ([15]-[19]). Compared with the results of MASs in integer-order case, the consensus problem of FOMASs is relatively few, which has the potential research value due to the memory of FOMASs. Because of practical constraints, some agents partial information may be unmeasurable. Thus, for the consensus tracking problems, agent output measurements are observed, and different techniques of observer-based control are studied ([20]-[27]). Compared with the published works in the literature, the obtained criteria improve the previous works. Therefore, it is of the great significance to study the observer-based control for the engineering application scopes of MASs.

A cyber-physical system (CPS) is an intelligence system consist of processing, communication, and control with both physical and cyber components. As established in ([28]-[31]), security concerns for CPSs differ from those in typical control systems because cyber-attacks in the cyber layer can be extended to the physical layer. With the advent of network information and broad spatial distributed systems, MASs which can be considered a subset of CPSs, are becoming vulnerable to cyber-attacks. In actuality, the network is very vulnerable to malicious signal attacks as a result of its openness and shareability ([32]-[37]). Thus, our results significance improve from former works.

The T-S fuzzy model is well known as a powerful tool for dealing with the leader-follower consensus in achieve MASs ([38]-[43]). Due to their significant usage of communication technologies, MASs are frequently exposed to various cyber-attacks. T-S fuzzy networked systems, which can be considered a class of CPSs, have been vulnerable to cyber-attacks as network information technology and large-

scale spatial distributed systems have advanced. These attacks could have a significant impact on tracking performance ([44]-[46]). Implementing performance distributed secure control techniques for FOMASs under attack remains a challenging and significant concern. To the best of our knowledge, no one has explored the observer-based consensus tracking problem of T-S fuzzy FOMASs with cyber-attacks, and it is, therefore, beneficial to further develop new techniques dealing. This motivates our study.

As narrated above, we focused on the T-S fuzzy observer-based consensus tracking control of FOMASs under cyber-attack. The main contributions are:

- (i) The secure consensus criteria is derived for FOMASs via T-S fuzzy approach under a cyber-attack scenario.
- (ii) Compared with the existing results for MAS under cyber-attacks ([32]-[34]), under malicious attacks, the security control analysis of both controllers and observers communication networks is unrelated, and over the duration of the attack in this study, these two topologies can change.
- (iii) We developed a useful technique for determining the coupling strengths and feedback gain matrices for the controllers and observers.
- (iv) We developed two optimization problems that solved sufficient criteria to achieve consensus tracking.
- (v) Finally, numerical simulations show that the suggested observer-based control scheme is used to the consensus tracking of a tunnel diode network circuit.

Notations: Let \mathcal{N} is the natural number; Real numbers, and $n \times 1$ real (complex) column vectors are referred to in \mathcal{R} , and $\mathcal{R}^n(\mathcal{C}^n)$ respectively. 'T' denotes the matrix transposition. \mathcal{I}_n represent identity matrix. $\lambda(\cdot)$ the eigenvalue of a matrix. \otimes stands for the Kronecker product.

II. SYSTEM DESCRIPTION AND PRELIMINARIES

A. Algebraic Graph Theory

When each agents is regarded a node, the FOMASs have \mathcal{M} followers, and a single node can be represented as a directed graph, where $\mathcal{G} = (\mathcal{V}, \mathcal{E}, \mathcal{A})$, where $\mathcal{V} = \{1, 2, \dots, \mathcal{M} + 1\}$ is the node set, $\mathcal{E} \subseteq \{(p, q), p, q \in \mathcal{V}\}$ is the edge set, and $\mathcal{A} = [a_{pq}] \in \mathcal{R}^{(\mathcal{M}+1) \times (\mathcal{M}+1)}$, which is called adjacent matrix of \mathcal{G} with non-negative elements, where if p is adjacent to q , $a_{pq} > 0$; otherwise $a_{pq} = 0$. If there is a node p such that there exists a directed from it to any other node, \mathcal{G} is said to contain a directed spanning-tree. The Laplacian matrix \mathcal{L} defined as $\mathcal{L} = [l_{pq}] \in \mathcal{R}^{(\mathcal{M}+1) \times (\mathcal{M}+1)}$ with $l_{pq} = -a_{pq}, p \neq q$; and $l_{pq} = \sum_{q=1}^{\mathcal{M}+1} a_{pq}, \forall p = 1, \dots, \mathcal{M} + 1$.

B. Model Formulation and Basic Lemmas

We give some definitions of fractional calculus and lemmas that will be required later. Then, consensus issue of FOMASs is formulated via T-S fuzzy.

Definition 1 [11]: For $0 < \alpha \leq 1$, the Caputo fractional derivative is known as

$${}^C D_t^\alpha h(t) = \frac{1}{\Gamma(1-\alpha)} \int_{t_0}^t \frac{h'(\xi)}{(t-\xi)^\alpha} d\xi, \quad (1)$$

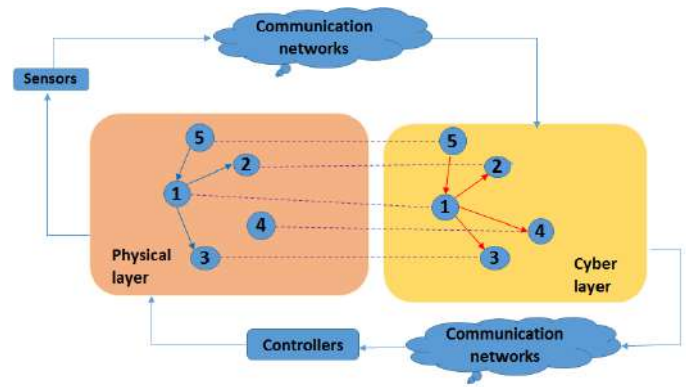


Fig. 1. Framework for networked agent systems with physical and cyber layers.

where $\Gamma(1-\alpha) = \int_0^\infty t^{-\alpha} e^{-\xi} d\xi$.

Definition 2 [14]: The Mittag-Leffler function are

$$\mathbb{E}_\alpha(z) = \sum_{m=0}^{\infty} \frac{z^m}{\Gamma(m\alpha + 1)}, \quad (2)$$

where $\alpha > 0$, and $z \in \mathcal{C}$.

Lemma 1 [14]: Let $\mathcal{V}(t)$ be a continuous function on $[t_0, +\infty)$ and satisfies ${}^C D_t^\alpha \mathcal{V}(t) \leq \Theta \mathcal{V}(t)$, then

$$\mathcal{V}(t) \leq \mathcal{V}(t_0) \mathbb{E}_\alpha(\Theta(t-t_0))^\alpha,$$

where $\alpha \in (0, 1)$ and Θ constant.

Lemma 2 [12]: For $0 < \alpha < 1$, $t \in \mathcal{R}$, $t > 0$, we have

$$\lim_{t \rightarrow +\infty} \mathbb{E}_\alpha(t) \leq \lim_{t \rightarrow +\infty} \frac{1}{\alpha} e^{t^\frac{1}{\alpha}}.$$

Lemma 3 [13]: Let $x(t)$ be a continuous and derivable vector valued function. Then for any $t \geq t_0$, $\frac{1}{2}({}^C D_t^\alpha x^T(t)x(t)) \leq x^T(t)({}^C D_t^\alpha x(t))$, where $0 < \alpha < 1$.

The security control for T-S fuzzy FOMASs, which consists of cyber-attacks, is displayed in Fig. 1 with cyber layer $p = 1, 2, \dots, \mathcal{M}, \mathcal{M} + 1$. A network channel, controller and sensor are included in this framework. In fact, when an attack happens, the network can not operate properly, and then after a period of time, the networks attempts to restore or recovery process must reconstruct the network so that the network will work effectively. Several well-studied results on recovery mechanisms have been published. In recent years, there has been a significant increase in research on the security control of complex cyber-physical networks (see in [28]-[30], [44], [45]). It is noteworthy that several authors have recently investigated the security control problem for MASs in integer-order case (see in [26], [27], [31]-[34]), but there is no results for fractional case. Moreover, fractional-order case has better characteristics than corresponding integer-order case.

The fractional-order physical-plant model of $\mathcal{M} + 1$ agents and $p(1 \leq p \leq \mathcal{M})$ followers as:

$$\begin{cases} {}^C D_t^\alpha \mathfrak{S}_p(t) = \mathcal{A} \mathfrak{S}_p(t) + \mathcal{B} \tilde{u}_p(t), \\ \varphi_p(t) = \mathcal{C} \mathfrak{S}_p(t), \end{cases} \quad (3)$$

where $0 < \alpha < 1$, $\mathfrak{S}_p(t) \in \mathcal{R}^n$, $\varphi_p \in \mathcal{R}^m$, and $\tilde{u}_p(t) \in \mathcal{R}^r$ denotes, respectively, the state, output, and control inputs. \mathcal{A} , \mathcal{B} , and \mathcal{C} is the constant matrices. The control aims to establish distributed consensus tracking protocols $\tilde{u}_p(t), p = 1, \dots, \mathcal{M}$ to make it asymptotic for the states of the followers to obey $\mathcal{M} + 1$, which will satisfy the leaders [7],

$${}^C_{t_0} D_t^\alpha \mathfrak{S}_{\mathcal{M}+1}(t) = \mathcal{A} \mathfrak{S}_{\mathcal{M}+1}(t). \quad (4)$$

C. T-S fuzzy and T-S fuzzy control models

Fuzzy logic systems directly address the imprecisions of the variables of input and output by describing them in linguistic terms with the fuzzy numbers (and fuzzy sets). The fractional physical plant system (3) is described in the T-S fuzzy approach are given:

Rule θ :

IF ϕ_1 is $\mathcal{M}_{\theta 1}$ and ϕ_2 is $\mathcal{M}_{\theta 2}$ and ... and ϕ_k is $\mathcal{M}_{\theta k}$.

THEN

$$\begin{cases} {}^C_{t_0} D_t^\alpha \mathfrak{S}_p(t) = \mathcal{A}_\theta \mathfrak{S}_p(t) + \mathcal{B}_\theta \tilde{u}_p(t), \\ \varphi_p(t) = \mathcal{C}_\theta \mathfrak{S}_p(t), \end{cases} \quad (5)$$

where $\phi_p(t)$ is the premise variable; $\mathcal{M}_{\theta k}$ for $\theta = 1, \dots, \beta$ represents the fuzzy sets, β are IF-THEN laws; The constant matrices are \mathcal{A}_θ , \mathcal{B}_θ and \mathcal{C}_θ .

By the T-S fuzzy with final output processes, we have

$$\begin{cases} {}^C_{t_0} D_t^\alpha \mathfrak{S}_p(t) = \sum_{\theta=1}^{\beta} \Psi_\theta(\phi_p(t)) \left(\frac{\mathcal{A}_\theta \mathfrak{S}_p(t) + \mathcal{B}_\theta \tilde{u}_p(t)}{\sum_{\theta=1}^{\beta} \Psi_\theta(\phi_p(t))} \right), \\ \varphi_p(t) = \sum_{\theta=1}^{\beta} \Psi_\theta(\phi_p(t)) \left(\frac{\mathcal{C}_\theta \mathfrak{S}_p(t)}{\sum_{\theta=1}^{\beta} \Psi_\theta(\phi_p(t))} \right), \end{cases} \quad (6)$$

where $\Psi_\theta(\phi_p(t)) = \prod_{k=1}^m \mathcal{M}_{\theta k}(\phi_p(t))$ with $\mathcal{M}_{\theta k}(\phi_p(t))$ representing the grade of memberships of ϕ_p in $\mathcal{M}_{\theta k}$, satisfy the following conditions:

$$\begin{cases} \sum_{\theta=1}^{\beta} \Psi_\theta(\phi_p(t)) > 0, \\ \Psi_\theta(\phi_p(t)) \geq 0, (\theta = 1, \dots, \beta). \end{cases} \quad (7)$$

Let $\mu_\theta(\phi_p(t)) = \frac{\Psi_\theta(\phi_p(t))}{\sum_{\theta=1}^{\beta} \Psi_\theta(\phi_p(t))}$, then the expression (7) is written as

$$\begin{cases} {}^C_{t_0} D_t^\alpha \mathfrak{S}_p(t) = \sum_{\theta=1}^{\beta} \mu_\theta(\phi_p(t)) (\mathcal{A}_\theta \mathfrak{S}_p(t) + \mathcal{B}_\theta \tilde{u}_p(t)), \\ \varphi_p(t) = \sum_{\theta=1}^{\beta} \mu_\theta(\phi_p(t)) \mathcal{C}_\theta \mathfrak{S}_p(t), \\ {}^C_{t_0} D_t^\alpha \mathfrak{S}_{\mathcal{M}+1} = \sum_{\theta=1}^{\beta} \mu_\theta(\phi(t)) \mathcal{A}_\theta \mathfrak{S}_{\mathcal{M}+1}, \end{cases} \quad (8)$$

where

$$\begin{cases} \sum_{\theta=1}^{\beta} \mu_\theta(\phi_p(t)) = 1, \\ \mu_\theta(\phi_p(t)) \geq 0, (\theta = 1, \dots, \beta), \end{cases}$$

where $\mu_\theta(\phi_p(t))$ are IF-THEN rules weights.

The fuzzy control design of distributed consensus tracking protocols $\tilde{u}_p(t)$ is given as

Rule θ :

IF ϕ_1 is $\mathcal{M}_{\theta 1}$ and ϕ_2 is $\mathcal{M}_{\theta 2}$ and ... and ϕ_k is $\mathcal{M}_{\theta k}$.

THEN

$$\tilde{u}_p(t) = \xi \sum_{q=1}^{\mathcal{M}+1} \mathcal{K}_\theta a_{pq}^{(\hat{\sigma}^{(k)})} (\mathfrak{S}_q(t) - \mathfrak{S}_p(t)), \quad (9)$$

where \mathcal{K}_θ are the control gain matrices, ξ are coupling strengths, $a_{pq}^{(\hat{\sigma}^{(k)})}$ is the adjacent matrix representing the communication network via attacks.

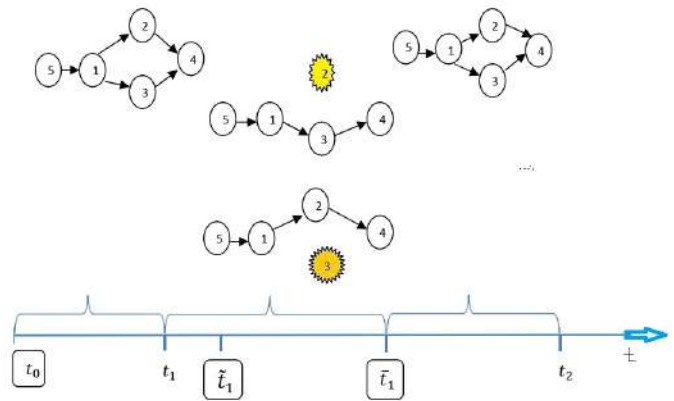


Fig. 2. Attack to communication network of controllers and observers.

The final output can be described as the fuzzy prediction controller by,

$$\tilde{u}_p(t) = \xi \sum_{\theta=1}^{\beta} \mu_\theta(\phi_p(t)) \sum_{q=1}^{\mathcal{M}+1} \mathcal{K}_\theta a_{pq}^{(\hat{\sigma}^{(k)})} (\mathfrak{S}_q(t) - \mathfrak{S}_p(t)). \quad (10)$$

Substitute (10) in (8), we obtain the complete controlled T-S fuzzy system as:

$$\begin{cases} {}^C_{t_0} D_t^\alpha \mathfrak{S}_p(t) = \sum_{\theta=1}^{\beta} \mu_\theta(\phi_p(t)) (\mathcal{A}_\theta \mathfrak{S}_p(t) + \xi \mathcal{B}_\theta \sum_{q=1}^{\mathcal{M}+1} \mathcal{K}_\theta a_{pq}^{(\hat{\sigma}^{(k)})} (\mathfrak{S}_q(t) - \mathfrak{S}_p(t))) \\ \varphi_p(t) = \sum_{\theta=1}^{\beta} \mu_\theta(\phi_p(t)) \mathcal{C}_\theta \mathfrak{S}_p(t). \end{cases} \quad (11)$$

The following distributed state T-S fuzzy observer is developed for the followers p ($1 \leq p \leq \mathcal{M}$) to estimate the unknown system states $\mathfrak{S}_p(t)$ in system (3):

$$\begin{cases} {}^C_{t_0} D_t^\alpha \hat{\mathfrak{S}}_p(t) = \sum_{\theta=1}^{\beta} \mu_\theta(\phi_p(t)) (\mathcal{A}_\theta \hat{\mathfrak{S}}_p(t) + \xi \mathcal{B}_\theta \sum_{q=1}^{\mathcal{M}+1} \mathcal{K}_\theta a_{pq}^{(\hat{\sigma}^{(k)})} (\hat{\mathfrak{S}}_q(t) - \hat{\mathfrak{S}}_p(t)) + \xi \Omega_\theta \sum_{q=1}^{\mathcal{M}+1} \mathcal{K}_\theta a_{pq}^{(\hat{\sigma}^{(k)})} (\rho_q(t) - \rho_p(t))) \\ \hat{\varphi}_p(t) = \sum_{\theta=1}^{\beta} \mu_\theta(\phi_p(t)) \mathcal{C}_\theta \hat{\mathfrak{S}}_p(t), \end{cases} \quad (12)$$

where $\hat{\mathfrak{S}}_p(t)$ is the observers state for agent p , and $\rho_p(t) = \hat{\varphi}_p(t) - \varphi_p(t) = \mathcal{C}(\hat{\mathfrak{S}}_p(t) - \mathfrak{S}_p(t))$, Ω_θ are the observer control gain matrices, ξ is coupling strength, $a_{pq}^{(\hat{\sigma}^{(k)})}$ is the adjacent matrix representing the observer-based communication network via attacks.

Remark 1: The states of system dynamics are not always completely accessible in a realistic application. As an outcome, the observer-based control technique has gradually evolved into a valuable tool for networked control systems. A high-order system can be viewed as FOMAS (3) and high dimensional system states can be seen in (12). It is well known that in practice the systems state $\mathfrak{S}_p(t)$ can be difficult to obtain, therefore the state observer $\hat{\mathfrak{S}}_p(t)$ is intended in this paper to estimate the state $\mathfrak{S}_p(t)$ (kindly refer [7]). In addition, the observer (12) also discusses gains \mathcal{K}_θ and Ω_θ , that are able to effectively improve the control characteristics for FOMAS and decrease the conservativeness of the output feedback control design. In this study, we focused on the general

dynamics of the leader-follower MAS, which varies from the established observer-based model in previous studies ([24], [25]). Compared with the previous studies in ([24], [25]), our obtained criteria improve the previous results. In this paper the malicious cyber-attacks are also considered for realizing output feedback controller.

However, the attacks method of targeting the controller is safer since manipulating the control signal $u(t)$ expressly reveals the system to vulnerabilities. Fig. 2 depicts the communication networks of controllers and observers during p^{th} attacks in the time interval $[\bar{t}_p, \bar{t}_p]$. The enhanced network containing of 4 followers and one leader in the presence of attacks on nodes. Node 2 (shade star) is attacked to the communication channel of controllers and node 3 (shade star) is attacked to the communication channel of observers. Here, t_0 and t_p are respectively initial, and p^{th} malicious attack occurs. \bar{t}_p and \bar{t}_p , $p = 1, 2, \dots$, are respectively instants of time during which the p^{th} attack and the node functions are recovered. It is believed that malicious assaults will have an independent impact on controller and observation channels. Attacks can be seen to occur at time instant t_1 , but the cyber command centre notices them at \bar{t}_1 . Then, beginning with \bar{t}_1 , the repair system will be turned on. From \bar{t}_1 to t_1 , the communication graphs are discontinuous. Specifically, node 3 is destroyed in the observation communication network and node 2 becomes inactive in the communication network of control inputs. The effect of the attacks will be eliminated at \bar{t}_1 , and during the time interval $[\bar{t}_1, t_2]$, the topology of the whole network will be recovered back to its initial setting, until the next attacks happen at t_2 .

By using Kronecker product, from (11) and (12) are given:

$$\begin{aligned} {}^c_{t_0} D_t^\alpha \mathfrak{S}(t) &= \sum_{\theta=1}^{\beta} \mu_\theta(\phi_p(t)) ((\mathcal{I}_M \otimes \mathcal{A}_\theta) \mathfrak{S}(t) \\ &\quad - \xi(\mathcal{L}_{\hat{\sigma}(k)} \otimes \mathcal{B}_\theta \mathcal{K}_\theta) \tilde{\mathfrak{S}}(t)), \end{aligned} \quad (13)$$

and

$$\begin{aligned} {}^c_{t_0} D_t^\alpha \hat{\mathfrak{S}}(t) &= \sum_{\theta=1}^{\beta} \mu_\theta(\phi_p(t)) ((\mathcal{I}_M \otimes \mathcal{A}_\theta) \hat{\mathfrak{S}}(t) \\ &\quad - \xi(\mathcal{L}_{\hat{\sigma}(k)} \otimes \mathcal{B}_\theta \mathcal{K}_\theta) \tilde{x}(t) - \tilde{\xi}(\mathcal{L}_{\hat{\sigma}(k)} \otimes \Omega_\theta) \rho(t)), \end{aligned} \quad (14)$$

where $\mathfrak{S}(t) = (\mathfrak{S}_1^T(t), \dots, \mathfrak{S}_M^T(t))^T$, $\hat{\mathfrak{S}}(t) = (\hat{\mathfrak{S}}_1^T(t), \dots, \hat{\mathfrak{S}}_M^T(t))^T$, $\rho(t) = (\rho_1^T(t), \dots, \rho_M^T(t))^T$ and $\tilde{\mathfrak{S}}(t) = (\tilde{\mathfrak{S}}_M^T(t), \tilde{\mathfrak{S}}_{M+1}^T(t))^T$, $\mathcal{L}_{\hat{\sigma}(k)} = \begin{bmatrix} \mathcal{L}_{\hat{\sigma}(k)} & \chi \\ 0_M^T & 0 \end{bmatrix}$, $\tilde{\mathcal{L}}_{\hat{\sigma}(k)} = \begin{bmatrix} \tilde{\mathcal{L}}_{\hat{\sigma}(k)} & \chi \\ 0_M^T & 0 \end{bmatrix}$, $\chi = (\chi_1, \dots, \chi_M)^T$, in which $\chi_p = 1$ if a relation from the leader to the follower p exists; otherwise, $\chi_p = 0$.

Define $\omega_p(t) = \mathfrak{S}_p(t) - \mathfrak{S}_{M+1}(t)$, $\varpi_p(t) = \hat{\mathfrak{S}}_p(t) - \hat{\mathfrak{S}}_p(t)$, $\omega^T(t) = (\omega_1^T(t), \dots, \omega_M^T(t))^T$, $\varpi^T(t) = (\varpi_1^T(t), \dots, \varpi_M^T(t))^T$.

From (13) and (14) can be written as:

$${}^c_{t_0} D_t^\alpha \varpi(t) = \sum_{\theta=1}^{\beta} \mu_\theta(\phi(t)) ((\mathcal{I}_M \otimes \mathcal{A}_\theta) \varpi(t)$$

$$- \tilde{\xi}(\mathcal{L}_{\hat{\sigma}(k)} \otimes \Omega_\theta \mathcal{C}_\theta) \varpi(t)), \quad (15)$$

$$\begin{aligned} {}^c_{t_0} D_t^\alpha \omega(t) &= \sum_{\theta=1}^{\beta} \mu_\theta(\phi(t)) ((\mathcal{I}_M \otimes \mathcal{A}_\theta) \omega(t) \\ &\quad - \xi(\mathcal{L}_{\hat{\sigma}(k)} \otimes \mathcal{B}_\theta \mathcal{K}_\theta) \tilde{x}(t)), \end{aligned} \quad (16)$$

with

$$\begin{aligned} &(\mathcal{L}_{\hat{\sigma}(k)} \otimes \mathcal{B}_\theta \mathcal{K}_\theta) \tilde{x}(t) \\ &= (\mathcal{L}_{\hat{\sigma}(k)} \otimes \mathcal{B}_\theta \mathcal{K}_\theta) (\tilde{x}(t) - 1_{M+1} \otimes x_{M+1}(t)) \\ &= (\mathcal{L}_{\hat{\sigma}(k)} \otimes \mathcal{B}_\theta \mathcal{K}_\theta) (\hat{x}(t) - 1_M \otimes x_{M+1}) \\ &= (\mathcal{L}_{\hat{\sigma}(k)} \otimes \mathcal{B}_\theta \mathcal{K}_\theta) (\omega(t) - \varpi(t)). \end{aligned} \quad (17)$$

From (15)-(17) we have,

$${}^c_{t_0} D_t^\alpha \hat{\omega}(t) = \sum_{\theta=1}^{\beta} \mu_\theta(\phi(t)) \mathcal{A} \hat{\omega}(t),$$

where $\mathcal{A} = \begin{bmatrix} \mathfrak{S}_1 & 0_{n_M \times n_M} \\ \xi(\mathcal{L}_{\hat{\sigma}(k)} \otimes \mathcal{B}_\theta \mathcal{K}_\theta) & \mathfrak{S}_2 \end{bmatrix}$, $\hat{\omega}(t) = [\varpi^T(t), \omega^T(t)]^T$, $\mathfrak{S}_1(\mathcal{I}_M \otimes \mathcal{A}_\theta) - \tilde{\xi}(\mathcal{L}_{\hat{\sigma}(k)} \otimes \Omega_\theta \mathcal{C}_\theta)$, $(\mathcal{I}_M \otimes \mathcal{A}_\theta) - \xi(\mathcal{L}_{\hat{\sigma}(k)} \otimes \mathcal{B}_\theta \mathcal{K}_\theta)$.

III. MAIN RESULT

Theorem 1: For positive scalars ϑ , $\hat{\vartheta}$, η , $\bar{\eta}$, $\tilde{\eta}$, $\hat{\eta}$, γ , α , the positive-definite matrices W, U with $\mathcal{K}_\theta = \mathcal{B}_\theta^T U^{-1}$ and $\Omega_\theta = W^{-1} \mathcal{C}_\theta^T$, FOMAS (3) and (4) can be achieved the consensus using tracking control (9), if the following inequalities hold,

$$W \mathcal{A}_\theta + \mathcal{A}_\theta^T W - \vartheta \mathcal{C}_\theta^T \mathcal{C}_\theta + \eta W < 0, \quad (18)$$

$$\mathcal{A}_\theta U + U \mathcal{A}_\theta^T - \hat{\vartheta} \mathcal{B}_\theta \mathcal{B}_\theta^T + \bar{\eta} U < 0, \quad (19)$$

$$\Xi = \begin{bmatrix} -\tilde{\eta}(\Upsilon \otimes W) & \\ \Lambda & -\tau \hat{\eta}(\Upsilon \otimes U^{-1}) \end{bmatrix} < 0, \quad (20)$$

where $\Lambda = \tau(\xi \Upsilon \mathcal{L} \otimes U^{-1} \mathcal{B}_\theta \mathcal{B}_\theta^T U^{-1})$ and for each $k \in \mathcal{N}$,

$$(\eta_{\min}(t_k - \bar{t}_{k-1}))^{\frac{1}{\alpha}} - (\Theta_{\min}(\bar{t}_k - t_k))^{\frac{1}{\alpha}} - \epsilon < 0, \quad (21)$$

and $\Theta_{\min} = \min\{\Theta_1, \Theta_2\}$.

The following optimization problem is obtained by solving:

Minimize Θ_1 , subject to

$$W \mathcal{A}_\theta + \mathcal{A}_\theta^T W - \xi \hat{\psi} \mathcal{C}_\theta^T \mathcal{C}_\theta - \Theta_1 W < 0. \quad (22)$$

Minimize Θ_2 , subject to

$$\mathcal{A}_\theta^T U^{-1} + U^{-1} \mathcal{A}_\theta - \hat{\xi} \check{\psi} U^{-1} \mathcal{B}_\theta \mathcal{B}_\theta^T U^{-1} - \Theta_2 U^{-1} < 0, \quad (23)$$

where $\hat{\psi}_{\min} = \frac{\lambda_{\min}}{\gamma_{\min}}$, $\hat{\lambda}_{\min} = \min_{\hat{\sigma}(k)} \{\mathcal{L}_{\hat{\sigma}(k)}^T \Upsilon + \Upsilon \mathcal{L}_{\hat{\sigma}(k)}\}$, $\check{\psi}_{\min} = \frac{\lambda_{\min}}{\gamma_{\min}}$, $\check{\lambda}_{\min} = \min_{\check{\sigma}(k)} \{\mathcal{L}_{\check{\sigma}(k)}^T \Upsilon + \Upsilon \mathcal{L}_{\check{\sigma}(k)}\}$, $\gamma_{\min} = \min_{1 \leq p \leq M} \{\gamma_p\}$.

Proof: Consider a Lyapunov function:

$$V(t) = \varpi^T(t) (\Upsilon \otimes W) \varpi(t) + \tau \omega^T(t) (\Upsilon \otimes U^{-1}) \omega(t), \quad (24)$$

where U and W are positive definite. Here denote $V_\pi = \varpi^T(t) (\Upsilon \otimes W) \varpi(t)$, and $V_\delta = \omega^T(t) (\Upsilon \otimes U^{-1}) \omega(t)$. For $t \in [\bar{t}_{k-1}, t_k]$, $k \in \mathcal{N}$ without attacks occur $\mathcal{L}_{\hat{\sigma}(k)} = \mathcal{L}_{\check{\sigma}(k)} =$

\mathcal{L} .

By applying Lemma 3, one has

$$\begin{aligned}
 {}^C_{t_0} D_t^\alpha V_\pi(t) &= {}^C_{t_0} D_t^\alpha (\varpi^T(t)(\Upsilon \otimes W)\varpi(t)) \\
 &\leq 2(\varpi^T(t)(\Upsilon \otimes W)) {}^C_{t_0} D_t^\alpha \varpi(t) \\
 &\leq 2 \sum_{\theta=1}^{\beta} \mu_\theta(\phi(t)) \left(\varpi^T(t)(\Upsilon \otimes W) ((\mathcal{L}_M \otimes \mathcal{A}_\theta) \right. \\
 &\quad \left. - \hat{\xi}(\mathcal{L} \otimes \Omega_\theta \mathcal{C}_\theta)) \varpi(t) \right) \\
 &\leq \sum_{\theta=1}^{\beta} \mu_\theta(\phi(t)) \varpi^T(t) \left(\Upsilon \otimes (W \mathcal{A}_\theta + \mathcal{A}_\theta^T W) \right. \\
 &\quad \left. - 2\hat{\xi}(\Upsilon \mathcal{L} \otimes W \Omega_\theta \mathcal{C}_\theta) \right) \varpi(t) \\
 &\leq \sum_{\theta=1}^{\beta} \mu_\theta(\phi(t)) \varpi^T(t) \left(\Upsilon \otimes (W \mathcal{A}_\theta + \mathcal{A}_\theta^T W) \right. \\
 &\quad \left. - 2(\Upsilon \mathcal{L} \otimes \mathcal{C}_\theta^T \mathcal{C}_\theta) \right) \varpi(t) \\
 &\leq \sum_{\theta=1}^{\beta} \mu_\theta(\phi(t)) \varpi^T(t) \left(\Upsilon \otimes (W \mathcal{A}_\theta + \mathcal{A}_\theta^T W \right. \\
 &\quad \left. - \frac{\hat{\xi}}{\gamma_{\max}} \lambda_{\min}(\Upsilon \mathcal{L} + \mathcal{L}^T \Upsilon) \Upsilon \mathcal{C}_\theta^T \mathcal{C}_\theta) \right) \varpi(t). \tag{25}
 \end{aligned}$$

For $\hat{\xi} > \vartheta/\zeta$, $\zeta = \frac{\lambda_{\min}(\Upsilon \mathcal{L} + \mathcal{L}^T \Upsilon)}{\gamma_{\max}}$, where $\gamma_{\max} = \max_{1 \leq p \leq \mathcal{M}} \{\gamma_p\}$, $\Upsilon = \text{diag}\{\gamma_1, \gamma_2, \dots, \gamma_{\mathcal{M}}\}$, $\mathcal{L}^T \gamma = \mathbf{1}_{\mathcal{M}}$. It follows that

$${}^C_{t_0} D_t^\alpha V_\pi(t) \leq \sum_{\theta=1}^{\beta} \mu_\theta(\phi(t)) \varpi^T(t) \left(\Upsilon \otimes (W \mathcal{A}_\theta + \mathcal{A}_\theta^T W - \vartheta \mathcal{C}_\theta^T \mathcal{C}_\theta) \right) \varpi(t). \tag{26}$$

Then,

$${}^C_{t_0} D_t^\alpha V_\pi(t) \leq - \sum_{\theta=1}^{\beta} \mu_\theta(\phi(t)) (\eta + \tilde{\eta}) \varpi^T(t) (\Upsilon \otimes W) \varpi(t), \tag{27}$$

where $\tilde{\eta}$ is a constant, $0 < \tilde{\eta} \ll \eta$.

Next, taking the fractional derivative of V_δ with system (16), one has

$$\begin{aligned}
 {}^C_{t_0} D_t^\alpha V_\delta(t) &= {}^C_{t_0} D_t^\alpha (\omega^T(t)(\Upsilon \otimes U^{-1})\omega(t)) \\
 &\leq \sum_{\theta=1}^{\beta} \mu_\theta(\phi(t)) 2\xi \left(\omega^T(t)(\Upsilon \mathcal{L} \otimes U^{-1} \mathcal{B}_\theta \mathcal{K}_\theta) \varpi(t) \right. \\
 &\quad \left. + \omega^T(t)(\Upsilon \mathcal{L} \otimes U^{-1} \mathcal{B}_\theta \mathcal{K}_\theta) \omega(t) \right) \\
 &\leq \sum_{\theta=1}^{\beta} \mu_\theta(\phi(t)) \left(2\xi \omega^T(t)(\Upsilon \mathcal{L} \otimes U^{-1} \mathcal{B}_\theta \mathcal{B}_\theta^T U^{-1}) \right. \\
 &\quad \times \varpi(t) + \omega^T(t)(\mathcal{A}_\theta U^{-1} + U^{-1} \mathcal{A}_\theta) \\
 &\quad \left. - \frac{\xi}{\gamma_{\max}} \lambda_{\min}(\Upsilon \mathcal{L} + \mathcal{L}^T \Upsilon) \right. \\
 &\quad \left. \times \Upsilon U^{-1} \mathcal{B}_\theta \mathcal{B}_\theta^T U^{-1} \right) \omega(t). \tag{28}
 \end{aligned}$$

For $\xi > \hat{\vartheta}/\hat{\zeta}$, $\hat{\zeta} = \frac{\lambda_{\min}(\Upsilon \mathcal{L} + \mathcal{L}^T \Upsilon)}{\gamma_{\max}}$, it follows that

$${}^C_{t_0} D_t^\alpha V_\delta(t) \leq \sum_{\theta=1}^{\beta} \mu_\theta(\phi(t)) \left(2\eta \omega^T(t)(\Upsilon \mathcal{L} \otimes U^{-1} \mathcal{B}_\theta \mathcal{B}_\theta^T U^{-1}) \right. \\
 \left. \times \varpi(t) - (\tilde{\eta} + \hat{\eta})(\Upsilon \otimes U^{-1})\omega(t) \right), \tag{29}$$

where $\hat{\eta}$ is a constant, $0 < \hat{\eta} \ll \tilde{\eta}$.

From (27) and (29), we obtain

$$\begin{aligned}
 {}^C_{t_0} D_t^\alpha V(t) &\leq \sum_{\theta=1}^{\beta} \mu_\theta(\phi(t)) \left(-(\eta + \tilde{\eta}) \varpi^T(t)(\Upsilon \otimes W) \varpi(t) \right. \\
 &\quad \left. + 2\eta \omega^T(t)(\Upsilon \mathcal{L} \otimes U^{-1} \mathcal{B}_\theta \mathcal{B}_\theta^T U^{-1}) \varpi(t) \right. \\
 &\quad \left. - (\tilde{\eta} + \hat{\eta})(\Upsilon \otimes U^{-1})\omega(t) \right) \\
 &\leq \sum_{\theta=1}^{\beta} \mu_\theta(\phi(t)) \left(-\eta \varpi^T(t)(\Upsilon \otimes W) \varpi(t) + \tilde{\omega}^T \Xi \tilde{\omega}(t) \right. \\
 &\quad \left. - \tilde{\eta} \varpi^T(t)(\Upsilon \otimes U^{-1}) \right) \\
 &< - \sum_{\theta=1}^{\beta} \mu_\theta(\phi(t)) \left(\eta \varpi^T(t)(\Upsilon \otimes W) \varpi(t) \right. \\
 &\quad \left. + \tilde{\eta} \varpi^T(t)(\Upsilon \otimes U^{-1}) \right) \\
 &< - \sum_{\theta=1}^{\beta} \mu_\theta(\phi(t)) \eta_{\min} V(t)
 \end{aligned}$$

$${}^C_{t_0} D_t^\alpha V(t) < -\eta_{\min} V(t), \quad t \in [\bar{t}_{k-1}, t_k), \tag{30}$$

where $\eta_{\min} = \min\{\eta, \tilde{\eta}\}$. By applying Lemma 1, we get

$$V(t_k) \leq V(\bar{t}_{k-1}) \mathbb{E}_\alpha(-\eta_{\min}(t_k - \bar{t}_{k-1}))^\alpha. \tag{31}$$

According to Lemma 2, we get

$$V(t_k) \leq V(\bar{t}_{k-1}) \frac{1}{\alpha} e^{-(\eta_{\min}(t_k - \bar{t}_{k-1}))^\alpha}. \tag{32}$$

When $t \in [t_k, \bar{t}_k)$, both controllers and observers communication network is destroyed by malicious attacks, i.e. $\mathcal{L}_{\hat{\sigma}(k)}$ and $\mathcal{L}_{\hat{\sigma}(k)}$ should both be considered. Calculating the Caputo fractional derivative of V_φ and V_δ along the trajectory of system (15) and (16) by selecting Θ_1 and Θ_2 in (22) and (23) respectively, we get

$$\begin{aligned}
 {}^C_{t_0} D_t^\alpha V_\pi(t) &= {}^C_{t_0} D_t^\alpha (\varpi^T(t)(\Upsilon \otimes W)\varpi(t)) \\
 &\leq 2(\varpi^T(t)(\Upsilon \otimes W)) {}^C_{t_0} D_t^\alpha \varpi(t) \\
 &\leq 2 \sum_{\theta=1}^{\beta} \mu_\theta(\phi(t)) \left(\varpi^T(t)(\Upsilon \otimes W) ((\mathcal{L}_M \otimes \mathcal{A}_\theta) \right. \\
 &\quad \left. - \hat{\xi}(\mathcal{L}_{\hat{\sigma}(k)} \otimes \Omega_\theta \mathcal{C}_\theta)) \varpi(t) \right) \\
 &\leq \sum_{\theta=1}^{\beta} \mu_\theta(\phi(t)) (\Theta_1 - \tilde{\eta}) \varpi^T(t)(\Upsilon \otimes W) \varpi(t), \tag{33}
 \end{aligned}$$

and

$$\begin{aligned}
 {}^C_{t_0} D_t^\alpha V_\delta(t) &= {}^C_{t_0} D_t^\alpha (\omega^T(t)(\Upsilon \otimes U^{-1})\omega(t)) \\
 &\leq \sum_{\theta=1}^{\beta} \mu_\theta(\phi(t)) 2\xi \left(\omega^T(t)(\Upsilon \mathcal{L}_{\hat{\sigma}(k)} \otimes U^{-1} \mathcal{B}_\theta \mathcal{K}_\theta) \varpi(t) \right.
 \end{aligned}$$

$$\begin{aligned}
 & + \omega^T(t) (\Upsilon \mathcal{L}_{\hat{\sigma}(k)} \otimes U^{-1} \mathcal{B}_\theta \mathcal{K}_\theta) \omega(t) \\
 & \leq \sum_{\theta=1}^{\beta} \mu_\theta(\phi(t)) \left(2\xi \omega^T(t) (\Upsilon \mathcal{L}_{\hat{\sigma}(k)} \otimes U^{-1} \mathcal{B}_\theta \mathcal{B}_\theta^T U^{-1}) \right. \\
 & \quad \times \varpi(t) + (\Theta_2 - \hat{\eta}) \omega^T(t) (\Upsilon \otimes U^{-1}) \omega(t) \Big). \tag{34}
 \end{aligned}$$

From (33) and (34), one has

$$\begin{aligned}
 {}^C_{t_0} D_t^\alpha V(t) & \leq \sum_{\theta=1}^{\beta} \mu_\theta(\phi(t)) \left(\Theta_1 \varpi^T(t) (\Upsilon \otimes W) \varpi(t) \right. \\
 & \quad \left. + \tilde{\omega}^T \Xi_{\sigma(k)} \tilde{\omega}(t) + \tau \Theta_2 \omega^T(t) (\Upsilon \otimes U^{-1}) \omega(t) \right) \\
 & < \sum_{\theta=1}^{\beta} \mu_\theta(\phi(t)) \left(\Theta_1 \varpi^T(t) (\Upsilon \otimes W) \varpi(t) \right. \\
 & \quad \left. + \tau \Theta_2 \varpi^T(t) (\Upsilon \otimes U^{-1}) \omega(t) \right) \\
 & < \sum_{\theta=1}^{\beta} \mu_\theta(\phi(t)) \Theta_{\min} V(t) \\
 & < \Theta_{\min} V(t). \tag{35}
 \end{aligned}$$

Applying Lemma 1 in (35) we get

$$V(\bar{t}_k) \leq V(t_k) \mathbb{E}_\alpha(\Theta_{\min}(\bar{t}_k - t_k))^\alpha. \tag{36}$$

By applying Lemma 2, one has

$$\begin{aligned}
 V(\bar{t}_k) & \leq V(t_k) \frac{1}{\alpha} e^{(\Theta_{\min}(\bar{t}_k - t_k)) \frac{1}{\alpha}} \\
 & \leq V(\bar{t}_{k-1}) \frac{1}{\alpha} e^{-(\eta_{\min}(t_k - \bar{t}_{k-1})) \frac{1}{\alpha}} \frac{1}{\alpha} e^{(\Theta_{\min}(\bar{t}_k - t_k)) \frac{1}{\alpha}} \\
 & \leq V(\bar{t}_{k-1}) \frac{1}{\alpha^2} e^{-((n_{\min}(t_k - \bar{t}_{k-1})) \frac{1}{\alpha}) - (\Theta_{\min}(\bar{t}_k - t_k)) \frac{1}{\alpha}} \\
 & < \frac{1}{\alpha^2} e^{-\epsilon} V(\bar{t}_{k-1}) < \frac{1}{\alpha^2} e^{-k\epsilon} V(t_0).
 \end{aligned}$$

Therefore, the FOMAS (3) and (4) can be reached the consensus, i.e., $\omega(t)$ and $\varpi(t)$ are converge to zero.

Corollary 1: For positive scalars $\vartheta, \hat{\vartheta}, \eta, \bar{\eta}, \tilde{\eta}, \hat{\eta}, \tau$ with $\mathcal{K}_\theta = \mathcal{B}_\theta^T U^{-1}$, $\Omega_\theta = W^{-1} \mathcal{C}_\theta^T$, and attacks occur only in the communication channel for the controllers, FOMAS (3) and (4) can achieve the consensus using tracking control (9), if (18)-(20) holds in Theorem 1 and for each $k \in \mathcal{N}$, $(\eta_{\min}(t_k - \bar{t}_{k-1})) \frac{1}{\alpha} - (\Theta_1(\bar{t}_k - t_k)) \frac{1}{\alpha} - \epsilon < 0$. The following optimization problem is obtained by solving:

Minimize Θ_1 , subject to

$$W \mathcal{A}_\theta + \mathcal{A}_\theta^T W - \xi \hat{\psi} \mathcal{C}_\theta^T \mathcal{C}_\theta - \Theta_1 W < 0. \tag{37}$$

where $\hat{\psi}_{\min} = \frac{\lambda_{\min}}{\gamma_{\min}}$, $\hat{\lambda}_{\min} = \min_{\hat{\sigma}(k)} \{ \mathcal{L}_{\hat{\sigma}(k)}^T \Upsilon + \Upsilon \mathcal{L}_{\hat{\sigma}(k)} \}$, $\gamma_{\min} = \min_{1 \leq p \leq \mathcal{M}} \{ \gamma_p \}$.

Corollary 2: For positive scalars $\vartheta, \hat{\vartheta}, \eta, \bar{\eta}, \tilde{\eta}, \hat{\eta}, \tau$ with $\mathcal{K}_\theta = \mathcal{B}_\theta^T U^{-1}$, $\Omega_\theta = W^{-1} \mathcal{C}_\theta^T$, and attacks occur only in the communication network for the observers, FOMAS (3) and (4) can achieve the consensus using tracking control (9), if (18)-(20) in Theorem 1 hold and for each $k \in \mathcal{N}$, $(\eta_{\min}(t_k - \bar{t}_{k-1})) \frac{1}{\alpha} - (\Theta_2(\bar{t}_k - t_k)) \frac{1}{\alpha} - \epsilon < 0$. The following

optimization problem is obtained by solving:

Minimize Θ_2 , subject to

$$\mathcal{A}_\theta^T U^{-1} + U^{-1} \mathcal{A}_\theta - \hat{\xi} \check{\psi} U^{-1} \mathcal{B}_\theta \mathcal{B}_\theta^T U^{-1} - \Theta_2 U^{-1} < 0, \tag{38}$$

where $\check{\psi}_{\min} = \frac{\lambda_{\min}}{\gamma_{\min}}$, $\check{\lambda}_{\min} = \min_{\check{\sigma}(k)} \{ \mathcal{L}_{\check{\sigma}(k)}^T \Upsilon + \Upsilon \mathcal{L}_{\check{\sigma}(k)} \}$, $\gamma_{\min} = \min_{1 \leq p \leq \mathcal{M}} \{ \gamma_p \}$.

Remark 2: In special case, when cyber attacks can not impact the security of topologies of the communication networks of both controllers and observers ([24], [25]) formation control of observer-based FOMAS without T-S fuzzy system. Next our investigated to Mittag-Leffler sense of T-S fuzzy observer-based FOMAS and also our proposed method valid with $\alpha \in (0, 1]$ in [24], [25]), so the following Corollary.

Corollary 3: For positive scalars $\vartheta, \hat{\vartheta}, \eta, \bar{\eta}, \tilde{\eta}, \hat{\eta}, \tau$ with $\mathcal{K}_\theta = \mathcal{B}_\theta^T U^{-1}$, and $\Omega_\theta = W^{-1} \mathcal{C}_\theta^T$, FOMAS (3) and (4) can be achieved the Mittag-Leffler sense of consensus using tracking control (9), if (18)-(20) holds and $\eta_{\min} > 0$.

Proof: Consider the Lyapunov functional (24) and taking the fractional derivative on system (15) and (16), we obtain that

$${}^C_{t_0} D_t^\alpha V(t) < -\eta_{\min} V(t),$$

where $\eta_{\min} = \min\{\eta, \bar{\eta}\}$. By using Lemma 1, we get

$$V(t) \leq V(t_0) \mathbb{E}_\alpha(-\eta_{\min}(t - t_0))^\alpha, \tag{39}$$

where $\eta_{\min} = \min\{\eta, \bar{\eta}\} > 0$. It follows from [14], the inequality (39) are satisfied. Therefore, the FOMAS (3) and (4) can be reached the consensus of Mittag-Leffler sense.

IV. NUMERICAL EXAMPLES

Two numerical examples are used in this section to demonstrate the effectiveness of the theoretical results achieved.

Example 1: We consider FOMAS system (3) and (4) with $\mathfrak{S}_p = [\mathfrak{S}_{p1}, \mathfrak{S}_{p2}, \mathfrak{S}_{p3}]^T, p = 1, \dots, 5$. Having 4 followers and one leader, allow these agents to get information from their neighbor in accordance with their communication topology. We analyze two scenarios, 1) When the cyber system is not under attack, the communication networks is represented in Fig. 3(a). 2) When a cyber system is under attack, the communication topology is depicted in Figs. 3(b) and 3(c). Suppose that attacks occur in the time interval $[t_p, \bar{t}_p]$, we take $p \in \mathcal{N}$, $t_p = 0.7(p - 1)$ and $\bar{t}_p = 0.7(p - 1) + 0.5$.

The T-S fuzzy model is:

Rule \mathcal{R}^1

$$\text{IF } \mathfrak{S}_{p1} \text{ is } \mathcal{M}_1, \text{ THEN } \begin{cases} {}^C D_t^\alpha \mathfrak{S}(t) = \mathcal{A}_1 \mathfrak{S}(t) + \mathcal{B}_1 \tilde{u}(t), \\ \varphi(t) = \mathcal{C}_1 \mathfrak{S}(t). \end{cases}$$

Rule \mathcal{R}^2

$$\text{IF } \mathfrak{S}_{p1} \text{ is } \mathcal{M}_2, \text{ THEN } \begin{cases} {}^C D_t^\alpha \mathfrak{S}(t) = \mathcal{A}_2 \mathfrak{S}(t) + \mathcal{B}_2 \tilde{u}(t), \\ \varphi(t) = \mathcal{C}_2 \mathfrak{S}(t), \end{cases}$$

where $\mathfrak{S}(t) = (\mathfrak{S}_{p1}, \mathfrak{S}_{p2}, \mathfrak{S}_{p3})$,

$$\begin{aligned}
 \mathcal{A}_1 = \mathcal{A}_2 & = \begin{bmatrix} -2.97 & 0.92 & -0.04 \\ -0.93 & 0 & -0.012 \\ 0.37 & -4.73 & -1.79 \end{bmatrix}, \\
 \mathcal{B}_1 = \mathcal{B}_2 & = \begin{bmatrix} -0.05 & 0.90 & 1.59 \\ 0 & 0 & 0 \\ -1.80 & 1.70 & -2 \end{bmatrix},
 \end{aligned}$$

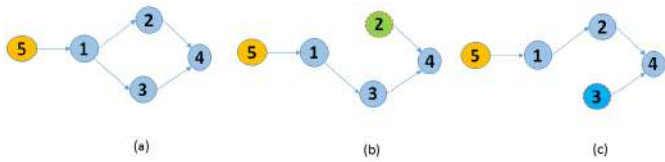


Fig. 3. The communication topology.

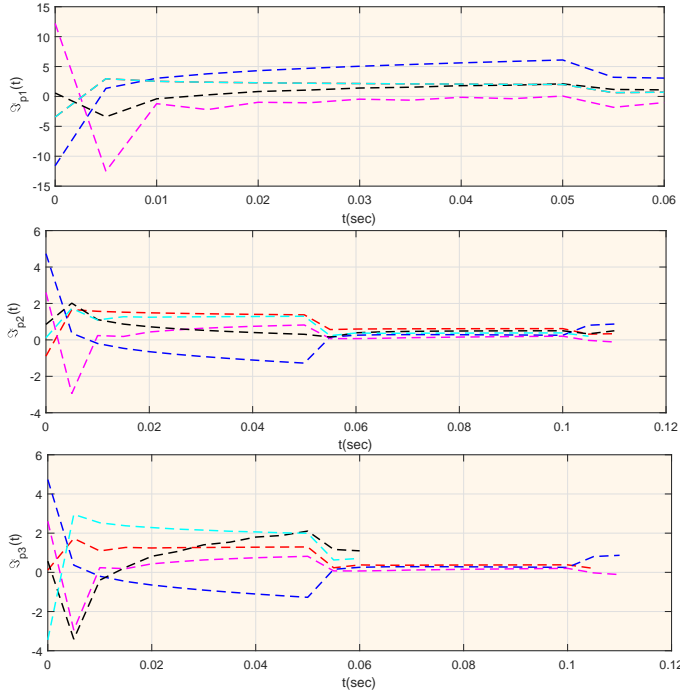


Fig. 4. State trajectories for FOMASs when attacks occur with no security control, where $\mathfrak{S}_p(t) = (\mathfrak{S}_{p1}(t), \mathfrak{S}_{p2}(t), \mathfrak{S}_{p3}(t))^T, p = 1, 2, \dots, 5$.

$$\mathcal{C}_1 = \mathcal{C}_2 = \begin{bmatrix} 2.50 & 0.98 & 1.70 \\ 0.73 & 1.70 & 0.97 \end{bmatrix},$$

$\mathcal{M}_1 = \frac{1}{2}(1 + \frac{\mathfrak{S}_{p1}}{d}), \mathcal{M}_2 = \frac{1}{2}(1 - \frac{\mathfrak{S}_{p1}}{d}), \mathfrak{S}_{p1} \in [-d, d]$ with $d > 0$.

The distributed control is taken as:

Rule \mathcal{R}^1 :

IF \mathfrak{S}_{p1} is \mathcal{M}_1 , THEN $\tilde{u}(t) = \xi \mathcal{K}_1 \mathfrak{S}(t)$,

Rule \mathcal{R}^2 :

IF \mathfrak{S}_{p1} is \mathcal{M}_2 , THEN $\tilde{u}(t) = \xi \mathcal{K}_2 \mathfrak{S}(t)$. We choose $\alpha = 0.91$, $\xi = 28$, $\hat{\xi} = 32$, $\eta = 7.2$, $\bar{\eta} = 5.7$. By solving (18)-(20), we obtain feedback gain matrices \mathcal{K}_1 and \mathcal{K}_2 , observer gain matrices Ω_1 and Ω_2 as

$$\mathcal{K}_1 = \mathcal{K}_2 = \begin{bmatrix} 0.0937 & 0.0385 & -0.0115 \\ -0.2005 & -0.0065 & -0.0304 \\ -0.1119 & 0.1005 & -0.0924 \end{bmatrix},$$

$$\Omega_1 = \Omega_2 = \begin{bmatrix} 0.0921 & 0.0823 \\ 0.0349 & -0.1197 \\ 0.1566 & 0.1117 \end{bmatrix},$$

with $\vartheta = 9.6406$ $\hat{\vartheta} = 29.8760$, $\Theta_{\min} = 187$.

Thus FOMAS (3) and (4) expressed by T-S fuzzy model obtained the cyber-security consensus for each $k \in \mathcal{N}$. Fig. 4 depicts trajectories of FOMASs when DoS at-

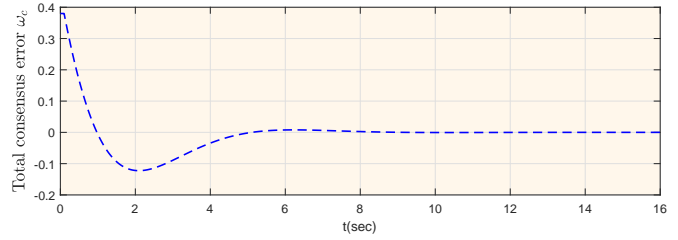


Fig. 5. Evolution of total consensus errors ω_c .

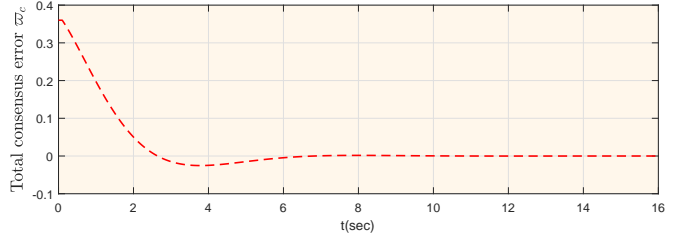


Fig. 6. Evolution of total observer errors ϖ_c .

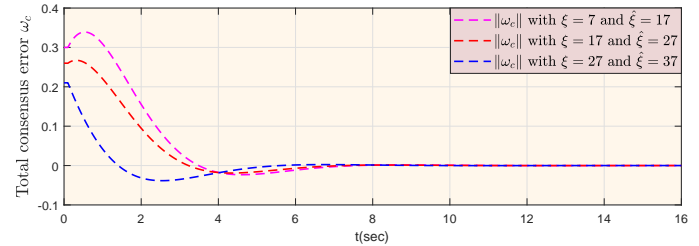


Fig. 7. Comparison of consensus errors ω_c , versus parameters ξ and $\hat{\xi}$ numerical simulations.

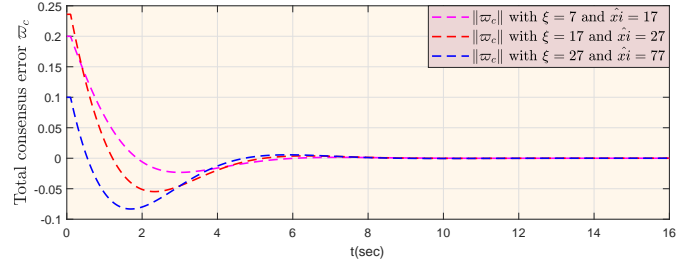


Fig. 8. Comparison of observer errors ϖ_c , versus parameters ξ and $\hat{\xi}$ numerical simulations.

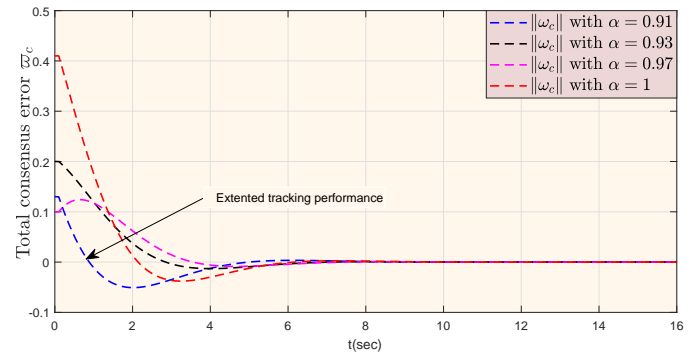


Fig. 9. Comparison of consensus errors ω_c , for differential orders. Notice that, for $\alpha = 0.91$ consensus errors performance effective manner when compared to order $\alpha = 1$.

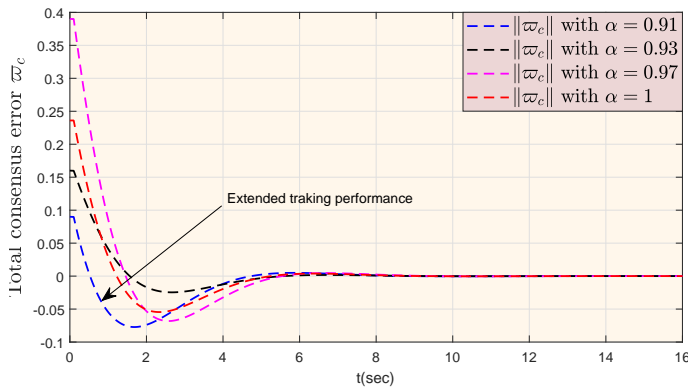


Fig. 10. Comparison of consensus errors ϖ_c , for differential orders. Notice that, for $\alpha = 0.91$ consensus errors performance effective manner when compared to order $\alpha = 1$.

tacks happen in the communication network connecting the three layers without security control, where $\mathfrak{S}_p(t) = (\mathfrak{S}_{p1}(t), \mathfrak{S}_{p2}(t), \mathfrak{S}_{p3}(t))^T, p = 1, 2, \dots, 5$. When $\omega_c = \frac{1}{4} \sum_{p=1}^4 |\omega_p|$, Fig. 5 denotes the consensus tracking error. When $\varpi_c = \frac{1}{4} \sum_{p=1}^4 |\varpi_p|$, the observer error of closed-loop systems is depicted in Fig. 6. Figs. 5 and 6 show that cyber attack occurs and the secure control mechanism still steers the system states to achieve consensus. Figs. 7 and 8 depict the comparison of the consensus tracking error ω_c , and observer error ϖ_c of systems of the different parameters ξ and $\hat{\xi}$. Figs. 9 and 10 show the comparison of the consensus tracking error ω_c , and observer error ϖ_c .

Remark 3: Moreover, numerical simulations demonstrate that increasing the coupling strengths ξ and $\hat{\xi}$ improves both the convergence rates for consensus tracking and states observing (see Figs. 7 and 8 for details). This implies that, while the consensus tracking problem can be solved by adjusting the coupling strengths $\xi > \hat{\vartheta}/\hat{\zeta}$, $\hat{\zeta} = \frac{\lambda_{\min}(\Upsilon\mathcal{L} + \mathcal{L}\Upsilon)}{\gamma_{\max}}$ and $\hat{\xi} > \vartheta/\zeta$, $\zeta = \frac{\lambda_{\min}(\Upsilon\mathcal{L} + \mathcal{L}\Upsilon)}{\gamma_{\max}}$, the convergence rates may be quite small when the coupling strengths ξ and $\hat{\xi}$ are, respectively. Addition, another advantage for comparison tracking error ω_c , and observer error ϖ_c (see Figs. 9 and 10 for details). Notice that, for $\alpha = 0.91$, consensus errors and observer error performance effective manner when compared to order $\alpha = 1$. Briefly, according to the presented results, the T-S fuzzy FOMASs outperforms the secure control scheme exploiting integer-order operators.

Example 2. In this example, the suggested observer-based design approach is used to track the consensus of a network circuit for a tunnel diode model. We proposed the tunnel diode network circuit model as depicted in Fig. 11, where C_1, C_2 denote the capacitor, R_D represents the impedance of tunnel diode, E is inductor, and R_L, R_E are the linear resistance. The fractional-order calculus model is used to rewrite the dynamic description of the three-state tunnel diode network circuit model provided in the literature [46]:

$$\begin{cases} {}^c D_t^\alpha \mathfrak{S}(t) = \mathcal{A}\mathfrak{S}(t) + \mathcal{B}\tilde{u}(t), \\ \varphi(t) = \mathcal{C}\mathfrak{S}(t) \end{cases} \quad (40)$$

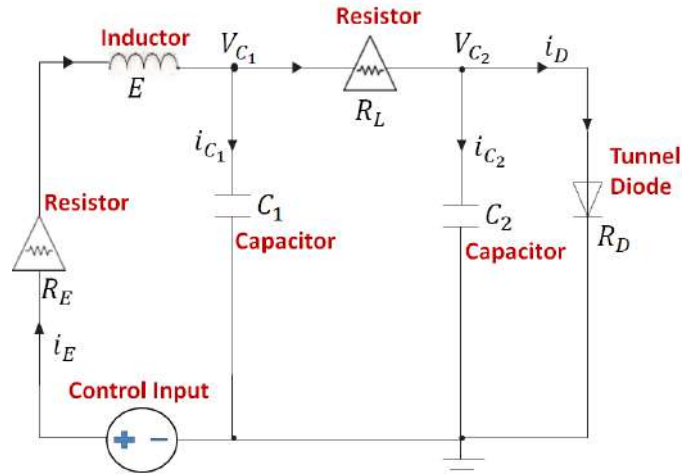


Fig. 11. The application network circuit of tunnel diode.

with

$$\mathcal{A} = \begin{bmatrix} -\frac{1}{R_L C_1} & \frac{1}{R_L C_1} & \frac{1}{C_1} \\ \frac{1}{R_L C_2} & -\frac{s_1 + s_2 \mathfrak{S}_1^2(t)}{C_2} - \frac{1}{R_L C_2} & 0 \\ -\frac{1}{E} & 0 & -\frac{R_E}{E} \end{bmatrix},$$

$$\mathcal{B} = \begin{bmatrix} 0 \\ 0 \\ \frac{1}{E} \end{bmatrix}, \mathcal{C} = I, \mathfrak{S}(t) = (\mathfrak{S}_1, \mathfrak{S}_2, \mathfrak{S}_3)^T,$$

$$\mathfrak{S}_1(t) \in [m_1, m_2], m_1 = \max\{m_1^2, m_2^2\},$$

and s_1, s_2 is a known scalars.

The following equations can be expressed in T-S fuzzy form:

$$\begin{cases} {}^c D_t^\alpha \mathfrak{S}_p(t) = \sum_{\theta=1}^2 \Psi_\theta(\phi_p(t)) [\mathcal{A}_\theta \mathfrak{S}_p(t) + \mathcal{B}_\theta \tilde{u}_p(t)], \\ \varphi_p(t) = \sum_{\theta=1}^2 \Psi_\theta(\phi_p(t)) [\mathcal{C}_\theta \mathfrak{S}_p(t)], \end{cases} \quad (41)$$

where

$$\mathfrak{S}_p(t) = [\mathfrak{S}_{p1}, \mathfrak{S}_{p2}, \mathfrak{S}_{p3}]^T,$$

$$\mathcal{A}_1 = \begin{bmatrix} -\frac{1}{R_L C_1} & \frac{1}{R_L C_1} & \frac{1}{C_1} \\ \frac{1}{R_L C_2} & -\frac{s_1 + s_2 m_1}{C_2} - \frac{1}{R_L C_2} & 0 \\ -\frac{1}{E} & 0 & -\frac{R_E}{E} \end{bmatrix},$$

$$\mathcal{A}_2 = \begin{bmatrix} -\frac{1}{R_L C_1} & \frac{1}{R_L C_1} & \frac{1}{C_1} \\ \frac{1}{R_L C_2} & -\frac{s_1}{C_2} - \frac{1}{R_L C_2} & 0 \\ -\frac{1}{E} & 0 & -\frac{R_E}{E} \end{bmatrix},$$

$$\mathcal{B}_1 = \mathcal{B}_2 = \begin{bmatrix} 0 \\ 0 \\ \frac{1}{E} \end{bmatrix}, \mathcal{C} = I,$$

$$\mathcal{M}_1 = \frac{\mathfrak{S}_{p1}^2(t)}{m_1}, \mathcal{M}_2 = 1 - \frac{\mathfrak{S}_{p1}^2(t)}{m_1}, \mathfrak{S}_{p1} \in [-4, 4].$$

Here, the order α is chosen as 0.93, and similar to [46], the values of $s_1, s_2, C_1, C_2, E, R_E, R_L$ are selected as 0.002, 0.01, 1F, 0.1F, 20H, 0 Ω and 1 Ω respectively. Select one tunnel diode network circuit model to act as the leader agent, generating the required state trajectory. With the network topology shown in Fig. 3, four tunnel diode circuit models operate as follower agents, and these agents can receive output information from their neighbours. Moreover, let $h = 0.02s$ and $t_p = 90ph$,

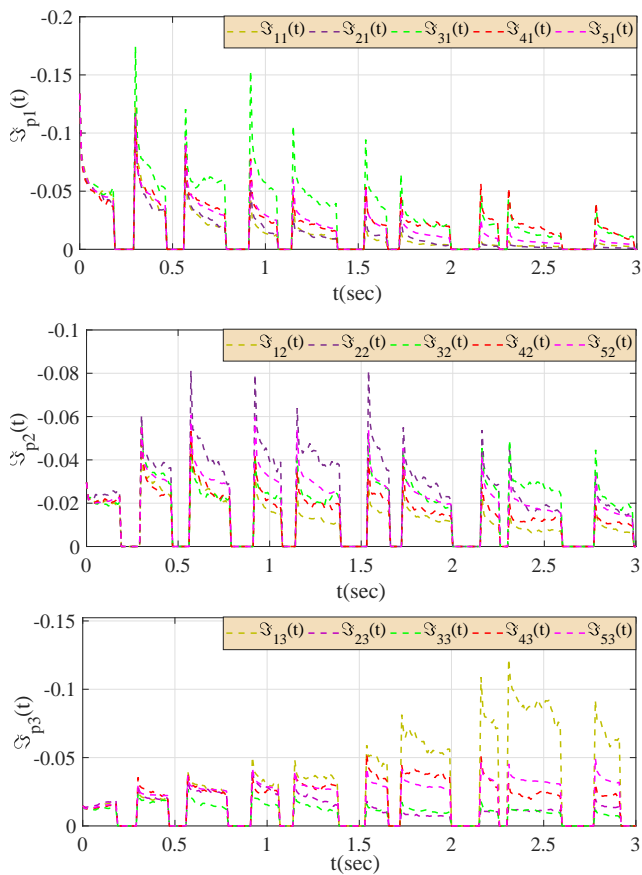


Fig. 12. State trajectories for tunnel diode circuit model when attacks occur with no security control, where $\mathfrak{S}_p(t) = (\mathfrak{S}_{p1}(t), \mathfrak{S}_{p2}(t), \mathfrak{S}_{p3}(t))^T$, $p = 1, 2, \dots, 5$.

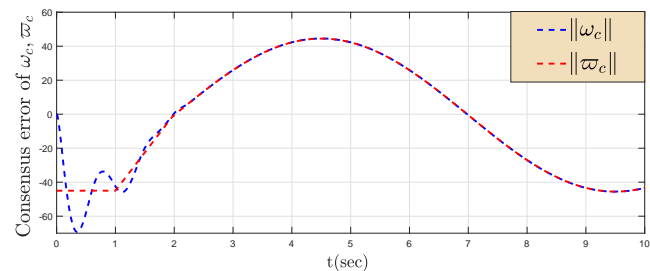


Fig. 13. Consensus error ω_c and ϖ_c , when attacks occur with no security control.

$\bar{t}_p = 91ph$, for $p \in \mathcal{N}$. Assume that attacks occur over the time interval $[t_p, \bar{t}_p]$. We choose $\xi = 13$, $\hat{\xi} = 19$, $\eta = 3.7$, $\bar{\eta} = 7.9$. By solving (18)-(20), we obtain feedback gain matrices \mathcal{K}_1 and \mathcal{K}_2 , observer gain matrices Ω_1 and Ω_2 as

$$\mathcal{K}_1 = \begin{bmatrix} -0.0794 & -0.0008 & 0 \\ 0.0008 & -0.0734 & 0 \\ 0 & 0 & -0.0974 \end{bmatrix},$$

$$\mathcal{K}_2 = \begin{bmatrix} 2.3741 & 0.1895 & 0 \\ 0 & 1.3604 & -0.9087 \\ 0.1895 & -0.9087 & 0.3761 \end{bmatrix},$$

$$\Omega_1 = \begin{bmatrix} -2.9031 & -0.7980 \\ 3.2080 & 0.3950 \\ -1.7935 & -0.9705 \end{bmatrix},$$

$$\Omega_2 = \begin{bmatrix} -1.9464 & 0.4488 \\ 0.8713 & -0.8736 \\ -1.3688 & -0.9125 \end{bmatrix}$$

with $\vartheta = 39.0318$, $\hat{\vartheta} = 38.4191$, $\Theta_{\min} = 374$. When no security controls are used and attacks occur at $t_1 = 1.4s$, the state trajectories of the 5 agents are represented in Fig. 12. The final tracking to the leader was not possible due to difficulties in the connectivity of the two communication networks. Fig. 13 shows that without secure control scheme of system model is still not achieve consensus error. As a result, to evaluate the distributed observer-based security control mechanism, the followers are implemented, and the consensus errors are presented in Fig. 14, indicating that good observation performance has been obtained.

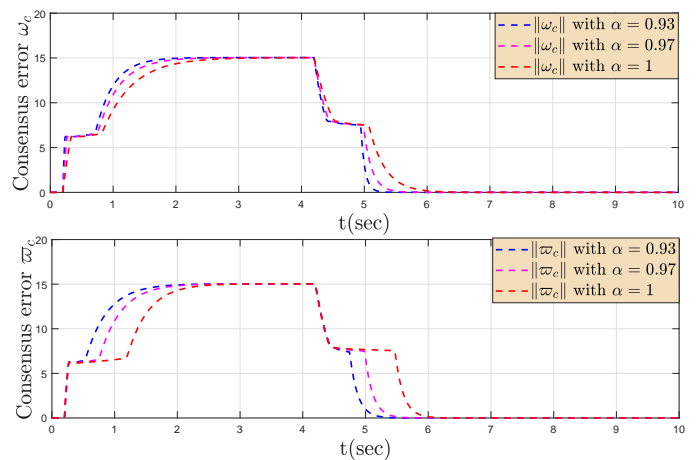


Fig. 14. Consensus errors ω_c and ϖ_c with different differential orders.

V. CONCLUSION

The security control for T-S fuzzy FOMASs with cyber-attacks has been examined. A cyber-attack model with malicious attacks are considered with both controllers and observers. For modeling recoverable cyber attacks a switched device has been employed. By utilizing the theory of fractional-calculus, Lyapunov functional and algebraic graph theory, an distributed control is designed to achieve the secure consensus of T-S fuzzy FOMASs. Finally, a simulation examples and an electronic circuit based on a tunnel diode are presented to demonstrate the effectiveness of the suggested strategy. In the future, we will investigate the networking of T-S fuzzy cascade multi-area power systems in a smart grid with electric vehicles (EVs) under DoS attacks.

REFERENCES

- [1] Y. Tang, X. Xing, H. Karimi, and L. Kocarev, "Tracking control of networked multi agent systems under new characterizations of impulses and its applications in robotic systems," *IEEE T. Ind. Electron.*, vol. 63, pp. 1299–1307, 2015.
- [2] C. Tomlin, G. Pappas, and S. Sastry, "Conflict resolution for air traffic management: A study in multi-agent hybrid systems," *IEEE Trans. Autom. Control.*, vol. 43, pp. 509–521, 1998.
- [3] R. W. Beard, T. W. McLain, M. A. Goodrich, and E. P. Anderson, "Coordinated target assignment and intercept for unmanned air vehicles," *IEEE Trans. Robot. Autom.*, vol. 18, pp. 911–92, 2002.

- [4] C. Dou, D. Yue, J. M. Guerrero, X. Xie and S. Hu, "Multi-agent system-based distributed coordinated control for radial dc micro grid considering transmission time delays," *IEEE T. Smart. Grid.*, vol. 8, pp. 2370–2381, 2017.
- [5] Y. Zheng, J. Ma, and L. Wang, "Consensus of hybrid multi-agent systems," *IEEE Trans. Neural Netw. Learn. Syst.*, vol. 29, pp. 1359–1365, 2018.
- [6] W. Zou, P. Shi, Z. Xiang, and Y. Shi, "Finite-time consensus of second-order switched nonlinear multi-agent systems," *IEEE Trans. Neural Netw. Learn. Syst.*, vol. 31, pp. 1757–1762, 2020.
- [7] G. Wen, W. Yu, Y. Xia, X. Yu, J. Hu, "Distributed tracking of non-linear multi-agent systems under directed switching topology: An observer-based protocol," *IEEE Trans. Syst. Man Cybern.*, vol. 47, pp. 869–881, 2017.
- [8] S. Liu, Z. Wang, G. Wei, and M. Li, "Distributed set-membership filtering for multirate systems under the Round-robin scheduling over sensor networks," *IEEE Trans. Cybern.*, vol. 50, pp. 1910–1920, 2020.
- [9] M. Syed Ali, R. Agalya, V. Shekher, and Y. H. Joo, "Non-fragile sampled data control for stabilization of non-linear multi-agent system with additive time varying delays, Markovian jump and uncertain parameters," *Nonlinear Anal. Hybri.*, vol. 36, 100830, 2020.
- [10] P. Gong, and W. Lan, "Adaptive robust tracking control for multiple unknown fractional-order nonlinear systems," *IEEE Trans. Cybern.*, vol. 49, pp. 1365–1376, 2019.
- [11] P. Mani, R. Rajan, L. Shanmugam, and Y. H. Joo, "Adaptive fractional fuzzy integral sliding mode control for PMSM model," *IEEE T. Fuzzy Syst.*, vol. 27, pp. 1674–1686, 2019.
- [12] F. Wang, Y. Yang, A. Hu, and X. Xu, "Exponential synchronization of fractional-order complex networks via pinning impulsive control," *Nonlinear Dyn.*, vol. 82, pp. 1979–1987, 2015.
- [13] S. Zhang, Y. Yu, and J. Yu, "LMI conditions for global stability of fractional-order neural networks," *IEEE Trans. Neural Netw. Learn. Syst.*, vol. 28, pp. 2423–2433, 2017.
- [14] M. Syed Ali, G. Narayanan, V. Shekher, A. Alsaedi, and B. Ahmad, "Global Mittag-Leffler stability analysis of impulsive fractional-order complex-valued BAM neural networks with time varying delays," *Commun. Nonlinear Sci. Numer. Simulat.*, vol. 83, 105088, 2020.
- [15] Y. Cao, Y. Li, W. Ren, and Y. Chen, "Distributed coordinative of networked fractional-order systems," *IEEE Trans. Syst. Man Cybern. Part B, Cybern.*, vol. 40, pp. 362–370, 2010.
- [16] H. Liu, L. Cheng, M. Tan, and Z. G. Hou, "Exponential finite-time consensus of fractional-order multiagent systems," *IEEE Trans. Syst. Man Cybern. B Cybern.*, vol. 50, pp. 1549–1558, 2020.
- [17] J. Chen, B. Chen, and Z. Zeng, "Synchronization and consensus in networks of linear fractional-order multi-agent systems via sampled-data control," *IEEE Trans. Neural Netw. Learn. Syst.*, vol. 31, pp. 2955–2964, 2020.
- [18] Z. Li, L. Gao, W. Chen, and Y. Xu, "Distributed adaptive cooperative tracking of uncertain nonlinear fractional-order multi-agent systems," *IEEE-CAA J. Automatic.*, vol. 7, pp. 292–300, 2020.
- [19] G. Ren, Y. Yu, C. Xu, and X. Hai, Consensus of fractional multi-agent systems by distributed event-triggered strategy, *Nonlinear Dyn.* vol. 95, pp. 541–555, 2019.
- [20] Y. Li, Y. Liu, and S. Tong, "Observer-based neuro-adaptive optimized control of strict-feedback nonlinear systems with state constraints," *IEEE Trans. Neural Netw. Learn. Syst.*, doi: 10.1109/TNNLS.2021.3051030, 2021.
- [21] Y. Yang, H. Xu, and D. Yue, "Observer-based distributed secure consensus control of a class of linear multi-agent systems subject to random attacks," *IEEE Trans. Circuits Syst. I, Reg. Papers.*, vol. 66, pp. 3089–3099, 2019.
- [22] L. Wang, Z. Wang, G. Wei, F. E. Alsaadi, "Observer-based consensus control for discrete-time multi agent systems with coding-decoding communication protocol," *IEEE Trans. Cybern.*, vol. 49, pp. 4335–4345, 2019.
- [23] Y. Wan, J. Cao, G. Chen, and W. Huang, "Distributed observer-based cyber-security control of complex dynamical networks," *IEEE Trans. Circuits Syst. I, Reg. Papers.*, vol. 64, pp. 2966–2975, 2017.
- [24] W. Yu, Y. Li, G. Wen, X. Yu, and J. Cao, "Observer design for tracking consensus in second-order multi-agent systems: fractional order less than two," *IEEE Trans. Autom. Control.*, vol. 62, pp. 894–900, 2017.
- [25] Y. Gong, G. Wen, Z. Peng, T. Huang and Y. Chen, "Observer-based time-varying formation control of fractional-order multi-agent systems with general linear dynamics," *IEEE Trans. Circuits Syst.,II, Exp. Briefs.*, vol. 67, pp. 82–86, 2020.
- [26] H. Yang, and D. Ye, "Observer-based fixed-time secure tracking consensus for networked high-order multi-agent systems against DoS attacks," *IEEE Trans. Cybern.*, doi: 10.1109/TCYB.2020.3005354, 2020.
- [27] D. Ding, Z. Wang, D. W. C. Ho, and G. Wei, "Observer-based event-triggering consensus control for multiagent systems with lossy sensors and cyber-attacks," *IEEE Trans. Cybern.*, vol. 47, pp. 1936–1947, 2017.
- [28] H. Sandberg, S. Amin, and K. Johansson, "Cyberphysical security in networked control systems: an introduction to the issue," *IEEE Control Syst.*, vol. 35, pp. 20–23, 2015.
- [29] D. Ding, Q. L. Han, X. Ge, and J. Wang, "Secure state estimation and control of cyber-physical systems: A survey," *IEEE Trans. Syst. Man Cybern.*, vol. 51, pp. 176–190, 2021.
- [30] H. Song, D. Ding, H. Dong, and X. Yi, "Distributed filtering based on Cauchy-kernel-based maximum correntropy subject to randomly occurring cyber-attacks," *Automatica.*, vol. 135, 110004, 2022.
- [31] J. Liu, T. Yin, D. Yue, H. R. Karimi, and J. Cao, "Event-based secure leader-following consensus control for multiagent systems with multiple cyber attacks," *IEEE Trans. Cybern.*, doi: 10.1109/TCYB.2020.2970556, 2020.
- [32] Y. Xu, M. Fang, Z. Wu, Y. Pan, M. Chadli, and T. Huang, "Input-based event-triggering consensus of multiagent systems under Denial-of-Service attacks," *IEEE Trans. Syst. Man Cybern.*, vol. 50, pp. 1455–1464, 2020.
- [33] Y. Wan, G. Wen, X. Yu, and T. Huang, "Distributed consensus tracking of networked agent systems under denial-of-service attacks," *IEEE Trans. Syst. Man Cybern.*, vol. 51, pp. 6183–6196, 2021.
- [34] W. L. He, X. Y. Gao, W. M. Zhong, and F. Qian, "Secure impulsive synchronization control of multi-agent systems under deception attacks," *Inf. Sci.*, vol. 459, pp. 354–68, 2018.
- [35] K. Shi, J. wang, S. Zhong, Y. Tang, and J. Cheng, "Hybrid-driven finite-time H_∞ sampling synchronization control for coupling memory complex networks with stochastic cyber attacks," *Neurocomputing.*, vol. 387, pp. 241–254, 2020.
- [36] Z. Feng, G. Hu, and G. Wen, "Distributed consensus tracking for multi-agent systems under two types of attacks," *Int. J. Robust Nonlinear Control.*, vol. 26, pp. 896–918, 2016.
- [37] M. M. Hossain, C. Peng, "Observer-based event triggering H_∞ LFC for multi-area power systems under DoS attacks," *Inf. Sci.*, vol. 543, pp. 437–453, 2021.
- [38] H. Shen, Y. Men, Z. Wu, and J. H. Park, "Nonfragile H_∞ control for fuzzy Markovian jump systems under fast sampling singular perturbation," *IEEE Trans. Syst. Man Cybern.*, vol. 48, pp. 2058–2069, 2018.
- [39] Y. Zhao, B. Li, J. Qin, H. Gao, and H. R. Karimi, " H_∞ consensus and synchronization of nonlinear systems based on a novel fuzzy model," *IEEE Trans. Cybern.*, vol. 43, pp. 2157–2169, 2013.
- [40] Q. Shen, B. Jiang, P. Shi, and J. Zhao, "Cooperative adaptive fuzzy tracking control for networked unknown nonlinear multiagent systems with time-varying actuator faults," *IEEE Trans. Fuzzy Syst.*, vol. 22, pp. 494–504, 2013.
- [41] Y. Ma, and J. Zhao, "Cooperative output regulation for nonlinear multi-agent systems described by T-S fuzzy models under jointly connected switching topology," *Neurocomputing.*, vol. 332, pp. 351–359, 2019.
- [42] J. H. Moon, and H. J. Lee, "Graph Laplacian-based leaderless consensus for multi-agent systems in T-S form," *Fuzzy Set Syst.*, vol. 368, pp. 119–136, 2019.
- [43] Y. Cheng, T. Hu, Y. Li, and S. Zhong, "Consensus of fractional-order multi-agent systems with uncertain topological structure: A Takagi-Sugeno fuzzy event-triggered control strategy," *Fuzzy Set Syst.*, vol. 416, pp. 64–85, 2021.
- [44] J. Liu, T. Yin, J. Cao, D. Yue, and H. R. Karimi, "Security control for TS fuzzy systems with adaptive event-triggered mechanism and multiple cyber-attacks," *IEEE Trans. Syst. Man Cybern.*, vol. 51, pp. 6544–6554, 2021.
- [45] J. Liu, L. Wei, X. Xie, E. Tian, and S. Fei, "Quantized stabilization for TS fuzzy systems with Hybrid-triggered mechanism and stochastic cyber-attacks," *IEEE Trans. Fuzzy Syst.*, vol. 26, pp. 3820–3834, 2018.
- [46] J. Liu, M. Yang, E. Tian, and J. Cao, "Event-based security control for state-dependent uncertain systems under hybrid-attacks and its application to electronic circuits," *IEEE Trans. Circuits Syst. I Regul. Pap.*, vol. 66, pp. 4817–4828, 2019.



G. Narayanan was born in 1994. He received the B.Sc degree in the field of Mathematics from C. Abdul Hakeem College, Melvisharam, Vellore affiliated to Thiruvalluvar University, Vellore, Tamil Nadu, India, in 2016. He received his post graduation in Mathematics from, Thiruvalluvar University, Vellore, Tamil Nadu, India, in 2018 and the Ph.D. degree in mathematics from Thiruvalluvar University, Vellore, India, in 2022 and the Ph.D. degree under the guidance of Dr. M. Syed Ali. He is currently working as a Assistant Professor in

Mathematics with Center for Computational Modeling, Chennai Institute of Technology, Chennai, India. He has authored and coauthored of many research articles in various SCI journals. His research interests are fractional-order nonlinear systems, wind turbine system, cyber security control, complex-valued & quaternion-valued of molecular systems, and multi-agent networked systems. He serves as a Reviewer for various SCI journals.



Dr. Ganesh Kumar Thakur has been associated with Krishna Engineering College, Ghaziabad for the last decade as a competent Associate Professor (Mathematics), Department of Applied Science. He has received his M.Sc.(Mathematics) degree by securing the first rank and awarded by Ph.D (Mathematics) from TMBU, Bhagalpur. As an ardent researcher, he has to his credit 25 research papers published in reputed referred journals. He has also co-guided one research scholar. He is a member of various Mathematical Societies.



Dr. M. Syed Ali graduated from the Department of Mathematics of Gobi Arts and Science College affiliated to Bharathiar University, Coimbatore, in 2002. He received his post-graduation in mathematics from Sri Ramakrishna Mission Vidyalaya College of Arts and Science affiliated to Bharathiar University, Coimbatore, Tamil Nadu, India, in 2005. He was awarded master of philosophy in 2006 in the field of mathematics with specialised area of numerical analysis from Gandhigram Rural University Gandhigram, India. He was conferred with doctor

of philosophy in 2010 in the field of mathematics specialised in the area of fuzzy neural networks in Gandhi gram Rural University, Gandhi gram, India. He was selected as a post-doctoral fellow in the year 2010 for promoting his research in the field of mathematics at Bharathidasan University, Trichy, Tamil Nadu and also worked there from November 2010 to February 2011. Since March 2011, he is working as an assistant professor in the Department of Mathematics, Thiruvalluvar University, Vellore, Tamil Nadu, India. He was awarded young scientist award 2016 by The Academy of Sciences, Chennai. Dr M. Syed Ali has been listed in 2 % of world scientists as released by Stanford University on 2020, 2021, and 2022. He has published more than 190 research papers in various SCI journals holding impact factors. He has also published research articles in national journals and international conference proceedings. He also serves as a reviewer for several SCI journals. His research interests include stochastic differential equations, dynamical systems, fuzzy neural networks, complex networks and cryptography.



Dr. Bandana Priya is working as a Professor (Mathematics) in the Department of Applied Sciences, G L Bajaj Institute of Technology, and Management, Greater Noida, UP, India. She is equipped with an extraordinary caliber and appreciable academic potency. She has published many research paper in journals of high repute. Her area of research includes Optimization technique, Fuzzy Graph theory, and Mathematical Control Theory.



Quanxin Zhu received the Ph.D. degree from Sun Yat-sen (Zhongshan) University, Guangzhou, China, in 2005. He is currently a Professor with Hunan Normal University. He received the Alexander von Humboldt Foundation of Germany. He is a Highly Cited Scientist in the world, in 2018 and 2020. He has authored or co-authored more than 200 journal papers. His research interests include stochastic control, stochastic delayed systems, stochastic stability, nonlinear systems, Markovian jump systems, and stochastic complex networks.

Robust dissipative observer-based control design for discrete-time switched systems with time-varying delay

ISSN 1751-8644
 Received on 26th July 2018
 Revised 10th July 2019
 Accepted on 29th August 2019
 E-First on 3rd October 2019
 doi: 10.1049/iet-cta.2018.5822
 www.ietdl.org

Mohamed Amin Regaieg^{1,2} ✉, Mourad Kchaou^{2,3}, Jérôme Bosche¹, Ahmed El-Hajjaji¹, Mohamed Chaabane²

¹Modeling, Information, and Systems Laboratory, University of Picardie Jules Verne, UFR of Sciences, 33 Rue St Leu Amiens 80000, France

²National School of Engineering of Sfax, University of Sfax, Lab-STA, LR11ES50, 3038, Sfax, Tunisia

³Electrical Department, College of Engineering, University of Hail, P.O. Box 2440, Hail, Kingdom of Saudi Arabia

✉ E-mail: med-amine.regaieg@enis.tn

Abstract: This study deals with $(\mathcal{Q}, \mathcal{S}, \mathcal{R})$ - γ -dissipative output feedback control design for a class of switched systems with time-varying delay and unmeasurable states. The purpose is to design an observer-based controller and a switching rule to ensure both exponential stability and strict dissipativity of the resulting closed-loop switched systems. Using an augmented switched Lyapunov–Krasovskii functional with triple sum and the improved reciprocally convex combination approach, new sufficient conditions are developed in terms of linear matrix inequalities. Simulation examples are included to demonstrate the validity and effectiveness of the proposed design technique.

1 Introduction

As a class of hybrid systems, switched systems can describe several physical processes. A switched system is defined by a collection of dynamical subsystems and a logical rule that supervises or monitors the inter-working status among the subsystems. Recently, switched systems have been used to describe many engineering processes including communication networks, flight and air traffic systems, chemical processes, power systems, etc. Significant research efforts have been devoted to the basic problems of stability and control design of switched systems. The reader can refer to papers [1–4] and the references cited therein. However, all the cited works are mainly interested to arbitrary switching signal to study the problem of stability and control design of switched systems. Thus, many switched systems fail to preserve stability under arbitrary switching signals, but may be stable under some prescribed switching signals. Then, the study of switched system under the average dwell time (ADT) approach is significant theoretically as well as practically. The ADT switching means that the number of switches in a finite interval is bounded and the average time interval between consecutive switching mode is no less than a specified τ_a^* . For slow switching systems, ADT technique has been suggested in several papers to cope with the stability problem (see [5–7] and the references therein).

As is well known, there always exists many real plants involving intrinsically a time delay which can be the main cause of instability and poor performance of dynamic systems. Many results towards time-delay systems have been developed (see [8, 9] and their bibliographies). The research on switched systems with delays has also received growing attention in recent years and several methods have been developed to deal with such systems.

By taking the advantage of a Lyapunov functional with triple sum terms, the problem of exponential $l_2 - l_\infty$ output controller has been studied in [10] for a class of discrete-time switched systems with time-varying delay. Based on the free-weighting matrix and the Jensen's integral inequality approaches, the problems of passivity and passification for a class of uncertain switched systems subject to stochastic disturbance and time-varying delay have been treated in [11].

In [12], a new summation inequality based on the Wirtinger-based integral inequality has been introduced to improve the usual Jensen inequality method and to cope with the problem of

dissipative and $l_2 - l_\infty$ filtering for discrete switched neural networks with constant time delay. Recently, the combination of Wirtinger-based inequality with the reciprocally convex method has been investigated in [13] to derive a less conservative criterion. Generally speaking, the use of reciprocally convex approach combined with Wirtinger-based inequality and the triple sum Lyapunov–Krasovskii functional usually yields less conservative results. This motivates us to combine the three techniques to revisit the stability analysis problem of discrete-time switched delayed systems.

On another research front, the notion of dissipativity, which is closely related to the notion of energy, is considered as a most important concept in system theory for theoretical considerations as well as from a practical point of view. Dissipative theory, which encompasses H_∞ performance and passivity, provides a framework for robust analysis and control design for different types of systems. Considerable attention has been devoted to the study of dissipativity for linear and non-linear systems and a variety of results has been reported. For example, the authors in [14] have considered the problem of a small-gain for stochastic network systems by the aid of conditional dissipativity. Based on parameterising the solutions of the constraint set, the problems of dissipative control and filtering of discrete-time singular systems have been investigated in [15]. The issue of reliable load frequency control design of an uncertain multi-area power system with constant time delays and disturbances via non-fragile sampled-data control approach has been studied in [16]. In [17], the problem of dissipative-based non-fragile controller for network-based singular systems with event-triggered sampling scheme has been treated. The problems arising from switched systems are significant. For a class of continuous switched systems and using ADT approach, sufficient conditions have been reported in [18–20] to design state feedback controller, sliding mode control and filter, respectively. For the class of discrete systems, the problem of stability has been developed in [21, 22]. In [23], the problem of dissipative control for a class of continuous Markov jump systems has been addressed.

It should be noted that the aforementioned results for switched systems are developed upon the premise that the system states are totally measured. However, the non-existence of appropriate sensors to measure some states, or the increased number of sensors make the whole system more complex, the state variables are generally partially available. The static output-feedback control

strategy has been studied and excellently implemented in various cases [13, 24]. The dynamic output feedback control design scheme has been also considered for switched systems in [25, 26]. It is noted that even the static output control strategy can be easily implemented, the controller synthesis becomes complex especially when the noise affects the measurement. For a such case, the design of observers to estimate the system states is more reasonable and promising. Accordingly, a great work of literature has appeared on the observer-based control problem for switched systems. In [27], the problem of observer-based control for a class of switched networked systems has been studied. The authors in [28] have considered the problem of observer fault detection for uncertain discrete-time switched systems with constant delay. For a class of switched systems, the problem of observer-based dissipative control design have been addressed in [29]. Recently, the issue of observer-based finite-time stabilisation for discrete-time switched singular systems with quadratically inner-bounded non-linear terms has been developed in [30]. Unfortunately, up to date, the problem of exponential dissipative control for discrete-time switched systems with state delay in the presence of unmeasurable states and external disturbances has not been fully investigated. This constitutes a further motivation to carry out this study.

This paper presents a new observer-based control scheme which may be a worthy addition of the output feedback approach for switched systems subject of unmeasured states, external disturbances and time delay. The key novelty covers the following:

- Based on the ADT approach, the exponential stability as well as the strict dissipativity of the system under consideration are analysed.
- Using the discrete Wirtinger-based inequality approach and an appropriate Lyapunov–Krasovskii functional with a triple sum term, a new delay-dependent sufficient criterion is derived which is expected to be less conservative.
- The cone complement linearisation (CCL) method is adopted to design a switched observer-based controller so that the corresponding closed loop system is exponential stable with a strict $(\mathcal{Q}, \mathcal{S}, \mathcal{R})$ -dissipativity. In fact, neither the SVD decomposition [31, 32] nor the pseudo inverse of the output matrix [33] are applied.

The rest of the paper is organised as follows. Preliminaries and system description are introduced in Section 2. Stability and dissipativity analyses are studied in Section 3. Section 4 is dedicated to dissipative observer-based control design for delayed switched systems. Section 5 shows the potential and the validity of the proposed strategy by three numerical examples. Conclusion and remarks are given in Section 6.

Notations Throughout the paper a real-symmetric matrix $Y > 0$ ($Y \geq 0$) denotes Y being a positive definite (or positive semi-definite) matrix. $\text{sym}(Y)$ stands for $Y + Y^T$. I and 0 symbolise the identity matrix and a zero matrix with appropriate dimension, respectively. Superscript ‘T’ stands for matrix transposition. $Y \in \mathbb{R}^s$ denotes the s -dimensional Euclidean space, while $Y \in \mathbb{R}^{s \times n}$ refers to the set of all $s \times n$ real matrices. $\lambda_{\min}(P)$ and $\lambda_{\max}(P)$ denote the minimum and maximum eigenvalues of P , respectively. $l_2[0, \infty)$ is the space of square summable vectors. In symmetric block matrices or long matrix expressions, we use a star * to represent a term that is induced by symmetry. Matrices, if their dimensions are not explicitly stated, are assumed to be compatible for algebraic operations. $\| \cdot \|$ denotes the Euclidean norm of a vector and its induced.

2 System description and preliminaries

A discrete-time switched linear system with time-varying delay in the presence of external disturbances can be described as follows:

$$\begin{cases} x(k+1) = A_{\sigma(k)}x(k) + A_{d\sigma(k)}x(k-d(k)) + B_{1\sigma(k)}u(k) \\ \quad + D_{1\sigma(k)}w(k) \\ y(k) = C_{\sigma(k)}x(k) + D_{2\sigma(k)}w(k) \\ z(k) = C_{z\sigma(k)}x(k) + B_{z\sigma(k)}u(k) \\ x(k) = \phi(k), k \in [-d_M, 0] \end{cases} \quad (1)$$

where $x(k) \in \mathbb{R}^n$ is the state vector, $u(k) \in \mathbb{R}^m$ is the control input vector, $w(k) \in \mathbb{R}^r$ is the disturbance input, $z(k) \in \mathbb{R}^q$ is the controller output vector, $y(k) \in \mathbb{R}^p$ is the measured output vector, switching signal $\sigma(k): \mathbb{Z}^+ \rightarrow \{1, 2, \dots, N\}$ defines which subsystem will be activated and N represents the number of subsystems. Delay $d(k)$ is time-varying and satisfies

$$0 < d_m \leq d(k) \leq d_M \quad (2)$$

with d_m and d_M are positive integers and represent, respectively, the lower and upper bounds of the time-varying delay. $A_{\sigma(k)}$, $A_{d\sigma(k)}$, $B_{1\sigma(k)}$, $D_{1\sigma(k)}$, $C_{\sigma(k)}$, $D_{2\sigma(k)}$, $C_{z\sigma(k)}$ and $B_{z\sigma(k)}$ are known constant matrices.

We state some definitions for later development.

Consider the following nominal unforced switched delay system with $u(k) = 0$:

$$\begin{cases} x(k+1) = A_{\sigma(k)}x(k) + A_{d\sigma(k)}x(k-d(k)) + D_{\sigma(k)}w(k) \\ z(k) = C_{z\sigma(k)}x(k) \end{cases} \quad (3)$$

To characterize the exponential stability and the switching signal, the following two definitions are recalled [34].

Definition 1: System (3) with $w(k) = 0$ is exponentially stable, if the solution $x(k)$ satisfies $\|x(k)\| \leq \delta \varpi^{k-k_0} \|x(k_0)\|$, $\forall k > k_0$, for constant $\delta > 0$ and $0 < \varpi < 1$, where $\|x(k)\|_L = \sup_{L=0, \dots, d_M} \{ \|x(k)\|, \dots, \|x(k-L)\|, \|x(k) - x(k-1)\|, \|x(k+1-L) - x(k-L)\| \}$

Definition 2: For switching signal $\sigma(k)$ and any $k_s > k_a > k_0$, let $N_{\sigma(k)}(k_a, k_s)$ be the switching numbers of $\sigma(k)$ over interval $[k_a, k_s]$. If for given $N_0 \geq 0$ and $\tau_a \geq 0$, we have $N_{\sigma(k)}(k_a, k_s) \leq N_0 + (k_s - k_a)/\tau_a$, then τ_a and N_0 are called ADT and the chatter bound. For simplicity, we choose $N_0 = 0$.

Similar to [35] the problem of dissipativity can be formulated as follows:

Definition 3: Given matrices \mathcal{Q} , \mathcal{S} , and \mathcal{R} where \mathcal{Q} and \mathcal{R} are symmetric. Switched system (3) is called strictly $(\mathcal{Q}, \mathcal{S}, \mathcal{R})$ - γ -dissipative, if for some scalar $\gamma > 0$ the following condition is satisfied under zero initial state:

$$\langle z, \mathcal{Q}z \rangle_T + 2\langle z, \mathcal{S}w \rangle_T + \langle w, \mathcal{R}w \rangle_T \geq \gamma \langle w, w \rangle_T, \quad \forall T \geq 0 \quad (4)$$

where γ is the dissipativity rate and $\langle r, s \rangle_T$ denotes $\sum_{k=0}^T r^T(k)s(k)$.

Remark 1: From Definition 3, the notion of $(\mathcal{Q}, \mathcal{S}, \mathcal{R})$ -dissipativity includes H_∞ performance and strict passivity as special cases by choosing different values for \mathcal{Q} , \mathcal{R} and \mathcal{S} .

- If $\mathcal{Q} = -I$, $\mathcal{R} = \gamma^2 I$ and $\mathcal{S} = 0$, inequality (4) reduces to an H_∞ performance requirement.
- If $\mathcal{Q} = 0$, $\mathcal{R} = 0$ and $\mathcal{S} = I$, inequality (4) corresponds to a strict passivity or strictly positive realness.
- If $\mathcal{Q} = -\theta I$, $\mathcal{R} = \theta \gamma^2 I$ and $\mathcal{S} = (1 - \theta)I$, $\theta \in [0, 1]$ be a given scalar weight representing a trade off between H_∞ and positive real performance, then $(\mathcal{Q}, \mathcal{S}, \mathcal{R})$ -dissipativity reduces to the mixed H_∞ and positive real performance.

Without loss of generality, it is assumed that $\mathcal{Q} < 0$.

For the purposes of development the following lemmas are reminded from [36] and [10].

Lemma 1: For a given positive definite matrix Z and three non-negative integers h_1, h_2 and k satisfying $h_1 \leq h_2 \leq k$, denote

$$\varphi(k, h_1, h_2) = \begin{cases} \frac{1}{h_2 - h_1} \left[2 \sum_{s=k-h_2}^{k-h_1-1} x(s) + x(k-h_1) + x(k-h_2) \right] & h_1 < h_2 \\ 2x(k-h_1) & h_1 = h_2 \end{cases}$$

Then we have

$$-(h_2 - h_1) \sum_{s=k-h_2}^{k-h_1-1} \eta^T(s) Z \eta(s) \leq - \begin{bmatrix} \chi_1 \\ \chi_2 \end{bmatrix}^T \begin{bmatrix} Z & 0 \\ 0 & 3Z \end{bmatrix} \times \begin{bmatrix} \chi_1 \\ \chi_2 \end{bmatrix},$$

where $\eta(k) = x(k+1) - x(k)$

$$\begin{aligned} \chi_1 &= x(k-h_1) - x(k-h_2), \\ \chi_2 &= x(k-h_1) + x(k-h_2) - \varphi(k, h_1, h_2). \end{aligned}$$

Lemma 2: Let Z_1 and Z_2 two positive matrices with appropriate dimensions. The improved reciprocally convex combination guarantees that, if there exists a matrix Y such that

$$\begin{bmatrix} Z_1 & Y \\ Y^T & Z_2 \end{bmatrix} \geq 0,$$

then the following inequality holds for any scalar κ in the interval $[0, 1]$:

$$\begin{bmatrix} \frac{1}{\kappa} Z_1 & 0 \\ 0 & \frac{1}{1-\kappa} Z_2 \end{bmatrix} \geq \begin{bmatrix} Z_1 & Y \\ Y^T & Z_2 \end{bmatrix}. \quad (5)$$

Lemma 3: For any matrix $V > 0$, R_1, R_2 and a scalar $d > 0$, the following inequality holds:

$$\begin{aligned} & - \sum_{n=-d}^1 \sum_{s=k+n}^{k-1} \eta(s)^T V \eta(s) \\ & \leq \zeta_1^T(k) \begin{bmatrix} dR_1^T + dR_1 & -R_1^T + dR_2 \\ * & -R_2^T - R_2 \end{bmatrix} \zeta_1(k) \quad (6) \\ & + \frac{d(d+1)}{2} \zeta_1^T(k) \begin{bmatrix} R_1^T \\ R_2^T \end{bmatrix} V^{-1} [R_1 \quad R_2] \zeta_1(k), \end{aligned}$$

where $\eta(k) = x(k+1) - x(k)$ and $\zeta_1 = [x^T(k) \quad (\sum_{s=k-d}^{k-1} x(s))^T]^T$.

3 ($\mathcal{Q}, \mathcal{S}, \mathcal{R}$)-dissipativity analysis

3.1 Stability analysis

In this section, the problem of exponential stability analysis based on the ADT approach is addressed. According to the lemmas presented above, sufficient conditions are developed to guarantee the exponential stability analysis of switched system (3) with $w(k) = 0$.

Theorem 1: Given two tunable scalars $0 < \alpha < 1$ and $\mu > 1$ and two positive integers d_m and d_M satisfying (2). Switched system (3), with $w(k) = 0$, is exponentially stable, if there exist matrices $P_i > 0, Q_{1i} > 0, Q_{2i} > 0, Q_{3i} > 0, Z_{1i} > 0, Z_{2i} > 0, Z_{3i} > 0, Z_{4i} > 0$

and Y, R_1, R_2 such that the following inequalities hold for all $(i, j) \in \mathbb{I} \times \mathbb{I}$

$$\Omega_i > 0, \quad (7)$$

$$\begin{bmatrix} Y_i & * \\ \sqrt{d_M} \mathbb{R} H_R & -\alpha^{d_M} Z_{4i} \end{bmatrix} < 0, \quad (8)$$

where

$$\begin{aligned} Y_i &= \Phi_i + H_1^T P_i H_1 - \alpha H_2^T P_i H_2 + H_3^T (d_m^2 Z_{1i} + d_r^2 Z_{2i} \\ & \quad + d_M^2 Z_{3i} + \tilde{d}_M Z_{4i}) H_3 - \Pi^T \Omega_i \Pi + H_R^T \Pi_R H_R, \\ \Phi_i &= \text{diag}(Q_{1i} + Q_{2i} + (d_r + 1) Q_{3i}, -\alpha^{d_m} Q_{1i}, -\alpha^{d_M} Q_{3i}, \\ & \quad -\alpha^{d_M} Q_{2i}; 0; 0; 0; 0; 0), \\ H_1 &= \begin{bmatrix} A_i & 0 & A_{di} & 0 & 0 & 0 & 0 & 0 & 0 \\ I_n & 0 & 0 & -I_n & 0 & 0 & 0 & 0 & I_n \end{bmatrix}, \\ H_2 &= \begin{bmatrix} I_n & 0 & 0 & 0 & 0 & 0 & 0 & 0 & 0 \\ 0 & 0 & 0 & 0 & 0 & 0 & 0 & 0 & I_n \end{bmatrix}, \\ H_R &= \begin{bmatrix} I_n & 0 & 0 & 0 & 0 & 0 & 0 & 0 & 0 \\ 0 & 0 & 0 & 0 & 0 & 0 & 0 & 0 & I_n \end{bmatrix}, \\ \Pi_R &= \begin{bmatrix} d_M R_1^T + d_M R_1 & -R_1^T + d_M R_2 \\ * & -R_2^T - R_2 \end{bmatrix}, \end{aligned} \quad (9)$$

$$\begin{aligned} \Omega_i &= \begin{bmatrix} Z_{1i} & 0 & 0 & 0 \\ 0 & Z_{2i} & Y & 0 \\ 0 & Y^T & Z_{2i} & 0 \\ 0 & 0 & 0 & Z_{3i} \end{bmatrix}, \\ Z_{1i} &= \begin{bmatrix} \alpha^{d_m-1} Z_{1i} & 0 \\ 0 & 3\alpha^{d_m-1} Z_{1i} \end{bmatrix}, \\ Z_{3i} &= \begin{bmatrix} \alpha^{d_M-1} Z_{3i} & 0 \\ 0 & 3\alpha^{d_M-1} Z_{3i} \end{bmatrix}, \\ H_3 &= [A_i - I_n \quad 0 \quad A_{di} \quad 0 \quad 0 \quad 0 \quad 0 \quad 0 \quad 0], \\ Z_{2i} &= \begin{bmatrix} \alpha^{d_M-1} Z_{2i} & 0 \\ 0 & 3\alpha^{d_M-1} Z_{2i} \end{bmatrix}, \end{aligned} \quad (10)$$

$$\Pi = \begin{bmatrix} I_n & -I_n & 0 & 0 & 0 & 0 & 0 & 0 & 0 \\ I_n & I_n & 0 & 0 & -I_n & 0 & 0 & 0 & 0 \\ 0 & I_n & -I_n & 0 & 0 & 0 & 0 & 0 & 0 \\ 0 & I_n & I_n & 0 & 0 & -I_n & 0 & 0 & 0 \\ 0 & 0 & I_n & -I_n & 0 & 0 & 0 & 0 & 0 \\ 0 & 0 & I_n & I_n & 0 & 0 & -I_n & 0 & 0 \\ I_n & 0 & 0 & -I_n & 0 & 0 & 0 & 0 & 0 \\ I_n & 0 & 0 & I_n & 0 & 0 & 0 & -I_n & 0 \end{bmatrix},$$

$$\mathbb{R} = [R_1 \quad R_2], d_r = d_M - d_m, \tilde{d}_M = \frac{d_M(d_M + 1)}{2},$$

then system (3) is exponentially stable under any switching sequence with ADT $\tilde{\tau}_a > \tau_a^* = -(\ln \mu / \ln \alpha)$, where μ satisfies

$$\begin{aligned} P_i - \mu P_j &< 0, \quad Q_{1i} - \mu Q_{1j} < 0, \quad Q_{2i} - \mu Q_{2j} < 0, \\ Q_{3i} - \mu Q_{3j} &< 0, \quad Z_{1i} - \mu Z_{1j} < 0, \quad Z_{2i} - \mu Z_{2j} < 0, \\ Z_{3i} - \mu Z_{3j} &< 0, \quad Z_{4i} - \mu Z_{4j} < 0. \end{aligned} \quad (11)$$

Proof: To establish the exponential stability of system (3), with $w(k) = 0$, we choose the following switched Lyapunov-Krasovskii functional candidate for the i th subsystem:

$$\begin{aligned}
V_i(k) &= \sum_{s=1}^6 V_{is}(k), \quad i \in \mathbb{I} \\
V_{i1}(k) &= v^T(k)P_i v(k), \\
V_{i2}(k) &= \sum_{s=k-d_m}^{k-1} x^T(s)\alpha^{k-1-s}Q_{i2}x(s), \\
V_{i3}(k) &= \sum_{s=k-d_M}^{k-1} x^T(s)\alpha^{k-1-s}Q_{i3}x(s), \\
V_{i4}(k) &= \sum_{n=-d_M}^{-d_m} \sum_{s=k+n}^{k-1} x^T(s)\alpha^{k-1-s}Q_{i4}x(s), \\
V_{i5}(k) &= d_m \sum_{n=-d_m+1}^0 \sum_{s=k+n}^{k-1} \eta^T(s)\alpha^{k-1-s}Z_{i1}\eta(s) \\
&\quad + d_r \sum_{n=-d_M}^{-d_m} \sum_{s=k+n}^{k-1} \eta^T(s)\alpha^{k-1-s}Z_{i2}\eta(s) \\
&\quad + d_M \sum_{n=-d_M+1}^0 \sum_{s=k+n}^{k-1} \eta^T(s)\alpha^{k-1-s}Z_{i3}\eta(s), \\
V_{i6}(k) &= \sum_{s=-d_M}^{-1} \sum_{n=s}^{-1} \sum_{m=k+n}^{k-1} \alpha^{k-1-m}\eta^T(m)Z_{i4}\eta(m),
\end{aligned} \tag{12}$$

where $\eta(k) = x(k+1) - x(k)$ and

$$v(k) = \begin{bmatrix} x(k) \\ \sum_{s=k-d_M}^{k-1} x(s) \end{bmatrix}. \tag{13}$$

Let $\psi_1(k) = \varphi(k, 0, d_m)$, $\psi_2(k) = \varphi(k, d_m, d(k))$, $\psi_3(k) = \varphi(k, d(k), d_M)$, $\psi_4(k) = \varphi(k, 0, d_M)$ and augmented vector (see (14)).

Defining $\Delta_\alpha V_i(k) = V_i(k+1) - \alpha V_i(k)$, for $k \in [k_r, k_{r+1})$, the following equations yield:

$$\Delta_\alpha V_{i1}(k) = v^T(k+1)P_i v(k+1) - \alpha v^T(k)P_i v(k), \tag{15}$$

where

$$\begin{aligned}
v(k+1) &= \begin{bmatrix} x(k+1) \\ \sum_{s=k+1-d_M}^k x(s) \end{bmatrix} \\
&= \begin{bmatrix} A_i x(k) + A_{di} x(k-d(k)) \\ x(k) - x(k-d_M) + \sum_{s=k-d_M}^{k-1} x(s) \end{bmatrix} \\
&= H_1 \zeta(k),
\end{aligned} \tag{16}$$

$$v(k) = H_2 \zeta(k), \tag{17}$$

Using (16) and (17), (15) can be written as

$$\begin{aligned}
\Delta_\alpha V_{i1}(k) &= \zeta^T(k)H_1^T P_i H_1 \zeta(k) - \zeta^T(k)H_2^T \alpha P_i H_2 \zeta(k), \\
\Delta_\alpha V_{i2}(k) &= x^T(k)Q_{i2}x(k) - x^T(k-d_m)\alpha^{d_m}Q_{i2}x(k-d_m), \\
\Delta_\alpha V_{i3}(k) &= x^T(k)Q_{i3}x(k) - x^T(k-d_M)\alpha^{d_M}Q_{i3}x(k-d_M), \\
\Delta_\alpha V_{i4}(k) &= (d_r+1)x^T(k)Q_{i4}x(k)
\end{aligned} \tag{18}$$

$$\begin{aligned}
&\quad - \sum_{s=k-d_M}^{k-d_m} x^T(s)\alpha^{k-s}Q_{i4}x(s) \\
&\leq (d_r+1)x^T(k)Q_{i4}x(k) \\
&\quad - x^T(k-d(k))\alpha^{d_M}Q_{i4}x(k-d(k)),
\end{aligned}$$

$$\begin{aligned}
\Delta_\alpha V_{i5}(k) &\leq \eta^T(k)(d_m^2 Z_{i1} + d_r^2 Z_{i2} + d_M^2 Z_{i3})\eta(k) \\
&\quad - d_m \sum_{s=k-d_m+1}^k \eta^T(s)\alpha^{d_m-1}Z_{i1}\eta(s) \\
&\quad - d_r \sum_{s=k-d(k)+1}^{k-d_m} \eta^T(s)\alpha^{d_M-1}Z_{i2}\eta(s) \\
&\quad - d_r \sum_{s=k-d_M+1}^{k-d(k)} \eta^T(s)\alpha^{d_M-1}Z_{i2}\eta(s) \\
&\quad - d_M \sum_{s=k-d_M+1}^k \eta^T(s)\alpha^{d_M-1}Z_{i3}\eta(s).
\end{aligned}$$

According to Lemma 1, we can deduce that

$$\begin{aligned}
&-d_m \sum_{s=k-d_m+1}^k \eta^T(s)\alpha^{d_m-1}Z_{i1}\eta(s) \\
&\leq - \begin{bmatrix} x(k) - x(k-d_m) \\ x(k) + x(k-d_m) - \psi_1(k) \end{bmatrix}^T \\
&\quad \times \mathbb{Z}_{i1} \begin{bmatrix} x(k) - x(k-d_m) \\ x(k) + x(k-d_m) - \psi_1(k) \end{bmatrix},
\end{aligned} \tag{19}$$

$$\begin{aligned}
&-d_r \sum_{s=k-d(k)+1}^{k-d_m} \eta^T(s)\alpha^{d_M-1}Z_{i2}\eta(s) \\
&\leq - \frac{d_r}{d(k)-d_m} \begin{bmatrix} x(k-d_m) - x(k-d(k)) \\ x(k-d_m) + x(k-d(k)) - \psi_2(k) \end{bmatrix}^T \\
&\quad \times \mathbb{Z}_{i2} \begin{bmatrix} x(k-d_m) - x(k-d(k)) \\ x(k-d_m) + x(k-d(k)) - \psi_2(k) \end{bmatrix},
\end{aligned} \tag{20}$$

$$\begin{aligned}
&-d_r \sum_{s=k-d_M+1}^{k-d(k)} \eta^T(s)\alpha^{d_M-1}Z_{i2}\eta(s) \\
&\leq - \frac{d_r}{d_M-d(k)} \begin{bmatrix} x(k-d(k)) - x(k-d_M) \\ x(k-d(k)) + x(k-d_M) - \psi_3(k) \end{bmatrix}^T \\
&\quad \times \mathbb{Z}_{i2} \begin{bmatrix} x(k-d(k)) - x(k-d_M) \\ x(k-d(k)) + x(k-d_M) - \psi_3(k) \end{bmatrix},
\end{aligned} \tag{21}$$

$$\begin{aligned}
&-d_M \sum_{s=k-d_M+1}^k \eta^T(s)\alpha^{d_M-1}Z_{i3}\eta(s) \\
&\leq - \begin{bmatrix} x(k) - x(k-d_M) \\ x(k) + x(k-d_M) - \psi_4(k) \end{bmatrix}^T \\
&\quad \times \mathbb{Z}_{i3} \begin{bmatrix} x(k) - x(k-d_M) \\ x(k) + x(k-d_M) - \psi_4(k) \end{bmatrix}.
\end{aligned} \tag{22}$$

$$\zeta(k) = \begin{bmatrix} x^T(k) & x^T(k-d_m) & x^T(k-d(k)) & x^T(k-d_M)\psi_1^T(k) & \psi_2^T(k) & \psi_3^T(k) & \psi_4^T(k) & \left(\sum_{s=k-d_M}^{k-1} x(s) \right)^T \end{bmatrix}^T. \tag{14}$$

From (19)–(22), $\Delta_\alpha V_{is}(k)$ can be expressed as follows:

$$\Delta_\alpha V_{is}(k) \leq \eta^T(k)(d_m^2 Z_{1i} + d_r^2 Z_{2i} + d_M^2 Z_{3i})\eta(k) - \zeta^T(k)\Pi^T \begin{bmatrix} Z_{1i} & 0 & 0 & 0 \\ 0 & \frac{1}{\kappa(k)}Z_{2i} & 0 & 0 \\ 0 & 0 & \frac{1}{1-\kappa(k)}Z_{2i} & 0 \\ 0 & 0 & 0 & Z_{3i} \end{bmatrix} \Pi \zeta(k), \quad (23)$$

where $\kappa(k) = (d(k) - d_m)/d_r$. Then, according to Lemma 2, the following inequality holds for a suitable matrix $Y \in \mathbb{R}^{2n \times 2n}$.

$$\Delta_\alpha V_{is}(k) \leq \zeta^T(k)(H_3^T(d_m^2 Z_{1i} + d_r^2 Z_{2i} + d_M^2 Z_{3i})H_3 - \Pi^T \Omega_i \Pi)\zeta(k). \quad (24)$$

Next, we calculate

$$\begin{aligned} \Delta_\alpha V_{i6}(k) &= \sum_{s=-d_M}^{-1} \sum_{n=s}^{-1} [\eta^T(k)Z_{4i}\eta(k) - \alpha^{-n}\eta^T(k+n)Z_{4i}\eta(k+n)] \\ &= \sum_{s=-d_M}^{-1} -s\eta^T(k)Z_{4i}\eta(k) \\ &\quad - \sum_{s=-d_M}^{-1} \sum_{n=k+s}^{k-1} \alpha^{-n}\eta^T(n)Z_{4i}\eta(n) \\ &\leq \frac{d_M(d_M+1)}{2}\eta^T(k)Z_{4i}\eta(k) \\ &\quad - \sum_{s=-d_M}^{-1} \sum_{n=k+s}^{k-1} \eta^T(n)\alpha^{d_M}Z_{4i}\eta(n). \end{aligned} \quad (25)$$

Based on Lemma 3, the following inequality holds:

$$\begin{aligned} \Delta_\alpha V_{i6}(k) &\leq \frac{d_M(d_M+1)}{2}\eta^T(k)Z_{4i}\eta(k) \\ &\quad + \zeta_1^T(k) \begin{bmatrix} d_M R_1^T + d_M R_1 & -R_1^T + d_M R_2 \\ * & -R_2^T - R_2 \end{bmatrix} \zeta_1(k) \\ &\quad + \frac{d_M(d_M+1)}{2}\zeta_1^T(k) \begin{bmatrix} R_1^T \\ R_2^T \end{bmatrix} (\alpha^{d_M} Z_{4i})^{-1} [R_1 \quad R_2] \zeta_1(k), \end{aligned} \quad (26)$$

where $\zeta_1(k) = [x^T(k) \quad (\sum_{s=k-d_M}^{k-1} x(s))^T]^T$.

From (18)–(26), we have

$$\Delta_\alpha V_i(k) \leq \zeta^T(k)(Y_i + (\tilde{d}_M \mathbb{R} H_R)^T (\alpha^{d_M} Z_{4i})^{-1} \times (\tilde{d}_M \mathbb{R} H_R))\zeta(k). \quad (27)$$

Performing to Schur complement, we can verify (8).

Now we are in a position to demonstrate the exponential stability.

For $k \in [k_r, k_{r+1})$, the i th subsystem is activated and the following inequality can be verified:

$$V_{\sigma(k)}(k) \leq \alpha^{k-k_r} V_{\sigma(k_r)}(k_r). \quad (28)$$

From (11), we get

$$\begin{aligned} V_{\sigma(k)}(k) &\leq \alpha^{k-k_r} \mu V_{\sigma(k_r-1)}(k_r) \\ &\leq \dots \leq \alpha^{k-k_0} \mu^{(k-k_0)/\bar{\tau}_a} V_{\sigma(k_0)}(k_0) \\ &= (\alpha \mu^{1/\bar{\tau}_a})^{k-k_0} V_{\sigma(k_0)}(k_0). \end{aligned} \quad (29)$$

Moreover, from the definition of the Lyapunov–Krasovskii function in (12), we have

$$\delta \|x(k)\|^2 \leq V_{\sigma(k)}(k); \quad V_{\sigma(k_0)}(k_0) \leq \rho \|x(k_0)\|_L^2, \quad (30)$$

where

$$\begin{aligned} \delta &= \min_{i \in \mathbb{I}} \lambda_{\min}(P_i), \\ \rho &= \max_{i \in \mathbb{I}} \left[\lambda_{\max}(P_i) + \frac{\alpha}{\alpha-1} \lambda_{\max}(Q_{1i}) + \frac{\alpha}{\alpha-1} \lambda_{\max}(Q_{2i}) \right. \\ &\quad + \frac{\alpha(d_M - d_m + 1)}{\alpha-1} \lambda_{\max}(Q_{3i}) + d_m^2 \frac{\alpha}{\alpha-1} \lambda_{\max}(Z_{1i}) \\ &\quad + d_r(d_r + 1) \frac{\alpha}{\alpha-1} \lambda_{\max}(Z_{2i}) + d_M^2 \frac{\alpha}{\alpha-1} \lambda_{\max}(Z_{3i}) \\ &\quad \left. + \frac{\alpha d_M(d_M + 1)}{2(\alpha-1)} \lambda_{\max}(Z_{4i}) \right]. \end{aligned}$$

Let $\varpi = \sqrt{\alpha \mu^{1/\bar{\tau}_a}}$. Combining (29) and (30), the system state satisfies

$$\|x(k)\|^2 \leq \frac{1}{\delta} V_{\sigma(k_r)}(k) \leq \frac{\rho}{\delta} \varpi^{2(k-k_0)} \|x(k_0)\|_L^2, \quad (31)$$

which further implies that

$$\|x(k)\| \leq \sqrt{\frac{\rho}{\delta}} \varpi^{(k-k_0)} \|x(k_0)\|_L. \quad (32)$$

Then, according to Definition 1, we can conclude that the system is exponentially stable with decay rate $\varpi = \sqrt{\alpha \mu^{1/\bar{\tau}_a}}$. This completes the proof. \square

Remark 2:

- The main feature of Theorem 1 is neither the model transformation nor the bounding techniques are used to estimate the upper bound of the cross product terms (see [34, 37, 38]).
- To bound the terms in $\Delta_\alpha V_{is}(k)$, different methods can be used from the literature to reduce the conservatism of the obtained criteria. In [11, 39], Jensen's inequality has been used, the Wirtinger inequality has been introduced in [12] and the input–output transformation with scaled small-gain approach has been suggested in [2]. However, the key merit of the proposed criterion lies in the combination of the Wirtinger-based integral and the improved reciprocally convex approaches. Different to [13], this study exhibits an appropriate Lyapunov–Krasovskii functional with triple sum terms to get less conservative results.

3.2 Dissipativity analysis

Based on the new stability condition developed in the above theorem, this subsection is deduced to investigate the $(\mathcal{Q}, \mathcal{S}, \mathcal{R})$ - γ -dissipativity problem for switched system with time-varying delay (3).

Theorem 2: Given positive integers d_m and d_M satisfying (2), scalars $0 < \alpha < 1$ and $\mu > 1$ and matrices $\mathcal{Q} < 0$, \mathcal{R} and \mathcal{S} . If there exist matrices $P_i > 0$, $Q_{1i} > 0$, $Q_{2i} > 0$, $Q_{3i} > 0$, $Z_{1i} > 0$, $Z_{2i} > 0$, $Z_{3i} > 0$, $Z_{4i} > 0$, Y , R_1 , R_2 and a scalar $\gamma_0 > 0$ such that the following inequalities hold for all $(i, j) \in \mathbb{I} \times \mathbb{I}$:

$$\Omega_i > 0, \quad (33)$$

$$\begin{bmatrix} \bar{Y}_i & * \\ \sqrt{\tilde{d}_M} \mathbb{R} \bar{H}_R & -\alpha^{d_M} Z_{4i} \end{bmatrix} < 0, \quad (34)$$

where

$$\begin{aligned} \tilde{Y}_i &= \tilde{\Phi}_i + \tilde{H}_1^T(d_i)P_i\tilde{H}_1 - \alpha\tilde{H}_2^T P_i\tilde{H}_2 + \tilde{H}_3^T(d_m^2 Z_{1i} + d_r^2 Z_{2i} \\ &\quad + d_M^2 Z_{3i} + \tilde{d}_M Z_{4i})\tilde{H}_3 + \tilde{H}_R^T \Pi_R \tilde{H}_R - \tilde{\Pi}^T \Omega_i \tilde{\Pi} \\ &\quad - \text{sym}(H_z \mathcal{S} H_w) - H_z^T \mathcal{Q} H_z, \\ \tilde{\Phi}_i &= \text{diag}(Q_{1i} + Q_{2i} + (d_r + 1)Q_{3i}; -\alpha^{d_m} Q_{1i}; \\ &\quad -\alpha^{d_M} Q_{3i}; -\alpha^{d_M} Q_{2i}; 0; 0; 0; 0; 0; 0; (-\mathcal{R} + \gamma_0 I)), \quad (35) \\ \tilde{H}_1 &= [H_1 \quad \mathbb{D}_{1i}], \quad \tilde{H}_2 = [H_2 \quad 0], \quad \tilde{H}_3 = [H_3 \quad D_{1i}], \\ \tilde{\Pi} &= [\Pi \quad 0], \quad \tilde{H}_R = [H_R \quad 0], \quad \mathbb{D}_{1i} = \begin{bmatrix} D_{1i} \\ 0 \end{bmatrix}, \\ H_w &= [0 \quad 0 \quad 0 \quad 0 \quad 0 \quad 0 \quad 0 \quad 0 \quad 0 \quad I], \\ H_z &= [C_{zi} \quad 0 \quad 0 \quad 0 \quad 0 \quad 0 \quad 0 \quad 0 \quad 0 \quad 0]. \end{aligned}$$

Then, system (3) is exponentially stable under a strict $(\mathcal{Q}, \mathcal{S}, \mathcal{R})$ - γ -dissipative rate γ , given by $\gamma = \gamma_0 \mu (\alpha^{\lambda+1} - \alpha^\lambda)$, with $\lambda > 1$ and for any switching sequence with ADT $\tau_a \geq \lambda \tau_a^*$ where μ satisfies

$$\begin{aligned} P_i - \mu P_j &< 0, \quad Q_{1i} - \mu Q_{1j} < 0, \quad Q_{2i} - \mu Q_{2j} < 0, \\ Q_{3i} - \mu Q_{3j} &< 0, \quad Z_{1i} - \mu Z_{1j} < 0, \quad Z_{2i} - \mu Z_{2j} < 0, \quad (36) \\ Z_{3i} - \mu Z_{3j} &< 0, \quad Z_{4i} - \mu Z_{4j} < 0. \end{aligned}$$

Proof: To deal with the dissipativity performance for system (3), we consider the Lyapunov–Krasovskii functional as in (12). Define

$$\mathcal{F}(k) = \mathcal{F}_1(k) + \gamma_0 w^T(k)w(k), \quad (37)$$

$$\mathcal{F}_1(k) = -z^T(k)\mathcal{Q}z(k) - 2z^T(k)\mathcal{S}w(k) - w^T(k)\mathcal{R}w(k). \quad (38)$$

By following the same procedure used in Theorem 1 with $w(k) \neq 0$, it is easy to verify from (34) that

$$V_i(k+1) - \alpha V_i(k) + \mathcal{F}(k) \leq 0, \quad i \in \mathbb{I} \quad (39)$$

Then, for $k \in [k_r, k_{r+1})$, we have

$$V_{\sigma(k)}(k) \leq \alpha^{k-k_r} V_{\sigma(k_r)}(k_r) - \sum_{s=k_r}^{k-1} \alpha^{k-1-s} \mathcal{F}(s). \quad (40)$$

By iteration operation, yields

$$\begin{aligned} V_{\sigma(k)}(k) &\leq \alpha^{k-k_r} \mu \left[\alpha^{k_r-k_{r-1}} V_{\sigma(k_{r-1})}(k_{r-1}) \right. \\ &\quad \left. - \sum_{s=k_{r-1}}^{k_r-1} \alpha^{k_r-1-s} \mathcal{F}(s) \right] - \sum_{s=k_r}^{k-1} \alpha^{k-1-s} \mathcal{F}(s) \\ &\leq \alpha^{k-k_{r-1}} \mu^2 \left[\alpha^{k_{r-1}-k_{r-2}} V_{\sigma(k_{r-2})}(k_{r-2}) \right. \\ &\quad \left. - \sum_{s=k_{r-2}}^{k_{r-1}-1} \alpha^{k_{r-1}-1-s} \mathcal{F}(s) \right] \\ &\quad - \alpha^{k-k_r} \mu \sum_{s=k_{r-1}}^{k_r-1} \alpha^{k_r-1-s} \mathcal{F}(s) \\ &\quad - \sum_{s=k_r}^{k-1} \alpha^{k-1-s} \mathcal{F}(s) \\ &\leq \dots \leq \alpha^{k-k_0} \mu^{N_{\sigma(k)}(k_0, k)} V_{\sigma(k_0)}(k_0) \\ &\quad - \sum_{s=k_0}^{k-1} \mu^{N_{\sigma(k)}(s, k)} \alpha^{k-1-s} \mathcal{F}(s). \end{aligned} \quad (41)$$

Due to the fact that $V_{\sigma(k)}(k) \geq 0$, under zero initial condition $\phi(k) = 0$, we have

$$\sum_{s=k_0}^{k-1} \mu^{N_{\sigma(k)}(s, k)} \alpha^{k-1-s} \mathcal{F}(s) \leq 0. \quad (42)$$

That is

$$\begin{aligned} \gamma_0 \sum_{s=k_0}^{k-1} \mu^{N_{\sigma(k)}(s, k)} \alpha^{k-1-s} w^T(s)w(s) \\ \leq \sum_{s=k_0}^{k-1} \mu^{N_{\sigma(k)}(s, k)} \alpha^{k-1-s} (-\mathcal{F}_1(s)). \end{aligned} \quad (43)$$

Which implies

$$\begin{aligned} \gamma_0 \sum_{s=k_0}^{k-1} \mu \alpha^{k-1-s} w^T(s)w(s) \\ \leq \sum_{s=k_0}^{k-1} \mu^{N_{\sigma(k)}(s, k)} \alpha^{k-1-s} (-\mathcal{F}_1(s)). \end{aligned} \quad (44)$$

Moreover, it follows from Definition 2 that

$$0 \leq N_i(s, k) \leq (k-s)/\tau_a \text{ which is equivalent to } \mu^{N_i(s, k)} = \alpha^{-(1/\lambda)(k-s)}. \text{ Then, we get}$$

$$\gamma_0 \sum_{s=k_0}^{k-1} \mu \alpha^{k-1-s} w^T(s)w(s) \leq \sum_{s=k_0}^{k-1} \alpha^{(1-\frac{1}{\lambda})(k-s)-1} (-\mathcal{F}_1(s)). \quad (45)$$

Thus see the following equation: (see (46))

$$\begin{aligned} \gamma_0 \mu \sum_{k=k_0+1}^{T+1} \sum_{s=k_0}^{k-1} \alpha^{k-s-1} w^T(s)w(s) &\leq \sum_{k=k_0+1}^{T+1} \sum_{s=k_0}^{k-1} \alpha^{(1-\frac{1}{\lambda})(k-s)-1} (-\mathcal{F}_1(s)), \\ \gamma_0 \mu \sum_{s=k_0}^T \sum_{k=s+1}^{T+1} \alpha^{k-s-1} w^T(s)w(s) &\leq \sum_{s=k_0}^T \sum_{k=s+1}^{T+1} \alpha^{(1-\frac{1}{\lambda})(k-s)-1} (-\mathcal{F}_1(s)), \\ \gamma_0 \mu \sum_{s=k_0}^T \alpha^{-s-1} \sum_{k=s+1}^{T+1} \alpha^k w^T(s)w(s) &\leq \sum_{s=k_0}^T \alpha^{(1-\frac{1}{\lambda})(k-s)-1} \sum_{k=s+1}^{T+1} \alpha^{(1-\frac{1}{\lambda})k} (-\mathcal{F}_1(s)), \\ \gamma_0 \mu \sum_{s=k_0}^T \frac{1-\alpha^{T-s+1}}{1-\alpha} w^T(s)w(s) &\leq \alpha^{(-\frac{1}{\lambda})} \sum_{s=k_0}^T \frac{1-\alpha^{(1-\frac{1}{\lambda})(T-s-1)}}{1-\alpha^{(1-\frac{1}{\lambda})}} (-\mathcal{F}_1(s)), \\ \gamma_0 \mu \sum_{s=k_0}^T w^T(s)w(s) &\leq \frac{\alpha^{(-\frac{1}{\lambda})}}{1-\alpha^{(1-\frac{1}{\lambda})}} \sum_{s=k_0}^T (-\mathcal{F}_1(s)). \end{aligned} \quad (46)$$

According to Definition 3, we can conclude that system (3) is strictly $(\mathcal{Q}, \mathcal{S}, \mathcal{R})$ - γ -dissipative with $\gamma = \gamma_0 \mu (\alpha^{\lambda+1} - \alpha^\lambda)$. This completes the proof. \square

Remark 3: As we remark, the ADT $\tilde{\tau}_a$ and the dissipativity rate γ are, respectively, increasing functions on parameter λ . As in [35], this positive scalar $\lambda > 1$ is introduced to make the dissipativity analysis in Theorem 2 easier.

4 Dissipative observer-based control synthesis

It is known that state feedback systems require the measurement of all system states. However, in practical applications, it is not always possible to have access to all state variables and only partial information is available via measured outputs. Hence, the observer-based control is probably well suited in such situation for feedback control. To deal with such problem for system (1), we introduce the following observer:

$$\begin{cases} \hat{x}(k+1) = A_{\sigma(k)}\hat{x}(k) + A_{d\sigma(k)}\hat{x}(k-d(k)) + B_{1\sigma(k)}u(k) \\ \quad + L_{\sigma(k)}(y(k) - \hat{y}(k)) \\ \hat{y}(k) = C_{\sigma(k)}\hat{x}(k) \end{cases} \quad (47)$$

where $\hat{x}(k)$ is the state estimation of $x(k)$, $\hat{y}(k)$ is the observer output and $L_{\sigma(k)} \in \mathbb{R}^{n \times p}$ are the observer gain matrices to be determined.

Including this observer, we are interested in the following form of the observer-based control:

$$u(k) = K_{\sigma(k)}\hat{x}(k), \quad (48)$$

where $K_{\sigma(k)}$ is the controller gain matrices.

Denoting the estimation error as $e(k) = x(k) - \hat{x}(k)$ and combining (1) and (47) with (48), the augmenting closed-loop systems is written as

$$\begin{cases} \tilde{x}(k+1) = \tilde{A}_{\sigma(k)}\tilde{x}(k) + \tilde{A}_{d\sigma(k)}\tilde{x}(k-d(k)) + \tilde{D}_{1\sigma(k)}w(k) \\ Z(k) = \tilde{C}_{z\sigma(k)}\tilde{x}(k) \end{cases} \quad (49)$$

where

$$\begin{aligned} \tilde{x}(k) &= \begin{bmatrix} x(k) \\ e(k) \end{bmatrix}, \quad \tilde{A}_{d\sigma(k)} = \begin{bmatrix} A_{d\sigma(k)} & 0 \\ 0 & A_{d\sigma(k)} \end{bmatrix}, \\ \tilde{A}_{\sigma(k)} &= \begin{bmatrix} A_{\sigma(k)} + B_{1\sigma(k)}K_{\sigma(k)} & -B_{1\sigma(k)}K_{\sigma(k)} \\ 0 & A_{\sigma(k)} - L_{\sigma(k)}C_{\sigma(k)} \end{bmatrix}, \\ \tilde{C}_{z\sigma(k)} &= [C_{z\sigma(k)} + B_{z\sigma(k)}K_{\sigma(k)} \quad -B_{z\sigma(k)}K_{\sigma(k)}], \\ \tilde{D}_{1\sigma(k)} &= \begin{bmatrix} D_{1\sigma(k)} \\ D_{1\sigma(k)} - L_{\sigma(k)}D_{2\sigma(k)} \end{bmatrix}. \end{aligned} \quad (50)$$

Theorem 3: Given two scalars $0 < \alpha < 1$ and $\mu > 1$, two positive integers d_m and d_M satisfying (2), symmetric matrices $\mathcal{Q} < 0$ and \mathcal{R} and matrix \mathcal{S} . Closed-loop system (49) is exponentially stable and strictly $(\mathcal{Q}, \mathcal{S}, \mathcal{R})$ - γ -dissipative, if there exist symmetric positive-definite matrices $\tilde{P}_i, \tilde{P}_i \in \mathbb{R}^{4n \times 4n}$, $\tilde{Q}_{1i}, \tilde{Q}_{2i}, \tilde{Q}_{3i}, \tilde{Z}_{1i}, \tilde{Z}_{2i}, \tilde{Z}_{3i}, \tilde{Z}_{4i}, \tilde{Z}_{1i}, \tilde{Z}_{2i}, \tilde{Z}_{3i}, \tilde{Z}_{4i} \in \mathbb{R}^{2n \times 2n}$ and matrices $\tilde{Y}, \tilde{R}_1, \tilde{R}_2, K_i, L_i$ with appropriate dimension and a scalar $\gamma_0 > 0$ satisfying

$$\tilde{\Gamma}_i < 0; \quad \tilde{\Omega}_i > 0 \quad (51)$$

$$\tilde{P}_i \tilde{P}_i = I, \quad \tilde{Z}_{1i} \tilde{Z}_{1i} = I, \quad \tilde{Z}_{2i} \tilde{Z}_{2i} = I, \quad \tilde{Z}_{3i} \tilde{Z}_{3i} = I, \quad \tilde{Z}_{4i} \tilde{Z}_{4i} = I, \quad (52)$$

where

(see equation below)
(see equation below)

$$\tilde{\Phi}_i = \text{diag}(\tilde{Q}_{1i} + \tilde{Q}_{2i} + (d_r + 1)\tilde{Q}_{3i}; \quad -\alpha^{d_m}\tilde{Q}_{1i}; \quad -\alpha^{d_M}\tilde{Q}_{3i}; \\ -\alpha^{d_M}\tilde{Q}_{2i}; \quad 0; \quad 0; \quad 0; \quad 0; \quad 0; \quad 0; \quad (-\mathcal{R} + \gamma_0 I)),$$

where system (49) is exponentially stable under switching sequence with ADT τ_a satisfies

$$\begin{aligned} \tilde{P}_i - \mu \tilde{P}_j &< 0, \quad \tilde{Q}_{1i} - \mu \tilde{Q}_{1j} < 0, \quad \tilde{Q}_{2i} - \mu \tilde{Q}_{2j} < 0, \\ \tilde{Q}_{3i} - \mu \tilde{Q}_{3j} &< 0, \quad \tilde{Z}_{1i} - \mu \tilde{Z}_{1j} < 0, \quad \tilde{Z}_{2i} - \mu \tilde{Z}_{2j} < 0, \\ \tilde{Z}_{3i} - \mu \tilde{Z}_{3j} &< 0, \quad \tilde{Z}_{4i} - \mu \tilde{Z}_{4j} < 0. \end{aligned}$$

Proof: Performing Theorem 2 to system (49), inequalities in (51) hold with $\tilde{P}_i = \tilde{P}_i^{-1}$, $\tilde{Z}_{1i} = \tilde{Z}_{1i}^{-1}$, $\tilde{Z}_{2i} = \tilde{Z}_{2i}^{-1}$, $\tilde{Z}_{3i} = \tilde{Z}_{3i}^{-1}$ and $\tilde{Z}_{4i} = \tilde{Z}_{4i}^{-1}$. This completes the proof. \square

Remark 4: Due to equality constraints (52), conditions in (51) are not in a strict linear matrix inequality (LMI) form which cannot be solved directly using the standard LMI procedures. For applying the LMI technique, we can formulate this non-convex feasibility problem into a sequential optimisation problem subject to LMIs constraints.

Based on the CCL technique [40], we propose the following minimisation problem involving LMI conditions instead of the original non-convex condition (52).

$$\min \text{Tr} \sum_{i=1}^N (\tilde{P}_i \tilde{P}_i + \tilde{Z}_{1i} \tilde{Z}_{1i} + \tilde{Z}_{2i} \tilde{Z}_{2i} + \tilde{Z}_{3i} \tilde{Z}_{3i} + \tilde{Z}_{4i} \tilde{Z}_{4i}). \quad (53)$$

s.t.:

$$\begin{cases} (51) \\ \begin{bmatrix} \tilde{P}_i & I_{4n} \\ I_{4n} & \tilde{P}_i \end{bmatrix} \geq 0, \quad \begin{bmatrix} \tilde{Z}_{1i} & I_{2n} \\ I_{2n} & \tilde{Z}_{1i} \end{bmatrix} \geq 0, \quad \begin{bmatrix} \tilde{Z}_{2i} & I_{2n} \\ I_{2n} & \tilde{Z}_{2i} \end{bmatrix} \geq 0 \\ \begin{bmatrix} \tilde{Z}_{3i} & I_{2n} \\ I_{2n} & \tilde{Z}_{3i} \end{bmatrix} \geq 0, \quad \begin{bmatrix} \tilde{Z}_{4i} & I_{2n} \\ I_{2n} & \tilde{Z}_{4i} \end{bmatrix} \geq 0 \end{cases} \quad (54)$$

If the solution of the above minimisation problem is $12n \times N$, i.e.

$$\begin{aligned} \min \text{Tr} \sum_{i=1}^N (\tilde{P}_i \tilde{P}_i + \tilde{Z}_{1i} \tilde{Z}_{1i} + \tilde{Z}_{2i} \tilde{Z}_{2i} \\ + \tilde{Z}_{3i} \tilde{Z}_{3i} + \tilde{Z}_{4i} \tilde{Z}_{4i}) = 12n \times N, \end{aligned} \quad (55)$$

then, the conditions in Theorem 3 are solvable. In order to find a feasible solution of the above minimisation problem, we suggest the following algorithm:

Algorithm 1:

Step 1: Find a feasible set $P^0_i, P^0_i, Z^0_{1i}, Z^0_{1i}, Z^0_{2i};$

$Z^0_{2i}, Z^0_{3i}, Z^0_{3i}, Z^0_{4i}, Z^0_{4i}$. Satisfying (51). Set $r = 0$.

Step 2: Solve the following optimisation problem:

$$\begin{aligned} \min \text{Tr} \sum_{i=1}^N (\tilde{P}_i^r \tilde{P}_i + \tilde{P}_i^r \tilde{P}_i + \tilde{Z}_{1i}^r \tilde{Z}_{1i} + \tilde{Z}_{1i}^r \tilde{Z}_{1i} + \tilde{Z}_{2i}^r \tilde{Z}_{2i} \\ + \tilde{Z}_{2i}^r \tilde{Z}_{2i} + \tilde{Z}_{3i}^r \tilde{Z}_{3i} + \tilde{Z}_{3i}^r \tilde{Z}_{3i} + \tilde{Z}_{4i}^r \tilde{Z}_{4i} + \tilde{Z}_{4i}^r \tilde{Z}_{4i}) \end{aligned} \quad (56)$$

s.t. (54).

Step 3: if $|\text{Tr} \sum_{i=1}^N (P_i P_i + Z_{1i} Z_{1i} + Z_{2i} Z_{2i} + Z_{3i} Z_{3i} + Z_{4i} Z_{4i}) - 12n \times N| \leq \theta$,

for a sufficiently small scalar $\theta > 0$, the solution K_i and L_i , $i=1, 2, \dots, N$, are the controller and the observer gains, respectively. **STOP**.

else

Set $r = r + 1$, set $(P_i^r; P_i^r; Z_{1i}^r; Z_{1i}^r; Z_{2i}^r) = (P_i; P_i; Z_{1i}; Z_{1i}; Z_{2i})$, and go to Step 2.

Step 4: If $r > N_m$, where N_m is the maximum number of iterations allowed, EXIT. Our method fails to find feasible gains.

Remark 5:

• In the design of the observer-based controller, we have two terms P_i and P_i^{-1} occur together, which results a non-linear condition. To overcome this problem, numerous methods have been introduced in the literature. In [28, 33, 41], the non-linear term P_i^{-1} is replaced by $2I - P_i$ using the fact that $(P_i - I)^T P_i^{-1} (P_i - I) \geq 0$. This method is very common to solve such problem. Nevertheless, as in [42], the cone complementarity approach is adopted in this work as a second alternative.

$$\begin{aligned} \tilde{\Omega}_i &= \begin{bmatrix} \tilde{Z}_{1i} & 0 & 0 & 0 \\ 0 & \tilde{Z}_{2i} & \tilde{Y} & 0 \\ 0 & \tilde{Y}^T & \tilde{Z}_{2i} & 0 \\ 0 & 0 & 0 & \tilde{Z}_{3i} \end{bmatrix}, \quad \tilde{Z}_{1i} = \begin{bmatrix} \alpha^{d_m-1} \tilde{Z}_{1i} & 0 \\ 0 & 3\alpha^{d_m-1} \tilde{Z}_{1i} \end{bmatrix}, \\ \tilde{Z}_{2i} &= \begin{bmatrix} \alpha^{d_M-1} \tilde{Z}_{2i} & 0 \\ 0 & 3\alpha^{d_M-1} \tilde{Z}_{2i} \end{bmatrix}, \\ \tilde{Z}_{3i} &= \begin{bmatrix} \alpha^{d_M-1} \tilde{Z}_{3i} & 0 \\ 0 & 3\alpha^{d_M-1} \tilde{Z}_{3i} \end{bmatrix}, \\ \tilde{\Gamma}_{11}^i &= \tilde{\Phi}_i - \alpha \tilde{H}_2^T \tilde{P}_i \tilde{H}_2 - \tilde{\Pi}^T \tilde{\Omega}_i \tilde{\Pi} + \tilde{H}_R^T \tilde{\Pi}_R \tilde{H}_R - \text{sym}(\tilde{H}_z \mathcal{S} \tilde{H}_w), \\ \tilde{H}_1 &= \begin{bmatrix} \tilde{A}_i & 0 & \tilde{A}_{di} & 0 & 0 & 0 & 0 & 0 & \tilde{D}_{1i} \\ I_{2n} & 0 & 0 & -I_{2n} & 0 & 0 & 0 & 0 & I_{2n} & 0 \end{bmatrix}, \\ \tilde{H}_2 &= \begin{bmatrix} I_{2n} & 0 & 0 & 0 & 0 & 0 & 0 & 0 & 0 & 0 \\ 0 & 0 & 0 & 0 & 0 & 0 & 0 & 0 & I_{2n} & 0 \end{bmatrix}, \\ \tilde{H}_3 &= [\tilde{A}_i - I_{2n} \quad 0 \quad \tilde{A}_{di} \quad 0 \quad 0 \quad 0 \quad 0 \quad 0 \quad 0 \quad \tilde{D}_{1i}], \\ \tilde{H}_w &= [0 \quad 0 \quad 0 \quad 0 \quad 0 \quad 0 \quad 0 \quad 0 \quad 0 \quad I], \\ \tilde{H}_z &= [\tilde{C}_{zi} \quad 0 \quad 0 \quad 0 \quad 0 \quad 0 \quad 0 \quad 0 \quad 0 \quad 0], \\ \tilde{H}_R &= \begin{bmatrix} I_{2n} & 0 & 0 & 0 & 0 & 0 & 0 & 0 & 0 & 0 \\ 0 & 0 & 0 & 0 & 0 & 0 & 0 & 0 & I_{2n} & 0 \end{bmatrix}, \\ \tilde{\Pi}_R &= \begin{bmatrix} d_M \tilde{R}_1^T + d_M \tilde{R}_1 & -\tilde{R}_1^T + d_M \tilde{R}_2 \\ * & -\tilde{R}_2^T - \tilde{R}_2 \end{bmatrix}, \quad \tilde{\mathbb{R}} = [\tilde{R}_1 \quad \tilde{R}_2], \end{aligned}$$

$$\tilde{\Gamma}_i = \begin{bmatrix} \tilde{\Gamma}_{11}^i & * & * & * & * & * & * & * \\ \sqrt{d_M} \tilde{\mathbb{R}} \tilde{H}_R & -\alpha^{d_M} \tilde{Z}_{4i} & * & * & * & * & * & * \\ \tilde{H}_3 & 0 & -\frac{1}{d_m} \tilde{Z}_{1i} & * & * & * & * & * \\ \tilde{H}_3 & 0 & 0 & -\frac{1}{d_r} \tilde{Z}_{2i} & * & * & * & * \\ \tilde{H}_3 & 0 & 0 & 0 & -\frac{1}{d_M} \tilde{Z}_{3i} & * & * & * \\ \tilde{H}_3 & 0 & 0 & 0 & 0 & -\frac{1}{d_M} \tilde{Z}_{4i} & * & * \\ \tilde{H}_1 & 0 & 0 & 0 & 0 & 0 & -\tilde{P}_i & * \\ \tilde{H}_z \mathcal{Q} & 0 & 0 & 0 & 0 & 0 & 0 & \mathcal{Q} \end{bmatrix},$$

$$\tilde{\Pi} = \begin{bmatrix} I_{2n} & -I_{2n} & 0 & 0 & 0 & 0 & 0 & 0 & 0 & 0 \\ I_{2n} & I_{2n} & 0 & 0 & -I_{2n} & 0 & 0 & 0 & 0 & 0 \\ 0 & I_{2n} & -I_{2n} & 0 & 0 & 0 & 0 & 0 & 0 & 0 \\ 0 & I_{2n} & I_{2n} & 0 & 0 & -I_{2n} & 0 & 0 & 0 & 0 \\ 0 & 0 & I_{2n} & -I_{2n} & 0 & 0 & 0 & 0 & 0 & 0 \\ 0 & 0 & I_{2n} & I_{2n} & 0 & 0 & -I_{2n} & 0 & 0 & 0 \\ I_{2n} & 0 & 0 & -I_{2n} & 0 & 0 & 0 & 0 & 0 & 0 \\ I_{2n} & 0 & 0 & I_{2n} & 0 & 0 & 0 & -I_{2n} & 0 & 0 \end{bmatrix},$$

Table 1 Upper bound d_M variation for different d_m

d_m	2	4	6	8	10	12	14	16	18
[45]	—	—	—	—	—	—	—	—	—
[10]	6	7	9	10	11	12	14	16	—
[46]	9	10	11	13	14	15	16	18	19
[47]	12	13	14	16	17	19	21	22	23
Theorem 1	15	16	17	18	20	21	23	24	26

Table 2 Upper bound d_M variation for different d_m with $\alpha = 1$

d_m	2	4	6	8	10	12	14	16	18
[13]	15	17	19	21	23	25	27	29	31
[2]	27	29	31	33	35	37	39	41	43
[37]	39	41	43	45	47	49	51	53	55
Theorem 1	47	49	51	53	55	57	59	61	63

• To synthesise the observer and controller gains, the SVD [31, 32, 43], the pseudo inverse of the output matrix [33], and the Finsler's lemma with a particular structure of some decision matrices [44] have been used. However, these techniques are difficult to apply when the disturbance affects the measurements. The CCL algorithm is used here to consider this case.

5 Numerical examples

In the sequel, we demonstrate the applicability of the suggested strategy by means of three simulation examples.

Example 1: Consider a switched system composed of two modes and the following system matrices:

$$A_1 = \begin{bmatrix} 0.2 & -0.1 \\ 0.1 & 0.4 \end{bmatrix}, A_2 = \begin{bmatrix} 0.4 & 0.2 \\ -0.1 & 0.3 \end{bmatrix},$$

$$A_{d1} = \begin{bmatrix} 0.1 & 0 \\ 0.1 & 0.1 \end{bmatrix}, A_{d2} = \begin{bmatrix} 0.1 & 0 \\ -0.01 & 0.1 \end{bmatrix}.$$

Our purpose is to determine the allowable time delay upper bounds d_M for various d_m such that system (3) will be stable. By choosing $\alpha = 0.95$ and $\mu = 1.1$, detailed comparison of the maximum allowed bounds d_M is given in Table 1.

In terms of conservatism, results in Table 1 clearly show that the strategy in Theorem 1 outperforms those in [45–47].

To further prove the merit of the proposed approach, the maximum allowed bounds d_M for different delay lower bounds d_m in Table 2 have been computed from Theorem 1 in our work for the case of arbitrary switching with $\alpha = 1$ and we eliminate conditions in (11), Theorem 1 in [2, 37] and the proposed strategy in [13]. From Tables 1 and 2, it is obvious that the combination Wirtinger-based inequality, improved reciprocally convex approach and Lyapunov–Krasovskii functional with triple sum term provides not only less conservative results, but also significantly improved bounds than [2] using input–output approach with scaled small gain condition, Qiu *et al.* [13] using only Wirtinger-based inequality and improved reciprocally convex approach, Mahmoud and Xia [37] using free matrices and null equations and Hou *et al.* [10] using Lyapunov functional with triple sum terms.

Example 2: For comparison purpose, the proposed control technique will be applied to the following switched system borrowed from [48]:

$$A_1 = \begin{bmatrix} -0.45 & -0.2 \\ 0.2 & 0.3 \end{bmatrix}, A_2 = \begin{bmatrix} -1.1 & 0.2 \\ -0.2 & 0.3 \end{bmatrix}, B_1 = \begin{bmatrix} 0.5 \\ 0.2 \end{bmatrix},$$

$$A_{d1} = \begin{bmatrix} 0.1 & 0 - 0.1 \\ 0 & 0.1 \end{bmatrix}, A_{d2} = \begin{bmatrix} 0.1 & -0.1 \\ 0.1 & 0 \end{bmatrix}, B_2 = \begin{bmatrix} 0.4 \\ 0.3 \end{bmatrix},$$

$$C_{z1} = \begin{bmatrix} 0.5 & 0 \\ 0 & 0.5 \end{bmatrix}, C_{z2} = \begin{bmatrix} 0.3 & 0 \\ 0 & -0.2 \end{bmatrix}, B_{z1} = \begin{bmatrix} 0.2 \\ 0.3 \end{bmatrix},$$

$$B_{z2} = \begin{bmatrix} 0.1 \\ -0.2 \end{bmatrix}, D_{11} = \begin{bmatrix} 0.5 & 0 \\ 0 & 0.5 \end{bmatrix}, D_{12} = \begin{bmatrix} 0.5 & 0 \\ 0 & 0.6 \end{bmatrix},$$

$$D_{21} = D_{22} = 0.$$

In order to highlight the effectiveness of the proposed control strategy, we will perform a comparison with the method in [42] extended to the problem of dissipativity performance with

$$\mathcal{Q} = \begin{bmatrix} -0.4 & 0 \\ 0 & -1 \end{bmatrix}, \mathcal{S} = \begin{bmatrix} 1 & 0.5 \\ 1 & 1 \end{bmatrix}, \mathcal{R} = \begin{bmatrix} 1 & 0 \\ 0 & 1 \end{bmatrix}.$$

Case 1: The method in this paper: Let $\alpha = 0.7$ and $\mu = 1.4$, which implies $\tau_a^* = 0.9434$, $\lambda = 2.7$.

Set $\theta = 10^{-3}$, Theorem 3 produces a feasible solution to the corresponding LMIs, using solver SDP3 of Yalmip toolbox, with minimum values $\gamma_0 = 0.5$ and $\gamma = 0.0901$ and

$$= [-0.7823 \quad -1.1801], K_2 = [1.3559 \quad -1.$$

$$= \begin{bmatrix} -0.3575 & -0.6879 \\ 0.2126 & -0.2466 \end{bmatrix}, L_2 = \begin{bmatrix} -1.8884 & 0. \\ -0.5908 & 0. \end{bmatrix} \quad (57)$$

Case 2: The method in [42]: The observer and control gains can be computed as

$$= [-0.2196 \quad -0.5968], K_2 = [1.2811 \quad -0.$$

$$= \begin{bmatrix} -0.4898 & 0.2238 \\ -0.2891 & 0.6276 \end{bmatrix}, L_2 = \begin{bmatrix} -1.6501 & 0.27 \\ -0.6638 & 0.3 \end{bmatrix} \quad (58)$$

The sampling period and initial states in this example are chosen as follows: $T_e = 0.32$ s and $\phi_0(k) = [12e^{-0.1k} \ 10.8]^T$, $k = -4, \dots, 0$. The delay is given by a repeating of sequence [4, 2, 3, 2, 1, 3].

The state and estimate trajectories are carried out by taking $w(k) = [\sin(4k)e^{-0.5k} \ \sin(4k)e^{-0.5k}]^T$ and repeated sequence [2, 1, 2] as a switching signal with $\tau_a = 3.2$.

Fig. 1 depicts the evolutions of state and estimate trajectories when the previous cases are adopted, while Fig. 1d shows evolution of the ratio under zero-initial condition. It is observed from the plotted figures that both control laws guarantee the convergence of the system state to zero. However, the proposed controller provides a better ratio than the controller designed in

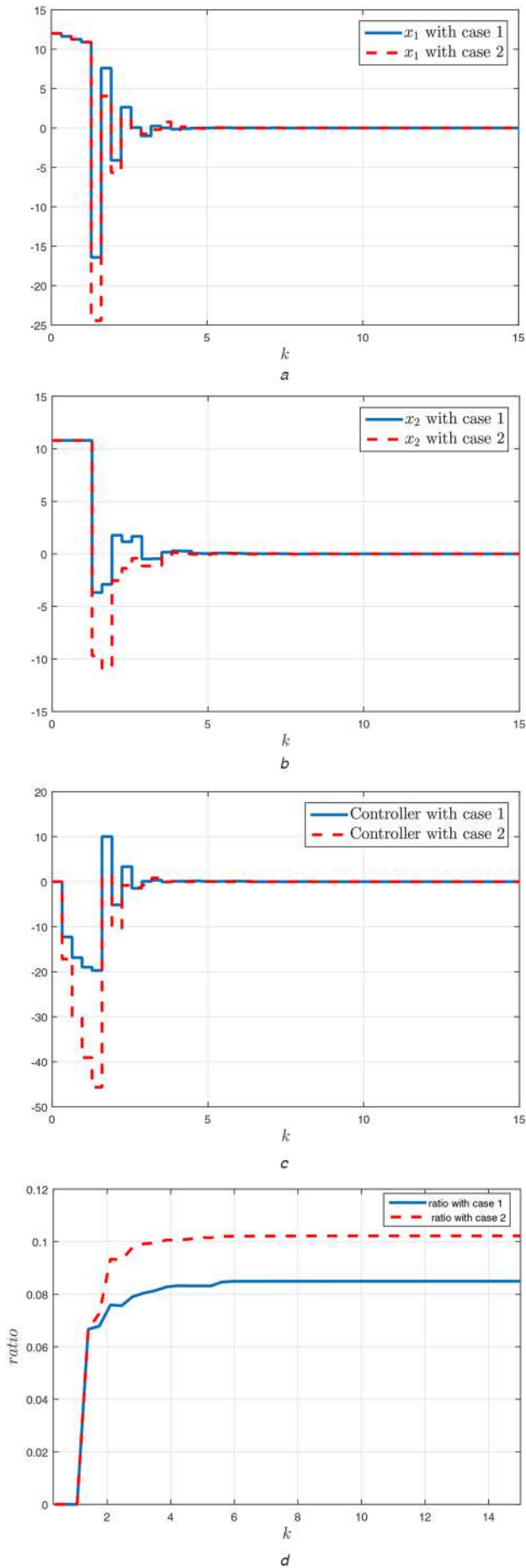


Fig. 1 Simulation results for Example 2 with cases 1 and 2
 (a) Response and estimate trajectories of x_1 , (b) Response and estimate trajectories of x_2 , (c) Control input, (d) Ratio evolution

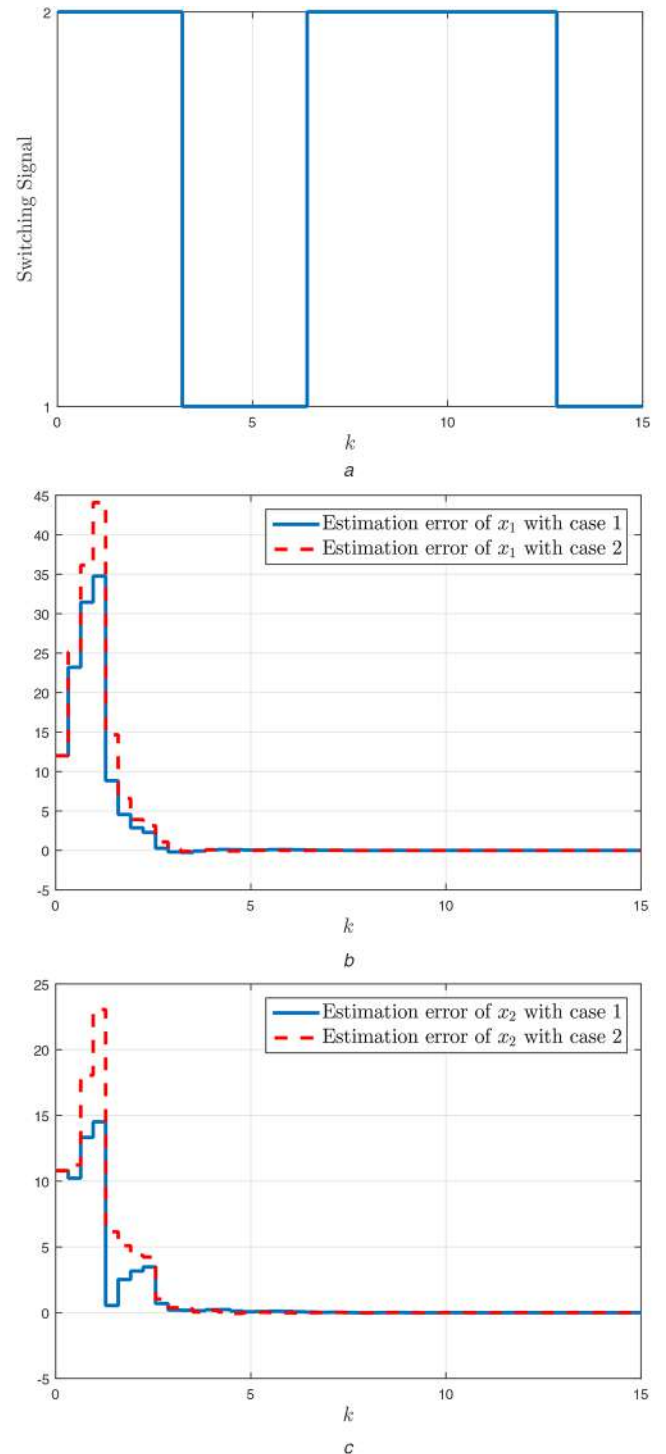


Fig. 2 Switching signal and errors evolutions
 (a) Switching signal, (b) Estimation error of x_1 , (c) Estimation error of x_2

case 2. Thus, the simulation results are satisfactory, which validate the theoretical findings (see Fig. 2).

Example 3: To evaluate the effectiveness of the proposed controller design approach, we consider the example of single-ended primary inductor converter (SEPIC) presented in [49]. This type of converter, shown in Fig. 3, can supply an output voltage less than, greater than or equals to the input voltage and it can be used in several application such GPS systems, CD/DVD players, digital cameras and cellular phones. The switching element V can give a switching behaviour at most once in each period T to the converter. The parameters of the proposed converter are summarised in Table 3.

Table 3 Converter parameters

Acronyms	Definitions	Values, units
L_1	input inductor	1×10^{-3} H
L_2	output inductor	0.5×10^{-3} H
C_1	input capacitor	0.1×10^{-3} F
C_2	output capacitor	0.1×10^{-3} F
R_1	resistor of input inductor	2 Ω
R_2	resistor of output inductor	0.2 Ω
R	load resistor	2 Ω

The inductive currents i_1 and i_2 , capacitor voltage u_{c1} , and output voltage u_0 , four states variables are chosen to characterise the system model described with the following differential equations:

When V switch on

$$\begin{cases} \dot{i}_1 = -\frac{R_1}{L_1}i_1 + \frac{1}{L_1}E \\ \dot{u}_{c1} = -\frac{1}{C_1}i_2 \\ \dot{u}_0 = -\frac{1}{RC_2}u_0 \\ \dot{i}_2 = -\frac{R_2}{L_2}i_2 + \frac{1}{L_2}u_{c1} \end{cases} \quad (59)$$

When V switch off

$$\begin{cases} \dot{i}_1 = -\frac{R_1}{L_1}i_1 - \frac{1}{L_1}u_{c1} - \frac{1}{L_1}u_0 + \frac{1}{L_1}E \\ \dot{u}_{c1} = \frac{1}{C_1}i_1 \\ \dot{u}_0 = \frac{1}{C_2}i_1 + \frac{1}{C_2}i_2 - \frac{1}{RC_2}u_0 \\ \dot{i}_2 = -\frac{R_2}{L_2}i_2 - \frac{1}{L_2}u_0 \end{cases} \quad (60)$$

Set the sampling time $T_e = 2 \times 10^{-5}$ s and choosing the state vector as $x(k) = [i_1(k) u_{c1}(k) u_0(k) i_2(k)]^T$ and the control input $u(k) = E$.

The aim is to apply the proposed design technique to model (1) described by the following data:

$$\begin{aligned} A_1 &= \begin{bmatrix} 0.96 & 0 & 0 & 0 \\ 0 & 1 & 0 & -0.2 \\ 0 & 0 & 0.99 & 0 \\ 0 & 0.04 & 0 & 0.992 \end{bmatrix}, & B_1 = B_2 &= \begin{bmatrix} 0.02 \\ 0 \\ 0 \\ 0 \end{bmatrix}, \\ A_2 &= \begin{bmatrix} 0.96 & -0.02 & -0.02 & 0 \\ 0.2 & 1 & 0 & 0 \\ 0.2 & 0 & 0.99 & 0.2 \\ 0 & 0 & -0.04 & 0.992 \end{bmatrix}, & D_{11} &= \begin{bmatrix} -0.1 \\ 0.1 \\ -0.5 \\ 0.1 \end{bmatrix}, \\ C_1 = C_2 &= \begin{bmatrix} 1 & 0 & 0 & 0 \\ 0 & 1 & 0 & 0 \\ 0 & 0 & 1 & 0 \end{bmatrix}, & D_{12} &= \begin{bmatrix} 0.5 \\ -0.1 \\ -0.1 \\ -0.5 \end{bmatrix}, & A_{d1} = A_{d2} &= 0, \\ C_{z1} &= [0.02 \ 0 \ 0 \ 0], & D_{z1} = D_{z2} &= \begin{bmatrix} 0 \\ 0 \\ 0 \end{bmatrix}, \\ C_{z2} &= [0.01 \ 0 \ 0 \ 0], & B_{z1} &= 0.01, B_{z2} = 0.02. \end{aligned} \quad (61)$$

Let $\mathcal{Q} = -1$, $\mathcal{R} = 1$, $\mathcal{S} = 0$ and the ADT parameters $\alpha = 0.94$ and $\mu = 1.5$, which gives $\tau_d^* = 6.5529$. Set $\theta = 10^{-1}$, Theorem 3 produces a feasible solution to the corresponding LMIs, using

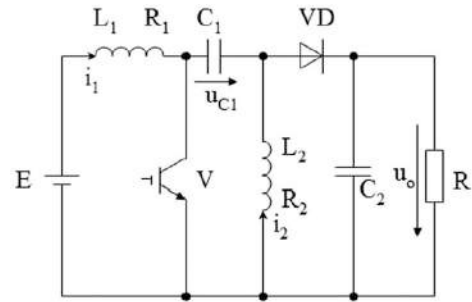


Fig. 3 Single-ended primary inductor converter

solver SDP3 with Yalmip toolbox, with the associated controller and observer gains:

$$\begin{aligned} K_1 &= [-19.0129 \quad -3.7921 \quad -3.3107 \quad -7.1217], \\ K_2 &= [-14.5563 \quad -0.9161 \quad -0.3893 \quad -6.6751], \\ L_1 &= \begin{bmatrix} 0.4081 & 0.1669 & 0.0882 \\ 0.4601 & 1.0845 & -0.0181 \\ 0.2778 & -0.0630 & 0.7716 \\ -0.3815 & -0.7171 & -0.0399 \end{bmatrix}, \\ L_2 &= \begin{bmatrix} 0.4448 & -0.0478 & 0.0512 \\ 0.1588 & 0.9432 & 0.1189 \\ -0.1689 & -0.0161 & 0.4380 \\ -0.3458 & -0.3748 & 0.1141 \end{bmatrix}. \end{aligned} \quad (62)$$

External disturbance $w(k)$ is chosen by

$$w(k) = \frac{\text{rand}(1)}{k+5}. \quad (63)$$

Given the initial conditions $x(0) = [1 \ 5 \ 1 \ 2]^T$ and $\hat{x}(0) = [0 \ 0 \ 0 \ 0]^T$, simulation results are depicted in Fig. 4–6. Fig. 4 denotes the open-loop response of the system states. The evolutions of the system states and the observer are given in Figs. 5 and 6. The result implies that the converter system is effectively stabilised even the presence of the external disturbance, and the output-feedback control problem can be achieved when the system states are incompletely available via the developed control strategy, which is in accordance with the analysis in the paper.

Assume that $D_{z1} = D_{z2} = [1 \ 0 \ 0]^T$. Theorem 3 produces a feasible solution to the corresponding LMIs with the following gains:

$$\begin{aligned} K_1 &= [-23.0016 \quad -4.8059 \quad -3.9610 \quad -9.4311], \\ K_2 &= [-24.7755 \quad -2.7291 \quad -2.0683 \quad -11.4085], \\ L_1 &= \begin{bmatrix} 0.0651 & -0.0150 & 0.4402 \\ 0.1213 & 0.9617 & -0.1551 \\ -0.4330 & -0.0331 & 0.9838 \\ 0.0502 & -0.4725 & 0.0515 \end{bmatrix}, \\ L_2 &= \begin{bmatrix} 0.3444 & -0.0606 & 0.1810 \\ -0.0667 & 0.9108 & 0.0537 \\ -0.1786 & -0.0769 & 0.9505 \\ -0.3661 & -0.1285 & 0.4675 \end{bmatrix}. \end{aligned} \quad (64)$$

To further prove the merit of the proposed strategy, two quality criteria are considered to evaluate the deviation of the estimated error $e(k) = x(k) - \hat{x}(k)$ with different stochastic noises: integral squared error (ISE) and integral absolute error (IAE). The comparison is listed in Table 4.

From the calculated results in Table 4, we can deduce that the total deviation of $e(k)$ is smaller when controller (64) is applied for both cases of noises.

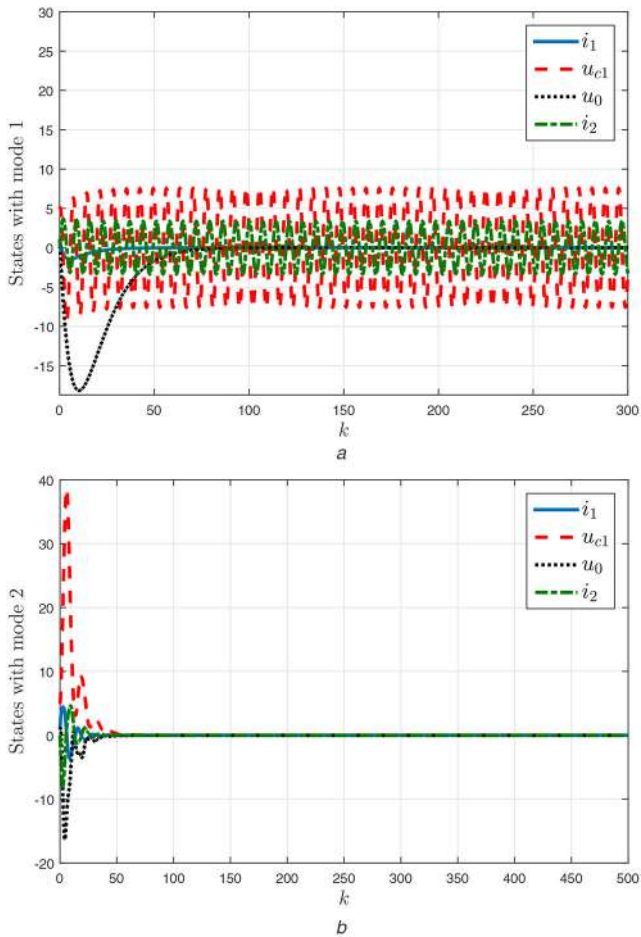


Fig. 4 Open-loop systems trajectories
 (a) State trajectories with mode 1, (b) State trajectories with mode 2

Regarding these results, we conclude that the disturbance attenuation property is evident and the proposed control scheme yields a good performance which validates the theoretical findings.

6 Conclusions

A novel $(\mathcal{Q}, \mathcal{S}, \mathcal{R})$ - γ -dissipative observer-based controller has been proposed in this paper for stabilising a discrete-time switched systems with time-varying delay. Based on the improved reciprocally convex technique and the ADT approach, a delay-dependent sufficient condition has been derived to guarantee the exponential stability of nominal switched systems. Moreover, using the cone complementarity algorithm, an observer-based control law has been designed to ensure the stability and dissipativity of the resulting closed-loop systems. The validity of the theoretical developments has been tested by three examples. It should be emphasised that the design procedure can be a promising procedure to be applied to a wide range of practical systems and the computational simplicity of the method can be another feature of this work.

For some practical systems, the lag time between the switching of the controller and the system modes is quite long and it can never be neglected. So it is interesting to deal with the asynchronous phenomenon as a future research topic. Furthermore, it is also interesting to experimentally validate the developed method on buck–boost converter for a photovoltaic system.

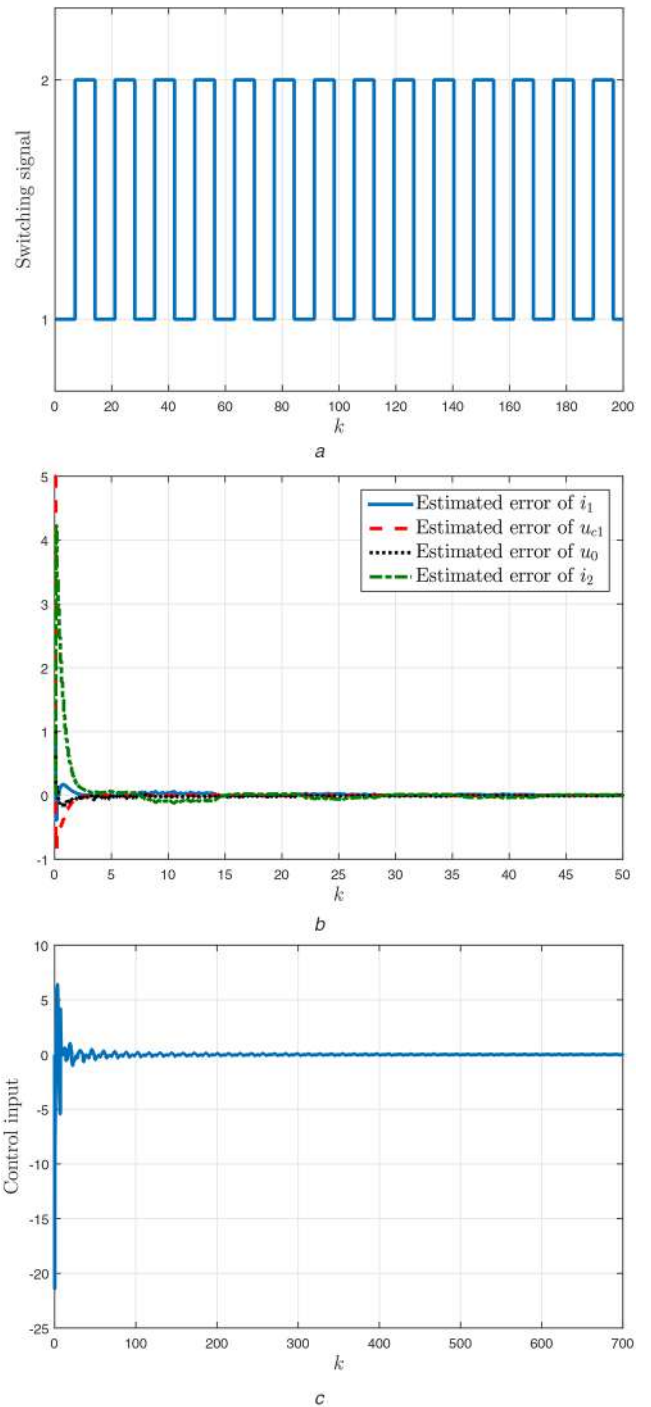


Fig. 5 Control input and estimation error
 (a) Switching signal, (b) State estimation error, (c) Response of control input u

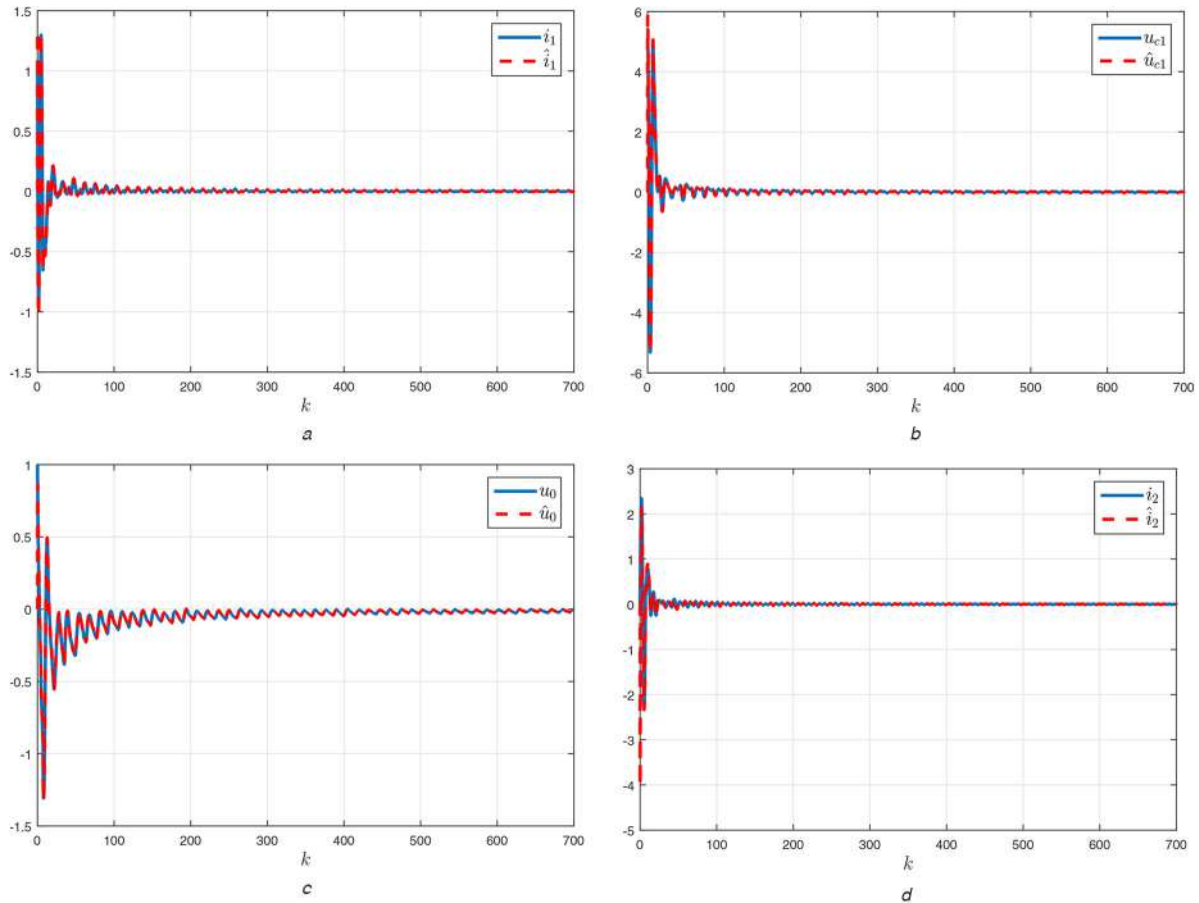


Fig. 6 Simulation results for example 3

(a) Response and estimate trajectories of i_1 , (b) Response and estimate trajectories of u_{c1} , (c) Response and estimate trajectories of u_0 , (d) Response and estimate trajectories of i_2

Table 4 Comparison of $e(k)$ for $k \in [0, 700]$

$w(k)$	$\frac{\text{rand}(1)}{k+5}$		$\text{rand}(1)\sin(k)\exp(-0.1k)$	
	ISE	IAE	ISE	IAE
controller (62)	9.2	11.8	11.1	12.8
controller (64)	6.34	7.16	6.8	7.9

7 References

- [1] Hetel, L., Daafouz, J., Jung, C.: 'Stabilization of arbitrary switched linear systems with unknown time-varying delays', *IEEE Trans. Autom. Control*, 2006, **51**, (10), pp. 1668–1674
- [2] Li, Z., Gao, H., Karimi, H.R.: 'Stability analysis and H_∞ controller synthesis of discrete-time switched systems with time delay', *Syst. Control Lett.*, 2014, **66**, pp. 85–93
- [3] Liu, L., Zhao, X.D., Niu, B., et al.: 'Global output-feedback stabilisation of switched stochastic non-linear time-delay systems under arbitrary switchings', *IET Control Theory Appl.*, 2014, **9**, (2), pp. 283–292
- [4] Li, Y., Sui, S., Tong, S.: 'Adaptive fuzzy control design for stochastic nonlinear switched systems with arbitrary switchings and unmodeled dynamics', *IEEE Trans. Cybern.*, 2017, **47**, (2), pp. 403–414
- [5] Zhang, J., Han, Z., Wu, H., et al.: 'Robust stabilization of discrete-time positive switched systems with uncertainties and average dwell time switching', *Circuits Syst. Signal Process.*, 2014, **33**, (1), pp. 71–95
- [6] Xiao, J., Xiang, W.: 'New results on asynchronous H_∞ control for switched discrete-time linear systems under dwell time constraint', *Appl. Math. Comput.*, 2014, **242**, pp. 601–611
- [7] Tian, Y., Cai, Y., Sun, Y.: 'Stability of switched nonlinear time-delay systems with stable and unstable subsystems', *Nonlinear Anal., Hybrid Syst.*, 2017, **24**, pp. 58–68
- [8] Gassara, H., Kchaou, M., El-Hajjaji, M., et al.: 'Control of time delay fuzzy descriptor systems with actuator saturation', *Circuits Syst. Signal Process.*, 2014, **33**, (12), pp. 3739–3756
- [9] Kchaou, M., El-Hajjaji, A.: 'Resilient H_∞ sliding mode control for discrete-time descriptor fuzzy systems with multiple time delays', *Int. J. Syst. Sci.*, 2016, **48**, (2), pp. 1–14
- [10] Hou, L., Zong, G., Wu, Y., et al.: 'Exponential $l_2 - l_\infty$ output tracking control for discrete-time switched system with time-varying delay', *Int. J. Robust Nonlinear Control*, 2012, **22**, (11), pp. 1175–1194
- [11] Lian, J., Shi, P., Feng, Z.: 'Passivity and passification for a class of uncertain switched stochastic time-delay systems', *IEEE Trans. Cybern.*, 2012, **43**, (1), pp. 3–13
- [12] Choi, H.D., Ahn, C.K., Karimi, H.R., et al.: 'Filtering of discrete-time switched neural networks ensuring exponential dissipative and $l_2 - l_\infty$ performances', *IEEE Trans. Cybern.*, 2017, **47**, (10), pp. 3195–3207
- [13] Qiu, J., Wei, Y., Karimi, H.R., et al.: 'Reliable control of discrete-time piecewise-affine time-delay systems via output feedback', *IEEE Trans. Reliab.*, 2017, **67**, (1), pp. 79–91
- [14] Wu, Z., Karimi, H.R., Shi, P.: 'Dissipativity-based small-gain theorems for stochastic network systems', *IEEE Trans. Autom. Control*, 2015, **61**, (8), pp. 2065–2078
- [15] Feng, Z., Lam, J.: 'Dissipative control and filtering of discrete-time singular systems', *Int. J. Syst. Sci.*, 2016, **47**, (11), pp. 2532–2542
- [16] Aravindh, D., Sakthivel, R., Anthoni, S.M.: 'Extended dissipativity-based non-fragile control for multi-area power systems with actuator fault', *Int. J. Syst. Sci.*, 2019, **50**, (2), pp. 256–272
- [17] Sakthivel, R., Santra, S., Kaviarasan, B., et al.: 'Dissipative analysis for network-based singular systems with non-fragile controller and event-triggered sampling scheme', *J. Franklin Inst.*, 2017, **354**, (12), pp. 4739–4761
- [18] Mahmoud, M.S.: 'Delay-dependent dissipativity analysis and synthesis of switched delay systems', *Int. J. Robust Nonlinear Control*, 2011, **21**, (1), pp. 1–20
- [19] Wu, L., Zheng, W.X., Gao, H.: 'Dissipativity-based sliding mode control of switched stochastic systems', *IEEE Trans. Autom. Control*, 2013, **58**, (3), pp. 785–791
- [20] Shi, P., Su, X., Li, F.: 'Dissipativity-based filtering for fuzzy switched systems with stochastic perturbation', *IEEE Trans. Autom. Control*, 2016, **61**, (6), pp. 1694–1699
- [21] Liu, B., Hill, D.J.: 'Decomposable dissipativity and related stability for discrete-time switched systems', *IEEE Trans. Autom. Control*, 2011, **56**, (7), pp. 1666–1671
- [22] McCourt, M.J., Antsaklis, P.J.: 'Stability of interconnected switched systems using qsr dissipativity with multiple supply rates'. American Control Conf. (ACC), Montreal, QC, Canada, 2012, pp. 4564–4569
- [23] Dong, S., Wu, Z.G., Su, H., et al.: 'Asynchronous control of continuous-time nonlinear markov jump systems subject to strict dissipativity', *IEEE Trans. Autom. Control*, 2018, **64**, (3), pp. 1250–1256
- [24] Ding, D.W., Yang, G.H.: ' H_∞ static output feedback control for discrete-time switched linear systems with average dwell time', *IET Control Theory Appl.*, 2010, **4**, (3), pp. 381–390
- [25] Yuan, C., Wu, F.: 'Asynchronous switching output feedback control of discrete-time switched linear systems', *Int. J. Control*, 2015, **88**, (9), pp. 1766–1774

- [26] Shi, S., Shi, S., Fei, Z., *et al.*: 'Finite-time output feedback control for discrete-time switched linear systems with mode-dependent persistent dwell-time', *J. Franklin Inst.*, 2018, **355**, (13), pp. 5560–5575
- [27] Sakthivel, R., Santra, S., Mathiyalagan, K., *et al.*: 'Observer-based control for switched networked control systems with missing data', *Int. J. Mach. Learn. Cybern.*, 2015, **6**, (4), pp. 677–686
- [28] Benzouia, A., Telbissi, K., Ouladsine, M., *et al.*: 'Based observer fault detection for uncertain delayed discrete-time switched systems: a reduced LMI size'. 2017 25th Mediterranean Conf. on Control and Automation (MED), Valetta, Malta, 2017, pp. 430–435
- [29] Mathiyalagan, K., Park, J.H., Sakthivel, R.: 'Observer-based dissipative control for networked control systems: a switched system approach', *Complexity*, 2015, **21**, (2), pp. 297–308
- [30] Sun, Y., Ma, S.: 'Observer-based finite-time stabilization for discrete-time switched singular systems with quadratically inner-bounded nonlinearities', *Int. J. Robust Nonlinear Control*, 2019, **29**, (6), pp. 2041–2062
- [31] Wang, C.L.J., Lu, J.: 'Observer-based robust stabilisation of a class of non-linear fractional-order uncertain systems: an linear matrix inequality approach', *IET Control Theory Appl.*, 2012, **6**, (18), pp. 2757–2764
- [32] Wang, D., Shi, P., Wang, W., *et al.*: 'Non-fragile H_∞ control for switched stochastic delay systems with application to water quality process', *Int. J. Robust Nonlinear Control*, 2014, **24**, (11), pp. 1677–1693
- [33] Xiang, X.L.Z.: 'Observer design of discrete-time impulsive switched nonlinear systems with time-varying delays', *Appl. Math. Comput.*, 2014, **229**, pp. 327–339
- [34] Wang, G., Xie, R., Zhang, H., *et al.*: 'Robust exponential H_∞ filtering for discrete-time switched fuzzy systems with time-varying delay', *Circuits Syst. Signal Process.*, 2016, **35**, (1), pp. 117–138
- [35] Lin, J., Shi, Y., Fei, S., *et al.*: 'Reliable dissipative control of discrete-time switched singular systems with mixed time delays and stochastic actuator failures', *IET Control Theory Appl.*, 2013, **7**, (11), pp. 1447–1462
- [36] Feng, Z., Li, W., Lam, J.: 'Dissipativity analysis for discrete singular systems with time-varying delay', *ISA Trans.*, 2016, **64**, pp. 86–91
- [37] Mahmoud, M.S., Xia, Y.: 'Multi-controller approach to uncertain discrete-time-delay systems', *Int. J. Syst. Control Commun.*, 2013, **5**, (3–4), pp. 328–346
- [38] Mao, Y., Zhang, H.: 'Exponential stability and robust H_∞ control of a class of discrete-time switched non-linear systems with time-varying delays via TS fuzzy model', *Int. J. Syst. Sci.*, 2012, **45**, (5), pp. 1112–1127
- [39] Kwon, O., Park, M., Park, J., *et al.*: 'Improved delay-partitioning approach to robust stability analysis for discrete-time systems with time-varying delays and randomly occurring parameter uncertainties', *Opt. Control Appl. Methods*, 2015, **36**, (4), pp. 496–511
- [40] Du, D., Jiang, B., Zhou, S.: 'Delay-dependent robust stabilisation of uncertain discrete-time switched systems with time-varying state delay', *Int. J. Syst. Sci.*, 2008, **39**, (3), pp. 305–313
- [41] Xie, X., Yue, D., Peng, C.: 'Relaxed observer design of discrete-time nonlinear systems via a novel ranking-based switching mechanism', *Appl. Soft Comput.*, 2016, **46**, pp. 162–169
- [42] Hou, L., Zong, G., Wu, Y.: 'Observer-based finite-time exponential $l_2 - l_\infty$ control for discrete-time switched delay systems with uncertainties', *Trans. Inst. Meas. Control*, 2013, **35**, (3), pp. 310–320
- [43] Sakthivel, R., Rathika, M., Santra, S., *et al.*: 'Observer-based dissipative control for markovian jump systems via delta operators', *Int. J. Syst. Sci.*, 2017, **48**, (2), pp. 247–256
- [44] Bibi, H., Bedouhene, F., Zemouche, A., *et al.*: 'Output feedback stabilization of switching discrete-time linear systems with parameter uncertainties', *J. Franklin Inst.*, 2017, **354**, (14), pp. 5895–5918
- [45] Wang, D., Shi, P., Wang, J., *et al.*: 'Delay-dependent exponential H_∞ filtering for discrete-time switched delay systems', *Int. J. Robust Nonlinear Control*, 2012, **22**, (13), pp. 1522–1536
- [46] Zhang, G., Han, C., Guan, Y., *et al.*: 'Exponential stability analysis and stabilization of discrete-time nonlinear switched systems with time delays', *Int. J. Innov. Comput. Inf. Control*, 2012, **8**, (3), pp. 1973–1986
- [47] Regaieg, M.A., Kchaou, M., Gassara, H., *et al.*: 'Average dwell-time approach to H_∞ control of time-varying delay switched systems'. 2016 17th Int. Conf. on Sciences and Techniques of Automatic Control and Computer Engineering (STA), Sousse, Tunisia, 2016, pp. 741–746
- [48] Song, Y., Fan, J., Fei, M., *et al.*: 'Robust H_∞ control of discrete switched system with time delay', *Appl. Math. Comput.*, 2008, **205**, (1), pp. 159–169
- [49] Guo, S., Zhu, F., Jiang, B.: 'Reduced-order switched UIO design for switched discrete-time descriptor systems', *Nonlinear Anal., Hybrid Syst.*, 2018, **30**, pp. 240–255

See discussions, stats, and author profiles for this publication at: <https://www.researchgate.net/publication/365348940>

Impulsive security control for fractional-order delayed multi-agent systems with uncertain parameters and switching topology under DoS attack

Article in *Information Sciences* · December 2022

DOI: 10.1016/j.ins.2022.10.123

CITATIONS

0

READS

81

6 authors, including:



Govindasamy Narayanan
Kunsan National University

18 PUBLICATIONS 332 CITATIONS

[SEE PROFILE](#)



M. Syed Ali
Thiruvalluvar University

190 PUBLICATIONS 3,675 CITATIONS

[SEE PROFILE](#)



Gani Stamov
University of Texas at San Antonio

145 PUBLICATIONS 1,925 CITATIONS

[SEE PROFILE](#)



Ivanka Stamova
University of Texas at San Antonio

167 PUBLICATIONS 2,693 CITATIONS

[SEE PROFILE](#)

Some of the authors of this publication are also working on these related projects:



Hilfer fractional integro differential equations [View project](#)



MATHEMATICS (MDPI): Special Issue "Computational Mathematics and Neural Systems" [View project](#)



Impulsive security control for fractional-order delayed multi-agent systems with uncertain parameters and switching topology under DoS attack

G. Narayanan^{a,b}, M. Syed Ali^a, Hamed Alsulami^c, Gani Stamov^d, Ivanka Stamova^{d,*}, Bashir Ahmad^c

^aComplex System Laboratory, Department of Mathematics, Thiruvalluvar University, Vellore 632 115, India

^bCenter for Computational Modeling, Chennai Institute of Technology, Chennai 600069, India

^cNonlinear Analysis and Applied Mathematics (NAAM)-Research Group, Department of Mathematics, Faculty of Science, P.O. Box 80203, King Abdulaziz University, Jeddah, Saudi Arabia

^dThe University of Texas at San Antonio, Department of Mathematics, San Antonio, TX 78249, USA

ARTICLE INFO

Article history:

Received 15 April 2022

Received in revised form 22 October 2022

Accepted 27 October 2022

Available online 7 November 2022

Keywords:

Caputo fractional derivative

Multi-agent systems

Secure consensus

Impulsive control

Uncertainty

ABSTRACT

This paper studies the problem of fractional-order impulsive security control for uncertain fractional-order delayed multi-agent systems (FDMASs) under Denial-of-Service (DoS) attack. New sufficient conditions to achieve impulsive secure consensus are analyzed. To determine the stability of the resulting error system, we utilized fractional-calculus theory, algebraic graph theory, Lyapunov functional. The influence of the impulsive control scheme depends on the order of the Caputo fractional-order systems addressed. It is shown that the agents can achieve an exponential consensus under the proposed impulsive control scheme. Finally, the effectiveness of the theoretical results is demonstrated by numerical examples and simulation results.

Published by Elsevier Inc.

1. Introduction

Multi-agent systems (MASs) consist of multiple interacting autonomous subsystems that can be used by means of shared information for the tough or complex task. Consensus is one of the key issues of the MASs collective actions, which ensures that by designing an effective distributed control based on local knowledge alone, each agent state converges into the desired common state. Several important results on consensus problems with limited communication, dynamically changing topologies, uniform or non-uniform time-delays, and external disturbances have been proposed in the existing literature [1–5], including some very recent publications [6–8]. It should be noticed that much of the existing MASs consensus analysis are focused on integer-order dynamics. However, some phenomena can not be adequately represented in most practical systems by integer-order dynamics such as electrical engineering [9,10], control systems [11,12], robotics systems [13,14], brain stimulation systems [15], while fractional-order dynamics are best illustrated when the operator order is an arbitrary real number. For more results on fractional-order non-linear dynamical systems where the problems of control and synchronization have been thoroughly explored we refer to [16–18].

* Corresponding author.

E-mail addresses: gani.stamov@utsa.edu (G. Stamov), ivanka.stamova@utsa.edu (I. Stamova).

In fact, many working environments have viscoelastic properties for agents, for instance, work spaces include taped, sandy, muddy or grass areas and so on, for agents with many micro organisms, viscous substances, or for agent work spaces can therefore be described as fractional-order systems. An important issue for fractional-order multi-agent systems (FOMASs) is the consensus control of MASs, which was studied by Cao and Ren [19] and then rapidly developed. Relevant findings can be used to solve the distributed FOMASs containment control problem [20]. In addition, because of the hardware efficiency, each agent requires a certain input time delay to communicate and process information. Considering time delays in the analysis and control of the system is therefore of a great importance. The special case of FDMASs containment control was tackled at [21,22]. In [23] also the problems of uncertain FOMASs were examined for distributed containment control.

Impulsive control is a typical discontinuous check among these control systems, which may be used in systems not controlled by a continuous control input. The conventional controller is slowly replaced by the digital controller with the advancement of information science and computer technology; thus the impulsive control mechanism has been improved greatly. The impulsive control has many excellent features compared with continuous controls, such as robustness, versatility and low cost [24–27]. This type of control is also very beneficial for MASs. Indeed, in order to achieve synchronization the exchange of information between interconnected agents should be ongoing, so that every agent gathers information from itself and its neighbors at all times. In the case of limited communication bandwidths, that will be a heavy burden. With impulsive control systems that have discontinuous inputs, it is natural to use sample data from each agent and its neighbors to develop the distributed impulsive controller only at a discrete time. Han et al., agreed with the impulsive consensus of discrete-time MASs [28], that the communication costs of MASs were significantly reduced thus maintaining system stability. Although a lot of work has been done to achieve consensus on integer-order MASs via impulsive control (see [29,30] and the references therein), the existing FOMASs works are fairly limited. It is noted, however, that some results on FOMASs via impulsive control strategy exist [31,32]. Wang and Yang (see [33]) investigated the distributed impulsive control problem of FOMASs with input delay based on leader-following case.

It is worth noting that agents are typically linked to each other via communication networks which are subject to different cyber attacks. The cyber attacks can be split into two categories in multi-agent networks. When a malicious agent attacks, the first ends up removing one object by the communication network graph and the result of the second is a damage of the communication. The second case involves DoS attacks and deceptions. MASs are especially vulnerable to DoS attacks, as it is virtually impossible to protect DoS attacks on all communication channels, whereas MASs agents are still individually interacting. As a result, the defense against attacks by distributed DoS is one of the key safety issues when designing the network control system. Some controllers have been designed to overcome the effect of DoS attack [34–37], including the impulsive control case [38,39]. Nonetheless, fewer network security studies have been published for FOMASs in the available literature, this means that network safety research at FOMASs is an ongoing topic. For example, the effects of uncertain parameters on their dynamical properties is not previously studied. Since uncertain terms may lead to poor performance and chaotic behavior [40–42], the study of the impulsive security control problems of uncertain FDMASs in presence of DoS attack is of a great importance.

In this paper, our attention is focused on the impulsive security control problem of uncertain FDMASs in presence of DoS attack. The main contributions of this paper are embodied in the three aspects as follows:

- (i) An impulsive secure consensus is proposed for leader-following FDMASs with uncertain parameters subject to DoS attacks. To reduce the contact consumption controllers and DoS attacks on the edges of controllers we utilized distributed impulsive controller. To ensure the acceptance of network disconnections, a switching method is suggested;
- (ii) The designed distributed impulsive controller still achieve the secure consensus of uncertain FDMASs. By utilizing the tools from fractional-calculus theory, algebraic graph theory, efficient algorithm is designed. Impulsive controller that depends on the Caputo fractional derivative is given to ensure exponential consensus tracking of the uncertain FDMASs under DoS attack scenarios;
- (iii) At last presented, numerical simulations verify that the obtained scheme is efficient on the designed impulsive controller for nonlinear FOMASs with networks of Chua's circuits in presence of DoS attack. A solution is given in this paper on how to change the impulse intervals against DoS attacks if the exact details of DoS attacks is identified.

Notations: ${}^c D_{t_0}^\beta$ denotes the β -order Caputo fractional derivative; Real numbers, and $n \times 1$ real (complex) column vectors are referred to \mathcal{R} and $\mathcal{R}^n(\mathcal{C}^n)$, respectively; \mathcal{I}_n represents an identity matrix; \otimes stands for the Kronecker product; $\sigma_{\max}(\cdot)$ is the maximum singular value; $\lambda_{\min}(\cdot)$ and $\lambda_{\max}(\cdot)$ represent the smallest and largest values of a real symmetric matrix, respectively.

2. Model introduction and preliminaries

In this section, some preliminaries of the graph theory, fractional calculus, model description, and some lemmas are given.

2.1. Communication topologies

Consider a weighted digraph $\mathcal{G}^{\sigma(t)} = (\mathcal{V}, \mathcal{E}^{\sigma(t)}, \mathcal{A}^{\sigma(t)})$, $\mathcal{V} = \{v_p, p \in \overline{\mathcal{N}}\}$, where $\overline{\mathcal{N}} = 1, 2, \dots, N$ is a nonempty node, $\mathcal{E}^{\sigma(t)} \subset \mathcal{V} \times \mathcal{V}$ is an edge set, and $\mathcal{A}^{\sigma(t)} = [a_{pq}^{\sigma(t)}] \in \mathcal{R}^{N \times N}$ is an adjacency matrix, where $a_{pq}^{\sigma(t)} > 0$ if and only if $(v_q, v_p) \in \mathcal{E}$ and $a_{pq}^{\sigma(t)} = 0$ otherwise. The Laplacian matrix is defined as $\mathcal{L}^{\sigma(t)} \in \mathcal{R}^{N \times N}$ with $\ell_{pq}^{\sigma(t)} = \sum_{q=1}^N a_{pq}^{\sigma(t)}$ and $\ell_{pq} = -a_{pq}, p \neq q$. Further more details on the communication topologies, kindly refer [36].

2.2. Some fractional calculus definitions

The fractional derivatives are classified in several ways. The definitions of Riemann–Liouville and Caputo type are commonly used. Let $\Gamma(\beta) = \int_0^{+\infty} t^{\beta-1} e^{-t} dt, \beta > 0$. Since the fractional derivative of Caputo type needs only initial conditions via an integral-order derivative, it reflects a well understood physical situation and makes it more applicable to problems in the real world. In this paper we deal with uncertain FDMASs involving the Caputo fractional derivative.

Definition 2.1. [18] The fractional integral ${}_{t_0}D_t^{-\beta}$ with fractional-order $\beta > 0$ of $\mathcal{F}(t)$ is defined as

$${}_{t_0}D_t^{-\beta} \mathcal{F}(t) = \frac{1}{\Gamma(\beta)} \int_{t_0}^t (t - \xi)^{\beta-1} \mathcal{F}(\xi) d\xi, \quad t \geq t_0 \geq 0. \tag{2.1}$$

The Caputo fractional derivative with order β of a function $\mathcal{F}(t) \in C^m([t_0, +\infty), \mathcal{R})$ is

$${}_{t_0}^C D_t^\beta \mathcal{F}(t) = \begin{cases} \frac{1}{\Gamma(m-\beta)} \int_{t_0}^t \frac{\mathcal{F}^{(m)}(\xi)}{(t-\xi)^{\beta+1-m}} d\xi, & m-1 < \beta < m, \\ \frac{d^m}{dt^m} \mathcal{F}(t), & \beta = m. \end{cases} \tag{2.2}$$

Specifically, when $\beta \in (0, 1), {}_{t_0}^C D_t^\beta \mathcal{F}(t) = (1/\Gamma(1-\beta)) \int_{t_0}^t (\mathcal{F}'(\xi)/(t-\xi)^\beta)$. For simplicity, we denote ${}_{t_0}^C D_t^\beta$ as the Caputo fractional derivative D^β .

Definition 2.2. [17] The two parameters Mittag–Leffler function with $\alpha > 0, \beta > 0$ is defined as

$$\mathbb{E}_{\alpha, \beta}(z) = \sum_{k=0}^{\infty} \frac{z^k}{\Gamma(k\alpha + \beta)},$$

where $z \in \mathcal{C}$.

Denoting $\beta=1$, with one parameter type, its Mittag–Leffler function is

$$\mathbb{E}_\alpha(z) = \sum_{k=0}^{\infty} \frac{z^k}{\Gamma(k\alpha + 1)} = \mathbb{E}_{\alpha, 1}(z).$$

Particularly, $\mathbb{E}_{1, 1}(z) = e^z$, when $\alpha = \beta = 1$.

2.3. Model introduction

We will investigate a FDMAS with one leader and \mathcal{N} followers and uncertain parameters, whose dynamics can be modeled by

$$\begin{aligned} D^\beta \mathfrak{S}_p(t) &= (E + \Delta E) \mathfrak{S}_p(t) + (F + \Delta F) \omega(\mathfrak{S}_p(t)) \\ &+ (G + \Delta G) \omega(\mathfrak{S}_p(t - \tau)) + u_p(t), \end{aligned} \tag{2.3}$$

where $p = 1, 2, \dots, \mathcal{N}, \mathfrak{S}_p(t) \in \mathcal{R}^n$ is the state variable of the p^{th} follower agent; E, F , and G are constant matrices; $\Delta E, \Delta F$, and ΔG are uncertain parameter matrices; $\omega(\mathfrak{S}_p(t)) = [\omega_1(\mathfrak{S}_p(t)), \omega_2(\mathfrak{S}_p(t)), \dots, \omega_n(\mathfrak{S}_p(t))]^\top, p = 1, 2, \dots, \mathcal{N}$ is a non-linear function; τ is the constant input time delay; $u_p(t)$ is the control input, which will be designed later; we denote $t - \tau = \chi_\tau$.

The dynamics of the leader is described as

$$\begin{aligned} D^\beta \mathfrak{S}_0(t) &= (E + \Delta E) \mathfrak{S}_0(t) + (F + \Delta F) \omega(\mathfrak{S}_0(t)) \\ &+ (G + \Delta G) \omega(\mathfrak{S}_0(\chi_\tau)), \end{aligned} \tag{2.4}$$

where $\mathfrak{S}_0(t) \in \mathcal{R}^n$.

Assumptions:

(\mathcal{A}_{H1}) For the continuous nonlinear function $\omega(\cdot)$ there exist nonnegative constants $\psi_{pq} > 0, p, q \in \{1, 2, \dots, n\}$ such that, for any $\mathfrak{S}_1, \mathfrak{S}_2 \in \mathcal{R}^n$,

$$|\omega_p(\mathfrak{I}_1) - \omega_p(\mathfrak{I}_2)| \leq \sum_{q=1}^n \psi_{pq} |\mathfrak{I}_{1q} - \mathfrak{I}_{2q}|. \tag{2.5}$$

(A_{H2}) The continuous nonlinear function $\omega(\cdot)$ satisfies the following Lipschitz condition, for $\mathfrak{I}_1 = (\mathfrak{I}_{11}, \mathfrak{I}_{12}, \dots, \mathfrak{I}_{1n})^\top$, $\mathfrak{I}_2 = (\mathfrak{I}_{21}, \mathfrak{I}_{22}, \dots, \mathfrak{I}_{2n})^\top \in \mathcal{R}^{2n}$,

$$|\omega_p(\mathfrak{I}_1) - \omega_p(\mathfrak{I}_2)| \leq \psi_p |\mathfrak{I}_{1p} - \mathfrak{I}_{2p}|, \tag{2.6}$$

where $\psi_p > 0, (p = 1, 2, \dots, n)$.

(A_{H3}) The uncertain parameter matrices $\Delta E, \Delta F, \Delta G$ satisfy the following constraints:

$$\Delta E^T \Delta E \leq (\alpha_i \otimes \mathcal{I}_n),$$

$$\Delta F^T \Delta F \leq (\alpha_\epsilon \otimes \mathcal{I}_n),$$

$$\Delta G^T \Delta G \leq (\alpha_\delta \otimes \mathcal{I}_n),$$

where $\alpha_i, \alpha_\epsilon$, and α_δ are known constants.

(A_{H4}) The leader is the root node of the directed spanning tree embedded in the augmented graph \mathcal{G}^1 , when no attack occurs.

(A_{H5}) The framework model (2.3) has a recovery mechanism, that is, the communication topology can be recovered after an attack.

Remark 2.3. Many authors have studied the secure consensus problem for MASs in the integer-order case [34–40], but still not focused on MASs in the fractional-order case. In practice, the problem of consensus tracking control for FOMAS was developed by the well-established works [19–21]. Moreover, since FOMASs have better characteristics than the corresponding integer-order ones, some sufficient consensus conditions for the FOMASs associated with the network structure and the fractional-order were given and the idea about choosing some appropriate varying orders with time to quicken the convergence speed were introduced in [19–21]. However, the control method in [19–21] cannot handle FOMASs under DoS attacks. So, in this paper, the impulsive secure consensus problem for FDMASs with uncertain parameters subject to DoS attacks described by a fractional-order model is first studied.

The states of agents in (2.3) may be changed at certain discrete moments under an impulsive control scheme due to which the states of agents jump to a certain value. We will propose an impulsive control scheme u_p that only depends on the agent p information, as indicated in the Fig. 1. Initially, we assume that at time t_r , each agent measures (samples) its own state $\mathfrak{I}_p(t_r)$, and send it to its neighbors through a communication link.

Remark 2.4. The controllers in [34–37] require a communication with neighbor agents constantly, which causes systems to be a subject to continuous DoS attacks. In order to avoid such attacks, we design an impulsive control method that only needs a communication with neighbor agents at sampling instants. Compared with the existing results on the continuous controllers for MASs with DoS attacks [34–37], the proposed impulsive controllers will further reduce the communication consumption of controllers.

2.4. An impulsive controller design based on switching mechanism

The communication topology between \mathcal{N} agents will be defined by directed switches over the given graph $\hat{\mathcal{G}}$, where $\hat{\mathcal{G}} = \{\mathcal{G}^{(1)}, \mathcal{G}^{(2)}, \dots, \mathcal{G}^{(s)}\}$. Let $\mathcal{G}^{\sigma(t)}$ be the communication topology of the considered MASs at time t , where $t \geq 0$. The piecewise

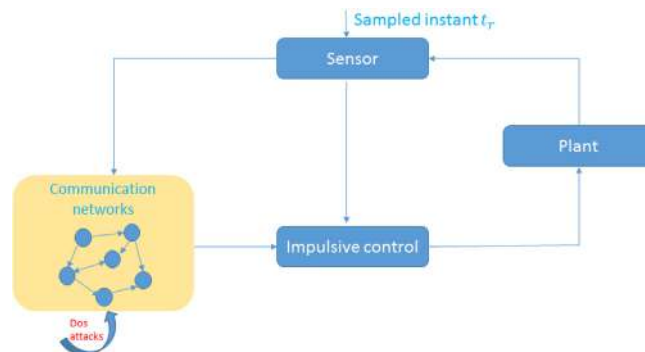


Fig. 1. The framework of MASs with impulsive control.

constant function $\sigma(t) : [0, \infty) \rightarrow \{1, 2, \dots, s\}$ is the switching signal. $\mathcal{G}^{(1)}$ is the topology graph without an attack, while $\mathcal{G}^{(2)}, \dots, \mathcal{G}^{(s)}$ are the topological graphs under attacks. Noticeably, $\mathcal{G}^{\sigma(t)} \in \widehat{\mathcal{G}}, \forall t \geq 0$.

To solve secure consensus problems, the distributed impulsive controller is designed as

$$u_p(t) = \sum_{r=1}^{\infty} -b_r \left[\sum_{q=1}^{\mathcal{N}} a_{pq}^{\sigma(t)} (\mathfrak{Z}_q(t) - \mathfrak{Z}_p(t)) + d_p^{\sigma(t)} (\mathfrak{Z}_p(t) - \mathfrak{Z}_0(t)) \right] \delta^*(t - t_r), \tag{2.7}$$

where $\delta^*(\cdot)$ is the Dirac delta function; $b_r, r \in \mathcal{N}_+$ is the impulsive control gain; $a_{pq}^{\sigma(t)}$ is an element of the weighted adjacency matrix of the digraph $\mathcal{G}^{\sigma(t)}$; $d_p^{\sigma(t)}$ describes the pinning link and $d_p^{\sigma(t)} > 0$ iff there is a directed link with positive weight $d_p^{\sigma(t)}$ from the leader to the p^{th} follower.

Definition 2.5. [12] An impulsive sequence $\varsigma = \{t_r\}, r \in \mathcal{N}_+$ is said to have an average impulsive interval h_b if there exist two positive numbers \mathcal{N}_0 and h_b such that

$$\frac{t - t_0}{h_b} - \mathcal{N}_0 \leq \mathcal{N}_{\varsigma}(t, t_0) \leq \frac{t - t_0}{h_b} + \mathcal{N}_0, \tag{2.8}$$

where $\mathcal{N}_{\varsigma}(t, t_0)$ is the number of impulsive instances during the interval (t_0, t) .

The following assumption will be also essential.

(A_{H6}) The average impulsive interval of the impulsive sequence $\{t_r, r \in \mathcal{N}_+\}$ is equal to h_b and there exist two constants $0 < \phi < \widehat{\phi} < +\infty$ such that $\phi \leq t_r - t_{r-1} \leq \widehat{\phi}, \forall r \in \mathcal{N}_+$.

Lemma 2.6. [18] Let $\mathfrak{Z}(t)$ be a continuous and differentiable for $t \geq t_0$. Then

$$\frac{1}{2} \left(D^\beta \mathfrak{Z}^\top(t) \mathfrak{Z}(t) \right) \leq \mathfrak{Z}^\top(t) D^\beta \mathfrak{Z}(t), t \geq t_0. \tag{2.9}$$

Lemma 2.7. [17] Let $\mathcal{V}(t)$ on $[t_0, +\infty)$ be a continuous function and satisfies $D^\beta \mathcal{V}(t) \leq \widehat{\gamma} \mathcal{V}(t)$. Then

$$\mathcal{V}(t) \leq \mathcal{V}(t_0) \mathbb{E}_\beta \left(\widehat{\gamma} (t - t_0)^\beta \right),$$

where $0 < \beta < 1$ and $\widehat{\gamma}$ are constant.

Lemma 2.8. [43] For real matrices E and F with appropriate dimensions, any positive constant θ and any symmetric matrix $\Phi > 0$, the following inequality holds:

$$E^T F + F^T E \leq \theta^{-1} E^T \Phi E + \theta F^T \Phi^{-1} F.$$

The controlled uncertain FDMASs (2.3) is considered as [12]:

$$\begin{cases} D^\beta \mathfrak{Z}_p(t) = (E + \Delta E) \mathfrak{Z}_p(t) + (F + \Delta F) \omega(\mathfrak{Z}_p(t)) \\ \quad + (G + \Delta G) \omega(\mathfrak{Z}_p(\chi_\tau)), \quad t \in (t_{r-1}, t_r], \\ \Delta \mathfrak{Z}_p(t_r) = \frac{-b_r}{\Gamma(\beta+1)} \left[\sum_{q=1}^{\mathcal{N}} a_{pq}^{\sigma(t_r)} (\mathfrak{Z}_q(t_r) - \mathfrak{Z}_p(t_r)) \right. \\ \quad \left. + d_p^{\sigma(t_r)} (\mathfrak{Z}_p(t_r) - \mathfrak{Z}_0(t_r)) \right], \quad r \in \mathcal{N}_+, \end{cases} \tag{2.10}$$

where $0 < \beta < 1$; $\Delta \mathfrak{Z}_p(t)$ is the leap of the state at an instant time t_r ; $t_r < t_{r+1}$, and $\lim_{r \rightarrow +\infty} t_r = +\infty$; $\mathfrak{Z}_p(t_0) = \mathfrak{Z}_p(t_0^+)$, and $\mathfrak{Z}_p(t_r) = \mathfrak{Z}_p(t_r^-)$ for $r \in \mathcal{N}_+$.

Define $\widehat{\mathfrak{Z}}_p(t) = \mathfrak{Z}_p(t) - \mathfrak{Z}_0(t)$. Then, the error system has the form:

$$\begin{cases} D^\beta \widehat{\mathfrak{Z}}_p(t) = (E + \Delta E) \widehat{\mathfrak{Z}}_p(t) + (F + \Delta F) \widehat{\omega}_i(\widehat{\mathfrak{Z}}_p(t)) \\ \quad + (G + \Delta G) H(\widehat{\mathfrak{Z}}_p(\chi_\tau)), \quad t \in (t_{r-1}, t_r], \\ \Delta \widehat{\mathfrak{Z}}_p(t_r) = \frac{-b_r}{\Gamma(\beta+1)} \left[\sum_{q=1}^{\mathcal{N}} a_{pq}^{\sigma(t_r)} (\widehat{\mathfrak{Z}}_q(t_r^+) - \widehat{\mathfrak{Z}}_p(t_r^+)) \right. \\ \quad \left. + d_p^{\sigma(t_r)} \widehat{\mathfrak{Z}}_p(t_r^+) \right], r \in \mathcal{N}_+, \end{cases} \tag{2.11}$$

where $\widehat{\omega}_i(\widehat{\mathfrak{Z}}_p(t)) = \omega(\widehat{\mathfrak{Z}}_p(t) + \mathfrak{Z}_0(t)) - \omega(\mathfrak{Z}_0(t))$.

Compact forms can be written from (2.11) as shown

$$\begin{cases} D^\beta \widehat{\mathfrak{Z}}(t) = (\mathcal{I}_N \otimes (E + \Delta E))\widehat{\mathfrak{Z}}(t) + (\mathcal{I}_N \otimes (F + \Delta F))H(\widehat{\mathfrak{Z}}(t)) \\ \quad + (\mathcal{I}_N \otimes (G + \Delta G))H(\widehat{\mathfrak{Z}}(\chi_\tau)), \\ \Delta \widehat{\mathfrak{Z}}(t_r^+) = \left(\mathcal{I}_N - \frac{b_r}{\Gamma(\beta+1)}(\mathcal{L}^{\sigma(t_r)} + \widehat{\Phi}^{\sigma(t_r)}) \otimes \mathcal{I}_n\right)\widehat{\mathfrak{Z}}(t_r^+), \end{cases} \tag{2.12}$$

where $\widehat{\Phi} = \text{diag}\{d_1, d_2, \dots, d_N\}$.

3. Main results

Theorem 3.1. Given non-zero scalars $\theta_i, \theta_\epsilon, \theta_\delta, \alpha_i, \alpha_\epsilon, \alpha_\delta, \phi, \Theta_\delta, \Theta_\phi$ and $\hat{\theta}$, suppose that Assumptions $(\mathcal{A}_{H2}) - (\mathcal{A}_{H6})$ are satisfied for positive symmetric matrices Ψ_κ, Ψ_σ , and $\Theta_\delta - \Theta_\phi \leq 0$, $r \in \mathcal{N}_+, \gamma(t_r)\mathbb{E}_\beta((\Theta_\delta - \Theta_\phi)\phi^\beta) < 1$. Then, the uncertain FDMAS (2.3) is exponentially stable under the suggested impulsive control strategy (2.7) if the following conditions are satisfied:

(i) $N\Psi_\sigma N + \theta_\delta N(\alpha_\delta \otimes \mathcal{I}_n)N \leq \Theta_\delta Q$, (3.1)

(ii) $\begin{bmatrix} \Gamma_\pi & Q & QF & QG \\ Q & -(\theta_i + \theta_\epsilon + \theta_\delta) \otimes \mathcal{I}_n & 0 & 0 \\ F^T Q & 0 & -\Psi_\kappa & 0 \\ G^T Q & 0 & 0 & -\Psi_\sigma \end{bmatrix} < 0$, (3.2)

(iii) $\hat{\eta}_\psi < \frac{\ln(\gamma_1 \mathbb{E}_\beta(\Theta_\delta - \Theta_\phi)\phi^\beta) + \hat{\theta}h_b}{(\ln(\gamma_1 \mathbb{E}_\beta(\Theta_\delta - \Theta_\phi)\phi^\beta) - \ln(\gamma_2 \mathbb{E}_\beta(\Theta_\delta - \Theta_\phi)\phi^\beta))}$, (3.3)

where $\Gamma_\pi = QE + E^T Q + \theta_i(\alpha_i \otimes \mathcal{I}_n) + N\Psi_\kappa N + \theta_\epsilon(\alpha_\epsilon \otimes \mathcal{I}_n) + \Theta_\phi Q$, $N = \text{diag}\{\psi_1, \dots, \psi_n\}$,

$$\gamma_1 = \sigma_{\max}^2 \left\{ \mathcal{I}_N - \frac{b_r}{\Gamma(\beta+1)}(\mathcal{L}^1 + \widehat{\Phi}^1) \otimes \mathcal{I}_n \right\},$$

$$\gamma_2 = \max_{\sigma(t_r) \in \{2, \dots, s\}} \sigma_{\max}^2 \left\{ \mathcal{I}_N - \frac{b_r}{\Gamma(\beta+1)}(\mathcal{L}^{\sigma(t_r)} + \widehat{\Phi}^{\sigma(t_r)}) \otimes \mathcal{I}_n \right\}.$$

Proof. We construct the Lyapunov functional candidate as follows:

$$\mathbb{V}(t) = \mathbb{V}(\widehat{\mathfrak{Z}}(t)) = \sum_{p=1}^N \widehat{\mathfrak{Z}}_p^T(t)(Q \otimes \mathcal{I}_n)\widehat{\mathfrak{Z}}_p(t). \tag{3.4}$$

For $t_{r-1} < t \leq t_r$, taking the Caputo fractional derivative of $\mathbb{V}(t)$ with system (2.11) and according to Lemma 2.6, for any $\widehat{\mathfrak{Z}}(t) \in \mathcal{R}^n$, we have

$$\begin{aligned} D^\beta \mathbb{V}(t) &\leq \sum_{p=1}^N 2\widehat{\mathfrak{Z}}_p^T(t)(Q \otimes \mathcal{I}_n)\mathbb{D}^\beta \widehat{\mathfrak{Z}}_p(t) \\ &\leq \sum_{p=1}^N 2\widehat{\mathfrak{Z}}_p^T(t)(Q \otimes \mathcal{I}_n) \left((E + \Delta E)\widehat{\mathfrak{Z}}_p(t) \right. \\ &\quad \left. + (F + \Delta F)H(\widehat{\mathfrak{Z}}_p(t)) + (G + \Delta G)H(\widehat{\mathfrak{Z}}_p(\chi_\tau)) \right) \\ &\leq \sum_{p=1}^N \left(\widehat{\mathfrak{Z}}_p^T(t)(QE + E^T Q)\widehat{\mathfrak{Z}}_p(t) \right. \\ &\quad \left. + 2\widehat{\mathfrak{Z}}_p^T(t)(Q\Delta E)\widehat{\mathfrak{Z}}_p(t) + 2\widehat{\mathfrak{Z}}_p^T(t)QFH(\widehat{\mathfrak{Z}}_p(t)) \right. \\ &\quad \left. + 2\widehat{\mathfrak{Z}}_p^T(t)Q\Delta FH(\widehat{\mathfrak{Z}}_p(t)) + 2\widehat{\mathfrak{Z}}_p^T(t)QGH(\widehat{\mathfrak{Z}}_p(\chi_\tau)) \right. \\ &\quad \left. + 2\widehat{\mathfrak{Z}}_p^T(t)Q\Delta GH(\widehat{\mathfrak{Z}}_p(\chi_\tau)) \right). \end{aligned} \tag{3.5}$$

Based on Assumptions $(\mathcal{A}_{H2}), (\mathcal{A}_{H3})$ and Lemma 2.8, we have

$$\begin{aligned}
 2\widehat{\mathfrak{Z}}_p^T(t)Q\Delta E\widehat{\mathfrak{Z}}_p(t) &\leq \theta_i^{-1}\widehat{\mathfrak{Z}}_p^T(t)QQ\widehat{\mathfrak{Z}}_p(t) + \theta_i\widehat{\mathfrak{Z}}_p^T(t)(\alpha_i \otimes \mathcal{I}_n)\widehat{\mathfrak{Z}}_p(t), \\
 2\widehat{\mathfrak{Z}}_p^T(t)QFH(\widehat{\mathfrak{Z}}_p(t)) &\leq \widehat{\mathfrak{Z}}_p^T(t)QF\Psi_\kappa^{-1}F^TQ\widehat{\mathfrak{Z}}_p(t) + \widehat{\mathfrak{Z}}_p^T(t)\aleph\Psi_\kappa\aleph\widehat{\mathfrak{Z}}_p(t), \\
 2\widehat{\mathfrak{Z}}_p^T(t)Q\Delta F\widehat{\mathfrak{Z}}_p(t) &\leq \theta_\epsilon^{-1}\widehat{\mathfrak{Z}}_p^T(t)QQ\widehat{\mathfrak{Z}}_p(t) + \theta_\epsilon\widehat{\mathfrak{Z}}_p^T(t)\aleph(\alpha_\epsilon \otimes \mathcal{I}_n)\aleph\widehat{\mathfrak{Z}}_p(t), \\
 2\widehat{\mathfrak{Z}}_p^T(t)QGH(\widehat{\mathfrak{Z}}_p(\chi_\tau)) &\leq \widehat{\mathfrak{Z}}_p^T(t)QG\Psi_\sigma^{-1}G^TQ\widehat{\mathfrak{Z}}_p(t) + H(\widehat{\mathfrak{Z}}_p(\chi_\tau))\aleph\Psi_\sigma\aleph H(\widehat{\mathfrak{Z}}_p(\chi_\tau)), \\
 2\widehat{\mathfrak{Z}}_p^T(t)Q\Delta GH(\widehat{\mathfrak{Z}}_p(\chi_\tau)) &\leq \theta_\delta^{-1}\widehat{\mathfrak{Z}}_p^T(t)QQ\widehat{\mathfrak{Z}}_p(t) + \theta_\delta\widehat{\mathfrak{Z}}_p^T(\chi_\tau)\aleph(\alpha_\delta \otimes \mathcal{I}_n)\aleph\widehat{\mathfrak{Z}}_p(\chi_\tau).
 \end{aligned}$$

Combing the above inequalities with (3.5), we have

$$\begin{aligned}
 D^\beta \mathbb{V}(\mathfrak{t}) &\leq \sum_{p=1}^N \widehat{\mathfrak{Z}}_p^T(\mathfrak{t})(QE + E^TQ \\
 &+ \theta_i^{-1}QQ + \theta_i(\alpha_i \otimes \mathcal{I}_n)\mathcal{I}_n + QE\Psi_\kappa^{-1}E^TQ + \aleph\Psi_\kappa\aleph \\
 &+ \theta_\epsilon^{-1}QQ + \theta_\epsilon(\alpha_\epsilon \otimes \mathcal{I}_n) + QG\Psi_\sigma^{-1}G^TQ + \theta_\delta^{-1}QQ) \widehat{\mathfrak{Z}}_p(\mathfrak{t}) \\
 &+ \sum_{p=1}^N \widehat{\mathfrak{Z}}_p^T(\chi_\tau)(\aleph\Psi_\sigma\aleph + \theta_\delta\aleph(\alpha_\delta \otimes \mathcal{I}_n)\aleph) \widehat{\mathfrak{Z}}_p(\chi_\tau).
 \end{aligned} \tag{3.6}$$

Then, it follows from (3.2) that

$$\begin{aligned}
 D^\beta \mathbb{V}(\mathfrak{t}) &\leq -\Theta_\varphi \sum_{p=1}^N \widehat{\mathfrak{Z}}_p^T(\mathfrak{t})(Q \otimes \mathcal{I}_n) \widehat{\mathfrak{Z}}_p(\mathfrak{t}) + \Theta_\delta \sum_{p=1}^N \widehat{\mathfrak{Z}}_p^T(\chi_\tau)(Q \otimes \mathcal{I}_n) \widehat{\mathfrak{Z}}_p(\chi_\tau) \\
 &\leq -\Theta_\varphi \mathbb{V}(\mathfrak{t}) + \Theta_\delta \sup_{\chi_\tau \leq \zeta \leq \mathfrak{t}} \mathbb{V}(\zeta).
 \end{aligned} \tag{3.7}$$

From (3.7), we get

$$D^\beta \mathbb{V}(\mathfrak{t}) \leq (\Theta_\delta - \Theta_\varphi) \mathbb{V}(\mathfrak{t}) \tag{3.8}$$

when the Razumikhin condition [17]

$$\sup_{\chi_\tau \leq \zeta \leq \mathfrak{t}} \mathbb{V}(\zeta) \leq \mathbb{V}(\mathfrak{t}) \tag{3.9}$$

is satisfied. When $r \in \mathcal{N}_+$,

$$\begin{aligned}
 \mathbb{V}(\mathfrak{t}_r^+) &= \widehat{\mathfrak{Z}}^T(\mathfrak{t}_r^+)(\mathcal{I}_N \otimes Q) \widehat{\mathfrak{Z}}(\mathfrak{t}_r^+) \\
 &= \left(\left(\mathcal{I}_N - \frac{\mathbb{b}_r}{\Gamma(\beta+1)} (\mathcal{L}^{\sigma(\mathfrak{t}_r)} + \widehat{\Phi}^{\sigma(\mathfrak{t}_r)}) \otimes \mathcal{I}_n \right) \widehat{\mathfrak{Z}}(\mathfrak{t}) \right)^T (\mathcal{I}_N \otimes Q) \left(\left(\mathcal{I}_N - \frac{\mathbb{b}_r}{\Gamma(\beta+1)} (\mathcal{L}^{\sigma(\mathfrak{t}_r)} + \widehat{\Phi}^{\sigma(\mathfrak{t}_r)}) \otimes \mathcal{I}_n \right) \widehat{\mathfrak{Z}}(\mathfrak{t}) \right) \\
 &\leq \gamma(\mathfrak{t}_r) \mathbb{V}(\mathfrak{t}_r),
 \end{aligned} \tag{3.10}$$

where $\gamma(\mathfrak{t}_r) = \sigma_{\max}^2 \left\{ \mathcal{I}_N - \frac{\mathbb{b}_r}{\Gamma(\beta+1)} (\mathcal{L}^{\sigma(\mathfrak{t}_r)} + \widehat{\Phi}^{\sigma(\mathfrak{t}_r)}) \otimes \mathcal{I}_n \right\}$.

From (3.8) and (3.10) we have

$$\begin{cases} D^\beta \mathbb{V}(\mathfrak{t}) \leq (\Theta_\delta - \Theta_\varphi) \mathbb{V}(\mathfrak{t}), & \mathfrak{t}_{r-1} < \mathfrak{t} \leq \mathfrak{t}_r, \\ \mathbb{V}(\mathfrak{t}_r^+) \leq \gamma(\mathfrak{t}_r) \mathbb{V}(\mathfrak{t}_r), & r \in \mathcal{N}_+. \end{cases} \tag{3.11}$$

According to Lemma 2.7 from (3.11), we get

$$\mathbb{V}(\mathfrak{t}) \leq \mathbb{V}(\mathfrak{t}_0) E_\beta \left((\Theta_\delta - \Theta_\varphi) (\mathfrak{t} - \mathfrak{t}_0)^\beta \right),$$

for $t \in [t_0, t_1]$, which shows that if $(\Theta_\delta - \Theta_\varphi) \leq 0$ and $\gamma(\mathfrak{t}_1) E_\beta \left((\Theta_\delta - \Theta_\varphi) \phi^\beta \right) < 1$,

$$\mathbb{V}(\mathfrak{t}) \leq \mathbb{V}(\mathfrak{t}_0) \leq \mathbb{V}(\mathfrak{t}_0) \mu, e^{\frac{\ln(\gamma(\mathfrak{t}_1) E_\beta \left((\Theta_\delta - \Theta_\varphi) \phi^\beta \right))}{h_b} (\mathfrak{t} - \mathfrak{t}_0)}. \tag{3.12}$$

On the other hand, for any $r \in \mathcal{N}_+$, by using Lemma 2.7 in (3.11), we have

$$\mathbb{V}(\mathfrak{t}_r^+) \leq \gamma(\mathfrak{t}_r) E_\beta \left((\Theta_\delta - \Theta_\varphi) (\mathfrak{t}_r - \mathfrak{t}_{r-1})^\beta \right). \tag{3.13}$$

Hence, by the use of recursion

$$\mathbb{V}(\mathbb{t}_r^+) \leq \mathbb{V}(\mathbb{t}_0)(\gamma(\mathbb{t}_r))^r \prod_{\xi=1}^r \mathbb{E}_\beta \left((\Theta_\delta - \Theta_\varphi)(\mathbb{t}_\xi - \mathbb{t}_{\xi-1})^\beta \right). \tag{3.14}$$

For $t > t_1$, there exists a non-negative integer k such that, $t_k < t \leq t_{k+1}$.

$$\begin{aligned} \mathbb{V}(\mathbb{t}) &\leq \mathbb{V}(\mathbb{t}_k^+) \mathbb{E}_\beta \left((\Theta_\delta - \Theta_\varphi)(\mathbb{t} - \mathbb{t}_k)^\beta \right) \\ &\leq \mathbb{V}(\mathbb{t}_0)(\gamma(\mathbb{t}_z))^k \prod_{\xi=1}^k \mathbb{E}_\beta \left((\Theta_\delta - \Theta_\varphi)(\mathbb{t}_\xi - \mathbb{t}_{\xi-1})^\beta \right) \\ &\times \mathbb{E}_\beta \left((\Theta_\delta - \Theta_\varphi)(\mathbb{t} - \mathbb{t}_k)^\beta \right). \end{aligned} \tag{3.15}$$

From Definition 2.5 and Assumption (A_{H6}), $k = \varpi_1 \leq \frac{t-t_0}{h_b} + \mathcal{N}_0$. When there are no attacks (i.e., $\sigma(t_r) = 1$), we have

$$\begin{aligned} \mathbb{V}(\mathbb{t}) &\leq \mathbb{V}(\mathbb{t}_0)(\gamma_1 \mathbb{E}_\beta((\Theta_\delta - \Theta_\varphi)\phi^\beta))^{\varpi_1} \\ &\leq \mathbb{V}(\mathbb{t}_0) \mu_\zeta e^{\frac{\ln(\gamma_1 \mathbb{E}_\beta((\Theta_\delta - \Theta_\varphi)\phi^\beta))}{h_b}(\mathbb{t} - \mathbb{t}_0)}, \end{aligned} \tag{3.16}$$

where $\mu_\zeta = (\gamma_1 \mathbb{E}_\beta((\Theta_\delta - \Theta_\varphi)\phi^\beta))^{-\mathcal{N}_0} > 1$, $\mu_t = (\gamma_1 \mathbb{E}_\beta((\Theta_\delta - \Theta_\varphi)\phi^\beta))^{-\frac{\hat{\theta}}{h_b}} > 1$. Define $\mu = \max\{\mu_1, \mu_2\}$. Then

$$\mathbb{V}(\mathbb{t}) \leq \mathbb{V}(\mathbb{t}_0) \mu e^{\frac{\ln(\gamma_1 \mathbb{E}_\beta((\Theta_\delta - \Theta_\varphi)\phi^\beta))}{h_b}(\mathbb{t} - \mathbb{t}_0)} \leq \mathbb{V}(\mathbb{t}_0) \mu e^{-(\Xi + \hat{\theta})(\mathbb{t} - \mathbb{t}_0)}, \tag{3.17}$$

where

$$\Xi = - \left(\frac{\ln(\gamma_1 \mathbb{E}_\beta((\Theta_\delta - \Theta_\varphi)\phi^\beta))}{h_b} + \hat{\theta} \right) > 0. \tag{3.18}$$

The FDMASs (2.3) is thus exponentially stable.

In the general case, when there is at least one attack,

$$\mathbb{V}(\mathbb{t}) \leq \mathbb{V}(\mathbb{t}_0)(\gamma_1 \mathbb{E}_\beta((\Theta_\delta - \Theta_\varphi)\phi^\beta))^{\varpi_1} (\gamma_2 \mathbb{E}_\beta((\Theta_\delta - \Theta_\varphi)\phi^\beta))^{\varpi_\zeta}.$$

By Definition 2.5, it follows that

$$\frac{\varpi_1}{\varpi_x} \left(\frac{t - t_0}{h_b} - \mathcal{N}_0 \right) \leq \varpi_1 \leq \frac{\varpi_1}{\varpi_x} \left(\frac{t - t_0}{h_b} + \mathcal{N}_0 \right), \tag{3.19}$$

$$\frac{\varpi_\zeta}{\varpi_x} \left(\frac{t - t_0}{h_b} - \mathcal{N}_0 \right) \leq \varpi_\zeta \leq \frac{\varpi_\zeta}{\varpi_x} \left(\frac{t - t_0}{h_b} + \mathcal{N}_0 \right), \tag{3.20}$$

where $\varpi_x = \varpi_1 + \varpi_\zeta$; ϖ_ζ denotes the number of impulsive moments when the system suffers from attacks over the interval (t_0, t) .

Case (i): $\gamma_2 \geq 1$, and $\gamma_2 \mathbb{E}_\beta((\Theta_\delta - \Theta_\varphi)\phi^\beta) < 1$, thus

$$\begin{aligned} \mathbb{V}(\mathbb{t}) &< \mathbb{V}(\mathbb{t}_0)(\gamma_1 \mathbb{E}_\beta((\Theta_\delta - \Theta_\varphi)\phi^\beta))^{\frac{\varpi_1}{\varpi_x} \left(\frac{t-t_0}{h_b} - \mathcal{N}_0 \right)} (\gamma_2 \mathbb{E}_\beta((\Theta_\delta - \Theta_\varphi)\phi^\beta))^{\frac{\varpi_\zeta}{\varpi_x} \left(\frac{t-t_0}{h_b} - \mathcal{N}_0 \right)} \\ &< \mathbb{V}(\mathbb{t}_0)(\gamma_1 \mathbb{E}_\beta((\Theta_\delta - \Theta_\varphi)\phi^\beta))^{-\frac{\varpi_1 \mathcal{N}_0}{\varpi_x}} (\gamma_2 \mathbb{E}_\beta((\Theta_\delta - \Theta_\varphi)\phi^\beta))^{-\frac{\varpi_\zeta \mathcal{N}_0}{\varpi_x}} \\ &\times e^{\left(\frac{\ln(\gamma_1 \mathbb{E}_\beta((\Theta_\delta - \Theta_\varphi)\phi^\beta))}{h_b} \frac{\varpi_1}{\varpi_x} + \frac{\ln(\gamma_2 \mathbb{E}_\beta((\Theta_\delta - \Theta_\varphi)\phi^\beta))}{h_b} \frac{\varpi_\zeta}{\varpi_x} \right) (\mathbb{t} - \mathbb{t}_0)}. \end{aligned} \tag{3.21}$$

Case (ii) $0 < \gamma_2 < 1$, and $\gamma_2 \mathbb{E}_\beta((\Theta_\delta - \Theta_\varphi)\phi^\beta) < 1$.

From case (i) and (ii), if $\Theta_\delta - \Theta_\varphi \leq 0$, similar to the result in (3.21), we have

$$\mathbb{V}(\mathbb{t}) < \mathbb{V}(\mathbb{t}_0) \hat{\mu}_\pi e^{\left(\frac{\ln(\gamma_1 \mathbb{E}_\beta((\Theta_\delta - \Theta_\varphi)\phi^\beta))}{h_b} \frac{\varpi_1}{\varpi_x} + \frac{\ln(\gamma_2 \mathbb{E}_\beta((\Theta_\delta - \Theta_\varphi)\phi^\beta))}{h_b} \frac{\varpi_\zeta}{\varpi_x} \right) (\mathbb{t} - \mathbb{t}_0)},$$

where $\hat{\mu}_\pi = (\gamma_1 \mathbb{E}_\beta((\Theta_\delta - \Theta_\varphi)\phi^\beta))^{\frac{\sigma_x \mathcal{N}_0}{\sigma_x \mathcal{N}_0}} (\gamma_2 \mathbb{E}_\beta((\Theta_\delta - \Theta_\varphi)\phi^\beta))^{-\frac{\sigma_x \mathcal{N}_0}{\sigma_x \mathcal{N}_0}} > \mathbb{1}$.

Then

$$\begin{aligned} \mathbb{V}(\hat{\mathbb{t}}) &< \mathbb{V}(\hat{\mathbb{t}}_0) \hat{\mu}_\pi e^{\left(\frac{\ln(\gamma_1 \mathbb{E}_\beta((\Theta_\delta - \Theta_\varphi)\phi^\beta))}{h_b}\right) (1 - \frac{\sigma_x}{\sigma_x}) + \frac{\ln(\gamma_2 \mathbb{E}_\beta((\Theta_\delta - \Theta_\varphi)\phi^\beta))}{h_b} \frac{\sigma_x}{\sigma_x}} (t - t_0) \\ &< \mathbb{V}(\hat{\mathbb{t}}_0) \hat{\mu}_\pi e^{-\hat{\chi}_\theta (t - t_0)}, \end{aligned}$$

where $\hat{\chi}_\theta = \hat{\chi} + \hat{\theta}$, $\hat{\chi} = -\left(\frac{\ln(\gamma_1 \mathbb{E}_\beta((\Theta_\delta - \Theta_\varphi)\phi^\beta))}{h_b}\right) (1 - \hat{\eta}_\varphi) + \frac{\ln(\gamma_2 \mathbb{E}_\beta((\Theta_\delta - \Theta_\varphi)\phi^\beta))}{h_b} \hat{\eta}_\varphi + \hat{\theta} > 0$, $\hat{\eta}_\varphi = \frac{\sigma_x}{\sigma_x}$.

We conclude that

$$\|\hat{\mathbb{S}}(t)\| < \sqrt{\frac{\mathbb{V}(\hat{\mathbb{t}}_0) \hat{\mu}_\pi e^{-\hat{\chi}_\theta (t - t_0)}}{\lambda_{\min}(Q)}}.$$

The proof is completed. \square

Remark 3.2. Based on an average impulsive interval, the average dwell time approach and Lyapunov stability theory, a novel impulsive secure consensus problem for systems (2.3) and (2.4) with uncertain parameters subject to DoS attacks is solved by the proposed impulsive protocol (2.7). Different from the existing controller design methods [34–36], the influence of the DoS attacks is considered. The DoS attacks on the edges might lead to unsatisfactory consensus performance. A switching mechanism is proposed to switch the underlying topologies to ensure the tolerance for network disconnections.

Remark 3.3. When the system (2.3) is not a subject to an attack, then by condition (3.18) in Theorem 3.1, the average impulsive interval satisfies $h_b < -\frac{\ln(\gamma_1 \mathbb{E}_\beta((\Theta_\delta - \Theta_\varphi)\phi^\beta))}{\hat{\theta}}$ and also when the system is subject to attacks, then by the impulsive attack ratio condition (3.3) in Theorem 3.1, the average impulsive interval

$$\hat{h}_b = h_b < \frac{\ln(\gamma_1 \mathbb{E}_\beta((\Theta_\delta - \Theta_\varphi)\phi^\beta)) (\hat{\eta}_\varphi - \mathbb{1}) - \ln(\gamma_2 \mathbb{E}_\beta((\Theta_\delta - \Theta_\varphi)\phi^\beta)) \hat{\eta}_\varphi}{\hat{\theta}},$$

i.e., the system can detect the attacks information (γ_2 and $\hat{\eta}_\varphi$ are known), which guarantees the secure performance of tracking consensus error system by adjusting the average impulsive interval \hat{h}_b .

Corollary 3.4. Given non-zero scalars $\theta_1, \theta_\epsilon, \theta_\delta, \alpha_1, \alpha_\epsilon, \alpha_\delta, \phi, \Theta_\delta, \Theta_\varphi$ and $\bar{\theta}$, suppose that Assumptions $(\mathcal{A}_{H2}) - (\mathcal{A}_{H6})$ are satisfied for positive symmetric matrices Ψ_κ, Ψ_σ and $\Theta_\delta - \Theta_\varphi > 0$, for $r \in \mathcal{N}_+, \gamma(t_r) \mathbb{E}_\beta((\Theta_\delta - \Theta_\varphi)\hat{\varphi}^\beta) < \mathbb{1}$. Then, under the suggested impulsive control strategy (2.7), the FDMAS (2.3) is exponentially stable under the following conditions:

$$(i) \quad \mathbb{N} \Psi_\sigma \mathbb{N} + \theta_\delta \mathbb{N} (\alpha_\delta \otimes \mathcal{I}_n) \mathbb{N} \leq \Theta_\delta Q, \tag{3.22}$$

$$(ii) \quad \begin{bmatrix} \Gamma_\pi & Q & QF & QG \\ Q & -(\theta_1 + \theta_\epsilon + \theta_\delta) \otimes \mathcal{I}_n & 0 & 0 \\ F^T Q & 0 & -\Psi_\kappa & 0 \\ G^T Q & 0 & 0 & -\Psi_\sigma \end{bmatrix} < 0, \tag{3.23}$$

$$(iii) \quad \hat{\eta}_\varphi < \frac{\ln(\gamma_1 \mathbb{E}_\beta(\Theta_\delta - \Theta_\varphi)\hat{\varphi}^\beta) + \bar{\theta} h_b}{(\ln(\gamma_1 \mathbb{E}_\beta(\Theta_\delta - \Theta_\varphi)\hat{\varphi}^\beta) - \ln(\gamma_2 \mathbb{E}_\beta(\Theta_\delta - \Theta_\varphi)\hat{\varphi}^\beta))}. \tag{3.24}$$

Proof. Corollary 3.4 can be proved using standard arguments close to these in the proof of Theorem 3.1. The set of inequalities (3.11) shows that if $\Theta_\delta - \Theta_\varphi > 0$, for any $t_0 \leq t \leq t_1$,

$$\begin{aligned} \mathbb{V}(\hat{\mathbb{t}}) &\leq \mathbb{V}(\hat{\mathbb{t}}_0) \gamma(\hat{\mathbb{t}}_r) \mathbb{E}_\beta((\Theta_\delta - \Theta_\varphi)\hat{\varphi}^\beta) \\ &\leq \mathbb{V}(\hat{\mathbb{t}}_0) \mu_\theta e^{\frac{\ln(\gamma(t_r) \mathbb{E}_\beta((\Theta_\delta - \Theta_\varphi)\hat{\varphi}^\beta))}{h_b} (t - t_0)}, \end{aligned}$$

where $\mu_\theta = \mathbb{E}_\beta((\Theta_\delta - \Theta_\varphi)\hat{\varphi}^\beta) (\gamma(\hat{\mathbb{t}}_r) \mathbb{E}_\beta((\Theta_\delta - \Theta_\varphi)\hat{\varphi}^\beta))^{-\frac{\sigma}{h_b}} > \mathbb{1}$.

On the other hand, it follows from Lemma 2.7, for any $r \in \mathcal{N}_+$, that if $\Theta_\delta - \Theta_\varphi > 0$,

$$\mathbb{V}(\hat{\mathbb{t}}_0) \leq \mathbb{V}(\hat{\mathbb{t}}_0) \mu_x e^{\frac{\ln(\gamma_1 \mathbb{E}_\beta(\Theta_\delta - \Theta_\varphi)\hat{\varphi}^\beta)}{h_b} (t - t_0)},$$

where $\mu_x = (\gamma_1 \mathbb{E}_\beta((\Theta_\delta - \Theta_\varphi)\hat{\varphi}^\beta))^{-\mathcal{N}_0} \mathbb{E}_\beta((\Theta_\delta - \Theta_\varphi)\hat{\varphi}^\beta) > \mathbb{1}$.

Define $\mu_{\varrho} = \max\{\mu_{\theta}, \mu_{\alpha}\}$, if $\Theta_{\delta} - \Theta_{\varphi} > 0$, and $\gamma_1 \mathbb{E}_{\beta}((\Theta_{\delta} - \Theta_{\varphi}) \widehat{\varphi}^{\beta}) < 1$,

$$\mathbb{V}(\mathfrak{t}) \leq \mathbb{V}(\mathfrak{t}_0) \mu_{\varrho} e^{\frac{\ln(\gamma_1 \mathbb{E}_{\beta}((\Theta_{\delta} - \Theta_{\varphi}) \widehat{\varphi}^{\beta}))}{h_b} (\mathfrak{t} - \mathfrak{t}_0)}.$$

For the general case, when there exist attacks,

$$\mathbb{V}(\mathfrak{t}) \leq \mathbb{V}(\mathfrak{t}_0) (\gamma_1 \mathbb{E}_{\beta}((\Theta_{\delta} - \Theta_{\varphi}) \widehat{\varphi}^{\beta}))^{\varpi_1} (\gamma_2 \mathbb{E}_{\beta}((\Theta_{\delta} - \Theta_{\varphi}) \widehat{\varphi}^{\beta}))^{\varpi_2}.$$

By Definition 2.5, $\gamma_2 \in \mathcal{R}_+$, $\gamma_2 \mathbb{E}_{\beta}((\Theta_{\delta} - \Theta_{\varphi}) \widehat{\varphi}^{\beta}) < 1$, and

$$\begin{aligned} \mathbb{V}(\mathfrak{t}) &< \mathbb{V}(\mathfrak{t}_0) \check{\mu}_{\xi} e^{\left(\frac{\ln(\gamma_1 \mathbb{E}_{\beta}((\Theta_{\delta} - \Theta_{\varphi}) \widehat{\varphi}^{\beta}))}{h_b} \frac{\varpi_1}{\varpi_2} + \frac{\ln(\gamma_2 \mathbb{E}_{\beta}((\Theta_{\delta} - \Theta_{\varphi}) \widehat{\varphi}^{\beta}))}{h_b} \frac{\varpi_2}{\varpi_2}\right) (\mathfrak{t} - \mathfrak{t}_0)} \\ &< \mathbb{V}(\mathfrak{t}_0) \check{\mu}_{\xi} e^{-\Upsilon_{\delta} (\mathfrak{t} - \mathfrak{t}_0)}, \end{aligned}$$

where $\check{\mu}_{\xi} = (\gamma_1 \mathbb{E}_{\beta}((\Theta_{\delta} - \Theta_{\varphi}) \widehat{\varphi}^{\beta}))^{\frac{\varpi_1}{\varpi_2} \mathcal{N}_{\theta}} (\gamma_2 \mathbb{E}_{\beta}((\Theta_{\delta} - \Theta_{\varphi}) \widehat{\varphi}^{\beta}))^{\frac{\varpi_2}{\varpi_2} \mathcal{N}_{\theta}} > 1$, $\Upsilon_{\delta} = \Upsilon + \bar{\theta}$,

$$\Upsilon = -\left(\frac{\ln(\gamma_1 \mathbb{E}_{\beta}((\Theta_{\delta} - \Theta_{\varphi}) \widehat{\varphi}^{\beta}))}{h_b} (1 - \widehat{\eta}_{\varphi}) + \frac{\ln(\gamma_2 \mathbb{E}_{\beta}((\Theta_{\delta} - \Theta_{\varphi}) \widehat{\varphi}^{\beta}))}{h_b} \widehat{\eta}_{\varphi} + \bar{\theta}\right) > 0, \widehat{\eta}_{\varphi} = \frac{\varpi_2}{\varpi_2}.$$

We conclude that

$$\|\widehat{\mathfrak{Z}}(\mathfrak{t})\| < \sqrt{\frac{\mathbb{V}(\mathfrak{t}_0) \check{\mu}_{\xi}}{\lambda_{\min}(\mathbb{Q})}} e^{-\frac{\Upsilon_{\delta}}{2} (\mathfrak{t} - \mathfrak{t}_0)}.$$

The proof is completed. \square

Theorem 3.5. Assume that Assumptions (\mathcal{A}_{H1}) and $(\mathcal{A}_{H3}) - (\mathcal{A}_{H6})$ are satisfied for non-zero scalars $\theta_1, \theta_{\epsilon}, \theta_{\delta}, \alpha_1, \alpha_{\epsilon}, \alpha_{\delta}, \phi, \Theta_{\delta}, \Theta_{\varphi}$ and $\hat{\theta}$, positive symmetric matrices $\widehat{\Psi}_{\kappa}, \widehat{\Psi}_{\sigma}$ exist and $\Theta_{\delta} - \Theta_{\varphi} \leq 0$, for $r \in \mathcal{N}_+$, $\gamma(t_r) \mathbb{E}_{\beta}((\Theta_{\delta} - \Theta_{\varphi}) \phi^{\beta}) < 1$. Then, the uncertain FDMAS (2.3) is exponentially stable in the context of the proposed impulsive control strategy (2.7), if the following conditions are satisfied,

$$(i) \begin{bmatrix} \Xi_{\pi} & Q & QF & QG \\ Q & -(\theta_1 + \theta_{\epsilon} + \theta_{\delta}) \otimes \mathcal{I}_n & 0 & 0 \\ F^T Q & 0 & -\widehat{\Psi}_{\kappa} & 0 \\ G^T Q & 0 & 0 & -\widehat{\Psi}_{\sigma} \end{bmatrix} < 0, \tag{3.25}$$

$$(ii) \lambda_{\max}(\mathcal{N}_{\theta}^T \mathcal{N}_{\theta}) \widehat{\Psi}_{\sigma} + \lambda_{\max}(\mathcal{N}_{\theta}^T \mathcal{N}_{\theta}) \theta_{\delta} (\alpha_{\delta} \otimes \mathcal{I}_n) \leq \Theta_{\delta} Q, \tag{3.26}$$

$$(iii) \widehat{\eta}_{\varphi} < \frac{\ln(\gamma_1 \mathbb{E}_{\beta}(\Theta_{\delta} - \Theta_{\varphi}) \phi^{\beta}) + \hat{\theta} h_b}{(\ln(\gamma_1 \mathbb{E}_{\beta}(\Theta_{\delta} - \Theta_{\varphi}) \phi^{\beta}) - \ln(\gamma_2 \mathbb{E}_{\beta}(\Theta_{\delta} - \Theta_{\varphi}) \phi^{\beta}))}, \tag{3.27}$$

where $\Xi_{\pi} = QE + E^T Q + \theta_1 (\alpha_1 \otimes \mathcal{I}_n) + \lambda_{\max}(\mathcal{N}_{\theta}^T \mathcal{N}_{\theta}) \widehat{\Psi}_{\kappa} + \theta_{\epsilon} (\alpha_{\epsilon} \otimes \mathcal{I}_n) + \Theta_{\varphi} Q$, $\mathcal{N}_{\theta} = (\psi_{pq})_{n \times n}$.

Theorem 3.5 can be proved using standard arguments similar to these used in the proof of Theorem 3.1.

Corollary 3.6. Let Assumptions (\mathcal{A}_{H1}) and $(\mathcal{A}_{H3}) - (\mathcal{A}_{H6})$ be satisfied for non-zero scalars $\theta_1, \theta_{\epsilon}, \theta_{\delta}, \alpha_1, \alpha_{\epsilon}, \alpha_{\delta}, \phi, \Theta_{\delta}, \Theta_{\varphi}$ and $\bar{\theta}$, positive symmetric matrices $\widehat{\Psi}_{\kappa}, \widehat{\Psi}_{\sigma}$, exist and $\Theta_{\delta} - \Theta_{\varphi} > 0$, for $\gamma(t_k) \mathbb{E}_{\beta}((\Theta_{\delta} - \Theta_{\varphi}) \widehat{\varphi}^{\beta}) < 1$. Then, the uncertain FDMAS (2.3) is exponentially stable in the context of the proposed impulsive control strategy (2.7), if the following conditions are satisfied,

$$(i) \begin{bmatrix} \Xi_{\pi} & Q & QF & QG \\ Q & -(\theta_1 + \theta_{\epsilon} + \theta_{\delta}) \otimes \mathcal{I}_n & 0 & 0 \\ F^T Q & 0 & -\widehat{\Psi}_{\kappa} & 0 \\ G^T Q & 0 & 0 & -\widehat{\Psi}_{\sigma} \end{bmatrix} < 0, \tag{3.28}$$

$$(ii) \lambda_{\max}(\mathcal{N}_{\theta}^T \mathcal{N}_{\theta}) \widehat{\Psi}_{\sigma} + \lambda_{\max}(\mathcal{N}_{\theta}^T \mathcal{N}_{\theta}) \theta_{\delta} (\alpha_{\delta} \otimes \mathcal{I}_n) \leq \Theta_{\delta} Q, \tag{3.29}$$

$$(iii) \widehat{\eta}_{\varphi} < \frac{\ln(\gamma_1 \mathbb{E}_{\beta}(\Theta_{\delta} - \Theta_{\varphi}) \widehat{\varphi}^{\beta}) + \hat{\theta} h_b}{(\ln(\gamma_1 \mathbb{E}_{\beta}(\Theta_{\delta} - \Theta_{\varphi}) \widehat{\varphi}^{\beta}) - \ln(\gamma_2 \mathbb{E}_{\beta}(\Theta_{\delta} - \Theta_{\varphi}) \widehat{\varphi}^{\beta}))}. \tag{3.30}$$

Remark 3.7. In a special case, we can also extend our results to common nonlinear FOMASs (2.3) under the impulsive control (2.7) without input time delay and uncertain parameters.

Consider a FOMAS consisting of \mathcal{N} followers with a nonlinear function:

$$D^{\beta} \mathfrak{Z}_p(t) = E \mathfrak{Z}_p(t) + F \omega(\mathfrak{Z}_p(t)) + u_p(t). \tag{3.31}$$

The dynamics leader is known as,

$$D^\beta \mathfrak{Z}_0(t) = E\mathfrak{Z}_0(t) + F\omega(\mathfrak{Z}_0(t)). \tag{3.32}$$

The nonlinear FOMAS (3.31) under the impulsive controller (2.7) is represented as

$$\begin{cases} D^\beta \mathfrak{Z}_p(t) = E\mathfrak{Z}_p(t) + F\omega(\mathfrak{Z}_p(t)), & t \in (t_{r-1}, t_r], \\ \Delta \mathfrak{Z}_p(t_r) = \frac{-b_r}{\Gamma(\beta+1)} \left[\sum_{q=1}^N a_{pq}^{\sigma(t_r)} (\mathfrak{Z}_q(t_r) - \mathfrak{Z}_p(t_r)) \right. \\ \qquad \qquad \qquad \left. + d_p^{\sigma(t_r)} (\mathfrak{Z}_p(t_r) - \mathfrak{Z}_0(t_r)) \right], & r \in \mathcal{N}_+. \end{cases} \tag{3.33}$$

From (3.32) and (3.33), the tracking error system is obtained as

$$\begin{cases} D^\beta \widehat{\mathfrak{Z}}_p(t) = E\widehat{\mathfrak{Z}}_p(t) + FH(\widehat{\mathfrak{Z}}_p(t)), & t \in (t_{r-1}, t_r], \\ \Delta \widehat{\mathfrak{Z}}_p(t_r) = \frac{-b_r}{\Gamma(\beta+1)} \left[\sum_{q=1}^N a_{pq}^{\sigma(t_r)} (\widehat{\mathfrak{Z}}_q(t_r^+) - \widehat{\mathfrak{Z}}_p(t_r^+)) \right. \\ \qquad \qquad \qquad \left. + d_p^{\sigma(t_r)} \widehat{\mathfrak{Z}}_p(t_r^+) \right], & r \in \mathcal{N}_+. \end{cases} \tag{3.34}$$

Theorem 3.8. Suppose that Assumption $(\mathcal{A}_{H2}) - (\mathcal{A}_{H6})$ are satisfied for a non-zero scalar $\check{\theta}$ and positive symmetric matrices $\Omega_\kappa, \widehat{\theta}_\delta \leq 0$ exists, and for $r \in \mathcal{N}_+, \gamma(t_r)\mathbb{E}_\beta(\widehat{\theta}_\delta\phi^\beta) < 1$. Then, the nonlinear FOMAS (3.31) achieves an exponential consensus using the impulsive control (2.7), if the following inequalities are satisfied,

$$(i) \quad \begin{bmatrix} QE + E^T Q + \aleph^T \Omega_\kappa \aleph - \widehat{\theta}_\delta Q & QF \\ F^T Q & -\Omega_\kappa \end{bmatrix} < 0, \tag{3.35}$$

$$(ii) \quad \widehat{\eta}_\ell < \frac{\ln(\gamma_1 \mathbb{E}_\beta(\widehat{\theta}_\delta \phi^\beta)) + \check{\theta} \check{h}_b}{\ln(\gamma_1 \mathbb{E}_\beta(\widehat{\theta}_\delta \phi^\beta)) - \ln(\gamma_2 \mathbb{E}_\beta(\widehat{\theta}_\delta \phi^\beta))}. \tag{3.36}$$

The proof of Theorem 3.8 is similar to that of Theorem 3.1 and, here it is omitted.

Corollary 3.9. Suppose that Assumptions $(\mathcal{A}_{H2}) - (\mathcal{A}_{H6})$ are satisfied for a non-zero scalar $\check{\theta}$ and positive symmetric matrices $\Omega_\kappa, \widehat{\theta}_\delta > 0$ exist, and for $r \in \mathcal{N}_+, \gamma(t_r)\mathbb{E}_\beta(\widehat{\theta}_\delta \widehat{\phi}^\beta) < 1$. Then, the nonlinear FOMAS (3.31) achieves an exponential consensus using the impulsive control (2.7), if the following inequalities are satisfied,

$$(i) \quad \begin{bmatrix} QE + E^T Q + \aleph^T \Omega_\kappa \aleph - \widehat{\theta}_\delta Q & QF \\ F^T Q & -\Omega_\kappa \end{bmatrix} < 0,$$

$$(ii) \quad \widehat{\eta}_\ell < \frac{\ln(\gamma_1 \mathbb{E}_\beta(\widehat{\theta}_\delta^\beta \widehat{\phi}^\beta)) + \check{\theta} \check{h}_b}{\ln(\gamma_1 \mathbb{E}_\beta(\widehat{\theta}_\delta \widehat{\phi}^\beta)) - \ln(\gamma_2 \mathbb{E}_\beta(\widehat{\theta}_\delta \widehat{\phi}^\beta))}.$$

Remark 3.10. The special case, when DoS attacks can not impact the security of topologies of the communication networks of nonlinear FOMASs via impulsive control has been studied in [31,32]. In [31,32], the authors considered nonlinear FOMASs of the type

$$\begin{cases} D^\beta \widehat{\mathfrak{Z}}_p(t) = E\widehat{\mathfrak{Z}}_p(t) + FH(\widehat{\mathfrak{Z}}_p(t)), & t \neq t_r, \\ \Delta \widehat{\mathfrak{Z}}_p(t_r) = -b_r \epsilon_p(t_r), & r \in \mathcal{N}_+, \end{cases} \tag{3.37}$$

where $\epsilon_p(t) = \sum_{q=1}^N a_{pq} \mathfrak{Z}_q(t) - \mathfrak{Z}_p(t) + d_p (\mathfrak{Z}_p(t) - \mathfrak{Z}_0(t))$.

In this paper compared with ([31,32]), we study a nonlinear FOMAS with an impulsive control law,

$$\begin{cases} D^\beta \widehat{\mathfrak{Z}}_p(xt) = E\widehat{\mathfrak{Z}}_p(t) + FH(\widehat{\mathfrak{Z}}_p(t)), & t \in (t_{r-1}, t_r], \\ \Delta \widehat{\mathfrak{Z}}_p(t_r) = \frac{-b_r}{\Gamma(\beta+1)} \epsilon_p(t_r), & r \in \mathcal{N}_+. \end{cases} \tag{3.38}$$

It follows from (3.38) that $\frac{b_r}{\Gamma(\beta+1)}$ is the impulsive change of the state at time t_r , which demonstrates that the impact of impulsive control on the controlled systems not only depends on the impulsive functions designed, but also on the fractional order β .

Remark 3.11. Ma et al. [31] investigated the coordinate impulsive control problem of nonlinear FOMASs. In [32], a class of nonlinear FOMASs with switching topology and time-delays was studied by an impulsive control method. An impulsive control scheme is proposed in [33] for a leader-following nonlinear FOMAS with hybrid time-varying delay. Differently from previous studies (see [31–33]), the memory effects of impulsive control are considered in this paper via the fractional derivative.

Corollary 3.12. Assume that the Assumptions (\mathcal{A}_{H2}) and (\mathcal{A}_{H6}) hold for a non-zero scalar $\tilde{\theta}$ and positive symmetric matrices $\Omega_\kappa, \hat{\theta}_\delta \leq 0$ exists, and $\gamma_0 \mathbb{E}_\beta(\hat{\theta}_\delta \phi^\beta) < 1$, where $\gamma_0 = \left(\mathcal{I}_{\mathcal{N}} - \frac{b_r}{\Gamma(\beta+1)}(\mathcal{L} + \hat{D})\right)$. Then, the nonlinear FOMAS (3.38) achieves an exponential consensus using the impulsive controller, if the following inequality is satisfied,

$$\begin{bmatrix} QE + E^T Q + \mathbb{N}^T \Omega_\kappa \mathbb{N} - \hat{\theta}_\delta Q & QF \\ F^T Q & -\Omega_\kappa \end{bmatrix} < 0.$$

Corollary 3.13. Assume that Assumptions (\mathcal{A}_{H2}) and (\mathcal{A}_{H6}) hold for a non-zero scalar $\tilde{\theta}$ and positive symmetric matrices $\Omega_\kappa, \hat{\theta}_\delta > 0, \gamma_0 \mathbb{E}_\beta(\hat{\theta}_\delta \phi^\beta) < 1$. Then, the nonlinear FOMAS (3.38) achieves an exponential consensus using the impulsive controller, if the following inequality is satisfied,

$$\begin{bmatrix} QE + E^T Q + \mathbb{N}^T \Omega_\kappa \mathbb{N} - \hat{\theta}_\delta Q & QF \\ F^T Q & -\Omega_\kappa \end{bmatrix} < 0.$$

Remark 3.14. Up to now, there are only few research results about impulsive consensus of MASs under DoS attacks [39,47]. In [39], the impulsive quasi synchronization problem of heterogeneous MASs under DoS attacks was investigated, and it was assumed that there was no control input when DoS attacks occurred. In [47], the impulsive consensus of fuzzy MASs under DoS attacks was studied, and the MASs was considered with switching topologies caused by DoS attacks. Compare the method proposed in this paper with the proposed in [39,47], there are the following disparities:

- (i) It follows from (2.10) that the impulsive change of the state at time t_r is $\frac{b_r}{\Gamma(\beta+1)}$, which shows that the effect of the impulsive control on the controlled systems not only depends on the impulsive gain designed, but also on the fractional order β ;
- (ii) The LMIs techniques employed in this paper utilizes more information for the secure consensus problem of FDMASs;
- (iii) The memory effects of impulsive controllers, fractional-order nonlinear dynamics and uncertainties are also considered in this paper.

4. Numerical simulations

In this section, two examples are provided to support the validity of the proposed control approach. Example 4.1 considers uncertain FDMASs subject to DoS attacks. Example 4.3 considers the networks of Chua’s circuits in presence of DoS attacks.

Example 4.1. We consider uncertain FDMASs of the type (2.3) and (2.4) with five followers and a leader. Let these agents receive information from their neighbor according to communication topology given in Fig. 2(a). When DoS attacks occur, the network topologies switches are shown in Fig. 2((b)-(d)) with system input matrices

$$E = \begin{bmatrix} -12.3 & 0 & -21 \\ 0 & -11.7 & 0 \\ 0 & 0 & -12.7 \end{bmatrix}, \quad F = \begin{bmatrix} 0 & -15.37 & 0 \\ -13.47 & 0 & 0 \\ 0 & 0 & -27 \end{bmatrix},$$

$$G = \begin{bmatrix} 10.98 & -11.37 & 0 \\ 0 & 0 & 0 \\ 0 & 0 & -11.07 \end{bmatrix}.$$

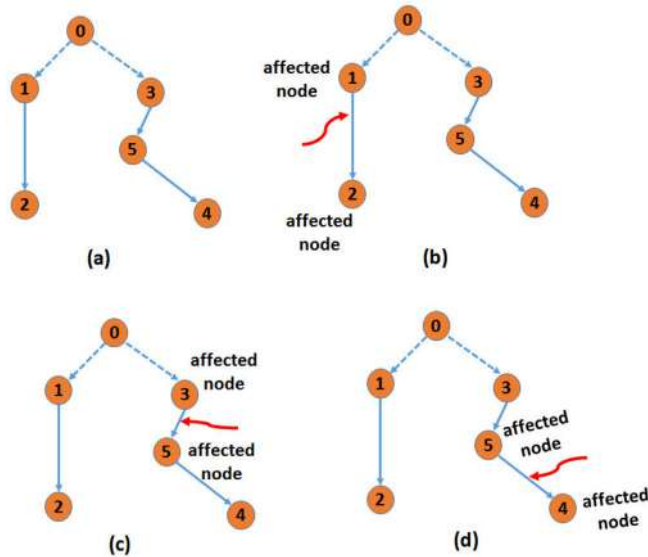


Fig. 2. (a) Networked communication structure, (b)-(d) Different switching topologies by DoS attacks.

In simulations, the nonlinear function $\omega(\mathfrak{T}_p(t)) = [\tanh(\mathfrak{T}_{p1}(t)), \tanh(\mathfrak{T}_{p2}(t))]^T$, and the dynamic parameters are $\beta = 0.97$, $\alpha_i = 0.4$, $\alpha_\epsilon = 1.2$, $\alpha_\delta = 0.4$, $\theta_i = -6.73$, $\theta_\epsilon = -5.02$, $\theta_\delta = 2.08$, $\hat{\theta} = 2.7$, $\tau = 0.1$, $\Theta_\delta = 3.27$, $\Theta_\phi = 5.09$, $\aleph = \text{diag}\{5, 3, 7\}$, $\phi = 0.07$, and control parameters $b_1 = 0.23$, $b_2 = 1.37$, $b_3 = 0.94$, $b_4 = 0.73$, $b_5 = 1.07$, and $\hat{\eta}_\sigma = 0.27$. Then, by solving the LMIs (3.1)–(3.3), we can get

$$Q = \begin{bmatrix} -0.0010 & 0.0010 & 0.0010 \\ 0.0010 & 0.0016 & -0.0006 \\ 0.0010 & -0.0060 & 0.0001 \end{bmatrix}, \quad \Psi_\kappa = \begin{bmatrix} 0.0681 & -0.0006 & 0.0007 \\ -0.0006 & 0.1950 & -0.0005 \\ 0.0007 & -0.0005 & 0.0336 \end{bmatrix},$$

$$\Psi_\sigma = \begin{bmatrix} 1.0686 & 0.0000 & 0.0000 \\ 0.0000 & 1.0686 & 0.0000 \\ 0.0000 & 0.0000 & 1.0686 \end{bmatrix}.$$

If the cyber system is not a subject to an attack, we get $h_b < 0.0970$. Fig. 3 shows the state trajectories and the consensus tracking error for MASs considered without DoS attacks in the communication networks connecting the two layers for $h_b = 0.09$. When DoS attacks meet conditions in Theorem 3.1, the impulsive interval should be adjusted as $\hat{h}_b < 0.0815$. For $\hat{h}_b = 0.08$, state trajectories and consensus monitoring error after adjusting the average impulsive interval after an attack on the FDMAS is shown in Fig. 4. Based on these simulation results, it is clear that the suggested impulsive controllers are effective in coping with DoS attacks in the considered FDMAS.

Remark 4.2. By virtue of their inherent properties of memory and heritage, fractional-order tools have been demonstrated to constitute useful techniques for modeling and control of advanced complex phenomena, such as industrial automation and robotic applications (see [9–15]). The studies and experiments indicated that the continuous controller in fractional-order systems could be controlled. However, the investigations on the application of fractional-order systems via impulsive control are still very few [12]. The impulsive control seems to be more efficient than the continuous control strategies since the former is implemented only at impulsive instants while the latter do so at every moment [12]. Moreover, in some cases, a continuous control (see [9–15]) is impossible, and only an impulsive control method can be used. Note that the impulsive control approach applied in our study has some similarities with the distributed optimization and data-driven control approaches proposed in [6–8] for multiagent systems where agents exchange information at discrete instants, but is quite different. Both approaches are applied for multiagent systems with integer-order dynamics. Also, the impulsive control framework is considered as more general and more appropriate in the cases of DoS attacks [38,39] which are not addressed in [6–8]. In addition, the authors in [6–8] didn’t investigated fractional-order controllers.

The Chua’s circuit is among the simplests non-linear circuits that show the most complex dynamical behavior [44,45]. In Fig. 5 each node represents a single Chua’s circuit. Recently, since the security issues have emerged as one of the major topics in the research and development of Chua’s networks circuits, some approaches have been proposed for the defense against cyber-attacks (see [46]). Moreover, the problem of impulsive control of fractional-order Chua’s networks circuit under cyber-

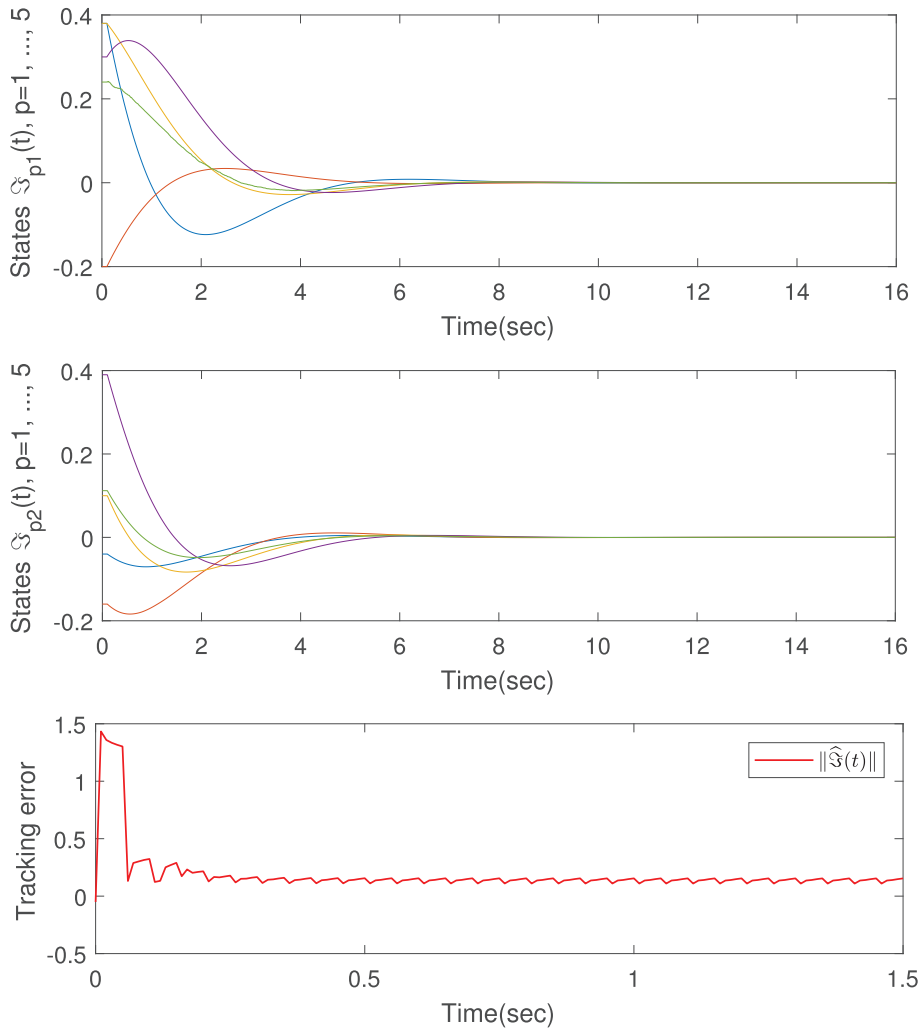


Fig. 3. The FDMASs without attacks on the communication networks of state trajectories and consensus tracking error, where $\mathfrak{S}_p(t) = (\mathfrak{S}_{p1}(t), \mathfrak{S}_{p2}(t))^T$, $p = 1, \dots, 5$.

attacks has not been studied previously. In such motivation in [Example 4.3](#), we consider a fractional-order Chua’s network circuit in the presence of DoS attacks, and also fractional-order impulsive controller approaches are investigated. Different from the existing continuous controllers proposed in the literature [\[44–46\]](#), the effects of DoS attacks are also considered in the input of the impulsive controller (2.7), which is more accordantly with practical circumstances. Therefore, we develop the fractional-order impulsive control approach based on the interactions with complex networks in sampling time so as prevent continued DoS attacks. The impulsive controller would further reduce the contact consumption of the fractional-order Chua’s network circuit compared to the continuous controllers elaborated in [\[44–46\]](#).

Example 4.3. In this example, we verified the control design method proposed using a well-known nonlinear Chua’s networks circuit ([\[44–46\]](#)),

$$\begin{cases} C_1 {}^C D_t^\beta \vartheta_1 &= \frac{1}{R}(-\vartheta_1 + \vartheta_2) - g(\vartheta_1), \\ C_2 {}^C D_t^\beta \vartheta_2 &= \frac{1}{R}(\vartheta_1 - \vartheta_2) + i_3, \\ L {}^C D_t^\beta i_3 &= -(\vartheta_2 + R_0 i_3), \end{cases} \tag{4.1}$$

where ϑ_1, ϑ_2 and i_3 are the voltage across the capacitor C_1 , the voltage across the capacitor C_2 , and current through the inductor L , respectively, $g(\vartheta_1)$ is the voltage versus current characteristic of Chua’s diode N_R defined by [\[44\]](#),

$$g(\vartheta_1) = \frac{1}{C_1} \left[\Upsilon_2 \vartheta_1 + \frac{1}{2} (\Upsilon_1 - \Upsilon_2) (|\vartheta_1 + B_p| - |\vartheta_1 - B_p|) \right],$$

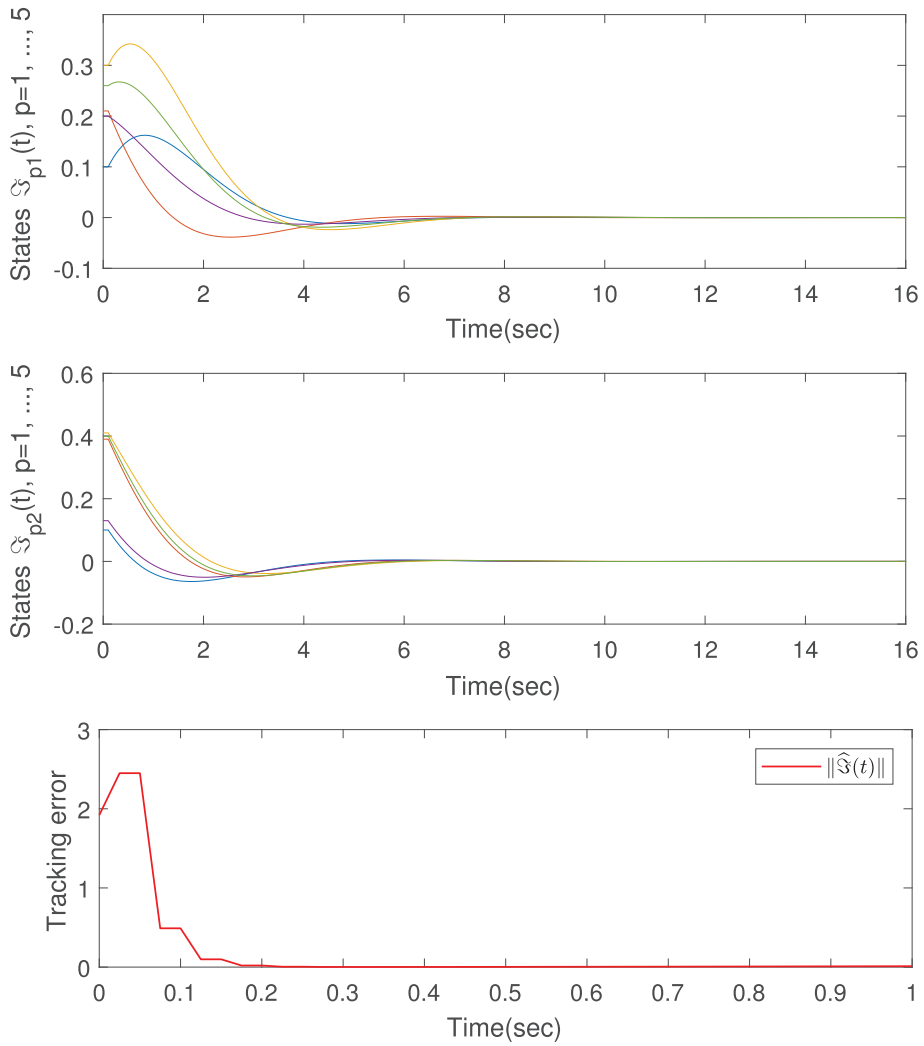


Fig. 4. The FDMASs with attacks on the communication networks of state trajectories and consensus tracking error, where $\mathfrak{S}_p(t) = (\mathfrak{S}_{p1}(t), \mathfrak{S}_{p2}(t))^T$, $p = 1, \dots, 5$.

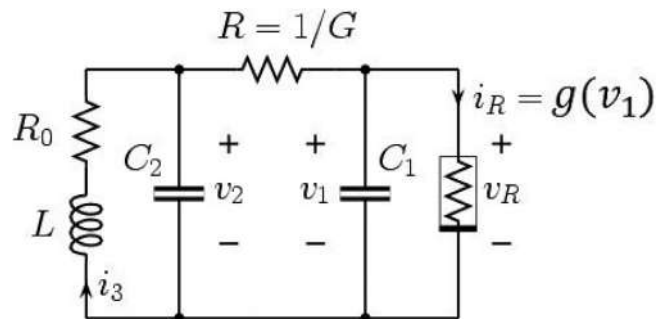


Fig. 5. Chua's circuit.

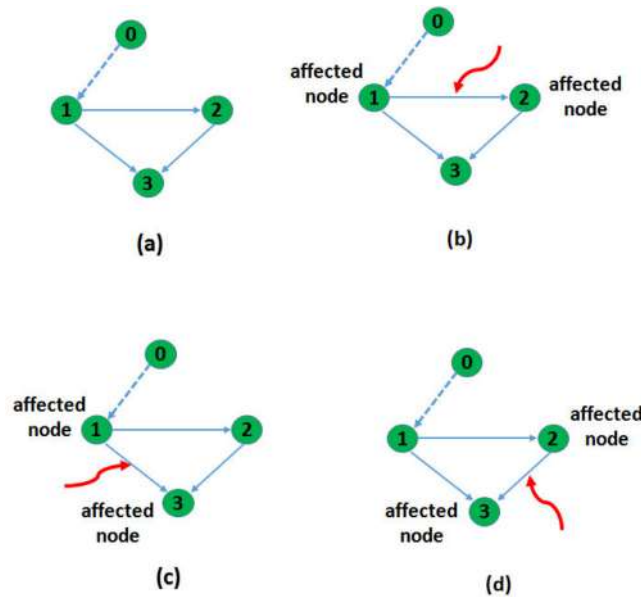


Fig. 6. (a) Networked communication structure, (b)-(d) Different switching topologies by DoS attacks.

the slopes in the inner and outer regions are Υ_1 and Υ_2 , respectively, while $\pm B_p$ denotes the breakpoints of Chua’s diode.

In this case, we consider a multi-agent network with one leader node and three followers communication topologies. The network topologies of three different DoS attacks are seen in Fig. 6((b)-(d)). The dynamics of each follower agent is described by Chua’s networks circuit. Let $\mathfrak{S}_{p1}(t) = \vartheta_1$, $\mathfrak{S}_{p2}(t) = \vartheta_2$, and $\mathfrak{S}_{p3}(t) = i_3$. The corresponding dynamics of agent p with control u_p is

$$D^\beta \mathfrak{S}_p(t) = E\mathfrak{S}_p(t) + F\omega(\mathfrak{S}_p(t)) + u_p(t), \tag{4.2}$$

where $\beta = 0.93$, $\mathfrak{S}_p = [\mathfrak{S}_{p1}, \mathfrak{S}_{p2}, \mathfrak{S}_{p3}]^T$, $E = \begin{bmatrix} -\Lambda_\zeta & \Lambda_\zeta & 0 \\ \Lambda_\theta & -\Lambda_\theta & \rho_\kappa \\ 0 & -\rho_\xi & -\aleph_l \end{bmatrix}$, $F = \begin{bmatrix} -\frac{\Upsilon_1 - \Upsilon_2}{c_1} & 0 & 0 \\ 0 & 0 & 0 \\ 0 & 0 & 0 \end{bmatrix}$, $\omega(\mathfrak{S}_p) = [\frac{1}{2}|\mathfrak{S}_{p1} + 1| - |\mathfrak{S}_{p1} - 1|, 0, 0]^T$

with $\Lambda_\zeta = \frac{1}{RC_1}$, $\Lambda_\theta = \frac{1}{RC_2}$, $\rho_\kappa = \frac{1}{C_2}$, $\rho_\xi = \frac{1}{L}$, $\aleph_l = \frac{R_0}{L}$, $p = 1, 2, 3$. Subsequently, we choose, $\Lambda_\zeta = 9.1$, $\Lambda_\theta = 1$, $\rho_\kappa = 1$, $\Upsilon_1 = -0.7559$, $\Upsilon_2 = -1.3938$, $\frac{1}{c_1} = 9.1$, $\rho_\xi = 16.5811$, $\aleph_l = 0.1380$, $\omega(\mathfrak{S}_{p1}) = \Upsilon_2 \mathfrak{S}_{p1} + 0.5(\Upsilon_1 - \Upsilon_2)(|\mathfrak{S}_{p1} + 1| - |\mathfrak{S}_{p1} - 1|)$. According to Theorem 3.8, we designed impulsive control parameters as $b_1 = b_2 = b_3 = 0.57$, and $\hat{\theta}_\delta = -0.37$, $\bar{\theta} = 1.73$, $\phi = 0.03$, $\hat{\eta}_\nu = 0.53$. Then, by feasibility of the conditions in Theorem 3.8, we obtain that

$$Q = \begin{bmatrix} 0.6254 & 0.7179 & -0.0452 \\ 0.7179 & 3.9136 & 1.0273 \\ -0.0452 & 1.0273 & 64.7185 \end{bmatrix},$$

$$\Omega_\kappa = \begin{bmatrix} -7.2613 & -4.1672 & 0.2627 \\ -4.1617 & 0.0002 & 0.0000 \\ 0.2627 & 0.0000 & 0.0005 \end{bmatrix}.$$

When the Chua’s networks circuit is not a subject to an attack, then $\hat{h}_b < 0.03917$. Fig. 7 displays the state trajectories, and consensus monitoring error for the considered Chua’s networks circuit without attacks in the communication networks for $\hat{h}_b = 0.03$. When DoS attacks satisfying conditions in Theorem 3.8, we should adjust the impulse interval as $\hat{h}_b < 0.0271$. For $\hat{h}_b = 0.02$, the state trajectories and consensus tracking error after adjusting the average impulse interval when the system is under attacks are shown in Fig. 8. The control responses are shown in Fig. 9 by employing different differential orders, from which we can see that the developed fractional-order impulsive controller design method is more effective to reduce the communication consumption of controllers than traditional impulsive control method in [39,47]. In addition, Fig. 10 illustrates with impulsive effects and no control inputs in [39] can no longer synchronize the error system when DoS attacks are involved.

Based on the description above, under the proposed controllers, the consensus of the considered MAS is still achieved in the presence of DoS attacks. Besides, Fig. 9 shows that the fractional-order impulsive controller provides faster convergence rate than the impulsive controllers considered in [39,47]. The impulsive consensus method in [39] cannot handle control

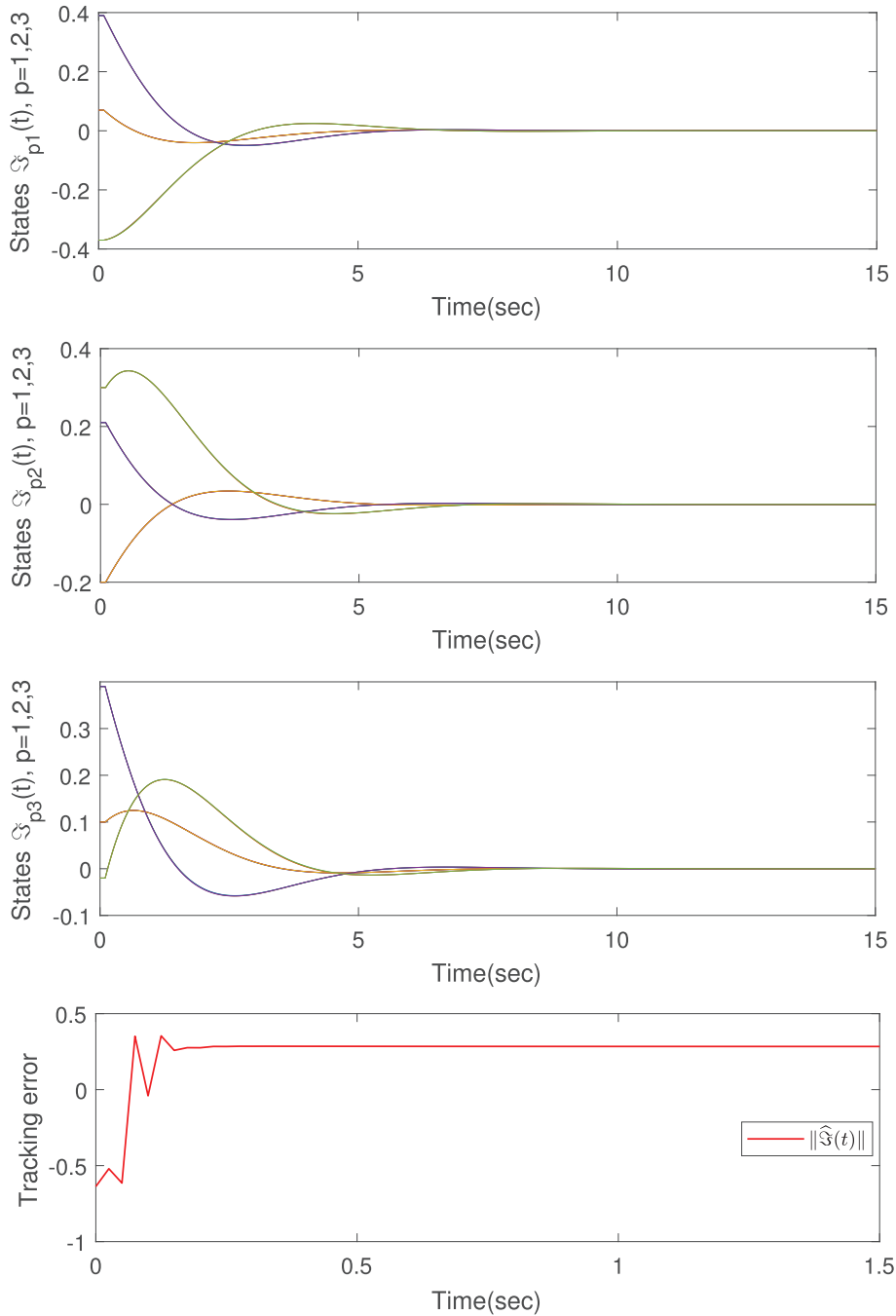


Fig. 7. The Chua's network circuit without attacks on the communication networks of state trajectories and consensus tracking error, where $\mathfrak{S}_p(t) = (\mathfrak{S}_{p1}(t), \mathfrak{S}_{p2}(t), \mathfrak{S}_{p3}(t))^T$, $p = 1, 2, 3$.

input when DoS attacks occurred. Different from the method used in the previous works [39,47], we provide an estimation of impulsive control parameters $b_r (r = 1, 2, \dots, n)$ which can be used to achieve a better performance if they are chosen as conditions in the following manner: if $\Theta_\delta - \Theta_\phi \leq 0$, for any $r = 1, 2, \dots, n$, one has

$$\Gamma(\beta + 1) \left(1 - \frac{1}{\mathbb{E}_\beta((\Theta_\delta - \Theta_\phi)\phi^\beta)} \right) < b_r < \Gamma(\beta + 1) \left(1 + \frac{1}{\mathbb{E}_\beta((\Theta_\delta - \Theta_\phi)\phi^\beta)} \right), \tag{4.3}$$

and if $\Theta_\delta - \Theta_\phi > 0$, one has

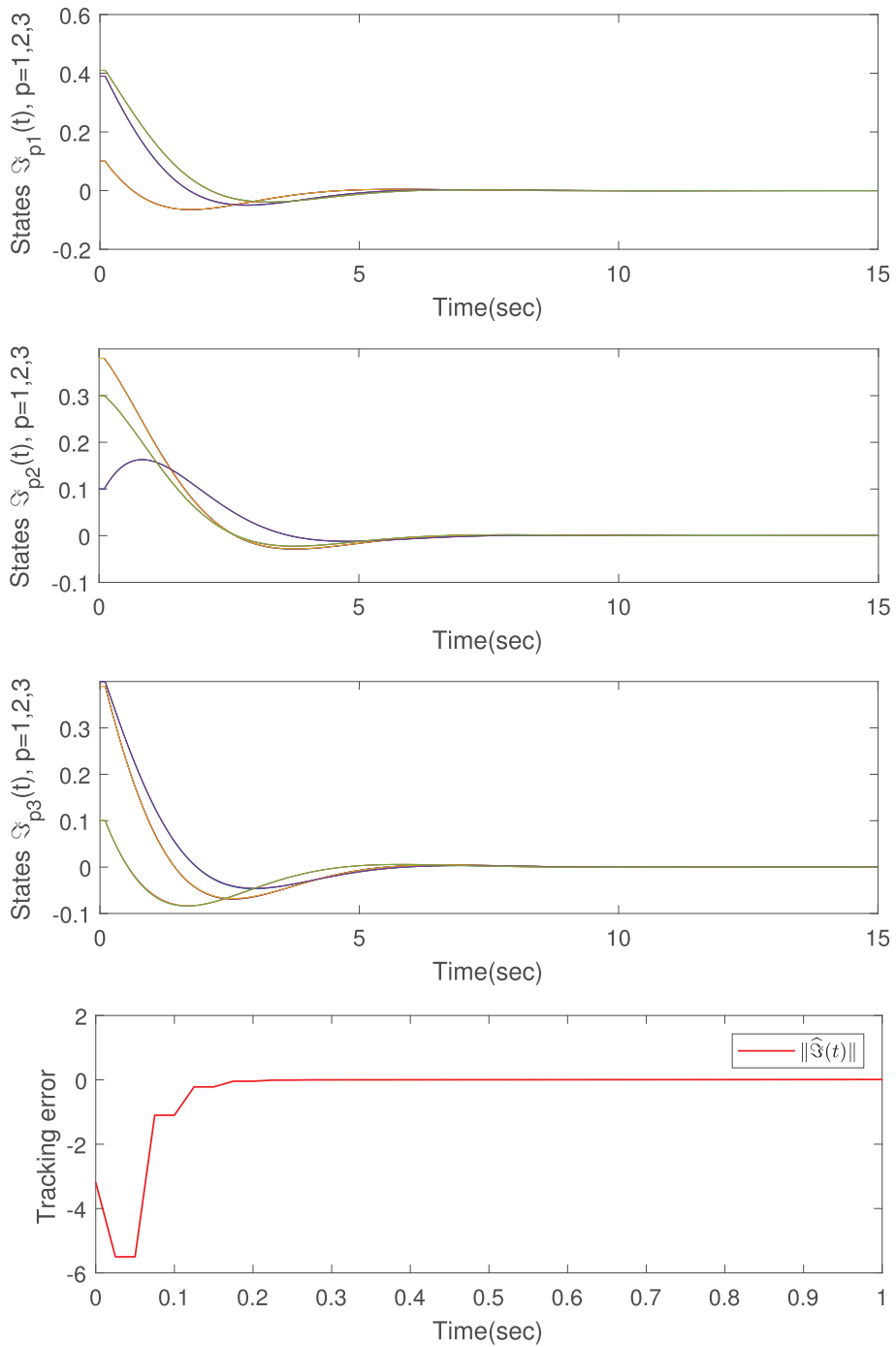


Fig. 8. The Chua's network circuit under attacks on the communication networks of state trajectories and consensus tracking error, where $\mathfrak{S}_p(t) = (\mathfrak{S}_{p1}(t), \mathfrak{S}_{p2}(t), \mathfrak{S}_{p3}(t))^T$, $p = 1, 2, 3$.

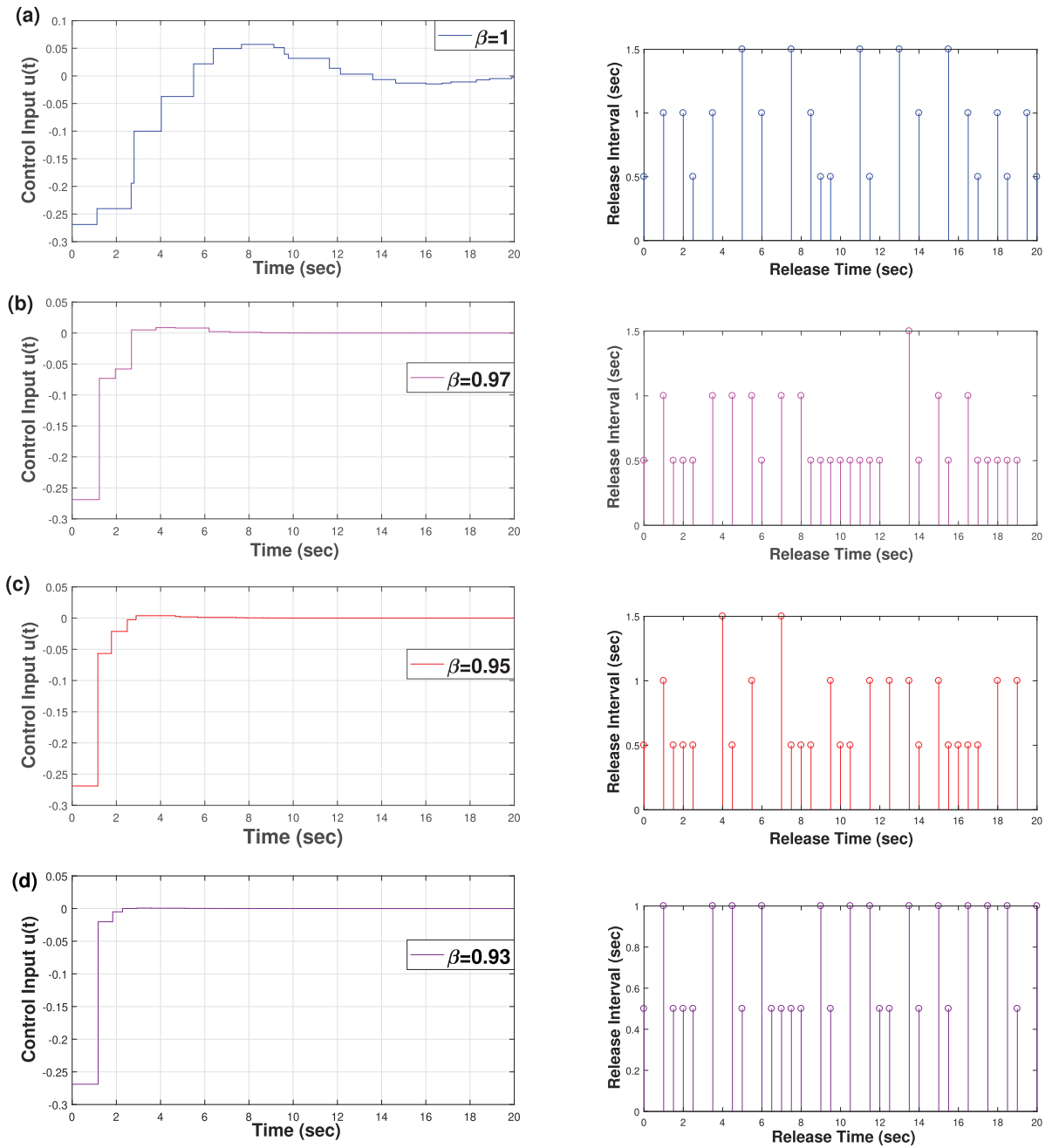


Fig. 9. Estimation of control responses and the release interval based on the impulsive control parameters b_r ($r = 1, 2, 3$) with different differential orders: (a) $\beta = 1$; (b) $\beta = 0.97$; $\beta = 0.95$; $\beta = 0.93$.

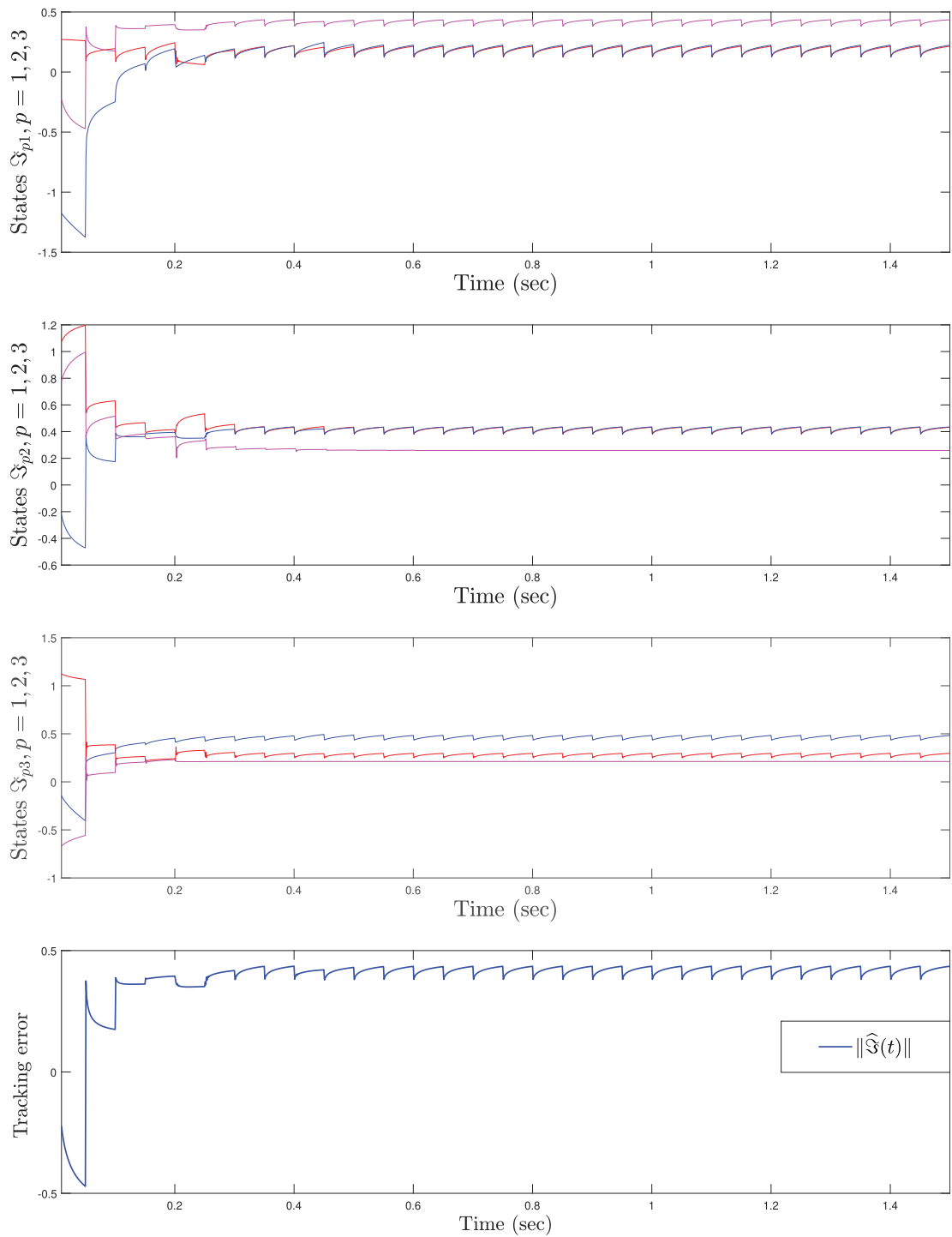


Fig. 10. The Chua's network circuit under attacks with impulsive effects and no control inputs.

$$\Gamma(\beta + 1) \left(1 - \frac{1}{\mathbb{E}_\beta((\Theta_\delta - \Theta_\varphi)\hat{\varphi}^\beta)} \right) < b_r < \Gamma(\beta + 1) \left(1 + \frac{1}{\mathbb{E}_\beta((\Theta_\delta - \Theta_\varphi)\hat{\varphi}^\beta)} \right). \quad (4.4)$$

From these simulation results, it can be observed that the proposed impulsive controllers are successful in dealing with DoS attacks in Chua's network circuit. It is clear that the secure consensus can be achieved under the DoS attacks, fractional-order nonlinear dynamics, impulsive controller, and uncertainties.

5. Conclusion

This paper investigates the secure tracking consensus issues for FDMASs with uncertain parameters in the presence of DoS attacks on communication networks. To guarantee the tolerance of network disconnections, a switching mechanism is proposed to switch the underlying communication network topologies. Subsequently, by utilizing the tools from fractional-calculus theory, Lyapunov-functional, an impulsive controller is developed for each agent, which guaranteed the secure performance of tracking exponential consensus. The impulsive attack ratio which reflects the systems tolerance for attacks is obtained and an appropriate average impulsive interval is designed. It is shown through case studies that the proposed method is an effective tool for secure consensus control of FDMASs subject to DoS attacks. Finally, simulation results are provided to verify the effectiveness of this method. In the future, we will focus on the consensus of FDMASs under distributed DoS attacks with an intermittently random character.

Declaration of Competing Interest

The authors declare that they have no known competing financial interests or personal relationships that could have appeared to influence the work reported in this paper.

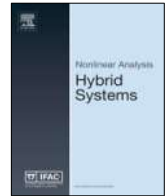
Acknowledgment

The Deanship of Scientific Research (DSR) at King Abdulaziz University, Jeddah, Saudi Arabia has funded this project, under grant no. (FP-133-43).

References

- [1] J. Dai, G. Guo, Event-triggered leader-following consensus for multi-agent systems with semi-Markov switching topologies, *Inf. Sci.* 459 (2018) 290–301.
- [2] X. Liu, K. Zhang, W.C. Xie, Consensus of multi-agent systems via hybrid impulsive protocols with time-delay, *Nonlinear Anal.: Hybrid Syst.* 30 (2018) 134–146.
- [3] Z. Ma, Z. Liu, Z. Chen, Leader-following consensus of multi-agent system with a smart leader, *Neurocomputing* 214 (2016) 401–408.
- [4] M. Syed Ali, R. Agalya, Z. Orman, S. Arik, Leader-following consensus of non-linear multi-agent systems with interval time-varying delay via impulsive control, *Neural Process. Lett.* 53 (2021) 69–83.
- [5] M. Syed Ali, R. Agalya, V. Shekher, Y.H. Joo, Non-fragile sampled data control for stabilization of non-linear multi-agent system with additive time varying delays, Markovian jump and uncertain parameters, *Nonlinear Anal.: Hybrid Syst.* 36 (2020) 100830.
- [6] G. Guo, J. Kang, R. Li, G. Yang, Distributed model reference adaptive optimization of disturbed multiagent systems with intermittent communications, *IEEE Trans. Cybern.* 52 (2022) 5464–5473.
- [7] G. Guo, J. Kang, Distributed optimization of multiagent systems against unmatched disturbances: a hierarchical integral control framework, *IEEE Trans. Syst. Man Cybern.* 52 (2022) 3556–3567.
- [8] G. Guo, R. Zhang, Lyapunov redesign-based optimal consensus control for multi-agent systems with uncertain dynamics, *IEEE Trans. Circuits Syst. II Express Briefs* 69 (2022) 2902–2906.
- [9] C. Zou, L. Zhang, X. Hu, Z. Wang, T. Wik, M. Pecht, A review of fractional-order techniques applied to lithium-ion batteries, lead-acid batteries, and supercapacitors, *J. Power Sources* 390 (2018) 286–296.
- [10] T. Stefanski, J. Gulgowski, Electromagnetic-based derivation of fractional-order circuit theory, *Commun. Nonlinear Sci. Numer. Simul.* 79 (2019) 104897.
- [11] P. Balasubramaniam, P. Muthukumar, K. Ratnavelu, Theoretical and practical applications of fuzzy fractional integral sliding mode control for fractional-order dynamical system, *Nonlinear Dyn.* 80 (2015) 249–267.
- [12] S. Yang, C. Hu, J. Yu, H. Jiang, Exponential stability of fractional-order impulsive control systems with applications in synchronization, *IEEE Trans. Cybern.* 50 (2020) 3157–3168.
- [13] L. Angel, J. Viola, Fractional order PID for tracking control of a parallel robotic manipulator type delta, *ISA Trans.* 79 (2018) 172–188.
- [14] Y. Xie, X. Zhang, W. Meng, S. Zheng, L. Jiang, J. Meng, S. Wang, Coupled fractional-order sliding mode control and obstacle avoidance of a four-wheeled steerable mobile robot, *ISA Trans.* 108 (2021) 282–294.
- [15] A. Coronel-Escamilla, J.F. Gomez-Aguilar, I. Stamova, F. Santamaria, Fractional order controllers increase the robustness of closed-loop deep brain stimulation systems, *Chaos Solitons Fractals* 140 (2020) 110149.
- [16] I. Stamova, Global Mittag-Leffler stability and synchronization of impulsive fractional-order neural networks with time-varying delays, *Nonlinear Dyn.* 77 (2014) 1251–1260.
- [17] M. Syed Ali, G. Narayanan, V. Shekher, A. Alsaedi, B. Ahmad, Global Mittag-Leffler stability analysis of impulsive fractional-order complex-valued BAM neural networks with time varying delays, *Commun. Nonlinear Sci. Numer. Simul.* 83 (2020) 105088.
- [18] S. Zhang, Y. Yu, J. Yu, LMI conditions for global stability of fractional-order neural networks, *EEE Trans. Neural Networks Learn. Syst.* 28 (2017) 2423–2433.
- [19] Y. Cao, W. Ren, Distributed formation control for fractional-order systems: Dynamic interaction and absolute/relative damping, *Syst. Control Lett.* 10 (2010) 233–240.
- [20] Y. Ye, H. Su, Leader-following consensus of nonlinear fractional-order multi-agent systems over directed networks, *Nonlinear Dyn.* 96 (2019) 1391–1403.
- [21] H. Yang, F. Wang, F. Han, Containment control of fractional-order multi-agent systems with time delays, *IEEE/CAA J. Autom. Sin.* 5 (2016) 727–732.

- [22] W. Yu, Y. Li, G. Wen, X. Yu, J. Cao, Observer design for tracking consensus in second-order multi-agent systems: Fractional-order less than two, *IEEE Trans. Autom. Control* 62 (2017) 894–900.
- [23] Z. Li, L. Gao, W. Chen, Y. Xu, Distributed adaptive cooperative tracking of uncertain nonlinear fractional-order multi-agent systems, *IEEE/CAA J. Autom. Sin.* 7 (2020) 292–300.
- [24] X. Li, X. Yang, T. Huang, Persistence of delayed cooperative models: Impulsive control method, *Appl. Math. Comput.* 342 (2019) 130–146.
- [25] X. Li, R. Rakkiyappan, Impulsive controller design for exponential synchronization of chaotic neural networks with mixed delays, *Commun. Nonlinear Sci. Numer. Simul.* 18 (2013) 1515–1523.
- [26] I. Stamova, G. Stamov, Mittag-Leffler synchronization of fractional neural networks with time-varying delays and reaction-diffusion terms using impulsive and linear controllers, *Neural Networks* 96 (2017) 22–32.
- [27] Q. Zhu, J. Cao, Stability of Markovian jump neural networks with impulse control and time varying delays, *Nonlinear Anal.: Real World Appl.* 13 (2012) 2259–2270.
- [28] Y. Han, C. Li, Second-order consensus of discrete-time multi-agent systems in directed networks with nonlinear dynamics via impulsive protocols, *Neurocomputing* 286 (2018) 51–57.
- [29] Y. Han, C. Li, Z. Zeng, H. Li, Exponential consensus of discrete-time non-linear multi-agent systems via relative state-dependent impulsive protocols, *Neural Networks* 108 (2018) 192–201.
- [30] X. Tan, J. Cao, X. Li, Consensus of leader-following multiagent systems: A distributed event-triggered impulsive control strategy, *IEEE Trans. Cybern.* 49 (2019) 792–801.
- [31] T. Ma, T. Li, B. Cui, Coordination of fractional-order nonlinear multi-agent systems via distributed impulsive control, *Int. J. Syst. Sci.* 49 (2018) 1–14.
- [32] Z. Yaghoubi, H.A. Talebi, Cluster consensus of fractional-order non-linear multi-agent systems with switching topology and time-delays via impulsive control, *Int. J. Syst. Sci.* 51 (2020) 1685–1698.
- [33] F. Wang, Y. Yang, Leader-following exponential consensus of fractional order nonlinear multi-agents system with hybrid time-varying delay: A heterogeneous impulsive method, *Phys. A* 482 (2017) 158–172.
- [34] B. Chang, X. Mu, Z. Yang, J. Fang, Event-based secure consensus of multi-agent systems under asynchronous DoS attacks, *Appl. Math. Comput.* 401 (2021) 126120.
- [35] Z. Feng, G. Hu, Secure cooperative event-triggered control of linear multiagent systems under DoS attacks, *IEEE Trans. Control Syst. Technol.* 28 (2020) 741–752.
- [36] D. Zhang, L. Liu, G. Feng, Consensus of heterogeneous linear multi agent systems subject to aperiodic sampled-data and DoS attack, *IEEE Trans. Cybern.* 49 (2019) 1501–1511.
- [37] L. Zhao, G. Yang, Adaptive fault-tolerant control for nonlinear multi-agent systems with DoS attacks, *Inf. Sci.* 526 (2020) 39–53.
- [38] W. He, X. Gao, W. Zhong, F. Qian, Secure impulsive synchronization control of multi-agent systems under deception attacks, *Inf. Sci.* 459 (2018) 354–368.
- [39] D. Ye, Y. Shao, Quasi-synchronization of heterogeneous nonlinear multi-agent systems subject to DOS attacks with impulsive effects, *Neurocomputing* 366 (2019) 131–139.
- [40] X. Chen, L. Yin, Y. Liu, H. Liu, Hybrid-triggered consensus for multi-agent systems with time-delays, uncertain switching topologies, and stochastic cyber-attacks, *Chin. Phys. B* 28 (2019) 090701.
- [41] G.T. Stamov, I.M. Stamova, J. Cao, Uncertain impulsive functional differential systems of fractional order and almost periodicity, *J. Franklin Inst.* 355 (2018) 5310–5323.
- [42] G. Wen, X. Zhai, Z. Peng, A. Rahmani, Fault-Tolerant secure consensus tracking of delayed nonlinear multi-agent systems with deception attacks and uncertain parameters via impulsive control, *Commun. Nonlinear Sci. Numer. Simul.* 80 (2020) 105043.
- [43] W. Zhang, J. Huang, P. Wei, Weak synchronization of chaotic neural networks with parameter mismatch via periodically intermittent control, *Appl. Math. Model.* 35 (2011) 612–620.
- [44] L. Ding, W.X. Zheng, Network-based practical consensus of heterogeneous nonlinear multiagent systems, *IEEE Trans. Cybern.* 47 (2017) 1841–1851.
- [45] X.J. Li, C.X. Shi, G.H. Yang, Observer-based adaptive output-feedback fault-tolerant control of a class of complex dynamical networks, *IEEE Trans. Syst. Man Cybern.* 48 (2018) 2407–2418.
- [46] K. Shi, J. Wang, S. Zhong, Y. Tang, J. Cheng, Hybrid-driven finite-time H_∞ sampling synchronization control for coupling memory complex networks with stochastic cyber attacks, *Neurocomputing* 387 (2020) 241–254.
- [47] T. Ma, Z. Zhang, B. Cui, Impulsive consensus of nonlinear fuzzy multi-agent systems under DoS attack, *Nonlinear Anal.: Hybrid Syst.* 44 (2022) 101155.



Mixed H_∞ and passivity-based resilient controller for nonhomogeneous Markov jump systems

M. Sathishkumar^a, R. Sakthivel^{b,*}, Faris Alzahrani^c, B. Kaviarasan^a, Yong Ren^{d,*}

^a Department of Mathematics, Anna University Regional Campus, Coimbatore 641046, India

^b Department of Mathematics, Bharathiar University, Coimbatore 641046, India

^c Department of Mathematics, Faculty of Science, King Abdulaziz University, Jeddah 21589, Saudi Arabia

^d Department of Mathematics, Anhui Normal University, Wuhu 241000, China

ARTICLE INFO

Article history:

Received 31 March 2018

Accepted 7 August 2018

Available online xxxx

Keywords:

Markovian jump nonlinear systems
Mixed H_∞ and passivity-based resilient controller
Polytope uncertainties
Mode-dependent quantizer

ABSTRACT

In this paper, the robust mixed H_∞ and passivity-based control problem is investigated for a class of discrete-time Markov jump nonlinear systems with uncertainties, quantization and time-varying transition probabilities. In addition, the time-varying transition probability matrices in the considered system are described by a polytope set. Further, the measurement size reduction technique is implemented which consists of two factors, namely, the logarithmic quantization and the measurement element selection scheme. In order to reflect the imprecision in controller implementation, the additive controller gain problem is considered. Based on the Lyapunov stability theory, a new set of conditions is derived such that the resulting closed-loop Markov jump system is stochastically stable with a prescribed mixed H_∞ and passivity performance index. Finally, the effectiveness of the proposed control scheme is illustrated by two numerical examples including an application example based on a DC motor device.

© 2018 Elsevier Ltd. All rights reserved.

1. Introduction

Over the past few decades, Markovian jump systems have received significant research interest of researchers because of their wide range of applications in many areas of engineering, such as mobile robots, modeling production systems, networked control systems, manufacturing systems and communication systems [1–4]. Markov jump systems are more appropriate to describe dynamical systems subject to random changes in their structures, which may be caused by component failures or repairs of subsystems, sudden environmental changes and system noise. Recently, many important and interesting results have been reported on Markovian jump systems, such as stochastic stability and stabilization [5,6], fault detection [7,8], filtering [9–11] and state estimation [12–15]. In most of the existing works, Markov jump systems are all under the hypothesis that the system must satisfy time invariant Markov process in which transition probabilities are constant matrix. However, in some real process, the transition probability may not be a constant matrix but a time-varying one. In such situations, polytope set can be used to describe the characteristics of time-varying transition probability-based uncertainties.

Even though the transition probability of the Markov process is not exactly known, polytope set can be used to evaluate some values in some points and it is assumed that the time-varying transition probabilities evolve in this polytope, which is in a convex set [16,17]. Also, it is more reasonable to model the system as Markovian jump system with nonhomogeneous

* Corresponding authors.

E-mail addresses: krsakthivel@yahoo.com (R. Sakthivel), brightry@hotmail.com (Y. Ren).

jump process, that is, the transition probabilities are time-varying. On another research frontier, the handling of quantization errors due to limited communication capacity has become an active research area in control systems since the quantization errors in actuators and sensors may provide poor performance and also be potential source of instability [18]. There are two types of quantizers in which the first one is static quantizers, such as uniform and logarithmic quantizers [19,20] and the second one is the dynamic quantizer which scales the quantization levels dynamically in order to improve the steady-state performance [21,22]. Therefore, the stabilization controller design problem for nonlinear systems containing ellipsoidal Lipschitz nonlinearities by incorporating the bounded quantization error and input saturation has been investigated in [23]. The authors in [24] studied the sampled-data model predictive control for linear parameter varying systems with input quantization by using new Lyapunov–Krasovskii functional.

Several important works based on the disturbance attenuation problems have been reported via various control design methods, such as H_∞ control [25,26], H_2/H_∞ control [27] and passivity-based control [28,29]. Among them, two control strategies, namely, H_∞ and passivity-based control methods have received much attention from the researchers due to their broad applications. In particular, the H_∞ controller is designed for several control systems because it deals with uncertainties so as to minimize the disturbance attenuation level. Moreover, passivity theory serves as an important concept of system theory and can characterize the stability of dynamical systems. The passive property of a system is that it can keep the system internally stable by using input–output characteristics and it has found powerful applications in diverse areas such as stability, signal processing, fuzzy control, chaos control and synchronization. For instance, in [30], the authors studied the problem of mixed H_∞ and passivity filter design for discrete time-delay neural networks with Markovian jump parameters represented by Takagi–Sugeno fuzzy model.

In some circumstances, inaccuracies and uncertainties may occur in the controller implementation. Thus, the controller should be designed in such a way that it is insensitive to some amount of uncertainties with respect to its gain, which is called as resilient or non-fragile controller [31]. Very recently, the problem of passivity-based resilient sampled-data control for Markovian jump systems subject to actuator faults via adaptive fault-tolerant mechanism has been reported in [32]. On the other hand, energy constraint causes a major problem in the stability analysis of dynamical systems since it limits the system performance. Further, it is one of the measurement size reduction techniques. The purpose of measurement size reduction scheme is that it significantly reduces the communication times. Compared with the literature results on linear networked systems with energy constraints, the filtering or control of nonlinear systems with energy constraints has not received adequate attention. Up to now, only a few works have been done related to this topic, for instance see [33,34] and [35]. Moreover, to the best of authors' knowledge, the mixed H_∞ and passivity-based resilient control design problem for Markov jump systems with energy constraints has not yet been solved, which is the motivation for this present study.

Based on the aforementioned discussions, the purpose of this paper is to solve the robust mixed H_∞ and passivity-based resilient control problem for Markov jump systems in the presence of nonhomogeneous jump processes, quantization and energy constraints. To be precise, we establish a new set of sufficient conditions such that the considered Markovian jump system is robustly stochastically stable with a prescribed mixed H_∞ and passive performance index. The main contributions of this work are summarized as follows:

- (1) A robust mixed H_∞ and passivity-based resilient control problem for nonhomogeneous Markov jump systems with quantization and energy constraints is considered.
- (2) The proposed system considers two common issues, namely, quantization and energy constraints, which may reflect the reality more closely.
- (3) Sufficient conditions subject to quantization and energy constraints are developed for obtaining the required results by using the Lyapunov stability theory and the corresponding control gains are obtained by solving a cone complementarity linearization algorithm.

At last, two numerical examples with simulation results are provided to illustrate the effectiveness of the proposed design method.

Notations. Throughout this paper, the following standard notations will be used. The superscripts “ T ” and “ (-1) ” stand for matrix transposition and matrix inverse, respectively. \mathbb{R}^n represents the n -dimensional Euclidean space. $\mathbb{R}^{n \times n}$ denotes the set of all $n \times n$ real matrices. $E\{\cdot\}$ denotes the mathematical expectation. $L_2^n[0, \infty)$ stands for the space of n -dimensional square integrable functions over $[0, \infty)$. $P > 0$ means that P is a positive definite matrix. I represents the identity matrix with compatible dimension. In symmetric block matrices or long matrix expressions, we use an asterisk (*) to represent a term that is induced by symmetry. Moreover, let $(\Omega, \mathcal{F}, \mathcal{P})$ be a complete probability space in which Ω is the sample space, \mathcal{F} is the σ -algebra of subsets of Ω and \mathcal{P} is the probability measure on \mathcal{F} . $\|\cdot\|$ refers to the Euclidean vector norm.

2. Problem formulation and preliminaries

In this paper, we consider a class of discrete-time Markovian jump systems in the following form:

$$\begin{aligned} x(k+1) &= A(r(k))x(k) + B(r(k))u(k) + C(r(k))v(k) + g(x(k), r(k)), \\ z(k) &= D(r(k))x(k) + E(r(k))v(k), \end{aligned} \quad (1)$$

where $A(r(k)), B(r(k)), C(r(k)), D(r(k))$ and $E(r(k))$ are mode-dependent constant matrices with appropriate dimensions at the working instant k ; $x(k) \in \mathbb{R}^n$ is the state vector of the system; $u(k) \in \mathbb{R}^p$ is the control input; $z(k)$ is the controlled output vector of the system; $v(k) \in L_2^q[0, \infty)$ is the external disturbance vector acting on the system; $g(\cdot)$ is the time-dependent norm-bounded uncertainties; $r(k), k \geq 0$ is the concerned discrete-time Markov stochastic process which takes the values in finite state set $\Lambda = \{1, 2, 3, \dots, N\}$, where $r(0)$ represents the initial mode. Further, the following condition is imposed on the uncertainty $g(x(k), r(k))$.

(H1) The norm bounded uncertainty $g(x(k), r(k))$ in system (1) is assumed to satisfy $g(x(k), r(k)) = \Delta A(r(k))x(k)$ and $\Delta A(r(k)) = M(r(k))\Upsilon(r(k))N(r(k))$, where $M(r(k))$ and $N(r(k))$ are constant matrices with appropriate dimensions, $\Upsilon(r(k))$ is an unknown matrix with Lebesgue measurable elements satisfying $\Upsilon^T(r(k))\Upsilon(r(k)) \leq I$. Further, we denote $r(k) = i, i \in \Lambda$, then the system (1) can be rewritten in the following form:

$$\begin{aligned} x(k+1) &= \mathcal{A}_i(k)x(k) + B_i u(k) + C_i v(k), \\ z(k) &= D_i x(k) + E_i v(k), \end{aligned} \tag{2}$$

where $\mathcal{A}_i(k) = (A_i + \Delta A_i(k))$. Also, the transition probability matrix is defined as $\Pi(k) = \{\pi_{ij}(k)\}, i, j \in \Lambda$, where $\pi_{ij}(k) = P(r(k+1) = j | r(k) = i)$ is the transition probability from mode i at time k to mode j at time $k+1$, such that $\pi_{ij}(k) \geq 0$ and $\sum_{j=1}^N \pi_{ij}(k) = 1$.

For given vertices $\Pi^s, s = 1, 2, \dots, w$, the time-varying transition matrix can be described as $\Pi(k) = \sum_{s=1}^w \alpha_s(k) \Pi^s$, where $0 \leq \alpha_s(k) \leq 1$ and $\sum_{s=1}^w \alpha_s(k) = 1$. In particular, such transition uncertainties are assumed to evolve in a polytope, which is described by several vertices. For more details about the polytope, one can refer the paper [17]. In practice, due to widespread usage of digital signals in control systems, the control signals are often needed to be quantized before the manipulation of feedback. Here, the quantized state feedback is considered in the following form:

$$u(k) = q_i(\varphi(k)) \quad \text{and} \quad \varphi(k) = K_i x(k), \tag{3}$$

where $q_i(\cdot)$ is a quantizer that is assumed to be symmetric, that is, $q_i(-\varphi) = -q_i(\varphi)$. In this paper, logarithmic static and time-invariant quantizers are employed for subsystems. Also, the set of quantized levels is described by

$$u = \{\pm u_i^j : u_i^j = \rho_i^j u_i^0, j = \pm 1, \pm 2, \dots\} \cup \{\pm u_i^0\} \cup \{0\}, \rho_i \in (0, 1), u_i^0 > 0, \tag{4}$$

where the parameter ρ_i represents the quantization density. Each of the quantization level u_i^j corresponds to a segment such that the quantizer maps the whole segment to this quantization level. The quantizer $q_i(\cdot)$ is represented by

$$q_i(\varphi(k)) = \begin{cases} u_i^j, & \text{if } \frac{1}{1+\delta_i} u_i^j < \varphi \leq \frac{1}{1-\delta_i} u_i^j, \\ 0, & \text{if } \varphi = 0, \\ -q_i(-\varphi), & \text{if } \varphi < 0, \end{cases}$$

where $\delta_i = \frac{1-\rho_i}{1+\rho_i}$. Moreover, by following the procedure carried out in [18], we can get

$$q_i(\varphi) = (I + \Delta_i)\varphi, \tag{5}$$

where $\Delta_i = \text{diag}\{\Delta_i^1, \Delta_i^2, \dots, \Delta_i^m\}$. Then it follows that $\Delta_i^j \in [-\delta_i^j, \delta_i^j], j = 1, 2, \dots, m$.

Now, we employ another measurement size reduction technique called energy constraint. Here, we consider n cases for the measurement scheduling scheme. According to works in [33–35], we define a structure matrix by $\Phi_{\sigma(k)} \in \{\text{diag}\{1, 0, \dots, 0\}, \dots, \text{diag}\{0, 0, \dots, 1\}\}$, where $\sigma(k) \in \Theta = \{1, 2, \dots, n\}$. Based on the above discussion, the modified

control signal is expressed by

$$u(k) = (I + \Delta_i)K_{i\sigma(k)}\Phi_{\sigma(k)}x(k). \tag{6}$$

It is assumed that the variation of the piecewise signal $\sigma(k)$ follows a Markov process with the transition probability matrix $\bar{\Pi} = \{\lambda_{ab}\}$, that is, for $\sigma(k) = a, \sigma(k+1) = b$, we have $\text{Prob}(\sigma(k+1) = b | \sigma(k) = a) = \lambda_{ab}$, where $\lambda_{ab} \geq 0$, and for each $a, b \in \Theta$, we have $\sum_{b=1}^n \lambda_{ab} = 1$.

Substituting (6) in (2), the closed-loop system can be described by

$$\begin{aligned} x(k+1) &= \mathcal{A}_i(k)x(k) + B_i(I + \Delta_i)K_{i\sigma(k)}\Phi_{\sigma(k)}x(k) + C_i v(k), \\ z(k) &= D_i x(k) + E_i v(k). \end{aligned} \tag{7}$$

Now, we present two definitions that are more essential to obtain the main results.

Definition 2.1 ([17]). System (7) with $v(k) = 0$ and $u(k) = 0$ is robustly stochastically stable, for any initial state $(x(0), r(0))$, if the following condition holds:

$$E\left\{\sum_{k=0}^{\infty} \|x(k)\|^2 \mid (x(0), r(0))\right\} < \infty, \tag{8}$$

where $x(k)$ denotes the solution of (7).

Definition 2.2 ([36]). System (7) is said to be stochastically stable with a prescribed mixed H_∞ and passive performance index γ , under zero initial condition, if there exists a scalar $\gamma > 0$ such that the following inequality holds:

$$E\left[\sum_{k=0}^{\infty} \gamma^{-1} \theta z^T(k)z(k) - 2(1 - \theta)z^T(k)v(k)\right] \leq E\left[\sum_{k=0}^{\infty} \gamma v^T(k)v(k)\right], \tag{9}$$

for any non-zero $v(k) \in L_2^q[0, \infty)$ and $\theta \in [0, 1]$.

Remark 2.3. The composition of proposed controller (6) is due to the following reasons. In practice, the signal quantization is an effective scheme to reduce the storage space or transmission bandwidth. However, if the plant is large, there may still need some signals to transmit the complete information. In such situation, the measurement size reduction technique can be employed, which reduces the measurement size by selecting one element signal for transmission. Therefore, the simultaneous utilization of signal quantization and measurement selection scheme is more effective in saving the transmission energy of the proposed controller (6).

Remark 2.4. In [37], Gaussian distribution is used to describe uncertain transition probabilities. In practice, it is very hard to meet such distribution. To overcome this issue, in this paper, a new technique is considered to improve such deficiency, which makes the theoretical results developed in this paper more practical. More precisely, the uncertain transition probabilities are described by a nonhomogeneous process, modeled as a polytope set.

3. Main results

This section presents a robust resilient control design based on the mixed H_∞ and passivity theory, which ensures the stochastic stability of the system (7).

3.1. Stochastic stability

In this subsection, first, we obtain a set of sufficient conditions for the stochastic stability of the system (7) with $u(k) = 0$ and $v(k) = 0$.

Theorem 3.1. For a given initial condition $x(0)$, the system (7) with $u(k) = 0$ and $v(k) = 0$ is robustly stochastically stable, if there exist a set of positive definite symmetric matrices P_{ia}^s and P_{jb}^q , such that

$$\begin{bmatrix} -\bar{P}_{ia}^s & \mathcal{A}_i^T(k) \\ * & -(P_{jb}^q)^{-1} \end{bmatrix} < 0, \tag{10}$$

holds for all $i \in \Lambda$ and $a \in \Theta$, where $\bar{P}_{ia}^s = \sum_{s=1}^w \alpha^s(k)P_{ia}^s$, $\bar{P}_{jb}^q = \sum_{j=1}^N \sum_{b=1}^n \sum_{s=1}^w \sum_{q=1}^w \alpha^s(k)\beta^q(k)\pi_{ij}^s \lambda_{ab} P_{jb}^q$, $0 \leq \alpha^s(k) \leq 1$, $\sum_{s=1}^w \alpha^s(k) = 1$ and $0 \leq \beta^q(k) \leq 1$, $\sum_{q=1}^w \beta^q(k) = 1$.

Proof. Consider the Lyapunov function for the system (7) in the following form:

$$V(x(k)) = x^T(k) \sum_{s=1}^w \alpha^s(k)P_{ia}^s x(k) \text{ for } i \in \Lambda, a \in \Theta,$$

where $0 \leq \alpha^s(k) \leq 1$, $\sum_{s=1}^w \alpha^s(k) = 1$ and $P_{ia}^s > 0$. By computing the forward difference of $\Delta V(x(k))$ along the trajectories of the system (7) and taking the mathematical expectation, we get

$$\begin{aligned} E\{\Delta V(x(k))\} &= E\{V(x(k+1)) - V(x(k))\} \\ &= E\left\{x^T(k) \left[\mathcal{A}_i^T(k) \left(\sum_{j=1}^N \sum_{b=1}^n \sum_{s=1}^w \sum_{q=1}^w \alpha^s(k)\beta^q(k)\pi_{ij}^s \lambda_{ab} P_{jb}^q \right) \mathcal{A}_i(k) \right] x(k) \right. \\ &\quad \left. - x^T(k) \sum_{s=1}^w \alpha^s(k)P_{ia}^s x(k) \right\} \\ &= E\{x^T(k)\Psi(k)x(k)\}, \end{aligned}$$

where $\Psi(k) = -\sum_{s=1}^w \alpha^s(k)P_{ia}^s + \mathcal{A}_i^T(k) \left(\sum_{j=1}^N \sum_{b=1}^n \sum_{s=1}^w \sum_{q=1}^w \alpha^s(k)\beta^q(k)\pi_{ij}^s \lambda_{ab} P_{jb}^q \right) \mathcal{A}_i(k)$.

By using Schur complement, $\Psi(k)$ can be equivalently viewed as the matrix term in (10). Thus, it follows from (10) that $E\{\Delta V(x(k))\} < 0$. Let $\mu = \min_k \{\lambda_{\min}(\Psi(k))\}$, where $\lambda_{\min}(\Psi(k))$ is the minimal eigenvalue of $-\Psi(k)$. Then, $E\{\Delta V(x(k))\} \leq -\mu E\{x^T(k)x(k)\}$. Further, by taking mathematical expectation, we have $E\{\sum_{k=0}^T \Delta V(x(k))\} = E\{V(x(T+1)) - V(x(0))\}$

$\leq -\mu E\{\sum_{k=0}^T \|x(k)\|^2\}$ from which it follows that $E\{\sum_{k=0}^T \|x(k)\|^2\} \leq -\frac{1}{\mu}(E\{V(x(T+1)) - V(x(0))\}) \leq \frac{1}{\mu}(E\{V(x(0)) - V(x(T+1))\})$. Also, we have $\lim_{T \rightarrow \infty} E\{\sum_{k=0}^T \|x(k)\|^2\} \leq \frac{1}{\mu}E\{V(x(0))\}$. It follows from Definition 2.1 that the system (7) with $u(k) = 0$ and $v(k) = 0$ is stochastically stable, and this completes the proof.

3.2. Robust mixed H_∞ and passivity-based control design

In the following theorem, we derive a set of criteria to obtain the controller gain that guarantees the stochastic stability of system (7).

Theorem 3.2. For given scalars $\gamma > 0, \theta \in [0, 1]$, quantization density $\rho > 0$ and the controller gain matrix K_{ia} , if there exist a set of positive definite symmetric matrices P_{ia}^s, Q_{jb}^q and some scalars v_{1i} and v_{2i} , such that the following condition hold for all $i \in \Lambda$ and $a \in \Theta$:

$$\hat{\Omega}_i = \begin{bmatrix} \bar{\Omega}_i & \bar{\Omega}_2^T & v_{1i}\bar{\Omega}_3 & \bar{N}_i^T & v_{2i}\bar{M}_i \\ * & -v_{1i} & 0 & 0 & 0 \\ * & * & -v_{1i} & 0 & 0 \\ * & * & * & -v_{2i} & 0 \\ * & * & * & * & -v_{2i} \end{bmatrix} < 0, \tag{11}$$

$$Q_{jb}^q \times P_{jb}^q = I, \tag{12}$$

where

$$\bar{\Omega}_i = \begin{bmatrix} -P_{ia}^s & -(1-\theta)D_i^T & \bar{\Omega}_{13i} & \dots & \bar{\Omega}_{14i} & \sqrt{\theta}D_i^T \\ * & -2(1-\theta)E_i^T - \gamma I & \bar{\Omega}_{17i} & \dots & \bar{\Omega}_{18i} & \sqrt{\theta}E_i^T \\ * & * & -Q_{11}^q & 0 & 0 & 0 \\ * & * & * & \ddots & 0 & 0 \\ * & * & * & * & -Q_{Nn}^q & 0 \\ * & * & * & * & * & -\gamma I \end{bmatrix},$$

$$\bar{\Omega}_{13i} = \sqrt{\pi_{i1}^s \lambda_{i1}}(\mathcal{A}_i^T(k) + \Phi_a^T K_{ia}^T B_i^T), \bar{\Omega}_{14i} = \sqrt{\pi_{iN}^s \lambda_{in}}(\mathcal{A}_i^T(k) + \Phi_a^T K_{ia}^T B_i^T), \bar{\Omega}_{17i} = \sqrt{\pi_{i1}^s \lambda_{i1}} C_i^T,$$

$$\bar{\Omega}_{18i} = \sqrt{\pi_{iN}^s \lambda_{in}} C_i^T, \bar{\Omega}_2 = [\delta_i K_{ia} \Phi_a \quad 0 \quad 0 \quad \dots \quad 0 \quad 0], \bar{\Omega}_3 = [0 \quad 0 \quad \sqrt{\pi_{i1}^s \lambda_{i1}} B_i^T \quad \dots \quad \sqrt{\pi_{iN}^s \lambda_{in}} B_i^T \quad 0]^T,$$

$$Q_{jb}^q = (P_{jb}^q)^{-1}, \bar{M}_i = [0 \quad 0 \quad \sqrt{\pi_{i1}^s \lambda_{i1}} M_i^T \quad \dots \quad \sqrt{\pi_{iN}^s \lambda_{in}} M_i^T \quad 0]^T, \bar{N}_i = [N_i \quad 0 \quad 0 \quad \dots \quad 0 \quad 0].$$

Then, the closed-loop system (7) is robustly stochastically stable and also satisfies a prescribed mixed H_∞ and passive performance index.

Proof. Here, we discuss the mixed H_∞ and passivity performance of the closed-loop system (7) with $v(k) \neq 0$ and $u(k) \neq 0$. For this, we consider the following performance index:

$$J = \sum_{k=0}^{\infty} [\gamma^{-1} \theta z^T(k) z(k) - 2(1-\theta) z^T(k) v(k) - \gamma v^T(k) v(k)].$$

Now, using the output vector $z(k)$ defined in (7) and following the similar derivations in Theorem 3.1, we get

$$E\{\Delta V(x(k)) + \gamma^{-1} \theta z^T(k) z(k) - 2(1-\theta) z^T(k) v(k) - \gamma v^T(k) v(k)\} \leq E\{\eta^T(k) \Omega_i \eta(k)\}, \tag{13}$$

where

$$\Omega_i = \begin{bmatrix} -P_{ia}^s & -(1-\theta)D_i^T \\ * & -2(1-\theta)E_i^T - \gamma I \end{bmatrix} + \pi_{i1}^s \lambda_{i1} \begin{bmatrix} \mathcal{A}_i(k) + B_i K_{ia} \Phi_a \\ C_i \end{bmatrix}^T P_{11}^q \begin{bmatrix} \mathcal{A}_i(k) + B_i K_{ia} \Phi_a \\ C_i \end{bmatrix} \\ + \dots + \pi_{iN}^s \lambda_{in} \begin{bmatrix} \mathcal{A}_i(k) + B_i K_{ia} \Phi_a \\ C_i \end{bmatrix}^T P_{Nn}^q \begin{bmatrix} \mathcal{A}_i(k) + B_i K_{ia} \Phi_a \\ C_i \end{bmatrix} + \theta \begin{bmatrix} D_i \\ E_i \end{bmatrix}^T \gamma^{-1} \begin{bmatrix} D_i \\ E_i \end{bmatrix}.$$

By using Schur complement to (13), we have

$$\Omega_i = \begin{bmatrix} -P_{ia}^s & -(1-\theta)D_i^T & \Omega_{13i} & \dots & \Omega_{14i} & \sqrt{\theta}D_i^T \\ * & -2(1-\theta)E_i^T - \gamma I & \Omega_{17i} & \dots & \Omega_{18i} & \sqrt{\theta}E_i^T \\ * & * & -(P_{11}^q)^{-1} & 0 & 0 & 0 \\ * & * & * & \ddots & 0 & 0 \\ * & * & * & * & -(P_{Nn}^q)^{-1} & 0 \\ * & * & * & * & * & -\gamma I \end{bmatrix},$$

$\Omega_{13i} = \sqrt{\pi_{i1}^s \lambda_{i1}} (\mathcal{A}_i^T(k) + \Phi_a^T K_{ia}^T B_i^T)$, $\Omega_{14i} = \sqrt{\pi_{iN}^s \lambda_{in}} (\mathcal{A}_i^T(k) + \Phi_a^T K_{ia}^T B_i^T)$, $\Omega_{17i} = \sqrt{\pi_{i1}^s \lambda_{i1}} C_i^T$, $\Omega_{18i} = \sqrt{\pi_{iN}^s \lambda_{in}} C_i^T$ and $\eta(k) = [x^T(k), w^T(k)]^T$. Hence, the performance level can be guaranteed provided that $\Omega_{2i} < 0$. Further, according to the definition of norm-bounded uncertainty in **(H1)**, we can get

$$\Omega_{2i} + \tilde{\Omega}_2 \Delta(k) \tilde{\Omega}_3 + \tilde{\Omega}_3^T \Delta^T(k) \tilde{\Omega}_2^T + \bar{M}_i \Upsilon(i) \bar{N}_i + \bar{N}_i^T \Upsilon(i)^T \bar{M}_i^T < 0, \tag{14}$$

where $\tilde{\Omega}_2, \tilde{\Omega}_3, \bar{M}_i$ and \bar{N}_i are defined in the theorem statement. By using **Lemmas A.1** and **A.2** in (14) and taking $Q_{jb}^q = (P_{jb}^q)^{-1}$, we can easily get the linear matrix inequality (LMI) in (11). Therefore, if the conditions in (11) and (12) are satisfied, the closed-loop system (7) is stochastically stable and also satisfies the mixed H_∞ and passivity performance index, which concludes the proof.

3.3. Robust mixed H_∞ and passivity-based resilient control design

It should be mentioned that the controller may be very sensitive or fragile with respect to some variations on feedback gains. Therefore, the resilient control concept is utilized to design a feedback control which will be insensitive to some extent of perturbations in control gains.

In this subsection, we will obtain mixed H_∞ and passivity-based resilient control design for the discrete-time Markovian jump system (1). Now, we consider the gain matrix as \bar{K}_i instead of K_i , which has the structure $\bar{K}_i = K_i + \Delta K_i(k)$ in which the perturbation $\Delta K_i(k)$ is defined by

$$\Delta K_i(k) = \mathcal{M}_i \Sigma_i(k) \mathcal{N}_i, \tag{15}$$

where \mathcal{M}_i and \mathcal{N}_i are known constant matrices and $\Sigma_i(k)$ is an unknown matrix satisfying $\Sigma_i(k)^T \Sigma_i(k) \leq I$. Then, the corresponding closed-loop system can be written as

$$\begin{aligned} x(k+1) &= \mathcal{A}_i(k)x(k) + B_i(I + \Delta_i) \bar{K}_{ia} \Phi_{\sigma(k)} x(k) + C_i v(k), \\ z(k) &= D_i x(k) + E_i v(k). \end{aligned} \tag{16}$$

Theorem 3.3. For given scalars $\gamma > 0, \theta \in [0, 1]$ and quantization density $\rho > 0$, the closed-loop system (16) is robustly stochastically stable if there exist a set of positive definite symmetric matrices P_{ia}^s, Q_{jb}^q and matrix K_i with appropriate dimensions, and some scalars ν_{1i}, ν_{2i} and ϵ_i , such that the following matrix inequalities together with (12) hold for all $i \in \Lambda$ and $a \in \Theta$:

$$\tilde{\Omega}_i = \begin{bmatrix} \hat{\Omega}_i & N_i^T & \epsilon_i M_i \\ * & -\epsilon_i & 0 \\ * & * & -\epsilon_i \end{bmatrix} < 0, \tag{17}$$

where $M_i = [0 \ 0 \ \sqrt{\pi_{i1}^s \lambda_{a1}} \mathcal{M}_i^T B_i^T \ \dots \ \sqrt{\pi_{iN}^s \lambda_{an}} \mathcal{M}_i^T B_i^T \ 0 \ \delta_i \mathcal{M}_i^T \ 0 \ 0 \ 0]^T$, $N_i = [\mathcal{N}_i \Phi_a \ 0 \ 0 \ \dots \ 0 \ 0 \ 0 \ 0 \ 0 \ 0]$ and other parameters are defined as in **Theorem 3.2**.

Proof. With the use of (15), the LMI condition (11) in **Theorem 3.2** can be written as

$$\mathcal{E} = \hat{\Omega}_i + M_i \Sigma_i(k) N_i + N_i^T \Sigma_i^T(k) M_i^T. \tag{18}$$

Applying **Lemma A.1** to the expression in (18), it is easy to get that

$$\mathcal{E} = \hat{\Omega}_i + \epsilon_i M_i M_i^T + \epsilon_i^{-1} N_i^T N_i. \tag{19}$$

Then, by using **Lemma A.2** in the above expression (19), it can be observed that (19) is equivalent to LMI (17). Thus, it can be concluded that the closed-loop system (16) is stochastically stable and satisfies the mixed H_∞ and passive performance index. This concludes the proof.

With the use of the cone complementarity linearization algorithm, it is easy to solve the LMI problem with bilinear matrix equation constraint. Therefore, the control gains formulated by (17) and (12) and can be converted into the following optimization problem:

$$\begin{aligned} \min \quad & \text{trace} \left\{ \sum_{j=1}^N \sum_{b=1}^n Q_{jb}^q \times P_{jb}^q \right\} \\ \text{subject to} \quad & (17) \text{ and } \begin{bmatrix} Q_{jb}^q & I \\ * & P_{jb}^q \end{bmatrix} \geq 0. \end{aligned} \tag{20}$$

To solve this optimization problem, the detailed controller design algorithm is given below:

Algorithm: Controller Design Algorithm**Step 1:** Set $k = 0$ and solve (12) and (17) to obtain the feasible set $(P_{jb}(0), Q_{jb}(0), K(0))$.**Step 2:** Solve the following LMI minimization problem:

$$\min \text{trace} \left\{ \sum_{j=1}^N \sum_{b=1}^n (Q_{jb}^q(k) \times P_{jb}^q + P_{jb}^q(k) \times Q_{jb}^q) \right\} \text{ subject to (17) and (20).}$$

Step 3: If the obtained matrix variable (P_{jb}, Q_{jb}, K) satisfies (19), then output of the feasible solution is (P_{jb}, Q_{jb}, K) . EXIT. Otherwise, set $k = k + 1$ and return to the **Step 2**.

Remark 3.4. It should be mentioned that the mixed H_∞ and passivity-based control problem studied in this paper is a special case of dissipative control problem, which combines the passivity and the H_∞ performances in a unified framework. It is well known that the dissipative analysis mostly studied for the systems with complex structure or sometimes chaotic structures, where interacting particles exhibit long-range correlations. But the special case considered in this paper does not have these restrictions on the considered system. On the other hand, inaccuracies or uncertainties may occur during the controller implementation in practice. Therefore, the controller should be designed in such a way that it is insensitive to some amount of uncertainties with respect to its gain. These are the facts to consider mixed H_∞ and passivity performance and resilient control together in this paper. Besides, a conventional controller may result in unsatisfactory performance, or even instability, in the event of malfunctions in actuators, sensors or other system components. To overcome this issue, many reliable control designs have been developed [38,39]. The difference between these two kinds of controllers is that the resilient controller is employed to precisely deal with gain fluctuations whereas the reliable controller is used to deal with components failures in the system, especially actuators and sensors.

Remark 3.5. Based on the cone complementarity linearization algorithm, sufficient conditions for the existence of robust mixed H_∞ and passivity-based control and robust mixed H_∞ and passivity-based resilient control for the considered closed-loop systems (7) and (16) are obtained, respectively, in Theorems 3.2 and 3.3 without using any zero equations and free-weighting matrices. This significantly reduces the computational complexity.

Remark 3.6. It is known that Markov jump system evolves according to a Markov stochastic process (or chain), wherein the transition probability plays a crucial role in Markov process (or chain). In the analysis and synthesis of Markov jump systems, transition probabilities are usually assumed to be fully accessible or exactly known [2,9]. However, transition probabilities are often expensive and sometimes, are not known precisely in many practical situations. Keeping these facts into consideration, in this paper, we adopt the time-varying transition probabilities, which are described by a polytope set. Therefore, the transition probabilities chosen in this paper are more general than those in [2,9]. In addition, the main advantage of considered system (1) is the flexibility in the transition probabilities that are changing over time.

4. Simulation results

In this section, two numerical examples including a DC motor device model are given to illustrate the effectiveness of the obtained results.

Example 4.1. We consider the speed control problem for a DC motor device driving an inertial load, which can be described by the discrete-time Markovian jump system (2). A DC motor device model is shown in Fig. 1, where $V_c(t)$ is the applied voltage to the motor, which represents the control input and $v(t)$ represents the angular rate of the load. We use T_k to denote the torque at the shaft of the motor, which is proportional to the current $i(t)$ induced by the applied voltage. $V_m(t)$ is the voltage proportional to the angular rate $v(t)$ seen at the shaft. Moreover, the corresponding system parameter values are borrowed from [17] which are given below:

$$\begin{aligned} A_1 &= \begin{bmatrix} -0.479908 & 5.1546 \\ -3.81625 & 14.4723 \end{bmatrix}; A_2 = \begin{bmatrix} -1.60261 & 9.1632 \\ -0.5918697 & 3.0317 \end{bmatrix}; A_3 = \begin{bmatrix} 0.634617 & 0.917836 \\ -0.50569 & 2.48116 \end{bmatrix}; \\ B_1 &= \begin{bmatrix} 5.87058212 \\ 15.50107 \end{bmatrix}; B_2 = \begin{bmatrix} 10.255129 \\ 2.2282663 \end{bmatrix}; B_3 = \begin{bmatrix} 0.7874647 \\ 1.5302844 \end{bmatrix}; C_1 = C_2 = C_3 = \begin{bmatrix} 0.1 \\ 0.2 \end{bmatrix}; \\ D_1 &= [1 \ 0]; D_2 = [0 \ 1]; D_3 = [0 \ 1]; \\ E_1 &= E_2 = E_3 = 0.1; M_1 = M_2 = M_3 = \begin{bmatrix} 0.1 \\ 0.1 \end{bmatrix}; N_1 = N_2 = N_3 = [0.1 \ 0.1]; \mathcal{M}_1 = \mathcal{M}_2 = \mathcal{M}_3 = 0.1; \\ \mathcal{N}_1 &= \mathcal{N}_2 = \mathcal{N}_3 = [0.1 \ 0.1]. \end{aligned}$$

The vertices of the time-varying transition probability matrix are given as follows:

$$\Pi^1 = \begin{bmatrix} 0.671 & 0.153 & 0.176 \\ 0.324 & 0.489 & 0.187 \\ 0.136 & 0.524 & 0.340 \end{bmatrix}; \quad \Pi^2 = \begin{bmatrix} 0.145 & 0.427 & 0.428 \\ 0.321 & 0.546 & 0.133 \\ 0.249 & 0.476 & 0.275 \end{bmatrix};$$

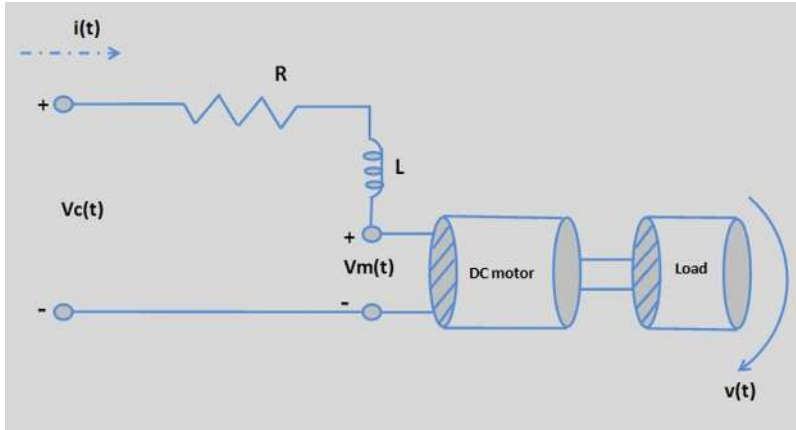


Fig. 1. DC motor device [17].

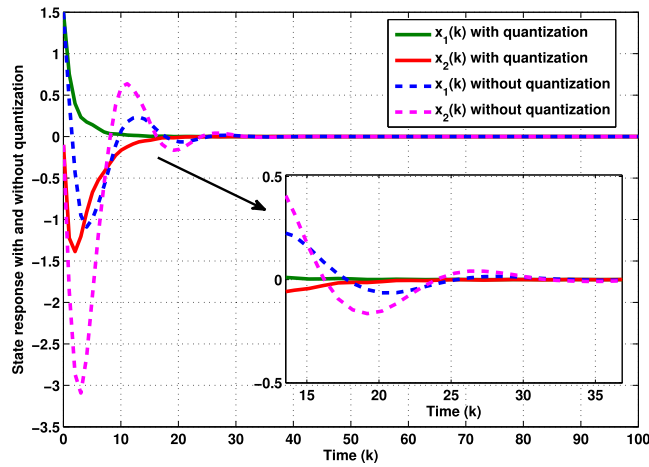


Fig. 2. State responses of (7) with and without quantization.

$$\Pi^3 = \begin{bmatrix} 0.368 & 0.435 & 0.197 \\ 0.243 & 0.457 & 0.300 \\ 0.162 & 0.622 & 0.216 \end{bmatrix}; \quad \Pi^4 = \begin{bmatrix} 0.419 & 0.536 & 0.045 \\ 0.782 & 0.136 & 0.082 \\ 0.167 & 0.346 & 0.487 \end{bmatrix}.$$

To reduce the measurement size during each transmission, we take $\sigma(k) \in \{1, 2\}$ and $\Phi_{\sigma(k)} \in \left\{ \begin{bmatrix} 1 & 0 \\ 0 & 0 \end{bmatrix}, \begin{bmatrix} 0 & 0 \\ 0 & 1 \end{bmatrix} \right\}$.

Also, the measurement scheduling method is modeled by Markov process, with the transition probability matrix $\bar{\Pi} = \begin{bmatrix} 0.2 & 0.7 & 0.1 \\ 0.35 & 0.2 & 0.45 \\ 0.1 & 0.4 & 0.5 \end{bmatrix}$.

For the simulation purposes, we choose $\theta = 0.5$, $\rho = 0.4$ and $\gamma = 0.2$. According to Theorem 3.3, we can get the following mode-dependent controller gain matrices with the use of above said parameter values:

$$K_{11} = [-0.2266 \ 0]; K_{12} = [0 \ -0.7727]; K_{21} = [-0.1232 \ 0]; \\ K_{22} = [0 \ -0.7447]; K_{31} = [-0.0034 \ 0]; K_{32} = [0 \ -0.0560].$$

Further, we take disturbance input as $v(k) = 0.1 \exp(-0.1k) \sin(\frac{\pi k}{2})$ and choose the initial condition of the system state $x(0) = [1.5 \ -0.1]^T$. Using the designed controller above, we can get the states of the closed-loop system with and without quantization, which are presented in Fig. 2. It can be observed from Fig. 2 that the time taken for convergence of the state trajectories with quantization is less than that of state trajectories without quantization. The control and output responses of the system with and without quantization are depicted in Fig. 3 and Fig. 4, respectively. In Fig. 5, the controlled output

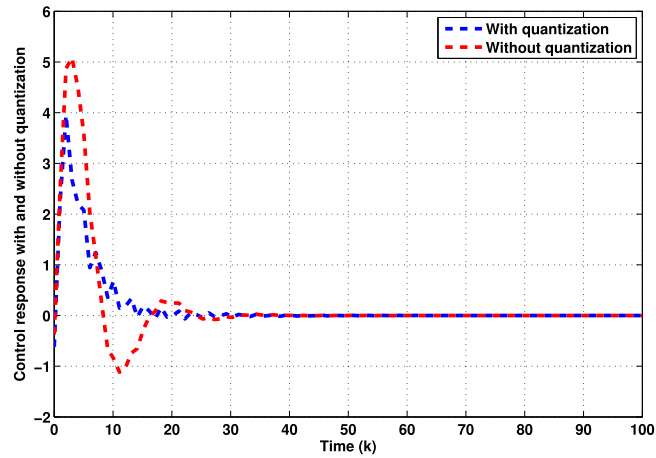


Fig. 3. Control response with and without quantization.

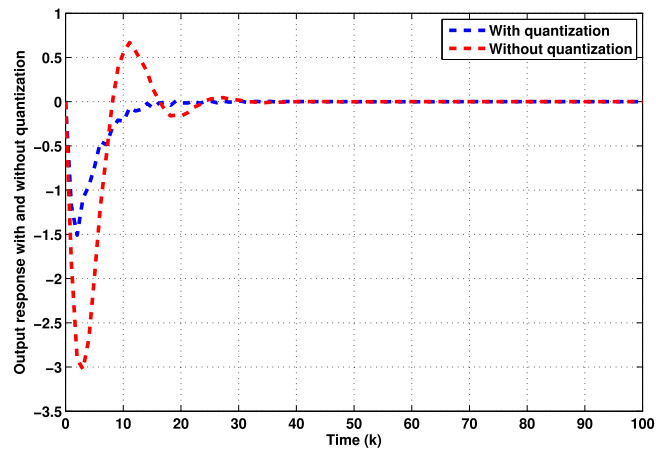


Fig. 4. Output response with and without quantization.

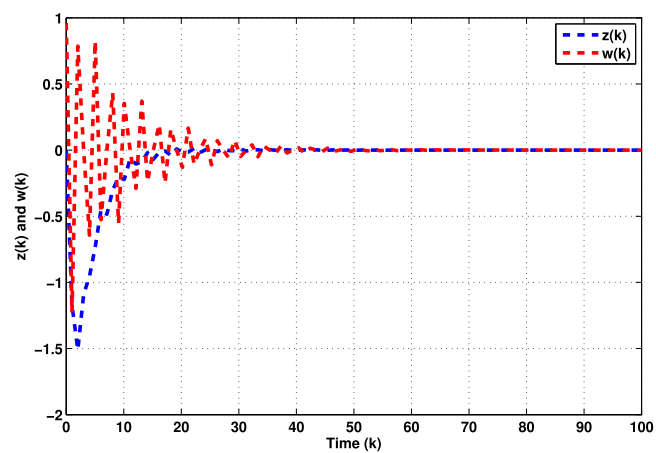


Fig. 5. Disturbance input and controlled output.

and disturbance input signal are given. Randomly generating jumping modes and variations of transition probabilities are displayed in Fig. 6 and Fig. 7, respectively. Furthermore, the calculated minimum γ value for different cases namely, passivity,

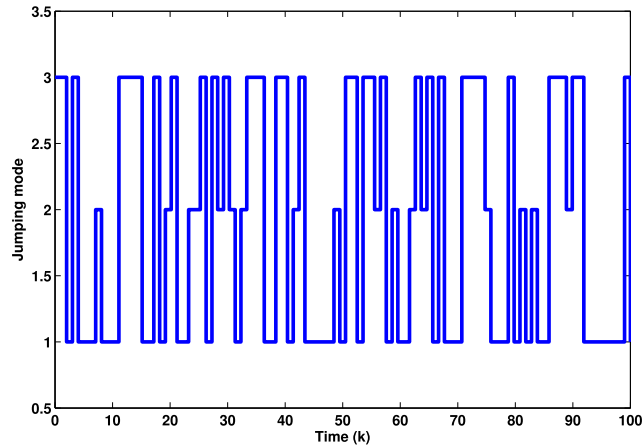


Fig. 6. Jumping modes.

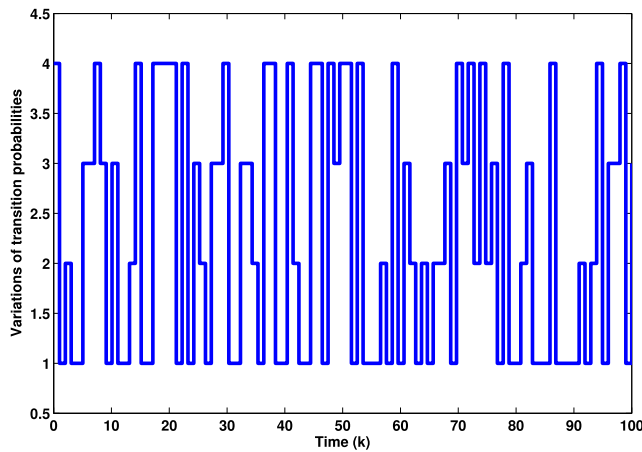


Fig. 7. Variations of transition probabilities.

Table 1
Calculated minimum γ for different cases.

Cases	γ_{\min}
Passivity ($\theta = 0$)	0.0001
Mixed H_∞ and passivity ($\theta = 0.5$)	0.0367
H_∞ ($\theta = 1$)	0.1001

Table 2
Calculated minimum γ for different θ values.

θ	0.2	0.3	0.4	0.5	0.6	0.7	0.8	0.9
Theorem 3.3	0.0117	0.0189	0.0272	0.0367	0.0472	0.0589	0.0718	0.0854

mixed H_∞ and passivity, and H_∞ cases is displayed in Table 1 and also the calculated minimum γ value for different values of θ is presented in Table 2. From the simulation results, it can be strongly concluded that the proposed control scheme is more appropriate in practical purposes since it is more generalized and can tolerate with uncertainties, quantization and time-varying transition probabilities.

Remark 4.2. If the quantization effect and energy constraints are not taken into account in the considered Markov jump system, it will be deduced to the systems in [17] and [40], respectively. The aforementioned factors could not be ignorable since they exemplify the real-world circumstances. Thus, the results presented in this paper are superior than those in [17] and [40]. In particular, the simulation results show that the designed controller has the ability to enforce system trajectories

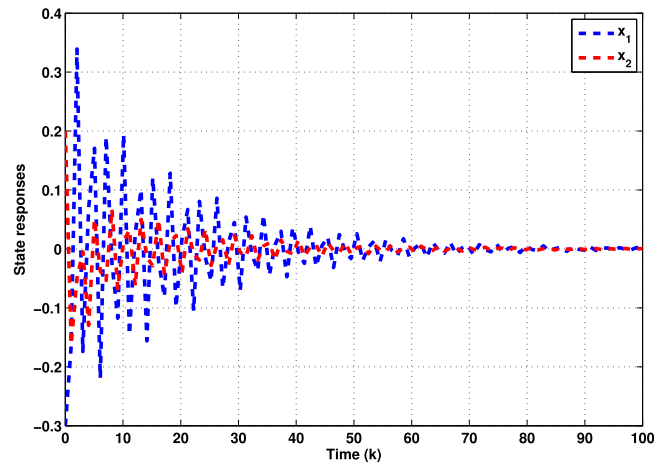


Fig. 8. State responses of (7).

to achieve desired performances even in the presence of quantization effect and energy constraints. On the other hand, delays frequently appear in control engineering systems, where time delays are the property of a physical system [41,42]. Though the effect of time delay is not considered in this study, it is possible to extend the results proposed in this paper to Markov jump system with time delay. This issue will be our near future work.

Example 4.3. We consider the discrete-time Markovian jump system (1) with the following jump parameters:

$$A_1 = \begin{bmatrix} 1.3 & -0.45 \\ 0.5 & 1.1 \end{bmatrix}; A_2 = \begin{bmatrix} 0.1 & -0.29 \\ 0.9 & 1.5 \end{bmatrix}; B_1 = \begin{bmatrix} 0.1 \\ 0.2 \end{bmatrix}; B_2 = \begin{bmatrix} 0.5 \\ 0.2 \end{bmatrix}; C_1 = C_2 = \begin{bmatrix} 0.1 \\ 0.2 \end{bmatrix};$$

$$D_1 = \begin{bmatrix} 0.1 & 0 \end{bmatrix}; D_2 = \begin{bmatrix} 0.1 & 0.1 \end{bmatrix}; E_1 = E_2 = 0.1; M_1 = M_2 = \begin{bmatrix} 0.05 \\ 0.05 \end{bmatrix}; N_1 = N_2 = \begin{bmatrix} 0.01 & 0.01 \end{bmatrix};$$

$$\mathcal{M}_1 = \mathcal{M}_2 = 0.05; \mathcal{N}_1 = \mathcal{N}_2 = \begin{bmatrix} 0.01 & 0.01 \end{bmatrix}.$$

We set the external disturbance as $v(k) = 1.5 \exp(-0.05k) \sin(-\frac{3\pi k}{4})$ and the initial condition as $x(0) = [-0.3 \ 0.2]^T$. Further, the vertices of the time-varying transition probability matrix are taken as follows:

$$\Pi^1 = \begin{bmatrix} 0.2 & 0.8 \\ 0.35 & 0.65 \end{bmatrix}; \Pi^2 = \begin{bmatrix} 0.55 & 0.45 \\ 0.48 & 0.52 \end{bmatrix}; \Pi^3 = \begin{bmatrix} 0.6 & 0.4 \\ 0.3 & 0.7 \end{bmatrix}; \Pi^4 = \begin{bmatrix} 0.4 & 0.6 \\ 0.9 & 0.1 \end{bmatrix}.$$

The measurement scheduling method is modeled by Markov chain, with the transition probability matrix defined by $\bar{\Pi} = \begin{bmatrix} 0.3 & 0.7 \\ 0.55 & 0.45 \end{bmatrix}$. In this example, we take $\theta = 0.5$, $\rho = 0.4$, $\gamma = 1.2$ and the same measurement size reduction matrix structure as defined in Example 4.1. Then, by solving the conditions (17) and (20) in Theorem 3.3, we can get the following controller gain matrices: $K_{11} = [-0.5730 \ 0]$, $K_{12} = [0 \ -0.7109]$, $K_{21} = [-0.4707 \ 0]$ and $K_{22} = [0 \ -0.6088]$. Based on these gain values, the state responses of the considered Markovian jump system (1) are presented in Fig. 8 and the associated control responses of the system are shown in Fig. 9. Fig. 10 depicts the controlled output and disturbance input. We present a prescribed variation between four transition probability matrices and the system jumping modes are plotted together in Fig. 11. The result reveals that the designed mixed H_∞ and passivity-based resilient control is effective for achieving the desired performance of the considered system.

5. Conclusion

In this paper, the mixed H_∞ and passivity-based resilient control problem for discrete-time nonhomogeneous Markov jump systems with uncertainties, quantization and energy constraints has been studied. In order to reduce the energy consumption, measurement size reduction technique has been used. In addition, the resilient property and the logarithmic quantization are also taken into account, which makes that the results of this work as a generalized one. Moreover, a polytope has been used to express time-varying transition probability matrices in which vertices are given prior and the parameter-dependent Lyapunov function has been utilized to ensure that the closed-loop system is stochastically stable with a prescribed mixed H_∞ and passivity performance index. Two numerical examples have been given to show the effectiveness of the proposed method. Further, the problems of non-fragile finite-time stability and non-fragile finite-time filtering are

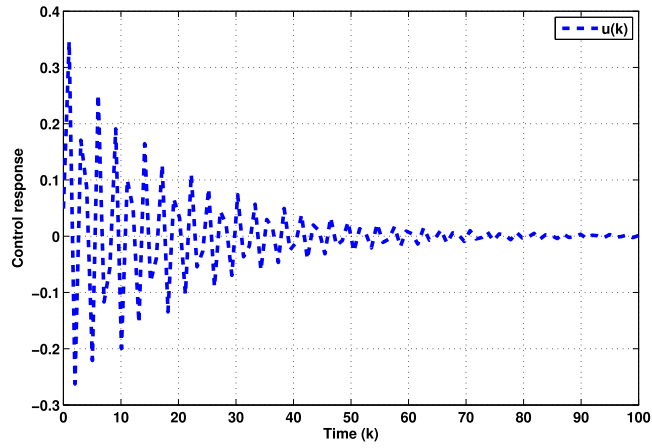


Fig. 9. Control response.

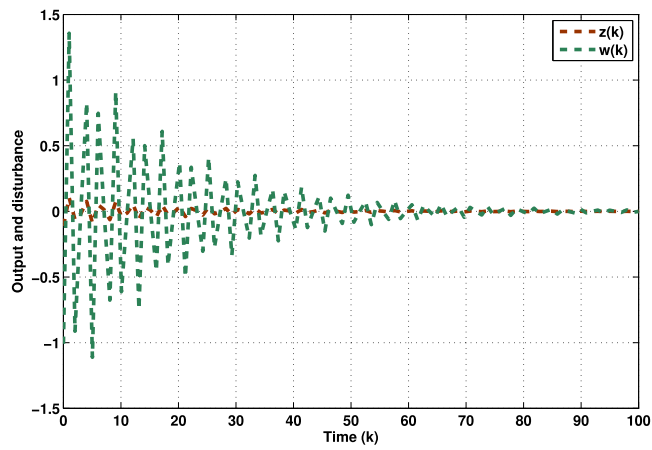


Fig. 10. Output and disturbance.

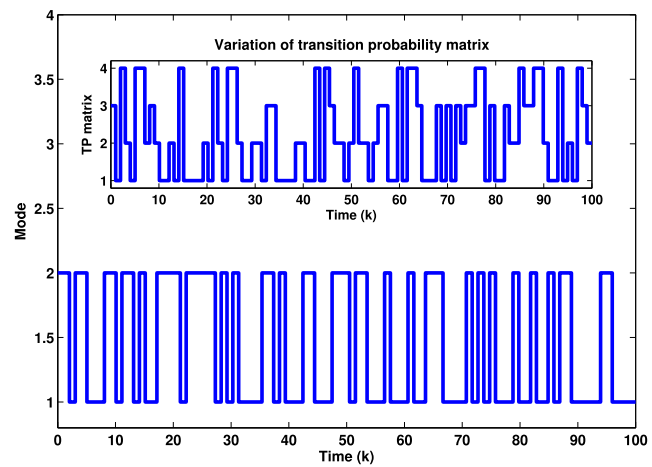


Fig. 11. Jumping mode.

untreated topics for the considered nonhomogeneous Markov jump systems with uncertainties, quantization and energy constraints. These issues will be our future research topics.

Acknowledgments

The work of Yong Ren is supported by the National Natural Science Foundation of China (10871076).

Appendix

Lemma A.1 ([3]). Assume that Ω , M and N are real matrices with appropriate dimensions and Υ is a matrix function satisfying $\Upsilon^T \Upsilon \leq I$, then $\Omega + M\Upsilon N + [M\Upsilon N]^T < 0$ holds, if and only if there exists a scalar $\epsilon > 0$ satisfying $\Omega + \epsilon^{-1}MM^T + \epsilon N^T N < 0$.

Lemma A.2 ([3]). Given constant matrices Ω_{11} , Ω_{12} and Ω_{22} with appropriate dimensions, where $\Omega_{11}^T = \Omega_{11}$ and $\Omega_{22}^T = \Omega_{22}$, then $\Omega_{11} + \Omega_{12}^T \Omega_{22}^{-1} \Omega_{12} < 0$ if and only if $\begin{bmatrix} \Omega_{11} & \Omega_{12}^T \\ * & -\Omega_{22} \end{bmatrix} < 0$.

References

- [1] H. Li, P. Shi, D. Yao, Adaptive sliding-mode control of Markov jump nonlinear systems with actuator faults, *IEEE Trans. Automat. Control* 62 (2017) 1933–1939.
- [2] S. Li, Z. Xiang, Stochastic stability analysis and L_∞ -gain controller design for positive Markov jump systems with time-varying delays, *Nonlinear Anal. Hybrid Syst.* 22 (2016) 31–42.
- [3] R. Sakthivel, M. Sathishkumar, K. Mathiyalagan, S. Marshal Anthoni, Robust reliable dissipative filtering for markovian jump nonlinear systems with uncertainties, *Internat. J. Adapt. Control Signal Process.* 31 (2017) 39–53.
- [4] S. Dong, Z.G. Wu, Y.J. Pan, H. Su, Y. Liu, Hidden-Markov-model-based asynchronous filter design of nonlinear Markov jump systems in continuous-time domain, *IEEE Trans. Cybern.* (2018) <http://dx.doi.org/10.1109/TCYB.2018.2824799>.
- [5] J. Wang, S. Ma, C. Zhang, Stability analysis and stabilization for nonlinear continuous-time descriptor semi-Markov jump systems, *Appl. Math. Comput.* 279 (2016) 90–102.
- [6] Z. Yan, Y. Song, J.H. Park, Finite-time stability and stabilization for stochastic Markov jump systems with mode-dependent time delays, *ISA Trans.* 68 (2017) 141–149.
- [7] F. Li, P. Shi, C.C. Lim, L. Wu, Fault detection filtering for nonhomogeneous Markovian jump systems via fuzzy approach, *IEEE Trans. Fuzzy Syst.* 26 (2018) 131–141.
- [8] S. Dong, Z.G. Wu, P. Shi, H.R. Karimi, H. Su, Networked fault detection for Markov jump nonlinear systems, *IEEE Trans. Fuzzy Syst.* (2018) <http://dx.doi.org/10.1109/TFUZZ.2018.2826467>.
- [9] P. Balasubramaniam, V.M. Revathi, H_∞ filtering for Markovian switching system with mode-dependent time-varying delays, *Circuits Syst. Signal Process.* 33 (2014) 347–369.
- [10] H. Shen, F. Li, Z.G. Wu, J.H. Park, Finite-time asynchronous H_∞ filtering for discrete-time Markov jump systems over a lossy network, *Internat. J. Robust Nonlinear Control* 26 (2016) 3831–3848.
- [11] J. Tao, Z.G. Wu, H. Su, Y. Wu, D. Zhang, Asynchronous and resilient filtering for markovian jump neural networks subject to extended dissipativity, *IEEE Trans. Cybern.* (2018) <http://dx.doi.org/10.1109/TCYB.2018.2824853>.
- [12] Q. Li, B. Shen, Y. Liu, F.E. Alsaadi, Event-triggered H_∞ state estimation for discrete-time stochastic genetic regulatory networks with Markovian jumping parameters and time-varying delays, *Neurocomputing* 174 (2016) 912–920.
- [13] S. Li, Z. Xiang, H. Lin, H.R. Karimi, State estimation on positive Markovian jump systems with time-varying delay and uncertain transition probabilities, *Inform. Sci.* 369 (2016) 251–266.
- [14] J. Tao, R. Lu, H. Su, Z.G. Wu, Y. Xu, Dissipativity-based asynchronous state estimation for Markov jump neural networks with jumping fading channels, *Neurocomputing* 241 (2017) 56–63.
- [15] Y. Liu, B.Z. Guo, J.H. Park, S.M. Lee, Event-based reliable dissipative filtering for T-S fuzzy systems with asynchronous constraints, *IEEE Trans. Fuzzy Syst.* (2017) <http://dx.doi.org/10.1109/TFUZZ.2017.2762633>.
- [16] J. Cheng, J.H. Park, H.R. Karimi, X. Zhao, Static output feedback control of nonhomogeneous Markovian jump systems with asynchronous time delays, *Inform. Sci.* 399 (2017) 219–238.
- [17] Y. Yin, P. Shi, F. Liu, C.C. Lim, Robust control for nonhomogeneous Markov jump processes: An application to DC motor device, *J. Franklin Inst. B* 351 (2014) 3322–3338.
- [18] M. Fu, L. Xie, The sector bound approach to quantized feedback control, *IEEE Trans. Automat. Control* 50 (2005) 1698–1711.
- [19] M.J. Park, O.M. Kwon, S.G. Choi, E.J. Cha, Consensus protocol design for discrete-time networks of multiagent with time-varying delay via logarithmic quantizer, *Complexity* 21 (2015) 163–176.
- [20] C. Wu, H. Li, H.K. Lam, H.R. Karimi, Fault detection for nonlinear networked systems based on quantization and dropout compensation: an interval type-2 fuzzy-model method, *Neurocomputing* 191 (2016) 409–420.
- [21] J. Li, J.H. Park, Fault detection filter design for switched systems with quantization effects, *J. Franklin Inst. B* 353 (2016) 2431–2450.
- [22] B.C. Zheng, G.H. Yang, Decentralized sliding mode quantized feedback control for a class of uncertain large-scale systems with dead-zone input, *Nonlinear Dynam.* 71 (2013) 417–427.
- [23] M. Rehan, M. Tufail, C.K. Ahn, M. Chadli, Stabilisation of locally Lipschitz non-linear systems under input saturation and quantisation, *IET Control Theory Appl.* 11 (2017) 1459–1466.
- [24] S.M. Lee, O.M. Kwon, Quantised MPC for LPV systems by using new Lyapunov-Krasovskii functional, *IET Control Theory Appl.* 11 (2016) 439–445.
- [25] J. Cheng, J.H. Park, Y. Liu, Z. Liu, L. Tang, Finite-time H_∞ fuzzy control of nonlinear Markovian jump delayed systems with partly uncertain transition descriptions, *Fuzzy Sets and Systems* 314 (2017) 99–115.
- [26] Q. Zhang, D. Zhao, Y. Zhu, Event-triggered H_∞ control for continuous-time nonlinear system via concurrent learning, *IEEE Trans. Syst. Man Cybern. A* 47 (2017) 1071–1081.
- [27] K.N. Wu, J. Wang, Mixed H_2/H_∞ control of synchronization for coupled partial differential systems, *Internat. J. Robust Nonlinear Control* 27 (2017) 1397–1418.
- [28] Z.G. Wu, P. Shi, Z. Shu, H. Su, R. Lu, Passivity-based asynchronous control for Markov jump systems, *IEEE Trans. Automat. Control* 62 (2017) 2020–2025.
- [29] Y. Liu, J.H. Park, B.Z. Guo, F. Fang, F. Zhou, Event-triggered dissipative synchronization for Markovian jump neural networks with general transition probabilities, *Internat. J. Robust Nonlinear Control* (2018) <http://dx.doi.org/10.1002/rnc.4110>.

- [30] P. Shi, Y. Zhang, M. Chadli, R.K. Agarwal, Mixed H_∞ and passive filtering for discrete fuzzy neural networks with stochastic jumps and time delays, *IEEE Trans. Neural Netw. Learn. Syst.* 27 (2016) 903–909.
- [31] T. Senthilkumar, P. Balasubramaniam, Non-fragile robust stabilization and H_∞ control for uncertain stochastic time delay systems with Markovian jump parameters and nonlinear disturbances, *Internat. J. Adapt. Control Signal Process.* 28 (2014) 464–478.
- [32] R. Sakthivel, H.R. Karimi, M. Joby, S. Santra, Resilient sampled-data control for Markovian jump systems with adaptive fault-tolerant mechanism, *IEEE Trans. Circuits Syst. II* 64 (2017) 1312–1316.
- [33] D. Zhang, D. Srinivasan, L. Yu, W. Zhang, K. Xing, Distributed non-fragile filtering in sensor networks with energy constraints, *Inform. Sci.* 370–371 (2016) 695–707.
- [34] D. Zhang, Z. Xu, D. Srinivasan, L. Yu, Leader-follower consensus of multiagent systems with energy constraints: A Markovian system approach, *IEEE Trans. Syst. Man Cybern. A* 47 (2017) 1727–1736.
- [35] D. Zhang, F. Yang, C. Yu, D. Srinivasan, L. Yu, Robust fuzzy-model-based filtering for nonlinear networked systems with energy constraints, *J. Franklin Inst. B* 354 (2017) 1957–1973.
- [36] M. Sathishkumar, R. Sakthivel, C. Wang, B. Kaviarasan, S. Marshal Anthoni, Non-fragile filtering for singular markovian jump systems with missing measurements, *Signal Process.* 142 (2018) 125–136.
- [37] X. Luan, S. Zhao, F. Liu, H_∞ control for discrete-time Markov jump systems with uncertain transition probabilities, *IEEE Trans. Automat. Control* 58 (2013) 1566–1572.
- [38] J. Qiu, Y. Wei, H.R. Karimi, H. Gao, Reliable control of discrete-time piecewise-affine time-delay systems via output feedback, *IEEE Trans. Reliab.* 67 (2018) 79–91.
- [39] Y. Wei, J. Qiu, H.R. Karimi, Reliable output feedback control of discrete-time fuzzy affine systems with actuator faults, *IEEE Trans. Circuits Syst. I. Regul. Pap.* 64 (2017) 170–181.
- [40] P. Shi, Y. Yin, F. Liu, J. Zhang, Robust control on saturated Markov jump systems with missing information, *Inform. Sci.* 265 (2014) 123–138.
- [41] H.R. Karimi, H. Gao, New delay-dependent exponential h_∞ synchronization for uncertain neural networks with mixed time delays, *IEEE Trans. Syst. Man Cybern. B* 40 (2010) 173–185.
- [42] H.R. Karimi, P. Maass, Delay-range-dependent exponential H_∞ synchronization of a class of delayed neural networks, *Chaos Solitons Fractals* 41 (2009) 1125–1135.

Date of publication xxxx 00, 0000, date of current version xxxx 00, 0000.

Digital Object Identifier 10.1109/ACCESS.2023.0322000

Finite-Time Boundedness of Switched Time-Varying Delay Systems with Actuator Saturation: Applications in Water Pollution Control

SARAVANAN SHANMUGAM¹, M. SYED ALI², G. NARAYANAN^{3,4} and MOHAMED RHAIMA⁵

¹Centre for Nonlinear Systems, Chennai Institute of Technology, Chennai 600 069, Tamilnadu, India (e-mail: saravans@citchennai.net)

²Department of Mathematics, Thiruvalluvar University, Vellore - 632 115, Tamilnadu, India (e-mail: syedgru@gmail.com)

³School of IT Information and Control Engineering, Kunsan National University, South Korea

⁴Centre for Computational Modeling, Chennai Institute of Technology, Chennai-600069, India, (e-mail: narayanantvu@gmail.com)

⁵Department of Statistics and Operations Research, College of Sciences, King Saud University, P.O. Box 2455 Riyadh 11451, Saudi Arabia. (e-mail: mrhaima.c@ksu.edu.sa)

Corresponding authors: M. Syed Ali (e-mail: syedgru@gmail.com) and Mohamed Rhaima (e-mail: mrhaima.c@ksu.edu.sa).

“This work was supported in part by the Centre for Nonlinear Systems, Chennai Institute of Technology (CIT), India, vide funding number CIT/CNS/2023/RP-005 and King Saud University, Riyadh, Saudi Arabia, Supporting Project number (RSPD2023R683)”

ABSTRACT This paper addresses the challenge of ensuring finite-time boundedness in switched time-varying delay systems with actuator saturation. Utilizing Lyapunov–Krasovskii functionals, we establish delay-dependent conditions through linear matrix inequalities, ensuring that switched systems with time-varying delays remain finite-time bounded. The paper also introduces the concept of average dwell time for switching signals, providing additional conditions for finite-time boundedness. Furthermore, the finite-time L_2 - L_∞ performance of switched systems with time-varying delays is investigated as a measure of disturbance capability within a finite-time interval. The estimator gain matrix can be determined by solving the linear matrix inequalities. The effectiveness of the proposed approach is illustrated through numerical examples.

INDEX TERMS Actuator saturation, Average dwell time, Finite-time boundedness, $L_2 - L_\infty$ performance, Lyapunov-Krasovskii method, Time-varying delay.

I. INTRODUCTION

SWITCHED systems have received much attention recently, with studies exploring stability, controllability, and performance. The notable topics include finite-time stabilization, robust filtering, L_2 gain, Finite-time boundedness, stochastic, and H_∞ control in switched systems [1]- [7]. These collective studies significantly contribute to understanding control and stability in switched time-delay systems. Switched systems have wide applications in chemical processes, mechanical systems, automotive industry, aircraft and air traffic control, and so on. Such a class of systems is composed of a finite number of subsystems and a logical rule orchestrating the switching between the subsystems. Basically, the switching rule in most existing literatures can be classified into three categories: arbitrary switching is investigated in [8], dwell time switching is given in [7], and state dependent switching is presented in [9]. It is well known that the first two categories of switching rules require that each subsystem of a switched system is stable or stabilized. In particular, it is

generally admitted that dwell time switching regime is more pliant than arbitrary switching rule to some extent.

Recently, researchers have employed two methods for dealing with slow switching: dwell time and average dwell time. However, these results are somewhat conservative. In the majority of the literature, the average dwell time scheme is preferred because it yields more general results compared to dwell time. In the average dwell time approach, the number of switches within a finite interval is bounded, and the average time between consecutive switchings is not less than a constant. This method has been demonstrated to be a successful and effective technique for analyzing the stability of switched systems and designing controllers. For example, refer to [10]- [12].

Actuator saturation are the key of control which is applicable to all areas of engineering and science. However, majority of actuators are not strictly accord with linearity, most of them subject to saturation in real physical systems. On the other hand, as a physical phenomenon, actuator saturation

often occurs in practical systems due to physical constraints. That can severely degrade the performance of closed-loop system and sometimes even make a stable closed-loop system unstable if the controller is designed without considering this kind of nonlinearity. During the past several decades, control systems with actuator saturation have received much attention, (see for examples [13]- [17], and the references therein). The analysis and synthesis of T-S fuzzy systems with actuator saturation nonlinearities is given in [18]. A problem of robust observer-based passive control for uncertain singular time-delay systems subject to actuator saturation has been investigated in [19]. In [20] passivity controller design for singular time-delay system and actuator saturation with nonlinear disturbance are employed. H_∞ observer design for stochastic time-delayed systems with Markovian switching under partly known transition rates and actuator saturations has been investigated in [21]. The problem of exponential stabilization for a class of singularly perturbed switched systems subject to actuator saturation is studied in [22]. Based on finite-time H_∞ control problem for a class of discrete-time switched singular time-delay with actuator saturation have been investigated in [23].

Finite-time stability addresses the stability of a system over a finite-time interval and holds significant importance. It's essential to note that finite-time stability and Lyapunov asymptotic stability are distinct concepts, and they are independent of each other. Therefore, it is important to emphasize the distinction between classical Lyapunov stability and finite-time stability. However, in many practical systems, people increasingly prefer to consider the behavior of system in a finite interval [24]- [26]. And in recent years, finite-time stability and finite-time boundedness problems have been widely spread and used in various systems [27]. The finite-time filtering and state observer design problems have been solved respectively in [28]. In the field of control systems, recent research has focused on achieving finite-time stability and control for various dynamic systems. [29] introduced a novel approach to fuzzy adaptive finite-time consensus control for high-order nonlinear multiagent systems based on event-triggered mechanisms, providing robustness against uncertainties and disturbances. [30] addressed finite-time event-triggered stabilization for discrete-time fuzzy Markov jump singularly perturbed systems, offering insights into stochastic systems with singularly perturbed dynamics. [31] contributed to the design of event-based finite-time control strategies for nonlinear multiagent systems with asymptotic tracking objectives, emphasizing finite-time convergence and asymptotic tracking behavior. Additionally, interval type-2 fuzzy systems with time delay and actuator faults were explored in an unidentified article, focusing on the finite-time boundedness of such systems in [32]. This growing body of research underscores the significance of finite-time control in addressing complex system dynamics.

To the best of our knowledge, the concept of finite-time boundedness represents a crucial aspect of control theory,

ensuring that a system's state variables remain within predetermined bounds within a finite time frame. This property is particularly significant in real-world applications where the system's behavior must be tightly controlled and constrained to meet performance and safety requirements. Additionally, the finite-time control of switched system with $L_2 - L_\infty$ performance criteria plays a major role in this paper. The main contribution of this work as given as follows:

- 1) We establish sufficient conditions for ensuring finite-time boundedness through the Lyapunov-Krasovskii functional, Jensen's inequality, Wirtinger's integral inequality, and a novel integral inequality, utilizing linear matrix inequalities (LMIs).
- 2) Exploring the finite-time $L_2 - L_\infty$ performance of switched systems with time-varying delays as a measure of disturbance capability within a finite-time interval.
- 3) We address the challenging problem of finite-time boundedness in switched time-delay systems while incorporating an actuator saturation controller gain. The design of the controller gain considers factors such as attenuation levels and the average dwell time, ensuring effective control under saturation constraints. Consequently, we determine the estimator gains required for the proposed control strategy's implementation.
- 4) Furthermore, we demonstrate the practical relevance of our approach by applying it to real-world scenarios, specifically addressing the water pollution control problem. Our approach's effectiveness and applicability are demonstrated through numerical examples, showcasing its potential for providing sustainable solutions to control problems.

Notation: The notation used in this paper is standard. \mathcal{R}^n denotes n -dimensional Euclidean space, the superscript " T " denotes the transpose and the notation $P > 0$ (≥ 0) means P is real symmetric positive definite matrix, $\lambda_{\max}(P)$ and $\lambda_{\min}(P)$ denote the maximum and minimum eigenvalues of matrix P , respectively. I is an identity matrix with appropriate dimension. The asterisk $*$ in a matrix is used to denote a term that is induced by symmetry.

II. PROBLEM FORMULATION AND PRELIMINARIES

Consider the following switched system with time varying delays as follows:

$$\left. \begin{aligned} \dot{x}(t) &= A_{p(t)}x(t) + A_{dp(t)}x(t - h(t)) + B_{p(t)}sat(u(t)) \\ &\quad + B_{wp(t)}w(t), \\ z(t) &= C_{p(t)}x(t) + C_{dp(t)}x(t - h(t)) + D_{wp(t)}w(t), \\ x(t) &= \phi(t), t \in [-h_M, 0], \end{aligned} \right\} (1)$$

where $x(\cdot) = [x_1(\cdot), x_2(\cdot), \dots, x_n(\cdot)]^T \in \mathcal{R}^n$ is the state vector, $u(t) \in \mathcal{R}^p$ is the control input $z(t) \in \mathcal{R}^m$ is the control output vector; $p(t) : [0, \infty) \rightarrow N = \{1, 2, \dots, n\}$ is the switching signal that is a piecewise constant function depending on time t or state $x(t)$, and n is the number of

subsystems; $w(t) \in \mathcal{R}^q$ is the disturbance and satisfies $\int_0^T w^T(t)w(t) \leq d, d \geq 0, h(t)$ is time-varying delay satisfies $0 \leq h(t) \leq h, \dot{h}(t) \leq h_M. \text{sat}(u(t)) : \mathcal{R}^p \rightarrow \mathcal{R}^p$ is the control input, $\text{sat}(\cdot)$ is the saturation nonlinearity function.

A. CONTROL FORMULATION

The saturation function $\text{sat}(u(\cdot)) : \mathcal{R}^p \rightarrow \mathcal{R}^p$ is defined as follows:

$$\text{sat}(u) := [\text{sat}(u_1), \text{sat}(u_2), \dots, \text{sat}(u_p)]^T,$$

where $\text{sat}(u_l) = \text{sig}(u_l) \min\{\vartheta_l, |u_l|\}$, or we can write as follows

$$\begin{cases} \vartheta_l & u_l > \vartheta_l, \\ u_l, & -\vartheta_l \leq u_l \leq \vartheta_l, \quad l = 1, 2, \dots, p, \\ -\vartheta_l, & u_l < -\vartheta_l. \end{cases}$$

The saturation function $\text{sat}(u(t))$ may be decomposed into a linear and a nonlinear segment, which helps elucidate its behavior and implications for the model at hand

$$\text{sat}(u(t)) = u(t) - \phi(u(t)), \quad (2)$$

where $\phi(u(t)) = [\phi_1(u(t)), \phi_2(u(t)), \dots, \phi_p(u(t))]^T \in \mathbb{R}^p$, and $\phi_l(u(t)) = u_l(t) - \text{sat}(u_l(t)), (l = 1, 2, \dots, p)$. Subsequently, a scalar value $0 < \epsilon < 1$ exists, satisfying the condition that

$$\epsilon u^T(t)u(t) \geq \phi^T(u(t))\phi(u(t)).$$

Therefore we design the controller as the following form:

$$u(t) = K_i x(t) \quad (3)$$

where $K_i \in \mathcal{R}^p$ is the gain matrix to be designed. Assuming that only a finite part of the non-linearity is considered during the actual system operation, i.e. the operation of the saturation is inside the sector $[\epsilon, 1], 0 < \epsilon < 1$. Corresponding to the switching signal $p(t)$, we have the following switching sequence, $\{x_0 : (i_0, t_0), \dots, (i_k, t_k), \dots, i_k \in \mathbb{N}, k = 0, 1, \dots\}$. Moreover, $p(t) = i$ which means that i_k th subsystem is activated when $t \in [t_k, t_{k+1})$.

From (1) the switched time-varying delayed system and replaced with $p(t) = i$ is written as follows,

$$\left. \begin{aligned} \dot{x}(t) &= A_i x(t) + A_{di} x(t-h(t)) + B_i \text{sat}(u(t)) + B_{wi} w(t), \\ z(t) &= C_i x(t) + C_{di} x(t-h(t)) + D_{wi} w(t), \\ x(t) &= \phi(t), t \in [-h_M, 0], \end{aligned} \right\} \quad (4)$$

Definition 2.1: [25] (Finite-time boundedness). For a given time constant $c_1 > 0, c_2 > 0, T$ and symmetric matrix $R > 0$, the system (1) is said to be finite-time bounded with respect to (c_1, c_2, T, R) if there exist constants $c_2 > c_1 > 0$, such that

$$x^T(t_0)Rx(t_0) \leq c_1 \Rightarrow x^T(t)Rx(t) \leq c_2, \quad \forall t \in [0, T].$$

Definition 2.2: [39] (L_2 - L_∞ performance). The time-varying delay switched system (1) is said to be finite-time bounded

with respect to (c_1, c_2, T, R, d) in the sense of Definition 2.1 and disturbance attenuation $\gamma > 0$ such that

$$\|z(t)\|_\infty^2 \leq \gamma^2 \|w(t)\|_2^2,$$

where $\|z(t)\|_\infty^2 = \sup_{t>0} [z^T(t)z(t)]$,

$$\|w(t)\|_2^2 = \int_0^T w^T(t)w(t)dt.$$

Definition 2.3: [34] For any switching signal $p(t)$ and $t_2 \geq t_1 \geq 0$, let $N_{p(t)}(t_2, t_1)$ denote the switching number of $p(t)$ on an interval (t_1, t_2) . We say that $p(t)$ has an average dwell time τ_a if

$$N_{p(t)}(t_1, t_2) \leq N_0 + \frac{t_2 - t_1}{\tau_a}$$

holds for given $N_0 \geq 0, \tau_a > 0, N_0$ is the chatter bound. Without loss of generality, we choose $N_0 = 0$ throughout this paper.

Lemma 2.4: [38] For any real vectors α, β and any matrix $Q > 0$ with appropriate dimensions, it follows that

$$2\alpha^T \beta \leq \alpha^T Q \alpha + \beta^T Q^{-1} \beta.$$

Lemma 2.5: For any positive matrices $\mathcal{M}_1, \mathcal{M}_2 \in \mathcal{R}^{n \times n}, \mathcal{L} \in \mathcal{R}^{n \times q}$, positive definite symmetric matrix $\mathcal{Q}_2 \in \mathcal{R}^{n \times n}$ and any time varying delays $h(t)$, we have

$$-\int_{t-d(t)}^t \dot{x}^T(s) \mathcal{Q}_2 \dot{x}(s) ds \leq \xi^T(t) \left[\Psi + h \Pi^T \mathcal{Q}_2^{-1} \Pi \right] \xi(t) \quad (5)$$

where

$$\begin{aligned} \Pi &= [\mathcal{M}_1 \quad \mathcal{M}_2 \quad \mathcal{L}], \\ \xi^T &= [x^T(t) \quad x^T(t-h(t)) \quad w^T(t)], \\ \Psi &= \begin{bmatrix} \mathcal{M}_1^T + \mathcal{M}_1 & -\mathcal{M}_1^T + \mathcal{M}_2 & \mathcal{L} \\ * & -\mathcal{M}_2^T - \mathcal{M}_2 & -\mathcal{L} \\ * & * & 0 \end{bmatrix} \end{aligned}$$

Proof From Lemma 2.4 we have

$$\begin{aligned} -\int_{t-h(t)}^t \dot{x}^T(s) \mathcal{Q}_2 \dot{x}(s) ds &\leq 2 \left(\int_{t-h(t)}^t \dot{x}(s) ds \right)^T \Pi \xi(t) \\ &\quad + \int_{t-h(t)}^t \xi^T(t) \Pi^T \mathcal{Q}_2^{-1} \Pi \xi(t) ds, \\ &\leq 2\xi^T(t) \begin{bmatrix} I \\ -I \\ 0 \end{bmatrix} \Pi \xi(t) \\ &\quad + h \xi^T(t) \Pi^T \mathcal{Q}_2^{-1} \Pi \xi(t), \\ &= \xi^T(t) \Psi \xi(t) + h \xi^T(t) \Pi^T \mathcal{Q}_2^{-1} \Pi \xi(t). \end{aligned} \quad (6)$$

Hence we conclude (5). \square

Lemma 2.6: [33] For any constant matrix $M > 0$, the following inequality holds for all continuously differentiable function φ on $[a, b] \rightarrow \mathcal{R}^{n \times n}$:

$$(b-a) \int_a^b \varphi^T(s) M \varphi(s) ds \geq \left(\int_a^b \varphi(s) ds \right)^T M \left(\int_a^b \varphi(s) ds \right) + 3\Omega^T M \Omega,$$

where

$$\Omega = \int_a^b \varphi(s)ds - \frac{2}{b-a} \int_a^b \int_a^s \varphi(\theta)d\theta ds.$$

III. MAIN RESULTS

A. FINITE-TIME BOUNDEDNESS

In this section, we first derive the finite-time boundedness condition for the switched system from (4) with $u(t) = K_i x(t)$, where K_i is known constant and $z(t) = 0$:

$$\left. \begin{aligned} \dot{x}(t) &= A_i x(t) + A_{di} x(t-h(t)) + B_i \text{sat}(K_i x(t)) + B_{wi} w(t), \\ x(t) &= \phi(t), t \in [-h_M, 0], \end{aligned} \right\} \quad (7)$$

Theorem 3.1: For given positive scalars $T, c_1, c_2, d, h, h_M, K_i, \epsilon, \epsilon_a$ and α the system (7) is finite-time boundedness if there exist symmetric positive definite matrices $P_i > 0, Q_{1i} > 0, Q_{2i} > 0, Z_i > 0, S_i > 0$ and the appropriate dimensional matrices $M_{1i} > 0, M_{2i} > 0$ and $L_i > 0$ such that the following LMIs holds:

$$\widetilde{\Sigma} = \begin{bmatrix} \sum & \Theta^T & h\Pi^T \\ * & -\frac{1}{h}Q_{2i} & 0 \\ * & * & -Q_{2i} \end{bmatrix} < 0, \quad (8)$$

$$e^{(\alpha + \frac{\ln \mu}{\tau_a})T} \left[\left(\lambda_2 + h\lambda_3 + \frac{h^2}{2}\lambda_4 + \frac{h^2}{2}\lambda_5 \right) c_1 + d\lambda_6 \right] < \lambda_1 c_2. \quad (9)$$

Then, under the following average dwell time scheme

$$\tau_a > \tau_a^* = \frac{T \ln \mu}{\ln(c_2 e^{-\alpha T}) - \ln[\beta c_1 + d\lambda_6]}, \quad (10)$$

where $\beta = \left(\lambda_2 + h\lambda_3 + \frac{h^2}{2}\lambda_4 + \frac{h^2}{2}\lambda_5 \right)$, the system is finite-time bounded with respect to $(c_1, c_2, T, R, p(t))$, where $\mu > 1$ satisfying

$$P_s < \mu P_i, Q_{1s} < \mu Q_{1i}, Q_{2s} < \mu Q_{2i}, Z_s < \mu Z_i, \quad \forall i, s \in \mathbb{N}. \quad (11)$$

where

$$\Sigma = \begin{bmatrix} \Phi_{11} & \Phi_{12} & 0 & 0 & 0 & 0 & B_{wi}L_i & -B_i \\ * & \Phi_{22} & 0 & 0 & 0 & 0 & -L_i & 0 \\ * & * & \Phi_{33} & 0 & 0 & \Phi_{36} & 0 & 0 \\ * & * & * & \Phi_{44} & \Phi_{45} & 0 & 0 & 0 \\ * & * & * & * & \Phi_{55} & 0 & 0 & 0 \\ * & * & * & * & * & \Phi_{66} & 0 & 0 \\ * & * & * & * & * & * & -S_i & -\epsilon_a B_i \end{bmatrix}.$$

$$\begin{aligned} \Phi_{11} &= 2P_i A_i + 2B_i K_i + Q_{1i} + dQ_{3i} + M_{1i} + M_{1i}^T - \alpha P_i, \\ \Phi_{12} &= A_{di} P_i - M_{1i}^T + M_{2i}, \Phi_{22} = e^{-\alpha h(t)} Q_{1i} - M_{2i}^T \\ &- M_{2i}, \Phi_{33} = \frac{e^{-\alpha h}}{h} Z_i - \frac{3e^{-\alpha h}}{h} Z_i, \Phi_{36} = \frac{6e^{-\alpha h}}{h^2} Z_i, \\ \Phi_{44} &= \frac{e^{-\alpha h}}{h} Z_i - \frac{3e^{-\alpha h}}{h} Z_i, \Phi_{45} = \frac{6e^{-\alpha h}}{h^2} Z_i, \end{aligned}$$

$$\begin{aligned} \Phi_{55} &= -\frac{12e^{-\alpha h}}{h^3} Z_i, \Phi_{66} = -\frac{12e^{-\alpha h}}{h^3} Z_i, \\ \Theta &= \begin{bmatrix} A_i Q_{2i} & A_{di} Q_{2i} & 0 & 0 & 0 & 0 & B_{wi} Q_{2i} & B_i Q_{2i} \end{bmatrix}, \\ \Pi &= \begin{bmatrix} M_{1i} & M_{2i} & 0 & 0 & 0 & 0 & L_i & 0 \end{bmatrix}. \\ \lambda_1 &= \lambda_{\min}(P_i), \lambda_2 = \lambda_{\max}(P_i), \lambda_3 = \lambda_{\max}(Q_{1i}), \\ \lambda_4 &= \lambda_{\max}(Q_{2i}), \lambda_5 = \lambda_{\max}(Z_i), \lambda_6 = \lambda_{\max}(S_i). \end{aligned}$$

Proof Choose the following Lyapunov functional for the system (7) as:

$$V(x(t), t) = \sum_{i=1}^4 V_i(x(t)), \quad (12)$$

where

$$\begin{aligned} V_1(x(t), t) &= x^T(t) P_i x(t), \\ V_2(x(t), t) &= \int_{t-h(t)}^t e^{\alpha(t-s)} x^T(s) Q_{1i} x(s) ds, \\ V_3(x(t), t) &= \int_{-h}^0 \int_{t+\theta}^t e^{\alpha(t-s)} \dot{x}^T(s) Q_{2i} \dot{x}(s) ds d\theta, \\ V_4(x(t), t) &= \int_{-h}^0 \int_{t+\theta}^t e^{\alpha(t-s)} x^T(t) Z_i x(s) ds d\theta. \end{aligned}$$

Calculating the time derivative of $V(x(t), t)$ along the trajectories of the system (7), we have

$$\dot{V}_1 = 2x^T(t) P_i \dot{x}(t), \quad (13)$$

$$\dot{V}_2 = x^T(t) Q_{1i} x(t) - (1-h_M) e^{-\alpha h(t)} x^T(t-h(t)) Q_{1i} x(t-h(t)), \quad (14)$$

$$\dot{V}_3 = h \dot{x}^T(t) Q_{2i} \dot{x}(t) - e^{-\alpha h} \int_{t-h}^t \dot{x}^T(s) Q_{2i} \dot{x}(s) ds, \quad (15)$$

$$\dot{V}_4 = h x^T(t) Z_i x(t) - e^{-\alpha h} \int_{t-h}^t x^T(s) Z_i x(s) ds. \quad (16)$$

By applying Lemma 2.5 in the integral term in (15), we can get,

$$- \int_{t-h}^t \dot{x}^T(s) Q_{2i} \dot{x}(s) ds \leq \xi^T(t) \left\{ \Psi + h\Pi^T Q_{2i}^{-1} \Pi \right\} \xi(t). \quad (17)$$

The integral term in (16) can be written as

$$\begin{aligned} - \int_{t-h}^t x^T(s) Z_i x(s) ds &= - \int_{t-h}^{t-h(t)} x^T(s) Z_i x(s) ds \\ &- \int_{t-h(t)}^t x^T(s) Z_i x(s) ds. \end{aligned} \quad (18)$$

By using Lemma 2.6, we have

$$\begin{aligned} - \int_{t-h}^{t-h(t)} x^T(s) Z_i x(s) ds &= -\frac{1}{h} \left(\int_{t-h}^{t-h(t)} x(s) ds \right)^T \\ &\times Z_i \left(\int_{t-h}^{t-h(t)} x(s) ds \right) - \frac{3}{h} \Omega_1^T Z_i \Omega_1, \end{aligned} \quad (19)$$

$$\begin{aligned} - \int_{t-h(t)}^t x^T(s) Z_i x(s) ds &= -\frac{1}{h} \left(\int_{t-h(t)}^t x(s) ds \right)^T \\ &\times Z_i \left(\int_{t-h(t)}^t x(s) ds \right) - \frac{3}{h} \Omega_2^T Z_i \Omega_2. \end{aligned} \quad (20)$$

where $\Omega_1 = \int_{t-h}^{t-h(t)} x(s)ds - \frac{2}{h} \int_{-h}^{-h(t)} \int_{t+\theta}^t x(s)dsd\theta$, $\Omega_2 = \int_{h(t)}^t x(s)ds - \frac{2}{h} \int_{-h(t)}^0 \int_{t+\theta}^t x(s)dsd\theta$. The saturation effect of the actuator considered in (2), we can get

$$\text{sat}(u(t)) = u(t) - \phi(u(t)), \quad (21)$$

Replacing $u(t)$ in (21) for the right hand side of (3)

$$\text{sat}(u(t)) = K_i x(t) - \phi(u(t)), \quad (22)$$

Moreover, there exists a scalar $0 < \epsilon < 1$ satisfying

$$\epsilon u^T(t)u(t) - \phi^T(u(t))\phi(u(t)) \geq 0, \quad (23)$$

Substitute (3) in (23) we have,

$$\epsilon x^T(t)K_i^T K_i x(t) - \phi^T(u(t))\phi(u(t)) \geq 0, \quad (24)$$

Therefore, for any constant $\epsilon_a > 0$, we can derive

$$\epsilon \epsilon_a x^T(t)K_i^T K_i x(t) - \epsilon_a \phi^T(u(t))\phi(u(t)) \geq 0, \quad (25)$$

Combining from (13) to (25), we have that

$$\begin{aligned} & \dot{V}(x(t)) - \alpha V(x(t)) - w^T(t)S_i w(t) \\ & = \Xi^T(t) \left\{ \Sigma + \Theta^T Q_{2i}^{-1} \Theta + h \Pi^T Q_{2i}^{-1} \Pi \right\} \Xi(t), \end{aligned} \quad (26)$$

where $\Xi^T(t) = \left[x^T(t) \quad x^T(t-h(t)) \quad \int_{t-h}^{t-h(t)} x^T(s)ds \quad \int_{t-h(t)}^t x^T(s)ds \quad \int_{-h(t)}^0 \int_{t+\theta}^t x^T(s)dsd\theta \quad \int_{-h}^{-h(t)} \int_{t+\theta}^t x^T(s)dsd\theta \quad w^T(t) \quad \phi(u(t)) \right]$

By applying Schur complement Lemma, in (26) we get,

$$\dot{V}(x(t)) - \alpha V(x(t)) - w^T(t)S_i w(t) < 0, \quad (27)$$

It can be obtained from (27), for $t \in [t_k, t_{k+1})$,

$$\begin{aligned} V(t) & < e^{\alpha(t-t_k)} V(t_k) + \int_{t_k}^t e^{\alpha(t-s)} w^T(s) S_i w(s) ds, \\ & < e^{\alpha(t-t_k)} \mu V(t_{k-}) + \int_{t_k}^t e^{\alpha(t-s)} w^T(s) S_i w(s) ds, \\ & < e^{\alpha(t-t_k)} \mu [e^{\alpha(t-t_{k-1})} V(t_{k-1}) \\ & \quad + \int_{t_{k-1}}^{t_k} e^{\alpha(t_k-s)} w^T(s) S_i w(s) ds] \\ & \quad + \int_{t_k}^t e^{\alpha(t-s)} w^T(s) S_i w(s) ds, \\ & = e^{\alpha(t-t_{k-1})} \mu V(t_{k-1}) + \mu \int_{t_{k-1}}^{t_k} e^{\alpha(t-s)} w^T(s) S_i w(s) ds \\ & \quad + \int_{t_k}^t e^{\alpha(t-s)} w^T(s) S_i w(s) ds < \dots \\ & \dots < e^{\alpha(t-0)} \mu^{N_p(0,t)} V(0) \\ & \quad + \mu^{N_p(0,t)} \int_0^{t_1} e^{\alpha(t-s)} w^T(s) S_i w(s) ds \\ & \quad + \mu^{N_p(t_1,t)} \int_{t_1}^{t_2} e^{\alpha(t-s)} w^T(s) S_i w(s) ds + \dots \\ & \quad + \mu \int_{t_{k-1}}^{t_k} e^{\alpha(t-s)} w^T(s) S_i w(s) ds \\ & \quad + \int_{t_k}^t e^{\alpha(t-s)} w^T(s) S_i w(s) ds, \\ & = e^{\alpha(t-0)} \mu^{N_p(0,t)} V(0) \\ & \quad + \int_0^t e^{\alpha(t-s)} \mu^{N_p(0,t)} w^T(s) S_i w(s) ds, \\ & < e^{\alpha t} \mu^{N_p(0,t)} V(0) \\ & \quad + \mu^{N_p(0,t)} e^{\alpha t} \int_0^t w^T(s) S_i w(s) ds, \\ & < e^{\alpha T} \mu^{N_p(0,T)} [V(0) + \int_0^T w^T(s) S_i w(s) ds] \\ & < e^{\alpha T} \mu^{N_p(0,T)} [V(0) + \lambda_{\max}(S_i) d]. \end{aligned} \quad (28)$$

From Definition 2.4, we know $N_p(0, t) < \frac{T}{\tau_a}$. Noting that $S_i < \lambda_6 I$, we have

$$V(t) < e^{(\alpha + \frac{\ln \mu}{\tau_a}) T} [V(0) + \lambda_6 d]. \quad (29)$$

Then

$$\begin{aligned} V(t) = V_i(t) & \geq x^T(t) \tilde{P}_i^{-1} x(t) = x^T(t) R^{\frac{1}{2}} P_i^{-1} R^{\frac{1}{2}} x(t) \\ & \geq \frac{1}{\lambda_{\max}(P_i)} x^T(t) R x(t). \end{aligned}$$

Noting that, $\lambda_1 R^{-1} < \tilde{P}_i < R^{-1}$ we have $\lambda_{\max}(P_i) < 1$, then

$$V(t) > V_{1i}(t) > x^T(t)Rx(t). \quad (30)$$

On other hand

$$\begin{aligned} V(x(0)) &= x^T(0)P_i x(0) + \int_{-h(0)}^0 e^{\alpha(-s)} x^T(s) Q_{1i} x(s) ds \\ &+ \int_{-h}^0 \int_{\theta}^0 e^{\alpha(-s)} \dot{x}^T(s) Q_{2i} \dot{x}(s) ds d\theta \\ &+ \int_{-h}^0 \int_{\theta}^0 e^{\alpha(-s)} x^T(0) Z_i x(s) ds d\theta. \\ &\leq \left(\lambda_2 + h\lambda_3 + \frac{h^2}{2}\lambda_4 + \frac{h^2}{2}\lambda_5 \right) \\ &\quad \sup_{-\bar{\tau} \leq \theta \leq 0} \{x^T(\theta)Rx(\theta), \dot{x}^T(\theta)R\dot{x}(\theta)\}. \end{aligned}$$

$$V(x(t)) \leq e^{(\alpha + \frac{\ln \mu}{\tau_a})T} \left[\left(\lambda_2 + h\lambda_3 + \frac{h^2}{2}\lambda_4 + \frac{h^2}{2}\lambda_5 \right) c_1 + d\lambda_6 \right]. \quad (31)$$

From (9) we have

$$x^T(t)Rx(t) < c_2. \quad (32)$$

By Definition 2.1, the system (7) is finite-time boundedness. This completes the proof. \square

Remark 3.2: Based on the theorem presented above, we can conclude that the system described in equation (7) shows finite-time boundedness. If we set the term $w(t) = 0$ in equation (7), we can conclude the theorem as representing finite-time stable.

Next, we focus on the finite-time boundedness of the (4).

B. FINITE-TIME $L_2 - L_\infty$ PERFORMANCE

Theorem 3.3: For given positive scalars $T, c_1, c_2, d, h, h_M, K_i, \epsilon, \epsilon_a$ and α the system (4) with $B_i = 0$ is finite-time boundedness with a prescribed level of noise attenuation $\gamma > 0$ if there exist symmetric positive definite matrices $P_i > 0, Q_{1i} > 0, Q_{2i} > 0, Z_i > 0$ and any appropriate dimensional matrices $M_{1i} > 0, M_{2i} > 0$ and $L_i > 0$ such that the following LMIs holds:

$$\widetilde{\Sigma}_2 = \begin{bmatrix} \Sigma_2 & \Theta^T & h\Pi^T & \widehat{A} \\ * & -\frac{1}{h}Q_{2i} & 0 & 0 \\ * & * & -Q_{2i} & 0 \\ * & * & * & -I \end{bmatrix} < 0, \quad (33)$$

$$e^{(\alpha + \frac{\ln \mu}{\tau_a})T} [(\beta)c_1] < \lambda_1 c_2. \quad (34)$$

Then, under the following average dwell time scheme

$$\tau_a > \tau_a^* = \frac{T \ln \mu}{\ln(c_2 e^{-\alpha T}) - \ln(\beta)c_1}, \quad (35)$$

the system is finite-time bounded with respect to $(c_1, c_2, T, R, p(t))$, where $\mu > 1$ satisfying

$$P_s < \mu P_i, Q_{1s} < \mu Q_{1i}, Q_{2s} < \mu Q_{2i}, Z_s < \mu Z_i, \quad \forall i, s \in \mathbb{N}. \quad (36)$$

and

$$\Sigma_2 = \begin{bmatrix} \Phi_{11} & \Phi_{12} & 0 & 0 & 0 & 0 & L_i & -B_i \\ * & \Phi_{22} & 0 & 0 & 0 & 0 & -L_i & 0 \\ * & * & \Phi_{33} & 0 & 0 & \Phi_{36} & 0 & 0 \\ * & * & * & \Phi_{44} & \Phi_{45} & 0 & 0 & 0 \\ * & * & * & * & \Phi_{55} & 0 & 0 & 0 \\ * & * & * & * & * & \Phi_{66} & 0 & 0 \\ * & * & * & * & * & * & -\gamma^2 I & 0 \\ * & * & * & * & * & * & 0 & -\epsilon_a B_i \end{bmatrix},$$

$$\widehat{A} = [C_i \quad C_{di} \quad 0 \quad 0 \quad 0 \quad 0 \quad D_{wi} \quad 0].$$

$\Phi_{11}, \Phi_{12}, \Phi_{22}, \Phi_{33}, \Phi_{36}, \Phi_{44}, \Phi_{45}, \Phi_{55}, \Phi_{66}$ are defined in theorem 3.1.

Proof By following similar lines in the proof of Theorem 3.1, we have,

$$\dot{V}(t, e(t)) - \alpha V(t) + z^T(t)z(t) - \gamma^2 w^T(t)w(t) < 0. \quad (37)$$

Define

$$J = \gamma^2 w^T(t)w(t) - z^T(t)z(t). \quad (38)$$

Multiplying (37) by $e^{-\delta t}$, we have,

$$\frac{d}{dt} \{e^{-\delta t} V(t)\} < e^{-\delta t} J(t). \quad (39)$$

Integrating this inequality on $[0, T]$ yields

$$0 \leq e^{-\delta T} V(t) < \int_0^T e^{-\delta t} J(t) dt. \quad (40)$$

We have

$$\begin{aligned} e^{-\delta T} \int_0^T z^T(t)z(t) dt &< \int_0^T e^{-\delta t} z^T(t)z(t) dt \\ &< \gamma^2 \int_0^T e^{-\delta t} w^T(t)w(t) dt \\ &< \gamma^2 \int_0^T w^T(t)w(t) dt. \end{aligned} \quad (41)$$

By Definition 2.2 the system (4) is finite-time bounded with respect to (c_1, c_2, T, R, d) and with a prescribed level of noise attenuation $\gamma > 0$. This completes the proof. \square

C. FINITE-TIME $L_2 - L_\infty$ ACTUATOR CONTROL

In this subsection, we will present a detailed procedure for actuator controller design, i.e., to find the controller gains K_i for each subsystem. The following theorem gives sufficient conditions for finite-time boundedness of the closed-loop system (4)

Theorem 3.4: For given positive scalars $T, c_1, c_2, d, h, h_M, \epsilon, \epsilon_a$ and α the system (4) is finite-time boundedness with a prescribed level of noise attenuation $\gamma > 0$ if there exist

symmetric positive definite matrices $P_i > 0$, $Q_{1i} > 0$, $Q_{2i} > 0$, $Z_i > 0$ and the appropriate matrices $M_{1i} > 0$, $M_{2i} > 0$ and $L_i > 0$ such that the following LMIs holds:

$$\widetilde{\Sigma}_3 = \begin{bmatrix} \Sigma_3 & \Theta^T & h\Pi_1^T & \widehat{A}_1 & B_i^T K_i^T \\ * & -\frac{1}{h}Q_{2i}^{-1} & 0 & 0 & 0 \\ * & * & -Q_{2i} & 0 & 0 \\ * & * & * & -I & 0 \\ * & * & * & 0 & -I \end{bmatrix} < 0, \quad (42)$$

$$e^{(\alpha + \frac{\ln \mu}{\tau_a})T} (\beta)c_1 < \lambda_1 c_2. \quad (43)$$

Then, under the following average dwell time scheme

$$\tau_a > \tau_a^* = \frac{T \ln \mu}{\ln(c_2 e^{-\alpha T}) - \ln(\beta)c_1}, \quad (44)$$

the system is finite-time bounded with respect to $(c_1, c_2, T, R, p(t))$, where $\mu > 1$ satisfying

$$P_s < \mu P_i, Q_{1s} < \mu Q_{1i}, Q_{2s} < \mu Q_{2i}, Z_s < \mu Z_i, \quad \forall i, s \in \mathbb{N}. \quad (45)$$

and

$$\Sigma_3 = \begin{bmatrix} \widehat{\Phi}_{11} & \widehat{\Phi}_{12} & 0 & 0 & 0 & 0 & L_i & -B_i \\ * & \widehat{\Phi}_{22} & 0 & 0 & 0 & 0 & -L_i & 0 \\ * & * & \widehat{\Phi}_{33} & 0 & 0 & \widehat{\Phi}_{36} & 0 & 0 \\ * & * & * & \widehat{\Phi}_{44} & \widehat{\Phi}_{45} & 0 & 0 & 0 \\ * & * & * & * & \widehat{\Phi}_{55} & 0 & 0 & 0 \\ * & * & * & * & * & \widehat{\Phi}_{66} & 0 & 0 \\ * & * & * & * & * & * & -\gamma^2 I & 0 \\ * & * & * & * & * & * & 0 & -\epsilon_a B_i \end{bmatrix}$$

$$\begin{aligned} \widehat{\Phi}_{11} &= 2P_i A_i + Q_{1i} + dQ_{3i} + M_{1i} + M_{1i}^T - \alpha P_i, \\ \widehat{\Phi}_{12} &= -A_{di} P_i - M_{1i}^T + M_{2i}, \widehat{\Phi}_{22} = e^{-\alpha h(t)} Q_1 - M_{2i}^T \\ &- M_{2i}, \widehat{\Phi}_{33} = \frac{e^{-\alpha h}}{h} Z_i - \frac{3e^{-\alpha h}}{h} Z_i, \widehat{\Phi}_{36} = \frac{6e^{-\alpha h}}{h^2} Z_i, \\ \widehat{\Phi}_{44} &= \frac{e^{-\alpha h}}{h} Z_i - \frac{3e^{-\alpha h}}{h} Z_i, \widehat{\Phi}_{45} = \frac{6e^{-\alpha h}}{h^2} Z_i, \widehat{\Phi}_{55} = -\frac{12e^{-\alpha h}}{h^3} Z_i, \\ \widehat{\Phi}_{66} &= -\frac{12e^{-\alpha h}}{h^3} Z_i, \\ \Theta &= [A_i Q_{2i} \quad A_{di} Q_{2i} \quad 0 \quad 0 \quad 0 \quad 0 \quad B_{wi} Q_{2i} \quad B_i Q_{2i}], \\ \widehat{\Pi} &= [M_{1i} \quad M_{2i} \quad 0 \quad 0 \quad 0 \quad 0 \quad L_i \quad 0], \\ \widehat{A} &= [C_i \quad C_{di} \quad 0 \quad 0 \quad 0 \quad 0 \quad D_{wi} \quad 0]. \end{aligned}$$

Proof Following the same line of proof as presented in the Theorem 3.3 and applying the Schur complement lemma to equation (33), we can draw a conclusion regarding the behavior of (42). Consequently, we establish that the switching system described in (4) shows finite-time boundedness. As a result, this completes the proof. \square

Remark 3.5: To obtain an optimal finite-time $L_2 - L_\infty$ performance against unknown inputs, the attenuation level γ^2 can be reduced to the minimum possible value such that LMIs (33)-(36) are satisfied with a fixed α . The optimization problem can be described as follows: $\min s.t:$ LMIs (33)-(36) with γ^2

IV. NUMERICAL EXAMPLES

In this section we have given numerical examples to verify the effectiveness of the presented method.

Example 4.1: Water Pollution Control Problem We present the simulation results in this section, based on [40] and [41] first simplifying this water pollution system into a switched linear time-delay one, then providing a switching control method, and finally presenting the simulation results for the system (7) without disturbance. **System Description:** As an

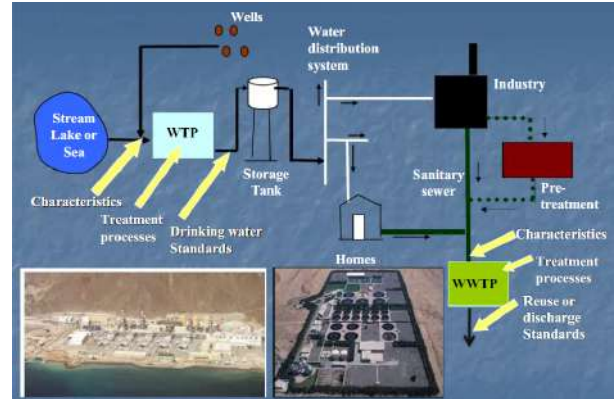


FIGURE 1. Water Pollution Control Problem

example, let us consider an area along a river that has a waste treatment facility at its beginning. At time t , $y(t)$ denotes biochemical oxygen demand (BOD) and $q(t)$ denote dissolved oxygen content in the reach. In this case, we assume constant flow rates and well-mixed water in the reach, and that when the flow enters the reach at instant $t - \tau$, BOD and DO are equal to their previous states [40]. The system dynamics are first described by defining two parameters $\varphi_1 = \frac{Q_E}{v}$ and $\varphi_2 = \frac{Q}{v}$, where Q_E and Q are the effluent flow and stream flow, respectively, and v defines the flow in the reach. By mass balance concentrations, we can obtain the following switched delay-differential equations that govern BOD and DO dynamics (where φ_1 and φ_2 are 0.1 : 0.9 and 0.2 : 0.8, respectively):

$$\begin{aligned} \dot{x}(t) &= A_i x(t) + A_{di} x(t - h(t)) + B_i \text{sat}(u(t)) \\ x(t) &= \phi(t), \quad t \in [-h_M, 0], \end{aligned} \quad (46)$$

where $x = [y(t) - y^*, q(t) - q^*]$, therein z^* and q^* are desired steady-state values of BOD and DO, respectively, and other parameters are listed as follows:

$$\begin{aligned} A_1 &= \begin{bmatrix} -\kappa_{10} - \varphi_1^1 - \varphi_2^1 & 0 \\ -\kappa_{30} & -\kappa_{20} - \varphi_1^1 - \varphi_2^1 \\ -\kappa_{10} - \varphi_1^2 - \varphi_2^2 & 0 \\ -\kappa_{30} & -\kappa_{20} - \varphi_1^2 - \varphi_2^2 \end{bmatrix}, \\ A_{d1} &= \begin{bmatrix} \varphi_2^1 & 0 \\ 0 & \varphi_2^1 \end{bmatrix}, A_{d2} = \begin{bmatrix} \varphi_2^2 & 0 \\ 0 & \varphi_2^2 \end{bmatrix}, \\ B_1 &= \begin{bmatrix} \varphi_1^1 & 0 \\ 0 & 1 \end{bmatrix}, B_2 = \begin{bmatrix} \varphi_1^2 & 0 \\ 0 & 1 \end{bmatrix}. \end{aligned}$$

Based on [40], the following values are chosen for the parameter values: $\varphi_1^1 = 0.1$, $\varphi_1^2 = 0.2$, $\varphi_2^1 = 0.9$, $\varphi_2^2 = 0.8$, $\kappa_{10} =$

1.6, $\kappa_{20} = 1.0, \kappa_{30} = 0.6, z^* = 1.3750, q^{ast} = 6.0, h = 5.2, h_M = 0.5, d = 0.2, T = 5, c_1 = 2.2, \mu = 1.2, \alpha = 0.005$. By solving the LMIs in Theorem 3.1, that the optimal value of c_2 depends on parameter α . By solving the matrix inequalities (8)-(11), we can get the optimal bound of c_2 with different value of α in each subsystems. The smallest bound can be obtained as $c_2 = 4.5651$ when $\alpha = 0.005$ and we obtain feasible solutions as follows:

$$\begin{aligned}
 P_1 &= \begin{bmatrix} 94.7613 & -9.7732 \\ -9.7732 & 79.0008 \end{bmatrix}, Q_{11} = \begin{bmatrix} 5.5558 & -0.5631 \\ -0.5631 & 4.5208 \end{bmatrix} \\
 Q_{21} &= \begin{bmatrix} 1.4102 & -0.1617 \\ -0.1617 & 1.0922 \end{bmatrix}, Z_1 = \begin{bmatrix} 2.6297 & -0.2707 \\ -0.2707 & 2.1399 \end{bmatrix}, \\
 S_1 &= \begin{bmatrix} 29.8679 & -2.9594 \\ -2.9594 & 49.4804 \end{bmatrix}, P_2 = \begin{bmatrix} 78.8410 & -3.6993 \\ -3.6993 & 65.5524 \end{bmatrix}, \\
 Q_{12} &= \begin{bmatrix} 49.4027 & 0.3073 \\ 0.3073 & 40.7624 \end{bmatrix}, Q_{22} = \begin{bmatrix} 7.3744 & -0.6521 \\ -0.6521 & 9.9667 \end{bmatrix}, \\
 Z_2 &= \begin{bmatrix} 48.2782 & 2.3655 \\ 2.3655 & 21.1940 \end{bmatrix}, S_2 = \begin{bmatrix} 38.7956 & -2.8749 \\ -2.8749 & 75.4845 \end{bmatrix}.
 \end{aligned}$$

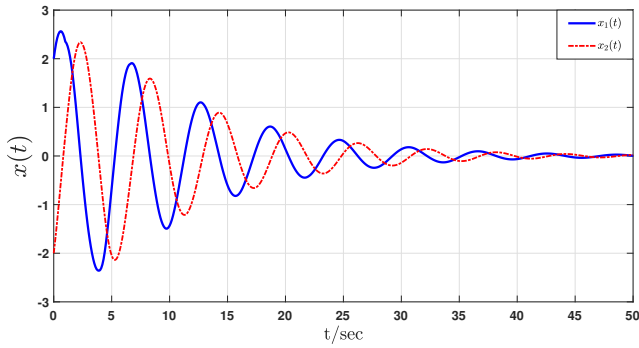


FIGURE 2. State trajectories of the considered model (46) without controller.

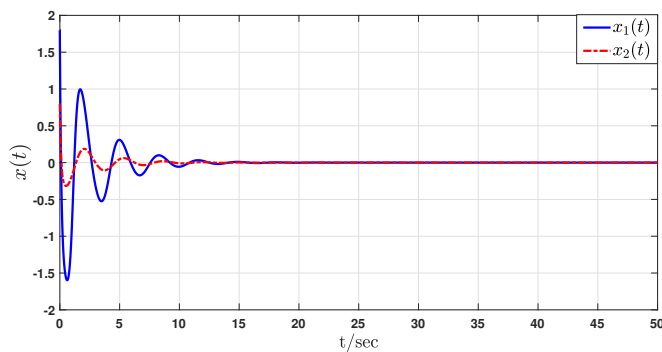


FIGURE 3. State trajectories of the considered model (46) with controller.

As a result of the above control gain matrices and $x(0) = [1.4 \ 2.7]^T$ as the initial value, the simulation results of the state response and control trajectory of the proposed model (46) are plotted in Figs. 1-4. Fig. 1 illustrates the state responses of the system (46) with uncontrolled. As shown in Fig. 2, the proposed control strategy can ensure the finite-time stability of the considered system (46). Fig. 3 shows the trajectory

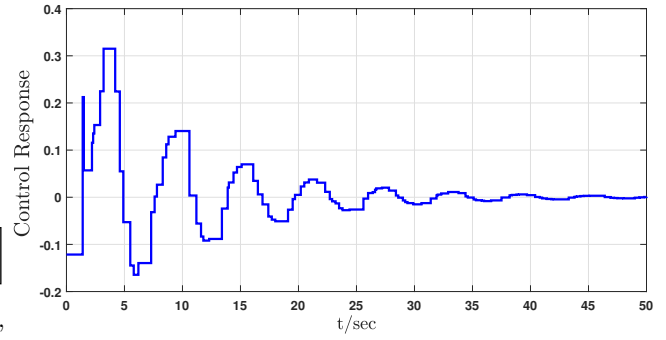


FIGURE 4. Control input response.

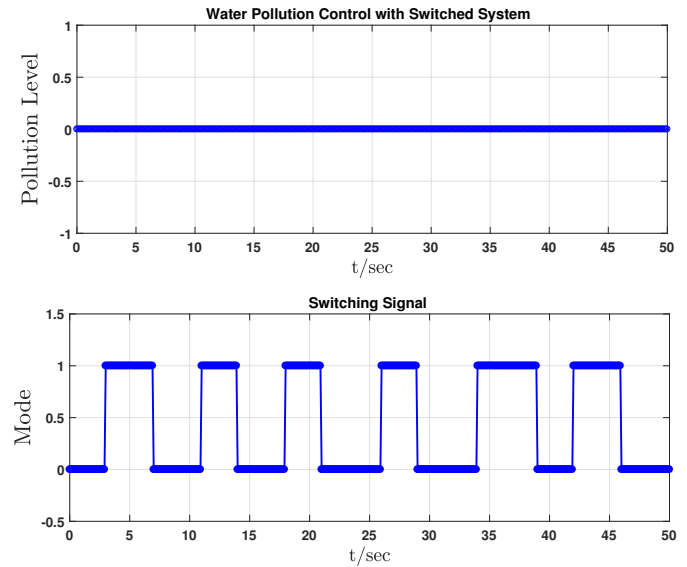


FIGURE 5. Evolution of switching signal.

of the saturated control input. Fig. 4 illustrates the estimate of the switching signal and its water pollution control with switched system. Compared to the existing results [42], Fig. 2 shows that our method provides better robust stability than [42] even when the saturation inputs, and it is obvious that our controller (3) consumes less control energy than the controller in [40], [42]. The asymptotic stability of [42] has been considered in addition to the comparison of the arbitrary switching signal strictness. When switching harshness varies arbitrary, the switched system may become unstable, while the same system can maintain stability when switching harshness is based on dwell time. Despite its random nature and variations in response to industrial discharges, the water pollution model does not have a high-frequency switching signal. For stream water quality control problems, slow switching signals that enforce remaining in subsystems are feasible, and saturation control inputs are practical and progressive. This confirms the superiority of the proposed method.

Remark 4.1: Note that the conditions (9) are dependent on the size of c_2 , then we can also get the optimal lower bound of c_2 to guarantee the finite-time stability by solving a simple optimal problem. For example, we can obtain the optimal lower bound of c_2 is 4.5651.

Example 4.2: Consider the actuator saturation with switched time-delay system (1) and the following parameters: $A_1 = \begin{bmatrix} 2.5 & 0 \\ 0 & 3.5 \end{bmatrix}$, $A_{d1} = \begin{bmatrix} 0.2 & 1.2 \\ -0.5 & 1.2 \end{bmatrix}$, $B_1 = \begin{bmatrix} -0.1 \\ -0.4 \end{bmatrix}$, $B_{w1} = \begin{bmatrix} 2 \\ 0.3 \end{bmatrix}$, $C_1 = \begin{bmatrix} -0.3 & 0.2 \\ 0.3 & -0.03 \end{bmatrix}$, $C_{d1} = \begin{bmatrix} -0.6 & 0.5 \\ 2.1 & 0.1 \end{bmatrix}$, $D_{w1} = \begin{bmatrix} 0.3 \\ 0.1 \end{bmatrix}$, $A_2 = \begin{bmatrix} 3 & 0 \\ 0 & 4 \end{bmatrix}$, $A_{d2} = \begin{bmatrix} 0.1 & -1.1 \\ 0.3 & -0.8 \end{bmatrix}$, $B_2 = \begin{bmatrix} 0.3 \\ -0.1 \end{bmatrix}$, $B_{w2} = \begin{bmatrix} 1 \\ 0.6 \end{bmatrix}$, $C_2 = \begin{bmatrix} -0.4 & 0.1 \\ 0.2 & -0.3 \end{bmatrix}$, $C_{d2} = \begin{bmatrix} -0.8 & 0.4 \\ -2.2 & 0.2 \end{bmatrix}$, $D_{w2} = \begin{bmatrix} 0.5 \\ 0.2 \end{bmatrix}$, $h = 0.7$, $h_M = 1.6$, $d = 0.003$, $T = 5$, $c_1 = 1.4$, $c_2 = 7.9$, $\mu = 1.3$, $\alpha = 0.02$. Solve the LMIs in Theorem 3.4, we obtain the feasible solutions as follows:

$$P_1 = \begin{bmatrix} 91.5023 & 59.5738 \\ 59.5738 & 59.3507 \end{bmatrix}, Q_{11} = \begin{bmatrix} 0.3870 & 0.2811 \\ 0.2811 & 0.2160 \end{bmatrix},$$

$$Q_{21} = \begin{bmatrix} 0.9370 & 0.6525 \\ 0.6525 & 0.5037 \end{bmatrix}, Z_1 = \begin{bmatrix} 17.6717 & 12.4013 \\ 12.4013 & 10.5504 \end{bmatrix},$$

$$P_2 = \begin{bmatrix} 7.9658 & 5.5558 \\ 5.5558 & 4.9213 \end{bmatrix}, Q_{21} = \begin{bmatrix} 29.0450 & 19.9782 \\ 19.9782 & 16.1920 \end{bmatrix},$$

$$Q_{22} = \begin{bmatrix} 0.3624 & 0.2719 \\ 0.2719 & 0.2129 \end{bmatrix}, Z_2 = \begin{bmatrix} 43.0322 & 27.1583 \\ 27.1583 & 28.3567 \end{bmatrix}.$$

We obtained the saturation gain matrices as,

$$K_1 = \begin{bmatrix} -0.1621 & -0.5423 \end{bmatrix}, K_2 = \begin{bmatrix} -1.7542 & -0.2486 \end{bmatrix}.$$

The system is finite time stabilizable with the prescribed $L_2 - L_\infty$ performance $\gamma^2 = 0.6$. Figure 6, Figure 7, Figure 8, and Figure 9 shows the state responses of the system with different initial values.

Remark 4.2: This work addresses the finite-time boundedness of switched time-varying systems with actuator saturation. In contrast to research results on finite-time boundedness in [2], [4], [23], [28]], which investigated switched, filtering, and discrete-time systems respectively, we explore finite-time switched systems with actuator saturation using LMIs and introduce new integral inequalities in this paper. Consequently, the approach presented in this work proves to be more effective while managing the system's complexity. In Table 1, a comparison table with previously published results is presented below.

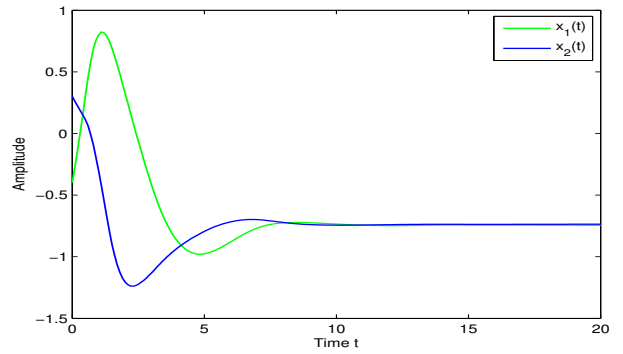


FIGURE 6. State responses of the closed-loop system (1) in Example 4.2.

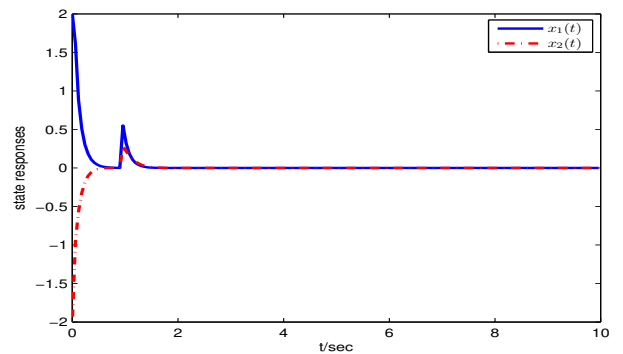


FIGURE 7. State responses of the closed-loop system (1) in Example 4.2.

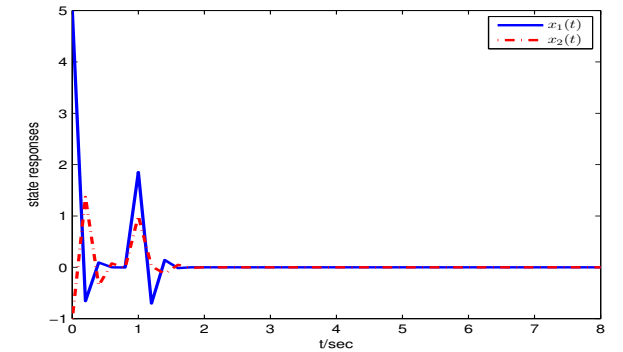


FIGURE 8. State responses of the closed-loop system (1) in Example 4.2.

V. CONCLUSION

In this study, we have investigated the intricate problem of finite-time $L_2 - L_\infty$ control for switched systems with time-varying delays and actuator saturation. Our primary contributions encompass the derivation of a sufficient condition for ensuring the finite-time boundedness of the closed-loop system, achieved through the application of the Lyapunov functional approach. We have demonstrated that the resulting controller can be efficiently obtained using cutting-edge Linear Matrix Inequality techniques. Extensive numerical examples

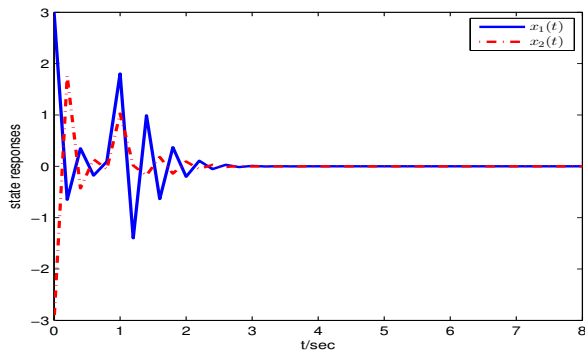


FIGURE 9. State responses of the closed-loop system (1) in Example 4.2.

	[2]	[4]	[28], [23]	[35]	Our Paper
Finite-time	✓	✓	✓	×	✓
Switched	✓	✓	✓	×	✓
$L_2 - L_\infty$	×	×	×	✓	✓
Actuator saturation	×	✓	✓	×	✓

TABLE 1. Comparison with other works.

and simulations have validated the practical effectiveness of our proposed methodology by MATLAB. Looking forward, our research opens avenues for future work, including the extension of our approach to tackle fractional-order systems with distributed delays and the exploration of solutions to address uncertainty mining and control challenges, promising advancements in the field of finite-time control.

ACKNOWLEDGMENT

M. Rhaima was supported by Researchers Supporting Project number (RSPD2023R683) King Saud University, Riyadh, Saudi Arabia. The first author gratefully acknowledge this work is funded by the Centre for Nonlinear Systems, Chennai Institute of Technology (CIT), India, vide funding number CIT/CNS/2023/RP-005.

REFERENCES

[1] M. Xiang, Z. Xiang, Stability, L_1 -gain and control synthesis for positive switched systems with time-varying delay, *Nonlinear Anal.: Hybrid Syst.* **9** (2013) 9-17.
 [2] X. Lin, H. Du, S. Li, Finite-time boundedness and L_2 -gain analysis for switched delay systems with norm-bounded disturbance, *Appl. Math. Comput.* **217** (2014) 5982-5993.
 [3] H. Chen, P. Shi, C.C. Lim, Stability of neutral stochastic switched time delay systems: An average dwell time approach, *Int. J. Robust Nonlinear Control* **27** (2017) 512-532.
 [4] X. Lin, S. Li, Y. Zou, Finite-time stabilization of switched linear time-delay systems with saturating actuators, *Appl. Math. Comput.* **299** (2017) 66-79.
 [5] G. Zong, L. Hou, Y. Wu, Robust $l_2 - l_\infty$ guaranteed cost filtering for uncertain discrete-time switched system with mode-dependent time-varying delays, *Circuits Syst. Signal Process.* **30** (2011) 17-33.
 [6] W. Sun, H. Gao, O. Kaynak, Finite frequency H_∞ control for vehicle active suspension systems, *IEEE Trans. Control Syst. Technol.* **19** (2011) 416-422.
 [7] L. Zhang, H. Gao, Asynchronously switched control of switched linear systems with average dwell time, *Automatica* **46** (2010) 953-958.

[8] X.Q. Zhao, D. Ye, G.X. Zhong, Passivity and passification of switched systems with the persistent dwell time switching, *Nonlinear Anal.-Hybrid Syst.* **34** (2019) 18-29.
 [9] D. Yang, X. Li, J. Qiu, Output tracking control of delayed switched systems via state-dependent switching and dynamic output feedback, *Nonlinear Anal.-Hybrid Syst.* **32** (2019) 294-305.
 [10] H. Chen, P. Shi, C.C. Lim, Stability of neutral stochastic switched time delay systems: An average dwell time approach, *Int. J. Robust Nonlinear Control* **27** (2017) 512-532.
 [11] M. Syed Ali, S. Saravanan, Finite-time stability for memristor based switched neural networks with time-varying delays via average dwell time approach, *Neurocomputing* **275** (2018) 1637-1649.
 [12] Y. Yin, X. Zhao, X. Zheng, New stability and stabilization conditions of switched systems with mode-dependent average dwell time, *Circuits Syst. Signal Process.* **36** (2017) 82-98.
 [13] X. Zhang, C. Su, Stability analysis and antiwindup design of switched linear systems with actuator saturation, *Automatica* **16** (2018) 1247-1253.
 [14] W. Qi, Y. Kao, X. Gao, Y. Wei, Controller design for time-delay system with stochastic disturbance and actuator saturation via a new criterion, *Appl. Math. Comput.* **320** (2018) 535-546.
 [15] S. Saravanan, R. Vadivel, N. Gunasekaran, Finite-Time Synchronization of Quantized Markovian-Jump Time-Varying Delayed Neural Networks via an Event-Triggered Control Scheme under Actuator Saturation, *Mathematics* **11** (2023) 2257.
 [16] H. Yang, P. Shi, Z. Li and C. Hua, Analysis and design for delta operator systems with actuator saturation, *Int. J. control* **87** (2014) 987-999.
 [17] H. Yang, Z. Li, C. Hua and Z. Liu, Stability analysis of delta operator systems with actuator saturation by a saturation-dependent Lyapunov function, *Circuits Syst. Signal Process.* **34** (2015) 971-986.
 [18] W. Guan, F. Liu, Finite-time H_∞ memory state feedback control for uncertain singular TS fuzzy time-delay system under actuator saturation, *Adv. Differ. Equ.* **2016** (2016) Article no. 52.
 [19] Y. Ma, P. Yang, Y. Yan, Q. Zhang, Robust observer-based passive control for uncertain singular time-delay systems subject to actuator saturation, *ISA Trans.* **67** (2017) 9-18.
 [20] L. Fu, Y. Ma, Passive control for singular time-delay system with actuator saturation, *Appl. Math. Comput.* **289** (2016) 181-193.
 [21] W. Qi, X. Gao, Robust H_∞ control for stochastic time-delayed Markovian switching systems under partly known transition rates and actuator saturation via anti-windup design *Optim. Control Appl. Methods* **37** (2016) 608-626.
 [22] J. Lian, X. Wang, Exponential stabilization of singularly perturbed switched systems subject to actuator saturation *Inform. Sci.* **320** (2015) 235-243.
 [23] Y. Ma, L. Fu, Finite time H_∞ control for discrete-time switched singular time-delay systems subject to actuator saturation via static output feedback *Int. J. Syst. Sci.* **47** (2016) 3394-3408.
 [24] F. Amato, M. Ariola, C. Cosentino, Finite-time stabilization via dynamic output feedback, *Automatica* **42** (2008) 337-342.
 [25] F. Amato, M. Ariola, C. Cosentino, Finite-time control of linear stochastic systems, *Int. J. Innov. Comput. Inform. Cont.* **4** (2008) 687-694.
 [26] F. Amato, M. Ariola, C. Cosentino, Robust finite-time stability of impulsive dynamical linear systems subject to norm-bounded uncertainties, *Int. J. Robust Nonlin. Control* **21** (2011) 1080-1093.
 [27] M. Syed Ali, S. Saravanan, Robust finite-time H_∞ control for a class of uncertain switched neural networks of neutral-type with distributed time varying delays, *Neurocomputing* **177** (2016) 454-468.
 [28] J. Cheng, H. Zhu, S. Zhong, F. Zheng, Y. Zeng, Finite-time filtering for switched linear systems with a mode-dependent average dwell time, *Nonlinear Anal.-Hybrid Syst.* **15** (2015) 145-156.
 [29] H. Zhou, S. Sui, and S. Tong, Fuzzy Adaptive Finite-Time Consensus Control for High-Order Nonlinear Multiagent Systems Based on Event-Triggered, *IEEE Transactions on Fuzzy Systems*, **30** (2022) 4891-4904.
 [30] W. Qi, C. Zhang, G. Zong, S.-F. Su, and M. Chadli, Finite-Time Event-Triggered Stabilization for Discrete-Time Fuzzy Markov Jump Singularly Perturbed Systems, *IEEE Transactions on Cybernetics*, **53** (2023) 4511-4520.
 [31] Y. Li, Y.-X. Li, and S. Tong, Event-Based Finite-Time Control for Nonlinear Multiagent Systems With Asymptotic Tracking," *IEEE Transactions on Automatic Control*, **68** (2023) 3790-3797.
 [32] R. Kavikumar, R. Sakthivel, O.M. Kwon, B. Kaviarasan, Finite-Time boundedness of interval type-2 Fuzzy systems with time delay and actuator faults, *Journal of the Franklin Institute* **356** (2019) 8296-8324.

- [33] A. Seuret, F. Gouaisbaut, Wirtinger-based integral inequality: Application to time-delay systems, *Automatica* **49** (2013) 2860-2866.
- [34] X. M. Sun, J. Zhao, D. J. Hill, Stability and L_2 -gain analysis for switched delay systems: A delay-dependent method, *Automatica* **42** (2006) 1769-1774.
- [35] S. He, F. Liu, $L_2 - L_\infty$ fuzzy control for Markov jump systems with neutral time-delays, *Math. Comput. Simul.* **92** (2013) 1-13.
- [36] T. Hu, Z. Lin, B. Chen, An analysis and design method for linear systems subject to actuator saturation and disturbance, *Automatica* **38** (2002) 351-359.
- [37] K. Gu, V. L. Kharitonov, J. Chen, *Stability of time delay systems*, Birkhuser, Boston, 2003.
- [38] O.M. Kwon, Ju H. Park, S.M. Lee, Augmented Lyapunov functional approach to stability of uncertain neutral systems with time-varying delays, *Appl. Math. Comput.* **207** (2009) 202-212.
- [39] J. Song, S. He, Nonfragile robust finite-time $L_2 - L_\infty$ controller Design for a class of uncertain Lipschitz nonlinear systems with time-delays, *Appl. Math. Comput.* (2013) 265473.
- [40] Y. Jin, Y. Zhang, Y. Jing and J. Fu, An average dwell-time method for fault-tolerant control of switched time-delay systems and its application, *IEEE Transactions on Industrial Electronics* **66** (2019) 3139-3147.
- [41] H. Sobhanipour and B. Rezaie, Enhanced exponential stability analysis for switched linear time-varying delay systems under admissible edge-dependent average dwell-time strategy, *IEEE Transactions on Systems, Man, and Cybernetics: Systems* **53** (2023) 5331-5342.
- [42] R. Ma, M. Ma, J. Li, J. Fu, C. Wu, Standard H_∞ performance of switched delay systems under minimum dwell time switching, *Journal of the Franklin Institute* **356** (2019) 3443-3456.



M. SYED ALI graduated from the Department of Mathematics of Gobi Arts and Science College affiliated to Bharathiar University, Coimbatore in 2002. He received his post-graduation in Mathematics from Sri Ramakrishna Mission Vidyalaya College of Arts and Science affiliated to Bharathiar University, Coimbatore, Tamil Nadu, India, in 2005. He was awarded Master of Philosophy in 2006 in the field of Mathematics with specialized area of Numerical Analysis from Gandhigram Rural University Gandhigram, India. He was conferred with Doctor of Philosophy in 2010 in the field of Mathematics specialized in the area of Fuzzy Neural Networks in Gandhigram Rural University, Gandhigram, India. He was selected as a Post-Doctoral Fellow in the year 2010 for promoting his research in the field of Mathematics at Bharathidasan University, Trichy, Tamil Nadu and also worked there from November 2010 to February 2011. Since March 2011 he is working as an Assistant Professor in Department of Mathematics, Thiruvalluvar University, Vellore, Tamil Nadu, India. He was awarded Young Scientist Award 2016 by The Academy of Sciences, Chennai. He has published more than 230 research papers in various SCI and Scopus indexed journals holding impact factors. He has also published research articles in national journals and international conference proceedings. He also serves as a reviewer for several SCI journals. His research interests include stochastic differential equations, dynamical systems, fuzzy neural networks, complex networks and cryptography.



G. NARAYANAN received the Ph.D. degree in mathematics from Thiruvalluvar University, Vellore, India, in 2022. He was a Research Faculty with Center for Nonlinear Systems, at Chennai Institute of Technology, Chennai, India. He is currently a Postdoctoral Research Fellow with the Research Center of Wind Energy Systems, Kunsan National University, Gunsan-si, South Korea. His current research interests include fractional-order nonlinear systems, wind turbine system and multi-agent networked systems.



SARAVANAN SHANMUGAM was born in 1990. He received the bachelor degree from Department of Mathematics, Government arts college Thiruvannamalai, affiliated to Thiruvalluvar University, Vellore, Tamil Nadu, India, in 2011. He post-graduated in Mathematics from Madras Christian College, University of Madras, Chennai, Tamil Nadu, India, in 2013. He received Doctor of Philosophy in Mathematics from Thiruvalluvar University, Vellore, Tamil Nadu, India, in 2018. He worked as a Visiting Research Fellow in Department of Industrial Engineering, Pusan National University, Busan, Korea during January 2018 to July 2018, he worked as a PNU Post-Doctoral Research Fellow in School of Mechanical Engineering, Pusan National University, Busan, Korea. Currently he is working in Centre for Nonlinear Systems, Chennai Institute of Technology, Chennai, India. He serves as a reviewer for various SCI journals. His current research interests finite-time control of time-delay system, stochastic stability, nonlinear systems, Markovian jump systems, H_∞ control and Multi-agent systems.



MOHAMED RHAIMA was born in 1984. He received his MSc degree in Mathematics from the Faculty of Sciences of Tunis, Tunisia, in 2012. He received his PhD in Mathematics from the University of Tunis El Manar, Tunisia and Tor Vergata University, Rome-Italy, in 2017. His research interests include nonlinear stochastic control systems, nonlinear stochastic dynamical systems, stochastic fractional-order systems and stochastic delay systems.

...

H_∞ control for discrete-time IT2 fuzzy system with infinite distributed-delay via adaptive event-triggered scheme and its application

M. Syed Ali¹, M. Mubeen Tajudeen², G. Rajchakit³ and A. Jirawattanapanit⁴

^{1,2}Complex Systems and Networked Science Research Laboratory, Department of Mathematics, Thiruvalluvar University, Vellore-632115, Tamil Nadu, India.

³Department of Mathematics, Faculty of Science, Maejo University, Chiang Mai 50290, Thailand.

⁴Department of Mathematics, Faculty of Science, Phuket Rajabhat University (PKRU), 6 Thekasattree Road, Raddasa, Phuket 83000, Thailand.

syedgru@gmail.com, mubeentajudeen19@gmail.com, kreangkri@mju.ac.th, anuwat.j@pkru.ac.th

Abstract

This article investigates the H_∞ control problem for discrete-time interval type-2 (IT2) fuzzy systems with infinite distributed delay via an adaptive event-triggered scheme. The IT2 T-S fuzzy system, which is a development over the (type-1) T-S fuzzy system, has greater effectiveness for the expression of system uncertainty, which will improve the difficulty of analysis. Our main goal is to make more efficient use of network resources by developing an adaptive event-triggered controller for interval type-2 fuzzy systems. In contrast to the traditional triggering method, an adaptive event-triggered technique is proposed to improve bandwidth consumption and network control performance. The triggering function's parameters are based on an adaptive law. Moreover, employing the Lyapunov functional method, the resultant criterion gives sufficient conditions to guarantee that discrete time IT2 fuzzy systems are mean-square exponentially stable with a H_∞ performance. Finally, a single-link robot arm model and a DC motor are employed to show the usefulness and efficiency of the obtained theoretical results.

Keywords: Adaptive event-triggered scheme, infinite-distributed delay, discrete-time IT2 fuzzy system.

1 Introduction

The Takagi-Sugeno(T-S) fuzzy model has been demonstrated in engineering applications and theoretical research fields to better deal with the nonlinearity of the system [2]. The T-S fuzzy model has received extensive attention from researchers in sliding mode control design, output feedback control, event-triggered control, and so on [13, 24, 25]. Due to its uniform approximation property, this model can be transformed into a linear system with a few local subsystems. The type-1 T-S model has been proven to be an effective tool for analyzing nonlinear systems by converting them into some sub-local linear systems with weighting summation. The parameter uncertainties in the membership functions, which are present in every practical application, cannot be handled by type-1 fuzzy systems [7]. Also, with the IT2 fuzzy system, the parameter uncertainties can be effectively extracted by the following bounds, that is, by the bounds of the upper member function and the lower member function. The T-S fuzzy system was proposed to describe such systems in [34] where there are unclear parameters in discrete-time systems. In fact, IT2 fuzzy systems are usually preferred due to their easy design and beneficial applicability to larger networks. It has been demonstrated that IT2 T-S fuzzy systems are superior in various fields compared to type-1 T-S fuzzy models [22]. Recently, dwell-time-dependent H_∞ bumpless transfer control for discrete-time switched interval type-2 fuzzy systems described in [33]. The IT2 fuzzy model has attracted a lot of interest from researchers in recent years [10, 35]. The sliding mode control problem of discrete-time IT2 Markov jump systems subject to external disturbances and time-varying delays is described in [18].

Discrete-time systems have a strong tradition in engineering applications. The study of time-delay systems stability analysis and controller design has become a popular research topic in recent years, with a number of famous results

being reported [5, 20, 27, 37]. Recent developments in discrete-time delay state systems involve tighter sum over bounds Wirtinger's inequality, resulting in less conservative analysis requirements. Synchronization and state estimation for discrete-time complex networks with distributed delays is studied in [14]. Quantized static output feedback control for discrete-time systems. The $l_2 - l_\infty$ control of discrete-time with randomly occurring delays via IT2 fuzzy model [36]. Time delay fuzzy system have been effectively employed in a wide range of domains, including system identification, modeling chemical plants and other industrial processes [12, 21, 30, 31]. The delay-dependent reliable control problem for discrete-time systems with H_∞ are discussed by many researchers [15, 19].

Event-triggered control (ETC) techniques are thought to be a good way to save communication resources. When compared to a traditional sampled-data control, an event-triggered control can help reduce the number of control tasks [9, 23, 29]. A number of control strategies are based on an event-triggered scheme as discussed in [1, 6]. However, the event-triggered scheme greatly aids in more efficient utilisation of network resources and decreases the transmission load of the broadband network, and many successful results have been attained. It has a wide range of applications since it is inspired by the event-triggered scheme [4]. Traditional ETC for nonlinear systems was developed into adaptive event-triggered control. In recent years, the literature has described a variety of event-triggered methods as an alternative methodology for reducing communication resources, one of which is event-triggered control (ETC) in [28]. Further, a new ETS with an adaptive law was proposed to reduce the use of communication resources, and it is utilised to address the challenging issue of fuzzy network systems in [26]. Some recent results about AETS is described in [11, 16, 17, 32]. H_∞ control problem for networked control system via AETS discussed in [26]. Resilient adaptive event-triggered fuzzy tracking control and filtering discussed in [3]. It is essential to develop a more effective AETS for discrete-time IT2 T-S fuzzy systems in light of the aforementioned concerns.

The goal of this research work is to develop a H_∞ control structure for discrete-time IT2 fuzzy systems via adaptive event-triggered scheme in order to increase effective communication while maintaining desirable control performance. The below are the major contributions:

- (1) We focus on the H_∞ control problem for the discrete-time IT2 fuzzy system with infinite distributed delay via adaptive event-triggered scheme.
- (2) In contrast to traditional triggering scheme, the adaptive event-triggered scheme is proposed to reduce energy consumption. Furthermore, we verify that this adaptive event-triggered scheme has no Zeno behaviour associated with it.
- (3) This study is distinct from previous work [7, 34], since it is the first to describe an IT2 fuzzy system with infinite distributed delay.
- (4) The fundamental aim is to create an adaptive event-triggered control and it ensure exponentially mean-square stable with H_∞ performance index.
- (5) The numerical results include a single-link robot arm model and a DC motor are employed to show the usefulness and efficiency of the obtained theoretical results.

Notations: In this study, \mathbb{R}^n denotes n -dimensional real vector space. The transpose of vector A is A^T . The space of summable sequences over $[0, \infty)$ is denoted as $l_2[0, \infty)$. Set of positive reals are denoted as $\mathbb{R}_{\geq 0}$. To establish symmetric structure, the symbol $*$ will be employed in matrix expressions. $n \times n$ identity matrix is denoted by I_n . $\mathbb{E}(x)$ represents the mathematical expectation of x . $\|\cdot\|$ denotes the Euclidean norm for vectors.

2 Preliminaries

2.1 System description:

The IT2 T-S fuzzy model can be used to estimate a class of nonlinear plants that are uncertain. Consider the discrete-time IT2 T-S fuzzy system is described as follows.

Plant Rule i: IF $g_1(\varpi(\varphi))$ is G_1^i and ... and $g_r(\varpi(\varphi))$ is G_r^i , THEN

$$\begin{cases} \varpi(\varphi + 1) &= A_i \varpi(\varphi) + A_{i1} \sum_{d=1}^{\infty} \lambda_d \varpi(\varphi - d) + B_{1i} w(\varphi) + C_{1i} u(\varphi), \\ z(\varphi) &= D_i \varpi(\varphi) + B_{2i} w(\varphi) + C_{2i} u(\varphi), \\ \varpi(\varphi) &= \theta(\varphi), \quad \varphi \in \mathcal{Z}^-. \end{cases} \quad (1)$$

where $G_{\bar{r}}^i$ ($\bar{r} = 1, 2, \dots, r$) and $g(\varpi(\varphi)) = [g_1(\varpi(\varphi)), g_2(\varpi(\varphi)), \dots, g_r(\varpi(\varphi))]$ denotes fuzzy sets and premise variables, respectively. The scalar q is the number of IF-THEN rules of the system. $u(\varphi) \in \mathcal{R}^m$ is the controlled input vector, $\phi(\varphi)$ is the initial state vector, $w(\varphi) \in \mathcal{R}^p$ is the disturbance input vector, $z(\varphi) \in \mathcal{R}^s$ is the output vector, which is unknown

but that belongs to $l_2[0, \infty)$ and $\varpi(\varphi) \in \mathcal{R}^n$ is the state vector. Constant matrices are $A_i, A_{li}, B_{1i}, B_{2i}, C_{1i}, C_{2i}, D_{1i}$. The constants $\lambda_d \geq 0, (d = 1, 2, \dots)$ satisfies the converging condition given below [27]:

$$\bar{\lambda} = \sum_{d=1}^{\infty} \lambda_d < \infty, \quad \sum_{d=1}^{\infty} d\lambda_d < \infty. \quad (2)$$

Remark 2.1. In system (1), the term $\sum_{d=1}^{\infty} \lambda_d \varpi(\varphi - d)$ represents the infinite distributed delay in discrete-time model [23], which is equivalent to the infinite-distributed delay $\int_{-\infty}^t \varphi(t - g) dg$ in continuous time system. The convergent condition (2) guarantees the fuzzy Lyapunov functional (to be developed later) convergent and $\int_{d=1}^{\infty} \lambda_d \varpi(\varphi - d)$ is ensured, which is necessary for the system's stability.

The interval firing strength corresponding to i th plant rule is represented as follows:

$$\Omega_i(\varpi(\varphi)) = [\underline{\alpha}_i(\varpi(\varphi)), \bar{\alpha}_i(\varpi(\varphi))], \quad (3)$$

where $\bar{\alpha}_i(\varpi(\varphi))$ and $\underline{\alpha}_i(\varpi(\varphi))$ the denote the upper and lower firing strengths,

$$\bar{\alpha}_i(\varpi(\varphi)) = \prod_{m=1}^r \bar{\varphi}_{G_{im}}(g_m(\varpi(\varphi))) \geq 0, \quad (4)$$

$$\underline{\alpha}_i(\varpi(\varphi)) = \prod_{m=1}^r \underline{\varphi}_{G_{im}}(g_m(\varpi(\varphi))) \geq 0. \quad (5)$$

where $\bar{\varphi}_{G_{im}}(g_m(\varpi(\varphi))) \in [0, 1]$ and $\underline{\varphi}_{G_{im}}(g_m(\varpi(\varphi))) \in [0, 1]$ are represent the upper and lower grade memberships of $(g_m(\varpi(\varphi)))$, respectively. $\bar{\varphi}_{G_{im}}(g_m(\varpi(\varphi))) \geq \underline{\varphi}_{G_{im}}(g_m(\varpi(\varphi))) \geq 0$ and $\bar{\alpha}_i(\varpi(\varphi)) \geq \underline{\alpha}_i(\varpi(\varphi)) \geq 0$.

The global model of system (1) is described as,

$$\begin{cases} \varpi(\varphi + 1) &= \sum_{i=1}^q \alpha_i(\varpi(\varphi)) [A_i \varpi(\varphi) + A_{li} \sum_{d=1}^{\infty} \lambda_d \varpi(\varphi - d) + B_{1i} w(\varphi) + C_{1i} u(\varphi)], \\ z(\varphi) &= \sum_{i=1}^q \alpha_i(\varpi(\varphi)) [D_i \varpi(\varphi) + B_{2i} w(\varphi) + C_{2i} u(\varphi)]. \end{cases} \quad (6)$$

The variable $\alpha_i(\varpi(\varphi))$ is the membership of the plant and satisfy $\sum_{i=1}^q \alpha_i(\varpi(\varphi)) = 1$, and $\alpha_i(\varpi(\varphi)) = \frac{\tilde{\alpha}_i(\varpi(\varphi))}{\sum_{\varepsilon=1}^q \tilde{\alpha}_\varepsilon(\varpi(\varphi))} \geq 0$ with $\tilde{\alpha}_i(\varpi(\varphi)) = \underline{\pi}_i(\varpi(\varphi)) \underline{\alpha}_i(\varpi(\varphi)) + \bar{\pi}_i(\varpi(\varphi)) \bar{\alpha}_i(\varpi(\varphi)) \geq 0$. $\underline{\pi}_i(\varpi(\varphi))$ and $\bar{\pi}_i(\varpi(\varphi))$ denote non-linear weighting functions and satisfy $\bar{\pi}_i(\varpi(\varphi)) + \underline{\pi}_i(\varpi(\varphi)) = 1$, $0 \leq \underline{\pi}_i(\varpi(\varphi)) \leq 1$ and $0 \leq \bar{\pi}_i(\varpi(\varphi)) \leq 1$.

Remark 2.2. In recent years, research on type-2 fuzzy systems has attracted a lot of attention [10, 35]. The non-linearities but not the uncertainties can be efficiently captured by type-1 fuzzy sets. The Type-2 fuzzy model handles uncertainty well, in contrast to the conventional T-S fuzzy model. The generalized type-2 fuzzy set can be computed more quickly using the IT2 fuzzy set while still having the additional benefit of being able to handle uncertainty with simplicity.

2.2 Adaptive event-triggered scheme:

An adaptive event-triggered scheme (AETS) introduced between the sensor and the controller to reduce effectively the communication burden of the shared network. $\varphi_l^i h (l = 0, 1, 2, \dots)$, where h is the sampling period, φ_l^i is non-negative integer. The initial instant is $\varphi_0^i h = 0$.

The mathematical model of the adaptive event-triggered law is written as follows

$$e_i^T(\varphi) \Theta e_i(\varphi) \leq \gamma_i(t) \varpi_i^T((\varphi_l^i + j)h) \Theta \varpi_i((\varphi_l^i + j)h), \quad (7)$$

where $e_i(\varphi) = \varpi_i(\varphi_l^i h) - \varpi_i((\varphi_l^i + j)h)$, $\Theta > 0$ is the parameter of adaptive event-triggered scheme to be determined, and $\gamma_i(\varphi)$ satisfies the following condition.

$$\gamma_i(\varphi) = \frac{\theta_i}{\gamma_i(\varphi)} \left[\frac{1}{\gamma_i(\varphi)} - \vartheta_i(\varphi) \right] e_i^T(\varphi) \Theta e_i(\varphi), \quad (8)$$

where $0 \leq \gamma_i(\varphi) < 1, \vartheta_i > 0, \theta_i > 0$.

Thus, based on the triggering law (8), the next released instant can be determined by the following expression.

$$\varphi_{l+1}^i h = \varphi_l^i h + \min\{jh | e_i^T(t) \Theta e_i(t) > \gamma_i(\varphi) \varpi_i^T((\varphi_l^i + j)h) \Theta \varpi_i((\varphi_l^i + j)h)\}. \quad (9)$$

It is unavoidable that the occurrence of communication delay when signals are transmitted in the network channels. One can assume that the delay is expressed by ι_i^i , where $\iota_i^i \in [0, \iota_M^i]$, then the time φ of the transmitted data arriving at controller satisfies $\varphi \in [\varphi_i^i + \iota_i^i, \varphi_{i+1}^i h + \iota_{k+1}^i]$.

Defining $\iota_i(\varphi) = \varphi - \varphi_{i+1}^i$, $\varphi \in [\varphi_i^i + \iota_i^i, \varphi_{i+1}^i h + \iota_{k+1}^i]$, the actual sensor measurement error $\bar{\omega}_i(\varphi)$ can be written as

$$\bar{\omega}(\varphi) = \varpi(\varphi_i^i h) = \varpi(\varphi - \iota(\varphi)) + e(\varphi). \quad (10)$$

Remark 2.3. Different from traditional event-triggered scheme [6, 9], the adaptive event-triggered scheme is introduced. According to equation (8) using the dynamically adjusted threshold $\gamma_i(\varphi)$ and reducing the number of unnecessary data packet transmissions is possible using the event generator with adaptive law. In (8), when the parameter $\vartheta_i(\varphi) = \frac{1}{\gamma(0)}$, one can get the adaptive event-triggered law $\dot{\gamma}(\varphi) = 0$. That indicates that the proposed AETS will become a standard time-triggered strategy. The adaptation law $\gamma(\varphi) \rightarrow 0$ indicates that the threshold of AETS does not need adjustment if the system gradually obtains stability.

2.3 Controller design:

The design interval type-2 fuzzy controller with mismatched premises can improve design flexibility against deception attacks.

The fuzzy control law is considered as follows:

Controller Rule j: IF $f_1(\varpi(\varphi))$ is F_1^j and $f_2(\varpi(\varphi))$ is F_2^j and $\dots, f_s(\varpi(\varphi))$ is F_s^j , THEN

$$u(\varphi) = K_j \bar{\omega}(\varphi), \quad (j = 1, \dots, q) \quad (11)$$

where F_s^j ($s = 1, 2, \dots, s$) and $f(\varpi(\varphi)) = [f_1(\varpi(\varphi)), f_2(\varpi(\varphi)), \dots, f_s(\varpi(\varphi))]$ denotes the related fuzzy set and premise variables, respectively. The scalar q is the number of IF-THEN rules of the system. K_j are controller gains to be designed, $\bar{\omega}(\nu)$ is the signals transmitted through the network to the controller.

The interval firing strength corresponding to j th plant rule is represented as,

$$\Gamma_i(\varpi(\varphi)) = [\underline{\beta}_i(\varpi(\varphi)), \bar{\beta}_i(\varpi(\varphi))], \quad (12)$$

where $\bar{\beta}_j(\varpi(\varphi))$ and $\underline{\beta}_j(\varpi(\varphi))$ are denotes the upper and lower firing strengths,

$$\bar{\beta}_j(\varpi(\varphi)) = \prod_{n=1}^s \bar{\varphi}_{F_{j_n}}(f_n(\varpi(\varphi))) \geq 0, \quad (13)$$

$$\underline{\beta}_j(\varpi(\varphi)) = \prod_{n=1}^s \underline{\varphi}_{F_{j_n}}(f_n(\varpi(\varphi))) \geq 0. \quad (14)$$

where $\bar{\varphi}_{F_{j_n}}(f_n(\varpi(\varphi))) \in [0, 1]$ and $\underline{\varphi}_{F_{j_n}}(f_n(\varpi(\varphi))) \in [0, 1]$ are represent the upper and lower grade memberships of $(f_n(\varpi(\varphi)))$, respectively. $\bar{\varphi}_{F_{j_n}}(f_n(\varpi(\varphi))) \geq \underline{\varphi}_{F_{j_n}}(f_n(\varpi(\varphi))) \geq 0$ and $\bar{\beta}_j(\varpi(\varphi)) \geq \underline{\beta}_j(\varpi(\varphi)) \geq 0$.

Based on fuzzy reasoning process, the over all controller is derived as:

$$u(\varphi) = \sum_{j=1}^q \beta_j(\varpi(\varphi)) K_j \bar{\omega}(\varphi), \quad (15)$$

where $\beta_j(\varpi(\varphi))$ represent the grade membership and satisfy $\sum_{j=1}^q \beta_j(\varpi(\varphi)) = 1$ and $\beta_j(\varpi(\varphi)) = \frac{\bar{\beta}_j(\varpi(\varphi))}{\sum_{\epsilon=1}^q \bar{\beta}_\epsilon(\varpi(\varphi))}$ with $\bar{\beta}_j(\varpi(\varphi)) = \underline{\nu}_j(\varpi(\varphi)) \underline{\beta}_j(\varpi(\varphi)) + \bar{\nu}_j(\varpi(\varphi)) \bar{\beta}_j(\varpi(\varphi)) \geq 0$. $\underline{\nu}_j(\varpi(\varphi))$ and $\bar{\nu}_j(\varpi(\varphi))$ denote non-linear weighting functions and satisfy $\bar{\nu}_j(\varpi(\varphi)) + \underline{\nu}_j(\varpi(\varphi)) = 1$, $0 \leq \underline{\nu}_j(\varpi(\varphi)) \leq 1$ and $0 \leq \bar{\nu}_j(\varpi(\varphi)) \leq 1$.

Substituting (15) into (10), the control input is described as follows:

$$u(\varphi) = \sum_{j=1}^q \beta_j(\varpi(\varphi)) K_j [\varpi(\varphi - \iota(\varphi)) + e(\varphi)]. \quad (16)$$

Based on the above discussions, by using (6) and (16), the closed-loop discrete-time IT2 fuzzy systems is formulated as follows:

$$\begin{cases} \varpi(\varphi + 1) &= \sum_{i=1}^q \sum_{j=1}^q \alpha_i \beta_j \{ A_i \varpi(\varphi) + A_{i\epsilon} \sum_{d=1}^{\infty} \lambda_d \varpi(\varphi - d) + B_{1i} w(\varphi) + C_{1i} K_j [e(\varphi) \\ &\quad + \varpi(\varphi - \iota(\varphi))] \}, \\ z(\varphi) &= \sum_{i=1}^q \sum_{j=1}^q \alpha_i \beta_j \{ D_i \varpi(\varphi) + B_{2i} w(\varphi) + C_{2i} K_j [\varpi(\varphi - \iota(\varphi)) + e(\varphi)] \}. \end{cases} \quad (17)$$

Let $A = \sum_{i=1}^q \alpha_i A_i$, $A_\iota = \sum_{i=1}^q \alpha_i A_{\iota i}$, $B_1 = \sum_{i=1}^q \alpha_i B_{1i}$, $B_2 = \sum_{i=1}^q \alpha_i B_{2i}$, $C_1 = \sum_{i=1}^q \sum_{j=1}^q \alpha_i \beta_j C_{1ij}$, and

$$C_2 = \sum_{i=1}^q \sum_{j=1}^q \alpha_i \beta_j C_{2ij}.$$

The equation (17) can be written in compact form as

$$\begin{cases} \varpi(\varphi + 1) &= A\varpi(\varphi) + A_\iota \sum_{d=1}^{\infty} \lambda_d \varpi(\varphi - d) + B_1 w(\varphi) + C_1 K_j [e(\varphi) + \varpi(\varphi - \iota(\varphi))], \\ z(\varphi) &= D\varpi(\varphi) + B_2 w(\varphi) + C_2 K_j [\varpi(\varphi - \iota(\varphi)) + e(\varphi)]. \end{cases} \quad (18)$$

Definition 2.4. [27] *In the mean square sense, the system (10) is considered to be exponentially stable, with initial condition $\psi(\varphi) = 0$, if there exist constants α and β with, $\alpha > 0$ and $0 < \beta < 1$, such that*

$$\|\varpi(\varphi)\|^2 < \alpha \beta^\varphi \sup_{s \in \mathcal{Z}^-} \|\psi(s)\|^2. \quad (19)$$

Definition 2.5. [27] *The system (10) with $w(\varphi) = 0$ is said to be exponentially mean-square stable. If for a given disturbance attention level $\delta > 0$, then the system (10) is said to be exponentially mean-square stable with H_∞ performance δ and under zero initial condition,*

$$\sum_{\varphi=0}^{\infty} \|z(\varphi)\|^2 < \delta^2 \sum_{\varphi=0}^{\infty} \|w(\varphi)\|^2, \quad (20)$$

is satisfied and $\omega(\varphi) \in l_2[0, +\infty)$.

Lemma 2.6. [14] *For any matrix $M > 0$, vectors $\varpi_i \in \mathcal{R}^n$ and scalar constants $a_i (i = 1, 2, \dots)$ if the series concerned are convergent, then the following inequality holds:*

$$\left(\sum_{i=1}^{\infty} a_i \varpi_i \right)^T M \left(\sum_{i=1}^{\infty} a_i \varpi_i \right) \leq \left(\sum_{i=1}^{\infty} a_i \right) \sum_{i=1}^{\infty} a_i \varpi_i^T M \varpi_i.$$

Lemma 2.7. [20] (Schur Complement) *Given constant matrices S_1, S_2, S_3 , where $S_1 = S_1^T$ and $S_3 < 0$, then $S_1 - S_2 S_3^{-1} S_2^T < 0$ if and only if*

$$\begin{bmatrix} S_1 & S_2 \\ S_2^T & S_3 \end{bmatrix} < 0.$$

Lemma 2.8. [15] *For any positive symmetric constant matrix $\mathcal{R} \in \mathbb{R}^{n \times n}$. ι_m, ι_M are any scalar which satisfies the condition $\iota_m \leq \iota_M$. The vector valued function $\xi(\varphi) = \eta(\varphi + 1) - \eta(\varphi)$, we have*

$$\begin{aligned} - \sum_{i=\varphi-\iota_M}^{\varphi-\iota_m-1} \xi^T(i) \mathcal{R} \xi(i) &\leq - \frac{1}{\iota_M - \iota_m} \sum_{i=\varphi-\iota_M}^{\varphi-\iota_m-1} \xi^T(i) \mathcal{R} \sum_{i=\varphi-\iota_M}^{\varphi-\iota_m-1} \xi(i), \\ - \sum_{j=-\iota_M}^{\iota_m-1} \sum_{i=\varphi+j}^{\varphi-1} \xi^T(i) \mathcal{R} \xi(i) &\leq - \frac{2}{(\iota_M - \iota_m)(\iota_M + \iota_m + 1)} \sum_{j=-\iota_M}^{\iota_m-1} \sum_{i=\varphi+j}^{\varphi-1} \xi^T(i) \mathcal{R} \xi(i) \sum_{j=-\iota_M}^{\iota_m-1} \sum_{i=\varphi+j}^{\varphi-1} \xi(i). \end{aligned}$$

3 Main Results

Theorem 3.1. *For a given constant $\delta > 0, \vartheta > 0$, discrete-time IT2 T-S fuzzy system (18) is mean-square exponentially stable with H_∞ performance δ , if there exist a positive definite matrices $R_1 > 0, Q_1 > 0, R_2 > 0, Q_2 > 0, R_3 > 0, W > 0, R > 0, P_i > 0$ and event triggered parameter matrix Θ , such that the following inequalities hold.*

$$\begin{bmatrix} \Phi & \delta I \\ * & -P_i \end{bmatrix} < 0, \quad (21)$$

$$\Phi = \begin{bmatrix} \Phi_{11} & \Phi_{12} & \Phi_{13} & 0 & \Phi_{15} & 0 & \Phi_{17} & \Phi_{18} & 0 & 0 & 0 \\ * & \Phi_{22} & 0 & 0 & 0 & 0 & \Phi_{27} & 0 & 0 & 0 & 0 \\ * & * & \Phi_{33} & 0 & 0 & 0 & \Phi_{37} & 0 & 0 & 0 & 0 \\ * & * & * & \Phi_{44} & \Phi_{45} & 0 & 0 & 0 & \Phi_{49} & 0 & 0 \\ * & * & * & * & \Phi_{55} & \Phi_{56} & \Phi_{57} & 0 & \Phi_{59} & \Phi_{5,10} & 0 \\ * & * & * & * & * & \Phi_{66} & 0 & 0 & 0 & 0 & \Phi_{6,11} \\ * & * & * & * & * & * & \Phi_{77} & \Phi_{78} & 0 & 0 & 0 \\ * & * & * & * & * & * & * & \Phi_{88} & 0 & 0 & 0 \\ * & * & * & * & * & * & * & * & \Phi_{99} & 0 & 0 \\ * & * & * & * & * & * & * & * & * & \Phi_{10,10} & 0 \\ * & * & * & * & * & * & * & * & * & * & \Phi_{11,11} \end{bmatrix}, \quad (22)$$

where,

$$\begin{aligned} \Phi_{11} &= -P_i + W + (\iota_*)R + R_{11} + R_{21} + R_{31} + \iota_2 R_1 - \frac{Q_2}{\iota_M} + 2N_1[A(\varphi) - I], & \Phi_{12} &= 2N_1A_\iota(\varphi), \\ \Phi_{13} &= 2N_1B_1(\varphi), & \Phi_{15} &= 2N_1KC_1(\varphi) + \gamma\Theta + \frac{Q_2}{\iota_M}, & \Phi_{17} &= 2N_1A[\varphi - I_1] - 2N_1 + R_{12} + R_{22} + R_{32}, \\ \Phi_{18} &= -2N_1KC_1(\varphi), & \Phi_{22} &= -\lambda^{-1}R, & \Phi_{27} &= 2N_1A_\iota(\varphi), & \Phi_{33} &= -\delta^2I, & \Phi_{37} &= 2N_1B_1(\varphi), \\ \Phi_{44} &= -R_{21} - \frac{Q_1}{\iota_*}, & \Phi_{45} &= \frac{Q_1}{\iota_*}, & \Phi_{49} &= -2R_{22}, & \Phi_{55} &= -W - R_{11} - \frac{2Q_1}{\iota_*} + \Theta - \frac{2Q_2}{\iota_*} - \frac{Q_2}{\iota_M}, \\ \Phi_{57} &= 2N_1C_1(\varphi), & \Phi_{5,10} &= -2R_{12}, & \Phi_{66} &= -\frac{Q_1}{\iota_*} - \frac{Q_2}{\iota_*} - R_{31}, & \Phi_{6,11} &= -R_{32}, & \Phi_{77} &= R_{13} + R_{23} + R_{33} + \iota_*R_1 + \\ & & & & & & & & & & \iota_*Q_1 + \iota_MQ_2 - 2N_1, & \Phi_{78} &= -2N_1KC_1(\varphi) & \Phi_{88} &= -\vartheta\Theta, & \Phi_{99} &= -R_{23}, \\ \Phi_{10,10} &= -R_{13}, & \Phi_{11,11} &= -R_{33}, & \Phi_{56} &= \frac{Q_1}{\iota_*} + \frac{Q_2}{\iota_*}, \text{ and } \iota_* = \iota_M - \iota_m \end{aligned}$$

Proof. The following Lyapunov functional candidate is considered:

$$\begin{aligned} V_1(\varphi) &= \varpi^T(\varphi)P_i(\varphi)\varpi(\varphi) + \sum_{d=1}^{\infty} \lambda_d \sum_{\bar{i}=\varphi-d}^{\varphi-1} \varpi(\bar{i})^T R \varpi(\bar{i}), \\ V_2(\varphi) &= \sum_{i=\varphi-\iota(\varphi)}^{\varphi-1} \varpi^T(i)W\varpi(i), \\ V_3(\varphi) &= \sum_{i=\varphi-\iota_M}^{\varphi-\iota_m} \varpi^T(i)W\varpi(i), \\ V_4(\varphi) &= \sum_{i=\varphi-\iota(\varphi)}^{\varphi-1} \mu^T(i)R_1\mu(i) + \sum_{i=\varphi-\iota_m}^{\varphi-1} \mu^T(i)R_2\mu(i) + \sum_{i=\varphi-\iota_m}^{\varphi-1} \mu^T(i)R_3\mu(i), \\ V_5(\varphi) &= \sum_{j=-\iota_M+1}^{-\iota_m} \sum_{i=\varphi+j}^{\varphi-1} \mu^T(i)R_1\mu(i) + \sum_{j=-\iota_M}^{-\iota_m-1} \sum_{i=\varphi+j}^{\varphi-1} x^T(i)Q_1x(i) + \sum_{j=\iota_M}^{-1} \sum_{i=\varphi+j}^{\varphi-1} x^T(i)Q_2x(i), \\ V_6(\varphi) &= \frac{1}{2}\gamma^T(\varphi)\gamma(\varphi). \end{aligned}$$

Here $\mu(\varphi) = [\varpi^T(\varphi) \quad x^T(\varphi)]^T$ and $x^T(\varphi) = \varpi(\varphi+1) - \varpi(\varphi)$.

$$J = \sum_{\varphi=0}^{N-1} (z^T(\varphi)z(\varphi) - \delta^2w^T(\varphi)w(\varphi)). \quad (23)$$

Then, we get

$$\dot{V}_1(\varphi) = \{\varpi(\varphi+1)^T P_i(\varphi+1)\varpi(\varphi+1) - \varpi(\varphi)^T P_i(\varphi)\varpi(\varphi) + \bar{\lambda}\varpi(\varphi)^T R \varpi(\varphi) - \sum_{d=1}^{\infty} \lambda_d \varpi(\varphi-d)^T R \varpi(\varphi-d)\}. \quad (24)$$

By applying (2) and Lemma [2.6](#), we get

$$-\sum_{d=1}^{\infty} \lambda_d \varpi(\varphi-d)^T R \varpi(\varphi-d) \leq -\bar{\lambda}^{-1} \left[\sum_{d=1}^{\infty} \lambda_d \varpi(\varphi-d) \right]^T R \left[\sum_{d=1}^{\infty} \lambda_d \varpi(\varphi-d) \right].$$

$$\begin{aligned}
 \dot{V}_2(\varphi) &= \left\{ \sum_{i=\varphi+1-\iota(\varphi+1)}^{\varphi} \varpi^T(i)W\varpi(i) - \sum_{i=\varphi-\iota(\varphi)}^{\varphi-1} \varpi^T(i)W\varpi(i) \right\}, \\
 &= \left\{ \varpi^T(\varphi)W\varpi(\varphi) - \varpi^T(\varphi-\iota(\varphi))W\varpi(\varphi-\iota(\varphi)) + \sum_{i=\varphi-\iota(\varphi+1)+1}^{\varphi} \varpi^T(i)W\varpi(i) - \sum_{i=\varphi-\iota(\varphi)+1}^{\varphi-1} \varpi^T(i)W\varpi(i) \right\}, \\
 &= \left\{ \varpi^T(\varphi)W\varpi(\varphi) - \varpi^T(\varphi-\iota(\varphi))W\varpi(\varphi-\iota(\varphi)) + \sum_{i=\varphi-\iota_M+1}^{\varphi-\iota_m} \varpi^T(i)W\varpi(i) \right\}. \tag{25}
 \end{aligned}$$

$$\begin{aligned}
 \dot{V}_3(\varphi) &= \left\{ \sum_{j=\varphi-\iota_M+2}^{\varphi-\iota_m+1} \sum_{i=j}^{\varphi} \varpi^T(i)W\varpi(i) - \sum_{j=\varphi-\iota_M+1}^{\varphi-\iota_m} \sum_{i=j}^{\varphi-1} \varpi^T(i)W\varpi(i) \right\}, \\
 &= \left\{ \sum_{j=\varphi-\iota_M+1}^{\varphi-\iota_m} \sum_{i=j+1}^{\varphi} \varpi^T(i)W\varpi(i) - \sum_{j=\varphi-\iota_M+1}^{\varphi-\iota_m} \sum_{i=j}^{\varphi-1} \varpi^T(i)W\varpi(i) \right\}, \\
 &= \left\{ (\iota_M - \iota_m) \varpi^T(i)W\varpi(i) - \sum_{j=\varphi-\iota_M+1}^{\varphi-\iota_m} \varpi^T(i)W\varpi(i) \right\}. \tag{26}
 \end{aligned}$$

$$\begin{aligned}
 \dot{V}_4(\varphi) &= \left\{ \mu^T(\varphi)R_1\mu(\varphi) - \mu^T(\varphi-\iota(\varphi))R_1\mu(\varphi-\iota(\varphi)) + \sum_{i=\varphi+1-\iota(\varphi+1)}^{\varphi-\iota_m} \mu^T(i)R_1\mu(i) \right. \\
 &\quad + \sum_{i=\varphi+1-\iota_m}^{\varphi-1} \mu^T(i)R_1\mu(i) - \sum_{i=\varphi+1-\iota(\varphi)}^{\varphi-1} \mu^T(i)R_1\mu(i) + \mu^T(\varphi)R_2\mu(\varphi) \\
 &\quad \left. - \mu^T(\varphi-\iota_m)R_2\mu(\varphi-\iota_m) + \mu^T(\varphi)R_3\mu(\varphi) - \mu^T(\varphi-\iota_M)R_3\mu(\varphi-\iota_M) \right\}, \\
 &\leq \left\{ \mu^T(\varphi)(R_1 + R_2 + R_3)\mu(\varphi) - \mu^T(\varphi-\iota(\varphi))R_1\mu(\varphi-\iota(\varphi)) + \sum_{i=\varphi+1-\iota_M}^{\varphi-\iota_m} \mu^T(i)R_1\mu(i) \right. \\
 &\quad \left. - \mu^T(\varphi-\iota_m)R_2\mu(\varphi-\iota_m) - \mu^T(\varphi-\iota_M)R_3\mu(\varphi-\iota_M) \right\}, \\
 &\leq \left\{ \varpi^T(\varphi)(R_{11} + R_{21} + R_{31})\varpi(\varphi) + 2\varpi^T(\varphi)(R_{12} + R_{22} + R_{32})x(\varphi) + x^T(\varphi)(R_{13} + R_{23} \right. \\
 &\quad + R_{33})x(\varphi) - \varpi^T(\varphi-\iota(\varphi))R_{11}\varpi(\varphi-\iota(\varphi)) - 2\varpi^T(\varphi-\iota(\varphi))R_{12}x(\varphi-\iota(\varphi)) \\
 &\quad - x^T(\varphi-\iota(\varphi))R_{13}x(\varphi-\iota(\varphi)) - \varpi^T(\varphi-\iota_m)R_{21}\varpi(\varphi-\iota_m) - 2\varpi^T(\varphi-\iota_m)R_{22}x(\varphi-\iota_m) \\
 &\quad - x^T(\varphi-\iota_m)R_{23}x(\varphi-\iota_m) - \varpi^T(\varphi-\iota_M)R_{31}\varpi(\varphi-\iota_M) - 2\varpi^T(\varphi-\iota_M)R_{32}x(\varphi-\iota_M) \\
 &\quad \left. - x^T(\varphi-\iota_M)R_{33}x(\varphi-\iota_M) + \sum_{i=\varphi+1-\iota_M}^{\varphi-\iota_m} \mu^T(i)R_1\mu(i) \right\}. \tag{27}
 \end{aligned}$$

$$\begin{aligned}
 \dot{V}_5(\varphi) &= \left(\sum_{j=-\iota_M+1}^{-\iota_m} \left[\sum_{i=\varphi+1+j}^i \mu^T(i)R_1\mu(i) - \sum_{i=\varphi+j}^{\varphi-1} \mu^T(i)R_1\mu(i) \right] + \sum_{j=-\iota_M}^{-\iota_m-1} \left[\sum_{i=\varphi+1+j}^{\varphi} x^T(i)Q_1x(i) \right. \right. \\
 &\quad \left. \left. - \sum_{i=\varphi+j}^{\varphi-1} x^T(i)Q_1x(i) \right] + \sum_{j=-\iota_M}^{-1} \left[\sum_{i=\varphi+1+j}^{\varphi} x^T(i)Q_2x(i) - \sum_{i=\varphi+j}^{\varphi-1} x^T(i)Q_2x(i) \right] \right), \\
 &= \left[\iota_2 \mu^T(\varphi)R_1\mu(\varphi) - \sum_{i=\varphi+1-\iota_M}^{\varphi-\iota_m} \mu^T(i)R_1\mu(i) + \iota_2 x^T(\varphi)R_1x(\varphi) - \sum_{i=\varphi-\iota_M}^{\varphi-\iota_m-1} x^T(i)Q_1x(i) \right. \\
 &\quad \left. + \iota_M x^T(\varphi)Q_2x(\varphi) - \sum_{i=\varphi-\iota_M}^{\varphi-1} x^T(i)Q_2x(i) \right]. \tag{28}
 \end{aligned}$$

By applying Lemma ??, we get

$$\begin{aligned}
-\sum_{i=\wp-\iota_M}^{\wp-\iota_m-1} x^T(i)Q_1x(i) &= -\sum_{i=\wp-\iota_M}^{\wp-\iota(\wp)-1} x^T(i)Q_1x(i) - \sum_{i=\wp-\iota(\wp)}^{\wp-\iota_m-1} x^T(i)Q_1x(i), \\
&\leq -\frac{1}{\iota_2} \sum_{i=\wp-\iota_M}^{\wp-\iota(\wp)-1} x^T(i)Q_1 \sum_{i=\wp-\iota_M}^{\wp-\iota(\wp)-1} x(i) - \frac{1}{\iota_2} \sum_{i=\wp-\iota(\wp)}^{\wp-\iota_m-1} x^T(i)Q_1 \sum_{i=\wp-\iota(\wp)}^{\wp-\iota_m-1} x(i), \\
&\leq -\frac{1}{\iota_2} \left(\{\varpi[\wp - \iota(\wp)] - \varpi[\wp - \iota_M]\}^T Q_1 \{\varpi[\wp - \iota(\wp)] - \varpi[\wp - \iota_M]\} + \right. \\
&\quad \left. \{\varpi[\wp - \iota_m] - \varpi[\wp - \iota(\wp)]\}^T \times Q_1 \{\varpi[\wp - \iota_m] - \varpi[\wp - \iota(\wp)]\} \right), \\
-\sum_{i=\wp-\iota_M}^{\wp-1} x^T(i)Q_2x(i) &= -\sum_{i=\wp-\iota_M}^{\wp-\iota(\wp)-1} x^T(i)Q_2x(i) - \sum_{i=\wp-\iota(\wp)}^{\wp-1} x^T(i)Q_2x(i), \\
&\leq -\frac{1}{\iota_2} \sum_{i=\wp-\iota_M}^{\wp-\iota(\wp)-1} x^T(i)Q_2 \sum_{i=\wp-\iota_M}^{\wp-\iota(\wp)-1} x(i) - \frac{1}{\iota_M} \sum_{i=\wp-\iota(\wp)}^{\wp-1} x^T(i)Q_2 \sum_{i=\wp-\iota(\wp)}^{\wp-1} x(i), \\
&\leq -\frac{1}{\iota_2} \left(\{\varpi[\wp - \iota(\wp)] - \varpi[\wp - \iota_M]\}^T Q_2 \{\varpi[\wp - \iota(\wp)] - \varpi[\wp - \iota_M]\} \right. \\
&\quad \left. - \frac{1}{\iota_M} \{\varpi[\wp] - \varpi[\wp - \iota(\wp)]\}^T \times Q_2 \{\varpi[\wp] - \varpi[\wp - \iota(\wp)]\} \right).
\end{aligned}$$

$$\begin{aligned}
\dot{V}_6(\wp) &= \gamma^T(\wp)\dot{\gamma}(\wp), \\
&= \theta_1 \left(\frac{1}{\gamma_1(\wp)} - \vartheta_1 \right) e_1^T(\wp) \Theta_1 e_1(\wp) + \theta_2 \left(\frac{1}{\gamma_2(\wp)} - \vartheta_2 \right) e_2^T(\wp) \Theta_2 e_2(\wp) + \dots + \theta_N \left(\frac{1}{\gamma_N(\wp)} - \vartheta_N \right) \\
&\quad \times e_N^T(\wp) \Theta_N e_N(\wp), \\
&= \frac{\theta_1}{\gamma_1}^T(\wp) \Theta_1 \gamma_1(\wp) + \frac{\theta_2}{\gamma_2}^T(\wp) \Theta_2 \gamma_2(\wp) + \dots + \frac{\theta_N}{\gamma_N}^T(\wp) \Theta_N \gamma_N(\wp) - \theta_1 \vartheta_1 e_1^T(\wp) \Theta_1 e_1(\wp) \\
&\quad - \theta_2 \vartheta_2 e_2^T(\wp) \Theta_2 e_2(\wp) - \dots - \theta_N \vartheta_N e_N^T(\wp) \Theta_N e_N(\wp).
\end{aligned} \tag{29}$$

Combining (8) and (29), one can get the following inequality

$$\begin{aligned}
\dot{V}_6(\wp) &\leq \theta_1 \varpi_1^T(\wp - \iota_1(\wp)) \Theta_1 \varpi_1(\wp - \iota_1(\wp)) + \theta_2 \varpi_2^T(\wp - \iota_2(\wp)) \Theta_2 \varpi_2(\wp - \iota_2(\wp)) + \dots \\
&\quad + \theta_N \varpi_N^T(\wp - \iota_N(\wp)) \Theta_N \varpi_N(\wp - \iota_N(\wp)) - \theta_1 \vartheta_1 e_1^T(\wp) \Theta_1 e_1(\wp) - \theta_2 \vartheta_2 e_2^T(\wp) \Theta_2 e_2(\wp) - \dots \\
&\quad - \theta_N \vartheta_N e_N^T(\wp) \Theta_N e_N(\wp), \\
&= \varpi^T(\iota - \iota(\wp)) \Theta \varpi(\iota - \iota(\wp)) - e^T(\wp) \Theta \vartheta e(\wp).
\end{aligned} \tag{30}$$

In addition, we have

$$\begin{aligned}
[x(\wp)] &= [\varpi(\wp + 1) - \varpi(\wp)], \\
0 &= \left[2 \left([x(\wp)N_1 + \varpi(\wp)N_1][\varpi(\wp + 1) - \varpi(\wp) - x(\wp)] \right) \right],
\end{aligned} \tag{31}$$

$$\begin{aligned}
0 &= \left[2 \left([x(\wp)N_1 + \varpi(\wp)N_1][A(\wp)\varpi(\wp) + A_\iota(\wp) \sum_{d=1}^{\infty} \lambda_d \varpi(\wp - d) + B_1(\wp)w(\wp) \right. \right. \\
&\quad \left. \left. + C_1(\wp)K\varpi(\wp - \iota(\wp)) - C_1K(k)e(i_\wp h) - \varpi(\wp) - x(\wp)] \right) \right].
\end{aligned} \tag{32}$$

From the equation (23)-(32), we get

$$\begin{aligned}
 \dot{V}(\varphi) = & \{ \varpi(\varphi+1)^T P_i(\varphi+1) \varpi(\varphi+1) - \varpi(\varphi)^T P_i(\varphi) \varpi(\varphi) + \bar{\lambda} \varpi(\varphi)^T R \varpi(\varphi) - \bar{\lambda}^{-1} \left[\sum_{d=1}^{\infty} \lambda_d \varpi(\varphi-d) \right]^T \\
 & R \left[\sum_{d=1}^{\infty} \lambda_d \varpi(\varphi-d) \right] + \varpi^T(\varphi) W \varpi(\varphi) - \varpi^T(\varphi-\iota(\varphi)) W \varpi(\varphi-\iota(\varphi)) + \sum_{i=\varphi-\iota_M+1}^{\varphi-\iota_m} \varpi^T(i) W \varpi(i) \\
 & + (\iota_M - \iota_m) \varpi^T(i) W \varpi(i) - \sum_{j=\varphi-\iota_M+1}^{\varphi-\iota_m} \varpi^T(i) W \varpi(i) + \sum_{i=\varphi+1-\iota_M}^{\varphi-\iota_m} \mu^T(i) R_1 \mu(i) - e^T(\varphi) \Theta \vartheta e(\varphi) \\
 & - \varpi^T(\varphi-\iota(\varphi)) R_{11} \varpi(\varphi-\iota(\varphi)) - 2\varpi^T(\varphi-\iota(\varphi)) R_{12} x(\varphi-\iota(\varphi)) - x^T(\varphi-\iota(\varphi)) R_{13} x(\varphi-\iota(\varphi)) \\
 & + \varpi^T(\varphi) (R_{11} + R_{21} + R_{31}) \varpi(\varphi) + 2\varpi^T(\varphi) (R_{12} + R_{22} + R_{32}) x(\varphi) + x^T(\varphi) (R_{13} + R_{23} + R_{33}) \\
 & x(\varphi) - \varpi^T(\varphi-\iota_m) R_{21} \varpi(\varphi-\iota_m) - 2\varpi^T(\varphi-\iota_m) R_{22} x(\varphi-\iota_m) - x^T(\varphi-\iota_m) R_{23} x(\varphi-\iota_m) \\
 & - \varpi^T(\varphi-\iota_M) R_{31} \varpi(\varphi-\iota_M) - 2\varpi^T(\varphi-\iota_M) R_{32} x(\varphi-\iota_M) - x^T(\varphi-\iota_M) R_{33} x(\varphi-\iota_M) \\
 & + \left[\iota_2 \mu^T(\varphi) R_1 \mu(\varphi) - \sum_{i=\varphi+1-\iota_M}^{\varphi-\iota_m} \mu^T(i) R_1 \mu(i) + \iota_2 x^T(\varphi) R_1 x(\varphi) + \iota_M x^T(\varphi) R_1 x(\varphi) \right] - \frac{1}{\iota_2} \\
 & \left(\{ \varpi[\varphi-\iota(\varphi)] - \varpi[\varphi-\iota_M] \}^T Q_1 \{ \varpi[\varphi-\iota(\varphi)] - \varpi[\varphi-\iota_M] \} + \{ \varpi[\varphi-\iota_m] - \varpi[\varphi-\iota(\varphi)] \}^T Q_1 \right. \\
 & \left. \{ \varpi[\varphi-\iota_m] - \varpi[\varphi-\iota(\varphi)] \} \right) - \frac{1}{\iota_2} \left(\{ \varpi[\varphi-\iota(\varphi)] - \varpi[\varphi-\iota_M] \}^T Q_2 \{ \varpi[\varphi-\iota(\varphi)] - \varpi[\varphi-\iota_M] \} \right. \\
 & \left. - \frac{1}{\iota_M} \{ \varpi[\varphi] - \varpi[\varphi-\iota(\varphi)] \}^T Q_2 \{ \varpi[\varphi] - \varpi[\varphi-\iota(\varphi)] \} \right) + \left[2N_1 \left([x(\varphi) + \varpi(\varphi)] [A(\varphi) \varpi(\varphi) A_\iota(\varphi)] \right. \right. \\
 & \left. \left. + \sum_{d=1}^{\infty} \lambda_d \varpi(\varphi-d) + B_1(\varphi) w(\varphi) + C_1(\varphi) K \varpi(\varphi-\iota(\varphi)) - C_1 K(\varphi) e(i_\varphi h) - \varpi(\varphi) - x(\varphi) \right) \right] \} \\
 & + \varpi^T(\iota-\iota(\varphi)) \Theta \varpi(\iota-\iota(\varphi)). \tag{33}
 \end{aligned}$$

Therefore, under zero initial condition, it follows from (23) and (33), we get

$$\begin{aligned}
 J & \leq \sum_{\varphi=0}^{N-1} (z^T(\varphi) z(\varphi) - \delta^2 w^T(\varphi) w(\varphi)) + V(\varphi+1) - V(\varphi) + V(0) - V(\infty), \\
 J & \leq \xi^T(\varphi) [\Phi + \Upsilon_1^T(P_i) \Upsilon_1 + \Upsilon_2^T I \Upsilon_2] \xi(\varphi). \tag{34}
 \end{aligned}$$

where,

$$\begin{aligned}
 \xi(\varphi) = & \left[\varpi^T(\varphi) \quad \sum_{d=1}^{\infty} \lambda_d \varpi^T(\varphi-d) \quad w^T(\varphi) \quad \varpi^T(\varphi-\iota_m(\varphi)) \quad \varpi^T(\varphi-\iota(\varphi)) \quad \varpi^T(\varphi-\iota_M(\varphi)) \right. \\
 & \left. x^T(\varphi) \quad e^T(i_\varphi h) \quad x^T(\varphi-\iota_m(\varphi)) \quad x^T(\varphi-\iota(\varphi)) \quad x^T(\varphi-\iota_M(\varphi)) \right]^T, \quad \Upsilon_1(\varphi) = \left[A^T(\varphi) \quad A_\iota^T(\varphi) \quad B_{1i}^T(\varphi) \right. \\
 & \left. 0 \quad KC_{1i}^T(\varphi) \quad 0 \quad 0 \quad -KC_{1i}^T(\varphi) \quad 0 \quad 0 \quad 0 \right]^T \text{ and } \Upsilon_2(\varphi) = \left[D_i^T(\varphi) \quad 0 \quad B_{2i}^T(\varphi) \quad 0 \quad KC_{2i}^T(\varphi) \quad 0 \quad 0 \right. \\
 & \left. -KC_{2i}^T(\varphi) \quad 0 \quad 0 \quad 0 \right]^T.
 \end{aligned}$$

By using the Schur Complement (Lemma 2.8), we get (21). Therefore, $J < 0$ for any nonzero $w(\varphi) \in l_2[0, \infty)$. Letting $N \rightarrow \infty$, then the inequality (20) holds. Therefore the system (18) is exponentially mean square stable with H_∞ performance. \square

Corollary 3.2. *The discrete-time IT2 T-S fuzzy system (18) with $w(\varphi) = 0$ is mean-square exponentially stable, if there exist a positive definite matrices $R_1 > 0, Q_1 > 0, R_2 > 0, Q_2 > 0, R_3 > 0, W > 0, R > 0, P_i > 0$, and event triggered parameter matrix Θ , such that the following inequalities hold.*

$$\begin{bmatrix} \bar{\Phi} & \delta I \\ * & -P_i \end{bmatrix} < 0, \tag{35}$$

$$\bar{\Phi} = \begin{bmatrix} \bar{\Phi}_{11} & \bar{\Phi}_{12} & 0 & \bar{\Phi}_{14} & 0 & \bar{\Phi}_{16} & \bar{\Phi}_{17} & 0 & 0 & 0 \\ * & \bar{\Phi}_{22} & 0 & 0 & 0 & \bar{\Phi}_{26} & 0 & 0 & 0 & 0 \\ * & * & \bar{\Phi}_{33} & \bar{\Phi}_{34} & 0 & 0 & 0 & \bar{\Phi}_{38} & 0 & 0 \\ * & * & * & \bar{\Phi}_{44} & \bar{\Phi}_{45} & \bar{\Phi}_{46} & 0 & \bar{\Phi}_{4,8} & \bar{\Phi}_{4,9} & 0 \\ * & * & * & * & \bar{\Phi}_{55} & 0 & 0 & 0 & 0 & \bar{\Phi}_{5,10} \\ * & * & * & * & * & \bar{\Phi}_{66} & \bar{\Phi}_{67} & 0 & 0 & 0 \\ * & * & * & * & * & * & \bar{\Phi}_{77} & 0 & 0 & 0 \\ * & * & * & * & * & * & * & \bar{\Phi}_{88} & 0 & 0 \\ * & * & * & * & * & * & * & * & \bar{\Phi}_{99} & 0 \\ * & * & * & * & * & * & * & * & * & \bar{\Phi}_{10,10} \end{bmatrix}, \quad (36)$$

where,

$$\begin{aligned} \bar{\Phi}_{11} &= -P_i + W + (\iota_*)R + R_{11} + R_{21} + R_{31} + \iota_2 R_1 - \frac{Q_2}{\iota_M} + 2N_1[A(\varphi) - I], & \bar{\Phi}_{12} &= 2N_1A_\iota(\varphi), \\ \bar{\Phi}_{14} &= 2N_1KC_1(\varphi) + \gamma_1\Theta + \frac{Q_2}{\iota_M}, & \bar{\Phi}_{16} &= 2N_1A[\varphi - I_1] - 2N_1 + R_{12} + R_{22} + R_{32}, & \bar{\Phi}_{17} &= -2N_1KC_1(\varphi), \\ \bar{\Phi}_{22} &= -\lambda^{-1}R, & \bar{\Phi}_{27} &= 2N_1A_\iota(\varphi), & \bar{\Phi}_{33} &= -R_{21} - \frac{Q_1}{\iota_*}, & \bar{\Phi}_{34} &= \frac{Q_1}{\iota_*}, & \bar{\Phi}_{38} &= -2R_{22}, & \bar{\Phi}_{4,9} &= -2R_{12}, \\ \bar{\Phi}_{44} &= -W - R_{11} - \frac{2Q_1}{\iota_*} + \Theta - \frac{2Q_2}{\iota_*} - \frac{Q_2}{\iota_M}, & \bar{\Phi}_{45} &= \frac{Q_1}{\iota_*} + \frac{Q_2}{\iota_*}, & \bar{\Phi}_{46} &= 2N_1C_1(\varphi), & \bar{\Phi}_{55} &= -\frac{Q_1}{\iota_*} - \frac{Q_2}{\iota_*} - R_{31}, \\ \bar{\Phi}_{5,10} &= -R_{32}, & \bar{\Phi}_{66} &= R_{13} + R_{23} + R_{33} + \iota_*R_1 + \iota_*Q_1 + \iota_MQ_2 - 2N_1, & \bar{\Phi}_{67} &= -2N_1KC_1(\varphi) \\ \bar{\Phi}_{77} &= -\vartheta\Theta, & \bar{\Phi}_{88} &= -R_{23}, & \bar{\Phi}_{9,9} &= -R_{13}, & \bar{\Phi}_{10,10} &= -R_{33}, & \bar{\Phi}_8 &= \gamma_1\Theta \text{ and } \iota_* = \iota_M - \iota_m. \end{aligned}$$

Proof. Following the same procedure in Theorem 3.1, we get

$$\dot{V}(\varphi) \leq \xi^T(\varphi) \left[\bar{\Phi} + \tilde{\Upsilon}_1^T(P_i)\tilde{\Upsilon}_1 + \tilde{\Upsilon}_2^T I \tilde{\Upsilon}_2 \right] \xi(\varphi) < -\kappa \|\varpi(\varphi)\|^2, \quad (37)$$

where,

$$\begin{aligned} \tilde{\xi}(\varphi) &= \left[\varpi^T(\varphi) \quad \sum_{d=1}^{\infty} \lambda_d \varpi^T(\varphi - d) \quad \varpi^T(\varphi - \iota_m(\varphi)) \quad \varpi^T(\varphi - \iota(\varphi)) \quad \varpi^T(\varphi - \iota_M(\varphi)) \quad x^T(\varphi) \quad e^T(i_\varphi h) \right. \\ & \left. x^T(\varphi - \iota_m(\varphi)) \quad x^T(\varphi - \iota(\varphi)) \quad x^T(\varphi - \iota_M(\varphi)) \right]^T, \quad \tilde{\Upsilon}_1(\varphi) = \left[A^T(\varphi) \quad A_{\iota i}^T(\varphi) \quad 0 \quad KC_{1i}^T(\varphi) \quad 0 \quad 0 \right. \\ & \left. - KC_{1i}^T(\varphi) \quad 0 \quad 0 \quad 0 \right]^T \text{ and } \tilde{\Upsilon}_2(\varphi) = \left[D_{1i}^T(\varphi) \quad 0 \quad 0 \quad KC_{2i}^T(\varphi) \quad 0 \quad 0 \quad -KC_2^T(\varphi) \quad 0 \quad 0 \quad 0 \right]^T. \end{aligned}$$

By using a method of analysis similar to that used in [9] and from Definition 2.4, system (18) with $w(\varphi) = 0$ is exponentially mean-square stable. This concludes the proof. \square

Theorem 3.3. *The discrete-time IT2 T-S fuzzy system (18) is mean-square exponentially stable with H_∞ performance δ , if there exist matrices $\tilde{R}_1 > 0, \tilde{Q}_1 > 0, \tilde{R}_2 > 0, \tilde{Q}_2 > 0, \tilde{R}_3 > 0, \tilde{R} > 0, \tilde{V} > 0, \tilde{P}_i > 0$, event triggered parameter matrix Θ and positive diagonal matrix \tilde{N}_1 with proper dimensions such that,*

$$\tilde{\Phi} = \begin{bmatrix} \tilde{\Phi}_{11} & \tilde{\Phi}_{12} & \tilde{\Phi}_{13} & 0 & \tilde{\Phi}_{15} & 0 & \tilde{\Phi}_{17} & \tilde{\Phi}_{18} & 0 & 0 & 0 & P_i A_i & D_i \\ * & \tilde{\Phi}_{22} & 0 & 0 & 0 & 0 & \tilde{\Phi}_{27} & 0 & 0 & 0 & 0 & P_i A_{\iota i} & 0 \\ * & * & \tilde{\Phi}_{33} & 0 & 0 & 0 & \tilde{\Phi}_{37} & 0 & 0 & 0 & 0 & P_i B_{1i} & B_{2i} \\ * & * & * & \tilde{\Phi}_{44} & \tilde{\Phi}_{45} & 0 & 0 & \tilde{\Phi}_{49} & 0 & 0 & 0 & 0 & 0 \\ * & * & * & * & \tilde{\Phi}_{55} & \tilde{\Phi}_{56} & \tilde{\Phi}_{57} & 0 & \tilde{\Phi}_{59} & \tilde{\Phi}_{5,10} & 0 & P_i C_{1i} K & C_{2i} K \\ * & * & * & * & * & \tilde{\Phi}_{66} & 0 & 0 & 0 & 0 & \tilde{\Phi}_{6,11} & 0 & 0 \\ * & * & * & * & * & * & \tilde{\Phi}_{77} & \tilde{\Phi}_{78} & 0 & 0 & 0 & 0 & 0 \\ * & * & * & * & * & * & * & \tilde{\Phi}_{88} & 0 & 0 & 0 & -P_i C_{1i} K & -C_{2i} K \\ * & * & * & * & * & * & * & * & \tilde{\Phi}_{99} & 0 & 0 & 0 & 0 \\ * & * & * & * & * & * & * & * & * & \tilde{\Phi}_{10,10} & 0 & 0 & 0 \\ * & * & * & * & * & * & * & * & * & * & \tilde{\Phi}_{11,11} & 0 & 0 \\ * & * & * & * & * & * & * & * & * & * & * & -P_i & 0 \\ * & * & * & * & * & * & * & * & * & * & * & * & -I \end{bmatrix} < 0 \quad (38)$$

where,

$$\begin{aligned} \tilde{\Phi}_{11} &= -\tilde{P}_i + \tilde{W} + (\iota_*)\tilde{R} + \tilde{R}_{11} + \tilde{R}_{21} + \tilde{R}_{31} + \iota_2 \tilde{R}_1 - \frac{\tilde{Q}_2}{\iota_M} + 2\epsilon \tilde{P}[A(\varphi) - I], & \tilde{\Phi}_{12} &= 2\epsilon \tilde{P}A_\iota(\varphi), \\ \tilde{\Phi}_{13} &= 2\epsilon \tilde{P}B_{1i}(\varphi), & \tilde{\Phi}_{15} &= 2\epsilon X C_1(\varphi) + \frac{Q_2}{\iota_M} + \gamma_1 \tilde{\Theta}, & \tilde{\Phi}_{17} &= 2\epsilon \tilde{P}A[\varphi - I_1] - 2\epsilon \tilde{P} + \tilde{R}_{12} + \tilde{R}_{22} + \tilde{R}_{32}, \\ \tilde{\Phi}_{18} &= -2\epsilon X C_1(\varphi), & \tilde{\Phi}_{1,12} &= \tilde{P}A_i(k) & \tilde{\Phi}_{1,13} &= \tilde{P}D_i, & \tilde{\Phi}_{22} &= -\lambda^{-1}\tilde{R}, & \tilde{\Phi}_{27} &= 2\epsilon \tilde{P}A_\iota(\varphi), \\ \tilde{\Phi}_{2,12} &= \tilde{P}A_{\iota i}(k), & \tilde{\Phi}_{33} &= -\delta^2 I, & \tilde{\Phi}_{37} &= 2\epsilon \tilde{P}B_{1i}(\varphi), & \tilde{\Phi}_{3,12} &= \tilde{P}B_{1i}, & \tilde{\Phi}_{3,13} &= B_{2i} \tilde{\Phi}_{44} = -\tilde{R}_{21} - \frac{\tilde{Q}_1}{\iota_*}, \end{aligned}$$

$$\begin{aligned} \tilde{\Phi}_{45} &= \frac{\tilde{Q}_1}{\iota_*}, \quad \tilde{\Phi}_{49} = -2\tilde{R}_{22}, \quad \tilde{\Phi}_{55} = -\tilde{W} - \tilde{R}_{11} + \tilde{\Theta} - \frac{2\tilde{Q}_1}{\iota_*} - \frac{2\tilde{Q}_2}{\iota_*} - \frac{\tilde{Q}_2}{\iota_M}, \quad \tilde{\Phi}_{56} = \frac{\tilde{Q}_1}{\iota_*} + \frac{\tilde{Q}_2}{\iota_*}, \\ \tilde{\Phi}_{5,10} &= -2\tilde{R}_{12}, \quad \tilde{\Phi}_{5,12} = XC_1, \quad \tilde{\Phi}_{5,13} = XC_2, \quad \tilde{\Phi}_{66} = -\frac{\tilde{Q}_1}{\iota_*} - \frac{\tilde{Q}_2}{\iota_*} - \tilde{R}_{31}, \quad \tilde{\Phi}_{6,11} = -\tilde{R}_{32}, \\ \tilde{\Phi}_{77} &= \tilde{R}_{13} + \tilde{R}_{23} + \tilde{R}_{33} + \iota_*\tilde{R}_1 + \iota_*\tilde{Q}_1 + \iota_M\tilde{Q}_2 - 2\epsilon\tilde{P}, \quad \tilde{\Phi}_{78} = -2\epsilon XC_1(\varphi), \quad \tilde{\Phi}_{88} = -\vartheta\tilde{\Theta}, \\ \tilde{\Phi}_{8,12} &= -XC_1, \quad \tilde{\Phi}_{8,13} = -XC_2, \quad \tilde{\Phi}_{99} = -\tilde{R}_{23}, \quad \tilde{\Phi}_{10,10} = -\tilde{R}_{13}, \quad \tilde{\Phi}_{11,11} = -\tilde{R}_{33}, \\ \tilde{\Phi}_{12,12} &= -\tilde{P}, \quad \tilde{\Phi}_{13,13} = -I, \quad \tilde{\Phi}_{57} = 2\epsilon\tilde{P}C_1(\varphi) \text{ and } \iota_* = \iota_M - \iota_m. \end{aligned}$$

$$K = \tilde{P}^{-1}X. \quad (39)$$

Proof. We calculate $\tilde{\Phi}_{ij} = \Lambda\Phi_{ij}\Lambda^T$ with

$$\Lambda = \text{diag}\{\tilde{P}, \tilde{P}, I, \tilde{P}, \tilde{P}, \tilde{P}, \tilde{P}, \tilde{P}, \tilde{P}, \tilde{P}, \tilde{P}, I\},$$

where $\tilde{P} = P^{-1}$. Defining $\tilde{W} = \tilde{P}W\tilde{P}$, $\tilde{Q}_i = \tilde{P}Q_i\tilde{P}$, ($i = 1, 2, 3$), $\tilde{R}_{ij} = \tilde{P}R_{ij}\tilde{P}$, ($i, j = 1, 2, 3$) and letting $N_1 = \epsilon\tilde{P}$, we obtain $\tilde{\Phi}_{ij}$ in (38). If the conditions (38) hold, event-triggered control gain matrices are K are given by (39). \square

4 Numerical examples

To illustrate the theoretical results, numerical examples are provided.

Example 4.1. Consider the following single link robot arm system in [25, 33].

$$\ddot{\varpi}(t) = \frac{LgM_k}{J_k}\sin(\varpi(t)) - \frac{Q_k}{J_k}\dot{\varpi}(t) + \frac{1}{J_k}u(t) + Bw(t) \quad (40)$$

In this example $w(t)$ and $u(t)$ represents the disturbance input and control input, respectively. $\dot{\varpi}$ and ϖ indicates the angular velocity of the robot arm and the angel, respectively. The system parameters include, L is the arm's length, g is the acceleration of gravity, the mass of the payload is M_k , J_k is the moment of inertia, ρ is retarded coefficient and the coefficient of viscous friction is Q_k .

The values of the parameters $g = 9.81$, $Q_1 = Q_2 = 2$, $L = 0.5$, $M_1 = J_1 = 1$, $M_2 = J_2 = 5$, $M_3 = J_3 = 10$, $\rho = 0.85$ and $T = 0.1$.

Then, the single-link robot arm system can be approximated by the following IT2 T-S fuzzy model.

Pant rule 1: IF $\varpi_1(\varphi)$ is $1 - \frac{\varpi_1^2(\varphi)}{3}$, THEN

$$\begin{cases} \varpi(\varphi + 1) &= \sum_{i=1}^q \sum_{j=1}^q \alpha_i \beta_j \{A_1 \varpi(\varphi) + A_{11} \sum_{d=1}^{\infty} \lambda_d \varpi(\varphi - d) + B_{11} w(\varphi) + C_{11} u(\varphi)\}, \\ z(\varphi) &= \sum_{i=1}^q \sum_{j=1}^q \alpha_i \beta_j \{D_1 \varpi(\varphi) + B_{21} w(\varphi) + C_{21} u(\varphi)\}. \end{cases} \quad (41)$$

Pant rule 2: IF $\varpi_1(\varphi)$ is $\frac{\varpi_1^2(\varphi)}{3}$, THEN

$$\begin{cases} \varpi(\varphi + 1) &= \sum_{i=1}^q \sum_{j=1}^q \alpha_i \beta_j \{A_2 \varpi(\varphi) + A_{12} \sum_{d=1}^{\infty} \lambda_d \varpi(\varphi - d) + B_{12} w(\varphi) + C_{12} u(\varphi)\}, \\ z(\varphi) &= \sum_{i=1}^q \sum_{j=1}^q \alpha_i \beta_j \{D_2 \varpi(\varphi) + B_{22} w(\varphi) + C_{22} u(\varphi)\}. \end{cases} \quad (42)$$

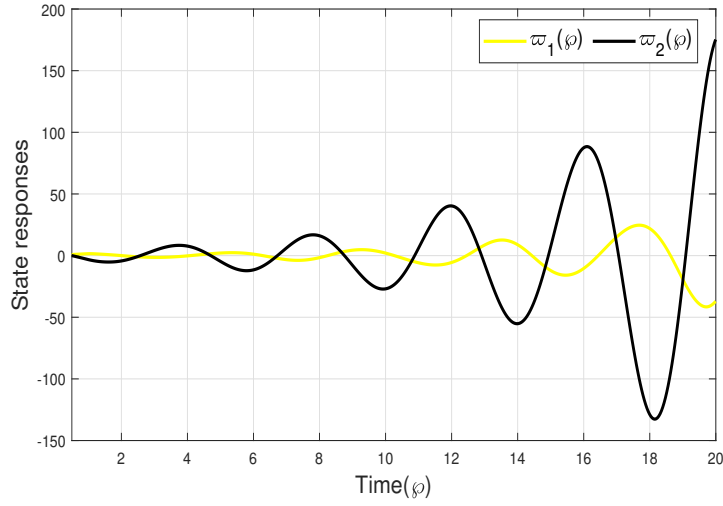


Figure 1: State response for discrete-time IT2 fuzzy system without control input.

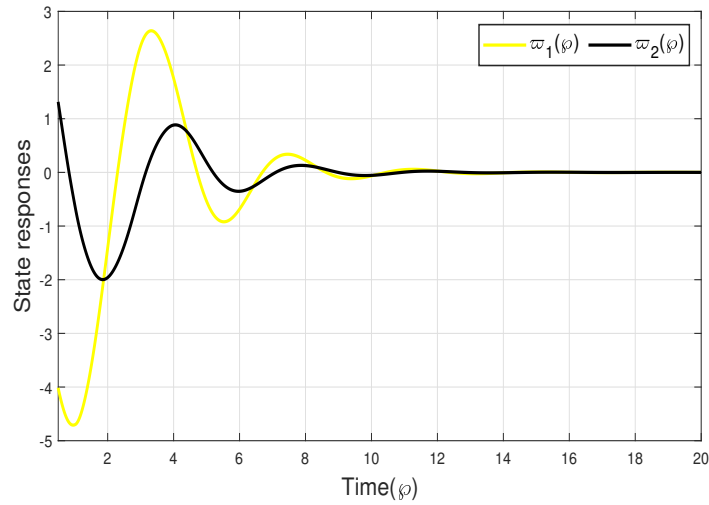


Figure 2: State response for discrete-time IT2 fuzzy system with control input.

where,

$$A_1 = \begin{bmatrix} 1 & T\rho \\ -\frac{TgLM_b}{J_b} & 1 - \frac{T\rho Q_a}{J_b} \end{bmatrix}, A_2 = \begin{bmatrix} 1 & T\rho \\ -\varsigma \frac{TgLM_b}{J_b} & 1 - \frac{T\rho Q_a}{J_b} \end{bmatrix}, A_{\iota 1} = A_{\iota 2} = \begin{bmatrix} 0 & T(1-\rho) \\ 0 & -\frac{T(1-\rho)Q_a}{J_b} \end{bmatrix},$$

$$B_{11} = B_{12} = \begin{bmatrix} 0 \\ T \end{bmatrix}, C_{11} = C_{12} = \begin{bmatrix} 0 \\ \frac{Q}{J_b} \end{bmatrix}, D_1 = D_2 = \begin{bmatrix} 1 \\ 0 \end{bmatrix}, B_{21} = B_{22} = 0.1, C_{21} = C_{22} = 0.$$

Choose $\lambda_d = 2^{-d-3}$, then we find that

$$\bar{\lambda}_d = \sum_{d=1}^{\infty} \lambda_d = \frac{1}{8} < \sum_{d=1}^{\infty} d\lambda_d = 2 < +\infty,$$

which satisfies the convergence condition (2).

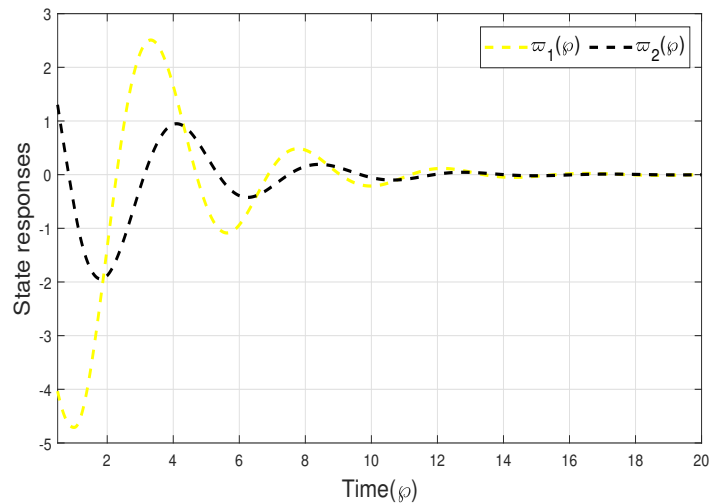


Figure 3: State response for discrete-time type-1 fuzzy system.

In addition, $\mathfrak{S} \in [9, 27]$ is the uncertain parameter. The IT2 fuzzy model can be used to effectively describe the uncertain parameters in this scenario. Table I and Table II, respectively, list the lower and upper membership functions of the original system and controller. Assume that the external disturbance $w(\varphi) = e^{1.5\varphi}$.

Table 1: The upper and lower membership functions of the original system.	
The upper membership functions	The lower membership functions
$\bar{\alpha}_1(\varpi(\varphi)) = 1 - \frac{e^{-\varpi_1^2(\varphi)}}{3}$	$\alpha_1(\varpi(\varphi)) = 1 - \frac{e^{-\varpi_1^2(\varphi)}}{6}$
$\bar{\alpha}_2(\varpi(\varphi)) = 1 - \bar{\alpha}_1(\varpi(\varphi))$	$\alpha_2(\varpi(\varphi)) = 1 - \alpha_1(\varpi(\varphi))$

Let $\underline{\pi}(\varpi(\varphi)) = 0.6\sin^2(\varpi(\varphi))$, $\bar{\pi}(\varpi(\varphi)) = 1 - \underline{\pi}(\varpi(\varphi))$, $\underline{\nu}(\varpi(\varphi)) = \bar{\nu}(\varphi(\varphi)) = 0.5$. Assume the generalized ETC performance be specified by $\iota_m = 1.2$, $\iota_M = 3.30$, $\lambda = 0.1$ and H_∞ performance level is chosen $\delta = 2.75$. By applying Theorem 3.3, the controller gain and event-triggered parameter matrices are obtained as follows:

$$K_1 = [0.5831 \quad 0.2233], K_2 = [-0.4992 \quad -0.3959], \Theta = \begin{bmatrix} 0.1856 & 0.0498 \\ 0.0493 & 0.1332 \end{bmatrix}. \quad (43)$$

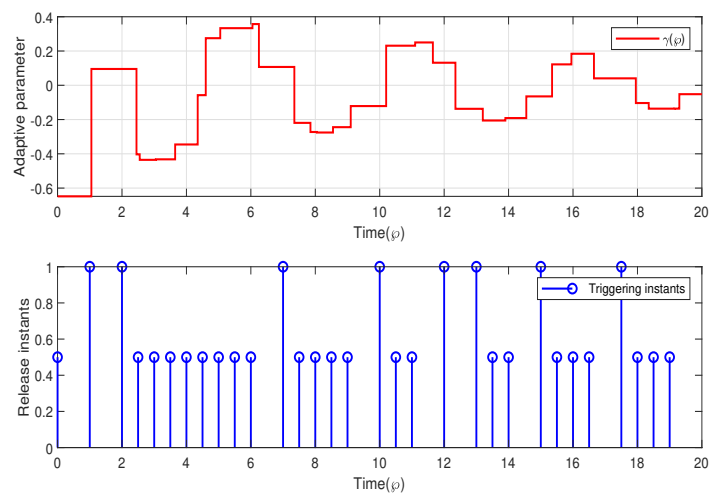


Figure 4: Curve of adaptive triggering parameter $\gamma(\varphi)$ and Triggering instants and intervals.

Table 2: The upper and lower membership functions for controller.	
The upper membership functions	The lower membership functions
$\bar{\beta}_1(\varpi(\varphi)) = \beta_1(\varpi(\varphi))$	$\beta_1(\varpi(\varphi)) = \frac{e^{-\varpi_1^2(\varphi)}}{6}$
$\bar{\beta}_2(\varpi(\varphi)) = 1 - \underline{\beta}_1(\varpi(\varphi))$	$\underline{\beta}_2(\varpi(\varphi)) = 1 - \underline{\beta}_1(\varpi(\varphi))$

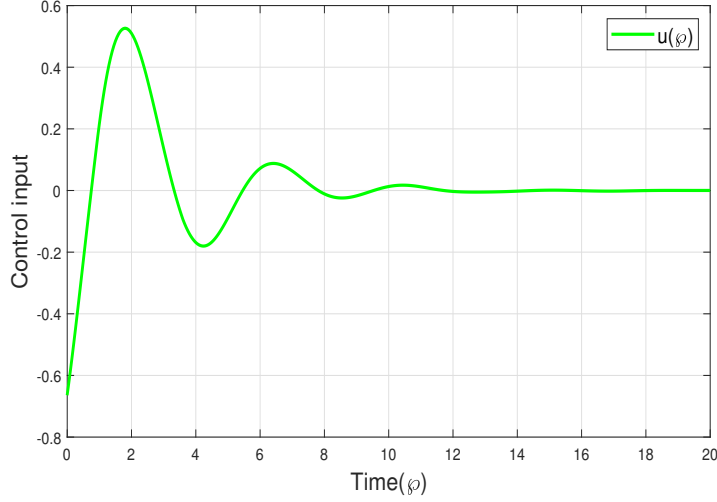


Figure 5: Trajectory of control input.

By choosing the sampling interval as $h = 0.05$ and assume the initial condition $\varpi(0) = [3.5, -1.5]^T$. State responses discrete-time IT2 fuzzy system without control input depicted in Fig. 1. When there is no control input, the system is unstable. State response for discrete-time IT2 fuzzy system with control input shown in Fig. 2. According to Fig. 2, it is clear that the state trajectories under the proposed control scheme are converging to zero within 10s. In Fig. 3, propose the state responses for discrete-time type-1 fuzzy system and its converging to zero within 14s. From Figure 2 and Figure 3, it is clear that the proposed IT2 fuzzy model is effective. The adaptive triggering parameter $\gamma(\varphi)$ and the triggered instants with intervals are described in Fig. 4. In Fig. 5, present trajectories of control input. We can conclude from the above simulation findings that the technique for discrete-time IT2 fuzzy system with designing AETS controllers in this work is effective.

Example 4.2. Consider an inverted pendulum controlled by a DC motor via a gear train [7] with discrete-time IT2 fuzzy systems under AETS.

We add some disturbance terms and a controllable output for simulation as follows.

Pant rule 1: IF $\varpi_1(\varphi)$ is $1 - \frac{\varpi_1^2(\varphi)}{3}$, THEN

$$\begin{cases} \varpi(\varphi + 1) &= \sum_{i=1}^q \sum_{j=1}^q \alpha_i \beta_j \{A_1 \varpi(\varphi) + A_{i1} \sum_{d=1}^{\infty} \lambda_d \varpi(\varphi - d) + B_{11} w(\varphi) + C_{11} u(\varphi)\}, \\ z(\varphi) &= \sum_{i=1}^q \sum_{j=1}^q \alpha_i \beta_j \{D_1 \varpi(\varphi) + B_{21} w(\varphi) + C_{21} u(\varphi)\}. \end{cases} \quad (44)$$

Pant rule 2: IF $\varpi_1(\varphi)$ is $\frac{\varpi_1^2(\varphi)}{3}$, THEN

$$\begin{cases} \varpi(\varphi + 1) &= \sum_{i=1}^q \sum_{j=1}^q \alpha_i \beta_j \{A_2 \varpi(\varphi) + A_{i2} \sum_{d=1}^{\infty} \lambda_d \varpi(\varphi - d) + B_{12} w(\varphi) + C_{12} u(\varphi)\}, \\ z(\varphi) &= \sum_{i=1}^q \sum_{j=1}^q \alpha_i \beta_j \{D_2 \varpi(\varphi) + B_{22} w(\varphi) + C_{22} u(\varphi)\}. \end{cases} \quad (45)$$

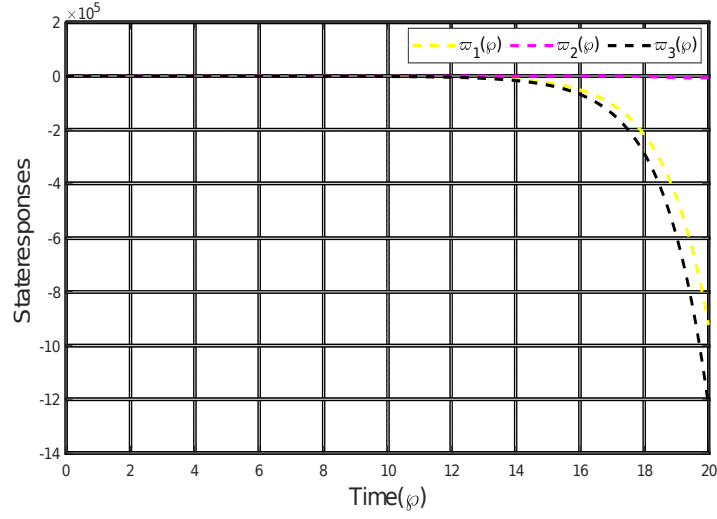


Figure 6: State response for discrete-time IT2 fuzzy system without control input.

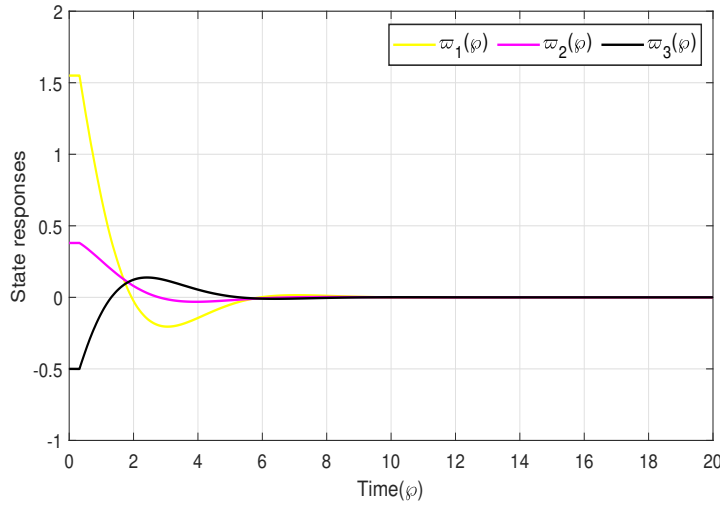


Figure 7: State response for discrete-time IT2 fuzzy system with control input.

where,

$$A_1 = \begin{bmatrix} 1.002 & 0.02 & 0.02 \\ 0.196 & 1.001 & 0.0181 \\ -0.0184 & -0.1813 & 0.8170 \end{bmatrix}, \quad A_2 = \begin{bmatrix} 1 & 0.02 & 0.0002 \\ 0 & 0.9981 & 0.0181 \\ 0 & -0.1811 & 0.8170 \end{bmatrix}, \quad B_{11} = \begin{bmatrix} 0.054 \\ 0.094 \\ 0 \end{bmatrix},$$

$$B_{12} = \begin{bmatrix} -0.054 \\ -0.094 \\ 0 \end{bmatrix}, \quad C_{11} = \begin{bmatrix} 0 \\ 0.0019 \\ 0.1811 \end{bmatrix}, \quad C_{12} = \begin{bmatrix} 0 \\ 0.0019 \\ 0.1811 \end{bmatrix}, \quad D_1 = \begin{bmatrix} 0.054 \\ 0.005 \\ 0.1 \end{bmatrix}, \quad D_2 = \begin{bmatrix} 0.054 \\ 0.005 \\ 0.1 \end{bmatrix},$$

$$B_{21} = 0.1, B_{22} = 0.1, C_{21} = 0.1, C_{22} = 0.1.$$

Choose $\lambda_d = 2^{-d-3}$, the we find that

$$\bar{\lambda}_d = \sum_{d=1}^{\infty} \lambda_d = \frac{1}{8} < \sum_{d=1}^{\infty} d\lambda_d = 2 < +\infty,$$

which satisfies the convergence condition (2).

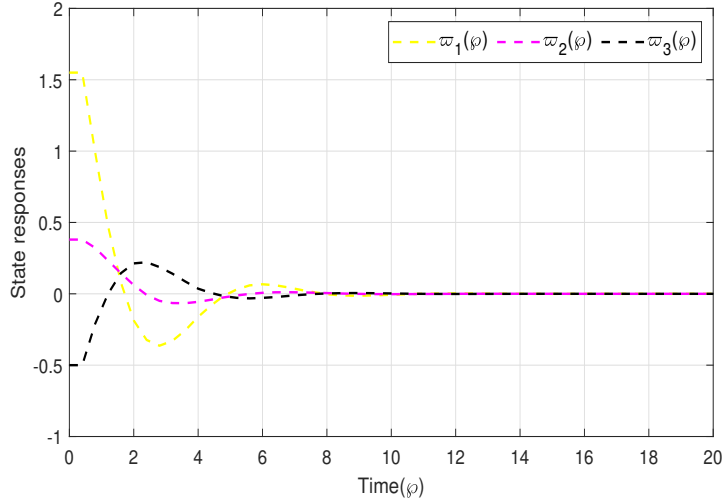


Figure 8: State response for discrete-time type-1 fuzzy system.

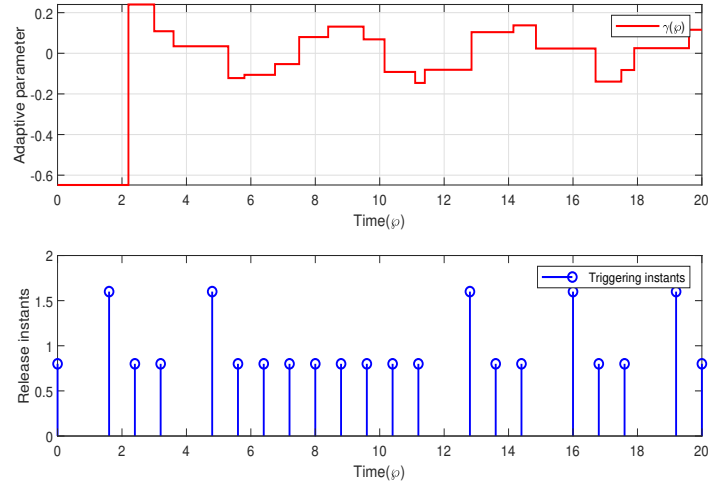


Figure 9: Curve of adaptive triggering parameter $\gamma(\varphi)$ and Triggering instants and intervals.

The IT2 fuzzy model can be used to effectively describe the uncertain parameters in this scenario. Table III and Table IV, respectively, list the lower and upper membership functions of the original system and controller. The external disturbance $w(\varphi)$ is assumed to be

$$w(\varphi) = \begin{cases} 0.2, & 0 \leq \varphi \leq 1 \\ -0.2, & 1 \leq \varphi \leq 2 \\ 0, & \text{others} \end{cases}$$

Table 3: The upper and lower membership functions of the original system.	
The upper membership functions	The lower membership functions
$\bar{\alpha}_1(\varpi(\varphi)) = 1 - \frac{1}{1+e^{-(2-\varpi_1(\varphi)+3)}}$	$\underline{\alpha}_1(\varpi(\varphi)) = 1 - \frac{1}{1+e^{-(2-\varpi_1(\varphi)+5)}}$
$\bar{\alpha}_2(\varpi(\varphi)) = 1 - \frac{1}{1+e^{-(2-\varpi_1(\varphi)-3)}}$	$\underline{\alpha}_2(\varpi(\varphi)) = 1 - \frac{1}{1+e^{-(2-\varpi_1(\varphi)-5)}}$

Let $\underline{\pi}(\varpi(\varphi)) = 0.4\sin^2(\varpi(\varphi))$, $\bar{\pi}(\varpi(\varphi)) = 1 - \underline{\pi}(\varpi(\varphi))$, $\underline{\nu}(\varpi(\varphi)) = \bar{\nu}(\varphi(\varphi)) = 0.6$. Assume the generalized ETC performance be specified by $\iota_m = 1.4$, $\iota_M = 3.10$, $\lambda = 0.2$, and H_∞ performance level is chosen as $\delta = 1.5$. By applying Theorem 3.3 for $\gamma_1 = 0.45$, the feedback controller gain can be obtained as

$$K_1 = [0.6844 \quad 0.0952 \quad 0.0479], K_2 = [0.6435 \quad -0.1995 \quad 0.0775].$$

Table 4: The upper and lower membership functions for controller.	
The upper membership functions	The lower membership functions
$\bar{\beta}_1(\varpi(\varphi)) = \beta_{-1}(\varpi(\varphi))$	$\beta_{-1}(\varpi(\varphi)) = \frac{e^{-\varpi_1^2(\varphi)}}{6}$
$\bar{\beta}_2(\varpi(\varphi)) = 1 - \beta_{-1}(\varpi(\varphi))$	$\beta_2(\varpi(\varphi)) = 1 - \beta_{-1}(\varpi(\varphi))$

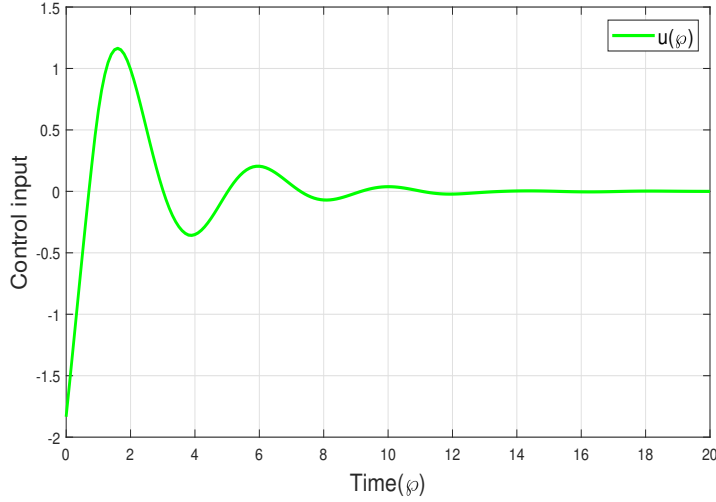


Figure 10: Trajectory of control input.

By choosing the sampling interval as $h = 0.07$ and assume the initial condition $\varpi(0) = [0.3, -0.8]^T$. State responses discrete-time IT2 fuzzy system without control input depicted in Fig. 6. State response for discrete-time IT2 fuzzy system with control input shown in Fig. 7. According to Fig. 7, it is clear that the state trajectories under the proposed control scheme are converging to zero within 5s. In Fig. 8. propose the state response for discrete-time type-1 fuzzy system are converging to zero within 7s. From Fig. 7 and Fig. 8, it is clear that the proposed IT2 fuzzy model is effective. The adaptive triggering parameter $\gamma(\varphi)$ and the triggered instants with intervals are is described in Fig. 9. In Fig. 10. present trajectories of control input. The simulation results clearly demonstrate the utility of the established theoretical results in the study of H_∞ control for discrete-time IT2 fuzzy systems via AETS.

Remark 4.3. *It must be observed that the type-1 fuzzy-model-based results cannot handle uncertain parameters. The lower and upper member functions in the IT2 fuzzy model of this paper are used to describe the uncertainties. The proposed IT2 fuzzy model approach is more general and effective in contrast to existing results [7, 24, 25]. In compared to existing work [18], our results are quickly converge, where the trajectories are converges to origin within 14s as shown in Fig.3.*

5 Conclusion

In this work, we have investigated the problem of H_∞ control for discrete-time IT2 fuzzy systems with infinite distributed delay via adaptive event-triggered scheme. Furthermore, the adaptive event-triggered technique was developed to reduce communication’s power consumption. The importance of the proposed technique in terms of state convergence, stability, and avoiding unwanted triggering events are illustrated by numerical simulations achieved with the examined discrete-time IT2 fuzzy system via an adaptive event-triggered scheme. In addition, IT2 is used to approximate the external disturbances of the system due to its better estimation ability to describe the fuzzy system uncertainties.

Also, by using the Lyapunov functional method, the resulting criterion guarantees that discrete-time IT2 fuzzy systems with efficiency H_∞ are mean-square exponentially stable. The effectiveness of the IT2 fuzzy system by using AETS approach is demonstrated by two examples of numerical simulation and real-world application. The authors will try to extend this in further studies by making resilient tracking control susceptible to a variety of attacks, including DoS, replay, and deception attacks. The theory's capacity to be applied to actual engineering practice is significantly improved.

Conflict of Interest The authors does not have any conflict of interest.

Acknowledgement:

The financial support from the National Research Council of Thailand (Talented Mid-Career Researchers) Grant Number N42A650250.

References

- [1] M. S. Ali, *Robust stability of stochastic uncertain recurrent neural networks with Markovian jumping parameters and time-varying delays*, International Journal of Machine Learning and Cybernetics, **5**(1) (2014), 13-22.
- [2] M. S. Aslam, X. Dai, T. Zhao, *Stability and stabilization of network T-S fuzzy systems with random packet-loss for synchronous machine*, Iranian Journal of Fuzzy Systems, **18**(1) (2021), 35-51.
- [3] P. Balasubramaniam, L. J. Banu, *Robust stability criterion for discrete-time nonlinear switched systems with randomly occurring delays via T-S fuzzy approach*, Information Sciences, **20**(6) (2015), 49-61.
- [4] B. Ding, B. Wang, R. Zhang, *Event-triggered control for hybrid power supply of fuel-cell heavy-duty truck*, Journal of Energy Storage, **41** (2021), 102985.
- [5] L. Fan, Q. Zhu, *Mean square exponential stability of discrete-time Markov switched stochastic neural networks with partially unstable subsystems and mixed delays*, Information Sciences, **580** (2021), 243-259.
- [6] M. Gao, L. Zhang, W. Qi, J. Cao, *Security control for T-S fuzzy systems with multi-sensor saturations and distributed event-triggered mechanism*, Journal of the Franklin Institute, **357**(5) (2020), 2851-2867.
- [7] H. Gao, Y. Zhao, T. Chen, *H_∞ fuzzy control of nonlinear systems under unreliable communication links*, ISA Transactions, **17**(2) (2009), 96-104.
- [8] A. Kazemy, J. Lam, Z. Chang, *Adaptive event-triggered mechanism for networked control systems under deception attacks with uncertain occurring probability*, International Journal of Systems Science, **52**(7) (2021), 1426-1439.
- [9] B. A. Khashoeei, D. J. Antunes, W. P. M. H. Heemels, *Output-based event-triggered control with performance guarantees*, IEEE Transactions on Automatic Control, **62**(7) (2017), 3646-3652.
- [10] Q. Li, Y. Pan, Z. Zhang, H. K. Lam, *Reliable dissipative interval type-2 fuzzy control for nonlinear systems with stochastic incomplete communication route and actuator failure*, International Journal of Fuzzy Systems, **22** (2020), 368-379.
- [11] Z. Lian, P. Shi, C. C. Lim, *Hybrid-triggered interval type-2 fuzzy control for networked systems under attacks*, Information Science, **567** (2021), 332-347.
- [12] Z. Lian, P. Shi, C. C. Lim, *Hybrid-triggered interval type-2 fuzzy control for networked systems under attacks*, Information Sciences, **567** (2022), 332-347.
- [13] J. Liu, Q. Liu, J. Cao, Y. Zhang, *Adaptive event-triggered H_∞ filtering for T-S fuzzy system with time delay*, Neurocomputing **189** (2015), 86-94.
- [14] Y. Liu, Z. Wang, J. Liang, X. Liu, *Synchronization and state estimation for discrete-time complex networks with distributed delays*, IEEE Transactions on Systems, Man, and Cybernetics: Systems, **38**(5) (2008), 1314-1325.
- [15] K. Mathiyalagan, R. Sakthivel, *Robust stabilization and H_∞ control for discrete-time stochastic genetic regulatory networks with time delays*, Canadian Journal of Physics, **90**(10) (2012), 939-953.

- [16] M. Mubeen Tajudeen, M. S. Ali, S. A. Kauser, K. Subkrajang, A. Jirawattanapanit, G. Rajchakit, *Adaptive event-triggered control for complex dynamical network with random coupling delay under stochastic deception attacks*, Hindawi Complexity, (2022). DOI: 10.1155/2022/8761612.
- [17] R. Pan, Y. Tana, D. Du, S. Fei, *Adaptive event-triggered synchronization control for complex networks with quantization and cyber-attacks*, Neurocomputing, **382** (2020), 249-258.
- [18] B. Priya, M. Mubeen Tajudeen, M. Syed Ali, G. Rajchakit, G. Kumar Thakur, *Event-triggered H_∞ control of complex dynamical networks subject to stochastic cyber-attacks by new two-sided delay-dependent LKF functional*, Journal of Control and Decision, (2023). Doi: 10.1080/23307706.2023.2240338.
- [19] Z. Qu, Z. Du, G. Zhang, *Sampled-Data H_∞ control for nonlinear dynamical intelligent fuzzy systems with time-varying delay*, 2022 34th Chinese Control and Decision Conference (CCDC), (2022), 4077-4084.
- [20] N. Rong, Z. Wang, *State-dependent asynchronous intermittent control for IT2 T-S fuzzy interconnected systems under deception attacks*, Nonlinear Dynamics, **100** (2020), 3433-3448.
- [21] A. W. A. Saif, M. Mudasar, M. Mysorewala, M. Elshafei, *Observer-based interval type-2 fuzzy logic control for nonlinear networked control systems with delays*, International Journal of Fuzzy Systems, **22** (2020), 380-399.
- [22] J. Sun, H. Zhang, Y. Wang, S. Sun, *Fault-tolerant control for stochastic switched IT2 fuzzy uncertain time-delayed nonlinear systems*, IEEE Transactions on Cybernetics, **52**(2) (2022), 1335-1346.
- [23] J. Suo, Z. Wang, B. Shen, *Pinning synchronization control for a class of discrete-time switched stochastic complex networks under event-triggered mechanism*, Nonlinear Analysis: Hybrid Systems, **37** (2020), 100886.
- [24] M. Syed Ali, M. Mubeen Tajudeen, G. Rajchakit, B. Priya, G. Kumar Thakur, *Adaptive event-triggered pinning synchronization control for complex networks with random saturation subject to hybrid cyber-attacks*, International Journal of Adaptive Control and Signal Processing, **37**(8) (2023), 2041-2062.
- [25] J. Tao, R. Lu, P. Shi, H. Su, Z. G. Wu, *Dissipativity-based reliable control for fuzzy Markov jump systems with actuator faults*, IEEE Transactions on Cybernetics, **47**(9) (2017), 2377-2388.
- [26] X. Wang, J. H. Park, H. Yang, Z. Yu, *Sampled-data-based \mathcal{H}_∞ fuzzy pinning synchronization of complex networked systems with adaptive event-triggered communications*, IEEE Transactions on Fuzzy Systems, **30**(7) (2022), 2254-2265.
- [27] G. Wei, G. Feng, Z. Wang, *Robust \mathcal{H}_∞ control for discrete-time fuzzy systems with infinite-distributed delays*, IEEE Transactions on Fuzzy Systems, **17**(1) (2009). DOI:10.1109/TFUZZ.2008.2006621.
- [28] Y. Yan, C. Yang, X. Ma, L. Zhou, *Observer-based event-triggered control for singularly perturbed systems with saturating actuator*, International Journal of Robust and Nonlinear Control, **29**(12) (2019), 3954-3970.
- [29] L. Yang, C. Guan, Z. Fei, *Finite-time asynchronous filtering for switched linear systems with an event-triggered mechanism*, Journal of the Franklin Institute, **356**(10) (2015), 5503-5520.
- [30] X. Yang, H. Wang, Q. Zhu, *Event-triggered predictive control of nonlinear stochastic systems with output delay*, Automatica, **140** (2022), 110230.
- [31] X. Yang, Q. Zhu, *Stabilization of stochastic retarded systems based on sampled-data feedback control*, IEEE Transactions on Systems, Man, and Cybernetics: Systems, **51**(9) (2021), 5895-5904.
- [32] H. Zhang, Q. Ma, J. Lu, Y. Chu, Y. Li, *Synchronization control of neutral-type neural networks with sampled-data via adaptive event-triggered communication scheme*, Journal of the Franklin Institute, **358**(3) (2021), 1999-2014.
- [33] S. Zhang, J. Zhao, *Dwell-time-dependent H_∞ bumpless transfer control for discrete-time switched interval type-2 fuzzy systems*, IEEE Transactions on Fuzzy Systems, **30**(7) (2022), 2426-2437.
- [34] D. Zhang, Z. Zhou, X. Ji, *Networked fuzzy output feedback control for discrete-time Takagi-Sugeno fuzzy systems with sensor saturation and measurement noise*, Information Sciences, **457**(8) (2018), 182-194.
- [35] N. Zhao, P. Shi, W. Xing, C. P. Lim, *Resilient adaptive event-triggered fuzzy tracking control and filtering for nonlinear networked systems under denial-of-service attacks*, IEEE Transactions on Fuzzy Systems, **30**(8) (2022), 3191-3201.

- [36] Y. Zeng, H. K. Lam, B. Xiao, L. Wu, *$l_2 - l_\infty$ control of discrete-time state-delay interval type-2 fuzzy systems via dynamic output feedback*, IEEE Transactions on Cybernetics, **52**(6) (2022), 4198-4208.
- [37] Q. Zhu, *Stabilization of stochastic nonlinear delay systems with exogenous disturbances and the event-triggered feedback control*, IEEE Transactions on Automatic Control, **64**(9) (2019), 3764-3771.



Research article

Security-guaranteed filter design for discrete-time Markovian jump delayed systems subject to deception attacks and sensor saturation

M. Syed Ali ^a [✉](#), M. Mubeen Tajudeen ^a [✉](#), Oh-Min Kwon ^b [✉](#), Banadana Priya ^c, Ganesh Kumar Thakur ^d[Show more](#) [✓](#)[Share](#) [Cite](#)<https://doi.org/10.1016/j.isatra.2023.10.020> [↗](#)[Get rights and content](#) [↗](#)

Abstract



This work is devoted the problem of a security-guaranteed filter design for a class of discrete-time Markov jump systems that are vulnerable to stochastic deception attacks and have random sensor saturation. Deception attacks, in particular, are taken into account in the filter when the attacker attempts to modify the broadcast signal in communication networks by inserting some misleading information data into the assessment output. The Bernoulli distribution is satisfied by two sets of introduced stochastic variables. It shows the likelihood that the broadcaster's data transmissions will be the focus of deception attacks and sensor saturation. The Lyapunov functional technique is established, and criteria are derived to ensure that the system is mean-square stable. Furthermore, explicit expression of the filter gains is obtained by solving a set of linear matrix inequalities. Lastly, two simulation examples including a synthetic genetic regulatory network are provided to further demonstrate the validity and efficiency of the suggested theoretical results.

Introduction

Discrete-time systems have a strong tradition in engineering applications. The study of time-delay systems with controller design and stability analysis has become a popular research topic in recent years, with a number of famous results being reported [1], [2], [3]. State bounding estimation of positive singular discrete-time systems with unbounded time-varying delays in [4]. Finite-time output feedback control for nonlinear networked discrete-time systems with an adaptive event-triggered scheme discussed in [5]. Recent developments in discrete-time delay state systems involve tighter sum over bounds Wirtinger's inequality, resulting in less conservative analysis requirements. H_∞ filtering for discrete-time systems with time-varying delay is studied in [6]. Discrete-time switched systems with randomly occurring delays via T-S fuzzy model [7].

Article

Global Asymptotic Stability and Synchronization of Fractional-Order Reaction–Diffusion Fuzzy BAM Neural Networks with Distributed Delays via Hybrid Feedback Controllers

M. Syed Ali ¹, Gani Stamov ^{2,*}, Ivanka Stamova ² , Tarek F. Ibrahim ³ , Arafa A. Dawood ⁴ and Fathea M. Osman Birkea ⁵

¹ Department of Mathematics, Thiruvalluvar University, Vellore 632115, Tamil Nadu, India; syed@tvu.edu.in

² Department of Mathematics, University of Texas at San Antonio, San Antonio, TX 78249, USA; ivanka.stamova@utsa.edu

³ Department of Mathematics, Faculty of Sciences and Arts (Mahayel), King Khalid University, Abha 62529, Saudi Arabia; tfoze@kku.edu.sa

⁴ Department of Mathematics, Faculty of Sciences and Arts in Sarat Abeda, King Khalid University, Abha 62529, Saudi Arabia; adawood@kku.edu.sa

⁵ Department of Mathematics, Faculty of Science, Northern Border University, Arar 1321, Saudi Arabia; fathia.birkea@nbu.edu.sa

* Correspondence: gani.stamov@utsa.edu

Abstract: In this paper, the global asymptotic stability and global Mittag–Leffler stability of a class of fractional-order fuzzy bidirectional associative memory (BAM) neural networks with distributed delays is investigated. Necessary conditions are obtained by means of the Lyapunov functional method and inequality techniques. The hybrid feedback controllers are then developed to ensure the global asymptotic synchronization of these neural networks, resulting in two additional synchronization criteria. The derived conditions are applied to check the fractional-order fuzzy BAM neural network’s Mittag–Leffler stability and synchronization. Three examples are given to demonstrate the effectiveness of the achieved results.

Keywords: fractional-order system; bidirectional associative memory neural networks; distributed delays; global asymptotic stability; global Mittag–Leffler stability; reaction–diffusion terms

MSC: 26A33; 34K36; 34K37; 34K20; 93D20



Citation: Syed Ali, M.; Stamov, G.; Stamova, I.; Ibrahim, T.F.; Dawood, A.A.; Osman Birkea, F.M. Global Asymptotic Stability and Synchronization of Fractional-Order Reaction–Diffusion Fuzzy BAM Neural Networks with Distributed Delays via Hybrid Feedback Controllers. *Mathematics* **2023**, *11*, 4248. <https://doi.org/10.3390/math11204248>

Academic Editors: Pedro Navas and Bo Li

Received: 4 September 2023

Revised: 2 October 2023

Accepted: 10 October 2023

Published: 11 October 2023



Copyright: © 2023 by the authors. Licensee MDPI, Basel, Switzerland. This article is an open access article distributed under the terms and conditions of the Creative Commons Attribution (CC BY) license (<https://creativecommons.org/licenses/by/4.0/>).

1. Introduction

On the parallel perspective, neural networks having fractional-order derivatives generally possess boundless memory, which finds an advantage in comparison with common integer-order neural networks. In fact, the memory and heredity properties of certain materials and processes are known to be better represented by fractional-order derivatives [1,2]. Because of its wide range of applications in areas such as neural networks, quantum physics, optical systems, and optical image processing, fractional-order systems have been extensively investigated during the last several decades as a technique for precisely describing real systems [3–11].

In addition, there is a class of fuzzy cellular neural networks with delays that has been studied by numerous researchers using a variety of analytical and numerical methodologies. In comparison to normal cellular neural networks, a fuzzy cellular neural network uses fuzzy logic between its template input and/or output in addition to the sum of product operations. Hence, there has been a lot of research activity in the area of delayed fuzzy cellular neural networks [12–14], including recently studied fractional-order cases [15,16].

Bidirectional associative memory (BAM) neural networks with two layers of neuronal cells were first introduced by Kosko [17]. The neurons in the first layer are fully interconnected with the neurons in the second layer, but there is no interconnect between neurons in the same layer. Due to their application in numerous disciplines such as image and signal processing, pattern recognition, optimization, and autonomous control, BAM neural networks have received a lot of attention in the last decade [18,19]. As a result, the stability of BAM neural networks has been extensively studied, and many stability requirements for BAM neural networks have been published [20–22].

Global asymptotic stability is one of the most investigated stability behavior of real-world neural systems and artificial neural network systems. This is due to the fact that a globally asymptotically stable neural network system is promising for a fast convergence rate to a state of interest. The global asymptotic stability of an error neural network is closely related to the global asymptotic synchronization of the master and response systems. That is why global asymptotic stability and global asymptotic synchronization have received much attention among researchers [1,13,20,22]. Both notions are studied for integer-order as well as for fractional-order problems.

Podlubny and his coauthors proposed in [23] the Mittag–Leffler stability notion and the fractional Lyapunov direct approach to extend the use of fractional calculus in nonlinear systems, with the goal of improving both system theory and fractional calculus knowledge. Since then, the stability of Mittag–Leffler, generalized Mittag–Leffler stability, and synchronization have been examined for different classes of fractional-order neural networks [24–27], including BAM neural network models [28,29].

It is evident from the literature that most research work on delayed neural networks are devoted to simple cases of discrete delays. However, due to the presence of numerous parallel ways, neural networks usually exhibit a unique nature, resulting in a distribution of conduction velocities and propagation delays along these pathways. Due to the presence of a large number of parallel routes with different axon diameters and lengths, neural networks usually have a spatial extent. As a result, there will be a distribution of conduction velocities and propagation delays along these pathways. In these cases, signal transmission is not instantaneous and cannot be described using discrete delays; instead, continuously distributed and infinite delays are more appropriate [1,16,22,30–33].

When electrons move in asymmetric electromagnetic fields, diffusion effects cannot be avoided in the complex network models strictly speaking [2,12,34–39]. In signal transmission, the signal becomes weak due to diffusion, so it is very important to consider that the activation varies in space as well as in time, and the reaction–diffusion effects cannot be neglected in both biological and man-made networks [40]. The models covering time delay and reaction–diffusion are good mimicry for real neural networks in terms of application, but the existence of time delays and reaction–diffusion could bring about some undesirable behavior.

Motivated by the above considerations, we have studied the global asymptotic stability of fractional-order fuzzy BAM reaction–diffusion neural networks with discrete and distributed delays via hybrid feedback controllers. The main contributions of this research are:

1. The global asymptotic stability and synchronization of fractional-order fuzzy BAM neural networks with reaction–diffusion terms and mixed delays, including distributed ones, are investigated via hybrid feedback controllers.
2. By applying of stability theory for fractional models together with some inequality strategies, efficient criteria are obtained to guarantee the global Mittag–Leffler stability and synchronization.
3. We establish a uniform approach to dealing with discrete and distributed time delays under more general activation function assumptions.
4. The established conditions include the positive influence of reaction–diffusion terms on the stability and synchronization behavior and reduce the conservatism of the existing ones.

5. Finally, numerical examples are provided to demonstrate the correctness of the proposed results.

The rest of the paper is organized as follows. Some preliminary definitions and results related to fractional calculus are given in Section 2. The fractional-order fuzzy BAM neural network model, together with the controlled one are also introduced. Section 3 is devoted to our global asymptotic stability results. Global Mittag–Leffler synchronization criteria are established in Section 4. In Section 5, we elaborate some examples to demonstrate the validity and feasibility of the established results. Some conclusion notes and future directions of our research are discussed in Section 6.

2. Preliminaries and Problem Definition

In the present section, we first introduce some basic definitions and the corresponding results that are used later. Then, the fractional-order fuzzy BAM neural network model is formulated.

Definition 1 ([41]). *The Caputo fractional derivative of order β for a function $f(t)$ is defined by*

$$D^\beta f(t) = \frac{1}{\Gamma(n - \beta)} \int_b^t (t - \tau)^{n-\beta-1} f^{(n)}(\tau) d\tau,$$

in which $t \geq b, t \in \mathbb{R}, n - 1 < \beta < n \in \mathbb{N}$, and Γ is the standard Gamma function.

In this paper, we consider the following fractional-order reaction–diffusion fuzzy BAM neural network with mixed delays

$$\begin{aligned} \frac{\partial^\lambda \zeta_\varphi(t, \wp)}{\partial t^\lambda} &= \sum_{k=1}^q \frac{\partial}{\partial \zeta_k} \left(m_{\varphi k} \frac{\partial \zeta_\varphi(t, \wp)}{\partial \wp_k} \right) - d_\varphi \zeta_\varphi(t, \wp) + \sum_{\omega=1}^n c_{\varphi\omega} f_\omega(\mathfrak{S}_\omega(t, \wp)) \\ &+ \sum_{\omega=1}^n a_{\varphi\omega} f_\omega(\mathfrak{S}_\omega(t - \tau, \wp)) \\ &+ \bigwedge_{\omega=1}^n u_{\varphi\omega} \int_0^\infty k_{\varphi\omega}(s) f_\omega(\mathfrak{S}_\omega(s - \tau, \wp)) ds + \bigwedge_{\omega=1}^n P_{\varphi\omega} \mathfrak{S}_\omega(t, \wp) \\ &+ \bigvee_{\omega=1}^n v_{\varphi\omega} \int_0^\infty k_{\varphi\omega}(s) f_\omega(\mathfrak{S}_\omega(s - \tau, \wp)) ds + \bigvee_{\omega=1}^n Q_{\varphi\omega} \mathfrak{S}_\omega(t, \wp) + I_\varphi, \varphi = 1, 2, \dots, o, \\ \frac{\partial^\lambda \mathfrak{S}_\omega(t, \wp)}{\partial t^\lambda} &= \sum_{k=1}^q \frac{\partial}{\partial \mathfrak{S}_k} \left(\tilde{m}_{\omega k} \frac{\partial \mathfrak{S}_\omega(t, \wp)}{\partial \wp_k} \right) - \tilde{d}_\omega \mathfrak{S}_\omega(t, \wp) + \sum_{\varphi=1}^o \tilde{c}_{\omega\varphi} g_\varphi(\zeta_\varphi(t, \wp)) \\ &+ \sum_{\varphi=1}^o \tilde{a}_{\omega\varphi} g_\varphi(\zeta_\varphi(t - \tau, \wp)) \\ &+ \bigwedge_{\varphi=1}^o \tilde{u}_{\omega\varphi} \int_0^\infty k_{\omega\varphi}(s) g_\varphi(\zeta_\varphi(s - \tau, \wp)) ds + \bigwedge_{\varphi=1}^o \tilde{P}_{\omega\varphi} \zeta_\varphi(t, \wp) \\ &+ \bigvee_{\varphi=1}^o \tilde{v}_{\omega\varphi} \int_0^\infty k_{\omega\varphi}(s) g_\varphi(\zeta_\varphi(s - \tau, \wp)) ds + \bigvee_{\varphi=1}^o \tilde{Q}_{\omega\varphi} \zeta_\varphi(t, \wp) + J_\omega, \omega = 1, 2, \dots, n, \end{aligned} \tag{1}$$

where n and o denote the number of neurons in the \mathfrak{S} -layer and ζ -layer, respectively. For $\varphi = 1, 2, \dots, o, \omega = 1, 2, \dots, n$, and $\wp = (\wp_1, \wp_2, \dots, \wp_q)^T \in \Omega \subset R^q, \Omega$ is a bounded compact set with a smooth boundary $\partial\Omega$, and $\text{mess}(\Omega) > 0$ in the space R^q ; $\zeta_\varphi(t, \wp)$ and $\mathfrak{S}_\omega(t, \wp)$ are the states of the φ th neuron and the ω th neurons at time t and space \wp , respectively; d_φ and \tilde{d}_ω indicate the rates with which the φ th neuron and ω th neuron will reset their potentials to the resting states in isolation when disconnecting the network and external inputs; $c_{\varphi\omega}, a_{\varphi\omega}, \tilde{c}_{\omega\varphi}$, and $\tilde{a}_{\omega\varphi}$ are elements of the fuzzy feedback MIN template and fuzzy feed-forward MIN template, fuzzy feedback MAX template, and fuzzy feed-

forward MAX template, respectively; τ is the discrete transmission delay; \wedge and \vee denote the fuzzy AND and fuzzy OR operations, respectively; I_φ and J_ω denote the external inputs on the φ th neurons in the \mathfrak{S} -layer and the ω th neurons in the ζ -layer, respectively. The smooth functions $m_{\varphi k} \geq 0$ and $\tilde{m}_{\omega k} \geq 0$ correspond to the transmission diffusion operators along the φ th neurons and the ω th neurons, respectively, $u_{\varphi\omega}$, $v_{\omega\varphi}$, $P_{\omega\varphi}$, and $Q_{\omega\varphi}$ are elements of the fuzzy feedback MIN template and fuzzy feedback MAX template in the \mathfrak{S} -layer, respectively. $\tilde{u}_{\varphi\omega}$, $\tilde{v}_{\omega\varphi}$, $\tilde{P}_{\omega\varphi}$, and $\tilde{Q}_{\omega\varphi}$ are elements of the fuzzy feedback MIN template and fuzzy feedback MAX template in the ζ -layer. $k_{\varphi\omega}(\cdot)$ and $k_{\omega\varphi}(\cdot)$ are delay kernels functions. $f_\omega(\cdot)$ and $g_\varphi(\cdot)$ are signal transmission functions of ω th neurons and φ th neurons, respectively, and

$$\frac{\partial^\lambda p(t, \varphi)}{\partial t^\lambda} = \frac{1}{\Gamma(1-\lambda)} \int_0^t \frac{\partial p(s, \varphi)}{\partial s} \frac{ds}{(t-s)^\lambda}, \quad t > 0, \quad 0 < \lambda < 1$$

for a function $p \in C^1[[0, b] \times \Omega, \mathbb{R}]$, $b > 0$ [7].

The corresponding response system with feedback controllers $\mathcal{U}_\varphi(t, \varphi)$ and $\mathcal{U}_\omega(t, \varphi)$ is described by

$$\begin{aligned} \frac{\partial^\lambda \bar{\zeta}_\varphi(t, \varphi)}{\partial t^\lambda} &= \sum_{k=1}^q \frac{\partial}{\partial \varphi_k} \left(m_{\varphi k} \frac{\partial \bar{\zeta}_\varphi(t, \varphi)}{\partial \varphi_k} \right) - d_\varphi \bar{\zeta}_\varphi(t, \varphi) + \sum_{\omega=1}^n c_{\varphi\omega} f_\omega(\bar{\mathfrak{S}}_\omega(t, \varphi)) \\ &+ \sum_{\omega=1}^n a_{\varphi\omega} f_\omega(\bar{\mathfrak{S}}_\omega(t-\tau, \varphi)) + \bigwedge_{\omega=1}^n u_{\varphi\omega} \int_0^\infty k_{\varphi\omega}(s) f_\omega(\bar{\mathfrak{S}}_\omega(s-\tau, \varphi)) ds \\ &+ \bigwedge_{\omega=1}^n P_{\varphi\omega} \bar{\mathfrak{S}}_\omega(t, \varphi) + \bigvee_{\omega=1}^n v_{\varphi\omega} \int_0^\infty k_{\varphi\omega}(s) f_\omega(\bar{\mathfrak{S}}_\omega(s-\tau, \varphi)) ds \\ &+ \bigvee_{\omega=1}^n Q_{\varphi\omega} \bar{\mathfrak{S}}_\omega(t, \varphi) + I_\varphi + \mathcal{U}_\varphi(t, \varphi), \quad \varphi = 1, 2, \dots, o, \\ \frac{\partial^\lambda \bar{\mathfrak{S}}_\omega(t, \varphi)}{\partial t^\lambda} &= \sum_{k=1}^q \frac{\partial}{\partial \varphi_k} \left(\tilde{m}_{\omega k} \frac{\partial \bar{\mathfrak{S}}_\omega(t, \varphi)}{\partial \varphi_k} \right) - \tilde{d}_\omega \bar{\mathfrak{S}}_\omega(t, \varphi) + \sum_{\varphi=1}^o \tilde{c}_{\omega\varphi} g_\varphi(\bar{\zeta}_\varphi(t, \varphi)) \\ &+ \sum_{\varphi=1}^o \tilde{a}_{\omega\varphi} g_\varphi(\bar{\zeta}_\varphi(t-\tau, \varphi)) + \bigwedge_{\varphi=1}^o \tilde{u}_{\omega\varphi} \int_0^\infty k_{\omega\varphi}(s) g_\varphi(\bar{\zeta}_\varphi(s-\tau, \varphi)) ds \\ &+ \bigwedge_{\varphi=1}^o \tilde{P}_{\omega\varphi} \bar{\zeta}_\varphi(t, \varphi) + \bigvee_{\varphi=1}^o \tilde{v}_{\omega\varphi} \int_0^\infty k_{\omega\varphi}(s) g_\varphi(\bar{\zeta}_\varphi(s-\tau, \varphi)) ds \\ &+ \bigvee_{\varphi=1}^o \tilde{Q}_{\omega\varphi} \bar{\zeta}_\varphi(t, \varphi) + J_\omega + \mathcal{U}_\omega(t, \varphi), \quad \omega = 1, 2, \dots, n. \end{aligned} \tag{2}$$

For $\xi_\varphi(t, \varphi) = \bar{\zeta}_\varphi(t, \varphi) - \zeta_\varphi(t, \varphi)$ and $\bar{\xi}_\omega(t, \varphi) = \bar{\mathfrak{S}}_\omega(t, \varphi) - \mathfrak{S}_\omega(t, \varphi)$, the error system is defined by

$$\begin{aligned} \frac{\partial^\lambda \xi_\varphi(t, \varphi)}{\partial t^\lambda} &= \sum_{k=1}^q \frac{\partial}{\partial \varphi_k} \left(m_{\varphi k} \frac{\partial \xi_\varphi(t, \varphi)}{\partial \varphi_k} \right) - d_\varphi \xi_\varphi(t, \varphi) \\ &+ \left[\sum_{\omega=1}^n c_{\varphi\omega} f_\omega(\tilde{\mathfrak{S}}_\omega(t, \varphi)) - \sum_{\omega=1}^n c_{\varphi\omega} f_\omega(\mathfrak{S}_\omega(t, \varphi)) \right] \\ &+ \left[\sum_{\omega=1}^n a_{\varphi\omega} f_\omega(\tilde{\mathfrak{S}}_\omega(t - \tau, \varphi)) - \sum_{\omega=1}^n a_{\varphi\omega} f_\omega(\mathfrak{S}_\omega(t - \tau, \varphi)) \right] \\ &+ \left[\bigwedge_{\omega=1}^n u_{\varphi\omega} \int_0^\infty k_{\varphi\omega}(s) f_\omega(\tilde{\mathfrak{S}}_\omega(s - \tau, \varphi)) ds - \bigwedge_{\omega=1}^n u_{\varphi\omega} \int_0^\infty k_{\varphi\omega}(s) f_\omega(\mathfrak{S}_\omega(s - \tau, \varphi)) ds \right] \\ &+ \left[\bigvee_{\omega=1}^n v_{\varphi\omega} \int_0^\infty k_{\varphi\omega}(s) f_\omega(\tilde{\mathfrak{S}}_\omega(s - \tau, \varphi)) ds - \bigvee_{\omega=1}^n v_{\varphi\omega} \int_0^\infty k_{\varphi\omega}(s) f_\omega(\mathfrak{S}_\omega(s - \tau, \varphi)) ds \right] \\ &+ \mathcal{U}_\varphi(t, \varphi), \quad \varphi = 1, 2, \dots, o, \end{aligned}$$

$$\begin{aligned} \frac{\partial^\lambda \bar{\xi}_\omega(t, \varphi)}{\partial t^\lambda} &= \sum_{k=1}^q \frac{\partial}{\partial \varphi_k} \left(\tilde{m}_{\omega k} \frac{\partial \bar{\xi}_\omega(t, \varphi)}{\partial \varphi_k} \right) - \tilde{d}_\omega \bar{\xi}_\omega(t, \varphi) \\ &+ \left[\sum_{\varphi=1}^o \tilde{c}_{\omega\varphi} g_\varphi(\bar{\xi}_\varphi(t, \varphi)) - \sum_{\varphi=1}^o \tilde{c}_{\omega\varphi} g_\varphi(\xi_\varphi(t, \varphi)) \right] \\ &+ \left[\sum_{\varphi=1}^o \tilde{a}_{\omega\varphi} g_\varphi(\bar{\xi}_\varphi(t - \tau, \varphi)) - \sum_{\varphi=1}^o \tilde{a}_{\omega\varphi} g_\varphi(\xi_\varphi(t - \tau, \varphi)) \right] \\ &+ \left[\bigwedge_{\varphi=1}^o \tilde{u}_{\omega\varphi} \int_0^\infty k_{\omega\varphi}(s) g_\varphi(\bar{\xi}_\varphi(s - \tau, \varphi)) ds - \bigwedge_{\varphi=1}^o \tilde{u}_{\omega\varphi} \int_0^\infty k_{\omega\varphi}(s) g_\varphi(\xi_\varphi(s - \tau, \varphi)) ds \right] \\ &+ \left[\bigvee_{\varphi=1}^o \tilde{v}_{\omega\varphi} \int_0^\infty k_{\omega\varphi}(s) g_\varphi(\bar{\xi}_\varphi(s - \tau, \varphi)) ds - \bigvee_{\varphi=1}^o \tilde{v}_{\omega\varphi} \int_0^\infty k_{\omega\varphi}(s) g_\varphi(\xi_\varphi(s - \tau, \varphi)) ds \right] \\ &+ \mathcal{U}_\omega(t, \varphi), \quad \omega = 1, 2, \dots, n. \end{aligned} \tag{3}$$

We design a suitable controller for the error system (3). Let $\mathcal{U}_\varphi(t, \varphi) = \mathcal{U}_{1\varphi}(t, \varphi) + \mathcal{U}_{2\varphi}(t, \varphi)$, where $\mathcal{U}_{1\varphi}(t, \varphi) = -\mathfrak{t}_\varphi \xi_\varphi(t, \varphi)$ and $\mathcal{U}_{2\varphi}(t, \varphi) = -\Psi_\varphi \xi_\varphi(t, \varphi)$ and $\mathcal{U}_\omega(t, \varphi) = \mathcal{U}_{1\omega}(t, \varphi) + \mathcal{U}_{2\omega}(t, \varphi)$, where $\mathcal{U}_{1\omega}(t, \varphi) = -\omega_\omega \bar{\xi}_\omega(t, \varphi)$ and $\mathcal{U}_{2\omega}(t, \varphi) = -\varrho_\omega \bar{\xi}_\omega(t, \varphi)$, where $\mathfrak{t}_\varphi, \Psi_\varphi, \omega_\omega$, and ϱ_ω are positive constants. Then, system (3) has the form

$$\begin{aligned} \frac{\partial^\lambda \xi_\varphi(t, \varphi)}{\partial t^\lambda} &= \sum_{k=1}^q \frac{\partial}{\partial \varphi_k} \left(m_{\varphi k} \frac{\partial \xi_\varphi(t, \varphi)}{\partial \varphi_k} \right) - d_\varphi \xi_\varphi(t, \varphi) \\ &+ \left[\sum_{\omega=1}^n c_{\varphi\omega} f_\omega(\tilde{\mathfrak{S}}_\omega(t, \varphi)) - \sum_{\omega=1}^n c_{\varphi\omega} f_\omega(\mathfrak{S}_\omega(t, \varphi)) \right] \\ &+ \left[\sum_{\omega=1}^n a_{\varphi\omega} f_\omega(\tilde{\mathfrak{S}}_\omega(t - \tau, \varphi)) - \sum_{\omega=1}^n a_{\varphi\omega} f_\omega(\mathfrak{S}_\omega(t - \tau, \varphi)) \right] \\ &+ \left[\bigwedge_{\omega=1}^n u_{\varphi\omega} \int_0^\infty k_{\varphi\omega}(s) f_\omega(\tilde{\mathfrak{S}}_\omega(s - \tau, \varphi)) ds - \bigwedge_{\omega=1}^n u_{\varphi\omega} \int_0^\infty k_{\varphi\omega}(s) f_\omega(\mathfrak{S}_\omega(s - \tau, \varphi)) ds \right] \\ &+ \left[\bigvee_{\omega=1}^n v_{\varphi\omega} \int_0^\infty k_{\varphi\omega}(s) f_\omega(\tilde{\mathfrak{S}}_\omega(s - \tau, \varphi)) ds - \bigvee_{\omega=1}^n v_{\varphi\omega} \int_0^\infty k_{\varphi\omega}(s) f_\omega(\mathfrak{S}_\omega(s - \tau, \varphi)) ds \right] \\ &- \mathfrak{t}_\varphi \xi_\varphi(t, \varphi) - \Psi_\varphi \xi_\varphi(t, \varphi), \quad \varphi = 1, 2, \dots, o, \end{aligned}$$

$$\begin{aligned}
 \frac{\partial^\lambda \bar{\xi}_\omega(t, \wp)}{\partial t^\lambda} &= \sum_{k=1}^q \frac{\partial}{\partial \wp_k} \left(\bar{m}_{\omega k} \frac{\partial \bar{\xi}_\omega(t, \wp)}{\partial \wp_k} \right) - \bar{d}_\omega \bar{\xi}_\omega(t, \wp) \\
 &+ \left[\sum_{\varphi=1}^o \bar{c}_{\omega\varphi} g_\varphi(\bar{\zeta}_\varphi(t, \wp)) - \sum_{\varphi=1}^o \bar{c}_{\omega\varphi} g_\varphi(\zeta_\varphi(t, \wp)) \right] \\
 &+ \left[\sum_{\varphi=1}^o \bar{a}_{\omega\varphi} g_\varphi(\bar{\zeta}_\varphi(t - \tau, \wp)) - \sum_{\varphi=1}^o \bar{a}_{\omega\varphi} g_\varphi(\zeta_\varphi(t - \tau, \wp)) \right] \\
 &+ \left[\bigwedge_{\varphi=1}^o \bar{u}_{\omega\varphi} \int_0^\infty k_{\omega\varphi}(s) g_\varphi(\bar{\zeta}_\varphi(s - \tau, \wp)) ds - \bigwedge_{\varphi=1}^o \bar{u}_{\omega\varphi} \int_0^\infty k_{\omega\varphi}(s) g_\varphi(\zeta_\varphi(s - \tau, \wp)) ds \right] \\
 &+ \left[\bigvee_{\varphi=1}^o \bar{v}_{\omega\varphi} \int_0^\infty k_{\omega\varphi}(s) g_\varphi(\bar{\zeta}_\varphi(s - \tau, \wp)) ds - \bigvee_{\varphi=1}^o \bar{v}_{\omega\varphi} \int_0^\infty k_{\omega\varphi}(s) g_\varphi(\zeta_\varphi(s - \tau, \wp)) ds \right] \\
 &- \omega_\omega \bar{\xi}_\omega(t, \wp) - \varrho_\omega \bar{\xi}_\omega(t, \wp), \quad \omega = 1, 2, \dots, n.
 \end{aligned} \tag{4}$$

We investigate the error system (4) under the following initial and boundary conditions:

$$\begin{aligned}
 \zeta_\varphi(\mathfrak{s}, \wp) &= \phi_\varphi(\mathfrak{s}, \wp), \quad \mathfrak{s} \in (-\infty, 0], \quad \wp \in \Omega, \\
 \bar{\xi}_\omega(\mathfrak{s}, \wp) &= \bar{\phi}_\omega(\mathfrak{s}, \wp), \quad \mathfrak{s} \in (-\infty, 0], \quad \wp \in \Omega, \\
 \zeta_\varphi(t, \wp) &= 0, \quad t \in \mathbb{R}, \quad \wp \in \partial\Omega, \\
 \bar{\xi}_\omega(t, \wp) &= 0, \quad t \in \mathbb{R}, \quad \wp \in \partial\Omega, \quad \varphi = 1, 2, \dots, o, \quad \omega = 1, 2, \dots, n,
 \end{aligned} \tag{5}$$

where ϕ_φ and $\bar{\phi}_\omega$ are continuous initial functions.

In our stability analysis, we need the following assumptions.

Assumption 1. For $\vartheta_\omega, \bar{\vartheta}_\omega \in \mathbb{R}$ and $\zeta_\varphi, \bar{\zeta}_\varphi \in \mathbb{R}$, the activation functions f_ω and g_φ satisfy

$$\begin{aligned}
 \left| \bigwedge_{\omega=1}^n u_{\omega\omega} f_\omega(\vartheta_\omega) - \bigwedge_{\omega=1}^n u_{\omega\omega} f_\omega(\bar{\vartheta}_\omega) \right| &\leq \sum_{\omega=1}^n |u_{\omega\omega}| |f_\omega(\vartheta_\omega) - f_\omega(\bar{\vartheta}_\omega)|, \quad \omega = 1, 2, \dots, n, \\
 \left| \bigvee_{\omega=1}^n v_{\omega\omega} f_\omega(\vartheta_\omega) - \bigvee_{\omega=1}^n v_{\omega\omega} f_\omega(\bar{\vartheta}_\omega) \right| &\leq \sum_{\omega=1}^n |v_{\omega\omega}| |f_\omega(\vartheta_\omega) - f_\omega(\bar{\vartheta}_\omega)|, \quad \omega = 1, 2, \dots, n, \\
 \left| \bigwedge_{\varphi=1}^o \bar{u}_{\omega\varphi} g_\varphi(\zeta_\varphi) - \bigwedge_{\varphi=1}^o \bar{u}_{\omega\varphi} g_\varphi(\bar{\zeta}_\varphi) \right| &\leq \sum_{\varphi=1}^o |\bar{u}_{\omega\varphi}| |g_\varphi(\zeta_\varphi) - g_\varphi(\bar{\zeta}_\varphi)|, \quad \varphi = 1, 2, \dots, o, \\
 \left| \bigvee_{\varphi=1}^o \bar{v}_{\omega\varphi} g_\varphi(\zeta_\varphi) - \bigvee_{\varphi=1}^o \bar{v}_{\omega\varphi} g_\varphi(\bar{\zeta}_\varphi) \right| &\leq \sum_{\varphi=1}^o |\bar{v}_{\omega\varphi}| |g_\varphi(\zeta_\varphi) - g_\varphi(\bar{\zeta}_\varphi)|, \quad \varphi = 1, 2, \dots, o.
 \end{aligned}$$

Assumption 2. For any $\vartheta_\omega, \bar{\vartheta}_\omega \in \mathbb{R}$ and $\zeta_\varphi, \bar{\zeta}_\varphi \in \mathbb{R}$, there exists positive constants F_φ, F_ω , such that

$$\begin{aligned}
 |f_\omega(\vartheta_\omega) - f_\omega(\bar{\vartheta}_\omega)| &\leq F_\omega |\vartheta_\omega - \bar{\vartheta}_\omega|, \quad \omega = 1, 2, \dots, n, \\
 |g_\varphi(\zeta_\varphi) - g_\varphi(\bar{\zeta}_\varphi)| &\leq G_\varphi |\zeta_\varphi - \bar{\zeta}_\varphi|, \quad \varphi = 1, 2, \dots, o.
 \end{aligned}$$

Assumption 3. The delay kernels $k_{\varphi\omega}(\cdot)$ and $k_{\omega\varphi}(\cdot)$ satisfy

$$\int_0^\infty k_{\varphi\omega}(s) ds \leq 1, \quad \int_0^\infty k_{\omega\varphi}(s) ds \leq 1$$

for $\varphi = 1, 2, \dots, o, \omega = 1, 2, \dots, n$.

The next lemmas are also used.

Lemma 1 ([34]). Let $p : [0, b] \times \Omega \rightarrow \mathbb{R}$ with $b > 0$ be a continuously differentiable function on $t, t > 0$ for any $\varphi \in \Omega$. Then, for any $t \geq 0, \varphi \in \Omega$

$$\frac{1}{2} \frac{\partial^\lambda p^2(t, \varphi)}{\partial t^\lambda} \leq p(t, \varphi) \frac{\partial^\lambda p(t, \varphi)}{\partial t^\lambda}$$

for $0 < \lambda < 1$.

Lemma 2 ([34]). For $0 < \beta < 1$, assume that the function $V(t)$ is continuous on $[0, \infty)$ satisfying

$$D^\beta V(t) \leq YV(t), Y \in \mathbb{R}$$

whenever

$$V(\gamma + \xi) \leq V(\gamma), -\infty < \xi \leq 0.$$

Then,

$$V(t) \leq \max_{-\infty < s \leq 0} V(s) E_\beta(Yt^\beta), t > 0,$$

where E_β is the corresponding Mittag–Leffler function.

Lemma 3 ([42]). Suppose that $V(t) \in \mathbb{R}$ is a continuous, differentiable, and non-negative function satisfying

$$D^\alpha V(t) \leq -bV(t) + cV(t - \tau), \quad 0 < \alpha < 1, \\ V(\gamma) = \varphi(\gamma) \geq 0, \quad \gamma \in [-\tau, 0].$$

If $b > \sqrt{2c}$ and $c > 0$, then for all $\varphi(\gamma) \geq 0, \tau > 0, \lim_{t \rightarrow +\infty} V(t) = 0$.

The assertion of Lemma 3 is true for $\tau = \infty$, too.

Lemma 4 (Fractional Barbalat’s Lemma [43]). If $\int_{t_0}^t \zeta(\xi) d\xi$ includes a finite limit as $t \rightarrow +\infty$, and $D^\lambda \zeta(t)$ is bounded, then $\zeta(t) \rightarrow 0$ as $t \rightarrow \infty$, whenever $0 < \lambda < 1$.

Lemma 5 ([44]). Given any scalar $\epsilon > 0, x, y \in \mathbb{R}^n$, and matrix A , then

$$x^T A y \leq \frac{1}{2\epsilon} x^T A A^T x + \frac{\epsilon}{2} y^T y.$$

Lemma 6 ([45]). Let Ω be a cube $|x_k| < l_q (k = 1, 2, \dots, q)$, and let $v(x)$ be a real-valued function belonging to $C^1(\Omega)$ which vanishes on the boundary $\partial\Omega$ of Ω , i.e., $v(x)|_\Omega = 0$. Then,

$$\int_\Omega v^2(x) dx \leq l_k^2 \int_\Omega \left| \frac{\partial v(x)}{\partial x_k} \right|^2 dx.$$

3. Global Asymptotic Stability via State Feedback Control

Definition 2. The error system (4) is said to be globally asymptotically stable under the given controllers if

$$\lim_{t \rightarrow \infty} (\|\xi(t, \varphi)\|_1 + \|\bar{\xi}(t, \varphi)\|_2) = 0,$$

where $\|\cdot\|_1$ and $\|\cdot\|_2$ are the corresponding norms of $\xi(t, \varphi) = (\xi_1(t, \varphi), \xi_2(t, \varphi), \dots, \xi_n(t, \varphi))^T \in \mathbb{R}^n$, and $\bar{\xi}(t, \varphi) = (\bar{\xi}_1(t, \varphi), \bar{\xi}_2(t, \varphi), \dots, \bar{\xi}_n(t, \varphi))^T \in \mathbb{R}^n$, respectively.

Remark 1. Since $\xi_\varphi(t, \varphi) = \bar{\xi}_\varphi(t, \varphi) - \zeta_\varphi(t, \varphi)$, $\varphi = 1, 2, \dots, o$ and $\bar{\xi}_\omega(t, \varphi) = \bar{\mathfrak{S}}_\omega(t, \varphi) - \mathfrak{S}_\omega(t, \varphi)$, $\omega = 1, 2, \dots, n$, the global asymptotic stability of the error system (4) is equivalent to a global asymptotic synchronization of the nodes of system (2) onto those of system (1) under the appropriate controllers.

Theorem 1. Suppose that Assumptions 1–3 and the conditions of Lemma 6 hold, and $\bar{M}_\varphi, \bar{\tilde{M}}_\omega$ are positive constants, such that $\bar{M}_\varphi = \sum_{k=1}^q \frac{m_{\varphi k}}{l_k^2}$, $\bar{\tilde{M}}_\omega = \sum_{k=1}^q \frac{\tilde{m}_{\omega k}}{l_k^2}$. The error system (4) is globally asymptotically stable, if there exist constants $\rho > 0$ and

$$\begin{aligned} \mu_{\min}^{(1)} &= \min_{1 \leq \varphi \leq o} \left\{ 2\bar{M}_\varphi + 2d_\varphi - \sum_{\omega=1}^n |c_{\varphi\omega}| F_\omega \rho^{-1} - \sum_{\omega=1}^n |a_{\varphi\omega}| F_\omega \rho^{-1} \right. \\ &\quad \left. - \sum_{\omega=1}^n |u_{\varphi\omega}| F_\omega \rho^{-1} - \sum_{\omega=1}^n |v_{\varphi\omega}| F_\omega \rho^{-1} + t_\varphi + \psi_\varphi - \sum_{\omega=1}^n |c_{\varphi\omega}| F_\omega \rho \right\} > 0, \\ \mu_{\min}^{(2)} &= \min_{1 \leq \omega \leq n} \left\{ 2\bar{\tilde{M}}_\omega + 2\tilde{d}_\omega - \sum_{\varphi=1}^o |\tilde{c}_{\omega\varphi}| G_\varphi \rho^{-1} - \sum_{\varphi=1}^o |\tilde{a}_{\omega\varphi}| G_\varphi \rho^{-1} - \sum_{\varphi=1}^o |\tilde{u}_{\omega\varphi}| G_\varphi \rho^{-1} \right. \\ &\quad \left. - \sum_{\varphi=1}^o |\tilde{v}_{\omega\varphi}| G_\varphi \rho^{-1} + \omega_\omega + \varrho_\omega - \sum_{\varphi=1}^o |\tilde{c}_{\omega\varphi}| G_\varphi \rho \right\} > 0, \\ \Lambda_1^\mu &= \max_{1 \leq \varphi \leq o} \left\{ \sum_{\omega=1}^n |\tilde{u}_{\omega\varphi}| G_\varphi \rho + \sum_{\omega=1}^n |\tilde{v}_{\omega\varphi}| G_\varphi \rho + \sum_{\omega=1}^n |\tilde{a}_{\omega\varphi}| G_\varphi \rho \right\} > 0, \\ \Lambda_2^\mu &= \max_{1 \leq \omega \leq n} \left\{ \sum_{\varphi=1}^o |u_{\varphi\omega}| F_\omega \rho + \sum_{\varphi=1}^o |v_{\varphi\omega}| F_\omega \rho + \sum_{\varphi=1}^o |a_{\varphi\omega}| F_\omega \rho \right\} > 0. \end{aligned}$$

such that

$$\min\{\mu_{\min}^{(1)}, \mu_{\min}^{(2)}\} > \sqrt{2} \max\{\Lambda_1^\mu, \Lambda_2^\mu\}.$$

Proof. We define a Lyapunov function as

$$V(t) = \int_\Omega \sum_{\varphi=1}^o \frac{1}{2} \xi_\varphi^2(t, \varphi) d\varphi + \int_\Omega \sum_{\omega=1}^n \frac{1}{2} \bar{\xi}_\omega^2(t, \varphi) d\varphi. \tag{6}$$

Then, for the fractional derivative of V of order λ , we have

$$\begin{aligned} \frac{d^\lambda V(t)}{dt^\lambda} &= \frac{1}{2} \frac{d^\lambda}{dt^\lambda} \left(\int_\Omega \frac{1}{2} \sum_{\varphi=1}^o \xi_\varphi^2(t, \varphi) d\varphi + \int_\Omega \frac{1}{2} \sum_{\omega=1}^n \bar{\xi}_\omega^2(t, \varphi) d\varphi \right) \\ &= \frac{1}{2} \sum_{\varphi=1}^o \left[\frac{d^\lambda}{dt^\lambda} \left(\int_\Omega \xi_\varphi^2(t, \varphi) d\varphi \right) \right] + \frac{1}{2} \sum_{\omega=1}^n \left[\frac{d^\lambda}{dt^\lambda} \left(\int_\Omega \bar{\xi}_\omega^2(t, \varphi) d\varphi \right) \right]. \end{aligned} \tag{7}$$

We have from Lemma 1 that

$$\begin{aligned} \frac{d^\lambda}{dt^\lambda} \left(\int_\Omega \xi_\varphi^2(t, \varphi) d\varphi \right) &\leq 2 \int_\Omega \xi_\varphi(t, \varphi) \frac{\partial^\lambda \xi_\varphi(t, \varphi)}{\partial t^\lambda} d\varphi, \\ \frac{d^\lambda}{dt^\lambda} \left(\int_\Omega \bar{\xi}_\omega^2(t, \varphi) d\varphi \right) &\leq 2 \int_\Omega \bar{\xi}_\omega(t, \varphi) \frac{\partial^\lambda \bar{\xi}_\omega(t, \varphi)}{\partial t^\lambda} d\varphi. \end{aligned}$$

Substituting the above inequalities in Equation (7), we obtain

$$\begin{aligned}
 D^\lambda V(t) &\leq \sum_{\varphi=1}^o \int_{\Omega} \zeta_{\varphi}(t, \wp)^c D^\lambda \zeta_{\varphi}(t, \wp) d\wp + \sum_{\omega=1}^n \int_{\Omega} \bar{\zeta}_{\omega}(t, \wp)^c D^\lambda \bar{\zeta}_{\omega}(t, \wp) d\wp \\
 &= \sum_{\varphi=1}^o \int_{\Omega} \zeta_{\varphi}(t, \wp) \left(\sum_{k=1}^q \frac{\partial}{\partial \zeta_k} \left(m_{\varphi k} \frac{\partial \zeta_{\varphi}(t, \wp)}{\partial \wp_k} \right) - d_{\varphi} \zeta_{\varphi}(t, \wp) \right. \\
 &\quad + \left[\sum_{\omega=1}^n c_{\varphi \omega} f_{\omega}(\bar{\mathfrak{S}}_{\omega}(t, \wp)) - \sum_{\omega=1}^n c_{\varphi \omega} f_{\omega}(\mathfrak{S}_{\omega}(t, \wp)) \right] \\
 &\quad + \left[\sum_{\omega=1}^n a_{\varphi \omega} f_{\omega}(\bar{\mathfrak{S}}_{\omega}(t - \tau, \wp)) - \sum_{\omega=1}^n a_{\varphi \omega} f_{\omega}(\mathfrak{S}_{\omega}(t - \tau, \wp)) \right] \\
 &\quad + \left[\bigwedge_{\omega=1}^n u_{\varphi \omega} \int_0^{\infty} k_{\varphi \omega}(s) f_{\omega}(\bar{\mathfrak{S}}_{\omega}(s - \tau, \wp)) ds \right. \\
 &\quad \left. - \bigwedge_{\omega=1}^n u_{\varphi \omega} \int_0^{\infty} k_{\varphi \omega}(s) f_{\omega}(\mathfrak{S}_{\omega}(s - \tau, \wp)) ds \right] \\
 &\quad + \left[\bigvee_{\omega=1}^n v_{\varphi \omega} \int_0^{\infty} k_{\varphi \omega}(s) f_{\omega}(\bar{\mathfrak{S}}_{\omega}(s - \tau, \wp)) ds \right. \\
 &\quad \left. - \bigvee_{\omega=1}^n v_{\varphi \omega} \int_0^{\infty} k_{\varphi \omega}(s) f_{\omega}(\mathfrak{S}_{\omega}(s - \tau, \wp)) ds \right] \\
 &\quad \left. - t_{\varphi} \zeta_{\varphi}(t, \wp) - \Psi_{\varphi} \zeta_{\varphi}(t, \wp) \right) d\wp \\
 &\quad + \sum_{\omega=1}^n \int_{\Omega} \bar{\zeta}_{\omega}(t, \wp) \left(\sum_{k=1}^q \frac{\partial}{\partial \bar{\zeta}_k} \left(\bar{m}_{\omega k} \frac{\partial \bar{\zeta}_{\omega}(t, \wp)}{\partial \wp_k} \right) - \bar{d}_{\omega} \bar{\zeta}_{\omega}(t, \wp) \right. \\
 &\quad + \left[\sum_{\varphi=1}^o \bar{c}_{\omega \varphi} g_{\varphi}(\bar{\zeta}_{\varphi}(t, \wp)) - \sum_{\varphi=1}^o \bar{c}_{\omega \varphi} g_{\varphi}(\zeta_{\varphi}(t, \wp)) \right] \\
 &\quad + \left[\sum_{\varphi=1}^o \bar{a}_{\omega \varphi} g_{\varphi}(\bar{\zeta}_{\varphi}(t - \tau, \wp)) - \sum_{\varphi=1}^o \bar{a}_{\omega \varphi} g_{\varphi}(\zeta_{\varphi}(t - \tau, \wp)) \right] \\
 &\quad + \left[\bigwedge_{\varphi=1}^o \bar{u}_{\omega \varphi} \int_0^{\infty} k_{\omega \varphi}(s) g_{\varphi}(\bar{\zeta}_{\varphi}(s - \tau, \wp)) ds \right. \\
 &\quad \left. - \bigwedge_{\varphi=1}^o \bar{u}_{\omega \varphi} \int_0^{\infty} k_{\omega \varphi}(s) g_{\varphi}(\zeta_{\varphi}(s - \tau, \wp)) ds \right] \\
 &\quad + \left[\bigvee_{\varphi=1}^o \bar{v}_{\omega \varphi} \int_0^{\infty} k_{\omega \varphi}(s) g_{\varphi}(\bar{\zeta}_{\varphi}(s - \tau, \wp)) ds \right. \\
 &\quad \left. - \bigvee_{\varphi=1}^o \bar{v}_{\omega \varphi} \int_0^{\infty} k_{\omega \varphi}(s) g_{\varphi}(\zeta_{\varphi}(s - \tau, \wp)) ds \right] \\
 &\quad \left. - \omega_{\omega} \bar{\zeta}_{\omega}(t, \wp) - \varrho_{\omega} \bar{\zeta}_{\omega}(t, \wp) \right) d\wp.
 \end{aligned}$$

By Green’s formula using the boundary conditions, we obtain

$$\sum_{k=1}^q \int_{\Omega} \zeta_{\varphi}(t, \wp) \frac{\partial}{\partial \wp_k} \left(m_{\varphi k} \frac{\partial \zeta_{\varphi}(t, \wp)}{\partial \wp_k} \right) d\wp = - \sum_{k=1}^q \int_{\Omega} m_{\varphi k} \left(\frac{\partial \zeta_{\varphi}(t, \wp)}{\partial \wp_k} \right)^2 d\wp,$$

$$\sum_{k=1}^q \int_{\Omega} \bar{\xi}_{\omega}(t, \wp) \frac{\partial}{\partial \wp_k} \left(\tilde{m}_{\omega k} \frac{\partial \bar{\xi}_{\omega}(t, \wp)}{\partial \wp_k} \right) d\wp = - \sum_{k=1}^q \int_{\Omega} \tilde{m}_{\omega k} \left(\frac{\partial \bar{\xi}_{\omega}(t, \wp)}{\partial \wp_k} \right)^2 d\wp.$$

From the above identities and Lemma 6, we obtain

$$\begin{aligned} \sum_{k=1}^q \int_{\Omega} \xi_{\varphi}(t, \wp) \frac{\partial}{\partial \wp_k} \left(m_{\varphi k} \frac{\partial \xi_{\varphi}(t, \wp)}{\partial \wp_k} \right) d\wp &= - \sum_{k=1}^q \int_{\Omega} m_{\varphi k} \left(\frac{\partial \xi_{\varphi}(t, \wp)}{\partial \wp_k} \right)^2 d\wp \\ &\leq - \sum_{k=1}^q \int_{\Omega} \frac{m_{\varphi k}}{l_k^2} \xi_{\varphi}^2(t, \wp) d\wp = -\bar{M}_{\varphi} \int_{\Omega} \xi_{\varphi}^2(t, \wp) d\wp. \end{aligned}$$

Similarly,

$$\begin{aligned} \sum_{k=1}^q \int_{\Omega} \bar{\xi}_{\omega}(t, \wp) \frac{\partial}{\partial \wp_k} \left(\tilde{m}_{\omega k} \frac{\partial \bar{\xi}_{\omega}(t, \wp)}{\partial \wp_k} \right) d\wp &= - \sum_{k=1}^q \int_{\Omega} \tilde{m}_{\omega k} \left(\frac{\partial \bar{\xi}_{\omega}(t, \wp)}{\partial \wp_k} \right)^2 d\wp \\ &\leq - \sum_{k=1}^q \int_{\Omega} \frac{\tilde{m}_{\omega k}}{l_k^2} \bar{\xi}_{\omega}^2(t, \wp) d\wp = -\tilde{M}_{\omega} \int_{\Omega} \bar{\xi}_{\omega}^2(t, \wp) d\wp. \end{aligned}$$

Then, using Assumptions 1 and 2, we obtain

$$\begin{aligned} D^{\lambda}V(t) \leq & \int_{\Omega} \left\{ - \sum_{\varphi=1}^o \bar{M}_{\varphi} \xi_{\varphi}^2(t, \wp) - \sum_{\varphi=1}^o d_{\varphi} \xi_{\varphi}^2(t, \wp) + \sum_{\varphi=1}^o \sum_{\omega=1}^n |c_{\varphi\omega}| F_{\omega} |\xi_{\varphi}(t, \wp)| |\bar{\xi}_{\omega}(t, \wp)| \right. \\ & + \sum_{\varphi=1}^o \sum_{\omega=1}^n |a_{\varphi\omega}| F_{\omega} |\xi_{\varphi}(t, \wp)| |\bar{\xi}_{\omega}(t - \tau, \wp)| \\ & + \sum_{\varphi=1}^o \sum_{\omega=1}^n |u_{\varphi\omega}| \int_0^{\infty} k_{\varphi\omega}(s) F_{\omega} |\xi_{\varphi}(s, \wp)| |\bar{\xi}_{\omega}(s - \tau, \wp)| ds \\ & + \sum_{\varphi=1}^o \sum_{\omega=1}^n |v_{\varphi\omega}| \int_0^{\infty} k_{\varphi\omega}(s) F_{\omega} |\xi_{\varphi}(s, \wp)| |\bar{\xi}_{\omega}(s - \tau, \wp)| ds - \sum_{\varphi=1}^o t_{\varphi} \xi_{\varphi}^2(t, \wp) \\ & - \sum_{\varphi=1}^o \Psi_{\varphi} \xi_{\varphi}^2(t, \wp) - \sum_{\omega=1}^n \bar{M}_{\omega} \bar{\xi}_{\omega}^2(t, \wp) - \sum_{\omega=1}^n \tilde{d}_{\omega} \bar{\xi}_{\omega}^2(t, \wp) \\ & + \sum_{\omega=1}^n \sum_{\varphi=1}^o |\tilde{c}_{\omega\varphi}| G_{\varphi} |\bar{\xi}_{\omega}(t, \wp)| |\xi_{\varphi}(t, \wp)| \\ & + \sum_{\omega=1}^n \sum_{\varphi=1}^o |\tilde{a}_{\omega\varphi}| G_{\varphi} |\bar{\xi}_{\omega}(t, \wp)| |\xi_{\varphi}(t - \tau, \wp)| \\ & + \sum_{\omega=1}^n \sum_{\varphi=1}^o |\tilde{u}_{\omega\varphi}| \int_0^{\infty} k_{\omega\varphi}(s) G_{\varphi} \bar{\xi}_{\omega}(s, \wp) |\xi_{\varphi}(s - \tau, \wp)| ds \\ & + \sum_{\omega=1}^n \sum_{\varphi=1}^o |\tilde{v}_{\omega\varphi}| \int_0^{\infty} k_{\omega\varphi}(s) G_{\varphi} \bar{\xi}_{\omega}(s, \wp) |\xi_{\varphi}(s - \tau, \wp)| ds \\ & \left. - \sum_{\varphi=1}^o \omega_{\varphi} \xi_{\varphi}^2(t, \wp) - \sum_{\varphi=1}^o \varrho_{\varphi} \xi_{\varphi}^2(t, \wp) \right\} d\wp. \end{aligned}$$

Lemma 5 implies the existence of a constant $\rho > 0$ such that

$$\begin{aligned}
 D^\lambda V(t) \leq & \int_{\Omega} \left\{ - \sum_{\varphi=1}^o \tilde{M}_\varphi \tilde{\zeta}_\varphi^2(t, \wp) - \sum_{\varphi=1}^o d_\varphi \tilde{\zeta}_\varphi^2(t, \wp) + \sum_{\varphi=1}^o \sum_{\omega=1}^n |c_{\varphi\omega}| F_\omega \left[\frac{\rho^{-1}}{2} \tilde{\zeta}_\varphi^2(t, \wp) + \frac{\rho}{2} \tilde{\zeta}_\omega^2(t, \wp) \right] \right. \\
 & + \sum_{\varphi=1}^o \sum_{\omega=1}^n |a_{\varphi\omega}| F_\omega \left[\frac{\rho^{-1}}{2} \tilde{\zeta}_\varphi^2(t, \wp) + \frac{\rho}{2} \tilde{\zeta}_\omega^2(t - \tau, \wp) \right] \\
 & + \sum_{\varphi=1}^o \sum_{\omega=1}^n |u_{\varphi\omega}| \int_0^\infty k_{\varphi\omega}(s) F_\omega \left[\frac{\rho^{-1}}{2} \tilde{\zeta}_\varphi^2(s, \wp) + \frac{\rho}{2} \tilde{\zeta}_\omega^2(s - \tau, \wp) \right] ds \\
 & + \sum_{\varphi=1}^o \sum_{\omega=1}^n |v_{\varphi\omega}| \int_0^\infty k_{\varphi\omega}(s) F_\omega \left[\frac{\rho^{-1}}{2} \tilde{\zeta}_\varphi^2(s, \wp) + \frac{\rho}{2} \tilde{\zeta}_\omega^2(s - \tau, \wp) \right] ds \\
 & - \sum_{\varphi=1}^o t_\varphi \tilde{\zeta}_\varphi^2(t, \wp) - \sum_{\varphi=1}^o \Psi_\varphi \tilde{\zeta}_\varphi^2(t, \wp) \\
 & - \sum_{\omega=1}^n \tilde{M}_\omega \tilde{\zeta}_\omega^2(t, \wp) - \sum_{\omega=1}^n \tilde{d}_\omega \tilde{\zeta}_\omega^2(t, \wp) + \sum_{\omega=1}^n \sum_{\varphi=1}^o |\tilde{c}_{\omega\varphi}| G_\varphi \left[\frac{\rho^{-1}}{2} \tilde{\zeta}_\omega^2(t, \wp) + \frac{\rho}{2} \tilde{\zeta}_\varphi^2(t, \wp) \right] \\
 & + \sum_{\omega=1}^n \sum_{\varphi=1}^o |\tilde{a}_{\omega\varphi}| G_\varphi \left[\frac{\rho^{-1}}{2} \tilde{\zeta}_\omega^2(t, \wp) + \frac{\rho}{2} \tilde{\zeta}_\varphi^2(t - \tau, \wp) \right] \\
 & + \sum_{\omega=1}^n \sum_{\varphi=1}^o |\tilde{u}_{\omega\varphi}| \int_0^\infty k_{\omega\varphi}(s) G_\varphi \left[\frac{\rho^{-1}}{2} \tilde{\zeta}_\omega^2(s, \wp) + \frac{\rho}{2} \tilde{\zeta}_\varphi^2(s - \tau, \wp) \right] ds \\
 & + \sum_{\omega=1}^n \sum_{\varphi=1}^o |\tilde{v}_{\omega\varphi}| \int_0^\infty k_{\omega\varphi}(s) G_\varphi \left[\frac{\rho^{-1}}{2} \tilde{\zeta}_\omega^2(s, \wp) + \frac{\rho}{2} \tilde{\zeta}_\varphi^2(s - \tau, \wp) \right] ds \\
 & \left. - \sum_{\omega=1}^n \omega_\omega \tilde{\zeta}_\omega^2(t, \wp) - \sum_{\omega=1}^n \varrho_\omega \tilde{\zeta}_\omega^2(t, \wp) \right\}.
 \end{aligned}$$

We apply Assumption 3 to obtain

$$\begin{aligned}
 D^\lambda V(t) \leq & \int_{\Omega} \tilde{\zeta}_\varphi^2(t, \wp) \left\{ - \sum_{\varphi=1}^o \tilde{M}_\varphi - \sum_{\varphi=1}^o d_\varphi + \sum_{\varphi=1}^o \sum_{\omega=1}^n |c_{\varphi\omega}| F_\omega \frac{\rho^{-1}}{2} + \sum_{\varphi=1}^o \sum_{\omega=1}^n |a_{\varphi\omega}| F_\omega \frac{\rho^{-1}}{2} \right. \\
 & + \sum_{\varphi=1}^o \sum_{\omega=1}^n |u_{\varphi\omega}| F_\omega \frac{\rho^{-1}}{2} + \sum_{\varphi=1}^o \sum_{\omega=1}^n |v_{\varphi\omega}| F_\omega \frac{\rho^{-1}}{2} - \sum_{\varphi=1}^o t_\varphi - \sum_{\varphi=1}^o \Psi_\varphi + \sum_{\omega=1}^n \sum_{\varphi=1}^o |\tilde{c}_{\omega\varphi}| G_\varphi \frac{\rho}{2} \left. \right\} \\
 & + \max_{-\infty < s \leq 0} \tilde{\zeta}_\varphi^2(s, \wp) \left\{ \sum_{\omega=1}^n \sum_{\varphi=1}^o |\tilde{a}_{\omega\varphi}| G_\varphi \frac{\rho}{2} + \sum_{\omega=1}^n \sum_{\varphi=1}^o |\tilde{v}_{\omega\varphi}| G_\varphi \frac{\rho}{2} + \sum_{\omega=1}^n \sum_{\varphi=1}^o |\tilde{u}_{\omega\varphi}| G_\varphi \frac{\rho}{2} \right\} \\
 & + \tilde{\zeta}_\omega^2(t, \wp) \left\{ - \sum_{\omega=1}^n \tilde{M}_\omega - \sum_{\omega=1}^n \tilde{d}_\omega + \sum_{\omega=1}^n \sum_{\varphi=1}^o |\tilde{c}_{\omega\varphi}| G_\varphi \frac{\rho^{-1}}{2} + \sum_{\omega=1}^n \sum_{\varphi=1}^o |\tilde{a}_{\omega\varphi}| G_\varphi \frac{\rho^{-1}}{2} \right. \\
 & + \sum_{\omega=1}^n \sum_{\varphi=1}^o |\tilde{u}_{\omega\varphi}| G_\varphi \frac{\rho^{-1}}{2} + \sum_{\omega=1}^n \sum_{\varphi=1}^o |\tilde{v}_{\omega\varphi}| G_\varphi \frac{\rho^{-1}}{2} - \sum_{\omega=1}^n \omega_\omega - \sum_{\omega=1}^n \varrho_\omega \\
 & + \sum_{\varphi=1}^o \sum_{\omega=1}^n |\tilde{c}_{\varphi\omega}| G_\omega \frac{\rho}{2} \left. \right\} + \max_{-\infty < s \leq 0} \tilde{\zeta}_\omega^2(s, \wp) \left\{ \sum_{\varphi=1}^o \sum_{\omega=1}^n |u_{\varphi\omega}| F_\omega \frac{\rho}{2} \right. \\
 & \left. + \sum_{\varphi=1}^o \sum_{\omega=1}^n |v_{\varphi\omega}| F_\omega \frac{\rho}{2} + \sum_{\varphi=1}^o \sum_{\omega=1}^n |a_{\varphi\omega}| F_\omega \frac{\rho}{2} \right\} d\wp,
 \end{aligned}$$

or

$$D^\lambda V(t) \leq \int_{\Omega} \left\{ -\mu_{\min}^{(1)} \sum_{\varphi=1}^o \bar{\xi}_{\varphi}^2(t, \varphi) - \mu_{\min}^{(2)} \sum_{\omega=1}^n \bar{\xi}_{\omega}^2(t, \varphi) + \Omega_{\max}^{(1)} \sum_{\varphi=1}^n \max_{-\infty < s \leq 0} \bar{\xi}_{\varphi}^2(s, \varphi) + \Omega_{\max}^{(2)} \sum_{\varphi=1}^n \max_{-\infty < s \leq 0} \bar{\xi}_{\omega}^2(s, \varphi) \right\} d\varphi \leq -\mu V(t) + \Lambda \max_{-\infty < s \leq 0} V(s),$$

where $\mu = \min\{\mu_{\min}^{(1)}, \mu_{\min}^{(2)}\}$, and $\Lambda = \max\{\Lambda_1^{\mu}, \Lambda_2^{\mu}\}$.

By Lemma 3, since $\mu > \sqrt{2}\Lambda$, we have $\lim_{t \rightarrow \infty} V(t) = 0$.

For $\|\bar{\xi}(t, \varphi)\|_1 + \|\bar{\xi}(t, \varphi)\|_2 = V(t)$, we can conclude that system (4) is globally asymptotically stable. This means that the drive system (1) and the response system (2) are globally asymptotically synchronized via the state feedback controllers. This completes the proof of the theorem. \square

Remark 2. Different from all existent synchronization results for neural network models, we consider a class of more general structures which include Caputo type fractional derivatives, reaction–diffusion terms, discrete and distributed delays which allow us to divide all nodes in the network into different classes, a BAM two-layer connection, fuzzy logic, and hybrid feedback controllers. Thus, the proposed results in Theorem 1 generalize and complement numerous asymptotic synchronization results. For example, our results generalize the results in [16] to the BAM case considering Caputo’s fractional differential operators. Moreover, the results established complement the results in [2] considering Caputo’s fractional differential operators and hybrid feedback controllers.

Remark 3. The proposed global asymptotic synchronization criteria in Theorem 1 are in the forms of inequalities between the system parameters. This form allows applied researchers to easily apply the established results. The presence of the terms that include $|u_{\varphi\omega}|$, $|v_{\varphi\omega}|$, $|\bar{u}_{\omega\varphi}|$, and $|\bar{v}_{\omega\varphi}|$ in the conditions for $\mu_{\min}^{(1)}$, $\mu_{\min}^{(2)}$, Λ_1^{μ} , and Λ_2^{μ} reflects the role of the distributed delays with delay kernels which satisfy Assumption 3. Furthermore, the terms $t_{\varphi} + \psi_{\varphi}$ and $\omega_{\omega} + \varrho_{\omega}$ reflect the design of the controllers.

Remark 4. Without feedback controllers, the error system (4) becomes

$$\begin{aligned} \frac{\partial^\lambda \bar{\xi}_{\varphi}(t, \varphi)}{\partial t^\lambda} &= \sum_{k=1}^q \frac{\partial}{\partial \varrho_k} \left(m_{\varphi k} \frac{\partial \bar{\xi}_{\varphi}(t, \varphi)}{\partial \varrho_k} \right) - d_{\varphi} \bar{\xi}_{\varphi}(t, \varphi) \\ &+ \left[\sum_{\omega=1}^n c_{\varphi\omega} f_{\omega}(\bar{\mathfrak{S}}_{\omega}(t, \varphi)) - \sum_{\omega=1}^n c_{\varphi\omega} f_{\omega}(\mathfrak{S}_{\omega}(t, \varphi)) \right] \\ &+ \left[\sum_{\omega=1}^n a_{\varphi\omega} f_{\omega}(\bar{\mathfrak{S}}_{\omega}(t - \tau, \varphi)) - \sum_{\omega=1}^n a_{\varphi\omega} f_{\omega}(\mathfrak{S}_{\omega}(t - \tau, \varphi)) \right] \\ &+ \left[\bigwedge_{\omega=1}^n u_{\varphi\omega} \int_0^\infty k_{\varphi\omega}(s) f_{\omega}(\bar{\mathfrak{S}}_{\omega}(s - \tau, \varphi)) ds \right. \\ &\quad \left. - \bigwedge_{\omega=1}^n u_{\varphi\omega} \int_0^\infty k_{\varphi\omega}(s) f_{\omega}(\mathfrak{S}_{\omega}(s - \tau, \varphi)) ds \right] \\ &+ \left[\bigvee_{\omega=1}^n v_{\varphi\omega} \int_0^\infty k_{\varphi\omega}(s) f_{\omega}(\bar{\mathfrak{S}}_{\omega}(s - \tau, \varphi)) ds \right. \\ &\quad \left. - \bigvee_{\omega=1}^n v_{\varphi\omega} \int_0^\infty k_{\varphi\omega}(s) f_{\omega}(\mathfrak{S}_{\omega}(s - \tau, \varphi)) ds \right], \varphi = 1, 2, \dots, o, \end{aligned}$$

$$\begin{aligned}
 \frac{\partial^\lambda \bar{\xi}_\omega(t, \wp)}{\partial t^\lambda} &= \sum_{k=1}^q \frac{\partial}{\partial \wp^k} (\tilde{m}_{\omega k} \frac{\partial \bar{\xi}_\omega(t, \wp)}{\partial \wp^k}) - \tilde{d}_\omega \bar{\xi}_\omega(t, \wp) \\
 &+ \left[\sum_{\varphi=1}^o \tilde{c}_{\omega\varphi} g_\varphi(\bar{\xi}_\varphi(t, \wp)) - \sum_{\varphi=1}^o \tilde{c}_{\omega\varphi} g_\varphi(\xi_\varphi(t, \wp)) \right] \\
 &+ \left[\sum_{\varphi=1}^o \tilde{a}_{\omega\varphi} g_\varphi(\bar{\xi}_\varphi(t - \tau, \wp)) - \sum_{\varphi=1}^o \tilde{a}_{\omega\varphi} g_\varphi(\xi_\varphi(t - \tau, \wp)) \right] \\
 &+ \left[\bigwedge_{\varphi=1}^o \tilde{u}_{\omega\varphi} \int_0^\infty k_{\omega\varphi}(s) g_\varphi(\bar{\xi}_\varphi(s - \tau, \wp)) ds \right. \\
 &\quad \left. - \bigwedge_{\varphi=1}^o \tilde{u}_{\omega\varphi} \int_0^\infty k_{\omega\varphi}(s) g_\varphi(\xi_\varphi(s - \tau, \wp)) ds \right] \\
 &+ \left[\bigvee_{\varphi=1}^o \tilde{v}_{\omega\varphi} \int_0^\infty k_{\omega\varphi}(s) g_\varphi(\bar{\xi}_\varphi(s - \tau, \wp)) ds \right. \\
 &\quad \left. - \bigvee_{\varphi=1}^o \tilde{v}_{\omega\varphi} \int_0^\infty k_{\omega\varphi}(s) g_\varphi(\xi_\varphi(s - \tau, \wp)) ds \right], \omega = 1, 2, \dots, n. \tag{8}
 \end{aligned}$$

Theorem 2. Suppose that Assumptions 1–3, $\tau < 1$, and conditions of Lemma 6 hold. The error system (8) is globally asymptotically stable, if there exist constants

$$\begin{aligned}
 \Theta_1 &= \min_{1 \leq \varphi \leq o} \left\{ (\tilde{M}_\varphi + d_\varphi) - \sum_{\omega=1}^n |\tilde{c}_{\omega\varphi}| G_\varphi \right\} > 0, \\
 \Theta_2 &= \min_{1 \leq \varphi \leq o} \left\{ (\tilde{M}_\omega + \tilde{d}_\omega) - \sum_{\varphi=1}^o |c_{\varphi\omega}| F_\omega \right\} > 0, \\
 \Lambda_1^\theta &= \left\{ \sum_{\omega=1}^n \sum_{\varphi=1}^o |\tilde{a}_{\omega\varphi}| G_\varphi + \sum_{\omega=1}^n \sum_{\varphi=1}^o |\tilde{u}_{\omega\varphi}| G_\varphi + \sum_{\omega=1}^n \sum_{\varphi=1}^o |\tilde{v}_{\omega\varphi}| G_\varphi \right\} > 0, \\
 \Lambda_2^\theta &= \left\{ \sum_{\varphi=1}^o \sum_{\omega=1}^n |a_{\varphi\omega}| F_\omega + \sum_{\varphi=1}^o \sum_{\omega=1}^n |u_{\varphi\omega}| F_\omega + \sum_{\varphi=1}^o \sum_{\omega=1}^n |v_{\varphi\omega}| F_\omega \right\} > 0,
 \end{aligned}$$

such that

$$\min\{\Theta_1, \Theta_2\} > \max\{\Lambda_1^\theta, \Lambda_2^\theta\}.$$

Proof. We define a Lyapunov function as

$$\begin{aligned}
 V(t) &= \int_\Omega D^{-(1-\lambda)} \left[\sum_{\varphi=1}^o |\xi_\varphi(t, \wp)| + \sum_{\omega=1}^n |\bar{\xi}_\omega(t, \wp)| \right] d\wp + \int_\Omega \sum_{\varphi=1}^o \int_{t-\tau}^t |\xi_\varphi(s, \wp)| ds d\wp \\
 &+ \int_\Omega \sum_{\omega=1}^n \int_{t-\tau}^t |\bar{\xi}_\omega(s, \wp)| ds d\wp. \tag{9}
 \end{aligned}$$

Taking the time derivative of (9), we obtain

$$\begin{aligned}
 \frac{dV(t)}{dt} &= \int_\Omega D^\lambda \left[\sum_{\varphi=1}^o |\xi_\varphi(t, \wp)| + \sum_{\omega=1}^n |\bar{\xi}_\omega(t, \wp)| \right] d\wp + \int_\Omega \sum_{\varphi=1}^o |\xi_\varphi(t, \wp)| d\wp - \int_\Omega \sum_{\varphi=1}^o |\xi_\varphi(t - \tau, \wp)| d\wp \\
 &+ \int_\Omega \sum_{\omega=1}^n |\bar{\xi}_\omega(t, \wp)| d\wp - \int_\Omega \sum_{\omega=1}^n |\bar{\xi}_\omega(t - \tau_1(t), \wp)| d\wp.
 \end{aligned}$$

The rest of the proof is similar to the proof of Theorem 1. Instead of Lemma 3, the fractional Barbalat’s Lemma is used. □

4. Global Mittag–Leffler Synchronization

For fractional-order systems, the concept of Mittag–Leffler stability was introduced in [23]. This notion generalizes the exponential stability notion for integer-order systems and has been investigated intensively [23–29,34,44]. In this section, we establish criteria for the global Mittag–Leffler stability of the error system (8).

Definition 3. The error system (8) is said to be globally Mittag–Leffler stable, if for any continuous initial functions $\phi, (\phi_1, \phi_2, \dots, \phi_o)^T$ and $\tilde{\phi}, (\tilde{\phi}_1, \tilde{\phi}_2, \dots, \tilde{\phi}_n)^T$, there exist positive constants δ and q such that

$$\|\xi(t, \varphi)\|_1 + \|\bar{\xi}(t, \varphi)\|_2 \leq \left\{ M(\|\phi\|_\infty^1 + \|\tilde{\phi}\|_\infty^2) E_\lambda(-\delta t^\lambda) \right\}^q$$

for $t \geq 0$, where E_λ is the corresponding Mittag–Leffler function, $\|\phi\|_\infty^1 = \max_{s \in (-\infty, 0]} \|\phi(s)\|_1$, $\|\tilde{\phi}\|_\infty^2 = \max_{s \in (-\infty, 0]} \|\tilde{\phi}(s)\|_2$, $M(0) = 0$, $M \geq 0$, and M is Lipschitz with respect to its argument.

The global Mittag–Leffler stability of the error system (8) is equivalent to the global Mittag–Leffler synchronization of the master and response systems.

Theorem 3. Suppose that Assumptions 1–3 and the conditions of Lemma 6 hold. The error system (8) is globally Mittag–Leffler stable if there exist constants $\rho > 0$ and

$$\begin{aligned} v_{\min}^{(1)} &= \min_{1 \leq \varphi \leq o} \left\{ 2\tilde{M}_\varphi + 2d_\varphi - \sum_{\omega=1}^n |c_{\varphi\omega}| F_\omega \rho^{-1} - \sum_{\omega=1}^n |a_{\varphi\omega}| F_\omega \rho^{-1} \right. \\ &\quad \left. - \sum_{\omega=1}^n |u_{\varphi\omega}| F_\omega \rho^{-1} - \sum_{\omega=1}^n |v_{\varphi\omega}| F_\omega \rho^{-1} - \sum_{\omega=1}^n |c_{\varphi\omega}| F_\omega \rho \right\} > 0, \\ v_{\min}^{(2)} &= \min_{1 \leq \omega \leq n} \left\{ 2\tilde{M}_\omega + 2\tilde{d}_\omega - \sum_{\varphi=1}^o |\tilde{c}_{\omega\varphi}| G_\varphi \rho^{-1} - \sum_{\varphi=1}^o |\tilde{a}_{\omega\varphi}| G_\varphi \rho^{-1} - \sum_{\varphi=1}^o |\tilde{u}_{\omega\varphi}| G_\varphi \rho^{-1} \right. \\ &\quad \left. - \sum_{\varphi=1}^o |\tilde{v}_{\omega\varphi}| G_\varphi \rho^{-1} - \sum_{\varphi=1}^o |\tilde{c}_{\omega\varphi}| G_\varphi \rho \right\} > 0, \\ \Lambda_1^v &= \max_{1 \leq \varphi \leq o} \left\{ \sum_{\omega=1}^n |\tilde{u}_{\omega\varphi}| G_\varphi \rho + \sum_{\omega=1}^n |\tilde{v}_{\omega\varphi}| G_\varphi \rho + \sum_{\omega=1}^n |\tilde{a}_{\omega\varphi}| G_\varphi \rho \right\} > 0, \\ \Lambda_2^v &= \max_{1 \leq \omega \leq n} \left\{ \sum_{\varphi=1}^o |u_{\varphi\omega}| F_\omega \rho + \sum_{\varphi=1}^o |v_{\varphi\omega}| F_\omega \rho + \sum_{\varphi=1}^o |a_{\varphi\omega}| F_\omega \rho \right\} > 0, \end{aligned}$$

such that

$$\min\{v_{\min}^{(1)}, v_{\min}^{(2)}\} \geq \max\{\Lambda_1^v, \Lambda_2^v\}.$$

Proof. We define again a Lyapunov function as

$$V(t) = \int_\Omega \sum_{\varphi=1}^o \frac{1}{2} \xi_\varphi^2(t, \varphi) d\varphi + \int_\Omega \sum_{\omega=1}^n \frac{1}{2} \bar{\xi}_\omega^2(t, \varphi) d\varphi. \tag{10}$$

Applying the same technique and steps as in the proof of Theorem 1, we obtain

$$D^\lambda V(t) \leq -\nu V(t) + \Lambda \max_{-\infty < s \leq 0} V(s),$$

where $\nu = \min\{v_{\min}^{(1)}, v_{\min}^{(2)}\}$ and $\Lambda = \max\{\Lambda_1^\mu, \Lambda_2^\mu\}$.

We apply the Razumikhin condition

$$V(s) \leq V(t), \quad -\infty < s \leq t \tag{11}$$

to the above inequality to obtain

$$D^\lambda V(t) \leq -(v - \Lambda)V(t).$$

Since $v \geq \Lambda$, there exists a positive constant δ , such that

$$D^\lambda V(t) \leq -\delta V(t).$$

Then, by Lemma 2, we have

$$V(t) \leq \max_{-\infty < s \leq 0} V(s) E_\lambda(-\delta t^\lambda), \quad t > 0.$$

Therefore,

$$\|\tilde{\zeta}(t, \varphi)\|_1 + \|\tilde{\zeta}(t, \varphi)\|_2 \leq \left(\|\phi\|_\infty^1 + \|\tilde{\phi}\|_\infty^2 \right) E_\lambda(-\delta t^\lambda),$$

i.e., according to Definition 3, the error system (8) is globally Mittag–Leffler stable, which means that the master and response systems are globally Mittag–Leffler synchronized. The proof is completed. \square

Remark 5. When the distributed delays and diffusion terms are not considered in model (1), the fractional-order fuzzy BAM neural network is denoted as follows:

$$\begin{aligned} \frac{\partial^\lambda \zeta_\varphi(t)}{\partial t^\lambda} &= -d_\varphi \zeta_\varphi(t) + \sum_{\omega=1}^n c_{\varphi\omega} f_\omega(\mathfrak{S}_\omega(t)) \\ &\quad + \sum_{\omega=1}^n a_{\varphi\omega} f_\omega(\mathfrak{S}_\omega(t - \tau)) + I_\varphi, \quad \varphi = 1, 2, \dots, o, \\ \frac{\partial^\lambda \mathfrak{S}_\omega(t)}{\partial t^\lambda} &= -\tilde{d}_\omega \mathfrak{S}_\omega(t) + \sum_{\varphi=1}^o \tilde{c}_{\omega\varphi} g_\varphi(\zeta_\varphi(t)) \\ &\quad + \sum_{\varphi=1}^o \tilde{a}_{\omega\varphi} g_\varphi(\zeta_\varphi(t - \tau)) + J_\omega, \quad \omega = 1, 2, \dots, n. \end{aligned} \tag{12}$$

Under the assumption that the activation functions f_ω and g_φ are bounded, the above neural network system (12) has an equilibrium point $(\zeta^*, \mathfrak{S}^*)^T$. Let $\hat{\zeta}(t) = \zeta(t) - \zeta^*$, $\check{\mathfrak{S}}(t) = \mathfrak{S}(t) - \mathfrak{S}^*$. Then, we can apply the established results for system (4) to the following system

$$\begin{aligned} \frac{\partial^\lambda \hat{\zeta}_\varphi(t)}{\partial t^\lambda} &= -d_\varphi \hat{\zeta}_\varphi(t) + \sum_{\omega=1}^n c_{\varphi\omega} f_\omega(\check{\mathfrak{S}}_\omega(t)) \\ &\quad + \sum_{\omega=1}^n a_{\varphi\omega} f_\omega(\check{\mathfrak{S}}_\omega(t - \tau)), \quad \varphi = 1, 2, \dots, o, \\ \frac{\partial^\lambda \check{\mathfrak{S}}_\omega(t)}{\partial t^\lambda} &= -\tilde{d}_\omega \check{\mathfrak{S}}_\omega(t) + \sum_{\varphi=1}^o \tilde{c}_{\omega\varphi} g_\varphi(\hat{\zeta}_\varphi(t)) \\ &\quad + \sum_{\varphi=1}^o \tilde{a}_{\omega\varphi} g_\varphi(\hat{\zeta}_\varphi(t - \tau)), \quad \omega = 1, 2, \dots, n. \end{aligned} \tag{13}$$

Theorem 4. Under Assumption 2, system (13) is globally Mittag–Leffler stable if the activation functions are bounded and $\delta = (\omega_1^\theta - \omega_2^\theta) > 0$, $\omega_1^\theta = \min\{\omega_1, \omega_2\}$, $\omega_2^\theta = \max\{\omega_3, \omega_4\}$,

$$\omega_1 = \min_{1 \leq \varphi \leq o} \{ [d_\varphi - |\tilde{c}_{\omega\varphi}|G_\varphi] \}, \omega_2 = \min_{1 \leq \varphi \leq o} \{ [\tilde{d}_\omega - |c_{\varphi\omega}|F_\omega] \}, \omega_3 = \min_{1 \leq \varphi \leq o} \sum_{\omega=1}^n |a_{\varphi\omega}|F_\omega, \omega_4 = \max_{1 \leq \omega \leq n} \sum_{\varphi=1}^o |\tilde{a}_{\omega\varphi}|G_\varphi.$$

Proof. We define a Lyapunov function as

$$V(t, \hat{\zeta}, \check{\mathfrak{S}}) = \sum_{\varphi=1}^o |\hat{\zeta}_\varphi(t)| + \sum_{\omega=1}^n |\check{\mathfrak{S}}_\omega(t)| \tag{14}$$

For the Caputo derivative along the trajectories of (13) and using Assumption 2, we have

$$\begin{aligned} D^\lambda V(t, \hat{\zeta}, \check{\mathfrak{S}}) &= D^\lambda \left[\sum_{\varphi=1}^o |\hat{\zeta}_\varphi(t)| + \sum_{\omega=1}^n |\check{\mathfrak{S}}_\omega(t)| \right] \\ &\leq \left\{ \sum_{\varphi=1}^o (-d_\varphi |\hat{\zeta}_\varphi(t)| + \sum_{\omega=1}^n |c_{\varphi\omega}|F_\omega |\check{\mathfrak{S}}_\omega(t)| \right. \\ &\quad + \sum_{\omega=1}^n |a_{\varphi\omega}|F_\omega |\check{\mathfrak{S}}_\omega(t-\tau)| + \sum_{\omega=1}^n (-\tilde{d}_\omega |\check{\mathfrak{S}}_\omega(t)| + \sum_{\varphi=1}^o |\tilde{c}_{\omega\varphi}|G_\varphi |\hat{\zeta}_\varphi(t)| \\ &\quad \left. + \sum_{\varphi=1}^o |\tilde{a}_{\omega\varphi}|G_\varphi |\hat{\zeta}_\varphi(t-\tau)| \right\} \\ &= - \left\{ \sum_{\varphi=1}^o [d_\varphi - |\tilde{c}_{\omega\varphi}|G_\varphi] |\hat{\zeta}_\varphi(t)| - \sum_{\omega=1}^n [\tilde{d}_\omega - |c_{\varphi\omega}|F_\omega] |\check{\mathfrak{S}}_\omega(t)| \right. \\ &\quad \left. + \sum_{\varphi=1}^o \sum_{\omega=1}^n |a_{\varphi\omega}|F_\omega |\check{\mathfrak{S}}_\omega(t-\tau)| + \sum_{\varphi=1}^o |\tilde{a}_{\omega\varphi}|G_\varphi |\hat{\zeta}_\varphi(t-\tau)| \right\}, \\ &= -\omega_1 \sum_{\varphi=1}^o |\hat{\zeta}_\varphi(t)| - \omega_2 \sum_{\omega=1}^n |\check{\mathfrak{S}}_\omega(t)| + \sum_{\varphi=1}^o \sum_{\omega=1}^n \omega_3 |\hat{\zeta}_\varphi(t-\tau)| \\ &\quad + \left\{ \sum_{\varphi=1}^o \sum_{\omega=1}^n \omega_4 |\check{\mathfrak{S}}_\omega(t-\tau)| \right\} \\ &\leq -\omega_1^\theta V(t, \hat{\zeta}(t), \check{\mathfrak{S}}_\omega(t)) + \omega_2^\theta \sup_{t-\tau \leq s \leq t} V(s, \hat{\zeta}(s), \check{\mathfrak{S}}(s)). \tag{15} \end{aligned}$$

We apply the Razumikhin condition,

$$\sup_{t-\tau \leq s \leq t} V(s, \hat{\zeta}(s), \check{\mathfrak{S}}(s)) \leq V(t, \hat{\zeta}(t), \check{\mathfrak{S}}(t)), \tag{16}$$

to (15) and obtain

$$D^\lambda V(t, \hat{\zeta}(t), \check{\mathfrak{S}}(t)) \leq -(\omega_1^\theta - \omega_2^\theta) V(t, \hat{\zeta}(t), \check{\mathfrak{S}}(t)). \tag{17}$$

We can choose a positive constant $\delta > 0$, such that

$$(\omega_1^\theta - \omega_2^\theta) \geq \delta \tag{18}$$

From (17) and (18), we obtain

$$D^\lambda V(t, \hat{\zeta}(t), \check{\mathfrak{S}}(t)) \leq -\delta V(t, \hat{\zeta}(t), \check{\mathfrak{S}}(t)). \tag{19}$$

According to Lemma 2,

$$V(t, \hat{\zeta}(t), \check{\mathfrak{S}}(t)) \leq \sup_{t-\tau \leq s \leq t} V(o, \hat{\zeta}(s), \check{\mathfrak{S}}(s)) E_\lambda(-\delta t^\lambda). \tag{20}$$

For

$$\begin{aligned}
 V(t, \zeta(t), \mathfrak{S}(t)) &= \|\zeta(t) - \zeta^*\|_1 + \|\mathfrak{S}(t) - \mathfrak{S}^*\|_2, \\
 &= \sum_{\varphi=1}^o |\zeta_{\varphi}(t) - \zeta^*| + \sum_{\omega=1}^n |\mathfrak{S}_{\omega}(t) - \mathfrak{S}^*|,
 \end{aligned}$$

we have from (20)

$$\|\zeta(t) - \zeta^*\|_1 + \|\mathfrak{S}(t) - \mathfrak{S}^*\|_2 \leq \left(\|\phi_{\varphi} - \zeta^*\|_{\tau}^1 + \|\phi_{\omega} - \mathfrak{S}^*\|_{\tau}^2 \right) E_{\lambda}(-\delta t^{\lambda}), \tag{21}$$

where ϕ_{φ} and $\tilde{\phi}_{\omega}$ are the initial functions that correspond to system (12), and $\|\phi\|_{\tau}^1 = \max_{s \in [-\tau, 0]} \|\phi(s)\|_1, \|\tilde{\phi}\|_{\tau}^2 = \max_{s \in [-\tau, 0]} \|\tilde{\phi}(s)\|_2$.

Therefore, system (13) is globally Mittag–Leffler stable, i.e., the equilibrium of system (12) is globally Mittag–Leffler stable. The proof is completed. \square

Remark 6. Notice that the results provided by Theorems 3 and 4 are particular cases of the results established in Theorem 1. In addition, it is seen that the Mittag–Leffler stability concept is a particular case of the asymptotic stability notion and generalizes the exponential stability in the fractional-order case.

5. Numerical Examples

In this section, numerical examples are addressed to demonstrate the usefulness of the proposed results.

Example 1. For $\varphi = \omega = 2$, we consider the master system (1) and response system (2) of fuzzy BAM NNs with the following parameters: $\lambda = 0.97, \tau = 0.2$,

$$\begin{aligned}
 D = \tilde{D} &= \begin{bmatrix} 1.5 & 0 \\ 0 & 1.5 \end{bmatrix}, c_{\varphi\omega} = \tilde{c}_{\omega\varphi} = \begin{bmatrix} 0.2 & -0.1 \\ 0.1 & 0.2 \end{bmatrix}, a_{\varphi\omega} = \tilde{a}_{\omega\varphi} = \begin{bmatrix} -0.4 & 0.5 \\ 0.4 & -2.5 \end{bmatrix}, \\
 u_{\varphi\omega} = \tilde{u}_{\omega\varphi} &= \begin{bmatrix} 0.5 & -0.5 \\ 0.6 & 0.8 \end{bmatrix}, P_{\varphi\omega} = \tilde{P}_{\omega\varphi} = \begin{bmatrix} -0.4 & -0.8 \\ 0.5 & 0.1 \end{bmatrix}, v_{\varphi\omega} = \tilde{v}_{\omega\varphi} = \begin{bmatrix} -0.5 & -0.1 \\ -0.2 & -0.5 \end{bmatrix}, \\
 Q_{\varphi\omega} = \tilde{Q}_{\omega\varphi} &= \begin{bmatrix} -0.4 & 0.5 \\ 0.4 & -2.5 \end{bmatrix}, M_1 = M_2 = \begin{bmatrix} 0 & 0 \\ 0 & 0 \end{bmatrix}, I_{\varphi} = J_{\omega} = \begin{bmatrix} -0.2 \cos(t) \\ -0.2 \sin(t) \end{bmatrix}, \\
 \tilde{M}_1 = \tilde{M}_2 &= \begin{bmatrix} 0 & 0 \\ 0 & 0 \end{bmatrix}.
 \end{aligned}$$

Consider the activation functions defined by

$$g_{\varphi}(\zeta_{\varphi}(t, \varphi)) = |\zeta_{\varphi}(t, \varphi) + 2| - |\zeta_{\varphi}(t, \varphi) - 2|,$$

$$f_{\omega}(\mathfrak{S}_{\omega}(t, \varphi)) = |\mathfrak{S}_{\omega}(t, \varphi) + 2| - |\mathfrak{S}_{\omega}(t, \varphi) - 2|,$$

which satisfy Assumption 2 for $F_{\omega} = \frac{1}{2}$ and $G_{\varphi} = \frac{1}{2}$.

Although Assumptions 1–3 are satisfied, the numerical simulations demonstrated in Figure 1 show that the global asymptotic synchronization cannot be realized for systems (1) and (2), or the corresponding error system is not globally asymptotically stable in the absence of a control input.

Now, let us consider feedback controllers with $t_{\varphi} = 2.1, \Psi_{\varphi} = 1.1, \omega_{\omega} = 0, \varrho_{\omega} = 2$, and let $\rho = 0.2$.

Substituting the above values in Theorem 1, we obtain

$$\begin{aligned} \mu_{\min}^{(1)} &= \min_{1 \leq \varphi \leq o} \left\{ 2\tilde{M}_\varphi + 2d_\varphi - \sum_{\omega=1}^n |c_{\varphi\omega}| F_\omega \rho^{-1} - \sum_{\omega=1}^n |a_{\varphi\omega}| F_\omega \rho^{-1} \right. \\ &\quad \left. - \sum_{\omega=1}^n |u_{\varphi\omega}| F_\omega \rho^{-1} - \sum_{\omega=1}^n |v_{\varphi\omega}| F_\omega \rho^{-1} + t_\varphi + \psi_\varphi - \sum_{\omega=1}^n |c_{\varphi\omega}| F_\omega \rho \right\} = 1.22 > 0, \\ \mu_{\min}^{(2)} &= \min_{1 \leq \omega \leq n} \left\{ 2\tilde{M}_\omega + 2\tilde{d}_\omega - \sum_{\varphi=1}^o |\tilde{c}_{\omega\varphi}| G_\varphi \rho^{-1} - \sum_{\varphi=1}^o |\tilde{a}_{\omega\varphi}| G_\varphi \rho^{-1} - \sum_{\varphi=1}^o |\tilde{u}_{\omega\varphi}| G_\varphi \rho^{-1} \right. \\ &\quad \left. - \sum_{\varphi=1}^o |\tilde{v}_{\omega\varphi}| G_\varphi \rho^{-1} + \omega_\omega + \varrho_\omega - \sum_{\varphi=1}^o |\tilde{c}_{\omega\varphi}| G_\varphi \rho \right\} = 1.29 > 0, \\ \Lambda_1^\mu &= \max_{1 \leq \varphi \leq o} \left\{ \sum_{\omega=1}^n |\tilde{u}_{\omega\varphi}| G_\varphi \rho + \sum_{\omega=1}^n |\tilde{v}_{\omega\varphi}| G_\varphi \rho + \sum_{\omega=1}^n |\tilde{a}_{\omega\varphi}| G_\varphi \rho \right\} = 0.86 > 0, \\ \Lambda_2^\mu &= \max_{1 \leq \omega \leq n} \left\{ \sum_{\varphi=1}^o |u_{\varphi\omega}| F_\omega \rho + \sum_{\varphi=1}^o |v_{\varphi\omega}| F_\omega \rho + \sum_{\varphi=1}^o |a_{\varphi\omega}| F_\omega \rho \right\} = 0.45 > 0. \end{aligned}$$

Hence, $\mu > \sqrt{2}\Lambda$, where $\mu = \min\{\mu_{\min}^{(1)}, \mu_{\min}^{(2)}\} = 1.22$ and $\Lambda = \max\{\Lambda_1^\mu, \Lambda_2^\mu\} = 0.86$, and by Theorem 1, systems (1) and (2) are globally asymptotically synchronized. This means that the corresponding error system is globally asymptotically stable via the controllers. The trajectories of the error system for $\lambda = 0.97$ are given in Figure 2.

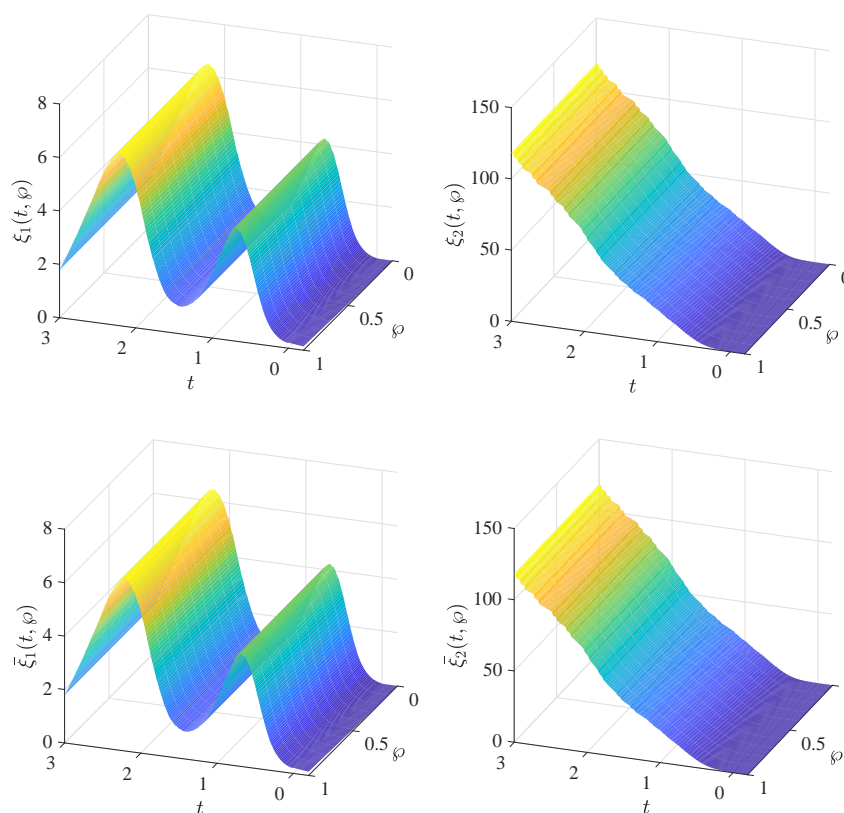


Figure 1. State trajectories of the error system corresponding to the fractional-order fuzzy BAM neural networks in Example 1 for $\lambda = 0.97$ without controllers.

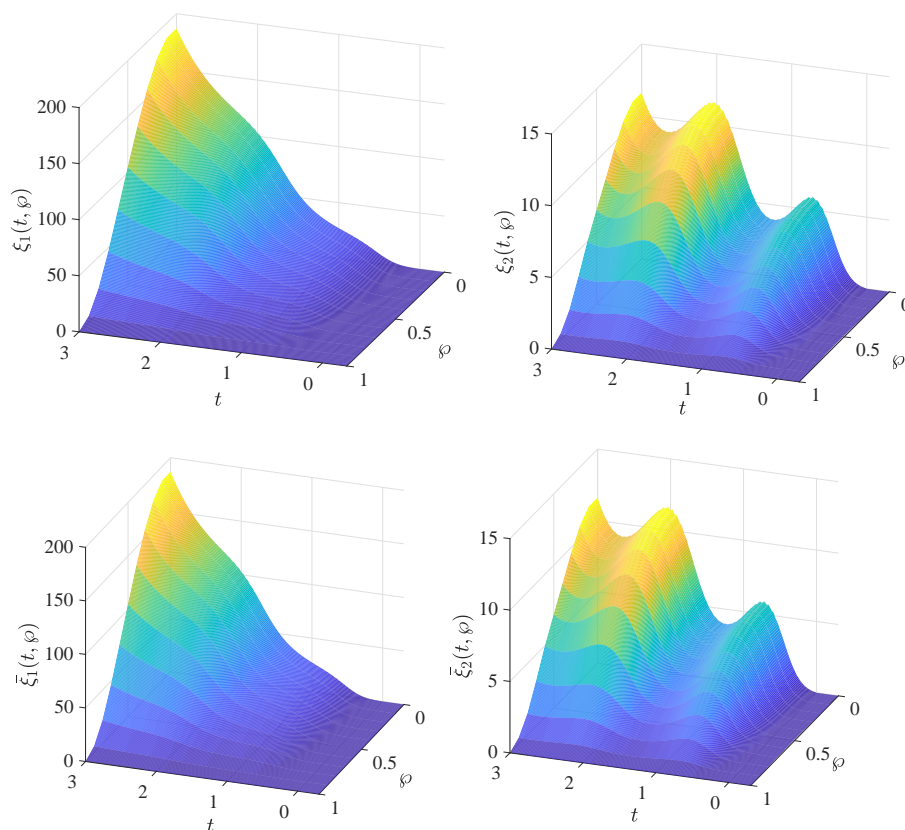


Figure 2. State trajectories of the error system corresponding to the fractional-order fuzzy BAM neural networks in Example 1 with fractional order $\lambda = 0.97$ with controllers.

Example 2. In this example, consider the error system (8) for $\varphi = \omega = 2$ and the following parameters: $\lambda = 0.95, \tau = 0.2$

$$\begin{aligned}
 D = \tilde{D} &= \begin{bmatrix} 1.5 & 0 \\ 0 & 1.5 \end{bmatrix}, c_{\varphi\omega} = \tilde{c}_{\varphi\omega} = \begin{bmatrix} 0.2 & -0.1 \\ 0.1 & 0.3 \end{bmatrix}, a_{\varphi\omega} = \tilde{a}_{\varphi\omega} = \begin{bmatrix} -0.2 & 0.6 \\ 0.5 & -3.5 \end{bmatrix}, \\
 u_{\varphi\omega} = u_{\omega\varphi} &= \begin{bmatrix} 0.4 & -0.4 \\ 0.7 & 0.6 \end{bmatrix}, P_{\varphi\omega} = \tilde{P}_{\varphi\omega} = \begin{bmatrix} -0.3 & -0.7 \\ 0.4 & -2 \end{bmatrix}, v_{\varphi\omega} = \tilde{v}_{\varphi\omega} = \begin{bmatrix} -0.7 & -0.2 \\ -0.1 & -0.5 \end{bmatrix}, \\
 Q_{\varphi\omega} = \tilde{Q}_{\varphi\omega} &= \begin{bmatrix} -0.3 & 0.4 \\ 0.3 & -2.6 \end{bmatrix}, M_1 = M_2 = 0, \tilde{M}_1 = \tilde{M}_2 = 0, I = \begin{bmatrix} -0.2 \cos(t) \\ -0.2 \sin(t) \end{bmatrix}.
 \end{aligned}$$

Then, the following functions are defined

$$g_{\varphi}(\zeta_{\varphi}(t, \varphi)) = |\zeta_{\varphi}(t, \varphi) + 2| - |\zeta_{\varphi}(t, \varphi) - 2|.$$

$$f_{\omega}(\mathfrak{S}_{\omega}(t, \varphi)) = |\mathfrak{S}_{\omega}(t, \varphi) + 2| - |\mathfrak{S}_{\omega}(t, \varphi) - 2|,$$

Substituting the above values in Theorem 3, we obtain

$$\begin{aligned}
 v_{\min}^{(1)} &= \min_{1 \leq \varphi \leq o} \left\{ 2\tilde{M}_\varphi + 2d_\varphi - \sum_{\omega=1}^n |c_{\varphi\omega}| F_{\omega\rho}^{-1} - \sum_{\omega=1}^n |a_{\varphi\omega}| F_{\omega\rho}^{-1} \right. \\
 &\quad \left. - \sum_{\omega=1}^n |u_{\varphi\omega}| F_{\omega\rho}^{-1} - \sum_{\omega=1}^n |v_{\varphi\omega}| F_{\omega\rho}^{-1} - \sum_{\omega=1}^n |c_{\varphi\omega}| F_{\omega\rho} \right\} = 2.10 > 0, \\
 v_{\min}^{(2)} &= \min_{1 \leq \omega \leq n} \left\{ 2\tilde{M}_\omega + 2\tilde{d}_\omega - \sum_{\varphi=1}^o |\tilde{c}_{\omega\varphi}| G_{\varphi\rho}^{-1} - \sum_{\varphi=1}^o |\tilde{a}_{\omega\varphi}| G_{\varphi\rho}^{-1} - \sum_{\varphi=1}^o |\tilde{u}_{\omega\varphi}| G_{\varphi\rho}^{-1} \right. \\
 &\quad \left. - \sum_{\varphi=1}^o |\tilde{v}_{\omega\varphi}| G_{\varphi\rho}^{-1} - \sum_{\varphi=1}^o |\tilde{c}_{\omega\varphi}| G_{\varphi\rho} \right\} = 2.10 > 0, \\
 \Lambda_1^v &= \max_{1 \leq \varphi \leq o} \left\{ \sum_{\omega=1}^n |\tilde{u}_{\omega\varphi}| G_{\varphi\rho} + \sum_{\omega=1}^n |\tilde{v}_{\omega\varphi}| G_{\varphi\rho} + \sum_{\omega=1}^n |\tilde{a}_{\omega\varphi}| G_{\varphi\rho} \right\} = 1.98 > 0, \\
 \Lambda_2^v &= \max_{1 \leq \omega \leq n} \left\{ \sum_{\varphi=1}^o |u_{\varphi\omega}| F_{\omega\rho} + \sum_{\varphi=1}^o |v_{\varphi\omega}| F_{\omega\rho} + \sum_{\varphi=1}^o |a_{\varphi\omega}| F_{\omega\rho} \right\} = 0.87 > 0.
 \end{aligned}$$

Hence, since $2.10 = \min\{v_{\min}^{(1)}, v_{\min}^{(2)}\} > \max\{\Lambda_1^v, \Lambda_2^v\} = 1.98$, Theorem 3 implies that the error system (8) is globally Mittag-Leffler stable. The state trajectories for the given system parameters are shown in Figure 3.

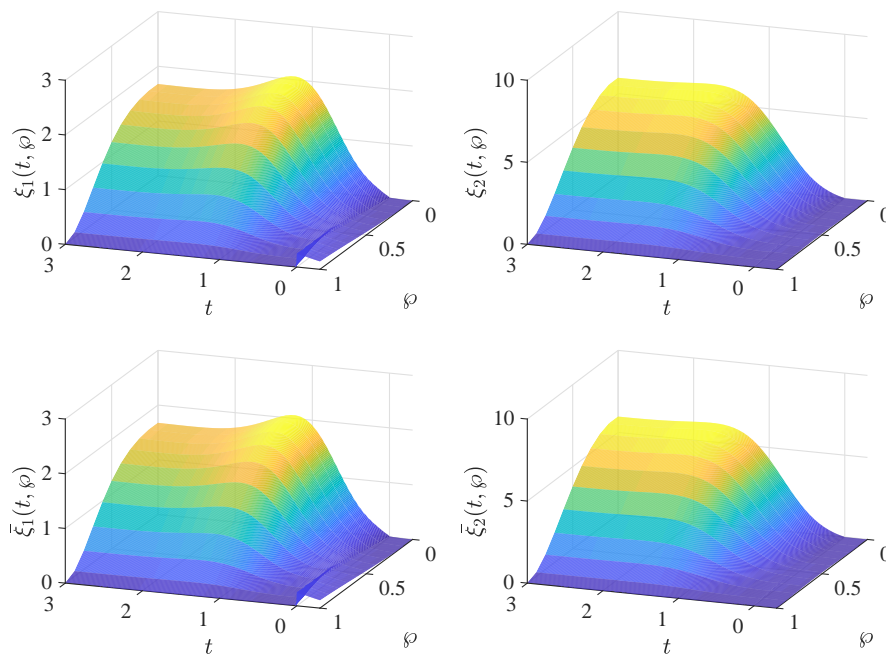


Figure 3. The state trajectories of the fractional-order fuzzy BAM neural network system (8) in Example 2.

Example 3. In this Example, we consider a model of type (13) with $\varphi = \omega = 2$ and $\lambda = 0.9, \tau = 0.2$,

$$c_{\varphi\omega} = \tilde{c}_{\omega\varphi} = \begin{bmatrix} 0.6 & -0.3 \\ 0.3 & 0.7 \end{bmatrix}, \quad a_{\varphi\omega} = \tilde{a}_{\omega\varphi} = \begin{bmatrix} -0.2 & 0.4 \\ 0.4 & -1.2 \end{bmatrix},$$

and activation functions defined by

$$g_\varphi(\hat{\zeta}_\varphi(t)) = |\hat{\zeta}_\varphi(t) + 2| - |\hat{\zeta}_\varphi(t) - 2|,$$

$$f_\omega(\check{\zeta}_\omega(t)) = |\check{\zeta}_\omega(t) + 2| - |\check{\zeta}_\omega(t) - 2|.$$

Substituting the above values in Theorem 3, we obtain $\omega_1 = \min_{1 \leq \varphi \leq o} \{[d_\varphi - |\tilde{c}_{\omega\varphi}|F_\varphi]\} = 2.87$, $\omega_2 = \min_{1 \leq \varphi \leq o} \{[\tilde{d}_\omega - |c_{\varphi\omega}|F_\omega]\} = 1.78$, $\omega_3 = \min_{1 \leq \varphi \leq o} [\sum_{\omega=1}^n |a_{\varphi\omega}|F_\omega] = 0.87$, $\omega_4 = \max_{1 \leq \omega \leq n} [\sum_{\varphi=1}^o |\tilde{a}_{\omega\varphi}|F_\varphi] = 0.87$.

By utilizing Theorem 4, we are able to ascertain that system (13) is globally Mittag-Leffler stable. The stable behavior of the states is shown in Figure 4.

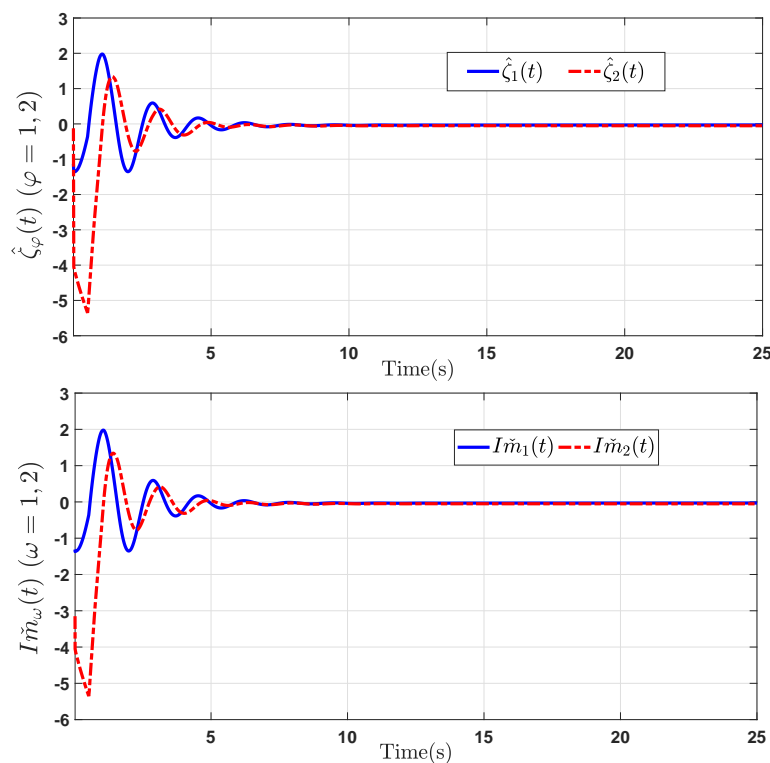


Figure 4. The state trajectories of the fractional-order BAM neural network system in Example 3.

Remark 7. The parameters, initial values, software, and computer configurations used in establishing numerical simulations were as follows:

Example 1: $N = 2000$; $d = [0.5; 0.5]$; $D_1 = \text{diag}(d)$; $f_1 = 2$; $f_2 = 2$; $g_1 = 1$; $g_2 = 1$; $\text{dis} = 1$; $ti = 3$; $a = 0.2$; $b = 0.1$; $\tau = 0.3$; $tstep = 0.01$; $dstep = 0.1$; $\tau no = \tau / tstep$; $t no = ti / tstep$; $d no = \text{dis} / dstep$; $N_1 = 10$; $T_1 = \text{zeros}(1, N_1)$; $\text{delta}2 = \text{zeros}(1, N_1)$; $T_1(1) = \tau no$; $\beta = \min(F_1) / \max(F)N = 2000$.

Example 2: $f_1 = 2$; $f_2 = 2$; $g_1 = 1$; $g_2 = 1$; $\text{Dis} = 1$; $ti = 3$; $a = 0.2$; $b = 0.1$; $\tau = 0.3$; $tstep = 0.01$; $dstep = 0.1$; $\tau no = \tau / tstep$; $t no = ti / tstep$; $d no = \text{dis} / dstep$; $N_1 = 10$; $T_1 = \text{zeros}(1, N_1)$; $\text{delta}2 = \text{zeros}(1, N_1)$; $T_1(1) = \tau no$; for $k = 2 : N_1$; $T_1(k) = \tau no + 30 * (k - 1) + (-1)^k * (\text{rem}((k - 1), 10))$; for $k = 1 : N_1 - 1$ $\text{delta}(k) = T_1(k) + \text{round}(0.6 * (T_1(k + 1) - T_1(k)))$; $\text{delta}(N_1) = T_1(N_1) + 20$.

Example 3: $et = 25$; $h = 0.02$; $t = -st : h : et$; $N_0 = \text{floor}(st/h)$; $N_1 = et/h$; $n = N_0 + N_1$; $q_1 = 0.95$; $q_2 = 0.95$; $q_3 = 0.95$; $q_4 = 0.95$

System configuration: Window 10 and Matlab 2017A software.

6. Conclusions

In this paper, we considered a reaction–diffusion fractional-order fuzzy BAM neural network with discrete and distributed delays. The global asymptotic stability and global asymptotic synchronization behaviors were investigated using novel hybrid feedback controllers. In addition, sufficient conditions ensuring the globally Mittag–Leffler stability of such systems were derived based on the inequality technique and an analysis method for the controller was also developed. The criteria were in the form of algebraic inequalities and were convenient for applications. The established global asymptotic synchronization results also reflected the presence of distributed delays and the design of the proposed controllers. Numerical examples were given to verify the effectiveness of the main results.

The obtained results advance the related state of the art by considering a more general structure which allows one to divide all nodes in the network into different classes and includes a BAM two-layer connection, fuzzy logic, and hybrid feedback controllers. The applied technique can be extended to systems under impulsive perturbations which can also be used as a control mechanism. Considering real case studies, such as proportional–integral–derivative controllers, variable-order fractional derivatives are also subjects for future development of the topic.

Author Contributions: Conceptualization, M.S.A., G.S., I.S., T.F.I., A.A.D. and F.M.O.B.; methodology, M.S.A., G.S., I.S., T.F.I., A.A.D. and F.M.O.B.; formal analysis, M.S.A., G.S., I.S., T.F.I., A.A.D. and F.M.O.B.; investigation, M.S.A., G.S., I.S., T.F.I., A.A.D. and F.M.O.B.; writing—original draft preparation, M.S.A. and I.S. All authors have read and agreed to the published version of the manuscript.

Funding: This research is founded through a project under grant number RGP2/141/44.

Data Availability Statement: Not applicable.

Acknowledgments: The authors extend their appreciation to the Deanship of Scientific Research at King Khalid University for funding this work through large groups (project under grant number RGP2/141/44).

Conflicts of Interest: The authors declare no conflict of interest.

References

1. Syed Ali, M.; Hymavathi, M.; Saroha, S.; Krishna Moorthy, R. Global asymptotic stability of neutral type fractional-order memristor-based neural networks with leakage term, discrete and distributed delays. *Math. Methods Appl. Sci.* **2021**, *44*, 5953–5973. [[CrossRef](#)]
2. Syed Ali, M.; Hymavathi, M.; Rajchakit, G.; Saroha, S.; Palanisamy, L.; Hammachukiattikul, P. Synchronization of fractional order fuzzy BAM neural networks with time varying delays and reaction diffusion terms. *IEEE Access* **2020**, *8*, 186551–186571.
3. Baleanu, D.; Diethelm, K.; Scalas, E.; Trujillo, J.J. *Fractional Calculus: Models and Numerical Methods*, 1st ed.; World Scientific: Singapore, 2012; ISBN 978-981-4355-20-9.
4. Bao, H.; Park, J.H.; Cao, J. Non-fragile state estimation for fractional-order delayed memristive BAM neural networks. *Neural Netw.* **2019**, *119*, 190–199. [[CrossRef](#)]
5. Bohner, M.; Jonnalagadda, J.M. Discrete fractional cobweb models. *Chaos Solit. Fract.* **2022**, *162*, 112451. [[CrossRef](#)]
6. Magin, R. *Fractional Calculus in Bioengineering*, 1st ed.; Begell House: Redding, CA, USA, 2006; ISBN 978-1567002157.
7. Podlubny, I. *Fractional Differential Equations*, 1st ed.; Academic Press: San Diego, CA, USA, 1999; ISBN 558840-2.
8. Singh, H.; Srivastava, H.M.; Nieto, J.J. (Eds.) *Handbook of Fractional Calculus for Engineering and Science*, 1st ed.; CRC Press, Taylor and Francis Group: Boca Raton, USA, 2022; ISBN 9781003263517.
9. Wang, Z.; Huang, X.; Shi, G. Analysis of nonlinear dynamics and chaos in a fractional order financial system with time delay. *Comput. Math. Appl.* **2011**, *62*, 1531–1539. [[CrossRef](#)]
10. Wang, L.; Song, Q.; Liu, Y.; Zhao, Z.; Alsaadi, F. Finite-time stability analysis of fractional order complex-valued memristor-based neural networks with both leakage and time-varying delays. *Neurocomputing* **2017**, *245*, 86–101. [[CrossRef](#)]
11. Zhang, L.; Yang, Y.; Wang, F. Synchronization analysis of fractional-order neural networks with time-varying delays via discontinuous neuron activations. *Neurocomputing* **2017**, *275*, 40–49. [[CrossRef](#)]
12. Abdurahman, A.; Jiang, H.; Teng, Z. Finite-time synchronization for fuzzy cellular neural networks with time-varying delays. *Fuzzy Sets Syst.* **2016**, *297*, 96–111. [[CrossRef](#)]
13. Li, X.; Rakkiyappan, R.; Balasubramaniam, P. Existence and global stability analysis of equilibrium of fuzzy cellular neural networks with time delay in the leakage term under impulsive perturbations. *J. Franklin Inst.* **2011**, *348*, 135–155. [[CrossRef](#)]

14. Kumar, A.; Das, S.; Yadav, V.K.; Jinde Cao, J.; Huang, C. Synchronizations of fuzzy cellular neural networks with proportional time-delay. *AIMS Math.* **2021**, *6*, 10620–10641. [[CrossRef](#)]
15. Du, F.; Lu, J.G. Finite-time stability of fractional-order fuzzy cellular neural networks with time delays. *Fuzzy Sets Syst.* **2022**, *438*, 107–120. [[CrossRef](#)]
16. Singh, A.; Rai, J.N. Stability of fractional order fuzzy cellular neural networks with distributed delays via hybrid feedback controllers. *Neural Process. Lett.* **2021**, *53*, 1469–1499. [[CrossRef](#)]
17. Kosko, B. Adaptive bidirectional associative memories. *Appl. Opt.* **1987**, *26*, 4947–4960. [[CrossRef](#)] [[PubMed](#)]
18. Huang, C.; Wang, J.; Chen, X.; Cao, J. Bifurcations in a fractional-order BAM neural network with four different delays. *Neural Netw.* **2021**, *141*, 344–354. [[CrossRef](#)] [[PubMed](#)]
19. Syed Ali, M.; Hymavathi, M.; Kausar, S.A.; Boonsatit, N.; Hammachukiattikul, P.; Rajchakit, G. Synchronization of fractional order uncertain BAM competitive neural networks. *Fractal Fract.* **2022**, *6*, 14. [[CrossRef](#)]
20. Li, Y.; Wang, C. Existence and global exponential stability of equilibrium for discrete-time fuzzy BAM neural networks with variable delays and impulses. *Fuzzy Sets Syst.* **2013**, *217*, 62–79. [[CrossRef](#)]
21. Zhang, Y.; Li, Z.; Jiang, W.; Liu, W. The stability of anti-periodic solutions for fractional-order inertial BAM neural networks with time-delays. *AIMS Math.* **2023**, *8*, 6176–6190. [[CrossRef](#)]
22. Zhu, Q.; Li, X.; Yang, X. Exponential stability for stochastic reaction–diffusion BAM neural networks with time-varying and distributed delays. *Appl. Math. Comput.* **2011**, *217*, 6078–6091. [[CrossRef](#)]
23. Li, Y.; Chen, Y.Q.; Podlubny, I. Stability of fractional-order nonlinear dynamic systems: Lyapunov direct method and generalized Mittag–Leffler stability. *Comput. Math. Appl.* **2010**, *24*, 1429–1468. [[CrossRef](#)]
24. Liu, S.; Li, X.Y.; Jiang, W.; Zhou, X.F. Mittag–Leffler stability of nonlinear fractional neutral singular systems. *Commun. Nonlinear Sci. Numer. Simul.* **2012**, *17*, 3961–3966. [[CrossRef](#)]
25. Stamov, T.; Stamova, I. Design of impulsive controllers and impulsive control strategy for the Mittag–Leffler stability behavior of fractional gene regulatory networks. *Neurocomputing* **2021**, *424*, 54–62. [[CrossRef](#)]
26. Wu, A.; Liu, L.; Huang, T.; Zeng, Z. Mittag–Leffler stability of fractional-order neural networks in the presence of generalized piecewise constant arguments. *Neural Netw.* **2017**, *85*, 118–127. [[CrossRef](#)] [[PubMed](#)]
27. Wu, A.; Zeng, Z. Global Mittag–Leffler stabilization of fractional-order memristive neural networks. *IEEE Trans. Neural Netw. Learn. Syst.* **2015**, *28*, 206–217. [[CrossRef](#)] [[PubMed](#)]
28. Xiao, J.; Zhong, S.; Li, Y.; Xu, F. Finite-time Mittag–Leffler synchronization of fractional-order memristive BAM neural networks with time delays. *Neurocomputing* **2017**, *219*, 431–439. [[CrossRef](#)]
29. Yan, H.; Qiao, Y.; Duan, L.; Zhang, L. Global Mittag–Leffler stabilization of fractional-order BAM neural networks with linear state feedback controllers. *Math. Probl. Eng.* **2020**, *2020*, 6398208. [[CrossRef](#)]
30. Li, X.; Caraballo, T.; Rakkiyappan, R.; Han, X. On the stability of impulsive functional differential equations with infinite delays. *Math. Methods Appl. Sci.* **2015**, *38*, 3130–3140. [[CrossRef](#)]
31. Song, Q.; Wang, Z. Neural networks with discrete and distributed time-varying delays: A general stability analysis. *Neural Netw.* **2008**, *37*, 1538–1547. [[CrossRef](#)]
32. Syed Ali, M.; Saravanan, S. Robust finite-time H_∞ control for a class of uncertain switched neural networks of neutral-type with distributed time varying delays. *Neurocomputing* **2016**, *177*, 454–468.
33. Zhang, G.; Zeng, Z.; Hu, J. New results on global exponential dissipativity analysis of memristive inertial neural networks with distributed time-varying delays. *Neural Netw.* **2018**, *97*, 183–191. [[CrossRef](#)]
34. Stamova, I.; Stamov, G. Mittag–Leffler synchronization of fractional neural networks with time-varying delays and reaction-diffusion terms using impulsive and linear controllers. *Neural Netw.* **2017**, *96*, 22–32. [[CrossRef](#)]
35. Li, R.; Cao, J.; Alsaedi, A.; Alsaadi, F. Exponential and fixed-time synchronization of Cohen–Grossberg neural networks with time-varying delays and reaction-diffusion terms. *Appl. Math. Comput.* **2017**, *313*, 37–51. [[CrossRef](#)]
36. Wang, C.; Zhang, H.; Stamova, I.; Cao, J. Global synchronization for BAM delayed reaction-diffusion neural networks with fractional partial differential operator. *J. Franklin Inst.* **2023**, *360*, 635–656. [[CrossRef](#)]
37. Wang, L.; Zhou, Q. Global exponential stability of BAM neural networks with time-varying delays and reaction-diffusion terms. *Phys. Lett. A* **2007**, *371*, 83–89.
38. Wei, T.; Li, X.; Stojanovic, V. Input-to-state stability of impulsive reaction–diffusion neural networks with infinite distributed delays. *Nonlinear Dyn.* **2021**, *103*, 1733–1755. [[CrossRef](#)]
39. Wu, X.; Liu, S.; Wang, Y. Stability analysis of Riemann–Liouville fractional-order neural networks with reaction-diffusion terms and mixed time-varying delays. *Neurocomputing* **2021**, *431*, 169–178. [[CrossRef](#)]
40. Antsaklis, P.J. Special issue on hybrid systems: theory and applications—a brief introduction to the theory and applications of hybrid systems. *Proc. IEEE* **2000**, *88*, 879–887. [[CrossRef](#)]
41. Diethelm, K.; Ford, N.J. Analysis of fractional differential equations. *J. Math. Anal. Appl.* **2002**, *265*, 229–248. [[CrossRef](#)]
42. Liang, S.; Wu, R.; Chen, L. Comparison principles and stability of nonlinear fractional-order cellular neural networks with multiple time delays. *Neurocomputing* **2015**, *168*, 618–625. [[CrossRef](#)]
43. Kuang, J.C. *Applied Inequalities*, 3rd ed.; Shandong Science and Technology Press: Jinan, China, 2004; ISBN 9787533136185. (In Chinese)

44. Wu, H.; Zhang, X.; Xue, S.; Wang, L.; Wang, Y. LMI conditions to global Mittag-Leffler stability of fractional-order neural networks with impulses. *Neurocomputing* **2016**, *193*, 148–154. [[CrossRef](#)]
45. Lu, J.G. Global exponential stability and periodicity of reaction-diffusion delayed recurrent neural networks with Dirichlet boundary conditions. *Chaos Solitons Fract.* **2008**, *35*, 116–125. [[CrossRef](#)]

Disclaimer/Publisher's Note: The statements, opinions and data contained in all publications are solely those of the individual author(s) and contributor(s) and not of MDPI and/or the editor(s). MDPI and/or the editor(s) disclaim responsibility for any injury to people or property resulting from any ideas, methods, instructions or products referred to in the content.

[Home](#) [Soft Computing](#) [Article](#)

Observer-based security control for Markov jump systems under hybrid cyber-attacks and its application via event-triggered scheme

[Application of soft computing](#) Published: 03 October 2023[\(2023\)](#) [Cite this article](#)[Soft Computing](#)[Aims and scope](#)[Submit manuscript](#)[M. Mubeen Tajudeen](#), [M. Syed Ali](#), [R. Perumal](#) , [Hamed Alsulami](#) & [Bashir Ahmad](#) **126** [Accesses](#) [Explore all metrics](#) →

Abstract

This article investigates the observer-based security control of discrete-time Markov jump systems (MJSS) subject to hybrid cyber-attacks and unmeasured states via event-triggered scheme. The event-triggered scheme (ETS) is being developed to relieve more network burdens. A Luenburger observer is used to estimate the unmeasured states. In this work, the hybrid cyber attack is addressed, which contains deception attacks and DoS attacks. It is anticipated that input control signals sent across a network are vulnerable to hybrid cyber-attacks in which adversaries could inject fake data into the control signals. Since system state information is usually not fully known, an observer-based controller is built to stabilize

[Journal of Control and Decision](#) >[Latest Articles](#)


61 | 0

Views | CrossRef citations to date | Altmetric

0

Research Article

Event-triggered H_∞ control of complex dynamical networks subject to stochastic cyber-attacks by new two-sided delay-dependent LKF functional

Bandana Priya, M. Mubeen Tajudeen, M. Syed Ali, Griengrai Rajchakit  & Ganesh Kumar Thakur

Received 16 Mar 2023, Accepted 19 Jul 2023, Published online: 02 Sep 2023

 Cite this article <https://doi.org/10.1080/23307706.2023.2240338>

Check for updates

 [Full Article](#) [Figures & data](#) [References](#) [Citations](#) [Metrics](#) [Reprints & Permissions](#)[Read this article](#)

ABSTRACT

This article deals with the problem of event-triggered control of complex dynamical networks (CDNs) subject to stochastic cyber-attacks and random coupling delays. Hackers may abuse the system by injecting malicious activity into communication networks. Two types of non-linear functions for cyber-attacks, time-varying coupling (), respectively, and a set of random variables satisfying the Bernoulli distribution

See discussions, stats, and author profiles for this publication at: <https://www.researchgate.net/publication/374594592>

Novel LMI-based adaptive boundary synchronisation of fractional-order fuzzy reaction-diffusion BAM neural networks with leakage delay

Article in *International Journal of Systems Science* - October 2023

DOI: 10.1080/00207721.2023.2250491

CITATIONS

0

READS

46

5 authors, including:



Gokulakrishnan Veeraragavan

SRM Institute of Science and Technology

8 PUBLICATIONS 17 CITATIONS

[SEE PROFILE](#)



M. Syed Ali

Thiruvalluvar University

203 PUBLICATIONS 4,320 CITATIONS

[SEE PROFILE](#)

Novel LMI-based adaptive boundary synchronisation of fractional-order fuzzy reaction–diffusion BAM neural networks with leakage delay

V. Gokulakrishnan, R. Srinivasan, M. Syed Ali, Grienggrai Rajchakit & Ganeshkumar Thakur

To cite this article: V. Gokulakrishnan, R. Srinivasan, M. Syed Ali, Grienggrai Rajchakit & Ganeshkumar Thakur (10 Oct 2023): Novel LMI-based adaptive boundary synchronisation of fractional-order fuzzy reaction–diffusion BAM neural networks with leakage delay, International Journal of Systems Science, DOI: [10.1080/00207721.2023.2250491](https://doi.org/10.1080/00207721.2023.2250491)

To link to this article: <https://doi.org/10.1080/00207721.2023.2250491>



Published online: 10 Oct 2023.



Submit your article to this journal [↗](#)



Article views: 4



View related articles [↗](#)



View Crossmark data [↗](#)



Novel LMI-based adaptive boundary synchronisation of fractional-order fuzzy reaction–diffusion BAM neural networks with leakage delay

V. Gokulakrishnan^a, R. Srinivasan^a, M. Syed Ali^b, Grienggrai Rajchakit^c and Ganeshkumar Thakur^d

^aDepartment of Mathematics, SRM Institute of Science and Technology, Chennai, India; ^bDepartment of Mathematics, Thiruvalluvar University, Vellore, India; ^cDepartment of Mathematics, Faculty of Science, Maejo University, Chiang Mai, Thailand; ^dDepartment of Applied Sciences, ABES Engineering College, Ghaziabad, India

ABSTRACT

The boundary synchronisation problem of fractional-order fuzzy reaction–diffusion BAM neural networks with leakage delay is investigated. A novel adaptive boundary controller, Neumann boundary condition, and fuzzy feedback MIN and MAX templates of nonlinear dynamic fuzzy modelling are employed. We developed adaptive sufficient criteria to check the asymptotic stability of error dynamical system by using suitable Lyapunov functional, Wirtinger's inequality and LMI method, which guarantee the drive-response dynamical systems achieve the synchronisation. Meanwhile, two different controllers, adaptive full-domain and boundary controllers are developed. At last, numerical simulations are presented to demonstrate the feasibility of the theoretical results.

ARTICLE HISTORY

Received 26 March 2023
Accepted 13 August 2023

KEYWORDS

Fuzzy BAM neural networks; reaction–diffusion terms; leakage delay; adaptive boundary control; linear matrix inequality; synchronisation

1. Introduction

In recent years, neural networks have performed exceptionally well in a variety of areas, including secure communication (Song et al., 2020), multi-channel audio encryption (Z. Dong et al., 2023), signal processing (Z. Wang, Eisen, et al., 2022), pattern formation (M. Li et al., 2022) and optimisation problems (Guan & Wang, 2022). In artificial neural networks, various architectures have been developed to model and analyse complicated patterns in data. Neural networks with bidirectional associative memory (BAM) are one of these architectures that can make bidirectional associations between patterns. Recurrent neural networks with specialised pattern recognition and pattern retrieval capabilities are referred to as BAM neural networks. BAM neural networks were initially proposed and studied by Kosko (1987), Kosko (1988). Synchronisation is a fundamental phenomenon in neural networks that has been studied in detail in the context of both integer-order and fractional-order systems (Sun et al., 2020; J. Wang, Tian, et al., 2023; Y. Wang et al., 2020). Understanding synchronisation in BAM neural networks is critical because synchronisation can facilitate information transfer, improve network efficiency and enable cooperative behaviour

among network elements. Studying synchronisation properties in these networks can provide insights into the emergence of collective behaviour, pattern formation and information integration. Recently, asymptotic synchronisation (D. Chen & Zhang, 2022), exponential synchronisation (Cao & Wan, 2014), finite-time synchronisation (Zhou et al., 2022), fixed-time synchronisation (Duan & Li, 2021) and H_∞ synchronisation (Shen et al., 2022) have been studied in BAM neural networks. Furthermore, diffusion effects are unavoidable in BAM neural networks because electrons move through nonuniform electromagnetic fields (T. Dong et al., 2022; Hu et al., 2022; M. Li & Zhao, 2022; Y. Li & Wei, 2022; Lin et al., 2020; Thakur et al., 2022; L. Wang et al., 2018).

Compared to traditional integer models, fractional models have been proven to be a valuable tool for defining the memory and associated properties of many materials (Nirvin et al., 2022; Udhayakumar, Rakkiyappan, et al., 2022; Udhayakumar, Rihan, et al., 2022; S. Yang et al., 2021). Based on the connections between neurons, fractional differential equations show how the concentration of neuron changes in response to what the brain does. Fractional-order BAM neural networks are strongly nonlinear

systems that exhibit a variety of dynamic behaviours, including bifurcation (C. Xu et al., 2021), chaos (Y. Wang et al., 2022), Mittag–Leffler stability (Stamov et al., 2019), passivity analysis (C. Wang, Zhang, Ye, et al., 2023), stabilisation (Wu et al., 2016) and synchronisation (C. Wang, Zhang, Stamova, et al., 2023). Time delays are important because many real-world phenomena have time dependencies. In neural networks, time delays can affect the dynamics of information transmission and processing. Investigating the time delays in neural networks can provide valuable insights into the stability, convergence and performance of these networks. In particular, leakage delays were introduced and studied in BAM neural networks by Gopalsamy (2007). Consequently, the dynamic behaviour of leakage delays in neural networks has paid much attention in the literature (Huang & Cao, 2018; Huang et al., 2021, 2017; Lin et al., 2019). However, the theory of fuzzy logic is required to solve the challenging biological problems that exceed the abilities of other existing techniques. Fractional fuzzy BAM neural networks have become a popular study in recent decades (Ratnavelu et al., 2017; Syed Ali, Hymavathi, et al., 2020; Syed Ali, Narayanan, et al., 2020; Z. Zhang & Yang, 2023).

Adaptive control, which is a continuous control strategy, has received much attention in real-world applications such as secure communications (Shanmugam et al., 2020) and image encryption (Mani et al., 2019) to save money in the temporal domain. The existing adaptive control methods include adaptive update laws. Adaptive control for the synchronisation of fractional-order BAM neural networks has attracted much attention in recent decades (C. Chen et al., 2018; Pratap et al., 2019; Rajivganthi et al., 2016; Shafiya et al., 2022; J. Yang et al., 2022; Z. Yang & Zhang, 2020). To achieve desired performance for neural networks while reducing the spatial domain cost and enabling easy implementation, a boundary controller can be introduced as unique control method for diffusion systems. In X. Z. Liu et al. (2023), R. J. Zhang et al. (2022), X. Z. Liu et al. (2020), the authors studied the synchronisation problem of fractional reaction–diffusion neural networks via boundary control. In recent years, a new paradigm, adaptive boundary control synchronisation, has emerged as a promising alternative. Adaptive boundary control synchronisation combines the principles of adaptive control with the concepts of boundary control and

Table 1. Comparison for fractional-order BAM neural networks (FOBAMNNs) with other works.

FOBAMNNs	Shafiya et al. (2022)	J. Yang et al. (2022)	Pratap et al. (2019)	This paper
Fuzzy approach	×	✓	×	✓
Reaction–diffusion	×	×	×	✓
Leakage delay	×	×	×	✓
LMI approach	✓	×	×	✓
Adaptive control	✓	×	✓	✓
Boundary control	×	×	×	✓
Synchronisation	✓	✓	✓	✓

synchronisation theory. In addition, adaptive boundary control provides better performance in terms of convergence speed and tracking accuracy compared to traditional adaptive control methods. Therefore, adaptive boundary control synchronisation is considered in this paper.

The previous discussion motivates us to do research on the new topic: LMI-based adaptive boundary synchronisation of fractional-order fuzzy reaction–diffusion BAM neural networks with leakage delay. The main contributions are listed as follows:

- The problem of boundary synchronisation of fractional-order fuzzy reaction–diffusion BAM neural networks with leakage time delay and adaptive boundary control is studied for the first time.
- By developing a set of adaptive boundary control strategies with adaptive updated laws in the fractional domain, new sufficient criteria are created to guarantee that the fractional-order fuzzy reaction–diffusion BAM neural networks achieve asymptotic synchronisation.
- Based on the Lyapunov stability theory and the LMI approach, asymptotic stability criteria are derived.
- The derived LMI stability criteria are less complicated to compute than the algebraic stability criteria suggested in C. Wang, Zhang, Stamova, et al. (2023), Syed Ali, Narayanan, et al. (2020), C. Chen et al. (2018), Z. Yang and Zhang (2020), J. Yang et al. (2022), Pratap et al. (2019), Rajivganthi et al. (2016).

We present Table 1 compared with existing works on fractional-order BAM neural networks with fuzzy approach, reaction–diffusion, leakage delay, LMI approach, adaptive control, boundary control and synchronisation to highlight the contributions and innovations of this work.

The rest of this work is organised as follows. In Section 2, system models and preliminaries are introduced. In Section 3, we investigate our main results: (i) designed both adaptive full-domain and boundary controllers. (ii) We obtain the synchronisation of the drive-response dynamical systems via adaptive full-domain controller. (iii) The adaptive boundary synchronisation of the drive-response dynamical systems is achieved. In Section 4, numerical simulations show that the designed adaptive controllers are effective. At last, conclusion and future works are shown in Section 5.

Notations: \mathbb{R} – set of all real numbers; \mathbb{R}^n – Euclidean space; $\mathcal{A}^T = \mathcal{A} < 0$ (respectively, $\mathcal{A}^T = \mathcal{A} > 0$) – negative definite matrix (positive definite matrix); \mathcal{A}^T – transpose of the matrix \mathcal{A} ; $\Pi_{\min}(\mathcal{A})$ – minimum eigen value of the matrix \mathcal{A} ; $\Pi_{\max}(\mathcal{A})$ – maximum eigen value of the matrix \mathcal{A} ; $*$ – the entry is symmetric; $\text{sym}(\mathcal{A}) = (\mathcal{A} + \mathcal{A}^T)$; $\|\cdot\|$ – Euclidean norm; $\mathcal{W}^{1,2}([0, \mathcal{L}]; \mathbb{R}^n)$ – absolutely continuous function in Soblev space; $(\int_0^1 \xi^T(t, z)\xi(t, z) dz)^{\frac{1}{2}} = \|\xi(t, z)\|_2$.

2. System description and preliminaries

Definition 2.1: (Y. Xu et al., 2021) The Caputo fractional derivative of state variable $\mathfrak{S}(t, z) : \mathbb{R}^n \times \mathbb{R}^+ \rightarrow \mathbb{R}$ with order $0 < \hbar < 1$ is defined by

$${}^C D_t^\hbar \mathfrak{S}(t, z) = \frac{1}{\Gamma(1 - \hbar)} \int_{t_0}^t \frac{\partial \mathfrak{S}(s, z)}{\partial s} \frac{ds}{(t - s)^\hbar}, \quad t > t_0.$$

Furthermore, the gamma function $\Gamma(\cdot)$ is defined by

$$\Gamma(x) = \int_0^\infty e^{-t} t^{x-1} dt.$$

Remark 2.2: To account for the ambiguity, an adaptive controller is integrated into the fractional BAM neural network with reaction–diffusion, and we found a new model where it is necessary to consider the adaptive controller in Neumann boundary conditions. In recent decades, some synchronisation results on fractional BAM neural networks with adaptive control have been reported. To best our knowledge, the synchronisation result of adaptive boundary controller based on fractional fuzzy reaction–diffusion BAM neural networks has not been published yet. Inspired by previous-mentioned works, we study the theoretical significance of adaptive boundary controller based on

fractional-order fuzzy reaction–diffusion BAM neural networks. Moreover, investigating the time delays and synchronisation in fractional-order fuzzy reaction–diffusion BAM neural networks is of significant importance. Understanding these aspects is crucial for gaining insights into the behaviour and dynamics of such networks, and it can have implications for various real-world applications. By studying the time delays and synchronisation, researchers can uncover essential characteristics and properties of these networks, leading to a deeper understanding of their capabilities and potential limitations.

Consider the following fractional-order fuzzy reaction–diffusion BAM neural networks with leakage time delay:

$$\left\{ \begin{array}{l} {}^C D_t^\hbar x_i^\zeta(t, z) = L_i \frac{\partial^2 x_i^\zeta(t, z)}{\partial z^2} - a_i x_i^\zeta(t - \sigma, z) \\ \quad + \sum_{j=1}^m b_{ij} f_j(y_j^\zeta(t - \tau(t), z)) \\ \quad + \bigwedge_{j=1}^m \mu_{ij} f_j(y_j^\zeta(t - \tau(t), z)) \\ \quad + \bigvee_{j=1}^m \varphi_{ij} f_j(y_j^\zeta(t - \tau(t), z)) \\ \quad + \mathcal{J}_i, \quad i = 1, 2, 3, \dots, n, \\ {}^C D_t^\hbar y_j^\zeta(t, z) = M_j \frac{\partial^2 y_j^\zeta(t, z)}{\partial z^2} - c_j y_j^\zeta(t - \delta, z) \\ \quad + \sum_{i=1}^n d_{ji} g_i(x_i^\zeta(t - \eta(t), z)) \\ \quad + \bigwedge_{i=1}^n \gamma_{ji} g_i(x_i^\zeta(t - \eta(t), z)) \\ \quad + \bigvee_{i=1}^n \rho_{ji} g_i(x_i^\zeta(t - \eta(t), z)) \\ \quad + \mathcal{K}_j, \quad j = 1, 2, 3, \dots, m, \end{array} \right. \quad (1)$$

with initial and Neumann boundary conditions as follows:

$$\left\{ \begin{array}{l} x_i^\zeta(t, z) = \phi_i^\zeta(t, z), \quad z \in (0, 1), \quad t \in [-\eta, 0], \\ y_j^\zeta(t, z) = \psi_j^\zeta(t, z), \quad z \in (0, 1), \quad t \in [-\tau, 0], \end{array} \right.$$

and

$$\begin{cases} \frac{\partial x_i^\zeta(t, z)}{\partial z} \Big|_{z=0} = 0, & \frac{\partial x_i^\zeta(t, z)}{\partial z} \Big|_{z=1} = 0, \\ \frac{\partial y_j^\zeta(t, z)}{\partial z} \Big|_{z=0} = 0, & \frac{\partial y_j^\zeta(t, z)}{\partial z} \Big|_{z=1} = 0, \end{cases}$$

where $x_i^\zeta(t, z) \in \mathbb{R}^n$ and $y_j^\zeta(t, z) \in \mathbb{R}^m$ are the neuron state variables; $t > 0$ denote the time variable; $z \in (0, 1)$ denote the space variable; ${}_0^C D_t^{\bar{h}}$ denote the fractional derivative with order $\bar{h} \in (0, 1)$. $\phi_i^\zeta(t, z) \in \mathbb{R}^n$ and $\psi_j^\zeta(t, z) \in \mathbb{R}^m$ are the initial functions. $L = \text{diag}\{L_1, L_2, \dots, L_n\}$ and $M = \text{diag}\{M_1, M_2, \dots, M_m\}$ are positive diffusion matrices. $A = \text{diag}\{a_1, a_2, \dots, a_n\}$ and $C = \text{diag}\{c_1, c_2, \dots, c_m\}$ are positive diagonal matrices. $f_j(y_j^\zeta(t - \tau(t), z))$ and $g_i(x_i^\zeta(t - \eta(t), z))$ are the activation nonlinear functions. $B = (b_{ij})_{n \times m}$ and $D = (d_{ji})_{m \times n}$ are the connection weight matrices. The fuzzy AND and fuzzy OR functions are denoted by the symbols \wedge and \vee , respectively. The components of fuzzy feedback MIN and MAX templates are (μ_{ij}, γ_{ji}) and $(\varphi_{ij}, \rho_{ji})$, respectively. The leakage delays are represented by σ and δ . The time-varying delays are represented by $\tau(t)$ and $\eta(t)$.

The nonlinear dynamics of the response system with adaptive full-domain control is described by

$$\begin{cases} {}_0^C D_t^{\bar{h}} x_i^\kappa(t, z) = L_i \frac{\partial^2 x_i^\kappa(t, z)}{\partial z^2} - a_i x_i^\kappa(t - \sigma, z) \\ \quad + \sum_{j=1}^m b_{ij} f_j(y_j^\kappa(t - \tau(t), z)) \\ \quad + \bigwedge_{j=1}^m \mu_{ij} f_j(y_j^\kappa(t - \tau(t), z)) \\ \quad + \bigvee_{j=1}^m \varphi_{ij} f_j(y_j^\kappa(t - \tau(t), z)) \\ \quad + u_i(t, z) + \mathcal{J}_i, \quad i = 1, 2, 3, \dots, n, \\ {}_0^C D_t^{\bar{h}} y_j^\kappa(t, z) = M_j \frac{\partial^2 y_j^\kappa(t, z)}{\partial z^2} - c_j y_j^\kappa(t - \delta, z) \\ \quad + \sum_{i=1}^n d_{ji} g_i(x_i^\kappa(t - \eta(t), z)) \\ \quad + \bigwedge_{i=1}^n \gamma_{ji} g_i(x_i^\kappa(t - \eta(t), z)) \\ \quad + \bigvee_{i=1}^n \rho_{ji} g_i(x_i^\kappa(t - \eta(t), z)) \\ \quad + v_j(t, z) + \mathcal{K}_j, \quad j = 1, 2, 3, \dots, m, \end{cases} \quad (2)$$

with initial and Neumann boundary conditions as follows:

$$\begin{cases} x_i^\kappa(t, z) = \phi_i^\kappa(t, z), & z \in (0, 1), t \in [-\eta, 0], \\ y_j^\kappa(t, z) = \psi_j^\kappa(t, z), & z \in (0, 1), t \in [-\tau, 0], \end{cases}$$

and

$$\begin{cases} \frac{\partial x_i^\kappa(t, z)}{\partial z} \Big|_{z=0} = 0, & \frac{\partial x_i^\kappa(t, z)}{\partial z} \Big|_{z=1} = 0, \\ \frac{\partial y_j^\kappa(t, z)}{\partial z} \Big|_{z=0} = 0, & \frac{\partial y_j^\kappa(t, z)}{\partial z} \Big|_{z=1} = 0, \end{cases}$$

where $u_i(t, z)$ and $v_j(t, z)$ are adaptive full-domain controllers.

The nonlinear dynamics of the response system with adaptive boundary control is described by

$$\begin{cases} {}_0^C D_t^{\bar{h}} x_i^\kappa(t, z) = L_i \frac{\partial^2 x_i^\kappa(t, z)}{\partial z^2} - a_i x_i^\kappa(t - \sigma, z) \\ \quad + \sum_{j=1}^m b_{ij} f_j(y_j^\kappa(t - \tau(t), z)) \\ \quad + \bigwedge_{j=1}^m \mu_{ij} f_j(y_j^\kappa(t - \tau(t), z)) \\ \quad + \bigvee_{j=1}^m \varphi_{ij} f_j(y_j^\kappa(t - \tau(t), z)) \\ \quad + \mathcal{J}_i, \quad i = 1, 2, 3, \dots, n, \\ {}_0^C D_t^{\bar{h}} y_j^\kappa(t, z) = M_j \frac{\partial^2 y_j^\kappa(t, z)}{\partial z^2} - c_j y_j^\kappa(t - \delta, z) \\ \quad + \sum_{i=1}^n d_{ji} g_i(x_i^\kappa(t - \eta(t), z)) \\ \quad + \bigwedge_{i=1}^n \gamma_{ji} g_i(x_i^\kappa(t - \eta(t), z)) \\ \quad + \bigvee_{i=1}^n \rho_{ji} g_i(x_i^\kappa(t - \eta(t), z)) \\ \quad + \mathcal{K}_j, \quad j = 1, 2, 3, \dots, m, \end{cases} \quad (3)$$

with initial and Neumann boundary conditions as follows:

$$\begin{cases} x_i^\kappa(t, z) = \phi_i^\kappa(t, z), & z \in (0, 1), t \in [-\eta, 0], \\ y_j^\kappa(t, z) = \psi_j^\kappa(t, z), & z \in (0, 1), t \in [-\tau, 0], \end{cases}$$

and

$$\begin{cases} \frac{\partial x_i^k(t, z)}{\partial z}|_{z=0} = 0, & \frac{\partial x_i^k(t, z)}{\partial z}|_{z=1} = u_i(t), \\ \frac{\partial y_j^k(t, z)}{\partial z}|_{z=0} = 0, & \frac{\partial y_j^k(t, z)}{\partial z}|_{z=1} = v_j(t), \end{cases}$$

where $u_i(t)$ and $v_j(t)$ are adaptive boundary controllers.

Assumption 2.3: The continuous nonlinear functions $f_j(\cdot)$ and $g_i(\cdot)$ satisfy the following conditions:

$$\begin{aligned} \alpha_i^- &\leq \frac{g_i(x_{1i}) - g_i(x_{2i})}{x_{1i} - x_{2i}} \leq \alpha_i^+, \\ \forall x_{1i}, x_{2i} &\in \mathbb{R}, x_{1i} \neq x_{2i}, i = 1, 2, \dots, n, \\ \beta_j^- &\leq \frac{f_j(y_{1j}) - f_j(y_{2j})}{y_{1j} - y_{2j}} \leq \beta_j^+, \\ \forall y_{1j}, y_{2j} &\in \mathbb{R}, y_{1j} \neq y_{2j}, j = 1, 2, \dots, m, \end{aligned}$$

where $\alpha_i^-, \alpha_i^+, \beta_j^-,$ and β_j^+ are real scalars. Furthermore, $f_j(0) = 0$ and $g_i(0) = 0$.

Lemma 2.4: (Mani et al., 2019) Let $\mathfrak{R}(t)$ be the differentiable state vector. Then the following inequality is hold for any matrix $\mathcal{Z} > 0$ and the time $t \geq 0$:

$$\begin{aligned} {}^C D_0^h \mathfrak{R}^T(t) \mathcal{Z} \mathfrak{R}(t) &\leq 2\mathfrak{R}^T(t) \mathcal{Z} \\ {}^C D_0^h \mathfrak{R}(t), \quad \forall h &\in (0, 1). \end{aligned}$$

Lemma 2.5: (Narayanan, Syed Ali, Karthikeyan, et al., 2022) If $x_{1i}, x_{2i}, y_{1j}, y_{2j}$ are the four state variables of system (1), then we get

$$\begin{aligned} &\left| \bigwedge_{i=1}^n \gamma_{ji} g_i(x_{1i}) - \bigwedge_{i=1}^n \gamma_{ji} g_i(x_{2i}) \right| \\ &\leq \sum_{i=1}^n |\gamma_{ji}| |g_i(x_{1i}) - g_i(x_{2i})|, \\ &\left| \bigvee_{i=1}^n \rho_{ji} g_i(x_{1i}) - \bigvee_{i=1}^n \rho_{ji} g_i(x_{2i}) \right| \\ &\leq \sum_{i=1}^n |\rho_{ji}| |g_i(x_{1i}) - g_i(x_{2i})|, \\ &\left| \bigwedge_{j=1}^m \mu_{ij} f_j(y_{1j}) - \bigwedge_{j=1}^m \mu_{ij} f_j(y_{2j}) \right| \\ &\leq \sum_{j=1}^m |\mu_{ij}| |f_j(y_{1j}) - f_j(y_{2j})|, \end{aligned}$$

$$\begin{aligned} &\left| \bigvee_{j=1}^m \varphi_{ij} f_j(y_{1j}) - \bigvee_{j=1}^m \varphi_{ij} f_j(y_{2j}) \right| \\ &\leq \sum_{j=1}^m |\varphi_{ij}| |f_j(y_{1j}) - f_j(y_{2j})|. \end{aligned}$$

Lemma 2.6: (Syed Ali, Hymavathi, et al., 2020) There exist real matrices \mathfrak{S}_1 and \mathfrak{S}_2 , and a matrix $\Pi > 0$, so that the following inequality is valid:

$$\mathfrak{S}_1^T \mathfrak{S}_2 + \mathfrak{S}_2^T \mathfrak{S}_1 \leq \mathfrak{S}_1^T \Pi^{-1} \mathfrak{S}_1 + \mathfrak{S}_2^T \Pi \mathfrak{S}_2.$$

Lemma 2.7: (X. Z. Liu et al., 2020) For a state variable $\mathfrak{R}(\cdot) \in \mathcal{W}^{1,2}([0, \mathcal{L}]; \mathbb{R}^n)$ with $\mathfrak{R}(0) = 0$ or $\mathfrak{R}(\mathcal{L}) = 0$ and a matrix $\mathcal{M} > 0$, we get

$$\begin{aligned} &\int_0^{\mathcal{L}} \mathfrak{R}^T(s) \mathcal{M} \mathfrak{R}(s) ds \\ &\leq \frac{4\mathcal{L}^2}{\pi^2} \int_0^{\mathcal{L}} \left(\frac{d\mathfrak{R}(s)}{ds} \right)^T \mathcal{M} \left(\frac{d\mathfrak{R}(s)}{ds} \right) ds. \end{aligned}$$

Lemma 2.8: (Thakur et al., 2022) Let $\mathfrak{U}_1, \mathfrak{U}_2, \mathfrak{U}_3$ be given matrices such that $\mathfrak{U}_1^T = \mathfrak{U}_1 > 0$ and $\mathfrak{U}_2^T = \mathfrak{U}_2 > 0$. Then, we have

$$\begin{aligned} \mathfrak{U}_1 + \mathfrak{U}_3^T \mathfrak{U}_2^{-1} \mathfrak{U}_3 < 0 &\Leftrightarrow \begin{bmatrix} \mathfrak{U}_1 & \mathfrak{U}_3^T \\ * & -\mathfrak{U}_2 \end{bmatrix} < 0 \quad \text{or} \\ \begin{bmatrix} -\mathfrak{U}_2 & \mathfrak{U}_3 \\ * & \mathfrak{U}_1 \end{bmatrix} < 0. \end{aligned}$$

Definition 2.9: (S. Yang et al., 2021) The system (1) achieve global asymptotic synchronisation if the synchronisation errors $\xi(t, z)$ and $\varpi(t, z)$ satisfy the following condition:

$$\lim_{t \rightarrow \infty} \left\{ \|\xi(t, z)\|_2 + \|\varpi(t, z)\|_2 \right\} = 0.$$

3. Main results

In this section, we obtain a sufficient criterion for adaptive full-domain synchronisation of drive-response systems (1) and (2). In addition, we obtain a new sufficient criterion for adaptive boundary synchronisation of drive-response systems (1) and (3).

3.1. Adaptive full-domain control synchronisation

To achieve these synchronisation criteria, the adaptive full-domain controllers $u_i(t, z)$ and $v_j(t, z)$ are

designed as follows:

$$\begin{cases} u_i(t, z) = -\theta_{1i}(t)\xi_i(t, z) - \theta_{2i}(t)\text{sign}(\xi_i(t, z)), \\ v_j(t, z) = -\vartheta_{1j}(t)\varpi_j(t, z) - \vartheta_{2j}(t)\text{sign}(\varpi_j(t, z)), \end{cases} \quad (4)$$

where $\text{sign}(\cdot)$ is the symbolic function, and $\theta_{1i}(t)$, $\theta_{2i}(t)$, $\vartheta_{1j}(t)$ and $\vartheta_{2j}(t)$ are control parameters.

Adaptive update laws:

$$\begin{cases} {}_0^C D_t^h \theta_{1i}(t) = \omega_{1i} \xi_i^2(t, z), \\ {}_0^C D_t^h \theta_{2i}(t) = -\omega_{2i} |\xi_i(t, z)|, \\ {}_0^C D_t^h \vartheta_{1j}(t) = \varrho_{1j} \varpi_j^2(t, z), \\ {}_0^C D_t^h \vartheta_{2j}(t) = -\varrho_{2j} |\varpi_j(t, z)|, \end{cases} \quad (5)$$

where ω_{1i} , ω_{2i} , ϱ_{1j} and ϱ_{2j} are positive real constants.

Next, the error dynamical system of drive-response systems (1) and (2) is described by

$$\begin{cases} {}_0^C D_t^h \xi_i(t, z) = L_i \frac{\partial^2 \xi_i(t, z)}{\partial z^2} - a_i \xi_i(t - \sigma, z) \\ \quad + \sum_{j=1}^m b_{ij} \mathcal{F}_j(\varpi_j(t - \tau(t), z)) \\ \quad + \bigwedge_{j=1}^m \mu_{ij} \mathcal{F}_j(\varpi_j(t - \tau(t), z)) \\ \quad + \bigvee_{j=1}^m \varphi_{ij} \mathcal{F}_j(\varpi_j(t - \tau(t), z)) \\ \quad + u_i(t, z), \quad i = 1, 2, 3, \dots, n, \\ {}_0^C D_t^h \varpi_j(t, z) = M_j \frac{\partial^2 \varpi_j(t, z)}{\partial z^2} - c_j \varpi_j(t - \delta, z) \\ \quad + \sum_{i=1}^n d_{ji} \mathcal{G}_i(\xi_i(t - \eta(t), z)) \\ \quad + \bigwedge_{i=1}^n \gamma_{ji} \mathcal{G}_i(\xi_i(t - \eta(t), z)) \\ \quad + \bigvee_{i=1}^n \rho_{ji} \mathcal{G}_i(\xi_i(t - \eta(t), z)) + v_j(t, z), \\ \quad j = 1, 2, 3, \dots, m, \end{cases} \quad (6)$$

with initial and Neumann boundary conditions as follows:

$$\begin{cases} \xi_i(t, z) = \phi_i(t, z), \quad z \in (0, 1), t \in [-\eta, 0], \\ \varpi_j(t, z) = \psi_j(t, z), \quad z \in (0, 1), t \in [-\tau, 0], \end{cases} \quad (7)$$

and

$$\begin{cases} \left. \begin{aligned} \frac{\partial \xi_i(t, z)}{\partial z} \Big|_{z=0} = 0, & \quad \frac{\partial \xi_i(t, z)}{\partial z} \Big|_{z=1} = 0, \\ \frac{\partial \varpi_j(t, z)}{\partial z} \Big|_{z=0} = 0, & \quad \frac{\partial \varpi_j(t, z)}{\partial z} \Big|_{z=1} = 0, \end{aligned} \right\} \quad (8)$$

where $\xi_i(t, z) = x_i^k(t, z) - x_i^s(t, z)$, $\varpi_j(t, z) = y_j^k(t, z) - y_j^s(t, z)$, $\mathcal{F}_j(\varpi_j(t - \tau(t), z)) = f_j(y_j^k(t - \tau(t), z)) - f_j(y_j^s(t - \tau(t), z))$, $\mathcal{G}_i(\xi_i(t - \eta(t), z)) = g_i(x_i^k(t - \eta(t), z)) - g_i(x_i^s(t - \eta(t), z))$, $\phi_i(t, z) = \phi_i^k(t, z) - \phi_i^s(t, z)$, $\psi_j(t, z) = \psi_j^k(t, z) - \psi_j^s(t, z)$, $\frac{\partial \xi_i(t, z)}{\partial z} = \frac{\partial x_i^k(t, z)}{\partial z} - \frac{\partial x_i^s(t, z)}{\partial z}$, $\frac{\partial \varpi_j(t, z)}{\partial z} = \frac{\partial y_j^k(t, z)}{\partial z} - \frac{\partial y_j^s(t, z)}{\partial z}$.

Theorem 3.1: Under Assumption 2.3 and adaptive full-domain controller (4) with adaptive update law (5), the error dynamical system (6) is said to be global asymptotically stable if there exist positive definite diagonal matrices $P, Q, \Pi_1, \Pi_2, \Gamma_1, \Gamma_2$, and symmetric positive definite matrices R, S such that the following LMI holds:

$$(i) \Xi = \begin{bmatrix} \Xi_{11} & 0 & 0 & 0 & \Xi_{15} & 0 & 0 \\ * & \Xi_{22} & 0 & 0 & 0 & \Xi_{26} & 0 \\ * & * & \Xi_{33} & 0 & 0 & 0 & 0 \\ * & * & * & \Xi_{44} & 0 & 0 & 0 \\ * & * & * & * & \Xi_{55} & 0 & 0 \\ * & * & * & * & * & \Xi_{66} & 0 \\ * & * & * & * & * & * & \Xi_{77} \\ * & * & * & * & * & * & * \\ * & * & * & * & * & * & * \\ * & * & * & * & * & * & * \\ * & * & * & * & * & * & * \\ * & * & * & * & * & * & * \\ * & * & * & * & * & * & * \\ * & * & * & * & * & * & * \\ 0 & 0 & \Xi_{110} & \Xi_{111} & 0 & & \\ 0 & \Xi_{29} & 0 & 0 & \Xi_{212} & & \\ 0 & 0 & 0 & 0 & 0 & & \\ 0 & 0 & 0 & 0 & 0 & & \\ 0 & 0 & 0 & 0 & 0 & & \\ 0 & 0 & 0 & 0 & 0 & & \\ 0 & \Xi_{79} & 0 & 0 & 0 & & \\ \Xi_{88} & 0 & \Xi_{810} & 0 & 0 & & \\ * & \Xi_{99} & 0 & 0 & 0 & & \\ * & * & \Xi_{1010} & 0 & 0 & & \\ * & * & * & \Xi_{1111} & 0 & & \\ * & * & * & * & \Xi_{1212} & & \end{bmatrix} < 0, \quad (9)$$

where

$$\begin{aligned}\Xi_{11} &= -\text{sym}\left(P\aleph_1 + \frac{\pi^2}{8}PL\right) + R, & \Xi_{15} &= -PA, \\ \Xi_{110} &= PB, & \Xi_{111} &= P(|\mu| + |\varphi|), \\ \Xi_{22} &= -\text{sym}\left(Q\aleph_2 + \frac{\pi^2}{8}QM\right) + S, & \Xi_{26} &= -QC, \\ \Xi_{29} &= QD, & \Xi_{212} &= Q(|\gamma| + |\rho|), \\ \Xi_{33} &= -\text{sym}\left(\frac{\pi^2}{8}PL\right), & \Xi_{44} &= -\text{sym}\left(\frac{\pi^2}{8}QM\right), \\ \Xi_{55} &= -R, & \Xi_{66} &= -S, & \Xi_{77} &= -\Lambda_1\Gamma_1, \\ \Xi_{79} &= \Lambda_2\Gamma_1, & \Xi_{88} &= -\Omega_1\Gamma_2, & \Xi_{810} &= \Omega_2\Gamma_2, \\ \Xi_{99} &= \Pi_2 - \Gamma_1, & \Xi_{1010} &= \Pi_1 - \Gamma_2, \\ \Xi_{1111} &= -\Pi_1, & \Xi_{1212} &= -\Pi_2, \\ P &= \text{diag}\{\hat{p}_1, \hat{p}_2, \dots, \hat{p}_n\}, & Q &= \text{diag}\{\hat{q}_1, \hat{q}_2, \dots, \hat{q}_m\}, \\ \aleph_1 &= \{\aleph_{11}, \aleph_{12}, \dots, \aleph_{1n}\}, \\ \aleph_2 &= \text{diag}\{\aleph_{21}, \aleph_{22}, \dots, \aleph_{2m}\}, \\ \Lambda_1 &= \text{diag}\{\alpha_1^-\alpha_1^+, \alpha_2^-\alpha_2^+, \dots, \alpha_n^-\alpha_n^+\}, \\ \Omega_1 &= \text{diag}\{\beta_1^-\beta_1^+, \beta_2^-\beta_2^+, \dots, \beta_m^-\beta_m^+\}, \\ \Lambda_2 &= \frac{1}{2} \text{diag}\{\alpha_1^- + \alpha_1^+, \alpha_2^- + \alpha_2^+, \dots, \alpha_n^- + \alpha_n^+\}, \\ \Omega_2 &= \frac{1}{2} \text{diag}\{\beta_1^- + \beta_1^+, \beta_2^- + \beta_2^+, \dots, \beta_m^- + \beta_m^+\}.\end{aligned}$$

Proof: Consider the following Lyapunov function candidates:

$$V(t) = V_1(t) + V_2(t) + V_3(t), \quad (10)$$

where

$$\begin{aligned}V_1(t) &= \int_0^1 \xi^T(t, z)P\xi(t, z) dz \\ &+ \int_0^1 \varpi^T(t, z)Q\varpi(t, z) dz, \\ V_2(t) &= \sum_{i=1}^n \int_0^1 \left[\frac{1}{\omega_{1i}} \hat{p}_i(\theta_{1i}(t) - \aleph_{1i})^2 + \frac{1}{\omega_{2i}} \hat{p}_i\theta_{2i}^2(t) \right] dz \\ &+ \sum_{j=1}^m \int_0^1 \left[\frac{1}{\varrho_{1j}} \hat{q}_j(\vartheta_{1j}(t) - \aleph_{2j})^2 \right. \\ &\left. + \frac{1}{\varrho_{2j}} \hat{q}_j\vartheta_{2j}^2(t) \right] dz, \\ V_3(t) &= {}_0^C D_t^{1-h} \left(\int_0^1 \int_{t-\sigma}^t \xi^T(s, z)R\xi(s, z) ds dz \right)\end{aligned}$$

$$+ {}_0^C D_t^{1-h} \left(\int_0^1 \int_{t-\delta}^t \varpi^T(s, z)S\varpi(s, z) ds dz \right),$$

with known constants $\aleph_{1i} \geq 0$ and $\aleph_{2j} \geq 0$. Calculating the fractional derivative of $V(t)$ with the error dynamical system (6) by Lemma 2.4, we find that

$${}_0^C D_t^h V(t) = {}_0^C D_t^h V_1(t) + {}_0^C D_t^h V_2(t) + {}_0^C D_t^h V_3(t). \quad (11)$$

Further, we have

$$\begin{aligned}{}_0^C D_t^h V_1(t) &= {}_0^C D_t^h \left(\int_0^1 \xi^T(t, z)P\xi(t, z) dz \right) \\ &+ {}_0^C D_t^h \left(\int_0^1 \varpi^T(t, z)Q\varpi(t, z) dz \right) \\ &\leq 2 \sum_{i=1}^n \int_0^1 \xi_i^T(t, z) \hat{p}_i {}_0^C D_t^h \xi_i(t, z) dz \\ &+ 2 \sum_{j=1}^m \int_0^1 \varpi_j^T(t, z) \hat{q}_j {}_0^C D_t^h \varpi_j(t, z) dz \\ &\leq 2 \sum_{i=1}^n \int_0^1 \xi_i^T(t, z) \hat{p}_i \left[L_i \frac{\partial^2 \xi_i(t, z)}{\partial z^2} \right. \\ &\quad - a_i \xi_i(t - \sigma, z) \\ &\quad + \sum_{j=1}^m b_{ij} \mathcal{F}_j(\varpi_j(t - \tau(t), z)) \\ &\quad + \bigwedge_{j=1}^m \mu_{ij} \mathcal{F}_j(\varpi_j(t - \tau(t), z)) \\ &\quad \left. + \bigvee_{j=1}^m \varphi_{ij} \mathcal{F}_j(\varpi_j(t - \tau(t), z)) + u_i(t, z) \right] dz \\ &+ 2 \sum_{j=1}^m \int_0^1 \varpi_j^T(t, z) \hat{q}_j \left[M_j \frac{\partial^2 \varpi_j(t, z)}{\partial z^2} \right. \\ &\quad - c_j \varpi_j(t - \delta, z) \\ &\quad + \sum_{i=1}^n d_{ji} \mathcal{G}_i(\xi_i(t - \eta(t), z)) \\ &\quad + \bigwedge_{i=1}^n \gamma_{ji} \mathcal{G}_i(\xi_i(t - \eta(t), z)) \\ &\quad \left. + \bigvee_{i=1}^n \rho_{ji} \mathcal{G}_i(\xi_i(t - \eta(t), z)) + v_j(t, z) \right] dz \\ &\leq 2 \int_0^1 \xi^T(t, z)P \left[L \frac{\partial^2 \xi(t, z)}{\partial z^2} \right.\end{aligned}$$

$$\begin{aligned}
& - A\xi(t - \sigma, z) \\
& + B\mathcal{F}(\varpi(t - \tau(t), z))] dz \\
& + \int_0^1 \xi^T(t, z)P(|\mu| + |\varphi|) \\
& \times \Pi_1^{-1}(|\mu| + |\varphi|)^T P\xi(t, z) dz \\
& + \int_0^1 \mathcal{F}^T(\varpi(t - \tau(t), z)) \\
& \times \Pi_1 \mathcal{F}(\varpi(t - \tau(t), z)) dz \\
& \times + 2 \sum_{i=1}^n \int_0^1 \xi_i^T(t, z) \hat{p}_i (-\theta_{1i}(t)\xi_i(t, z) \\
& - \theta_{2i}(t)\text{sign}(\xi_i(t, z))) dz \\
& + 2 \int_0^1 \varpi^T(t, z)Q \left[M \frac{\partial^2 \varpi(t, z)}{\partial z^2} \right. \\
& - C\varpi(t - \delta, z) + D\mathcal{G}(\xi(t - \eta(t), z))] dz \\
& + \int_0^1 \varpi^T(t, z)Q(|\gamma| + |\rho|) \\
& \times \Pi_2^{-1}(|\gamma| + |\rho|)^T Q\varpi(t, z) dz \\
& + \int_0^1 \mathcal{G}^T(\xi(t - \eta(t), z)) \\
& \times \Pi_2 \mathcal{G}(\xi(t - \eta(t), z)) dz \\
& + 2 \sum_{j=1}^m \int_0^1 \varpi_j^T(t, z) \hat{q}_j (-\vartheta_{1j}(t)\varpi_j(t, z) \\
& - \vartheta_{2j}\text{sign}(\varpi_j(t, z))) dz, \tag{12} \\
{}_0^C D_t^h V_2(t) &= \sum_{i=1}^n \int_0^1 \left[\frac{1}{\omega_{1i}} \hat{p}_{i0} {}_0^C D_t^h (\theta_{1i}(t) - \aleph_{1i})^2 \right. \\
& \left. + \frac{1}{\omega_{2i}} \hat{p}_{i0} {}_0^C D_t^h (\theta_{2i}(t)) \right] dz \\
& + \sum_{j=1}^m \int_0^1 \left[\frac{1}{\varrho_{1j}} \hat{q}_{j0} {}_0^C D_t^h (\vartheta_{1j}(t) - \aleph_{2j})^2 \right. \\
& \left. + \frac{1}{\varrho_{2j}} \hat{q}_{j0} {}_0^C D_t^h (\vartheta_{2j}(t)) \right] dz \\
& = \sum_{i=1}^n \int_0^1 [2\hat{p}_i (\theta_{1i}(t) - \aleph_{1i}) \xi_i^2(t, z) \\
& + 2\hat{p}_i \theta_{2i}(t) \xi_i(t, z) \text{sign}(\xi_i(t, z))] dz \\
& + \sum_{j=1}^m \int_0^1 [2\hat{q}_j (\vartheta_{1j}(t) - \aleph_{2j}) \varpi_j^2(t, z)
\end{aligned}$$

$$\begin{aligned}
& + 2\hat{q}_j \vartheta_{2j}(t) \varpi_j(t, z) \text{sign}(\varpi_j(t, z))] dz, \tag{13} \\
{}_0^C D_t^h V_3(t) &= {}_0^C D_t^h \left({}_0^C D_t^{1-h} \int_0^1 \int_{t-\sigma}^t \right. \\
& \times \xi^T(s, z) R\xi(s, z) ds dz \Big) \\
& + {}_0^C D_t^h \left({}_0^C D_t^{1-h} \int_0^1 \int_{t-\delta}^t \right. \\
& \times \varpi^T(s, z) S\varpi(s, z) ds dz \Big) \\
& = \int_0^1 \xi^T(t, z) R\xi(t, z) dz \\
& - \int_0^1 \xi^T(t - \sigma, z) R\xi(t - \sigma, z) dz \\
& + \int_0^1 \varpi^T(t, z) S\varpi(t, z) dz \\
& - \int_0^1 \varpi^T(t - \delta, z) S\varpi(t - \delta, z) dz. \tag{14}
\end{aligned}$$

Using the integration by parts approach and boundary condition (8), we get

$$\begin{aligned}
& \int_0^1 \xi^T(t, z) PL \frac{\partial^2 \xi(t, z)}{\partial z^2} dz \\
& = \left[\xi^T(t, z) PL \frac{\partial \xi(t, z)}{\partial z} \right]_{z=0}^{z=1} \\
& - \int_0^1 \frac{\partial \xi^T(t, z)}{\partial z} PL \frac{\partial \xi(t, z)}{\partial z} dz \\
& = - \int_0^1 \frac{\partial \xi^T(t, z)}{\partial z} PL \frac{\partial \xi(t, z)}{\partial z} dz \tag{15}
\end{aligned}$$

and

$$\begin{aligned}
& \int_0^1 \varpi^T(t, z) QM \frac{\partial^2 \varpi(t, z)}{\partial z^2} dz \\
& = \left[\varpi^T(t, z) QM \frac{\partial \varpi(t, z)}{\partial z} \right]_{z=0}^{z=1} \\
& - \int_0^1 \frac{\partial \varpi^T(t, z)}{\partial z} QM \frac{\partial \varpi(t, z)}{\partial z} dz \\
& = - \int_0^1 \frac{\partial \varpi^T(t, z)}{\partial z} QM \frac{\partial \varpi(t, z)}{\partial z} dz. \tag{16}
\end{aligned}$$

To get $\hat{\xi}(t, z) = 0$ and $\hat{\varpi}(t, z) = 0$, we introduce the new state variables $\hat{\xi}(t, z) = \xi(t, z) - \xi(t, 1)$ and

$\hat{\omega}(t, z) = \varpi(t, z) - \varpi(t, 1)$. Furthermore, the following conditions hold:

$$\frac{\partial \xi^T(t, z)}{\partial z} PL \frac{\partial \xi(t, z)}{\partial z} = \frac{\partial \hat{\xi}^T(t, z)}{\partial z} PL \frac{\partial \hat{\xi}(t, z)}{\partial z}, \quad (17)$$

$$\frac{\partial \varpi^T(t, z)}{\partial z} QM \frac{\partial \varpi(t, z)}{\partial z} = \frac{\partial \hat{\omega}^T(t, z)}{\partial z} QM \frac{\partial \hat{\omega}(t, z)}{\partial z}. \quad (18)$$

Applying Wirtinger's inequality, we get

$$\begin{aligned} & \int_0^1 \xi^T(t, z) PL \frac{\partial^2 \xi(t, z)}{\partial z^2} dz \\ &= -\frac{1}{2} \int_0^1 \frac{\partial \xi^T(t, z)}{\partial z} PL \frac{\partial \xi(t, z)}{\partial z} dz \\ & \quad - \frac{1}{2} \int_0^1 \frac{\partial \hat{\xi}^T(t, z)}{\partial z} PL \frac{\partial \hat{\xi}(t, z)}{\partial z} dz \\ & \leq -\frac{\pi^2}{8} \int_0^1 \xi^T(t, z) PL \xi(t, z) dz \\ & \quad - \frac{\pi^2}{8} \int_0^1 \hat{\xi}^T(t, z) PL \hat{\xi}(t, z) dz \end{aligned} \quad (19)$$

and

$$\begin{aligned} & \int_0^1 \varpi^T(t, z) QM \frac{\partial^2 \varpi(t, z)}{\partial z^2} dz \\ &= -\frac{1}{2} \int_0^1 \frac{\partial \varpi^T(t, z)}{\partial z} QM \frac{\partial \varpi(t, z)}{\partial z} dz \\ & \quad - \frac{1}{2} \int_0^1 \frac{\partial \hat{\omega}^T(t, z)}{\partial z} QM \frac{\partial \hat{\omega}(t, z)}{\partial z} dz \\ & \leq -\frac{\pi^2}{8} \int_0^1 \varpi^T(t, z) QM \varpi(t, z) dz \\ & \quad - \frac{\pi^2}{8} \int_0^1 \hat{\omega}^T(t, z) QM \hat{\omega}(t, z) dz. \end{aligned} \quad (20)$$

By virtue of Assumption 2.3, we get

$$\begin{aligned} & [\mathcal{G}_i(\xi_i(t - \eta(t), z)) - \alpha_i^+ \xi_i(t - \eta(t), z)] \\ & [\mathcal{G}_i(\xi_i(t - \eta(t), z)) - \alpha_i^- \xi_i(t - \eta(t), z)] \leq 0, \\ & [\mathcal{F}_j(\varpi_j(t - \tau(t), z)) - \beta_j^+ \varpi_j(t - \tau(t), z)] \\ & [\mathcal{F}_j(\varpi_j(t - \tau(t), z)) - \beta_j^- \varpi_j(t - \tau(t), z)] \leq 0. \end{aligned}$$

Thus, for diagonal matrices $\Gamma_1 = \text{diag}\{\Gamma_{11}, \Gamma_{12}, \dots, \Gamma_{1n}\} > 0$ and $\Gamma_2 = \text{diag}\{\Gamma_{21}, \Gamma_{22}, \dots, \Gamma_{2m}\} > 0$, it

follows that

$$\begin{aligned} & \sum_{i=1}^n \Gamma_{1i} \begin{bmatrix} \xi_i(t - \eta(t), z) \\ \mathcal{G}_i(\xi_i(t - \eta(t), z)) \end{bmatrix}^T \\ & \begin{bmatrix} \alpha_i^+ \alpha_i^- e_i e_i^T & -\frac{\alpha_i^+ + \alpha_i^-}{2} e_i e_i^T \\ -\frac{\alpha_i^+ + \alpha_i^-}{2} e_i e_i^T & e_i e_i^T \end{bmatrix} \\ & \begin{bmatrix} \xi_i(t - \eta(t), z) \\ \mathcal{G}_i(\xi_i(t - \eta(t), z)) \end{bmatrix} \leq 0, \\ & \sum_{j=1}^m \Gamma_{2j} \begin{bmatrix} \varpi_j(t - \tau(t), z) \\ \mathcal{F}_j(\varpi_j(t - \tau(t), z)) \end{bmatrix}^T \\ & \begin{bmatrix} \beta_j^+ \beta_j^- \hat{e}_j \hat{e}_j^T & -\frac{\beta_j^+ + \beta_j^-}{2} \hat{e}_j \hat{e}_j^T \\ -\frac{\beta_j^+ + \beta_j^-}{2} \hat{e}_j \hat{e}_j^T & \hat{e}_j \hat{e}_j^T \end{bmatrix} \\ & \begin{bmatrix} \varpi_j(t - \tau(t), z) \\ \mathcal{F}_j(\varpi_j(t - \tau(t), z)) \end{bmatrix} \leq 0, \end{aligned}$$

where e_i and \hat{e}_j denote unit column vectors which has a '1' element in its i th and j th rows, respectively, and zeros otherwise. Furthermore, we have

$$\begin{aligned} & \begin{bmatrix} \xi(t - \eta(t), z) \\ \mathcal{G}(\xi(t - \eta(t), z)) \end{bmatrix}^T \\ & \begin{bmatrix} \Lambda_1 \Gamma_1 & -\Lambda_2 \Gamma_1 \\ * & \Gamma_1 \end{bmatrix} \\ & \begin{bmatrix} \xi(t - \eta(t), z) \\ \mathcal{G}(\xi(t - \eta(t), z)) \end{bmatrix} \leq 0, \end{aligned} \quad (21)$$

$$\begin{aligned} & \begin{bmatrix} \varpi(t - \tau(t), z) \\ \mathcal{F}(\varpi(t - \tau(t), z)) \end{bmatrix}^T \begin{bmatrix} \Omega_1 \Gamma_2 & -\Omega_2 \Gamma_2 \\ * & \Gamma_2 \end{bmatrix} \\ & \begin{bmatrix} \varpi(t - \tau(t), z) \\ \mathcal{F}(\varpi(t - \tau(t), z)) \end{bmatrix} \leq 0. \end{aligned} \quad (22)$$

From the inequalities (11)–(22), we have

$$\begin{aligned} {}_0^C D_t^h V(t) & \leq \int_0^1 \left[\xi^T(t, z) \left(-\text{sym}(P\mathfrak{N}_1) - \frac{\pi^2}{4} PL + R \right. \right. \\ & \quad \left. \left. + P(|\mu| + |\varphi|) \Pi_1^{-1} (|\mu| + |\varphi|)^T P \right) \xi(t, z) \right. \\ & \quad \left. - 2\xi^T(t, z) PA \xi(t - \sigma, z) \right. \\ & \quad \left. + 2\xi^T(t, z) PB \mathcal{F}(\varpi(t - \tau(t), z)) \right. \\ & \quad \left. + \varpi^T(t, z) (-\text{sym}(Q\mathfrak{N}_2)) \right. \end{aligned}$$

$$\begin{aligned}
& -\frac{\pi^2}{4}QM + S + Q(|\gamma| + |\rho|) \\
& \times \Pi_2^{-1}(|\gamma| + |\rho|)^T Q \varpi(t, z) \\
& - 2\varpi^T(t, z)QC\varpi(t - \delta, z) \\
& + 2\varpi^T(t, z)QDG(\varpi(t - \eta(t), z)) \\
& - \hat{\xi}^T(t, z) \left(\frac{\pi^2 PL}{4} \right) \hat{\xi}(t, z) \\
& - \hat{\varpi}^T(t, z) \left(\frac{\pi^2 QM}{4} \right) \hat{\varpi}(t, z) \\
& - \xi^T(t - \sigma, z)R\xi(t - \sigma, z) \\
& - \varpi^T(t - \delta, z)S\varpi(t - \delta, z) \\
& - \xi^T(t - \eta(t), z)\Lambda_1\Gamma_1\xi(t - \eta(t), z) \\
& + 2\xi^T(t - \eta(t), z)\Lambda_2\Gamma_1\mathcal{G}(\xi(t - \eta(t), z)) \\
& - \varpi^T(t - \tau(t), z)\Omega_1\Gamma_2\varpi(t - \tau(t), z) \\
& + 2\varpi^T(t - \tau(t), z) \\
& \times \Omega_2\Gamma_2\mathcal{F}(\varpi(t - \tau(t), z)) \\
& + \mathcal{G}^T(\xi(t - \eta(t), z)(\Pi_2 - \Gamma_1) \\
& \times \mathcal{G}(\xi(t - \eta(t), z)) \\
& + \mathcal{F}^T(\varpi(t - \tau(t), z)(\Pi_1 - \Gamma_2) \\
& \times \mathcal{F}(\varpi(t - \tau(t), z))] dz \\
& \leq \int_0^1 \Upsilon^T(t, z)\Xi\Upsilon(t, z) dz, \quad (23)
\end{aligned}$$

where

$$\begin{aligned}
\Upsilon^T(t, z) = & \left[\xi^T(t, z)\varpi^T(t, z)\hat{\xi}^T(t, z)\hat{\varpi}^T(t, z)\xi^T \right. \\
& (t - \sigma, z)\varpi^T(t - \delta, z)\xi^T(t - \eta(t), z) \\
& \varpi^T(t - \tau(t), z)\mathcal{G}^T(\xi(t - \eta(t), z)) \\
& \left. \mathcal{F}^T(\varpi(t - \tau(t), z)) \right].
\end{aligned}$$

If the LMI $\Xi < 0$, we can conclude that the error dynamical system (6) is globally asymptotically stable. The proof is completed. \blacksquare

3.2. Adaptive boundary control synchronisation

To achieve these synchronisation criteria, the adaptive boundary controllers $u_i(t)$ and $v_j(t)$ are designed as

follows:

$$\left\{ \begin{aligned} u_i(t) = & -\theta_{3i}(t) \int_0^1 \frac{\xi_i^2(t, z)}{\xi_i(t, 1)} dz \\ & - \theta_{4i}(t) \int_0^1 \frac{\xi_i(t, z)\text{sign}(\xi_i(t, z))}{\xi_i(t, 1)} dz, \\ v_j(t) = & -\vartheta_{3j}(t) \int_0^1 \frac{\varpi_j^2(t, z)}{\varpi_j(t, 1)} dz \\ & - \vartheta_{4j}(t) \int_0^1 \frac{\varpi_j(t, z)\text{sign}(\varpi_j(t, z))}{\varpi_j(t, 1)} dz, \end{aligned} \right. \quad (24)$$

where $\theta_{3i}(t)$, $\theta_{4i}(t)$, $\vartheta_{3j}(t)$ and $\vartheta_{4j}(t)$ are control parameters.

Adaptive update laws:

$$\left\{ \begin{aligned} {}_0^C D_t^h \theta_{3i}(t) = & \omega_{3i} \xi_i^2(t, z), \\ {}_0^C D_t^h \theta_{4i}(t) = & -\omega_{4i} |\xi_i(t, z)|, \\ {}_0^C D_t^h \vartheta_{3j}(t) = & \varrho_{3j} \varpi_j^2(t, z), \\ {}_0^C D_t^h \vartheta_{4j}(t) = & -\varrho_{4j} |\varpi_j(t, z)|, \end{aligned} \right. \quad (25)$$

where ω_{3i} , ω_{4i} , ϱ_{3j} , and ϱ_{4j} are real constants.

Next, the error dynamical system of drive-response systems (1) and (3) is described by

$$\left\{ \begin{aligned} {}_0^C D_t^h \xi_i(t, z) = & L_i \frac{\partial^2 \xi_i(t, z)}{\partial z^2} - a_i \xi_i(t - \sigma, z) \\ & + \sum_{j=1}^m b_{ij} \mathcal{F}_j(\varpi_j(t - \tau(t), z)) \\ & + \bigwedge_{j=1}^m \mu_{ij} \mathcal{F}_j(\varpi_j(t - \tau(t), z)) \\ & + \bigvee_{j=1}^m \varphi_{ij} \mathcal{F}_j(\varpi_j(t - \tau(t), z)), \\ {}_0^C D_t^h \varpi_j(t, z) = & M_j \frac{\partial^2 \varpi_j(t, z)}{\partial z^2} - c_j \varpi_j(t - \delta, z) \\ & + \sum_{i=1}^n d_{ji} \mathcal{G}_i(\xi_i(t - \eta(t), z)) \\ & + \bigwedge_{i=1}^n \gamma_{ji} \mathcal{G}_i(\xi_i(t - \eta(t), z)) \\ & + \bigvee_{i=1}^n \rho_{ji} \mathcal{G}_i(\xi_i(t - \eta(t), z)), \end{aligned} \right. \quad (26)$$

with initial and Neumann boundary conditions as follows:

$$\begin{cases} \xi_i(t, z) = \phi_i(t, z), & z \in (0, 1), t \in [-\eta, 0], \\ \varpi_j(t, z) = \psi_j(t, z), & z \in (0, 1), t \in [-\tau, 0], \end{cases} \quad (27)$$

and

$$\begin{cases} \frac{\partial \xi_i(t, z)}{\partial z}|_{z=0} = 0, & \frac{\partial \xi_i(t, z)}{\partial z}|_{z=1} = u_i(t), \\ \frac{\partial \varpi_j(t, z)}{\partial z}|_{z=0} = 0, & \frac{\partial \varpi_j(t, z)}{\partial z}|_{z=1} = v_j(t). \end{cases} \quad (28)$$

Theorem 3.2: Under Assumption 2.3 and adaptive boundary controller (24) with adaptive update law (25), the error dynamical system (26) is said to be global asymptotically stable if there exist positive definite diagonal matrices $P, Q, \Pi_1, \Pi_2, \Gamma_1, \Gamma_2$, and symmetric positive definite matrices R, S such that the following LMI holds:

$$(i)\Delta = \begin{bmatrix} \Delta_{11} & 0 & 0 & 0 & \Xi_{15} & 0 \\ * & \Delta_{22} & 0 & 0 & 0 & \Xi_{26} \\ * & * & \Xi_{33} & 0 & 0 & 0 \\ * & * & * & \Xi_{44} & 0 & 0 \\ * & * & * & * & \Xi_{55} & 0 \\ * & * & * & * & * & \Xi_{66} \\ * & * & * & * & * & * \\ * & * & * & * & * & * \\ * & * & * & * & * & * \\ * & * & * & * & * & * \\ * & * & * & * & * & * \\ 0 & 0 & 0 & \Xi_{110} & \Xi_{111} & 0 \\ 0 & 0 & \Xi_{29} & 0 & 0 & \Xi_{212} \\ 0 & 0 & 0 & 0 & 0 & 0 \\ 0 & 0 & 0 & 0 & 0 & 0 \\ 0 & 0 & 0 & 0 & 0 & 0 \\ 0 & 0 & 0 & 0 & 0 & 0 \\ \Xi_{77} & 0 & \Xi_{79} & 0 & 0 & 0 \\ * & \Xi_{88} & 0 & \Xi_{810} & 0 & 0 \\ * & * & \Xi_{99} & 0 & 0 & 0 \\ * & * & * & \Xi_{1010} & 0 & 0 \\ * & * & * & * & \Xi_{1111} & 0 \\ * & * & * & * & * & \Xi_{1212} \end{bmatrix} < 0, \quad (29)$$

where

$$\Delta_{11} = -\text{sym} \left(P\aleph_3 + \frac{\pi^2}{8} PL \right) + R,$$

$$\Delta_{22} = -\text{sym} \left(Q\aleph_4 + \frac{\pi^2}{8} QM \right) + S,$$

$$\aleph_3 = \text{diag}\{\aleph_{31}, \aleph_{32}, \dots, \aleph_{3n}\},$$

$$\aleph_4 = \text{diag}\{\aleph_{41}, \aleph_{42}, \dots, \aleph_{4m}\},$$

the remaining values are defined in

Theorem 3.1.

Proof: Consider the following Lyapunov function candidates:

$$\bar{V}(t) = V_1(t) + \bar{V}_2(t) + V_3(t), \quad (30)$$

where

$$\begin{aligned} \bar{V}_2(t) = & \sum_{i=1}^n \int_0^1 \left[\frac{L_i}{\omega_{3i}} \hat{p}_i(\theta_{3i}(t) - \aleph_{3i})^2 \right. \\ & \left. + \frac{L_i}{\omega_{4i}} \hat{p}_i \theta_{4i}^2(t) \right] dz \\ & + \sum_{j=1}^m \left[\frac{M_j}{\varrho_{3j}} \hat{q}_j(\vartheta_{3j}(t) - \aleph_{4j})^2 + \frac{M_j}{\varrho_{4j}} \hat{q}_j \vartheta_{4j}^2(t) \right], \end{aligned}$$

$V_1(t)$ and $V_3(t)$ are defined in Theorem 3.1. Calculating the fractional derivative of $\bar{V}(t)$ along the error dynamical system (26) using similar methods as in Theorem 3.1, we find that

$$\begin{aligned} {}_0^C D_t^h \bar{V}(t) \leq & \int_0^1 \left\{ 2\xi^T(t, z) P \left[L \frac{\partial^2 \xi(t, z)}{\partial z^2} \right. \right. \\ & \left. \left. - A\xi(t - \sigma, z) + B\mathcal{F}(\varpi(t - \tau(t), z)) \right] \right. \\ & \left. + \xi^T(t, z) P(|\mu| + |\varphi|) \right. \\ & \left. \times \Pi_1^{-1}(|\mu| + |\varphi|)^T P \xi(t, z) \right. \\ & \left. + \mathcal{F}^T(\varpi(t - \tau(t), z)) \right. \\ & \left. \times \Pi_1 \mathcal{F}(\varpi(t - \tau(t), z)) \right. \\ & \left. + 2\varpi^T(t, z) Q \left[M \frac{\partial^2 \varpi(t, z)}{\partial z^2} \right. \right. \\ & \left. \left. - C\varpi(t - \delta, z) + D\mathcal{G}(\xi(t - \eta(t), z)) \right] \right. \\ & \left. + \varpi^T(t, z) Q(|\gamma| + |\rho|) \right. \\ & \left. \times \Pi_2^{-1}(|\gamma| + |\rho|)^T Q \varpi(t, z) \right. \\ & \left. + \mathcal{G}^T(\xi(t - \eta(t), z)) \Pi_2 \mathcal{G}(\xi(t - \eta(t), z)) \right. \\ & \left. + \sum_{i=1}^n \left[2\hat{p}_i L_i(\theta_{3i}(t) \right. \right. \\ & \left. \left. - \aleph_{3i}) \xi_i^2(t, z) \right. \right. \end{aligned}$$

$$\begin{aligned}
& + 2\hat{p}_i L_i \theta_{4i}(t) \xi_i(t, z) \text{sign}(\xi_i(t, z)) \\
& + \sum_{j=1}^m \left[2\hat{q}_j M_j (\vartheta_{3j}(t) - \aleph_{4j}) \varpi_j^2(t, z) \right. \\
& + 2\hat{q}_j M_j \vartheta_{4j}(t) \varpi_j(t, z) \text{sign}(\varpi_j(t, z)) \\
& + \xi^T(t, z) R \xi(t, z) \\
& - \xi^T(t - \sigma, z) R \xi(t - \sigma, z) \\
& + \varpi^T(t, z) S \varpi(t, z) \\
& \left. - \varpi^T(t - \delta, z) S \varpi(t - \delta, z) \right] dz. \quad (31)
\end{aligned}$$

Using the integration by parts approach and boundary condition (28), we get

$$\begin{aligned}
& \sum_{i=1}^n \int_0^1 \xi_i^T(t, z) \hat{p}_i L_i \frac{\partial^2 \xi_i(t, z)}{\partial z^2} dz \\
& = \sum_{i=1}^n \left[\xi_i^T(t, z) \hat{p}_i L_i \frac{\partial \xi_i(t, z)}{\partial z} \right]_{z=0}^{z=1} \\
& - \sum_{i=1}^n \int_0^1 \frac{\partial \xi_i^T(t, z)}{\partial z} \hat{p}_i L_i \frac{\partial \xi_i(t, z)}{\partial z} dz \\
& = \sum_{i=1}^n \xi_i^T(t, 1) \hat{p}_i L_i u_i(t) \\
& - \sum_{i=1}^n \int_0^1 \frac{\partial \xi_i^T(t, z)}{\partial z} \hat{p}_i L_i \frac{\partial \xi_i(t, z)}{\partial z} dz \\
& = \sum_{i=1}^n \xi_i^T(t, 1) \hat{p}_i L_i \left[-\theta_{3i}(t) \int_0^1 \frac{\xi_i^2(t, z)}{\xi_i(t, 1)} dz \right. \\
& \left. - \theta_{4i}(t) \int_0^1 \frac{\xi_i(t, z) \text{sign}(\xi_i(t, z))}{\xi_i(t, 1)} dz \right] \\
& - \sum_{i=1}^n \int_0^1 \frac{\partial \xi_i^T(t, z)}{\partial z} \hat{p}_i L_i \frac{\partial \xi_i(t, z)}{\partial z} dz \\
& = - \sum_{i=1}^n \int_0^1 \hat{p}_i L_i \theta_{3i}(t) \xi_i^2(t, z) dz \\
& - \sum_{i=1}^n \int_0^1 \hat{p}_i L_i \theta_{4i}(t) \xi_i(t, z) \\
& \times \text{sign}(\xi_i(t, z)) dz \\
& - \sum_{i=1}^n \int_0^1 \frac{\partial \xi_i^T(t, z)}{\partial z} \hat{p}_i L_i \frac{\partial \xi_i(t, z)}{\partial z} dz, \quad (32)
\end{aligned}$$

similarly

$$\begin{aligned}
& \sum_{j=1}^m \int_0^1 \varpi_j^T(t, z) \hat{q}_j M_j \frac{\partial^2 \varpi_j(t, z)}{\partial z^2} dz \\
& = - \sum_{j=1}^m \int_0^1 \hat{q}_j M_j \vartheta_{3j}(t) \varpi_j^2(t, z) dz \\
& - \sum_{j=1}^m \int_0^1 \hat{q}_j M_j \vartheta_{4j}(t) \varpi_j(t, z) \text{sign}(\varpi_j(t, z)) dz \\
& - \sum_{j=1}^m \int_0^1 \frac{\partial \varpi_j^T(t, z)}{\partial z} \hat{q}_j M_j \frac{\partial \varpi_j(t, z)}{\partial z} dz. \quad (33)
\end{aligned}$$

To get $\hat{\xi}(t, z) = 0$ and $\hat{\varpi}(t, z) = 0$, we introduce the new state variables $\hat{\xi}(t, z) = \xi(t, z) - \xi(t, 1)$ and $\hat{\varpi}(t, z) = \varpi(t, z) - \varpi(t, 1)$. Furthermore, the conditions (17) and (18) are holds. Applying Wirtinger's inequality, we get

$$\begin{aligned}
& \sum_{i=1}^n \int_0^1 \xi_i^T(t, z) \hat{p}_i L_i \frac{\partial^2 \xi_i(t, z)}{\partial z^2} dz \\
& = - \sum_{i=1}^n \int_0^1 \hat{p}_i L_i \theta_{3i}(t) \xi_i^2(t, z) dz \\
& - \sum_{i=1}^n \int_0^1 \hat{p}_i L_i \theta_{4i}(t) \xi_i(t, z) \text{sign}(\xi_i(t, z)) dz \\
& - \frac{1}{2} \sum_{i=1}^n \int_0^1 \frac{\partial \xi_i^T(t, z)}{\partial z} \hat{p}_i L_i \frac{\partial \xi_i(t, z)}{\partial z} dz \\
& - \frac{1}{2} \sum_{i=1}^n \int_0^1 \frac{\partial \hat{\xi}_i^T(t, z)}{\partial z} \hat{p}_i L_i \frac{\partial \hat{\xi}_i(t, z)}{\partial z} dz \\
& \leq - \sum_{i=1}^n \int_0^1 \hat{p}_i L_i \theta_{3i}(t) \xi_i^2(t, z) dz \\
& - \sum_{i=1}^n \int_0^1 \hat{p}_i L_i \theta_{4i}(t) \xi_i(t, z) \text{sign}(\xi_i(t, z)) dz \\
& - \frac{\pi^2}{8} \sum_{i=1}^n \int_0^1 \xi_i^T(t, z) \hat{p}_i L_i \xi_i(t, z) dz \\
& - \frac{\pi^2}{8} \sum_{i=1}^n \int_0^1 \hat{\xi}_i^T(t, z) \hat{p}_i L_i \hat{\xi}_i(t, z) dz, \quad (34)
\end{aligned}$$

similarly

$$\sum_{j=1}^m \int_0^1 \varpi_j^T(t, z) \hat{q}_j M_j \frac{\partial^2 \varpi_j(t, z)}{\partial z^2} dz$$

$$\begin{aligned}
&\leq - \sum_{j=1}^m \int_0^1 \hat{q}_j M_j \vartheta_{3j}(t) \varpi_j^2(t, z) dz \\
&- \sum_{j=1}^m \int_0^1 \hat{q}_j M_j \vartheta_{4j}(t) \varpi_j(t, z) \text{sign}(\varpi_j(t, z)) dz \\
&- \frac{\pi^2}{8} \sum_{j=1}^m \int_0^1 \varpi_j^T(t, z) \hat{q}_j M_j \varpi_j(t, z) dz \\
&- \frac{\pi^2}{8} \sum_{j=1}^m \int_0^1 \hat{\varpi}_j^T(t, z) \hat{q}_j M_j \hat{\varpi}_j(t, z) dz. \quad (35)
\end{aligned}$$

Combining the inequalities (31)–(35), (21) and (22), we find that

$${}^C_0 D_t^h \bar{V}(t) \leq \int_0^1 \Upsilon^T(t, z) \Delta \Upsilon(t, z) dz, \quad (36)$$

where

$$\begin{aligned}
\Upsilon^T(t, z) = &\left[\xi^T(t, z) \varpi^T(t, z) \hat{\xi}^T(t, z) \right. \\
&\varpi^T(t, z) \xi^T(t - \sigma, z) \\
&\varpi^T(t - \delta, z) \xi^T(t - \eta(t), z) \\
&\varpi^T(t - \tau(t), z) \mathcal{G}^T(\xi(t - \eta(t), z)) \\
&\left. \mathcal{F}^T(\varpi(t - \tau(t), z)) \right].
\end{aligned}$$

If the LMI $\Delta < 0$, we conclude that the error dynamical system (26) is globally asymptotically stable. The proof is completed. \blacksquare

Remark 3.3: Theorem 3.2 is new because no one has investigated the results of adaptive boundary controller on synchronisation of fractional-order fuzzy reaction–diffusion BAM neural networks. Compared with existing results in C. Wang, Zhang, Stamova, et al. (2023), Syed Ali, Hymavathi, et al. (2020), C. Chen et al. (2018), we deal with fractional-order fuzzy reaction–diffusion BAM neural networks and asymptotic boundary control synchronisation, which is better than that of asymptotic full-domain control synchronisation because boundary control can save the cost of spatial domain.

Remark 3.4: Compared with the existing results (Pratap et al., 2019; Rajivganthi et al., 2016; Shafiya et al., 2022; J. Yang et al., 2022), the following are the main aspects and advantages of this paper:

- In Theorems 3.1 and 3.2, new sufficient criteria for fractional-order fuzzy reaction–diffusion BAM neural networks are investigated by constructing suitable Lyapunov function and using Neumann boundary condition, Wirtinger’s inequality, and the LMI approach to guarantee asymptotic full-domain control synchronisation and asymptotic boundary control synchronisation, respectively. The derived LMI stability criteria are less complicated to compute than algebraic stability criteria suggested in Shafiya et al. (2022), J. Yang et al. (2022), Pratap et al. (2019), Rajivganthi et al. (2016).
- We used novel adaptive boundary controllers in this study may have incorporated certain optimisations that resulted in reduced computational complexity. These could be unique to the problem at hand and may not have been extended in Shafiya et al. (2022), J. Yang et al. (2022), Pratap et al. (2019), Rajivganthi et al. (2016).
- The nonlinear dynamics of reaction–diffusion BAM neural networks with changing structural properties was effectively treated by using the well-known fuzzy model (fuzzy AND and fuzzy OR) and fractional derivative.

Remark 3.5: Reaction–diffusion BAM neural networks have attracted the attention of numerous researchers due to their potential and wide applications in various fields, such as pattern formation (T. Dong et al., 2022) and image encryption (Lin et al., 2020). In contrast, the boundary control method offers significant advantages since it employs the controllers only at the boundary positions and not in the entire spatial domain (X. Z. Liu et al., 2020, 2023; R. J. Zhang et al., 2022). Moreover, it even overcomes the problem of uncontrollable internal spatial points within networks (X. Z. Liu et al., 2020, 2023; R. J. Zhang et al., 2022). Consequently, the design of boundary controllers becomes necessary to account for the dynamic behaviour of reaction–diffusion BAM neural networks. Regrettably, the synchronisation problem for fractional-order fuzzy reaction–diffusion BAM neural networks with boundary control has not been explored yet. As far as we know, our work is the first to solve the synchronisation problem of systems (1) and (3) with adaptive boundary control under Neumann boundary conditions. In general, the image encryption application of complex-valued BAM neural network model is more difficult to study the

synchronisation analysis (Guo et al., 2020; A. Liu et al., 2022). Therefore, it will be interesting and challenging how to develop the adaptive boundary controller for fractional-order complex-valued BAM neural networks model in the near future.

If the fuzzy feedback MIN templates $\mu_{ij} = \gamma_{ji} = 0$ and MAX templates $\varphi_{ij} = \rho_{ji} = 0$ in the systems (1)–(3), then the systems (1)–(3) can be rewritten as follows:

$$\left\{ \begin{array}{l} {}_0^C D_t^h x_i^\zeta(t, z) = L_i \frac{\partial^2 x_i^\zeta(t, z)}{\partial z^2} - a_i x_i^\zeta(t - \sigma, z) \\ \quad + \sum_{j=1}^m b_{ij} f_j(y_j^\zeta(t - \tau(t), z)) + \mathcal{J}_i, \\ {}_0^C D_t^h y_j^\zeta(t, z) = M_j \frac{\partial^2 y_j^\zeta(t, z)}{\partial z^2} - c_j y_j^\zeta(t - \delta, z) \\ \quad + \sum_{i=1}^n d_{ji} g_i(x_i^\zeta(t - \eta(t), z)) + \mathcal{K}_j, \end{array} \right. \quad (37)$$

and

$$\left\{ \begin{array}{l} {}_0^C D_t^h x_i^\kappa(t, z) = L_i \frac{\partial^2 x_i^\kappa(t, z)}{\partial z^2} - a_i x_i^\kappa(t - \sigma, z) \\ \quad + \sum_{j=1}^m b_{ij} f_j(y_j^\kappa(t - \tau(t), z)) \\ \quad + u_i(t, z) + \mathcal{J}_i, \\ {}_0^C D_t^h y_j^\kappa(t, z) = M_j \frac{\partial^2 y_j^\kappa(t, z)}{\partial z^2} - c_j y_j^\kappa(t - \delta, z) \\ \quad + \sum_{i=1}^n d_{ji} g_i(x_i^\kappa(t - \eta(t), z)) \\ \quad + v_j(t, z) + \mathcal{K}_j, \\ {}_0^C D_t^h x_i^\kappa(t, z) = L_i \frac{\partial^2 x_i^\kappa(t, z)}{\partial z^2} - a_i x_i^\kappa(t - \sigma, z) \\ \quad + \sum_{j=1}^m b_{ij} f_j(y_j^\kappa(t - \tau(t), z)) + \mathcal{J}_i, \\ {}_0^C D_t^h y_j^\kappa(t, z) = M_j \frac{\partial^2 y_j^\kappa(t, z)}{\partial z^2} - c_j y_j^\kappa(t - \delta, z) \\ \quad + \sum_{i=1}^n d_{ji} g_i(x_i^\kappa(t - \eta(t), z)) + \mathcal{K}_j. \end{array} \right. \quad (38)$$

$$\left\{ \begin{array}{l} {}_0^C D_t^h x_i^\kappa(t, z) = L_i \frac{\partial^2 x_i^\kappa(t, z)}{\partial z^2} - a_i x_i^\kappa(t - \sigma, z) \\ \quad + \sum_{j=1}^m b_{ij} f_j(y_j^\kappa(t - \tau(t), z)) + \mathcal{J}_i, \\ {}_0^C D_t^h y_j^\kappa(t, z) = M_j \frac{\partial^2 y_j^\kappa(t, z)}{\partial z^2} - c_j y_j^\kappa(t - \delta, z) \\ \quad + \sum_{i=1}^n d_{ji} g_i(x_i^\kappa(t - \eta(t), z)) + \mathcal{K}_j. \end{array} \right. \quad (39)$$

The error dynamical system of above drive-response systems is defined as follows:

$$\left\{ \begin{array}{l} {}_0^C D_t^h \xi_i(t, z) = L_i \frac{\partial^2 \xi_i(t, z)}{\partial z^2} - a_i \xi_i(t - \sigma, z) \\ \quad + \sum_{j=1}^m b_{ij} \mathcal{F}_j(\varpi_j(t - \tau(t), z)) \\ \quad + u_i(t, z), \\ {}_0^C D_t^h \varpi_j(t, z) = M_j \frac{\partial^2 \varpi_j(t, z)}{\partial z^2} - c_j \varpi_j(t - \delta, z) \\ \quad + \sum_{i=1}^n d_{ji} \mathcal{G}_i(\xi_i(t - \eta(t), z)) + v_j(t, z), \end{array} \right. \quad (40)$$

and

$$\left\{ \begin{array}{l} {}_0^C D_t^h \xi_i(t, z) = L_i \frac{\partial^2 \xi_i(t, z)}{\partial z^2} - a_i \xi_i(t - \sigma, z) \\ \quad + \sum_{j=1}^m b_{ij} \mathcal{F}_j(\varpi_j(t - \tau(t), z)), \\ {}_0^C D_t^h \varpi_j(t, z) = M_j \frac{\partial^2 \varpi_j(t, z)}{\partial z^2} - c_j \varpi_j(t - \delta, z) \\ \quad + \sum_{i=1}^n d_{ji} \mathcal{G}_i(\xi_i(t - \eta(t), z)). \end{array} \right. \quad (41)$$

Corollary 3.6: Under Assumption 2.3 and adaptive full-domain controller (4) with adaptive update law (5), the error dynamical system (40) is said to be globally asymptotically stable if there exist positive definite diagonal matrices $P, Q, \Pi_1, \Pi_2, \Gamma_1, \Gamma_2$, and symmetric positive definite matrices R, S such that the following LMI holds:

$$(iii) \Phi = \begin{bmatrix} \Xi_{11} & 0 & 0 & 0 & \Xi_{15} \\ * & \Xi_{22} & 0 & 0 & 0 \\ * & * & \Xi_{33} & 0 & 0 \\ * & * & * & \Xi_{44} & 0 \\ * & * & * & * & \Xi_{55} \\ * & * & * & * & * \\ * & * & * & * & * \\ * & * & * & * & * \\ * & * & * & * & * \\ * & * & * & * & * \end{bmatrix}$$

$$\begin{bmatrix} 0 & 0 & 0 & 0 & \Xi_{110} \\ \Xi_{26} & 0 & 0 & \Xi_{29} & 0 \\ 0 & 0 & 0 & 0 & 0 \\ 0 & 0 & 0 & 0 & 0 \\ \Xi_{66} & 0 & 0 & 0 & 0 \\ * & \Xi_{77} & 0 & \Xi_{79} & 0 \\ * & * & \Xi_{88} & 0 & \Xi_{810} \\ * & * & * & -\Gamma_1 & 0 \\ * & * & * & * & -\Gamma_2 \end{bmatrix} < 0, \tag{42}$$

where $\Xi_{11}, \Xi_{15}, \Xi_{110}, \Xi_{22}, \Xi_{26}, \Xi_{29}, \Xi_{33}, \Xi_{44}, \Xi_{55}, \Xi_{66}, \Xi_{77}, \Xi_{79}, \Xi_{88}$ and Ξ_{810} are defined in Theorem 3.1.

Corollary 3.7: Under Assumption 2.3 and adaptive boundary controller (24) with adaptive update law (25), the error dynamical system (41) is said to be globally asymptotically stable if there exist positive definite diagonal matrices $P, Q, \Pi_1, \Pi_2, \Gamma_1, \Gamma_2$, and symmetric positive definite matrices R, S such that the following LMI holds:

$$(iii) \Psi = \begin{bmatrix} \Delta_{11} & 0 & 0 & 0 & \Xi_{15} \\ * & \Delta_{22} & 0 & 0 & 0 \\ * & * & \Xi_{33} & 0 & 0 \\ * & * & * & \Xi_{44} & 0 \\ * & * & * & * & \Xi_{55} \\ * & * & * & * & * \\ * & * & * & * & * \\ * & * & * & * & * \\ * & * & * & * & * \\ * & * & * & * & * \end{bmatrix} < 0, \tag{43}$$

$$\begin{bmatrix} 0 & 0 & 0 & 0 & \Xi_{110} \\ \Xi_{26} & 0 & 0 & \Xi_{29} & 0 \\ 0 & 0 & 0 & 0 & 0 \\ 0 & 0 & 0 & 0 & 0 \\ \Xi_{66} & 0 & 0 & 0 & 0 \\ * & \Xi_{77} & 0 & \Xi_{79} & 0 \\ * & * & \Xi_{88} & 0 & \Xi_{810} \\ * & * & * & -\Gamma_1 & 0 \\ * & * & * & * & -\Gamma_2 \end{bmatrix} < 0,$$

where $\Xi_{15}, \Xi_{110}, \Xi_{26}, \Xi_{29}, \Xi_{33}, \Xi_{44}, \Xi_{55}, \Xi_{66}, \Xi_{77}, \Xi_{79}, \Xi_{88}$ and Ξ_{810} are defined in Theorem 3.1, and Δ_{11}, Δ_{22} are defined in Theorem 3.2.

4. Numerical simulations

This section presents a numerical example with two cases to illustrate the feasibility of the main results.

Example 4.1: Consider the following fractional-order fuzzy reaction–diffusion BAM neural networks with leakage time delay:

$$\left\{ \begin{aligned} {}^C D_t^h x_i^s(t, z) &= L_i \frac{\partial^2 x_i^s(t, z)}{\partial z^2} - a_i x_i^s(t - \sigma, z) \\ &+ \sum_{j=1}^3 b_{ijf_j} (y_j^s(t - \tau(t), z)) \\ &+ \bigwedge_{j=1}^3 \mu_{ijf_j} (y_j^s(t - \tau(t), z)) \\ &+ \bigvee_{j=1}^3 \varphi_{ijf_j} (y_j^s(t - \tau(t), z)) + \mathcal{J}_i, \\ {}^C D_t^h y_j^s(t, z) &= M_j \frac{\partial^2 y_j^s(t, z)}{\partial z^2} - c_j y_j^s(t - \delta, z) \\ &+ \sum_{i=1}^3 d_{jig_i} (x_i^s(t - \eta(t), z)) \\ &+ \bigwedge_{i=1}^3 \gamma_{jig_i} (x_i^s(t - \eta(t), z)) \\ &+ \bigvee_{i=1}^3 \rho_{ijg_i} (x_i^s(t - \eta(t), z)) + \mathcal{K}_j, \end{aligned} \right. \tag{44}$$

with initial and Neumann boundary conditions are as follows:

$$\begin{cases} x_i^s(t, z) = \phi_i^s(t, z), z \in (0, 1), t \in [-\eta, 0], \\ y_j^s(t, z) = \psi_j^s(t, z), z \in (0, 1), t \in [-\tau, 0], \end{cases}$$

and

$$\begin{cases} \frac{\partial x_r^s(t, z)}{\partial z} \Big|_{z=0} = 0, & \frac{\partial x_r^s(t, z)}{\partial z} \Big|_{z=1} = 0, \\ \frac{\partial y_s^s(t, z)}{\partial z} \Big|_{z=0} = 0, & \frac{\partial y_s^s(t, z)}{\partial z} \Big|_{z=1} = 0, \end{cases}$$

where $h = 0.96$, the nonlinear functions chosen as $f(y) = \frac{y^2}{1+y^2}$ and $g(x) = \frac{x^2}{1+x^2}$, which gives $\Lambda_1 = \Omega_1 = \text{diag}\{0, 0, 0\}$ and $\Lambda_2 = \Omega_2 = \text{diag}\{1, 1, 1\}$, $\sigma = \delta = 0.5$, and $\eta(t) = 0.5 |\cos(t)|, \tau(t) = 0.5 |\cos(t)|$.

The real matrices for drive system (44) can be chosen as follows:

$$L = M = \begin{bmatrix} 0.5 & 0 & 0 \\ 0 & 0.5 & 0 \\ 0 & 0 & 0.5 \end{bmatrix}, A = \begin{bmatrix} 6 & 0 & 0 \\ 0 & 6 & 0 \\ 0 & 0 & 6 \end{bmatrix},$$

$$B = \begin{bmatrix} -2.2 & -3.5 & 1.5 \\ 2.5 & -2.2 & 3.2 \\ 1.1 & -2.1 & 3.3 \end{bmatrix},$$

$$C = \begin{bmatrix} 5 & 0 & 0 \\ 0 & 5 & 0 \\ 0 & 0 & 5 \end{bmatrix}, D = \begin{bmatrix} -2.5 & -1.2 & 2.6 \\ 2.3 & 1.2 & 1.6 \\ -2.1 & 1.1 & 2.2 \end{bmatrix},$$

$$\mu = \begin{bmatrix} -0.02 & 0.05 & 0.05 \\ 0.05 & -0.02 & 0.02 \\ -0.01 & 0.01 & -0.03 \end{bmatrix},$$

$$\varphi = \begin{bmatrix} -0.03 & 0.02 & 0.06 \\ -0.02 & 0.03 & -0.06 \\ 0.05 & 0.01 & -0.02 \end{bmatrix},$$

$$\gamma = \begin{bmatrix} -0.01 & 0.02 & -0.01 \\ 0.02 & 0.02 & -0.05 \\ 0.01 & 0.08 & 0.03 \end{bmatrix},$$

$$\rho = \begin{bmatrix} -0.01 & 0.01 & -0.08 \\ -0.01 & 0.01 & 0.05 \\ -0.06 & 0.05 & 0.03 \end{bmatrix},$$

$$\aleph_1 = \aleph_2 = \begin{bmatrix} 7 & 0 & 0 \\ 0 & 7 & 0 \\ 0 & 0 & 7 \end{bmatrix},$$

$$\aleph_3 = \aleph_4 = \begin{bmatrix} 10 & 0 & 0 \\ 0 & 10 & 0 \\ 0 & 0 & 10 \end{bmatrix}.$$

The initial values of (44) are as follows:

$$\begin{cases} x_1^\zeta(t, z) = 0.5 \sin(t) + 0.5 \sin(0.5\pi z), \\ \quad t \in [-0.5, 0], \\ x_2^\zeta(t, z) = 0.3 \sin(t) + 0.5 \sin(0.9\pi z), \\ \quad t \in [-0.5, 0], \\ x_3^\zeta(t, z) = 0.8 \sin(t) + 0.6 \sin(0.4\pi z), \\ \quad t \in [-0.5, 0], \end{cases}$$

and

$$\begin{cases} y_1^\zeta(t, z) = 0.5 \sin(t) + 0.5 \sin(0.5\pi z), \\ \quad t \in [-0.5, 0], \\ y_2^\zeta(t, z) = 0.3 \sin(t) + 0.5 \sin(0.9\pi z), \\ \quad t \in [-0.5, 0], \\ y_3^\zeta(t, z) = 0.8 \sin(t) + 0.6 \sin(0.4\pi z), \\ \quad t \in [-0.5, 0]. \end{cases}$$

Next, the nonlinear dynamics of full-domain controlled response system is defined by

$$\begin{cases} {}_0^C D_t^h x_i^\kappa(t, z) = L_i \frac{\partial^2 x_i^\kappa(t, z)}{\partial z^2} - a_i x_i^\kappa(t - \sigma, z) \\ \quad + \sum_{j=1}^3 b_{ij} f_j(y_j^\kappa(t - \tau(t), z)) \\ \quad + \bigwedge_{j=1}^3 \mu_{ij} f_j(y_j^\kappa(t - \tau(t), z)) \\ \quad + \bigvee_{j=1}^3 \varphi_{ij} f_j(y_j^\kappa(t - \tau(t), z)) \\ \quad + u_i(t, z) + \mathcal{J}_i, \\ {}_0^C D_t^h y_j^\kappa(t, z) = M_j \frac{\partial^2 y_j^\kappa(t, z)}{\partial z^2} - c_j y_j^\kappa(t - \delta, z) \\ \quad + \sum_{i=1}^3 d_{ji} g_i(x_i^\kappa(t - \eta(t), z)) \\ \quad + \bigwedge_{i=1}^3 \gamma_{ji} g_i(x_i^\kappa(t - \eta(t), z)) \\ \quad + \bigvee_{i=1}^3 \rho_{ji} g_i(x_i^\kappa(t - \eta(t), z)) \\ \quad + v_j(t, z) + \mathcal{K}_j, \end{cases} \quad (45)$$

with initial and Neumann boundary conditions are as follows:

$$\begin{cases} x_i^\kappa(t, z) = \phi_i^\kappa(t, z), \quad z \in (0, 1), t \in [-\eta, 0], \\ y_j^\kappa(t, z) = \psi_j^\kappa(t, z), \quad z \in (0, 1), t \in [-\tau, 0], \end{cases}$$

and

$$\begin{cases} \frac{\partial x_i^\kappa(t, z)}{\partial z} \Big|_{z=0} = 0, \quad \frac{\partial x_i^\kappa(t, z)}{\partial z} \Big|_{z=1} = 0, \\ \frac{\partial y_j^\kappa(t, z)}{\partial z} \Big|_{z=0} = 0, \quad \frac{\partial y_j^\kappa(t, z)}{\partial z} \Big|_{z=1} = 0, \end{cases}$$

the parameters are identical with those in (44).

The nonlinear dynamics of boundary controlled response system is defined by

$$\left\{ \begin{array}{l} {}^C_0 D_t^h x_i^k(t, z) = L_i \frac{\partial^2 x_i^k(t, z)}{\partial z^2} - a_i x_i^k(t - \sigma, z) \\ \quad + \sum_{j=1}^3 b_{ij} f_j(y_j^k(t - \tau(t), z)) \\ \quad + \bigwedge_{j=1}^3 \mu_{ij} f_j(y_j^k(t - \tau(t), z)) \\ \quad + \bigvee_{j=1}^3 \varphi_{ij} f_j(y_j^k(t - \tau(t), z)) + \mathcal{J}_i, \\ {}^C_0 D_t^h y_j^k(t, z) = M_j \frac{\partial^2 y_j^k(t, z)}{\partial z^2} - c_j y_j^k(t - \delta, z) \\ \quad + \sum_{i=1}^3 d_{ji} g_i(x_i^k(t - \eta(t), z)) \\ \quad + \bigwedge_{i=1}^3 \gamma_{ji} g_i(x_i^k(t - \eta(t), z)) \\ \quad + \bigvee_{i=1}^3 \rho_{ji} g_i(x_i^k(t - \eta(t), z)) + \mathcal{K}_j, \end{array} \right. \quad (46)$$

with initial and Neumann boundary conditions as follows:

$$\left\{ \begin{array}{l} x_i^k(t, z) = \phi_i^k(t, z), \quad z \in (0, 1), t \in [-\eta, 0], \\ y_j^k(t, z) = \psi_j^k(t, z), \quad z \in (0, 1), t \in [-\tau, 0], \end{array} \right.$$

and

$$\left\{ \begin{array}{l} \frac{\partial x_i^k(t, z)}{\partial z} \Big|_{z=0} = 0, \quad \frac{\partial x_i^k(t, z)}{\partial z} \Big|_{z=1} = u_i(t), \\ \frac{\partial y_j^k(t, z)}{\partial z} \Big|_{z=0} = 0, \quad \frac{\partial y_j^k(t, z)}{\partial z} \Big|_{z=1} = v_j(t), \end{array} \right.$$

the parameters are identical with those in (44)

Case I: Adaptive full-domain control synchronisation.

Now, the controller parameters values are chosen as follows: $\theta_{11} = 1.7304$, $\theta_{12} = 0.8923$, $\theta_{13} = 0.4103$, $\theta_{21} = 1.0229$, $\theta_{22} = 1.5683$, $\theta_{23} = 0.4743$, $\vartheta_{11} = 0.6164$, $\vartheta_{12} = 0.0813$, $\vartheta_{13} = 2.8414$, $\vartheta_{21} = 1.8458$, $\vartheta_{22} = 0.8782$, $\vartheta_{23} = 0.4682$, $\omega_{11} = 1.0722$, $\omega_{12} = 1.6682$, $\omega_{13} = 1.0219$, $\omega_{21} = 0.6456$, $\omega_{22} = 0.8652$, $\omega_{23} = 2.3523$, $\varrho_{11} = 1.5684$, $\varrho_{12} = 0.4103$, $\varrho_{13} = 2.8215$, $\varrho_{21} = 0.3812$, $\varrho_{22} = 0.9414$, and $\varrho_{23} = 1.8548$.

By virtue of Theorem 3.1 to check the adaptive full-domain synchronisation, we solve the LMI (9) with the MATLAB LMI toolbox, the feasible solutions are determined as follows:

$$\begin{aligned} P &= \begin{bmatrix} 0.7539 & 0 & 0 \\ 0 & 0.7539 & 0 \\ 0 & 0 & 0.7539 \end{bmatrix}, \\ Q &= \begin{bmatrix} 0.7149 & 0 & 0 \\ 0 & 0.7149 & 0 \\ 0 & 0 & 0.7149 \end{bmatrix}, \\ R &= \begin{bmatrix} 4.6387 & 0.1610 & 0.1936 \\ 0.1610 & 4.7155 & 0.3303 \\ 0.1936 & 0.3303 & 4.6404 \end{bmatrix}, \\ S &= \begin{bmatrix} 3.8373 & -0.0941 & 0.3128 \\ -0.0941 & 3.6081 & -0.0238 \\ 0.3128 & -0.0238 & 3.7032 \end{bmatrix}, \\ \Pi_1 &= \begin{bmatrix} 1.1482 & 0 & 0 \\ 0 & 1.1482 & 0 \\ 0 & 0 & 1.1482 \end{bmatrix}, \\ \Pi_2 &= \begin{bmatrix} 1.2357 & 0 & 0 \\ 0 & 1.2357 & 0 \\ 0 & 0 & 1.2357 \end{bmatrix}, \\ \Gamma_1 &= \begin{bmatrix} 14.8054 & 0 & 0 \\ 0 & 14.8054 & 0 \\ 0 & 0 & 14.8054 \end{bmatrix}, \\ \Gamma_2 &= \begin{bmatrix} 46.5009 & 0 & 0 \\ 0 & 46.5009 & 0 \\ 0 & 0 & 46.5009 \end{bmatrix}. \end{aligned}$$

Case II: Adaptive boundary control synchronisation.

Now, the controller parameter values are chosen as follows: $\theta_{31} = 2.7304$, $\theta_{32} = 2.8923$, $\theta_{33} = 2.3410$, $\theta_{41} = 1.2523$, $\theta_{42} = 2.9534$, $\theta_{43} = 1.7523$, $\vartheta_{31} = 0.8535$, $\vartheta_{32} = 0.9345$, $\vartheta_{33} = 1.4212$, $\vartheta_{41} = 3.4510$, $\vartheta_{42} = 2.9230$, $\vartheta_{43} = 3.1423$, $\omega_{31} = 1.7525$, $\omega_{32} = 2.3525$, $\omega_{33} = 1.7678$, $\omega_{41} = 4.7987$, $\omega_{42} = 2.9878$, $\omega_{43} = 3.7890$, $\varrho_{31} = 1.8535$, $\varrho_{32} = 1.9898$, $\varrho_{33} = 1.2525$, $\varrho_{41} = 1.8593$, $\varrho_{42} = 1.9520$, and $\varrho_{43} = 1.8513$. By virtue of Theorem 3.2 to check the adaptive boundary synchronisation, we solve the LMI (29) with the MATLAB LMI toolbox, the feasible solutions are determined as follows:

$$P = \begin{bmatrix} 2.2202 & 0 & 0 \\ 0 & 2.2202 & 0 \\ 0 & 0 & 2.2202 \end{bmatrix},$$

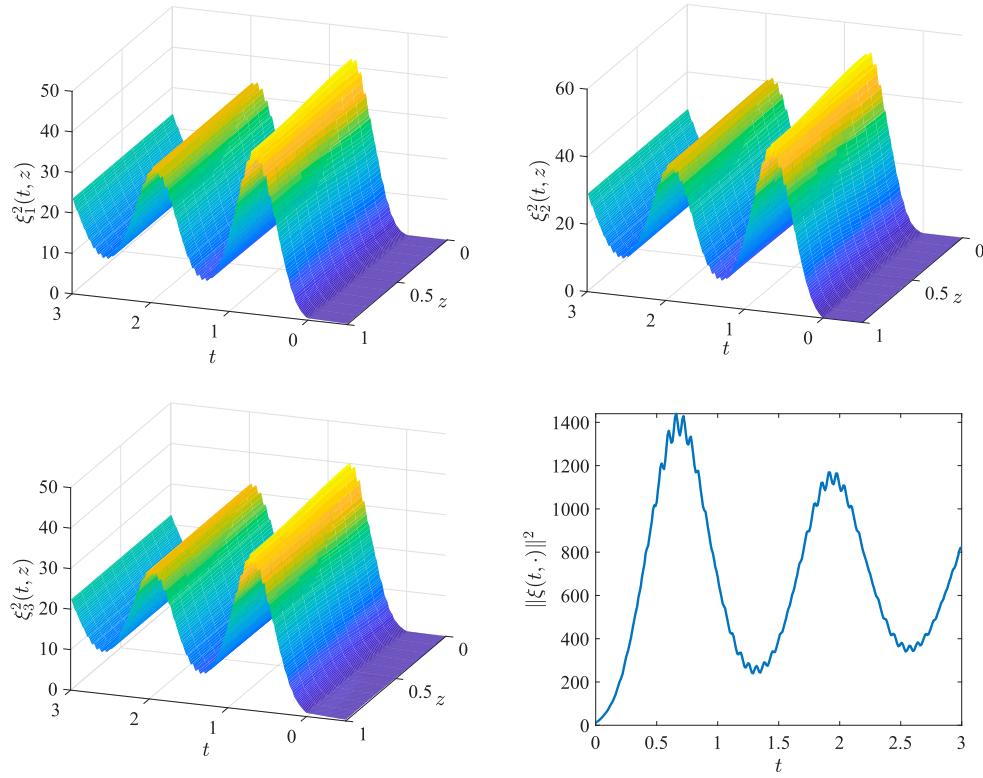


Figure 1. The errors $\xi^2(t, z)$ and norm $\|\xi(t, \cdot)\|^2$ of drive–response systems (44) and (45) without control.

$$Q = \begin{bmatrix} 1.8155 & 0 & 0 \\ 0 & 1.8155 & 0 \\ 0 & 0 & 1.8155 \end{bmatrix},$$

$$R = \begin{bmatrix} 9.6870 & 0.0166 & -0.0237 \\ 0.0166 & 9.7216 & -0.0636 \\ -0.0237 & -0.0636 & 9.7466 \end{bmatrix},$$

$$S = \begin{bmatrix} 12.6321 & -0.2754 & 0.7928 \\ -0.2754 & 12.0612 & -0.0586 \\ 0.7928 & -0.0586 & 12.2944 \end{bmatrix},$$

$$\Pi_1 = \begin{bmatrix} 4.5872 & 0 & 0 \\ 0 & 4.5872 & 0 \\ 0 & 0 & 4.5872 \end{bmatrix},$$

$$\Pi_2 = \begin{bmatrix} 3.9407 & 0 & 0 \\ 0 & 3.9407 & 0 \\ 0 & 0 & 3.9407 \end{bmatrix},$$

$$\Gamma_1 = \begin{bmatrix} 31.7901 & 0 & 0 \\ 0 & 31.7901 & 0 \\ 0 & 0 & 31.7901 \end{bmatrix},$$

$$\Gamma_2 = \begin{bmatrix} 24.6728 & 0 & 0 \\ 0 & 24.6728 & 0 \\ 0 & 0 & 24.6728 \end{bmatrix}.$$

The synchronisation errors $\xi^2(t, z)$ and norm $\|\xi(t, \cdot)\|^2$ of drive–response systems (44) and (45) without control are depicted in Figure 1. The synchronisation errors $\varpi^2(t, z)$ and norm $\|\varpi(t, \cdot)\|^2$ of drive–response systems (44) and (45) without control are depicted in Figure 2. It is clearly shown that the drive–response systems (44) and (45) do not realise synchronisation without control. Under the adaptive boundary controllers (24) with fractional update laws (25), Figures 3 and 4 show that the adaptive boundary controllers (24) can achieve guaranteed asymptotic synchronisation of the drive–response systems (44) and (46). Under the adaptive full-domain controllers (4) with fractional update laws (5), Figures 5 and 6 show that the adaptive full-domain controllers (4) cannot achieve asymptotic synchronisation of the drive–response systems (44) and (45).

Remark 4.1: To demonstrate the superiority of our synchronisation strategy, we choose the adaptive boundary control gains $(\theta_{3i}, \theta_{4i}, \vartheta_{3j}, \vartheta_{4j})$, than several comparison results are displayed in Figures 3 and 4. According to Figures 3 and 4, we find convergence rates of synchronisation errors in this work are quicker

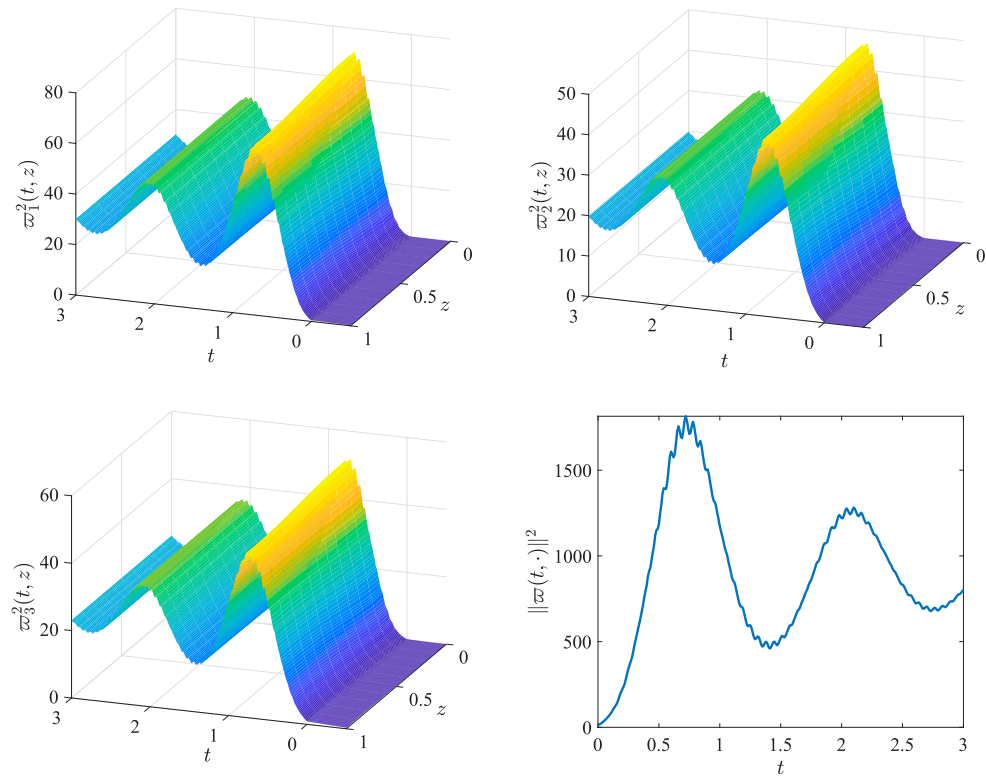


Figure 2. The errors $w^2(t, z)$ and norm $\|w(t, \cdot)\|^2$ of drive–response systems (44) and (45) without control.

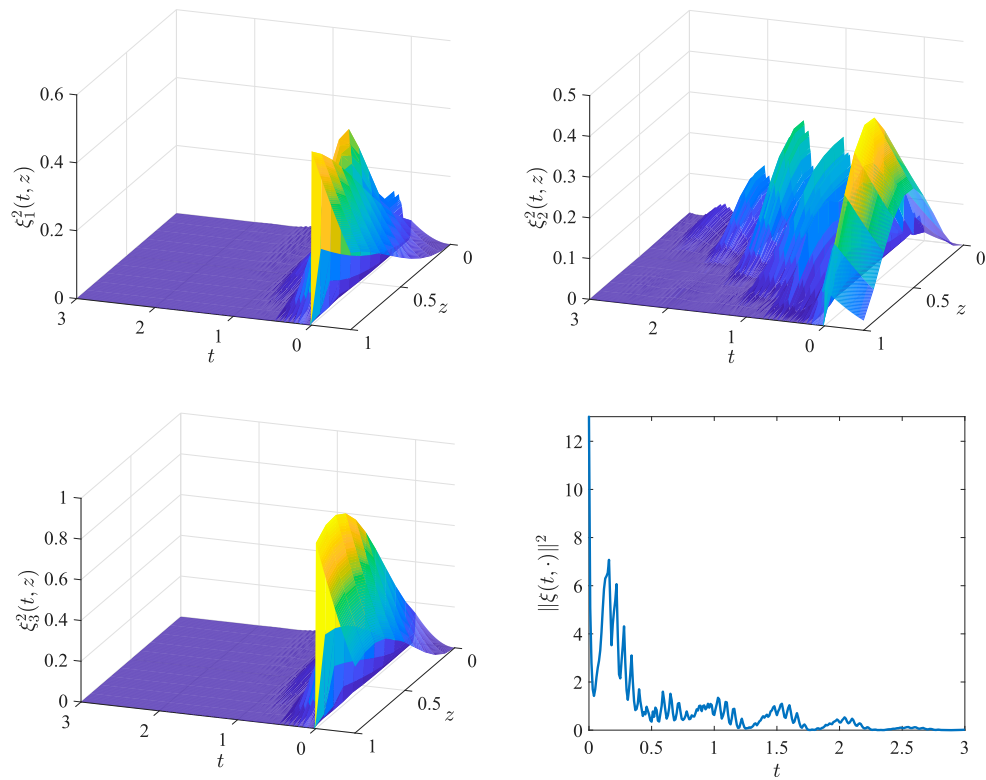


Figure 3. The errors $\xi^2(t, z)$ and norm $\|\xi(t, \cdot)\|^2$ of drive–response systems (44) and (46) with adaptive boundary controller (24) and fractional update law (25).

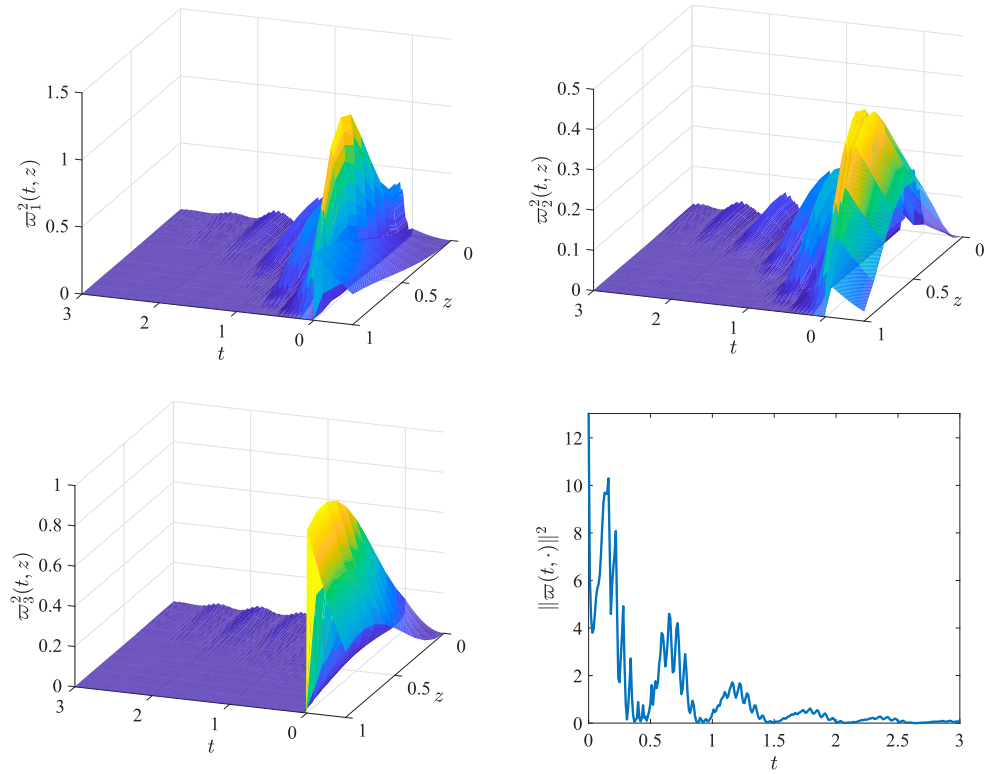


Figure 4. The errors $w^2(t, z)$ and norm $\|w(t, \cdot)\|^2$ of drive–response systems (44) and (46) with adaptive boundary controller (24) and fractional update law (25).

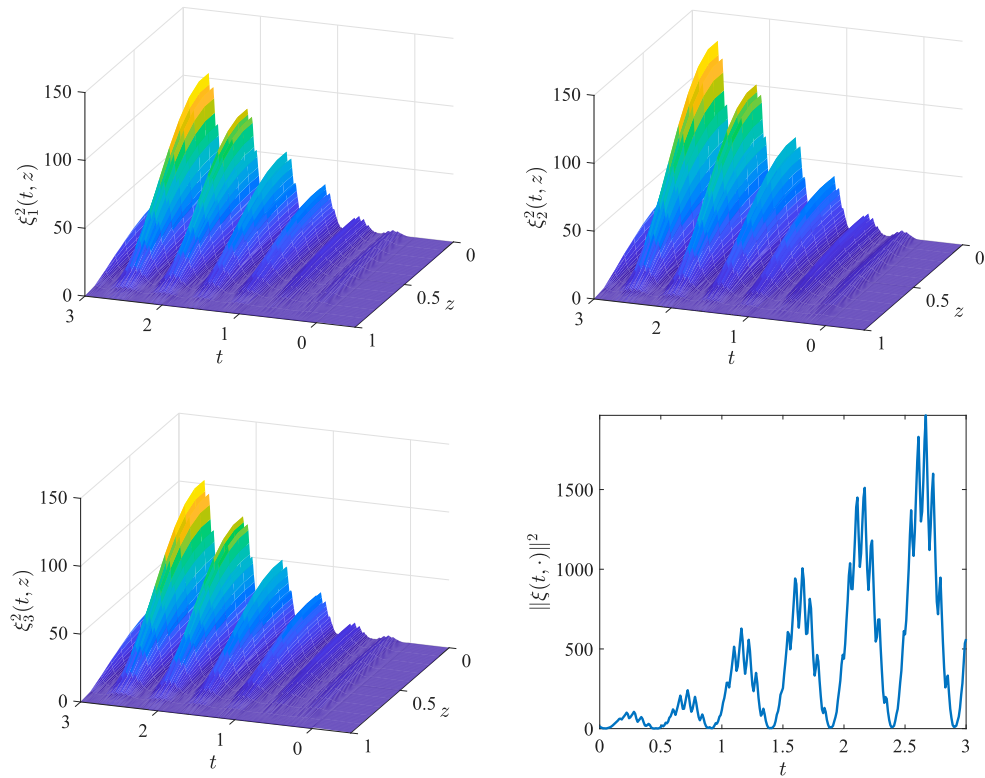


Figure 5. The errors $\xi^2(t, z)$ and norm $\|\xi(t, \cdot)\|^2$ of drive–response systems (44) and (45) with adaptive full-domain controller (4) and fractional update law (5).

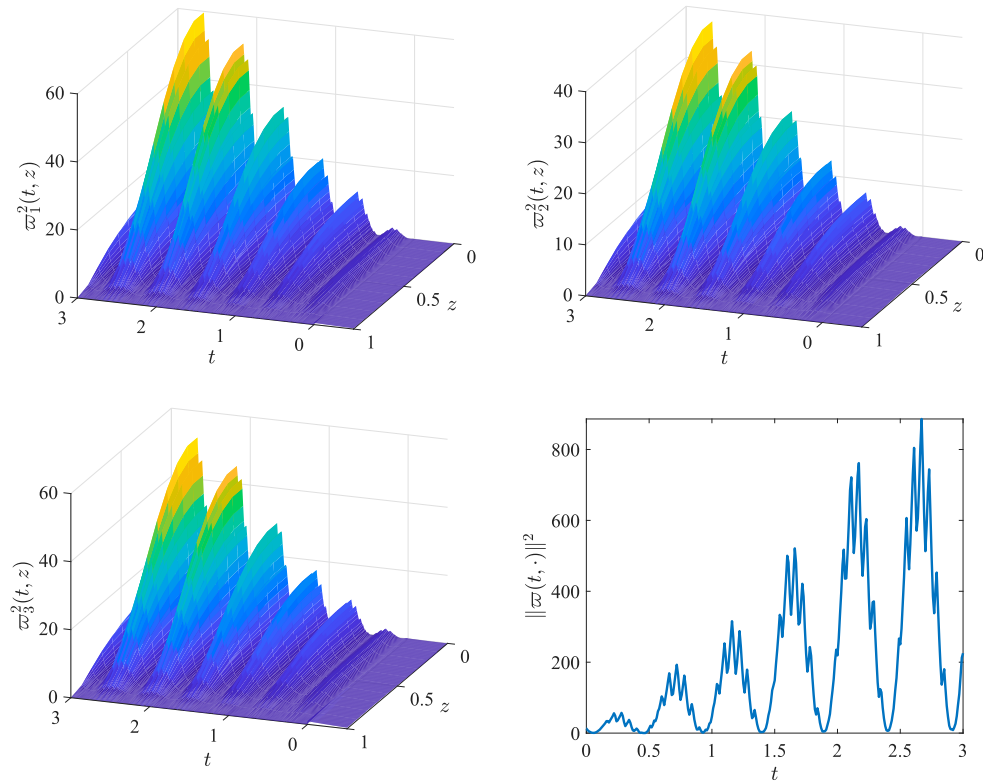


Figure 6. The errors $\varpi^2(t, z)$ and norm $\|\varpi(t, \cdot)\|^2$ of drive–response systems (44) and (45) with adaptive full-domain controller (4) and fractional update law (5).

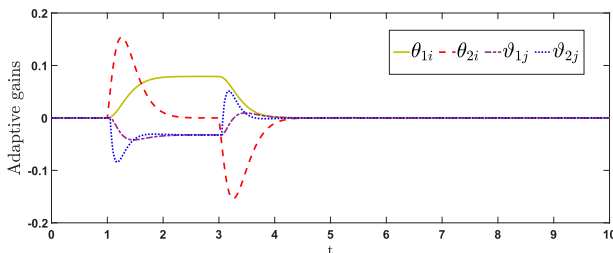


Figure 7. Control gain curve of the adaptive controllers.

than other control approaches in C. Wang, Zhang, Stamova, et al. (2023), C. Chen et al. (2018).

5. Conclusion

A new class of nonlinear dynamic fuzzy modelling of fractional-order reaction–diffusion BAM neural networks with adaptive boundary control and leakage time delay is considered in this paper. By developing a set of adaptive boundary control strategies with adaptive updated laws in the fractional domain, new sufficient criteria are derived to guarantee that the fractional-order fuzzy reaction–diffusion BAM neural networks achieve asymptotic synchronisation in terms of LMI. In light of these criteria, the impacts of

both the adaptive full-domain controller and the adaptive boundary controller on asymptotic stability are studied. Finally, numerical simulations are presented to illustrate the efficiency of our main results. In the future, we will investigate the adaptive boundary synchronisation of fractional-order fuzzy complex-valued BAM neural networks with reaction–diffusion and its application of image encryption.

Disclosure statement

No potential conflict of interest was reported by the author(s).

Funding

We thank the financial support from the National Research Council of Thailand (Talented Mid-Career Researchers) Grant Number N42A650250.

Data Availability Statement

Data sharing is not applicable to this article as no new data were created or analysed in this study.

References

Cao, J., & Wan, Y. (2014). Matrix measure strategies for stability and synchronisation of inertial BAM neural network with

- time delays. *Neural Networks*, 53, 165–172. <https://doi.org/10.1016/j.neunet.2014.02.003>
- Chen, C., Li, L., Peng, H., & Yang, Y. (2018). Adaptive synchronization of memristor-based BAM neural networks with mixed delays. *Applied Mathematics and Computation*, 322, 100–110. <https://doi.org/10.1016/j.amc.2017.11.037>
- Chen, D., & Zhang, Z. (2022). Globally asymptotic synchronization for complex-valued BAM neural networks by the differential inequality way. *Chaos, Solitons and Fractals*, 164, Article 112681. <https://doi.org/10.1016/j.chaos.2022.112681>
- Dong, T., Xiang, W., Huang, T., & Li, H. (2022). Pattern formation in a reaction-diffusion BAM neural network with time delay: (k_1, k_2) mode Hopf-zero bifurcation case. *IEEE Transactions on Neural Networks and Learning Systems*, 33, 7266–7276. <https://doi.org/10.1109/TNNLS.2021.3084693>
- Dong, Z., Wang, X., Zhang, X., Hu, M., & Dinh, T. N. (2023). Global exponential synchronization of discrete-time high-order switched neural networks and its application to multi-channel audio encryption. *Nonlinear Analysis: Hybrid Systems*, 47, Article 101291.
- Duan, L., & Li, J. (2021). Fixed-time synchronization of fuzzy neutral-type BAM memristive inertial neural networks with proportional delays. *Information Sciences*, 576, 522–541. <https://doi.org/10.1016/j.ins.2021.06.093>
- Gopalsamy, K. (2007). Leakage delays in BAM. *Journal of Mathematical Analysis and Applications*, 325, 1117–1132. <https://doi.org/10.1016/j.jmaa.2006.02.039>
- Guan, S., & Wang, X. (2022). Optimization analysis of football match prediction model based on neural network. *Neural Computing and Applications*, 34, 2525–2541. <https://doi.org/10.1007/s00521-021-05930-x>
- Guo, Y., Luo, Y., Wang, W., Luo, X., Ge, C., Kurths, J., Yuan, M., & Gao, Y. (2020). Fixed-time synchronization of complex-valued memristive BAM neural network and applications in image encryption and decryption. *International Journal of Control, Automation and Systems*, 18, 462–476. <https://doi.org/10.1007/s12555-018-0676-7>
- Hu, J., Zhang, Q., Baese, A. M., & Ye, M. (2022). Finite-time stability and optimal control of a stochastic reaction-diffusion model for Alzheimer's disease with impulse and time-varying delay. *Applied Mathematical Modelling*, 102, 511–539. <https://doi.org/10.1016/j.apm.2021.10.004>
- Huang, C., & Cao, J. (2018). Impact of leakage delay on bifurcation in high-order fractional BAM neural networks. *Neural Networks*, 98, 223–235. <https://doi.org/10.1016/j.neunet.2017.11.020>
- Huang, C., Liu, H., Chen, Y., Chen, X., & Song, F. (2021). Dynamics of a fractional-order BAM neural network with leakage delay and communication delay. *Fractals*, 29, Article 2150073. <https://doi.org/10.1142/S0218348X21500730>
- Huang, C., Meng, Y., Cao, J., Alsaedi, A., & Alsaadi, F. E. (2017). New bifurcation results for fractional BAM neural network with leakage delay. *Chaos, Solitons and Fractals*, 100, 31–44. <https://doi.org/10.1016/j.chaos.2017.04.037>
- Kosko, B. (1987). Adaptive bidirectional associative memories. *Applied Optics*, 26, 4947–4960. <https://doi.org/10.1364/AO.26.004947>
- Kosko, B. (1988). Bidirectional associative memories. *IEEE Transactions on Systems, Man, and Cybernetics*, 18, 49–60. <https://doi.org/10.1109/21.87054>
- Li, M., Hong, Q., & Wang, X. (2022). Memristor-based circuit implementation of competitive neural network based on online unsupervised Hebbian learning rule for pattern recognition. *Neural Computing and Applications*, 34, 319–331. <https://doi.org/10.1007/s00521-021-06361-4>
- Li, M., & Zhao, H. (2022). Dynamics of a reaction-diffusion dengue fever model with incubation periods and vertical transmission in heterogeneous environments. *Journal of Applied Mathematics and Computing*, 68, 3673–3703. <https://doi.org/10.1007/s12190-021-01676-w>
- Li, Y., & Wei, Z. (2022). Dynamics and optimal control of a stochastic coronavirus (COVID-19) epidemic model with diffusion. *Nonlinear Dynamics*, 109, 91–120. <https://doi.org/10.1007/s11071-021-06998-9>
- Lin, J., Xu, R., & Li, L. (2019). Effect of leakage delay on Hopf bifurcation in a fractional BAM neural network. *International Journal of Bifurcation and Chaos*, 29, Article 1950077. <https://doi.org/10.1142/S0218127419500779>
- Lin, J., Xu, R., & Li, L. (2020). Spatio-temporal synchronization of reaction-diffusion BAM neural networks via impulsive pinning control. *Neurocomputing*, 418, 300–313. <https://doi.org/10.1016/j.neucom.2020.08.039>
- Liu, A., Zhao, H., Wang, Q., Niu, S., Gao, X., Chen, C., & Li, L. (2022). A new predefined-time stability theorem and its application in the synchronization of memristive complex-valued BAM neural networks. *Neural Networks*, 153, 152–163. <https://doi.org/10.1016/j.neunet.2022.05.031>
- Liu, X. Z., Li, Z. T., & Wu, K. N. (2020). Boundary Mittag-Leffler stabilization of fractional reaction-diffusion cellular neural networks. *Neural Networks*, 132, 269–280. <https://doi.org/10.1016/j.neunet.2020.09.009>
- Liu, X. Z., Wu, K. N., & Ahn, C. K. (2023). Intermittent boundary control for synchronization of fractional delay neural networks with diffusion terms. *IEEE Transactions on Systems, Man, and Cybernetics: Systems*, 53, 2900–2912. <https://doi.org/10.1109/TSMC.2022.3220650>
- Mani, P., Rajan, R., Shanmugam, L., & Joo, Y. H. (2019). Adaptive control for fractional-order induced chaotic fuzzy cellular neural networks and its application to image encryption. *Information Sciences*, 491, 74–89. <https://doi.org/10.1016/j.ins.2019.04.007>
- Narayanan, G., Syed Ali, M., Karthikeyan, R., Rajchakit, G., & Jirawattanapanit, A. (2022). Novel adaptive strategies for synchronization control mechanism in nonlinear dynamic fuzzy modeling of fractional-order genetic regulatory networks. *Chaos, Solitons and Fractals*, 165, Article 112748. <https://doi.org/10.1016/j.chaos.2022.112748>
- Nirvin, P., Rihan, F. A., Rakkiyappan, R., & Pradeep, C. (2022). Impulsive sampled-data controller design for synchronization of delayed T-S fuzzy Hindmarsh-Rose neuron model.

- Mathematics and Computers in Simulation*, 201, 588–602. <https://doi.org/10.1016/j.matcom.2021.03.022>
- Pratap, A., Raja, R., Rajchakit, G., Cao, J., & Bagdasar, O. (2019). Mittag–Leffler state estimator design and synchronization analysis for fractional-order BAM neural networks with time delays. *International Journal of Adaptive Control and Signal Processing*, 33, 855–874. <https://doi.org/10.1002/acs.v33.5>
- Rajivganthi, C., Rihan, F. A., Lakshmanan, S., Rakkiyappan, R., & Muthukumar, P. (2016). Synchronization of memristor-based delayed BAM neural networks with fractional-order derivatives. *Complexity*, 21, 412–426. <https://doi.org/10.1002/cplx.v21.S2>
- Ratnavelu, K., Manikandan, M., & Balasubramaniam, P. (2017). Design of state estimator for BAM fuzzy cellular neural networks with leakage and unbounded distributed delays. *Information Sciences*, 398, 91–109. <https://doi.org/10.1016/j.ins.2017.02.056>
- Shafiya, M., Nagamani, G., & Dafik, D. (2022). Global synchronization of uncertain fractional-order BAM neural networks with time delay via improved fractional-order integral inequality. *Mathematics and Computers in Simulation*, 191, 168–186. <https://doi.org/10.1016/j.matcom.2021.08.001>
- Shanmugam, L., Mani, P., Rajan, R., & Joo, Y. H. (2020). Adaptive synchronization of reaction–diffusion neural networks and its application to secure communication. *IEEE Transactions on Cybernetics*, 50, 911–922. <https://doi.org/10.1109/TCYB.6221036>
- Shen, H., Huang, Z., Park, Z., & Wu, J. H. (2022). Non-fragile H_∞ synchronization of BAM inertial neural networks subject to persistent dwell-time switching regularity. *IEEE Transactions on Cybernetics*, 52, 6591–6602. <https://doi.org/10.1109/TCYB.2021.3119199>
- Song, X., Man, J., Song, S., Zhang, Y., & Ning, Z. (2020). Finite/fixed-time synchronization for Markovian complex-valued memristive neural networks with reaction–diffusion terms and its application. *Neurocomputing*, 414, 131–142. <https://doi.org/10.1016/j.neucom.2020.07.024>
- Stamov, G., Stamova, I., & Spirova, C. (2019). Reaction–diffusion impulsive fractional-order bidirectional neural networks with distributed delays: Mittag–Leffler stability along manifolds. *AIP Conference Proceedings*, 2172, Article 050002.
- Sun, B., Cao, Y., Guo, Z., Yan, Z., & Wen, S. (2020). Synchronization of discrete-time recurrent neural networks with time-varying delays via quantized sliding mode control. *Applied Mathematics and Computation*, 375, Article 125093. <https://doi.org/10.1016/j.amc.2020.125093>
- Syed Ali, M., Hymavathi, M., Rajchakit, G., Saroha, S., Palanisamy, L., & Hammachukiattikul, P. (2020). Synchronization of fractional-order fuzzy BAM neural networks with time-varying delays and reaction–diffusion terms. *IEEE Access*, 8, 186551–186571. <https://doi.org/10.1109/Access.6287639>
- Syed Ali, M., Narayanan, G., Shekher, V., Alsulami, H., & Saeed, T. (2020). Dynamic stability analysis of stochastic fractional-order memristor fuzzy BAM neural networks with delay and leakage terms. *Applied Mathematics and Computation*, 369, 124896. <https://doi.org/10.1016/j.amc.2019.124896>
- Thakur, G. K., Syed Ali, M., Priya, B., Gokulakrishnan, V., & Asma Kauser, S. (2022). Impulsive effects on stochastic bidirectional associative memory neural networks with reaction–diffusion and leakage delays. *International Journal of Computer Mathematics*, 99, 1669–1686. <https://doi.org/10.1080/00207160.2021.1999428>
- Udhayakumar, K., Rakkiyappan, R., Rihan, F. A., & Banerjee, S. (2022). Projective multi-synchronization of fractional-order complex-valued coupled multi-stable neural networks with impulsive control. *Neurocomputing*, 467, 392–405. <https://doi.org/10.1016/j.neucom.2021.10.003>
- Udhayakumar, K., Rihan, F. A., Rakkiyappan, R., & Cao, J. (2022). Fractional-order discontinuous systems with indefinite LKFs: An application to fractional-order neural networks with time delays. *Neural Networks*, 145, 319–330. <https://doi.org/10.1016/j.neunet.2021.10.027>
- Wang, C., Zhang, H., Stamova, I., & Cao, J. (2023). Global synchronization for BAM delayed reaction–diffusion neural networks with fractional partial differential operator. *Journal of the Franklin Institute*, 360, 635–656. <https://doi.org/10.1016/j.jfranklin.2022.08.038>
- Wang, C., Zhang, H., Ye, R., Zhang, W., & Zhang, H. (2023). Finite time passivity analysis for Caputo fractional BAM reaction–diffusion delayed neural networks. *Mathematics and Computers in Simulation*, 208, 424–443. <https://doi.org/10.1016/j.matcom.2023.01.042>
- Wang, J., Tian, Y., Hua, L., Shi, K., Zhong, S., & Wen, S. (2023). New results on finite-time synchronization control of chaotic memristor-based inertial neural networks with time-varying delays. *Mathematics*, 11, Article 684. <https://doi.org/10.3390/math11030684>
- Wang, L., Ding, X., & Li, M. (2018). Global asymptotic stability of a class of generalized BAM neural networks with reaction–diffusion terms and mixed time delays. *Neurocomputing*, 321, 251–265. <https://doi.org/10.1016/j.neucom.2018.09.016>
- Wang, Y., Cao, J., & Huang, C. (2022). Exploration of bifurcation for a fractional-order BAM neural network with $n+2$ neurons and mixed time delays. *Chaos, Solitons and Fractals*, 159, Article 112117. <https://doi.org/10.1016/j.chaos.2022.112117>
- Wang, Y., Cao, Y., Guo, Z., Huang, T., & Wen, S. (2020). Event-based sliding-mode synchronization of delayed memristive neural networks via continuous/periodic sampling algorithm. *Applied Mathematics and Computation*, 383, Article 125379. <https://doi.org/10.1016/j.amc.2020.125379>
- Wang, Z., Eisen, M., & Ribeiro, A. (2022). Learning decentralized wireless resource allocations with graph neural networks. *IEEE Transactions on Signal Processing*, 70, 1850–1863. <https://doi.org/10.1109/TSP.2022.3163626>
- Wu, A., Zeng, Z., & Song, X. (2016). Global Mittag–Leffler stabilization of fractional-order bidirectional associative memory neural networks. *Neurocomputing*, 177, 489–496. <https://doi.org/10.1016/j.neucom.2015.11.055>
- Xu, C., Liu, Z., Liao, M., Li, P., Xiao, Q., & Yuan, S. (2021). Fractional-order bidirectional associate memory (BAM) neural networks with multiple delays: The case of Hopf

- bifurcation. *Mathematics and Computers in Simulation*, 182, 471–494. <https://doi.org/10.1016/j.matcom.2020.11.023>
- Xu, Y., Sun, F., & Li, W. (2021). Exponential synchronization of fractional-order multilayer coupled neural networks with reaction–diffusion terms via intermittent control. *Neural Computing and Applications*, 33, 16019–16032. <https://doi.org/10.1007/s00521-021-06214-0>
- Yang, J., Li, H., Yang, J., Zhang, L., & Jiang, H. (2022). Quasi-synchronization and complete synchronization of fractional-order fuzzy BAM neural networks via nonlinear control. *Neural Processing Letters*, 54, 3303–3319. <https://doi.org/10.1007/s11063-022-10769-x>
- Yang, S., Jiang, H., Hu, C., & Yu, J. (2021). Synchronization for fractional-order reaction–diffusion competitive neural networks with leakage and discrete delays. *Neurocomputing*, 436, 47–57. <https://doi.org/10.1016/j.neucom.2021.01.009>
- Yang, Z., & Zhang, J. (2020). Global stabilization of fractional-order bidirectional associative memory neural networks with mixed time delays via adaptive feedback control. *International Journal of Computer Mathematics*, 97, 2074–2090. <https://doi.org/10.1080/00207160.2019.1677897>
- Zhang, R. J., Wang, L., & Wu, K. N. (2022). Finite-time boundary stabilization of fractional reaction–diffusion systems. *Mathematical Methods in the Applied Sciences*, 46, 4612–4627. <https://doi.org/10.1002/mma.v46.4>
- Zhang, Z., & Yang, Z. (2023). Asymptotic stability for quaternion-valued fuzzy BAM neural networks via integral inequality approach. *Chaos, Solitons and Fractals*, 169, Article 113227. <https://doi.org/10.1016/j.chaos.2023.113227>
- Zhou, Z., Zhang, Z., & Chen, M. (2022). Finite-time synchronization for fuzzy delayed neutral-type inertial BAM neural networks via the figure analysis approach. *International Journal of Fuzzy Systems*, 24, 229–246. <https://doi.org/10.1007/s40815-021-01132-8>

See discussions, stats, and author profiles for this publication at: <https://www.researchgate.net/publication/373183496>

Robust Adaptive Fractional Sliding-Mode Controller Design for Mittag-Leffler Synchronization of Fractional-Order PMSG-Based Wind Turbine System

Article in IEEE Transactions on Systems Man and Cybernetics Systems · December 2023

DOI: 10.1109/TSMC.2023.3296682

CITATIONS

0

READS

127

6 authors, including:



Govindasamy Narayanan
Kunsan National University

22 PUBLICATIONS 526 CITATIONS

SEE PROFILE



M. Syed Ali
Thiruvalluvar University

203 PUBLICATIONS 4,320 CITATIONS

SEE PROFILE



Young Hoon Joo
Kunsan National University

596 PUBLICATIONS 7,781 CITATIONS

SEE PROFILE



Bashir Ahmad
Université de Paris 1 Panthéon-Sorbonne

730 PUBLICATIONS 20,353 CITATIONS

SEE PROFILE

Robust Adaptive Fractional Sliding-Mode Controller Design for Mittag-Leffler Synchronization of Fractional-Order PMSG-Based Wind Turbine System

G. Narayanan, M. Syed Ali¹, Young Hoon Joo², R. Perumal, Bashir Ahmad, and Hamed Alsulami

Abstract—In this article, the Mittag-Leffler synchronization (MLS) problem of a fractional-order permanent magnet synchronous generator (FOPMSG)-based wind turbine system against unknown disturbances, such as external load torque variations and system parameter uncertainties, an adaptive fractional sliding-mode control (AFSMC) method is proposed based on improved convergence rate performance of the FOPMSG to track accuracy, response speed, and robustness. The AFSMC method is based on a fractional-order term incorporated into the new law for reaching the sliding mode, improves the chattering in the control signal, and reduces the time required for the system to reach the sliding-mode surface. Sufficient conditions are derived to ensure the robust MLS for the sliding-mode dynamics by the designed robust controller. In this article, for the first time, an adaptive sliding-mode control (ASMC) with a terminal function that accurately controls the FOPMSG model at a prespecified time is proposed. Moreover, the designed ASMC can effectively attenuate the existence of disturbances and uncertainties by eliminating the reaching phase based on the Lyapunov stability theory. Finally, the simulation results applied to the FOPMSG model show that the proposed control method has better disturbance rejection ability, fast dynamic response, and suppression of the chattering effect.

Index Terms—Adaptive sliding-mode control (ASMC), fractional-order, Mittag-Leffler synchronization (MLS), permanent magnet synchronous generator (PMSG).

Manuscript received 5 November 2022; revised 25 March 2023 and 31 May 2023; accepted 1 July 2023. This work was supported by the Deanship of Scientific Research (DSR) at King Abdulaziz University, Jeddah, Saudi Arabia, under Grant FP-134-43. This article was recommended by Associate Editor Q. Yang. (Corresponding author: R. Perumal.)

G. Narayanan is with the School of IT Information and Control Engineering, Kunsan National University, Gunsan 54150, Jeonbuk, Republic of Korea, and also with the Center for Nonlinear Systems, Chennai Institute of Technology, Chennai 600069, India (e-mail: narayanantvu@gmail.com).

M. Syed Ali is with the Department of Mathematics, Thiruvalluvar University, Vellore 632115, India (e-mail: syedgru@gmail.com).

Young Hoon Joo is with the School of IT Information and Control Engineering, Kunsan National University, Gunsan 54150, Jeonbuk, Republic of Korea (e-mail: yhjoo@kunsan.ac.kr).

R. Perumal is with the Department of Mathematics, Faculty of Engineering and Technology, SRM Institute of Science and Technology, Chennai 603203, India (e-mail: perumalr@srmist.edu.in).

Bashir Ahmad and Hamed Alsulami are with the Department of Mathematics, King Abdulaziz University, Jeddah 21589, Saudi Arabia (e-mail: bahmad@kau.edu.sa; hhaalsalmi@kau.edu.sa).

Color versions of one or more figures in this article are available at <https://doi.org/10.1109/TSMC.2023.3296682>.

Digital Object Identifier 10.1109/TSMC.2023.3296682

I. INTRODUCTION

THE GENERATION of electricity from renewable energy sources, including solar and wind power, has become increasingly popular in recent years because of environmental concerns. Wind energy plays an important role in current and future electricity generation strategies because of its environmentally friendly nature and lower impact on the environment. Many studies focus on improving the wind turbine system (WTS) by stabilizing the power, controlling the trajectories, and observing the point of maximum power during stochastic natural reflections. WTSs that generate electricity can use a variety of generators, including the permanent magnet synchronous generator (PMSG), the doubly salient electromagnetic generator, the doubly fed induction generator, and others. The main advantage of using a PMSG instead of a doubly fed induction generator in WTS is the high power-to-weight ratio, low maintenance, and elimination of dc excitation [1]. There are also two types of WTS models: 1) fixed-speed WTS and 2) variable-speed WTS, where variable-speed WTS is far more effective than WTS with fixed speed, which has been recognized as an important area of research. For example, Shanmugam and Joo [2] studied a generalized model of power system dynamics that reflects the characteristics of all forms of variable-speed WTS, as well as their simulations. In addition, it has been widely used by researchers to verify their wind power generation technologies, a specific simulation and field testing has been planned and procedure is carried out on the concerned variable-speed WTS in various platforms that include MATLAB control toolbox [3], Garrad Hassan's Bladed [4], and FAST code [5]. Given its potential to operate in a gearless excitation system, direct-drive variable-speed WTS-based on PMSG is a particularly attractive topic (see [6], [7], [8]). Although fractional-order calculus provides a powerful and effective tool for describing the inheritance and unlimited memory properties of various substances it is evident from previous studies that PMSG-based WTS are integer-order PMSG model, which requires further investigation. The objective of this study is to establish the PMSG-based WTS for fractional-order area instead of the traditional control systems. The key principle behind the fractional domain is to increase the stability domain, i.e., the stability of the WTS [9]. Therefore, the main aim of this

research is to investigate the dynamic behavior of PMSG-based WTS using a fractional domain control technique.

Real dynamic object and process models of fractional order have applications in various scientific and engineering fields [10], [11], [12]. Nowadays, the dynamical systems of synchronization of chaotic fractional differential systems are challenging because of potential applications, such as secure communication, information theory, etc. Fractional-order calculus provides more reliable system models than integral calculus and has been recently proposed for synchronization control systems for chaotic fractional-order systems (see [13]). In addition, various practical systems, such as dc-dc converters [14], electrical circuits [15], and permanent magnet synchronous motors (PMSMs) [16], can be elegantly represented and accurately modeled using fractional calculus. Recently, many types of fractional-order synchronization results have been obtained, which include integrated synchronization [17], quasi-synchronization [18], and Mittag-Leffler synchronization (MLS) [19]. Li et al. [20] proposed to use MLS and the direct fractional Lyapunov technique to extend the application of fractional calculus to nonlinear systems in order to improve the study of both systems theory and fractional calculus. MLS extends the concept of exponential synchronization to nonlinear fractional-order systems [21]. To the best of our knowledge, MLS results have not yet been studied for PMSG-based WTS with the Caputo fractional operator, which provides the motivation for the current study.

Control theory provides a better foundation for understanding WTS and for subsequent improvements to maximize performance while minimizing leakage. With the rapid advances in modern control theory, various studies have contributed to the improvement of nonlinear control methods for the integer-order case of PMSG model, for example, predictive control [22], sliding-mode control (SMC) [23], adaptive control [24], and among these approaches, the SMC guarantees better control performance. Considering the superior performance in dealing with uncertainties/disturbances, extensive research has been conducted on SMC for various types of systems, including stochastic systems [25], uncertain systems [26], and fuzzy systems [27]. SMC has several practical properties, including fast reflexes, ease of implementation, robustness to system uncertainties, and low sensitivity to external disturbances [28]. In [29], adaptive control strategies were developed to solve robust fixed-time synchronization problems in the presence of unknown parameters. Khanzadeh and Pourgholi [30] and Pourgholi and Khanzadeh [31] studied adaptive SMC (ASMC) for synchronization of fractional-order chaotic systems, which is completely robust to uncertainties and disturbances by eliminating the reaching phase. Fractional-order control has recently emerged as a new control approach in which the order of the controlled object is part of a fractional domain. The fractional-order operator, unlike the rational transfer function of integer order, has infinite memory and takes into account the entire history of incoming signals, which greatly reduces the chattering phenomena of traditional SMC. The fusion of fractional control and SMC has been studied for a variety of topics [14], which makes the controlled system more accurate. Xiong et al. [32] discussed a fractional-order SMC approach for grid-connected DFIGs,

which are a key component in WTS. The adaptive fractional SMC (AFSMC) was recently used to study the stabilization of PMSM-based WTS in two different situations: with and without a smooth air gap [9]. However, the development of the AFSMC for PMSG-based WTS against external load torque variations and system parameter uncertainties still require much attention from researchers, which is the main objective of this study. So far, the AFSMC design of a nonlinear fractional-order PMSG (FOPMSG)-based WTS based on the fractional domain memory using the MLS technique has not been studied in detail.

Motivated by the above observations, we investigate the robust controller scheme for the MLS problem of FOPMSG against unknown disturbances, such as external load torque variations and system parameter uncertainties. In this study, the application of fractional-calculus theory is a very important activity in practice to improve the AFSMC of FOPMSG, and also the AFSMC strategy is applied to an FOPMSG model in this study to improve system robustness against external load torque variations and system parameter uncertainties. The main contributions of this study are as follows.

- 1) An AFSMC scheme is proposed to improve the robustness of the dynamics of the FOPMSG-based WTS in the presence of disturbances and uncertainties, and a reaching law-based fractional sliding-mode surface is designed to achieve faster response and higher precision as well as lower chattering compared with the conventional SMC.
- 2) Most researchers have focused on local stability analysis of a PMSG-based WTS (see [6], [7], [8]). However, unlike the existing results [6], [7], [8], this study uses the MLS conditions for FOPMSG developed via the AFSMC scheme with exponential reaching Law.
- 3) Furthermore, we have extended our results to the robust prespecified time, which enables the synchronization of the FOPMSG model in the presence of uncertainties and disturbances, an ASMC scheme with terminal functions is proposed.
- 4) The obtained algebraic stability criteria have a simpler form than the LMI stability criteria presented in [6], [7], [8], [9], [16], and [23], which reduces the computational complexity.

Notations: We use the following notations in this article, ${}^C_0D_t^\beta$ stands for the Caputo fractional derivative; \Re represents the real number; \mathbb{C} represents the complex number; and \Re^m and \mathbb{C}^m represent the real and complex vector spaces of dimension m .

II. MODEL DESCRIPTION AND PRELIMINARIES

In this section, we present a mathematical model of the FOPMSG and some definitions and lemmas used in this article.

A. Fractional-Order Calculus

Definition 1 [9]: The fractional integral of a function $f(t)$ is given as

$${}^{RL}I_t^\beta f(t) = \frac{1}{\Gamma(\beta)} \int_0^t (t-\xi)^{\beta-1} f(\xi) d\xi \quad (1)$$

where $t \geq 0$, $\beta > 0$, and $\Gamma(\beta) = \int_0^\infty t^{\beta-1} e^{-t} dt$.

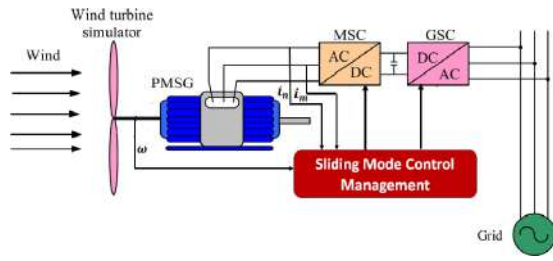


Fig. 1. Schematic of a PMSG-based generator side SMC system.

Definition 2 [9]: The Caputo fractional derivative of a function $f(t) \in \mathcal{C}^m([0, +\infty), \mathfrak{R}^m)$ is given as

$${}_0^C D_t^\beta f(t) = \frac{1}{\Gamma(m-\beta)} \int_0^t \frac{f^m(\zeta)}{(t-\zeta)^{\beta-m+1}} d\zeta \quad (2)$$

where $t \geq 0$, $\beta > 0$, and $0 < m-1 < \beta < m$.

Furthermore, if $0 < \beta < 1$ therefore

$${}_0^C D_t^\beta f(t) = \frac{1}{\Gamma(1-\beta)} \int_0^t \frac{f'(\zeta)}{(t-\zeta)^\beta} d\zeta. \quad (3)$$

Definition 3 [31]: The extension of the Beta functions, the incomplete Beta function, is described as follows:

$$B_x(p, q) = \int_0^x u^{p-1} (1-u)^{q-1} du, \quad \text{Re}(p) > 0 \\ \text{Re}(q) > 0, \quad 0 \leq x \leq 1. \quad (4)$$

B. PMSG-Based WTS

PMSG is usually used for small wind turbines that are freestanding because they have high performance and low maintenance. It consists of four components: 1) wind turbine; 2) PMSG; 3) converter; and 4) controller between them, as shown in Fig. 1. According to the energy conversion theory, the wind turbine converts the wind energy into mechanical energy, the PMSG converts the mechanical energy into electrical energy, and the converter feeds the electrical energy into the power grid [7]. The mathematical model of the three-phase symmetrical winding PMSG is based on an n - m reference frame and is constructed using Betz's aerodynamic theory and a coordinate transformation based on the mechanical torque equation. The analog circuit of PMSG under rated operating conditions is shown in Fig. 2. The mathematical model of fractional-order PMSG-based WTS in terms of m - n reference frame is as follows [8]:

$$\begin{cases} {}_0^C D_t^\beta \omega = \frac{\mathcal{P}}{\mathcal{J}} (\phi_f i_m + (\mathcal{L}_n - \mathcal{L}_m) i_n i_m) - \frac{f}{\mathcal{J}} \omega - \frac{\mathcal{T}_L}{\mathcal{J}} \\ {}_0^C D_t^\beta i_m = -\frac{\mathcal{R}_s}{\mathcal{L}_m} i_m + \frac{\mathcal{L}_n}{\mathcal{L}_m} \mathcal{P} \omega i_n - \mathcal{P} \frac{\phi_f}{\mathcal{L}_m} \omega + \frac{u_m}{\mathcal{L}_m} \\ {}_0^C D_t^\beta i_n = -\frac{\mathcal{R}_s}{\mathcal{L}_n} i_n + \frac{\mathcal{L}_m}{\mathcal{L}_n} \mathcal{P} \omega i_m + \frac{u_n}{\mathcal{L}_n} \end{cases} \quad (5)$$

where i_n , i_m and u_n , u_m denote the n - m axis currents and voltages, respectively; and ω denotes the rotor angular velocity of the generator and other parameters used in model as shown in Table I (as similar in [7]).

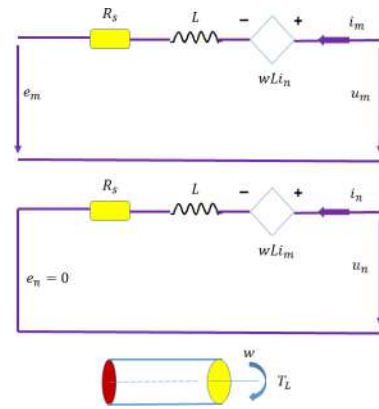


Fig. 2. Equivalent circuit of the PMSG.

 TABLE I
PARAMETERS OF PMSG MODEL [7]

Parameters	Description	Numerical Value
\mathcal{L}_n	n-axis stator inductance	3.34 mH
\mathcal{L}_m	m-axis stator inductance	3.58 mH
\mathcal{R}_s	Winding resistance	0.4578 Ω
\mathcal{P}	Generator pole pair	2
\mathcal{J}	Moment of inertia	50 kg.m ²
ϕ_f	Magnetic flux linkage	0.3 wb
f	Friction coefficient	0.0003035 N.m.rad ⁻¹ .s ⁻¹
\mathcal{R}	Turbine radius	14 m

The FOPMSG model (5) can be transformed into (6) using an affine transformation and a time scaling transform

$$\begin{cases} {}_0^C D_t^\beta \varpi = \alpha (\tilde{i}_m - \varpi) + \vartheta \tilde{i}_n \tilde{i}_m - \hat{\mathcal{T}} \\ {}_0^C D_t^\beta \tilde{i}_m = -\tilde{i}_m - \varpi \tilde{i}_n + \rho \varpi + \tilde{u}_m \\ {}_0^C D_t^\beta \tilde{i}_n = -\tilde{i}_n + \varpi \tilde{i}_m + \tilde{u}_n \end{cases} \quad (6)$$

where $\vartheta = ((\mathcal{L}_m - \mathcal{L}_n) \mathcal{P} b \mathcal{L}_m^2 \kappa^2) / (\mathcal{J} \mathcal{R}_s^2)$, $\alpha = (\mathcal{L}_m f / \mathcal{J} \mathcal{R}_s)$, $\rho = -(\phi_f / \kappa \mathcal{L}_m)$, $b = (\mathcal{L}_m / \mathcal{L}_n)$, $\kappa = (f \mathcal{R} / [\mathcal{L}_m \mathcal{P} \phi_f])$, $\tilde{i}_n = (\mathcal{L}_n \mathcal{P} \phi_f i_n / f \mathcal{R}_s)$, $\tilde{i}_m = (\mathcal{L}_m \mathcal{P} \phi_f i_m / f \mathcal{R}_s)$, $\varpi = (\mathcal{L}_m \omega / \mathcal{R}_s)$, $\tilde{u}_n = (u_n / \mathcal{R}_s \kappa)$, $\tilde{u}_m = (u_m / \mathcal{R}_s \kappa)$, and $\hat{\mathcal{T}} = (\mathcal{L}_m^2 \mathcal{T}_L / \mathcal{J} \mathcal{R}_s^2)$. The chaos phenomena of the FOPMSG model with nonsmooth air gap (6) have been fully studied in [8]. We choose the system parameters and initial conditions $\alpha = 5.45$, $\rho = 20$, and $(\varpi(0), \tilde{i}_n(0), \tilde{i}_m(0)) = (7, 2, -1)$, respectively. Fig. 3 shows the typical characteristic (chaotic motion) and the state responses for different differential orders (a) $\beta = 0.93$ and (b) $\beta = 1$ of the considered system (6) without control. The FOPMSG model may exhibit chaotic oscillations, which can seriously affect power quality and stability and even lead to the collapse of the win farm. The advantageous control methods eliminate the chaotic oscillations and ensure the stable operation of the FOPMSG model [8], [9]. The objective of this study is to develop an AFSMC in the fractional domain for the MLS problem of FOPMSG-based WTS.

C. Synchronizing of FOPMSG Control System

In the case of the smooth air gap, $\mathcal{L} = \mathcal{L}_m = \mathcal{L}_n$ and the external inputs vanish, i.e., $\tilde{u}_n = 0$, $\tilde{u}_m = 0$, and $\hat{\mathcal{T}} = 0$. Here, α and ρ are positive constants. We have $\varpi = \mathfrak{S}_1$, $\tilde{i}_m = \mathfrak{S}_2$,

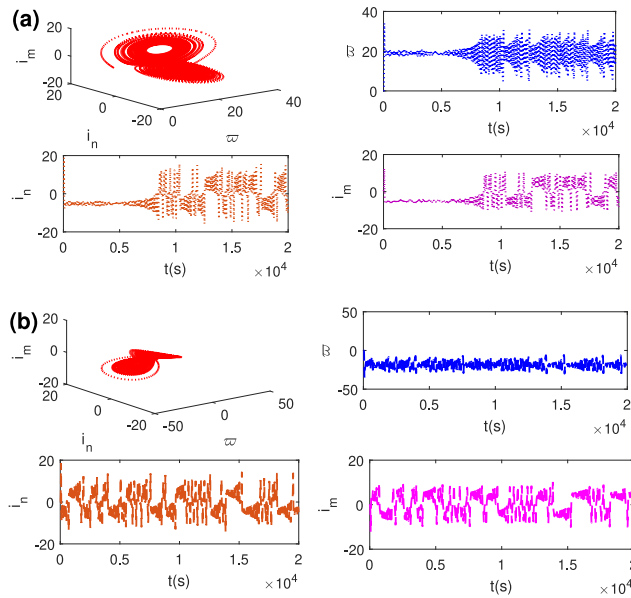


Fig. 3. Behavior of the FOPMSG (2) without control input for various differential-order values. (a) $\beta = 0.93$. (b) $\beta = 1$.

and $\tilde{i}_n = \tilde{\mathfrak{S}}_3$, the system (6) can be expressed as

$$\begin{cases} {}_0^C D_t^\beta \tilde{\mathfrak{S}}_1(t) = \alpha(\tilde{\mathfrak{S}}_2 - \tilde{\mathfrak{S}}_1) \\ {}_0^C D_t^\beta \tilde{\mathfrak{S}}_2(t) = -\tilde{\mathfrak{S}}_2 - \tilde{\mathfrak{S}}_1 \tilde{\mathfrak{S}}_3 + \rho \tilde{\mathfrak{S}}_1 \\ {}_0^C D_t^\beta \tilde{\mathfrak{S}}_3(t) = -\tilde{\mathfrak{S}}_3 + \tilde{\mathfrak{S}}_1 \tilde{\mathfrak{S}}_2. \end{cases} \quad (7)$$

By considering parametric uncertainties and external disturbances in the system (7), the following drive FOPMSG system is obtained as:

$$\begin{cases} {}_0^C D_t^\beta \tilde{\mathfrak{S}}_1(t) = \alpha(\tilde{\mathfrak{S}}_2 - \tilde{\mathfrak{S}}_1) \\ {}_0^C D_t^\beta \tilde{\mathfrak{S}}_2(t) = -\tilde{\mathfrak{S}}_2 - \tilde{\mathfrak{S}}_1 \tilde{\mathfrak{S}}_3 + (\rho + \Delta_i) \tilde{\mathfrak{S}}_1 + d_i \\ {}_0^C D_t^\beta \tilde{\mathfrak{S}}_3(t) = -\tilde{\mathfrak{S}}_3 + \tilde{\mathfrak{S}}_1 \tilde{\mathfrak{S}}_2 + d_\sigma. \end{cases} \quad (8)$$

The considered response FOPMSG system has the similar form of (8)

$$\begin{cases} {}_0^C D_t^\beta \hat{\tilde{\mathfrak{S}}}_1(t) = \alpha(\hat{\tilde{\mathfrak{S}}}_2 - \hat{\tilde{\mathfrak{S}}}_1) + u_i^{<\varphi>} \\ {}_0^C D_t^\beta \hat{\tilde{\mathfrak{S}}}_2(t) = -\hat{\tilde{\mathfrak{S}}}_2 - \hat{\tilde{\mathfrak{S}}}_1 \hat{\tilde{\mathfrak{S}}}_3 + (\rho + \Delta_\kappa) \hat{\tilde{\mathfrak{S}}}_1 \\ \quad + d_\kappa + u_i^{<\sigma>} \\ {}_0^C D_t^\beta \hat{\tilde{\mathfrak{S}}}_3(t) = -\hat{\tilde{\mathfrak{S}}}_3 + \hat{\tilde{\mathfrak{S}}}_1 \hat{\tilde{\mathfrak{S}}}_2 + d_\tau + u_i^{<\lambda>} \end{cases} \quad (9)$$

where $u_i^{<\varphi>}$, $u_i^{<\sigma>}$, $u_i^{<\lambda>}$ is the control function to be designed.

For $\varphi_1 = \hat{\tilde{\mathfrak{S}}}_1 - \tilde{\mathfrak{S}}_1$, $\varphi_2 = \hat{\tilde{\mathfrak{S}}}_2 - \tilde{\mathfrak{S}}_2$, and $\varphi_3 = \hat{\tilde{\mathfrak{S}}}_3 - \tilde{\mathfrak{S}}_3$, then the error dynamic system of the drive FOPMSG system (8) and response FOPMSG system (9) is obtained as follows:

$$\begin{cases} {}_0^C D_t^\beta \varphi_1(t) = \alpha(\varphi_2 - \varphi_1) + u_i^{<\varphi>} \\ {}_0^C D_t^\beta \varphi_2(t) = -\varphi_2 - (\hat{\tilde{\mathfrak{S}}}_1 \hat{\tilde{\mathfrak{S}}}_3 - \tilde{\mathfrak{S}}_1 \tilde{\mathfrak{S}}_3) + \rho \varphi_1 \\ \quad + (\Delta_\kappa \hat{\tilde{\mathfrak{S}}}_1 - \Delta_i \tilde{\mathfrak{S}}_1) + d_\kappa - d_i + u_i^{<\sigma>} \\ {}_0^C D_t^\beta \varphi_3(t) = -\varphi_3 + (\hat{\tilde{\mathfrak{S}}}_1 \hat{\tilde{\mathfrak{S}}}_2 - \tilde{\mathfrak{S}}_1 \tilde{\mathfrak{S}}_2) \\ \quad + d_\tau - d_\sigma + u_i^{<\lambda>}. \end{cases} \quad (10)$$

In accordance with the fact that

$$\begin{cases} \hat{\tilde{\mathfrak{S}}}_1 \hat{\tilde{\mathfrak{S}}}_3 - \tilde{\mathfrak{S}}_1 \tilde{\mathfrak{S}}_3 = -\varphi_1 \varphi_3 + \varphi_1 \hat{\tilde{\mathfrak{S}}}_3 + \varphi_3 \hat{\tilde{\mathfrak{S}}}_1 \\ \Delta_\kappa \hat{\tilde{\mathfrak{S}}}_1 - \Delta_i \tilde{\mathfrak{S}}_1 = (\Delta_\kappa - \Delta_i) \hat{\tilde{\mathfrak{S}}}_1 + \Delta_i \varphi_1 \\ \hat{\tilde{\mathfrak{S}}}_1 \hat{\tilde{\mathfrak{S}}}_2 - \tilde{\mathfrak{S}}_1 \tilde{\mathfrak{S}}_2 = -\varphi_1 \varphi_2 + \varphi_1 \hat{\tilde{\mathfrak{S}}}_2 + \varphi_2 \hat{\tilde{\mathfrak{S}}}_1. \end{cases} \quad (11)$$

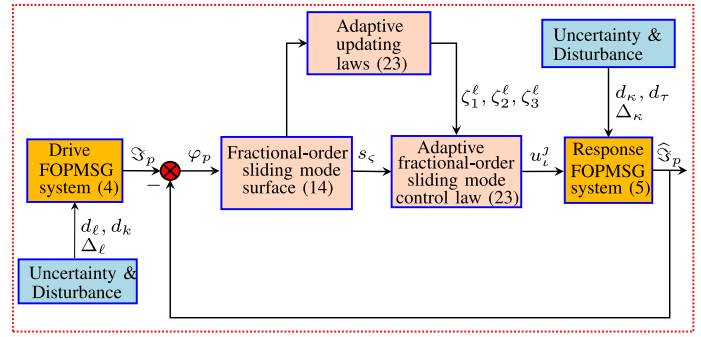


Fig. 4. Block diagram of the proposed AFSMC scheme, where $p = 1, 2, 3$; $\varsigma = 1, 2, 3$, and $J = \langle \varphi \rangle, \langle \sigma \rangle, \langle \lambda \rangle$.

System (10) can be rewritten as

$$\begin{cases} {}_0^C D_t^\beta \varphi_1(t) = \alpha(\varphi_2 - \varphi_1) + u_i^{<\varphi>} \\ {}_0^C D_t^\beta \varphi_2(t) = -\varphi_2 - (\varphi_1 \hat{\tilde{\mathfrak{S}}}_3 + \varphi_3 \hat{\tilde{\mathfrak{S}}}_1 - \varphi_1 \varphi_3) + \rho \varphi_1 \\ \quad + (\Delta_\kappa - \Delta_i) \hat{\tilde{\mathfrak{S}}}_1 + \Delta_i \varphi_1 + d_\kappa - d_i + u_i^{<\sigma>} \\ {}_0^C D_t^\beta \varphi_3(t) = -\varphi_3 + \varphi_1 \hat{\tilde{\mathfrak{S}}}_2 + \varphi_2 \hat{\tilde{\mathfrak{S}}}_1 - \varphi_1 \varphi_2 \\ \quad + d_\tau - d_\sigma + u_i^{<\lambda>}. \end{cases} \quad (12)$$

Assumption 1: The external disturbance d_i , d_κ , d_σ , d_τ , and uncertainties Δ_i , Δ_κ are bounded, i.e., there exist non-negative constants, respectively, ξ^{d_i} , ξ^{d_κ} , ξ^{d_σ} , ξ^{d_τ} , and ξ^{Δ_i} , ξ^{Δ_κ} such as $|d_i| \leq \xi^{d_i}$, $|d_\kappa| \leq \xi^{d_\kappa}$, $|d_\sigma| \leq \xi^{d_\sigma}$, $|d_\tau| \leq \xi^{d_\tau}$, $|\Delta_i| \leq \xi^{\Delta_i}$, $|\Delta_\kappa| \leq \xi^{\Delta_\kappa}$.

Definition 4 [119]: The drive FOPMSG system (8) will achieve MLS on the response FOPMSG system (9) under the proposed controller when $\|\varphi(t)\| \leq \mathcal{M}(\vartheta(t)) t^{-\theta} \mathbb{E}_{\theta, \hat{\sigma}}(-\hat{\eta}t)$ in which $0 < \theta, \hat{\sigma} \leq 1$, $\vartheta(0) = 0$, and $\mathcal{M}(\vartheta(t)) \geq 0$. Here, $\mathcal{M}(\vartheta(t))$ is locally Lipschitz on $\vartheta \in \mathfrak{R}^n$ with Lipschitz constant \mathcal{M}_0 .

Lemma 1 [31]: If $f(t) \in \mathcal{C}^1[0, T]$ for some $T > 0$, then ${}_0^C D_t^\theta ({}_0^C D_t^{\hat{\sigma}} f(t)) = {}_0^C D_t^{\theta + \hat{\sigma}} f(t)$, $t \in [0, T]$, where $\theta, \hat{\sigma} \in \mathfrak{R}^+$ and $\theta + \hat{\sigma} \leq 1$.

Lemma 2 [30]: If $g(t) \in \mathcal{C}^1([0, +\infty), \mathfrak{R})$, then for any $\hat{\sigma} \in (0, 1)$, ${}_0^C D_t^{\hat{\sigma}} |g(t)| \leq \text{sign}(g(t)) {}_0^C D_t^{\hat{\sigma}} \text{sign}(g(t))$.

III. MAIN RESULTS

In this section, we study the robust controller design for the MLS problem of the FOPMSG model using different control strategies.

A. MLS via Fractional Sliding-Mode Control

The main superiority of FSMC is its robustness in overcoming uncertainties and external disturbances of the system. In Fig. 4, the block diagram of the proposed control schemes is shown schematically for the convenience of the readers.

Define a fractional sliding surface as

$$s_\varsigma(t) = {}_0^C D_t^{\beta-1} \varphi_\varsigma(t), \quad \varsigma = 1, 2, 3. \quad (13)$$

The FSMC scheme is designed in this section to provide the MLS of the drive FOPMSG system (8) and the response FOPMSG system (9).

Theorem 1: Given constant $\mu > 0$, control gains $\gamma_\theta > 0$, $\gamma_\tau > 0$, and $\gamma_\varsigma > 0$, considering the dynamics of drive and

response FOPMSG system are modeled by Caputo fractional derivative. Robust MLS between (8) and (9) can be achieved, if $\Psi_{\min} < 0$ and the control law is chosen as

$$\begin{cases} u_i^{<\varphi>} = \alpha\varphi_1 - (\alpha\varphi_2 + \gamma_\theta s_1), \\ u_i^{<\sigma>} = \varphi_2 + (\varphi_1 \widehat{s}_3 + \varphi_3 \widehat{s}_1 - \varphi_1 \varphi_3) \\ \quad - \rho\varphi_1 - ((\xi^{\Delta_k} + \xi^{\Delta_i})|\widehat{s}_1| + \xi^{\Delta_i}|\varphi_1| \\ \quad + \xi^{d_k} + \xi^{d_i} + \gamma_\tau s_2), \\ u_i^{<\lambda>} = \varphi_3 - \varphi_1 \widehat{s}_2 - \varphi_2 \widehat{s}_1 + \varphi_1 \varphi_2 \\ \quad - (\xi^{d_\sigma} + \xi^{d_\tau} + \gamma_\varsigma s_3) \end{cases} \quad (14)$$

where $\Psi_{\min} = \min_{1 \leq \varsigma \leq 3} \{\psi_\varsigma^\delta\}$, $\psi_1^\delta = \mu - 2\gamma_\theta$, $\psi_2^\delta = \mu - 2\gamma_\tau$, and $\psi_3^\delta = \mu - 2\gamma_\varsigma$.

Proof: Consider the Lyapunov function

$$\mathcal{V}(t) = \sum_{\varsigma=1}^3 \widehat{\mathcal{V}}_\varsigma(t) = \sum_{\varsigma=1}^3 e^{\mu t} s_\varsigma^T(t) s_\varsigma(t) \quad (15)$$

where $\widehat{\mathcal{V}}_1(t) = e^{\mu t} s_1^T(t) s_1(t)$, $\widehat{\mathcal{V}}_2(t) = e^{\mu t} s_2^T(t) s_2(t)$, $\widehat{\mathcal{V}}_3(t) = e^{\mu t} s_3^T(t) s_3(t)$. The time derivative of $\widehat{\mathcal{V}}_1$ can be calculated using Lemma 1 and gives that

$$\frac{d\widehat{\mathcal{V}}_1}{dt} = e^{\mu t} (\mu s_1^T(t) s_1(t) + 2s_1^T(t) D^\beta \varphi_1(t)) \leq \psi_1^\delta \widehat{\mathcal{V}}_1(t). \quad (16)$$

Based on Assumption 1, we then obtain

$$\frac{d\widehat{\mathcal{V}}_2}{dt} \leq (\mu - 2\gamma_\tau) e^{\mu t} s_2^T s_2 \leq \psi_2^\delta \widehat{\mathcal{V}}_2(t) \quad (17)$$

$$\frac{d\widehat{\mathcal{V}}_3}{dt} \leq (\mu - 2\gamma_\varsigma) e^{\mu t} s_3^T s_3 \leq \psi_3^\delta \widehat{\mathcal{V}}_3(t). \quad (18)$$

From (15)–(18), $\dot{\mathcal{V}}(t) \leq \min_{1 \leq \varsigma \leq 3} \{\psi_\varsigma^\delta\} \mathcal{V}(t) \leq \Psi_{\min} \mathcal{V}(t)$. Therefore, $\mathcal{V}(t) \leq \Psi_{\min} \mathcal{V}(0)$, $t \geq 0$, which implies that $e^{\mu t} \|s(t)\|^2 \leq \Psi_{\min} \mathcal{V}(0)$. That is, $\|s(t)\| \leq (\Psi_{\min} \mathcal{V}(0))^{(1/2)} e^{-(\mu t/2)}$. Combining (13) with above, $\|{}_0^C D_t^{\beta-1} \varphi(t)\| \leq \chi_\epsilon e^{-(\mu t/2)}$, where $\chi_\epsilon = (\Psi_{\min} \mathcal{V}(0))^{(1/2)}$. By the ς element of the vector $\varphi(t)$, $-\chi_\epsilon e^{-(\mu t/2)} \leq {}_0^C D_t^{\beta-1} \varphi_\varsigma(t) \leq \chi_\epsilon e^{-(\mu t/2)}$. By the Laplace transformation of both sides, we get $(-\chi_\epsilon/s + \frac{\mu}{2}) \leq s^{\beta-1} \varphi_\varsigma(s) \leq (\chi_\epsilon/s + [\mu/2])$. Consequently, based on Laplace inverse transformation, we have the following inequality, that is, $|\varphi_\varsigma| \leq (\chi_\epsilon/t^{1-\beta}) \mathbb{E}_{1,\beta}(-[\mu t/2])$. So one concludes that $\|\varphi(t)\| \leq [\mathcal{M}(\vartheta)/t^{1-\beta}] \mathbb{E}_{1,\beta}(-\mu t/2)$, where $\mathcal{M}(\vartheta) = \chi_\epsilon \sqrt{3} = (\Psi_{\min} \mathcal{V}(0))^{(1/2)} \sqrt{3}$. Thus, the sliding-mode surface $s(t)$ and error trajectory $\varphi(t)$ converge exponentially to zero. According to Definition 4, the MLS between FOPMSG system (8) and (9) is achieved by using three robust controllers (14), i.e., $u_i^{<\varphi>}$, $u_i^{<\sigma>}$, and $u_i^{<\lambda>}$.

Remark 1: In [6], the observer-based impulsive control scheme was studied based on chaotic behavior without smooth air gap in PMSG-based WTS. In [7], the suppression of chaotic behavior of predictive control problem of PMSG-based WTS with local stability analysis was studied. In these studies, the MLS approach was not used for uncertainties and external disturbances of PMSG-based WTS over FSMC. Therefore, in this study, the fractional domain memory of FSMC is developed for PMSG-based WTS with uncertainties and external disturbances. Therefore, the development of the FSMC approach based on the fractional domain memory is beneficial from both theoretical and practical perspectives when compared with previous studies [6], [7].

B. Adaptive Sliding-Mode Controller Design

We consider the MLS problem of system (8) and (9) using the AFSMC method. Motivated by, Kao et al. [19] theoretically designed the adaptive control with MLS criteria for fractional-order system and proved its effectiveness. The adaptive control strategies designed (19) differ from existing adaptive control strategies for PMSG-based WTS (see [9], [23], [24]), there are no reports on the MLS problem of FOPMSG-based WTS using AFSMC. Therefore, we investigated AFSMC strategies with MLS to distinguish the system (8) between system (9) in this section.

We design an adaptive controller as follows:

$$\begin{cases} \dot{\zeta}_1^\ell(t) = 2e^{\mu t} \|s_1\|^2 - \eta_\theta (\zeta_1^\ell(t) - \varrho_1^\kappa) \\ \dot{\zeta}_2^\ell(t) = 2e^{\mu t} \|s_2\|^2 - \eta_i (\zeta_2^\ell(t) - \varrho_2^\kappa) \\ \dot{\zeta}_3^\ell(t) = 2e^{\mu t} \|s_3\|^2 - \eta_\kappa (\zeta_3^\ell(t) - \varrho_3^\kappa) \end{cases} \quad (19)$$

where $\zeta_\varsigma^\ell(t)$ are tunable functions; ϱ_ς^κ are tunable constants; and η_θ , η_i , and η_κ are control gains.

Theorem 2: Given constant $\mu > 0$, control gains $\eta_\theta > 0$, $\eta_i > 0$, and $\eta_\kappa > 0$. The robust MLS between drive FOPMSG system (8) and response FOPMSG system (9) can be achieved, if $\Psi_{\min}^{<\delta>} < 0$, for the adaptive law (19) and the designed control law

$$\begin{cases} u_i^{<\varphi>} = \alpha\varphi_1 - \alpha\varphi_2 - \zeta_1^\ell s_1 \\ u_i^{<\sigma>} = \varphi_2 + (\varphi_1 \widehat{s}_3 + \varphi_3 \widehat{s}_1 - \varphi_1 \varphi_3) - \rho\varphi_1 \\ \quad - ((\xi^{\Delta_k} + \xi^{\Delta_i})|\widehat{s}_1| \\ \quad + \xi^{\Delta_i}|\varphi_1| + (\xi^{d_k} + \xi^{d_i}) - \zeta_2^\ell s_2) \\ u_i^{<\lambda>} = \varphi_3 - \varphi_1 \widehat{s}_2 - \varphi_2 \widehat{s}_1 + \varphi_1 \varphi_2 \\ \quad - (\xi^{d_\sigma} + \xi^{d_\tau} + \zeta_3^\ell s_3) \end{cases} \quad (20)$$

where $\Psi_{\min}^{<\delta>} = \min_{1 \leq \varsigma \leq 3} \{\Phi_\varsigma^{<\delta>}\}$, $\Phi_1^{<\delta>} = \min\{(\mu - 2\varrho_1^\kappa), 2\eta_\theta\}$, $\Phi_2^{<\delta>} = \min\{(\mu - 2\varrho_2^\kappa), 2\eta_i\}$, $\Phi_3^{<\delta>} = \min\{(\mu - 2\varrho_3^\kappa), 2\eta_\kappa\}$.

Proof: Consider the Lyapunov function as follows: $\mathcal{V}(t) = \sum_{\varsigma=1}^3 \widehat{\mathcal{V}}_\varsigma(t)$, where $\widehat{\mathcal{V}}_1(t) = e^{\mu t} s_1^T(t) s_1(t) + (1/2)(\zeta_1^\ell(t) - \varrho_1^\kappa)^2$, $\widehat{\mathcal{V}}_2(t) = e^{\mu t} s_2^T(t) s_2(t) + (1/2)(\zeta_2^\ell(t) - \varrho_2^\kappa)^2$, $\widehat{\mathcal{V}}_3(t) = e^{\mu t} s_3^T(t) s_3(t) + (1/2)(\zeta_3^\ell(t) - \varrho_3^\kappa)^2$. Time derivative $\dot{\mathcal{V}}$ can be calculated by

$$\frac{d\widehat{\mathcal{V}}_1}{dt} \leq \Phi_1^{<\delta>} \widehat{\mathcal{V}}_1(t), \quad \frac{d\widehat{\mathcal{V}}_2}{dt} \leq \Phi_2^{<\delta>} \widehat{\mathcal{V}}_2(t), \quad \frac{d\widehat{\mathcal{V}}_3}{dt} \leq \Phi_3^{<\delta>} \widehat{\mathcal{V}}_3(t). \quad (21)$$

From (21), we get $\dot{\mathcal{V}}(t) \leq \min_{1 \leq \varsigma \leq 3} \{\Phi_\varsigma^{<\delta>}\} \mathcal{V}(t) \leq \Psi_{\min}^{<\delta>} \mathcal{V}(t)$. Therefore, $\mathcal{V}(t) \leq \Psi_{\min}^{<\delta>} \mathcal{V}(0)$, $t \geq 0$. It means that $\sum_{\varsigma=1}^3 e^{\mu t} s_\varsigma^T(t) s_\varsigma(t) \leq \sum_{\varsigma=1}^3 [e^{\mu t} s_\varsigma^T(t) s_\varsigma(t) + (1/2)(\zeta_\varsigma^\ell(t) - \varrho_\varsigma^\kappa)^2] \leq \Psi_{\min}^{<\delta>} \mathcal{V}(0)$, $t \geq 0$, that is

$$e^{\mu t} \|s(t)\|^2 \leq \Psi_{\min}^{<\delta>} \sum_{\varsigma=1}^3 \left(s_\varsigma^T(0) s_\varsigma(0) + \frac{1}{2} (\zeta_\varsigma^\ell(0) - \varrho_\varsigma^\kappa)^2 \right). \quad (22)$$

In view of $\zeta_\varsigma^\ell(0) - \varrho_\varsigma^\kappa$ is finite, it is clear that there exists a positive constant \mathcal{M}_i leading to $\sum_{\varsigma=1}^3 (s_\varsigma^T(0) s_\varsigma(0) + (1/2)$

$(\zeta_\varepsilon^\ell(0) - \varrho_\varepsilon^k)^2 \leq \mathcal{M}_t$. From (22), we obtained the following:

$$\|s(t)\| \leq (\Psi_{\min}^{<\delta>} \mathcal{M}_t)^{\frac{1}{2}} e^{-\frac{\mu t}{2}}. \quad (23)$$

Combining (13) and (23), we have $\|{}_0^C D_t^{\beta-1} \varphi(t)\| \leq \widehat{\chi}_\delta e^{-(\mu t/2)}$, where $\widehat{\chi}_\delta = (\Psi_{\min}^{<\delta>} \mathcal{M}_t)^{(1/2)}$. It follows that Theorem 1:

$$\|\varphi(t)\| \leq \frac{\mathcal{M}(\widehat{\vartheta})}{t^{1-\beta}} \mathbb{E}_{1,\beta} \left(-\frac{\mu t}{2} \right) \quad (24)$$

where $\mathcal{M}(\widehat{\vartheta}) = \widehat{\chi}_\delta \sqrt{3}$. From (23), it follows that the sliding-mode surface $s(t)$ converges exponentially to zero. According to Definition 4, it follows from (24) that the error system (3) will be MLS under the proposed adaptive laws (19) and the robust control laws (20).

Remark 2: Some pioneering studies have focused on investigating the local stability control problem for FOPMSG-based WTS. In particular, Karthikeyan et al. [8] studied the dynamic properties of a variable-speed and current-dependent control for FOPMSG-based WTS via Lyapunov exponents, bicoherence, bifurcation, and the equilibrium points. The predictive controller for suppressing chaos in an FOPMSG-based WTS and its nonlinear dynamical behavior from Hopf bifurcation to local stability analysis are discussed in [7]. Unlike previous studies, the MLS criterion analyzed in this study is more practical than those proposed by [7] and [8], because this study discusses the AFSMC for FOPMSG-based WTS, which investigates the characteristics of the unique industrial challenge. Moreover, the results of robust controller design of MLS for FOPMSG have not been seen yet, so Theorems 1 and 2 are new. In this study, not only MLS criteria studies are conducted but also a fractional domain memory-based AFSMC is improved to achieve the MLS conditions in FOPMSG-based WTS, which are susceptible to nonlinear disturbances to external perturbations.

C. Design of Terminal Functions

Following [30], in this article, a novel switching surfaces is defined as

$$s_\varsigma(t) = \varphi_\varsigma(t) - \widehat{h}_\varsigma(t), \quad \varsigma = 1, 2, 3 \quad (25)$$

where $\widehat{h}_\varsigma(t)$ are known as terminal functions. It is expected that we can develop a controller that enforcing the synchronization error to completely follow the terminal function. Thus, complete robustness is achieved provided that

$$\widehat{h}_\varsigma(t_0) = \varphi_\varsigma(t_0) \quad (26)$$

where t_0 is the initial time. Synchronization is achieved at a predetermined time when $\widehat{h}_\varsigma(\mathbb{T}) = 0$, where \mathbb{T} is the synchronization time. For $t > \mathbb{T}$, the terminal functions must be zero, and it is assumed without loss of generality that $t_0 = 0$. We choose the specific information of the terminal functions $\widehat{h}_\varsigma(t)$ ($\varsigma = 1, 2, 3$) as follows:

$$\widehat{h}_\varsigma(t) = \begin{cases} -\frac{\varphi_\varsigma(0)}{\mathbb{T}^2} (t - \mathbb{T})^2, & t \leq \mathbb{T} \\ 0, & t \geq \mathbb{T}. \end{cases} \quad (27)$$

It is clear that the terminal function (27) satisfies two conditions (25) and (26).

Assumption 2 [31]: The uncertainties Δ_l , Δ_κ , and external disturbances d_l , d_κ , d_σ , d_τ are bounded, i.e., there exist positive constants λ^{Δ_l} , λ^{Δ_κ} , λ^{d_l} , λ^{d_κ} , λ^{d_σ} , λ^{d_τ}

$$\begin{aligned} |{}_0^C D_t^{1-\beta}(\Delta_l)| &\leq \lambda^{\Delta_l}, |{}_0^C D_t^{1-\beta}(\Delta_\kappa)| \leq \lambda^{\Delta_\kappa} \\ |{}_0^C D_t^{1-\beta}(d_l)| &\leq \lambda^{d_l}, |{}_0^C D_t^{1-\beta}(d_\kappa)| \leq \lambda^{d_\kappa} \\ |{}_0^C D_t^{1-\beta}(d_\sigma)| &\leq \lambda^{d_\sigma}, |{}_0^C D_t^{1-\beta}(d_\tau)| \leq \lambda^{d_\tau}. \end{aligned} \quad (28)$$

Theorem 3: Given constant $\widehat{\mu} > 0$, control gains $\psi_\theta > 0$, $\psi_\tau > 0$ and $\psi_\kappa > 0$. The drive FOPMSG system (8) and response FOPMSG system (9) can be achieved MLS at a prespecified time \mathbb{T} for the designed control law

$$\begin{cases} u_i^{<\varphi>} = \alpha\varphi_1 - \alpha\varphi_2 + {}_0^C D_t^\beta \widehat{h}_1 \\ \quad - {}_0^{RL} D_t^{-(1-\beta)} (\psi_\theta s_1) \\ u_i^{<\sigma>} = \varphi_2 + (\varphi_1 \widehat{\mathfrak{S}}_3 + \varphi_3 \widehat{\mathfrak{S}}_1 - \varphi_1 \varphi_3) - \rho\varphi_1 + {}_0^C D_t^\beta \widehat{h}_2 \\ \quad - {}_0^{RL} D_t^{-(1-\beta)} ((\lambda^{\Delta_\kappa} + \lambda^{\Delta_l}) |\widehat{\mathfrak{S}}_1| \\ \quad + \lambda^{\Delta_l} |\varphi_1| + \lambda^{d_\kappa} + \lambda^{d_l} + \psi_\tau s_2) \\ u_i^{<\lambda>} = \varphi_3 - \varphi_1 \widehat{\mathfrak{S}}_2 - \varphi_2 \widehat{\mathfrak{S}}_1 + \varphi_1 \varphi_2 + {}_0^C D_t^\beta \widehat{h}_3 \\ \quad - {}_0^{RL} D_t^{-(1-\beta)} (\lambda^{d_\sigma} + \lambda^{d_\tau} + \psi_\varsigma s_3) \end{cases} \quad (29)$$

if the following conditions hold: 1) $\|\varphi\| \leq \|\varphi - \widehat{h}\|$ and 2) $\Upsilon_{\min}^{<\delta>} < 0$, where $\Upsilon_{\min}^{<\delta>} = \min_{1 \leq \varsigma \leq 3} \{\Upsilon_\varsigma^{<\delta>}\}$, $\Upsilon_1^{<\delta>} = \{\widehat{\mu} - 2\psi_\theta\}$, $\Upsilon_2^{<\delta>} = \{\widehat{\mu} - 2\psi_\tau\}$, and $\Upsilon_3^{<\delta>} = \{\widehat{\mu} - 2\psi_\varsigma\}$.

Proof: Select the Lyapunov function as

$$\mathcal{V}(t) = \sum_{\varsigma=1}^3 \widehat{\mathcal{V}}_\varsigma(t) = \sum_{\varsigma=1}^3 e^{\widehat{\mu}t} s_\varsigma^T(t) s_\varsigma(t). \quad (30)$$

Then, by calculating the time derivative of $\widehat{\mathcal{V}}_1$, $\widehat{\mathcal{V}}_2$, $\widehat{\mathcal{V}}_3$ and applying Lemma 1, we obtain

$$\frac{d\widehat{\mathcal{V}}_1}{dt} = e^{\widehat{\mu}t} (\widehat{\mu} s_1^T s_1 - 2\psi_\theta s_1^T s_1) \leq (\widehat{\mu} - 2\psi_\theta) \widehat{\mathcal{V}}_1(t). \quad (31)$$

Based on Assumption 2, one has

$$\frac{d\widehat{\mathcal{V}}_2}{dt} \leq e^{\widehat{\mu}t} (\widehat{\mu} s_2^T s_2 - 2\psi_\tau s_2^T s_2) \leq (\widehat{\mu} - 2\psi_\tau) \widehat{\mathcal{V}}_2(t). \quad (32)$$

$$\frac{d\widehat{\mathcal{V}}_3}{dt} \leq (\widehat{\mu} - 2\psi_\varsigma) \widehat{\mathcal{V}}_3(t). \quad (33)$$

Adding (31)–(33), we can obtain $\dot{\mathcal{V}}(t) \leq \Upsilon_{\min}^{<\delta>} \mathcal{V}(t)$. According to Definition 4, the error system (12) is achieved the robust MLS under designed control laws (29).

Corollary 1: Given constant $\widehat{\mu} > 0$, control gains $\eta_\theta > 0$, $\eta_l > 0$ and $\eta_\kappa > 0$. The drive FOPMSG system (8) and response FOPMSG system (9) can be achieved MLS at a prespecified time \mathbb{T} , for adaptive law (19) and the designed control law

$$\begin{cases} u_i^{<\varphi>} = \alpha\varphi_1 - \alpha\varphi_2 + {}_0^C D_t^\beta \widehat{h}_1 - {}_0^{RL} D_t^{-(1-\beta)} (\zeta_1^\ell s_1) \\ u_i^{<\sigma>} = \varphi_2 + (\varphi_1 \widehat{\mathfrak{S}}_3 + \varphi_3 \widehat{\mathfrak{S}}_1 - \varphi_1 \varphi_3) - \rho\varphi_1 \\ \quad + {}_0^C D_t^\beta \widehat{h}_2 - {}_0^{RL} D_t^{-(1-\beta)} ((\lambda^{\Delta_\kappa} + \lambda^{\Delta_l}) |\widehat{\mathfrak{S}}_1| \\ \quad + \lambda^{\Delta_l} |\varphi_1| + \lambda^{d_\kappa} + \lambda^{d_l} + \zeta_2^\ell s_2) \\ u_i^{<\lambda>} = \varphi_3 - \varphi_1 \widehat{\mathfrak{S}}_2 - \varphi_2 \widehat{\mathfrak{S}}_1 + \varphi_1 \varphi_2 + {}_0^C D_t^\beta \widehat{h}_3 \\ \quad - {}_0^{RL} D_t^{-(1-\beta)} (\lambda^{d_\sigma} + \lambda^{d_\tau} + \zeta_3^\ell s_3) \end{cases} \quad (34)$$

if the following condition holds: 1) $\|\varphi\| \leq \|\varphi - \widehat{h}\|$ and 2) $\widehat{\Psi}_{\min}^{<\delta>} < 0$, where $\widehat{\Psi}_{\min}^{<\delta>} = \min_{1 \leq \varsigma \leq 3} \{\widehat{\Psi}_\varsigma^{<\delta>}\}$, $\widehat{\Psi}_1^{<\delta>} = \min\{(\widehat{\mu} - 2\varrho_1^k), 2\eta_\theta\}$, $\widehat{\Psi}_2^{<\delta>} = \min\{(\widehat{\mu} - 2\varrho_2^k), 2\eta_l\}$, $\widehat{\Psi}_3^{<\delta>} = \min\{(\widehat{\mu} - 2\varrho_3^k), 2\eta_\kappa\}$.

Theorem 4: Given nonzero positive parameters $\hat{\psi}_\theta$, $\hat{\psi}_\tau$, $\hat{\psi}_\zeta$, $\hat{\phi}_1^\delta$, $\hat{\phi}_2^\delta$, $\hat{\phi}_3^\delta$. The drive FOPMSG system (8) and the response FOPMSG system (9) can be achieve synchronization at a prespecified time Υ , for the control law

$$\begin{cases} u_i^{<\phi>} = \alpha\varphi_1 - \alpha\varphi_2 + {}_0^C D_t^\beta \hat{h}_1 - \hat{\psi}_\theta s_1 \\ \quad - {}_0^{RL} D_t^{-(1-\beta)} (\hat{\phi}_1^\delta \text{sign}(s_1)), \\ u_i^{<\sigma>} = \varphi_2 + (\varphi_1 \hat{\mathfrak{S}}_3 + \varphi_3 \hat{\mathfrak{S}}_1 - \varphi_1 \varphi_3) - \rho\varphi_1 + {}_0^C D_t^\beta \hat{h}_2 \\ \quad - \hat{\psi}_\tau s_2 - {}_0^{RL} D_t^{-(1-\beta)} ((\lambda^{\Delta_\kappa} + \lambda^{\Delta_\iota}) |\hat{\mathfrak{S}}_1| \\ \quad + \lambda^{\Delta_\iota} |\varphi_1| + \lambda^{d_\kappa} + \lambda^{d_\iota} + \hat{\phi}_2^\delta \text{sign}(s_2)), \\ u_i^{<\lambda>} = \varphi_3 - \varphi_1 \hat{\mathfrak{S}}_2 - \varphi_2 \hat{\mathfrak{S}}_1 + \varphi_1 \varphi_2 + {}_0^C D_t^\beta \hat{h}_3 \\ \quad - \hat{\psi}_\zeta s_3 - {}_0^{RL} D_t^{-(1-\beta)} (\lambda^{d_\sigma} + \lambda^{d_\tau} + \hat{\phi}_3^\delta \text{sign}(s_3)) \end{cases} \quad (35)$$

if the following parameter condition holds $\Psi^\theta > 0$, $\Theta_i > 0$, where $\Psi^\theta = \min_{1 \leq \zeta \leq 3} \{\hat{\psi}_\theta, \hat{\psi}_\tau, \hat{\psi}_\zeta\}$, $\Theta_i = \min_{1 \leq \zeta \leq 3} \{\hat{\phi}_\zeta^\delta \kappa_\zeta\}$, $\kappa_\zeta = \text{sign}(s_\zeta) \text{sign}(s_\zeta)$.

Proof: Choose the Lyapunov function as

$$\mathcal{V}(t) = \sum_{\zeta=1}^3 {}_0^C D_t^{1-\beta} (|s_\zeta(t)|).$$

Taking the Caputo fractional derivative of $\mathcal{V}(t)$ and applying Lemma 2, one has

$${}_0^C D_t^\beta \mathcal{V}(t) = \dot{s}_1 \text{sign}(s_1) + \dot{s}_2 \text{sign}(s_2) + \dot{s}_3 \text{sign}(s_3). \quad (36)$$

In particular, we have

$$\begin{aligned} \dot{s}_1 &= {}_0^C D_t^{1-\beta} (\alpha\varphi_2 - \alpha\varphi_1 + u_i^{<\phi>} - {}_0^C D_t^\beta \hat{h}) \\ &\leq -\hat{\psi}_\theta {}_0^C D_t^{1-\beta} s_1 - \hat{\phi}_1^\delta \text{sign}(s_1). \end{aligned} \quad (37)$$

Based on Assumption 2, we get $\dot{s}_2 \leq -\hat{\psi}_\tau {}_0^C D_t^{1-\beta} s_2 - \hat{\phi}_2^\delta \text{sign}(s_2)$. $\dot{s}_3 \leq -\hat{\psi}_\zeta {}_0^C D_t^{1-\beta} s_3 - \hat{\phi}_3^\delta \text{sign}(s_3)$. Combining the inequalities, we get that

$$\begin{aligned} {}_0^C D_t^\beta \mathcal{V}(t) &\leq -\hat{\psi}_\theta {}_0^C D_t^{1-\beta} |s_1| - \hat{\phi}_1^\delta \kappa_1 - \hat{\psi}_\tau {}_0^C D_t^{1-\beta} |s_2| \\ &\quad - \hat{\phi}_2^\delta \kappa_2 - \hat{\psi}_\zeta {}_0^C D_t^{1-\beta} |s_3| - \hat{\phi}_3^\delta \kappa_3 \leq -\min_{1 \leq \zeta \leq 3} \{\hat{\phi}_\zeta^\delta \kappa_\zeta\} \leq -\Theta_i. \end{aligned}$$

There is a positive function $g(t)$ such that ${}_0^C D_t^\beta \mathcal{V}(t) + g(t) = -\Theta_i$. The Riemann–Liouville fractional integral on both sides from 0 to t , one has

$$\begin{aligned} \mathcal{V}(t) - \mathcal{V}(0) + \frac{1}{\Gamma(\beta)} \int_0^t \frac{g(s)}{(t-s)^{1-\beta}} ds \\ = \frac{1}{\Gamma(\beta)} \int_0^t \frac{-\Theta_i}{(t-s)^{1-\beta}} ds. \end{aligned} \quad (38)$$

Because $\Gamma(\beta) > 0$, and $(t-s)^{\beta-1} g(s) \geq 0$, for $s \in [0, t]$, it follows that ${}_0^{RL} I_t^\beta g(t) \geq 0$. In particular

$$\frac{1}{\Gamma(\beta)} \int_0^t \frac{-\Theta_i}{(t-s)^{1-\beta}} ds = \frac{-\Theta_i}{\Gamma(\beta)} \int_0^t (t-s)^{\beta-1} ds = \frac{-\Theta_i t^\beta}{\beta \Gamma(\beta)}. \quad (39)$$

From (38) and (39), we obtain that

$$-\mathcal{V}(0) \leq \mathcal{V}(t) - \mathcal{V}(0) + {}_0^{RL} I_t^\beta g(t) = \frac{-\Theta_i t^\beta}{\beta \Gamma(\beta)}. \quad (40)$$

From (40), it can be seen that $t \leq [(\beta \Gamma(\beta) \mathcal{V}(0)) / \Theta_i]^{(1/\beta)}$.

Remark 3: The terminal function $\hat{h}_\zeta(t)$ ($\zeta = 1, 2, 3$) in (25) gets and adds to the control law (29). In this study, we used [30] to derive the fractional derivative of terminal function $\hat{h}_\zeta(t)$ and to find the β -order Caputo derivative of the function t^ϕ as

$${}_0^C D_t^\beta t^\phi = \frac{\Gamma(\phi+1)}{\Gamma(\phi-\beta+1)} t^{\phi-\beta}, \quad t > 0, \phi > -1. \quad (41)$$

For $t \leq \Upsilon$, and

$${}_0^C D_t^\beta \hat{h}_\zeta(t) = \frac{\varphi_\zeta(0)}{\Upsilon^2} \left(2\Upsilon \frac{\Gamma(2)}{\Gamma(2-\beta)} t^{1-\beta} - \frac{\Gamma(3)}{\Gamma(3-\beta)} t^{2-\beta} \right). \quad (42)$$

For $t > \Upsilon$, next we find the Caputo derivative of the function $H(t)$ as $H(t) = \begin{cases} t^\phi, & t \leq \Upsilon, \\ 0, & t > \Upsilon, \end{cases}$ where $\phi > 0$. According to

Definitions 2 and 3, for $t > \Upsilon$, we calculated ${}_0^C D_t^\beta \hat{h}_\zeta(t)$ as

$$\begin{aligned} {}_0^C D_t^\beta \hat{h}_\zeta(t) &= \frac{\varphi_\zeta(0)}{\Upsilon^2} \left(\frac{2\Upsilon}{\Gamma(1-\beta)} t^{1-\beta} B_{\Upsilon/t}(1, 1-\beta) \right. \\ &\quad \left. - \frac{2}{\Gamma(1-\beta)} t^{2-\beta} B_{\Upsilon/t}(2, 1-\beta) \right). \end{aligned} \quad (43)$$

IV. NUMERICAL EXAMPLE

In this section, two examples have been presented to validate our proposed theoretical results of this article.

Example 1: We consider the FOPMSG between drive system (8) and response system (9) as follows. The system parameters are selected as in [7], $\alpha = 5.45$, $\rho = 20$, and $\beta = 0.93$. The initial values of system (8) and (9) are set as $(\mathfrak{S}_1(0), \mathfrak{S}_2(0), \mathfrak{S}_3(0)) = (17, 0.8, 2.7)$ and $(\hat{\mathfrak{S}}_1(0), \hat{\mathfrak{S}}_2(0), \hat{\mathfrak{S}}_3(0)) = (5.7, 2.3, 1.5)$, respectively.

Case (i): We chose the following parameters $\gamma_\theta = 0.7$, $\gamma_\tau = 0.9$, $\gamma_\zeta = 1.3$, $\xi^{\Delta_\kappa} = 3.7$, $\xi^{\Delta_\iota} = 2.9$, $\xi^{d_\kappa} = 2.3$, $\xi^{d_\iota} = 3.1$, $\xi^{d_\sigma} = 1.5$, $\xi^{d_\tau} = 2.3$, and $\mu = 1.2$, combining with the proposed criteria in Theorem 1, one obtains the following results: $\psi_1^\delta = \mu - 2\gamma_\theta = -0.2$, $\psi_2^\delta = \mu - 2\gamma_\tau = -0.6$, $\psi_3^\delta = \mu - 2\gamma_\zeta = -1.4$, then $\Psi_{\min} = \min_{1 \leq \zeta \leq 3} \{\psi_\zeta^\delta\} < 0$ holds and applying the control scheme in the form of (14), then response FOPMSG system (9) can achieve MLS with drive FOPMSG system (8). Simulation results are as follows. The tracking error trajectory for various differential orders is given in Fig. 5. Fig. 6 shows the control input signals of $u_i^{<\phi>}$, $u_i^{<\sigma>}$, and $u_i^{<\lambda>}$.

Case (ii): We select the parameters $\xi^{\Delta_\kappa} = 1.3$, $\xi^{\Delta_\iota} = 3.7$, $\xi^{d_\kappa} = 3.1$, $\xi^{d_\iota} = 4.3$, $\xi^{d_\sigma} = 2.5$, $\xi^{d_\tau} = 2.9$, $\varrho_1^\kappa = 1.3$, $\varrho_2^\kappa = 1.5$, $\varrho_3^\kappa = 1.9$, $\eta_\theta = 0.9$, $\eta_\iota = 0.7$, $\eta_\kappa = 1.3$, and $\mu = 1.2$. By Theorem 2, we get the results $\Phi_1^{<\delta>} = \min\{(\mu - 2\varrho_1^\kappa), 2\eta_\theta\} = -1.4$, $\Phi_2^{<\delta>} = \min\{(\mu - 2\varrho_2^\kappa), 2\eta_\iota\} = -1.8$, $\Phi_3^{<\delta>} = \min\{(\mu - 2\varrho_3^\kappa), 2\eta_\kappa\} = -2.6$, then $\Psi_{\min}^{<\delta>} < 0$ holds, and the synchronization between FOPMSG systems (8) and (9) is achieved MLS by adaptive law (19) and designed control scheme (20). The tracking error trajectory performance test for different orders is depicted in Fig. 7. Fig. 8 shows the simulated responses of control inputs, the identifications of uncertain parameters, and tuning parameters. It can be distinguished from Figs. 5 and 7 that the proposed AFSMC technique has much better results in comparison with the other FSMC in the presence of high perturbations. If we use the error information ζ_1^ℓ , ζ_2^ℓ , and ζ_3^ℓ in the identification law, the

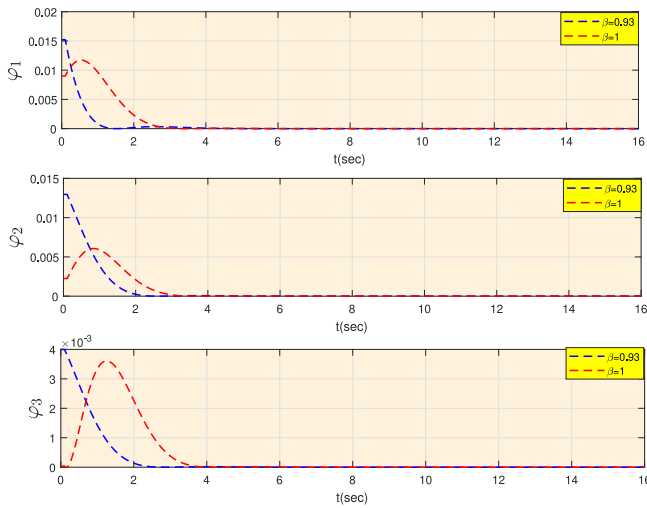


Fig. 5. Tracking error φ_ζ ($\zeta = 1, 2, 3$) for various differential order considered with $\beta = 0.93$ and $\beta = 1$.

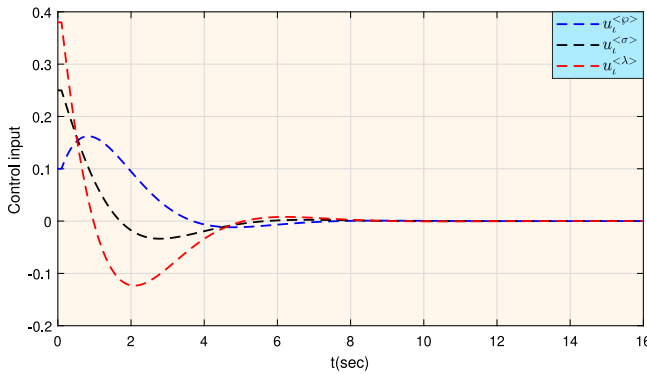


Fig. 6. Simulated responses of control inputs $u_i^{<\phi>}$, $u_i^{<\sigma>}$, $u_i^{<\lambda>}$.

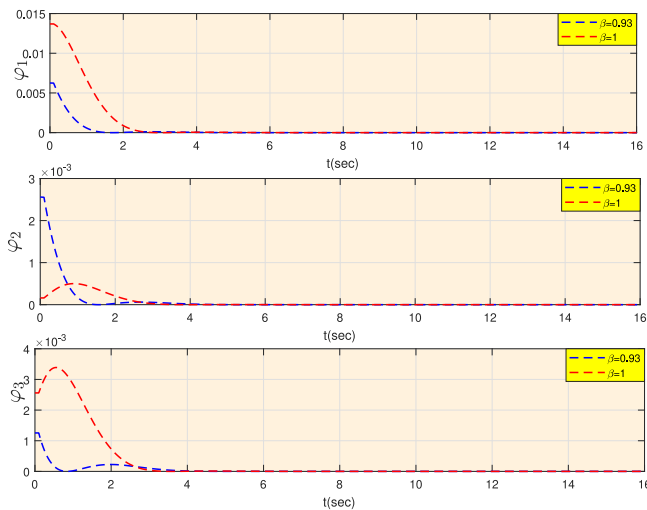


Fig. 7. Tracking error φ_ζ ($\zeta = 1, 2, 3$) for various differential order considered with $\beta = 0.93$ and $\beta = 1$.

identification of unknown parameters can be as quick as any speed. And at this situation, the MLS achieves very quickly as shown in Fig. 7. Comparison results about the SMC problem of PMSG-based WTS on enhanced exponential reaching law in [23], it follows from the simulation results that the proposed

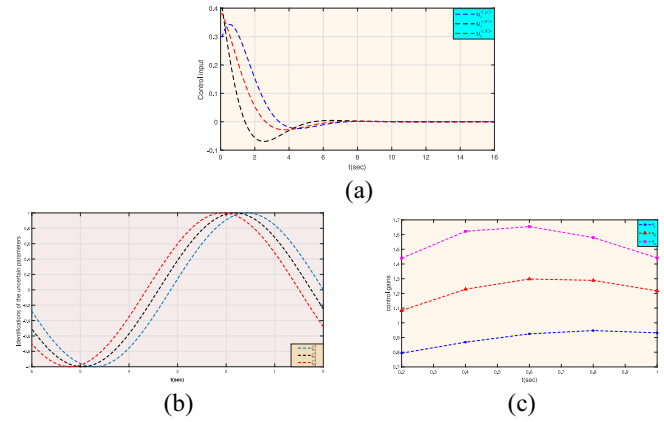


Fig. 8. (a) Control inputs $u_i^{<\phi>}$, $u_i^{<\sigma>}$, $u_i^{<\lambda>}$. (b) Identifications of the uncertain parameters ζ_1^l , ζ_2^l , ζ_3^l . (c) Tuning control gains of η_θ , η_l , and η_κ .

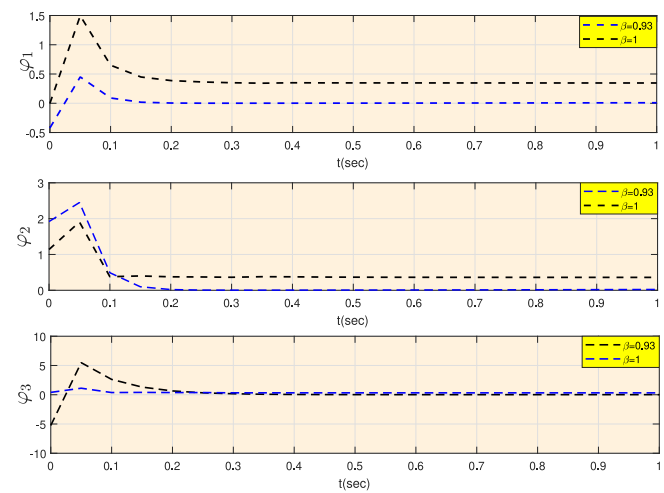


Fig. 9. Tracking error φ_ζ ($\zeta = 1, 2, 3$) for various differential order considered with $\beta = 0.93$ and $\beta = 1$.

MLS with in this article could get a faster convergent speed fractional-order ($\beta = 0.93$) tuning than integer order ($\beta = 1$).

Example 2: Consider a drive system (8) and response system (9) with the same initial condition and system parameters in Example 1.

Case (i): We choose the control parameters as $\psi_\theta = 1.7$, $\psi_\tau = 2.3$, $\psi_\zeta = 2.7$, $\lambda^{\Delta_\kappa} = 0.7$, $\lambda^{\Delta_l} = 0.9$, $\lambda^{d_\kappa} = 1.5$, $\lambda^{d_l} = 0.9$, $\lambda^{d_\sigma} = 1.8$, $\lambda^{d_\tau} = 2.2$, and $\hat{\mu} = 2.7$. By Theorem 3, we get the results $\Upsilon_1^{<\delta>} = \{\hat{\mu} - 2\psi_\theta\} = -0.7$, $\Upsilon_2^{<\delta>} = \{\hat{\mu} - 2\psi_\tau\} = -1.9$, $\Upsilon_3^{<\delta>} = \{\hat{\mu} - 2\psi_\zeta\} = -2.7$, then $\Upsilon_{\min}^{<\delta>} < 0$ holds, and the drive FOPMSG system (8) and response FOPMSG system (9) is reached MLS via designed control scheme (29). The simulations for synchronization errors and control input are presented in Figs. 9 and 10.

Case (ii): We choose $\lambda^{\Delta_\kappa} = 2.7$, $\lambda^{\Delta_l} = 3.9$, $\lambda^{d_\kappa} = 4.5$, $\lambda^{d_l} = 2.9$, $\lambda^{d_\sigma} = 2.8$, $\lambda^{d_\tau} = 1.2$, $\varrho_1^K = 2.3$, $\varrho_2^K = 3.5$, $\varrho_3^K = 2.9$, $\eta_\theta = 1.9$, $\eta_l = 2.1$, $\eta_\kappa = 2.7$, and $\mu = 2.7$, combining with the proposed criteria in Corollary 1, one obtains the following results: $\hat{\Psi}_1^{<\delta>} = \min\{(\hat{\mu} - 2\varrho_1^K), 2\eta_\theta\} = -1.9$, $\hat{\Psi}_2^{<\delta>} = \min\{(\hat{\mu} - 2\varrho_2^K), 2\eta_l\} = -4.3$, $\hat{\Psi}_3^{<\delta>} = \min\{(\hat{\mu} - 2\varrho_3^K), 2\eta_\kappa\} = -3.1$, then $\hat{\Psi}_{\min}^{<\delta>} < 0$ holds, it is clear that drive FOPMSG system (8) is reached MLS with response FOPMSG

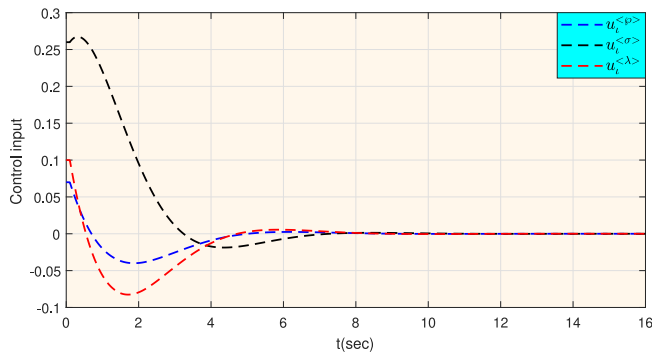


Fig. 10. Simulated responses of control inputs $u_t^{<\phi>}$, $u_t^{<\sigma>}$, $u_t^{<\lambda>}$.

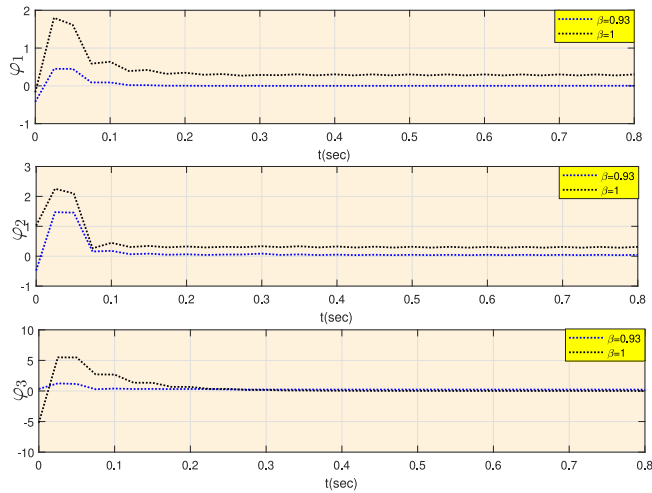


Fig. 11. Tracking error φ_ζ ($\zeta = 1, 2, 3$) for various differential order considered with $\beta = 0.93$ and $\beta = 1$.

system (9) under adaptive laws (19) and designed control scheme (35). Fig. 11 shows the convergence of the tracking errors φ_ζ , ($\alpha = 1, 2, 3$) which demonstrates that synchronization can be achieved for the drive FOPMSG system (8) and response FOPMSG system (9) under the proposed control (19) and (35). Fig. 12 shows the simulated responses of control inputs, the identifications of uncertain parameters, and tuning parameters.

The simulations were carried out to compare control schemes: AFSMC and ASMC, with terminal functions. Fig. 7 shows that FOPMSG system (8) can realize synchronization with response FOPMSG system (9) under AFSMC scheme reaches at the origin at $t = 1$ s ($\beta = 0.93$). Fig. 11 demonstrates the time response of the FOPMSG system with the improved performance of robust controller design with various differential order. The tracking error has reached the origin exactly at $t = 0.1$ s ($\beta = 0.93$). Hence, the FOPMSG system (8) and (9) in ASMC, with fractional terminal functions, is better than AFSMC, more robust and faster transient performance against uncertainly and disturbances due to eliminating the reaching phase completely, followed by the terminal functions. The advantages of our method concerning AFSMC and ASMC with terminal function are shown in various differential orders. This detailed analysis of the FOPMSG system proves the effectiveness of the proposed control scheme. Next, to show the efficiency of the proposed controller, we compare our observations with the existing research [9] and [22]. Sun

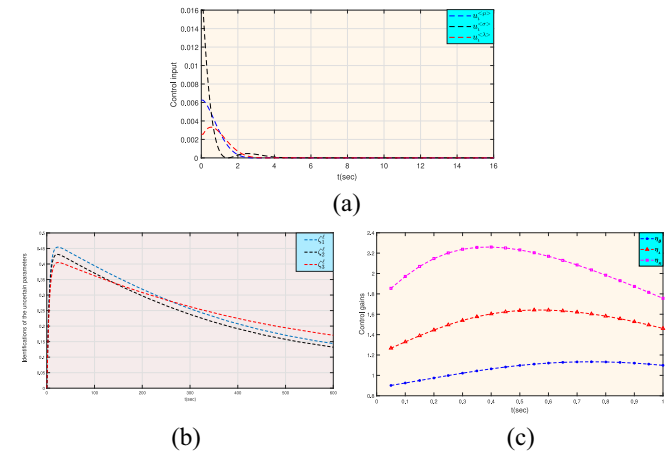


Fig. 12. (a) Control inputs $u_t^{<\phi>}$, $u_t^{<\sigma>}$, $u_t^{<\lambda>}$. (b) Identifications of the uncertain parameters ζ_1^l , ζ_2^l , ζ_3^l . (c) Tuning control gains of η_θ , η_l , and η_κ .

et al. [22] discussed the tuning parameters, a robust adaptive finite-time synchronization control problems of the PMSM with uncertain parameters, and Prakash et al. [9] further proposed an adaptive fractional fuzzy integral SMC method for PMSM with exogenous disturbances and estimate the unknown parameters. To make a fair comparison with these results, the designed values for tuning factors to be updated in (19) are chosen as $\varrho_1^K = 2.3$, $\varrho_2^K = 3.5$, and $\varrho_3^K = 2.9$, the gains of terminal attractors in [22] are chosen as $\eta_\theta = 1.9$, $\eta_l = 2.1$, and $\eta_\kappa = 2.7$, a shorter convergent speed could be obtained by using Corollary 1. The synchronization error has reached the origin at $t = 2$ s (see [22, Fig. 2]), and the system state can take almost the origin at $t = 2.5$ s (see [9, Fig. 5]). But, our designed control law (19) with terminal functions (26) observed from these simulation results that the synchronization error has become zero accurately at $t = 0.2$ s (see Fig. 11). Comparison results about the convergent speed are discussed above, it follows from the simulation results that the proposed MLS with AFSMC scheme in this study could get a faster convergent speed than those in [9] and [22].

V. CONCLUSION

In this article, the MLS problem for the FOPMSG-based WTS with uncertainties, and disturbance has been studied via fractional domain memory-based AFSMC. Novel AFSMC has been introduced in the fractional domain memory-based suitable sliding-mode surface function has been designed for the concerned FOPMSG model to derive the MLS conditions. Based on the Lyapunov function and the improved fractional differential inequality, sufficient conditions have been addressed in the form of algebraic criteria, guaranteeing that the considered FOPMSG model is MLS under the designed controller. Moreover, the robust prespecified time achieved the FOPMSG model with the help of time-varying switching surfaces ASMC. The simulation results show that the MLS performances of the FOPMSG-based WTS under fractional domain memory-based AFSMC and ASMC with terminal function are better with shorter convergence time, faster convergence speed, which reveals good transient performance and outperforms prevailing research [9], [22].

REFERENCES

- [1] P. Mani and Y. H. Joo, "Fuzzy event-triggered control for back-to-back converter involved PMSG-based wind turbine systems," *IEEE Trans. Fuzzy Syst.*, vol. 30, no. 5, pp. 1409–1420, May 2022.
- [2] L. Shanmugam and Y. H. Joo, "Stability and stabilization for T-S fuzzy large-scale interconnected power system with wind farm via sampled-data control," *IEEE Trans. Syst., Man, Cybern., Syst.*, vol. 51, no. 4, pp. 2134–2144, Apr. 2021.
- [3] S. Luo, Y. Song, F. L. Lewis, R. Garrappa, and S. Li, "Dynamic analysis and fuzzy fixed-time optimal synchronization control of unidirectionally coupled FO permanent magnet synchronous generator system," *IEEE Trans. Fuzzy Syst.*, vol. 31, no. 5, pp. 1742–1755, May 2023.
- [4] X. Jiao, Q. Yang, and B. Xu, "Hybrid intelligent feedforward-feedback pitch control for VSWT with predicted wind speed," *IEEE Trans. Energy Convers.*, vol. 36, no. 4, pp. 2770–2781, Dec. 2021.
- [5] X. Tang, M. Yin, C. Shen, Y. Xu, Z. Y. Dong, and Y. Zou, "Active power control of wind turbine generators via coordinated rotor speed and pitch angle regulation," *IEEE Trans. Sustain. Energy*, vol. 10, no. 2, pp. 822–832, Apr. 2019.
- [6] R. Vadeivel and Y. H. Joo, "Reliable fuzzy H_∞ control for permanent magnet synchronous motor against stochastic actuator faults," *IEEE Trans. Syst., Man, Cybern., Syst.*, vol. 51, no. 4, pp. 2232–2245, Apr. 2021.
- [7] M. Messadi, A. Mellit, K. Kemih, and M. Ghanes, "Predictive control of a chaotic permanent magnet synchronous generator in a wind turbine system," *Chin. Phys. B*, vol. 24, no. 1, 2015, Art. no. 10502.
- [8] A. Karthikeyan, K. Rajagopal, and D. Mathew, "Fractional-order nonlinear variable speed and current regulation of a permanent magnet synchronous generator wind turbine system," *Alexandria Eng. J.*, vol. 57, pp. 159–167, Mar. 2018.
- [9] M. Prakash, R. Rakkiyappan, S. Lakshmanan, and Y. H. Joo, "Adaptive fractional fuzzy integral sliding mode control for PMSM model," *IEEE Trans. Fuzzy Syst.*, vol. 27, no. 8, pp. 1674–1686, Aug. 2019.
- [10] D. Kui, and Q. Zhu, "Impulsive method to reliable sampled-data control for uncertain fractional-order memristive neural networks with stochastic sensor faults and its applications," *Nonlinear Dyn.*, vol. 100, pp. 2595–2608, May 2020.
- [11] S. Sui and S. Tong, "FTC design for switched fractional-order nonlinear systems: An application in a permanent magnet synchronous motor system," *IEEE Trans. Cybern.*, vol. 53, no. 4, pp. 2506–2515, Apr. 2023, doi: [10.1109/TCYB.2021.3123377](https://doi.org/10.1109/TCYB.2021.3123377).
- [12] Z. Yu, Y. Zhang, B. Jiang, J. Fu, Y. Jin, and T. Chai, "Composite adaptive disturbance observer-based decentralized fractional-order fault-tolerant control of networked UAVs," *IEEE Trans. Syst., Man, Cybern., Syst.*, vol. 52, no. 2, pp. 799–813, Feb. 2022.
- [13] Z. Yu, Y. Sun, and X. Dai, "Stability and stabilization of the fractional-order power system with time delay," *IEEE Trans. Circuits Syst. II, Exp. Briefs*, vol. 68, no. 11, pp. 3446–3450, Nov. 2021.
- [14] J. Fei, H. Wang, and Y. Fang, "Novel neural network fractional-order sliding-mode control with application to active power filter," *IEEE Trans. Syst., Man, Cybern., Syst.*, vol. 52, no. 6, pp. 3508–3518, Jun. 2022.
- [15] C. Chen, S. Zhu, Y. Wei, and C. Chen, "Finite-time stability of delayed memristor-based fractional-order neural networks," *IEEE Trans. Cybern.*, vol. 50, no. 4, pp. 1607–1616, Apr. 2020.
- [16] P. Mani, R. Rajan, and Y. H. Joo, "Design of observer-based event-triggered fuzzy ISMC for T-S fuzzy model and its application to PMSG," *IEEE Trans. Syst., Man, Cybern., Syst.*, vol. 51, no. 4, pp. 2221–2231, Apr. 2021.
- [17] B. Kaviarasan, O. M. Kwon, M. J. Park, and R. Sakthivel, "Integrated synchronization and anti-disturbance control design for fuzzy model-based multiweighted complex network," *IEEE Trans. Syst., Man, Cybern., Syst.*, vol. 51, no. 10, pp. 6330–6341, Oct. 2021.
- [18] F. Wang, Z. Zheng, and Y. Yang, "Quasi-synchronization of heterogeneous fractional-order dynamical networks with time-varying delay via distributed impulsive control," *Chaos, Solitons Fractals*, vol. 142, Jan. 2021, Art. no. 110465.
- [19] Y. Kao, Y. Li, J. H. Park, and X. Chen, "Mittag-Leffler synchronization of delayed fractional memristor neural networks via adaptive control," *IEEE Trans. Neural Netw. Learn. Syst.*, vol. 32, no. 5, pp. 2279–2284, May 2021.
- [20] Y.-X. Li, Q.-Y. Wang, and S. Tong, "Fuzzy adaptive fault-tolerant control of fractional-order nonlinear systems," *IEEE Trans. Syst., Man, Cybern., Syst.*, vol. 51, no. 3, pp. 1372–1379, Mar. 2021.
- [21] J. Chen, B. Chen, and Z. Zeng, "Global asymptotic stability and adaptive ultimate Mittag-Leffler synchronization for a fractional-order complex-valued memristive neural networks with delays," *IEEE Trans. Syst., Man, Cybern., Syst.*, vol. 49, no. 12, pp. 2519–2535, Dec. 2019.
- [22] Y. Sun, X. Wu, L. Bai, Z. Wei, and G. Sun, "Finite-time synchronization control and parameter identification of uncertain permanent magnet synchronous motor," *Neurocomputing*, vol. 207, pp. 511–518, Sep. 2016.
- [23] R. Subramaniam and Y. H. Joo, "Passivity-based fuzzy ISMC for wind energy conversion systems with PMSG," *IEEE Trans. Syst., Man, Cybern., Syst.*, vol. 51, no. 4, pp. 2212–2220, Apr. 2021.
- [24] H. Kord and S. M. Barakati, "Design an adaptive sliding mode controller for an advanced hybrid energy storage system in a wind dominated RAPS system based on PMSG," *Sustain. Energy, Grids Netw.*, vol. 21, Mar. 2020, Art. no. 100310.
- [25] M. Li, Y. Chen, Y. Zhang, and Y. Liu, "Adaptive sliding-mode tracking control of networked control systems with false data injection attacks," *Inf. Sci.*, vol. 585, pp. 194–208, Mar. 2022.
- [26] Q. Zhu, "Stabilization of stochastic nonlinear delay systems with exogenous disturbances and the event-triggered feedback control," *IEEE Trans. Autom. Control*, vol. 64, no. 9, pp. 3764–3771, Sep. 2019.
- [27] H. Li, J. Wang, H. Du, and H. R. Karimi, "Adaptive sliding mode control for Takagi-Sugeno fuzzy systems and its applications," *IEEE Trans. Fuzzy Syst.*, vol. 26, no. 2, pp. 531–542, Apr. 2018.
- [28] W. Qi, X. Gao, C. K. Ahn, J. Cao, and J. Cheng, "Fuzzy integral sliding-mode control for nonlinear semi-Markovian switching systems with application," *IEEE Trans. Syst., Man, Cybern., Syst.*, vol. 52, no. 3, pp. 1674–1683, Mar. 2022.
- [29] M. Shirkavand and M. Pourgholi, "Robust fixed-time synchronization of fractional-order chaotic using free chattering nonsingular adaptive fractional sliding mode controller design," *Chaos, Solitons Fractals*, vol. 113, pp. 135–147, Aug. 2018.
- [30] A. Khanzadeh and M. Pourgholi, "A novel continuous time-varying sliding mode controller for robustly synchronizing non-identical fractional-order pre-specified time using sliding mode controller with time-varying chaotic systems precisely at any arbitrary pre-specified time," *Nonlinear Dyn.*, vol. 86, pp. 543–558, Jun. 2016.
- [31] M. Pourgholi and A. Khanzadeh, "Robust synchronization of fractional-order chaotic systems at a pre-specified time using sliding mode controller with time-varying switching surfaces," *Chaos, Solitons Fractals*, vol. 91, pp. 69–77, Oct. 2016.
- [32] L. Xiong, J. Wang, X. Mi, and M. W. Khan, "Fractional-order sliding mode based direct power control of grid-connected DFIG," *IEEE Trans. Power Syst.*, vol. 33, no. 3, pp. 3087–3096, May 2018.

[< Back](#)

Advertise

[International Journal of Adaptive Control and Signal Processing / Volume 37, Issue 8 / p. 2041-2062](#)

RESEARCH ARTICLE

Adaptive event-triggered pinning synchronization control for complex networks with random saturation subject to hybrid cyber-attacks

M. Syed Ali, M. Mubeen Tajudeen, Grienggrai Rajchakit , Bandana Priya, Ganesh Kumar Thakur

First published: 23 May 2023

<https://doi.org/10.1002/acs.3625>

Summary

This research is concerned with the problem of pinning based output synchronization control for a complex networks with random saturation vulnerable to hybrid cyber-attacks via an adaptive event-triggered scheme (AETS). The output synchronization error systems are subject to suffer from deception attacks, replay attacks, and denial-of-service attacks. A novel hybrid cyber-attack model is first constructed to integrate the three kinds of attacks into a synchronization of complex network. AETSs based on output synchronization errors with the consideration of hybrid cyber-attacks, have been proposed to reduce the burden of communication. A pinning control strategy is used to decrease the control signal's input. By constructing a Lyapunov functional and using the linear matrix inequality technique, sufficient conditions are provided to ensure the output synchronization error system. Finally, a numerical simulation results are developed to illustrate the efficacy of the proposed theoretical methodology.

CONFLICT OF INTEREST STATEMENT

The authors does not have any conflict of interest.

REFERENCES





Article

Synchronization of Discrete-Time Fractional-Order Complex-Valued Neural Networks with Distributed Delays

R. Perumal¹ , M. Hymavathi², M. Syed Ali^{2,*} , Batul A. A. Mahmoud³, Waleed M. Osman⁴
and Tarek F. Ibrahim⁵

¹ Department of Mathematics, Faculty of Engineering and Technology, SRM Institute of Science and Technology, Kattankulathur 603203, Tamil Nadu, India

² Complex Systems and Networked Science Research Laboratory, Department of Mathematics, Thiruvalluvar University, Vellore 632115, Tamil Nadu, India

³ Department of Mathematics, Faculty of Sciences and Arts in Sarat Abeda, King Khalid University, Abha 62521, Saudi Arabia

⁴ Department of Mathematics, Faculty of Science and Arts, King Khalid University, Abha 62529, Saudi Arabia

⁵ Department of Mathematics, Faculty of Sciences and Arts (Mahayel), King Khalid University, Abha 62529, Saudi Arabia

* Correspondence: syedgru@gmail.com

Abstract: This research investigates the synchronization of distributed delayed discrete-time fractional-order complex-valued neural networks. The necessary conditions have been established for the stability of the proposed networks using the theory of discrete fractional calculus, the discrete Laplace transform, and the theory of fractional-order discrete Mittag–Leffler functions. In order to guarantee the global asymptotic stability, adequate criteria are determined using Lyapunov’s direct technique, the Lyapunov approach, and some novel analysis techniques of fractional calculation. Thus, some sufficient conditions are obtained to guarantee the global stability. The validity of the theoretical results are finally shown using numerical examples.

Keywords: fractional order; synchronization; complex-valued; discrete-time; neural networks



Citation: Perumal, R.; Hymavathi, M.; Ali, M.S.; Mahmoud, B.A.A.; Osman, W.M.; Ibrahim, T.F.

Synchronization of Discrete-Time Fractional-Order Complex-Valued Neural Networks with Distributed Delays. *Fractal Fract.* **2023**, *7*, 452. <https://doi.org/10.3390/fractalfract7060452>

Academic Editors: Carlo Cattani and Alicia Cordero

Received: 22 March 2023

Revised: 8 May 2023

Accepted: 24 May 2023

Published: 1 June 2023



Copyright: © 2023 by the authors. Licensee MDPI, Basel, Switzerland. This article is an open access article distributed under the terms and conditions of the Creative Commons Attribution (CC BY) license (<https://creativecommons.org/licenses/by/4.0/>).

1. Introduction

The 19th century witnessed the majority of the development of fractional calculus theory. More than 300 years ago, in Leibniz’s letter to L’Hospital from 1695, fractional calculus was first introduced. The distinct advantage of fractional-order systems over traditional integer-order systems is that they provide an ideal instrument for describing the memory and hereditary features of diverse materials and processes. Fractional calculus did not receive much attention for a very long time due to the complexity and lack of application for the background. Fractional-order differential equations have recently been demonstrated to be useful modelling tools in a variety of scientific and engineering domains, as shown in [1–3]. The dynamical characteristics of neural networks have drawn significant attention during the last few decades. Due to neural networks’ effective application in optimization, signal processing, associative memory, parallel computing, pattern recognition, artificial intelligence, etc., their dynamical features have come under intense scrutiny during the past few decades. As fractional calculus advanced quickly, several researchers astonishingly found that fractional calculus could be implemented into neural networks [4–10].

Despite the significant progress made by continuous fractional calculus, discrete fractional calculus research is still in its early stages. In order to explore discrete fractional calculus, Diaz and Osler introduced an infinite series in 1974. However, continuous-time and discrete-time systems are two complementary characteristics in real-world applications, therefore the question of whether discrete-time systems have similar dynamical behaviors to their continuous-time counterparts has emerged. It is crucial to study the dynamic

behavior of discrete fractional calculus since not all discrete operators in theoretical research have the same properties as continuous operators. Researchers often take continuous-time systems into consideration when simulating and analyzing dynamic behavior on computers. However, in a digital network, signal reception and operation are based on discrete time rather than continuous time [11–18].

The networks that process complex-valued input by employing complex-valued parameters and variables are known as complex-valued neural networks (CVNNs) [19–27]. In comparison to real-valued neural networks, complex-valued neural networks have a favoured superiority in easier network layout, quicker training times, and increased power throughout complex signal processing. However, according to Liouville's theorem, every bounded and smooth activation function in CVNNs simplifies to a constant. Therefore, it is more difficult and important to understand the dynamical behaviors of CVNNs. Additionally, they have better solutions than real-valued neural networks for resolving several challenging real-life problems, such as the XOR problem. A variety of techniques have been used to evaluate the stability of CVNNs based on the outcomes so far. Some scholars provided numerous significant results in recent years to guarantee the dynamics of complex-valued neural networks with temporal delays [28–38].

Synchronization for time-delayed neural networks has received particular attention due to their numerous potential applications in the areas of image processing, signal processing, associative memory, and secure communication. Synchronization has grown in popularity as a neural network research issue during the past decade. There are several different types of fractional neural network synchronization issues in use today [39,40]. These synchronization analyses are carried out using a singular Gronwall inequality and Filippov solution theorem [41–43].

The broad field of science and engineering known as stability theory examines how dynamical structures affect both linear and nonlinear systems. Most stability studies conducted in recent decades have focused on stability in the Lyapunov sense, including asymptotic, exponential, and uniform stability. The well-known methods for time-domain stability analysis for systems with integer orders, such as the Lyapunov functional method and those combined with Razumikhin-type techniques, cannot be easily generalised to FO systems with time delay because it is challenging to calculate the FO derivatives of Lyapunov functions. The Caputo definition is used. A numerical example is used to demonstrate the accuracy of the suggested procedure. The novelties of the study are given below:

- (1) We studied the global synchronization of discrete-time fractional-order complex-valued neural networks with distributed delays.
- (2) Unlike the previous literature, this paper explicitly examines the stability for discrete fractional-order complex-valued neural networks using the stability theory in complex fields as opposed to breaking down complex-valued systems into real-valued systems.
- (3) Using the Lyapunov direct technique, the synchronization condition of FOCVNNs with temporal delays is determined. In light of the definition of the Caputo fractional difference, it is simple to calculate the first-order backward difference of the Lyapunov function that we design, which includes discrete fractional sum terms.
- (4) Some conditions regarding the global Mittag-Leffler stability of fractional-order CVNNs are established using fractional derivative inequalities and fractional-order appropriate Lyapunov functions.
- (5) It is necessary to investigate the essential characteristics of the discrete Mittag-Leffler function and the Nabla discrete Laplace transform.
- (6) Finally, numerical illustrations are provided.

2. Preliminaries

Let $\nabla q(\hbar) := q(\hbar) - q(\hbar - 1)$ be a backward difference operator and $\nabla^m q(\hbar) := \nabla(\nabla^{(m-1)} q(\hbar))$ be the operator, where $m \in N^+$.

Definition 1 ([44]). The Nabla discrete fractional sum of order $\beta > 0$ is defined as:

$$\nabla_a^{-\beta} \varrho(\hbar) = \frac{1}{\Gamma(\beta)} \sum_{s=a}^{\hbar} (\hbar - \rho(s))^{\overline{\beta-1}} \varrho(s),$$

where $a \in \mathbb{R}$, $\rho(s) = s - 1$, $\hbar \in N_a = \{a, a + 1, a + 2, \dots\}$.

Definition 2 ([45]). The Riemann–Liouville fractional difference of order $\beta > 0$ is defined as

$${}^C\nabla_a^n \varrho(\hbar) = \nabla^m (\nabla_a^{-(m-n)} \varrho(\hbar)),$$

where $m - 1 < \beta \leq m$, $m \in \mathbb{N}^+$, $t \in N_{a+m}$.

Definition 3 ([46]). (Global Mittag–Leffler stability) The origin of System (1) is Mittag–Leffler stable if

$$\|x(\hbar)\| \leq \left\{ R(x(\hbar_0)) E_q \left(-\delta(\hbar - \hbar_0)^q \right) \right\}^\sigma,$$

where t_0 denotes the initial instant, $q \in (0, 1)$, $\delta > 0$, $\sigma > 0$, $R(0) = 0$, $R(x) \geq 0$, and $R(x)$ is locally Lipschitz on $x \in \mathbb{R}$ with respect to the Lipschitz constant R_0 .

Lemma 1 ([47]). Let $q(\hbar) = (q_1(\hbar), \dots, q_m(\hbar))^T \in \mathbb{R}^m$ be a positive definite matrix, which, if $H \in \mathbb{R}^{m \times m}$ is a positive definite matrix, implies

$${}^C\nabla_0^\beta q^T(\hbar) H q(\hbar) \leq 2q^T(\hbar) H {}^C\nabla_0^\beta q(\hbar), \beta \in (0, 1).$$

Lemma 2 ([48]). For $0 < \beta \leq 1$, $\hbar = a + n$,

$$\nabla_a^\beta \varrho^2(\hbar) \leq 2\varrho(\hbar) \nabla_a^\beta \varrho(\hbar).$$

Lemma 3 ([49]). Suppose that $V(\hbar) \in \mathbb{R}$ is a continuous, differentiable, and non-negative function satisfying

$$\begin{aligned} D^\beta V(\hbar) &\leq -bV(\hbar) + cV(\hbar - \omega), \quad 0 < \beta < 1, \\ V(\hbar) &= \varphi(\hbar) \geq 0. \quad \hbar \in [-\omega, 0]. \end{aligned}$$

If $b > \sqrt{2c}$ and $c > 0$, then for all $\varphi(\hbar) \geq 0$, $\omega > 0$, $\lim_{\hbar \rightarrow +\infty} V(\hbar) = 0$.

Lemma 4 ([50]). Let $V(\hbar)$ be a continuous function on $[0, +\infty)$ satisfying

$$D^\beta V(\hbar) \leq \delta V(\hbar), \beta \in (0, 1)$$

and let δ be a constant. Then,

$$V(\hbar) \leq V(0) E_\beta(\delta \hbar^\beta).$$

3. Main Results

We consider the following discrete-time fractional-order complex-valued neural networks with time-varying delays:

$$\begin{aligned} {}^C\nabla_0^\beta \gamma_\psi(\hbar) &= -c_\psi \gamma_\psi(\hbar) + \sum_{\phi=1}^m a_{\psi\phi} f_\phi(\gamma_\phi(\hbar)) + \sum_{\phi=1}^m b_{\psi\phi} f_\phi(\gamma_\phi(\hbar - \omega)) \\ &+ \sum_{\phi=1}^m d_{\psi\phi} \int_0^\infty K_{\psi\phi}(s) f_\phi(\gamma_\phi(s)) ds + I_\psi, t \in N_1, \end{aligned} \tag{1}$$

$$\gamma_\psi(\hbar) = \Phi_\psi(\hbar), t \in N_1,$$

where ${}^C\nabla_0^\beta$ denotes the Caputo fractional difference operator with the order $\beta(0 < \beta < 1)$. $\gamma_\psi(\hbar) = [\gamma_{\psi 1}(\hbar), \gamma_{\psi 2}(\hbar), \dots, \gamma_{\psi m}(\hbar)]^T \in R^n$ denotes the state vector, $f(\gamma_\psi(\hbar)) = [f_1(\gamma_{\psi 1}(\hbar)), f_2(\gamma_{\psi 2}(\hbar)), \dots, f_\psi(\gamma_{\psi m}(\hbar))]^T : C^m \rightarrow C^m$ are vector-valued activation functions, $c_\psi, a_{\psi\phi}, b_{\psi\phi}, d_{\psi\phi}$ are connection weight matrices, and $\tau, \sigma(\hbar)$ are time-varying delays.

The response system is designed as

$$\begin{aligned} {}^C\nabla_0^\beta \delta_\psi(\hbar) &= -c_\psi \delta_\psi(\hbar) + \sum_{\phi=1}^m a_{\psi\phi} f_\phi(\delta_\phi(\hbar)) + \sum_{\phi=1}^m b_{\psi\phi} f_\phi(\delta_\phi(\hbar - \omega)) \\ &+ \sum_{\phi=1}^m d_{\psi\phi} \int_0^\infty K_{\psi\phi}(s) f_\phi(\gamma_\phi(s)) ds + I_\psi + u_\psi(\hbar), \\ \delta_\psi(\hbar) &= \tilde{\Phi}_\psi(\hbar), \hbar \in N_1, \end{aligned} \tag{2}$$

where $\delta_1(\hbar) = (\delta_{11}(\hbar), \delta_{12}(\hbar), \dots, \delta_{1n}(\hbar))^T \in C^n, u_\psi(\hbar) = [u_{\psi 1}(\hbar), u_{\psi 2}(\hbar), \dots, u_{\psi m}(\hbar)]^T \in R^n$ is the control input.

Here, we study their solutions using Filippov regularization. Then, System (1) can be expressed as

$$\begin{aligned} {}^C\nabla_0^\beta \gamma_\psi(\hbar) &= -c_\psi \gamma_\psi(\hbar) + \sum_{\phi=1}^m a_{\psi\phi} F[f_\phi(\gamma_\phi(\hbar))] + \sum_{\phi=1}^m b_{\psi\phi} F[f_\phi(\gamma_\phi(\hbar - \omega))] \\ &+ \sum_{\phi=1}^m d_{\psi\phi} \int_0^\infty K_{\psi\phi}(s) F[f_\phi(\gamma_\phi(s))] ds, \\ \gamma_\psi(\hbar) &= F[\Phi_\psi(\hbar)], t \in N_1. \end{aligned} \tag{3}$$

If there exist $p_j(\hbar) \in F[f_j(x)]$, then

$$\begin{aligned} {}^C\nabla_0^\beta \gamma_\psi(t) &= -c_\psi \gamma_\psi(\hbar) + \sum_{\phi=1}^m a_{\psi\phi} p_\phi(\gamma_\phi(\hbar)) + \sum_{\phi=1}^m b_{\psi\phi} p_\phi(\gamma_\phi(\hbar - \omega)) \\ &+ \sum_{\phi=1}^m d_{\psi\phi} \int_0^\infty K_{\psi\phi}(s) p_\phi(\gamma_\phi(s)) ds, \\ \gamma_\psi(\hbar) &= p_\psi(t), \hbar \in N_1. \end{aligned} \tag{4}$$

Similarly, from System (2), we have

$$\begin{aligned} {}^C\nabla_0^\beta \delta_\psi(\hbar) &= -c_\psi \delta_\psi(\hbar) + \sum_{\phi=1}^m a_{\psi\phi} p_\phi(\delta_\phi(\hbar)) + \sum_{\phi=1}^m b_{\psi\phi} p_\phi(\delta_\phi(\hbar - \omega)) \\ &+ \sum_{\phi=1}^m d_{\psi\phi} \int_0^\infty K_{\psi\phi}(s) p_\phi(\delta_\phi(s)) ds + u_\psi(\hbar), \\ \delta_\psi(\hbar) &= \tilde{p}_\psi(\hbar), t \in N_1. \end{aligned} \tag{5}$$

Assumptions:

(H₁): Let $\gamma(\hbar) = \zeta(\hbar) + i\chi(\hbar)$ and $\delta(\hbar) = \xi(\hbar) + i\chi(\hbar)$; then, we have

$$p_\phi(\gamma_j(\hbar - \omega_s)) = p_\phi^R(\gamma_j(\hbar - \omega_s), \delta_j(\hbar - \omega_s)) + ip_\phi^I(\gamma_j(\hbar - \omega_s), \delta_j(\hbar - \omega_s)),$$

$$(H_2) : |\phi_i^R(\gamma_j(\hbar - \omega_s) - k_i^R(\delta_j(\hbar - \omega_s)))| \leq \lambda_i^{RR} |\gamma_j(\hbar - \omega_s) - \delta_j(\hbar - \omega_s)| + \lambda_i^{RI} |\gamma_j(\hbar - \omega_s) - \delta_j(\hbar - \omega_s)|,$$

$$|\phi_i^I(\gamma_j(\hbar - \omega_s) - k_i^I(\delta_j(\hbar - \omega_s)))| \leq \lambda_i^{IR} |\gamma_j(\hbar - \omega_s) - \delta_j(\hbar - \omega_s)| + \lambda_i^{II} |\gamma_j(\hbar - \omega_s) - \delta_j(\hbar - \omega_s)|.$$

From (H1) and (H2), Systems (4) and (5) can be expressed as

$$\begin{aligned}
 {}^C\nabla_0^\beta \zeta_\psi(\hbar) &= -c_\psi \zeta_\psi(\hbar) + \sum_{l=1}^m a_{\psi\phi}^R p_\phi^R(\zeta_\phi(\hbar), \chi_\phi(\hbar)) - \sum_{\phi=1}^m a_{\psi\phi}^I p_\phi^I(\zeta_\phi(\hbar), \chi_\phi(\hbar)) \\
 &+ \sum_{\phi=1}^m b_{\psi\phi}^R p_\phi^R(\zeta_\phi(\hbar - \omega), \chi_\phi(\hbar - \omega)) - \sum_{\phi=1}^m b_{\psi\phi}^I p_\phi^I(\zeta_\phi(\hbar - \omega), \chi_\phi(\hbar - \omega)) \\
 &+ \sum_{\phi=1}^m d_{\psi\phi}^R \int_0^\infty K_{\psi\phi}(s) p_\phi^R(\zeta_\phi(s), \chi_\phi(s)) ds - \sum_{\phi=1}^m d_{\psi\phi}^I \int_0^\infty K_{\psi\phi}(s) p_\phi^I(\zeta_\phi(s), \chi_\phi(s)) ds,
 \end{aligned} \tag{6}$$

$$\begin{aligned}
 {}^C\nabla_0^\beta \chi_\psi(\hbar) &= -c_\psi \chi_\psi(\hbar) + \sum_{\phi=1}^m a_{\psi\phi}^R p_\phi^I(\zeta_\phi(\hbar), \chi_\phi(\hbar)) + \sum_{\phi=1}^m a_{\psi\phi}^I p_\phi^R(\zeta_\phi(\hbar), \chi_\phi(\hbar)) \\
 &+ \sum_{\phi=1}^m b_{\psi\phi}^R p_\phi^I(\zeta_\phi(\hbar - \omega), \chi_\phi(\hbar - \omega)) + \sum_{\phi=1}^m b_{\psi\phi}^I p_\phi^R(\zeta_\phi(\hbar - \omega), \chi_\phi(\hbar - \omega)) \\
 &+ \sum_{\phi=1}^m d_{\psi\phi}^R \int_0^\infty K_{\psi\phi}(s) p_\phi^I(\zeta_\phi(s), \chi_\phi(s)) ds + \sum_{\phi=1}^m d_{\psi\phi}^I \int_0^\infty K_{\psi\phi}(s) p_\phi^R(\zeta_\phi(s), \chi_\phi(s)) ds,
 \end{aligned} \tag{7}$$

$$\begin{aligned}
 {}^C\nabla_0^\beta \zeta'_\psi(\hbar) &= -c_\psi \zeta'_\psi(\hbar) + \sum_{l=1}^m a_{\psi\phi}^R p_\phi^R(\zeta'_\phi(\hbar), \chi'_\phi(\hbar)) - \sum_{\phi=1}^m a_{\psi\phi}^I p_\phi^I(\zeta'_\phi(\hbar), \chi'_\phi(\hbar)) \\
 &+ \sum_{\phi=1}^m b_{\psi\phi}^R p_\phi^R(\zeta'_\phi(\hbar - \omega), \chi'_\phi(\hbar - \omega)) - \sum_{\phi=1}^m b_{\psi\phi}^I p_\phi^I(\zeta'_\phi(\hbar - \omega), \chi'_\phi(\hbar - \omega)) \\
 &+ \sum_{\phi=1}^m d_{\psi\phi}^R \int_0^\infty K_{\psi\phi}(s) p_\phi^R(\zeta'_\phi(s), \chi'_\phi(s)) ds - \sum_{\phi=1}^m d_{\psi\phi}^I \int_0^\infty K_{\psi\phi}(s) p_\phi^I(\zeta'_\phi(s), \chi'_\phi(s)) ds,
 \end{aligned} \tag{8}$$

$$\begin{aligned}
 {}^C\nabla_0^\beta \chi'_\psi(t) &= -c_\psi \chi'_\psi(t) + \sum_{\phi=1}^m a_{\psi\phi}^R p_\phi^I(\zeta'_\phi(\hbar), \chi'_\phi(t)) + \sum_{\phi=1}^m a_{\psi\phi}^I p_\phi^R(\zeta'_\phi(\hbar), \chi'_\phi(t)) \\
 &+ \sum_{\phi=1}^m b_{\psi\phi}^R p_\phi^I(\zeta'_\phi(\hbar - \omega), \chi'_\phi(t - \omega)) + \sum_{\phi=1}^m b_{\psi\phi}^I p_\phi^R(\zeta'_\phi(\hbar - \omega), \chi'_\phi(t - \omega)) \\
 &+ \sum_{\phi=1}^m d_{\psi\phi}^R \int_0^\infty K_{\psi\phi}(s) p_\phi^I(\zeta'_\phi(s), \chi'_\phi(s)) ds + \sum_{\phi=1}^m d_{\psi\phi}^I \int_0^\infty K_{\psi\phi}(s) p_\phi^R(\zeta'_\phi(s), \chi'_\phi(s)) ds,
 \end{aligned} \tag{9}$$

We define $\wp^R(\hbar) = \zeta'(\hbar) - \zeta(\hbar)$, $\wp^I(\hbar) = \chi'(\hbar) - \chi(\hbar)$ as the synchronization errors. Let $u_\psi(\hbar) = 0$. Then, the system's error is defined as

$$\begin{aligned}
 {}^C\nabla_0^\beta [\wp_\psi^R(\hbar)] &= -c_\psi \wp_\psi^R(\hbar) + \sum_{\phi=1}^m a_{\psi\phi}^R [p_\phi^R(\zeta'_\phi(\hbar), \chi'_\phi(\hbar)) - p_\phi^R(\zeta_\phi(\hbar), \chi_\phi(\hbar))] \\
 &- \sum_{\phi=1}^m a_{\psi\phi}^I [p_\phi^I(\zeta'_\phi(\hbar), \chi'_\phi(\hbar)) - p_\phi^I(\zeta_\phi(\hbar), \chi_\phi(\hbar))] \\
 &+ \sum_{\phi=1}^m b_{\psi\phi}^R [p_\phi^R(\zeta'_\phi(\hbar - \omega), \chi'_\phi(\hbar - \omega)) - p_\phi^R(\zeta_\phi(\hbar - \omega), \chi_\phi(\hbar - \omega))] \\
 &- \sum_{\phi=1}^m b_{\psi\phi}^I [p_\phi^I(\zeta'_\phi(\hbar - \omega), \chi'_\phi(\hbar - \omega)) - p_\phi^I(\zeta_\phi(\hbar - \omega), \chi_\phi(\hbar - \omega))] \\
 &+ \sum_{\phi=1}^m d_{\psi\phi}^R \int_0^\infty K_{\psi\phi}(s) [p_\phi^R(\zeta'_\phi(s), \chi'_\phi(s)) - p_\phi^R(\zeta_\phi(s), \chi_\phi(s))] ds
 \end{aligned} \tag{10}$$

$$\begin{aligned}
 & - \sum_{\phi=1}^m d_{\psi\phi}^I \int_0^\infty K_{\psi\phi}(s) [p_\phi^I(\zeta'_\phi(s), \chi'_\phi(s)) - p_\phi^I(\zeta_\phi^R(s), \chi_\phi(s))] ds. \\
 {}^C\nabla_0^\beta [|\varrho_\psi^I(\hbar)] & = -c_\psi \varrho_\psi^I(\hbar) + \sum_{\phi=1}^m a_{\psi\phi}^R [p_\phi^I(\zeta'_\phi(\hbar), \chi'_\phi(\hbar)) - p_\phi^I(\zeta_\phi(\hbar), \chi_\phi(\hbar))] \\
 & + \sum_{\phi=1}^m a_{\psi\phi}^I [p_\phi^R(\zeta'_\phi(\hbar), \chi'_\phi(\hbar)) - p_\phi^R(\gamma_\phi(\hbar), \gamma_\phi(\hbar))] \\
 & + \sum_{\phi=1}^m b_{\psi\phi}^R [p_\phi^I(\zeta'_\phi(\hbar - \omega), \chi'_\phi(\hbar - \omega)) - p_\phi^I(\zeta_\phi(\hbar - \omega), \chi_\phi(\hbar - \omega))] \\
 & + \sum_{\phi=1}^m b_{\psi\phi}^I [p_\phi^R(\zeta'_\phi(\hbar - \omega), \chi'_\phi(\hbar - \omega)) - p_\phi^R(\zeta_\phi(\hbar - \omega), \chi_\phi(\hbar - \omega))] \\
 & + \sum_{\phi=1}^m d_{\psi\phi}^R \int_0^\infty K_{\psi\phi}(s) [p_\phi^I(\zeta'_\phi(s), \chi'_\phi(s)) - p_\phi^I(\zeta_\phi(s), \chi_\phi(s))] \\
 & + \sum_{\phi=1}^m d_{\psi\phi}^I \int_0^\infty K_{\psi\phi}(s) [p_\phi^R(\zeta'_\phi(s), \chi'_\phi(s)) - p_\phi^R(\zeta_\phi(s), \chi_\phi(s))] ds.
 \end{aligned} \tag{11}$$

Theorem 1. Under Assumptions (H1) and (H2) and Lemma 3, Systems (10) and (11) are globally asymptotically stable and satisfy $\theta_1 > \sqrt{2}\theta_2, \theta_2 > 0$.

Proof. We construct a Lyapunov functional

$$V(\hbar) = \sum_{\psi=1}^m [|\varrho_\psi^R(\hbar)| + |\varrho_\psi^I(\hbar)|]. \tag{12}$$

In the light of Lemma 1, we can calculate the fractional difference of $V(\hbar)$,

$$\begin{aligned}
 {}^C\nabla_0^\beta V(\hbar) & \leq \sum_{\psi=1}^m {}^C\nabla_0^\beta [|\varrho_\psi^R(t)| + |\varrho_\psi^I(\hbar)|], \\
 {}^C\nabla_0^\beta V(\hbar) & = \sum_{\psi=1}^m [\text{sign}(\varrho_\psi^R(\hbar)) \left\{ -c_\psi \varrho_\psi^R(\hbar) + \sum_{\phi=1}^m a_{\psi\phi}^R [p_\phi^R(\zeta'_\phi(\hbar), \chi'_\phi(\hbar)) - p_\phi^R(\zeta_\phi(\hbar), \chi_\phi(\hbar))] \right. \\
 & - \sum_{\phi=1}^m a_{\psi\phi}^I [p_\phi^I(\zeta'_\phi(\hbar), \chi'_\phi(\hbar)) - p_\phi^I(\zeta_\phi(\hbar), \chi_\phi(\hbar))] \\
 & + \sum_{\phi=1}^m b_{\psi\phi}^R [p_\phi^R(\zeta'_\phi(\hbar - \omega), \chi'_\phi(\hbar - \omega)) - p_\phi^R(\zeta_\phi(\hbar - \omega), \chi_\phi(\hbar - \omega))] \\
 & - \sum_{\phi=1}^m b_{\psi\phi}^I [p_\phi^I(\zeta'_\phi(\hbar - \omega), \chi'_\phi(\hbar - \omega)) - p_\phi^I(\zeta_\phi(\hbar - \omega), \chi_\phi(\hbar - \omega))] \\
 & + \sum_{\phi=1}^m d_{\psi\phi}^R \int_0^\infty K_{\psi\phi}(s) [p_\phi^R(\zeta'_\phi(s), \chi'_\phi(s)) - p_\phi^R(\zeta_\phi(s), \chi_\phi(s))] ds \\
 & \left. - \sum_{\phi=1}^m d_{\psi\phi}^I \int_0^\infty K_{\psi\phi}(s) [p_\phi^I(\zeta'_\phi(s), \chi'_\phi(s)) - p_\phi^I(\zeta_\phi^R(s), \chi_\phi(s))] ds \right\} \\
 & + \sum_{\psi=1}^m \text{sign}(\varrho_\psi^I(\hbar)) \left\{ -c_\psi \varrho_\psi^I(\hbar) + \sum_{\phi=1}^m a_{\psi\phi}^R [p_\phi^I(\zeta'_\phi(\hbar), \chi'_\phi(\hbar)) - p_\phi^I(\zeta_\phi(t), \chi_\phi(\hbar))] \right. \\
 & + \sum_{\phi=1}^m a_{\psi\phi}^I [p_\phi^R(\zeta'_\phi(\hbar), \chi'_\phi(\hbar)) - p_\phi^R(\gamma_\phi(\hbar), \gamma_\phi(\hbar))]
 \end{aligned} \tag{13}$$

$$\begin{aligned}
 & + \sum_{\phi=1}^m b_{\psi\phi}^R [p_{\phi}^I(\zeta'_{\phi}(t - \omega), \chi'_{\phi}(\hbar - \omega)) - p_{\phi}^I(\zeta_{\phi}(\hbar - \omega), \chi_{\phi}(\hbar - \omega))] \\
 & + \sum_{\phi=1}^m b_{\psi\phi}^I [p_{\phi}^R(\zeta'_{\phi}(\hbar - \omega), \chi'_{\phi}(\hbar - \omega)) - p_{\phi}^R(\zeta_{\phi}(\hbar - \omega), \chi_{\phi}(\hbar - \omega))] \\
 & + \sum_{\phi=1}^m d_{\psi\phi}^R \int_0^{\infty} K_{\psi\phi}(s) [p_{\phi}^I(\zeta'_{\phi}(s), \chi'_{\phi}(s)) - p_{\phi}^I(\zeta_{\phi}(s), \chi_{\phi}(s))] \\
 & + \sum_{\phi=1}^m d_{\psi\phi}^I \int_0^{\infty} K_{\psi\phi}(s) [p_{\phi}^R(\zeta'_{\phi}(s), \chi'_{\phi}(s)) - p_{\phi}^R(\zeta_{\phi}(s), \chi_{\phi}(s))] ds \Big\}
 \end{aligned}$$

Under Assumptions (H1) and (H2), Systems (10) and (11) can be expressed as:

$$\begin{aligned}
 {}^C\nabla_0^{\beta} V(\hbar) & \leq \sum_{\psi=1}^m \left\{ -c_{\psi} |\wp_{\psi}^R(\hbar)| + \sum_{\phi=1}^m |a_{\psi\phi}^R| [|\lambda_{\phi}^{RR}| |\wp_{\phi}^R(\hbar)| + \lambda_{\phi}^{RI} |\wp_{\phi}^I(\hbar)|] \right. \\
 & + \sum_{\phi=1}^m |a_{\psi\phi}^I| [|\lambda_{\phi}^{IR}| |\wp_{\phi}^R(\hbar)| + \lambda_{\phi}^{II} |\wp_{\phi}^I(\hbar)|] \\
 & + \sum_{\phi=1}^m |b_{\psi\phi}^R| [|\lambda_{\phi}^{RR}| |\wp_{\phi}^R(\hbar - \omega)| + \lambda_{\phi}^{RI} |\wp_{\phi}^I(\hbar - \omega)|] \\
 & + \sum_{\phi=1}^m |b_{\psi\phi}^I| [|\lambda_{\phi}^{IR}| |\wp_{\phi}^R(\hbar - \omega)| + \lambda_{\phi}^{II} |\wp_{\phi}^I(\hbar - \omega)|] \\
 & + \sum_{\phi=1}^m |d_{\psi\phi}^R| \int_0^{\infty} K_{\psi\phi}(s) [|\lambda_{\phi}^{RR}| |\wp_{\phi}^R(s)| + \lambda_{\phi}^{RI} |\wp_{\phi}^I(s)|] ds \\
 & + \sum_{\phi=1}^m |d_{\psi\phi}^I| \int_0^{\infty} K_{\psi\phi}(s) [|\lambda_{\phi}^{IR}| |\wp_{\phi}^R(s)| + \lambda_{\phi}^{II} |\wp_{\phi}^I(s)|] ds \Big\} \\
 & + \sum_{\psi=1}^m \left\{ -c_{\psi} |\wp_{\psi}^I(\hbar)| + \sum_{\phi=1}^m |a_{\psi\phi}^R| [|\lambda_{\phi}^{IR}| |\wp_{\phi}^R(\hbar)| + \lambda_{\phi}^{II} |\wp_{\phi}^I(\hbar)|] \right. \\
 & + \sum_{\phi=1}^m |a_{\psi\phi}^I| [|\lambda_{\phi}^{RR}| |\wp_{\phi}^R(\hbar)| + \lambda_{\phi}^{RI} |\wp_{\phi}^I(\hbar)|] \\
 & + \sum_{\phi=1}^m |b_{\psi\phi}^R| [|\lambda_{\phi}^{IR}| |\wp_{\phi}^R(\hbar - \omega)| + \lambda_{\phi}^{II} |\wp_{\phi}^I(\hbar - \omega)|] \\
 & + \sum_{\phi=1}^m |b_{\psi\phi}^I| [|\lambda_{\phi}^{RR}| |\wp_{\phi}^R(\hbar - \omega)| + \lambda_{\phi}^{RI} |\wp_{\phi}^I(\hbar - \omega)|] \\
 & + \sum_{\phi=1}^m |d_{\psi\phi}^R| \int_0^{\infty} K_{\psi\phi}(s) [|\lambda_{\phi}^{IR}| |\wp_{\phi}^R(s)| + \lambda_{\phi}^{II} |\wp_{\phi}^I(s)|] ds \\
 & + \sum_{\phi=1}^m |d_{\psi\phi}^I| \int_0^{\infty} K_{\psi\phi}(s) [|\lambda_{\phi}^{RR}| |\wp_{\phi}^R(s)| + \lambda_{\phi}^{RI} |\wp_{\phi}^I(s)|] ds \Big\} \\
 & \leq \sum_{\psi=1}^m \left\{ -c_{\psi} |\wp_{\psi}^R(\hbar)| + \sum_{\phi=1}^m |a_{\psi\phi}^R| \lambda_{\phi}^{RR} |\wp_{\phi}^R(\hbar)| + \sum_{\phi=1}^m |a_{\psi\phi}^R| \lambda_{\phi}^{RI} |\wp_{\phi}^I(\hbar)| \right. \\
 & + \sum_{\phi=1}^m |a_{\psi\phi}^I| \lambda_{\phi}^{IR} |\wp_{\phi}^R(\hbar)| + \sum_{\phi=1}^m |a_{\psi\phi}^I| \lambda_{\phi}^{II} |\wp_{\phi}^I(\hbar)| \\
 & + \sum_{\phi=1}^m |b_{\psi\phi}^R| \lambda_{\phi}^{RR} |\wp_{\phi}^R(\hbar - \omega)| + \sum_{\phi=1}^m |b_{\psi\phi}^R| \lambda_{\phi}^{RI} |\wp_{\phi}^I(\hbar - \omega)| \\
 & + \sum_{\phi=1}^m |b_{\psi\phi}^I| \lambda_{\phi}^{IR} |\wp_{\phi}^R(\hbar - \omega)| + \sum_{\phi=1}^m |b_{\psi\phi}^I| \lambda_{\phi}^{II} |\wp_{\phi}^I(\hbar - \omega)|
 \end{aligned}$$

$$\begin{aligned}
 & + \sum_{\phi=1}^m |d_{\psi\phi}^R| \int_0^\infty K_{\psi\phi}(s) \lambda_\phi^{RR} |\wp_\phi^R(s)| ds + \sum_{\phi=1}^m |d_{\psi\phi}^R| \int_0^\infty K_{\psi\phi}(s) \lambda_\phi^{RI} |\wp_\phi^I(s)| ds \\
 & + \sum_{\phi=1}^m |d_{\psi\phi}^I| \int_0^\infty K_{\psi\phi}(s) \lambda_\phi^{IR} |\wp_\phi^R(s)| ds + \sum_{\phi=1}^m |d_{\psi\phi}^I| \int_0^\infty K_{\psi\phi}(s) \lambda_\phi^{II} |\wp_\phi^I(s)| ds \Big\} \\
 & + \sum_{\psi=1}^m \left\{ -c_\psi |\wp_\psi^I(\hbar)| + \sum_{\phi=1}^m |a_{\psi\phi}^R| \lambda_\phi^{IR} |\wp_\phi^R(\hbar)| + \sum_{\phi=1}^m |a_{\psi\phi}^R| \lambda_\phi^{II} |\wp_\phi^I(\hbar)| \right. \\
 & + \sum_{\phi=1}^m |a_{\psi\phi}^I| \lambda_\phi^{RR} |\wp_\phi^R(\hbar)| + \sum_{\phi=1}^m |a_{\psi\phi}^I| \lambda_\phi^{RI} |\wp_\phi^I(\hbar)| \\
 & + \sum_{\phi=1}^m |b_{\psi\phi}^R| \lambda_\phi^{IR} |\wp_\phi^R(\hbar - \omega)| + \sum_{\phi=1}^m |b_{\psi\phi}^R| \lambda_\phi^{II} |\wp_\phi^I(\hbar - \omega)| \\
 & + \sum_{\phi=1}^m |b_{\psi\phi}^I| \lambda_\phi^{RR} |\wp_\phi^R(\hbar - \omega)| + \sum_{\phi=1}^m |b_{\psi\phi}^I| \lambda_\phi^{RI} |\wp_\phi^I(\hbar - \omega)| \Big\} \tag{14} \\
 & + \sum_{\phi=1}^m |d_{\psi\phi}^R| \int_0^\infty K_{\psi\phi}(s) \lambda_\phi^{IR} |\wp_\phi^R(s)| ds + \sum_{\phi=1}^m |d_{\psi\phi}^R| \int_0^\infty K_{\psi\phi}(s) \lambda_\phi^{II} |\wp_\phi^I(s)| ds \\
 & + \sum_{\phi=1}^m |d_{\psi\phi}^I| \int_0^\infty K_{\psi\phi}(s) \lambda_\phi^{RR} |\wp_\phi^R(s)| ds + \sum_{\phi=1}^m |d_{\psi\phi}^I| \int_0^\infty K_{\psi\phi}(s) \lambda_\phi^{RI} |\wp_\phi^I(s)| ds \Big\} \\
 & \leq \sum_{\psi=1}^m \left\{ -c_\psi |\wp_\psi^R(\hbar)| + \sum_{\phi=1}^m |a_{\psi\phi}^R| \lambda_\phi^{RR} |\wp_\phi^R(\hbar)| + \sum_{\phi=1}^m |a_{\psi\phi}^R| \lambda_\phi^{RI} |\wp_\phi^I(\hbar)| \right. \\
 & + \sum_{\phi=1}^m |a_{\psi\phi}^I| \lambda_\phi^{IR} |\wp_\phi^R(\hbar)| + \sum_{\phi=1}^m |a_{\psi\phi}^I| \lambda_\phi^{II} |\wp_\phi^I(\hbar)| \\
 & + \sum_{\phi=1}^m |b_{\psi\phi}^R| \lambda_\phi^{RR} |\wp_\phi^R(\hbar - \omega)| + \sum_{\phi=1}^m |b_{\psi\phi}^R| \lambda_\phi^{RI} |\wp_\phi^I(\hbar - \omega)| \\
 & + \sum_{\phi=1}^m |b_{\psi\phi}^I| \lambda_\phi^{IR} |\wp_\phi^R(\hbar - \omega)| + \sum_{\phi=1}^m |b_{\psi\phi}^I| \lambda_\phi^{II} |\wp_\phi^I(\hbar - \omega)| \\
 & + \sum_{\phi=1}^m |d_{\psi\phi}^R| \lambda_\phi^{RR} |\wp_\phi^R(\hbar)| + \sum_{\phi=1}^m |d_{\psi\phi}^R| \lambda_\phi^{RI} |\wp_\phi^I(\hbar)| \\
 & + \sum_{\phi=1}^m |d_{\psi\phi}^I| \lambda_\phi^{IR} |\wp_\phi^R(\hbar)| + \sum_{\phi=1}^m |d_{\psi\phi}^I| \lambda_\phi^{II} |\wp_\phi^I(\hbar)| \Big\} \\
 & + \sum_{\psi=1}^m \left\{ -c_\psi |\wp_\psi^I(\hbar)| + \sum_{\phi=1}^m |a_{\psi\phi}^R| \lambda_\phi^{IR} |\wp_\phi^R(\hbar)| + \sum_{\phi=1}^m |a_{\psi\phi}^R| \lambda_\phi^{II} |\wp_\phi^I(\hbar)| \right. \\
 & + \sum_{\phi=1}^m |a_{\psi\phi}^I| \lambda_\phi^{RR} |\wp_\phi^R(\hbar)| + \sum_{\phi=1}^m |a_{\psi\phi}^I| \lambda_\phi^{RI} |\wp_\phi^I(\hbar)| \\
 & + \sum_{\phi=1}^m |b_{\psi\phi}^R| \lambda_\phi^{IR} |\wp_\phi^R(\hbar - \omega)| + \sum_{\phi=1}^m |b_{\psi\phi}^R| \lambda_\phi^{II} |\wp_\phi^I(\hbar - \omega)| \\
 & + \sum_{\phi=1}^m |b_{\psi\phi}^I| \lambda_\phi^{RR} |\wp_\phi^R(\hbar - \omega)| + \sum_{\phi=1}^m |b_{\psi\phi}^I| \lambda_\phi^{RI} |\wp_\phi^I(\hbar - \omega)| \\
 & + \sum_{\phi=1}^m |d_{\psi\phi}^R| \lambda_\phi^{IR} |\wp_\phi^R(\hbar)| + \sum_{\phi=1}^m |d_{\psi\phi}^R| \lambda_\phi^{II} |\wp_\phi^I(\hbar)| \\
 & + \sum_{\phi=1}^m |d_{\psi\phi}^I| \lambda_\phi^{RR} |\wp_\phi^R(\hbar)| + \sum_{\phi=1}^m |d_{\psi\phi}^I| \lambda_\phi^{RI} |\wp_\phi^I(\hbar)| \Big\}
 \end{aligned}$$

$$\begin{aligned} &\leq -\theta_{\min}^{(1)} \sum_{\psi=1}^m |\wp_{\phi}^R(\hbar)| - \theta_{\min}^{(2)} \sum_{\psi=1}^m |\wp_{\phi}^I(\hbar)| + \theta_{\max}^{(1)} \sum_{\psi=1}^m |\wp_{\phi}^R(\hbar - \omega)| + \theta_{\max}^{(2)} \sum_{\psi=1}^m |\wp_{\phi}^I(\hbar - \omega)|, \\ &= -\theta_1 V(\hbar) + \theta_2 V(\hbar - \omega), \end{aligned}$$

where

$$\begin{aligned} \theta_{\min}^{(1)} &= \left\{ c_{\psi} - \sum_{\phi}^m |a_{\phi\psi}^R| \lambda_{\psi}^{RR} - \sum_{\phi=1}^m |a_{\phi\psi}^I| \lambda_{\psi}^{IR} - \sum_{\phi=1}^m |d_{\phi\psi}^R| \lambda_{\psi}^{RR} - \sum_{\phi=1}^m |d_{\phi\psi}^I| \lambda_{\psi}^{IR} \right. \\ &\quad \left. - \sum_{\phi=1}^m |a_{\phi\psi}^R| \lambda_{\psi}^{IR} - \sum_{\phi=1}^m |a_{\phi\psi}^I| \lambda_{\psi}^{RR} - \sum_{\phi=1}^m |d_{\phi\psi}^R| \lambda_{\psi}^{IR} - \sum_{\phi=1}^m |d_{\phi\psi}^I| \lambda_{\psi}^{RR} \right\}, \\ \theta_{\min}^{(2)} &= \left\{ c_{\psi} - \sum_{\phi}^m |a_{\phi\psi}^R| \lambda_{\psi}^{RI} - \sum_{\phi=1}^m |a_{\phi\psi}^I| \lambda_{\psi}^{II} - \sum_{\phi=1}^m |d_{\phi\psi}^R| \lambda_{\psi}^{RI} - \sum_{\phi=1}^m |d_{\phi\psi}^I| \lambda_{\psi}^{II} \right. \\ &\quad \left. - \sum_{\phi=1}^m |a_{\phi\psi}^R| \lambda_{\psi}^{II} - \sum_{\phi=1}^m |a_{\phi\psi}^I| \lambda_{\psi}^{RI} - \sum_{\phi=1}^m |d_{\phi\psi}^R| \lambda_{\psi}^{II} - \sum_{\phi=1}^m |d_{\phi\psi}^I| \lambda_{\psi}^{RI} \right\}, \\ \theta_{\max}^{(1)} &= \sum_{\psi=1}^m \left\{ \sum_{\phi=1}^m |b_{\psi\phi}^I| \lambda_{\phi}^{RR} + \sum_{\phi=1}^m |b_{\psi\phi}^I| \lambda_{\phi}^{IR} + \sum_{\phi=1}^m |b_{\psi\phi}^R| \lambda_{\phi}^{IR} + \sum_{\phi=1}^m |b_{\psi\phi}^I| \lambda_{\phi}^{RR} \right\}, \\ \theta_{\max}^{(2)} &= \sum_{\psi=1}^m \left\{ \sum_{\phi=1}^m |b_{\psi\phi}^R| \lambda_{\phi}^{IR} + \sum_{\phi=1}^m |b_{\psi\phi}^I| \lambda_{\phi}^{II} + \sum_{\phi=1}^m |b_{\psi\phi}^R| \lambda_{\phi}^{II} + \sum_{\phi=1}^m |b_{\psi\phi}^I| \lambda_{\phi}^{RI} \right\}, \end{aligned}$$

By Lemma 3, $\theta_1 > \sqrt{2}\theta_2, \theta_2 > 0$.

Consequently, Systems (10) and (11) are globally asymptotically stable. \square

Theorem 2. Under Assumptions (H1) and (H2) and Lemma 3, Systems (10) and (11) are globally asymptotically stable and satisfy $\Theta_1 > \sqrt{2}\Theta_2, \Theta_2 > 0$.

Proof. Consider the auxiliary function

$$V(\hbar) = \sum_{\psi=1}^m \frac{1}{2} (\wp_{\psi}^R(\hbar))^2 + \sum_{\psi=1}^m \frac{1}{2} (\wp_{\psi}^I(\hbar))^2. \tag{15}$$

In light of Lemma 2, calculating the fractional difference of $V(t)$, we have

$$\begin{aligned} {}^C\nabla_0^{\beta} V(\hbar) &\leq \sum_{\psi=1}^m \left\{ -c_{\psi} (\wp_{\psi}^R(\hbar))^2 + \sum_{\phi=1}^m a_{\psi\phi}^R \wp_{\psi}^R(t) [\lambda_{\phi}^{RR} \wp_{\phi}^R(\hbar) + \lambda_{\phi}^{RI} \wp_{\phi}^I(t)] \right. \\ &\quad + \sum_{\phi=1}^m a_{\psi\phi}^I \wp_{\psi}^R(\hbar) [\lambda_{\phi}^{IR} \wp_{\phi}^R(\hbar) + \lambda_{\phi}^{II} \wp_{\phi}^I(\hbar)] \\ &\quad + \sum_{\phi=1}^m b_{\psi\phi}^R \wp_{\psi}^R(\hbar) [\lambda_{\phi}^{RR} \wp_{\phi}^R(\hbar - \omega) + \lambda_{\phi}^{RI} \wp_{\phi}^I(\hbar - \omega)] \\ &\quad + \sum_{\phi=1}^m b_{\psi\phi}^I \wp_{\psi}^R(\hbar) [\lambda_{\phi}^{IR} \wp_{\phi}^R(\hbar - \omega) + \lambda_{\phi}^{II} \wp_{\phi}^I(\hbar - \omega)] \\ &\quad + \sum_{\phi=1}^m d_{\psi\phi}^R \wp_{\psi}^R(\hbar) \int_0^{\infty} K_{\psi\phi}(s) [\lambda_{\phi}^{RR} \wp_{\phi}^R(s) + \lambda_{\phi}^{RI} \wp_{\phi}^I(s)] ds \\ &\quad + \sum_{\phi=1}^m d_{\psi\phi}^I \wp_{\psi}^R(\hbar) \int_0^{\infty} K_{\psi\phi}(s) [\lambda_{\phi}^{IR} \wp_{\phi}^R(s) + \lambda_{\phi}^{II} \wp_{\phi}^I(s)] ds \left. \right\} \\ &\quad + \sum_{\psi=1}^m \left\{ -c_{\psi} (\wp_{\psi}^I(\hbar))^2 + \sum_{\phi=1}^m a_{\psi\phi}^R \wp_{\psi}^I(\hbar) [\lambda_{\phi}^{IR} \wp_{\phi}^R(\hbar) + \lambda_{\phi}^{II} \wp_{\phi}^I(\hbar)] \right. \end{aligned}$$

$$\begin{aligned}
 & + \sum_{\phi=1}^m a_{\psi\phi}^I \wp_{\psi}^I(t) [\lambda_k^{RR} \wp_{\phi}^R(\hbar) + \lambda_{\phi}^{RI} \wp_{\phi}^I(\hbar)] \\
 & + \sum_{\phi=1}^m b_{\psi\phi}^R \wp_{\psi}^I(\hbar) [\lambda_{\phi}^{IR} \wp_{\phi}^R(\hbar - \omega) + \lambda_{\phi}^{II} \wp_{\phi}^I(\hbar - \omega)] \\
 & + \sum_{\phi=1}^m b_{\psi\phi}^I \wp_{\psi}^I(\hbar) [\lambda_{\phi}^{RR} \wp_{\phi}^R(\hbar - \omega) + \lambda_{\phi}^{RI} \wp_{\phi}^I(\hbar - \omega)] \\
 & + \sum_{\phi=1}^m d_{\psi\phi}^R \wp_{\psi}^I(\hbar) \int_0^{\infty} K_{\psi\phi}(s) [\lambda_{\phi}^{IR} \wp_{\phi}^R(s) + \lambda_{\phi}^{II} \wp_{\phi}^I(s)] ds \\
 & + \sum_{\phi=1}^m d_{\psi\phi}^I \wp_{\psi}^I(\hbar) \int_0^{\infty} K_{\psi\phi}(s) [\lambda_{\phi}^{RR} \wp_{\phi}^R(s) + \lambda_{\phi}^{RI} \wp_{\phi}^I(s)] ds \Big\} \\
 & \leq \sum_{\psi=1}^m \left\{ -c_{\psi} (\wp_{\psi}^R(\hbar))^2 + \left[\sum_{\phi=1}^m a_{\psi\phi}^R \wp_{\psi}^R(\hbar) \lambda_{\phi}^{RR} \wp_{\phi}^R(\hbar) + \sum_{\phi=1}^m a_{\psi\phi}^R \wp_{\psi}^R(\hbar) \lambda_{\phi}^{RI} \wp_{\phi}^I(\hbar) \right] \right. \\
 & + \left[\sum_{\phi=1}^m a_{\psi\phi}^I \wp_{\psi}^R(\hbar) \lambda_k^{IR} \wp_{\phi}^R(\hbar) + \sum_{\phi=1}^m a_{\psi\phi}^I \wp_{\psi}^R(\hbar) \lambda_{\phi}^{II} \wp_{\phi}^I(\hbar) \right] \\
 & + \left[\sum_{\phi=1}^m b_{\psi\phi}^R \wp_{\psi}^R(\hbar) \sum_{\phi=1}^m b_{\psi\phi}^R \wp_{\psi}^R(\hbar) \lambda_{\phi}^{RR} \wp_{\phi}^R(t - \omega) + \sum_{\phi=1}^m b_{\psi\phi}^R \wp_{\psi}^R(\hbar) \lambda_{\phi}^{RI} \wp_{\phi}^I(\hbar - \omega) \right] \\
 & + \left[\sum_{\phi=1}^m b_{\psi\phi}^I \wp_{\psi}^R(\hbar) \lambda_{\phi}^{IR} \wp_{\phi}^R(\hbar - \omega) + \sum_{\phi=1}^m b_{\psi\phi}^I \wp_{\psi}^R(\hbar) \lambda_{\phi}^{II} \wp_{\phi}^I(\hbar - \omega) \right] \\
 & + \left[\sum_{\phi=1}^m d_{\psi\phi}^R \wp_{\psi}^R(\hbar) \int_0^{\infty} K_{\psi\phi}(s) \lambda_{\phi}^{RR} \wp_{\phi}^R(s) + \sum_{\phi=1}^m d_{\psi\phi}^R \wp_{\psi}^R(\hbar) \int_0^{\infty} K_{\psi\phi}(s) \lambda_{\phi}^{RI} \wp_{\phi}^I(s) \right] ds \\
 & + \left. \left[\sum_{\phi=1}^m d_{\psi\phi}^I \wp_{\psi}^R(\hbar) \int_0^{\infty} K_{\psi\phi}(s) \lambda_{\phi}^{IR} \wp_{\phi}^R(s) + \sum_{\phi=1}^m d_{\psi\phi}^I \wp_{\psi}^R(\hbar) \int_0^{\infty} K_{\psi\phi}(s) \lambda_{\phi}^{II} \wp_{\phi}^I(s) \right] ds \right\} \\
 & + \sum_{\psi=1}^m \left\{ -c_{\psi} (\wp_{\psi}^I(\hbar))^2 + \left[\sum_{\phi=1}^m a_{\psi\phi}^R \wp_{\psi}^I(\hbar) \lambda_k^{IR} \wp_{\phi}^R(\hbar) + \sum_{\phi=1}^m a_{\psi\phi}^R \wp_{\psi}^I(\hbar) \lambda_{\phi}^{II} \wp_{\phi}^I(\hbar) \right] \right. \\
 & + \sum_{\phi=1}^m a_{\psi\phi}^I \wp_{\psi}^I(\hbar) \lambda_k^{RR} \wp_{\phi}^R(\hbar) + \sum_{\phi=1}^m a_{\psi\phi}^I \wp_{\psi}^I(\hbar) \lambda_{\phi}^{RI} \wp_{\phi}^I(\hbar) \\
 & + \left[\sum_{\phi=1}^m b_{\psi\phi}^R \wp_{\psi}^I(\hbar) \lambda_{\phi}^{IR} \wp_{\phi}^R(\hbar - \omega) + \sum_{\phi=1}^m b_{\psi\phi}^R \wp_{\psi}^I(\hbar) \lambda_{\phi}^{II} \wp_{\phi}^I(\hbar - \omega) \right] \\
 & + \left[\sum_{\phi=1}^m b_{\psi\phi}^I \wp_{\psi}^I(\hbar) \lambda_{\phi}^{RR} \wp_{\phi}^R(\hbar - \omega) + \sum_{\phi=1}^m b_{\psi\phi}^I \wp_{\psi}^I(\hbar) \lambda_{\phi}^{RI} \wp_{\phi}^I(t - \omega) \right] \\
 & + \left[\sum_{\phi=1}^m d_{\psi\phi}^R \wp_{\psi}^I(t) \int_0^{\infty} K_{\psi\phi}(s) \lambda_{\phi}^{IR} \wp_{\phi}^R(s) ds + \sum_{\phi=1}^m d_{\psi\phi}^R \wp_{\psi}^I(\hbar) \int_0^{\infty} K_{\psi\phi}(s) \lambda_{\phi}^{II} \wp_{\phi}^I(s) ds \right] \\
 & + \left. \left[\sum_{\phi=1}^m d_{\psi\phi}^I \wp_{\psi}^I(\hbar) \int_0^{\infty} K_{\psi\phi}(s) \lambda_{\phi}^{RR} \wp_{\phi}^R(s) ds + \sum_{\phi=1}^m d_{\psi\phi}^I \wp_{\psi}^I(\hbar) \int_0^{\infty} K_{\psi\phi}(s) \lambda_{\phi}^{RI} \wp_{\phi}^I(s) ds \right] \right\} \\
 & \leq \sum_{\psi=1}^m \left\{ -c_{\psi} (\wp_{\psi}^R(\hbar))^2 + \left[\sum_{\phi=1}^m a_{\psi\phi}^R \wp_{\psi}^R(\hbar) \lambda_{\phi}^{RR} \wp_{\phi}^R(\hbar) + \sum_{\phi=1}^m a_{\psi\phi}^R \wp_{\psi}^R(\hbar) \lambda_{\phi}^{RI} \wp_{\phi}^I(\hbar) \right] \right. \\
 & + \left[\sum_{\phi=1}^m a_{\psi\phi}^I \wp_{\psi}^R(\hbar) \lambda_k^{IR} \wp_{\phi}^R(t) + \sum_{\phi=1}^m a_{\psi\phi}^I \wp_{\psi}^R(\hbar) \lambda_{\phi}^{II} \wp_{\phi}^I(\hbar) \right] \\
 & + \left. \left[\sum_{\phi=1}^m b_{\psi\phi}^R \wp_{\psi}^R(\hbar) \sum_{\phi=1}^m b_{\psi\phi}^R \wp_{\psi}^R(\hbar - \omega) \lambda_{\phi}^{RR} \wp_{\phi}^R(\hbar - \omega) + \sum_{\phi=1}^m b_{\psi\phi}^R \wp_{\psi}^R(t) \lambda_{\phi}^{RI} \wp_{\phi}^I(t - \tau) \right] \right\}
 \end{aligned}$$

$$\begin{aligned}
 & + \left[\sum_{\phi=1}^m b_{\psi\phi}^I \wp_{\psi}^R(\hbar) \lambda_{\phi}^{IR} \wp_{\phi}^R(\hbar - \omega) + \sum_{\phi=1}^m b_{\psi\phi}^I \wp_{\psi}^R(\hbar) \lambda_{\phi}^{II} \wp_{\phi}^I(\hbar - \omega) \right] \\
 & + \left[\sum_{\phi=1}^m d_{\psi\phi}^R \wp_{\psi}^R(\hbar) \lambda_{\phi}^{RR} \wp_{\phi}^R(\hbar) + \sum_{\phi=1}^m d_{\psi\phi}^R \wp_{\psi}^R(\hbar) \lambda_{\phi}^{RI} \wp_{\phi}^I(t) \right] \\
 & + \left. \left[\sum_{\phi=1}^m d_{\psi\phi}^I \wp_{\psi}^R(\hbar) \lambda_{\phi}^{IR} \wp_{\phi}^R(\hbar) + \sum_{\phi=1}^m d_{\psi\phi}^I \wp_{\psi}^R(\hbar) \lambda_{\phi}^{II} \wp_{\phi}^I(\hbar) \right] \right\} \\
 & + \sum_{\psi=1}^m \left\{ -c_{\psi}(\wp_{\psi}^I(\hbar))^2 + \left[\sum_{\phi=1}^m a_{\psi\phi}^R \wp_{\psi}^I(\hbar) \lambda_{\phi}^{IR} \wp_{\phi}^R(\hbar) + \sum_{\phi=1}^m a_{\psi\phi}^R \wp_{\psi}^I(\hbar) \lambda_{\phi}^{II} \wp_{\phi}^I(\hbar) \right] \right. \\
 & + \left[\sum_{\phi=1}^m a_{\psi\phi}^I \wp_{\psi}^I(\hbar) \lambda_{\phi}^{RR} \wp_{\phi}^R(\hbar) + \sum_{\phi=1}^m a_{\psi\phi}^I \wp_{\psi}^I(t) \lambda_{\phi}^{RI} \wp_{\phi}^I(t) \right] \\
 & + \left[\sum_{\phi=1}^m b_{\psi\phi}^R \wp_{\psi}^I(\hbar) \lambda_{\phi}^{IR} \wp_{\phi}^R(\hbar - \omega) + \sum_{\phi=1}^m b_{\psi\phi}^R \wp_{\psi}^I(\hbar) \lambda_{\phi}^{II} \wp_{\phi}^I(\hbar - \omega) \right] \\
 & + \left[\sum_{\phi=1}^m b_{\psi\phi}^I \wp_{\psi}^I(\hbar) \lambda_{\phi}^{RR} \wp_{\phi}^R(\hbar - \omega) + \sum_{\phi=1}^m b_{\psi\phi}^I \wp_{\psi}^I(\hbar) \lambda_{\phi}^{RI} \wp_{\phi}^I(\hbar - \omega) \right] \\
 & + \left[\sum_{\phi=1}^m d_{\psi\phi}^R \wp_{\psi}^I(\hbar) \lambda_{\phi}^{IR} \wp_{\phi}^R(\hbar) + \sum_{\phi=1}^m d_{\psi\phi}^R \wp_{\psi}^I(t) \lambda_{\phi}^{II} \wp_{\phi}^I(\hbar) \right] \\
 & + \left. \left[\sum_{\phi=1}^m d_{\psi\phi}^I \wp_{\psi}^I(\hbar) \lambda_{\phi}^{RR} \wp_{\phi}^R(\hbar) + \sum_{\phi=1}^m d_{\psi\phi}^I \wp_{\psi}^I(\hbar) \lambda_{\phi}^{RI} \wp_{\phi}^I(t) \right] \right\} \\
 & \leq \sum_{\psi=1}^m \left\{ -c_{\psi}(\wp_{\psi}^R(\hbar))^2 + \left[\frac{1}{2} \sum_{\phi=1}^m a_{\psi\phi}^R \lambda_{\phi}^{RR} [(\wp_{\psi}^R(\hbar))^2 + (\wp_{\phi}^R(\hbar))^2] \right. \right. \\
 & + \frac{1}{2} \sum_{\phi=1}^m a_{\psi\phi}^R \lambda_{\phi}^{RI} [(\wp_{\psi}^R(t))^2 + (\wp_{\phi}^I(\hbar))^2] + \left[\frac{1}{2} \sum_{\phi=1}^m a_{\psi\phi}^I \lambda_{\phi}^{IR} [(\wp_{\psi}^R(\hbar))^2 + (\wp_{\phi}^R(\hbar))^2] \right. \\
 & + \frac{1}{2} \sum_{\phi=1}^m a_{\psi\phi}^I \lambda_{\phi}^{II} [(\wp_{\psi}^R(\hbar))^2 + (\wp_{\phi}^I(\hbar))^2] + \left. \left. \left[\frac{1}{2} \sum_{\phi=1}^m b_{\psi\phi}^R \lambda_{\phi}^{RR} [(\wp_{\psi}^R(\hbar))^2 + (\wp_{\psi}^R(\hbar - \omega))^2] \right. \right. \right. \\
 & + \left. \left. \frac{1}{2} \sum_{\phi=1}^m b_{\psi\phi}^R \lambda_{\phi}^{RI} [(\wp_{\psi}^R(\hbar))^2 + (\wp_{\phi}^I(\hbar - \omega))^2] \right] \right. \\
 & + \left. \left[\frac{1}{2} \sum_{\phi=1}^m b_{\psi\phi}^I \lambda_{\phi}^{RR} [(\wp_{\psi}^R(\hbar))^2 + (\wp_{\phi}^R(\hbar - \tau))^2] + \frac{1}{2} \sum_{\phi=1}^m b_{\psi\phi}^I \lambda_{\phi}^{RI} [(\wp_{\psi}^R(\hbar))^2 + (\wp_{\phi}^I(\hbar - \tau))^2] \right] \right. \\
 & + \left. \left[\frac{1}{2} \sum_{\phi=1}^m d_{\psi\phi}^R \lambda_{\phi}^{RR} [(\wp_{\psi}^R(\hbar))^2 + (\wp_{\phi}^R(\hbar))^2] + \frac{1}{2} \sum_{\phi=1}^m d_{\psi\phi}^R \lambda_{\phi}^{RI} [(\wp_{\psi}^R(\hbar))^2 + (\wp_{\phi}^I(\hbar))^2] \right] \right. \\
 & + \left. \left. \left[\frac{1}{2} \sum_{\phi=1}^m d_{\psi\phi}^I \lambda_{\phi}^{IR} [(\wp_{\psi}^R(\hbar))^2 + (\wp_{\phi}^R(\hbar))^2] + \frac{1}{2} \sum_{\phi=1}^m d_{\psi\phi}^I \lambda_{\phi}^{II} [(\wp_{\psi}^R(\hbar))^2 + (\wp_{\phi}^I(\hbar))^2] \right] \right\} \\
 & + \frac{1}{2} \sum_{\psi=1}^m \left\{ -c_{\psi}(\wp_{\psi}^I(\hbar))^2 + \left[\frac{1}{2} \sum_{\phi=1}^m a_{\psi\phi}^R \lambda_{\phi}^{IR} [(\wp_{\psi}^I(\hbar))^2 + (\wp_{\phi}^R(t))^2] + \frac{1}{2} \sum_{\phi=1}^m a_{\psi\phi}^R \lambda_{\phi}^{II} [(\wp_{\psi}^I(t))^2 + (\wp_{\phi}^I(\hbar))^2] \right] \right. \\
 & + \left[\frac{1}{2} \sum_{\phi=1}^m a_{\psi\phi}^I \lambda_{\phi}^{RR} [(\wp_{\psi}^I(\hbar))^2 + (\wp_{\phi}^R(\hbar))^2] + \frac{1}{2} \sum_{\phi=1}^m a_{\psi\phi}^I \lambda_{\phi}^{RI} [(\wp_{\psi}^I(\hbar))^2 + (\wp_{\phi}^I(\hbar))^2] \right] \\
 & + \left. \left[\frac{1}{2} \sum_{\phi=1}^m b_{\psi\phi}^R \lambda_{\phi}^{IR} [(\wp_{\psi}^I(\hbar))^2 + (\wp_{\phi}^R(\hbar - \omega))^2] + \frac{1}{2} \sum_{\phi=1}^m b_{\psi\phi}^R \lambda_{\phi}^{II} [(\wp_{\psi}^I(\hbar))^2 + (\wp_{\phi}^I(\hbar - \omega))^2] \right] \right. \\
 & + \left. \left. \left[\frac{1}{2} \sum_{\phi=1}^m b_{\psi\phi}^I \lambda_{\phi}^{RR} [(\wp_{\psi}^I(\hbar))^2 + (\wp_{\phi}^R(\hbar - \omega))^2] + \frac{1}{2} \sum_{\phi=1}^m b_{\psi\phi}^I \lambda_{\phi}^{RI} [(\wp_{\psi}^I(\hbar))^2 + (\wp_{\phi}^I(\hbar - \omega))^2] \right] \right\}
 \end{aligned}
 \tag{16}$$

$$\begin{aligned}
 &+ \left[\frac{1}{2} \sum_{\phi=1}^m d_{\psi\phi}^R \lambda_{\phi}^{IR} [(\varphi_{\psi}^I(\hbar))^2 + (\varphi_{\phi}^R(\hbar))^2] + \frac{1}{2} \sum_{\phi=1}^m d_{\psi\phi}^R \lambda_{\phi}^{II} [(\varphi_{\psi}^I(\hbar))^2 + (\varphi_{\phi}^I(\hbar))^2] \right. \\
 &+ \left. \left[\frac{1}{2} \sum_{\phi=1}^m d_{\psi\phi}^I \lambda_{\phi}^{RR} [(\varphi_{\psi}^I(\hbar))^2 + (\varphi_{\phi}^R(s))^2] + \frac{1}{2} \sum_{\phi=1}^m d_{\psi\phi}^I \lambda_{\phi}^{RI} [(\varphi_{\psi}^I(\hbar))^2 + (\varphi_{\phi}^I(s))^2] \right] \right\} \\
 &\leq -\Theta_{\min}^{(1)} \frac{1}{2} \sum_{\psi=1}^m (\varphi_{\psi}^R(t))^2 - \Theta_{\min}^{(2)} \frac{1}{2} \sum_{\psi=1}^m (\varphi_{\psi}^I(t))^2 + \Theta_{\max}^{(1)} \frac{1}{2} \sum_{\psi=1}^m (\varphi_{\psi}^R(\hbar - \omega))^2 + \Theta_{\max}^{(2)} \frac{1}{2} \sum_{\psi=1}^m (\varphi_{\psi}^I(\hbar - \omega))^2, \\
 &= -\Theta_1 V(\hbar) + \Theta_2 V(\hbar - \omega),
 \end{aligned}$$

where

$$\begin{aligned}
 \Theta_{\min}^{(1)} &= \left\{ c_{\psi} - \frac{1}{2} \sum_{\phi=1}^m a_{\psi\phi}^R \lambda_{\phi}^{RR} - \frac{1}{2} \sum_{\phi=1}^m a_{\phi\psi}^R \lambda_{\psi}^{RR} - \frac{1}{2} \sum_{\phi=1}^m a_{\phi\psi}^R \lambda_{\psi}^{RI} - \frac{1}{2} \sum_{\phi=1}^m a_{\psi\phi}^I \lambda_{\phi}^{IR} \right. \\
 &- \frac{1}{2} \sum_{\phi=1}^m a_{\phi\psi}^I \lambda_{\psi}^{IR} - \frac{1}{2} \sum_{\phi=1}^m a_{\phi\psi}^I \lambda_{\phi}^{II} - \frac{1}{2} \sum_{\phi=1}^m b_{\psi\phi}^R \lambda_{\phi}^{RR} - \frac{1}{2} \sum_{\phi=1}^m b_{\psi\phi}^R \lambda_{\phi}^{RI} - \frac{1}{2} \sum_{\phi=1}^m b_{\psi\phi}^I \lambda_{\phi}^{RR} \\
 &- \frac{1}{2} \sum_{\phi=1}^m b_{\psi\phi}^I \lambda_{\phi}^{RI} - \frac{1}{2} \sum_{\phi=1}^m d_{\psi\phi}^R \lambda_{\phi}^{RR} - \frac{1}{2} \sum_{\phi=1}^m d_{\phi\psi}^R \lambda_{\psi}^{RR} - \frac{1}{2} \sum_{\phi=1}^m d_{\psi\phi}^R \lambda_{\phi}^{RI} \\
 &- \frac{1}{2} \sum_{\phi=1}^m d_{\phi\psi}^I \lambda_{\psi}^{IR} - \frac{1}{2} \sum_{\phi=1}^m d_{\phi\psi}^I \lambda_{\psi}^{IR} - \frac{1}{2} \sum_{\phi=1}^m d_{\psi\phi}^I \lambda_{\phi}^{II} - \frac{1}{2} \sum_{\phi=1}^m a_{\psi\phi}^R \lambda_{\phi}^{IR} \\
 &\left. - \frac{1}{2} \sum_{\phi=1}^m a_{\phi\psi}^I \lambda_{\psi}^{RR} - \frac{1}{2} \sum_{\phi=1}^m d_{\psi\phi}^R \lambda_{\psi}^{IR} - \frac{1}{2} \sum_{\phi=1}^m d_{\phi\psi}^I \lambda_{\psi}^{RR} \right\}, \\
 \Theta_{\min}^{(2)} &= \left\{ c_{\psi} - \frac{1}{2} \sum_{\phi=1}^m a_{\psi\phi}^R \lambda_{\phi}^{IR} - \frac{1}{2} \sum_{\phi=1}^m a_{\psi\phi}^R \lambda_{\phi}^{II} - \frac{1}{2} \sum_{\phi=1}^m a_{\phi\psi}^R \lambda_{\psi}^{II} - \frac{1}{2} \sum_{\phi=1}^m a_{\psi\phi}^I \lambda_{\phi}^{RR} \right. \\
 &- \frac{1}{2} \sum_{\phi=1}^m a_{\psi\phi}^I \lambda_{\phi}^{RI} - \frac{1}{2} \sum_{\phi=1}^m a_{\phi\psi}^I \lambda_{\psi}^{RI} - \frac{1}{2} \sum_{\phi=1}^m b_{\psi\phi}^R \lambda_{\phi}^{IR} - \frac{1}{2} \sum_{\phi=1}^m b_{\psi\phi}^R \lambda_{\phi}^{II} \\
 &- \frac{1}{2} \sum_{\phi=1}^m b_{\psi\phi}^I \lambda_{\phi}^{RR} - \frac{1}{2} \sum_{\phi=1}^m b_{\psi\phi}^I \lambda_{\phi}^{RI} - \frac{1}{2} \sum_{\phi=1}^m d_{\psi\phi}^R \lambda_{\psi}^{IR} - \frac{1}{2} \sum_{\phi=1}^m d_{\psi\phi}^R \lambda_{\phi}^{II} \\
 &- \frac{1}{2} \sum_{\phi=1}^m d_{\phi\psi}^R \lambda_{\psi}^{II} - \frac{1}{2} \sum_{\phi=1}^m d_{\psi\phi}^I \lambda_{\phi}^{RR} - \frac{1}{2} \sum_{\phi=1}^m d_{\psi\phi}^I \lambda_{\phi}^{RI} - \frac{1}{2} \sum_{\phi=1}^m d_{\phi\psi}^I \lambda_{\psi}^{RI} \\
 &\left. - \frac{1}{2} \sum_{\phi=1}^m a_{\phi\psi}^R \lambda_{\psi}^{RI} - \frac{1}{2} \sum_{\phi=1}^m a_{\phi\psi}^I \lambda_{\phi}^{II} - \frac{1}{2} \sum_{\phi=1}^m d_{\phi\psi}^I \lambda_{\psi}^{RI} - \frac{1}{2} \sum_{\phi=1}^m d_{\phi\psi}^I \lambda_{\psi}^{II} \right\}, \\
 \Theta_{\max}^{(1)} &= \sum_{\psi=1}^m \left\{ \sum_{\phi=1}^m b_{\psi\phi}^I \lambda_{\phi}^{RR} + \sum_{\phi=1}^m b_{\psi\phi}^I \lambda_{\phi}^{IR} + \sum_{\phi=1}^m b_{\psi\phi}^R \lambda_{\phi}^{IR} + \sum_{\phi=1}^m b_{\psi\phi}^I \lambda_{\phi}^{RR} \right\}, \\
 \Theta_{\max}^{(2)} &= \sum_{\psi=1}^m \left\{ \sum_{\phi=1}^m |b_{\psi\phi}^R \lambda_{\phi}^{IR} + \sum_{\phi=1}^m b_{\psi\phi}^I \lambda_{\phi}^{II} + \sum_{\phi=1}^m b_{\psi\phi}^R \lambda_{\phi}^{II} + \sum_{\phi=1}^m b_{\psi\phi}^I \lambda_{\phi}^{RI} \right\},
 \end{aligned}$$

By Lemma 3, $\Theta_1 > \sqrt{2}\Theta_2$, and $\Theta_2 > 0$.

Consequently, Systems (10) and (11) are globally asymptotically stable. \square

Remark 1. Consider the master system

$$\begin{aligned}
 {}^C \nabla_0^{\beta} \gamma_{\psi}(\hbar) &= -c_{\psi} \gamma_{\psi}(\hbar) + \sum_{\phi=1}^m a_{\psi\phi} f_{\phi}(\gamma_{\phi}(\hbar)) + \sum_{\phi=1}^m b_{\psi\phi} f_{\phi}(\gamma_{\phi}(\hbar - \omega)) \\
 &+ \sum_{\phi=1}^m d_{\psi\phi} \int_0^{\infty} K_{\psi\phi}(s) f_{\phi}(\gamma_{\phi}(s)) ds + I_{\psi}, \hbar \in N_1,
 \end{aligned} \tag{17}$$

Consider the slave system

$$\begin{aligned}
 {}^C\nabla_0^\beta \tilde{\gamma}_\psi(\hbar) &= -c_\psi \tilde{\gamma}_\psi(\hbar) + \sum_{\phi=1}^m a_{\psi\phi} f_\phi(\tilde{\gamma}_\phi(\hbar)) + \sum_{\phi=1}^m b_{\psi\phi} f_\phi(\tilde{\gamma}_\phi(\hbar - \omega)) \\
 &+ \sum_{\phi=1}^m d_{\psi\phi} \int_0^\infty K_{\psi\phi}(s) f_\phi(\tilde{\gamma}_\phi(s)) ds + I_\psi + u_\psi(\hbar), \hbar \in N_1,
 \end{aligned}
 \tag{18}$$

The error system is defined as

$$\begin{aligned}
 {}^C\nabla_0^\beta \wp_\psi(\hbar) &= -c_\psi \wp_\psi(\hbar) + \sum_{\phi=1}^m a_{\psi\phi} f_\phi(\wp_\phi(\hbar)) + \sum_{\phi=1}^m b_{\psi\phi} f_\phi(\wp_\phi(\hbar - \omega)) \\
 &+ \sum_{\phi=1}^m d_{\psi\phi} \int_0^\infty K_{\psi\phi}(s) f_\phi(\wp_\phi(s)) ds + u_\psi(\hbar), \hbar \in N_1,
 \end{aligned}
 \tag{19}$$

Theorem 3. Under Assumptions (H1) and (H2), the system is globally Mittag–Leffler stable if the activation functions are bounded. Let $u_\psi(\hbar) = 0$; then,

$$0 < \rho = \rho_1 - \rho_2 < 1,$$

$$\rho_1 = \min_{1 \leq \psi \leq m} \left\{ c_\psi - \sum_{\phi=1}^m |a_{\psi\phi}| L_\psi - \sum_{\phi=1}^m |d_{\psi\phi}^I| L_\psi \right\} \tag{20}$$

$$\rho_2 = \max_{1 \leq \psi \leq m} \left\{ \sum_{\phi=1}^n |b_{\psi\phi}| L_\phi \right\} > 0$$

Proof. Let us consider the Lyapunov functional

$$V(t, \zeta(t)) = \sum_{\psi=1}^m |\wp_\psi(t)|. \tag{21}$$

By calculating the Nabla–Caputo left-fractional difference of $V(t)$ along the trajectories of System (1), we obtain

$$\begin{aligned}
 {}^C\nabla_0^\beta V(t, \wp(\hbar)) &\leq \sum_{\psi=1}^m \text{sign}(\wp(\hbar)) \left\{ -c_\psi \wp_\psi(\hbar) + \sum_{\phi=1}^m a_{\psi\phi} f_\phi(\wp_\phi(\hbar)) + \sum_{\phi=1}^m b_{\psi\phi} f_\phi(\wp_\phi(\hbar - \tau)) \right. \\
 &+ \left. \sum_{\phi=1}^m d_{\psi\phi} \int_0^\infty K_{\psi\phi}(s) f_\phi(\wp_\phi(s)) ds \right\} \\
 &\leq \sum_{\psi=1}^m \left\{ -c_\psi |\wp_\psi(\hbar)| + \sum_{\phi=1}^m |a_{\psi\phi}| f_\phi(\wp_\phi(\hbar)) + \sum_{\phi=1}^m |b_{\psi\phi}| f_\phi(\wp_\phi(\hbar - \omega)) \right. \\
 &+ \left. \sum_{\phi=1}^m |d_{\psi\phi}| \int_0^\infty K_{\psi\phi}(s) f_\phi(\wp_\phi(s)) ds \right\} \tag{22} \\
 &\leq \sum_{\psi=1}^m \left\{ -c_\psi |\wp_\psi(\hbar)| + \sum_{\phi=1}^m |a_{\psi\phi}| f_\phi(\wp_\phi(\hbar)) + \sum_{\phi=1}^m |b_{\psi\phi}| f_\phi(\wp_\phi(\hbar - \omega)) + \sum_{\phi=1}^m |d_{\psi\phi}| f_\phi(\wp_\phi(\hbar)) \right\} \\
 &\leq \sum_{\psi=1}^m \left\{ -c_\psi |\wp_\psi(\hbar)| + \sum_{\phi=1}^m |a_{\psi\phi}| f_\phi(\wp_\phi(\hbar)) + \sum_{\phi=1}^m |d_{\psi\phi}| f_\phi(\wp_\phi(\hbar)) \right\} \\
 &+ \sum_{\psi=1}^m \sum_{\phi=1}^m |b_{\psi\phi}| f_\phi(\wp_\phi(\hbar - \omega)) \\
 &\leq -\rho_1 V(\hbar, \wp(\hbar)) + \rho_2 \sup_{\hbar - \tau \leq s \leq \hbar} V(s, \wp(s))
 \end{aligned}$$

as any solution $\varphi(t)$ of Error System (22), which satisfies the Razumikhin condition. Hence, on the basis of the Razumikhin technique, one has the criteria

$$\sup_{\hbar-\omega \leq s \leq t} V(s, \varphi(s)) \leq V(\hbar, \varphi(\hbar)) \tag{23}$$

Next, based on Systems (22) and (23), assume that there exists a constant $\Delta > 0$. One can then obtain

$$\begin{aligned} D^\beta V(\hbar, \varphi(\hbar)) &\leq -(\rho_1 - \rho_2)V(\hbar, \varphi(\hbar)), \\ \rho_1 - \rho_2 &\geq \Delta, \end{aligned} \tag{24}$$

and from (24), one observes that

$$D^\beta V(\hbar, \varphi(\hbar)) \leq -\Delta V(\hbar, \varphi(\hbar)) \tag{25}$$

Then, from (25) and Lemma 1, one has

$$V(\hbar, \varphi(\hbar)) \leq V(0)E_\beta(-\Delta\hbar^\alpha), \hbar \in [0, \infty) \tag{26}$$

Therefore, one concludes that

$$\begin{aligned} \|\varphi(\hbar)\| &= \|\tilde{\gamma}(\hbar) - \gamma(\hbar)\|, \\ &= \sum_{\psi=1}^m |\gamma_\psi(\hbar) - \gamma(\hbar)|, \\ &\leq \|\psi_0 - \phi_0\| E_\alpha(-\delta\hbar^\alpha) \end{aligned} \tag{27}$$

According to Definition 3, the fractional-order complex-valued neural network (1) achieves global Mittag–Leffler synchronization with fractional Systems (10) and (11). This completes the proof of Theorem 3. \square

4. Numerical Examples

Numerical examples are provided to demonstrate the validity of the results in this section.

Example 1. Consider the following discrete-time fractional-order complex-valued neural networks:

$${}^C\nabla_0^\beta \gamma_\psi(\hbar) = -c_\psi \gamma_\psi(\hbar) + \sum_{\phi=1}^m a_{\psi\phi} f_\phi(\gamma_\phi(\hbar)) + \sum_{\phi=1}^m b_{\psi\phi} f_\phi(\gamma_\phi(\hbar - \omega)) + \sum_{\phi=1}^m d_{\psi\phi} \int_0^\infty f_\phi(\gamma_\phi(s)) ds \tag{28}$$

Suppose $\beta = 0.95$ and $\omega = 0.2$ and suppose the parameters and the function are defined by

$$\begin{aligned} C &= \begin{bmatrix} 16 & 8 \\ 4 & 16 \end{bmatrix}, \\ A &= \begin{bmatrix} -0.4 - 0.2i & 0.2 + 0i \\ 0.2 - 0.5i & 0.4 + 0.2i \end{bmatrix}, \\ B &= \begin{bmatrix} 0.7 - 0.7i & 0.4 + 0.4i \\ 0.3 + 0.9i & -0.4 + 0.1i \end{bmatrix}, \\ D &= \begin{bmatrix} 0.6 - 0.8i & 0.3 + 0.4i \\ 0.2 + 0.3i & -0.7 + 0.7i \end{bmatrix}. \end{aligned}$$

$$U^R = [0.1\tan(t) \quad 0.4\cot(t)] U^I = [0.3\tan(t) \quad 0.7\cot(t)]$$

Assumptions H_1 and H_2 are satisfied for $\lambda_1^{RI}, \lambda_1^{II}, \lambda_1^{RR}, \lambda_1^{IR} = 1, c_1 = 28.95, |a_{11}^R| = 0.75, |a_{11}^I| = 0.97, |b_{11}^R| = 0.95, |b_{11}^I| = 0.87, |d_{11}^I| = 0.28, |d_{11}^R| = 0.29.$

From Theorem 1, $\theta_{\min}^{(1)} = 24.3700, \theta_{\min}^{(2)} = 24.3700, \theta_{\max}^{(1)} = 3.56, \theta_{\max}^{(2)} = 3.64.$ and $\theta_1 = 48.7400, \theta_2 = 7.2000$

For these conditions, we have $48.7400 < 10.1823.$ Hence, it follows from Theorem 1 that the system can achieve global asymptotic synchronization.

Example 2. Consider the following discrete-time fractional-order complex-valued neural networks:

$${}^C\nabla_0^\beta \gamma_\psi(\hbar) = -c_\psi \gamma_\psi(\hbar) + \sum_{\phi=1}^m a_{\psi\phi} f_\phi(\gamma_\phi(\hbar)) + \sum_{\phi=1}^m b_{\psi\phi} f_\phi(\gamma_\phi(\hbar - \omega)) + \sum_{\phi=1}^m d_{\psi\phi} \int_0^\infty f_\phi(\gamma_\phi(s)) ds \tag{29}$$

where $\beta = 0.56, \gamma_\psi(\hbar) = \gamma_\psi^R + \gamma_\psi^I(\hbar)i, \gamma_\psi^R(t), \gamma_\psi^I(t) \in R, f_\psi(\gamma_\psi) = 0.3 \tanh(\gamma_\psi^R) + 0.3 \tanh(\gamma_\psi^I)i, g_\psi(\gamma_\psi) = 0.65 \tanh(\gamma_\psi^R) + 0.65 \tanh(\gamma_\psi^I)i, \tau = 3,$ and

$$C = \begin{bmatrix} 0.9 & 0 & 0 \\ 0 & 0.9 & 0 \\ 0 & 0 & 0.9 \end{bmatrix},$$

$$A = \begin{bmatrix} 0.1 + 0.97i & 0.6 + 0.3i & 0.5 + 0.2i \\ 0.9 + 0.2i & 0.2 + 0.7i & 0.6 + 0.5i \\ 0.5 + 0.1i & 0.6 + 0.5i & 0.6 + 0.7i \end{bmatrix},$$

$$B = \begin{bmatrix} 0.2 + 0.87i & 5.56 + 3.45i & 3.56 + 5.45i \\ 0.56 + 2.45i & 4.56 + 2.45i & 0.56 + 6.45i \\ 1.56 + 0.35i & 2.56 + 4.45i & 0.56 + 8.45i \end{bmatrix},$$

$$D = \begin{bmatrix} 0.3 + 0.29i & 3.56 + 4.45i & 4.56 + 2.45i \\ 0.56 + 2.55i & 2.56 + 5.45i & 1.56 + 3.45i \\ 3.56 + 0.45i & 1.56 + 4.35i & 4.56 + 3.45i \end{bmatrix}.$$

Assumptions H_1 and H_2 are satisfied for $\lambda_1^{RI}, \lambda_1^{II}, \lambda_1^{RR}, \lambda_1^{IR} = 1, c_1 = 29.1456, |a_{11}^R| = 0.74, |a_{11}^I| = 0.96, |b_{11}^R| = 0.94, |b_{11}^I| = 0.86, |d_{11}^I| = 0.27, |d_{11}^R| = 0.27.$

From Theorem 2, $\Theta_{\min}^{(1)} = 16.44, \Theta_{\min}^{(2)} = 15.2956, \Theta_{\max}^{(1)} = 3.52, \Theta_{\max}^{(2)} = 3.20,$ and $\Theta_1 = 31.7356, \Theta_2 = 6.72.$

For these conditions, we have $31.7356 > 9.5035.$ Hence, it follows from Theorem 2 that this system can achieve global asymptotic synchronization. Refer Figures 1 and 2 for the graphical representation of the obtained result.

Example 3. Consider the following discrete-time fractional order complex-valued neural networks:

$${}^C\nabla_0^\beta \gamma_\psi(\hbar) = -c_\psi \gamma_\psi(\hbar) + \sum_{\phi=1}^m a_{\psi\phi} f_\phi(\gamma_\phi(\hbar)) + \sum_{\phi=1}^m b_{\psi\phi} f_\phi(\gamma_\phi(\hbar - \omega)) + \sum_{\phi=1}^m d_{\psi\phi} \int_0^\infty f_\phi(\gamma_\phi(s)) ds \tag{30}$$

Suppose $\beta = 0.98$ and $\omega = 0.2$ and suppose the parameters and the function are defined by $\lambda_1^{RI}, \lambda_1^{II}, \lambda_1^{RR}, \lambda_1^{IR} = 1, c_1 = 19.95, |a_{11}^R| = 0.72, |a_{11}^I| = 0.77, |b_{11}^R| = 0.94, |b_{11}^I| = 0.27, |d_{11}^I| = 0.23, |d_{11}^R| = 0.69.$

$$C = \begin{bmatrix} 16 & 8 \\ 4 & 16 \end{bmatrix},$$

$$A = \begin{bmatrix} -0.4 - 0.2i & 0.2 + 0i \\ 0.2 + 0.5i & 0.4 + 0.2i \end{bmatrix},$$

$$B = \begin{bmatrix} 0.7 - 0.7i & 0.4 + 0.4i \\ 0.3 + 0.9i & -0.4 + 0.1i \end{bmatrix},$$

$$D = \begin{bmatrix} 0.6 - 0.8i & 0.3 + 0.4i \\ 0.2 + 0.3i & -0.7 + 0.7i \end{bmatrix}.$$

$$U^R = [0.2\tan(t) \quad 0.5\cot(t)] U^I = [0.3\tan(t) \quad 0.7\cot(t)]$$

$\Theta_{\min}^{(1)} = 7.8300, \Theta_{\min}^{(2)} = 8.35, \Theta_{\max}^{(1)} = 2.75, \Theta_{\max}^{(2)} = 2.48.$ and $\Theta_1 = 16.1800, \Theta_2 = 5.23.$

For these conditions, we have $16.1800 > 7.3963.$ Hence, it follows from Theorem 2 that this system can achieve global asymptotic synchronization.

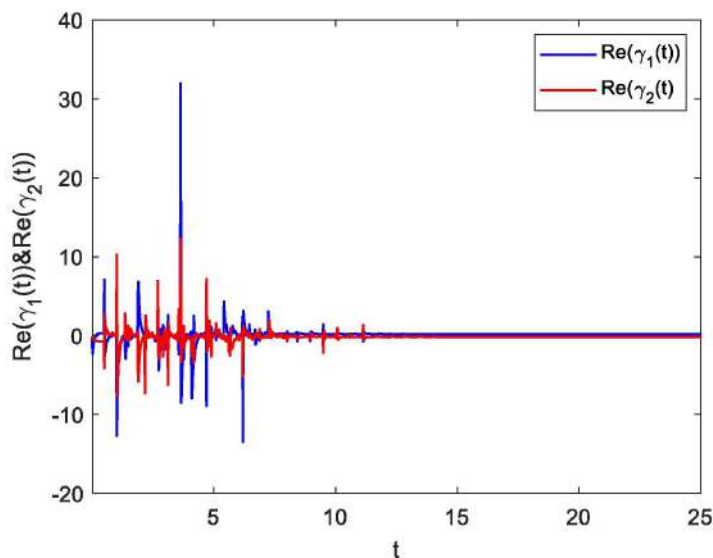


Figure 1. State trajectories of the FOCNNs (29) with fractional-order $\alpha = 0.45$ in the real axis.

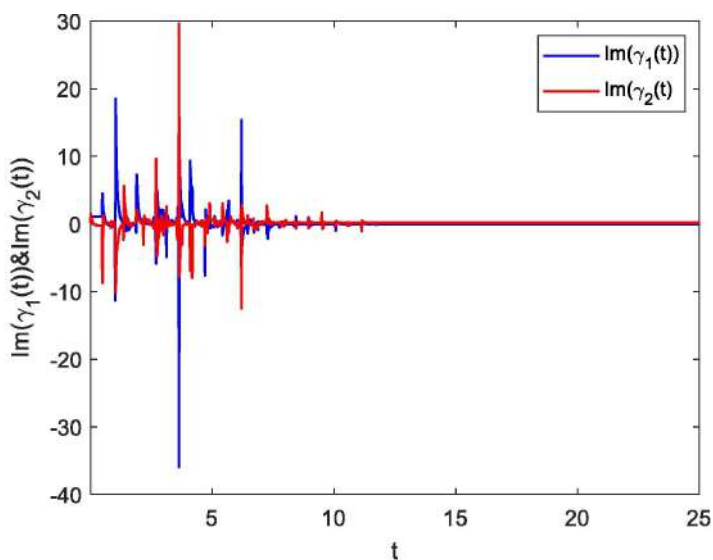


Figure 2. State trajectories of the FOCNNs (29) with fractional-order $\alpha = 0.45$ in the imaginary axis.

Example 4. Consider the discrete-time fractional-order complex-valued neural network

$${}^C\nabla_0^\beta \gamma_\psi(\hbar) = -c_\psi \gamma_\psi(\hbar) + \sum_{\phi=1}^m a_{\psi\phi} f_\phi(\gamma_\phi(\hbar)) + \sum_{\phi=1}^m b_{\psi\phi} f_\phi(\gamma_\phi(\hbar - \omega)) + \sum_{\phi=1}^m d_{\psi\phi} \int_0^\infty f_\phi(\gamma_\phi(s)) ds \tag{31}$$

Suppose $\beta = 0.98$ and $\omega = 0.2$ and suppose the parameters and the function are defined by

$$C = \begin{bmatrix} 0.9 & 0 & 0 \\ 0 & 0.9 & 0 \\ 0 & 0 & 0.9 \end{bmatrix},$$

$$A = \begin{bmatrix} 0.1 + 0.97i & 0.6 + 0.3i & 0.5 + 0.2i \\ 0.9 + 0.2i & 0.2 + 0.7i & 0.6 + 0.5i \\ 0.5 + 0.1i & 0.6 + 0.5i & 0.6 + 0.7i \end{bmatrix},$$

$$B = \begin{bmatrix} 0.2 + 0.87i & 5.56 + 3.45i & 3.56 + 5.45i \\ 0.56 + 2.45i & 4.56 + 2.45i & 0.56 + 6.45i \\ 1.56 + 0.35i & 2.56 + 4.45i & 0.56 + 8.45i \end{bmatrix},$$

$$D = \begin{bmatrix} 0.3 + 0.29i & 3.56 + 4.45i & 4.56 + 2.45i \\ 0.56 + 2.55i & 2.56 + 5.45i & 1.56 + 3.45i \\ 3.56 + 0.45i & 1.56 + 4.35i & 4.56 + 3.45i \end{bmatrix}.$$

Assumptions H_1, H_2 are satisfied for $c_1 = 2.14, a_{11} = 0.94, d_{11} = 0.92, b_{11} = 0.87, L_1 = 1$. By Theorem 3, we find that $\rho_1 = 1.28 > 0, \rho_2 = 0.87 > 0$.

Hence, $0 < \rho_1 - \rho_2 = 0.41 < 1$, and Theorem 3 holds. Therefore, (31) is globally Mittag–Leffler stable.

Remark 2. Many scholars have discussed the uniform stability, global asymptotic stability, and finite-time stability of fractional-order CVNNs with time delays Zhang et al. [30], Rakkiyappan et al. [21], Wang et al. [19], and Song et al. [22]. Most of these scholars considered that the activation functions of complex-valued systems can be separated into their real parts and imaginary parts. Thus, they transformed CVNNs to equivalent RVNNs to analyze their dynamic behavior. However, this method increases the dimension of systems and brings difficulties upon analysis. Compared with the existing literature, regardless of the activity, functions are separable, and the provided existence and finite-time stability criteria for discrete fractional-order CVNNs are valid and feasible in this paper.

Remark 3. Many authors studied the dynamics prosperities of discrete fractional difference equations in a real field. However, there are very few results about discrete fractional-order system in complex fields. Different from the existing literature, we first investigated discrete fractional-order CVNNs and analyzed their dynamic behavior.

Remark 4. In the aforementioned works, it is noted that only the discrete constant delays are involved in the network models. In this situation, discrete delays cannot well characterize the neural networks since the signal propagation is no longer instantaneous. Consequently, the distributed delays should also be taken into account in the description of neural network models. In recent decades, many researchers have made great efforts to the dynamics of neural networks with both discrete and distributed delays, and there have been some excellent results. Notice that these works were mainly concerned with integer-order neural networks. Research on fractional-order neural networks with discrete and distributed time delays has received little attention.

5. Conclusions

The synchronization of discrete-time fractional-order complex-valued neural networks with distributed delays is examined in this research. By building suitable Lyapunov functions, sufficient conditions are attained. The resulting results are fresh and add to the global Mittag–Leffler synchronization findings for fractional networks that already exist. Some adequate requirements are derived from the theory of discrete fractional calculus, the discrete Laplace transform, the theory of complex functions, and discrete Mittag–Leffler functions in order to guarantee the global stability and synchronization of the Mittag–Leffler function for the suggested networks. In future research, we will further study the dynamical behaviors, such as projective synchronization and finite time stability, of more

sophisticated neural networks, including fractional-order coupled discontinuous neural networks with time-varying delays.

Author Contributions: Methodology, R.P. and M.H.; Software, T.F.I.; Validation, M.S.A.; Formal analysis, B.A.A.M.; Investigation, W.M.O. All authors have read and agreed to the published version of the manuscript.

Funding: This research was funded by the Deanship of Scientific Research at King Khalid University under grant number RGP2/141/44.

Data Availability Statement: There is no data associated with this study.

Acknowledgments: The authors extend their appreciation to the Deanship of Scientific Research at King Khalid University for funding this work through large groups (project under grant number RGP2/141/44).

Conflicts of Interest: The authors declare no conflict of interest.

References

- Ahmeda, E.; Elgazzar, A. On fractional order differential equations model for nonlocal epidemics. *Physica A* **2007**, *379*, 607–614. [[CrossRef](#)] [[PubMed](#)]
- Moaddy, K.; Radwan, A.; Salama, K.; Momani, S.; Hashim, I. The fractional-order modeling and synchronization of electrically coupled neuron systems. *Comput. Math. Appl.* **2012**, *64*, 3329–3339. [[CrossRef](#)]
- Bhalekar, S.; Daftardar-Gejji, V. Synchronization of differential fractional-order chaotic systems using active control. *Commun. Nonlinear Sci. Numer. Simul.* **2010**, *15*, 3536–3546. [[CrossRef](#)]
- Narayanan, G.; Ali, M.S.; Karthikeyan, R.; Rajchakit, G.; Jirawattanapanit, A. Impulsive control strategies of mRNA and protein dynamics on fractional-order genetic regulatory networks with actuator saturation and its oscillations in repressilator model. *Biomed. Process. Control* **2023**, *82*, 104576. [[CrossRef](#)]
- Jmal, A.; Makhoulouf, A.B.; Nagy, A.M. Finite-Time Stability for Caputo Katugampola Fractional-Order Time-Delayed Neural Networks. *Neural Process Lett.* **2019**, *50*, 607–621. [[CrossRef](#)]
- Li, H.L.; Jiang, H.; Cao, J. Global synchronization of fractional-order quaternion-valued neural networks with leakage and discrete delays. *Neurocomputing* **2020**, *385*, 211–219. [[CrossRef](#)]
- Chen, S.; An, Q.; Ye, Y.; Su, H. Positive consensus of fractional-order multi-agent systems. *Neural Comput. Appl.* **2021**, *33*, 16139–16148. [[CrossRef](#)]
- Chen, S.; An, Q.; Zhou, H.; Su, H. Observer-based consensus for fractional-order multi-agent systems with positive constraint. Author links open overlay panel. *Neurocomputing* **2022**, *501*, 489–498. [[CrossRef](#)]
- Li, Z.Y.; Wei, Y.H.; Wang, J.; Li, A.; Wang, J.; Wang, Y. Fractional-order ADRC framework for fractional-order parallel systems. In Proceedings of the 2020 39th Chinese Control Conference (CCC), Shenyang, China, 27–29 July 2020; pp. 1813–1818.
- Wang, L. Symmetry and conserved quantities of Hamilton system with comfortable fractional derivatives. In Proceedings of the 2020 Chinese Control And Decision Conference (CCDC), Hefei, China, 22–24 August 2020; pp. 3430–3436.
- Castañeda, C.E.; López-Mancilla, D.; Chiu, R.; Villafana-Rauda, E.; Orozco-López, O.; Casillas-Rodríguez, F.; Sevilla-Escoboza, R. Discrete-time neural synchronization between an arduino microcontroller and a compact development system using multiscroll chaotic signals. *Chaos Solitons Fractals* **2019**, *119*, 269–275. [[CrossRef](#)]
- Atici, F.M.; Eloe, P.W. Gronwalls inequality on discrete fractional calculus. *Comput. Math. Appl.* **2012**, *64*, 3193–3200. [[CrossRef](#)]
- Ostalczyk, P. *Discrete Fractional Calculus: Applications in Control and Image Processing*; World Scientific: Singapore, 2015.
- Ganji, M.; Gharari, F. The discrete delta and nabla Mittag-Leffler distributions. *Commun. Stat. Theory Methods* **2018**, *47*, 4568–4589. [[CrossRef](#)]
- Wyrwas, M.; Mozyrska, D.; Girejko, E. Stability of discrete fractional-order nonlinear systems with the nabla Caputo difference. *IFAC Proc. Vol.* **2013**, *46*, 167–171. [[CrossRef](#)]
- Gray, H.L.; Zhang, N.F. On a new definition of the fractional difference. *Math. Comput.* **1988**, *50*, 513–529. [[CrossRef](#)]
- Wu, G.C.; Baleanu, D.; Luo, W.H. Lyapunov functions for Riemann-Liouville-like fractional difference equations. *Appl. Math. Comput.* **2017**, *314*, 228–236. [[CrossRef](#)]
- Baleanu, D.; Wu, G.C.; Bai, Y.R.; Chen, F.L. Stability analysis of Caputolike discrete fractional systems. *Commun. Nonlinear Sci. Numer. Simul.* **2017**, *48*, 520–530. [[CrossRef](#)]
- Hu, J.; Wang, J. Global stability of complex-valued recurrent neural networks with time-delays. *IEEE Trans. Neural Netw. Learn. Syst.* **2012**, *23*, 853–865. [[CrossRef](#)] [[PubMed](#)]
- Ozdemir, N.; Iskender, B.B.; Ozgur, N.Y. Complex valued neural network with Mobius activation function. *Commun. Nonlinear Sci. Numer. Simul.* **2011**, *16*, 4698–4703. [[CrossRef](#)]
- Rakkiyappan, R.; Cao, J.; Velmurugan, G. Existence and uniform stability analysis of fractional-order complex-valued neural networks with time delays. *IEEE Trans. Neural Netw. Learn. Syst.* **2015**, *26*, 84–97. [[CrossRef](#)]

22. Song, Q.; Zhao, Z.; Liu, Y. Stability analysis of complex-valued neural networks with probabilistic time-varying delays. *Neurocomputing* **2015**, *159*, 96–104. [[CrossRef](#)]
23. Pan, J.; Liu, X.; Xie, W. Exponential stability of a class of complex-valued neural networks with time-varying delays. *Neurocomputing* **2015**, *164*, 293–299. [[CrossRef](#)]
24. Li, X.; Rakkiyappan, R.; Velmurugan, G. Dissipativity analysis of memristor-based complex-valued neural networks with time-varying delays. *Inf. Sci.* **2015**, *294*, 645–665. [[CrossRef](#)]
25. Rakkiyappan, R.; Sivaranjani, K.; Velmurugan, G. Passivity and passification of memristor-based complex-valued recurrent neural networks with interval time-varying delays. *Neurocomputing* **2014**, *144*, 391–407. [[CrossRef](#)]
26. Chen, L.P.; Chai, Y.; Wu, R.C.; Ma, T.D.; Zhai, H.Z. Dynamic analysis of a class of fractional-order neural networks with delay. *Neurocomputing* **2013**, *111*, 190–194. [[CrossRef](#)]
27. Song, Q.; Yan, H.; Zhao, Z.; Liu, Y. Global exponential stability of complex-valued neural networks with both time-varying delays and impulsive effects. *Neural Netw.* **2016**, *79*, 108–116. [[CrossRef](#)]
28. Syed Ali, M.; Yogambigai, J.; Kwon, O.M. Finite-time robust passive control for a class of switched reaction-diffusion stochastic complex dynamical networks with coupling delays and impulsive control. *Int. J. Syst. Sci.* **2018**, *49*, 718–735. [[CrossRef](#)]
29. Zhou, B.; Song, Q. Boundedness and complete stability of complex valued neural networks with time delay. *IEEE Trans. Neural Netw. Learn. Syst.* **2013**, *24*, 1227–1238. [[CrossRef](#)]
30. Zhang, Z.; Lin, C.; Chen, B. Global stability criterion for delayed complex-valued recurrent neural networks. *IEEE Trans. Neural Netw. Learn. Syst.* **2014**, *25*, 1704–1708. [[CrossRef](#)]
31. Song, Q.; Zhao, Z. Stability criterion of complex-valued neural networks with both leakage delay and time-varying delays on time scales. *Neurocomputing* **2016**, *171*, 179–184. [[CrossRef](#)]
32. Sakthivel, R.; Sakthivel, R.; Kwon, O.M.; Selvaraj, P.; Anthoni, S.M. Observer-based robust synchronization of fractional-order multi-weighted complex dynamical networks. *Nonlinear Dyn.* **2019**, *98*, 1231–1246. [[CrossRef](#)]
33. Chen, X.; Song, Q. Global stability of complex-valued neural networks with both leakage time delay and discrete time delay on time scales. *Neurocomputing* **2013**, *121*, 254–264. [[CrossRef](#)]
34. Zhang, Z.; Yu, S. Global asymptotic stability for a class of complex valued Cohen-Grossberg neural networks with time delays. *Neurocomputing* **2016**, *171*, 1158–1166. [[CrossRef](#)]
35. Gong, W.; Liang, J.; Cao, J. Matrix measure method for global exponential stability of complex-valued recurrent neural networks with time-varying delays. *Neural Netw.* **2015**, *70*, 81–89. [[CrossRef](#)]
36. Syed Ali, M.; Yogambigai, J.; Cao, J. Synchronization of master-slave Markovian switching complex dynamical networks with time-varying delays in nonlinear function via sliding mode control. *Acta Math. Sci.* **2017**, *37*, 368–384.
37. Zhou, J.; Liu, Y.; Xia, J.; Wang, Z.; Arik, S. Resilient fault-tolerant antisynchronization for stochastic delayed reaction-diffusion neural networks with semi-Markov jump parameters. *Neural Netw.* **2020**, *125*, 194–204. [[CrossRef](#)] [[PubMed](#)]
38. Syed Ali, M.; Yogambigai, J. Finite-time robust stochastic synchronization of uncertain Markovian complex dynamical networks with mixed time-varying delays and reaction-diffusion terms via impulsive control. *J. Frankl. Inst.* **2017**, *354*, 2415–2436.
39. Narayanan, G.; Syed Ali, M.; Karthikeyan, R.; Rajchakit, G.; Jirawattanapanit, A. Novel adaptive strategies for synchronization mechanism in nonlinear dynamic fuzzy modeling of fractional-order genetic regulatory networks. *Chaos Solitons Fractals* **2022**, *165*, 112748. [[CrossRef](#)]
40. Yogambigai, J.; Syed Ali, M. Exponential Synchronization of switched complex dynamical networks with time varying delay via periodically intermittent control. *Int. J. Differ. Equ.* **2017**, *12*, 41–53.
41. Yogambigai, J.; Syed Ali, M. Finite-time and Sampled-data Synchronization of Delayed Markovian Jump Complex Dynamical Networks Based on Passive Theory. In Proceedings of the Third International Conference on Science Technology Engineering and Management (ICONSTEM), Chennai, India, 23–24 March 2017.
42. Yang, L.X.; Jiang, J. Adaptive synchronization of driveresponse fractional-order complex dynamical networks with uncertain parameters. *Commun. Nonlinear Sci. Numer. Simul.* **2014**, *19*, 1496–1506. [[CrossRef](#)]
43. Wong, W.K.; Li, H.; Leung, S.Y.S. Robust synchronization of fractional-order complex dynamical networks with parametric uncertainties. *Commun. Nonlinear Sci. Numer. Simul.* **2012**, *17*, 4877–4890. [[CrossRef](#)]
44. Bao, H.; Park, J.H.; Cao, J. Synchronization of fractional order complex-valued neural networks with time delay. *Neural Netw.* **2016**, *81*, 16–28. [[CrossRef](#)]
45. Qi, D.L.; Liu, M.Q.; Qiu, M.K.; Zhang, S.L. Exponential H_∞ synchronization of general discrete-time chaotic neural networks with or without time delays. *IEEE Trans. Neural Netw. Learn. Syst.* **2010**, *21*, 1358–1365.
46. Li, Z.Y.; Liu, H.; Lu, J.A.; Zeng, Z.G.; Lü, J. Synchronization regions of discrete-time dynamical networks with impulsive couplings. *Inf. Sci.* **2018**, *459*, 265–277. [[CrossRef](#)]
47. You, X.; Song, Q.; Zhao, Z. Global Mittag-Leffler stability and synchronization of discrete-time fractional-order complex-valued neural networks with time delay. *Neural Netw.* **2020**, *122*, 382–394. [[CrossRef](#)]
48. Atici, F.M.; Eloe, P.W. Discrete fractional calculus with the nabla operator. *Electron. J. Qual. Theory Differ. Equ.* **2009**, *3*, 1–12. [[CrossRef](#)]

49. Mu, X.X.; Chen, Y.G. Synchronization of delayed discrete-time neural networks subject to saturated time-delay feedback. *Neurocomputing* **2016**, *175*, 293–299. [[CrossRef](#)]
50. Liang, S.; Wu, R.C.; Chen, L.P. Comparison principles and stability of nonlinear fractional-order cellular neural networks with multiple time delays. *Neurocomputing* **2015**, *168*, 618–625. [[CrossRef](#)]

Disclaimer/Publisher's Note: The statements, opinions and data contained in all publications are solely those of the individual author(s) and contributor(s) and not of MDPI and/or the editor(s). MDPI and/or the editor(s) disclaim responsibility for any injury to people or property resulting from any ideas, methods, instructions or products referred to in the content.

Synchronization of T–S Fuzzy Fractional–Order Discrete–Time Complex–Valued Molecular Models of mRNA and Protein in Regulatory Mechanisms with Leakage Effects

Published: 01 September 2022

Volume 55, pages 3305–3331, (2023) [Cite this article](#)



Neural Processing Letters

[Aims and scope](#)

[Submit manuscript](#)

[G. Narayanan](#), [M. Syed Ali](#) , [Hamed Alsulami](#), [Tareq Saeed](#) & [Bashir Ahmad](#)

 213 Accesses  1 Citation  1 Altmetric [Explore all metrics](#) →

Abstract

This paper addresses the problem of Mittag–Leffler synchronization of T–S fuzzy fractional-order discrete-time complex-valued molecular models of mRNA and protein in regulatory mechanisms with two kinds of regulation functions, respectively. A novel approach is proposed to effectively deal with the joint effects from leakage delay and time varying delay for the class of T–S fuzzy fractional-order discrete-time complex-valued genetic regulatory networks (FDTCVGRNs). By employing Lyapunov stability method and Caputo fractional difference inequalities, several effective conditions according to algebraic inequality and

See discussions, stats, and author profiles for this publication at: <https://www.researchgate.net/publication/367263936>

Finite-time guaranteed cost control for stochastic nonlinear switched systems with time-varying delays and reaction-diffusion

Article in *International Journal of Computer Mathematics* · January 2023

DOI: 10.1080/00207160.2023.2169576

CITATIONS

3

READS

92

3 authors, including:

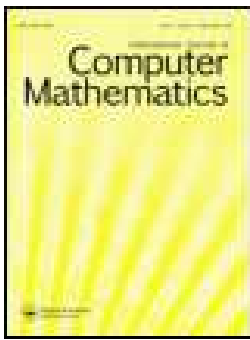


Gokulakrishnan Veeraragavan

SRM Institute of Science and Technology

8 PUBLICATIONS 17 CITATIONS

SEE PROFILE



Finite-time guaranteed cost control for stochastic nonlinear switched systems with time-varying delays and reaction-diffusion

V. Gokulakrishnan, R. Srinivasan, M. Syed Ali & Grienggrai Rajchakit

To cite this article: V. Gokulakrishnan, R. Srinivasan, M. Syed Ali & Grienggrai Rajchakit (2023): Finite-time guaranteed cost control for stochastic nonlinear switched systems with time-varying delays and reaction-diffusion, International Journal of Computer Mathematics, DOI: [10.1080/00207160.2023.2169576](https://doi.org/10.1080/00207160.2023.2169576)

To link to this article: <https://doi.org/10.1080/00207160.2023.2169576>



Published online: 06 Feb 2023.



Submit your article to this journal [↗](#)



Article views: 17



View related articles [↗](#)



View Crossmark data [↗](#)

Finite-time guaranteed cost control for stochastic nonlinear switched systems with time-varying delays and reaction-diffusion

V. Gokulakrishnan^a, R. Srinivasan^a, M. Syed Ali^b and Grienggrai Rajchakit^c

^aDepartment of Mathematics, SRM Institute of Science and Technology, Chennai, Tamilnadu, India; ^bDepartment of Mathematics, Thiruvalluvar University, Vellore, Tamilnadu, India; ^cFaculty of Science, Department of Mathematics, Maejo University, Chiang Mai, Thailand

ABSTRACT

This study considers the finite-time guaranteed cost control problem for a class of stochastic nonlinear switched systems (SNSs) with time-varying delays, reaction-diffusion and actuator faults. The reliable control strategy is designed to finite-time stabilization for SNSs. By virtue of the Lyapunov method, Neumann boundary condition, some famous inequality techniques and average dwell-time approach, sufficient criterion are obtained to ensure finite-time stability of proposed controlled systems. We investigate the finite-time stabilization results by designing the control gain matrices for reliable controller. The sufficient criteria are expressed in terms of linear matrix inequalities (LMIs) that can be verified by MATLAB LMI toolbox. Furthermore, a new sufficient criterion is presented to guarantee the finite-time cost control of proposed controlled systems. Based on this criterion, the effects of control gains, switching signals and time-varying delays on finite-time stability are also analysed. At last, numerical simulations are presented to illustrate the efficiency and superiority of designed reliable controller.

ARTICLE HISTORY

Received 29 March 2022
Revised 20 December 2022
Accepted 10 January 2023

KEYWORDS

Stochastic nonlinear switched systems; reaction-diffusion; reliable control; average dwell-time approach; stabilization; finite-time cost control

2000 AMS SUBJECT CLASSIFICATIONS

93-10; 93-08; 93-05

1. Introduction

In recent decades, switched systems have been used to unify the description of a wide range of practical applications, including circuit systems [4,13], networked systems [27], aircraft systems [22] and power systems [24,50]. Switched systems consist of multiple subsystems and a logical rule for switching that specifies which subsystem is selected at a certain time. The average dwell-time (ADT) scheme can ensure the stability properties of switched systems [14,21,26,49,52]. Recently an in-depth theoretical study on the dynamic theory of switched systems has been launched and some interesting results have been reported in the literatures [12,25,32,33,43,47,51]. Switched systems are a type of stochastic systems that consists of a finite family of discrete time or continuous time subsystems with active subsystems specified at each time instant by a random switching signal. Meanwhile, stochastic processes have played an essential role and attracted a lot of attention in various domains of scientific and technical applications over the last few decades [1,3,17,45,53].

In real-world applications such as secure communications [20,31], chemical reaction process [30], Alzheimer's disease model [16], virus transmission [23] and food web model [40] are well recognized to be accurately described by partial differential equations. The complete structure and non-linear dynamical behaviours of nonlinear systems depend not only on the temporal evolution and space

Table 1. Comparison for switched systems with other works.

Switched systems	[14]	[26]	[11,21,34]	[52]	[46]	[19]	[15]	[54]	This paper
Stochastic inputs	×	×	✓	×	×	✓	×	×	✓
Reaction-diffusion	✓	✓	✓	✓	✓	×	×	×	✓
Time-varying delays	✓	×	×	✓	×	✓	×	✓	✓
Actuator faults	×	×	×	✓	✓	✓	✓	×	✓
Reliable control	×	×	×	✓	✓	✓	✓	×	✓
Cost control	×	×	×	×	×	×	✓	✓	✓

position of all variable, but also on its connections stemming from the space-distributed configuration of entire networks. Therefore, the dynamics behaviours of reaction-diffusion systems create increased research attention among the researchers [6–8,10,11,34,36–38].

The work on the regulation of switched systems has a critical significance to the advancement of control theory as well as control engineering. Due to a tough work environment, power supply stability, inescapable component ageing and so on, the problem of actuator failures is unavoidable in actual control systems [5,9,29,42,46,48]. A considerable attention have been paid to designing a reliable control that can operate successfully on admissible failures. Such as the reliable T-S fuzzy filter design [35,44] and reliable state feedback controller design issue for continuous time systems [18,19,41]. Over the past decades, the theory of guaranteed cost control (GCC) has been developed and there have been many important results proposed [2,15,39,54]. The key concept is to stabilize the systems while maintaining an acceptable degree of efficiency as a quadratic cost function. The GCC has the advantage of establishing an upper bound on a particular system performance index and ensuring that system performance is not affected by uncertainty or time delays. To best of our knowledge, finite-time GCC for SNSSs with reaction-diffusion has been not yet published (Table 1).

Inspired by the above discussion, we aim to investigate the finite-time guaranteed cost control for a class of stochastic nonlinear switched systems (SNSSs) with time-varying delays, reaction-diffusion and actuator faults. The main contributions of this paper are as follows:

- A reliable controller was designed to guarantee finite-time stabilization of SNSSs with time-varying delays, reaction-diffusion and actuator faults.
- By utilizing suitable Lyapunov–Krasovskii functional, Neumann boundary condition, inequality techniques, average dwell-time (ADT) approach and linear matrix inequalities (LMIs), sufficient criteria are derived to guarantee the proposed controlled systems achieve the finite-time stability.
- The effects of control gains, switching signals and time-varying delays on finite-time stability are reflected from our obtained theoretical results.
- Furthermore, a new sufficient criterion is presented to guarantee the finite-time cost control of SNSSs with reaction-diffusion.
- Finally, simulation results show the efficiency of the proposed reliable controller.

Notations: \mathbb{Z} – set of all integers; \mathbb{R} – set of all real numbers; \mathbb{R}_+ – set of all positive real numbers; \mathbb{R}^n – Euclidean space of n -dimensions; $\mathbb{R}^{m \times n}$ – Euclidean space of $(m \times n)$ -dimensions; $\mathcal{A} < 0$ – real symmetric negative definite matrix; $\mathcal{A} > 0$ – real symmetric positive definite matrix; \mathcal{A}^T – transpose of \mathcal{A} ; $\lambda_{\min}(\mathcal{A})$ – minimum eigenvalue of \mathcal{A} ; $\lambda_{\max}(\mathcal{A})$ – maximum eigenvalue of \mathcal{A} ; $*$ – the entries are implied by symmetric; $He\{\mathcal{A}\} = (\mathcal{A} + \mathcal{A}^T)$; $\text{diag}\{\cdot \cdot \cdot\}$ – block diagonal matrix; $\sigma(t) = p$ – switching signal; $\|\cdot\|$ – Euclidean norms; $\mathbb{E}(X)$ – mathematical expectation of X ; $\mathcal{W}^{1,2}([0, L]; \mathbb{R}^n)$ – Soblev n -dimensional space of continuous functions; $\int_0^1 \mathfrak{S}^T(x, t) \mathfrak{S}(x, t) dx = \|\mathfrak{S}(x, t)\|^2$; ✓ – this item is included in that paper; × – this item is not included in that paper.

The remaining section of this paper is organized as follows. In Section 2, system model, reliable control problem and some preliminaries are introduced. In Section 3, we investigate our main results:

(i) to obtain the finite-time stability for proposed controlled system; (ii) to prove the finite-time stabilization result by designing control gains for reliable controller and (iii) to investigate the finite-time cost control for SNSSs with time-varying delays, reaction-diffusion and actuator faults. In Section 4, simulation results show that the proposed reliable controller is effective. Finally, conclusion and our future works are shown in Section 5.

2. Problem description and preliminaries

Consider the following SNSSs with time-varying delays, reaction-diffusion and actuator faults:

$$\begin{aligned} d\mathfrak{S}(x, t) = & \left[\mathcal{D}_{\sigma(t)} \frac{\partial^2 \mathfrak{S}(x, t)}{\partial x^2} + \mathcal{Q}_{\sigma(t)} \mathfrak{S}(x, t) + \mathcal{R}_{\sigma(t)} \mathfrak{S}(x, t - \eta(t)) \right. \\ & \left. + f_{\sigma(t)}(t, \mathfrak{S}(x, t)) + g_{\sigma(t)}(t, \mathfrak{S}(x, t - \eta(t))) + \mathcal{S}_{\sigma(t)} u^{\mathcal{F}}(x, t) \right] dt \\ & + h_{\sigma(t)}(t, \mathfrak{S}(x, t), \mathfrak{S}(x, t - \eta(t))) d\omega(t), \quad x \in (0, 1), t > 0, \end{aligned} \quad (1)$$

with initial and Neumann boundary conditions as follows:

$$\mathfrak{S}(x, s) = \psi(x, s), \quad s \in [-\eta, 0], \quad (2)$$

$$\left. \frac{\partial \mathfrak{S}(x, t)}{\partial x} \right|_{x=0} = 0, \quad \left. \frac{\partial \mathfrak{S}(x, t)}{\partial x} \right|_{x=1} = 0, \quad (3)$$

where $\mathfrak{S}(x, t) = [\mathfrak{S}_1(x, t), \mathfrak{S}_2(x, t), \dots, \mathfrak{S}_n(x, t)]^T \in \mathbb{R}^n$ is a state vector; $t > 0$ is a time variable; x is a space variable. $u^{\mathcal{F}}(x, t) = [u_1^{\mathcal{F}}(x, t), u_2^{\mathcal{F}}(x, t), \dots, u_n^{\mathcal{F}}(x, t)]^T \in \mathbb{R}^n$ denotes a control input of actuator faults to be designed later. $\psi(x, s) = [\psi_1(x, s), \psi_2(x, s), \dots, \psi_n(x, s)]^T \in \mathbb{R}^n$ is the initial continuous functions. $f_{\sigma(t)}, g_{\sigma(t)} : \mathbb{R}_+ \times \mathbb{R}^n \rightarrow \mathbb{R}^n$ and $h_{\sigma(t)} : \mathbb{R}_+ \times \mathbb{R}^n \times \mathbb{R}^n \rightarrow \mathbb{R}^{n \times m}$ are the non-linear continuous functions. $\eta(t)$ denotes the time-varying delays and satisfying the conditions $0 \leq \eta(t) \leq \eta$ and $\dot{\eta}(t) \leq \kappa$. $\omega(t) = [\omega_1(t), \omega_2(t), \dots, \omega_m(t)]^T \in \mathbb{R}^m$ denotes a Brownian motions. $\sigma(t) : [0, \infty) \rightarrow \mathcal{N} = \{1, 2, \dots, N\}$ denotes the switching piecewise constant function. The switching instants are expressed by a switching sequence $\{(p_0, t_0), \dots, (p_1, t_1), \dots, p_k \in \mathcal{N}, k = 0, 1, \dots\}$ which means the p_k th subsystems is activated when $t \in [t_k, t_{k+1})$. $\mathcal{D}_{\sigma(t)}$ is a positive definite diffusion matrix. $\mathcal{Q}_{\sigma(t)}, \mathcal{R}_{\sigma(t)}$ and $\mathcal{S}_{\sigma(t)}$ are constant matrices with suitable dimensions.

The actuator faults control input $u^{\mathcal{F}}(x, t)$ is designed as follows:

$$u^{\mathcal{F}}(x, t) = \mathcal{X}_{\mathcal{H}_{\sigma(t)}} u(x, t), \quad \mathcal{H} = 0, 1, 2, \dots, h_m, h_m \leq 2^l - 1, \quad (4)$$

where $u(x, t) = \mathcal{K}_{\sigma(t)} \mathfrak{S}(x, t)$ and scaling factor $\mathcal{X}_{\mathcal{H}_{\sigma(t)}}$ satisfies

$$\begin{aligned} \mathcal{X}_{\mathcal{H}_{\sigma(t)}} \in \mathcal{W} = & \{\mathcal{X}_{\mathcal{H}_{\sigma(t)}} = \text{diag}\{\mathcal{X}_{\mathcal{H}_{1\sigma(t)}}, \dots, \mathcal{X}_{\mathcal{H}_{l\sigma(t)}}\}, \\ & \mathcal{X}_{\mathcal{H}_{\alpha\sigma(t)}} = 0 \quad \text{or } 1, \alpha = 1, 2, \dots, l. \end{aligned}$$

Remark 2.1: The faults model (1) corresponds to the scenario of the α th-actuator outage when $\mathcal{X}_{\mathcal{H}_{\alpha\sigma(t)}} = 0$ for $1 \leq \alpha \leq l$. When $\mathcal{X}_{\mathcal{H}_{\alpha\sigma(t)}} = 1$, there is no faults in the α th -actuator. Suppose that $\mathcal{X}_{0\sigma(t)} = I$, $\mathcal{H} = 0$, corresponds to the normal control input $u^{\mathcal{F}}(x, t) = u(x, t)$.

Hence from Equations (1) and (4), we have

$$\begin{aligned} d\mathfrak{Z}(x, t) = & \left[\mathcal{D}_{\sigma(t)} \frac{\partial^2 \mathfrak{Z}(x, t)}{\partial x^2} + (\mathcal{Q}_{\sigma(t)} + \mathcal{S}_{\sigma(t)} \mathcal{X}_{\mathcal{H}_{\sigma(t)}} \mathcal{K}_{\sigma(t)}) \mathfrak{Z}(x, t) \right. \\ & \left. + \mathcal{R}_{\sigma(t)} \mathfrak{Z}(x, t - \eta(t)) + f_{\sigma(t)}(t, \mathfrak{Z}(x, t)) + g_{\sigma(t)}(t, \mathfrak{Z}(x, t - \eta(t))) \right] dt \\ & + h_{\sigma(t)}(t, \mathfrak{Z}(x, t), \mathfrak{Z}(x, t - \eta(t))) d\omega(t), \quad x \in (0, 1), t > 0. \end{aligned} \quad (5)$$

Remark 2.2: From system (1), the control input can be ignored. Then, system (1) can be rewritten as

$$\begin{aligned} d\mathfrak{Z}(x, t) = & \left[\mathcal{D}_{\sigma(t)} \frac{\partial^2 \mathfrak{Z}(x, t)}{\partial x^2} + \mathcal{Q}_{\sigma(t)} \mathfrak{Z}(x, t) + \mathcal{R}_{\sigma(t)} \mathfrak{Z}(x, t - \eta(t)) + f_{\sigma(t)}(t, \mathfrak{Z}(x, t)) \right. \\ & \left. + g_{\sigma(t)}(t, \mathfrak{Z}(x, t - \eta(t))) \right] dt + h_{\sigma(t)}(t, \mathfrak{Z}(x, t), \mathfrak{Z}(x, t - \eta(t))) d\omega(t), \quad x \in (0, 1), t > 0. \end{aligned} \quad (6)$$

The cost function of system (1) is given by

$$J = \mathbb{E} \left\{ \int_0^1 \int_0^\infty e^{-\gamma t} \left[\mathfrak{Z}^T(x, t) \mathcal{U}_{\sigma(t)} \mathfrak{Z}(x, t) + (u^{\mathcal{F}}(x, t))^T \mathcal{V}_{\sigma(t)} (u^{\mathcal{F}}(x, t)) \right] dt dx \right\}, \quad (7)$$

where $\mathcal{U}_{\sigma(t)}$, $\mathcal{V}_{\sigma(t)}$ are symmetric positive definite matrices and $\gamma > 0$ is a real constants.

Assumption (H): The nonlinear continuous functions $f(\cdot)$, $g(\cdot)$ and $h(\cdot)$ are satisfying the global Lipschitz conditions: there exist positive constants $\alpha, \beta, \lambda, \mu$ such that

$$\begin{aligned} |f(t, y_1) - f(t, y_2)|^2 & \leq \alpha |y_1 - y_2|^2, \\ |g(t, y_1) - g(t, y_2)|^2 & \leq \beta |y_1 - y_2|^2, \\ |h(t, y_1, y_3) - h(t, y_2, y_4)|^2 & \leq \lambda |y_1 - y_2|^2 + \mu |y_3 - y_4|^2, \end{aligned}$$

where $t \in \mathbb{R}_+$ and $y_1, y_2, y_3, y_4 \in \mathbb{R}^n$. Furthermore, $f(t, 0) = 0$, $g(t, 0) = 0$ and $h(t, 0, 0) = 0$.

Lemma 2.3 ([53]): The following matrix inequality applies to any real matrices M, N and a positive definite matrix Ψ :

$$M^T N + N^T M \leq M^T \Psi^{-1} M + N^T \Psi N.$$

Lemma 2.4 ([10]): For a state vector $y \in \mathcal{W}^{1,2}([0, L]; \mathbb{R}^n)$ with $y(0) = 0$ or $y(L) = 0$ and a matrix $\mathcal{M} > 0$, we get

$$\int_0^L y^T(s) \mathcal{M} y(s) ds \leq \frac{4L^2}{\pi^2} \int_0^L \left(\frac{dy(s)}{ds} \right)^T \mathcal{M} \left(\frac{dy(s)}{ds} \right) ds.$$

Lemma 2.5 ([37]): The following inequality applies for any symmetric matrix $\mathcal{M} > 0$, any scalars c and d with $c < d$, and vector function $\varpi(t) : [c, d] \rightarrow \mathbb{R}^n$ such that the integral is properly defined:

$$\left[\int_c^d \varpi(s) ds \right]^T \mathcal{M} \left[\int_c^d \varpi(s) ds \right] \leq (d - c) \int_c^d \varpi^T(s) \mathcal{M} \varpi(s) ds.$$

Lemma 2.6 ([38]): Let $\Omega_1, \Omega_2, \Omega_3$ be given matrices such that $\Omega_1^T = \Omega_1$ and $\Omega_2^T = \Omega_2 > 0$, then

$$\Omega_1 + \Omega_3^T \Omega_2^{-1} \Omega_3 < 0 \Leftrightarrow \begin{bmatrix} \Omega_1 & \Omega_3^T \\ * & -\Omega_2 \end{bmatrix} < 0 \quad \text{or} \quad \begin{bmatrix} -\Omega_2 & \Omega_3 \\ * & \Omega_1 \end{bmatrix} < 0.$$

Definition 2.7 ([47]): Let $\mathcal{N}_{\sigma(\mathcal{T}_\gamma, \mathcal{T}_\delta)}$ denote the number of switches of $\sigma(t)$ across $(\mathcal{T}_\gamma, \mathcal{T}_\delta)$ for any $\mathcal{T}_\delta > \mathcal{T}_\gamma \geq 0$. When $\mathcal{N}_{\sigma(\mathcal{T}_\gamma, \mathcal{T}_\delta)} \leq \mathcal{N}_0 + \frac{(\mathcal{T}_\delta - \mathcal{T}_\gamma)}{\tau_\epsilon}$ holds for $\tau_\epsilon > 0, \mathcal{N}_0 \geq 0, \tau_\epsilon$ is referred to as the ADT. We use $\mathcal{N}_0 = 0$ in this paper.

Definition 2.8 ([43]): Given three constants $\kappa_1 > 0, \kappa_2 > 0, \mathcal{T} > 0$ with $\kappa_1 < \kappa_2$ and symmetric matrix $\mathcal{P} > 0$, the system (6) is said to be finite-time stable (FTS) with respect to $(\kappa_1, \kappa_2, \mathcal{P}, \mathcal{T})$ if

$$\mathbb{E} \left\{ \int_0^1 \sup_{-\eta \leq s \leq 0} \{\psi^T(x, s) \mathcal{P} \psi(x, s)\} dx \right\} \leq \kappa_1 \Rightarrow \mathbb{E} \left\{ \int_0^1 \mathfrak{S}^T(x, t) \mathcal{P} \mathfrak{S}(x, t) dx \right\} < \kappa_2, \quad \forall t \in [0, \mathcal{T}].$$

Definition 2.9 ([7]): System (5) is said to be finite-time stabilizable if there exist control gain matrices for reliable controller (4) such that system (5) is FTS with respect to given constants $(\kappa_1, \kappa_2, \mathcal{P}, \mathcal{T})$.

Definition 2.10 ([54]): System (1) is taken into account. Assume there is a control law (4) and a real number $J^* > 0$ such that system (5) is FTS and the cost function (7) satisfies $J \leq J^*$. Then J^* is called a guaranteed cost and (4) is called a guaranteed control law for system (5).

3. Main results

In this section, we use the Lyapunov method and ADT approach to investigate the finite-time stability condition of system (6). In addition, we investigate the finite-time stabilization of system (5) by designing the control matrices for the reliable controller. Furthermore, we obtain the finite-time cost control of system (5).

For our convenience, we let

$$\begin{aligned} \Xi_p^* &= \mathcal{P}^{-\frac{1}{2}} \Xi_p \mathcal{P}^{-\frac{1}{2}}, & \Theta_p^* &= \mathcal{P}^{-\frac{1}{2}} \Theta_p \mathcal{P}^{-\frac{1}{2}}, & \Lambda_p^* &= \mathcal{P}^{-\frac{1}{2}} \Lambda_p \mathcal{P}^{-\frac{1}{2}}, & \Upsilon_p^* &= \mathcal{P}^{-\frac{1}{2}} \Upsilon_p \mathcal{P}^{-\frac{1}{2}}, \\ \lambda_1 &= \lambda_{\min}(\Xi_p^*), & \lambda_2 &= \lambda_{\max}(\Xi_p^*), & \lambda_3 &= \lambda_{\max}(\Theta_p^*), & \lambda_4 &= \lambda_{\max}(\Lambda_p^*), & \lambda_5 &= \lambda_{\max}(\Upsilon_p^*), \\ \Delta &= \lambda_2 + \eta e^{\gamma \eta} \lambda_3 + \eta e^{\gamma \eta} \lambda_4 + \eta^2 e^{\gamma \eta} \lambda_5. \end{aligned}$$

Theorem 3.1: Under Assumption (H), system (6) is said to be FTS with respect to given constants $(\kappa_1, \kappa_2, \mathcal{P}, \mathcal{T})$ if there exist constants $\gamma > 0, \varrho \geq 1$ and symmetric positive definite matrices $\Xi_p, \Theta_p, \Lambda_p, \Upsilon_p, \Psi_{1p}, \Psi_{2p}$ such that the following LMIs holds:

$$(i) \quad \mathcal{A} = \begin{bmatrix} \mathcal{A}_{11} & \mathcal{A}_{12} & \mathcal{A}_{13} & \mathcal{A}_{14} & \mathcal{A}_{15} & \mathcal{A}_{16} & \mathcal{A}_{17} \\ * & \mathcal{A}_{22} & \mathcal{A}_{23} & \mathcal{A}_{24} & \mathcal{A}_{25} & \mathcal{A}_{26} & \mathcal{A}_{27} \\ * & * & \mathcal{A}_{33} & \mathcal{A}_{34} & \mathcal{A}_{35} & \mathcal{A}_{36} & \mathcal{A}_{37} \\ * & * & * & \mathcal{A}_{44} & \mathcal{A}_{45} & \mathcal{A}_{46} & \mathcal{A}_{47} \\ * & * & * & * & \mathcal{A}_{55} & \mathcal{A}_{56} & \mathcal{A}_{57} \\ * & * & * & * & * & \mathcal{A}_{66} & \mathcal{A}_{67} \\ * & * & * & * & * & * & \mathcal{A}_{77} \end{bmatrix} < 0, \quad (8)$$

$$(ii) \quad \Xi_p \leq \varrho \Xi_q, \quad \Theta_p \leq \varrho \Theta_q, \quad \Lambda_p \leq \varrho \Lambda_q, \quad \Upsilon_p \leq \varrho \Upsilon_q, \quad (9)$$

$$(iii) \quad \lambda_1 \mathcal{P} \leq \Xi_p \leq \lambda_2 \mathcal{P}, \quad \Theta_p \leq \lambda_3 \mathcal{P}, \quad \Lambda_p \leq \lambda_4 \mathcal{P}, \quad \Upsilon_p \leq \lambda_5 \mathcal{P}, \quad (10)$$

$$(iv) \quad \Delta \kappa_1 - e^{-\gamma \mathcal{T}} \lambda_1 \kappa_2 < 0, \quad (11)$$

and the ADT of $\sigma(t)$ satisfies

$$(v) \quad \tau_\epsilon > \tau_\epsilon^* = \frac{\mathcal{T}(\ln \varrho)}{\ln(\lambda_1 \kappa_2) - \ln(\Delta \kappa_1) - \gamma \mathcal{T}}, \quad (12)$$

where

$$\begin{aligned} \mathcal{A}_{11} &= He(\Xi_p \mathcal{Q}_p) + \alpha_p \Psi_{1p} + \lambda_p \Xi_p + \Theta_p + \Lambda_p + \eta \Upsilon_p - \frac{1}{2} \pi^2 \Xi_p \mathcal{D}_p - \gamma \Xi_p, & \mathcal{A}_{12} &= \frac{1}{2} \pi^2 \Xi_p \mathcal{D}_p, \\ \mathcal{A}_{13} &= \Xi_p \mathcal{R}_p, \mathcal{A}_{14} = 0, & \mathcal{A}_{15} &= 0, \quad \mathcal{A}_{16} = \Xi_p, \quad \mathcal{A}_{17} = \Xi_p, & \mathcal{A}_{22} &= -\frac{1}{2} \pi^2 \Xi_p \mathcal{D}_p, \\ \mathcal{A}_{23} &= 0, \quad \mathcal{A}_{24} = 0, \quad \mathcal{A}_{25} = 0, \quad \mathcal{A}_{26} = 0, \quad \mathcal{A}_{27} = 0, \\ \mathcal{A}_{33} &= -(1 - \kappa) e^{\gamma \eta} \Theta_p + \beta_p \Psi_{2p} + \mu_p \Xi_p, & \mathcal{A}_{34} &= 0, \quad \mathcal{A}_{35} = 0, \quad \mathcal{A}_{36} = 0, \quad \mathcal{A}_{37} = 0, \\ \mathcal{A}_{44} &= -e^{\gamma \eta} \Lambda_p, \quad \mathcal{A}_{45} = 0, \quad \mathcal{A}_{46} = 0, \quad \mathcal{A}_{47} = 0, & \mathcal{A}_{55} &= -\frac{e^{\gamma \eta}}{\eta} \Upsilon_p, \quad \mathcal{A}_{56} = 0, \quad \mathcal{A}_{57} = 0, \\ \mathcal{A}_{66} &= -\Psi_{1p}, \quad \mathcal{A}_{67} = 0, \quad \mathcal{A}_{77} = -\Psi_{2p}. \end{aligned}$$

Proof: Let us consider the following Lyapunov–Krasovskii functional (LKF) candidate as

$$V_{\sigma(t)}(\mathfrak{S}(x, t)) = \sum_{r=1}^4 V_{r\sigma(t)}(\mathfrak{S}(x, t)),$$

where

$$\begin{aligned} V_{1\sigma(t)}(\mathfrak{S}(x, t)) &= \int_0^1 \mathfrak{S}^T(x, t) \Xi_{\sigma(t)} \mathfrak{S}(x, t) dx, \\ V_{2\sigma(t)}(\mathfrak{S}(x, t)) &= \int_0^1 \int_{t-\eta(t)}^t e^{\gamma(t-s)} \mathfrak{S}^T(x, s) \Theta_{\sigma(t)} \mathfrak{S}(x, s) ds dx, \\ V_{3\sigma(t)}(\mathfrak{S}(x, t)) &= \int_0^1 \int_{t-\eta}^t e^{\gamma(t-s)} \mathfrak{S}^T(x, s) \Lambda_{\sigma(t)} \mathfrak{S}(x, s) ds dx, \\ V_{4\sigma(t)}(\mathfrak{S}(x, t)) &= \int_0^1 \int_{-\eta}^0 \int_{t+\theta}^t e^{\gamma(t-s)} \mathfrak{S}^T(x, s) \Upsilon_{\sigma(t)} \mathfrak{S}(x, s) ds d\theta dx. \end{aligned}$$

Calculating $\mathcal{L}V_p(\mathfrak{S}(x, t))$ along the trajectories of system (6) by using Ito's formula, we get

$$\mathcal{L}V_p(\mathfrak{S}(x, t)) = \mathcal{L}V_{1p}(\mathfrak{S}(x, t)) + \mathcal{L}V_{2p}(\mathfrak{S}(x, t)) + \mathcal{L}V_{3p}(\mathfrak{S}(x, t)) + \mathcal{L}V_{4p}(\mathfrak{S}(x, t)). \quad (13)$$

Further, we have

$$\begin{aligned} \mathcal{L}V_{1p}(\mathfrak{S}(x, t)) &= 2 \int_0^1 \mathfrak{S}^T(x, t) \Xi_p \left[\mathcal{D}_p \frac{\partial^2 \mathfrak{S}(x, t)}{\partial x^2} + \mathcal{Q}_p \mathfrak{S}(x, t) + \mathcal{R}_p \mathfrak{S}(x, t - \eta(t)) \right. \\ &\quad \left. + f_p(t, \mathfrak{S}(x, t)) + g_p(t, \mathfrak{S}(x, t - \eta(t))) \right] dx + \int_0^1 \text{trace} \left[h_p^T(t) \Xi_p h_p(t) \right] dx \\ &\quad - \gamma \int_0^1 \mathfrak{S}^T(x, t) \Xi_p \mathfrak{S}(x, t) dx + \gamma V_{1p}(\mathfrak{S}(x, t)), \end{aligned} \quad (14)$$

where $h_p(t) = h_p(t, \mathfrak{S}(x, t), \mathfrak{S}(x, t - \eta(t)))$.

$$\begin{aligned} \mathcal{L}V_{2p}(\mathfrak{S}(x, t)) &= \gamma V_{2p}(\mathfrak{S}(x, t)) + \int_0^1 \mathfrak{S}^T(x, t) \Theta_p \mathfrak{S}(x, t) dx \\ &\quad - (1 - \eta(t)) \int_0^1 e^{\gamma \eta(t)} \mathfrak{S}^T(x, t - \eta(t)) \Theta_p \mathfrak{S}(x, t - \eta(t)) dx \\ &\leq \gamma V_{2p}(\mathfrak{S}(x, t)) + \int_0^1 \mathfrak{S}^T(x, t) \Theta_p \mathfrak{S}(x, t) dx \\ &\quad - (1 - \kappa) \int_0^1 e^{\gamma \eta} \mathfrak{S}^T(x, t - \eta(t)) \Theta_p \mathfrak{S}(x, t - \eta(t)) dx, \end{aligned} \quad (15)$$

$$\begin{aligned} \mathcal{L}V_{3p}(\mathfrak{S}(x, t)) &= \gamma V_{3p}(\mathfrak{S}(x, t)) + \int_0^1 \mathfrak{S}^T(x, t) \Lambda_p \mathfrak{S}(x, t) dx \\ &\quad - \int_0^1 e^{\gamma \eta} \mathfrak{S}^T(x, t - \eta) \Lambda_p \mathfrak{S}(x, t - \eta) dx, \end{aligned} \quad (16)$$

$$\begin{aligned} \mathcal{L}V_{4p}(\mathfrak{S}(x, t)) &= \gamma V_{4p}(\mathfrak{S}(x, t)) + \eta \int_0^1 \mathfrak{S}^T(x, t) \Upsilon_p \mathfrak{S}(x, t) dx \\ &\quad - \int_0^1 \int_{t-\eta}^t e^{\gamma \eta} \mathfrak{S}^T(x, s) \Upsilon_p \mathfrak{S}(x, s) ds dx. \end{aligned} \quad (17)$$

According to Lemma 2.3 and Assumption (7), we have

$$\begin{aligned} 2\mathfrak{S}^T(x, t) \Xi_p f_p(t, \mathfrak{S}(x, t)) &\leq \mathfrak{S}^T(x, t) \Xi_p \Psi_{1p}^{-1} \Xi_p \mathfrak{S}(x, t) + f_p^T(t, \mathfrak{S}(x, t)) \Psi_{1p} f_p(t, \mathfrak{S}(x, t)) \\ &\leq \mathfrak{S}^T(x, t) \Xi_p \Psi_{1p}^{-1} \Xi_p \mathfrak{S}(x, t) + \mathfrak{S}^T(x, t) \alpha_p \Psi_{1p} \mathfrak{S}(x, t), \end{aligned} \quad (18)$$

similarly

$$2\mathfrak{S}^T(x, t) \Xi_p g(t, \mathfrak{S}(x, t - \tau(t))) \leq \mathfrak{S}^T(x, t) \Xi_p \Psi_{2p}^{-1} \Xi_p \mathfrak{S}(x, t) + \mathfrak{S}^T(x, t - \tau(t)) \beta_p \Psi_{2p} \mathfrak{S}(x, t - \tau(t)). \quad (19)$$

Based on Assumption (7), we obtain

$$\text{trace}[h_p^T(t) \Xi_p h_p(t)] \leq \mathfrak{S}^T(x, t) \lambda_p \Xi_p \mathfrak{S}(x, t) + \mathfrak{S}^T(x, t - \tau(t)) \mu_p \Xi_p \mathfrak{S}(x, t - \tau(t)). \quad (20)$$

By virtue of integration by parts and Neumann boundary conditions (3), we obtain that

$$\begin{aligned} \int_0^1 \mathfrak{S}^T(x, t) \mathcal{D}_p \frac{\partial^2 \mathfrak{S}(x, t)}{\partial x^2} dx &= \left[\mathfrak{S}^T(x, t) \mathcal{D}_p \frac{\partial \mathfrak{S}(x, t)}{\partial x} \right]_{x=0}^{x=1} - \int_0^1 \frac{\partial \mathfrak{S}^T(x, t)}{\partial x} \mathcal{D}_p \frac{\partial \mathfrak{S}(x, t)}{\partial x} dx \\ &= - \int_0^1 \frac{\partial \mathfrak{S}^T(x, t)}{\partial x} \mathcal{D}_p \frac{\partial \mathfrak{S}(x, t)}{\partial x} dx. \end{aligned} \quad (21)$$

To obtain $\bar{\mathfrak{S}}(x, t) = 0$, we introduce a new state variable $\bar{\mathfrak{S}}(x, t) = \mathfrak{S}(x, t) - \mathfrak{S}(1, t)$ and satisfy the following condition:

$$\frac{\partial \mathfrak{S}^T(x, t)}{\partial x} \mathcal{D}_p \frac{\partial \mathfrak{S}(x, t)}{\partial x} = \frac{\partial \bar{\mathfrak{S}}^T(x, t)}{\partial x} \mathcal{D}_p \frac{\partial \bar{\mathfrak{S}}(x, t)}{\partial x}. \quad (22)$$

By virtue of Lemma 2.4, we obtain

$$\begin{aligned} \int_0^1 \mathfrak{S}^T(x, t) \mathcal{D}_p \frac{\partial^2 \mathfrak{S}(x, t)}{\partial x^2} dx &\leq -\frac{1}{4} \pi^2 \int_0^1 \tilde{\mathfrak{S}}^T(x, t) \mathcal{D}_p \tilde{\mathfrak{S}}(x, t) dx \\ &\leq -\frac{1}{4} \pi^2 \int_0^1 \mathfrak{S}^T(x, t) \mathcal{D}_p \mathfrak{S}(x, t) dx + \frac{1}{2} \pi^2 \int_0^1 \mathfrak{S}^T(x, t) \mathcal{D}_p \mathfrak{S}(1, t) dx \\ &\quad - \frac{1}{4} \pi^2 \int_0^1 \mathfrak{S}^T(1, t) \mathcal{D}_p \mathfrak{S}(1, t) dx. \end{aligned} \quad (23)$$

Based on Lemma 2.5, we obtain

$$-\int_{t-\eta}^t \mathfrak{S}^T(x, s) \Upsilon_p \mathfrak{S}(x, s) ds \leq -\frac{1}{\eta} \left(\int_{t-\eta}^t \mathfrak{S}(x, s) ds \right)^T \Upsilon_p \left(\int_{t-\eta}^t \mathfrak{S}(x, s) ds \right). \quad (24)$$

Combining the inequalities (13)–(24) and using Lemma 2.6, we have

$$\mathcal{L}V_p(\mathfrak{S}(x, t)) \leq \int_0^1 \xi^T(x, t) \mathcal{A} \xi(x, t) dx + \gamma V_p(\mathfrak{S}(x, t)), \quad (25)$$

where $\xi(x, t) = [\mathfrak{S}^T(x, t) \mathfrak{S}^T(1, t) \mathfrak{S}^T(x, t - \eta(t)) \mathfrak{S}^T(x, t - \eta) (\int_{t-\eta}^t \mathfrak{S}(x, s) ds)^T]^T$.

By virtue of inequality (8), we have

$$\mathcal{L}V_p(\mathfrak{S}(x, t)) \leq \gamma V_p(\mathfrak{S}(x, t)). \quad (26)$$

Multiplying the inequality (26) by $e^{-\gamma t}$, we get

$$\mathcal{L}(e^{-\gamma t} V_{\sigma(t)}(\mathfrak{S}(x, t))) < 0. \quad (27)$$

Then by taking mathematical expectation and integrating on both sides from t_k to t , we obtain that

$$\mathbb{E}\{V_{\sigma(t)}(\mathfrak{S}(x, t))\} < e^{\gamma(t-t_k)} \mathbb{E}\{V_{\sigma(t_k)}(\mathfrak{S}(x, t_k))\}, \quad (28)$$

for any $t \in [t_k, t_{k+1})$. Note that $\mathfrak{S}(x, t_k) = \mathfrak{S}(x, t_k^-)$ and applying the inequality (9) in $V_{\sigma(t)}(\mathfrak{S}(x, t))$, we obtain that

$$V_{\sigma(t_k)}(\mathfrak{S}(x, t_k)) \leq \varrho V_{\sigma(t_k^-)}(\mathfrak{S}(x, t_k^-)). \quad (29)$$

For any $t \in [0, T]$, there exist $n \in \mathbb{Z}$ such that $t \in [t_n, t_{n+1})$. Thus, it follows from the inequality (28) and (29) that

$$\begin{aligned} \mathbb{E}\{V_{\sigma(t)}(\mathfrak{S}(x, t))\} &< e^{\gamma(t-t_n)} \mathbb{E}\{V_{\sigma(t_n)}(\mathfrak{S}(x, t_n))\} \\ &\leq \varrho e^{\gamma(t-t_n)} \mathbb{E}\{V_{\sigma(t_n^-)}(\mathfrak{S}(x, t_n^-))\} \\ &\leq \dots \leq \varrho^{\mathcal{N}_{\sigma}(0, t)} e^{\gamma t} \mathbb{E}\{V_{\sigma(0)}(\mathfrak{S}(x, 0))\}. \end{aligned} \quad (30)$$

According to Definition 2.7, we obtain

$$\mathbb{E}\{V_{\sigma(t)}(\mathfrak{S}(x, t))\} < \varrho^{\frac{T}{\tau_c}} e^{\gamma T} \mathbb{E}\{V_{\sigma(0)}(\mathfrak{S}(x, 0))\}. \quad (31)$$

By virtue of inequality (10) and definition of $V_{\sigma(t)}(\mathfrak{S}(x, t))$, we have

$$\mathbb{E}\{V_{\sigma(t)}(\mathfrak{S}(x, t))\} \geq \mathbb{E}\left\{ \int_0^1 \mathfrak{S}^T(x, t) \Xi_{\sigma(t)} \mathfrak{S}(x, t) dx \right\} \geq \lambda_1 \mathbb{E}\left\{ \int_0^1 \mathfrak{S}^T(x, t) \mathcal{P} \mathfrak{S}(x, t) dx \right\}, \quad (32)$$

and

$$\begin{aligned} \mathbb{E}\{V_{\sigma(0)}(\mathfrak{Z}(x, 0))\} &= \mathbb{E}\left\{\int_0^1 \mathfrak{Z}^T(x, 0)\Xi_{\sigma(0)}\mathfrak{Z}(x, 0) dx + \int_0^1 \int_{-\eta(t)}^0 e^{-\gamma s}\mathfrak{Z}^T(x, s)\Theta_{\sigma(0)}\mathfrak{Z}(x, s) ds dx \right. \\ &\quad + \int_0^1 \int_{-\eta}^0 e^{-\gamma s}\mathfrak{Z}^T(x, s)\Lambda_{\sigma(0)}\mathfrak{Z}(x, s) ds dx \\ &\quad \left. + \int_0^1 \int_{-\eta}^0 \int_{\theta}^0 e^{-\gamma s}\mathfrak{Z}^T(x, s)\Upsilon_{\sigma(0)}\mathfrak{Z}(x, s) ds d\theta dx\right\} \\ &\leq (\lambda_2 + \eta e^{\gamma\eta}\lambda_3 + \eta e^{\gamma\eta}\lambda_4 + \eta^2 e^{\gamma\eta}\lambda_5) \\ &\quad \times \mathbb{E}\left\{\int_0^1 \sup_{-\eta \leq s \leq 0} \{\psi^T(x, s)\mathcal{P}\psi(x, s)\} dx\right\} = \Delta\kappa_1. \end{aligned} \tag{33}$$

From inequalities (31)–(33), we have

$$\mathbb{E}\left\{\int_0^1 \mathfrak{Z}^T(x, t)\mathcal{P}\mathfrak{Z}(x, t) dx\right\} \leq \frac{\Delta\kappa_1}{\lambda_1} \varrho^{\frac{T}{\tau_\epsilon}} e^{\gamma T}. \tag{34}$$

When $\varrho = 1$, clearly $\mathbb{E}\{\int_0^1 \mathfrak{Z}^T(x, t)\mathcal{P}\mathfrak{Z}(x, t) dx\} < \kappa_2 e^{-\gamma T} e^{\gamma T} = \kappa_2$. When $\varrho > 1$, from (11) and (12), we have

$$\ln(\lambda_1\kappa_2) - \ln(\Delta\kappa_1) - \gamma T > 0, \tag{35}$$

$$\frac{T}{\tau_\epsilon} < \frac{\ln(\lambda_1\kappa_2) - \ln(\Delta\kappa_1) - \gamma T}{\ln \varrho}. \tag{36}$$

Substituting the inequality (36) into (34), we obtain that

$$\mathbb{E}\left\{\int_0^1 \mathfrak{Z}^T(x, t)\mathcal{P}\mathfrak{Z}(x, t) dx\right\} \leq \frac{\Delta\kappa_1}{\lambda_1} e^{\gamma T} e^{\ln(\lambda_1\kappa_2) - \ln(\Delta\kappa_1) - \gamma T} = \kappa_2.$$

According to Definition 2.8, system (6) is FTS with respect to given constants $(\kappa_1, \kappa_2, \mathcal{P}, T)$. The proof is completed. ■

The following theorem states that the control gain matrices \mathcal{K}_p for the reliable controller (4) can be designed to obtain the finite-time stabilization for system (5).

Theorem 3.2: *The system (5) is said to be finite-time stabilizable if there exist constants $\gamma > 0, \varrho \geq 1$, symmetric positive definite matrices $\mathfrak{A}_p, \Theta_p, \tilde{\Lambda}_p, \tilde{\Upsilon}_p, \tilde{\Psi}_{1p}, \tilde{\Psi}_{2p}$ and constant matrix \mathfrak{B}_p such that the following LMIs (9)–(12) and*

$$(vi) \quad \mathcal{B} = \begin{bmatrix} \mathcal{B}_{11} & \mathcal{B}_{12} & \mathcal{B}_{13} & \mathcal{B}_{14} & \mathcal{B}_{15} & \mathcal{B}_{16} & \mathcal{B}_{17} \\ * & \mathcal{B}_{22} & \mathcal{B}_{23} & \mathcal{B}_{24} & \mathcal{B}_{25} & \mathcal{B}_{26} & \mathcal{B}_{27} \\ * & * & \mathcal{B}_{33} & \mathcal{B}_{34} & \mathcal{B}_{35} & \mathcal{B}_{36} & \mathcal{B}_{37} \\ * & * & * & \mathcal{B}_{44} & \mathcal{B}_{45} & \mathcal{B}_{46} & \mathcal{B}_{47} \\ * & * & * & * & \mathcal{B}_{55} & \mathcal{B}_{56} & \mathcal{B}_{57} \\ * & * & * & * & * & \mathcal{B}_{66} & \mathcal{B}_{67} \\ * & * & * & * & * & * & \mathcal{B}_{77} \end{bmatrix} < 0, \tag{37}$$

where

$$\begin{aligned}
\mathcal{B}_{11} &= He(\mathcal{Q}_p \mathfrak{A}_p + \mathcal{S}_p \mathcal{X}_{\mathcal{H}_p} \mathfrak{B}_p) + \alpha_p \tilde{\Psi}_{1p} + \mathfrak{A}_p \lambda_p + \tilde{\Theta}_p + \tilde{\Lambda}_p + \eta \tilde{\Upsilon}_p - \frac{1}{2} \pi^2 \mathcal{D}_p \mathfrak{A}_p - \gamma \mathfrak{A}_p, \\
\mathcal{B}_{12} &= \frac{1}{2} \pi^2 \mathcal{D}_p \mathfrak{A}_p, \quad \mathcal{B}_{13} = \mathcal{R}_p \mathfrak{A}_p, \quad \mathcal{B}_{14} = 0, \quad \mathcal{B}_{15} = 0, \quad \mathcal{B}_{16} = \mathfrak{A}_p, \quad \mathcal{B}_{17} = \mathfrak{A}_p, \\
\mathcal{B}_{22} &= -\frac{1}{2} \pi^2 \mathcal{D}_p \mathfrak{A}_p, \quad \mathcal{B}_{23} = 0, \quad \mathcal{B}_{24} = 0, \quad \mathcal{B}_{25} = 0, \quad \mathcal{B}_{26} = 0, \quad \mathcal{B}_{27} = 0, \\
\mathcal{B}_{33} &= -(1 - \kappa) e^{\gamma \eta} \tilde{\Theta}_p + \beta_p \tilde{\Psi}_{2p} + \mathfrak{A}_p \mu_p, \quad \mathcal{B}_{34} = 0, \\
\mathcal{B}_{35} &= 0, \quad \mathcal{B}_{36} = 0, \quad \mathcal{B}_{37} = 0, \quad \mathcal{B}_{44} = -e^{\gamma \eta} \tilde{\Lambda}_p, \quad \mathcal{B}_{45} = 0, \quad \mathcal{B}_{46} = 0, \quad \mathcal{B}_{47} = 0, \\
\mathcal{B}_{55} &= -\frac{e^{\gamma \eta}}{\eta} \tilde{\Upsilon}_p, \quad \mathcal{B}_{56} = 0, \quad \mathcal{B}_{57} = 0, \quad \mathcal{B}_{66} = -\tilde{\Psi}_{1p}, \quad \mathcal{B}_{67} = 0, \quad \mathcal{B}_{77} = -\tilde{\Psi}_{2p}
\end{aligned}$$

are satisfied. Furthermore, the control gain matrices are designed by

$$(vii) \quad \mathcal{K}_p = \mathfrak{B}_p \mathfrak{A}_p^{-1}. \quad (38)$$

Proof: Construct the same LKF candidate as in Theorem 3.1 and replacing \mathcal{Q}_p in (8) by $(\mathcal{Q}_p + \mathcal{S}_p \mathcal{X}_{\mathcal{H}_p} \mathcal{K}_p)$, we have

$$\mathcal{A} = \begin{bmatrix} \mathcal{A}_{11} & \mathcal{A}_{12} & \mathcal{A}_{13} & \mathcal{A}_{14} & \mathcal{A}_{15} & \mathcal{A}_{16} & \mathcal{A}_{17} \\ * & \mathcal{A}_{22} & \mathcal{A}_{23} & \mathcal{A}_{24} & \mathcal{A}_{25} & \mathcal{A}_{26} & \mathcal{A}_{27} \\ * & * & \mathcal{A}_{33} & \mathcal{A}_{34} & \mathcal{A}_{35} & \mathcal{A}_{36} & \mathcal{A}_{37} \\ * & * & * & \mathcal{A}_{44} & \mathcal{A}_{45} & \mathcal{A}_{46} & \mathcal{A}_{47} \\ * & * & * & * & \mathcal{A}_{55} & \mathcal{A}_{56} & \mathcal{A}_{57} \\ * & * & * & * & * & \mathcal{A}_{66} & \mathcal{A}_{67} \\ * & * & * & * & * & * & \mathcal{A}_{77} \end{bmatrix} < 0, \quad (39)$$

where

$$\begin{aligned}
\mathcal{A}_{11} &= He(\Xi_p(\mathcal{Q}_p + \mathcal{S}_p \mathcal{X}_{\mathcal{H}_p} \mathcal{K}_p)) + \alpha_p \Psi_{1p} + \lambda_p \Xi_p + \Theta_p + \Lambda_p + \eta \Upsilon_p - \frac{1}{2} \pi^2 \Xi_p \mathcal{D}_p - \gamma \Xi_p, \\
\mathcal{A}_{12} &= \frac{1}{2} \pi^2 \Xi_p \mathcal{D}_p, \quad \mathcal{A}_{13} = \Xi_p \mathcal{R}_p, \quad \mathcal{A}_{14} = 0, \quad \mathcal{A}_{15} = 0, \quad \mathcal{A}_{16} = \Xi_p, \quad \mathcal{A}_{17} = \Xi_p, \\
\mathcal{A}_{22} &= -\frac{1}{2} \pi^2 \Xi_p \mathcal{D}_p, \quad \mathcal{A}_{23} = 0, \quad \mathcal{A}_{24} = 0, \quad \mathcal{A}_{25} = 0, \quad \mathcal{A}_{26} = 0, \quad \mathcal{A}_{27} = 0, \\
\mathcal{A}_{33} &= -(1 - \kappa) e^{\gamma \eta} \Theta_p + \beta_p \Psi_{2p} + \mu_p \Xi_p, \quad \mathcal{A}_{34} = 0, \quad \mathcal{A}_{35} = 0, \quad \mathcal{A}_{36} = 0, \\
\mathcal{A}_{37} &= 0, \quad \mathcal{A}_{44} = -e^{\gamma \eta} \Lambda_p, \quad \mathcal{A}_{45} = 0, \quad \mathcal{A}_{46} = 0, \quad \mathcal{A}_{47} = 0, \quad \mathcal{A}_{55} = -\frac{e^{\gamma \eta}}{\eta} \Upsilon_p, \quad \mathcal{A}_{56} = 0, \\
\mathcal{A}_{57} &= 0, \quad \mathcal{A}_{66} = -\Psi_{1p}, \quad \mathcal{A}_{67} = 0, \quad \mathcal{A}_{77} = -\Psi_{2p}.
\end{aligned}$$

Now, pre and post multiplying (39) by $\text{diag}\{\Xi_p^{-1}, \Xi_p^{-1}, \Xi_p^{-1}, \Xi_p^{-1}, \Xi_p^{-1}, \Xi_p^{-1}, \Xi_p^{-1}\}$ and setting $\mathfrak{A}_p = \Xi_p^{-1}$, $\mathfrak{B}_p = \mathcal{K}_p \mathfrak{A}_p$, $\tilde{\Theta}_p = \mathfrak{A}_p \Theta_p \mathfrak{A}_p$, $\tilde{\Lambda}_p = \mathfrak{A}_p \Lambda_p \mathfrak{A}_p$, $\tilde{\Upsilon}_p = \mathfrak{A}_p \Upsilon_p \mathfrak{A}_p$, $\tilde{\Psi}_{1p} = \mathfrak{A}_p \Psi_{1p} \mathfrak{A}_p$, $\tilde{\Psi}_{2p} = \mathfrak{A}_p \Psi_{2p} \mathfrak{A}_p$, one can obtain $\mathcal{B} < 0$. By virtue of Theorem 3.1 and Definition 2.9, system (5) is finite-time stabilizable. The proof is completed. \blacksquare

The next theorem is to investigate the finite-time cost control for system (5).

Theorem 3.3: System (5) is said to be finite-time stabilizable if there exist constants $\gamma > 0, \varrho \geq 1$, symmetric positive definite matrices $\mathfrak{A}_p, \tilde{\Theta}_p, \tilde{\Lambda}_p, \tilde{\Upsilon}_p, \tilde{\Psi}_{1p}, \tilde{\Psi}_{2p}$ and constant matrix \mathfrak{B}_p such that they satisfy the following LMIs (9)–(12) and

$$(viii) \quad \Gamma = \begin{bmatrix} [\mathfrak{B}]_{7 \times 7} & \Gamma_{12} & \Gamma_{13} \\ * & \Gamma_{22} & \Gamma_{23} \\ * & * & \Gamma_{33} \end{bmatrix} < 0, \quad (40)$$

where

$$\begin{aligned} \Gamma_{12} &= [\mathcal{U}_p \mathfrak{A}_p \quad 0 \quad 0 \quad 0 \quad 0 \quad 0 \quad 0]^T, \quad \Gamma_{13} = [\mathcal{V}_p \mathcal{X}_{\mathcal{H}_p} \mathfrak{B}_p \quad 0 \quad 0 \quad 0 \quad 0 \quad 0 \quad 0]^T, \\ \Gamma_{22} &= -\mathcal{U}_p, \quad \Gamma_{23} = 0, \quad \Gamma_{33} = -\mathcal{V}_p, \end{aligned}$$

and $[\mathfrak{B}]_{7 \times 7}$ is defined in Theorem 3.2. Furthermore, the control gain matrices are designed by (38) and the GCC value is defined by

$$(ix) \quad J^* = \Delta \kappa_1. \quad (41)$$

Proof: Construct the same LKF candidate as in Theorem 3.1, and introduce the following inequality from Theorems 3.1, 3.2 and cost function (7):

$$\begin{aligned} \mathcal{L}V_{\sigma(t)}(\mathfrak{S}(x, t)) - \gamma V_{\sigma(t)}(\mathfrak{S}(x, t)) &\leq \int_0^1 \xi^T(x, t) \mathfrak{B} \xi(x, t) dx + \int_0^1 \left[\mathfrak{S}^T(x, t) (\mathcal{U}_{\sigma(t)} - \mathcal{U}_{\sigma(t)}) \mathfrak{S}(x, t) \right. \\ &\quad \left. + (u^{\mathcal{F}}(x, t))^T (\mathcal{V}_{\sigma(t)} - V_{\sigma(t)}) (u^{\mathcal{F}}(x, t)) \right] dx \\ &\leq \int_0^1 \xi^T(x, t) \mathfrak{B} \xi(x, t) dx + \int_0^1 \mathfrak{S}^T(x, t) [\mathcal{U}_p \\ &\quad + \mathcal{K}_p^T \mathcal{X}_{\mathcal{H}_p}^T \mathcal{V}_p \mathcal{X}_{\mathcal{H}_p} \mathcal{K}_p] \mathfrak{S}(x, t) dx \\ &\quad - \int_0^1 \mathfrak{S}^T(x, t) [\mathcal{U}_p + \mathcal{K}_p^T \mathcal{X}_{\mathcal{H}_p}^T \mathcal{V}_p \mathcal{X}_{\mathcal{H}_p} \mathcal{K}_p] \mathfrak{S}(x, t) dx. \end{aligned}$$

By virtue of Lemma 2.6 and inequality (40), we obtain

$$\mathcal{L}V_{\sigma(t)}(\mathfrak{S}(x, t)) - \gamma V_{\sigma(t)}(\mathfrak{S}(x, t)) \leq - \int_0^1 \mathfrak{S}^T(x, t) [\mathcal{U}_p + \mathcal{K}_p^T \mathcal{X}_{\mathcal{H}_p}^T \mathcal{V}_p \mathcal{X}_{\mathcal{H}_p} \mathcal{K}_p] \mathfrak{S}(x, t) dx. \quad (42)$$

From the given symmetric positive definite matrices $\mathcal{U}_p > 0, \mathcal{V}_p > 0$, Theorems 3.1 and 3.2, system (5) is finite-time stabilizable.

Furthermore, to obtain the GCC value, for inequality (42) multiplying by $e^{-\gamma t}$ and integrating from 0 to ∞ , we get

$$\begin{aligned} J &= \mathbb{E} \left\{ \int_0^1 \int_0^\infty e^{-\gamma t} \left[\mathfrak{S}^T(x, t) \mathcal{U}_p \mathfrak{S}(x, t) + (u^{\mathcal{F}}(x, t))^T \mathcal{V}_p (u^{\mathcal{F}}(x, t)) \right] dt dx \right\} \\ &\leq \mathbb{E} \{ V_{\sigma(0)}(\mathfrak{S}(x, 0)) \} \leq \Delta \kappa_1 = J^*. \end{aligned}$$

The proof is completed. ■

Remark 3.4: We compare it with some existing results in the literature [15,39,54]. In [15], the author investigated the GCC for switched delta operator systems with actuator faults. In [39], the author investigated the robust finite-time GCC for positive systems with delays. In [54], robust finite-time

GCC for switched impulsive systems was investigated. However, diffusion effects and stochastic disturbances are not considered in the above mentioned results. In fact, noise presented a fundamental issue in the transmission of information impacting all facets of the neuron systems operating within the neuron systems. Strictly speaking, the diffusion effects are unavoidable in nonlinear systems when electrons flow in nonuniform electromagnetic fields. It is worth noting the introduction of stochastic disturbances and diffusion systems into the nonlinear switched systems. It is suitable for dealing with real-life applications such as secure communication, image encryption and Alzheimer’s disease.

Remark 3.5: In [48], the author studied the membership-function-dependent based fuzzy control for memristive reaction-diffusion neural networks with sensors and actuators faults. In [9,28], the authors studied the fault-tolerant control for switched systems with actuator faults. In [42], the author studied a finite-time fuzzy adaptive control for nonlinear systems with actuator faults. In [29], author studied the finite-time control of switched systems with actuator faults. However, for the finite-time cost control of SNSSs with time-varying delays, reaction-diffusion and actuator faults related results have not been studied in previous works. To shorten the gap, this paper studied the finite-time guaranteed cost control for SNSSs with time-varying delays, reaction-diffusion and actuator faults via reliable control.

Remark 3.6: In this paper, Theorem 3.2 presents a sufficient criterion finite-time stabilization for SNSSs with time-varying delays, reaction-diffusion and actuator faults via reliable control. It should be pointed out that the control gain matrices \mathcal{K}_p are more flexible for the feasibility of LMIs (9)–(12) and (37) than those designed reliable controller in the literature [2]–[44].

Remark 3.7: The obtained results in this paper are extended with improved results in [11]. In [11], the author discussed the FTS and stabilization for stochastic Markovian switching reaction-diffusion systems via boundary control. In this paper, we discussed the FTS, stabilization and finite-time cost control for SNSSs with time-varying delays, reaction-diffusion and actuator faults via reliable control.

Remark 3.8: For system (5), let the reaction-diffusion terms be ignored. Then, system (5) can be rewritten as

$$d\mathfrak{S}(t) = \left[(\mathcal{Q}_{\sigma(t)} + \mathcal{S}_{\sigma(t)} \mathcal{X}_{\mathcal{H}_{\sigma(t)}} \mathcal{K}_{\sigma(t)}) \mathfrak{S}(t) + \mathcal{R}_{\sigma(t)} \mathfrak{S}(t - \eta(t)) + f_{\sigma(t)}(t, \mathfrak{S}(t)) + g_{\sigma(t)}(t, \mathfrak{S}(t - \eta(t))) \right] dt + h_{\sigma(t)}(t, \mathfrak{S}(t), \mathfrak{S}(t - \eta(t))) d\omega(t). \tag{43}$$

The following corollary follows from Theorem 3.3.

Corollary 3.9: System (43) is said to be finite-time stabilizable if there exist constants $\gamma > 0, \varrho \geq 1$, symmetric positive definite matrices $\mathfrak{A}_p, \tilde{\Theta}_p, \tilde{\Lambda}_p, \tilde{\Upsilon}_p, \tilde{\Psi}_{1p}, \tilde{\Psi}_{2p}$, and constant matrix \mathfrak{B}_p such that the following LMIs (9)–(12), and

$$(x) \quad \mathfrak{G} = \begin{bmatrix} \mathfrak{G}_{11} & \mathfrak{G}_{12} & \mathfrak{G}_{13} & \mathfrak{G}_{14} & \mathfrak{G}_{15} & \mathfrak{G}_{16} & \mathfrak{G}_{17} & \mathfrak{G}_{18} \\ * & \mathfrak{G}_{22} & \mathfrak{G}_{23} & \mathfrak{G}_{24} & \mathfrak{G}_{25} & \mathfrak{G}_{26} & \mathfrak{G}_{27} & \mathfrak{G}_{28} \\ * & * & \mathfrak{G}_{33} & \mathfrak{G}_{34} & \mathfrak{G}_{35} & \mathfrak{G}_{36} & \mathfrak{G}_{37} & \mathfrak{G}_{38} \\ * & * & * & \mathfrak{G}_{44} & \mathfrak{G}_{45} & \mathfrak{G}_{46} & \mathfrak{G}_{47} & \mathfrak{G}_{48} \\ * & * & * & * & \mathfrak{G}_{55} & \mathfrak{G}_{56} & \mathfrak{G}_{57} & \mathfrak{G}_{58} \\ * & * & * & * & * & \mathfrak{G}_{66} & \mathfrak{G}_{67} & \mathfrak{G}_{68} \\ * & * & * & * & * & * & \mathfrak{G}_{77} & \mathfrak{G}_{78} \\ * & * & * & * & * & * & * & \mathfrak{G}_{88} \end{bmatrix} < 0, \tag{44}$$

where

$$\begin{aligned}
 \mathfrak{G}_{11} &= He(\mathcal{Q}_p \mathfrak{A}_p + \mathcal{S}_p \mathcal{X}_{\mathcal{H}_p} \mathfrak{B}_p) + \alpha_p \tilde{\Psi}_{1p} + \mathfrak{A}_p \lambda_p + \tilde{\Theta}_p + \tilde{\Lambda}_p + \eta \tilde{\Upsilon}_p - \gamma \mathfrak{A}_p, & \mathfrak{G}_{12} &= \mathcal{R}_p \mathfrak{A}_p, \\
 \mathfrak{G}_{13} &= 0, & \mathfrak{G}_{14} &= 0, & \mathfrak{G}_{15} &= \mathfrak{A}_p, & \mathfrak{G}_{16} &= \mathfrak{A}_p, & \mathfrak{G}_{17} &= \mathcal{U}_p \mathfrak{A}_p, & \mathfrak{G}_{18} &= \mathcal{V}_p \mathcal{X}_{\mathcal{H}_p} \mathfrak{B}_p, \\
 \mathfrak{G}_{22} &= -(1 - \kappa) e^{\gamma \eta} \tilde{\Theta}_p + \beta_p \tilde{\Psi}_{2p} + \mathfrak{A}_p \mu_p, & \mathfrak{G}_{23} &= 0, & \mathfrak{G}_{24} &= 0, & \mathfrak{G}_{25} &= 0, & \mathfrak{G}_{26} &= 0, \\
 \mathfrak{G}_{27} &= 0, & \mathfrak{G}_{28} &= 0, & \mathfrak{G}_{33} &= -e^{\gamma \eta} \tilde{\Lambda}_p, & \mathfrak{G}_{34} &= 0, & \mathfrak{G}_{35} &= 0, & \mathfrak{G}_{36} &= 0, & \mathfrak{G}_{37} &= 0, \\
 \mathfrak{G}_{38} &= 0, & \mathfrak{G}_{44} &= -\frac{e^{\gamma \eta}}{\eta} \tilde{\Upsilon}_p, & \mathfrak{G}_{45} &= 0, & \mathfrak{G}_{46} &= 0, & \mathfrak{G}_{47} &= 0, & \mathfrak{G}_{48} &= 0, & \mathfrak{G}_{55} &= -\tilde{\Psi}_{1p}, \\
 \mathfrak{G}_{56} &= 0, & \mathfrak{G}_{57} &= 0, & \mathfrak{G}_{58} &= 0, & \mathfrak{G}_{66} &= -\tilde{\Psi}_{2p}, & \mathfrak{G}_{67} &= 0, & \mathfrak{G}_{68} &= 0, & \mathfrak{G}_{77} &= -\mathcal{U}_p, \\
 \mathfrak{G}_{78} &= 0, & \mathfrak{G}_{88} &= -\mathcal{V}_p,
 \end{aligned}$$

are satisfied. Furthermore, the control gain matrices are designed by (38) and the GCC value is defined by (41).

Remark 3.10: In system (5), if the stochastic disturbances $h_p(t) = 0$, then system (5) is turned into the following nonlinear switched systems (NSSs) with time-varying delays, reaction-diffusion and actuator faults:

$$\begin{aligned}
 \frac{\partial \mathfrak{Z}(x, t)}{\partial t} &= \mathcal{D}_{\sigma(t)} \frac{\partial^2 \mathfrak{Z}(x, t)}{\partial x^2} + (\mathcal{Q}_{\sigma(t)} + \mathcal{S}_{\sigma(t)} \mathcal{X}_{\mathcal{H}_{\sigma(t)}} \mathcal{K}_{\sigma(t)}) \mathfrak{Z}(x, t) + \mathcal{R}_{\sigma(t)} \mathfrak{Z}(x, t - \eta(t)) \\
 &+ f_{\sigma(t)}(t, \mathfrak{Z}(x, t)) + g_{\sigma(t)}(t, \mathfrak{Z}(x, t - \eta(t))).
 \end{aligned} \tag{45}$$

The next corollary is to investigate the finite-time cost control for system (45).

Corollary 3.11: System (45) is said to be finite-time stabilizable if there exist constants $\gamma > 0, \varrho \geq 1$, symmetric positive definite matrices $\mathfrak{A}_p, \tilde{\Theta}_p, \tilde{\Lambda}_p, \tilde{\Upsilon}_p, \tilde{\Psi}_{1p}, \tilde{\Psi}_{2p}$, and constant matrix \mathfrak{B}_p such that the following LMIs (9)-(12) and

$$\text{(xi) } \mathfrak{M} = \begin{bmatrix} \mathfrak{M}_{11} & \mathfrak{M}_{12} & \mathfrak{M}_{13} & \mathfrak{M}_{14} & \mathfrak{M}_{15} & \mathfrak{M}_{16} & \mathfrak{M}_{17} & \mathfrak{M}_{18} & \mathfrak{M}_{19} \\ * & \mathfrak{M}_{22} & \mathfrak{M}_{23} & \mathfrak{M}_{24} & \mathfrak{M}_{25} & \mathfrak{M}_{26} & \mathfrak{M}_{27} & \mathfrak{M}_{28} & \mathfrak{M}_{29} \\ * & * & \mathfrak{M}_{33} & \mathfrak{M}_{34} & \mathfrak{M}_{35} & \mathfrak{M}_{36} & \mathfrak{M}_{37} & \mathfrak{M}_{38} & \mathfrak{M}_{39} \\ * & * & * & \mathfrak{M}_{44} & \mathfrak{M}_{45} & \mathfrak{M}_{46} & \mathfrak{M}_{47} & \mathfrak{M}_{48} & \mathfrak{M}_{49} \\ * & * & * & * & \mathfrak{M}_{55} & \mathfrak{M}_{56} & \mathfrak{M}_{57} & \mathfrak{M}_{58} & \mathfrak{M}_{59} \\ * & * & * & * & * & \mathfrak{M}_{66} & \mathfrak{M}_{67} & \mathfrak{M}_{68} & \mathfrak{M}_{69} \\ * & * & * & * & * & * & \mathfrak{M}_{77} & \mathfrak{M}_{78} & \mathfrak{M}_{79} \\ * & * & * & * & * & * & * & \mathfrak{M}_{88} & \mathfrak{M}_{89} \\ * & * & * & * & * & * & * & * & \mathfrak{M}_{99} \end{bmatrix} < 0, \tag{46}$$

where

$$\begin{aligned}
 \mathfrak{M}_{11} &= He(\mathcal{Q}_p \mathfrak{A}_p + \mathcal{S}_p \mathcal{X}_{\mathcal{H}_p} \mathfrak{B}_p) + \alpha_p \tilde{\Psi}_{1p} + \tilde{\Theta}_p + \tilde{\Lambda}_p + \eta \tilde{\Upsilon}_p - \frac{1}{2} \pi^2 \mathcal{D}_p \mathfrak{A}_p - \gamma \mathfrak{A}_p, \\
 \mathfrak{M}_{12} &= \frac{1}{2} \pi^2 \mathcal{D}_p \mathfrak{A}_p, & \mathfrak{M}_{13} &= \mathcal{R}_p \mathfrak{A}_p, & \mathfrak{M}_{14} &= 0, & \mathfrak{M}_{15} &= 0, & \mathfrak{M}_{16} &= \mathfrak{A}_p, & \mathfrak{M}_{17} &= \mathfrak{A}_p, \\
 \mathfrak{M}_{18} &= \mathcal{U}_p \mathfrak{A}_p, & \mathfrak{M}_{19} &= \mathcal{V}_p \mathcal{X}_{\mathcal{H}_p} \mathfrak{B}_p, & \mathfrak{M}_{22} &= -\frac{1}{2} \pi^2 \mathcal{D}_p \mathfrak{A}_p, & \mathfrak{M}_{23} &= 0, & \mathfrak{M}_{24} &= 0, & \mathfrak{M}_{25} &= 0, \\
 \mathfrak{M}_{26} &= 0, & \mathfrak{M}_{27} &= 0, & \mathfrak{M}_{28} &= 0, & \mathfrak{M}_{29} &= 0, & \mathfrak{M}_{33} &= -(1 - \kappa) e^{\gamma \eta} \tilde{\Theta}_p + \beta_p \tilde{\Psi}_{2p},
 \end{aligned}$$

$$\begin{aligned}
\mathfrak{M}_{34} &= 0, & \mathfrak{M}_{35} &= 0, & \mathfrak{M}_{36} &= 0, & \mathfrak{M}_{37} &= 0, & \mathfrak{M}_{38} &= 0, & \mathfrak{M}_{39} &= 0, & \mathfrak{M}_{44} &= -e^{\gamma\eta} \tilde{\Lambda}_p, \\
\mathfrak{M}_{45} &= 0, & \mathfrak{M}_{46} &= 0, & \mathfrak{M}_{47} &= 0, & \mathfrak{M}_{48} &= 0, & \mathfrak{M}_{49} &= 0, & \mathfrak{M}_{55} &= -\frac{e^{\gamma\eta}}{\eta} \tilde{\Upsilon}_p, & \mathfrak{M}_{56} &= 0, \\
\mathfrak{M}_{57} &= 0, & \mathfrak{M}_{58} &= 0, & \mathfrak{M}_{59} &= 0, & \mathfrak{M}_{66} &= -\tilde{\Psi}_{1p}, & \mathfrak{M}_{67} &= 0, & \mathfrak{M}_{68} &= 0, & \mathfrak{M}_{69} &= 0, \\
\mathfrak{M}_{77} &= -\tilde{\Psi}_{2p}, & \mathfrak{M}_{78} &= 0, & \mathfrak{M}_{79} &= 0, & \mathfrak{M}_{88} &= -\mathcal{U}_p, & \mathfrak{M}_{89} &= 0, & \mathfrak{M}_{99} &= -\mathcal{V}_p,
\end{aligned}$$

are satisfied. Furthermore, the control gain matrices are designed by (38) and the GCC value is defined by (41).

4. Numerical example

In this section, one numerical example with two cases are presented to illustrates the effectiveness and validity of proposed reliable controller.

Consider the following two-mode SNSSs with time-varying delays, reaction-diffusion and actuator faults:

$$\left\{ \begin{aligned}
d\mathfrak{S}(x, t) &= \left[\mathcal{D}_{\sigma(t)} \frac{\partial^2 \mathfrak{S}(x, t)}{\partial x^2} + \mathcal{Q}_{\sigma(t)} \mathfrak{S}(x, t) + \mathcal{R}_{\sigma(t)} \mathfrak{S}(x, t - (0.3 + 0.2 \cos(t))) \right. \\
&\quad \left. + 2 \sin(\mathfrak{S}(x, t)) + \sin(\mathfrak{S}(x, t - (0.3 + 0.2 \cos(t)))) + \mathcal{S}_{\sigma(t)} u^{\mathcal{F}}(x, t) \right] dt \\
&\quad + [0.2 \mathfrak{S}(x, t) + 0.3 \mathfrak{S}(x, t - (0.3 + 0.2 \cos(t)))] d\omega(t), \\
\mathfrak{S}(x, s) &= \phi(x, s), \quad x \in (0, 1), \quad s \in [-0.5, 0], \\
\frac{\partial \mathfrak{S}(x, t)}{\partial x} \Big|_{x=0} &= 0, \quad \frac{\partial \mathfrak{S}(x, t)}{\partial x} \Big|_{x=1} = 0.
\end{aligned} \right. \quad (47)$$

Mode: 1.

$$\begin{aligned}
\mathcal{D}_1 &= \begin{bmatrix} 0.5 & 0 \\ 0 & 0.5 \end{bmatrix}, & \mathcal{Q}_1 &= \begin{bmatrix} 0.3 & 0.2 \\ -0.3 & -0.8 \end{bmatrix}, & \mathcal{R}_1 &= \begin{bmatrix} -1.01 & 0.2 \\ 0.03 & -1.2 \end{bmatrix}, & \mathcal{S}_1 &= \begin{bmatrix} -1.3 & 0.5 \\ 0.3 & -1.3 \end{bmatrix}, \\
\mathcal{U}_1 &= \begin{bmatrix} 0.1 & 0 \\ 0 & 0.3 \end{bmatrix}, & \mathcal{V}_1 &= \begin{bmatrix} 0.5 & 0 \\ 0 & 0.4 \end{bmatrix}, & \mathcal{X}_{1_1} &= \begin{bmatrix} 1 & 0 \\ 0 & 0 \end{bmatrix}.
\end{aligned}$$

Mode: 2.

$$\begin{aligned}
\mathcal{D}_2 &= \begin{bmatrix} 0.5 & 0 \\ 0 & 0.5 \end{bmatrix}, & \mathcal{Q}_2 &= \begin{bmatrix} -0.8 & -0.1 \\ 0.3 & 0.1 \end{bmatrix}, & \mathcal{R}_2 &= \begin{bmatrix} 0.6 & -0.4 \\ 0.7 & 0.2 \end{bmatrix}, & \mathcal{S}_2 &= \begin{bmatrix} -0.5 & 1.0 \\ 0.2 & -0.3 \end{bmatrix}, \\
\mathcal{U}_2 &= \begin{bmatrix} 0.1 & 0 \\ 0 & 0.3 \end{bmatrix}, & \mathcal{V}_2 &= \begin{bmatrix} 0.5 & 0 \\ 0 & 0.4 \end{bmatrix}, & \mathcal{X}_{1_2} &= \begin{bmatrix} 1 & 0 \\ 0 & 0 \end{bmatrix}.
\end{aligned}$$

The initial values of system (47) are

$$\begin{cases} \mathfrak{S}_1(x, s) = 0.4 \sin(0.4\pi x) + 0.4 \cos(s), & s \in [-0.5, 0], \\ \mathfrak{S}_2(x, s) = 0.3 \sin(0.9\pi x) + 0.2 \cos(s), & s \in [-0.5, 0], \\ \mathfrak{S}_3(x, s) = 0.4 \sin(0.6\pi x) + 0.3 \cos(s), & s \in [-0.5, 0]. \end{cases}$$

Figure 1 illustrates the state responses $\mathbb{E}\mathfrak{S}^2(x, t)$ and state norm $\mathbb{E}\|\mathfrak{S}(\cdot, t)\|^2$ of system (47) without control. It clearly shows that system (47) does not realize the stabilization without control.

Case 1: System (47) with stochastic disturbances.

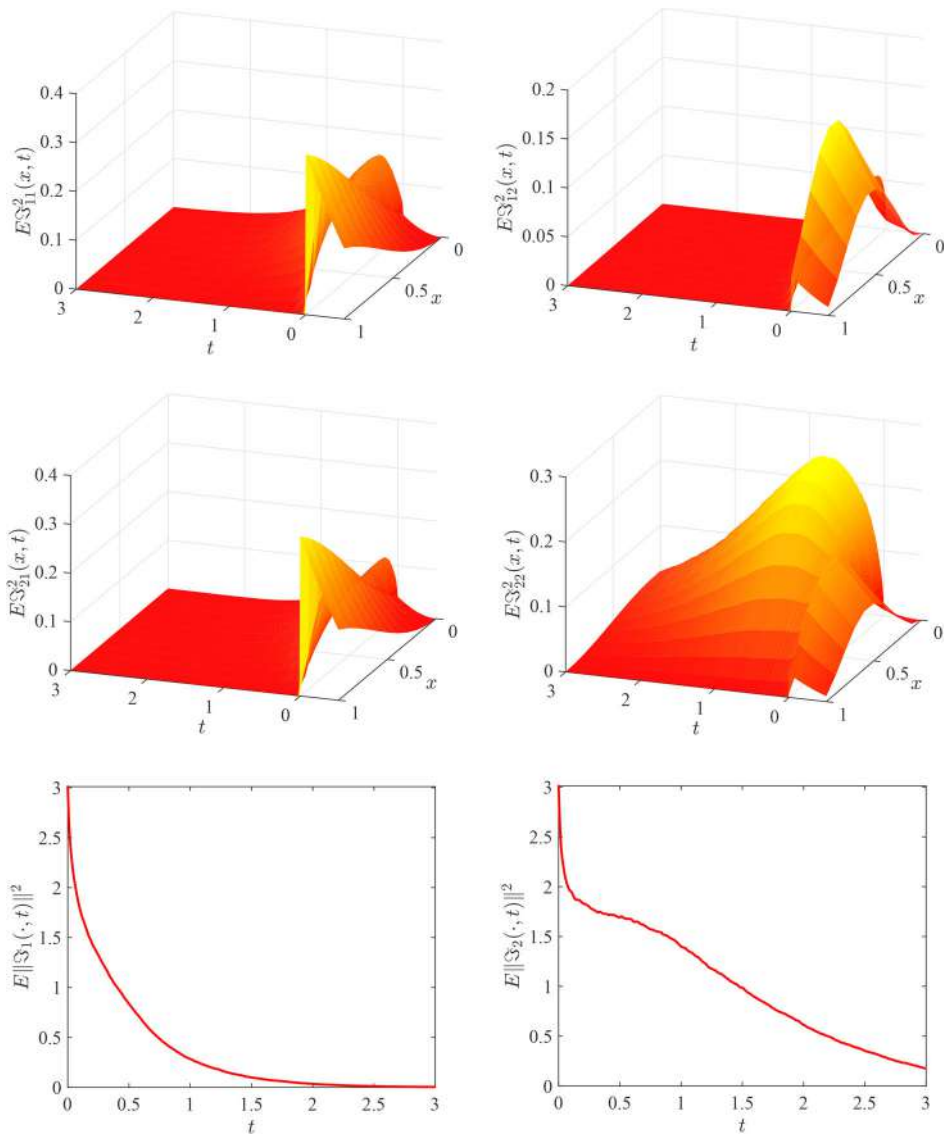


Figure 1. State responses $\mathbb{E}\mathfrak{S}^2(x, t)$ and state norm $\mathbb{E}\|\mathfrak{S}(\cdot, t)\|^2$ of system (47) without control.

We let, $\eta = 0.7$, $\kappa = 0.3$, $\gamma = 2.5$, $\varrho = 1.05$, $\kappa_1 = 1/2$, $\kappa_2 = 29/3$, $\mathcal{T} = 0.2$ and $\mathcal{P} = I$. Solve the LMIs in Theorem 3.3 by using the MATLAB LMI toolbox, we obtain the following feasible solutions:

$$\mathfrak{A}_1 = \begin{bmatrix} 0.3080 & 0.0557 \\ 0.0557 & 0.4998 \end{bmatrix}, \quad \mathfrak{A}_2 = \begin{bmatrix} 0.4352 & 0.0284 \\ 0.0284 & 0.6410 \end{bmatrix}, \quad \mathfrak{B}_1 = \begin{bmatrix} 0.7749 & -0.0484 \\ -0.0484 & 0.0000 \end{bmatrix},$$

$$\mathfrak{B}_2 = \begin{bmatrix} 0.3758 & -0.2355 \\ -0.2355 & 0.0000 \end{bmatrix}, \quad \tilde{\Theta}_1 = \begin{bmatrix} 0.4518 & -0.0161 \\ -0.0161 & 0.4422 \end{bmatrix}, \quad \tilde{\Theta}_2 = \begin{bmatrix} 0.4533 & -0.0392 \\ -0.0392 & 0.2659 \end{bmatrix},$$

$$\tilde{\Lambda}_1 = \begin{bmatrix} 0.2985 & -0.0200 \\ -0.0200 & 0.2330 \end{bmatrix}, \quad \tilde{\Lambda}_2 = \begin{bmatrix} 0.2613 & -0.0279 \\ -0.0279 & 0.1691 \end{bmatrix}, \quad \tilde{\Upsilon}_1 = \begin{bmatrix} 0.2231 & -0.0088 \\ -0.0088 & 0.1942 \end{bmatrix},$$

$$\begin{aligned}
\tilde{\Upsilon}_2 &= \begin{bmatrix} 0.2072 & -0.0147 \\ -0.0147 & 0.1591 \end{bmatrix}, & \tilde{\Psi}_{11} &= \begin{bmatrix} 2.0458 & 0.0779 \\ 0.0779 & 2.3221 \end{bmatrix}, & \tilde{\Psi}_{12} &= \begin{bmatrix} 2.1813 & 0.1282 \\ 0.1282 & 2.7498 \end{bmatrix}, \\
\tilde{\Psi}_{21} &= \begin{bmatrix} 2.0584 & 0.0867 \\ 0.0867 & 2.3642 \end{bmatrix}, & \tilde{\Psi}_{22} &= \begin{bmatrix} 2.2100 & 0.1505 \\ 0.1505 & 2.8530 \end{bmatrix}, & \Xi_1 &= \begin{bmatrix} 3.3130 & -0.3690 \\ -0.3690 & 2.0417 \end{bmatrix}, \\
\Xi_2 &= \begin{bmatrix} 2.3043 & -0.1022 \\ -0.1022 & 1.5645 \end{bmatrix}, & \Theta_1 &= \begin{bmatrix} 5.0580 & -0.9965 \\ -0.9965 & 1.9291 \end{bmatrix}, & \Theta_2 &= \begin{bmatrix} 2.4280 & -0.2911 \\ -0.2911 & 0.6682 \end{bmatrix}, \\
\Lambda_1 &= \begin{bmatrix} 3.3565 & -0.6786 \\ -0.6786 & 1.0421 \end{bmatrix}, & \Lambda_2 &= \begin{bmatrix} 1.4026 & -0.1896 \\ -0.1896 & 0.4255 \end{bmatrix}, & \Upsilon_1 &= \begin{bmatrix} 2.4969 & -0.4798 \\ -0.4798 & 0.8532 \end{bmatrix}, \\
\Upsilon_2 &= \begin{bmatrix} 2.4109 & -0.2354 \\ -0.2354 & 1.0922 \end{bmatrix}, & \Psi_{11} &= \begin{bmatrix} 22.5797 & -3.7128 \\ -3.7128 & 9.8415 \end{bmatrix}, & \Psi_{12} &= \begin{bmatrix} 11.5508 & -0.4902 \\ -0.4902 & 6.7123 \end{bmatrix}, \\
\Psi_{21} &= \begin{bmatrix} 22.7028 & -3.6991 \\ -3.6991 & 10.0053 \end{bmatrix}, & \Psi_{22} &= \begin{bmatrix} 11.6936 & -0.4329 \\ -0.4329 & 6.9581 \end{bmatrix}.
\end{aligned}$$

Furthermore, the control gains, ADT and GCC are obtained as follows:

$$\mathcal{K}_1 = \begin{bmatrix} 2.5852 & -0.3847 \\ -0.1603 & 0.0179 \end{bmatrix}, \quad \mathcal{K}_2 = \begin{bmatrix} 0.8901 & -0.4068 \\ -0.5426 & 0.0241 \end{bmatrix}, \quad \tau_{\epsilon^*} = 0.0155, \quad J^* = 13.4835. \quad (48)$$

By virtue of (4) and (48), Figure 2 shows that the reliable controller (4) can guarantee finite-time stabilization for system (47) with stochastic disturbances. Furthermore, Figure 3 illustrates the effects of switching signals $\sigma(t)$ and Figure 4 illustrates the state responses $\mathbb{E}\mathbb{S}^2(x, t)$ of system (47) with different time-varying delays.

Case 2: System (47) without stochastic disturbances.

Solve the LMIs in Corollary 3.11 by using the MATLAB LMI toolbox, we obtain the following feasible solutions:

$$\begin{aligned}
\mathfrak{A}_1 &= \begin{bmatrix} 0.0678 & 0.0102 \\ 0.0102 & 0.0992 \end{bmatrix}, & \mathfrak{A}_2 &= \begin{bmatrix} 0.0804 & 0.0113 \\ 0.0113 & 0.1119 \end{bmatrix}, & \mathfrak{B}_1 &= \begin{bmatrix} 0.1901 & -0.0193 \\ -0.0193 & 0.0000 \end{bmatrix}, \\
\mathfrak{B}_2 &= \begin{bmatrix} 0.2025 & -0.1174 \\ -0.1174 & 0.0000 \end{bmatrix}, & \tilde{\Theta}_1 &= \begin{bmatrix} 0.1149 & -0.0035 \\ -0.0035 & 0.1047 \end{bmatrix}, & \tilde{\Theta}_2 &= \begin{bmatrix} 0.1092 & -0.0067 \\ -0.0067 & 0.0880 \end{bmatrix}, \\
\tilde{\Lambda}_1 &= \begin{bmatrix} 0.0788 & -0.0020 \\ -0.0020 & 0.0708 \end{bmatrix}, & \tilde{\Lambda}_2 &= \begin{bmatrix} 0.0753 & -0.0036 \\ -0.0036 & 0.0708 \end{bmatrix}, & \tilde{\Upsilon}_1 &= \begin{bmatrix} 0.0544 & -0.0007 \\ -0.0007 & 0.0528 \end{bmatrix}, \\
\tilde{\Upsilon}_2 &= \begin{bmatrix} 0.0544 & -0.0013 \\ -0.0013 & 0.0507 \end{bmatrix}, & \tilde{\Psi}_{11} &= \begin{bmatrix} 0.4701 & 0.0032 \\ 0.0032 & 0.4802 \end{bmatrix}, & \tilde{\Psi}_{12} &= \begin{bmatrix} 0.4735 & 0.0047 \\ 0.0047 & 0.4875 \end{bmatrix}, \\
\tilde{\Psi}_{21} &= \begin{bmatrix} 0.4705 & 0.0038 \\ 0.0038 & 0.4828 \end{bmatrix}, & \tilde{\Psi}_{22} &= \begin{bmatrix} 0.4748 & 0.0057 \\ 0.0057 & 0.4917 \end{bmatrix}, & \Xi_1 &= \begin{bmatrix} 14.9766 & -1.5371 \\ -1.5371 & 10.2386 \end{bmatrix}, \\
\Xi_2 &= \begin{bmatrix} 12.6084 & -1.2689 \\ -1.2689 & 9.0667 \end{bmatrix}, & \Theta_1 &= \begin{bmatrix} 26.1796 & -4.8411 \\ -4.8411 & 11.3586 \end{bmatrix}, & \Theta_2 &= \begin{bmatrix} 17.7094 & -3.5406 \\ -3.5406 & 7.5679 \end{bmatrix}, \\
\Lambda_1 &= \begin{bmatrix} 17.9264 & -3.2452 \\ -3.2452 & 7.6739 \end{bmatrix}, & \Lambda_2 &= \begin{bmatrix} 12.1884 & -2.3752 \\ -2.3752 & 5.5705 \end{bmatrix}, & \Upsilon_1 &= \begin{bmatrix} 12.6427 & -2.2267 \\ -2.2267 & 5.6894 \end{bmatrix}, \\
\Upsilon_2 &= \begin{bmatrix} 18.5459 & -3.4512 \\ -3.4512 & 8.8736 \end{bmatrix}, & \Psi_{11} &= \begin{bmatrix} 106.4272 & -17.8779 \\ -17.8779 & 51.3473 \end{bmatrix}, \\
\Psi_{12} &= \begin{bmatrix} 75.9033 & -12.6401 \\ -12.6401 & 40.7263 \end{bmatrix}, & \Psi_{21} &= \begin{bmatrix} 106.4952 & -17.8401 \\ -17.8401 & 51.5999 \end{bmatrix},
\end{aligned}$$

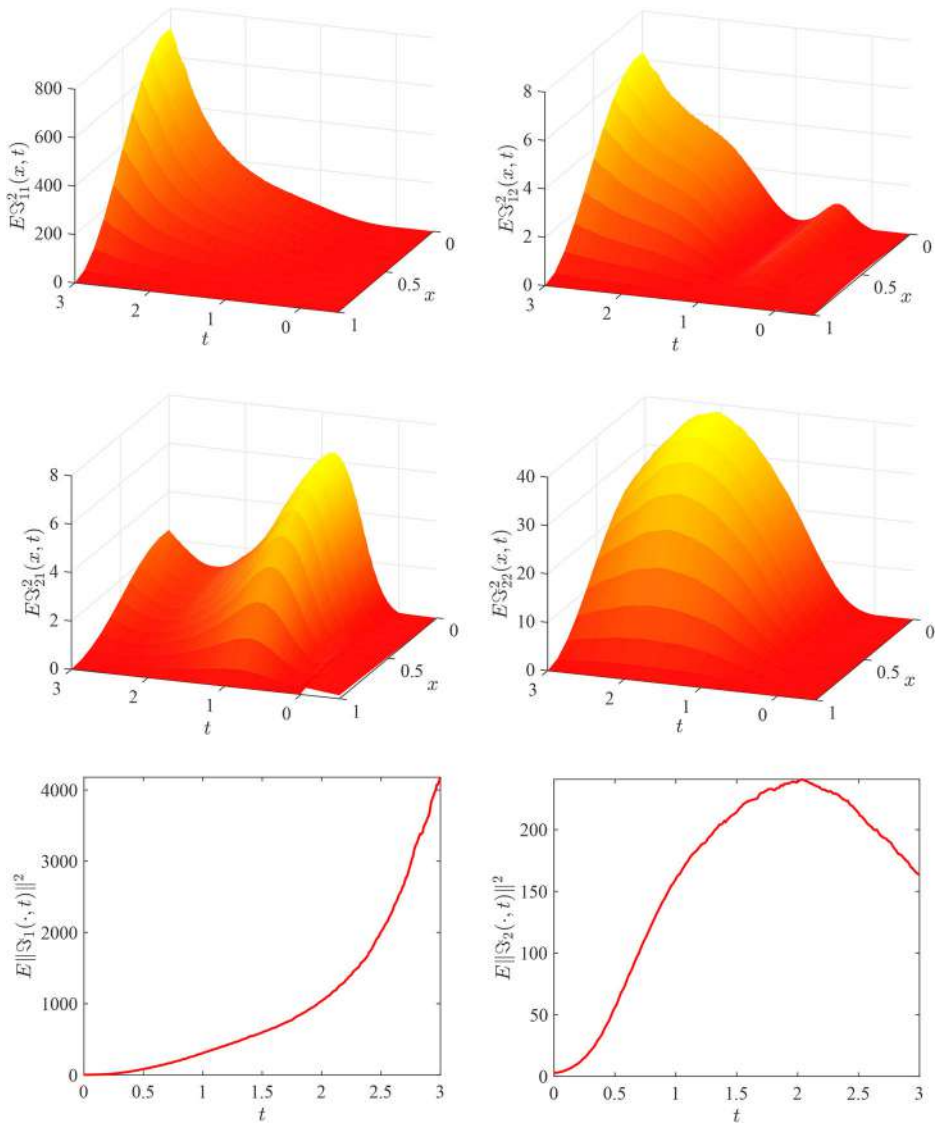


Figure 2. State responses $E\|S^2(x,t)$ and state norm $E\|S(\cdot, t)\|^2$ of system (47) with control and stochastic disturbances.

$$\Psi_{22} = \begin{bmatrix} 76.0871 & -12.5877 \\ -12.5877 & 41.0553 \end{bmatrix}.$$

Furthermore, the control gains, ADT and GCC are obtained as follows:

$$\mathcal{K}_1 = \begin{bmatrix} 2.8773 & -0.4900 \\ -0.2893 & 0.0297 \end{bmatrix}, \quad \mathcal{K}_2 = \begin{bmatrix} 2.7023 & -1.3212 \\ -1.4799 & 0.1489 \end{bmatrix}, \quad \tau_{\epsilon^*} = 0.0666, \quad J^* = 7.6544. \quad (49)$$

By virtue of (4) and (49), Figure 5 shows that the reliable controller (4) cannot guarantee finite-time stabilization for system (47) without stochastic disturbances.

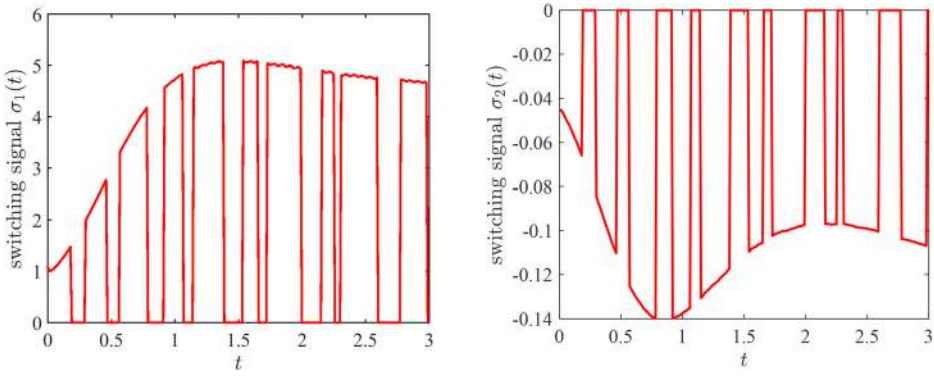


Figure 3. Effects of switching signals $\sigma(t)$.

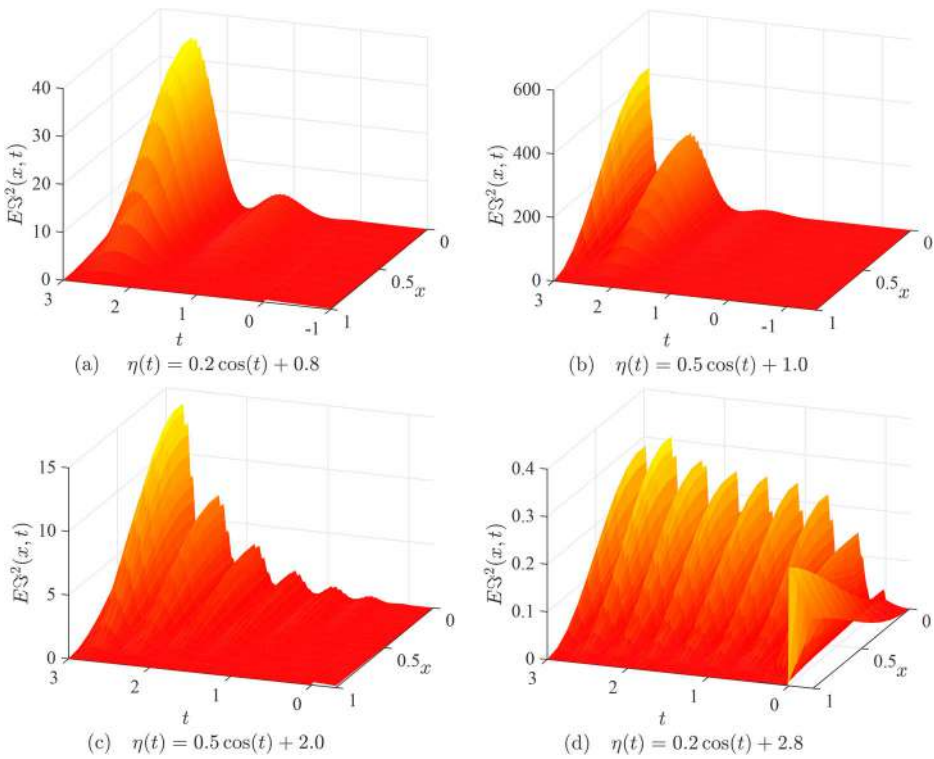


Figure 4. Effects of time-varying delays $\eta(t)$.

5. Conclusion

This paper investigated the finite-time guaranteed cost control for a class of stochastic nonlinear switched systems, where time-varying delays, reaction-diffusion, actuator faults, Neumann boundary condition and reliable control are considered. Then, the finite-time stability criterion is obtained by virtue of the Lyapunov method, some famous inequality techniques and average dwell-time approach. It should be pointed out that the finite-time stabilization performance was investigated through the control gains for reliable controller. Furthermore, we obtained the finite-time cost control for proposed controlled systems. Finally, the numerical simulations show the effectiveness of the designed reliable controller and obtained theoretical results. Since intermittent boundary control methods

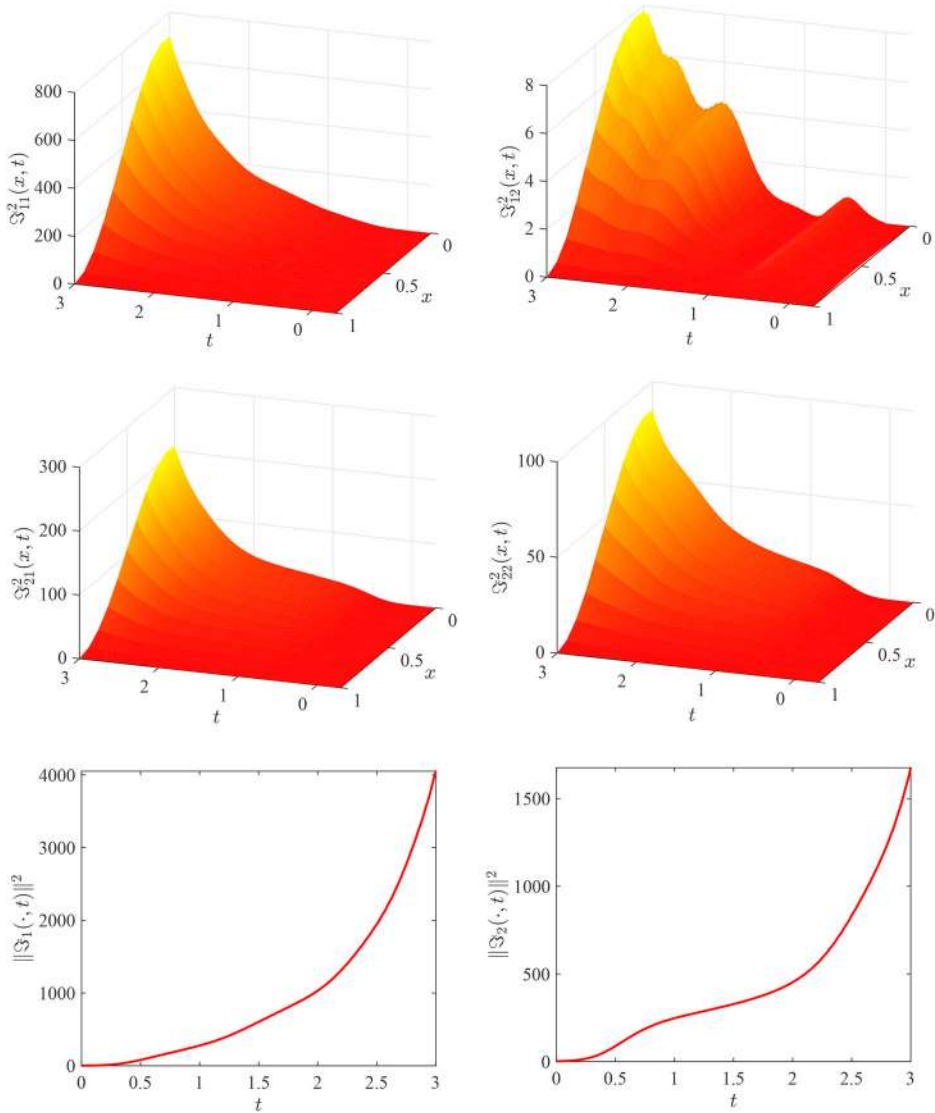


Figure 5. State responses $\mathbb{E}\mathfrak{S}^2(x, t)$ and state norm $\mathbb{E}\|\mathfrak{S}(\cdot, t)\|^2$ of system (47) with control and without stochastic disturbances.

can save control cost of both spatial and temporal domain, future work will focus on the intermittent boundary synchronization and stabilization problems of fractional-order stochastic nonlinear switched reaction-diffusion systems via intermittent boundary control.

Disclosure statement

No potential conflict of interest was reported by the author(s).

References

- [1] A. Cetinkaya, H. Ishii, and T. Hayakawa, *Analysis of stochastic switched systems with application to networked control under jamming attacks*, IEEE Trans. Automat. Contr. 64 (2018), pp. 2013–2028.
- [2] X.H. Chang, R. Huang, and J.H. Park, *Robust guaranteed cost control under digital communication channels*, IEEE Trans. Ind. Inform. 16 (2019), pp. 319–327.

- [3] Y. Chen, Q. Liu, R. Lu, and A. Xue, *Finite-time control of switched stochastic delayed systems*, Neurocomputing 191 (2016), pp. 374–379.
- [4] P. Cheng, S. He, X. Luan, and F. Liu, *Finite-region asynchronous control for 2D Markov jump systems*, Automatica 129 (2021), p. 109590.
- [5] D. Ding, J. Liu, M. Li, and L. Liu, *Double switchings reliable control of positive switched systems with unfixed actuator faults*, IEEE. Access. 8 (2020), pp. 65734–65744.
- [6] X. Fan, X. Zhang, L. Wu, and M. Shi, *Finite-time stability analysis of reaction-diffusion genetic regulatory networks with time-varying delays*, IEEE/ACM Trans. Comput. Biol. Bioinform. 14 (2017), pp. 868–879.
- [7] V. Gokulakrishnan and R. Srinivasan, *Finite-time boundedness of stochastic nonlinear reaction-diffusion systems with time delays and exogenous disturbances via boundary control*, Int. J. Nonlinear Anal. Appl. 13 (2022), pp. 1821–1832.
- [8] V. Gokulakrishnan and R. Srinivasan, *Impulsive effects on stabilization of stochastic nonlinear reaction-diffusion systems with time delays and boundary feedback control*, J. Math. Comput. Sci. 28 (2023), pp. 350–362.
- [9] J. Han, X. Liu, X. Wei, X. Hu, and H. Zhang, *Reduced-order observer based fault estimation and fault-tolerant control for switched stochastic systems with actuator and sensor faults*, ISA. Trans. 88 (2019), pp. 91–101.
- [10] X.X. Han, K.N. Wu, X. Ding, and B. Yang, *Boundary control of stochastic reaction-diffusion systems with Markovian switching*, Int. J. Robust Nonlinear Control 30 (2020), pp. 4129–4148.
- [11] X.X. Han, K.N. Wu, and X. Ding, *Finite-time stabilization for stochastic reaction-diffusion systems with Markovian switching via boundary control*, Appl. Math. Comput. 385 (2020), p. 125422.
- [12] X.X. Han, K.N. Wu, and Y. Niu, *Asynchronous boundary stabilization of stochastic Markov jump reaction-diffusion systems*, IEEE Trans. Syst. Man Cybern. Syst. 52 (2022), pp. 5668–5678.
- [13] S. He, Q. Ai, C. Ren, J. Dong, and F. Liu, *Finite-time resilient controller design of a class of uncertain nonlinear systems with time-delays under asynchronous switching*, IEEE Trans. Syst. Man Cybern. Syst. 49 (2019), pp. 281–286.
- [14] D. Hu, J. Tan, K. Shi, and K. Ding, *Switching synchronization of reaction-diffusion neural networks with time-varying delays*, Chaos Solitons Fract. 155 (2022), p. 111766.
- [15] H. Hu, B. Jiang, and H. Yang, *Reliable guaranteed-cost control of delta operator switched systems with actuator faults: Mode-dependent average dwell-time approach*, IET Control Theory Appl. 10 (2016), pp. 17–23.
- [16] J. Hu, Q. Zhang, A.M. Baese, and M. Ye, *Stability in distribution for a stochastic Alzheimer’s disease model with reaction-diffusion*, Nonlinear. Dyn. 108 (2022), pp. 4243–4260.
- [17] S. Huang and Z. Xiang, *Finite-time stabilization of switched stochastic nonlinear systems with mixed odd and even powers*, Automatica 73 (2016), pp. 130–137.
- [18] X. Huang and J. Dong, *Reliable control policy of cyber-physical systems against a class of frequency-constrained sensor and actuator attacks*, IEEE. Trans. Cybern. 48 (2018), pp. 3432–3439.
- [19] H. Jia, Z. Xiang, and H.R. Karimi, *Robust reliable passive control of uncertain stochastic switched time-delay systems*, Appl. Math. Comput. 231 (2014), pp. 254–267.
- [20] S. Lakshmanan, M. Prakash, R. Rakkiyappan, and J.H. Young, *Adaptive synchronization of reaction-diffusion neural networks and its application to secure communication*, IEEE. Trans. Cybern. 50 (2020), pp. 911–922.
- [21] Y. Li and Y. Ren, *Stability of switched stochastic reaction-diffusion systems*, Int. J. Control. (2022). <https://doi.org/10.1080/00207179.2022.2097958>
- [22] J. Lian, C. Li, and B. Xia, *Sampled-data control of switched linear systems with application to an F-18 aircraft*, IEEE Trans. Ind. Electron. 64 (2016), pp. 1332–1340.
- [23] H. Lin and F. Wang, *Global dynamics of a nonlocal reaction-diffusion system modeling the west nile virus transmission*, Nonlinear Anal. Real World Appl. 46 (2019), pp. 352–373.
- [24] L. Liu, Y.J. Liu, D. Li, S. Tong, and Z. Wang, *Barrier Lyapunov function-based adaptive fuzzy FTC for switched systems and its applications to resistance-inductance-capacitance circuit system*, IEEE. Trans. Cybern. 50 (2019), pp. 3491–3502.
- [25] X. Lyu, Q. Ai, Z. Yan, S. He, X. Luan, and F. Liu, *Finite-time asynchronous resilient observer design of a class of non-linear switched systems with time-delays and uncertainties*, IET Control Theory Appl. 14 (2020), pp. 952–963.
- [26] J. Man, Z. Zeng, Q. Xiao, and H. Zhang, *Exponential stabilization of semi-Markov reaction-diffusion memristive NNs via event-based spatially pointwise-piecewise switching control*, IEEE. Trans. Neural. Netw. Learn. Syst. (2022). <https://doi.org/10.1109/TNNLS.2022.3190694>
- [27] H. Ren, G. Zong, and H.R. Karimi, *Asynchronous finite-time filtering of networked switched systems and its application: An event-driven method*, IEEE Trans. Circuits Syst. 66 (2018), pp. 391–402.
- [28] H. Shen, M. Xing, Z.G. Wu, and J.H. Park, *Fault-tolerant control for fuzzy switched singular systems with persistent dwell-time subject to actuator fault*, Fuzzy Sets Syst. 392 (2020), pp. 60–76.
- [29] J. Song, Y. Niu, and Y. Zou, *A parameter-dependent sliding mode approach for finite-time bounded control of uncertain stochastic systems with randomly varying actuator faults and its application to a parallel active suspension system*, IEEE Trans. Ind. Electron. 65 (2018), pp. 8124–8132.
- [30] X. Song, M. Wang, J.H. Park, and S. Song, *Spatial- L_∞ -norm-based finite-time bounded control for semilinear parabolic PDE systems with applications to chemical-reaction processes*, IEEE. Trans. Cybern. 52 (2022), pp. 178–191.


- [31] X. Song, Q. Zhang, S. Song, and C.K. Ahn, *Sampled-data-based event-triggered fuzzy control for PDE systems under cyber-attacks*, IEEE. Trans. Fuzzy Syst. 30 (2022), pp. 2693–2705.
- [32] M. Syed Ali and S. Saravanan, *Finite-time L_2 -gain analysis for switched neural networks with time-varying delay*, Neural Comput. Appl. 29 (2016), pp. 975–984.
- [33] M. Syed Ali and J. Yogambigai, *Exponential stability of semi-Markovian switching complex dynamical networks with mixed time varying delays and impulsive control*, Neural Process. Lett. 46 (2016), pp. 113–133.
- [34] M. Syed Ali, R. Saravanakumar, and H.R. Karimi, *Robust H_∞ control of uncertain stochastic Markovian jump systems with mixed time-varying delays*, Int. J. Syst. Sci. 48 (2017), pp. 862–872.
- [35] M. Syed Ali, R. Vadivel, and R. Saravanakumar, *Design of robust reliable control for T-S fuzzy Markovian jumping delayed neutral type neural networks with probabilistic actuator faults and leakage delays: An event-triggered communication scheme*, ISA. Trans. 77 (2018), pp. 30–48.
- [36] M. Syed Ali, J. Yogambigai, and O.M. Kwon, *Finite-time robust passive control for a class of switched reaction-diffusion stochastic complex dynamical networks with coupling delays and impulsive control*, Int. J. Syst. Sci. 49 (2018), pp. 718–735.
- [37] M. Syed Ali, L. Palanisamy, J. Yogambigai, and L. Wang, *Passivity-based synchronization of Markovian jump complex dynamical networks with time-varying delays, parameter uncertainties, reaction-diffusion terms, and sampled-data control*, J. Comput. Appl. Math. 352 (2019), pp. 79–92.
- [38] G.K. Thakur, M. Syed Ali, B. Priya, V. Gokulakrishnan, and S. Asma Kauser, *Impulsive effects on stochastic bidirectional associative memory neural networks with reaction-diffusion and leakage delays*, Int. J. Comput. Math. 28 (2023), pp. 350–362.
- [39] M.V. Thuan, *Robust finite-time guaranteed cost control for positive systems with multiple time delays*, J. Syst. Sci. Complex. 32 (2019), pp. 496–509.
- [40] J. Wang and H. Wu, *Passivity of delayed reaction-diffusion networks with application to a food web model*, Appl. Math. Comput. 219 (2013), pp. 11311–11326.
- [41] Y. Wang, P. Shi, and H. Yan, *Reliable control of fuzzy singularly perturbed systems and its application to electronic circuits*, IEEE Trans. Circuits Syst. 65 (2018), pp. 3519–3528.
- [42] H. Wang, P.X. Liu, X. Zhao, and X. Liu, *Adaptive fuzzy finite-time control of nonlinear systems with actuator faults*, IEEE. Trans. Cybern. 50 (2019), pp. 1786–1797.
- [43] Y. Wu, J. Cao, A. Alofi, A.A. Mazrooei, and A. Elaiw, *Finite-time boundedness and stabilization of uncertain switched neural networks with time-varying delay*, Neural. Netw. 69 (2015), pp. 135–143.
- [44] Z.G. Wu, S. Dong, P. Shi, H. Su, and T. Huang, *Reliable filtering of nonlinear Markovian jump systems: The continuous-time case*, IEEE Trans. Syst. Man Cybern. Syst. 49 (2017), pp. 386–394.
- [45] Z. Xiang, C. Qiao, and M.S. Mahmoud, *Finite-time analysis and H_∞ control for switched stochastic systems*, J. Franklin. Inst. 349 (2012), pp. 915–927.
- [46] Z. Yan, T. Guo, A. Zhao, Q. Kong, and J. Zhou, *Reliable exponential H_∞ filtering for a class of switched reaction-diffusion neural networks*, Appl. Math. Comput. 414 (2022), p. 126661.
- [47] X. Yang, Y. Tian, and X. Li, *Finite-time boundedness and stabilization of uncertain switched delayed neural networks of neutral type*, Neurocomputing 314 (2018), pp. 468–478.
- [48] X.W. Zhang, H.N. Wu, J.L. Wang, Z. Liu, and R. Li, *Membership-function-dependent fuzzy control of reaction-diffusion memristive neural networks with a finite number of actuators and sensors*, Neurocomputing 514 (2022), pp. 94–100.
- [49] H. Zhao, Y. Niu, and T. Jia, *Security control of cyber-physical switched systems under round-robin protocol: Input-to-state stability in probability*, Inf. Sci. (Ny) 508 (2020), pp. 121–134.
- [50] S. Zheng and W. Li, *Fuzzy finite-time control for switched systems via adding a barrier power integrator*, IEEE. Trans. Cybern. 49 (2018), pp. 2693–2706.
- [51] C. Zho and X. Wang, *Robust stability of delayed Markovian switching genetic regulatory networks with reaction-diffusion terms*, Comput. Math. Appl. 79 (2020), pp. 1150–1164.
- [52] J. Zhou, Y. Liu, J.H. Park, Q. Kong, and Z. Wang, *Fault-tolerant anti-synchronization control for chaotic switched neural networks with time delay and reaction-diffusion*, Discrete Contin. Dyn. Syst. Ser. S 14 (2021), pp. 1569–1589.
- [53] Q. Zhu, *Stabilization of stochastic nonlinear delay systems with exogenous disturbances and the event-triggered feedback control*, IEEE. Trans. Automat. Contr. 64 (2019), pp. 3764–3771.
- [54] G. Zong, X. Wang, and H. Zhao, *Robust finite-time guaranteed cost control for impulsive switched systems with time-varying delay*, Int. J. Control Autom. Syst. 15 (2016), pp. 113–121.



Impulsive control strategies of mRNA and protein dynamics on fractional-order genetic regulatory networks with actuator saturation and its oscillations in repressilator model

G. Narayanan^a , M. Syed Ali^b , Rajagopal Karthikeyan^c , Grienggrai Rajchakit^d  , Anuwat Jirawattanapanit^e 

[Show more](#) 

 Share  Cite

<https://doi.org/10.1016/j.bspc.2023.104576> 

[Get rights and content](#) 

Abstract

In genetic regulatory networks (GRNs), the control strategies of messenger RNA (mRNA) and protein play a key role in regulatory mechanisms of gene expression, especially in translation and transcription. However, the influence of impulsive control strategies on oscillatory gene expression is not well understood. In this article, by considering the impulsive control strategies of mRNA and protein, a novel fractional-order genetic regulatory networks with actuator saturation is proposed. By applying polytopic representation technique, the actuator saturation term is first considered into the design of impulsive controller, and less conservative linear matrix inequalities (LMIs) criteria that guarantee finite-time Mittag-Leffler stabilization problem for fractional-order genetic regulatory networks are given. The derived sufficient conditions can easily be verified by designing impulsive control gains and solving simple LMIs. Finally, to investigate the effectiveness and applicability of the control strategies, an interesting simulation example as a synthetic oscillatory network of transcriptional regulators in Escherichia coli is illustrated.

Introduction

Genetic regulatory networks (GRNs) are biochemical networks that regulate gene expression and perform complex biological functions (via direct or indirect interactions between deoxyribonucleic acid (DNA), ribonucleic acid (RNA), proteins, and small molecules) as shown in Fig. 1. GRNs are a significant topic in bioscience and biomedical engineering, as they can help many biologists, engineers, and scientists understand a variety of complex challenges in living cells [1], [2], [3]. Because many traits and diseases are linked to dysfunctional transcriptional regulators or mutations in regulatory sequences, understanding gene expression regulation has an immediate impact on biology and medicine. Acquiring precise information about the states of GRNs is particularly useful in biological and biomedical sciences for applications such as gene identification and medical diagnosis/treatment [4], [5]. One of the key challenges in this area